AIR POLLUTION CONFERENCE
5th CMAS SOUTH AMERICA
COMMUNITY MODELING ANALYSIS SYSTEM

PROCEEDINGS OF THE

AIR POLLUTION CONFERENCE 2024

And 5th CMAS South America









Maria de Fátima Andrade
Taciana Toledo de A. Albuquerque
Jane Meri Santos

ISBN: 978-65-985800-0-1
Version - 3

Proceedings

AIR POLLUTION CONFERENCE 2024

And 5th CMAS South America

CONFERENCE
05 - 07 JUNE 2024

Maria de Fátima Andrade
Taciana Toledo de A. Albuquerque
Jane Meri Santos

ISBN: 978-65-985800-0-1

Version - 3

SÃO PAULO, 2024

www.aripollutionconference/2024

Proceedings

We are pleased to present the proceedings of the Air Pollution Conference Brazil 2024, held in June in São Paulo city at the University of São Paulo (USP). This event brought together leading experts, policymakers, industry representatives, scientists, and students to address the critical challenges posed by air pollution and its wide-ranging impacts on public health, ecosystems, and climate.

São Paulo, as one of Brazil's largest urban centers, provided an ideal setting for this important dialogue. The conference showcased a diverse program, highlighting innovative research, practical solutions, and interdisciplinary approaches to understanding and mitigating air pollution. Key topics included the impact of mining activities on air quality, urban and industrial emissions, the effects of biomass burning and deforestation, and the intersection of air pollution with public health and climate change.

The abstracts included in this program book reflect the richness of the discussions that took place during the conference. They represent the latest advancements in air quality monitoring, mitigation strategies, policy frameworks, and collaborative initiatives aimed at tackling the pressing issue of air pollution in Brazil and beyond.

We extend our deepest gratitude to the University of São Paulo for hosting this event, to the organizing committee for their dedication, and to all participants for their valuable contributions. This compilation of abstracts serves not only as a record of the conference but also as a resource to inspire continued efforts in addressing air pollution and its far-reaching consequences.
We hope this program book will serve as a reference and a catalyst for further research, collaboration, and action toward achieving cleaner air and a healthier environment for all.

Sincerely,
Maria de Fátima Andrade
Chair, Air Pollution Conference Brazil 2024

SUMMARY

UNIVERSITIES ORGANIZERS 6

PREMIUM SPONSORSHIP 7

SPONSORS 8

EXHIBITOR 9

SUPPORT 10

SCIENTIFIC COMMITTEE 10

ORGANIZING COMMITTEE 11

SESSION 01
AIR QUALITY, CLIMATE AND ENERGY 13

SESSION 02
AIR POLLUTION CONTROL 52

SESSION 03 EMERGING TRENDS AND INNOVATIONS
IN AIR POLLUTION RESEARCH 112

SESSION 04
EMISSIONS INVENTORIES, MODELS, AND
PROCESSES 130

SESSION 05
ENVIRONMENTAL ODOURS 156

SESSION 06
INDOOR AIR QUALITY AND ITS IMPLICATIONS 161

SUMMARY

SESSION 07
MACHINE LEARNING AND REDUCED FORM MODELS DEVELOPMENTS AND APPLICATIONS 179

SESSION 09
MODELING TO SUPPORT EXPOSURE AND HEALTH STUDIES AND COMMUNITY-SCALE APPLICATIONS 190

SESSION 10
MULTISCALE MODEL APPLICATIONS AND EVALUATIONS 204

SESSION 11
PARTICULATE MATTER AND ITS EFFECTS ON HUMAN HEALTH AND THE ENVIRONMENT 227

SESSION 12
POLICY AND REGULATORY FRAMEWORKS FOR AIR POLLUTION CONTROL 353

SESSION 13
REMOTE SENSING/SENSOR TECHNOLOGY AND MEASUREMENTS STUDIES 371

SESSION 14
URBAN CLIMATE PROCESSES AND METHODS 402

SESSION 15
STREET SCALE AIR QUALITY MODELING 425



UNIVERSITIES ORGANIZERS

USP

UFMG

UFES

THE UNIVERSITY of NORTH CAROLINA at CHAPEL HILL



PREMIUM SPONSORSHIP

ArcelorMittal

www.aripollutionconference/2024

SPONSORS







EXHIBITOR


QualityAmb


FPI
Focused Photonics Inc.


EcoSoft


DURAG BRASIL
DURAG GROUP


envex
engenharia e consultoria


NASAL RANGER


acoem


AEROSOL
MAGEE SCIENTIFIC

SUPPORT

WORLD METEOROLOGICAL ORGANIZATION

GURME

KLIMAPOLIS BRASIL

FAPEMIG

AngloAmerican

MINISTÉRIO DO MEIO AMBIENTE E MUDANÇA DO CLIMA

GOVERNO FEDERAL BRASIL UNIÃO E RECONSTRUÇÃO

SCIENTIFIC COMMITTEE



- Maria de Fátima Andrade (USP) (Chair)
- Taciana Toledo de A. Albuquerque (UFMG) (Co-Chair)
- Jane Meri Santos (UFES) (Co-Chair)
- Sarav Arunachalam (UNC)
- Yang Zhang (Northeastern University)
- Prashant Kumar (U.SURREY)
- Edmilson Dias Freitas (USP)
- Eduardo Landulfo (IPEN)
- Rita Y. Ynoue (USP)
- Lucia Andrade (USP)
- Pedro Jose Perez Martinez (UNICAMP)
- Neyval Costa Reis Junior (UFES)
- Jorge Alberto Martins (UFTPR)
- Leila Droprinchinski Martins (UFTPR)
- Leonardo Hoinaski (UFSC)
- Judith Hoelzemann (UFRN)
- Helber Barros Gomes (UFAL)
- Rafael Sartim (UFES)

ORGANIZING COMMITTEE



- Maria de Fátima Andrade (USP) (Chair)
- Taciana Toledo de A. Albuquerque (UFMG) (Co-Chair)
- Jane Meri Santos (UFES) (Co-Chair)
- Sarav Arunachalam (UNC)
- Yang Zhang (Northeastern University)
- Edmilson Dias Freitas (USP)
- Regina Maura de Miranda (USP)
- Mario Eduardo Gavidia Calderón (USP)
- Thiago Nogueira (USP)
- Janaina Antonino (UNICAMP)
- Rizzieri Pedruzzi (UERJ)
- Guilherme Martins Pereira (USP)
- Rafaela Squizzato (USP)
- João Ernani Antunes Costa Jr. (SEADFLIX)

PROCEEDINGS OF THE

2024 AIR POLLUTION CONFERENCE

And 5th CMAS South America

SESSION 01
Air Quality, Climate and Energy

The energy system is currently responsible for the majority of U.S. emissions of criteria air pollutants, greenhouse gases, and short-lived climate forcing pollutants. Understanding how the energy system may evolve in the future and the resulting implications on the environment is critical if environmental decision-makers are to address these challenges proactively and efficiently. The goal of this session is to highlight research efforts involved in exploring the linkages among air quality, climate and energy, with focus on supporting decision-making at federal, state or local levels. Among the topics that are appropriate for inclusion are:

- Scenario approaches for examining energy system futures, including exploring linkages between population growth, economic growth, land use change, climate change, technology change (in including cleantech), policy and energy
- Impact of the future energy system on sustainability and vulnerability metrics
- Translating energy system modeling into climate and air quality impacts
- Identifying interactions between strategies for climate mitigation and air quality management, including quantification of co-benefits and holistic management strategies that simultaneously meet both goals
- Models, tools and methodologies for assessing air, climate and energy linkages

SESSION 1

PM CHEMICAL CHARACTERIZATION AT A SEMI-ARID URBAN ENVIRONMENT IN CENTRAL MEXICO 15

EVALUATİON OF AİR QUALİTY İN THE CİTY OF FORTALEZA, BRAZİL, İN 2022 AND 2023: A COMPARİSON BETWEEN LOCAL AND INTERNATİONAL STANDARDS FOR PARTİCULATE MATTER (PM10 AND PM2.5) 17

SOURCE APPORTIONMENT AND THERMODYNAMIC MODELING OF ATMOSPHERIC AEROSOLS IN THE CENTRAL AMAZONIA 20

WİLL RİO DE JANEİRO FULFİLL SDG 11.6 OF THE 2030 AGENDA? AN ANALYSİS OF AİR QUALİTY FROM 2015 TO 2023 AND PROJECTİON TO 2030 23

BIOMASP+: TACKLING THE BIOSPHERE-ATMOSPHERE EXCHANGES AND THEIR IMPACT ON AIR POLLUTION IN AN EMBLEMATIC SUBTROPICAL MEGACITY: THE METROPOLITAN AREA OF SÃO PAULO, BRAZIL 26

ASSESSMENT OF AİR QUALİTY İN RİO DE JANEİRO: TRENDS, VİOLATİONS, AND IMPLİCATİONS (2019-2022) 28

GREENHOUSE GAS EMISSIONS FOR BIODIESEL PRODUCTION IN BRAZIL FROM DIFFERENT FEEDSTOCKS USING LIFE CYCLE ASSESSMENT 31

EVALUATİON OF THE RESULTS OF THE FİRST CYCLE OF SUBMİSSİONS OF THE NEW GREENHOUSE GAS EMİSSİONS REPORTİNG PROGRAM İN RİO DE JANEİRO 34

ASSESSING THE MITIGATING IMPACT OF GREEN AND BLUE INFRASTRUCTURE ON ENVIRONMENTAL STRESSORS 37

COOL AND CLEAN AIR PLACES: INTEGRATING PUBLIC PERCEPTION WITH URBAN GREEN SPACE 40

IMPACT OF OZONE ON MORTALİTY AND HOSPİTALİZATİONS İN THE MEGALOPOLİS OF THE VALLEY OF MEXİCO 43

DISPERSION STUDY OF NOX AND NH3 WITH THE AERMOD MODEL FOR A PRODUCTION PLANT OF GREEN HYDROGEN AN GREEN AMMONIA 46

TRENDS IN NITROGEN OXIDES AND OZONE CONCENTRATIONS AND THEIR RELATIONSHIPS WITH GLOBAL SOLAR RADIATION AND TEMPERATURE 49

AIR POLLUTION CONFERENCE BRAZIL
CMAS SOUTH AMERICA
COMMUNITY MODELING AND ANALYSIS SYSTEM

PM CHEMICAL CHARACTERIZATION AT A SEMI-ARID URBAN ENVIRONMENT IN CENTRAL MEXICO

Dara Salcedo[1], Harry Alvarez-Ospina[2], Sara E. Olivares-Salazar[3], Rafael N. Liñan-Abanto[4], Telma Castro[5]

[1] *UMDI-J Facultad de Ciencias, Universidad Nacional Autónoma de México*
dara.salcedo@ciencias.unam.mx
[2] *Facultad de Ciencias, Universidad Nacional Autónoma de México*
harry02co@gmail.com
[3] *UMDI-J Facultad de Ciencias, Universidad Nacional Autónoma de México*
erikaolivares.31@gmail.com
[4] *Departamento de Física, Facultad de Ciencias, Universidad Nacional Jorge Basadre Grohmann*
rafael.linian@gmail.com
[5] *ICAyCC, Universidad Nacional Autónoma de México*
telma@atmosfera.unam.mx

Abstract: We will present the analysis of one year of real-time data of the concentration and chemical composition of particulate matter in Queretaro (an important urban and industrial area in the central part of Mexico), together with meteorological variables and concentrations of criteria pollutants, to gain insight into the major emission sources and processes involved in the formation of particles in this region. The composition of the NR-PM_1 was measured using an aerosol mass spectrometer (ACSM), which speciated the aerosol into sulfate, nitrate, ammonium, chloride, and an organic fraction. Further analysis of the organic component using the PMF model yielded three factors: HOA, a primary fresh component; MO-OOA, a very oxidized (aged) regional aerosol; and LO-OOA, a less oxidized locally produced aerosol. Secondary components were the most abundant in $PM_{2.5}$, followed by resuspended non-refractory components and primary components. Regional photochemical and meteorology played a very important role in the formation of secondary aerosols. This work has been published by Salcedo et al. (2023).

Keywords: Queretaro, Bajio, source apportionment, resuspension, dust

INTRODUCTION

The central part of Mexico, a semi-arid region, hosts many anthropogenic activities (transport, industry, agriculture) that might affect the air quality of the several large cities within; however, the processes that occur in its atmosphere are poorly understood. Among air pollutants, particulate matter (PM) is the one that produces major concern due to its adverse health effects and climate forcing (Kim et al., 2015; Shrivastava et al., 2017). In order to control the air quality in this region, it is crucial to make ambient measurements and to understand the processes that determine the air pollutant concentration.

METHODS

The measuring site was located north of the Metropolitan area of Queretaro (MAQ) (20.7030◦ N, 100.4473◦ W, 1820 m.a.s.l.), in the Juriquilla Campus of the Universidad Nacional Autonoma de Mexico. The surrounding area is mainly residential and commercial. A major highway runs 500 m east with light vehicles and heavy-duty trucks. Several industrial parks are within 15 km to the north and south of the site. All the instruments used for this study were placed in the station of the Atmospheric Observatories University Network (RUOA, Spanish acronym), on the roof of a two-story building, with the air inlets located approximately 15 m.a.g.l..

Non-refractory components in submicron particles (NR-PM_1) were measured using an Aerosol Chemical Speciation Monitor (Aerodyne Research Inc., Billerica MA, USA). The NR-PM_1 organics fraction was further analyzed using the Positive Matrix Factorization (PMF) model.

A Photoacoustic Extinctiometer (PAX, Droplet Measurement Technologies, Longmont CO, USA) was used to measure the black carbon mass concentration in ambient air (Linan-Abanto et al. 2019). Temperature, relative humidity, wind speed and direction, as well as concentrations of carbon monoxide, ozone, sulfur dioxide, and nitrogen dioxide at the JUR site, were obtained from the RUOA database (www.ruoa.unam.mx). Total mass concentrations of particulate matter with diameter <10 μm and 2.5 μm were also obtained from the RUOA database.

FINDINGS

Figure 1 shows the average composition of $PM_{2.5}$ measured at the site, where OTHER is the difference between $PM_{2.5}$ and PM_1 and probably corresponds to resuspended non-refractory material.

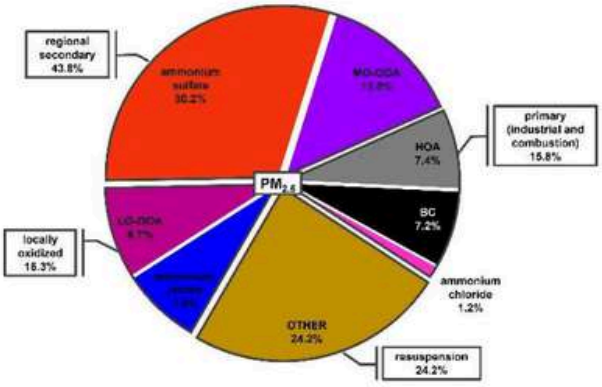


Figure 1. $PM_{2.5}$ reconstruction
(Salcedo et al., 2023).

Seasonal differences were found for all species measured. In general, those species with a local character such as primary pollutants (CO, BC, NO_2, chloride, and organics) or locally produced secondary components (nitrate and organics) were higher during the dry-cold season, probably due to lower temperatures, a lower boundary layer height, and more stable weather conditions. In addition, nitrate and chloride tend to partition towards the aerosol phase at lower temperatures. PM_{10} and $PM_{2.5}$ also showed similar concentrations during the two dry seasons, probably due to the importance of resuspension. As expected, ozone showed the largest concentrations during the dry-warm season due to higher radiation and very stable conditions. The largest concentrations of SO_2 occurred during the dry seasons, which might be related to the regional winds from the west, where an important industrial area and the Salamanca refinery are located, as Rozanes-Valenzuela et al. (2023) have suggested. On the other hand, the highest sulfate concentrations were observed during the rainy season because the oxidation of SO_2 is enhanced under high relative humidities and the presence of clouds.

CONCLUSIONS

The results of this study showed that even though the MAQ is only 250 km from the Mexico City Metropolitan Area (MCMA), the chemistry that determines its air quality is very different due to dissimilar emission sources and environmental conditions. This is probably also true for many of the largest urban areas located in the Bajio region, and the northern part of Mexico, where industrial and agricultural sources are larger compared to urban sources in the MCMA, and climatic conditions are very different. This work suggests that the regional interplay of emissions and meteorological conditions are determinants for the observed PM concentrations in addition to local processing.

REFERENCES

Kim, K. H., E. Kabir and S. Kabir. "A review on the human health impact of airborne particulate matter." İn Environment International (2015) 74, 136-143.

Linan-Abanto, R.N., O. Peralta, D. Salcedo, L.G. Ruiz-Suarez, P. Arnott, G. Paredes-Miranda, H. Alvarez-Ospina, and T. Castro. "Optical properties of atmospheric particles over an urban site in Mexico City and a peri-urban site in Queretaro." in Journal of Atmospheric Chemistry (2019) 76, 201-228.

Rozanes-Valenzuela, D., A.V. Magaldi and D. Salcedo. "Regional flow climatology for central Mexico (Querétaro): A first case study." in Atmósfera (2023, 36 (2), 239-252.

Salcedo, D., H. Alvarez-Ospina, S.E. Olivares-Salazar, R. Liñan-Abanto, and T. Castro. "PM chemical characterization at a semi-arid urban environment in Central Mexico." in Urban Climate (2023) 52, 101723.

Shrivastava, M., et al. "Recent advances in understanding secondary organic aerosol: Implications for global climate forcing." in Reviews of Geophysics (2017) 55, 509-559.

AIR POLLUTION CONFERENCE BRAZIL
CMAS SOUTH AMERICA
COMMUNITY MODELING AND ANALYSIS SYSTEM

EVALUATİON OF AİR QUALİTY İN THE CİTY OF FORTALEZA, BRAZİL, İN 2022 AND 2023: A COMPARİSON BETWEEN LOCAL AND INTERNATİONAL STANDARDS FOR PARTİCULATE MATTER (PM_{10} AND $PM_{2.5}$)

Amanda P. M. P. Alcantara[1], Débora L. Perazzoli[1], Maria Raquel L. do Vale[2], André L. Malheiros[1], Helder R. Nocko[1]

[1]*Envex Engenharia e Consultoria*

amanda.alcantara@envexengenharia.com.br
debora.perazzoli@envexengenharia.com.br
andre@envexengenharia.com.br
helder@envexengenharia.com.br

[2]*Secretaria Municipal do Urbanismo e Meio Ambiente de Fortaleza (SEUMA)*

raquel.lima@seuma.fortaleza.ce.gov.br

Abstract: The evaluation of air pollution is an important tool for environmental management and public health. In Brazil, air quality policies do not oblige municipalities to monitor air pollutant levels, only states. However, some cities, such as Fortaleza, in the state of Ceará, Brazil, have stood out for implementing air quality monitoring networks. The aim of this study is to assess air quality in the city of Fortaleza, Brazil, by a comparative analysis of local air quality levels in relation to the concentrations established by CONAMA Resolution 491/2018, in parallel with the guide values established by the World Health Organization (WHO) and other national agencies from countries such as the United States, China, India, as well as South American countries and the European Union. The city's air quality situation was assessed using the levels of particulate matter with aerodynamic sizes of less than 2.5µm ($PM_{2.5}$) and 10µm (PM_{10}), which were measured by the Fortaleza mobile air quality monitoring station (FMAQS). These parameters were selected because they are the most relevant in terms of human health impact. The pollutant data analyzed refer to the years 2022 and 2023, the post-pandemic period. During these years, the FMAQS was located at 8 strategic points in the city, 4 of which were bus terminals. For the $PM_{2.5}$ concentrations measured in Fortaleza, there was compliance with the national standards established in the two years evaluated, and the air quality in the region was considered "GOOD" on 98% of the days in 2022 and 100% of the days in 2023. For PM_{10}, air quality was also considered "GOOD" on 98% of the days in 2022 and 99% in 2023. Fortaleza's air quality complied with the WHO guideline values for 24-hour averages of $PM_{2.5}$ on 82% and 74% of the days in 2022 and 2023, respectively. For PM_{10}, concentrations in the city met WHO recommendations on 97% and 95% of days in 2022 and 2023, respectively. The levels of PM2.5 and PM10 measured in Fortaleza would be considered within the "GOOD" classification for 100% of the 2022-2023 period according to Chile's criteria, which has the most flexible levels among the countries studied. Compared to the more restrictive European criteria, air quality would be considered "FAIR" for 80% of the year 2023, in relation to $PM_{2.5}$, and 84% for PM_{10}. The annual average concentrations of $PM_{2.5}$ and PM_{10} were 13µg/m³ and 32µg/m³ (in 2022) and 13µg/m³ and 34µg/m³ (in 2023), respectively. These levels are above the annual guideline values stipulated by the WHO for $PM_{2.5}$ and PM_{10} (5µg/m³ and 15µg/m³, respectively), despite being in line with Brazilian legislation (20µg/m³ and 40µg/m³, respectively). It was also noted that the maximum 24-hour concentrations and monthly averages of $PM_{2.5}$ and PM_{10} were higher at the city's urban bus terminals than at the other points monitored, which indicate the need for actions for reducing pollutant levels in these environments, as they are strategic locations for public authorities and have a large number of people circulating daily, which are exposed to these pollution levels.

Keywords: Outdoor Air Quality. Air Quality Index. Particulate matter. Air Quality Standards.

INTRODUCTION

The air quality of large urban centers is a growing concern at global level, as it directly impacts environmental management and public health (Manisalidis et al. 2020). The challenge of maintaining healthy air becomes is more complex in developing countries as Brazil, where environmental legislation and monitoring practices vary significantly between states and cities.

According to MMA (2019), Particulate Matter (PM) is the priority parameter to be monitored in Brazil (BR), especially in the form of fine particles ($PM_{2.5}$ and PM_{10}). PM penetrates deep into the lungs and reaches the bloodstream causing various respiratory and cardiovascular diseases (Manisalidis et al. 2020). Therefore, the present study aimed to evaluate air quality in Fortaleza, comparing local levels of $PM_{2.5}$ and PM_{10} with the standards established by Brazil's CONAMA Resolution 491/2018 and the World Health Organization (WHO) guidelines, in addition to standards from other countries and economic blocs such as the United States, China, India, the European Union and South American countries.

METHODS

The data used in this study come from the Fortaleza Mobile Air Quality Station (FMAQS), obtained in 2022 and 2023. The station operated in 8 strategic points in the city, including urban bus terminals, important due to intense heavy vehicle traffic (SEUMA, 2024).

$PM_{2.5}$ and PM_{10} data were collected, measured and recorded, continuously and automatically, by Spirant™ BAM 1020 monitors. This equipment uses the method of attenuating beta rays emitted by a carbon-14 source that passes through a continuous filter. The difference in radiation intensity measured before and after PM collection is directly proportional to the mass of particles accumulated in the filter (ACOEM, 2024).

The levels of PM_{10} and $PM_{2.5}$ were compared with the standards established by CONAMA Resolution 491/2018 and the (WHO) air quality guidelines, in addition to Air Quality Indices (AQI) from other countries and economic blocs such as the United States (US), China (CN), India (IN), European Union (EU) and South American countries, such as Chile (CL), Mexico (MX) and Peru (PE) and Colombia (CO), that were obtained from regulations available on the websites of their environmental agencies.

FINDINGS AND ARGUMENTS

The concentrations of $PM_{2.5}$ and PM_{10} in Fortaleza indicated compliance with the BR AQI due to the showed compliance with AQI from BR, being classified mostly as 'GOOD' in the two years evaluated (Figure 1). If the CL's AQI criteria were considered, 100% of the data would be classified as 'GOOD'. However, when using the EU criteria, a marked negative change was observed with the appearance of the "UNHEALTHY" classification (2% of days for PM_{10} and 1% for $PM_{2.5}$ in 2022). In Figure 1 it is visible that the international classifications for PM_{10} are more homogeneous between countries than for $PM_{2.5}$, except in relation to EU, which differs significantly for both parameters. For $PM_{2.5}$, US, CO and PE also have significantly more restrictive criteria than the other countries. This suggests that differences between international AQIs can significantly influence the perception of local air quality, which points to the importance of a careful assessment of adopted standards and their suitability to local realities (Tan et al. 2021), as well as to the need to adopt global quality standards that allow comparison between the air quality of different countries.

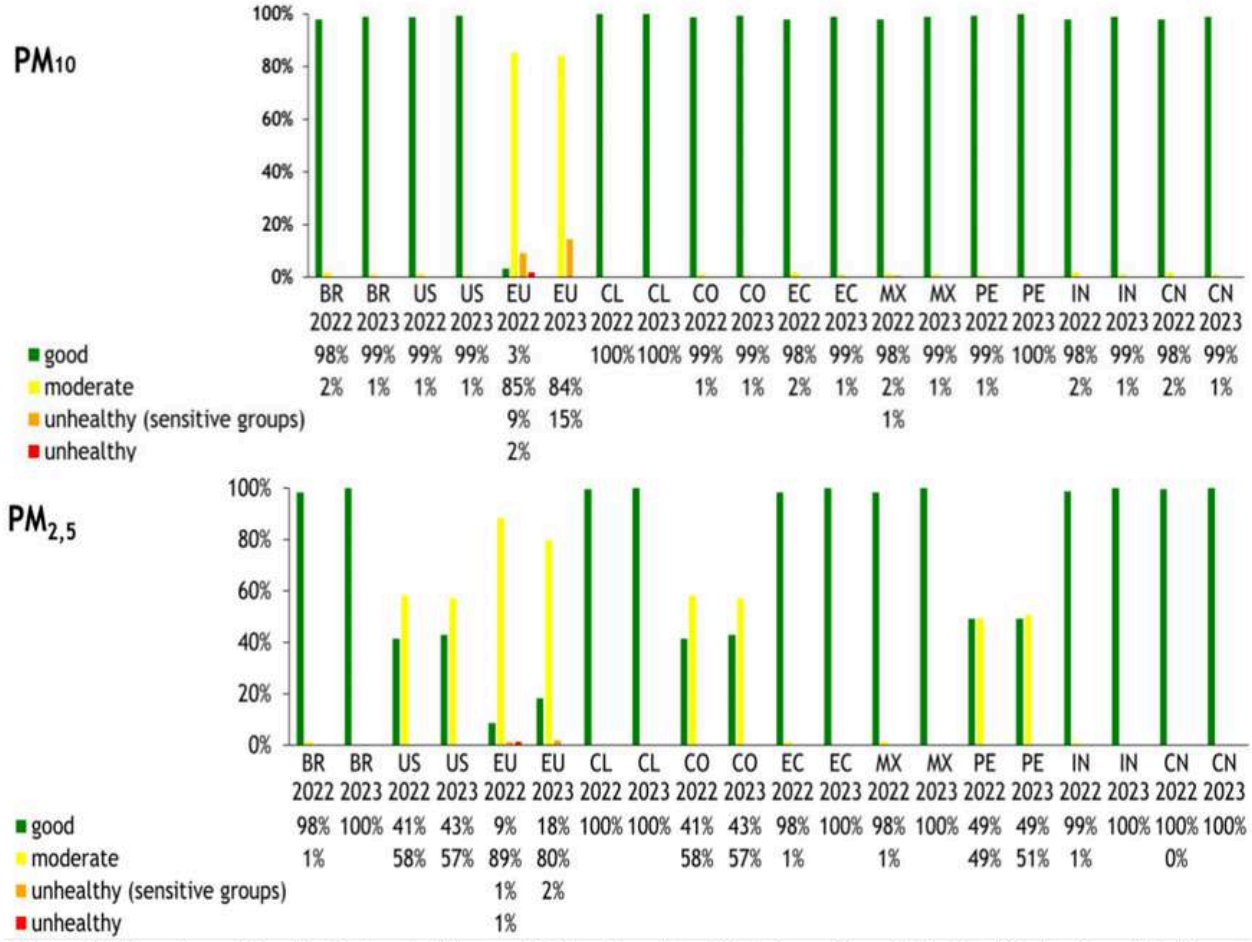


Figure 1. Benchmarking Fortaleza's PM_{10} and $PM_{2.5}$ Levels with International Air Quality Indices (Authors, 2024)

Table 1 shows the annual average values of $PM_{2.5}$ and PM_{10} in Fortaleza.

Table 1. Annual Average Concentrations of PM10 and PM2.5 in Fortaleza for 2022 and 2023.

Pollutant/Year	2022	2023
Average $PM_{2.5}$ (µg/m³)	13	13
Average PM_{10} (µg/m³)	32	34

Reference: (Authors, 2024)

The comparative analysis shows that these values met the limits of Brazil's CONAMA Resolution 491/2018 in the years evaluated (maximum of 20µg/m³, for $PM_{2.5}$, and 40µg/m³ for PM_{10}). However, the annual averages did not meet the levels recommended by WHO guidelines (maximum of 5µg/m³ for $PM_{2.5}$ and 15µg/m³ for PM_{10}).

Tan et al. 2021 shows that these variations in each agency/country's AQI point to the critical importance of developing a robust and internationally comparable Air Quality Index (AQI) system that is more accurate and consistent, thus helping both researchers and governments improve human well-being and achieve sustainable development. The adoption of holistic approaches to air quality assessment, such as AQI oriented to multiple contaminants, can bring benefits to air quality monitoring and analysis; however, these approaches are more complex than the traditional one and are sometimes unfeasible due to to the incipient monitoring of pollutants (Tan et al. 2021).

Above all, working with these disparities in recommendations is challenging from the point of view of strategic planning for the implementation of public policies aimed at improving air quality, since conservative guiding values imply the need for robust mitigating strategies, while flexible values end up for masking and delaying viable solutions to the serious environmental and public health problem of air pollution (EPA, 2024).

Monitoring air quality is essential for several reasons, including public health, environmental and socioeconomic issues, urban planning and infrastructure (Manisalidis et al. 2020). Failure to monitor air quality, therefore, brings a variety of systemic losses, ranging from misinformation to preventing the correct assessment of risks and the implementation of effective policies.

CONCLUSIONS

This work provided an accurate assessment of current air quality conditions in Fortaleza, considering both Brazilian and international AQIs, and contributed to the planning of effective public policies and the continuous improvement of the city's urban environment.

Although Brazilian Air Quality standards were met in the years evaluated, it is observed that more restrictive criteria, such as those of the European Union, were exceeded and Air Quality in relation to $PM_{2.5}$ would be classified as "GOOD" in just 9% and 18% of days in 2022 and 2023, respectively, and just 3% in 2022, considering PM_{10}. The WHO guidelines were not achieved in any of the years evaluated (2022 and 2023). Additionally, the importance of developing a robust and internationally comparable Air Quality Index system that meet, or is close to, WHO recommendations was highlighted. This system would contribute to accurate analysis of air quality in urban environments.

REFERENCES

ACOEM - "Spirant BAM Particulate Monitor: User Manual." Available at: < https://www.acoem.com/brasil/pt-br/products/ar-ambiente/monitores-de-particulas-de-ar/bam/spirant-bam/#> Acessed in: 22 apr. 2024

CONAMA - Conselho Nacional do Meio Ambiente. "Resolução 491/2018". Brasil. 2018.

EPA - U.S. Environmental Protection Agency. "Managing Air Quality - Control Strategies to Achieve Air Pollution Reduction." Available at: https://www.epa.gov/air-quality-management-process/managing-air-quality-control-strategies-achieve-air-pollution. Acessed in: 22 apr. 2024.

IQAir. "2023 World Air Quality Report: Region & City PM2.5 Ranking" Suíça, 2024. Available in: < https://www.iqair.com/> Acessed in: 22 apr. 2024.

Manisalidis et at. "Environmental and Health Impacts of Air Pollution: A Review" *Frontiers in Public Health* 8 (2020):14. DOI: 10.3389/fpubh.2020.00014.

MMA - Ministério do Meio Ambiente. "Guia Técnico Para o Monitoramento e Avaliação da Qualidade do Ar." Brasília, 2019. Disponível em: <https://www.mma.gov.br/agenda-ambiental-urbana/qualidade-do-ar.html>. Acessed in: 22 apr. 2020

SEUMA - Secretaria de Urbanismo e Meio Ambiente. "Painel do Monitoramento da Qualidade do Ar". Fortaleza, 2024. Disponível em: <https://urbanismoemeioambiente.fortaleza.ce.gov.br/urbanismo-e-meio-ambiente/1027-painel-do-monitoramento-da-qualidade-do-ar> Acessed in:: 22 abr. 2024.

Tan, et al. "A review of current air quality indexes and improvements under the multi-contaminant air pollution exposure". *Journal of Environmental Management* 279 (2021): 111681. DOI: 10.1016/j.jenvman.2020.111681

AIR POLLUTION CONFERENCE BRAZIL
CMAS SOUTH AMERICA
COMMUNITY MODELING AND ANALYSIS SYSTEM

SOURCE APPORTIONMENT AND THERMODYNAMIC MODELING OF ATMOSPHERIC AEROSOLS IN THE CENTRAL AMAZONIA

Guilherme Martins Pereira[1], Fernando Morais[2], Paulo Artaxo[2], Maria de Fátima Andrade[1], Samara Carbone[3], Christopher Pöhlker[4], Marco A. Franco[1]

[1]*Institute of Astronomy, Geophysics and Atmospheric Sciences, University of São Paulo, São Paulo, Brazil*

guilherme.martins.pereira@usp.br
marco.franco@usp.br

[2]*Institute of Physics, University of São Paulo, São Paulo, Brazil*

[3]*Federal University of Uberlândia, Uberlândia, Brazil*

[4]*Multiphase Chemistry Department, Max Planck Institute of Chemistry, Mainz, Germany*

Abstract: The Amazon Tall Tower Observatory (ATTO) is a research facility in central Amazonia, approximately 150 km northeast of Manaus, Brazil. It consists of two 80 m towers and a 325 m tower and is designed to monitor the region's climatic, biogeochemical, and atmospheric conditions over the long term. The site's location in a pristine rainforest region makes it an important resource for studying the impacts of human-made and climate change-related forest perturbations. By employing source apportionment techniques and thermodynamic modeling, we aim to indicate the origins of atmospheric aerosols, differentiating them between the most relevant sources. For aerosol sampling on nuclepore filters, a Thermo Scientific $PM_{2.5}$ aerodynamic cut inlet sampler with a flow rate of 16.67 LPM was employed at an elevation of 42 meters at the ATTO tower. The filters underwent Energy Dispersive X-ray Fluorescence Spectrometry (EDXRF) to quantify the concentration of chemical elements present in aerosol particle-containing samples. Simultaneously, measurements were performed with the Aerosol Chemical Speciation Monitor (ACSM) Instrument. Distinct aerosol peaks in the elemental aerosol concentration were observed in Figure 1. As observed in previous studies, the first two peaks between March and May were associated with the long-range transport of Saharan dust and the western and central African biomass-burning aerosols. These peaks were characterized by a high presence of K, Si, Ca, and Fe. The third peak is characteristic of the dry season in the Amazon rainforest between August and October, with strong particulate emissions related to local and regional biomass burning. With the thermodynamic model ISORROPIA, it was possible to estimate that the main solid species in the aerosol phase were K_2SO_4 and $CaSO_4$, with an increase of these species during the dry season, suggesting that they may be linked with biomass burning. Positive Matrix Factorization (PMF) was used for source apportionment, and a four-factor solution presented the best result with well-interpreted factors. Factor 1 was characterized by biomass-burning-related species such as K, Na, and BC and some other carbonaceous species fractions. Factor 1 was the second most abundant. Factor 2 represented the major fraction of $PM_{2.5}$ (38%) and presented loadings of secondarily formed species as NH_4^+, NO_3^-, SO_4^{2-}. The presence of Organic contribution is likely related to the local formation of secondary organic aerosol. Factor 3 was loaded with soil resuspension-related species, such as Al, Si, and Fe, although it also presented V, found in oil burning and industrial sources, likely associated with the site's diesel-powered generator. Factor 4 presented loadings of P, which are attributed to biogenic sources. Therefore, this study at the Amazon Tall Tower Observatory revealed a seasonal increase in K_2SO_4 and $CaSO_4$ aerosols. Positive Matrix Factorization identified four distinct sources, including biomass burning, secondary organic aerosol formation, soil resuspension, and biogenic emissions. These findings contribute crucial insights into the aerosol composition and sources in the central Amazon Basin, informing the region's climate research and sustainable development efforts.

Keywords: Particulate matter, receptor model, positive matrix factorization, ATTO site, central Amazon.

INTRODUCTION

The Amazon Tall Tower Observatory (ATTO) is a research facility in central Amazon, approximately 150 km northeast (upwind) of Manaus, Brazil (2°08.6470 S and 58°59.9920 W). It consists of two 80 m towers and a 325 m high tower and is designed to monitor the region's climatic, biogeochemical, and atmospheric conditions over the long term (Andreae et al., 2015). The site's location in a pristine rainforest region makes it an important resource for studying the impacts of human-made and climate change-related forest perturbations (Pöhlker et al., 2019). By employing source apportionment techniques and thermodynamic modeling, we aim to indicate the origins of atmospheric aerosols, differentiating them between the most relevant sources.

METHODS

Fine particulate matter ($PM_{2.5}$) was sampled on nuclepore filters with a Thermo Scientific sampler (17 LPM flow). This sampler was installed at 42 m height at the ATTO site. The filters were stored in a container adjacent to the tower, which maintained controlled temperature and humidity conditions (approximately 27°C and 38% RH). The sampling for each filter was conducted over approximately seven days, varying with weather conditions and sampled mass. Thus, a total of 34 filters were collected between March 26 and October 31, 2019, encompassing dry periods with a significant influence of wildfires, the wet season, and a period with dust influence originating from Northern Africa to the central Amazon.

Simultaneously, the chemical composition of the aerosol was monitored in near real-time using a Quadrupole Aerosol Chemical Speciation Monitor (ACSM), measuring the mass concentration of nitrate (NO_3^-), sulfate (SO_4^{2-}), ammonium (NH_4^+), chloride (Cl^-) and organics with a temporal resolution of about 10 to 30 minutes. An advantage of using a mass spectrometer of this type is that they can externally and continuously measure aerosols with sizes between 75-650 nm (Ng et al., 2011).

After sampling, the filters were analyzed with Energy Dispersive X-ray Fluorescence Spectrometry (EDXRF), an analytical method that relies on the emission of high-energy X-rays to identify and quantify the concentration of chemical elements present in aerosol particle-containing samples (Van Grieken and Markowicz, 2001; Van Meel et al., 2010). A PANalytical B.V Epsilon 5 X-ray Fluorescence spectrometer from the atmospheric physics laboratory of the Institute of Physics at the University of São Paulo was employed in this analysis.

In addition to the previous methods, the thermodynamic model ISORROPIA was used to estimate the different aerosol phases in the central Amazon atmosphere (Fountoukis and Nenes, 2007, Nenes et al., 1998). ISORROPIA computes the equilibrium distribution of inorganic aerosol components between gas and particle phases. ISORROPIA requires inputs including temperature, relative humidity, and total concentrations (gas and aerosols) of various species such as sulfate, nitrate, ammonium, sodium, chloride, calcium, magnesium, and potassium, and yields the corresponding equilibrium concentrations.

FINDINGS AND ARGUMENT

The FRX analysis results and the estimated dust concentration (red curve) are presented in Figure 1. Distinct aerosol peaks were observed. The first peaks between March and May may be correlated with the transport of Dust from the Sahara, as observed by Holanda et al. (2019), which is also suggested by backward air mass trajectories. The peaks observed after July may be associated with wildfires in central Africa, aligning with the findings of Holanda et al. (2019) and are characteristic of the dry season in the Amazon (between August and September), with strong emissions related to local biomass burning and enhanced potassium concentrations. It is important to note that the dust mass does not follow the sum of trace elements since the fraction of carbonaceous material is not considered in these calculations, and the sulfate component is relevant to the total mass. With ISORROPIA, it was possible to estimate that the main solid species in the aerosol phase were K_2SO_4 and $CaSO_4$, and an increase in these species during the dry season suggests that they may be linked with biomass burning.

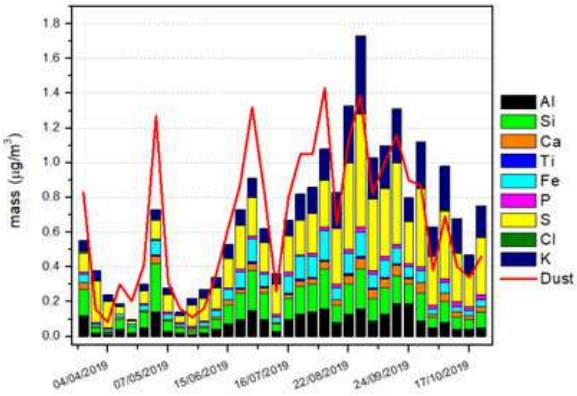


Figure 1. Elemental concentration of $PM_{2.5}$ and calculated dust mass.

Positive Matrix Factorization (PMF) was used for source apportionment with twenty strong chemical species (Org, BC, SO_4^{2-}, NO_3^-, NH_4^+, Cl^-, Na, Mg, Al, Si P, K, Ca, V, Mn, Fe, Zn, and Br) and four weak chemical species (Ti, Cr, Ni, and Cu). The $PM_{2.5}$ concentration was set as a total variable (weak). The final model was obtained with an additional 10% modeling uncertainty. A four-factor solution presented the best result, with well-interpreted factors. Bootstrap mapping (BS) was applied and most of the markers used to identify the sources were within the interquartile ranges.

The PMF receptor model generated four factors, and polar plots were obtained for their contributions, associating them with meteorological parameters, such as wind speed and direction (Figure 2).

Factor 1 was characterized by biomass-burning-related species such as K, Na, and BC and some carbonaceous species fractions (Liang et al., 2015). Some elements also appeared in the biomass burning profile, such as Mg, Zn, and Br. This factor increased with NE and SE winds.

Factor 2 presented loadings of secondarily formed species as NH_4^+, NO_3^-, and SO_4^{2-}. (Pereira et al., 2017). The presence of organic aerosols is related to the formation of secondary organic aerosol, and the presence of Cl^- may be related to secondary reactions of HCl. Furthermore, this factor also presented loadings of some primary emission species, possibly vehicular or industrial, such as Cu and Ni (Calvo et al., 2013). The factor contribution increased with calmer winds, suggesting that it is related to the local secondary formation of aerosols.

Factor 3 was loaded with soil resuspension-related species, such as Al, Si, and Fe. Although it also presents V, found in oil burning and industrial sources, which may indicate some power generator

contamination (Calvo et al., 2013). The polar plots suggest an increase in SE winds, with higher wind speed. Some soil-resuspension contribution peaks coincide with those observed for dust mass in Figure 1. Factor 4 presented loadings of P, which is attributed to biogenic sources, with a polar plot pointing to SE directions, which represent cleaner air masses.

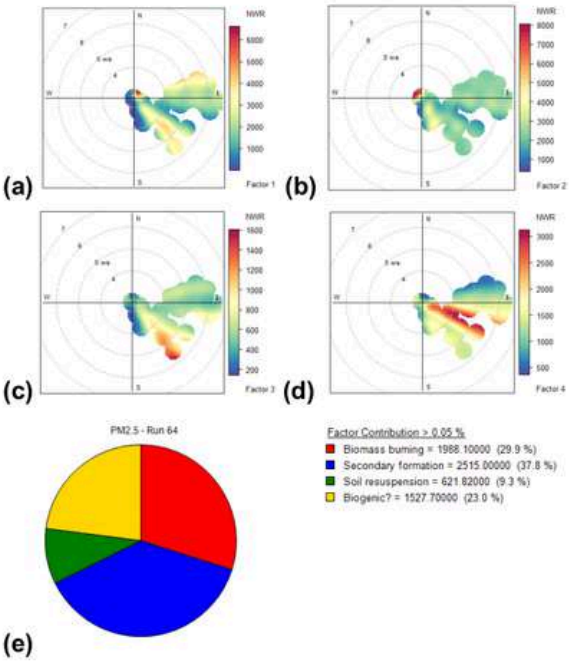


Figure 2. Polar plots for PMF factor contributions (a to d) and factor contributions to $PM_{2.5}$ (e).

CONCLUSIONS

Distinct aerosol peaks were observed: the first ones can be associated with the transport of dust from the Sahara (before the dry season), which is supported by the air mass trajectories, while the other peaks were observed in the dry season, and may be related to the contribution of biomass burning, a significant increase in the level of potassium was observed in the latter. The increase in pollution events in the dry season revealed a seasonal increase in K_2SO_4 and $CaSO_4$ species, possibly associated with biomass burning. Four distinct factors were observed in the PMF receptor. The greater contributors to $PM_{2.5}$ were secondary formation and biomass burning. The latter increased in the dry season. Soil dust and biogenic emissions were also apportioned.

REFERENCES

Andreae, Meinrat et al. The Amazon Tall Tower Observatory (ATTO): overview of pilot measurements on ecosystem ecology, meteorology, trace gases, and aerosols, *Atmospheric Chemistry & Physics* 15 (2015): 10723–10776.

Calvo, Ana et al. Research on aerosol sources and chemical composition: Past, current and emerging issues. *Atmospheric Research* 120–121 (2013): 1–28.

Fountoukis, Christos and Nenes, Athanasios. ISORROPIA II: a computationally efficient thermodynamic equilibrium model for K^+–Ca^{2+}–Mg^{2+}–NH_4^+–Na^+–SO_4^{2-}–NO_3^-–Cl^-–H_2O aerosols, *Atmospheric Chemistry & Physics* 7 (2007): 4639–4659.

Holanda, Bruna et al. Influx of African biomass burning aerosol during the Amazonian dry season through layered transatlantic transport of black carbon-rich smoke, *Atmospheric Chemistry & Physics* 20 (2020): 4757–4785.

Lang, Yin-Hai et al. Combination of Unmix and PMF receptor model to apportion the potential sources and contributions of PAHs in wetland soils from Jiaozhou Bay, China. *Marine Pollution Bulletin* 90 (2015): 129–134.

Nenes, Athanasios et al.. ISORROPIA: A New Thermodynamic Equilibrium Model for Multiphase Multicomponent Inorganic Aerosols. *Aquatic Geochemistry* 4 (1998): 123–152.

Ng, Nga Lee et al. An Aerosol Chemical Speciation Monitor (ACSM) for Routine Monitoring of the Composition and Mass Concentrations of Ambient Aerosol. *Aerosol Science and Technology* 45 (2011): 780–794.

Pereira, Guilherme Martins et al. Particulate pollutants in the Brazilian city of São Paulo: 1-year investigation for the chemical composition and source apportionment. *Atmospheric Chemistry and Physics* 17 (2017): 11943–11969.

Pöhlker, Christopher et al. Land cover and its transformation in the backward trajectory footprint region of the Amazon Tall Tower Observatory, *Atmospheric Chemistry and Physics* 19 (2019): 8425–8470.

Van Grieken, Rene and Markowicz, Andrzej. *Handbook of X-Ray Spectrometry.* Boca Raton: CRC Press, 2001.

Van Meel, Katleen et al. Elemental concentrations in 115 aerosols at the Belgian coast versus seasons and air mass trajectories. *Environmental Chemistry Letters* 8 (2010): 157–163.

AIR POLLUTION CONFERENCE BRAZIL
CMAS SOUTH AMERICA
COMMUNITY MODELING AND ANALYSIS SYSTEM

WİLL RİO DE JANEİRO FULFİLL SDG 11.6 OF THE 2030 AGENDA? AN ANALYSİS OF AİR QUALİTY FROM 2015 TO 2023 AND PROJECTİON TO 2030

Rebekah Bon Oliveira[1,2], Ana Drummond[2], Brenda Novaes[2], Leonardo Hoinaski[3], Rafael Barbosa Campos[1], Taciana Toledo de Almeida Albuquerque[4], Rizzieri Pedruzzi[2]

[1]*The State Institute for the Environment - Inea*

[2]*Department of Sanitary and Environmental Engineering - Uerj*

[3]*Department of Sanitary Engineering - UFSC*

[4]*Department of Sanitary Engineering - UFMG*

Corresponding author: rebekahbon@gmail.com , rizzieri.pedruzzi@gmail.com

Abstract *It is estimated that 7 million premature deaths occur every year due to exposure to air pollution, according to the United Nations (UN). Every day, the world's population is affected by the effects of industrial and vehicular emissions, developing various respiratory diseases. With anthropogenic actions intensifying, the UN has established goals that are considered a global call to action to protect the climate and the environment, end hunger and poverty, and ensure that people enjoy peace and prosperity. These were the Millennium Development Goals (MDGs) and later the Sustainable Development Goals (SDGs). Considering the importance of monitoring and controlling atmospheric emissions to preserve human health, SDG 11, Sustainable cities and Communities, set forth target 11.6 to enhance air quality in cities by 2030. Rio de Janeiro is a state that, from the perspective of the impact caused by air pollution, is no different from other brazilian metropolitan regions. Industrial activities and heavy motor vehicle traffic are the main sources of pollutants. In addition, its climatic and topographical characteristics also influence the dispersion of pollution. The state has automatic and semi-automatic stations run by the State Institute for the Environment (Inea) to assess air quality standards. Nowadays, violations of current national CONAMA 491/2018 standards and World Health Organization (WHO) standards are observed. This study aims to verify whether the metropolitan region of the state of Rio de Janeiro can meet target 11.6 of SDG 11, looking only at air quality. To achieve it, Inea's network data was used, collecting particulate matter pollutants below 10 µm (PM_{10}) and below 2.5 µm ($PM_{2.5}$), available on the Environmental Information System - SIA, a platform for exclusive use by Inea. After processing the data, the evolution of pollutant concentrations was analyzed from 2015 to 2023, based on the monthly and annual arithmetic mean, and it was then possible to perform a linear regression to determine the evolution of concentrations, determining an equation for air basin I. Finally, the concentrations were projected for the year 2030, verifying whether or not Air Basin I can achieve target 11.6, which has the annual average level of inhalable particles as its indicator. The result was that Air Basin I will not be able to meet target 11.6 of SDG 11, with the annual average 2030 projected to be above the limits set by the new WHO Global Air Quality Guidelines (AQG) and the legislation of Rio de Janeiro.*

Keywords: Air Quality, Atmospheric pollutants, Rio de Janeiro, SDG, 2030 Agenda.

INTRODUCTION

Air pollution became one of the biggest environmental threats to the health of living beings after the start of the Industrial Revolution. Air is considered polluted when contaminants or polluting substances in its composition, such as particulate matter, gases and volatile organic compounds (JACOBSON, 2010), alter human health and well-being.

With anthropogenic actions intensifying, the United Nations (UN) established the Millennium Development Goals (MDGs), which set 8 objectives to be achieved by 2015, these referring to accessibility to drinking water and improvement of precarious settlements, among others. At the time, air quality and its effects on human health were still not being addressed. At the end of the MDGs, new goals were set to guide society in the implementation of public policies, known as the Sustainable Development Goals (SDGs), signed in the UN's 2030 Agenda, to be achieved by 2030.

SDG 11, on sustainable cities and communities, aims to make cities and human settlements inclusive and safe. To achieve this goal, the SDG presents target 11.6, which aims to reduce the negative environmental impact per capita of cities, with an emphasis on air quality and solid waste management. In Brazil, one of the targets is to ensure that cities over 500,000 inhabitants have implemented air quality monitoring and solid waste management systems.

Rio de Janeiro is the second largest metropolitan region in Brazil and has a wide range of industrial and agricultural activities, as well as energy generation and vehicle emissions. Considering that all this complexity has a negative impact on air quality, with the population exposed to levels of atmospheric pollution on a daily basis, the aim of this work is to verify, based on particulate matter air quality monitoring data, whether the air basins of the metropolitan region of the state of Rio de Janeiro will be able to achieve target 11.6 of SDG 11 by the year 2030, only about air quality.

AIR POLLUTION CONFERENCE BRAZIL
CMAS SOUTH AMERICA
COMMUNITY MODELING AND ANALYSIS SYSTEM

METHODS

Although the Brazilian target considers the criterion of cities with over 500,000 inhabitants, it is important to note that there are cities with small populations that are affected by air pollution on a daily basis. Furthermore, a population criterion does not take into account the dispersion capacity of pollutants. For this reason, this study analyzed the data segmented under the concept of an air basin and not by municipal division, using population criteria.

By definition, an air basin is an area delimited by topography that induces characteristic atmospheric circulation and is responsible for the dispersion of pollutants in the air (Rio de Janeiro, 2023). The metropolitan region of Rio de Janeiro is divided into four air basins, as shown in Figure 1, due to the presence of massifs that act as physical barriers to the prevailing winds.



Figure 1. Air basins in the metropolitan region of RJ

Reference: Image extracted from AQMIS Software. 04/30/2024

Only the analyses for air basin I will be presented in this paper. Air Basin I is in the western part of the metropolitan region of the state of Rio de Janeiro, covering the municipalities of Seropédica, Itaguaí and Queimados, with an area of around 730 km^2 (FARIAS, 2013). In addition, 17 air quality stations monitoring particulate matter were used, 8 of which were semi-automatic and 9 automatic.

In the ATMOS module, the data was extracted from the Environmental Information System (SIA), a platform used exclusively by Inea employees. Daily averages of particulate matter below 10 µm (PM_{10}) and below 2.5 µm ($PM_{2,5}$) were collected, with at least 67% of hourly averages valid during the day from 2015 to 2023.

After collecting the data, the evolution of $PM_{2,5}$ and PM_{10} concentrations over the proposed period was analyzed based on the monthly and annual arithmetic average. The averages were calculated considering the representativeness criteria in the table below, in accordance with the MMA's technical guide to air quality.

Table 1. Minimum sampling time for data to be considered representative

Type of average	Validation Criteria
Monthly average	2/3 of the daily averages valid in the month
Annual average	1/2 of the valid daily averages obtained in each four-month period (Jan-Apr; May-Aug; and Sep-Dec)

Reference: MMA.2019

Finally, a linear regression was carried out to determine the evolution of pollutant concentrations, making it possible to project concentrations in 2030 and check whether the defined region will be able to meet target 11.6 of SDG 11, which establishes the annual average level of inhalable particles in cities as an indicator. The results were compared with the new WHO Global Air Quality Guidelines (AQG) and the legislation of the state of Rio de Janeiro.

FINDINGS AND ARGUMENT

After calculating the monthly and yearly averages of air basin I, the following PM_{10} trend line was found between the years 2015 to 2023, as indicated in Figure 2.

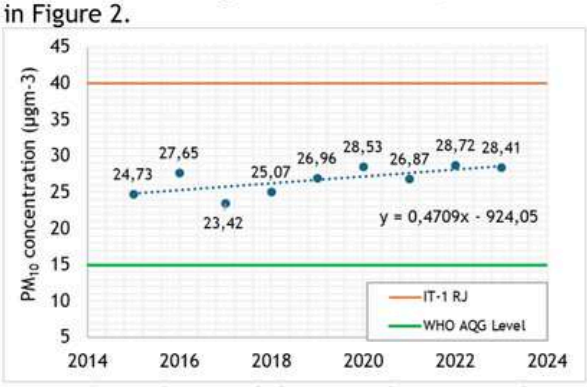


Figure 2. Evolution of the annual average of PM_{10} over the years, for air basin I

Figure 2 shows the evolution of the annual average over the years, also comparing the interim target set by the state of Rio de Janeiro, based on Decree 48668/2023, in addition to WHO AQG Level.

From the equation of line y= 0.4709x-924.05, it was possible to project the annual average of PM_{10} for the year 2030, obtaining the value of 31,87 μgm^{-3}. The trend shows an increasing annual average, indicating that in addition to being more than 100% above the WHO AQG Level of 15μgm^{-3}, it is also approaching the average established by the state of Rio de Janeiro of 40μgm^{-3}.

Figure 3 shows the evolution of the annual average $PM_{2,5}$, where there is a slight decrease in the average for air basin I.

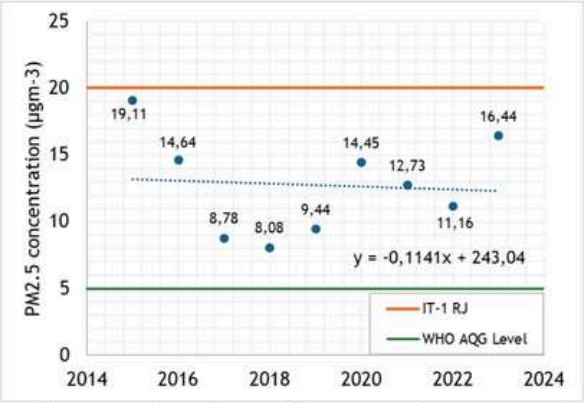


Figure 3. Evolution of the annual average of $PM_{2,5}$ over the years, for air basin I

From the linear regression, it was possible to make a projection for the year 2030, with the straight line equation y= -0.1141x+243.04, which obtained an annual average of 11.4 μgm^{-3}. The annual average projection of $PM_{2,5}$ is decreasing. However, it has not yet reached the WHO AQG level proposed in the 2021 review, which is 5 μgm^{-3}. The annual averages of $PM_{2,5}$ for the years 2015 to 2023 do not violate the air quality standards decreed by the state of RJ.

CONCLUSIONS

Based on the study carried out, it was possible to conclude that air basin I, which includes the municipalities of Itaguaí, Seropédica and Queimados, is unlikely to achieve target 11.6 of SDG 11 on Sustainable Cities and Communities, looking only at air quality. This is due to the fact that, even with a decrease in the annual average of $PM_{2,5}$, the linear projection is above the WHO AQG Level. In addition, the annual average of PM_{10} showed an increase in the linear projection, moving further away from the WHO AQG Level.

Regarding Rio de Janeiro's state legislation, it was possible to observe that air basin I already meets interim target I. However, for PM_{10}, the projection for the year 2030 is getting closer and closer to the established limit of 40μgm^{-3}. This indicates that, in the future, when a new interim target is set in the state, the region will most likely be outside the new established limit.

It is important to note that for PM_{10}, 100% of the minimum representativeness established (table 1) was achieved for the monthly and annual averages. When calculating the monthly averages for $PM_{2,5}$, around 94.4% of the months achieved the minimum representativeness, while for the annual average, only 2020 failed to meet the target.

Finally, if new interim targets are not set for the state of Rio de Janeiro, it will become increasingly difficult for the region to achieve its goal. Future work will be carried out to analyze the other air basins in the metropolitan region of Rio de Janeiro and also for the entire state of Rio de Janeiro, evaluating by government regions, which will be divided into Northwest Fluminense, North Fluminense, Baixadas Litorâneas, Serrana, Center-South Fluminense, Médio Paraíba and Costa Verde.

REFERENCES

DECRETO Nº 48.668 DE 01 DE SETEMBRO DE 2023. Regulamenta os padrões de qualidade do ar no estado do rio de janeiro, tendo por base padrões nacionais e as diretrizes e recomendações da organização mundial de saúde, e dá outras providências. Rio de Janeiro, 2023

Farias, Heitor & Oliveira, Jorge. (2013). BACIAS AÉREAS: Uma proposta metodológica para o estudo da qualidade do ar em áreas influenciadas pelo relevo. Revista Brasileira de Climatologia. 12. 10.5380/abclima.v12i1.30081.

Guia técnico para o monitoramento e avaliação da qualidade do ar / Ministério do Meio Ambiente. Secretaria de Qualidade Ambiental. Departamento de Qualidade Ambiental e Gestão de Resíduos. - Brasília, DF: MMA, 2020. 136 p. : il. color

JACOBSON, MZ. Short-term effects of controlling fossil-fuel soot, biofuel soot and gases, and methane on climate, arctic ice, and air pollution health. Journal of Geophysical Research: Atmospheres, v. 115, n. D14, 2010.

Sustainable Development Goal 11: Cidades e comunidades sustentáveis | As Nações Unidas no Brasil. (n.d.). Brasil.un.org. https://brasil.un.org/pt-br/sdgs/11

AIR POLLUTION CONFERENCE BRAZIL
CMAS SOUTH AMERICA
COMMUNITY MODELING AND ANALYSIS SYSTEM

BIOMASP+: tackling the biosphere-atmosphere exchanges and their impact on air pollution in an emblematic subtropical megacity: the Metropolitan Area of São Paulo, Brazil

Adalgiza Fornaro[1], Agnès Borbon[2], Silvia R. Souza[3], Amauri P. Oliveira[1], Rita Y. Ynoue[1], Joel Brito[4], Jean-Luc Jaffrezo[5], Michael Staudt[6], and other researchers from the BIOMASP project

[1]Depto. Ciências Atmosféricas, IAG-USP, Brazil
adalgiza.fornaro@iag.usp.br; apdolive@usp.br; rita.ynoue@iag.usp.br
[2]LaMP/CNRS/OPGC, Université Clermont Auvergne, France
A.Borbon@opgc.fr
[3]Instituto de Pesquisas Ambientais, IPA-SP, Brazil
sribeiro@sp.gov.br
[4]IMT Nord Europe, Université de Lille, France
joel.brito@imt-nord-europe.fr
[5]CEFE/CNR, Montpellier, France
michael.staudt@cefe.cnrs.fr
[6]IGE-CNRS, Grenoble, France
jean-luc.jaffrezo@univ-grenoble-alpes.fr

Abstract: Urban air pollution endangers human health and ecosystems. Despite anthropogenic emission control, ongoing climate change potentially reduces its effect by favoring biogenic volatile organic compounds (BVOC) emissions, key precursors of key pollutants, namely tropospheric ozone and secondary organic aerosol (SOA). However, such a scenario is uncertain due to the complexity of the processes involved in biosphere-atmosphere interactions. The critical role of biosphere-atmosphere interactions in urban pollution has been recognized for a long time but is far from being fully understood. Those interactions were first demonstrated in ozone production mechanisms, a well-known harmful photooxidant, in Atlanta thanks to the seminal work of Chameides et al. (1988) followed by many others (Calfapietra et al., 2013, Fitzky et al., 2019, Ji-Won et., 2022). BVOCs are usually unsaturated, including isoprene (2-methyl-1,3-butadiene), monoterpenes, sesquiterpenes and many others. São Paulo megacity (MASP) is surrounded by the Atlantic forest (Mata Atlântica), whose green infrastructures distribution is unequal, covering 45% of its area (Arantes et al., 2021). This relatively high prevalence of green areas in association with a subtropical climate favors biogenic emissions and photochemical processes. The modelled emission fluxes of the BVOCs isoprene and terpenes from the vegetation of Brazil are expected to be up to 3 orders of magnitude higher than the ones from temperate latitudes (Sindelarova et al., 2014). Previous studies estimated high ozone formation potentials for isoprene compared to aromatics VOCs in São Paulo (Santos et al., 2022). By taking MASP as a target natural laboratory, the Franco-Brazilian project BIOMASP+ is a unmatched opportunity to reduce gaps in our understanding of the atmospheric processes resulting from the complex anthropogenic and biogenic urban mixing. This is needed to properly quantify the impact of pollutants on air quality, health and climate change. The main objective of BIOMASP+ is to evaluate the impact of biosphere-atmosphere interactions on gaseous and particulate urban pollution in a changing climate by addressing the following questions:

- How does the biosphere-atmosphere interaction affect the ozone production?
- How does this alter the secondary organic aerosol (SOA) formation and aging?
- How does this affect health and, in return, the biosphere?

The infrastructure is based on micrometeorological towers, one 20 meters high at the top of Matão-IAG-USP main building, representative of a densely urbanized area and another tower in the Morro Grande Reserve (RMG) 30 m high, representative of a region of Atlantic Forest remnant, out of the densely urbanized area in MASP. Both towers have instrumentation, for extensive campaigns, that includes everything from conventional meteorological variables (precipitation, pressure, temperature, relative humidity, wind speed and direction), to energy balance components (sensible and latent heat flux, soil heat flux and CO_2) and radiation (net radiation and its components: solar and terrestrial radiation incident on and emerging from the surface), in addition to low-cost sensors (Petaja et al., 2021) for atmospheric pollutants (CO, O_3, NO_2, $PM_{2.5}$ and PM_{10}). The vegetation characterization, including species, height, canopy coverage area has been evaluated seasonally in both sites (RMG and Matão). It is important to highlight the intensive campaign with instrumentation to evaluate the chemical composition of gases and aerosols in both sites simultaneously between April and June 2023, in addition to studies in chambers considering the atmosphere of the Atlantic Forest and individually representative species. This campaign featured different instruments such as ACSM and PTR-MS with high resolution time analysis, in addition to GC-FID, gas monitors and PM10 (Hivol) samplers in both study sites. In this presentation, more details of the BIOMASP+ infrastructure will be shown, as well as the primary results of the 2023 intensive campaign.

Keywords: Biogenic volatile organic compounds (BVOCs), air pollution, atmospheric photochemistry, urban forest.

REFERENCES

Calfapietra, C. et al. (2013). Role of Biogenic Volatile Organic Compounds (BVOC) emitted by urban trees on ozone concentration in cities: A review. Environ. Pollut., 183, 71–80. https://linkinghub.elsevier.com/retrieve/pii/S0269749113001310.

Chameides, W. L. et al. (1988). The Role of Biogenic Hydrocarbons in Urban Photochemical Smog: Atlanta as a Case Study. Science, 241(4872), 1473–1475. Doi/10.1126/science.3420404

Fitzky et al. (2019). The Interplay Between Ozone and Urban Vegetation—BVOC Emissions, Ozone Deposition, and Tree Ecophysiology, Front. For. Glob. Change 2:50. Doi: 10.3389/ffgc.2019.00050

Ji-Won, et al., (2022). Characteristics of biogenic volatile organic compounds emitted from major species of street trees and urban forests, Atmos. Pollut. Res., 13(7), 101470, Doi: 10.1016/j.apr.2022.101470.

Petaja, T. et al. (2021). Added Value of Vaisala AQT530 Sensors as a Part of a Sensor Network for Comprehensive Air Quality Monitoring. Frontiers in Environ. Science, 9, Doi: 10.3389/fenvs.2021.719567

Santos, T. C. et al. (2022) Isoprene in urban Atlantic forests: Variability, origin, and implications on the air quality of a subtropical megacity. Sci. of the Total Environ., 824, 824:153728. https://doi.org/10.1016/j.scitotenv.2022.153728

Sindelarova, K. et al. (2014) Global data set of biogenic VOC emissions calculated by the MEGAN model over the last 30 years. Atmospheric Chemistry and Physics, 14(17), 9317–9341 https://acp.copernicus.org/articles/14/9317/2014/.

AIR POLLUTION CONFERENCE BRAZIL
CMAS SOUTH AMERICA
COMMUNITY MODELING AND ANALYSIS SYSTEM

ASSESSMENT OF AİR QUALİTY İN RİO DE JANEİRO: TRENDS, VİOLATİONS, AND IMPLİCATİONS (2019-2022)

Rafael Barbosa Campos[1], Leonardo Abreu Jorge Justo[1], Silvia Patrícia Araujo[2], Caroline Menegussi Soares[2], Vitor Alves de Souza Ferreira[2], Paulo Eduardo Hofacker[2]

[1] *Instituto Estadual do Ambiente – INEA , Rio de Janeiro, RJ, Brazil*
rcampos@inea.rj.gov.br
leonardojusto@inea.rj.gov.br
JCTM Comércio e Tecnologia LTDA[2]
silviaaraujo@jctm-hidromet.com
carolinemenegussi@jctm-hidromet.com
vitoralvess@jctm-hidromet.com
paulohofacker@ jctm-hidromet.com

Abstract: The State of Rio de Janeiro covers an area of 43,750.425 km², ranking as the 2nd state with the highest demographic density at 365.23 inhabitants/km². It is the 3rd most populous state in Brazil, with an estimated population of 17,463,349 people. The state boasts significant physiographic diversity, evident in various landscapes and distinct forms of anthropogenic intervention in the environment. Air quality in the state has been monitored since 1967, initiated by the former Institute of Sanitary Engineering (IES).

For air quality monitoring, the Environmental Institute of Rio de Janeiro State (INEA) has divided the state into subregions: Costa Verde Region (RCV), Medio Paraiba Region (RMP), Metropolitan Region of Rio de Janeiro (RMRJ), North Fluminense Region (RNF), and Mountain Region (RS). The primary aim of this research was to provide accurate and updated information on air quality in the state of Rio de Janeiro, using data from the Official Air Quality Monitoring Network (RMQAr), comprising automatic and semi-automatic monitoring stations, spanning the years 2019, 2020, 2021, and 2022. The air quality assessment followed the standards outlined by CONAMA Resolution nº 491/2018 and the National Technical Guide for Air Quality Monitoring and Assessment.

The study employed various parameters to characterize meteorological conditions and measure pollutant concentrations, including air temperature, relative humidity, rainfall, total suspended particles (PTS), particulate matter with diameters of up to 10 µm (PM_{10}) and 2.5 µm ($PM_{2.5}$), sulfur dioxide (SO_2), nitrogen dioxide (NO_2), ozone (O_3), and carbon monoxide (CO).

Through RMQAr, the research gathered information on major atmospheric pollutants, their sources, concentration levels, temporal trends, and potential impacts on public health and the environment, alongside observed meteorological conditions. The results reveal that in 2019, the RMP witnessed 33 exceedances of air quality standards, followed by 74 violations in the RMRJ, 2 in the North Fluminense Region, 1 in the Costa Verde Region, and 8 in the Mountain Region. In 2020, 15 violations were identified in the RMP, with 135 in the RMRJ, 5 in the North Fluminense Region, and 2 in the Costa Verde Region; the Mountain Region had no violations. In 2021, 4 violations occurred in RMP, 95 in RMRJ, 8 in the Mountain Region, and 9 in RCV, with the North Fluminense Region presenting no violations. In 2022, the RMP had 1 violations, followed by 65 violations in the RMRJ and 2 in the RS; the Costa Verde and North Fluminense Region had no violations. The significant increase in total violations, approximately 82% in 2020 compared to 2019, for the pollutant ozone and particulate, is linked to the reduction in NOx emissions, primarily from vehicles. Notably, this report covers a brief pre-pandemic period and the pandemic era, discussing the effects of health measures during the COVID-19 period on air quality.

Keywords: Air Quality Monitoring, meteorological conditions, Rio de Janeiro, urban air pollution pollutants.

INTRODUCTION (Heading Trebuchet MS, 11 font size, bold)

The climate of the state of Rio de Janeiro is influenced by synoptic and mesoscale meteorological phenomena. The passage of Frontal Systems (FSs), establishment of the South Atlantic Convergence Zone (SACZ), occurrence of Mesoscale Convective Systems (MCSs), and maritime circulation interact with the local orography, producing spatial irregularities in the precipitation field. According to Silva, Luiz Wanderson et al. 2014, the spatial distribution pattern of precipitation remains throughout the year, but in the summer, rainfall indices are higher, especially due to the establishment of SACZ and local convection. In winter, there is a sharp reduction in precipitation totals, with rainfall during this period being primarily a consequence of FSs. It is important to emphasize that climate and meteorological conditions are influenced by a series of complex and interconnected factors, such as ocean currents, topography, latitude and other global climate

phenomena, such as El Niño and La Niña. These factors affect the meteorological conditions in the state of Rio de Janeiro on different time scales, from daily variations to seasonal changes. Consequently, they influence the dispersion of pollutants, with the unfavorable period being the dispersion of primary pollutants mainly during winter, which spans from June to September. During this season, meteorological conditions favor the concentration of pollutants in the atmosphere, especially in urban areas with high concentrations of industries, vehicles, and other emission sources.

Pollutants can be classified into two main categories: primary pollutants and secondary pollutants. This classification is based on how they are emitted into the environment and their chemical forms. Primary pollutants are those released directly into the environment from specific sources. They do not undergo significant chemical reactions in the atmosphere and are emitted in their original form (SO2, CO, NO2, particulate matter). On the other hand, secondary pollutants are formed by chemical reactions in the atmosphere, resulting from the interaction of primary pollutants with other air components. These chemical reactions are typically triggered by sunlight (O3, H2SO2, NHO3). Through these pollutants, it is possible to determine the air quality in the region. The air quality assessment was carried out considering only pollutants whose standards for short- and long-term exposure are established by CONAMA Resolution No. 491/18. Through this resolution, thresholds for each pollutant are defined, determining a violation when atmospheric pollutant levels exceed the limits established by regulatory agencies responsible for protecting air quality.

The aim of this study is to provide accurate and up-to-date information on air quality in the state of Rio de Janeiro, based on data from the INEA Air Quality Monitoring Network (RMQAr), comprising automatic and semi-automatic monitoring stations for the years 2019, 2020, 2021, and 2022. The RMQAr consists of 81 continuous monitors for Total Suspended Particles (PTS), 67 for PM10, 30 for PM2.5, 30 for SO2, 36 for NOx, 43 for O3, and 30 for CO. These continuous monitors are distributed across regions as follows: 9 in the Coastal Rural Area (RCV), 67 in the Metropolitan Region of Rio de Janeiro (RMP), 173 in the Rio de Janeiro Metropolitan Region (RMRJ), 54 in the Northern Fluminense Region (RNF), and 14 in the Southern Region (RS).

METHODS

The method for monitoring the automatic air quality network in Rio de involves collecting data in real time, processing and analyzing this data and disseminating the results to the population. This information is crucial for decision-making and the implementation of measures to control and reduce air pollution. The data obtained is transmitted online and in real-time to the INEA telemetry center and stored in the Institute's database. For the semi-automatic network monitoring, the stations monitor particulate matter parameters for 24 uninterrupted hours, every six days. These network stations are visited weekly by INEA technicians, who measure, programming, and replacement of sampled filters. The filters are weighed, particulate matter concentration is calculated, and the results are entered into the semi-automatic network database. In addition to its own air quality monitoring stations, INEA uses data from private stations belonging to the main industrial and infrastructure projects with significant polluting potential, defined and implemented as required by environmental licensing. These stations are operated and maintained by the enterprises and transmit real-time data to INEA's Air Quality Supervisory Center, which monitors, audits and manages the results.

For the utilization of these data, criteria of representativeness have been adopted to ensure that the collected information is accurate and reliable. The representativeness criteria adopted in this study follow the standards published in the "Best Practices for Review and Validation of Ambient Air Monitoring Data" (EPA-454/B-21-007) and "Standard Operating Procedures for Data Review and Validation" (AQSB SOP 610 Third Edition).

For short-term exposure, the first and second maximum daily concentrations were calculated for the years 2019 to 2022, divided by region (RCV, RMP, RMRJ, RNF, RS). For long-term exposure, annual average concentrations were calculated for the period from 2013 to 2022. Additionally, the Air Quality Index (AQI) was calculated. Annex IV of Resolution Conama No. 491/18 provides the atmospheric pollutants that are part of the AQI calculation, the concentration values related to the air classification at the "good" level, and the mathematical equation for converting monitored concentrations into index values. Thus, it was possible to identify and evaluate, according to their classification, the levels of the AQI, as well as the violations that occurred during this period..

FINDINGS AND ARGUMENT

Figure 1 shows the total number of violations per region from 2019 to 2022. It can be observed that in 2019, there were 33 exceedances of the air quality standard in RMP, followed by 74 violations in RMRJ, 2 in the North Fluminense Region, 1 in the Costa Verde Region, and 8 in the Serrana Region of the state. In the year 2020, 15 violations were identified

in RMP, 135 in RMRJ, followed by 5 exceedances in RNF and 2 in the Costa Verde Region. The Serrana Region did not present any violations in 2020.

In 2021, 4 violations occurred in RMP, 95 in RMRJ, 4 exceedances in RS and 9 in RCV. RNF did not present any violations in 2021. Finally, in 2022, RMP presented 1 violation, followed by 65 violations in RMRJ and 2 in RS. The Costa Verde and Serrana regions did not present any violations.



Figure 1. Total number of violations for the years 2019 to 2022.
Reference: INEA 2024

Table 1 presents the distribution of the number of days per year for the air quality classification at the automatic stations of RMQAr INEA from 2019 to 2022. It can be observed that the worst scenarios were recorded in RMRJ, which may be related to the higher number of vehicular fleet and industrial activities in the state.

Table 1. Distribution of AQI by day count

YEAR	REGION	GOOD	MODERATE	POOR	VERY POOR	HAZARDOUS	NM
2019	RNF	337	26	2	0	0	0
	RS	207	144	8	4	0	2
	RCV	335	28	2	0	0	0
	RMP	139	176	47	3	0	0
	RMRJ	41	221	100	3	0	0
2020	RNF	277	74	14	1	0	0
	RS	351	15	0	0	0	0
	RCV	338	26	2	0	0	0
	RMP	129	221	12	4	0	0
	RMRJ	38	191	127	10	0	0
2021	RNF	351	14	0	0	0	0
	RS	349	14	1	1	0	0
	RCV	327	25	11	2	0	0
	RMP	199	166	0	0	0	0
	RMRJ	58	220	87	0	0	0
2022	RNF	355	10	0	0	0	0
	RS	351	13	0	0	1	0
	RCV	122	241	1	0	0	1
	RMP	207	157	1	0	0	0
	RMRJ	57	222	83	3	0	0

Reference: INEA 2024

CONCLUSIONS

The Metropolitan Region of Rio de Janeiro presents a greater diversity of violated pollutants compared to other regions of the state. This is a reflection of the population density, industrial activities, and vehicular traffic in the region.
Additionally, RMRJ has 173 continuous monitors, followed by 67 in RMP, which represents a difference of 158% in the number of continuous monitors. Due to the majority quantity of stations and continuous monitors, it is expected that RMRJ would indicate a higher number of violations. The significant increase in total violations in RMRJ, approximately 82% in 2020 compared to 2019, for the total pollutants, was mainly due to the increase in ozone and particulate matter. The increase in O3 is related to the reduction in NOx emissions, which are primarily emitted by vehicles.

REFERENCES

BRASIL. MMA. CONAMA. Resolução CONAMA nº 3, de 28 de junho de 1990. Dispõe sobre padrões de qualidade do ar, previstos no PRONAR. Brasília, DF: MMA, 1990. Com complementação e revogação posteriores. Publicada originalmente no Diário Oficial [da] República Federativa do Brasil: seção 1: Poder Executivo, Brasília, DF, p. 15937-15939, 22 ago. 1990. Disponível em: http://conama.mma.gov.br/?option=com_sisconama&task=arquivo.download&id=100. Acesso em: junho de 2023.

BRASIL. MMA, Ministério do Meio Ambiente. Guia Técnico para o Monitoramento e Avaliação da Qualidade do Ar. Brasília, DF, 2020. Disponível em: https://www.gov.br/mma/pt-br/centrais-de-conteudo/mma-guia-tecnico-qualidade-do-ar-pdf.

Silva, Wanderson Luiz, and Claudine Pereira Dereczynski. "Caracterização climatológica e tendências observadas em extremos climáticos no estado do Rio de Janeiro." Anuário do Instituto de Geociências 37.2 (2014): 123-138.

U. S. Department of Energy, Oak Ridge, TN.. U.S. Environmental Protection Agency (US EPA). Best Practices for Review and Validation of Ambient Air Monitoring Data. EPA-454/B-21-007. August 2021.

U.S. Environmental Protection Agency (US EPA). Standard Operating Procedures for Data Review and Validation. AQSB SOP 610 Third Edition. November 2019.

AIR POLLUTION CONFERENCE BRAZIL
CMAS SOUTH AMERICA
COMMUNITY MODELING AND ANALYSIS SYSTEM

Greenhouse gas emissions for biodiesel production in Brazil from different feedstocks using life cycle assessment

Sarah Dantas Rothéia Carvalho[1], Marcela Cravo Ferreira[1]
[1]*Faculdade de Tecnologia, Universidade Estadual de Campinas (UNICAMP)*
E-mail: mcravo@unicamp.br

Abstract: In the face of environmental and energy challenges, the search for cleaner and sustainable energy sources has become a global priority. In this scenario, biodiesel is an important biofuel for diversifying the Brazilian energy matrix and mitigating greenhouse gas emissions. Biodiesel is commercially produced through the transesterification process of vegetable oils or animal fats with a short-chain alcohol in the presence of a catalyst. Various oilseeds can be used for biodiesel production, with soybeans being the most commonly used in the national context, using methanol as the alcohol and sodium hydroxide as the catalyst. RenovaBio is Brazil's National Biofuels Policy established in 2017. Its main objective is to rejuvenate the bioenergy industry in Brazil and reduce greenhouse gas emissions. It aims to stimulate a more sustainable biofuel production based on performance assessments of production units, reflecting individual performance in mitigating emissions compared to fossil fuels for carbon credit issuance. Since different raw materials generate different environmental burdens in biodiesel production, evaluating various production alternatives is essential within the perspectives of new public policies incentivizing the production of biofuels with a lower carbon footprint. In this context, the objective of this study was to analyze the environmental impact resulting from biodiesel production using different feedstocks in the Brazilian scenario through a Life Cycle Assessment (LCA) methodology. The SimaPro software was used for LCA analyses, utilizing the Ecoinvent 3 database. For the assessment of the potential impact of climate change, the IPCC 2021 method with a 100-year methodology was employed. The following raw materials were compared: Brazilian soybean mix, cotton, and animal fat, with the analysis indicating the best environmental performance for animal fat biodiesel. A comparison was made between soybean biodiesel produced in four different states in Brazil - Goiás, Paraná, Rio Grande do Sul, and Mato Grosso. Small variations in emissions were observed based on the production of each state, with a higher contribution from the agricultural phase of soybean production in the emissions impact during the biodiesel production chain. Finally, an analysis was conducted on the substitution of methanol with ethanol during production, revealing an increase in greenhouse gas emissions related to the agricultural phase of sugarcane production.

Keywords: Biodiesel, Life Cycle Assessment (LCA), Soybean, CO_2 emissions.

INTRODUCTION

Biodiesel can be produced from plant or animal sources, such as vegetable oils, animal fats, and used cooking oil (KNOTHE et al., 2006), obtained through the transesterification process with a short-chain alcohol in the presence of a catalyst. Currently, the main raw material used for biodiesel production in Brazil is soybean oil, which accounted for approximately 69% of the country's biodiesel production in 2023 (ANP, 2024).

In Brazil, Law No. 13,576/2017 established the National Biofuels Program (RenovaBio), aimed at encouraging the production and use of biofuels, setting targets for reducing greenhouse gas emissions, and recognizing the environmental benefits of biofuels through the issuance of Decarbonization Credit (BRASIL, 2017). In the context of this public policy, along with the increasing participation of biodiesel in the energy sector, the demand for raw materials becomes greater, as does the need for lipid materials capable of positively contributing to a production chain with sustainable foundations.

Life Cycle Assessment (LCA) plays a crucial role in selecting potential raw materials for biodiesel production, as it allows for a comprehensive comparison between them. Through this methodology, it is possible to quantify and assess environmental impacts throughout all stages of the product life cycle, from raw material extraction to its final disposal.

The aim of this study was to assess the environmental impact arising from biodiesel production employing various feedstocks within the Brazilian context, utilizing a Life Cycle Assessment (LCA) methodology.

METHODS

The Life Cycle Analysis was conducted following the methodology outlined in ISO 14040 and 14044 (ASSOCIAÇÃO BRASILEIRA DE NORMAS TÉCNICAS, 2009a, 2009b). The SimaPro software (PRé Sustainability, Amersfoort Netherlands) was employed for inventory analysis and calculations. The analysis utilized the Ecoinvent 3 database. To evaluate the potential impact of climate change, the IPCC 2021 method employing a 100-year timeframe was applied. All the analyses were carried out considering 1kg of biodiesel.

Some comparisons were made between raw materials for biodiesel production using the traditional production route, employing basic catalysis with methanol as the alcohol. Initially, the

production of Brazilian biodiesel present in the database was evaluated, referred to in this study as "Brazil Mix". This mixture reflects the Brazilian distribution of raw materials for biodiesel production. This blend consists of 80.3% soybean oil, 18.6% tallow, and 1.1% cottonseed oil. Next, scenarios were simulated considering the biodiesel production from 100% soybean, tallow or cottonseed oil, in order to assess the raw material with the greatest impact.

Then, a comparative analysis was conducted specifically for soybean oil biodiesel. The four states with the highest soybean production in the country were considered: Mato Grosso (30.3% of national production), Paraná (18%), Goiás (11.1%), and Rio Grande do Sul (9.8%), with the remaining states together accounting for 30.8% of the total, according to the Brazilian soybean mix available in the software's database.

For biodiesel produced from soybean oil from Mato Grosso, an analysis of the contribution of impacts in each subsystem was carried out: soybean cultivation, oil extraction, and biodiesel production.

Finally, a comparative analysis was conducted between biodiesel from the Brazilian mix using the ethyl and methyl routes. For this purpose, a simplification was made considering only the change of solvent, taking into account the different mass ratios, but without considering changes in the process.

FINDINGS AND ARGUMENT

The fossil CO_{2eq} emissions for the first analysis considering the Brazil Mix and the respective emissions considering the biodiesels from each oil separately can be observed in Figure 1.

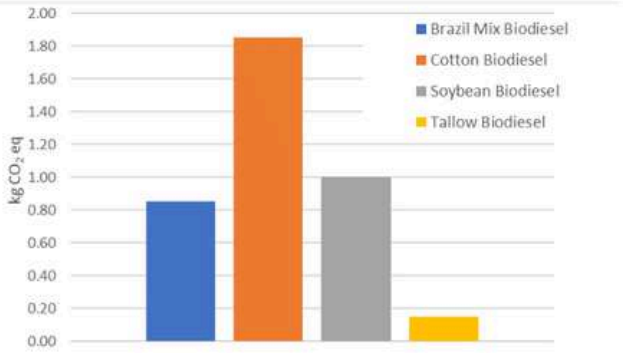


Figure 1. Comparison of CO_2 emissions between different raw materials for biodiesel production

It is possible to observe that the biodiesel with the lowest environmental impact is tallow, and the one with the highest is soybean oil biodiesel. The fact that tallow has a lower impact is because it is livestock waste, and during the LCA analysis no greenhouse gas emissions are attributed to its generation, only to its collection and transportation stages.

Figure 2 presents a comparison between soybean oil biodiesel from soybeans originating from different Brazilian states. The state with the highest emissions is Mato Grosso, however the difference in values between the states is very small, ranging from 0.92 kg CO_{2eq}(RS) to 1.02 (MT).

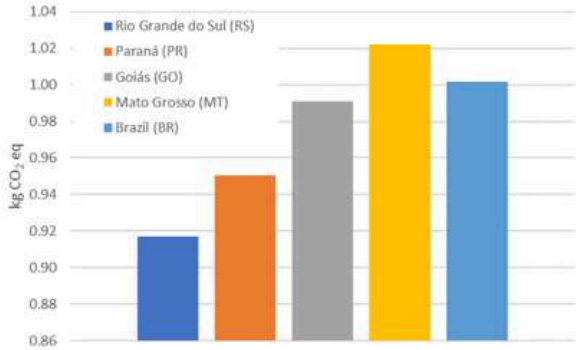


Figure 2. Comparison of soybean oil biodiesel from different Brazilian states

Analyzing the results obtained for the soybean biodiesel production subsystem (Figure 3), it is possible to observe that soybean oil has the highest contribution (79%) of CO_{2eq} emissions.

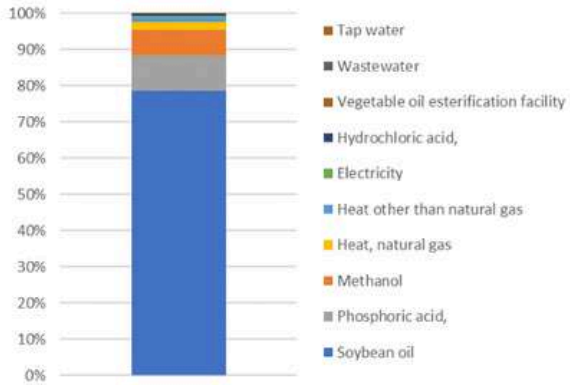


Figure 3. Contribution of impacts on the biodiesel production subsystem

Regarding the soybean oil extraction and production subsystem (Figure 4), it can be observed that soybeans contribute 90% of the impacts, highlighting the importance of the agricultural system in impact calculations.

For the agricultural phase, the main contributors to emissions are presented in Figure 5. The contributions are attributed to the crop management itself and to the chemicals used to provide nutrients and increase productivity.

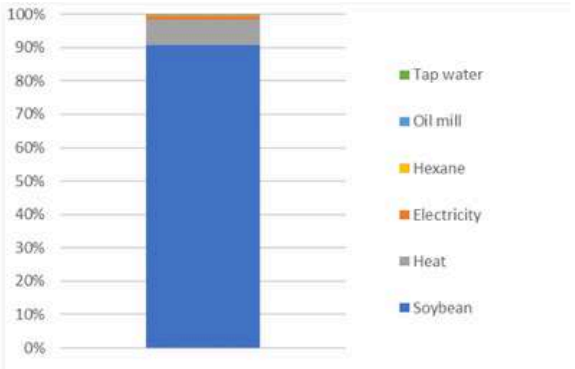


Figure 4. Contribution of impacts on the soybean oil production subsystem

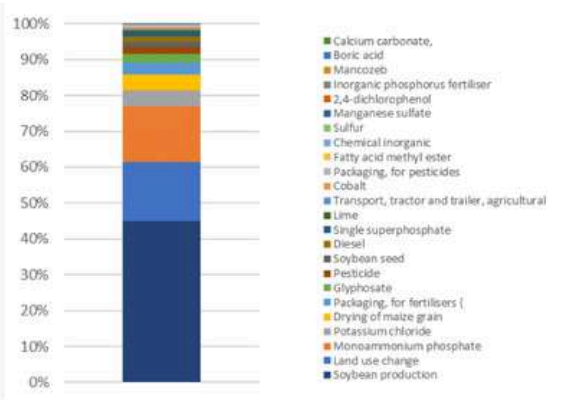


Figure 5. Contribution of impacts on the soybean production subsystem in the state of Mato Grosso

Regarding the short-chain alcohol used in biodiesel production, the ethyl route contributes to slightly greater environmental impacts compared to the methyl route (Figure 6). The detrimental performance of the ethyl route for soybean biodiesel is associated with ethanol production and the monoculture of sugarcane, which generates atmospheric emissions due to the burning of sugarcane straw and bagasse.

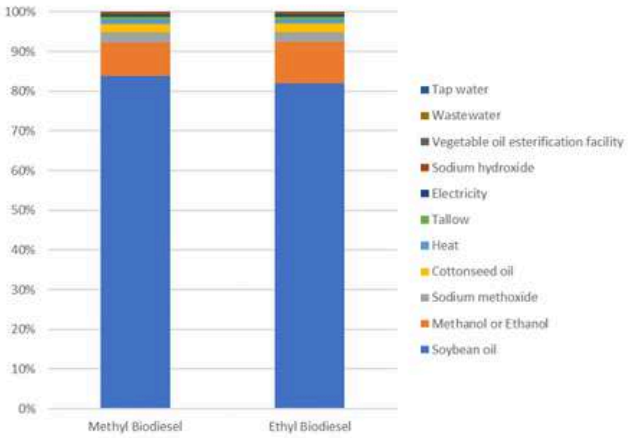


Figure 6. Contribution to the impacts of biodiesel Brazil Mix from the methyl and ethyl routes

CONCLUSIONS

From the analyses, it was possible to verify that tallow biodiesel showed better environmental performance. Therefore, it can be used to diversify the production scenario of this biofuel in response to the growing demand from the energy sector for more sustainable sources.

The results also showed that the agricultural phase has a significant influence on the emissions of soybean oil biodiesel. However, the soybean production region did not show a significant influence on impact calculations.

REFERENCES

ANP - Agência Nacional de Petróleo, Gás Natural e Biocombustíveis. Painel Dinâmico de Produtores de Biodiesel. Available at: https://www.gov.br/anp/pt-br/centrais-de-conteudo/paineis-dinamicos-da-anp/paineis-e-mapa-dinamicos-de-produtores-de-combustiveis-e-derivados/painel-dinamico-de-produtores-de-biodiesel. Accessed April 23, 2024.

Associação Brasileira De Normas Técnicas. ABNT NBR ISO 14040:2009 - Gestão ambiental - Avaliação do ciclo de vida - Princípios e estrutura. Rio de Janeiro: ABNT, 2009a.

Associação Brasileira De Normas Técnicas. ABNT NBR 14044:2009 - Gestão ambiental - Avaliação do ciclo de vida - Requisitos e orientações. Rio de Janeiro: ABNT, 2009b.

Brasil. Lei nº 13.576 de 26 de Dezembro de 2017a. Dispõe sobre a política nacional de biocombustíveis (RenovaBio) e dá outras providências. Diário Oficial da União: Seção 1, Brasília, DF, p. 4, 27 dez. 2017. Available at: https://www.planalto.gov.br/ccivil_03/_ato2015-2018/2017/lei/l13576.htm. Accessed April 23, 2024.

Knothe, G.; Van Gerpen, J.; Krahl, J.; Ramos, L. P. Manual de biodiesel. 1. ed. São Paulo: Edgard Blucher, 2006.

AIR POLLUTION CONFERENCE BRAZIL
CMAS SOUTH AMERICA
COMMUNITY MODELING AND ANALYSIS SYSTEM

EVALUATİON OF THE RESULTS OF THE FİRST CYCLE OF SUBMİSSİONS OF THE NEW GREENHOUSE GAS EMİSSİONS REPORTİNG PROGRAM İN RİO DE JANEİRO

Isabela Angelloti Costa [1], Pedro Henrique Rocha Valle [2], Gustavo Mota Rodrigues [3], Rafael Campos [4], Renato Vieira da Silva[5]

[1] *MJV Technology & Innovation; isabela.angelloti@mjv.com.br*

[2] *Environmental Institute of Rio de Janeiro State (INEA); pedrovalle@inea.rj.gov.br*

[3] *Environmental Institute of Rio de Janeiro State (INEA); gmota@inea.rj.gov.br*

[4] *Environmental Institute of Rio de Janeiro State (INEA); rcampos@inea.rj.gov.br*

[5] *Environmental Institute of Rio de Janeiro State (INEA); renvisil@inea.rj.gov.br*

Abstract: Concern about climate change and its impacts has encouraged governments, companies, and society to seek more efficient ways to monitor and reduce their greenhouse gas emissions. The State of Rio de Janeiro then approved the Operational Standard NOP-INEA-52, which replaced and modernized the Instituto Estadual do Ambiente (INEA) Resolution N°64/2012. This work aims to evaluate the results of the first cycle of inventory submission referring to the new Greenhouse Gas Emissions Reporting Program in Rio de Janeiro. This Program focused on improving the monitoring of emissions in the state, updating the program's coverage, presenting the responsibilities of the actors involved, bringing the option of voluntary participation, providing an online reporting platform, and creating a public emissions record. The evaluation of the different aspects of the Program will be presented, both concerning the engagement of interested parties, the ease of meeting their obligations, and the transparency and effectiveness of monitoring the evolution of greenhouse gas emissions in the territory of the state of Rio de Janeiro. To carry out this analysis, the information available on the INEA website was considered. Compared to previous legislation, the new Program enriched the program's coverage by increasing the list of mandatory activities in the areas of waste and effluents, industry and energy and transport, as well as establishing a minimum cut of 10,000 tCO2e considering emissions from scope 1 and 2 of the projects to compulsorily comply with the Program, focusing on large emitters, in addition to enabling voluntary participation. The results point to great efficiency in the use of the GHG Reporting Program. However, they also indicate the need to verify possible mandatory reporting projects that remained outside the first cycle, and increase engagement in specific sectors, in addition to pointing to the need to review the applicability requirements following the expected objectives.

Keywords: greenhouse gas, emission inventory, reporting program.

INTRODUCTION

This article aims to analyze the impacts of the first year of implementation of the Greenhouse Gas Emissions Reporting Program in Rio de Janeiro. The program was developed to serve as a benchmark model in measurement, reporting, and verification (MRV), aligned with the main instruments, methodologies, and standards already established both in Brazil and on the international scene, encouraging active participation and compliance with its guidelines. The structure and criteria adopted were based primarily on the ABNT 14064 standards, the WRI manual for creating mandatory programs, the National Emissions Registration System, and the GHG Protocol Brazil.

To implement the State Emissions Registry and update INEA/PRES Resolution No. 64, activities were initiated involving various stakeholders. Contributions were received from reporting entities, the Federation of Industries of the State of Rio de Janeiro, the National Institute of Metrology, Quality, and Technology (Inmetro), members of the Public Ministry, and specialized consultancies during the legislative update process.

The Resolution's modernization aimed to adjust to best practices, clarify rules, streamline communication between the State and inventory-presenting entities, and expand participant numbers, extending its application beyond environmental licensing.

As a result, Conema Resolution N° 97, approving Operational Standard NOP-INEA-52, was published in the Official Gazette on November 30, 2022. This standard establishes procedures, requirements, and criteria for the greenhouse gas emissions reporting program and forms the state registry of greenhouse gas emissions in Rio de Janeiro.

METHODS

This study evaluated the effectiveness of the standard in achieving its objectives, with a special focus on its new features:

(i) The transition from an INEA Resolution to an Operational Standard approved by the State Environmental Council, which expanded the participation of other stakeholders in its elaboration.

(ii) The clarity in its structure. NOP-52 sought to address the main elements of a measurement, reporting, and verification (MRV) program: What are the objectives? Who should report what? How to calculate and measure emissions? What information should be provided and how often? Where should they be reported? Who verifies? Who has access to the reported information?

(iii) The expansion of the program's coverage, maintaining the focus on the main emitters and the implementation of an online platform for reports.

The database used in this study was provided by INEA-RJ, referring to the year 2022, the first cycle of program submissions. This base includes inventories that may be subject to future adjustments, so updated information may be disclosed later.

The data will be evaluated both qualitatively and quantitatively, focusing on the results already obtained and compliance with its initial objectives. As defined in the Program, all inventories were made with mandatory scopes 1 and 2, and optional scope 3, minimally reporting the emissions of the gases Carbon Dioxide (CO2), Methane (CH4), Nitrous Oxide (N2O), Hydrofluorocarbons (HFCs), Perfluorocarbons (PFCs), Sulfur Hexafluoride (SF6), and Nitrogen Trifluoride (NF3). All third party verifications by an independent body must be made by bodies accredited by Inmetro.

The obligation to present an annual inventory of GHG emissions and its respective Verification Statement applies to enterprises classified as classes 4, 5, and 6, as provided for in state decree n° 46.890, of December 23, 2019, and that emit annually the equivalent to or above 10,000 tCO2eq (adding scopes 1 and 2). The calculation methodology adopted to determine the GHG emissions to be used by the entrepreneur for the preparation of the GHG Emissions Inventory is that of the GHG Protocol Brazil. For this cycle, all emission values in tons of carbon dioxide equivalent were converted considering the values of the Fifth Assessment Report of the IPCC.

FINDINGS AND ARGUMENT

In this study, significant adherence to the Greenhouse Gas Emissions Reporting Program (NOP-INEA-52) was observed in the first year of its implementation. The standard expanded the list of sectors that must report their emissions inventories but established a minimum emissions limit for this obligation to be applied. In 2022, 129 inventories were reported (Figure 1), a number close to the record in 2017, when the highest number of inventories was sent to Inea.

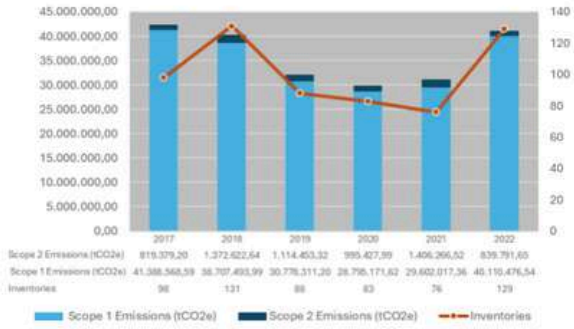


Figure 1: GHG Emissions by Year

A relevant fact is that, even being the first year of the program, 10% of the reported inventories were submitted voluntarily. Some of these voluntary inventories were from economic activities that were not foreseen in the resolution. In addition, 95% of the inventories that make up the database were verified by a third party.

Figure 2 shows the number of emissions reported in 2022 for each inventoried scope. Both for mandatory and voluntary reports, scope 3 is optional and was reported by 37 (28%) of the participating enterprises. The emissions from this scope represented about 10% of the total emissions from scopes 1 and 2.

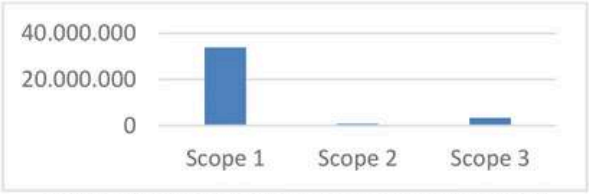


Figure 2: GHG Emissions by scopes in 2022 Report

Regarding the category of scope 1 sources, stationary combustion stood out as the main emitting source, corresponding to approximately 70% of all direct emissions from inventoried enterprises (Figure 3).

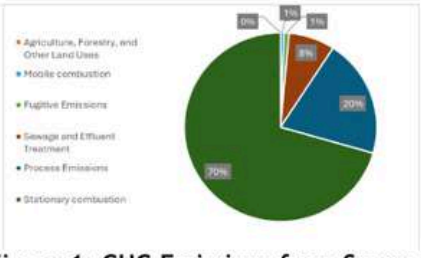


Figure 1: GHG Emissions from Scope 1

About the type of participating enterprise, the chemical industry stood out, followed by sewage and effluent treatment stations, sanitary landfills, and the oil, gas, and fuel alcohol industry. These three groups represented approximately 60% of the total inventories sent (Table 1). However, in terms

of tons of CO2 equivalents emitted, the steel, metallurgy, and petrochemical sectors represented approximately 73% of the total scope 1 and 2 emissions reported under the program (Figure 4).

Table 1: Number of inventories by activities

Activities	Number of Inventories
Chemical Industry	22
Sewage and liquid effluent treatment plants	20
Landfills	15
Oil, gas, and fuel alcohol industry	11
Steel, and metallurgy industry	9
Nonmetallic mineral industry	8
Others	44

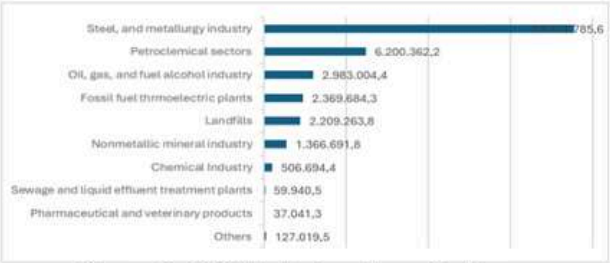


Figure 2: GHG Emissions by activities

As for the spatial distribution of participating enterprises (Figure 5), of the 92 municipalities in the state of Rio de Janeiro, 29 of them had participating enterprises. Four of these cities (Table 2) were responsible for more than half of these enterprises. These data demonstrate the breadth and significant impact of the program in its first year of implementation. The analysis of these results provides valuable insights to further improve and expand the program in the coming years.



Figure 3: Distribution of participating companies

Table 2: Number of inventories by municipalities

Municipalities	Number of inventories
Rio de Janeiro	33
Duque de Caxias	16
São Pedro da Aldeia	11
Macaé	8
Resende	6
Niterói	5
Araruama	4
Others	46

CONCLUSIONS

When specifically analysing the year 2022, the late publication of the standard may have limited comprehensive dissemination and engagement of Rio de Janeiro enterprises with new obligations, indicating potential for increased emissions and monitored enterprises.

Examining the state inventory of ghg emissions, a significant portion of emissions were not covered in the 2022 cycle of NOP-INEA-52, focused on corporate emissions. Two action fronts emerge: evaluating program coverage adjustment and applicability requirements and identifying enterprises that should comply with current legislation but haven't reported emissions. Freight and passenger transport activities, significant regional emissions contributors, along with some industrial activities, showed weak program adherence.

Despite gaps, the program demonstrates capacity to expand reporting entities, both mandatory and voluntary, showing potential in its first year. The large percentage of third-party verified inventories creates a powerful database for public policies aimed at mitigating and reducing greenhouse gas emissions, and potentially creating a carbon market.

These conclusions provide a comprehensive view of the program's first-year performance, highlighting areas for improvement and expansion. The analysis underscores the importance of effective engagement and clear communication with enterprises to ensure compliance and maximize impact.

REFERENCES

ABNT (2006). ABNT NBR ISO 14064: Gases de efeito estufa - Parte 1: Especificação com orientação, ao nível das organizações, para quantificação e relato de emissões e remoções de gases de efeito estufa. Rio de Janeiro: ABNT.

WRI World Resources Institute (2015), "Guia para elaboração de programas mandatórios de relato de gases de efeito estufa", 2015.

CONEMA (2022). Resolução nº 97 de 10 de novembro de 2022, que aprova a Nop-Inea-52. Conselho Estadual de Meio Ambiente do Estado do Rio de Janeiro.

Rio de Janeiro, Secretaria do Ambiente (2017). Inventário de emissões de Gases de Efeito Estufa (GEE) do Estado do Rio de Janeiro : ano base 2015 : resumo técnico / Secretaria do Ambiente. - Rio de Janeiro.

IPCC (2014). Climate Change 2014: Synthesis Report. Contribution of Working Groups I, II and III to the Fifth Assessment Report of the Intergovernmental Panel on Climate Change [Core Writing Team, R.K. Pachauri and L.A. Meyer (eds.)]. IPCC, Geneva, Switzerland.

AIR POLLUTION CONFERENCE BRAZIL
CMAS SOUTH AMERICA
COMMUNITY MODELING AND ANALYSIS SYSTEM

Assessing the Mitigating Impact of Green and Blue Infrastructure on Environmental Stressors

Patrick Connerton[1,2], Thiago Nogueira[1], Prashant Kumar[2,3], and Helena Ribeiro[1]
[1]*Universidade de São Paulo - Faculdade de Saúde Pública*
pjconnerton@usp.br
[2]*Global Centre for Clean Air Research (GCARE), University of Surrey*
[3]*Institute for Sustainability, University of Surrey*

Abstract: Ambient air pollution is the most important environmental factor impacting human health. Exposure to unsafe levels of air pollutants such as particulate matter has been linked to increased risk of respiratory and cardiovascular diseases. Cities present unique air quality challenges, being areas that typically have higher concentrations of air pollutants and exposed population. In such urban areas, green and blue infrastructure has shown potential for alleviating environmental stressors, including air pollution and heat wave abatement. However, such solutions must be correctly designed in order to maximize mitigation and not inadvertently increase pollutant exposure. This study utilizes low-cost sensors to examine the relationship between green and blue infrastructure and a series of environmental parameters. While previous studies have investigated green infrastructure and air quality mitigation, few have employed low-cost sensors to obtain highly localized data to demonstrate this relationship. In this study, as a part of NERC-FAPESP funded GreenCities project, low-cost sensors were validated through lab testing and then deployed in the field in locations in São Paulo, Brazil. The locations selected for this study allow for a comparison of built versus green and blue areas. Lidar data was used characterize the profile of each site based on surrounding vegetation area, canopy height, building area and building height. Distance to the closest roadways was also measured for each sensor location. These profiles are analyzed against the data obtained through the low-cost sensors, considering both meteorological (temperature, humidity and pressure) and particulate matter (PM1.0, PM2.5 and PM10) parameters. Data collection for this study is ongoing, but this analysis focuses on data collected during the period from August through December of 2023. Preliminary findings show that the sites with higher NDVI values had higher humidity. The impact of green and blue infrastructure on particulate matter and temperature is mixed, with a mitigating impact observed only at one of the two sites for each variable.

Keywords: Low-cost sensors, particulate matter, air quality, green infrastructure, cities

INTRODUCTION (Heading Trebuchet MS, 11 font size, bold)

Ambient air pollution has emerged as a critical issue impacting human health on a global scale (GBD 2019 Risk Factors Collaborators, 2020). Exposure to air pollution is especially critical in urban landscapes, where both population and emission sources tend to be more concentrated (Castells-Quintana et al., 2021). Green-blue infrastructure has emerged as a tool to mitigate exposure to air pollution (Kumar et al., 2019), however not all green infrastructure solutions offer similar benefits, and in some cases, factors such as decreased dispersion may offset gains (Gromke & Ruck, 2007; Nowak et al., 2018). Due to this range of possible outcomes, it is important to analyse each setting to understand how green-blue infrastructure is designed and what benefits it can offer.

In this context, the present study explores the influence of green-blue infrastructure in an urban setting by examining air pollution and climate data collected using low-cost sensors at four locations in São Paulo, Brazil (hereafter EACH, FSP, ETEC and CIENTEC). The goal of this research is to demonstrate whether these features present any air quality or climate mitigating benefits, and the extent to which this can be measured.

METHODS

The sensors used in this study are PurpleAir Flex Air Quality Monitors, which use a pair of PMS-6003 laser particle counters and one BME688 instrument for meteorological readings. Prior to installation, the sensors deployed in this study were validated via colocation within a chamber at the Global Centre for Clean Air Research (GCARE). A variety of scenarios were simulated, with the sensors showing adequate performance for particulate, temperature and humidity readings. Therefore, no calibration of the sensor readings was performed in this study.

The sensors were installed in four locations throughout the city of São Paulo. These locations were selected due to their unique characteristics, containing both green and built areas. The site characteristics, specifically vegetation area, tree crown height, building area and building height, were assessed using lidar data collected and made public by the Municipal Government of São Paulo. These parameters were calculated for a 50-meter radius around each site. Distance to nearest road and road classification were also obatined for each site.

AIR POLLUTION CONFERENCE BRAZIL
CMAS SOUTH AMERICA
COMMUNITY MODELING AND ANALYSIS SYSTEM

Transmitted sensor data were downloaded electronically by using the PurpleAir download tool. Standard data cleaning steps were followed to eliminate outliners and ensure agreement between the two particle counters for each sensor. Hourly and daily averages were calculated for the four sites, as well as the correlation between daily averages among the sites.

Background concentrations for each site were estimated, according to minimum hourly concentrations (generally observed around midday). From this, the percentage increase was calculated for different periods of the day, to estimate the mitigating impact of local features.

QGIS was used for site characterization and R Studio was used to analyze the sensor data.

FINDINGS AND ARGUMENT

The site characterization (Figure 1) revealed highly divergant characteristics for each site, with the ETEC site possessing a significantly higher area occupied by built infrastructure, while also having the second highest average tree crown height. The FSP site, on the other hand, while corresponding to the highest average building height, also possessed the largest area occupied by trees.

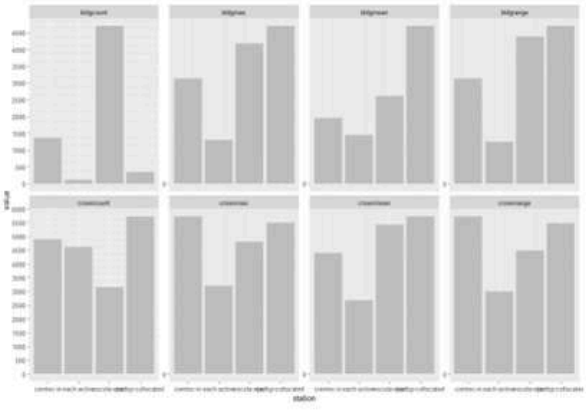


Figure 1. Lidar site characterization, based on canopy and building heights

The daily average particulate matter concentrations at each site followed the same trend and were highly correlated, with correlation coeficient values ranging from .74 to .92.

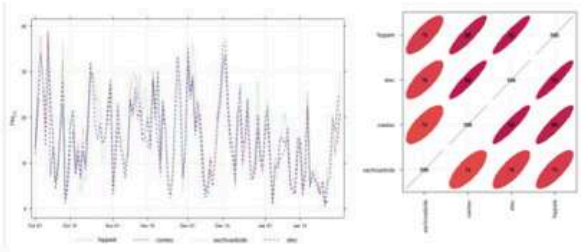
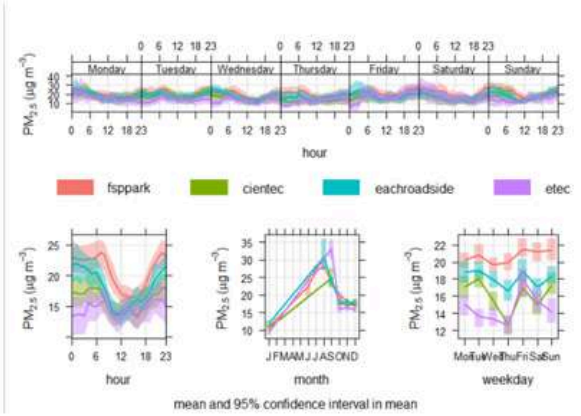


Figure 2. Temporal variation of fine particulate matter (PM2.5) measured by low-cost sensors at each site; (a) daily average values; (b) correlation between daily average values among the four sites

The temporal analysis of the data provides a more granular view of variation among the sites. While all sites follow the same overall daily variation pattern, we observe that the FSP location has higher concentrations for all periods, followed by EACH, CIENTEC and finally the ETEC location.



CONCLUSIONS

The results of this study reinforce the important role that green-blue infrastructure can play in mitigating environmental and climate impacts. It also shows how different site characteristics can affect the magnitude of this mitigating effect. This information should be taken into account when designing green-blue infrastructure, so as to maximize benefits and reduce population exposure.

REFERENCES

Castells-Quintana, D., Dienesch, E., & Krause, M. (2021). Air pollution in an urban world: A global view on density, cities and emissions. In Ecological Economics. https://doi.org/10.1016/j.ecolecon.2021.107153

GBD 2019 Risk Factors Collaborators. (2020). Global burden of 87 risk factors in 204 countries and territories, 1990–2019: a systematic analysis for the Global Burden of Disease Study 2019. The Lancet, 396(10258), 1223–1249. https://doi.org/10.1016/S0140-6736(20)30752-2

Gromke, C., & Ruck, B. (2007). Influence of trees on the dispersion of pollutants in an urban street canyon-Experimental investigation of the flow and concentration field. Atmospheric Environment. https://doi.org/10.1016/j.atmosenv.2006.12.043

Kumar, P., Druckman, A., Gallagher, J., Gatersleben, B., Allison, S., Eisenman, T. S., Hoang, U., Hama, S., Tiwari, A., Sharma, A., Abhijith, K. V., Adlakha, D., McNabola, A., Astell-Burt, T., Feng, X., Skeldon, A. C., de Lusignan, S., & Morawska, L. (2019). The nexus between air pollution, green infrastructure and human health. In Environment International. https://doi.org/10.1016/j.envint.2019.105181

Nowak, D. J., Hirabayashi, S., Doyle, M., McGovern, M., & Pasher, J. (2018). Air pollution removal by urban forests in Canada and its effect on air quality and human health. Urban Forestry and Urban Greening. https://doi.org/10.1016/j.ufug.2017.10.019

AIR POLLUTION CONFERENCE BRAZIL
CMAS SOUTH AMERICA
COMMUNITY MODELING AND ANALYSIS SYSTEM

COOL AND CLEAN AİR PLACES: INTEGRATİNG PUBLİC PERCEPTİON WİTH URBAN GREEN SPACE

Leticia Figueiredo Candido[1,3], Patrick Connerton[2,3] , Giuliano Maselli Locosselli[1,4], Prashant Kumar[3]
1 Cluster of Ecology, Institute of Environmental Research of the State of São Paulo, São Paulo, Brazil
leticia.fcandido@outlook.com
2 Faculty of Public Health, Universidade of São Paulo, São Paulo, Brazil
pjconnerton@usp.br
3 Global Centre for Clean Air Research (GCARE), School of Sustainability, Civil and Environmental Engineering, Faculty of Engineering and Physical Sciences, University of Surrey, Guildford, UK
locosselli@yahoo.com.br
4 Center for Nuclear Energy in Agriculture, University of São Paulo, Piracicaba, Brazil
p.kumar@surrey.ac.uk

Abstract: Cities growth and anthropogenic activities change the landscape and increase the levels of CO2 concentration, contributing to severe environmental issues and climate change. The decline in green spaces and the use of heat-retaining materials in grey infrastructure affect thermal comfort and air quality, impacting the well-being of citizens. Faced with these challenges, it is necessary to understand how to plan cities adapted to climate change. This study aims to discover cool and clean air places within the community, assess the impact of different types of blue and green infrastructure on air quality and urban temperature, and evaluate public perception. To achieve these objectives, a questionnaire was administered to Guildford (United Kingdom) citizens to evaluate their knowledge of cooling, air pollution, and perceptions of cool and clean places in the town. Based on the answers were selected areas for monitoring covering five different types of urban spaces: green infrastructure, blue and gray infrastructure, green and gray infrastructure, green and blue infrastructure, and gray infrastructure (built environment) the answers were based on the least polluted, most polluted, coolest and the hottest places. The places were monitored for 10 days, 3 times a day: morning peak - 8:00 to 9:30, off-peak - 12:30 to 14:00, and evening peak - 16:30 to 18:00, during December 2023 and January 2024. The data collection includes particulate matter 2.5, temperature, relative humidity, globe temperature, CO2 concentration, black carbon, and noise. Preliminary findings reveal a positive perception of green and blue infrastructure among citizens, although awareness of certain physical aspects remains low. Disparities were identified between perceived and actual pollution and temperature levels in urban green spaces. The study also shows that 45.16% of the public expressed curiosity about air quality issues. This ongoing study bridges the gap between public perception and environmental monitoring, providing valuable insights for evidence-based policies in sustainable urban planning. After measurements on the cool and clean air places the information will bring awareness and provide guidelines for healthier living environments in Guildford.

Keywords: particulate matter 2.5, black carbon, green infrastructure, blue infrastructure, air quality.

INTRODUCTION

In 2007, more than half of the global population became urbanized, reaching an estimated 55% of the world population (Baklanov et al., 2016). While urbanization has led to significant social advancements, also introduced substantial environmental challenges affecting citizen well-being. The growth of urban areas often results in the loss of green infrastructure and the expansion of grey infrastructure, which alters cities' radiation balance and contributes to local temperature increases (Seto et al., 2011). These changes, including the formation of heat islands due to the use of heat-retaining materials, lead to higher land surface temperatures, impacting microclimate conditions and resident comfort (Portner et al., 2022).

Urbanization also significantly alters local atmospheric composition, with vehicle emissions being a primary source of air pollution in cities. Black carbon and particle number concentrations (PNCs), such as PM2.5, are ultrafine particles linked to adverse health effects. The relationship between black carbon, PM2.5, temperature, and CO2 in urban settings is crucial for understanding air quality and climate change. Black carbon significantly contributes to global warming and aerosol formation, directly affecting local air quality and public health (Kumar et al. 2015).

Addressing these complex environmental challenges requires multifunctional solutions, including the integration of green and blue infrastructure (GBI). GBI, such as green spaces, green roofs, and rain gardens, provides ecosystem services that benefit both the environment and human well-being by improving water quality, and contributing to urban cooling and air quality improvement (Haase et al. 2014). Facing these challenges, this study aimed at unveiling cool and clean air paths within the community of the city of Guildford based on public perception, and scientifically assess the impact of different types of blue and green infrastructure on air quality and urban temperature.

AIR POLLUTION CONFERENCE BRAZIL
CMAS SOUTH AMERICA
COMMUNITY MODELING AND ANALYSIS SYSTEM

METHODS

Guildford is a historic market town located in Southeastern England (51.2362° N, 0.5704° W). The city provides an interesting framework for studying green and blue infrastructure, given its diverse array of green and blue spaces interspersed within the urban landscape. The city also presents determinate traffic peak periods allowing for a reliable assessment of the air pollution concentrations.

We applied a questionnaire to Guildford citizens to evaluate the public perception *of* the role of the GBI (green-blue infrastructure) on thermal comfort and air pollution mitigation. The questionnaire pursues public perception about the coolest and hottest places in Guildford as well as the most polluted and least polluted areas (Figure *1*). After analysing the questionnaire responses, we selected a path through the highlighted places to monitor climate and pollutant variables. The selected places were The Mount, Alice and The Rabbit Statue, Castle grounds, Stoke Park gardens, and built patches (Figure 2).

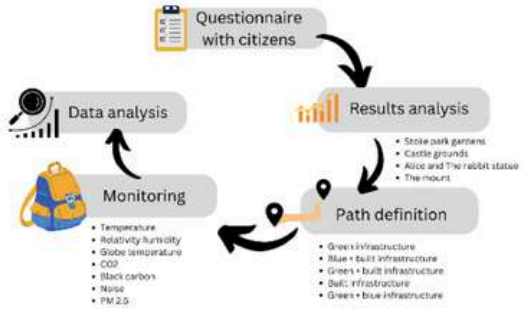


Figure 1. Methodological Framework.

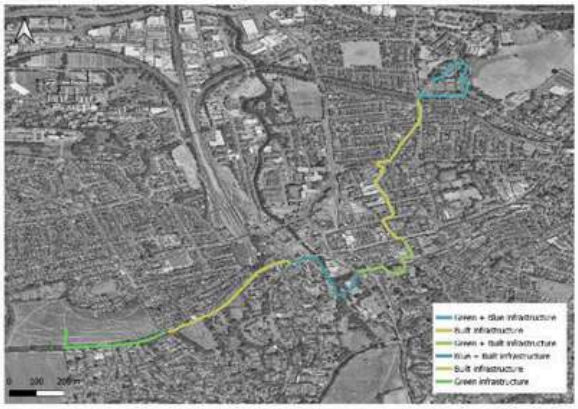


Figure 2. The selected route for monitoring. The map shows the path walked along the monitoring in the city of Guildford, the different colors indicate the different GBI infrastructures.

The data collected was an array of environmental parameters, including particulate matter 2.5 (PM2.5), temperature, relative humidity, globe temperature, CO2 concentration, black carbon levels, and ambient noise. We used the following instruments: pDR-1500 Aerosol Monitor, MicroAeth AE51 (Aethlabs), Testo 400, sound Level Meter (RS-1150. All the equipment was carried on a backpack for walking monitoring. The route was submitted to ten samples of the monitoring period for each variable, encompassing three distinct time intervals throughout the day according to traffic: morning peak (from 8:00 to 9:30), off-peak hours (from 12:30 to 14:00), and evening peak (from 16:30 to 18:00), decided based on previous studies to access the different variations along the day (Harrison et al., 2012; Kumar et al. 2018; Singh et al. 2018). From 10 samples, 8 were collected on weekdays and 2 on weekend days.The data is being processed and analyzed in R and QGIS software.

FINDINGS AND ARGUMENT

Based on feedback from 31 respondents, the coolest places in Guildford were identified as Stoke Park Gardens and The Mount, while the hottest places were Guildford Castle and Alice and The Rabbit. The least polluted areas were The Mount and Stoke Park Gardens, whereas the most polluted were Alice and The Rabbit statue and Allen House grounds. They generally understood the benefits of blue-green infrastructure (BGI) in reducing air temperature and pollution, but lacked knowledge about physical environmental aspects such as elevation and wind speed (Figure 3).

Interestingly, respondents had a positive perception of GBI's impact on air quality, a contrast to typical findings where functional benefits of GBI are often underestimated by the public. Previous studies suggest that citizens are more attracted to the aesthetic and recreational benefits of GBI rather than its functional aspects like microclimate regulation or water management (Syrbe et al., 2021). This study fills a gap in research on public perception of different types of GBI, aligning with findings that the public values air quality regulation provided by green infrastructure despite potential drawbacks.

The decision-making factors for ranking spaces by climate and pollution were primarily the presence of green and blue infrastructure, space structure, and traffic. Green infrastructure and elevation played significant roles in climate perception, while traffic and urban density were major determinants of perceived pollution levels. This highlights the importance of these elements in urban planning and public awareness campaigns.

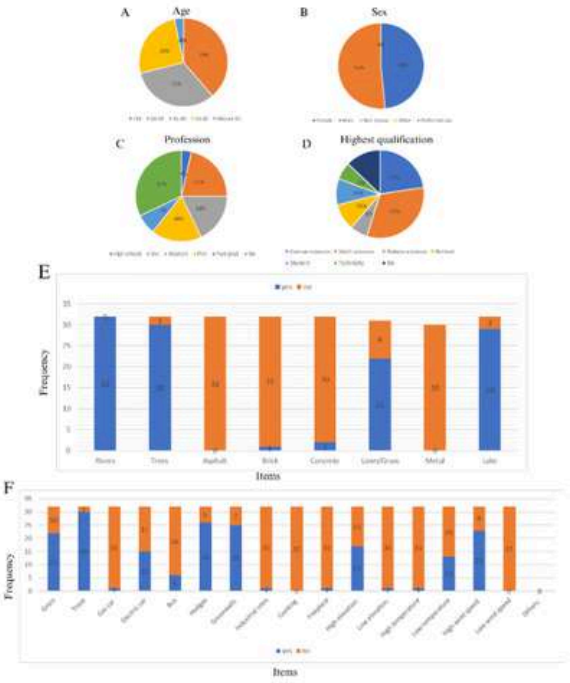


Figure 3. Questionnaire results. A, B, C, and D: Public profile; E. 1. Items that can lower air temperature and improve cooling; F. Items that can decrease air pollution.

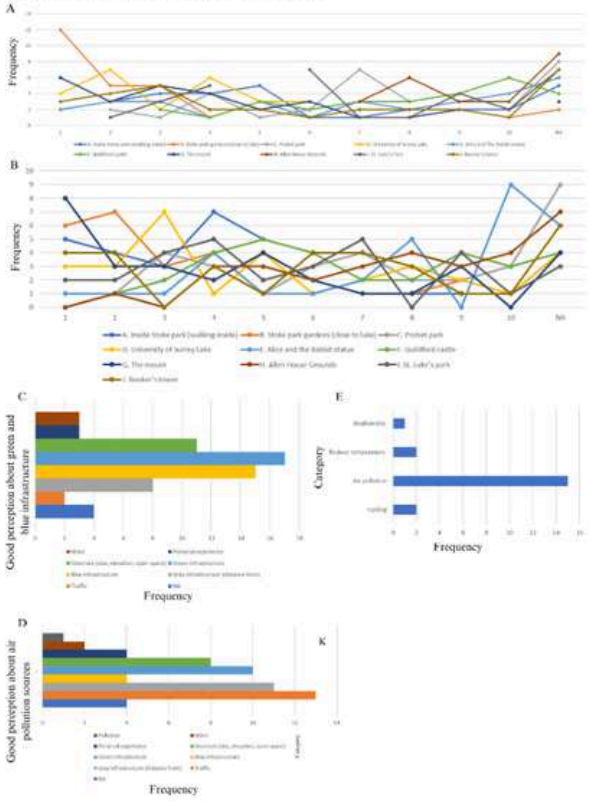


Figure 4. Questionnaire results. A. Frequency for places ranked from coolest to hottest; B. Frequency for places ranked from least polluted air to most polluted air; C. Reasons to rank the places according to the climate; D. Reasons to rank the places according to air pollution; E. Research interest by public.

Preliminary findings indicate a generally positive perception of green and blue infrastructure among citizens, though awareness of specific physical environmental factors remains limited. The study also reveals a strong public interest in air quality issues, with 45.16% of respondents curious about various aspects such as cycling routes, the health impacts of air pollution, ways to reduce pollution, and comparisons of air quality in different urban settings. This interest underscores the need for continued public education and engagement on the benefits of BGI and air quality improvement initiatives.

CONCLUSIONS

The study presents intriguing findings concerning public perception and favorable outcomes for both climate and air pollution variables. Overall, public perception towards Green and Blue Infrastructure (GBI) was positive, which constitutes an unexpected result. Perception studies regarding GBI remain scarce, underscoring the importance of comprehending public opinion on this matter. Preliminary findings regarding air pollution reveal discernible trends, with peak traffic and GBI exerting influence on pollutant concentrations. These results are currently undergoing further analysis, with public perception set to be juxtaposed against monitoring outcomes.

REFERENCES

Baklanov, Alexander, Molina, Luisa. T., and Gauss, Michael. "Megacities, Air Quality and Climate." Atmospheric Environment 126 (2016): 235-249. Accessed May, 2024. doi:10.1016/j.atmosenv.2015.11.059

Kumar, Prashant, et al. "New Directions: Air Pollution Challenges for Developing Megacities Like Delhi." Atmospheric Environment 122 (2015): 657-661. Accessed May, 2024. doi: 10.1016/j.atmosenv.2015.10.032

Pörtner, H. O., Roberts, D. C., Adams, H., Adler, C., Aldunce, P., Ali, E., ... and Ibrahim, Z. Z. "Climate Change 2022: Impacts, Adaptation and Vulnerability." Geneva, Switzerland: IPCC, 2022. Accessed May, 2024.

Seto, K. C., Fragkias, M., and Güneralp, B. "A Meta-Analysis of Global Urban Land Expansion." PLoS One 6, no. 8 (2011): e23777. Accessed May, 2024. doi.org/10.1371/journal.pone.0023777

Syrbe, R. U., Neumann, I., Grunewald, K., Brzoska, P., Louda, J., Kochan, B., ... and Bastian, O. "The Value of Urban Nature in Terms of Providing Ecosystem Services Related to Health and Well-Being: An Empirical Comparative Pilot Study of Cities in Germany and the Czech Republic." Land 10, no. 4 (2021): 341.

AIR POLLUTION CONFERENCE BRAZIL
CMAS SOUTH AMERICA
COMMUNITY MODELING AND ANALYSIS SYSTEM

IMPACT OF OZONE ON MORTALİTY AND HOSPİTALİZATİONS İN THE MEGALOPOLİS OF THE VALLEY OF MEXİCO

Blanca Rios[1], Francisco Estrada[2], Graciela B. Raga[1]
[1] *Instituto de Ciencias de la Atmósfera y Cambio Climático, Universidad Nacional Autónoma de México,Ciudad de México, México*
berr86@gmail.com, raga.graciela@gmail.com
[2] *Programa de Investigación en Cambio Climático,Universidad Nacional Autónoma de México,Ciudad de México, México*
feporrua@atmosfera.unam.mx

Abstract: Air pollution is a complex mixture of gaseous and particulate components, each of which has detrimental effects on human health. Ground-level ozone is a highly reactive oxidative gas commonly found in urban and suburban environments, primarily derived from anthropogenic emissions. Numerous epidemiological studies and several reviews from environmental and health agencies around the world have reported that exposure to these contaminants is associated with adverse health outcomes, including increased short-term mortality and morbidity. This project aims to quantify the excess mortality and short-term hospitalizations associated with ozone contingencies, with and without biomass burning emissions, in the megalopolis of the Valley of Mexico. Ozone concentrations are simulated using the regional chemical Weather Research and Forecasting (WRF) model coupled with Chemistry version 4.2.1.1. The model outputs and data from the Institute for Health Metrics and Evaluation (IHME) estimate morbidity and mortality caused by ozone exposition with the Environmental Benefits Mapping and Analysis Program - Community Edition (BenMAP-CE).
Keywords: Ozone, WRF-Chem, BenMAP-CE, Megalopolis of the Valley of Mexico

INTRODUCTION

Air pollution is a complex mixture of gaseous and particulate components, each of which has detrimental effects on human health(Manisalidis et al.). Gaseous pollutants such as nitrogen dioxide (NO2), sulfur dioxide (SO2), carbon monoxide (CO), and ground-level ozone (O3) are commonly found in urban and industrial areas. These pollutants primarily originate from vehicle emissions, industrial processes, and the burning of fossil fuels.(Ramanathan and Feng). Tropospheric ozone is a compound formed from the photochemical reactions of volatile organic compounds (VOCs) and nitrogen oxides (NOx) in the presence of sunlight (Lelieveld and Dentener). Numerous epidemiological studies and environmental health reviews have linked exposure to elevated ozone levels with adverse health outcomes.(Fleming et al.; Lefohn et al.). Short-term exposure can cause respiratory and cardiovascular issues, aggravate asthma, and lead to increased hospital admissions. Long-term exposure is even more concerning, as it can contribute to chronic respiratory diseases like chronic obstructive pulmonary disease (COPD), lung cancer, and heart disease, and can even reduce life expectancy. Vulnerable populations such as children, the elderly, and individuals with preexisting health conditions are particularly at risk (Wang et al.).

The Megalopolis of the Valley of Mexico, which includes Mexico City and its surrounding metropolitan areas, is home to over 21 million people, making it one of the most densely populated regions in the country and the world. The region is situated in a high-altitude basin surrounded by mountains, which can trap pollutants and exacerbate air quality problems. and experiences frequent and severe air pollution episodes. This research aims to quantify the impact of ozone on mortality and short-term hospitalizations within this megalopolis. Simulating ozone concentrations using the regional chemical Weather Research and Forecasting (WRF) model coupled with Chemistry version 4.2.1.1.

Combining model outputs with health data from the Institute for Health Metrics and Evaluation (IHME), the research will estimate health effects using the Environmental Benefits Mapping and Analysis Program - Community Edition (BenMAP-CE). This study is crucial for understanding the public health implications of ozone pollution in one of the world's most populated urban areas. It will inform strategies to mitigate the health impacts of air pollution in the Valley of Mexico.

METHODS

Configuration of the regional chemical model

The WRF-Chem model version 4.2.1.1 was run for the Megalopolis of the Valley of Mexico using the T1-MOZCART chemical mechanism to obtain hourly ozone concentrations for the 3 months (Mach-May) with most contingency events in 2016 with and without the biomass burning emissions. The largest domain is centered at Lon=-98.941 and Lat=19.252, with 75 x 72 grid cells in the longitudinal and latitudinal directions, respectively, at a spatial resolution of 10 x 10 km. For the Megalopolis of the Valley of Mexico, a second domain was created with a spatial resolution of 2.5 x 2.5 km, encompassing 133 x 113 grid cells in the longitudinal and

latitudinal directions. The model will be run with 45 vertical levels from the surface to 50 hPa (Figure 1). Initial and boundary meteorological conditions were obtained from the European Centre for Medium-Range Weather Forecasts (ECMWF) ERA5 reanalysis. The main physical options used are based on previous studies in the same region (Table 1).

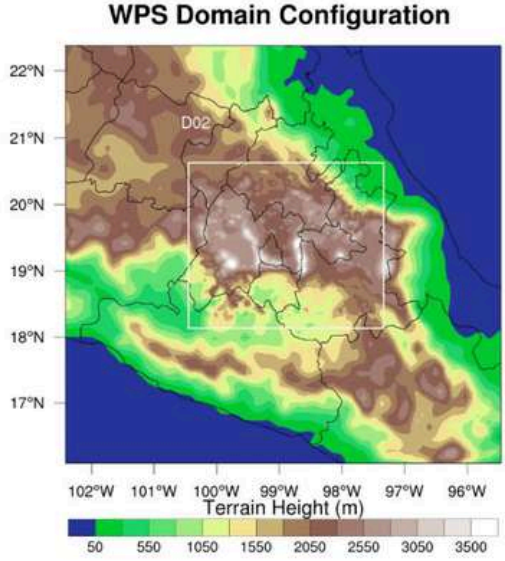


Figure 1. Selected domains for running the WRF-Chem simulations and the terrain height

Table 1. Configurations of the WRF-Chem

Attributes	WRF-Chem Option
Land surface model	Unified Noah land surface model
Microphysics	Thompson et al. scheme
Boundary layer scheme	Yonsei University scheme
Long wave radiation	RRTMG scheme
Short wave radiation	RRTMG shortwave scheme
Cumulus parameterization	Grell 3D Ensemble scheme
Surface layer	Monin-Obukhov
Photolysis scheme	Madronich F-TUV
Gas phase chemistry	T1-MOZCART

The land use/land cover was based on INEGI's land cover data at a resolution of 1 km. Anthropogenic emissions were sourced from the EDGAR-HTAP V3 (Emissions Database for Global Atmospheric) inventory. Biogenic emissions were incorporated through the Model of Emissions of Gases and Aerosols from Nature (MEGAN). Biomass burning emissions were obtained from the NCAR Fire Inventory Version 2.5 (FINN). Initial and lateral boundary conditions for atmospheric chemistry were taken from the CAM-chem dataset. Upper boundary conditions for chemical species were also utilized. Simulations were conducted monthly with a 10-day spin-up period for each month.

The simulations generated by the WRF-Chem model underwent validation utilizing data obtained from the atmospheric monitoring network of Mexico City (RAMA).

Health Effects

BenMAP-CE is a valuable tool for estimating the quantified number and economic valuation of health impacts associated with variations in air pollution concentrations. Our study focused on assessing these changes utilizing simulations derived from the WRF-Chem model, specifically targeting ozone concentration levels at the surface, both with and without biomass burning during environmental contingencies spanning from March to May 2016. Additionally, data from the Institute for Health Metrics and Evaluation (IHME) about the study region were incorporated into our analysis. Population data, a crucial component for BenMAP-CE calculations, were sourced from the National Institute of Statistics and Geography (INEGI) for 2016.

FINDINGS AND ARGUMENT

Model evaluation

We assess the performance of the WRF-Chem model in replicating regional hourly observational data for the month of April 2016. The hourly simulated values are spatially interpolated to match the locations of the monitoring station sites obtained from RAMA. Concurrently, the hourly observed values are aggregated and averaged over the entire month to compare with the simulated data comprehensively. This evaluation aims to gauge the model's ability to accurately represent the spatiotemporal variability of atmospheric constituents during the specified period.

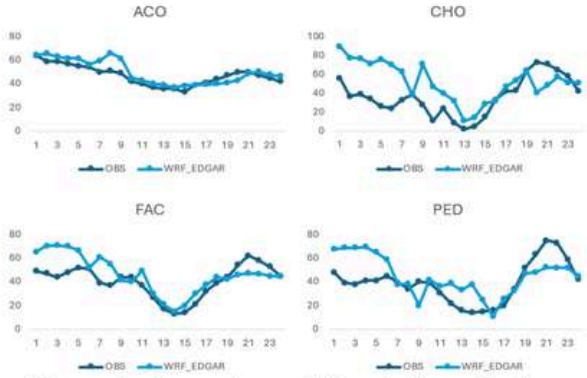


Figure 2. Comparison of Hourly Mean Surface Ozone Concentrations from Monitoring Sites

Overall, the WRF-Chem model demonstrates a strong capability to accurately simulate ozone concentrations across most monitoring sites within the Megalopolis region. It effectively captures the daily trends in ozone levels and generally aligns closely with observed data, typically within one standard deviation of the observations. Specifically, the model performs exceptionally well in replicating

ozone concentrations over Mexico City, particularly during the contingencies season, as depicted in Figure 2. This indicates the model's proficiency in capturing the complex dynamics of ozone formation and dispersion within urban environments, enhancing our understanding of air quality dynamics in the region.

Surface Ozone

Due to the high computational demands associated with running WRF-Chem simulations at such a fine spatial resolution, not all simulations have been completed at this time. Consequently, only preliminary results for the month of April 2016 will be presented in this study. In Figure 3, we display the 24-hour average ozone concentrations for the month of April within the second domain. These preliminary results provide an initial insight into the model's performance and the spatial distribution of ozone levels across the region, setting the stage for a more comprehensive analysis once all simulations are finalized. The detailed examination of these results will help to evaluate the effectiveness of WRF-Chem in capturing the intricate patterns of air pollution and its temporal variability in the Megalopolis of the Valley of Mexico.

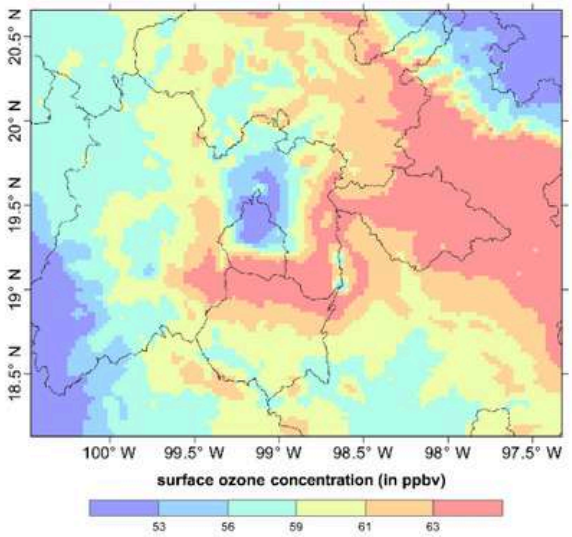


Figure 3. Average 24-hour surface ozone for April 2016

Figure 3 illustrates the distribution of population exposure to ozone (O3) across the Megalopolis of the Valley of Mexico. The highest levels of exposure are predominantly observed in the southern parts of the Megalopolis, particularly in Mexico City, the State of Mexico, and Morelos. This heightened exposure is primarily attributed to the increased emissions of O3 precursors in these areas, combined with prevailing wind patterns that facilitate the transport and concentration of ozone. These precursor emissions, originating from various anthropogenic activities such as vehicular traffic and industrial processes, interact with sunlight to produce ozone, leading to elevated levels that pose significant health risks to the local population.

CONCLUSIONS

The WRF-Chem model performed strongly in simulating ozone concentrations, accurately reflecting observed data from the RAMA network for April 2016. This validation confirms the model's reliability for air quality studies in the Megalopolis.
The highest ozone exposure levels were observed in the southern parts of the Megalopolis, particularly in Mexico City, the State of Mexico, and Morelos. These areas are characterized by significant emissions of ozone precursors, mainly from vehicular traffic and industrial activities.
Integrating simulated ozone data with health impact assessments using BenMAP-CE will highlight the severe health consequences of ozone pollution. This tool enabled the quantification of health impacts and the economic valuation of these effects, providing a comprehensive understanding of the public health burden associated with ozone exposure.

REFERENCES

Ebi, Kristie L., and Glenn McGregor. "Climate Change, Tropospheric Ozone and Particulate Matter, and Health Impacts." Environmental Health Perspectives, vol. 116, no. 11, 2008, pp. 1449–55, https://doi.org/10.1289/ehp.11463.

Fleming, Zoë L., et al. "Tropospheric Ozone Assessment Report: Present-Day Ozone Distribution and Trends Relevant to Human Health." Elementa, vol. 6, 2018, https://doi.org/10.1525/elementa.273.

Lefohn, Allen S., et al. "Tropospheric Ozone Assessment Report: Global Ozone Metrics for Climate Change, Human Health, and Crop/Ecosystem Research." Elementa, vol. 6, 2018, https://doi.org/10.1525/elementa.279.

Lelieveld, Jos, and Frank J. Dentener. "What Controls Tropospheric Ozone?" Journal of Geophysical Research Atmospheres, vol. 105, no. D3, 2000, pp. 3531–51, https://doi.org/10.1029/1999JD901011.

Manisalidis, Ioannis, et al. "Environmental and Health Impacts of Air Pollution: A Review." Frontiers in Public Health, vol. 8, Frontiers Media S.A., 20 Feb. 2020, https://doi.org/10.3389/fpubh.2020.00014.

Ramanathan, V., and Y. Feng. "Air Pollution, Greenhouse Gases and Climate Change: Global and Regional Perspectives." Atmospheric Environment, vol. 43, no. 1, 2009, pp. 37–50, https://doi.org/10.1016/j.atmosenv.2008.09.063.

Wang, Yuanlin, et al. "Health Impacts of Long-Term Ozone Exposure in China over 2013–2017." Environment International, vol. 144, 2020, p. 106030, https://doi.org/https://doi.org/10.1016/j.envint.2020.106030.

AIR POLLUTION CONFERENCE BRAZIL
CMAS SOUTH AMERICA
COMMUNITY MODELING AND ANALYSIS SYSTEM

DISPERSION STUDY OF NO_X AND NH_3 WITH THE AERMOD MODEL FOR A PRODUCTION PLANT OF GREEN HYDROGEN AN GREEN AMMONIA

Silvio de Oliveira[1], Oscar Alejandro Reyes Martinez[1],
[1] SECA Consultoria em Clima e Meio Ambiente; seca@seca-ambiental.com.br

Abstract: The present dispersion modeling study aimed to compose the Environmental Impact Study (EIS) of a green Hydrogen Plant to obtain the Prior Environmental License (LP). The present study aimed to evaluate the impact on air quality of NOX and NH3 emissions from a Green Hydrogen Plant Flare."Hydrogen (H_2)" is increasingly recognized as a clean and reliable energy vector for decarbonization and defossilization by various sectors, which is also called Green Hydrogen, whose development should meet the seventh goal of generating 'affordable energy' and clean' proposed by the United Nations. In Brazil, in Caucaia city, Ceará state, the first Green Hydrogen Production Plant should be installed, which will also be converted into Green Ammonia. The project's electrical energy demand will be supplied by solar and wind energy generation units available in the State of Ceará. For the production of green hydrogen, in addition to clean energy, the water component is necessary, which will be supplied by the direct capture of seawater extracted between 10 and 20 meters deep and subjected to a desalination process to obtain raw water, through the phenomenon of osmosis reverse, which uses the difference in osmotic pressure between salt water and pure water to remove salts, plus the use of other filters to obtain ultrapure water, called "permeated". The Green Hydrogen Production Plant will be designed according to the "zero vent" and "zero burn" philosophy during its normal operation. During its operation in emergency cases, the safety valve system will direct the gases produced in combustion to a safety burner that consists of a header dedicated to the Flare Stack flame, which has a pilot flame fed with natural gas. This flame, in contact with air, generates NO_X and NH_3 gases. The emission rates of these substances were estimated using the emission factors published in document AP-42, Compilation of Air Pollutant Emissions Factors, plus 3 years of hourly meteorological data for input into the AERMOD numerical model and obtaining the concentrations of NO_X and NH_3. The maximum concentration of 1h was 24 times lower than the hourly standard for NO2 under Brazilian legislation. The maximum concentration hourly of NH_3 was 28 times less than 1 digit, since Brazilian legislation did not define a standard for NH3. The simulation results demonstrated that the low concentrations of NO_X and NH_3 ensured the project's philosophy of generating clean energy without compromising the environment.

Keywords: Air quality, NO_X, nitrogen oxide, NH_3, ammonia, numerical modeling.

INTRODUCTION

Hydrogen is the most abundant element in the universe, and due to its reactivity, it only exists on earth in compounds such as water and organic materials. It is an odourless, flammable and colourless gas, which is leading to its safety concern, especially if a leak is not detected and gas collects in a confined area; it can ultimately ignite and causes explosions, Wood Group (2022). The higher heating value (HHV) of hydrogen is 141.8 MJ/kg at 298 K, and the lower heating value is 120 MJ/kg at the same temperature. This is significantly higher than that of most fuels such as gasoline with a value of 44 MJ/kg at 298 K. However, liquid hydrogen has a lower energy density by volume than hydrocarbon fuels such as gasoline by a factor of four with a density of 8 MJ/l versus density of 32 MJ/l. While hydrogen gas has a high energy density by weight but a low energy density by volume compared to hydrocarbons, it requires a larger tank to store. Green hydrogen is produced using renewable energy sources such as solar or wind energy, followed by water electrolysis. Water is typically purified and then sent to an electrolyser, which produces hydrogen and oxygen. The hydrogen is then dried, purified and compressed from a 10.3 to 413.7 bar pressure, and then stored in a tank. Hydrogen development must also meet the United Nations' seventh 'affordable and clean energy' target. The ammonia synthesis process is promoted by the catalytic reaction between hydrogen and nitrogen elements through the Haber process (Arora et al. 2018). The present study aimed to evaluate the impact on air quality of NO_X and NH_3 emissions from a Green Hydrogen Plant Flare.

METHODS

The methodology consisted of a general assessment of the site area of the green hydrogen industrial unit considering : topography analysis, estimation of NOX and NH3 emission rates from a Flare, analysis of 3 years of hourly meteorological data to produce the files for the AERMOD model and calculate NO_X and NH_3 concentrations. The planned location for installing the project is in the municipality of Caucaia, Ceará State, at the geographic coordinates of Latitude 3° 37´ 22.11" S and Longitude 38° 50´ 14.43" W, the average annual temperature varies between 26.6°C and 30.4°C, The prevailing winds blow from the east and east-southeast directions Caucaia Climate data (2016). The altitude of the municipality varies between 19m and 21m, therefore almost flat with few irregularities in the terrain that should not obstruct the path of the natural wind flow at atmospheric dispersion. as shown in Figure 1, Wood Group Map (2022).

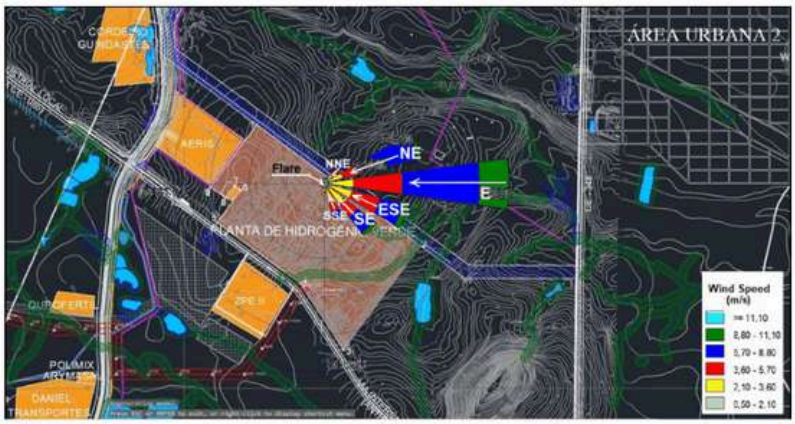


Figure 1. Wind Rose over the future location of the Hydrogen plant Wood Group Map (2022).

FINDINGS AND ARGUMENT

The AERMODView Gaussian model was used to calculate NO_X and NH_3 concentrations, Thé(2022). The Cartesian grid was centered at the coordinates of The hourly meteorological data were obtained from Fortaleza airport, located 16 km from Caucaia, for the period from January 1, 2020 to December 31, 2022, which were processed in the AERMET preprocessor, to produce the input files in the AERMOD model, for calculating pollutant concentrations. The Green Hydrogen Production Plant will be designed according to the philosophy of "zero vent" and "zero flaring" during normal operation. But, in cases of emergencies, the control system and/or safety valves will direct the residual gases produced to the safe burning system or Flare Stack, connected to the pressure relief systems located in the current separation vessels 1 of the Gas stream. and Liquid 7, operational technical details of the Flare Stack are found in Stack Flare (2022). Table 1 presents the technical characteristics of fluid streams 1 and 7. Stream 1 will be directed to burning in the Flare and has a natural gas flow rate equal to 65 Nm3/h (composed of 93% volumetric fraction of CH_4 and 7% of N_2. Fluid stream 7 (Flash gas), which will also be directed to burning in the Flare with a flow rate equal to 1190 Nm^3/h, and this stream will not be affected by combustion due to the low concentration of ammonia that varies between 50 and 100 ppm. in Flare. Therefore, as stream 7 contains the presence of residual NH_3 gas, it will be necessary to calculate the emission rate of this gas for atmospheric dispersion analysis.

Table 1 - Parameters of gas streams1 and 7, gas emissions, and Normal Flows.

Gas Stream	Emission source	Gaseous emissions	Operation mode	Time	Normal Flow (Nm^3/h)
1	Flare pilot burner	Hydrogen, H_2	Normal	Continuous	65
7	Flash Gas for Flare	Flash Gas	Normal	Continuous	1.190

Reference - Wood Group (2022) - Engineering and Production Facilities Brazil.

Table 2 presents the physical and quantitative parameters that were used to calculate the NO_X and NH_3 emission rate, as well as the effective flame height in the flare, which is defined by the physical height of the stack plus the flame rises. The calculation of the effective height of the flare stack was carried out using formula 2 *Beychok, M.R. (2005).*

$$h_{sl} = h_s + (4.56 \times 10^{-3}) \left({}^{(1-f)}/_{4.1868}\right) H)^{0.478} \ (metros) + \Delta h, \qquad (2)$$

Table 2. Presents the physical-chemical parameters for calculating NO_X and NH_3.

Item	Parameters	Units	Values
1	Heat release rate	MW	14.94
2	Heat loss fraction	-	0.00
3	Enthalpy of methane used	kJ/mol	890.40
4	Flame temperature	°C [default]	1000.00
5	Chimney outlet velocity	m/s [default]	20.00
6	Exhaust flow in the chimney	Nm^3/h	14.40
7	NOX emission factor (as NO_2)	lb/mmBtu	0.068
8	Composition of Natural Gas - CH_4	%	93.00
9	Composition of Natural Gas - N_2	%	7.00

Reference: Wood Group (2022) - Engineering and Production Facilities Brazil.

The burning of post-combustion gases CH_4=0.00 [v/v(%)]; O_2 = 0.00 [v/v(%)]; N_2 = 72.00 [v/v(%)]; CO_2 = 9.00 [v/v(%)]; NO_2 = 0.00000533 [v/v(%)]; H_2O = [19.00 v/v(%)]; form in the Flare's pilot flame. Understanding that the natural gas that keeps the pilot flame lit has 93% methane gas in its composition. In calculating the Emission Rate, ET, the formula ET[NO_X] = [EF].[Ec.1] was used, where the Emission Factor [EF] = 0.068[lb/MBTU],

RTI International (2015), substituting the data in these formulas resulted in a NOx emission rate equal to 20.90[g/s]. When calculating the NH_3 Emission Rate in the flash gas of Stream 7, the formula was used: TE[NH_3] = C [NH_3].Vgfhash and the result of TE [NH_3] was equal to 0.193[g/s]. Using emission rates, meteorological data and topography in the AERMOD model, NO_X and NH_3 concentrations were estimated. Table 4 presents the results of the maximum hourly NO_X concentration equal to 11.0 [$\mu g/m^3$], which represents 4.2% of the CONAMA 491/2018 NO_2 Standard of 260 [$\mu g/m^3$]. The maximum hourly concentration of NH_3 was equal to 0.036[$\mu g/m^3$]. Brazilian legislation has not defined a standard for NH_3. Figures 4.1 and 4.2 present maps of NO_X and NH_3 isoconcentrations, where it is observed that the concentrations of NO_X and NH_3 decrease radially with distance as they move away from the point of maximum concentration, tending towards zero.

Table 4 - Maximum concentration of NO_X and NH_3 resulting from dispersion modeling with AERMOD.

Source/pollutant	Average Time	Maximum Concentration			NO_2 Standard CONAMA 491/2018
		$\mu g/m^3$	Maximum location		
			Local	Coordinates	($\mu g/m^3$)
Flare Stack (NO_X)	1 hour	11.0	To the west, 3.5km away from Flare	X = 512676 Y = 9599386	260
Flare Stack (NH_3)	1 hour	0.036	To the west 1.0 km away	X = 516728 Y = 9599247	Undefined

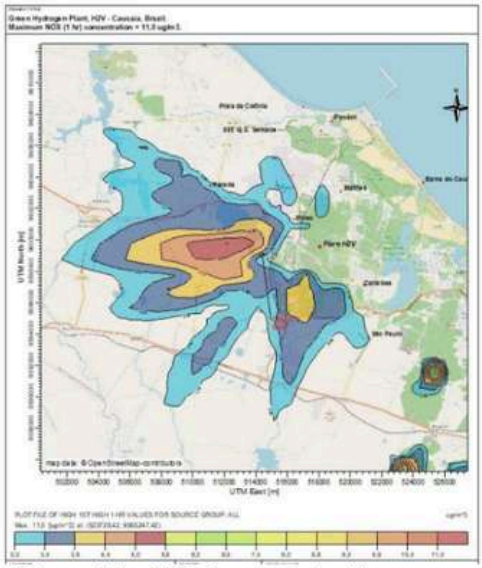


Figure 4.1 - NO_X isoconcentrations map.

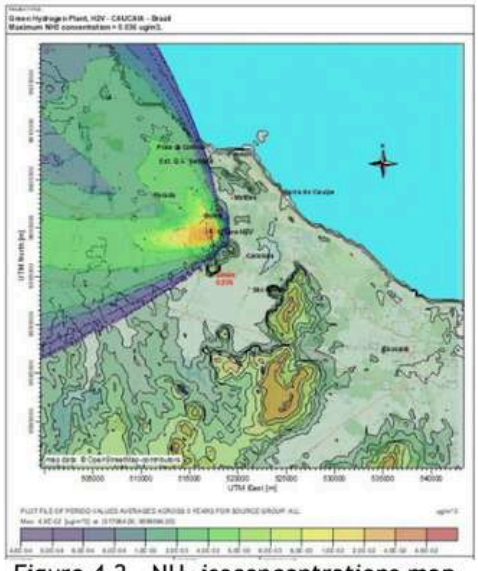


Figure 4.2 - NH_3 isoconcentrations map.

CONCLUSIONS

The present study aimed to evaluate the impact on air quality of NO_X and NH_3 emissions from a Green Hydrogen Plant Flare. The hydrogen production factory is made up of hermetically sealed hydrogen and ammonia production modules and the waste produced is sent to be burned in the flame of a flare. The flare stack dispersion study showed that the maximum 1-hour concentration was 24 times lower than the hourly NO_2 standard under Brazilian legislation. The maximum concentration hourly of NH_3 was 28 times less than 1 digit, since Brazilian legislation did not define a standard for NH_3. The results of atmospheric dispersion modeling demonstrated that low concentrations of NO_X and NH_3 guaranteed the project philosophy of generating clean energy without impacting the environment.

REFERENCES

Arora P et al (2018) Remote, small-scale, 'greener' routes of ammonia production. J Clean Prod 199:177-192. https://doi.org/10.1016/j.jclepro.2018.06.130.
Beychok, M.R. (2005), "Fundamentals of Stack Gas Dispersion", 4th edition, Beychok, Newport Beach, CA.
Clima: Caucaia. Climate Data. Consultado em 19 de maio de 2016. https://pt.climate-data.org/location/42582
CONAMA, Resolução (2018) nº 491, *Diário Oficial da União - Seção 1, Nº. 223, de 21 de novembro 2018*
RTI International (2015). https://annualreport.rti.org/2015/index.html
Stack Flare (2022) Versatile Business by Firely Themes. https://freeoil.ind.br/flare/Versatile.
Thé, J. L., and et al., User's Guide ISC-AERMOD View Version 11.2.0, Windows Interface for the USEPA. Lakes Environmental Software, Volume I, 2022.
USGS, 2006a, *Shuttle Radar Topography Mission (SRTM) "Finished" 3-arc second SRTM Format Documentation, Available online at*: http://edc.usgs.gov/products/elevation/srtmbil.html (accessed 01/08/2022).
Wood Group (2022) - Engineering and Production Facilities Brazil.

AIR POLLUTION CONFERENCE BRAZIL
CMAS SOUTH AMERICA
COMMUNITY MODELING AND ANALYSIS SYSTEM

TRENDS IN NITROGEN OXIDES AND OZONE CONCENTRATIONS AND THEIR RELATIONSHIPS WITH GLOBAL SOLAR RADIATION AND TEMPERATURE

Erick M. Delgado Moya[1], Marco A. Franco[2], Simone Andréa Pozza[3], Diego Samuel Rodrigues[3]
[1]*Pós-Doutorado Estratégico PDPG-CAPES, Programa de Pós-Graduação em Tecnologia, UNICAMP*
erickmat@unicamp.br
[2]*Departamento de Ciências Atmosféricas, IAG-USP*
marco.franco@usp.br
[3]*FT-UNICAMP*
simone.pozza@ft.unicamp.br / diego.rodrigues@ft.unicamp.br

Abstract: This study evaluated the correlations between the O_3, NO and NO_2 concentrations with the global solar radiation (RADG) and temperature (TEMP). In addition, the correlation of these quantities was also obtained for pairs of close monitoring stations in the same municipality. We used data from QUALAR-CETESB for NO, NO_2, and O_3 concentrations, global solar radiation, and temperature for the period from 01/01/2018 to 31/07/2023, measured in 18 monitoring stations in the state of São Paulo. We aim to trend and quantify all the correlations between NO, NO_2, O_3, RADG, and TEMP concentrations. Methodologically, the correlations between the variables of interest (NO, NO_2, O_3, RADG, TEMP) were analyzed by calculating the Pearson correlation coefficient (r). In cases where a very weak correlation was found ($|r| < 0.1$) or the Pearson correlation was not statistically significant (i.e., p-value > 0.05), we also calculated the Kendall and Spearman correlation coefficients to account for possible nonlinearities. The Pearson correlations between O_3-TEMP, O_3-RADG, TEMP-RADG, and NO-NO_2 were observed to be positive-moderate to strong. The Pearson correlations between NO-O_3, NO-TEMP, NO-RADG, NO_2-O_3, NO_2-RADG, and NO_2-TEMP were all negative-weak to moderate. In the case of NO_2-TEMP, we observed 3 cases where the Pearson correlation was not significant, and then we proceeded with Kendall and Spearman correlation analysis, resulting in values with statistical significance but very weak (< 0.1). Regarding Pearson's correlations for the same variable observed in pairs of close stations, all of the three pairs of stations studied were classified as strongly positive, except for NO in Santos, for which, due to the lack of Pearson correlation, Kendall and Spearman correlations were 0.660 and 0.795, respectively. The reported results are consistent with what is expected from the tropospheric ozone cycle. They also suggest different atmospheric processes occur at different observation sites.

Keywords: air pollutants, tropospheric ozone cycle, temperature, solar radiation, correlation analysis.

INTRODUCTION

Urban air pollution is the result of several activities, both natural and anthropogenic. The primary pollutant, nitrogen oxide (NO), oxidizes to nitrogen dioxide (NO_2). NO_2 is emitted as NO_x (= NO + NO_2), the main sources of which are urban fossil fuel combustion, mainly from vehicle emissions and affects human health, the ecosystem, and the climate (Sharma et al., 2023). Tropospheric ozone (O_3) formation is a consequence of the photodissociation of nitrogen dioxide (NO_2) by sunlight. Intense solar radiation, high temperature, and other factors can influence O3 levels, which has effects on ecosystems and human health and is even considered a greenhouse gas (de Oliveira et al., 2021).

This work aims to study the relationships between NO, NO_2, and O_3 with global radiation (RADG) and temperature (TEMP) using Pearson's correlation as the main strategy and, in some cases, Kendall and Spearman correlations with pollution data provided by CETESB (Environmental Agency of the State of São Paulo).

METHODS

The methodology is aimed at the statistical correlations between NO, NO_2, O_3, RADG, and TEMP. We used data provided by CETESB at QUALAR (https://cetesb.sp.gov.br/ar/qualar) for the period spanning from 01/01/2018 to 31/07/2023, with a total of 48,913 hours monitored at 18 stations in the state of São Paulo: Campinas-Taquaral, Campinas-Vila União, Capão Redondo, Carapicuíba, Catanduva, Guaratinguetá, Guarulhos-Paço Municipal, Guarulhos-Pimentas, Limeira, Marília, Parque D. Pedro II, Paulínia, Ribeirão Preto, São Bernardo-Centro, São José dos Campos-Jardim Satélite, Santos, Santos-Ponta da Praia, and Taubaté.

For correlation analysis, we firstly used Person's correlation (r) (Sedgwick, 2012; El-Hashash and Raga Hassan, 2022). The r correlation was classified as weak ($|r| < 0.3$), moderate ($0.3 \leq |r| < 0.5$), and strong ($|r| \geq 0.5$). For each correlation, we also compute the 95% confidence interval aimed at constructing a maximum interval for correlations (MIC). Pearson's correlation was considered statistically significant for the p-value < 0.05 (Sedgwick, 2012; El-Hashash and Raga Hassan, 2022). In these particular cases, we used the Kendall and Spearman correlations to assess the existence of a non-linear correlation (Taylor, 1987; El-Hashash and Raga Hassan, 2022).

FINDINGS AND ARGUMENT

The Pearson correlations between NO-NO_2 were positive for all the studied stations, and classified as strong in 15 of 18 stations. The other 3 stations had a moderate Pearson correlation. The station with the lowest correlation was Paulínia, with r = 0.466. In contrast, the highest correlation was observed for Catanduva (0.972), followed by Guarulhos-Paço Municipal (0.690). Considering the confidence intervals, the maximum interval of correlations (MIC) for all stations was [0.457; 1].

The correlations for the pair NO-O_3 were always negative for all stations, showing the production-consumption relationship between the variables. In 14 stations, r was classified as negatively moderate. The highest anticorrelation was found at Santos-Ponta da Praia with r = -0.605 and the lowest at Campinas Taquaral with -0.263. MIC: [-0.611; -0.253].

The correlations between NO-RADG were weak and negative for all the 18 stations studied. On average, the Pearson coefficient was -0.079. MIC: [-0.238; -0.009].

The correlations between NO-TEMP were negative in all stations, for which 15 stations presented a weak r, and 3 of them a moderate r. The highest anticorrelation was found in Riberão Preto, with r = -0.376, and the lowest in Marilía, with r = -0.068. MIC: [-0.385, -0.058].

The correlations between NO_2-O_3 resulted to be always negative for all stations, with a strong r in 7 stations, a moderate r in 7 stations, and weak in 2 stations, also showing the production-consumption relationship between the variables. The highest anticorrelation was obtained in Santos-Ponta da Praia, with r = -0.670, and the lowest in Marilia, with r = -0.212 (weak). MIC: [-0.675; -0.202].

The correlations of NO_2-RADG were always negative in all the stations, being classified as moderate in 10 stations, and weak in 8 stations. The highest anticorrelation was obtained for the Ribeirão Preto station, with r = -0.433. MIC: [-0.442; -0.089].

For the pair NO_2-TEMP, the correlations were negative, where 5 stations had moderate correlations and 10 stations had weak correlations. The highest anticorrelation was found for Taubaté, with r = -0.385. The lowest anticorrelation was obtained for Capão Redondo, with r = - 0.128, and the correlation interval was [-0.391; -0.107]. Still, regarding the pair NO_2-TEMP, only 3 stations (Marília, Parque Dom Pedro II, and São Bernardo-Centro) showed a p-value > 0.05, with no statistical significance. We studied the Kendall and Spearman correlations for these stations to account for non-linear effects. All the results were significant: for Marilia, the Kendall correlation was 0.001, and the Spearman correlation was 0.011. For Parque Dom Pedro II, the Kendall and Spearman correlations were 0.011 and 0.012, respectively. Finally, for São Bernardo-Centro, the Kendall and Spearman correlations were 0.025 and 0.037, respectively. As shown, the Kendall and Spearman correlations were weak and positive in contrast to the Pearson correlations, which were weak and negative (for Marilia; -0.006, for Parque Dom Pedro II, 0.002; for São Bernardo-Centro, -0.008).

All the Pearson correlations between O_3-RADG were positive and were observed to be strong in 16 stations and moderate in 2 stations. The highest correlation was obtained for Guarulhos-Pimentas, with r = 0.659, and the lowest r was obtained for Marilia, with r = 0.448. MCI: [0.437; 0.673].

The Pearson correlations between O_3-TEMP were positive and strong in 16 stations and moderate in 2 stations. The station with the highest correlation was Limeira, with r = 0.774, and the lowest was Santos-Ponta da Praia, with r = 0.483. MIC: [0.475; 0.779].

The Pearson correlations between RADG-TEMP were positive and strong in all the stations studied. The station with the highest correlation was Taubaté, with r = 0.625, and the lowest was Paulínia, with r = 0.587. MIC: [0.580; 0.631].

Table 1 summarizes the aforementioned results for the average Pearson correlations with the respective number of stations involved.

In addition to the previous analysis, the correlation between the same variable measured in pairs of close monitoring stations in the same municipality is also addressed. For this, the availability of data exists only for the stations in Campinas, Guarulhos, and Santos, as presented in Table 2 and discussed in the sequel.

Table 1. Average values of the Pearson's correlations for each of the referred pairs of variables (NO, NO_2, O_3, RADG, TEMP) within the respective number of stations.

Variable	NO_2	O_3	RADG	TEMP
NO	+ 0.585 (18 stations, all)	- 0.375 (18 stations, all)	- 0.079 (18 stations, all)	- 0.232 (18 stations, all)
NO_2	-	- 0.455	- 0.277	- 0.246

		(18 stations, all)	(18 stations, all)	(15 stations, 83%)
O_3	-	-	+ 0.574 (18 stations, all)	+ 0.636 (18 stations, all)
RADG	-	-	-	+ 0.589 (18 stations, all)

Considering the Campinas-V. União and Campinas-Taquaral station, the Pearson correlations of NO, NO_2, O_3, RADG, and TEMP all are positive and strong. The strongest Pearson correlation was for TEMP, with 0.974. For NO, NO_2, O_3, and RADG, we obtained 0.703, 0.891, 0.912, and 0.932, respectively.

For the Guarulhos-Pimentas and Guarulhos-Paço Municipal stations, TEMP also showed the strongest Pearson correlation with 0.986, and NO, NO_2, O_3, and RADG were 0.658, 0.842, 0.908 and 0.909, respectively.

The Pearson correlations for the Santos and Santos-Ponta da Praia stations for NO_2, O_3, RADG, and TEMP were positive and strong: 0.842, 0.921, 0.937, and 0.987, respectively. For NO, the correlation was negative and weak. In this case, we investigated the existence of a non-linear correlation using Kendall and Spearman correlations. For Kendall, such a correlation is 0.660, and for Spearman, it is 0.795, resulting in a positive and strong non-linear correlation between these stations for NO.

Table 2. Pearson's correlations for the same variable measured in different stations in the same municipality.

Variables	Campinas (Vila União/ Taquaral)	Guarulhos (Pimentas/ Paço Municipal)	Santos (Santos/ Ponta da Praia)
NO	+ 0.703	+ 0.658	- 0.272
NO_2	+ 0.890	+ 0.842	+ 0.841
O_3	+ 0.911	+ 0.908	+ 0.921
RADG	+ 0.930	+ 0.937	+ 0.909
TEMP	+ 0.974	+ 0.986	+ 0.987

CONCLUSIONS

In the study of the 18 CETESB stations in the selected time, we found that the Pearson correlations of O_3-TEMP, O_3-RADG, TEMP-RADG, and NO-NO_2 are positive, moderate and strong. Therefore, days with higher temperatures and higher solar radiation will have higher O_3 concentration, and an increase in NO concentration will also imply an increase in NO_2 concentration (Marco, 2022). The Pearson correlations for NO-O_3, NO-TEMP, NO-RADG, NO_2-O_3, NO-RADG, and NO_2-TEMP are all negative, moderate, and weak on average. In the case of NO_2-TEMP, we have 3 stations where the Pearson correlation is not significant, and we tested with Kendall and Spearman correlations that it was significant but very weak (<0.1).

In the study of the pairs stations in Campinas, Santos, and Guarulhos, the Pearson correlations for NO_2, O_3, RADG, and TEMP were positive and strong. In the case of NO, it was positive and strong for the stations in Campinas and Guarulhos but negative and moderate for Santos. For NO in Santos, we studied Kendall and Spearman correlations and obtained that it was strong but less than for the other variables.

ACKNOWLEDGMENTS

EMDM and DSR thank PDPG-CAPES for the postdoctoral scholarship funding of EMDM. MAF acknowledges FAPESP, São Paulo Research Foundation (#2016/18438-0) and CNPq (#07752/2023-4) for the research grants.

REFERENCES

Sedgwick, Philip. "Pearson's correlation coefficient." *BMJ* 345 (2012): e4483. doi:10.1136/bmj.e4483

El-Hashash, Essam F. and Ali Shiekh, Raga Hassan. "A Comparison of the Pearson, Spearman Rank and Kendall Tau Correlation Coefficients Using Quantitative Variables." *Asian Journal of Probability and Statistics.* 20(3): 36-48, 2022. doi:10.9734/ajpas/2022/v20i3425

Taylor, Jeremy M. G. "Kendall's and Spearman's Correlation Coefficients in the Presence of a Blocking Variable." *Biometrics.* 43(2): 409-416, 1987. doi:10.2307/2531822

de Oliveira, R. C. G., Cunha, C. L., Tôrres, A. R., and Corrêa, S. M. (2021). Forecasts of tropospheric ozone in the Metropolitan Area of Rio de Janeiro based on missing data imputation and multivariate calibration techniques. Environmental Monitoring and Assessment, 193(8). doi:10.1007/s10661-021-09333-2

Sharma, B. R., Kuttippurath, J., Gopikrishnan, G. S., and Pathak, M. (2023). Trends in atmospheric pollution in the Third Pole: analyses of tropospheric NO2 for the period 2005-2020. Environmental Science: Atmospheres. doi:10.1039/d2ea00075j.

PROCEEDINGS OF THE

2024 AIR POLLUTION CONFERENCE

And 5th CMAS South America

SESSION 02
Air Pollution Control

Air Pollution Control is an important area for the air pollution issue aiming to reduce or eliminate the emission into the atmosphere of substances that can affect the air quality. The performance of the techniques used to control the emissions must be effective in order to achieve the legal limitations imposed by the country or states government for the protection of the environment and public health. Therefore, with the increase of the restrictions of emission, the Research for efficiency improvements of these techniques is a very important subject. Also it is crucial to develop technologies with low Capital and Operational costs. This session is about the studies dedicated to the Air Pollution Control innovative techniques to control the emissions of particulate and gases. This session topics include:

- Particulate Control
- SOx Control
- NOx Control
- Acid Gas Control
- Dioxin and Furan Control
- Mercury Control
- VOC Control

SESSION 2

AIR POLLUTION DURING COVID-19 IN A MID-SIZED INDUSTRIAL CITY IN SOUTHERN BRAZIL: FROM ONSET TO POST-PANDEMIC 55

THE IMPACT OF PUBLIC POLICIES ON AIR QUALITY: A CASE STUDY IN THE METROPOLITAN AREA OF SÃO PAULO 58

OPTIMIZING INDUSTRIAL SITE MANAGEMENT: CFD SIMULATIONS AND ENVIRONMENTAL IMPACT ASSESSMENT OF WIND EROSION FROM STOCKPILES 61

COMPUTATIONAL FLUID DYNAMICS INVESTIGATION ON PARTICULATE MATTER EMISSION FROM ROADS, GRANULAR MATERIAL STORAGE AND HANDLING 64

NON-ERODIBLE PARTICLES EFFECTS IN TURBULENT STRUCTURES DEVELOPMENT: ON THE ROLE OF PARTICLE SHAPE INFLUENCE 67

ARTIFICIAL BARRIERS APPLIED TO AEOLIAN EROSION CONTROL: EVALUATION OF POROSITY AND TURBULENT MODELS ON FRICTION VELOCITY REDUCTION 70

INFLUENCE OF FILTER MEDIA MANUFACTURING METHOD ON THE FILTRATION PERFORMANCE OF BAG FILTERS 73

CFD ANALYSIS OF THE EFFICIENCY OF A CANOPY HOOD FOR HOT PROCESSES 76

FLOW BEHAVIOR INSIDE BAG FILTERS: A REVIEW OF EXPERIMENTAL STUDIES 79

CASE STUDY: LOW NOX BURNER İN A PELLETİZİNG PLANT 82

STUDY ON HIGH CONCENTRATION OF PM10 AND PLANETARY BOUNDARY LAYER STRUCTURE AT THE PORT OF PORTO ALEGRE - RS IN 2022 85

COMPARATİVE ANALYSİS OF CONTİNUOUS AND PERİODİC MONİTORİNG METHODS İN CEMENT PLANTS: A CASE STUDY İN THE STATE OF RİO DE JANEİRO 88

A COMPARATIVE AANALYSIS OF AIR QUALITY SCENARIOS IN BRAZIL FOR 2050 USING WRF-CHEM 91

CFD SIMULATION OF THE GAS FLOW DISTRIBUTION INSIDE AN INDUSTRIAL BAG FILTER 94

SESSION 2

IN SITU DESULFURIZATION OF BRAZILIAN COAL COMBUSTION USING DIFFERENT LIMESTONES IN A BUBBLING FLUIDIZED BED BENCH SCALE 97

ANALYSIS OF THE TEMPERATURE VARIATION AND Ca/S RATIO IN THE DESSULFURIZATION OF BRAZILIAN COAL IN A BUBBLING FLUIDIZED BED COMBUSTOR 100

POLYMER DUST SUPRESSANT PRODUCED FROM POLYETHYLENE TEREPHTHALATE (PET) AND ITS APPLICATIONS 103

IMPACT OF VEGETATION COVER ON THE CONCENTRATION OF CARBON DIOXIDE IN THE METROPOLITAN AREA OF SÃO PAULO 106

ANALYSIS OF THE TEMPERATURE VARIATION AND Ca/S RATIO IN THE DESSULFURIZATION OF BRAZILIAN COAL IN A BUBBLING FLUIDIZED BED COMBUSTOR 109

AIR POLLUTION CONFERENCE BRAZIL
CMAS SOUTH AMERICA
COMMUNITY MODELING AND ANALYSIS SYSTEM

AIR POLLUTION DURING COVID-19 IN A MID-SIZED INDUSTRIAL CITY IN SOUTHERN BRAZIL: FROM ONSET TO POST-PANDEMIC

Ronan Adler Tavella[1], Flavio Manoel Rodrigues da Silva Júnior [2]
[1] *Universidade Federal do Rio Grande e Universidade Federal de São Paulo*
ronan.adler@unifesp.br
[2] Universidade Federal do Rio Grande
f.m.r.silvajunior@gmail.com

Abstract: Our study assessed atmospheric pollutant levels (O_3, $PM_{2.5}$ and PM_{10}) in Rio Grande during and after the COVID-19 pandemic. Investigating how the restrictive measures adopted in the city affected the levels of these pollutants. Concurrently, we examined different parameters such as the weekend effect compared to the Controlled Distancing Model adopted by the state of Rio Grande do Sul in the city and the Interruption-Recovery pattern of these pollutants. Our findings revealed that Rio Grande experienced a significant decrease in ozone levels (up to 66% below average), alongside decreases in particulate matter in the first stages of the pandemic. Levels remained below usual until early 2021, coinciding with the end of state-imposed restrictions. Weekend effects shifted based on restriction stringency, with higher positive intensities observed during stricter measures, indicating non-compliance of restriction measures, by the population, during weekends. The Interruption-Recovery pattern showed a gradual return to usual pollutant levels by 2022. This investigation highlights the complex impact of the COVID-19 pandemic on air quality and offers guidance for future air quality control strategies and policies in similar contexts.

Keywords: Air quality, Interruption-recovery pattern, Machine learning, Particulate matter, Weekend effect.

INTRODUCTION

To curb the dissemination of coronavirus disease 2019 (COVID-19), nations worldwide implemented restriction measures that severely limited personal mobility. While these measures aimed primarily to flatten the COVID-19 infection curve and alleviate strain on healthcare systems, they created a unique test bed to assess the effect of anthropogenic activities on air pollution (Diffenbaugh et al. 2020).

However, despite this unique test bed, research in this topic has predominantly focused on large cities and metropolises, with limited investigations into small and medium-sized cities (Tavella and da Silva Júnior, 2021). This study addresses this gap, by investigating air pollution in Rio Grande, a medium-sized city in southern Brazil.

In this sense, our investigation sought to assess the levels of different atmospheric pollutants (O_3, $PM_{2.5}$ and PM_{10}) during and after the COVID-19 period in Rio Grande. Understanding how the restrictive measures adopted in the city affected the levels and behavior of these pollutants.

METHODS

Study Area and Monitoring Period

The study was conducted in the city of Rio Grande, a medium-sized city located in Rio Grande do Sul, Brazil (Figure 1). Rio Grande is home to approximately 200,000 inhabitants and serves as a significant industrial hub in the state. Due to its industrial activities, atmospheric pollutant levels in Rio Grande rank second only to the metropolitan region of the state.

Monitoring was conducted monthly from April 2020 to December 2022, encompassing the entire period during which social distancing measures recommended by the state government of Rio Grande do Sul were in effect. Notably, the primary restriction measures were implemented until the end of 2020, with subsequent relaxation in early 2021.

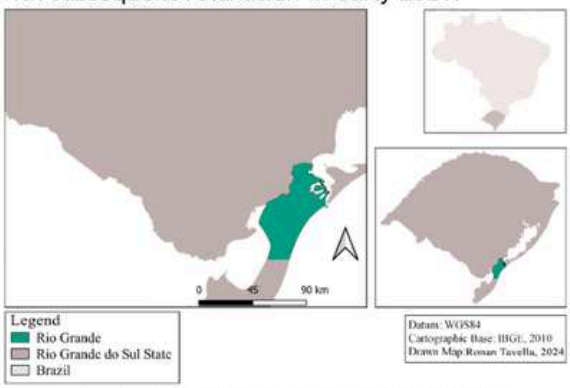


Figure 1. Location of Rio Grande city.

Controle Distance Model (MDC)

The MDC was a statewide policy implemented by the government of Rio Grande do Sul to prevent and manage the spread of COVID-19. This system classified regions of the state into four risk levels using "flags" as indicators (Figure 2). The color of the flags corresponded to the severity of the COVID-19 situation in a region, determined through weekly analysis of 11 health indicators. These indicators considered both the capacity of the health system and the rate of virus transmission. Stricter measures were imposed as the flag color intensified. The rigor of the measures increased as the flag's tone darkened.

Data Sampling

Sampling for this study involved two distinct approaches conducted at different stages of the CO-

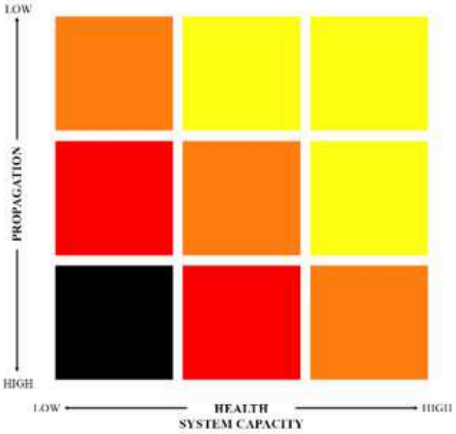


Figure 2. Criteria used by the MDC to determine the color of the flags

VID-19 pandemic: (1) Passive sampling of O_3 during the initial week of restriction measures in the city, in April 2020; and (2) Remote sensing sampling of the three atmospheric pollutants (O_3, $PM_{2.5}$, and PM_{10}) throughout the study period.

Passive sampling of O_3 measurements followed the method outlined by stablished methodology, where cellulose filters (37 mm) were used as diffusive surfaces in samplers placed on lampposts at a height of 2 meters. More information in Tavella et al. (2022).

Levels of O_3, $PM_{2.5}$ and PM_{10} obtained through remote sensing were derived from satellite data provided by the Copernicus Atmospheric Monitoring Service (CAMS) of the European Centre for Medium-Range Weather Forecasts (ECMWF) and real-time data manually retrieved from The Weather Channel app (IBM, USA). The unit of measurement adopted for all pollutants was $\mu g/m^3$.

Meteorological data for the city, including temperature, humidity, precipitation, wind speed, and atmospheric pressure, was obtained from the Brazilian National Institute of Meteorology (INMET).

Data analysis

The data was analyzed considering (1) passive sampling of O_3 at the onset of restriction measures, (2) the weekend effect of air pollutants concerning the MDC flags adopted in the city, and (3) the behavior of air pollutant levels during and after pandemic restriction measures compared to expected levels in predictive scenarios evaluated using machine learning.

The passive O_3 measurements were statistically compared to historical levels before the restrictive measures in Rio Grande. The weekend effect analysis followed the equation used by Tavella et al. (2023), calculating the average air pollutant concentration for weekends and weekdays to determine the weekend-weekday difference.

Annual mean and median concentrations for each pollutant were calculated based on observed data from the three-year study period. Expected data for 2021 and 2022 were estimated using a machine learning model.

A Support Vector Machine model, as described by da Tavella and da Silva Júnior (2023), was employed for machine learning. The model utilized observed meteorological and pollutant data from April to December 2020 as the training sample, while actual meteorological data from January 2021 to December 2022 was used as the test sample to estimate pollutant concentrations in a scenario with restricted urban mobility. The continuous dependent variables were the concentrations of the individual air pollutants, and the predictor variables were the meteorological parameters. Monthly concentrations of observed and expected pollutant values for 2021 and 2022 were plotted to compare their behavior.

FINDINGS AND ARGUMENT

Our study uncovered several findings regarding the impact of COVID-19 restriction measures on air pollution levels in Rio Grande, Brazil. Emphazis on the four main results are outlined below.

Firstly, contrary to the observed increase in O_3 levels reported in many large cities and metropolises during the early stages of restriction measures, Rio Grande exhibited a consistent decrease in O_3 levels. Passive sampling data indicated a significant reduction of up to 66% below the average for the period, a trend corroborated by satellite data. Additionally, reductions in $PM_{2.5}$ and PM_{10} levels, approximately 33% and 21% respectively, were observed through satellite data.

Secondly, our investigation into the weekend effect under the MDC revealed intriguing patterns. In scenarios characterized by less restrictive policies, we observed a negative weekend effect, with higher levels of air pollutants during the week. However, as more stringent measures were implemented, this trend reversed, with higher intensities of positive weekend effect observed (Figure 3).

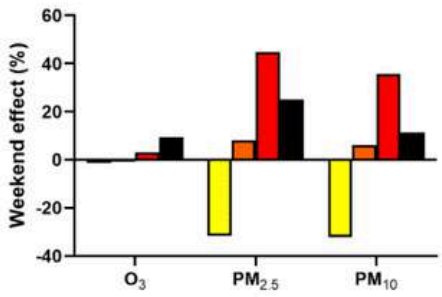


Figure 3. Weekend effect of air pollutants.

This likely occurred due to how the restriction measures were applied, because although human mobility on weekdays was affected by measures that involved the work format and the functioning of business, the weekend suffered less significant impacts, with the population still moving around for leisure or other outdoor recreational activities.

Thirdly, the machine learning model demonstrate that the pollutant levels remained below usual levels until the early months of 2021, aligning with the conclusion of the MDC in April 2021 (Figure 4). This suggests that the restriction measures played a crucial role in maintaining reduced pollution levels during this period.

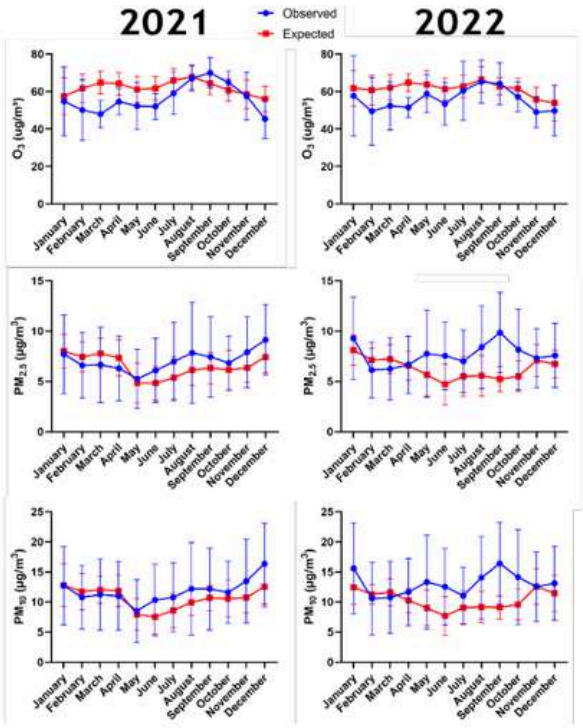


Figure 4. Observed and expected averages of air pollutants based on the prediction scenary.

Lastly, our analysis of the Interruption-Recovery pattern unveiled a transitional year in 2021, with pollutant levels gradually returning to usual levels by 2022. A behavior that is observed when analyzing Figure 4 together with Figure 5. This gradual recovery indicates a shift towards a 'new normal' for air pollutants in the region in the year 2022, emphasizing the long-lasting effects of the pandemic on atmospheric pollution dynamics.

These findings are part of my doctoral thesis, which encompasses multiple investigations into the behavior of air pollutants in various cities in Rio Grande do Sul (Tavella and da Silva Júnior, 2021; Tavella et al., 2022; Tavella and da Silva Júnior, 2023; Tavella et al., 2023a; Tavella et al., 2023b). They shed light on how air pollutants respond to human activity restrictions in different city contexts.

CONCLUSIONS

Our study provided valuable information regarding the impact of COVID-19 on air pollutant levels, demonstrating that the COVID-19 pandemic has had a complex and varying impact on atmospheric pollution. Additionally, it enabled an investigation and a glimpse into pollutant behaviour during major human-activity interruptions, offering guidance to responsible authorities for future air quality control strategies and policies.

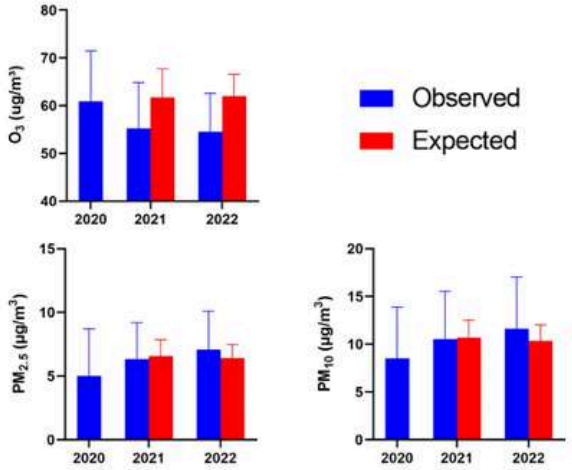


Figure 5. Median averages of air pollutants in the three investigated years.

REFERENCES

Diffenbaugh, Noah. S. et al. The COVID-19 lockdowns: a window into the Earth System. *Nature Reviews Earth & Environment* 1(9) (2020): 470-481.

Tavella, Ronan A., and da Silva Júnior, Flavio. M.R. Watch out for trends: did ozone increased or decreased during the COVID-19 pandemic?. *Environmental Science and Pollution Research* 28 (2021): 67880-67885.

Tavella, Ronan A. et al. Unexpected reduction in ozone levels in a mid-size city during COVID-19 lockdown. *International Journal of Environmental Health Research* 32(8) (2022) 1801-1814.

Tavella, Ronan A., and da Silva Júnior, Flavio M.R. Exploring the Interruption-Recovery Pattern of Air Pollutants During the COVID-19 Pandemic in Southern Brazil: An Analysis of the New Normal. *MAPAN* (2023):1-10.

Tavella, Ronan A. et al. Weekend effect of air pollutants in small and medium-sized cities: The role of policies stringency to COVID-19 containment. *Atmospheric Pollution Research* 14 (2023a): 101662.

Tavella, Ronan. A. et al. Better understanding the behavior of air pollutants at shutdown times–results of a short full lockdown. *International Journal of Environmental Health Research*, 33(12) (2023b) 1525-1532.

AIR POLLUTION CONFERENCE BRAZIL
CMAS SOUTH AMERICA
COMMUNITY MODELING AND ANALYSIS SYSTEM

THE IMPACT OF PUBLIC POLICIES ON AIR QUALITY: A CASE STUDY IN THE METROPOLITAN AREA OF SÃO PAULO

Maria Carla Queiroz Diniz Oliveira[1], Regina Maura de Miranda[1]
[1] *University of São Paulo - School of Arts, Sciences and Humanities*
mariaqueiroz@usp.br

Abstract: Air pollution represents a growing problem for human and public health in large urban centers, a consequence of the lack of effective urban mobility planning resulting in the predominance of the use of individual transport, the main emission source in large metropolises. International experiences show the importance of a set of public policies and local/municipal management for mitigating atmospheric pollution and its effects. Thus, a study was carried out focused on the Metropolitan Area of São Paulo (MASP), an important economic center in Latin America, analyzing the evolution of air quality, through the temporal analysis of 18 monitoring stations distributed throughout MASP, between the years of 2005 and 2023, for the pollutants PM_{10}, $PM_{2.5}$, SO_2 and NO_2 and their relationship with public policies, as well as the mapping of persistent exceedance periods, that is, events of high concentration of pollutants occurring in a large part of MASP and which have persisted for several days, 80% percentile. It was observed that there were improvements in pollutant concentrations, especially in the reduction of SO_2 and PM_{10}, with an average reduction of 10 ug/m³ of SO_2 between 2005 and 2023, attributed to public policies such as the Vehicle Emissions Control Program (PROCONVE) and fuel updates, with the reduction of sulfur in diesel and gasoline. Municipal intervention was also important, such as the implementation of the Maximum Restriction Zone on truck circulation. These public policies and municipal actions influenced the reduction of persistent events of poor air quality, as is the case of PM_{10}, with an average decrease of 3 persistent exceedance periods from 2015. Therefore, strengthening legislation and specific policies are essential to manage air quality regionally and municipally in order to continue reducing the concentrations of pollutants in large urban centers, mitigating the impacts that air pollution has on the health of populations in these regions of high density.

Keywords: Air pollution, Metropolitan Area of São Paulo, Public Policies and Air quality.

INTRODUCTION

Environmental degradation, particularly air quality deterioration, poses a significant threat to major urban centers worldwide. The Metropolitan Area of São Paulo (MASP), one of Latin America's largest economic hubs, comprises 39 municipalities and a population of approximately 21 million people, hosts 48% of the vehicle fleet of the State of São Paulo, making vehicular emissions the primary source of air pollutants, contributing to 95% of carbon monoxide (CO), 60% of nitrogen oxides (NO_x), 69% of hydrocarbons (HC), 9% of sulfur oxides (SO_x), and 40% of inhalable particulate matter (PM_{10}) (CETESB, 2022).

In addition to vehicular emissions, industrial activities also play a role in the air quality of the MASP. However, their impact has diminished due to emission control programs and industrial migration away from the metropolitan area since the 1990s (Kumar *et al.*, 2016; Andrade *et al.*, 2017). Despite these changes, industrial emissions remain significant near large complexes, such as the petrochemical in Capuava, Santo André, which emits primarily SO_2, NOx, and hydrocarbons (CETESB, 2018). Beyond these regulated sources, other pollution sources, like biomass burning, waste incineration, and regional transport of pollutants, also contribute to air quality issues (Kumar et al., 2016).

This way, this study aims to examine the long-term trends of air quality in the MASP from 2005 to 2023, focusing on persistent exceedance periods (PEPs) for pollutants like PM_{10}, $PM_{2.5}$, NO_2, and SO_2. The ultimate goal is to provide insights for public policy to reduce pollutant emissions and improve public health outcomes. Through a comprehensive analysis of air quality data, this study aims to offer recommendations for future policy measures and health-related guidelines.

METHODS

For this study on air pollution in the Metropolitan Area of São Paulo (MASP) and public policies, data from 18 automatic air quality monitoring stations f the São Paulo State Environmental Agency (CETESB) across the MASP were analyzed from 2005 to 2023. The selected stations included Diadema, Ibirapuera, Mauá, Osasco, Parque Dom Pedro II, Pinheiros, Santana, Santo Amaro, Congonhas, São Caetano do Sul, Taboão da Serra, Mooca, Guarulhos, Itaim Paulista, Grajaú, Nossa Senhora do Ó, Santo André - Capuava, and Marginal Tiête, representing a wide geographic distribution. These stations were chosen for their data availability and characteristics related to vehicular, industrial, and biogenic emissions. The hourly concentration data of PM_{10}, $PM_{2.5}$, NO_2, and SO_2 were extracted from the CETESB's (São Paulo State Environmental Company) QUALAR -

(https://qualar.cetesb.sp.gov.br/) system for the period from January 2005 to December 2023 and reduced to a daily basis using the maximum daily moving average. Daily time series of exceedances were constructed for the period between 2005 and 2023, based on the World Health Organization (WHO) air quality standards. An algorithm was developed to identify persistent exceedance periods (PEPs) for pollutants, considering events that occur simultaneously in at least 50% of the stations and last for a duration equal to or greater than the 80% percentile. For example, for PM_{10}, episodes are identified when they occur in at least 9 monitoring stations with a minimum duration of 5 consecutive days.

The study examined PEPs about public policies to understand the impact of government actions on air quality. This analysis involved reviewing public documents such as municipal Master Plans, reports from the National Environment Council (CONAMA), and the CETESB, along with secondary data on urban and environmental management. Legal frameworks at the municipal, state, and federal levels were also scrutinized to assess the regulations and policies in place during the study period.

FINDINGS AND ARGUMENT

Vehicle emissions are one of the primary sources of air pollution in major global metropolises, including the MASP, accounting for 60% of NOx emissions and 40% of particulate matter (PM) emissions (CETESB, 2022). This study analyzed the persistent exceedance events (PEPs) of PM_{10}, $PM_{2.5}$, NO_2, and SO_2 (Figures 1 and 2). The analysis revealed a significant reduction over time in persistent events for PM_{10} and NO_2. For PM_{10}, there was an average decrease of three events over the study period, each with a minimum duration of 5 consecutive days. For NO_2, the average decrease was 5 events, each with a minimum duration of 8 consecutive days. This reduction suggests an improvement in the quality of life for residents of the MASP.

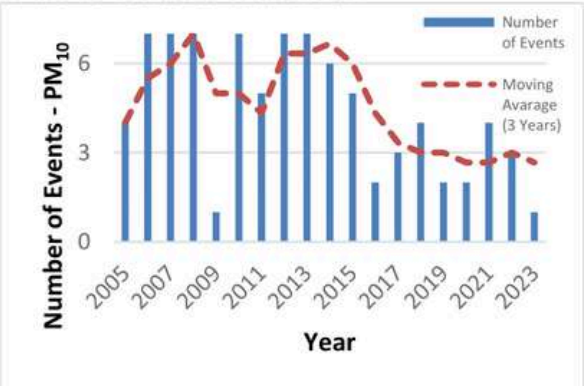


Figure 1. Number of persistent exceedance periods (PEPs) for PM_{10} for the MASP from 2005 to 2023.

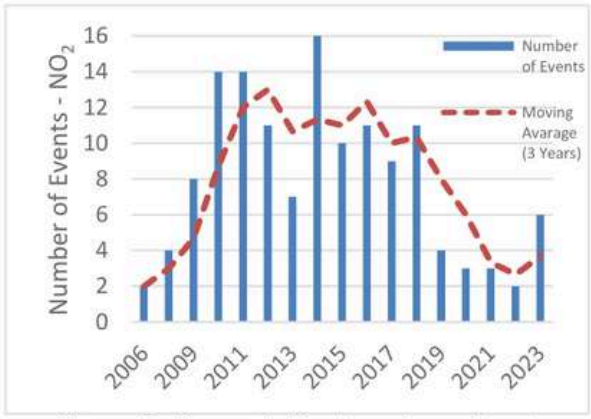


Figure 2. Figure 1. Number of persistent exceedance periods (PEPs) for NO_2 for the MASP from 2005 to 2023.

These trends might be linked to various public policies and initiatives implemented to improve air quality in the MASP (Andrade *et al.*, 2017). The introduction of phase L6 for light vehicles in 2015 and phase P7 for heavy vehicles in 2012 could have contributed to the reduction of PEPs for PM_{10} and NO_2. Phase P7, for example, aimed to cut NO_x emissions by 60%, setting a limit of 2 g/kWh for NO_x emissions (Nogueira et al., 2015; Dominutti et al., 2016). These phases were part of the Vehicle Emission Control Program (Proconve). In addition to federal and state regulations, municipal policies also play a crucial role in reducing pollution. The restriction of trucks in Maximum Restriction Zones has helped lower concentrations of NO_x and PM, especially in high-traffic areas like Congonhas.

Regarding SO_2, the study did not identify PEPs, due to the low concentrations of this pollutant in the MASP. Figure 3 shows a reduction in SO_2 concentrations starting in 2009, with a sharp decline in 2014. This reduction—averaging 65% compared to concentrations before 2014—coincided with the switch from diesel S-50 to diesel S-10, which contains only 10 ppm of sulfur (Nogueira et al., 2015; Andrade et al., 2017; CETESB, 2022).

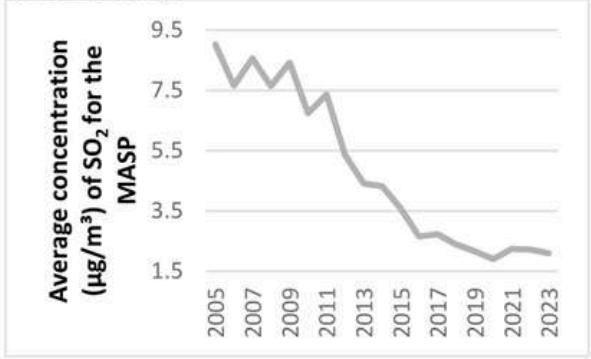


Figure 3. Avarage concentrarion of SO_2 for the MASP.

The MASP is aligning with global trends by adopting strategies to reduce vehicle emissions and encourage the use of non-motorized transport and public transportation (Slovic and Ribeiro, 2018). The city of São Paulo introduced a bike-sharing program in 2012, followed by the expansion of bike lanes and cycle paths.

This study is ongoing to fully understand the impact of public policies at the federal, state, and municipal levels on PEPs and how economic incentives may have contributed to reducing air pollution in the MASP. This phase of the study aims to identify which measures have been most effective in reducing emissions and whether these policies can be replicated or improved to provide ongoing enhancements to air quality. The continuation of the study will allow for a more in-depth exploration of the effectiveness of these policies and provide insights for future regulatory decisions.

CONCLUSIONS

Based on the analysis of air quality monitoring data from 18 stations across the MASP from 2005 to 2023, several key principles and generalizations can be inferred. First, the implementation of public policies and regulations aimed at reducing vehicle emissions appears to have had a positive impact on air quality, particularly in reducing PEPs for PM_{10} and NO_2. Policies such as vehicular emission control programs alongside municipal measures like the restriction of trucks in Maximum Restriction Zones, have contributed to these reductions. Furthermore, the reduction in the content of sulfur in diesel
coincided with a significant decrease in SO_2 concentrations.

However, the study identified exceptions to these trends, specifically regarding $PM_{2.5}$. Despite reductions in PM_{10} and NO_2, there was no clear trend for $PM_{2.5}$ concentrations during the study period. This inconsistency can be attributed to the complex nature of fine inhalable particles, primarily composed of secondary pollutants formed through chemical reactions in the atmosphere. This complexity suggests that reductions in primary sources like vehicle emissions may not always lead to proportional decreases in $PM_{2.5}$.

The findings of this study suggest several key recommendations to address air pollution in the MASP. Effective air quality policies require collaboration among government agencies, industry stakeholders, and environmental organizations, emphasizing the importance of public awareness to encourage practices that reduce pollution. In summary, the continuous review and update of public policies, informed by ongoing research, is crucial to guide decision-makers and achieve sustainable air quality improvements in MASP and other major urban areas.

REFERENCES

Andrade, M. de F. *et al.* (2017) "Air quality in the megacity of São Paulo: Evolution over the last 30 years and future perspectives," *Atmospheric Environment*, 159, pp. 66–82. Available at: https://doi.org/10.1016/j.atmosenv.2017.03.051.

Dominutti, P.A. *et al.* (2016) "One-year of NMHCs hourly observations in Sao Paulo megacity: meteorological and traffic emissions effects in a large ethanol burning context," *Atmospheric Environment*, 142(August), pp. 371–382. Available at: https://doi.org/10.1016/j.atmosenv.2016.08.008.

Kumar, P. *et al.* (2016) "New directions: From biofuels to wood stoves: The modern and ancient air quality challenges in the megacity of São Paulo," *Atmospheric Environment*, 140, pp. 364–369. Available at: https://doi.org/10.1016/j.atmosenv.2016.05.059.

Nogueira, T. *et al.* (2015) "On-road emissions of carbonyls from vehicles powered by biofuel blends in traffic tunnels in the Metropolitan Area of Sao Paulo, Brazil," *Atmospheric Environment*, 108, pp. 88–97. Available at: https://doi.org/10.1016/j.atmosenv.2015.02.064.

Slovic, A.D. and Ribeiro, H. (2018) "Policy instruments surrounding urban air quality: The cases of São Paulo, New York City and Paris," *Environmental Science and Policy*, 81(March 2017), pp. 1–9. Available at: https://doi.org/10.1016/j.envsci.2017.12.001.

AIR POLLUTION CONFERENCE BRAZIL
CMAS SOUTH AMERICA
COMMUNITY MODELING AND ANALYSIS SYSTEM

OPTIMIZING INDUSTRIAL SITE MANAGEMENT: CFD SIMULATIONS AND ENVIRONMENTAL IMPACT ASSESSMENT OF WIND EROSION FROM STOCKPILES

Cristina Lima de Morais, Jamily Fae Stocco, Bruno Furieri, Jane Meri Santos, Jose Gustavo da Costa

[1]*Universidade Federal do Espirito Santo*
E-mail: cristinalimademorais@gmail.com
[2]*ArcelorMittal Tubarao*

Abstract: The ongoing industrialization and expansion of urban areas have significantly increased the emission of particulate matter (PM) from various sources, including transportation networks and industrial storage yards. This paper aims to address the critical environmental challenge posed by PM emissions. The focus is on understanding and quantifying emissions from roads and granular material storage yards at the industrial site, a significant contributor to the particulate levels in the surrounding atmosphere. Particulate matter, especially PM10 and PM2.5, poses severe risks to environmental quality and human health, impacting respiratory and cardiovascular systems. This concern is particularly acute in industrial regions where the concentration of particulate matter often exceeds safe levels due to both mechanical disruptions and natural meteorological conditions. The primary objective of this project is to provide a scientific basis for the assessment and management of particulate emissions, enhancing the capability to predict dispersion patterns and their impacts on urban air quality. The methodology employed in this project integrates field measurements and advanced computational modeling to simulate the emission and dispersion processes. By employing Computational Fluid Dynamics (CFD) and Gaussian dispersion models, the project quantifies the dynamic processes influencing particulate matter behavior. These models facilitate a detailed understanding of how particulate matter disperses across different environmental barriers and under varying meteorological conditions. In conclusion, the insights gained from this research are expected to significantly contribute to the strategies for managing environmental impacts associated with industrial activities. The findings will aid policymakers and environmental managers in developing more effective emission control and mitigation strategies, ultimately leading to improved air quality and public health. The subsequent sections of this paper will detail the objectives, literature review, methodologies, results, and discussions derived from the comprehensive study of particulate matter emissions and dispersion at the industrial site.

Keywords: Particulate Matter Emissions; Computational Fluid Dynamics (CFD); Environmental Impact; Industrial Site Management; Wind Erosion.

INTRODUCTION

The present work intends to study the significant environmental impacts of particulate matter emissions from industrial storage yards and roads, highlighting the need for effective management and quantification of these emissions. This necessity is particularly pressing in the Metropolitan Region of Vitória (MRV), Brazil, where industrial activities contribute substantially to local air pollution. The paper references data from a local environmental agency which shows that mining and steel industries are responsible for approximately 23% of the particulate emissions in the area. Such emissions pose risks including reduced visibility, surface soiling, and various health hazards, underscoring the urgency of addressing these environmental challenges.

To effectively manage and mitigate the environmental risks posed by particulate matter, accurate quantification of emissions is essential. This is typically achieved through either field measurements or mathematical modeling. While field measurements provide direct data, they are often costly and challenging to execute due to the complexity of industrial sites and operational variability. Conversely, mathematical modeling offers a flexible and less expensive alternative, allowing for the assessment of different scenarios and the adaptation of control strategies accordingly. The most commonly utilized model in this context is developed by the United States Environmental Protection Agency (USEPA), which facilitates the estimation of emissions from various sources based on specific criteria related to erosion potential and particle detachment mechanisms.

Despite the utility of the USEPA model, its application has limitations, particularly in its assumption of standardized pile shapes and wind directions which may not accurately represent conditions at all industrial sites. The model's guidelines, based on simplified geometric and meteorological data, often fail to capture the nuanced dynamics at complex sites where multiple

environmental factors interact. Consequently, this can lead to significant discrepancies in emission estimates, as demonstrated by comparisons between model predictions and detailed Computational Fluid Dynamics (CFD) simulations. For instance, the emission rates calculated through the USEPA model can vary greatly when validated against more localized, CFD-derived data.

The paper emphasizes the need for ongoing research and methodological improvements to better understand and manage particulate emissions from industrial sources. The collaboration between academic research and industrial application is vital for advancing emission quantification techniques, ultimately contributing to more sustainable environmental practices. This will not only aid in compliance with regulatory standards but also in the protection of public health and the environment in regions affected by industrial activities.

METHODS

The strategy applied to the present paper aims to provide a thorough understanding of the dynamics of particulate matter generated by roads and granular material storage yards at an industrial site. Computational Fluid Dynamics (CFD) is primarily used to model the fluid flow and particulate dispersion within the industrial environment. This approach allows for the examination of complex interactions between particulate matter and various environmental barriers under different meteorological conditions.

It details the use of CFD simulations to analyze the effects of physical barriers, such as buildings and vegetation, on the dispersion of particulate matter. These simulations help to predict how changes in the physical layout of the site and the positioning of barriers can influence particulate trajectories and concentrations. The methodology involves generating a digital representation of the industrial site, including all significant physical features and potential emission sources. Various scenarios are modeled to assess the impact of different wind directions and barrier configurations on particulate dispersion patterns.

A critical component of the methodology is the mathematical modeling of particulate emissions using the USEPA's AP 42 "13.2.5 - Industrial Wind Erosion" model. This model estimates emissions based on factors such as the physical characteristics of the piles, local meteorological data, and site-specific conditions such as surface roughness and barrier effects. The model divides the pile surfaces into grid sections, each with calculated erosion potential, allowing for detailed analysis of particulate release and dispersion across the site.

To validate the computational models, the paper describes field measurements conducted at the site to gather real-time data on particulate matter concentrations and meteorological conditions. These measurements provide baseline data to calibrate the CFD models and ensure their accuracy. The integration of empirical data with computational predictions is crucial for refining the models and enhancing their predictive capabilities.

FINDINGS AND ARGUMENT

The paper presents a detailed analysis of the data obtained from both computational simulations and field measurements at the industrial site. The section primarily focuses on the outcomes of CFD simulations, which illustrate how different environmental and operational variables affect particulate matter emissions and dispersion patterns. These results are critical in understanding the effectiveness of current mitigation strategies and in developing new approaches to control particulate emissions effectively.

A significant portion of the work is dedicated to discussing the impact of wind erosion on storage piles within the industrial site, as demonstrated by the CFD models. The simulations reveal that wind direction and speed significantly influence emission rates, with certain directions exacerbating particulate release due to the alignment of wind flow with the orientation of storage piles. The data suggest that modifications to pile arrangement and the strategic placement of wind barriers could significantly reduce particulate emissions.

The work presents a validation of the CFD models against field measurements. The comparative analysis indicates a good correlation between the simulated data and actual measurements, reinforcing the reliability of the computational approach. Discrepancies noted are primarily attributed to unforeseen operational changes and environmental factors that were not accounted for in the initial simulations. These insights are used to refine the models further, improving their predictive accuracy.

Figure 1, which includes parts (a) and (b), provides a visual representation of the emission rate time series for the meteorological year of 2021 from two specific yards. These figures illustrate the temporal evolution of emitted mass and emitted mass flux from the piles, highlighting the fluctuations in emission rates over time. Figure 1a displays a relatively steadier emission rate, suggesting more consistent conditions at this yard. Figure 1b shows a more variable emission pattern, likely due to operational activities such as the addition or removal of material, which periodically alters the surface characteristics of the piles.

The discussion around these figures emphasizes the complexity of predicting particulate emissions, which are influenced by a myriad of factors including but not limited to wind speed and direction, pile configuration, surface treatment, and operational practices. The variability observed in the emission patterns underscores the necessity for continuous monitoring and adaptive management strategies to mitigate the impact of particulate matter on the environment.

Finally, the results concludes with an overview of the broader implications of these findings for environmental policy and site management. The validated models offer a robust tool for predicting the impacts of different control strategies, providing a scientific basis for decision-making processes related to environmental protection and compliance. This section not only highlights the successes of the current methodologies but also points towards areas for future research and development in the field of industrial particulate matter dispersion.

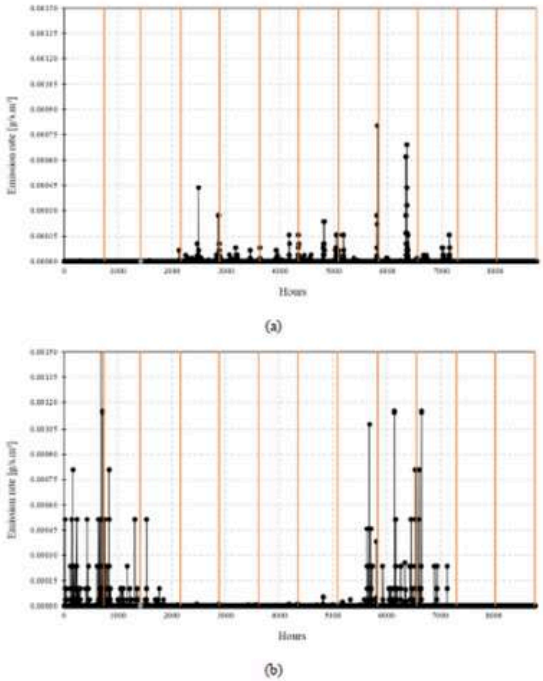


Figure 1. Emission rate time series for the meteorological year of 2021.

CONCLUSIONS

The comprehensive analysis presented in this paper offers a detailed quantification of particulate matter emissions from roads and granular material storage yards at the industrial site, utilizing a robust combination of Computational Fluid Dynamics (CFD) simulations and field measurements. The findings underscore the significant impact of wind direction, pile configuration, and operational practices on emission rates, demonstrating the critical need for strategically placed barriers and optimized yard layouts to mitigate particulate dispersion. Validation of the computational models with empirical data has not only reinforced the accuracy of the simulations but also highlighted areas for refinement, ensuring that the models remain relevant under varying operational conditions. Overall, this research significantly contributes to our understanding of particulate matter dynamics in industrial settings and provides a valuable tool for environmental management, facilitating informed decision-making to enhance air quality and compliance with environmental regulations.

REFERENCES

IEMA (2019). Atmospheric Emissions Inventory.

U.S. Environmental Protection Agency (USEPA) (2006). Guideline on Air Quality Models.

TURPIN, B. J., & HARION, J. L. (2010). "Limitations of the Standard USEPA Dispersion Model: A Case Study for Industrial Pile Emissions".

DIEGO, I., et al. (2009). "Computational Fluid Dynamics Studies to Enhance Understanding of Particulate Matter Emission Dynamics".

CONG, X., et al. (2012). "Advancements in Particulate Emission Modelling: Implications for Industrial Applications".

AIR POLLUTION CONFERENCE BRAZIL
CMAS SOUTH AMERICA
COMMUNITY MODELING AND ANALYSIS SYSTEM

COMPUTATIONAL FLUID DYNAMICS INVESTIGATION ON PARTICULATE MATTER EMISSION FROM ROADS, GRANULAR MATERIAL STORAGE AND HANDLING

Eduardo de Souza Pescada Miranda[2], Cristina Lima de Morais[1], Bruno Furieri[1], Bruna Lima Véras Maia[2], Taciana Toledo de Almeida Albuquerque[2]

[1]*Universidade Federal do Espírito Santo*

E-mail: bruno.furieri@ufes.br

[2]*Universidade Federal de Minas Gerais*

Abstract: The present paper refers to a simplified description of the theoretical and numerical methodology to be used in estimating particulate matter emissions from diffuse sources found in mines and steelworks operating in the city of Congonhas. The emission estimate of the diffuse sources will be carried out using the emission model proposed by the US EPA (United States Environmental Protection Agency) including improvements developed and published in the literature over the last decade (USEPA, 2006). Input data for the model include knowledge of the distribution of winds incident on the sources - the friction velocity distribution (generated by wind shear over the surfaces of the diffuse sources - mines and piles) estimated from the velocity at 25 cm from the surface of the mines or piles, as will be explained in the following sections, both obtained by numerical simulation. With this data in hand, the calculation is also carried out considering the properties of the particulate material that makes up the mines and piles, in addition to operational data on movement, removal, or reintroduction of material. The main objective of this document is to emphasize the importance of all required data and highlight the type of result expected at the end of the project.

Keywords: Computational Fluid Dynamics (CFD); Fugitive Dust Emissions; Wind Erosion; USEPA Emission Model; Industrial Stockpiles.

INTRODUCTION

The quantification of particulate matter emissions from industrial operations, especially those associated with mines and steelworks, is a crucial aspect of environmental management and regulatory compliance. Diffuse sources, such as open aggregate piles and large-scale industrial yards, represent significant challenges due to their exposure to environmental elements and the variability in particle emission behaviors under different meteorological conditions (Shao & Lu, 2000; USEPA, 2006). Accurately modeling these emissions is essential for improving air quality predictions and developing effective mitigation strategies.

Recent advancements in emission modeling have been driven by the integration of computational fluid dynamics (CFD) and empirical data from controlled experiments, such as wind tunnel testing. These methodologies enhance the understanding of complex flow dynamics around stockpiles and the resultant particulate dispersion (Badr & Harion, 2005; Turpin & Harion, 2010). This report builds on the foundation laid by the US Environmental Protection Agency (USEPA) models, incorporating the latest developments and insights from the last decade to refine emission estimates more accurately.

The primary focus of this report is on the theoretical and numerical approaches used to estimate emissions from diffuse sources found in the Congonhas region. These methodologies consider the unique industrial and environmental conditions of the area, employing a model that has been adapted to better reflect local wind shear effects and material characteristics (De Morais et al., 2018). This approach ensures that the model not only aligns with global standards such as those set by the USEPA but also addresses specific local challenges.

To achieve this, the paper details the use of numerical simulation tools to determine friction velocity distributions and the interaction of these velocities with various stockpile configurations. This methodology allows for a more nuanced understanding of how different geometrical setups and operational practices influence particulate emissions. The results from these models provide critical data that can guide operational changes and policy adjustments to minimize environmental impacts (Ferreira et al., 2019a; 2019b). Through a combination of advanced modeling techniques and comprehensive field data, this report aims to set a new standard for emission estimation from diffuse sources in industrial settings.

METHODS

The emission estimation model from diffuse sources due to wind erosion primarily utilizes the US EPA framework, which is widely recognized for its robustness in various industrial applications. This model adapts to the specific geometries of stockpiles and surface conditions, acknowledging that the wind flow and friction velocities are not constant and are significantly altered by the

physical presence of the piles. These modifications in wind flow create distinct shear stress distributions across the pile surfaces, which are then divided into zones of similar normalized velocity for emission calculation.

Recent improvements in the model have incorporated results from wind tunnel experiments, providing refined data on velocity distribution for different pile shapes and wind incidence angles. This enhancement allows for a more accurate simulation of real-world conditions where piles serve as both barriers and sources of particulate emissions. The model treats each segment of the pile according to its exposure to wind, ensuring that the emission estimates reflect the varying potential for particle entrainment across different areas of the pile.

The US EPA model's sophisticated approach to calculating friction velocity at the source incorporates a logarithmic wind profile equation. This method provides a detailed understanding of the interaction between wind speed, surface roughness, and particulate emission, critical for predicting the behavior of particulate matter under different environmental conditions. This refined modeling capability is essential for industries seeking to mitigate the impacts of fugitive dust and comply with environmental regulations.

FINDINGS AND ARGUMENT

The use of Computational Fluid Dynamics (CFD) has significantly advanced the ability to simulate friction velocities that affect erosion and emission from industrial stockpiles. By providing a direct estimation of friction velocity ($u*$) and the surface velocity at 25 cm above the pile (us), CFD simulations contribute crucial data necessary for refining emission models. This numerical approach addresses scenarios beyond the standard configurations provided by existing models, catering to the unique conditions found in operational industrial sites.

The simulation efforts detailed in the paper cover various pile geometries and wind directions, exploring how these factors influence the shear stress distribution and hence the dust emission rates. For instance, studies have shown that the configuration of the pile, whether semicircular or conical, dramatically affects the wind flow patterns and thus the potential for erosion. These findings help in adjusting the model to predict emissions more accurately by considering the specific pile configurations that occur in practice.

Moreover, the simulation results are integrated with the emission model to predict the overall dust emissions from the piles. This integration is critical in environments where the physical layout of stockpiles can vary widely, necessitating a flexible and dynamic approach to emission estimation. Through CFD, the emission model becomes a powerful tool for environmental management, providing stakeholders with the ability to forecast and control particulate matter emissions effectively.

Determining the threshold friction velocity ($ut*$) is an essential aspect of accurately estimating dust emissions. This velocity marks the minimum wind speed required to initiate particle movement, which varies based on particle size, density, and surface conditions. The most recent and comprehensive model for calculating this threshold velocity integrates both gravitational and cohesive forces affecting particles, offering a more detailed and realistic estimate of when erosion might occur.

Challenges remain in applying the threshold velocity model to diverse particle sizes and materials, particularly due to the variability in cohesive forces, which include electrostatic and van der Waals forces. These forces are notoriously difficult to quantify, yet they play a crucial role in determining whether particles will become airborne under given environmental conditions. As such, the model must continually adapt to incorporate new empirical data and theoretical insights to remain effective.

The ongoing development of the threshold friction velocity model underscores the complexity of fugitive dust emissions and highlights the need for robust, scientifically grounded approaches to managing environmental impacts. By refining the understanding of how different forces interact to cause particle entrainment, industries can better predict and mitigate the adverse effects of wind erosion on both local air quality and broader ecological systems.

Accurate emission estimation requires detailed operational data from diffuse sources, which involves understanding the material characteristics, pile configurations, and specific operational activities that influence particulate matter emissions. The data demand encompasses not only the physical dimensions and material properties of the piles but also the operational context, such as the frequency and methods of material movement, which can significantly affect emission rates. This comprehensive data collection is crucial for applying the emission model effectively.

Meteorological data also play a vital role in emission estimation, providing the necessary context for selecting appropriate CFD results and applying them to specific operational scenarios. The integration of meteorological and operational data allows for a dynamic assessment of emission rates, adjusting for temporal variations in weather conditions and

operational activities. This approach ensures that emission estimates are both accurate and relevant to current conditions.

Lastly, the need for a refined data set is critical for the continual improvement of emission models. As new information becomes available through ongoing research and technological advancements, it is incorporated into the model to enhance its accuracy and applicability. This iterative process ensures that the emission estimation remains a robust tool for environmental management, helping industries to meet regulatory requirements and minimize their environmental footprint.

CONCLUSIONS

This paper has presented an advanced approach to estimating particulate matter emissions from diffuse sources in mines and steelworks, emphasizing the integration of Computational Fluid Dynamics (CFD) and modifications to the USEPA emission model. By incorporating recent advancements in simulation technologies and experimental data, the revised methodology offers a more accurate and realistic assessment of fugitive dust emissions. The ability to predict emissions based on specific pile geometries and operational conditions not only aligns with environmental compliance requirements but also aids in the development of targeted mitigation strategies to reduce the environmental impact of industrial operations.

The enhanced emission model reflects a significant improvement over traditional approaches by accounting for the complex dynamics of wind erosion influenced by non-erodible particles. The introduction of variable friction velocities and detailed analysis of shear stress distributions provides a granular view of emission potentials across different sections of a stockpile. Such detailed modeling is crucial for industries located in regions like Congonhas, where localized environmental factors play a significant role in the dispersion of particulate matter. As a result, the model serves as a critical tool for both regulatory bodies and industrial operators, ensuring that emission estimates are both scientifically sound and practically applicable.

Looking forward, the continued refinement of emission models will require ongoing collaboration between researchers, industry stakeholders, and regulators. Incorporating real-time data acquisition systems for monitoring wind speeds and particulate emissions could further enhance the accuracy of predictions. Additionally, expanding the model to include a wider range of particle sizes and more diverse material characteristics will broaden its applicability, enabling more industries to benefit from precise emission estimations. By advancing these modeling techniques, we can better address the environmental challenges posed by industrial emissions and contribute to the sustainability of industrial practices worldwide.

REFERENCES

Badr, T., Harion, J.L., 2005. Numerical modelling of flow over stockpiles: Implications on dust emissions. Atmos Environ 39, 5576–5584. https://doi.org/10.1016/j.atmosenv.2005.05.053

De Morais, C.L., Ferreira, M.C.S., Santos, J.M., Furieri, B., Harion, J.L., 2018. Influence of non-erodible particles with multimodal size distribution on aeolian erosion of storage piles of granular materials. Environmental Fluid Mechanics. https://doi.org/10.1007/s10652-018-9640-6

Ferreira, M.C.S., Furieri, B., A., O.E.M., Harion, J.L., Valance, A., Dupont, P., Reis, N.C., Santos, J.M., 2019a. A simple model to estimate emission of wind-blown particles from a granular bed in comparison to wind tunnel experiments. Geomorphology 335, 1–13. https://doi.org/10.1016/j.geomorph.2019.03.004

Ferreira, M.C.S., Furieri, B., de Morais, C.L., Stocco, J.F., Reis Jr, N.C., Harion, J.-L., Santos, J.M., 2020. Experimental and numerical investigation of building effects on wind erosion of a granular material stockpile. Environmental Science and Pollution Research 27, 14.

Ferreira, M.C.S., Furieri, B., Santos, J.M., El Moctar, A.O., Harion, J.-L., Valance, A., Dupont, P., Reis, N.C., 2019b. An experimental and numerical study of the aeolian erosion of isolated and successive piles. Environmental Fluid Mechanics. https://doi.org/10.1007/s10652-019-09702-z

Shao, Y., Lu, H., 2000. A simple expression for wind erosion threshold friction velocity. J Geophys Res 105, 437–443.

USEPA, 2006. 13.2.5 Industrial wind erosion. Compil Air Pollut Emiss Factors 1. https://doi.org/10.1130/0091-7613(1998)026<0363

AIR POLLUTION CONFERENCE BRAZIL
CMAS SOUTH AMERICA
COMMUNITY MODELING AND ANALYSIS SYSTEM

NON-ERODIBLE PARTICLES EFFECTS IN TURBULENT STRUCTURES DEVELOPMENT: ON THE ROLE OF PARTICLE SHAPE INFLUENCE

Cristina Lima de Morais1, Geisiely do Espírito Santo1, Bruno Furieri1, Jane Meri Santos1, Maria Clara S. Ferreira2, Jean-Luc Harion3

[1]*Universidade Federal do Espírito Santo*
E-mail:
cristinalimademorais@gmail.com; geisielyes@gmail.com; bruno.furieri@ufes.br; jane.m.santos@ufes.br

[2]*Instituto Federal do Espírito Santo*
E-mail:
mclarascferreira@gmail.com

[3]*IMT Nord Europe*
E-mail:
jean-luc.harion@imt-nord-europe.fr

Abstract: The interaction between non-erodible particles and turbulent structures in aeolian plays a crucial role in understanding sediment dynamics. In recent decades, the degradation of air quality due to the suspension of fine particulate matter has become a global concern. Aeolian erosion is a significant source of airborne particles, including dust and pollutants, which can cause damaging impacts on human health and on the environment. The role of non-erodible roughness elements in shaping turbulent flow and influencing particle entrainment is central to understanding and develop more accurate emission models that underlies mitigating actions. This study investigates the effects of non-erodible particles on turbulent structures development foccusing on the influence of particle representation in cylindrical shape. Large-Eddy Simulations (LES) of the wind flow over particle beds using both particles shapes were perfomed. The governing equations used are those based on the filtered Navier-Stokes equations for mass and momentum. The physical model consists of an infinite bed formed by a mixture of erodible and non-erodible particles in a neutral atmosphere. Non-erodible particles are represented by random fixed cylindrical roughness elements and the erodible particles by the smooth surface around them. Just one portion of the bed is considered in the numerical simulations. Ansys Meshing® 19.0 software was used to construct a hexahedral mesh of 4,188,797 elements. The mesh was built by extrusion of hexahedral cells defined on the ground and cylinders walls with a growth rate of 1.1. To reach LES model requirements, the minimum element size on the walls was setup same order as 10^{-4} m and the time step 2.5×10^{-5} s. The minimum size was obtained considering that for LES, $y^+ < 1$. For upstream and downstream (x-direction) boundaries the periodicity condition with mass flow rate of 0.0051 was assumed. On the lateral sides (z-direction), the periodicity condition was also assumed, but the fluid flows in order that the mass balance within the domain is guaranteed. For top and bottom boundaries and rough surface it was assumed non-slip conditions. As one of the objectives of the present work is to evaluate the evolution of the flow from a smooth surface to the appearance of rough elements, it is also necessary to evaluate a smooth surface. To avoid additional computational costs, it was considered that the top of the domain could keep all the characteristics of a smooth bed as long as the distance of up to $y^+ = 30$ from the wall is respected. The results reveal that rough surfaces exhibit considerably higher friction velocity and that non-erodible elements affect the emission rate of erodible particles. Overall, the study contributes to a better understanding of wind erosion mechanisms, providing insights for the development of more accurate emission models and the implementation of mitigation measures.

Keywords: Aeolian erosion, particle emission, turbulent structures, particles shape, Large-Eddy Simulations.

INTRODUCTION

Industrial activities, although important for human life, have a significant impact on air pollution, especially due to the emission of particulate matter (PM), which is a set of pollutants consisting of dust, smoke, and other solid and liquid materials suspended in the atmosphere (CETESB, 2018). Storage yards in industrial facilities stand out as critical points because direct exposure to winds can lead to PM emissions due to wind erosion (NASCIMENTO, 2014).

Wind erosion is a natural process that drives the movement of granular materials, resulting in the lifting of particles into the atmosphere or rolling them along the surface (NASCIMENTO, 2014). Granular material is a set of distinct solid particles that can vary in size, shape, and positioning relative to the bed and the incident wind (SILVA, 2005). When subjected to wind erosion, they are classified based on their inertia as erodible or non-erodible (FURIERI et al., 2013).

AIR POLLUTION CONFERENCE BRAZIL
CMAS SOUTH AMERICA
COMMUNITY MODELING AND ANALYSIS SYSTEM

The interaction between erodible and non-erodible particles, along with turbulent structures in the atmosphere, is fundamental to understanding sediment dynamics. Studies like Durán, Claudin, and Andreotti (2011) show that when the wind reaches a threshold friction velocity over surfaces with particle clusters, the movement of these particles begins, leading to their dispersion to other areas. Determining this threshold friction velocity is influenced by the properties of the material that makes up the surface as well as the wind speed in the area (RIVERA, 2016).

Several studies have been conducted on non-erodible particles and surface erodibility (Gillette and Stockton, 1989; Roney, White, 2006; Brown, Nickling, Gillies, 2008; Webb, Strong, 2011; Furieri et al., 2013; Tan et al., 2013; Webb, Okin, Brown, 2014; De Morais et al., 2019; Pi et al., 2023). These studies demonstrate that the quantity of particles emitted due to wind erosion is significantly reduced by the presence of non-erodible particles and that there is an increase in the threshold friction velocity with the increase in the proportion of non-erodible particles. Thus, this work aimed to investigate the evolution and effects of flow generated from a smooth surface to the appearance of rough elements, represented by non-erodible cylindrical particles.

METHODS

Large Scale Simulations (LES) of wind flow over particle beds were conducted using both particle formats. The governing equations used are those based on the filtered Navier-Stokes equations for mass and momentum, as described below:

$$\frac{\partial \bar{u}_i}{\partial x_i} = 0$$

$$\frac{\partial \bar{u}_i}{\partial t} + \frac{\partial}{\partial x_j}\left(\bar{u}_i \bar{u}_j\right) = -\frac{\partial \bar{p}}{\partial x_i} + \nu \frac{\partial}{\partial x_j}\left(\frac{\partial \bar{u}_i}{\partial x_j} + \frac{\partial \bar{u}_j}{\partial x_i}\right) - \frac{\partial \tau_{ij}}{\partial x_j}$$

The physical model describes an infinite bed composed of a mixture of particles, some erodible and others non-erodible, in a neutral atmosphere. Non-erodible particles are represented by randomly arranged cylinder-shaped roughness elements, while erodible particles are symbolized by the smooth surface around these elements.

The Ansys Meshing® software was used to create the 4,188,797-element hexahedral mesh, which was constructed by extruding hexahedral cells defined on the ground and on the walls of the cylinders. To avoid additional computational costs, it was considered that the tops of the domains could maintain all the characteristics of a smooth bed as long as the distance of up to $y^+ = 30$ from the wall was respected.

Based on the physical model, computational domains were configured as illustrated in Figure 1, with base dimensions of 0.050 m × 0.040 m and a height of 0.037 m.

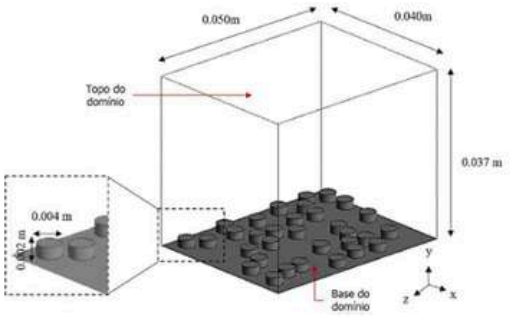


Figure 1. Computational domain scheme and its dimensions

The periodic condition was applied at both the inlet and outlet of the domains since the expected flow pattern has a periodic nature. The base of the domains and the roughness elements were treated as walls, and the no-slip condition was imposed.

Additionally, to evaluate the effects of friction velocity *(u*)* on smooth and rough planes, the obtained data were subjected to descriptive statistics analysis using R software version 4.1.1. Descriptive statistics are useful in creating data visualizations, making the communication of research results more accessible to other individuals (ALABI; BUKOLA, 2023).

FINDINGS AND ARGUMENT

From the descriptive statistics of the u* data in m/s, for points 16, 17, 18, 19, and 20 on the smooth surface and points 83, 84, 90, 91, and 93 on the rough plane, it is possible to observe that for the smooth surface, the mean values of u* are very close. As for the rough surface, the means also approached the values of the medians.

Figures 2 and 3 depict the histograms of the smooth and rough planes from the previous data. One common observation in these histograms is their right-skewed shape. This is also observed in the descriptive statistics, where all values of skewness and kurtosis are greater than zero, indicating positive skewness and a non-normal distribution.

The histograms of the smooth surface, Figure 2, appeared quite similar, with almost identical frequencies across all points, unlike what is observed in the rough surface, Figure 3. Points like 84, 90, and 91, which are positioned more freely and are not as close to non-erodible particles, exhibited very similar histograms, indicating that the flow velocity followed a consistent pattern.

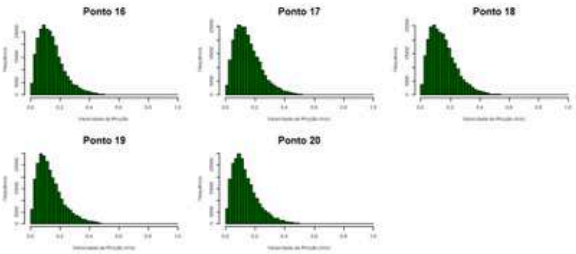


Figure 2. Histogram of each point on the smooth surface

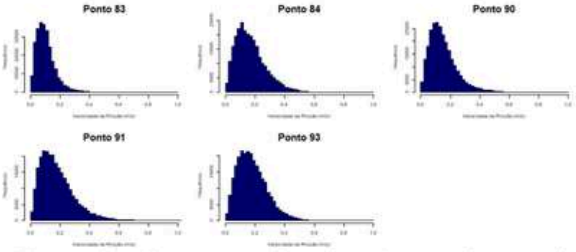


Figure 3. Histogram of each point on the rough surface

The results obtained indicate that the arrangement of points on a rough plane shows some differences in u*, while for smooth planes, no major divergences were identified. This behavior was already expected, as according to one of the results in the study by De Morais et al. (2019), the higher the proportion of non-erodible particles, the greater the protective effect on the observed points, the lower the number of emitted particles, and the smaller the changes observed on the surface of the pile.

CONCLUSIONS

From the results obtained, it was possible to identify that on rough surfaces, the u* is significantly higher compared to smooth surfaces. This indicates that erodible particles represented by points on the rough plane will have a higher emission rate when positioned farther away from non-erodible elements, as opposed to points closer to non-erodible particles.

The findings contribute to a detailed understanding of u* mechanisms on surfaces with non-erodible particles and their relationship with the emission of granular material near industries with stockpiles. The results of this study have the potential to assist in adapting and developing more accurate emission models to control air pollution. These measures aim to minimize negative impacts on both public health and the environment.

For future work, it is recommended to analyse how roughness could influence if treated as a hemisphere and what the effect would be on turbulence formation when analysing a bed with a greater or lesser quantity of particles.

REFERENCES

Alabı, O.; Bukola, T. Introduction to Descriptive Statistics. *Recent Advances in Biostatistics*, 2023.

Brown, S.; Nıcklıng, W. G.; Gıllıes, J. A. A wind tunnel examination of shear stress partitioning for an assortment of surface roughness distributions. *Journal of Geophysical Research: Earth Surface*, v. 113, n. 2, 24 jun. 2008.

CETESB. *Poluentes*. Disponível em: <https://cetesb.sp.gov.br/ar/poluentes/>. Accessed April 01, 2024.

De Morais, C. L. et al. Influence of non-erodible particles with multimodal size distribution on aeolian erosion of storage piles of granular materials. *Environmental Fluid Mechanics*, v. 19, n. 3, p. 583–599, 15 jun. 2019.

Durán, O.; Claudin, P.; Andreotti, B. On aeolian transport: Grain-scale interactions, dynamical mechanisms and scaling laws. *Aeolian Research*, v. 3, n. 3, p. 243– 270, Dez. 2011.

Furıerı, B. et al. Effects of non-erodible particles on aeolian erosion: Wind-tunnel simulations of a sand oblong storage pile. *Atmospheric Environment*, v. 79, p. 672–680, nov. 2013.

Gillette, D. A.; Stockton, P. H. The Effect of Nonerodible Particles On Wind Erosion of Erodible Surfaces. *Journal of Geophysical Research*, v. 94, n. D10, p. 885–897, 1989.

Nascimento, E. L. do. *Suspensão e deposição de material particulado emitido por pilhas de estocagem de granulados: uma abordagem numérica empregando LES*. Tese de doutorado em Engenharia Ambiental—Vitória, ES: UFES, 2014.

Pi, H. et al. Effects of secondary soil aggregates on threshold friction velocity and wind erosion. *Land Degradation and Development*, v. 34, n. 1, 2023.

Rivera, J. A. *Simulação da dispersão de poluentes atmosféricos numa microrregião do Município do Rio de Janeiro em escala real*. Dissertação de Mestrado em Engenharia Mecânica, RJ, PUC, 2016.

Roney, J. A.; Whıte, B. R. Estimating fugitive dust emission rates using an environmental boundary layer wind tunnel. *Atmospheric Environment*, v. 40, n. 40, p. 7668–7685, dez. 2006.

Tan, L. et al. Aeolian sand transport over gobi with different gravel coverages under limited sand supply: A mobile wind tunnel investigation. *Aeolian Research*, v. 11, p. 67–74, dez. 2013.

Webb, N. P.; Okin, G. S.; Brown, S. The effect of roughness elements on wind erosion: The importance of surface shear stress distribution. *Journal of Geophysical Research*, v. 119, n. 10, p. 6066–6084, 27 Maio 2014.

Webb, N. P.; Strong, C. L. Soil erodibility dynamics and its representation for wind erosion and dust emission models. *Aeolian Research*, Nov. 2011.

AIR POLLUTION CONFERENCE BRAZIL
CMAS SOUTH AMERICA
COMMUNITY MODELING AND ANALYSIS SYSTEM

ARTIFICIAL BARRIERS APPLIED TO AEOLIAN EROSION CONTROL: EVALUATION OF POROSITY AND TURBULENT MODELS ON FRICTION VELOCITY REDUCTION

Jamily Fae Stocco[1], Cristina Lima de Morais[1], Bruno Furieri[1], Jane Meri Santos[1], Jean-Luc Harion[2], Neyval Costa Reis Jr[1].

[1]*Universidade Federal do Espírito Santo*
E-mail: cristinalimademorais@gmail.com
[2]*IMT Nord Europe*

Abstract: *The work focuses on the influence of artificial wind barriers on the flow characteristics and erosion control effectiveness. The paper thoroughly analyzes the performance of turbulence models in simulating airflow modification due to wind barriers and assesses the effect of barrier porosity on the downstream surface wind velocity. The findings and discussions presented in this section are grounded in a comprehensive set of simulations that utilize different turbulence models and varying conditions of barrier porosity to model the airflow. Artificial wind barriers, typically solid or porous, are implemented to mitigate the erosive force of wind on granular storage piles by altering the airflow pattern around the barrier, effectively reducing wind velocity in the lee of the barrier which decreases the potential for wind erosion. The simulations compare various turbulence models to understand their accuracy in capturing the dynamics of wind flow around porous barriers. The results from these simulations are validated against experimental wind tunnel data, providing a robust framework for evaluating the models' effectiveness in realistic settings. This approach allows for a detailed investigation into how different porosity levels affect the wind flow, particularly how they influence the reduction in wind speed and the extent of the protected area downstream of the barrier. The discussion in this section is critical for designing effective erosion control strategies in industrial environments, where granular materials are often stored in large piles that are susceptible to wind erosion. By understanding the interaction between wind barriers and airflow, it is possible to optimize the design of these barriers to achieve maximum protection against erosion while minimizing the impact on the surrounding environment. In conclusion, the insights gained from the rigorous analysis provide valuable guidelines for the implementation of artificial wind barriers in industrial settings. The findings not only contribute to better environmental management practices but also enhance the understanding of turbulent flow dynamics in the presence of porous barriers, which is essential for the development of more effective erosion control measures.*

Keywords: Artificial Wind Barriers; Turbulent Flow Dynamics; Erosion Control; Computational Fluid Dynamics (CFD); Barrier Porosity.

INTRODUCTION

Wind erosion of granular material storage piles in industrial units results in the entrainment of particles into the atmosphere, leading to increased particulate concentrations, air quality degradation, and potential health risks. For instance, mining and steel industries located in the Metropolitan Region of Greater Vitória (RMGV), in the state of Espírito Santo, according to data from the environmental agency's source inventory for the base year of 2015, are responsible for 68.0% of the total particulate matter emission rate, 70.4% of PM10 (particulate matter with an aerodynamic diameter less than 10μm), and 71.6% of PM2.5 (particulate matter with an aerodynamic diameter less than 2.5μm). Of these, the emission rate from piles in storage yards corresponds to 33.2 kg/h, which is equivalent to 4% of total particulate matter, 16.4 kg/h equivalent to 3% of PM10, and 3.28 kg/h equivalent to 1% of PM2.5 (IEMA, 2019).

One strategy for controlling wind erosion on piles is the implementation of wind barriers around storage yards in industrial units. Wind barriers create resistance to wind flow, acting as momentum sinks that modify atmospheric flow and form regions with different flow characteristics around them (LYU; WANG; MASON, 2020; SPECKART; PARDYJAK, 2014), thus providing a sheltering effect in their vicinity (SANTIAGO et al., 2007; FERREIRA; LAMBERT, 2011; SAN; WANG; QIU, 2018). The barriers can be natural, such as tree belts, or artificial, such as porous screens made from various construction materials.

The effects caused by these barriers on the flow and their protection capability can be evaluated using different approaches. Commonly used are: field measurement techniques, reduced-scale physical modeling in wind tunnels, and mathematical and computational modeling (BADR; HARION, 2005; HONG; LEE; SEO, 2015; LIU et al., 2014; LIU et al., 2018; LYU; WANG; MASON, 2020).

AIR POLLUTION CONFERENCE BRAZIL
CMAS SOUTH AMERICA
COMMUNITY MODELING AND ANALYSIS SYSTEM

The correct prediction of the flow depends on the models used to represent the physical phenomena. Thus, the choice of the turbulence model, for example, is relevant for evaluating the modifications of the flow caused by the wind barrier and the effects on particle emission by wind erosion (DUPONT; BERGAMETTI; SIMOËNS, 2014; HONG; LEE; SEO, 2015; ROSENFELD; MAROM; BITAN, 2010; SAN; WANG; QIU, 2018; SAN; ZHAO; QIU, 2019). It is important to note, however, that the response time and computational cost of the simulations are highlighted as decisive factors in choosing the turbulence model to be used.

METHODS

Artificial porous barriers are described as constructs used to disrupt the airflow in a manner that reduces the wind velocity near granular material storage areas. These barriers are designed with specific porosity levels to achieve desired airflow characteristics. Both experimental data, particularly from wind tunnel tests, and computational fluid dynamics (CFD) models are employed to study the effectiveness of these barriers. The section explains how the experiments are set up to replicate real-world conditions as closely as possible and how these physical experiments help validate the CFD

he CFD simulations are designed to capture the complex interactions between the wind and the barrier. The models consider various factors such as the porosity of the barriers, the wind speed, and the physical geometry of the barriers. The simulations aim to predict how changes in these variables affect the wind flow patterns and erosion potential. The section discusses the results of the CFD simulations in terms of how effectively the barriers modify the flow. This includes a detailed analysis of the reduction in wind velocity behind the barriers and the creation of sheltered areas where the risk of erosion is significantly lowered.

A critical aspect of the analysis is understanding how the porosity of the barriers affects their performance. Different levels of porosity change the barrier's ability to reduce wind speeds and protect against erosion. The section explores optimal porosity levels that offer effective protection while maintaining sufficient airflow to prevent other unwanted environmental effects. Overall, section 4.1.2 provides a thorough examination of artificial porous barriers and their role in controlling erosion through detailed experimental and computational studies. The findings from this section contribute to the broader field of environmental engineering by offering insights into how to design and implement effective erosion control solutions in industrial settings.

FINDINGS AND ARGUMENT

CFD Model Validation and Analysis: The section begins by detailing the validation of CFD models against experimental data from wind tunnel studies, ensuring the models' accuracy in simulating real-world conditions. This validation is crucial for establishing the reliability of the simulations in predicting the effects of artificial barriers on wind patterns. Impact of Porosity on Airflow: Through simulations, the section explores how different levels of porosity in barriers affect the wind flow, particularly focusing on the reduction of wind velocity behind the barriers. It investigates how porosity variations influence the formation of low-velocity zones that are critical for reducing erosion potential.

Figure 1 illustrates the computed vorticity fields in the airflow around a 40% porous barrier, as obtained from the κ-ε Realizable and κ-ω SST turbulence models. The vorticity fields are compared to experimental data from Dong et al. (2010), highlighting the models' effectiveness in capturing the complex flow structures induced by the barrier. The analysis demonstrates that while both models provide a close approximation, there are subtle differences in the vorticity patterns that could influence the design of effective wind barriers.

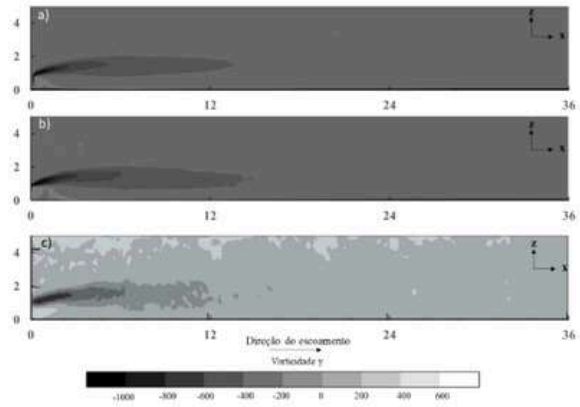


Figure 1. Result of the vorticity calculated in y in the xz plane at y=0.25 of the airflow through a wind barrier with 20% porosity obtained by the κ-ε Realizable (a) and κ-ω SST turbulence models compared to the experimental data from Dong et al. 2010 (c).

Figure 2 and Figure 3 figures demonstrate the impact of barrier porosity on the distribution of friction velocity in the protection region downstream of the barrier, particularly for barriers with 40% and 60% porosity, respectively. These figures show how increasing porosity affects the reduction in friction velocity, indicating a less aggressive decrease in wind speeds with higher

porosity levels. This suggests that while higher porosity might extend the protected area, it may not reduce wind speeds as effectively as lower porosity, which is crucial for controlling erosion.

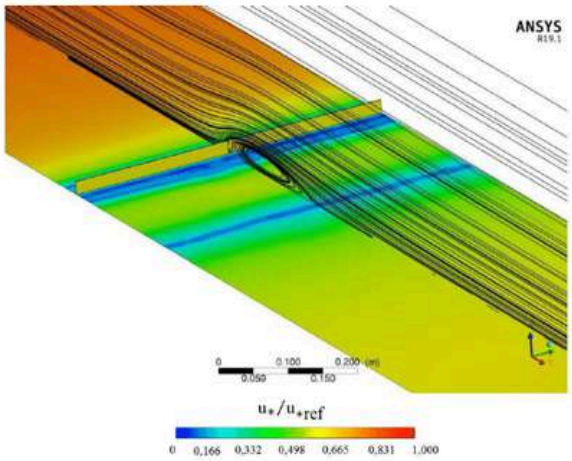


Figure 2. Friction velocity distribution and fluid flow pathlines for 20% porosity.

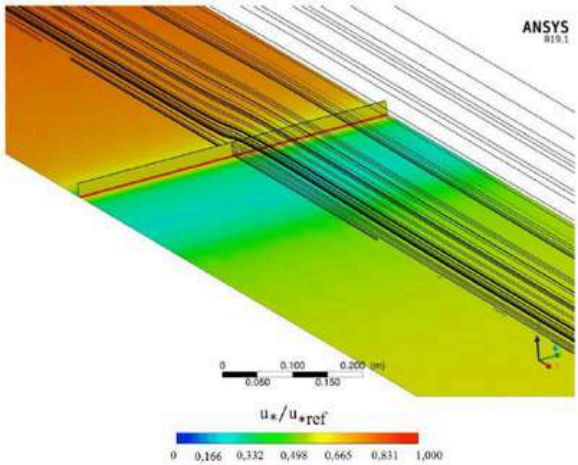


Figure 3. Friction velocity distribution and fluid flow pathlines for 60% porosity.

Based on the findings, the section discusses recommendations for optimizing barrier design, considering both erosion control effectiveness and environmental impacts. It emphasizes the need for a balanced approach in selecting barrier porosity, which must sufficiently disrupt wind flow to reduce erosion while avoiding adverse environmental impacts such as excessive airflow stagnation.

In conclusion, it provides a comprehensive analysis of how artificial wind barriers can be designed and implemented to control erosion effectively. The insights gained from the CFD simulations and experimental validations form a robust basis for enhancing barrier designs, contributing significantly to environmental management practices in industrial settings.

CONCLUSIONS

This paper investigated the turbulent atmospheric flow modified by artificial porous barriers applied to control wind erosion of granular materials. The main focus was on the analysis of how these barriers influence the reduction of airflow speed and the formation of a sheltered region due to their presence. The results obtained through numerical simulations showed that these barriers, when adequately dimensioned and positioned, are effective in reducing wind speed at ground level, thus diminishing the erosion process of granular materials. The simulations also highlighted the importance of the geometric configuration and porosity of the barriers, parameters that significantly affect the performance of these control mechanisms. Among the artificial barriers studied, those with porosity between 40% and 60% showed a balance between the reduction of wind speed and the extent of the protected area, proving to be the most efficient in controlling erosion. This optimal porosity range provides effective protection against erosion while allowing enough airflow to prevent the accumulation of airborne pollutants behind the barrier.

Additionally, the study confirmed that the correct application of CFD tools, complemented by experimental data, allows for accurate predictions of the effects of barriers on the airflow dynamics around storage yards. This approach facilitates the optimization of barrier designs, enhancing their effectiveness in practical applications.

REFERENCES

DONG, Z. et al. A wind tunnel simulation of the turbulence fields behind upright porous wind fences. Journal of Arid Environments, v. 74, n. 2, p. 193–207, Fev. 2010.

LIU, C. et al. Airflow around single and multiple plants. Agricultural and Forest Meteorology, v. 252, n. June 2017, p. 27–38, 2018.

SANTIAGO, J. L. et al. Evaluation of a CFD-based approach to estimate pollutant distribution within a real urban canopy by means of passive samplers. Science of the Total Environment, v. 576, p. 46–58, 2017.

SONG, C. F. et al. Numerical simulation of airflow structure and dust emissions behind porous fences used to shelter open storage piles. Aerosol and Air Quality Research, v. 14, n. 6, p. 1584–1592, 2014.

XU, Y.; CALAY, R. K.; MUSTAFA, M. Y. Feasibility of Computational Fluid Dynamics for Analyzing Airflow Around Porous Fences. Heat Transfer Engineering, v. 0, n. 0, p. 1–16, 2019. Disponível em: <https://doi.org/10.1080/01457632.2018.1546663>.

AIR POLLUTION CONFERENCE BRAZIL
CMAS SOUTH AMERICA
COMMUNITY MODELING AND ANALYSIS SYSTEM

INFLUENCE OF FILTER MEDIA MANUFACTURING METHOD ON THE FILTRATION PERFORMANCE OF BAG FILTERS

Ana Cristina Coelho Vieira[1*], Bruno José Chiaramonte de Castro[2], Rafael Sartim[2,3], Mônica Lopes Aguiar[1]

[1]*Graduate Program of Chemical Engineering, Federal University of São Carlos, Rodovia Washington Luís, s/n, 13565-905, São Carlos, SP, Brazil.*

[2]*Global R&D Brazil, ArcelorMittal, Avenida Brigadeiro Eduardo Gomes, nº 526, Polo Industrial Tubarão, 29160-904, Serra, ES, Brazil.*

[3]*Department of Industrial Technology, Federal University of Espírito Santo, Avenida Fernando Ferrari, 514, 29075-910, Goiabeiras, Vitória, ES, Brazil.*

**anacriscv21@gmail.com*

Abstract: Emissions of ultrafine particulate matter into the air are considered a global problem. These particles are inhalable and exposure to them can cause various types of diseases or even lead to death. As a result, there was a need to develop and optimize methods and equipment for controlling their emissions. In this context, the bag filter stands out as one of the most used devices nowadays, due to its high filtration efficiency, stability, reliability, and even resistance to high temperatures and chemical attack, depending on the bag material used. The way in which the filter medium is manufactured, such as needle felt and hydroentanglement, also affects its filtration efficiency and service life. The objective of this research is to analyze and compare the filtration performance of meta-aramid filter media, manufactured using the needle felt and hydroentanglement techniques, with times of use of 3 and 4 years in the bag filter of the desulfurization process of the steel industry. Filtration tests were performed on a filtration device based on the VDI 3926 standard, with pulse jet cleaning, in which the collection efficiency and the evolution of the pressure drop were evaluated during 30 filtration cycles. The hydroentangled filter medium had a twice as low permeability compared to the needle felt, in addition to a 25% larger average fiber diameter. The penetration of particulate matter was more challenging in the hydroentangled filter medium, thereby facilitating the cleaning process of the bags and enhancing filtration efficiency. After the 30 filtration cycles, the hydroentangled filter medium presented an efficiency of 99.9%, while the needled filter medium had an efficiency of 99.7%. The filtration cycles of the hydroentangled filter medium were longer than the cycles of the needled one, showing that the hydroentangled filter medium was less saturated with particles. As for the useful life over the years, the bags with 4 years of use showed greater residual pressure drop than the bags with 3 years of use, as expected, due to the accumulation of particulate matter in the filter medium over time. However, the increase in residual pressure drop was lower for the hydroentangled bag than for the needled one, which, for industrial use, means a longer service life.

Keywords: Gas Filtration, Bag Filter, Filter Media, Needle Felt, Hydroentanglement.

INTRODUCTION

At present, air pollution is acknowledged as the primary peril to human and environmental well-being. Among the diverse sources of air pollution, industries currently bear the principal responsibility for emitting particulate matter, $PM_{2.5}$ and PM_{10}, alongside gaseous pollutants such as sulfur dioxide (SO_2), carbon monoxide (CO), ozone (O_3), lead (Pb) and nitrogen dioxide (NO_2) (WHO 2023). Industries primarily rely on bag filters to mitigate the emission of particulate matter, owing to their high removal efficiency, resistance to elevated temperatures, and diverse chemical conditions. The bags, which are the filter media of the bag filters, can be made from a range of materials, including polyester and polyamides. Needle felt and hydroentanglement stand out as fiber bonding methods (Mukhopadhyay 2009; Karthik, C., e Rathinamoorthy 2016).

The manufacturing of the filter medium has a direct impact on the quality and efficiency of the filtration process. In the needle felt process, fibers are mechanically interconnected using barbed needle, yielding around 100 punctures per cm^2 and speeds reaching up to 2,000 needles per minute. Hydroentanglement represents an alternative to needle felt, employing ultra-fine water jets with high pressures and velocity. Pressures commonly fall within the range of 0.5 to 25 MPa (Hutten 2016; Cornier e Pursche 2023; Sutherland e Chase 2008).

The objective of this research is to analyse and compare the filtration performance of meta-aramid filter media, manufactured using the needle felt and hydroentanglement techniques, with times of use of 3 and 4 years in the bag filter of the desulfurization process of the steel industry. The particulate matter used in the experiments, taken from the industrial bag filter hopper, was also characterized. Filtration tests were performed on a filtration device based on the VDI 3926 standard, with pulse jet cleaning, in which the collection efficiency and the evolution of the pressure drop were evaluated during 30 filtration cycles (VDI 2004).

AIR POLLUTION CONFERENCE BRAZIL
CMAS SOUTH AMERICA
COMMUNITY MODELING AND ANALYSIS SYSTEM

METHODS

The particulate matter was characterized through analyses of specific mass, particle size distribution, and chemical composition. The filter media used, made of meta-aramid, were characterized by analyses of average fiber diameter, grammage, and air permeability. The filtration tests were conducted following the VDI 3926 standard, whose parameters are described in Table 1.

Table 1. Parameters of the VDI 3926 standard.

Parameter	Value
Surface velocity	2 m/min
Particle concentration	5.0 g/m³ ± 10 %
Temperature	20°C - 25°C
Relative humidity	< 50%
Cleaning tank pressure	5 bar ± 3 %
Maximum pressure drop	1000 Pa

Reference: Adapted from VDI, 2004.

Three samples were taken from each used bag along their length - one from the top, one from the middle, and one from the bottom - for the filtration tests. Thirty filtration cycles were performed on each filter medium sample. Each cycle was performed until the pressure drop reached 1000 Pa, when a pulse jet was activated to clean the sample.

FINDINGS AND ARGUMENT

The particulate matter characterization results are presented in Table 2. The average volumetric diameter of the particles was 26.95 µm, with 90% of them having a diameter smaller than 63.72 µm, with calcium and iron being the predominant elements in the chemical composition of the material. Additionally, other chemical compounds, including sulfur, chlorine and aluminum, have also been identified.

Table 2. Particulate matter characterization.

Characterization		Value
Specific mass (g/cm³)		2.85 ± 0.01
Chemical composition (% mass)	Ca	58.37 ± 0.18
	Fe	30.51 ± 0.11
	Others	11.12 ± 0.02

The results of the characterization of the filter media can be seen in Tables 3 and 4.

The hydroentangled filter medium exhibited lower values of grammage and permeability compared to the needled one. Additionally, the hydroentangled filter medium showed a larger diameter compared to the needled one. These results suggested greater airflow resistance through the hydroentangled medium. The high grammage of the used filter media were due to the presence of accumulated dust, while the considerable deviation resulted from the measurements taken in different regions of the bag.

Table 3. Characterizations of needled filter medium.

Characterization	Needled filter medium	
	3 years of use	4 years of use
Grammage (g/m²)	2199.80 ± 424.94	2215.39 ± 911.76
Permeability at 125 Pa (m³/m².min)	5.31 ± 0.23	5.94 ± 1.88
Fiber Diameter (µm)	12.58 ± 2.22	12.77 ± 2.32

Table 4. Characterizations of hydroentangled filter medium.

Characterization	Hydroentangled filter medium	
	3 years of use	4 years of use
Grammage (g/m²)	996.94 ± 65.68	1032.02 ± 42.41
Permeability at 125 Pa (m³/m².min)	2.19 ± 0.05	3.25 ± 0.09
Fiber Diameter (µm)	16.47 ± 2.74	15.31 ± 2.46

Figures 1 and 2 depict the pressure drop results over time for the 30 filtration cycles of the three samples of each filter medium utilized.

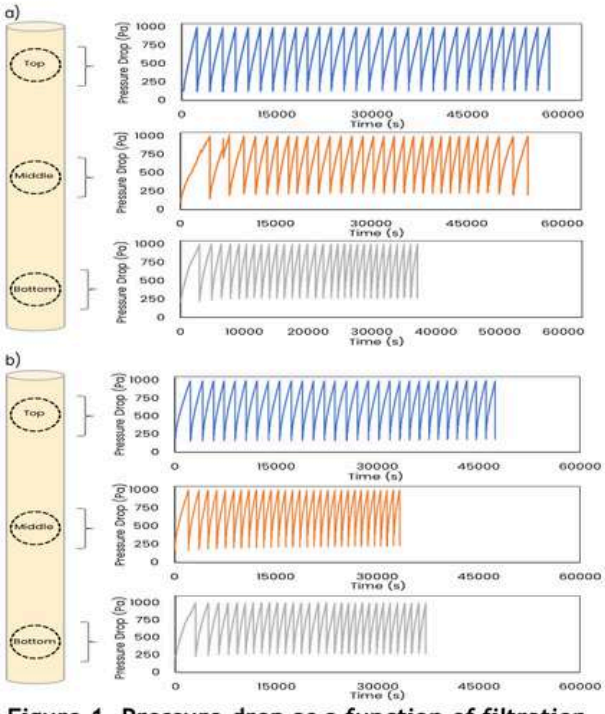


Figure 1. Pressure drop as a function of filtration time in the needled filter media of 3 years (a) and 4 years (b).

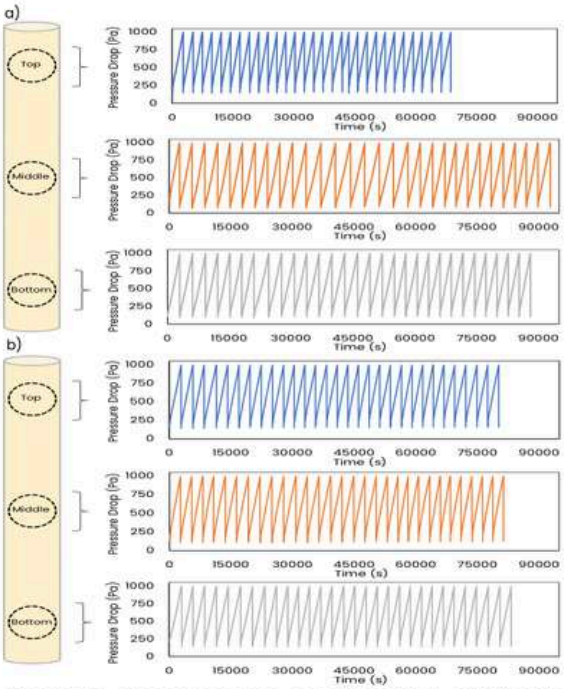


Figure 2. Pressure drop as a function of filtration time in the hydroentangled filter media of 3 years (a) and 4 years (b).

A significant distinction in behavior was observed along the length of the needled felt bag. The residual pressure drop in the sample from the bottom was considerably higher than the one of the samples of the top and middle, making the pressure drop to reach 1000 Pa faster, and the pulse jet to occur in a shorter time interval. This disparity may be attributed to the heterogeneous distribution of particulate matter inside the bag filter, with a higher concentration reaching the bottom of the bags.

Regarding the period of use, transitioning from 3 to 4 years, there was an increase in the residual pressure drop and a decrease in filtration time across all samples of the needled felt filter medium. This outcome was expected, as the residual pressure drop tends to increase over the time of use, due to the particle accumulation among the fibers.

The behavior of the hydroentangled filter medium was clearly different from the behavior of the needled felt filter medium. Despite the high dust concentrations at the bottom of the bag, the hydroentangled medium was not affected as much as the needled felt medium, which resulted in a lower and consistent pressure drop over time across the entire length of the bag. Additionally, the hydroentangled medium exhibited a longer filtration time. When comparing the 3- and 4-year intervals, the reduction in filtration time was not pronounced.

The hydroentangled filter medium presented a higher efficiency, of over 99.9%, while the the needled felt achieved an efficiency of approximately 99.7%. This result suggests more effective filtration and a more stable retention of particles in the hydroentangled medium.

CONCLUSIONS

The needled felt medium exhibited a smaller fiber diameter and a higher permeability than the hydroentangled one. The smaller fiber diameter may facilitate particle penetration into the medium, while the higher permeability can lead to more significant clogging, with particle deposition occurring inside the filter medium. These characteristics of the needled felt medium resulted in higher residual pressure drops and made the cleaning process more challenging during filtration, consequently reducing the total filtration time.

In contrast, the hydroentangled bag presented a more homogeneous behavior along its length regarding the residual pressure drop and the duration of the filtration cycles. It maintained superior efficiency and lower residual pressure drop during filtration, even after 3- and 4-years of use. This highlights its ability to maintain a stable and efficient performance.

REFERENCES

Cornier, Jean, e Franz Pursche, orgs. 2023. *Particle Technology and Textiles*. De Gruyter. https://doi.org/10.1515/9783110670776.

Hutten, Irwin M. 2016. *Handbook of Nonwoven Filter Media*. 2nd ed. Oxford: Butterworth-Heinemann.

Karthik, T., Prabha Karan C., e R. Rathinamoorthy. 2016. *Nonwovens: Process, structure, properties and applications*. 1st ed. New Delhi: Woodhead Publishing India Pvt. Ltd.

Mukhopadhyay, Arunangshu. 2009. "Pulse-jet filtration: An effective way to control industrial pollution Part I: Theory, selection and design of pulse-jet filter". *Textile Progress* 41 (4): 195–315. https://doi.org/10.1080/00405160903437948.

Sutherland, Kenneth S, e George Chase. 2008. *Filters and Filtration Handbook*. 5th ed. Oxford: Elsevier Science.

VDI. 2004. "VDI 3926: Testing of filter media for cleanable filters Standard test for the evaluation of cleanable filter media". Düsseldorf: Verein Deutscher Ingenieure. outubro de 2004. https://www.vdi.de/en/home/vdi-standards/details/vdi-3926-blatt-1-testing-of-cleanable-filter-media-standard-test-for-the-evaluation-of-cleanable-filter-media.

WHO. 2023. "WHO ambient air quality database, 2022 update". World Health Organization. 2023. https://iris.who.int/bitstream/handle/10665/368432/9789240047693-eng.pdf?sequence=1.

AIR POLLUTION CONFERENCE BRAZIL
CMAS SOUTH AMERICA
COMMUNITY MODELING AND ANALYSIS SYSTEM

CFD ANALYSIS OF THE EFFICIENCY OF A CANOPY HOOD FOR HOT PROCESSES

Andre Palmiro Storch[1,2], Bruno Furieri[1], Rafael Sartim[1,2]
[1]*Universidade Federal do Espírito Santo*
andre.pstorch@gmail.com
[2]*ArcelorMittal Global R&D Brazil*

Abstract: To minimize the health hazards by fugitive emissions of gases and particulate matter in high temperature industrial processes, local exhaust ventilation is often used. Overhead canopy hoods are typically used to receive contaminants from operations in which direct extracting the emissions from their sources is not possible. Due to the distance from the source and the hood, air entrainment in the plume induces a large airflow requirement at the hood. To estimate the necessary flow rate to capture the emissions, the Industrial Ventilation Manual (ACGIH) presents empirical equations that guide the design of a canopy hood. Previous works have shown the benefits of using CFD as a tool for evaluating an exhisting canopy hood design and proposing modifications to increase its efficiency. The present work aims to investigate the efficiency of a canopy hood designed using the best practice equations from the Industrial Ventilation Manual. The results show that although the best practice equations offer a baseline to start the project of a canopy hood, it has low efficiency in capturing the emissions from hot processes that emit gases an particulate matter at high flow rates.

Keywords: CFD, fugitive emissions, air pollution control, local exhaust ventilation.

INTRODUCTION

Air pollution with particulate matter and gases emitted from industrial processes can negatively affect the environment and, therefore, human health. The World Health Organization estimates the combined effects of ambient air pollution and household air pollution is associated with 7 million premature deaths annually (World Health Organization, 2022). Particles with a size less than 2.5 μm can be especially dangerous when inhaled, as they can penetrate the body, causing long term lung and heart diseases (El Morabet, 2019). In many industrial processes, workers can be exposed to levels higher than acceptable of air pollutants, and the indoor air pollution of these workplaces is one of the main causes of work-related diseases. In addition to its negative effects on human health, poor air quality affects the workers' comfortability and their productivity (Alzboon; Forton, 2019).

To minimize the risks of exposure to hazardous gases and particulate matter in the workplace, a local exhaust ventilation system can be implemented, in which the emissions are extracted directly from the source using exhaust hoods that direct the gases and particulate matter from the emission source to an air cleaning equipment, before releasing the gases to atmosphere (Macintyre, 1990; ACGIH, 2019). On the many different industrial ventilation solutions, Overhead canopy hoods are typically used to receive contaminants from operations in which directly extracting the emissions from their sources is not possible (ACGIH, 2019). The required airflow for these hoods then becomes proportional do their distance from the sources (ACGIH, 2019). Nevertheless, the dynamics of the operation can change the capturing efficiency of the hood, given that the flow rate of emissions can change over time (Macintyre, 1990; ACGIH, 2019)

The industrial ventilation manuals and best practice's equations for designing a new canopy hood assume that the hood will have 100 % efficiency for a given set of source constant parameters (temperature difference between source and ambient air) (Macintyre, 1990; ACGIH, 2019). However, studies of hood capturing efficiency of transient buoyant plumes from industrial operations have shown that a 100 % efficiency is not always the case in industrial installations, either because of geometric factors related to hood design or source parameters that are not foreseen by the industrial ventilation manuals, namely the velocity of emission at its source (Nielsen; Madsen; Tveit, 1991; Cascetta; Rosano, 2001; Kulmala et al., 2007) In steelmaking applications, for instance, the temperature and reaction rates of one process that emit dust and gases can have different ranges, because of the different composition that the liquid metal has from one heat to another (Fruehan, 1998).

The present work proposes the analysis of the effect that the velocity of a high temperature emission has in the capture efficiency of a canopy hood designed by the ACGIH Industrial Ventilation equations, to identify the cause for the differences found between the equations and real applications, using Computation Fluid Dynamics (CFD).

METHODS

The emission source used in this work was selected from the study of Huang *et al.* (2021), in which the authors study the turbulent characteristics of a buoyant jet with constant velocity of 1 m/s and varying temperature from 30 °C to 1200 °C, using experimental and numerical methods. The apparatus consists in a plume generator with diameter 0.38 m placed 0.8 m from the floor, and the dimensions of the room is 6 m x 6 m x 8 m (width x length x height). Although they varied the source temperature from 30 °C to 1200 °C, only their results for 1200 °C are used in the present work.
In the present study, a canopy hood was designed following the Industrial Ventilation Manual equations (ACGIH, 2019) to investigate the efficiency of a hood designed by those equations in capturing the high temperature emission. Figure 1 shows the necessary parameters to design a canopy hood for a hot source.

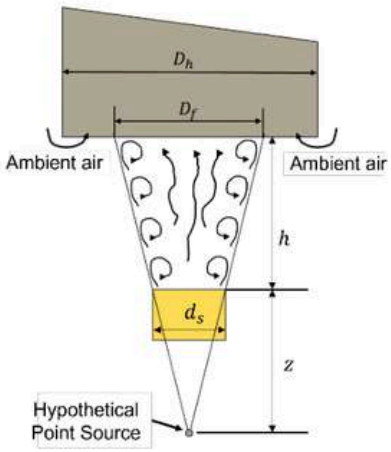


Figure 1. Canopy hood representation above a hot source, showing the parameters needed for calculating its position and dimensions. Source: Adapted from (ACGIH, 2019).

The set of equations bellow (Equation 1) determines each parameter necessary to design the canopy hood. All of the dimensions are in the International System of Units.

$$D_f = 0.43(h+z)^{0.88}$$

$$z = (2.6d_s)^{1.138}$$

$$v_f = 0.084(A_s)^{0.33}\frac{\Delta T^{0.42}}{(h+z)^{0.25}} \qquad (1)$$

$$D_h = D_f + 0.8(h+z)$$

$$Q_t = v_f A_f + v_r(A_h - A_f)$$

where D_f is the emission plume diameter when it reaches the hood, h is the distance of the canopy hood's face from the top of the plume's source, z is the distance from the source surface with diameter d_s to a hypothetical point source (when simplifying the plume as a cone), v_f is the velocity of the plume at the hood face, A_s is the area of the source, ΔT is the temperature difference between the hot source and the ambient air, Q_t is the total volume flow rate entering the hood, A_f is the cross sectional area of the plume at the hood face, A_h is the area of the face of the hood and v_r is the required air velocity through the remaining hood area. Figure 2 shows the canopy hood designed by the equations aforementioned. It has a rectangular entrance, as it is a common design used in industry (ACGIH, 2019). The distance between the source and the hood face is equal to 4 d_s. The exhaust duct diameter is calculated so that the airflow have a velocity of $v_d = 20\,m/s$ inside the duct, using the relation $Qt = v_d/Area_d$.

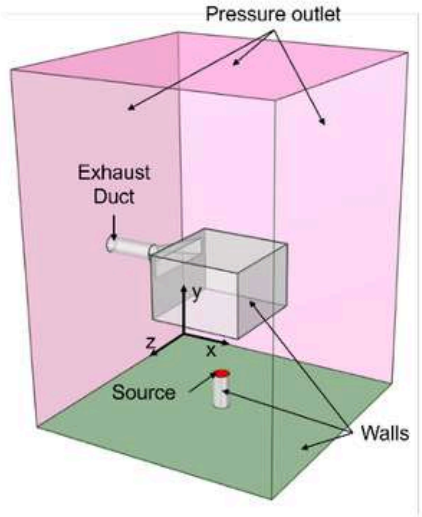


Figure 2. Boundary conditions used in the CFD model. Source: Author.

The high temperature is modelled as a buoyant jet with varying velocity boundary condition of 1 - 18 m/s at the source at temperature of 1200 °C. The exhaust flow of 20 m/s is imposed at the exit of the exhaust duct. The outer surfaces of the numerical domain are pressure outlets operating at 1 atm, and the walls are in no-slip condition.
The numerical model is solved using the commercial CFD code ANSYS Fluent 2020 R1 ©. The emission is taken as ideal gas air, where the density is a function of temperature following the equation of state for ideal gases. The flow is considered as steady-state. To model the turbulence, the Reynolds Stress Model (RSM) is used. Finally, in order to calculate the exhaust efficiency of the canopy hood, a passive scalar transport equation is used to trace the concentration of the emission throughout the domain. The efficiency of the canopy hood is calculated using Equation 2 at the exit of the exhaust duct.

$$\eta(\%) = \frac{\phi \cdot \dot{m}_d}{\dot{m}_s} \qquad (2)$$

where ϕ is the passive scalar concentration, $\dot{m}_d$ is the mass flow rate at the exit of the exhaust duct and $\dot{m}_s$ is the mass flow rate at the source.

FINDINGS AND ARGUMENT

Figure 3 shows the plume capture efficiency curve of the canopy hood in terms of source velocity. From a source velocity of 1 m/s to 12 m/s, the hood presents an efficiency of approximately 100 %. From a source velocity of 12 m/s to 14 m/s, there is a sharp decrease in the efficiency, from 99.87 % to 85 %, showing that, for the designed canopy hood of this study, the limit source velocity for most of the emission capture is between 12 m/s and 14 m/s.

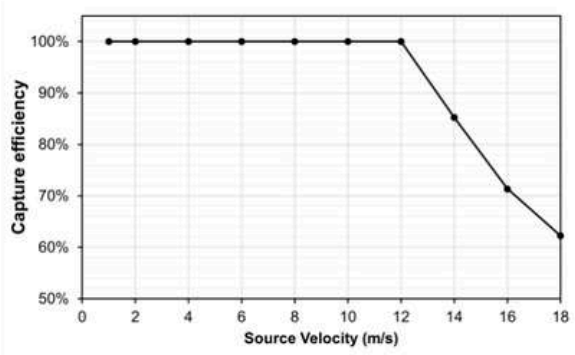


Figure 3. Airflow ratio and plume capture efficiency curves. Source: Author.

When ploting the velocity vector field at the face of the hood for the cases where the source velocity is 12 m/s and 14 m/s, one can see the effect of the buoyant jet entering the hood, where the velocity follows a gaussian distribution with its maximum magnitude at the center of the jet (Figure 4a). However, for the 14 m/s case, as the source velocity increases, some of the airflow start to exit the hood at the corners of its face, as shown in Figure 4b.

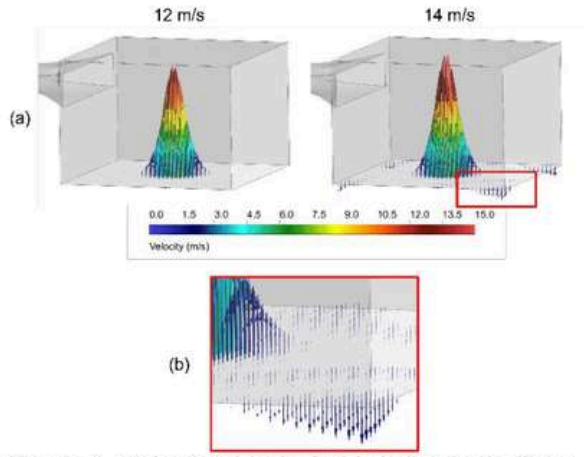


Figure 4. Velocity vector field at the face of the hood. Source: Author.

CONCLUSIONS

The present work used CFD to evaluate the efficiency of canopy hood when capturing an emission from a high temperature source with varying velocity. The equations to design the hood do not consider the initial velocity of the emission at the source. Given that some industrial processes can have different states where the flow rate of the emission changes, it is important to evaluate the limits of a canopy hood designed by those equations. The results showed that for an emission source velocity varying from 1 m/s to 12 m/s, the efficiency of its canopy hood is approximately 100 %. For greater source velocities, its efficiency sharply decreases, meaning that fugitive emissions occur in the vicinity of the process. However, for future works, it is recommended that different heights of the canopy hood to the source be simulated in order to investigate the efficiency curve of the canopy hood.

REFERENCES

ACGIH. American Conference of Governmental Industrial Hygienists. *Industrial Ventilation: A manual of recommended practice for design*. 30. ed. Cincinnati, OH: ACGIH, 2019.

Alzboon, K.; Forton, O. *Indoor air quality in steel making industries*. Environmental Management and Sustainable Development, v. 8, p. 147, 02 2019.

Cascetta, F.; Rosano, F. *Assessment of velocity fields in the vicinity of rectangular exhaust hood openings*. Building and Environment, v. 36, n. 10, p. 1137–1141, 2001.
ISSN 0360-132

El Morabet, R. *Effects of outdoor air pollution on human health*. Elsevier, 2019.

Fruehan, R. J. *The making, shaping and treating of steel: steelmaking and refining volume*. AISE Steel Foundation, 1998.

Huang, Y. et al. *Flow-field evolution and vortex structure characteristics of a high-temperature buoyant jet*. Building and Environment, v. 187, 2021. ISSN 03601323.

Kulmala, I. et al. *Local ventilation solution for large, warm emission sources*. The Annals of occupational hygiene, v. 51, p. 35–43, 02 2007.

Macintyre, A. J. *Ventilação industrial e controle da poluição*. 2. ed. Rio de Janeiro, RJ: LTC, 1990. p. 403.

Nielsen, P. V.; Madsen, U.; Tveit, D. J. *Experiments on an exhaust hood for the paint industry*. Dept. of Building Technology and Structural Engineering, 1991.

World Health Organization. *Air pollution*. 2022. Url https://www.who.int/health-topics/air-pollutiontab=tab2

AIR POLLUTION CONFERENCE BRAZIL
CMAS SOUTH AMERICA
COMMUNITY MODELING AND ANALYSIS SYSTEM

FLOW BEHAVIOR INSIDE BAG FILTERS: A REVIEW OF EXPERIMENTAL STUDIES

Bruna Lima Veras Maia, Msc[1], Renata Drumond Corrêa[1], Taciana Toledo de Almeida Albuquerque PhD[1],*, Rafael Sartim, PhD[2]

[1] *Federal University of Minas Gerais, Department of Sanitary and Environmental Engineering, Avenida Antonio Carlos, 31270-901, Brazil*

brunaveras@ufmg.br, redrummondc@outlook.com, taciana@desa.ufmg.br

[2] *ArcelorMittal - Global R&D Brazil, Avenida Brigadeiro Eduardo Gomes, Polo Industrial Tubarão, 29160-904, Brazil.*

rafael.sartim@arcelormittal.com.br

Abstract: Bag filters can be considered the main equipment adopted by industries to control particulate matter emissions. Its advantage over other equipments is related to high collection efficiency. Studies show that the high performance of this equipment depends not only on the filter media adopted but also on the flow behavior. Flow analysis inside bag filters using computational fluid dynamics has appeared in the literature. However, despite the majority one showing the potential of this tool, validation studies of mathematical modeling are still lacking in the scope of these works. Therefore, within this context, the present work aims to present a compilation of works from the open literature that carried out experiments on bag filters, highlighting the trends observed as well as the methodologies adopted for data collection to provide as a reference for researchers looking for ways to obtain experimental data for validation CFD studies in bag filters.

Keywords: Bag filters, pulse-jet baghouse, CFD, empirical data collection.

INTRODUCTION

Particulate matter, a significant air pollutant, consists of suspended particles, liquid, or solid, with composition varying according to emission sources [1]. Its adverse effects, according to World Health Organization, can manifest after short or long-term exposure [2]. Studies show a range of health issues linked to particulate matter exposure, from cognitive function changes to increased cardiovascular events [3, 4]. There is a significant association between respiratory hospitalizations and exposure to high particulate matter environments [5]. Moreover, smaller particulate matter sizes are associated with greater health risks [6].

The industrial sector, especially energy production, and vehicular emissions are major sources of this pollutant [7]. Bag filters are commonly used to control PM emissions. These filters use a filter medium to capture particles from gas flow, with a pulse jet cleaning system being widely adopted for its efficiency [8]. However, maintaining high collection efficiency requires proper equipment functioning, often associated with the cleaning system used. Bag wear, impacting collection efficiency, is a major maintenance issue associated with flow behavior during filtration or cleaning [9-12].

Computational Fluid Dynamics (CFD) has been used to study bag filter flow behavior, aiding in retrofitting existing systems or designing new ones. Studies have shown that gas entrance geometry and position influence flow distribution [10], and that bag wear can be associated with specific bag positions relative to intense gas flow regions [11]. Additionally, the manner in which pulse cleaning is guided by cleaning nozzles influences dust cake removal [14, 15].

While many CFD studies have been conducted, few have validated numerical data [13, 14]. Validation is crucial to ensure the reliability of CFD models [16]. A comparative test between calculated and experimental data is the main method used for validation [17]. Therefore, this study aims to compile existing experimental data on bag filters from open literature, highlighting observed trends and methodologies for data collection, to serve as a reference for researchers conducting CFD validation studies in bag filters.

METHODS

The methodology involved a systematic search for experimental studies to validate computational fluid dynamics simulations of bag filters and their cleaning systems. The search was conducted using Elsevier, Scopus, Periodicos Capes, Google Scholar, and SciELO portals. Keywords were established according to a prior study and the search string was defined: ("bag filter" OR "fabric filter bag" OR "fabric filter" OR "bag house") AND ("pulse-jet cleaning system" OR "pulse-jet baghouse") AND ("computational fluid dynamics" OR "CFD") AND ("experiment" OR "experimental" OR "empirical").

FINDINGS AND ARGUMENT

Tab. 1 presents a summary of the experiments performed by the works presented in this review.

These are studies related to understanding flow behavior, so the parameters measured are velocity and pressure. The position of the sensors will depend on the aim of the study. Yoa et al. [18] and Chen [19] aimed to investigate the influence of equipment design on pressure drop, while Fu and Zhao [20] and Saleem et al. [21] aimed to verify velocity profiles to understand the flow behavior in the equipment. Li et al. [24] and Qian et al. [23] aimed to evaluate the influence of tube and nozzle characteristics, respectively, on the uniformity of pulse jet cleaning. Li et al. [25] verified the performance of pulse jet cleaning under different particle sizes. For cases with transient states, it is important to be aware of the collection frequency.

Table 1. Equipment design, experimental conditions and data collection information from the works presented in the review.

Reference	Bag Filter and Cleaning System	Sensors
Simon et al. (2007)	Bag Filter Scale: pilot Number of bags: 24 Bag type: fabric Bag dimensions: 1500 mm length, 130 mm diameter Flow Conditions Gas: air with particulate Tank volume: - Pulse duration: 100 - 1000 ms Parameters measured Pressure drop, medium acceleration, face velocity at filter surface and axial velocity	Sensor: PD-41/ 8885.D-0.05, Brüel and Kjaer Type 4393 V, AFS-200, AVS-1024D1W224, respectively Collection points and sensors positions Fixed at location: Yes Number of points: 4 Position: points were set inner the bag in diferente positions along the length of the bag Frequency 100 Hz, 2048 Hz, 100Hz and 100 Hz, respectively
Qian et al. (2018)	Cleaning System Scale: pilot Number of bags: 2 Bag type: cartridge Bag dimensions: 660 mm length, 215 mm internal diameter, 325 mm external diameter Flow Conditions Gas: air without particulate Tank volume: 0.0268 m^3 Pulse duration: 0.08 s Parameters measured Peak pressure	Sensor: MYD-1540A Collection points and sensors positions Fixed at location: Yes Number of points: 3 Position: points were set inner the bag in different positions along the length of the cartridge Frequency 40kHz

Reference: Authors, 2024.

Yoa et al. [18] investigated the influence of gas feed position and particle energization on the pressure drop and collection efficiency of bag filters. They found that the position of the gas inlet significantly affects the performance of the equipment. Tangential gas inlets showed lower pressure drops compared to the central inlet, especially at high velocities. Additionally, tangential entries demonstrated higher collection efficiencies due to the centrifugal movement of the flow, favoring inertial particle collection.

Chen [19] studied the impact of baffle plate design on pressure drop in bag filters. Three cases were examined: distributor 1, with three plates perpendicular to the inlet flow; distributor 2, with two plates, one inclined at 60° and the other perpendicular to the flow; and no distributor. Results showed that while all cases exhibited similar pressure drops at low filtration velocities, distributor 1 increased pressure drop as velocity increased, while distributor 2 reduced it. This was explained by the barrier effect, more pronounced in case 1 due to the perpendicular positioning of the plates.

Fu and Zhao [20] investigated flow distribution between bags in a bag filter. They found non-homogeneous flow distribution, with bags closest to the gas inlet wall experiencing higher velocities compared to other bags. This behavior was attributed to the gas jet effect directing flow to the opposite wall, resulting in higher gas flow and filtration velocities. Most collected data showed velocities above the design filtration velocity, indicating non-ideal filtration conditions.

Saleem et al. [21] analyzed flow behavior during bag regeneration in pulse jet bag filters. They observed that axial velocity profiles varied according to the cleaning of neighboring bags, with a reduction in measured velocities during regeneration and an increase after regeneration. Flow distribution was strongly influenced by the dust load on the filter medium surface, affecting cake formation properties.

Simon et al. [22] characterized flow behavior during the cleaning process in pulse jet bag filters. They found uneven regeneration of bags due to non-uniform pressure and velocity distribution on bag surfaces. Other studies have investigated the influence of cleaning system accessories design on bag cleaning performance.

Qian et al. [23] evaluated various operating parameters' impact on cleaning effectiveness in

pulse jet cartridge filters. They found that higher peak pressures were associated with greater uniformity in cleaning. Additionally, they identified an optimal total nozzle area in the blow tube.
Li et al. [24] investigated the influence of compressed air tank pressure on pulse jet flow. They observed that higher tank pressures resulted in higher pressure peaks and transient pressures below injection holes, affecting cleaning efficiency. Li et al. [25] studied the effect of cleaning mode on cartridge filter performance under different particle sizes. They observed that smaller particles resulted in greater pressure drops and residual pressure, indicating poorer cleaning efficiency.

CONCLUSIONS

This review highlights investigations into flow dynamics within key particulate matter emission control equipment. Findings reveal discrepancies between design hypotheses and actual flow behavior in bag filters: non-homogeneous flow distribution, ineffective flow distributor plates, and uneven dust cake dislodgment. Data collection, including velocity and pressure profiles, proved crucial for understanding these phenomena. With the advancement of instrumentation technology, it is possible to obtain more efficient sensors in addition to those adopted by the works presented here. However, the location and choice of collection points remains relevant. In view of the growing demand for computational fluid dynamics analysis and the importance of validating the numerical data, the present work presents a compilation of information regarding the expected trends of the flow behavior inside the bag filter as well as guidelines from the literature for empirical data collection.

REFERENCES

J. I. Steinfeld, S. N. Pandis, *Atmospheric Chemistry and Physics: From Air Pollution to Climate Change*, 2nd ed., John Wiley & Sons, New Jersey **1998**.
World Health Organization. Air quality guidelines for particulate matter, ozone, nitrogen dioxide and sulfur dioxide: Global update 2005 - Summary of risk assessment. Suíça: WHO, 2005.
J. A. Ailshire, P. Clarke, *J. Gerontol.* **2014**, *70 (2)*, 322-328. DOI: doi:10.1093/geronb/gbu064
S. Koton, N. Molshatzki, Yuval, V. Myers, D. M. Broday, Y. Drory, D. M. Steinberg, Y. Gerber, *Prev. Med.* **2013**, *57 (4)*, 339-334. DOI: http://dx.doi.org/10.1016/j.ypmed.2013.06.009
E. S. Coker, R. Buralli, A. F. Manrique, C. M. Kanai, A. K. Amegah, N. Gouveia, *Environmental Research*. **2022**, *214* (1), 1-10. DOI: https://doi.org/10.1016/j.envres.2022.113738
K. Kim, E. Kabir, S. Kabir, *Environ. Int.* **2015**, *74*, 136-143. DOI: http://dx.doi.org/10.1016/j.envint.2014.10.005
D. Pimentel, S. Cooperstein, H. Randell, D. Filiberto, S. Sorrentino, B. Kaye, C. Nicklin, J. Yagi, J. Brian, J. O'Hern, A. Habas, C. Weinstein, *Hum. Eco.* **2007**, *35*, 653-668. DOI: DOI 10.1007/s10745-007-9128-3
Y. Cuiping, L. Guijian, C. Haiyan, *Powder Technol.* **2013**, *249*, 424-430. DOI: https://doi.org/10.1016/j.powtec.2013.09.017
S. M. S. Rocha, F. B. Marques, F. A. R. Pereira, D. C. Ribeiro, *Chem. Eng. Trans.* **2014**, *39*, 1369-1374. DOI: https://doi.org/10.3303/CET1439229
T. W. C. Pereira, F. B. Marques, F. A. R. Pereira, D. C. R. Ribeiro, S. M. S. Rocha, *J. Clean. Prod.* **2016**, *111*, 117-124. DOI: http://dx.doi.org/10.1016/j.jclepro.2015.09.070
W. F. Lima, R. Huebner, *ETASR* **2019**, *9 (4)*, 4452-4456. DOI: https://doi.org/10.48084/etasr.2732
C.P. Yan, G.J. Liu, H.Y. Chen. *Powder Technol.* **2013**, *249*, 424-430. DOI: https://doi.org/10.1016/j.powtec.2015.06.071
S. Park, Y. H. Joe, J. Shimb, H. Park, W. G. Shina, *J. Hazard. Mater.* **2019**, *365*, 440-447. DOI: https://doi.org/10.1016/j.jhazmat.2018.10.098
B.O. Andersen, N.F. Nielsen, J.H. Walther, *Powder Technol.* **2016**, *291*, 284-298. DOI: http://dx.doi.org/10.1016/j.powtec.2015.12.028
L. Lin, T. Liu, N. Yuan, Z. Xu, H. Chen. *Powder Technol.* **2021**, *377*, 139-148. DOI: https://doi.org/10.1016/j.powtec.2020.08.097
W. L. Oberkampf, T. G. Trucano, *Prog. Aerosp. Sci.* **2002**, *38*, 209-273. DOI: https://doi.org/10.1016/S0376-0421(02)00005-2
H. K. Versteeg, W. Malalasekera, *An Introduction to Computational Fluid Dynamics: The Finite Volume Method*, 2nd ed., Pearson Prentice Hall, Essex **2007**.
S. Yoa, Y. Cho, Y. Choi, J., *Korean J. Chem. Eng.* **2001**, *18 (4)*, 539-546.
C. Chen, *J. Air Waste Manag. Assoc.* **2001**, *51 (10)*, 1471-1475. DOI: https://doi.org/10.1080/10473289.2001.10464364
H. M. Fu, Y. J. Zhao, *Adv. Mat. Res.* **2012**, *508*, 254-258. DOI: https://doi.org/10.4028/www.scientific.net/amr.508.254
M. Saleem, M. S. Tahir, G. Krammer, *Chem. Eng. Technol.* **2012**, *35 (12)*, 2161-2169. DOI: https://doi.org/10.1002/ceat.201200287
X. Simon, S. Chazelet, D. Thomas, D. Bémer, R. Régnier, *Powder Technol.* **2007**, *172*, 67-81. DOI: https://doi.org/10.1016/j.powtec.2006.10.005
Y. Qian, H. Chen, H. Dai, T. Liu, T. Kuang, L. Bian, *Sep. Purif. Technol.* **2018**, *191*, 244-249. DOI: http://dx.doi.org/10.1016/j.seppur.2017.09.037
S. Li, F. Zhou, B. Xie, F. Wang, *Powder Technol.* **2018**, *328*, 264-274. DOI: https://doi.org/10.1016/j.powtec.2018.01.013
S. Li, S. Song, F. Wang, H. Jin, S. Zhou, B. Xie, S. Hu, F. Zhou, C. Liu, *Adv. Powder Technol.* **2019**, *30*, 1835-1841. DOI: https://doi.org/10.1016/j.apt.2019.05.029

AIR POLLUTION CONFERENCE BRAZIL
CMAS SOUTH AMERICA
COMMUNITY MODELING AND ANALYSIS SYSTEM

CASE STUDY: LOW NO_X BURNER İN A PELLETİZİNG PLANT

Andrielly Moutinho Knupp[1], Rossano Augusto Pilon Nunes[2], Ricardo Costa[3], Renata Favalli[4], Ana Buzatti[5], Diego Bernhard[6]

[1]*Vale*
andrielly.knupp@vale.com
[2]*Vale*
rossano.pilon@vale.com
[3]*FCTCombustion*
ricardo.costa@fctinternational.com
[4]*FCT Combustion*
renata.favalli@fctinternational.com
[5]*FCT Combustion*
ana.buzatti@fctinternational.com
[6]*FCT Combustion*
diego.bernhard@fctinternational.com

Abstract: *Nitrogen oxides (NO_x) are pollutants that can be produced by natural or anthropogenic processes. NO_x emissions of anthropogenic origin are mainly the result of the burning of fossil fuels at high temperatures. In pelletizing furnaces, mineral coals are used, and natural gas is burned, both processes contributing to nitrogen oxides emissions. Vale has a target to reduce 10% of all NO_x emissions by 2030. Given this scenario and aiming to reduce NO_x emissions at the Tubarão Unit - Vitoria, Espirito Santo/Brazil, a case study is proposed for the development of a burner for pelletizing furnaces with low NO_x emission. To better understand the NO_x formation in pellet furnaces, as well as what can be done to reduce NO_x emissions in existing plants, a series of CFD (Computation Fluid Dynamics) modelling scenarios were studied. The working scenarios were: Scenario number 1 - a 4,9 MW burner firing 3MW of natural gas in atmospheric air, defined as Base Case; Scenarios 2, 3, 4 and 5, respectively: i) a 4,9 MW burner firing 3MW of natural gas in atmospheric air, with addition of water at a flow rate of 60 l/h (75 µm droplet size and 36 degrees open cone spray spray); ii) 120 l/h (75 µm droplet size and 36 degrees open cone spray spray); iii) 120 l/h (120 µm droplet size and 88 degrees open cone spray spray); 160 l/h (120 µm droplet size and 88 degrees open cone spray spray). For the CFD modelling, the integral geometric model of one combustion chamber was considered. The computational mesh created had 1 million cells, which was refined during calculations in regions with high gradients. The models used were: k-ε for for turbulence, EDC (Eddy Dissipation Concept) for turbulence-chemistry interactions, the reduced mechanism DRM19 (19 species and 84 reactions), and DPM (Discrete Phase Model) for water droplets calculations. Regarding NO_x simulation, just the thermal NO_x generation was considered as this is the main mechanism of NO_x formation in pelletizing furnaces. With the modelled scenarios, no significant changes in flame shape, as per iso-surfaces of carbon monoxide (CO), were observed due to water addition. Up to 50 oC reduction in peak temperatures in the flame core was observed on the scenarios with water injection at the 120 l/h and 160 l/h flow rates. Considering the evaluated scenarios, a reduction in the range of 30% to 50% in NO_x emission was observed, with the scenarios applying 120 l/h with droplets of 75 mm and 160 l/h with droplets of 120 mm, the ones with the greatest NO_x reduction (50%). Given the results obtained, a water injection nozzle to fit into the central part of the burner was developed and will be tested in an industrial environment to validate the NO_x reduction observed in the simulations.*

Keywords: NO_x emissions, emissions control, low NO_x burner, pelletizing plant.

INTRODUCTION

The emission of nitrogen oxides (NO_x) poses a challenge for the pelletizing industries mainly due to the fuels that are burned. In general, there are several technologies that have been applied to reduce NO_x emissions such as Low- NO_x burners (LNBs) and post combustion NO_x control - like the Selective Catalytic Reduction (SCR-DeNO_x). Low-NO_x burner (LNB) is one of the most popular NO_x control technologies (Ballester et al., 1996) for retrofitting applications (Chen; Xing; Li, 2017) as it is water/steam addition into the flame region (Anufriev, 2021; Huang et al. 2024). Usually, post combustion NO_x control has a higher cost due the capital e operating costs when compared with the Low NO_x burners (Cheng and Bi, 2014; Farzan et al., 2002).

The pelletizing plants located at the Tubarão Unit - Vitoria, Espirito Santo/Brazil, account for a significant fraction of Vale's NO_x emissions, corresponding to around 982 g per tonne of pellets produced, in the base year of 2015. Vale has a target to reduce 10% of all NO_x emissions by 2030.

Considering technologies for reducing NO_x emissions, a case study is proposed to evaluate the application of burners with low NO_x emissions using water injection in the Vale Pelletizing Plant located at Tubarão Unit - Vitoria, Espirito Santo/Brazil. To

evaluate the development, a CFD (Computation Fluid Dynamics) modelling was applied.

METHODS

To better understand the NO_x formation in pellet furnaces, as well as what can be done to reduce NO_x emissions in existing plants, a series of CFD (Computation Fluid Dynamics) modelling scenarios were studied. The working scenarios were: Scenario number 1 - a 4,9 MW burner firing 3MW of natural gas in atmospheric air, defined as Base Case; Scenarios 2, 3, 4 and 5, respectively: i) a 4,9 MW burner firing 3MW of natural gas in atmospheric air, with addition of water at a flow rate of 60 l/h (75 µm droplet size and 36 degrees open cone spray spray); ii) 120 l/h (75 µm droplet size and 36 degrees open cone spray); iii) 120 l/h (120 µm droplet size and 88 degrees open cone spray); 160 l/h (120 µm droplet size and 88 degrees open cone spray).

For the CFD modelling, the integral geometric model of one combustion chamber was considered. The computational mesh created had 1 million cells, which was refined during calculations in regions with high gradients. The models used were: k-ε for turbulence, EDC (Eddy Dissipation Concept) for turbulence-chemistry interactions, the reduced mechanism DRM19 (19 species and 84 reactions), and DPM (Discrete Phase Model) for water droplets calculations. Regarding NO_x simulation, just the thermal NO_x generation was considered as this is the main mechanism of NO_x formation in pelletizing furnaces.

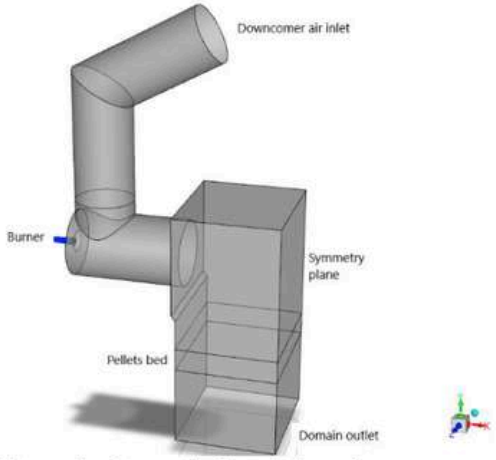


Figure 1. Computational domain

FINDINGS AND ARGUMENT

The first case modelled was the Base Case. This case is the starting point for any CFD modelling as it is used to adjust the proposed model to the real process data obtained in the plant. For this case it was considered an I-Jet™ burner with nominal capacity of 4,9MW, firing 3MW of natural gas. After adjusting the Base Case, it was possible to run the scenarios considering water injection. Table 1 presents the main parameters used on this simulation. The Figure 1 presents the Base Case velocity vectors coloured by velocity magnitude.

Table 1. Base Case parameters

Natural Gas flow rate (kg/h)	Air flow rate (kg/h)	Downcomer air flow rate (kg/h)	Downcomer air temperature (°C)
224,2	258,5	20160	930

Reference: Authors (2024).

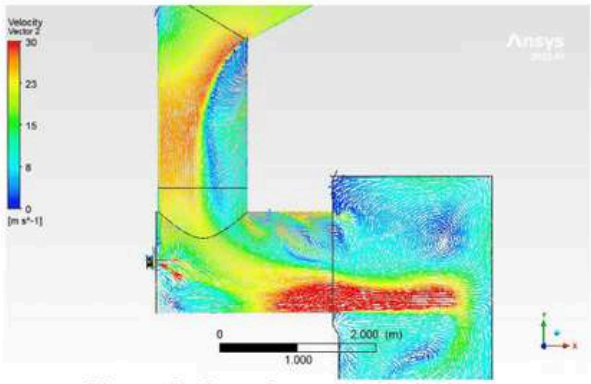


Figure 2. Base Case velocity vectors

The first scenario was modelled considering the same burner used on the Base Case, with addition of water at a flow rate of 60 l/h, 75 µm droplet size and 36 degrees open cone spray. In this modelling, it was possible to observe that the main burning parameters - velocities temperature, oxygen and flame shape - were not extensively affected by water injection. In this scenario, a reduction of approximately 30% in NO_x emissions was observed.

In the second scenario, it was proposed an analysis of the influence of increasing the water flow rate on NO_x reduction. For this scenario, the same burner was considered, with addition of water at a flow rate of 120 l/h, 75 µm droplet size and 36 degrees open cone spray. This scenario presented a reduction in NO_x of approximately 50%.

For the third scenario, it was proposed an analysis of the droplet size on NO_x reduction. For that, it was considered the same burner with addition of water at a flow rate of 120 l/h, 120 µm droplet size and 88 degrees open cone spray. This scenario presented a reduction of approximately 40% in NO_x emissions.

Considering the three scenarios evaluated, the scenario with the smallest droplet size was the one that presented the greatest reduction in NO_x emissions. However, due to the difficulty of achieving this droplet size with commercial injection nozzles, for the fourth scenario it was considered the droplet characteristics of the third scenario (120 µm droplet size and 88 degrees open

cone spray). Also, considering the good results obtained in the second scenario with the increase in water flow (further 20% reduction in NO_x when compared to the first scenario), an increase in water flow was also proposed.

Therefore, the fourth scenario considered the same burner with addition of water at a flow rate of 160 l/h with 120 µm droplet size and 88 degrees open cone spray. This scenario presented a reduction of approximately 50% in NO_x emissions.

Throughout all simulations, the main burning parameters - velocities, temperatures, oxygen concentrations, flame shape, etc - were analysed and considered suitable for the combustion process. With the modelled scenarios, no significant changes in flame shape, as per iso-surfaces of carbon monoxide (CO), were observed due to water addition. Up to 50°C reduction in peak temperatures in the flame core was observed on the scenarios with water injection at the 120 l/h and 160 l/h flow rates. Figure 3 presents the flame shape, coloured by temperature, obtained on the fourth scenario.

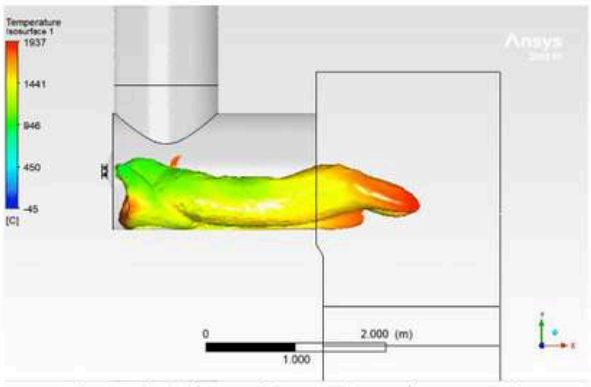


Figure 3. Flame shape - Fourth scenario

Figure 4 presents the NO_x emissions in the Base Case and in all scenarios studied here. Table 2 presents the summary of the considerations used on each scenario and the NO_x reduction achieved.

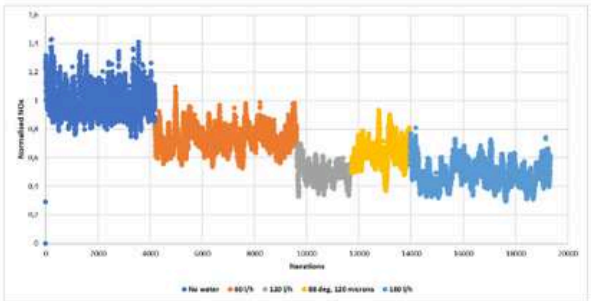


Figure 4. NO_x emission

Table 2. Simulations summary

Scenario	Water flow (l/h)	Droplet size (µm)	Injection nozzle	NO_x reduction (%)
1	60	75	36° open cone spray	30%
2	120	75	36° open cone spray	50%
3	120	120	88° open cone spray	40%
4	160	120	88° open cone spray	50%

NOTE: The NO_x reduction is based on the Base Case NO_x emission. Reference: Authors (2024).

CONCLUSIONS

Using CFD modelling, it was possible to observe reduction from 30% to 50% on NO_x emissions in a combustion chamber of a pelletizing furnace. These results indicate that the injection of water spray in this type of system is effective in terms of reducing NO_x emissions.

For future work, it is recommended to implement similar system to the modelled one and investigate the adequacy of the results obtained with the CFD simulation.

REFERENCES

Anufriev, I. S. "Review of water/steam addition in liquid-fuel combustion systems for NO_x reduction: Waste-to-energy trends." Renewable and Sustainable Energy Reviews 138 (2021): 110665. Accessed April 27, 2024. doi: 10.1016/j.rser.2020.110665.

Ballester, Javier M.; Dopazo, César; Fueyo, Norberto; Hernández, Manuel; Vidal, Pedro J. "Investigation of low- NO_x strategies for natural gas combustion." Fuel 76 (1997): 435-46. Accessed April 27, 2024. doi: 10.1016/S0016-2361(97)85521-4.

Chen, Sheng; Xing, Yuming; Li, Aojin. "CFD investigation on Low- NO_x strategy of folded flame pattern based on fuel-staging natural gas burner." Applied Thermal Engineering 112 (2017): 1487-96. Accessed April 04, 2024. doi: 10.1016/j.applthermaleng.2016.11.005.

Cheng, X., and Bi, X.T. "A review of recent advances in selective catalytic NO_x reduction reactor technologies". Particuology 16 (2014): 1-18. Accessed April 27, 2024. doi: 10.1016/j.partic.2014.01.006.

Farzan, H.; Sivy, J.; Sayre, A.; Boyle, J. Cost-effective control of NO_x with integrated Ultra Low-NO_x burners and SNCR. Ohio: Alliance, 2002.

Huang, Haiyu; Xue, Xufeng; Liu, Yi; Zhao, Jun; Tian, Mao; Niu, Yanqing. "Numerical studies of a water-cooled premixed burner for low NO_x combustion of natural gas." Journal of the Energy Institute 114 (2024): 101647. Accessed April 27, 2024. doi: 10.1016/j.joei.2024.101647.

AIR POLLUTION CONFERENCE BRAZIL
CMAS SOUTH AMERICA
COMMUNITY MODELING AND ANALYSIS SYSTEM

STUDY ON HIGH CONCENTRATION OF PM10 AND PLANETARY BOUNDARY LAYER STRUCTURE AT THE PORT OF PORTO ALEGRE - RS IN 2022

Joshua Budde[1], Ricardo Antonio Mollmann junior[2], *Rita de Cássia Marques Alves*[3]
[1]*Graduation in environmental engineering*
joshuabuddesegundo@gmail.com
[2]*Postgraduete Program in Remote Sensing, Universidade Federal do Rio Grande do Sul*
mollmannr@gmail.com
[3]*Institute of Geosciences, Universidade Federal do Rio Grande do Sul*
rita.cma@terra.com.br

Abstract: This study analyzes the PBL structure in episodes of high concentration of PM 10 in the operational area from the Port of Porto Alegre-RS in the year of 2022. The measurements of concentration and meteorological variables were extracted from the monitoring station and air quality installed in the operational area from the port of Porto Alegre-RS. The structures of the PBL were analyzed from the data of sounding and meteorological reports of visibility from the airport of Porto Alegre Salgado Filho, Located approximately 3 Km from the monitoring station. In the year 2022 eighteen episodes of high concentration of PM10 were registered by the station, which indicated condition's close or that surpassed the intermediary stage one of 120 µg/m³ per day of PM 10 from the National Quality Air Control Standard of CONAMA. The maximum concentration occurred during a stable boundary layer(night and after dawn). During these episodes the surface wind remained below 2 m/s between NE e S and the vertical profile of the wind reached at a maximum of 10 m/s, these were condition prone to deposit of pollutants in the surface. The relative Humidity kept at 86% or higher with only one day at 75 %. The visibility remained low with only two days beyond 5 Km.

Keywords: PM10, relative humidity, fog.

INTRODUCTION

Atmospheric pollutants have a significant impact on human health, causing a variety of respiratory and cardiovascular problems. Additionally, these pollutants interfere with the natural rain cycle, contributing to water and soil acidification. They also affect the distribution of solar radiation, potentially leading to an increase in global temperature, and influence fog formation, affecting visibility and air quality (World Health Organization,2018).

During low temperatures, such as during winter, atmospheric pollution becomes more dangerous due to the possibility of fog occurrence, which intensifies pollutant concentrations such as Fine Particulate Matter (PM2.5) and Coarse (PM10) (Bulbul et al., 2018). PM particles are solid or liquid particles found in the air, subdivided based on their diameter (USEPA, 2024). Particles with a diameter of 10 microns or less (PM10) can be inhaled into the lungs and can induce adverse health effects.

Air quality monitoring is considered essential for developing environmental management tools, mainly because it provides temporal-spatial aspects and information on causes and effects. This is further reinforced in the national context since there are various devices for regulating air pollution, such as environmental licenses and maximum emission limits per pollutant source (Gurgatz, 2018).

Port facilities play an important role in degrading air quality, but their effects are particularly difficult to characterize due to the inherent multimodal nature of the installations (Steffens et al., 2017). However, port facilities are also susceptible to fog/mist formation. Fog can form when moist air moves over a colder surface, such as water from a lake. The cooling of moist air in contact with the cold surface can cause condensation and fog formation. These, in turn, can influence pollutant measurements due to some limitation of a monitoring sensor.

Thus, the present study aims to investigate the behavior of the planetary boundary layer at the Port of Porto Alegre during the period when the station recorded high concentrations of the pollutant PM10, approaching or exceeding the limits established by CONAMA standards, and verifying whether the monitoring result was related to fog conditions or not.

METHODS

The study was formulated based on the monitored data from the year 2022 by the meteorological and air quality station located in the operational area

of the Port of Porto Alegre. This monitoring is a sub-area of the Environmental Management Program of the Port of Porto Alegre (PGA-POA), conducted by the Federal University of Rio Grande do Sul (UFRGS) in partnership with Portos RS. The automatic weather station used for surface measurements is made by VAISALA and consists of a sensor for air quality and meteorological measurements. The Air Quality Transmitter AQT400 sensor performs measurements of fine particulate matter at 2.5 µm and coarse particulate matter up to 10 µm using a Laser Particle Counter (LPC). However, the sensor manual states that high concentrations of humidity can affect the LPC performance and distort measurements. The meteorological sensor is responsible for measuring atmospheric pressure, air temperature, wind speed and direction, relative humidity, solar radiation, and precipitation.

For the analysis of wind speed, relative humidity, and the pollutant PM10, data from the meteorological station were used. The selected episodes for the study were chosen for the year 2022, during which the pollutant approached or exceeded the daily concentration standards established by the National Environment Council (CONAMA) law nº 491, which sets the limits for PM10 at 120 µg/m³. For the analysis of the vertical structure of the planetary boundary layer (PBL), data on vertical wind speed and potential temperature(THTA) from radiosondes released at 00Z and 12Z by the Salgado Filho airport, located about 4 km from the installation point of the monitoring station, were used. In addition to the radiosondes, the airport releases visibility data every hour.



Figure 1. Red represent the Airport and Purple the Meteorological station (30° South and 51° West)

FINDINGS AND ARGUMENT

In the year 2022, 18 days exceeded or approached the limit of 120 µg/m³ of PM10 established by CONAMA. A characteristic of these days is that during the night and early morning, there is a rapid increase in pollutant concentration, as shown in Figure 2.

Figures 2 also depict a common surface wind speed among all studied days. It can be observed that the wind is very weak in moments of high pollution, causing the pollutant to accumulate near the surface (Xin et al., 2020).

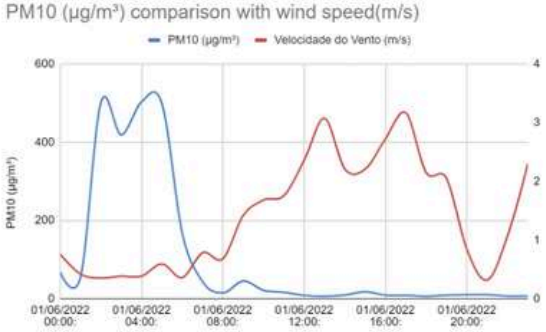


Figure 2. PM10 and Wind speed-01/06/2022

Figure 3 shows the THTA, which can imply if the PBL is stable or not. When an air parcel rises, and so does the temperature, the PBL is stable and less turbulent. Day 03/03 was the only day with an unstable PBL while 21/04 was the only neutral.

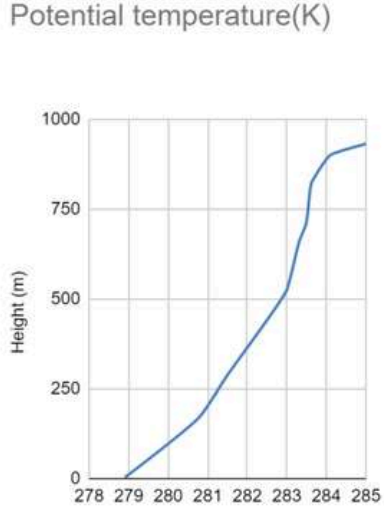


Figure 3. Potential temperature 12Z- 01/06/2022

In Table 1, we have the days when PM10 approached and overshot the limit of 120 µg/m³ in comparison to meteorological conditions.

Table 1. Days of High PM10 concentration

Data	PM10 24h (µg/m³)	Wind Speed (m/s)	Visibility (Km)	Relative humidity (%)
03/03/2022 05:00:00	299,03	1,57	2,5	89,75
20/04/2022 07:00:00	496,2	0,98	0,2	88,79
21/04/2022 07:00:00	333,08	0,95	0,3	88,78
07/05/2022 08:00:00	128,43	0,83	0,2	88,47
08/05/2022 07:00:00	498,23	0,77	0,15	88,72
09/05/2022 05:00:00	131,03	0,42	0,9	88,47
12/05/2022 00:00:00	127,59	1,67	0,9	88,53
21/05/2022 06:00:00	307,64	1,02	0,05	88,6
23/05/2022 07:00:00	668,87	0,86	0,1	89,1
01/06/2022 01:00:00	102,79	0,38	10	75,23
04/06/2022 07:00:00	255,38	0,17	9	88,33
15/06/2022 09:00:00	106,39	1,28	5	86,96
20/06/2022 06:00:00	349,01	0,48	0,1	88,13
22/07/2022 07:00:00	115,2	0,6	4	88,33
27/07/2022 02:00:00	716,54	0,67	0,3	88,3
28/07/2022 03:00:00	253,77	0,61	1	88,98
31/07/2022 08:00:00	128,56	0,53	0,2	88,19
01/08/2022 03:00:00	243,23	0,74	0,3	88,68

Joshua Budde, may 2024

Figure 4 shows the visibility for June 1st. Due to its high visibility and low humidity, the formation of fog is not possible, indicating that there was no distortion in the air quality sensor due to fog.

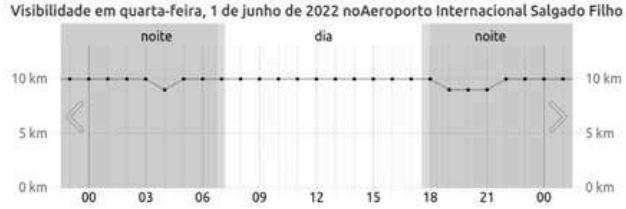


Figure 4. Visibility(Km)- 01/06/2022

CONCLUSIONS

In the year 2022, 18 days approached or exceeded the limit of 120 µg/m³ of PM10 concentration in 24 hours period established by CONAMA. Understanding the sensor distortion and its relationship to fog, we can conclude that June 1st was the only day with a real increase in PM10 pollutant concentration, reaching 102.79 µg/m³. Due to the Stable boundary Layer, the vertical wind movement that would disperse the pollutant is very weak, and since the horizontal wind in the surface is also weak, the PM10 stays closer to the surface from which it was emitted. These conditions are optimal for the formation of fog, but since the Relative Humidity was low, there was not enough to condensate and disturb the sensor.

The other 17 days had high levels of PM10 recorded due to meteorological conditions.The PBL was stable, creating a colder wind layer above the surface,which enabled the Humidity in the air to condensate. Since the winds were too weak to mix and scatter the air, fog formed, causing the distortion predicted by the air quality sensor manual.

REFERENCES

Souza Corrêa, Cleber. " *Estudo micrometeorológico da camada limite planetária estável na região de Porto Alegre*" diss., Universidade Federal do Rio Grande do Sul, 1997.

Bulbul, Gufran. "*PM10 Sampling and AOD Trends during 2016 Winter Fog Season in Islamabad Region*" article in Aerosol., Tufts University, 2017.

Wu, Sen. " Particle number size distribution of PM1 and PM10 in fogs and implications on fog droplets evolution" presented at the journal Atmospheric environment: Atmospheric composition and its impacts, 2022.

Li, Xin. "Atmospheric boundary layer turbulence structure for severe foggy haze episodes in north China in December 2016" Paper, 2020.

Maurer, Maylin and Klemm, Otto and Lokys, Hanna. "Trends of Fog and PBL visibility in Taiwan: Climate Change or Air Quality Improvement?" Journal of Aerosol and Air Quality Research, 2019.

Pineda Rojas, Andrea. "High PM10 concentrations in the city of Buenos Aires and their relationship with meteorological conditions" Atmospheric Environment Journal, 2020.

AIR POLLUTION CONFERENCE BRAZIL
CMAS SOUTH AMERICA
COMMUNITY MODELING AND ANALYSIS SYSTEM

COMPARATİVE ANALYSİS OF CONTİNUOUS AND PERİODİC MONİTORİNG METHODS İN CEMENT PLANTS: A CASE STUDY İN THE STATE OF RİO DE JANEİRO

Rafael Campos[1] , Renato Vieira[1] , Pedro Valle[1] , Silvia Araújo[2] , Josiane Loyola[2] , Solimar José[2]
1 Environmental Institute of Rio de Janeiro State (INEA), Rio de Janeiro, CEP 20081-312, Brazil
rcampos@inea.rj.gov.br
renvisil@inea.rj.gov.br
pedrovalle@inea.rj.gov.br
2 JCTM Comércio e Tecnologia LTDA, Rio de Janeiro, CEP 26130-200, Brazil
silviaaraujo@jctm-hidromet.com
josianeloyola@jctm-hidromet.com
solimarsilva@jctm-hidromet.com

Abstract: The research aims to make public the data from the case study of atmospheric pollutant emissions (PM and SOX) from three cement factories in the mountainous region of the State of Rio de Janeiro, comparing the parameters, the continuous and periodic monitoring methods and the companies, in a historical series from 2019 to 2023. The data was processed with the Estatistica 7.0 program and the correlation between the monitoring methods and chemical parameters was proven.

Keywords: Fixed sources, Monitoring, Chimney, Continuous and Periodic.

INTRODUCTION

Periodic Monitoring occurs at least every six months and the group of pollutants monitored varies according to the specificities of the process of each piece of equipment linked to its chimney or outlet duct. CONAMA resolutions 382/2006, 436/2011, 499/2020 and Operating standard (NOP-INEA 01) deal with the monitoring of pollutants in emissions from stationary (industrial) sources, specifying how, when, which and what is the limit for emission of pollutants into the atmosphere, however, states have autonomy to enact more restrictive limit depending on the nature of the enterprise, the polluting load, the terms of conduct adjustment, among other factors, the company with the greatest polluting potential must, in addition to carrying out periodic monitoring, install equipment to carry out continuous measurement of its pollutants. It is in these cases that CEMS (Continuous Emissions Monitoring Systems) are integrated to continuously measure pollutant concentrations or emission rates and generally consists of a probe for measuring samples at specific points in the chimney, a pollutant analyzer, a datalogger recorder data and a telemetry system for sending data to a server. must be employed (IN.gov, 2022). This study aims to verify the effectiveness of the methods used to monitor emissions from three cement plants registered in the INEA monitoring program, from 2019 to 2023.

METHODS

Data on Particulate Material (PM) and Sulfur Oxides (SOx) were collected isokinetically from three cement plants in the mountainous region of the state of Rio de Janeiro that participate in the periodic and continuous monitoring program of GERAR (Air Quality Management), these data of PM and SOx were collected using EPA method 5 and 8 respectively in the period from 2019 to 2023. The data matrix was treated with the aid of the STATISTICA 7.0 software, to study possible correlations and similarities between the chemical parameters PM and SOX, the Periodic and CEMS monitoring methods and the three cement plants in this case study, the program's correlation and dendrogram analysis resources (method ward and Euclidean distance) were used.

FINDINGS AND ARGUMENT

The data found show results of correlations and similarities of emissions of the chemical parameters of PM and SOx from Cement Plant 1, Cement Plant 2 and Cement Plant 3, and also the comparison between the continuous monitoring method (CEMS) and periodic, using data from a historical series from 2019 to 2023.

Cement Factory 1 has a correlation of 0.59 with Cement Factory 3, while Cement Factory 2 does not have a good correlation with any of the other projects. In Cement Plants 1 and 2, the chemical parameters and sampling methods present correlations between 0.75 and 0.96, thus validating

the continuous monitoring method. Cement plant 2 presented only two representative correlations of 0.86 and 0.77, in kilns 1 and 2 between CEMS and periodic in Kiln1 and 2 respectively with the PM parameter, Table 1 and Figure 2. In Cement Plant 2, SOX did not showed considerable correlation with no variable in this study.

In the dendrogram analysis of Figure 1, three large groups were observed, representing the three companies. The group that represents Cement Plant 2 is subdivided into three other groups with greater dissimilarity. Cement plant 3 has greater similarity between the studied variables as it has a shorter connection distance between them, but does not present good similarity with the other two cement plants. Cement Plant 2 showed greater dissimilarity between the kilns, parameters and monitoring methods.

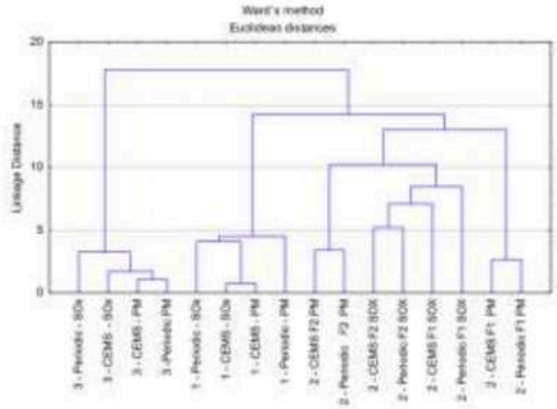


Figure 1. Conglomerate analysis for PM and SOx concentrations in the Periodic and CEMS monitoring method of the three Cement Plants.

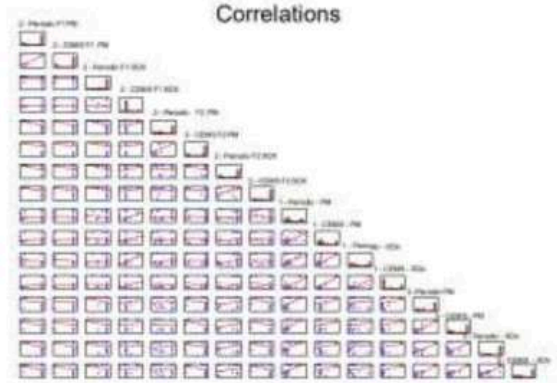


Figure 2. Correlation coefficient of chemical parameters, monitoring methods and companies.

Table 1. Correlation coefficient of chemical parameters, monitoring methods and companies.

	1 Per PM	1 CEMS PM	1 Per Sox	3 Per MP	3 CEMS PM	3 Per SOx
1 CEMS PM	0,75	-	-	-	-	-
1 Per - SO_x	-	0,80	-	-	-	-
1 CEMS - SO_x	0,76	0,99	0,78	-	-	-
3 Per-PM	-	-	-	-	-	-
3 CEMS PM	-	-	-	0,98	-	-
3 Per - Sox	-	-	-	0,82	0,86	-
3 CEMS - Sox	-	-	-	0,94	0,96	0,90

CONCLUSIONS

The results presented show that there are similarities in emissions between the chemical parameters MP and SOX in cement companies. It can be seen that company 2 did not show correlation and representative similarity with companies 1 and 3. However, companies 1 and 3 demonstrated correlations and similar, with 11 correlation values above 0.75 between the variables in this study. I emphasize that all companies had a good correlation between periodic and CEMS in the historical series studied, showing reliability of data from periodic analyzes and continuous monitoring throughout this period.
As a continuation of this study, it is suggested that analyzes be carried out with more samples over a longer period.

REFERENCES

CETESB - Air Quality. Available at: https://cetesb.sp.gov.br/ar/poluentes/ Accessed on 11/29/2023.
CETESB - Particulate Material. Available at: https://cetesb.sp.gov.br › uploads › sites › Accessed on 05/02/2023.
Compliance Monitoring Using Continuous Emissions Monitoring Systems (CEMS) Doc. ID: EAD-EQ-PCE-SOP-08 Issue Date: June 2010 Rev. Date: 14 April 2014 Rev. No.: 01 Page No.: 3 of 37
CONEMA RESOLUTION No. 026, OF NOVEMBER 22, 2010/APPROVES NOP - INEA - 01 - program for monitoring emissions from fixed sources into the atmosphere - PROMON AR.
IN- Indiana Department of Environmental Management Available at: https://www.in.gov/idem/aircompliance/cemscoms/ Accessed on 11/29/2022.
NATIONAL ENVIRONMENT COUNCIL (CONAMA). Resolution No. 382, of December 26, 2006. Establishes the maximum emission limits of atmospheric pollutants for fixed sources.
NATIONAL ENVIRONMENT COUNCIL (CONAMA). Resolution No. 436, of December 22, 2011. Establishes the maximum emission limits of

atmospheric pollutants for fixed sources installed or with an installation license request prior to January 2, 2007
https://www.staticfreesoft.com/index.html/› uploads › sites › Accessed on 02/05/2023. Accessed on 02/05/2023

AIR POLLUTION CONFERENCE BRAZIL
CMAS SOUTH AMERICA
COMMUNITY MODELING AND ANALYSIS SYSTEM

A COMPARATIVE ANALYSIS OF AIR QUALITY SCENARIOS IN BRAZIL FOR 2050 USING WRF-CHEM

Daniel Schuch[1], Yang Zhang[1], Mariana Império[2], Roberto Schaeffer[2], Sergio Ibarra-Espinosa[3,4], Maria de Fatima Andrade[5], Mario Eduardo Gavidia Calderón[5], and Michelle L. Bell[6]

[1] *Department of Civil and Environmental Engineering, Northeastern University, Boston, MA, USA*
d.schuch@northeastern.edu, ya.zhang@northeastern.edu

[2] *Instituto Alberto Luiz Coimbra de Pós Graduação e Pesquisa de Engenharia, Universidade Federal do Rio de Janeiro, RJ, Brazil*
marianaimperio@ppe.ufrj.br, roberto@ppe.ufrj.br

[3] *Cooperative Institute for Research in Environmental Sciences, CU Boulder; 216 UCB University of Colorado Boulder, CO, USA*
[4] *Global Monitoring Laboratory, National Oceanic and Atmospheric Administration (NOAA), Boulder, CO, USA*
sergio.ibarra-espinosa@noaa.gov

[5] *Instituto de Astronomia, Geofísica e Ciências Atmosféricas, Universidade de São Paulo, São Paulo, SP, Brazil*
maria.andrade@iag.usp.br, mario.calderon@iag.usp.br

[6] *School of the Environment, Yale University, New Haven, CT, USA*
michelle.bell@yale.edu

Abstract: Understanding how different emission control policies will affect future air quality is crucial to evaluate the effectiveness of these policies and determine their implications for human health across different socioeconomic groups. The objective of this work is to compare the effect of different emission projection scenarios on estimated air quality using the Weather Research and Forecasting model coupled with Chemistry (WRF-Chem) with a triple-nested domain configuration for Brazil, Southwest region, Metropolitan Area of São Paulo (MASP) and Metropolitan Area of Rio de Janeiro (MARJ). Anthropogenic emissions for baseline simulations are generated by combining the Emissions Database for Global Atmospheric Research (EDGAR), the local inventory for Rio de Janeiro and emissions estimated using the Vehicular Emissions Inventories model (VEIN) for the Metropolitan Area of São Paulo. For each future scenario, the baseline emissions for 2015 are projected for 2050 using emission change factors (ECFs) calculated from the Brazilian Land Use and Energy Systems (BLUES) model outputs for each region, sector, and pollutant. Two emission scenarios are compared: Current polices or business as usual (BAU) and Net-Zero/Control (NZC). The BAU scenario considers the maintenance and expansion of the current Brazil installed power capacity, control of deforestation levels, and the implementation of existing control measures for reducing emissions from stationary sources and fleet renovation. The NZC includes additional measures to achieve zero greenhouse gas emissions by 2050, along with measures to reduce primary pollutants and precursors. The BAU scenario projects an increase of emissions of nitrogen oxides (NO_x) by 25.3%, sulfur dioxide (SO_2) by 3.7%, and particulate matter lesson larger than 2.5 micrometers ($PM_{2.5}$) by 30.6%, while in the NZC there is a reduction of 37.8% for NO_x, 42.5% for SO_2, and 28.1% for $PM_{2.5}$. In future work, these simulations will be used to assess the health impact of O_3 and $PM_{2.5}$ and demonstrate the impacts of BAU and NZC emission reduction polices on both air quality and human health in MASP and MARJ, Brazil.

Keywords: *Air quality projection, Emission Scenarios, WRF-Chem, Brazil.*

INTRODUCTION

In recent decades, global concerns over air quality have escalated, leading many countries to implement various measures aimed at reducing atmospheric emissions. These efforts have resulted in improvements in air quality, particularly in developed regions such as Europe and United State. However, developed countries like Brazil continue to face challenges in implementing a consistent policy to improve air quality, especially in controlling secondary pollutants such as ozone (O_3) and particulate matter no larger than 2.5 micrometers ($PM_{2.5}$) (Andrade et al., 2017).

As Brazil's development progresses, projections indicate significant shifts in economics and population growth and aging, making its population more vulnerable to pollutant exposure (Carvalho & L. Rodríguez-Wong, 2008 . Additionally urban expansion, industrial growth, and increase in the number of vehicles in circulation will increase emissions.

AIR POLLUTION CONFERENCE BRAZIL
CMAS SOUTH AMERICA
COMMUNITY MODELING AND ANALYSIS SYSTEM

This work presents a comparative analysis of two emission scenarios for Brazil for the year 2050, utilizing the Weather Research and Forecasting model coupled with Chemistry (WRF-Chem). Through this study, we aim to simulate potential future trajectories of air pollution, exploring the effect of different mitigation strategies and policy interventions on anthropogenic emissions and the resulting effect on air quality. Our results will be used in studies to assess adverse effects on human health and can provide quantitative information to guide policymakers and stakeholders to foster informed decision-making and sustainable development practices.

MODELS AND SCENARIOS

WRF-Chem is an online-coupled, multi-scale 3-D air quality model consisting of a non-hydrostatic model with several physical parameterizations representing the unsolved processes as sub-grid processes (Skamarock et al., 2019) . The chemical module (Chem) is designed to simulate a variety of additional physical and chemical processes related to atmospheric chemistry, such as atmospheric emissions, transport, chemical reactions, aerosol formation and interactions with radiation and clouds, as well as wet and dry deposition. One key feature of WRF-Chem is that all modeled processes (e.g., emissions, transport, radiation, and chemistry) are fully coupled (Grell et al., 2005) , enabling its ability in simulating various meteorology and chemistry feedback in the atmosphere.

The simulation for the period of 2012-2016 is considered the BASELINE case. This simulation was performed using meteorological variables from Global reanalysis from National Centers for Environmental Prediction (NCEP-FNL) and Community Atmosphere Model with Chemistry (CAM-CHEM) model for Initial and boundary conditions of gases and aerosol species. Anthropogenic emissions from Emissions Database for Global Atmospheric Research (EDGAR), Vehicular Emissions INventories model (VEIN) for MASP, and a Local inventory for MARJ were combined for each domain. Natural emissions are from Fire emission inventory from NCAR (FINN), Model of Emissions of Gases and Aerosols from Nature (MEGAN 2); dust and sea salt emissions are from Global Ozone Chemistry Aerosol Radiation and Transport Model (GODART). Simulations from the BASELINE are evaluated against observations of meteorological variables and chemical species from surface stations and satellite, and the performance is considered good following criteria from the literature (Emery et al., 2017; Emery & Tai., 2001; Monk et al., 2019; Ramboll, 2018).

Simulations for two future emission scenarios: Business as Usual (BAU) and Net Zero/Control (NZC) are performed for the years of 2048-2052. In these simulations all inputs are kept the same and anthropogenic emissions are projected using emission change factors calculated from outputs from the Brazilian Land-Use and Energy Systems (BLUES) model (Köberle, 2018) . The BLUES model is an integrated assessment model (IAM) that considers the interactions between the major demand sectors (transportation, industry, residential, services, agriculture, and energy), land-use and land-use change driven by population projections from the Instituto Brasileiro de Geografia e Estatistica (IBGE, 2016) , and GDP growth rates based on SSP2 (Dellink et al., 2017) , adjusted to reflect current economic activity in Brazil based on BCB (2017) . The BAU scenario assumes that there are no changes in environmental legislation; deforestation levels are controlled; and the continuation of fleet renovation, existing control measures for stationary sources and the maintenance of existing energy assets and expansion of contracted facilities. The NZC scenario assumes that in addition to the current legislation, measures to reduce net greenhouse gas emissions to zero by 2050, and additional measures to reduce short-lived pollutants such as restricted control of stationary sources, improvements in energy efficiency in the industrial sector, reduction in the number of diesel vehicles, and improvements inroad conditions to reduce fuel consumption.

RESULTS AND DISCUSSION

The comparison of projected emissions for the BAU scenario for Brazil (excluding emissions over the ocean and other counties within the simulation domain) in relation to the BASELINE emissions show an increase in nitrogen oxides (NO_x) by 25.3%, sulfur dioxide (SO_2) by 3.7% and $PM_{2.5}$ by 30.6%, while volatile organic compounds (VOCs) and carbon monoxide (CO) emissions are reduced by 31.4% and 17.8%, respectively. Emissions of the NZC scenario show a reduction of NO_x of 37.8%, SO_2 of 42.5% and $PM_{2.5}$ of 28.1%, and a reduction of VOC and CO emissions of 36.1% and 27.8%, respectively.

For BAU scenario, the daily maximum 8-hour average (MDA8) O_3 concentrations increase over most of the domain when compared to the BASELINE, the southwest region shows a significant increase of MDA8, affecting especially urban areas, however there is a decrease of MDA8 in the states of Amazon and Acre. On the other hand, the BZC scenario shows a small change on MDA8 O_3; there is a larger reduction over the north region and a small increase of MDA8 over the two largest metropolitan areas MASP and MARJ.

$PM_{2.5}$ concentrations are higher in both BAU and NZC scenarios when compared to the baseline. For the BAU scenario, there is a $PM_{2.5}$ increase in major urban areas in the southwest and an increase in the northeast region. The NZC scenario shows a smaller increase of concentration, while major urban areas show a decrease of $PM_{2.5}$ compared to BAU.

CONCLUSIONS and FUTURE WORK

The BAU scenario projects a degradation of the air quality for both O_3 and $PM_{2.5}$, while in the NZC scenario there is an improvement in air quality compared to BAU at the national level. However, there are still some locations that exhibit lower air quality compared to the BASELINE. Therefore, the adoption of different measures to further restrict emissions and replace technologies is an additional step needed to make a significant improvement in terms of air quality.

Results presented in this work are derived from 36-km resolution WRF-Chem (input emissions and output concentrations). However, for more local analysis the model is being applied using higher resolution simulations: 9-km over the southeast region (where most of the economic and industrial activities and population are located) and 3-km domain over MASP and MARJ (the two major urban metropolitan areas in the country).

REFERENCES

Andrade, M. de F., Kumar, P., de Freitas, E. D., Ynoue, R. Y., Martins, J., Martins, L. D., Nogueira, T., Perez-Martinez, P., de Miranda, R. M., Albuquerque, T., Gonçalves, F. L. T., Oyama, B., & Zhang, Y. Air quality in the megacity of São Paulo: Evolution over the last 30 years and future perspectives. *Atmospheric Environment*, *159*, 66–82. (2017). https://doi.org/10.1016/j.atmosenv.2017.03.051

BCB. *Sistema de Expectativas de Mercado*. Https://Www3.Bcb.Gov.Br/Expectativas/Publico/Consulta/Serieestatisticas. (2017, September 1).

Carvalho, J. A. M., & L. Rodríguez-Wong, L. A transição da estrutura etária da população brasileira na primeira metade do século XXI. *Cadernos de Saúde Pública*, *24*(3), 597–605. (2008).

Dellink, R., Chateau, J., Lanzi, E., & Magné, B. Long-term economic growth projections in the Shared Socioeconomic Pathways. *Global Environmental Change*, *42*, 200–214. (2017). https://doi.org/10.1016/j.gloenvcha.2015.06.004

Emery, C., Liu, Z., Russell, A. G., Odman, M. T., Yarwood, G., & Kumar, N. Recommendations on statistics and benchmarks to assess photochemical model performance. *Journal of the Air & Waste Management Association*, *67*(5), 582–598. (2017). https://doi.org/10.1080/10962247.2016.1265027

Emery, C., & Tai., E. *Enhanced Meteorological Modeling and Performance Evaluation for Two Texas Ozone Episodes*. (2001).

Grell, G. A., Peckham, S. E., Schmitz, R., McKeen, S. A., Frost, G., Skamarock, W. C., & Eder, B. Fully coupled "online" chemistry within the WRF model. *Atmospheric Environment*, *39*(37), 6957–6975. (2005). https://doi.org/10.1016/j.atmosenv.2005.04.027

IBGE. *Projeção da População do Brasil por sexo e idade: 2000-2060. Instituto Brasileiro de Geografia e Estatistica*. Https://Ww2.Ibge.Gov.Br/Home/Estatistica/Populacao/Projecao_da_populacao/2013/Default.Shtm. (2016).

Köberle, de C. *Implementation of Land Use in an Energy System Model to Study the Long-Term Impacts of Bioenergy in Brazil and its Sensitivity to the Choice of Agricultural Greenhouse Gas Emission Factors*. Universidade Federal do Rio de Janeiro. (2018).

Monk, K., Guérette, E.-A., Paton-Walsh, C., Silver, J. D., Emmerson, K. M., Utembe, S. R., Zhang, Y., Griffiths, A. D., Chang, L. T.-C., Duc, H. N., Trieu, T., Scorgie, Y., & Cope, M. E. Evaluation of Regional Air Quality Models over Sydney and Australia: Part 1—Meteorological Model Comparison. *Atmosphere*, *10*(7), 374. (2019). https://doi.org/10.3390/atmos10070374

Ramboll. *PacWest Newport Meteorological Performance Evaluation*. (2018).

Skamarock, W. C., Klemp, J. B., Dudhia, J., Gill, D. O., Liu, Z., Berner, J., & Huang, X. Y. *A description of the advanced research WRF version 4* . (2019).

AIR POLLUTION CONFERENCE BRAZIL
CMAS SOUTH AMERICA
COMMUNITY MODELING AND ANALYSIS SYSTEM

CFD SIMULATION OF THE GAS FLOW DISTRIBUTION INSIDE AN INDUSTRIAL BAG FILTER

Julia Vargas[1]*, Matheus Leite[2], Bruno Castro[1], Rafael Sartim[1]
[1]*ArcelorMittal Tubarão, Serra, Espírito Santo, Brazil*
**julia.vargas@arcelormittal.com.br*
[2]*Federal University of Espírito Santo, Vitória, Espírito Santo, Brazil*

Abstract: *This study investigated, through Computational Fluid Dynamics (CFD) simulations, the gas flow behavior inside an industrial bag filter, aiming to identify the potential causes of the current uneven distribution of particles to each chamber of the equipment. To perform the analysis, three different geometries were evaluated and compared: (1) considering just the inlet duct and spark arrestor; (2) adding the chambers and outlet duct; (3) adding a porous block inside each chamber to represent the resistance provided by the bags. The results of all three cases showed that the way the gas flow enters the inlet duct significantly influences its distribution to each chamber. As it leaves the spark arrestor and enters the duct, the gas flow experiences a substantial acceleration due to abrupt changes in direction, creating a tendency for the gas and, potentially the particles, to go directly to the last chambers. Despite certain similarities, geometries 1 and 2 exhibited reverse flow issues in the first chamber inlet, which was not observed in the real bag filter. This behavior was solved with geometry 3, with the incorporation of porous blocks inside the chambers, obtaining flow distribution results compatible with reality. Therefore, it is also highlighted the importance of making correct assumptions to get consistent CFD results.*

Keywords: *Bag filter, CFD, flow distribution, geometry, control.*

INTRODUCTION

Among the pollutants found in the air, particulate matter is a significant concern due to its potential to harm fauna, flora, and human health. Consequently, strict regulations have been imposed to control particulate matter emissions, resulting in the constant research for efficient and reliable technologies, such as bag filters, widely used in industries to remove particles from gas streams.

Computational Fluid Dynamics (CFD) simulation can be a powerful tool for flow analysis in bag filters, allowing to evaluate the current situation of industrial devices, as well as to propose improvements to extend the equipment's service life and increase filtration efficiency, which can result in environmental benefits and in operational costs reduction. The flow behavior in bag filters has already been investigated through CFD simulations, with various objectives [1-5].

This study aimed to assess the gas flow behavior inside an industrial bag filter with five chambers, which is currently presenting significant uneven distribution of particles to each compartment. The objective with the CFD simulations was to investigate the potential causes of this non-uniform condition, which impacts the equipment performance. To perform the analysis, three different geometries were evaluated and compared.

METHODS

The three geometries are presented in Figure 1: (1) considering just the inlet duct and spark arrestor (Figure 1a); (2) adding the chambers and outlet duct (Figure 1b); (3) adding a porous block inside each chamber to represent the resistance provided by the bags (Figure 1c).

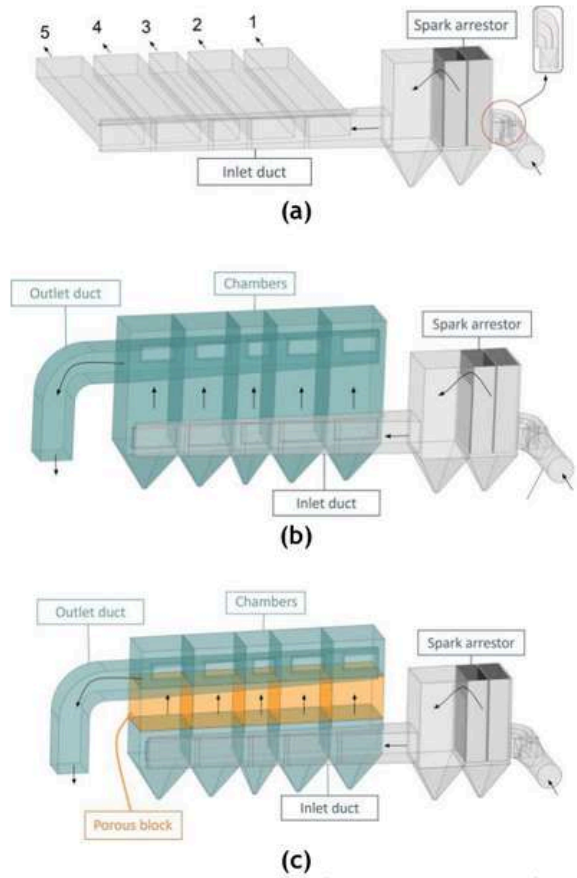


Figure 1. (a) Geometry 1, (b) geometry 2 and (c) geometry 3.

ANSYS Fluent 2020R1 was used, and the flow field was assumed to be incompressible, steady state and with no heat transfer. The simulations were performed using Realizable κ-ε turbulence model, as adopted in similar studies of bag filters [1-5], and a mesh independence test was performed, totaling 7.6, 8.3 and 8.5 million elements for geometries 1, 2 and 3, respectively.

A gas flow velocity of 24 m/s at the inlet and a gauge pressure equal to 0 Pa at the outlet of the domain were adopted in the three cases. In geometry 3, the porous block within each chamber was incorporated in a manner that its pressure variation was equal to the pressure variation induced by the existing bags, allowing the resistance representation with reduced computational costs. For this consideration, Porous Media model was adopted with specific values for the inertial resistance factor, C, and permeability, α. These constants can be obtained by performing simulations with the geometry of a single chamber with the presence of the bags and varying the inlet velocity to obtain an adjusted quadratic curve of pressure drop as a function of the velocity.

RESULTS

Gas flow distribution analysis

Figure 2 shows the velocity contour in a vertical plane inside the spark arrestor. Since the three geometries yielded very similar behavior results for this part of the domain, only the result for geometry 3 is presented. In addition, Figure 3 shows the velocity contour with vectors in a horizontal plane for geometries 1, 2 and 3, restricting the analysis to the inlet duct part.

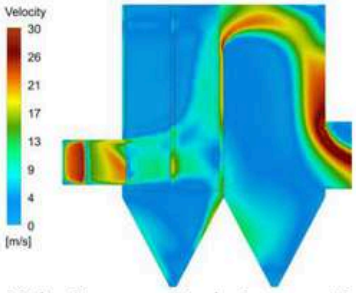
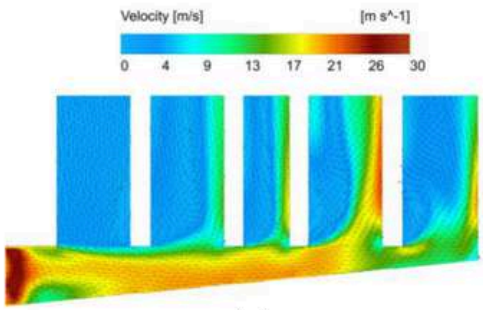
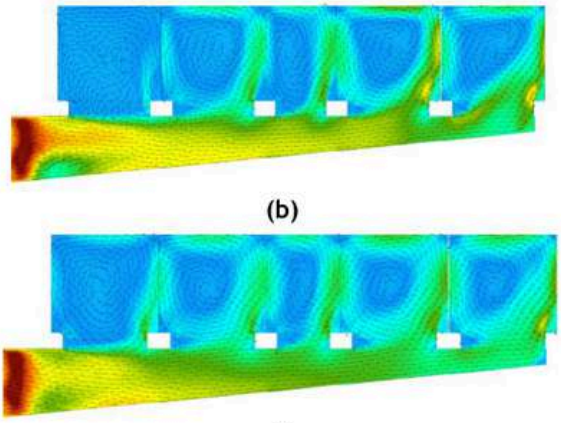


Figure 2. Velocity magnitude in a vertical plane inside the spark arrestor.



(a)



(b)

(c)

Figure 3. Velocity contour and vectors in a horizontal plane inside the inlet duct for geometries (a) 1, (b) 2 and (c) 3.

Abrupt changes of direction are noticed in Figure 2, which results in substantial acceleration of the flow, especially as it leaves the spark arrestor and enters the duct. This specific acceleration is also seen in Figure 3 for all the cases, which can significantly contribute to the uneven distribution seen in reality. When experiencing this acceleration upon entering the duct, the gas flow, and potentially the particles, tend to go directly to the last chambers, bypassing the first compartments.

However, despite the similarity observed with the three geometries, a reverse flow can be noticed when analyzing the vectors in geometries 1 and 2, where the gas flow enters the first outlet of the inlet duct instead of leaving it toward the chamber. This behavior is not observed only in geometry 3, with the addition of the porous blocks. In this context, it is important to highlight that real industrial bag filters, especially the analyzed equipment, do not exhibit this reverse phenomenon.

Table 1 shows the mass flow rates to each chamber, obtained with the CFD simulations of the three geometries. The negative values of flow rate entering chamber 1 for geometries 1 and 2 confirm the unexpected reverse flow behavior previously highlighted, where the gas enters the duct rather than leaving it. The relationship between this phenomenon and the spark arrestor presence will be further explored when assessing the pressure distribution results.

Table 1. Mass flow rates to each chamber.

Mass Flow Rate (kg/s)	Chamber				
	1	2	3	4	5
Geometry 1	-12	13	15	43	36
Geometry 2	-2	17	15	29	37
Geometry 3	8	18	15	36	29

In addition, considering the flow rate distribution of geometry 3, which presented no reverse flow, it can be seen that chambers 4 and 5 receive a considerably greater amount of mass flow compared to the first three compartments, especially chamber 1. This uneven distribution is in accordance with the current real situation, in which the highest particle load is directed to the last chambers.

Static pressure analysis

To understand better the reasons of the reverse flow and the effect of including the porous blocks, Figure 4 shows the static pressure contour for geometries 1, 2 and 3. The abrupt flow acceleration right after the spark arrestor generates a low-pressure zone in this area, as seen in the three geometries.

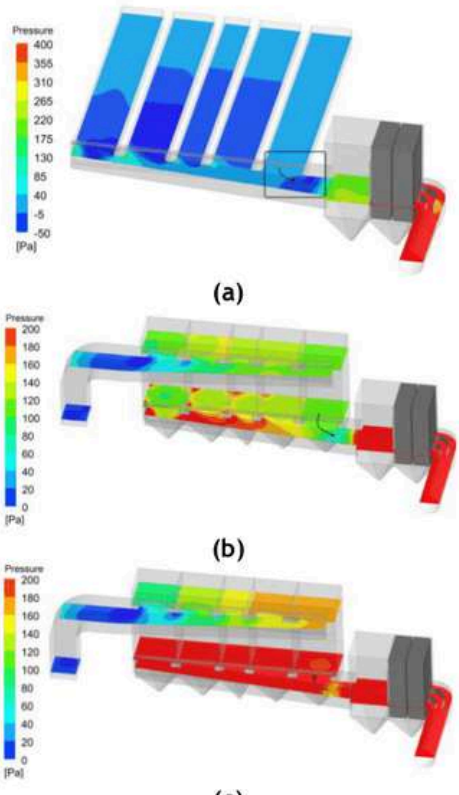


Figure 4. Static pressure contours for geometries (a) 1, (b) 2 and (c) 3.

Since this region is very close to the first chamber, the reverse flow phenomenon happens in geometries 1 and 2, where the gas goes from the region of higher to the lower pressure, as indicated by the arrows in the figures. For geometry 1, it goes from the duct of outlet 1 to the low-pressure zone inside the inlet duct. For geometry 2, with the influence of this low-pressure region, the pressure along the first chamber inlet is lower compared to its outlet, resulting in this reverse phenomenon as well. On the other hand, in geometry 3, the pressure at the chamber inlet exceeds the pressure at its outlet, even with the presence of the low-pressure zone after the spark arrestor. This happens because the porous blocks introduce an additional pressure variation along the chambers, preventing reverse flow in the first compartment. This fact is in accordance with real-world scenarios, where the bags provide an additional resistance to the flow.

CONCLUSIONS

This study investigated the gas flow behavior inside an industrial bag filter, aiming to identify the potential causes behind the current uneven distribution of particles to each chamber. In addition, the influence on the results of considering three different geometries was evaluated.

In all three cases, it became evident that the manner in which the gas flow enters the inlet duct significantly influences its distribution to each chamber. As it leaves the spark arrestor, the gas flow experiences a substantial acceleration, creating a tendency for the gas and, potentially the particles, to go directly to the last chambers and bypass the first compartments.

Despite certain similarities between the geometries, reverse flow was noticed in the first chamber inlet for geometries 1 and 2, contradicting to what is typically seen in real bag filters. The static pressure results revealed that this phenomenon happens due to particularities of the flow behavior. This unrealistic phenomenon just has been solved with the incorporation of porous blocks inside the chambers, which introduced additional pressure variation along the compartments. Therefore, it is also highlighted the importance of making correct assumptions to get consistent CFD results, as well as always critically assess the validity of the results.

REFERENCES

[1] Park, S. et al. Non-uniform filtration velocity of process gas passing through a long bag filter. Journal of Hazardous Materials 365 (2019): 440-447.
[2] Pereira, T. et al. The influence of the fabric filter layout of in a flow mass filtrate. Journal of Cleaner Production 111 (2016): 117-124.
[3] Rocha, S. et al. Applications of CFD Techniques in the Design of Fabric Filters. Chemical Engineering Transactions 39 (2014): 1369-1374.
[4] Solari, F. et al. "CFD MODEL VALIDATION OF A BAG FILTER FOR AIR FILTRATION IN A MILLING PLANT". In: Proceedings of the International Food Operations and Processing Simulation Workshop, 2017.
[5] Zhang, F. et al. Effects of flow distributor structures and particle-wall interaction on baghouse gas-solid flow. Separation and Purification Technology 335 (2024): 1383-5866.

AIR POLLUTION CONFERENCE BRAZIL
CMAS SOUTH AMERICA
COMMUNITY MODELING AND ANALYSIS SYSTEM

IN SITU DESULFURIZATION OF BRAZILIAN COAL COMBUSTION USING DIFFERENT LIMESTONES IN A BUBBLING FLUIDIZED BED BENCH SCALE

Flavio Michels Bianchi[1], Pedro Rodrigo Silva Moura[1], Josiane da Rocha Silvano das Neves[1], Raiane da Cruz[1], Thiago Luís Zanin[2], Luiz Fernando de Lima Luz Junior[2],Thiago Fernandes de Aquino[1]

[1]*Beneficent Association of the Santa Catarina Coal Industry (SATC). Criciúma, SC, Brazil*
flavio.bianchi@satc.edu.br

[2]*Department of Chemical Engineering at UFPR, Administration, 1st floor, DEQ/TC/UFPR Polytechnic Center, Curitiba, PR, Brazil*
thiago.zanin@ufpr.br

Abstract: To reach the limits of sulfur oxides emissions allowed for Brazilian legislation when burning coal in Brazil, some system for attenuation of these gases is often necessary to reduce emissions Fluidized bed combustors reduces this emmisions by adding limestone directly to the burning bed. Aiming guidance for better decision-making in the use of available limestones, a technical analysis was carried out to economically evaluate the best solution for a given equipment, additionally to compare the efficiency of removing SO_2 from the flue gas. In this way, both the base fuel and the limestones were embedded and tested in a bench-scale combustor where four different limestones were mixed to the fuel. Molar ratios of 3 and 4 to calcium and sulfur were defined to use for an average bed combustion temperature of 850°C. Emissions measurements were performed with specific portable analyzers with electrochemical cells for carbom monoxide, nitrous oxide, sulfur dioxide, oxygen and carbon dioxide. The resultant bottom and fly ashes from the burn were evaluated and classified. Eight desulfurization tests and one single coal combustion test were carried out. Compared with single coal combustion, the desulfurization test points removal ranged from 71.3% to 90.4% of sulfur from the gas stream. The total sulfur results in the bed (bottom ash) and fly ashes samples revealed that the sulfur concentration is higher in the fly ash.

Keywords: *In Situ* Desulfurization, Gas Composition, Brazilian Coal Combustion, Limestone.

INTRODUCTION

Due to the necessity to reach environmental limits for sulfur emissions in coal power plants, a study must be made to select the best way to mitigate those gases for technical and economic evaluation.
According to Hayashi (1996), there are three ways to reduce the emission of pollutants in combustion processes, cleaning fuel before burning, cleaning combustion fumes and modifying the process.
In bubbling fluidized bed boilers, a good path to strike this objective is by in situ desulfurization using limestone injection directly in bed.
Her, four different limestones were tested in a bench scale of a bubbling fluidized bed combustor. Coal from Cambuí's mine in Paraná State was used as a base for power generation and different ratios of limestone were used when a typical fluidized bed temperature was set.
Both coal and limestones have been characterized, thus they could be used after the ratio of calcium/sulfur (Ca/S) was calculated.
To compare, only coal was even fired to define the percentage of sulfur removal in each test in the presence of limestone.

METHODS

To run tests and evaluate the desulfurization of coal combustion with limestone, the materials involved were characterized to know those properties and calculate the process parameters.
The fuel used was named Cambuí coal from Paraná State, Brazil. It is a typical high ash content coal with a substantial amount of sulfur in its constitution and reasonable heat value. The analyses were performed using a calorimeter, thermogravimetric analyzer, and CHNS analyzer. The coal particle size was between 0,60 to 1,68 mm after preparation.
In the same way, four different limestones named B, C, F, and K were characterized using X-ray fluorescence spectrometry and by Pettijohn (1957) classification defined as calcitic limestone (B and C), and dolomitic limestone (F and K).
Based on this, the coal and limestone mixtures were prepared to reach 3 and 4 Ca/S ratio. Table 1 shows the limestone-coal mass ratio.

Table 1. Limestone-Coal Mass Ratios

Limestone (kg/kg)	Ca/S Ratio 3	4
B	0.339	0.452
C	0.337	0.450
F	0.382	0.509
K	0.409	0.547

The combustor used for the experimental tests was a bubbling fluidized bed. This technology permits sulfur removal using calcium compounds directly in the bed (Bragança and Castelan, 2009; Shimizu *et al.*, 2002).
As the main parts of the equipment (Figure 1) there is an air preheater (1), plenum chamber (2), combustion chamber (3), fuel storage and feeder

(4), thermocouples (5), cyclone separator (6), fly ash reservoir (7), and gas outlet (8).

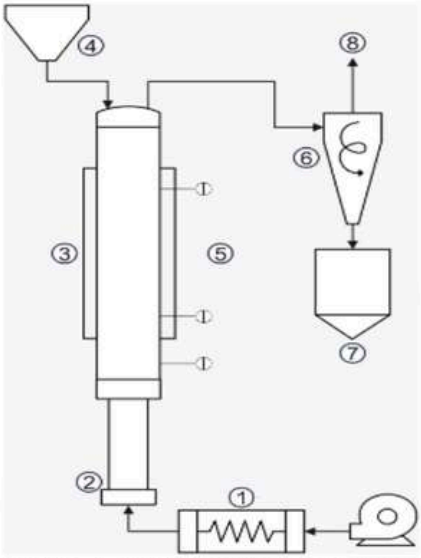


Figure 1. Fluidized Bed Combustor

The tests were carried out on a bubbling fluidized bed bench, with an average temperature of 850°C. The control of the fuel supply flow, air supply flow, bed and reactor temperature is carried out through a supervisory system. Sand with granulometry in the range of 0.20 x 0.35 mm was used as the bed.

At start-up, the combustor was heated using electrical resistances in the reactor and hot air from preheater. Fuel was fed when the bed temperature reached 550°C. After the fuel supply began, the electrical resistances was stoped and the combustion started suppling the heat necessary to reach the desired temperature.

Table 2. Experimental Conditions

Parameter	Value	Unit
Fuel Particle Size	0.60 x 1.68	mm
Limestone Particle Size	0.60 x 1.68	mm
Bed Particle Size	0.20 x 0.35	mm
Bed Temperature	850 ± 8	°C
Inlet Air Temperature	180 - 250	°C
Air Flow	150 - 200	L/min
Fuel Feed Rate	0.68 - 0.81	kg/h

The excess of air controls heat generated during combustion, avoiding temperatures higher than desired. As a premise, the fuel flow rate was maintained constant, so that eventual temperature variations were controlled by variations in the air supply. The sand in the bed reached operating temperatures simultaneously with the adjustment of air flow rates. The analysis of the exhaust gas composition began when the bed temperature stabilized at 850 ± 8°C. Table 2 summarizes the experimental conditions.

Eight tests were carried out with limestone, and in each test, only one Ca/S ratio was used. The time of operation with stabilized bed temperature was approximately five hours. A combustion test was carried out with only coal for comparing SO_x emissions, under the same conditions as the other tests but without the addition of limestone.

The quantification of the flue gas composition regarding NO_x, CO, CO_2, and SO_x emissions was carried out using the CHEMIST 502B and CHEMIST 504X portable flue gas analyzers.

Three determinations were carried out for each parameter under analysis. Each determination lasted ten minutes with a sampling time of one minute each. The results were expressed on mg/Nm³, and corrected for 7% O_2 excess. The values presented by the gas analyzer were corrected for the exhaust gas temperature, which is determined by the equipment.

Ash with particles below 0.1 mm was dragged by the hot gases and collected in the cyclone separator. Bottom ash was mixed into the bed.

After each desulfurization test, mass was collected from the bed with the bottom ash and fly ash deposited in the cyclone reservoir. The samples were analyzed by X-ray fluorescence spectrometry and X-ray diffraction, and the percentage of total sulfur was quantified according to the ASTM 4239 standard.

FINDINGS AND ARGUMENT

As a result of fuel characterization, Table 3 shows the chemical analysis of Cambuí's coal, which was a typical high ash content coal (about 30%) with low moisture.

Table 3. Chemical Analysis of Cambuí Coal

Parameter	Result
Hygroscopy moisture (%)	2.33
Volatile matter (%)	26.74
Ash (%)	29.25
Fixed carbon (%)	44.01
Total sulfur (%)	3.66
Carbon (%)	57.02
Hydrogen (%)	4.02
Nitrogen (%)	1.29
Oxygen (%)	4.76
HHV (cal/g)	5326
LHV (cal/g)	5101

The high heating value of about 5300 cal/g is enough to have good application in energy production. Nevertheless, their 3.66% of sulfur shows that this coal needs to be treated to reach the environmental limits of sulfur emissions.

Regarding to the limestones, the characterization leads to CaO higher than 45.81% in all samples including higher than 55% for B and C samples,

placing the latter as calcitic limestones. İn another other way, the MgO in samples F and K have percentages of 5.22 and 5.66% respectively placing them as dolomitic limestones. Table 4 resumes that characterization.

Table 4. Chemical Analysis of Limestones

Oxides (%)	B	C	F	K
CaO	55.36	55.68	49.14	45.81
SiO2	0.54	2.44	4.82	9.31
MgO	0.49	0.53	5.22	5.6
Others	0.72	0.61	2.00	5.66
LOI	42.90	41.44	38.81	33.61

From the ash analysis, Table 5 summarizes the amount of sulfur in the bottom and fly ashes. There was no direct correlation with the Ca/S ratio in relation to sulfur trapped in ashes, but there is a considerable increase of sulfur when compared with ashes from coal. Although the concentrations of sulfur were higher in fly ash, we must consider there was no bottom ash removal during operation and this ash is mixed with the initial bed. This leads to higher sulfur content in bottom ash for continuous operation.

Table 5. Total sulfur in bottom and fly ash

Sample	Bed+ Bottom Ash (%)	Fly Ash (%)
Coal	0.27	0.86
B3	0.58	1.51
B4	0.52	1.28
C3	0.67	1.57
C4	0.39	1.47
F3	1.06	1.13
F4	0.45	1.19
K3	0.89	2.55
K4	0.36	1.05

Table 6 shows that SO_2 was strongly affected by limestone injection and only the mixtures F3, F4, and K3 did not reach 1300 mg/m³ as emission limits of environmental legislation from Paraná State. Compared with single coal combustion, the desulfurization test points removal ranging from 71.3% to 90.4% of sulfur from the gas stream.

Table 6. Experimental Results

Parameter	Coal	B	B	C	C	F	F	K	K	Unit
Ca/S		3	4	3	4	3	4	3	4	-
O2	7.65	3.4	5.3	3.9	6.5	6.9	5.2	10.7	8.1	%
CO (7.0%)	31	56	35	53	24	15	28	13	12	ppm
CO_2IR (7.0%)	14.7	15.6	15.3	15.2	15	10.7	10.2	11.3	10.4	%
SO_2 (7.0%)	6081	1087	863	1195	580	1743	1405	1408	1171	mg/m³
NO_x (7.0%)	427	281	354	333	389	360	275	376	426	ppm
AVG Bed Temperature	852.0	846.5	852.6	851.3	850.0	850.8	850.3	850.8	849.7	°C
AVG Air Flow	209.0	159.0	177.0	159.0	180.0	182.5	157.5	182.5	155.0	l/min
AVG Fuel Feed Rate	0.75	0.93	1.09	1.04	1.03	1.12	1.10	1.04	1.05	kg/h

CONCLUSIONS

The sulfur results in the bottom and fly ashes samples showed that the sulfur concentration was higher in the fly ash. Nevertheless, bottom ash was mixed with bed sand and it needs to be considered. All tests showed SO_2 concentrations below the limit of 1300 mg/m³, except F3, F4, and K3.

The results points out the use of four limestones tested, and in the cases of F3, F4, and K3 they need to be corrected to achieve the emissions set out in legislation.

REFERENCES

Bragança, Saulo R., and Castellan, Jorge L., "FBC desulfurization process using coal with low sulfur content, high oxidizing conditions and metamorphic limestones." *Brazilian Journal of Chemical Engineering* 26 (2009): 375-383. Accessed April 10, 2024.

Hayashi, Angela M., "Estudo do efeito dos parâmetros físicos e químicos de adsorvente sólido no processo de adsorção de SO_2 em calcário." Master diss., Universe of Campinas - Unicamp, 1996.

Pettijohn, Francis J., *Sedimentary Rocks*. New York: Harper and Brothers, 1957.

Shimizu, Tadaaki., Satoh, Masato., Sato, Kazuma., Tonsho, Masaru., and Inagaki, Makoto.,. "Reduction of SO2 and N2O emissions without increasing NOxemission from a fluidized bed combustor by using fine limestone particles." *Energy & Fuels 16 (2002)*.

AIR POLLUTION CONFERENCE BRAZIL
CMAS SOUTH AMERICA
COMMUNITY MODELING AND ANALYSIS SYSTEM

ANALYSIS OF THE TEMPERATURE VARIATION AND Ca/S RATIO IN THE DESSULFURIZATION OF BRAZILIAN COAL IN A BUBBLING FLUIDIZED BED COMBUSTOR

Pedro Rodrigo Silva Moura[1], Flavio Michels Bianchi[1], Josiane da Rocha Silvano Neves[1], Raiane da Cruz[1], Thiago Luis Zanin[2], Luiz Fernando de Lima Junior[2], Thiago Fernandes de Aquino[1]

[1]*Beneficent Association of the Santa Catarina Coal Industry (SATC), Criciúma, SC, Brazil*
pedro.moura@satc.edu.br
[2]*Department of Chemical Engineering at UFPR, Administration, 1st floor, DEQ/TC/UFPR Polytechnic Center, Curitiba, PR, Brazil*
thiago.zanin@ufpr.br

Abstract: Despite worldwide calls to reduce its use, coal continues to be widely used for thermoelectric generation. Based on this, using it in a way that minimizes its harmful effects on the environment and the health of the population is essential. As it contains a significant percentage of sulfur in its composition, Brazilian coals after conversion must have their emissions strictly controlled to comply with legislation and mitigate their effects on the environment. In this way, experimental tests were carried out on a bench scale with the combustion of Brazilian coal from the state of Paraná using limestone to reduce sulfur oxides from the exhaust gas stream. To this end, a bubbling fluidized bed combustor was used where tests were carried out in addition to burning coal without adding limestone as a basis for comparison, as well as mixtures containing a Ca/S molar ratio in the order of 2, 3, and 4. The influence of temperature on sulfur reduction considering typical to the technology values was applied too. The gas compositions during combustion tests were obtained through a portable gas analyzer and the thermal behavior of the fuel was carried out using a thermogravimetric analyzer (TGA). From the tests carried out, it was found that the limestone used showed degradation peaks below 790°C on a thermobalance. This phenomenon could be confirmed in bench combustion tests, since for milder temperatures (around 815°C) the sulfur reduction was greater than those tested at higher temperatures (around 850°C). In terms of sulfur reduction, molar ratios 3 and 4 achieved reductions that comply with current legislation for the State of Paraná while ratio 2 did not reach values appropriate to the legislation.

Keywords: Desulfurization, Combustion, Fluidized Bed, Brazilian Coal, Limestone.

INTRODUCTION

Energy conversion technology using fluidized beds is modern and environmentally friendly when compared to traditional energy conversion methods, for example, combustors in fixed and pulverized fluidized bed (Basu, 2006; Wander et al., 2020).

This type of combustor works based on the suspension and combustion of solid fuels by a gas flow (Basu, 2006), allowing the combustion to happen faster, with good heat transfer rate as a function of turbulence and the possibility of burning solid materials of difficult ignition, as for example coals with high level of ashes. The fuel granulometry and the possibility of sulfur removal using calcium compounds in the bed are pointed to be another good advantage of this technology (Bragança e Castelan, 2009).

Therefore, this work experimentally evaluated on a bench scale the combustion of Brazilian coal from Paraná using in situ limestone to reduce sulfur oxides from the exhaust gas stream to meet the legal emission limits of this component.

METHODS

For the experimental tests, a bubbling fluidized bed reactor (capacity up to 3 kg/h) on a bench scale was used (see Figure 1), consisting of a cylindrical combustion chamber with an internal diameter of 160 mm and a height of 1200 mm, manufactured in 316 stainless steel.

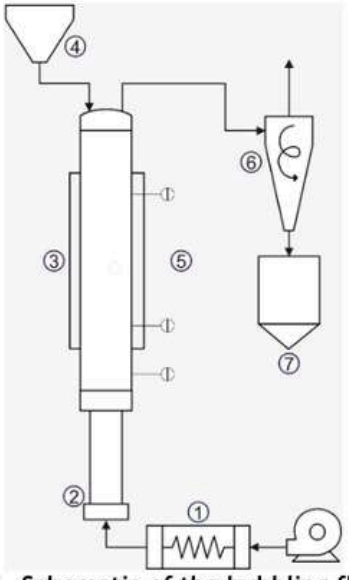


Figure 1. Schematic of the bubbling fluidized bed combustor. 1 - inlet air pre-heater, 2 - plenum chamber, 3 - combustion chamber, 4 - silo, 5 - thermocouples, 6 - cyclone, and 7 - ash hopper.

The combustor has a full chamber at its base, responsible for stabilizing the flow and absorbing pressure fluctuations of the incoming gas, before the perforated air distribution plate at the lower base of the combustion chamber. The distributor plate is made of ceramic fiber and is 12 mm thick with 1 mm diameter holes.
A portable gas analyzer of ECIL brand Chemist 600 brand was used to evaluate the concentration of combustion gases in terms of O_2, CO, CO_2, NO (corrected internally to NOx), and SO_2.
The tests were performed at average temperatures of 815 °C and 850 °C. The control of fuel flow, airflow, and bed temperature were carried out by supervision. The excess air and fuel flow rate were adjusted in each test to maintain the bed temperature close to 815 °C and 850 °C.
Casting sand was used as bed material. The size of the casting sand was in the range of 0.2-0.35 mm. The limestone used was the limestone supplied by Copel GeT with an average diameter of 402 µm, bulk density of 1560 kg/m^3, and chemical composition of 51.47% CaO, 5.18% MgO, 1.00% others and 42.35% LOI.
The diameter of selected coal particles was in the range of 0.60-2.00 mm aiming at stability of operation. The limestone was fed in a proportion expressed as a Ca/S molar ratio: 2, 3 and 4.
Two main parameters were evaluated for carrying out the combustion tests: temperature and the Ca/S molar ratio. Eight combustion tests were carried out. For comparison purposes, two of them considered only coal at 815 °C and 850 °C. For each Ca/S molar relationship used, two temperatures were used.

FINDINGS AND ARGUMENT

Table 1 shows the characteristics of the fuel.

Table 1 - Characteristics of the fuel.

Characteristic	Methods	Coal
HHV [kJ/kg]	ASTM D5865-13	5.559,0
LHV [kJ/kg]	---	5.340,6
Proximate analysis		
Ashes [%]	ASTM D3174-12	25.05
Volatile matter [%]	ASTM D3175-20	26.76
Fixed carbon [%]	ASTM D5865-20	48.18
Total humidity [%]	ASTM D3173M-17	3.22
Ultimate analysis		
Carbon [%]	ASTM D5373-21	56.20
Hydrogen [%]	ASTM D5373-21	3.80
Oxygen [%]	ASTM D3176-21	10.59
Nitrogen [%]	ASTM D5373-21	1.13
Sulfur	ASTM D4239-18	3.23

HHV - Higher heating value.
LHV - Lower heating value.

Thermogravimetric analysis was carried out on the coal sample to evaluate the volatile release temperature and possible events that may occur with the sample when subjected to high temperature conditions (up to 1000 °C) in an oxidizing atmosphere (representing the normal conditions of a possible burn). This behavior can be seen in Figure 2.

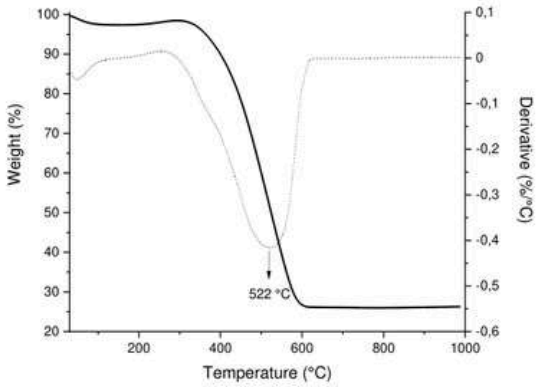


Figure 2 - Thermogravimetric analysis of coal.

The total mass loss obtained for the sample was 73.61%, with an exothermic mass loss event observed at a temperature of 522°C, that is related to the char combustion process. The thermogravimetric analysis of the limestone is shown in Figure 3. The temperature of 789°C indicates the break of the mineral structure of limestone.

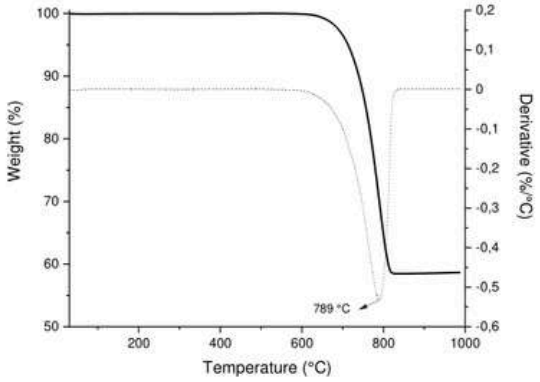


Figure 3 - Thermogravimetric analysis of limestone.

Gas emissions from the combustion of coal and limestone mixtures were analyzed. The exhaust gas composition and main operating conditions are shown in Table 2.
Analyzing Table 2, a significant reduction in the average concentrations of SO_2 in the exhaust gases is noted in comparison to the tests without the addition of limestone. The desulfurization efficiency increases as the Ca/S molar ratio increases.

Table 2 - Exhaust gas composition and operating conditions

	Coal		Ca/S = 2		Ca/S = 3		Ca/S = 4	
Parameter	T=815 °C	T=850 °C	T=815 °C	T=850 °C	T=815 °C	T=850 °C	T=815 °C	T=850 °C
O_2 (%)	8.69	7.76	6.97	6.10	8.95	7.04	7.69	6.03
CO_2 (%)	12.21	13.14	13.93	14.80	11.95	13.87	13.21	15.18
CO (mg/Nm³)	82.00	30.00	103.90	30.20	43.68	31.45	26.11	---
NO (mg/Nm³)	557.71	691.06	733.50	659.05	722.05	689.05	735.11	698.63
SO_2 (mg/Nm³)	5840.00	6116.50	1349.30	1726.80	938.74	1262.35	872.37	1055.89
SO_2 (7.0%)	6641.63	6468.97	1344.17	1617.20	1089.71	1261.10	918.17	985.30
T_{bed} (°C)(1)	807.19	849.98	813.30	857.38	814.91	859.92	813.37	852.16
$\dot{m}_{air}$ (L/min)(2)	189.16	185.17	175.13	190.54	178.79	198.47	180.99	197.47
$\dot{m}_{fuel}$ (kg/h)(3)	---	---	1.212	1.154	1.212	1.207	1.071	1.151
$\dot{m}_{coal}$ (kg/h)(4)	0.65	0.80	0.99	0.95	0.91	0.91	0.74	0.80
Excess air (%)	192.5	130.3	76.0	100.0	95.8	118.3	143.3	146.6
SO_2 removal (%)	---	---	79.8	75.0	83.6	80.5	86.2	84.8

(1) Bed average temperature.
(2) Volumetric air flow.
(3) Mass flow rate of fuel+limestone.
(4) Mass flow rate of coal.

The maximum desulfurization of 86.2% (T=813.4 °C) and 84.8% (T=852.2 °C) stands out for a Ca/S molar ratio of 4. Desulfurization tests at temperatures of 815 °C showed higher percentages of sulfur removal compared to tests at temperatures of 850 °C, for all molar ratios. This is due to the breakdown of limestone occurring at a temperature lower than that indicated in the literature, which is around 825°C. The limestone used in the tests showed, through thermogravimetric analysis, its breakdown at 789 °C (see Figure 3), thus enabling sulfur abatement at lower temperatures.

The test for the mixture with a Ca/S molar ratio equal to 4 at 850 °C showed an average SO_2 concentration of 985.3 mg/Nm³, corrected for 7% O_2. A significant drop in SO_2 concentrations in combustion gases is noted compared to the test without limestone addition (6468.97 mg/Nm³), as shown in Table 2. The SO_2 emission limit required by Resolution SEMA 016/2014 is 3000 mg/Nm³ for powers greater than 10 MW and less than 20 MW.

CONCLUSIONS

Tests without adding limestone to the fuel showed average SO_2 emissions of 6641.6 and 6468.9 mg/Nm³ for temperatures 815 and 850 °C, respectively.

Desulfurization tests at temperatures of 815 °C showed higher SO_2 conversion efficiencies compared to tests at temperatures of 850 °C, for all molar ratios. The limestone used showed, through thermogravimetric analysis, its breakdown at 789°C, thus enabling the reduction of sulfur at lower temperatures.

The tests with molar ratios 3 and 4 obtained reductions that comply with current legislation, while ratio 2 did not reach values appropriate to the legislation.

REFERENCES

Basu, Prabir. Combustion and Gasification in Fluidized Beds, 1a. ed. CRC Press. Boca Raton (2006).

Bragança, Saulo. R., and Castellan, Jorge. L. FBC desulfurization process using coal with low sulfur content, high oxidizing conditions and metamorphic limestones. Brazilian J. Chem. Eng. 26, 375-383 (2009).

Wander, Paulo. R., Bianchi, Flavio. M., Caetano, Nattan. R., Klunk, Marcos. A., Indrusiak, Maria. Luiza. S., Cofiring low-rank coal and biomass in a bubbling fluidized bed with varying excess air ratio and fluidization velocity. Energy 203. (2020). doi:10.1016/j.energy.2020.117882

AIR POLLUTION CONFERENCE BRAZIL
CMAS SOUTH AMERICA
COMMUNITY MODELING AND ANALYSIS SYSTEM

POLYMER DUST SUPRESSANT PRODUCED FROM POLYETHYLENE TEREPHTHALATE (PET) AND İTS APPLİCATİONS

Andrielly Moutinho Knupp[1], Vinícius Sampaio[2], Juliana Santos[3], Viviane Fontes[4], Roberta Link[5], Luiz Borges[6], Rafael Valadares[7], Elói Silva[8], Gustavo Gonçalves[9], Fabrício Uliana[10], Carolini Spadetto[11], Natalia Portela[12] and Paulo Filgueiras[13]

[1]Vale
andrielly.knupp@vale.com
[2]Vale (The Bakery)
c0650341@vale.com
[3]Vale
juliana.santos@vale.com
[4]Vale
viviane.fontes@vale.com
[5]Vale
roberta.link@vale.com
[6]Vale
luiz.borges@vale.com
[7]Vale
rafael.valadares@vale.com
[8]Vale
eloi.silv@gmail.com
[9]UFES
gustavo.rgoncalves@hotmail.com
[10]UFES
fabriciouliana6@gmail.com
[11]UFES
carolinispadetto@gmail.com
[12]UFES
nataliaportela@hotmail.com
[13]UFES
filgueiras.pr@gmail.com

Abstract: The Sustainable Suppressor was developed by Vale and the Federal University of Espirito Santo as a research and development project. The goal was to use PET (Polyethylene Terephthalate) as a raw material to create a chemically stable, biodegradable, non-hazardous polymer that could efficiency control particulate matter emissions. The Sustainable Suppressor is produced throughout the depolymerization of PET is based on the alkaline hydrolysis reaction. The suppressor was tested in a wind tunnel and on industrial scale. In the wind tunnel tests, 20 commercial suppressors and the PET suppressor were evaluated and compared using a Chevron configuration of iron ore piles under controlled conditions of wind speed, humidity, and temperature. The results were reported in percentage of dry ore mass loss, with lower percentages indicating the best performing suppressor. The PET was among the best-performing of dust suppressants between the products evaluated with an efficient coverage after 12 hours in the oven through the formation of a film-like or protective layer. The industrial-scale tests were conducted on iron ore fines and burned pellets stockpiles, with the application of the PET product and 4 others commercial dust suppressants. The concentration of Total Suspended Particles (TSP) was monitored over a period of 4 to 6 hours after the application of the suppressors. The monitoring of TSP results showed 0.06 kg/h of emission rate and 0.03 g/h.m² of emission factor from suppressor PET. The Sustainable Suppressor proved to be an effective emission control agent, without the need for operational interventions. The adoption of Sustainable Suppressor will bring operational optimization, cost reductions and will benefit 1,000 people with increased income and about 1 million tons of PET plastic will be removed from the environment per year.

Keywords: Circular economy, Polyethylene Terephthalate, Dust supressant, Sustainable Suppressor.

AIR POLLUTION CONFERENCE BRAZIL
CMAS SOUTH AMERICA
COMMUNITY MODELING AND ANALYSIS SYSTEM

INTRODUCTION

In the mining industry due to the various activities that include the materials handling and storage occurs particulate matter emissions in the atmosphere. Such activities require control of atmospheric emissions to mitigate the impact on air quality, and consequently, on human health.

To control emissions of particulate matter in the atmosphere and prevent their dispersion, the suppression technique is applied using water sprays or polymeric solutions to (WRAP, 2006; Santos Jr et al., 2017; Li et al., 2022; Zhou et al., 2023). The main mechanisms of suppressors to prevent the entrainment of particulate matter are humidification or particle agglomeration (Copeland and Kwatra, 2005).

With the aim of creating a sustainable suppressor, this work proposes the PET (Polyethylene Terephthalate) as a raw material to create a chemically stable, biodegradable, non-hazardous polymer that could efficiently control particulate matter emissions (Vanini et al, 2013; Dos Santos et al., 2024). The plastic pollution affects the quality of air, soil, water supply systems and biota (terrestrial or marine). According to the Brazilian Plastics Industry Association (Abiplast, 2021) in Brazil, just 2% of resins and 1,9% of plastics produced by recycling.

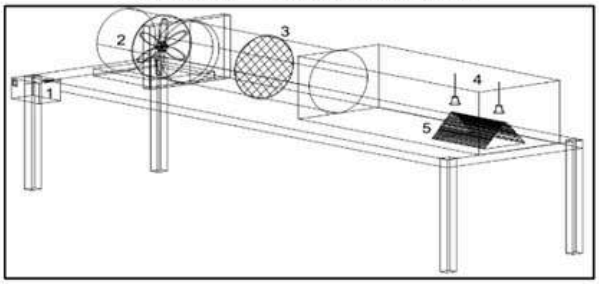
By using PET, the project would also contribute to the circular economy and increase the income of people with a social vulnerability condition by purchasing PET from recycling associations.

METHODS

Dust suppressor PET was produced under alkaline hydrolysis condition in an industrial reactor with a capacity of 2 tons. PET materials were obtained from the recycling associations and theirs labels and caps removed. Subsequently, the selected PET was transformed into flakes and micronized with the aim to increase the surface area and optimize the size of the particles to 0.35 mm. Thus, micronized PET reacted in the reactor with NaOH (50% solution), a special cationic catalyst (QACs), and water. This mixture is heated to 100°C and reacts for about 3 hours. As described in the patent BR 10 2013 001662-4 A2, any leftover PET waste is reused in the next batch.

The sustainable suppressor has been tested on a laboratory and industrial scale. A methodology shows in Figure 1, for evaluating the performance of dust suppressors in iron ore stockpiles using a wind tunnel was developed to assist in the evaluation of the best products under controlled conditions. The controlled conditions were wind speed (simulating the days of strong winds); humidity content of the iron ore (characteristic of relevant interference in the real-scale tests); humidity and ambient temperature.

Figure 1. Wind tunnel scheme



Notes: 1: Motor controller; 2: Motor and helices; 3: Wind flow rectifier; 4: Incandescent lamps and 5: Sample - iron ore stockpile.

The industrial-scale tests were conducted in an Industrial Complex located at the Tubarao Unit - Vitoria, Espirito Santo/Brazil, on 5 piles of iron ore fines and 1 pile of burned pellets, with the application of the Sustainable Suppressor at a concentration of 0.5% (m/m) and the usual concentration of the conventional suppressors. The concentration of Total Suspended Particles (TSP) was monitored by 3 verticals particulate monitors and 1 wind and direction speed sensor over a period of 4 to 6 hours after the application of the suppressors. The rates and factors of emission were determined, considering the following variables: amount of material, wind speed and direction, TSP concentration upwind and downwind of the emission source, main characteristics of the emission source and the fugitive emission plume.

FINDINGS AND ARGUMENT

The wind tunnel tests results of 21 samples analyzed of iron ore dust suppressors commercial products evaluated by the mass loss as emission of each one, which is inversely proportional to suppressor performance. The Figure 2 demonstrates the difference in performance between the dust suppressors analyzed. It shows that PET suppressant (sample S07) excels at keeping fine particles adhered to the piles.

In the industrial scale tests evaluated 5 dust suppressants products at iron ore stockpiles. The monitoring of TSP results showed 0.06 kg/h of emission rate and 0.029 g/h.m² of emission factor from suppressor PET (sample S04) (Figure 3). During the industrial tests, the Sustainable Suppressor proved to be an effective emission control agent

compared with the others dust suppressants, without the need for operational interventions to applying it.

Figure 2. Graph of the mass loss of dry iron ore by dust suppressor samples.

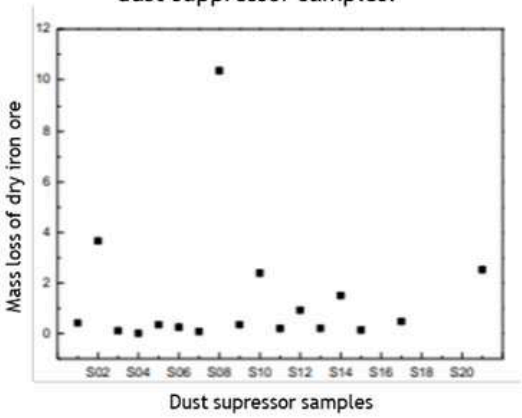
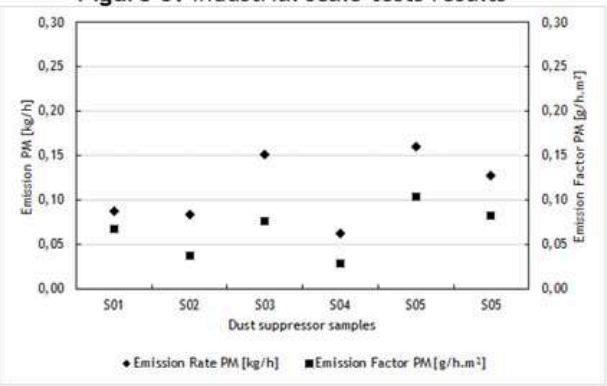


Figure 3. Industrial scale tests results



CONCLUSIONS

The process of chemical recycling PET to produce Sustainable Suppressant proved to be suitable (biodegradable, non-hazardous and non-toxic to the environment), combining an industrial dust control with circular economy and social improvements for waste collectors' associations.

In the laboratory and industrial tests scale the dust suppressor was satisfactory for the purpose, providing the efficiency between commercially available dust suppressor samples tested with a significantly outperformed.

Its industrial use has been validated for protecting iron ore stockpiles, but it can also be used on wagons and other materials stockpiles, considering a residence time of up to 18 days due to its biodegradability.

By using PET, the project would also contribute to recycling associations through social partnerships in 6 cities with 12 associations, new collection points and educate people on recycling, creating a closed-loop system for a sustainable future.

The implementation and scalability of the project is part of the business model developed that meets the commitment of environmental and social impact, risk mitigation, and operationalization, through the licensing of the technology and strategic partnerships with startups that are experts in the chemical industry and waste management, for the exclusive supply to Vale.

REFERENCES

Abiplast (Associação Brasileira da Indústria do Plástico). "Perfil 2021." Accessed March 28, 2023. https://www.abiplast.org.br/publicacoes/perfil-2021/.

Copeland, C. R., and Kwatra S. K. "Dust suppression in iron ore processing plants." Mining & Metallurgical Processing 22 (2005): 177-91. doi: 10.1007/BF03403321.

Li, M.; Wang, R.; Li, G.; Song, X.; Yang, H.; Lai, H. "Comprehensive chemical dust suppressant performance evaluation and optimization method." Environmental Research and Public Health 19 (2022): 5617. Accessed April 28, 2024. doi: 0.3390/Ijerph19095617.

Dos Santos, Gabriel F S.; Rodrigues, José G A.; Gomes Junior, Sidnei B.; da Silva, Tárcila M N.; Schaffel, Izabela F.; Conceição, Nathalia S.; Gonçalves, Gustavo R.; Filho, Eloi A Silva.; Ferreira, Rafael Q. "From Waste to Protection: A Green Industrial Recycling Approach to Generate an Eco-Friendly Corrosion Inhibitor for 304 Stainless Steel in Saline Solutions." Journal of materials engineering and performance, 25 mar. 2024.

Santos Jr, R.M., Fontana, A.R.L., Cunha, A.J.L., Mesquita, A.L.A., Gontijo, C. F., Leal Filho, L.S. "Experimentos em túnel de vento para secagem e emissão de particulados de minério de ferro em modelo de vagões de trem." Paper presented at the 27th National Meeting on Ore Treatment and Extractive Metallurgy, Belém, Pará, October 23-27, 2017.

Vanini, Gabriela.; Castro, Eustáquio V R de.; Silva Filho, Eloi Alves da.; Romão, Wanderson. "Despolimerização Química de PET Grau Garrafa Pós consumo na Presença de um Catalisador Catiônico, o Brometo de Hexadeciltrimetrilamônio (CTAB)." Polímeros, v. 23, n. 3, p. 425–431, 1 jan. 2013.

WRAP (Western Regional Air Partnership's). *Fugitive Dust Handbook, 1-14.* Denver: Countess Environmental, 2006.

Zhou, G.; Xu, Y.; Wang, Q.; Jiang, B. Ren, B. Zhang, X.; Yi, L. "Wetting-consolidation type dust suppressant based on sugarcane bagasse as an environmental material: Preparation, characterization and dust suppression mechanism." Journal of Environmental Management 330 (2023): 117097. Accessed April 28, 2024. doi: 10.1016/j.jenvman.2022.117097.

AIR POLLUTION CONFERENCE BRAZIL
CMAS SOUTH AMERICA
COMMUNITY MODELING AND ANALYSIS SYSTEM

Impact of vegetation cover on the concentration of carbon dioxide in the metropolitan area of São Paulo

Jorge A. Piscoya Santibañez[1] , Maria de Fátima Andrade[1] , Marco A. Franco[1]
[1]University of São Paulo, IAG, Department of Atmospheric Sciences
j.piscoya@usp.br / maria.andrade@iag.usp.br / marco.franco@usp.br

Abstract: This study aims to investigate the role of vegetation in regulating carbon dioxide (CO_2) concentration in the Metropolitan Region of São Paulo (MRSP), collaborating with the METROCLIMA project. On-site measurements and statistical analysis were conducted at four stations from the METROCLIMA network, named Pico do Jaraguá, ICESP, IAG, and UNICID, each surrounded by varying degrees of vegetation cover. Data from Picarro monitors spanning 2019 to 2022 focused on correcting measurement errors and analyzing seasonal concentration frequencies. The results show that CO_2 concentrations in the MRSP generally range between 400 to 500 ppm throughout the year, with a consistent trend around 425 ppm. Temporal variations show a diurnal pattern, with concentrations decreasing during the day and increasing at night. However, the ICESP station exhibited a unique behavior possibly attributed to the measurement height, which directly impacts the detection of the boundary layer evolution throughout the day. Additionally, all analyses showed that IAG has a higher concentration variability than the other stations. Statistical data indicates that Pico do Jaraguá has a lower and more stable CO_2 concentration, averaging around 420 ppm, with a standard deviation of 9 ppm, likely due to the nearby vegetation. In contrast, IAG has the highest standard deviation for all annual stations (spring: 20.1 ppm, summer: 17.6 ppm, fall: 22.2 ppm, and winter: 27.1 ppm), followed by UNICID (spring: 14.3 ppm, summer: 13.1 ppm, fall: 16.1 ppm, winter: 20.4 ppm). The analysis of distribution by annual seasons demonstrated that the data follow a Johnson's Su-type behavior, whose parameters (μ, σ, ν, τ), accurately describe the seasonal behavior of the data. To obtain the direct impact of vegetation on CO_2, the analyses were divided into winter and summer, observing a maximum variation in solar radiation intensity, focusing on the time interval between 13h - 16h LT. Pico do Jaraguá has the lowest average CO_2 concentration, with values of 412.6 ± 0.3 ppm in summer and 415.8 ± 0.2 ppm in winter. These concentrations were considered background to extract the gradient due to vegetation on the other sites. Differences in CO_2 in the region were observed in summer and winter, with 2.1, 2.7, and 8.5 ppm in summer and 2.7, 8.8, and 8.8 ppm in winter for IAG, ICESP, and UNICID, respectively. Therefore, regions with higher urbanization are also regions with higher CO_2 gradients. IAG, the site with intermediate urbanization and vegetation cover, presented the lowest values among the three more urbanized areas. The results found in the behavior of CO_2, contrasted with the calculated gradients, highlight the importance of vegetation in regulating CO_2 concentration in MASP.

Keywords: Carbon Dioxide, Metropolitan Region of São Paulo, vegetation, Temporal Variation, Statistical Analysis

INTRODUCTION

Carbon dioxide (CO_2) in the atmosphere, primarily generated by human activities, strongly increases globally (Gratani L, 2016). Numerous atmospheric components from human activities, especially in urban centers, directly contribute to the greenhouse effect. For instance, more than 50% of the world's population lives in cities, which is expected to increase by more than two-thirds up to 2050 (UN, United Nations, 2010). Therefore, the CO_2 concentration in cities is an important issue that needs to be urgently addressed.
Green spaces, which include parks, gardens, sports fields, tree-lined avenues, and hedges, play a crucial role in the carbon cycle within cities (Svirejeva-Hopkins A,2006). Plants absorb CO_2 by acting as sinks, storing carbon in photosynthesis to form biomass (Gratani L, 2016).

Brazil has one of the largest territories in the world, and it has one of the largest cities, São Paulo, which faces significant challenges concerning CO_2 emissions and air quality. To face these challenges, São Paulo seeks to implement policies and programs to mitigate CO_2 emissions and promote environmental sustainability. This study aims to investigate the impact of vegetation coverage on atmospheric CO_2 concentration in the Metropolitan Region of São Paulo (MRSP).

The methodology includes in-situ measurement of CO_2 concentration and detailed statistical data analysis. The measurements were carried out with monitoring instruments from PICARRO between 2019 and 2022, whose time series are shown in Figure 1, and its statistical analysis, correlating it with meteorological and vegetation coverage components. Data were collected at four stations belonging to the METROCLIMA network: Pico do Jaraguá, ICESP (Institute of Cancer of the State of São Paulo), IAG (Institute of Astronomy, Geophysics, and Atmospheric Sciences of the University of São Paulo), and UNICID (City University of São Paulo), selected due to differences in their vegetation coverage. Pico do Jaraguá is the station with the highest vegetation coverage, followed by IAG, while ICESP and UNICID are the stations with the most urbanized areas.

METHODS

This study performs a detailed statistical characterization of the available data on CO_2 concentration based on the following metrics: median, mean, minimum and maximum values,

standard deviation, and standard error. Additionally, classification by seasons (spring, summer, autumn, and winter) was carried out to identify data trends influenced by each season and subsequently analyzed concerning meteorological factors. External factors such as human activity and vegetation influence were also included. Daily cycle plots were produced to visualize and understand the data better, considering the temporal variation between the annual seasons (spring, summer, autumn, and winter) daily and hourly. A parametric distribution study based on histograms for annual seasons was added to find the spatial and temporal behavior of CO_2. The model used was the GAMLSS model (Generalized Additive Models for Location, Scale, and Shape), considering a parametrization of 4 parameters (μ,σ,ν,τ) to determine location (e.g., mean), scale (e.g., standard deviation), and shape (e.g., skewness and kurtosis), determining the type of function through density curves.

FINDINGS AND ARGUMENT

The statistical characterization shows that IAG and UNICID exhibit identical mean CO_2 concentrations during spring of 427.5 ± 0.2 ppm and 427.2 ± 0.2 ppm, respectively. The widest variability range in measurements is found at IAG, with 225.6 ppm, while the narrowest corresponds to ICESP, with 95.4 ppm. Notably, IAG displays the highest standard deviation of 20.1 ppm, indicating significant impacts of different CO_2 sources compared to the other locations, with the lowest being Pico do Jaraguá, at 8.8 ppm. IAG and UNICID display almost identical means in summer, at 425.9 ppm ± 0.2 and 425.7 ± 0.2 ppm, respectively.

The widest concentration range is found at IAG, with 258.3 ppm, while the narrowest corresponds to ICESP, with 51.4 ppm. Once more, IAG exhibits the highest standard deviation, at 17.6 ppm, while ICESP has the lowest at 8.9 ppm. In autumn, statistical data shows differing means among the locations. The widest range is found at ICESP with 210.2 ppm, while the narrowest ranges are observed at Pico do Jaraguá and UNICID. Again, IAG presents the highest standard deviation, at 22.2 ppm, while Pico do Jaraguá displays the lowest, at 8.9 ppm. Considering the statistical data for winter, similarities in means are observed between IAG and UNICID, at 433 ppm and 432 ppm, respectively. The widest range is observed at ICESP, with 238.5 ppm, and the narrowest at UNICID, with 162.2 ppm. The highest standard deviation is present at IAG with 27.1 ppm, and the lowest is found at Pico do Jaraguá with 8.8 ppm.

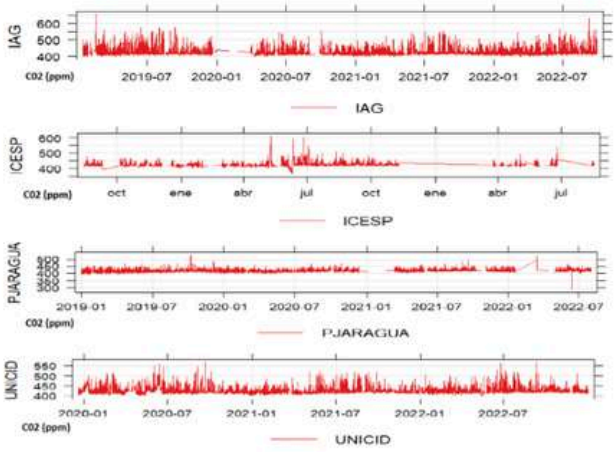


Figure 1: Time series of the four measurement locations (IAG, ICESP, Pico do Jaraguá, and UNICID) from 2019 to 2022.

Figure 2 shows the diurnal cycle of CO_2 concentration at the four stations. A clear trend pattern is observed in IAG, UNICID, and Pico do Jaraguá, where CO_2 concentrations decrease during the day due to the establishment of the mixing boundary layer and increase at night when the stable boundary layer is established. However, in ICESP, despite displaying similar behavior, the diurnal cycle is temporally shifted compared to the other stations. This particular behavior is likely due to the height at which the CO_2 is collected, as it detects the evolution of the boundary layer shifted in time compared to stations closer to the surface. IAG exhibits the highest nocturnal concentration peaks in almost all seasons, surpassed only in spring by ICESP. Additionally, it is observed that Pico do Jaraguá has the diurnal cycle with the lowest CO_2 concentrations compared to other locations.

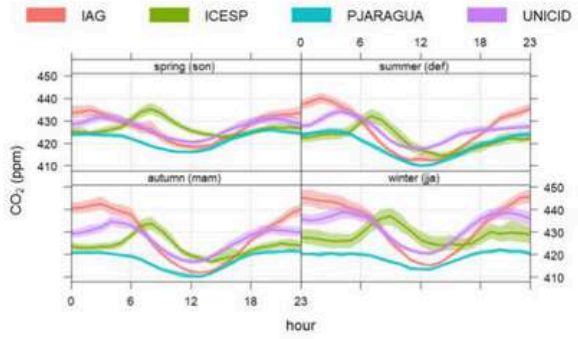


Figure 2. Diurnal cycles of CO2 concentrations discriminated by seasons of the year.

In the distribution analysis, the GAIC (generalized Akaike information criterion) metric was used to quantify the adjustment of the data distribution. The gamlssML package in R was applied, which uses the GAIC metric, discriminates different

distributions for each data arrangement, and provides the data seasonally (spring, summer, autumn, and winter). The obtained result showed that the distribution that best corresponded coupled to seasonal data is the Johnson's Su function.

To examine how vegetation impacts CO_2 concentration across various experimental sites, we selected the period of the highest mixing boundary layer in RMSP, which corresponds to 1:00 pm to 4:00 pm (Dos Santos A.V. et al., 2023). Also, the analysis was performed during the summer and winter due to the clear differences in solar radiation incidence. During the summer, it was observed that the average CO_2 concentration decreased compared to the total data. Pico do Jaraguá, which had the lowest average CO_2 concentration, with values of 412.6 ± 0.3 ppm in summer and 415.8 ± 0.2 ppm in winter, was selected as the background site. CO_2 differences were observed in summer and winter regions, with 2.1, 2.7, and 8.5 ppm in summer and 2.7, 8.8, and 8.8 ppm in winter for IAG, ICESP, and UNICID, respectively. Hence, areas characterized by increased urbanization exhibit correspondingly elevated CO_2 gradients. Notably, IAG, distinguished by intermediate urbanization and vegetation coverage, demonstrated the lowest CO_2 levels among the three most urbanized regions examined.

CONCLUSIONS

In conclusion, this study reveals significant seasonal and temporal variations in CO_2 concentrations across diverse measurement locations. Despite similar average levels at IAG and UNICID, IAG demonstrates larger concentration variability, potentially influenced by vegetation percentage and local sources such as important highways nearby. ICESP exhibits temporal changes due to installation height, which affects boundary layer detection. IAG consistently records the highest CO2 peaks, except in spring, where ICESP outperforms. Pico do Jaraguá consistently shows the lowest CO_2 concentrations, suggesting vegetation's crucial role in CO_2 regulation. The study emphasizes the importance of location characteristics and the boundary layer in understanding CO_2 dynamics, alongside the impact of vegetation percentage on CO_2 levels.

REFERENCES

Castelo, Daniel Prado, and Maria de Fátima Andrade. "Análise da concentração de dióxido de carbono nos sítios experimentais do projeto metroclima na cidade de São Paulo." (2022).

Gratani, Loretta, Laura Varone, and Andrea Bonito. "Carbon sequestration of four urban parks in Rome." Urban Forestry & Urban Greening 19 (2016): 184-193.

Kristal R. Verhulst1, Anna Karion, Jooil Kim, Peter K. Salameh, Ralph F. Keeling, Sally Newman, John Miller, Christopher Sloop, Thomas Pongettil, Preeti Rao, Clare Wong, Francesca M. Hopkinsl,Vineet Svirejeva-Hopkins A, Schellnhuber H. Modelling carbon dynamics from urban land conversion: fundamental model of city in relation to alocal carbon cycle. Carbon Bal Manag 2006

Vieira dos Santos, A.; Cristina Araújo, E.; da Silva Andrade, I.; Corrêa, T.; Talita Amorim Marques, M.; Eduardo Souto-Oliveira, C.; Franchi Leonardo, N.; de Mendonça Macedo, F.; Souza, G.; Pereira de Queiroz Lopes, P.; et al. Comparison of PBL Heights from Ceilometer Measurements and Greenhouse Gases Concentrations in São Paulo. Atmosphere 2023

AIR POLLUTION CONFERENCE BRAZIL
CMAS SOUTH AMERICA
COMMUNITY MODELING AND ANALYSIS SYSTEM

ANALYSIS OF THE TEMPERATURE VARIATION AND Ca/S RATIO IN THE DESSULFURIZATION OF BRAZILIAN COAL IN A BUBBLING FLUIDIZED BED COMBUSTOR

Pedro Rodrigo Silva Moura[1], Flavio Michels Bianchi[1], Josiane da Rocha Silvano Neves[1], Raiane da Cruz[1], Thiago Luis Zanin[2], Thiago Fernandes de Aquino[1]

[1]Beneficent Association of the Santa Catarina Coal Industry (SATC), Criciúma, SC, Brazil
pedro.moura@satc.edu.br
[2]COPEL Geração e Transmissão S.A, Curitiba, PR, Brazil
thiago.zanin@copel.com

Abstract: Despite worldwide calls to reduce its use, coal continues to be widely used for thermoelectric generation. Based on this, using it in a way that minimizes its harmful effects on the environment and the health of the population is essential. As it contains a significant percentage of sulfur in its composition, Brazilian coals after conversion must have their emissions strictly controlled to comply with legislation and mitigate their effects on the environment. In this way, experimental tests were carried out on a bench scale with the combustion of Brazilian coal from the state of Paraná using limestone to reduce sulfur oxides from the exhaust gas stream. To this end, a bubbling fluidized bed combustor was used where tests were carried out in addition to burning coal without adding limestone as a basis for comparison, as well as mixtures containing a Ca/S molar ratio in the order of 2, 3, and 4. The influence of temperature on sulfur reduction considering typical to the technology values was applied too. The gas compositions during combustion tests were obtained through a portable gas analyzer and the thermal behavior of the fuel was carried out using a thermogravimetric analyzer (TGA). From the tests carried out, it was found that the limestone used showed degradation peaks below 790°C on a thermobalance. This phenomenon could be confirmed in bench combustion tests, since for milder temperatures (around 815°C) the sulfur reduction was greater than those tested at higher temperatures (around 850°C). In terms of sulfur reduction, molar ratios 3 and 4 achieved reductions that comply with current legislation for the State of Paraná while ratio 2 did not reach values appropriate to the legislation.

Keywords: Desulfurization, Combustion, Fluidized Bed, Brazilian Coal, Limestone.

INTRODUCTION

Energy conversion technology using fluidized beds is modern and environmentally friendly when compared to traditional energy conversion methods, for example, combustors in fixed and pulverized fluidized bed (Basu, 2006; Wander et al., 2020).

This type of combustor works based on the suspension and combustion of solid fuels by a gas flow (Basu, 2006), allowing the combustion to happen faster, with good heat transfer rate as a function of turbulence and the possibility of burning solid materials of difficult ignition, as for example coals with high level of ashes. The fuel granulometry and the possibility of sulfur removal using calcium compounds in the bed are pointed to be another good advantage of this technology (Bragança e Castelan, 2009).

Therefore, this work experimentally evaluated on a bench scale the combustion of Brazilian coal from Paraná using in situ limestone to reduce sulfur oxides from the exhaust gas stream to meet the legal emission limits of this component.

METHODS

For the experimental tests, a bubbling fluidized bed reactor (capacity up to 3 kg/h) on a bench scale was used (see Figure 1), consisting of a cylindrical combustion chamber with an internal diameter of 160 mm and a height of 1200 mm, manufactured in 316 stainless steel.

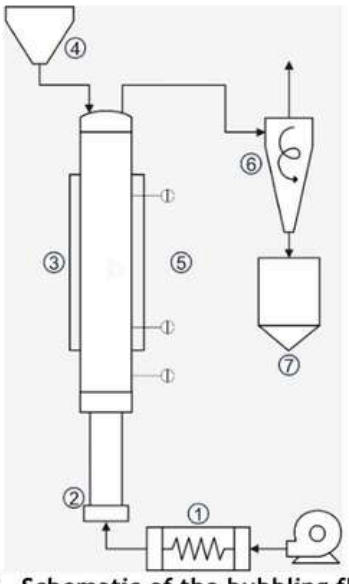


Figure 1. Schematic of the bubbling fluidized bed combustor. 1 - inlet air pre-heater, 2 - plenum chamber, 3 - combustion chamber, 4 - silo, 5 - thermocouples, 6 - cyclone, and 7 - ash hopper.

The combustor has a full chamber at its base, responsible for stabilizing the flow and absorbing pressure fluctuations of the incoming gas, before the perforated air distribution plate at the lower base of the combustion chamber. The distributor plate is made of ceramic fiber and is 12 mm thick with 1 mm diameter holes.

A portable gas analyzer of ECIL brand Chemist 600 brand was used to evaluate the concentration of combustion gases in terms of O_2, CO, CO_2, NO (corrected internally to NOx), and SO_2.

The tests were performed at average temperatures of 815 °C and 850 °C. The control of fuel flow, airflow, and bed temperature were carried out by supervision. The excess air and fuel flow rate were adjusted in each test to maintain the bed temperature close to 815 °C and 850 °C.

Casting sand was used as bed material. The size of the casting sand was in the range of 0.2-0.35 mm. The limestone used was the limestone supplied by Copel GeT with an average diameter of 402 µm, bulk density of 1560 kg/m^3, and chemical composition of 51.47% CaO, 5.18% MgO, 1.00% others and 42.35% LOI.

The diameter of selected coal particles was in the range of 0.60-2.00 mm aiming at stability of operation. The limestone was fed in a proportion expressed as a Ca/S molar ratio: 2, 3 and 4.

Two main parameters were evaluated for carrying out the combustion tests: temperature and the Ca/S molar ratio. Eight combustion tests were carried out. For comparison purposes, two of them considered only coal at 815 °C and 850 °C. For each Ca/S molar relationship used, two temperatures were used.

FINDINGS AND ARGUMENT

Table 1 shows the characteristics of the fuel.

Table 1 - Characteristics of the fuel.

Characteristic	Methods	Coal
HHV [kJ/kg]	ASTM D5865-13	5.559,0
LHV [kJ/kg]	---	5.340,6
Proximate analysis		
Ashes [%]	ASTM D3174-12	25.05
Volatile matter [%]	ASTM D3175-20	26.76
Fixed carbon [%]	ASTM D5865-20	48.18
Total humidity [%]	ASTM D3173M-17	3.22
Ultimate analysis		
Carbon [%]	ASTM D5373-21	56.20
Hydrogen [%]	ASTM D5373-21	3.80
Oxygen [%]	ASTM D3176-21	10.59
Nitrogen [%]	ASTM D5373-21	1.13
Sulfur	ASTM D4239-18	3.23

HHV - Higher heating value.
LHV - Lower heating value.

Thermogravimetric analysis was carried out on the coal sample to evaluate the volatile release temperature and possible events that may occur with the sample when subjected to high temperature conditions (up to 1000 °C) in an oxidizing atmosphere (representing the normal conditions of a possible burn). This behavior can be seen in Figure 2.

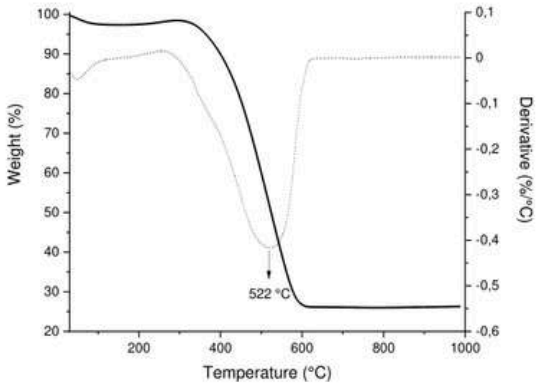


Figure 2 - Thermogravimetric analysis of coal.

The total mass loss obtained for the sample was 73.61%, with an exothermic mass loss event observed at a temperature of 522°C, that is related to the char combustion process. The thermogravimetric analysis of the limestone is shown in Figure 3. The temperature of 789°C indicates the break of the mineral structure of limestone.

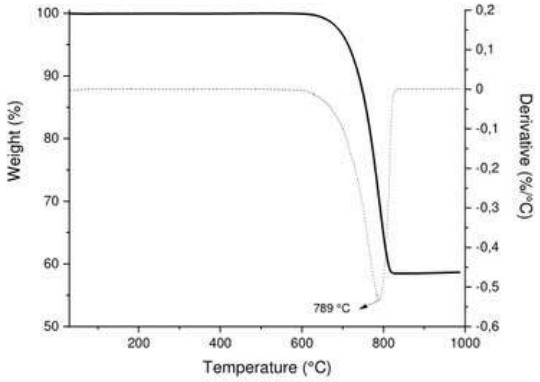


Figure 3 - Thermogravimetric analysis of limestone.

Gas emissions from the combustion of coal and limestone mixtures were analyzed. The exhaust gas composition and main operating conditions are shown in Table 2.

Analyzing Table 2, a significant reduction in the average concentrations of SO_2 in the exhaust gases is noted in comparison to the tests without the addition of limestone. The desulfurization efficiency increases as the Ca/S molar ratio increases.

Table 2 - Exhaust gas composition and operating conditions

	Coal		Ca/S = 2		Ca/S = 3		Ca/S = 4	
Parameter	T=815 °C	T=850 °C	T=815 °C	T=850 °C	T=815 °C	T=850 °C	T=815 °C	T=850 °C
O_2 (%)	8.69	7.76	6.97	6.10	8.95	7.04	7.69	6.03
CO_2 (%)	12.21	13.14	13.93	14.80	11.95	13.87	13.21	15.18
CO (mg/Nm³)	82.00	30.00	103.90	30.20	43.68	31.45	26.11	---
NO (mg/Nm³)	557.71	691.06	733.50	659.05	722.05	689.05	735.11	698.63
SO_2 (mg/Nm³)	5840.00	6116.50	1349.30	1726.80	938.74	1262.35	872.37	1055.89
SO_2 (7.0%)	6641.63	6468.97	1344.17	1617.20	1089.71	1261.10	918.17	985.30
T_{bed} (°C)(1)	807.19	849.98	813.30	857.38	814.91	859.92	813.37	852.16
$\dot{m}_{air}$ (L/min)(2)	189.16	185.17	175.13	190.54	178.79	198.47	180.99	197.47
$\dot{m}_{fuel}$ (kg/h)(3)	---	---	1.212	1.154	1.212	1.207	1.071	1.151
$\dot{m}_{coal}$ (kg/h)(4)	0.65	0.80	0.99	0.95	0.91	0.91	0.74	0.80
Excess air (%)	192.5	130.3	76.0	100.0	95.8	118.3	143.3	146.6
SO_2 removal (%)	---	---	79.8	75.0	83.6	80.5	86.2	84.8

(1) Bed average temperature.
(2) Volumetric air flow.
(3) Mass flow rate of fuel+limestone.
(4) Mass flow rate of coal.

The maximum desulfurization of 86.2% (T=813.4 °C) and 84.8% (T=852.2 °C) stands out for a Ca/S molar ratio of 4. Desulfurization tests at temperatures of 815 °C showed higher percentages of sulfur removal compared to tests at temperatures of 850 °C, for all molar ratios. This is due to the breakdown of limestone occurring at a temperature lower than that indicated in the literature, which is around 825°C. The limestone used in the tests showed, through thermogravimetric analysis, its breakdown at 789 °C (see Figure 3), thus enabling sulfur abatement at lower temperatures.
The test for the mixture with a Ca/S molar ratio equal to 4 at 850 °C showed an average SO_2 concentration of 985.3 mg/Nm³, corrected for 7% O_2. A significant drop in SO_2 concentrations in combustion gases is noted compared to the test without limestone addition (6468.97 mg/Nm³), as shown in Table 2. The SO_2 emission limit required by Resolution SEMA 016/2014 is 3000 mg/Nm³ for powers greater than 10 MW and less than 20 MW.

CONCLUSIONS

Tests without adding limestone to the fuel showed average SO_2 emissions of 6641.6 and 6468.9 mg/Nm³ for temperatures 815 and 850 °C, respectively.
Desulfurization tests at temperatures of 815 °C showed higher SO_2 conversion efficiencies compared to tests at temperatures of 850 °C, for all molar ratios. The limestone used showed, through thermogravimetric analysis, its breakdown at 789°C, thus enabling the reduction of sulfur at lower temperatures.
The tests with molar ratios 3 and 4 obtained reductions that comply with current legislation, while ratio 2 did not reach values appropriate to the legislation.

ACKNOWLEDGEMENTS

The authors would like to thank the company COPEL Geração e Transmissão S.A. for financial support for the project PD-06491-0417/2016 and the R&D program of the National Electric Energy Agency (ANEEL).

REFERENCES

Basu, Prabir. Combustion and Gasification in Fluidized Beds, 1a. ed. CRC Press. Boca Raton (2006).
Bragança, Saulo. R., and Castellan, Jorge. L. FBC desulfurization process using coal with low sulfur content, high oxidizing conditions and metamorphic limestones. Brazilian J. Chem. Eng. 26, 375-383 (2009).
Wander, Paulo. R., Bianchi, Flavio. M., Caetano, Nattan. R., Klunk, Marcos. A., Indrusiak, Maria. Luiza. S., Cofiring low-rank coal and biomass in a bubbling fluidized bed with varying excess air ratio and fluidization velocity. Energy 203. (2020). doi:10.1016/j.energy.2020.117882

PROCEEDINGS OF THE

2024 AIR POLLUTION CONFERENCE

And 5th CMAS South America

SESSION 03
Emerging trends and innovations in air pollution research

Air pollution remains a significant threat to both public health and the environment. Rapid industrialization, urbanization, and increased transportation have intensified this issue, demanding innovative solutions to mitigate its adverse effects. During this session, we will delve into the emerging trends and explore pioneering research that addresses air pollution at various scales, ranging from local to global.

On this session you will explore the latest advancements and cutting-edge research in the field of air pollution. This session aims to bring together scientists, researchers, policymakers, and industry experts to share their knowledge, experiences, and insights into tackling one of the most pressing global environmental challenges.

SESSION 3

ESTIMATION OF THE CARBONACEOUS FRACTION OF PM2.5 IN AN URBAN CENTER SITE OF THE ABURRÁ VALLEY, COLOMBIA 114

CHEMICAL CHARACTERIZATION AND MORPHOLOGICAL ANALYSIS OF PARTICULATE MATTER USING SEM-EDS IN THE ABURRÁ VALLEY, COLOMBIA. 117

CHEMICAL CHARACTERIZATION OF IONS AND METALS AND SOURCE IDENTIFICATION OF PM10 IN THE ABURRÁ VALLEY, COLOMBIA. 117

RAMP ROADS: A MONITORING SYSTEM TO IMPROVE KNOWLEDGE, MANAGEMENT AND CONTROL OF PARTICULATE MATTER FUGITIVE EMISSIONS FROM TRAFFIC ROADS 123

RADON EXHALATION RATE MEASUREMENT IN AMAZON FOREST SOIL 127

AIR POLLUTION CONFERENCE BRAZIL
CMAS SOUTH AMERICA
COMMUNITY MODELING AND ANALYSIS SYSTEM

ESTIMATION OF THE CARBONACEOUS FRACTION OF $PM_{2.5}$ IN AN URBAN CENTER SITE OF THE ABURRÁ VALLEY, COLOMBIA

Roxana Bedoya Saldarriaga[1], David Aguiar Gil[1], Luisa María Gómez[1], Mauricio Correa Ochoa[1], Henry A. Colorado [2]

[1]*Grupo de Investigación y Laboratorio de Monitoreo Ambiental G-LIMA, Universidad de Antioquia*
roxana.bedoya@udea.edu.co, david.aguiar@udea.edu.co, luisam.gomez@udea.edu.co, mandres.correa@udea.edu.co, henry.colorado@udea.edu.co
[2] *CCComposites Laboratory, Universidad de Antioquia*

Abstract:
The Aburrá Valley is one of the most populated metropolitan regions in Colombia. Due to its demographic conditions, large vehicle fleet and industrial production, it generates a large amount of pollutant emissions. The topographic conditions of a narrow valley and the climatic and meteorological conditions make it difficult to disperse the pollutants generated, making it one of the most polluted areas in the country. Twice a year in this area, contingency episodes are declared due to atmospheric pollution, especially for $PM_{2.5}$. Particulate matter can be composed of up to 50% carbonaceous compounds, which have received special attention due to their effects on health and the environment. In the Aburrá Valley there are not enough studies focused on this component of PM. In this study, daily samples of particulate matter $PM_{2.5}$ were collected during the first contingency episode of the year 2023 (in March-April), to estimate the carbonaceous fraction present in the particulate matter and their OC/EC ratio, to obtain inferences regarding the possible sources of carbonaceous particles. The particulate material was collected on quartz fiber filters and subsequently analyzed in thermo-optical equipment. The results showed that TC represents 32.82% of the mass of $PM_{2.5}$. Elemental carbon represented 6.44% and organic carbon represented 26.38%. It was observed that there is a contribution of secondary organic carbon during sampling, due to atmospheric reactions. The average OC/EC ratio showed a value of 4.24, which may represent a possible influence of biomass burning. Also, during the season, hot spots with back trajectories were identified to know if the air mass can be transported to the monitoring site.

Keywords: *$PM_{2.5}$,Organic Carbon, Elemental Carbon, OC/EC ratio*

INTRODUCTION

High concentrations of particulate matter are one of the main problems associated with air quality due to the impacts generated on health and the environment. Previously, studies focused on particle size, but more recently they have focused on the physicochemical and morphological characterization of this pollutant, since not only its size and concentration, but also its composition is directly linked to its potential to cause health problems.

For the year 2021, it was estimated that 15,681 deaths in Colombia were associated with poor air quality, mainly due to cardiac and pulmonary affectations (*Minsalud*). According to the Institute of Hydrology, Meteorology and Environmental Studies -IDEAM, particulate matter is one of the pollutants that generates more affectations in the Colombian territory. At the national level, the Aburrá Valley is one o (*IDEAM*) of the areas with the worst air quality and has been catalogued as a source area of contamination (*AMVA*). The topographic conditions of the valley, industrialization processes, transportation, and fast population growth have influenced the high concentrations of particulate matter generated in the area. However, external sources such as forest fires in other regions inside and outside the country, open burning for land preparation, have been considered factors influencing PM concentrations in the valley (*AMVA*). All these factors, together with the meteorological conditions in the area when there is a transition from dry to wet season, lead to an accumulation and an increase in the concentrations of particulate matter in the valley at two times of the year (February-March and September-October), which historically have been called contingency episodes.

The carbonaceous fraction, composed of organic carbon (OC) and elemental carbon (EC) of PM can represent up to 50% of its composition (*Jamhari et al.)*. These carbonaceous aerosols have received special attention due to the impacts generated not only on health, but also on the environment, since they represent problems not only of visibility, but also of climate change at a global level (*Jamhari et al.*).

Elemental carbon is mainly generated from incomplete primary combustion and thanks to its physical properties of light absorption, it is considered as one of the main contributors to climate change; while organic carbon can be of primary origin emitted by biogenic and anthropogenic sources (POC) and of secondary origin (SOC), formed from chemical reactions in the atmosphere by gaseous precursors (*Correa-Ochoa et al.*).

Currently there are limited data on the contribution of this fraction to PM concentrations in the Aburrá Valley, so this study aims to generate information on the concentrations of OC and EC, and their OC/EC ratio, to obtain inferences regarding the possible sources of carbonaceous particles.

AIR POLLUTION CONFERENCE BRAZIL
CMAS SOUTH AMERICA
COMMUNITY MODELING AND ANALYSIS SYSTEM

METHODS

SAMPLING OF PM2.5

The sampling site is in the center of the Metropolitan Region of Aburrá Valley, in the facilities of the Universidad de Antioquia (6°16'7''N,75°34'5''O). Sampling was carried out in one of the contingency periods of the year 2023, in March-April. A high-volume manual equipment with a flow rate of 1.13 m^3/min, Hivol Tisch reference (EPA approved) was used. Samples were collected every 24 hours on Whatman brand quartz fiber filters previously pre-baked at a temperature of 550°C for 6 hours and subsequently stored under 4°C. A total of 10 samples were collected.

CARBON ANALYSIS

Carbonaceous compounds were determined with a thermo-optical analyser (Sunset Lab) which determines the concentration of the carbonaceous fraction using the Thermal-optical transmittance (TOT) technique using the NIOHS 5040 method. Before the measurement, firstly, the filters were pre-baked at 550 °C for 6 hours, to avoid the presence of organic compounds in them. A 1.5 cm^2 quartz filter cut from the whole sampled was placed in a quartz vessel proceeded with different temperature programs in an inert helium atmosphere for measurement.

ESTİMATİON OF SECONDARY ORGANİC CARBON (SOC)

Due to the physical and chemical processes involved in the formation of secondary organic carbon, direct measurements of SOC are not possible. Therefore, it is necessary to employ other methodologies for its estimation. For this case, the EC tracer method, which is based on minimum OC/EC ratios, was used. This method uses EC as a tracer for primary OC and assumes that EC is not affected by chemical reactions occurring in the atmosphere such as photochemical oxidation, and that the OC/EC ratio remains constant during the sampling period (*Hama et al.*). SOC was calculated using the following equation:

$$SOC = OC_{total} - \frac{OC}{EC}_{min} \times EC$$

where SOC is secondary organic carbon, and OC total and EC are the respective environmental concentrations.

FINDINGS AND ARGUMENT

The concentration of particulate matter during the sampling period did not exceed the maximum permissible limits established in Colombian regulations. Daily $PM_{2.5}$ concentrations during the monitoring period ranged between 10.98 and 29.80 µg/m^3. Although the measurements were taken on contingency days, they coincided with a national holiday period, when educational and work activities are suspended, which reduces vehicle circulation and other activities.

For OC, concentrations were in the range of 1.41 and 11.34 µg/m^3. For EC, 0.33 and 1.88 µg/ m^3 were the minimum and maximum values, respectively. Table 1 shows the averages for each compound analyzed.

Table 1. Average values of the analyzed compounds in µg/m^3

$PM_{2.5}$	OC	EC	TC	OC/EC
20.00 ± 6.77	4.66 ± 3.20	1.07 ± 0.55	5.74 ± 3.58	4.41 ± 1.51

Figure 1 shows that organic carbon concentrations were always above elemental carbon, these significant contributions of this species are highly influenced by the high formation of secondary organic carbon.

Additionally, it is observed that OC/EC ratio, all days presented values above 2, indicating SOC formation, and several days presented values higher than 4, indicating a possible influence of biomass burning on the concentrations of particulate matter, according to the ratio values established by the environmental authority in the area (*AMVA*). This result coincides with a study conducted in Bogota by *Ramirez, et al.*, and what was established by *Watson* in 2002, where they indicated that values higher than 4 were influenced by biomass burning.

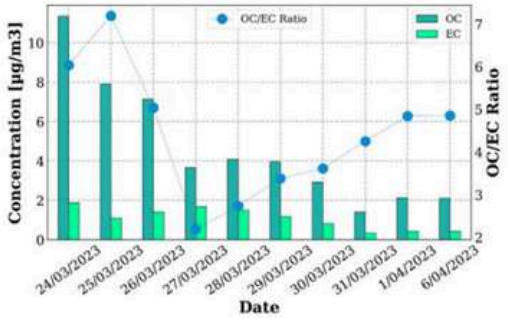


Figure 1. OC and EC concentrations in $PM_{2.5}$ and OC/EC ratio

Having OC/EC ratio greater than 2 on different days suggests that there is a contribution of secondary organic carbon to the PM mass because of atmospheric chemical reactions. This is reflected in figure 2. Being an area with an industry dependent on fossil fuels and a high vehicle fleet, a large amount of volatile organic compounds can be emitted into the atmosphere, which can produce higher concentrations of secondary organic carbon through photochemical reactions at high temperatures (*Li et al.*). Additionally, gases generated during biomass burning are also precursors for SOC formation.

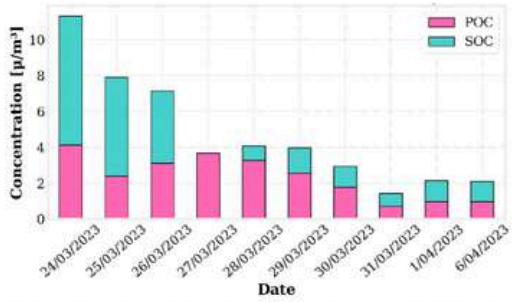


Figure 2. Contribution of SOC and POC to OC fraction in $PM_{2.5}$

Total Carbon (OC+EC) contributed to the PM mass up to 32.82%. The contributions of OC and EC to $PM_{2.5}$ were, on average, 26.36 ± 9.1 % and 6.44± 3.9 % respectively, these values indicate that most of the particulate matter is composed of the carbonaceous fraction. These results again agree with what was found in the study by Ramirez et al., where it was observed that for the city of Bogotá TC represented 33% of the total mass of particulate matter.

During the monitoring, backtrajectories were also carried out, in which the following were observed that during the march-april season, the wind plumes came from the northeastern of South America, where the greatest number of hot spots, associated with forest fires, were identified.

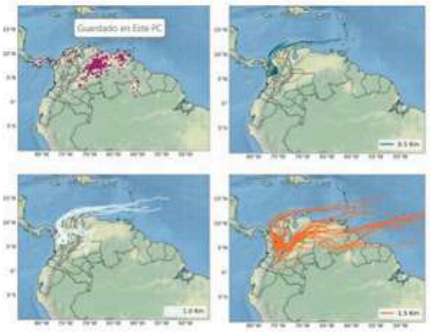


Figure 3. Hotspots and air mass trajectories al different heights, during monitoring period.

While this may represent an influence on the valley's air quality, it is important to keep in mind that, not only biomass burning by open burning or fires can contribute to $PM_{2.5}$ concentrations, but also biomass is used as fuel within industrial processes and that by 2022 it accounted for 17% of $PM_{2.5}$ emissions.

CONCLUSIONS

It was found that the carbonaceous fraction may represent an important percentage within the $PM_{2.5}$ composition. During the sampling days, organic carbon presented higher concentrations compared to elemental carbon and was highly influenced by secondary organic carbon. The OC/EC ratio presented an average value of 4.41, which could represent a possible influence of biomass burning, additionally, and a formation of secondary organic carbon. This ratio allows inferring emission sources of these particles and photochemical aging processes of the general emissions. It is important that these results are complemented with the analysis of back trajectories and hot spots associated with forest fires, in addition to the identification of other compounds present in the particulate matter, which would allow a clearer identification of the emission sources.

REFERENCES

AMVA. "El valle de Aburrá como Cuenca atmosférica y área fuente de contaminación". Calidad del aire, https://www.metropol.gov.co/ambientales/calidad-del-ire/generalidades/condiciones-especiales#:~:text=La%20regi%C3%B3n%20metropolitana%20del%20Valle,prevengan%20los%20da%C3%B1os%20de%20las

Correa-Ochoa, Mauricio A., et al. "A Review on the Characterization and Measurement of the Carbonaceous Fraction of Particulate Matter." *Sustainability (Switzerland)*, vol. 15, no. 11, 2023, https://doi.org/10.3390/su15118717.

IDEAM. "*Calidad del aire*", Contaminación atmosférica,http://www.ideam.gov.co/web/contaminacion-y-calidad-ambiental/calidad-del-aire

Galindo, N., et al. "Insights into the Origin and Evolution of Carbonaceous Aerosols in a Mediterranean Urban Environment." *Chemosphere*, vol. 235, Nov. 2019, pp. 636–42, https://doi.org/10.1016/J.CHEMOSPHERE.2019.06.202.

Hama, Sarkawt, et al. "Carbonaceous Aerosols in Five European Cities: Insights into Primary Emissions and Secondary Particle Formation." *Atmospheric Research*, vol. 274, Aug. 2022, p. 106180, https://doi.org/10.1016/J.ATMOSRES.2022.106180.

Jamhari, Anas Ahmad, et al. "Seasonal Variation and Size Distribution of Inorganic and Carbonaceous Components, Source Identification of Size-Fractioned Urban Air Particles in Kuala Lumpur, Malaysia." *Chemosphere*, vol. 287, Jan. 2022, p. 132309, https://doi.org/10.1016/J.CHEMOSPHERE.2021.132309.

Li, M., et al. "Comparison of Pm2.5 Chemical Compositions during Haze and Non-Haze Days in a Heavy Industrial City in North China." *Aerosol and Air Quality Research*, vol. 20, no. 9, 2020, pp. 1950–60, https://doi.org/10.4209/aaqr.2019.11.0591.

Ministerio de salud. "Minsalud comprometido con la calidad delaire", 2021, https://www.minsalud.gov.co/Paginas/Minsalud-comprometido-con-la-calidad-del-aire-.aspx

Ramírez, Omar, et al. "Ramírez, O., Sánchez de La Campa, A. M., & de La Rosa, J. (2018). Characteristics and Temporal Variations of Organic and Elemental Carbon Aerosols in a High–Altitude, Tropical Latin American Megacity. Atmospheric Research, 210(May), 110–122. Https://Doi.O." *Atmospheric Research*, vol. 210, no. May, 2018, pp. 110–22, https://doi.org/10.1016/j.atmosres.2018.04.006.

Watson, John G. "Visibility: Science and Regulation." *Journal of the Air and Waste Management Association*, vol. 52, no. 6, 2002, pp. 628–713, https://doi.org/10.1080/10473289.2002.10470813.

AIR POLLUTION CONFERENCE BRAZIL
CMAS SOUTH AMERICA
COMMUNITY MODELING AND ANALYSIS SYSTEM

CHEMICAL CHARACTERIZATION AND MORPHOLOGICAL ANALYSIS OF PARTICULATE MATTER USING SEM-EDS IN THE ABURRÁ VALLEY, COLOMBIA.

Juliana Rojas Villa [1], Mauricio A. Correa [1], Luisa M. Gómez [1], David Aguiar[1], Henry Colorado[1]
[11]Grupo de Investigación y Laboratorio de Monitoreo Ambiental G-LIMA, Universidad de Antioquia UdeA, Calle 70 N°. 52-21, Medellín 050010, Colombia

Abstract: Particulate Matter (PM) is a complex mixture of particles of natural and anthropogenic origin, classified according to their size into $PM_{2.5}$, PM_{10} and TPS. The Metropolitan Area of the Aburrá Valley (AMVA), Colombia is one of the regions most affected by air quality problems. This is due to its characteristic topography, which limits the circulation of winds, and consequently of pollutants. Advanced microscopy techniques such as Scanning Electron Microscopy (SEM) and Field Emission Electron Microscopy Dual Beam (FIB - FESEM), coupled with EDS, were used for the morphological and chemical characterization of PM_{10}. Samples were collected at monitoring stations located in the AMVA, selecting those strategic points affected by industrial and vehicular sources. A great diversity of particles was found, classified according to their morphology and chemical composition into: brocosomes, soot, fly ash, calcium carbonates and mixed particles (aluminosilicates-carbonates-Mg-rich particles). These findings allowed understanding the composition and associating possible sources of PM emissions, which facilitates the development of effective policies for air pollution control.

Keywords: PM_{10}, Advanced microscopy, SEM-EDS, FIB - FESEM, morphology

INTRODUCTION

PM is a complex mixture of particles of both natural and anthropogenic origin; it is classified according to its aerodynamic diameter particle (Dp) into $PM_{2.5}$ (Dp<2.5µm), PM_{10} (Dp<10µm) and TPS (total suspended particles)(Morantes et al.). PM is probably the air pollutant with the greatest influence on daily premature mortality rates, and is responsible for a large portion of the economic losses associated with public health and air quality(Aguiar-Gil et al.). Its composition is diverse, comprising organic and inorganic compounds. Inorganic compounds include sulfates, metals and nitrates, while the organic fraction consists of biological material, soot and hydrocarbons, both aromatic and polycyclic (González et al.).

In the year 2023, in Colombia, the regions of Bogotá, Bucaramanga, Cali and Aburrá Valley exceeded the maximum permissible threshold of PM_{10} recommended by the WHO by 4.8, 2.6, 3.1 and 3.1 times, respectively (IDEAM). One of the highest concentrations was recorded in the Metropolitan Area of the Aburrá Valley (AMVA). This problem is associated with the climatic conditions in the Aburrá Valley (VA), which are unique due to its topography and mountainous barriers that hinder the circulation of winds and the dispersion of atmospheric pollutants. In addition, in this area there has been a notable change in emission sources over time. According to the 2022 emissions inventory, PM_{10} emissions from stationary sources such as ceramic, food and textile industries were 84%, with the textile industry predominating with a contribution of 49% of these emissions (Bolivariana y Aburrá).

Advanced microscopy, especially scanning electron microscopy (SEM) coupled with energy dispersive spectrometry (EDS), has been used to chemically and morphologically characterize particulate matter (PM). This technique provides details on the size, shape and elemental composition of the PM. Given the diversity of emission sources, such as vehicular traffic, industry, metallurgy and biomass combustion, it is crucial to have detailed information on the chemical and morphological characteristics of this pollutant in order to develop effective air pollution control policies. For this reason, the analysis of PM by SEM has been fundamental in several studies (Pipal et al.; Yadav y Satsangi; González et al.)

The objective of this study is to determine the composition and emission sources of PM_{10} in the Aburrá Valley, Colombia, through the evaluation of its chemical and morphological characteristics using SEM-EDS and FIB-FESEM.

METHODS

The sampling location is within the AMVA, a subregion located in the department of Antioquia, Colombia. PM_{10} samples were collected at 10 stations of the Environmental Authority's air quality monitoring network. The collection and measurement of PM concentration was carried out using manual high-volume samplers (Hi-Vol), which operate for periods of 24 hours ± 1 hour, at a constant flow rate of 1.13 m^3/min. Whatman®1851-865 QM-A 20 cm x 25 cm quartz fiber filters with a pore size of 2.2 microns (µm) were used. The analysis was performed following the protocols established by the EPA (Environmental Protection Agency). This sampling was conducted in April 2019 and October 2023. The selected sampling stations

are influenced by various stationary sources, such as the ceramic and metalmechanical industries. In addition, they are affected by mobile sources, mainly due to emissions from vehicular traffic. A JEOL -JSM 6490LV thermionic Scanning Electron Microscope (SEM), equipped with an INCA PentaFETx3 X-ray microanalyzer (Oxford Instrument), and a Thermo Fisher Scientific Scios 2 LoVac Dual Beam Field Emission Electron Microscope (FIB - FESEM), with EDS Microanalysis System (UltraDry 129 eV 30 mm^2 model No: SDBX-30PM-B), were used to perform the morphological and compositional analysis. To carry out the analysis, a fraction of approximately 2 cm^2 was removed from the filter and fixed with double-sided graphite tape. Finally, a thin layer of gold (Au) was deposited by sputtering to generate conductivity in the sample.

FINDINGS AND ARGUMENT

From the results obtained by SEM-EDS and FIB-FESEM it was possible to classify PM_{10} into different groups of particles according to their chemical and morphological characteristics.

Figure 1 shows two types of particles that, due to their C-rich composition and morphology, have been classified as brocosomes (marked with red circles) and soot (marked with green arrows). As seen in the SEM image, the brocosomes exhibit a spherical shape with pentagonal recesses, similar to the geometry of a soccer ball or honeycomb structure. This type of particle is associated with leafhoppers, a species that is coated with brocosomes to acquire an external surface with a superhydrophobic character*(Yadav y Satsangi)*.

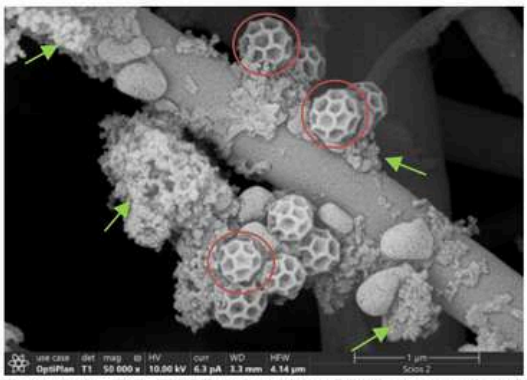


Figure 1. FIB-FESEM image of PM atmospheric particles. Red circles: Brocosomes, green arrows: soot.

On the other hand, soot particles show short-chain spherical morphologies with an average size of 0.3 µm. The shape of soot is influenced by atmospheric processes, the conditions under which combustion takes place and the types of fuels used. Its emission is associated with the incomplete combustion of diesel engines, widely used in transportation and heavy industries. The presence of soot at the sampling site is mainly due to heavy vehicular traffic near the sampling stations *(Yadav y Satsangi)*.

In Figure 2a and b, regular spherical morphologies with a smooth surface are observed, which have been identified as fly ash. In addition, irregularly agglomerated particles are present. Fly ash was classified as such due to its characteristic geometry and composition. The elemental composition of these particles revealed high contents of Al (between 13-18.8%), Ca and Na, as well as minor amounts of Mg, K, Ti, Fe, Cu. According to the literature, fly ash usually consists of different oxides, such as alumina (Al_2O_3), silica (SiO_2), calcium oxide (CaO) and iron oxides (Fe_2O_3). Comparing the composition of these oxides with the elemental composition found, it is confirmed that the analyzed particles correspond to fly ash.

According to the chemical composition, the emission sources of these particles are: industrial activities such as ceramics or metal industries located in the vicinity of the study areas. In addition, they are associated with fires (Apithanyasai et al.)

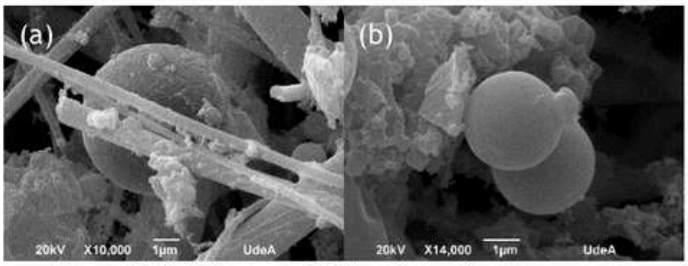


Figure 2. SEM image of PM_{10} atmospheric particles classified as fly ash (a) southern sample (b) northern sample

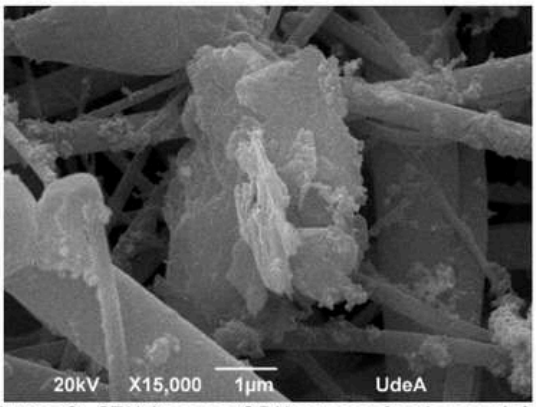


Figure 3. SEM image of PM atmospheric particles classified as calcium carbonate.

Another group of particles found corresponds to calcium carbonates, which are characterized by high contents of Ca, C and O, with traces of Al, Na, K, Fe (Figure 3). According to *(Santacatalina et al.)* these carbonates can adopt both regular and irregular morphologies. In particular, an irregular

particle with a size ranging from 5 to 8 µm can be observed in Figure 3. The ceramic and refractory industries located in the vicinity of the sampling points were the main contributors to the chemical composition of this type of particles.

The mixed particles rich in Al, Ca and Mg were characterized by forming aggregates with laminar and irregular morphologies, as shown in Figure 4. These particles have a variable chemical composition, with a high content of Al (32.84%), Ca (27.18%) and Mg (20%), in addition to traces of Na (4.78%), K (5.81%) and Fe (9.23%). This composition indicates that the analyzed particles consist of aluminosilicates, carbonates and Mg-rich particles, which justifies their classification as mixed particles. The aluminosilicate-carbonate composition is associated with ceramic industries, which use various minerals such as mullites, cordierite, dolomites, among others *(González et al.)*. On the other hand, Mg-rich particles are related to vehicular activity and are also linked to soil dust that is suspended by wind.

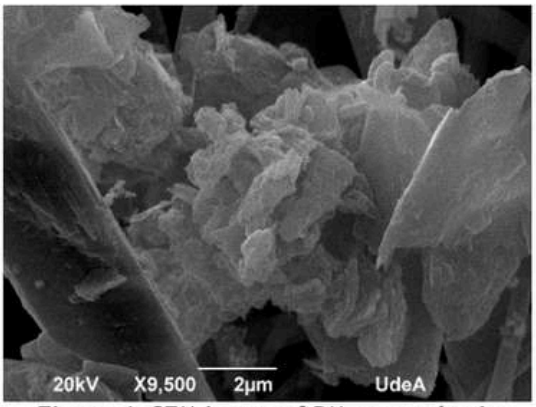


Figure 4. SEM image of PM atmospheric particulate matter classified as fly ash

CONCLUSIONS

The identification and classification of PM_{10} according to its chemical composition was possible thanks to the use of SEM and FE-SEM microscopy, combined with X-ray energy dispersive analysis (EDS). The presence of compounds such as aluminosilicates, calcium carbonates, soot, fly ash and biological material was evidenced. The morphological and chemical analysis allowed linking each classified compound with possible emission sources in the AMVA, such as natural sources, vehicular traffic, and ceramic and metalworking industries. These findings provide a solid basis for the design and implementation of effective air pollution control policies in the region.

It is recommended to continue with the characterization studies in the Aburrá Valley with complementary techniques to obtain a more detailed analysis of the microstructure, mineralogy and chemical composition of the PM.

REFERENCES

Aguiar-Gil, David, et al. «Evaluating the impact of PM2.5 atmospheric pollution on population mortality in an urbanized valley in the American tropics». *Atmospheric Environment*, vol. 224, n.º June 2019, 2020, https://doi.org/10.1016/j.atmosenv.2020.117343.

Apithanyasai, Suchanya, et al. «The potential of industrial waste: using foundry sand with fly ash and electric arc furnace slag for geopolymer brick production». *Heliyon*, vol. 6, n.º 3, marzo de 2020, https://doi.org/10.1016/J.HELIYON.2020.E03697.

Bolivariana, Universidad Pontificia, y Área Metropolitana del Valle de Aburrá. *Estudio de emisiones de fuentes industriales en el Área Metropolitana del Valle de Aburrá*. 2022, https://www.metropol.gov.co/ambiental/calidad-del-aire/Documents/Inventario-de-emisiones/Inventario-Emisiones-Fuentes-Fijas-2022.pdf.

González, Lucy T., et al. «Seasonal variation and chemical composition of particulate matter: A study by XPS, ICP-AES and sequential microanalysis using Raman with SEM/EDS». *Journal of Environmental Sciences (China)*, vol. 74, diciembre de 2018, pp. 32-49, https://doi.org/10.1016/J.JES.2018.02.002.

Morantes, Giobertti, et al. «Characterisation of particulate matter and identification of emission sources in Greater Caracas, Venezuela». *Air Quality, Atmosphere and Health*, 2021, https://doi.org/10.1007/S11869-021-01070-2.

Pipal, A. S., et al. «Study of surface morphology, elemental composition and origin of atmospheric aerosols (PM2.5 and PM10) over Agra, India». *Aerosol and Air Quality Research*, vol. 14, n.º 6, 2014, pp. 1685-700, https://doi.org/10.4209/aaqr.2014.01.0017.

Santacatalina, M., et al. «Impact of fugitive emissions in ambient PM levels and composition: A case study in Southeast Spain». *Science of The Total Environment*, vol. 408, n.º 21, octubre de 2010, pp. 4999-5009, https://doi.org/10.1016/J.SCITOTENV.2010.07.040.

Yadav, S., y P. G. Satsangi. «Chemical and morphological study of PM10 and PM2.5 in Pune, India». *International Journal of Environment and Waste Management*, vol. 13, n.º 2, 2014, pp. 199-216, https://doi.org/10.1504/IJEWM.2014.059617.

AIR POLLUTION CONFERENCE BRAZIL
CMAS SOUTH AMERICA
COMMUNITY MODELING AND ANALYSIS SYSTEM

CHEMICAL CHARACTERIZATION OF IONS AND METALS AND SOURCE IDENTIFICATION OF PM_{10} IN THE ABURRÁ VALLEY, COLOMBIA.

Santiago A. Franco[1], Luisa M. Gómez[1], David Aguiar[1], Mauricio A. Correa[1] and Henry A. Colorado[2]
[1]*Grupo de Investigación y Laboratorio de Monitoreo Ambiental—GLIMA, Universidad de Antioquia UdeA, Calle 70 N. 52-21, Medellín 050010, Colombia*
santiago.franco2@udea.edu.co, luisam.gomez@udea.edu.co, david.aguiar@udea.edu.co, mandres.correa@udea.edu.co
[2]*CCComposites Laboratory, Universidad de Antioquia UdeA, Calle 70 N_. 52-21, Medellín 050010, Colombia*
henry.colorado@udea.edu.co

Abstract: In this study, the sources of ions and metals in particulate matter (PM_{10}) were investigated in the Aburrá Valley (AV), an urbanized valley with conditions that encompass atmospheric pollution issues. The samples were collected at 10 stations of the air quality network of the AV on 20 dates between 2018 and 2021, which covered different specific conditions such as periods of environmental contingency due to atmospheric pollution, pyrotechnics events and everyday conditions. These stations are situated in urban areas and are affected by different conditions such as traffic and industrial emissions, among others. Samples were collected using high-volume particulate manual equipment with quartz fiber filters. The samples were chemically analyzed to determine their ionic and metal content using ionic chromatography and atomic absorption spectroscopy, respectively. Principal Component Analysis (PCA) and Positive Matrix Factorization (PMF) were used to determine the sources of the chemical species and to obtain their contributions to the total PM_{10} mass. The results indicate that both models found similar emission sources for the pollutants in the valley, including secondary aerosols, vehicular emissions, industrial emission, suspended dust, biomass burning and mixtures of the sources. The ions constitute the largest proportion of the PM_{10} in the AV, with sulphate being the most prominent, with an average concentration of 4.75μg/m^3, representing the 12% of the average concentration of PM_{10} (40.7μg/m^3). The PCA and PMF analyses results showed that secondary aerosols were the most significant contributor to the PM_{10} mass, accounting for 38% and 31% of the total variance of the data, respectively. Customized to the valley's distinctive geography, the methods and findings of this case study are an important tool to understand the implications of PM pollution in both local and global contexts.

Keywords: Atmospheric pollution, PM_{10}, Source identification, PCA, PMF.

INTRODUCTION

Particulate matter (PM) is an airborne pollutant with diverse physical and chemical characteristics, comprising solid and/or liquid suspended particles. PM arises from primary sources when particles are emitted directly by sources of pollution and from secondary origin when particles undergo transformations through interactions with other pollutants and atmospheric processes. Anthropogenic activities such as vehicular and industrial emissions are significant contributors to PM concentration, alongside natural phenomena such as the suspension of crustal matter or sea salts (Correa-Ochoa et al).

Consequently, the chemical composition of PM exhibits variability, according to factors such as emission sources and meteorological conditions. Inorganic compounds as ions and metals are part of the composition of PM, as are organic compounds like Organic Carbon (OC) and Volatile Organic Compounds (VOC), among others (Correa-Ochoa et al).

Due to the public health and environmental complications generated by this pollutant, it is widely used as a criterion to estimate air quality (Gómez-Peláez et al). PM_{10} (Particle matter with and aerodynamic diameter Dp<10μm) can penetrate the lungs, causing health problems such as respiratory and cardiovascular damage, and premature deaths (Aguiar-Gil et al). PM compounds present specific health and environmental risks. For instance, sulfate and nitrate contribute to respiratory issues and haze, impacting visibility and leading to global warming.

To estimate the emission sources of the PM, several statistical techniques have been employed worldwide, such as regression models or factor analysis. Principal Component Analysis (PCA), and the Positive Matrix Factorization (PMF), are the most employed models of multivariate statistical analysis for the estimation of the emission sources and the contribution of each pollutant. The study area is the Aburrá Valley (AV) an urban Valley situated in the Colombian Andes between 6.0° and 6.5° N and -75.5° and -75.7° W. Diverse emission sources, coupled with tropical climate and topographical factors, contribute to severe pollution, surpassing national regulations and WHO guidelines in the AV (Correa et al). To comprehend pollutant sources, ions and metals components of PM_{10} were characterized and statistically analyzed

using PCA and PMF to understand the emission sources in the case study.

SAMPLING AND CHEMICAL ANALYSIS

Ten air quality monitoring stations in the AV strategically placed in areas influenced by traffic, industry, urbanization and other factors were used (AMVA). 94 samples were collected across 20 different dates in which different conditions were presented such as environmental contingency, fireworks events and everyday condition spanning from December 2018 to October 2021. High-volume manual equipment with a flow rate of 1.13 m^3/min, Hivol Tisch and Graseby reference (EPA approved) were used to collect the samples with Whatman quartz-fiber filters (Whatman®1851-865QM-A). Ionic chromatography (Dionex Ion Chromatograph Model ICS-1100) analyzed ions (Cl^-, NO_3^-, PO_4^{-3}, SO_4^{-2}, Na^+, NH_4^+, K^+, Mg^{+2}, Ca^{+2}), while atomic absorption spectrometry (Thermo Model A.A S4 series GE712311) examined metals (Ni, Al, Zn, Fe). Anion concentrations followed SM 4110B method, and cations were assessed via ASTM D6919. Metal analysis adhered to US EPA IO 3.1 protocol.

SOURCE APPORTIONMENT ANALYSIS

Principal Component Analysis (PCA) is a prominent multivariate statistical tool that simplifies sample complexity by identifying components (sources) that explain sample variance. PCA identifies patterns in data by analyzing the correlation matrix, followed by standardization of chemical species concentrations. It generates Principal Components (PCi), interpreted as emission sources. RStudio version 4.3.0 was utilized for that analysis, the considered sources accounted for the 82% of the total variance of the data.
On the other hand, Positive Matrix Factorization (PMF), endorsed by the US Environmental Protection Agency (EPA) for source apportionment is a factor analysis technique to estimate pollutant contributions from various sources. This approach, assumes that sample data are influenced by linear combinations of emission sources. PMF identifies emission sources and quantifies compound contributions to each source (Paatero). In this study, EPA PMF 5.0 software was employed. A set of 14 chemical species across 94 samples were analyzed through PCA and PMF.

FINDINGS AND ARGUMENT

Table 1 summarizes the main findings. PM_{10} average concentration was 40.6µg/m^3, these average approaches the WHO limit of 45µg/m^3 for PM_{10} daily concentrations (WHO), with 40 of the 94 PM_{10} samples concentrations surpassing that threshold. From highest to lowest, the average concentration of the chemical species was PM_{10}> SO_4^{-2}> Na^+> NO_3^-> PO_4^{-3}> NH_4^+> K^+> Ca^{+2}> Fe^{+2}> Al> Mg^{+2}> Cl^-> Zn> Ni. SO_4^{-2} and NO_3^- were the dominant anions, Na^+ and NH_4^+ were the most abundant cations. Ions contributed to around 10.57µg/m^3 of the PM_{10} average mass, while metals comprised 1.22µg/m^3. By the other hand, the figure 1, illustrates the average distribution of PM_{10} for the analyzed samples.

Table 1. Summary statistics for the main measured species

Specie	Avg. (µg.m^{-3})	Min (µg.m^{-3})	Max. (µg.m^{-3})
PM_{10}	40.65	6.97	72.82
Sulphate	4.74	0.03	8.74
Sodium	1.36	0.20	4.09
Nitrate	0.99	0.05	3.18

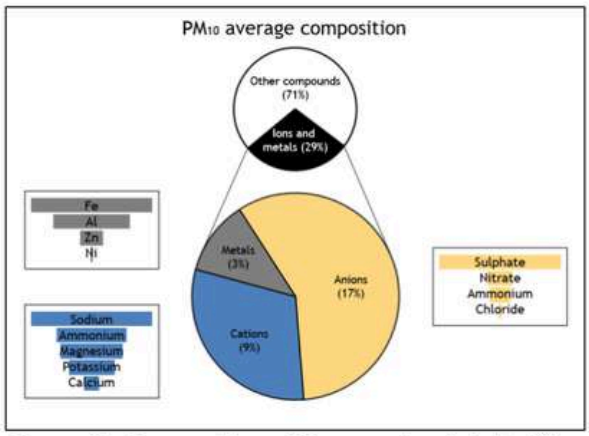


Figure 1. Composition of ions and metals in PM_{10}

The results of the source apportionment analysis can be interpreted from the perspective of previous studies, the working hypothesis and the current conditions of the study area, the findings and their implications must be analyzed in the broadest context possible. PCA identified 5 Principal Components (PCi), while PMF identified 5 Factor Sources (FSi), these sources are:
Secondary Aerosols (SA), comprising SO_4^{-2}, NO_3^-, and NH_4^+, originate from precursor gases SO_x, NO_x, and NH_3, respectively, sourced from both natural phenomena and human activities. SO_4^{-2} formation predominantly arises from the oxidation of SO_2 emitted from carbon combustion, diesel engines and industrial processes. This source was identified by PC_1 (grouping NO_3^- and SO_4^{-2}) and SF_1 (Grouping NH_4^+ and SO_4^{-2} in combination with K^+ and Al) accounting for 38% and 32% of the total variance respectively.
Biomass Burning (BB): Arising predominantly from fires and waste incineration, it significantly contributes to the formation of PM_{10} due to its diverse compound composition. K^+ is a key biomarker for biomass burning, while one of the most important sources of Na^+ is urban waste incineration, highlighting the substantial role of

biomass and waste combustion in urban air pollution. This source was identified by the PC_2 (PO_4^{-3}, Na^+, and K^+) and the SF_2 (PO_4^{-3} and Na^+), accounting for the 17% and 26% of the total variance.

Suspended dust (SD): consists of mineral elements from the earth, intensified by human actions. Distinguishing natural from human-induced sources is difficult. Soil and paved/road dust are primary contributors in cities, rich in Ca^{+2} and Mg^{+2}, Al and Fe. This source was identified in the Identified in the PC_3 (Mg^{+2}, Ca^{+2}) the FS_3 (K^+, Al, Fe) representing the 7% and 17% of the total variance.

Vehicular Emissions (VE): include primary PM pollutants from exhausts, as well as particles from brake and tire wear, notably Zn. The increasing vehicle count in the AV intensifies emissions, posing a major concern. PC_4 (Cl^-, Zn) accounts for 7% of the total variance, while FS_4 comprises (Zn) 8%.

Industrial emissions (IE): originate from diverse manufacturing processes like petrochemical, metallurgical, ceramics, and pharmaceutical industries, often escalating with population growth. Marker species such as Cu, Cr, Ba, Al, and Ni indicate industrial emissions, while SO_4^{-2}, NH_4^+, and Al serve as tracers. This source was identified in the FS_1 for the combination of K^+ and Al with SA.

Results suggest the combination of the SA with the chemical species characteristics of other sources as the FS_1 is a mixture of SA/IE, the PC_5 (13% of the total variance) and FS_5 (17% of total variance) are mixtures of SA/SD, the first groups Fe and Al with NH_4^+, the second Cl^-, NO_3^- and NH_4^+ with Mg^{+2} and Ca^{+2}. Table 2a and 2b shows the summary of the PCA and PMF results, respectively.

Table 2a. Summary of PCA source identification

Source (PCi)	Chemical species	%VAR
Secondary aerosols	NO_3^- SO_4^{-2}	38
Biomass burning	K^+ Na^+ PO_4^{-3}	17
Suspended dust	Mg^{+2} Ca^{+2}	7
Vehicular Emission	Cl- Zn	7
Secondary aerosol/SD	Fe, NH_4^+, Al	13

Table 2b. Summary of PMF source identification

Source	Chemical species	%VAR
SA/Industrial emission	NO_3^- SO_4^{-2} K^+ Al	32
Biomass burning	PO_4^{-3} Na^+	26
Suspended dust	K^+ Al Fe	17
Vehicular Emission	Zn	8
Secondary aerosol/SD	Cl-, NO_3^- NH_4^+ Mg^{+2} Ca^{+2}	17

CONCLUSIONS

PCA and PMF and showed similar results and 5 main sources of PM_{10} in the valley, these are SA, BB, SD, VE, IE, each contributing to the study region atmospheric pollution. SA, comprising SO_4^{-2}, NO_3^-, and NH_4^+ was the most highlighted source, results showed that the formation of this pollutants leads the combination of the species with other chemical species characteristics of other sources as IE and SD. SO_4^{-2} holds the largest mass fraction of PM_{10}. Further research is essential for understanding temporal-spatial pollutant behavior and interaction between emission sources, facilitating the development of more effective air pollution control strategies. These findings underscore the health risks of air pollution to the local population, emphasizing the importance of reducing emissions through initiatives such as promoting sustainable consumption practices, public transportation, and reducing reliance on internal combustion vehicles and promoting the energetical transition.

REFERENCES

AMVA. (2019). Diseño y Operacion SVCA Valle de Aburra. Área metropolitana Valle de Aburrá. Recuperado 24 de enero de 2024, de https://www.metropol.gov.co/ambiental/calidad-del-aire/Biblioteca-aire/Estudios-calidad-del-aire/Diseno-y-Operacion-SVCA-Valle-de-Aburra.pdf

Correa, M., Franco, S. A., Gómez, L. M. H., Aguiar, D., & Colorado, H. A. (2023). Characterization Methods of Ions and Metals in Particulate Matter Pollutants on PM2.5 and PM10 Samples from Several Emission Sources. Sustainability, 15(5), 4402. https://doi.org/10.3390/su15054402

Correa, M., Bedoya, R., Gómez, L. M. H., Aguiar, D., Tobón, C. a. P., & Colorado, H. A. (2023). A review on the characterization and measurement of the carbonaceous fraction of particulate matter. Sustainability, 15(11), 8717. https://doi.org/10.3390/su15118717

Aguiar-Gil, D., Gómez-Peláez, L. M., Álvarez-Jaramillo, T., Correa, M., & Saldarriaga-Molina, J. C. (2020). Evaluating the impact of PM2.5 atmospheric pollution on population mortality in an urbanized valley in the American tropics. Atmospheric Environment, 224, 117343. https://doi.org/10.1016/j.atmosenv.2020.117343

Correa, M., Zuluaga, C., Palacio, C., Pérez, J., Jiménez, J., 2009. Surface wind coupling from free atmosphere winds to local winds in a tropical region within complex terrain. Case of study: aburra Valley Antioquia, Colombia. Dyna 76 (158), 17-27.

Gómez-Peláez, Luisa & Santos, Jane Meri & Albuquerque, Taciana & Jr, Neyval & Andreão, Willian & Andrade, Maria. (2020). Air quality status and trends over large cities in South America. Environmental Science & Policy. 114. 422-435. 10.1016/j.envsci.2020.09.009.

Paatero, P. (1997). Least squares formulation of robust non-negative factor analysis. Chemometrics and Intelligent Laboratory Systems, 37(1), 23-35. https://doi.org/10.1016/s0169-7439(96)00044-5

AIR POLLUTION CONFERENCE BRAZIL
CMAS SOUTH AMERICA
COMMUNITY MODELING AND ANALYSIS SYSTEM

RAMP ROADS: A MONITORING SYSTEM TO IMPROVE KNOWLEDGE, MANAGEMENT AND CONTROL OF PARTICULATE MATTER FUGITIVE EMISSIONS FROM TRAFFIC ROADS

Luiz Cláudio D.Santolim[1], Luiz Antônio Radaeli[1], Adalberto José Mathias[1], Mayko Rodrigues Vieira[1], Victor Ferrão Santolim[1], Caio Almeida Giugni[1],
[1]*EcoSoft Soluções Ambientais*
luiz.radaeli@ecosoft.com.br

Abstract: Fugitive emissions of particulate matter (PM) may occur whenever vehicles travel over roads, which is one of the many fugitive emission sources that exists in different industrial and urban sectors due to the necessity of transportation and movement of people and materials. Quantification of the emission rates of PM from roads is a complex task that sometimes challenges those who study atmospheric emissions and the managers responsible for this control. We have been working on the development of an integrated solution (PM sensors, software, communication systems) that can obtain reliable data on PM emission factors and PM emission rates from roads. RAMP Roads is a system capable of real time measuring of fugitive PM emissions originated from roads, composed of a set of PM monitors strategically placed around a vehicle, that measures the flux of total suspended particles concentrations originated from the movement of the vehicle itself. Based on variations in dust concentrations detected by monitors installed at the front and rear of the vehicle, together with the speed and spatial positioning of the vehicle on the road, the RAMP Roads system calculates the PM emission factor for the monitored road. RAMP Roads particle concentration monitors are calibrated by intercomparison to traceable standards. The monitors are protected from interference from air humidity, temperature, lightness, mists, rain and vibration. The data is generated at very short time intervals (every 4 to 6 seconds) and sent to SSED (Supervisory System of Diffuse Emissions) for processing. The SSED is an application that can interpret and integrate the information received from the RAMP Roads, calculating PM emission factors and PM emission rates generated by each monitored road. The emissions of the monitored roads can be displayed in real time by the web-based application SaaS Ambion. Under dust emission events beyond a certain pre-set value, the RAMP Roads can send alerts to those responsible for the affected road, making it possible to take immediate action to neutralize the causes of the problem, at the time of occurrence or when it is about to occur. The monitors that make up RAMP Roads are designed and built to withstand harsh operating conditions of the production area for long periods of monitoring, usually operating on site up to 8 hours a day. This is an innovative solution that has helped companies in one of the most complex environmental management tasks, which is the effective control of fugitive dust emissions from roads. In addition to improving the management of dust emissions on roads in real time, RAMP Roads makes it possible to establish the real gains from implementing control actions (wetting, washing, sweeping, polymers, paving, etc.), evaluating the long-term evolution of emission factors or emission rates of monitored roads. This paper presents the results of RAMP Roads measurements applied to the environmental management of an Industrial Complex and of a Mining Plant containing several PM fugitive emitting roads. It also contains a comparison of emission factors calculated through a USEPA approved silt sampling procedure (Appendix C.1) on an industrial site paved roads and the emission factors calculated by RAMP Roads on the same roads.

Keywords: Continuous measurement, dust control, management tool, real-time monitoring, PM profile.

INTRODUCTION

Diffuse emissions of particulate matter (PM) originating from resuspension processes caused by vehicle movement and road dirtiness can represent a significant portion of total PM emissions in urban and industrial areas.

In the atmospheric emissions inventory of the Metropolitan Region of Vitória-ES Brazil, developed by EcoSoft in 2019, emissions from roadways accounted for 84% of the total PM emissions. In mining areas, this percentage can vary between 70 and 75% of total emissions.

Diffuse emissions of PM on roadways are difficult to quantify due to the dynamic nature of various factors influencing this process, such as the flow and characteristics of circulating vehicles, traffic speed, pavement type and the level of surface dirtiness susceptible to suspension (silt), among other factors.

The traditional method used to estimate fugitive emissions from roadways is the procedure described in Appendix C.1 of the AP-42, "Procedures for Sampling Surface/Bulk Dust Loading" (USEPA, 1993). Atmospheric emissions inventories conducted using the AP-42 method tend to be time-consuming, costly and typically based on silt sampling with a limited number of collections. In addition to low statistical representativeness and high uncertainty, silt collection involves the closure of roadway lanes, posing risks to the team involved and causing disruptions to local traffic.

Alternative methodologies for estimating emissions from roadways have been proposed by other authors, such as Kuhns et al. (2000), Amato et al. (2012), Sehyun Han & Yong-Won Jung (2012), and Padoan et al. (2017).

The RAMP Roads system was designed to measure in real time the emission factor of particulate matter on roadways with a high degree of detail, providing valuable information for the sizing and optimized management of dust emission control resources on roadways.

In comparison to the method described in the AP-42, the RAMP Roads accelerates this survey immensely, providing even greater quality, representativeness, and scope to the process, enabling the development of a more detailed atmospheric emissions inventory.

METHODS

The RAMP Roads system consists of at least one vehicle equipped with particle monitors specifically developed to measure synchronously the variations in PM concentrations generated by the vehicle's own movement on a roadway, along with its spatial positioning, speed, and direction of movement. The monitors operate based on particle counters and are calibrated by comparison with a reference method approved by USEPA (beta monitor).

Based on the mass balance between the concentrations measured by the monitors, RAMP Roads calculates the PM emission factors more quickly and accurately than the traditional method proposed in the AP-42.

The set of monitors is positioned in a way that prevents the determination of the emission factor from being influenced by suspended dust before the vehicle passes, for example, by dust emitted by another vehicle traveling ahead of the measuring vehicle.

As a validation method for the proposed technique, measurements were conducted using RAMP Roads and the silt determination procedure from the AP-42 at the same points located on specific roadways in an industrial area.

Figure 1 shows a scatter plot between the PM emission factors calculated by RAMP Roads and the amount of silt determined based on the AP-42 method. A high degree of correlation between the two variables is observed (R^2 = 0,95).

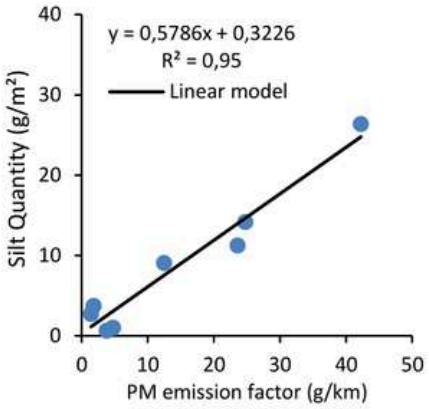


Figure 1. Scatter plot between silt quantity and emission factor results (Samarco, Mar/2023).

FINDINGS AND ARGUMENT

As fugitive PM emissions from roadways occur in a highly dynamic way, monitoring carried out with RAMP Roads offers the following benefits:

- Detailed knowledge of PM emission factors from monitored roadways, enabling the development of atmospheric emissions inventories more quickly and in greater detail;
- Monitoring is conducted along the entire length of the roadways, providing greater representativeness, specificity, and lower uncertainty of the obtained results;
- Obtaining data in a less costly and more efficient manner than traditional methods;
- Methodology applicable to both paved and unpaved roadways;
- Real-time monitoring of emission factors provided by RAMP Roads enables the optimization of resource application for control and response to detected anomalies, as opposed to predefined control routes;
- The RAMP Roads system can also operate in conjunction with a tracking system developed by EcoSoft, allowing the monitoring of water trucks and sweepers' operation alongside real-time monitoring of roadways.

Figure 2 shows results of PM emission factors from the main traffic roadways in a typical industrial area predominantly consisting of paved roads.



Figure 2. Average of emission factor (g/vkt) of PM for the main traffic roadways of the Tubarão Complex (Vale, Oct/23 to Mar/24).

RAMP Roads also provides real-time calculation of the PM emission rate from traffic roadways when integrated with the automated vehicle flow monitoring system called "EcoVision," which performs automated counting of light and heavy vehicle traffic in real-time.

Figure 3 shows the results of PM emission rate from the main traffic roadways in the same industrial area mentioned above.



Figure 3. Average of emission rate (kg/h) of PM for the main traffic roadways of the Tubarão Complex (Vale, Oct/23 to Mar/24).

Figure 4 shows the PM emission factors measured by RAMP Roads from the main traffic roadways in an open pit iron mining area, predominantly consisting of unpaved roads.

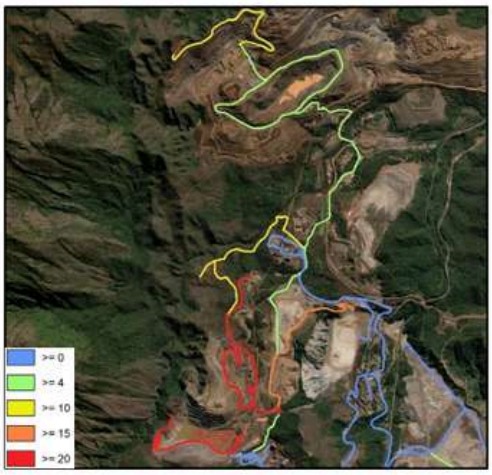


Figure 4. Average of emission factor (g/vkt) for the main roads of the Germano Mine (Samarco, Feb/23 to Nov/23).

Figure 5 shows the results of PM emission factors from the main traffic roadways in the urban area of Matozinhos/MG city, composed mainly of paved roads.

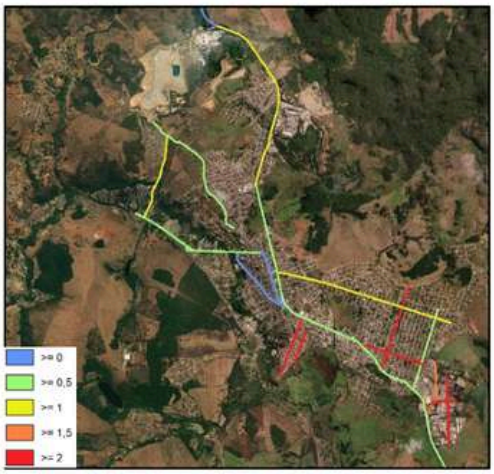


Figure 5. Average of emission factor (g/vkt) for the main roads of Matozinhos/MG (Nov/23).

CONCLUSIONS

The RAMP Roads system emerges as a new tool to enhance the management of atmospheric emissions on urban and industrial traffic roadways, as it enables the acquisition of PM emission factors in a more detailed, rapid, and less costly manner compared to the PM emission factors calculated through the USEPA's AP-42 method.

A new perspective emerges for the development of atmospheric particulate matter (PM) resuspension emissions inventories on traffic roadways, as well as

the management and control of these emissions on both paved and unpaved roads, as results can be obtained and monitored in real-time.

By combining RAMP Roads measurements with traffic flow and type counting conducted by smart cameras (EcoVision system), PM emission rates can be updated in real-time, providing total control to managers of these significant potential sources of atmospheric emissions.

ACKNOWLEDGMENTS

The authors would like to thank Vale S.A., Samarco Mineração S.A., and the Ministério Público do Estado de Minas Gerais for providing the data from the operation of RAMP Roads in their respective monitoring projects.

REFERENCES

United States Environmental Protection Agency (USEPA), 1993. AP-42 Appendix C.1 - Procedures for Sampling Surface/Bulk Dust Loading.

H. Kuhns, V. Etyemezian, D. Landwehr, C. MacDougall, M. Pitchford, M. Green, 2000. Testing Re-entrained Aerosol Kinetic Emissions from Roads (TRAKER): a new approach to infer silt loading on roadways.

H. Kuhnsa, V. Etyemezianb, M. Greenb, Karin Hendricksonc, Michael McGownc, Kevin Bartond, Marc Pitchford, 2003. Vehicle-based road dust emission measurement—Part II: Effect of precipitation, wintertime road sanding, and street sweepers on inferred PM_{10} emission potentials from paved and unpaved roads.

V. Etyemeziana, H. Kuhnsb, J. Gilliesb, J. Chowb, K. Hendricksonc, M. McGownc, M. Pitchford, 2003. Vehicle-based road dust emission measurement (III): effect of speed, traffic volume, location, and season on PM_{10} road dust emissions in the Treasure Valley, ID.

F. Amato, A. Karanasiou, T. Moreno, A. Alastuey, J.A.G. Orza, J. Lumbreras, R. Borge, E. Boldo, C. Linares, X. Querol, 2012. Emission factors from road dust resuspension in a Mediterranean freeway.

H. Sehyun, J. Yong-Won, 2012. A study on the characteristics of silt loading on paved roads in the Seoul metropolitan area using a mobile monitoring system. Journal of the Air & Waste Management Association, 62:7, 846-862.

E. Padoan, F. Ajmone-Marsan, X. Querol, F. Amato, 2017. An empirical model to predict road dust emissions based on pavement and traffic characteristics.

AIR POLLUTION CONFERENCE BRAZIL
CMAS SOUTH AMERICA
COMMUNITY MODELING AND ANALYSIS SYSTEM

RADON EXHALATION RATE MEASUREMENT IN AMAZON FOREST SOIL

O. Lakis[1], M. Moralles[2], B. Tappiz[3], C. K. Ostermann[4], J. O. V. Bustillos[5] and P. S. C. Da Silva[6]

[1,2,3,4,5,6] *Institute for Energy and Nuclear Research, IPEN/USP*

lakisomar@usp.br; mmoralles@gmail.com; brunotappiz@alumni.usp.br; carol.kako@gmail.com; ovega0000@gmail.com; pscsilva@usp.br

Abstract Measurements of terrestrial residual gas emissions are important for investigations of atmospheric, biological, and geophysical processes. Terrestrial high-frequency flows of the radioactive noble gas ^{222}Rn are useful for evaluating the performance of regional atmospheric models through the use of validated radon flux maps. In this sense, this work aims to validate a laboratory method for determining soil parameters that can influence the flow of ^{222}Rn in samples collected at the Amazon Tall Tower Observatory (ATTO). Specifically, the pH and humidity values were determined for three soil types. Although more observations are still necessary, we concluded that, in comparison with works reported in the literature, the exhalation rate is in good agreement for tropical forest soils. However, no clear correlation could be observed between the ^{222}Rn exhalation rate and soil humidity or pH.

Keywords: Radon Flux, Amazon Soil, Validation

INTRODUCTION

The soil is the main source of all life-supporting ingredients, directly or indirectly. It is also the primary contributor to the natural background radiation dose received by humans [1]. High-quality and long-term measurements of terrestrial gas emissions are important for investigations of atmospheric, biological, and geophysical processes. Soil is the upper part of the Earth's crust and is formed due to the deformation of rocks by physical and chemical processes, including weathering, decomposition, addition of organic matter, and water movement. It contains not only organic and inorganic matter but also various natural radionuclides, namely uranium (^{238}U), thorium (^{232}Th), their decay products and potassium (^{40}K), as inherent soil contents. The distribution of primordial radionuclides and their radiological effects are important factors for human health [2]. Radon gasses (^{222}Rn) and thoron (^{220}Rn) are decay products of radium (^{226}Ra) and thorium (^{232}Th), respectively [1]. As ^{238}U and ^{232}Th exist in all types of soils and rocks on the Earth's surface, after generation, these gasses escape from the soil matrix. This escape consists of a two-step process, emanation, and exhalation. In emanation, ^{222}Rn and ^{220}Rn atoms escape from solid mineral grains to air-filled pores, and in the exhalation process, they are transported to the atmosphere through convection and diffusion process. The exhalation rate is a pre-indicator of natural radioactivity levels; this rate is the emission of ^{222}Rn per unit area per unit time and depends on various factors such as the concentration of parent radium content in soil and rocks, emanation power or fraction of ^{222}Rn released from the mineral, geographical location, soil or rock porosity, grain size, water saturation degree, variable atmospheric conditions such as wind speed, temperature, and soil moisture content [2]. This work aimed to characterize the different types of soil found in the region of the High Tower Amazon Observatory (ATTO) and determine the ^{222}Rn exhalation rates. By understanding how soil parameters influence ^{222}Rn exhalation, researchers can infer information about gas dynamics in the tropical forest, its implications for the carbon cycle, and greenhouse gas emissions.

METHODS

A. Study area

Soil samples were collected from 3 distinct ecosystems existing at the ATTO site: the Terrace, an area next to the Uatumã river that is periodically flooded (Igapó Forest), the Plateau, a region of dense and non- flooded forest (Terra Firme Forest), and the Campina, an area of transition between the river terraces and the plateau [3].

B. Determination of pH and moisture

For pH determination, soil samples were placed in a 100 mL plastic beaker, and then 25 mL of 1 mol L^{-1} potassium chloride (KCl) solution was added and stirred with a glass rod. After one hour of settling, the samples were stirred again with a glass rod, and then pH readings were taken. This procedure was also performed for the pH determination in water medium [4]. For moisture determination, a soil sample was collected, and the wet mass of the sample was recorded. The soil sample was dried in a hot air oven at 105 °C until constant weight to obtain the dry weight. The moisture content is calculated by the difference in mass between the two weighing.

C. Radon (^{222}Rn) measurements

For ^{222}Rn measurements, a RAD7 detector (manufactured by Durridge Co., Inc.) was used, which is capable of detecting alpha particles by converting radiation into an electrical signal, distinguishing the energy of each particle, allowing the identification of isotopes (^{218}Po and ^{214}Po of ^{222}Rn and ^{216}Po of ^{220}Rn) produced by the decay of radon.

The calibration of RAD7 was performed at Durridge's internal facilities using a radon chamber with a radium source (^{226}Ra) to provide a known flux of ^{222}Rn. According to the RAD7 User Manual, reproducibility is generally better than 2%, and calibration accuracy is in the range of 5% [5]. The radon (^{222}Rn) exhalation rate was calculated following the formula given by Equation (1).

$$E0 = C\,\lambda eff V \,/\, 1-e^{-\lambda eff t} \quad \text{Eq.1}$$

The approach used in this study followed De Martino et al. [6], applying a nonlinear curve fitting to the experimental data C versus t, in the form $y = a\,(1 - e^{-bx})$, where $a = E0/\lambda eff \times V$ and $b = \lambda^{eff}$, where $E0$ is the exhalation rate, λeff is the effective decay constant, and V is the effective volume.

FINDINGS AND ARGUMENT

In Table 1 it is possible to see a variation from 0.92 to 12.7% in the organic matter content of the soil. The Campina soil sample had the lowest value, followed by terrace and plateau, with the higher. Studies show that in forest soils the organic matter content is generally between 1 and 5% [6], the current study shows a corresponding value in the Campina region, nevertheless, Plateau and Terrace were above this value.

Table 2 shows the soil pH measurements in water (H_2O) and potassium chloride (KCl), and also the delta pH values (ΔpH), which is the numerical difference in the pH values measured in KCl and H_2O (pH KCl - pH H_2O). The pH of the Terrace sample presented values similar to that observed in the Plateau sample, for the value observed for Campina sample, the pH was lower. In a KCl all the values were lower than in water, but the pattern remains the same, with higher values in Terraço and Plateau and lower in Campina. The ΔpH variation showed negative values in all three regions. When this difference is negative, the colloid has a negative net charge (cation exchange capacity), and when it is positive, it has a positive net charge (anion exchange capacity) [7].

Three different types of soil were analyzed from the Amazon region - site ATTO, in which the ^{222}Rn exhalation rate was presented according to Fig. 1 that shows an example of the nonlinear exponential regression fit used for determining the exhalation rate from the activity concentration values as a function of time [8].

Table 1: Moisture, organic matter, and loss on ignition - Soil samples collected at ATTO.

Samples	Temperature	Mean (% loss)	Standard Deviation
TERRAÇO	105 °C (after 24h)	0.89	0.16
	550 °C (after 4h)	7.72	0.09
	1000 °C (after 2h)	1.74	0.11
CAMPINA	105 °C (after 24h)	0.09	0.02
	550 °C (after 4h)	0.92	0.04
	1000 °C (after 2h)	0.27	0.30
PLATEAU	105 °C (after 24h)	1.27	0.15
	550 °C (after 4h)	12.7	0.64
	1000 °C (after 2h)	3.35	0.08

105°C (Moisture); 550°C (Organic matter); 1000°C (Loss on ignition)

Three different types of soil were analyzed from the Amazon region - site ATTO, in which the ^{222}Rn exhalation rate was presented according to Fig. 1 that shows an example of the nonlinear exponential regression fit used for determining the exhalation rate from the activity concentration values as a function of time [8].

The samples were collected during August 2023. The highest ^{222}Rn exhalation rate was found in the Terraço region, with the value from 32±7 mBq/cm² s. The Plateau and Campina region presented close values of 18±2 mBq/cm² s and 12±6 mBq/cm² s, respectively. The values found are close to the literature where samples analyzed in Atlantic Forest soils showed an exhalation rate of 13.5±1.6 mBq/cm² s to 20±2 mBq/cm² s [9].

Table 2: pH Amazon Soil - ATTO site

Samples	pH (H_2O)	pH (KCl)	Δ pH
TERRAÇO	4.01	3.65	-0.36
	4.07	3.68	-0.39
	4.09	3.64	-0.45
CAMPINA	3.57	3.06	-0.51
	3.69	3.07	-0.62
	3.65	3.08	-0.57
PLATEAU	4.03	3.60	-0.43
	4.05	3.78	-0.27
	4.05	3.78	-0.27

ΔpH=pH KCl - pH H_2O

CONCLUSIONS

In this study, three types of soil from the Amazon region were analyzed - ATTO site, in which the exhalation rate of ^{222}Rn showed the different soils present different exhalation rates. In comparison with works reported in the literature, the exhalation rate was in good agreement for tropical forest soils. No clear correlation could be observed between ^{222}Rn exhalation rate and humidity, or soil pH and more observations are still necessary.

ACKNOWLEDGMENT

Especially to the co-authors, technicians from ATTO and IPEN/CNEN for all their collaboration. To INPA for all logistical support and to CAPES for the scholarship granted.

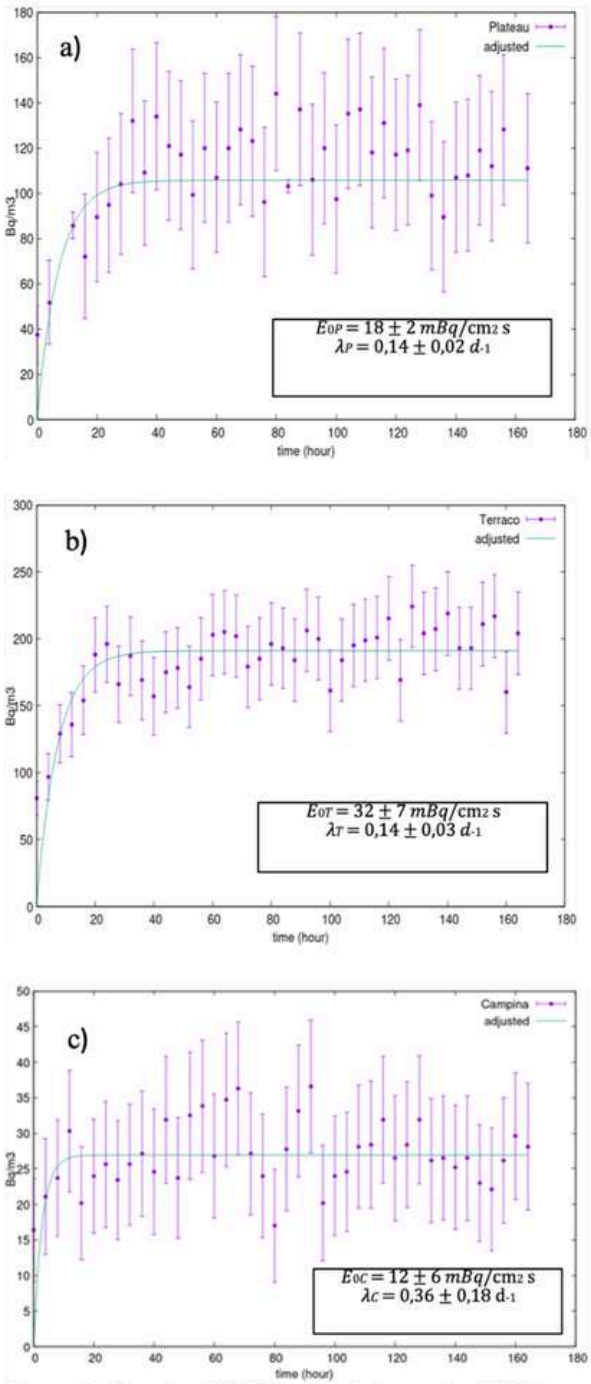


Figure 1: Graphs of 222Rn exhalation rates (E0C) as a function of time in three different regions (Campina, Terraço and Plateau) with the respective effective constant decay (λ).

REFERENCES

Andreae, M. O., Acevedo, O. C., Araùjo, A., Artaxo, P., Barbosa, C. G. G., Barbosa, H. M. J., Brito, J., Carbone, S., Chi, X., Cintra, B. B. L., da Silva, N. F., Dias, N. L., Dias-Júnior, C. Q., Ditas, F., Ditz, R., Godoi, A. F. L., Godoi, R. H. M., Heimann, M.; et al (2015). The Amazon Tall Tower Observatory (ATTO): overview of pilot measurements on ecosystem ecology, meteorology, trace gases, and aerosols. Atmospheric Chemistry and Physics, 15, 10723-10776. [3]

de Farias, E. E. G., da Silva Neto, P. C., de Souza, E. M., de França, E. J., & Hazin, C. A. (2016). Radon levels and transport parameters in Atlantic Forest soils. Journal of Radioanalytical and Nuclear Chemistry, 307, 811-815. [9]

de Martino, S., Sabbarese, C., & Monetti, G. (1998). Radon emanation and exhalation rates from soils measured with an electrostatic collector. Applied Radiation and Isotopes, 49(4), 407-413. [8]

DURRIDGE COMPANY INC. (2023). RAD7 Radon detector. User manual. Disponível em: <http://www.durridge.com/documentation/RAD7 Manual.pdf> Acesso em: 27 fev. 2023. [5]

Empresa Brasileira de Agropecuária, EMBRAPA. (1997). Manual de métodos de análise de solo. Centro Nacional de Pesquisas de Solos, Rio de Janeiro, 2ª ed. [4]

Kome, G. K., Enang, R. K., Yerima, B. P. K., & Lontsi, M. G. R. (2018). Models relating soil pH measurements in H2O, KCl and CaCl2 for volcanic ash soils of Cameroon. Geoderma Regional, 14, e00185. [7]

Kumar, M., & Sharma, N. (2022). Estimation of 222Rn, 220Rn exhalation rate and 226Ra, 232Th, 40K radionuclides in the soil samples of different regions of Gurdaspur district, Punjab. Materials Today: Proceedings, 49(8), 3396-3402. [1]

Nazaroff, W. W., & Nero Jr., A. V. (Eds.). (1988). Radon and Its Decay Products in Indoor Air. Wiley, New York, pp. 65-69. [2]

Osman, K. T. (2013). Organic Matter of Forest Soils. Forest Soils, 63-76. [6]

PROCEEDINGS OF THE

2024 AIR POLLUTION CONFERENCE

And 5th CMAS South America

SESSION 04
Emissions Inventories, Models, and Processes

This session is dedicated to the application of innovative methodologies for preparing and processing emissions for air quality modeling applications. Techniques to improve estimates of wild fires, dust and biogenic emissions, and temporal allocation of anthropogenic sources are of special interest for this session. Session topics include:

- Updates to inventories and emissions processing
- Emissions from alternative fuel use (e.g., bio-fuels in the transportation sector)
- Emissions from aviation activities
- Projection of emissions to future-year scenarios
- Inverse modeling

SESSION 4

IDENTIFICATION AND QUANTIFICATION OF SOURCES OF PARTICULATE MATTER AND POLLUTANTS GASES IN THE AMAZON: A STUDY IN FIVE COMMUNITIES WITH DIFFERENT USES AND LAND OCCUPATION IN NORTHEASTERN PARÁ 132

ASSESSMENT OF GREENHOUSE GAS EMISSIONS INVENTORY FROM A PHOTOVOLTAIC SOLAR PLANT IN RIO GRANDE DO NORTE 135

OZONE AND PM2.5 MODELING IN QUITO, ECUADOR 138

IDENTİFİCATİON AND QUANTİFİCATİON OF FİNE PARTİCLES İN THE TULA-TEPEJİ İNDUSTRİAL CORRİDOR İN TULA, USİNG PMF RECEPTOR MODEL 141

IMPACT OF COVID-19 ON METHANE EMISSIONS OVER THE US 144

CFD MODELING OF A PARTICULATE EMISSIONS MONITOR DEVICE IN QUENCH TOWERS EXHAUST 147

ROAD TRANSPORTATION EMISSIONS IN BRAZIL BETWEEN 1960 AND 2100 AND IMPACTS ON AIR QUALITY 150

SÃO PAULO URBAN GREENHOUSE GAS NETWORK – METROCLIMA PRELIMINARY RESULTS AND PROCESSES 153

AIR POLLUTION CONFERENCE BRAZIL
CMAS SOUTH AMERICA
COMMUNITY MODELING AND ANALYSIS SYSTEM

IDENTIFICATION AND QUANTIFICATION OF SOURCES OF PARTICULATE MATTER AND POLLUTANTS GASES IN THE AMAZON: A STUDY IN FIVE COMMUNITIES WITH DIFFERENT USES AND LAND OCCUPATION IN NORTHEASTERN PARÁ

Francisco Daniel Mota Lima[1], Glauber Guimarães Cirino[2], Julia Clarinda Paiva Cohen[3], David Kenton Adams[4]

[1] *Federal University of Pará*
francisco.lima@ifpa.edu.br
[2] *Federal University of Pará*
glaubercirino@ufpa.edu.br
[3] *Federal University of Pará*
jcpcohen@ufpa.edu.br
[4] *University of Arizona*
dave.k.adams@gmail.com

Abstract: Anthropic sources of air pollution are important emitters of different pollutants. The northeast of the Pará Amazon is going through an intense process of growth due to the different uses and occupation of the soil, constituting as potential sources of air pollution. Given the complexity and heterogeneity of the organization to that of space, it is difficult to identify and quantify accurately to all these sources, however, the vehicle emissions, activities in factories and industries, construction, burning of fossil fuel and burning of biomass are considered as the main anthropogenic sources of particulate matter and pollutants gases. On the other hand, the State of Pará still does not have systematized information on these sources of pollution, added to the fact that the State will host in 2025 COP 30 in the City of Belém, with significant structural changes in land use and occupation that can release large amounts of particulates and other pollutants into the atmosphere. Thus, this work aims to identify and quantify the stationary sources of pollutants in 05 Municipalities: an urbanized area in Belém-Pa; a coastal area of mangrove located in Bragança-Pa, an area near the sea located in Salinópolis-Pa and a pasture area, affected by mining, in Barcarena-Pa. The municipalities were chosen due to the different uses and occupation of the soil and potential emission of particulate matter. For this, this study has been carried out following the following steps: (1) academic and documentary survey, this and, searches on government websites, research platforms for (inter)national studies, through papers published in the area; (2) by geolocation and mapping of sources, taking into account the local economic activities, including the energy and vehicle matrices (different types of fleet and supply stations); and (3) visits and observations in loco, in the study municipalities. Industrial, agricultural and commercial areas will also be considered. it was possible to identify and quantify in the city of Belém: gas stations (145 points), ports (57) and airport (1) and service and commerce activities resulting from the burning of fossil fuels or biomass, such as activities in bakeries (248), pizzerias (231) and steakhouses (123). The pollutants SO_2 and O_3 were identified mainly in less central neighborhoods, while CO and NO_2 are better distributed throughout the city Belém.

Keywords : Atmospheric pollution, Stationary sources of pollution, Atmospheric pollutants, Land use, Pará Amazon.

INTRODUCTION

Atmospheric pollution is one of the main contemporary environmental problems. And stationary sources of air pollution, also known as fixed sources, are potential sources of pollutants with harmful effects on the environment and human health (Jacobson, 2002, Seinfeld and Pandis , 2016). On the other hand, they are less researched when compared to mobile sources of pollution, for example motor vehicles (Gomes, 2009). Examples of stationary sources of pollution are: thermoelectric plants, factories and industries, gas stations, ports and airports, landfills and service activities such as activities in bakeries, pizzerias and brick kilns (Jacobson, 2002; Seinfeld and Pandis, 2016; Kumar et al.,2015, Lima et al., 2020). In this sense, it is necessary to identify and quantify these sources of pollution in order to think about better environmental management and the use and occupation of urban space, in this study, in five municipalities in the State of Pará-Pa : Barcarena, Bragança, Capanema, Salinópolis and the capital Belém. The city of Belém is going through an intense process of metropolization and has been happening with little or no urban and environmental planning, especially in the run-up to COP 30 in the city of in 2025. Barcarena is approximately 70 km away from Belém and stands out for the production of ores, mainly aluminum and kaolin, in addition to the recent opening of a natural gas plant. Approximately 210 km from the capital, Bragança is the municipality with bigger production in flour It is activity fishing of the State, in addition to

activities in brickworks and the burning of biomass in flour mills, with potential in of particulate matter and polluting gases, in addition to the proximity to the sea and a mangrove area. Capanema stands out for the presence of a large cement factory and is approximately 165 km away from the capital Belém. Finally, the municipality of Salinópolis located on the coast of the State of Pará, approximately 215 km away from the capital, is one of the main tourist destinations of State. On the other hand, little is known about mapping and quantifying these sources of air pollution. In this study, the main focus is stationary sources of pollution that are still little studied. Among the pollutants, (CO, SO_2 , NO_2 and O_3) were considered as they are important parameters of air quality according to national and international legislation and by environmental and health bodies, such as USEPA, CETESB and WHO and, routinely they are associated with air quality degradation events and are possible to be estimated using the methodology of this study. In 2023, the first emissions inventory for Belém was published, however, the focus of the inventory was Greenhouse Gas (GHG) emissions, not including the pollutants treated in this research. Furthermore, the inventory does not consider sources of pollution such as ports, airports, gas stations and sources related to commerce and service activities which, although less harmful, are more numerous and sometimes the accumulated effect can generate potential damage to the environment and human health. (Gomes, 2009, Kumar et al., 2015, Lima et al., 2020,).

METHODS

Study area

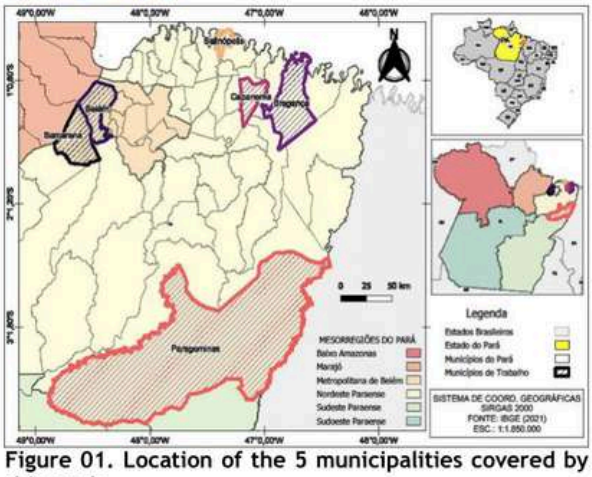


Figure 01. Location of the 5 municipalities covered by this study.

Location, identification and quantification of pollution sources

The data relating to the quantification and location of pollution sources were obtained through the computational technique of web scraping on Google maps, collecting the coordinates of each project or work, which were later inserted into the QGIS software to generate kernel maps . Density , to estimate the presence of polluting gases , was calculated based on the number of points at a location, with larger numbers of points grouped together resulting in larger values. In this study, the point density and the area covered by the data were used to define the radius values and the minimum number of grouped points, empirically adjusting the scale factor in order to achieve the greatest possible generalization. Grid smoothing was also applied to better visualization . The choices for kernel density they were based mainly at dimension of data extracted from *Sentinel* 5P OFFL L3 available in *Earth Engine* (EE) that has resolution space of approximately 1 km, to standardize the data and avoid that the analysis stay biased towards variables with greater order of magnitude, see table 01 .

Table 01: collections and their respective bands in the period from 2020 to 2023.

Collection	Band
COPERNICUS/S5P/OFFL/L3_CO	CO_column_number_density
COPERNICUS/S5P/NRTI/L3_SO2	SO2_column_number_density
COPERNICUS/S5P/OFFL/L3_NO2	NO2_column_number_density
COPERNICUS/S5P/OFFL/L3_O3	O3_column_number_density

FINDINGS AND ARGUMENTS

Using the proposed methodology, it was possible to identify and quantify: gas stations (145 points), ports (57) and airport (1) and service and commerce activities resulting from the burning of fossil fuels or biomass, such as activities in bakeries (248), pizzerias (231) and steakhouses (123), illustrated in figure 02.

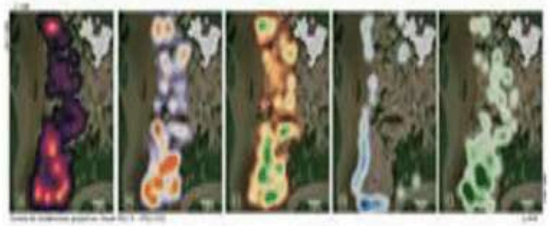


Figure 02. Identifies and quantifies stationary sources of pollution identified at city of Belém.

A place with the greatest presence of sources and density of pollutants, which is why it is most prominent in the study. The municipality of Salinópolis, followed by Capanema, Barcarena and Bragança, presented the lowest number and variation in the type of sources. The most significant sources of pollution in Salinópolis are of biogenic origin, represented by the sea and mangrove vegetation. It is a growing tourist city, with civil construction being a potential source of pollution, mainly PM_{10} , due to the construction of hotels, inns and resorts. In Capanema, apart from the cement factory, no other source of great magnitude was identified. Only sources related to commercial and service activities such as pizzerias, restaurants and

bakeries, with the burning of biomass still being an important source of energy. An industrial hub for the extraction and processing of kaolin, and the production of aluminum and derivatives, was identified in Barcarena. At the beginning of the year, a natural gas terminal was opened, which reinforces the industrial and mining vocation of this municipality. Concentrations of heavy metals and organic compounds are likely to be predominant due to the type of pollution source present. The methodology used in this work did not allow estimating the density for these pollutants. On the other hand, Belém presented the greatest number and diversity of stationary sources of pollution, as well as the highest density of pollutants, as shown in figure 03.

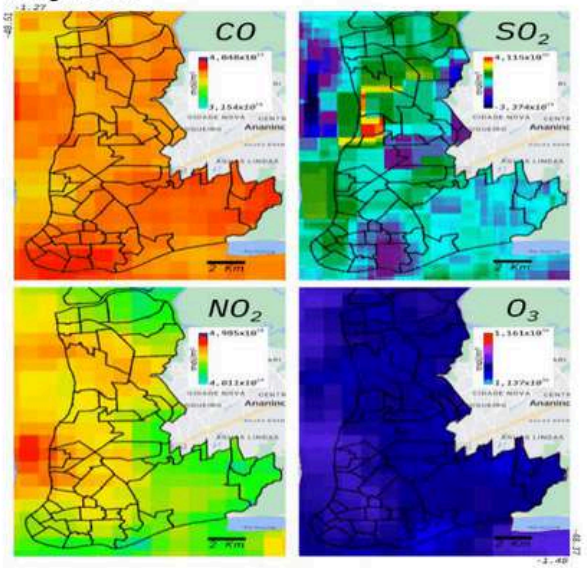


Figure 03. Time series from 2020 to 2023 of the pollutants CO, NO_2, SO_2 and O_3 at city of Belém.

The CO appeared in a better spatialized in the entire city, but with density bigger at Central region. The relative homogeneity he can to be assigned to the circulation of vehicles light and motorcycles at city arising from the high fleet of vehicles and motorcycles. The increase in the number of vehicles and the increase of around 85% in fleet of motorcycles, places Bethlehem like the fourth country city in fleet growth vehicle, currently with 511 thousand vehicles and approximately 150 thousand motorcycles (IBGE, 2022). The NO_2 showed good homogeneity at density, mainly at zone north and south of the city explained for the proximity to the airport, due to presence of numerous ports from where depart vessels of various sizes for the island region and other states, such as Amapá and Manaus. In addition to the airport, the ports of the city of Belém are the main sources SO_2 broadcasters. Sulfur is one of the main constituents of the diesel oil used us called vehicles heavy, like buses and trucks. Furthermore, it is one of the constituents of kerosene and oils, used at aviation and transport aquatic respectively. SO_2 was identified mainly in less central neighborhoods and closer to the city's international airport due to the burning of aviation fuel, in addition to the proximity to the main roads that connect the only access road to the city, BR-316, with high circulation of buses and trucks. O_3 is a pollutant secondary, or that is, it is not issued directly for the source of pollution, therefore, its density and distribution depends on other factors to be formed at atmosphere, like presence of solar radiation and pollutants precursors as hydrocarbons (HC) and nitrogen oxides (NOx). The location of the airport justifies the high density of pollutants in adjacent neighborhoods. Important access roads and vehicular traffic to the airport are located in these neighborhoods, in addition to the ozone generated at the airport itself resulting from the use of fossil fuels to fuel aircraft.

CONCLUSIONS

In this research it was possible to identify, quantify and map important stationary sources of air pollution not yet considered in the city's emission inventory. As expected, Belém presented a greater diversity of sources and a higher density of pollutants due to the larger population and different land uses, hence the greater focus in this study. Biogenic sources such as the sea and mangroves were identified in Salinópolis and Bragança. Capanema has an important cement factory and Barcarena has an important industrial complex, reinforced by the opening of a gas plant. The pollutants SO_2 and $_{03}$ were identified mainly in less central neighborhoods, while CO and NO_2 are better distributed throughout the city.

REFERENCES

Gomes, Edson, P. Survey of the main sources of atmospheric emissions in the city of Manaus, Master's Dissertation, 2009 UFAM.

IBGE: Institute Brazilian Geography and Statistics , 2022.

Kumar, P., Khare, M., Harrison, R.M., Bloss, W.J., Lewis, A.C., Coe, H., Morawsk, L., 2015. The air pollution changes for developing megacities like Delhi.Atmos. Environ. 122, 657-661.

Lima, F, Daniel Mota Lima., Pedro José Perez-Martinez., Maria De Fátima Andrade., Prashant Kumar., Regina Maura De Miranda. Characterization of particles emitted by pizzerias burning wood and briquettes : a case study at São Paulo, Brazil. Environmental Science and Pollution Research. 2020. https://doi.org/10.1007/s11356-019-07508-6

Jacobson, MZ Atmospheric Pollution - History, Science and Regulation, Cambridge University Press, 2002.

Seinfeid, JH ; Pandis, SN Atmospheric chemistry and physics: from air pollution to climate change. New York: John Wiley and Sons, 2016.

AIR POLLUTION CONFERENCE BRAZIL
CMAS SOUTH AMERICA
COMMUNITY MODELING AND ANALYSIS SYSTEM

ASSESSMENT OF GREENHOUSE GAS EMİSSİONS İNVENTORY FROM A PHOTOVOLTAİC SOLAR PLANT İN RİO GRANDE DO NORTE

Brenda Novaes[1], Ana Drummond[1], Rebekah Bon Oliveira[1], Taciana Toledo de Almeida Albuquerque[2], Leonardo Hoinaski[3], Alena Torres Netto[1], Rizzieri Pedruzzi[1]
[1]Department of Sanitary and Environmental Engineering - UERJ
[2]Department of Sanitary and Environmental Engineering - UFMG
[3]Department of Sanitary and Environmental Engineering - UFSC
Corresponding author: casanovabrenda13@gmail.com, rizzieri.pedruzzi@gmail.com

Abstract: Climate change has been studied for decades, but today, the Earth feels its impact, such as extreme temperatures, severe thunderstorms, hurricanes, droughts, and flooding. The world has witnessed catastrophic events recently as global temperatures have reached alarming levels. In this context, it is understood that it is necessary to reduce greenhouse gas emissions considerably. In order to avoid the effects of climate change, the world is changing the energy matrix from fossil fuel to renewable energy sources, such as wind and photovoltaic. These energy sources are in the spotlight because they claim to be clean and environmentally friendly, with few emissions of greenhouse gases. However, the supply chain of these energies is not 100% clean. Some studies state that greenhouse gas emissions are associated with specific stages of their life cycles, such as in the processes of raw material removal, manufacturing, construction, maintenance, and decommissioning, as in Schreiber (2019) and Schultz (2022). Therefore, it is essential to understand the effects of renewable energy on climate change and biodiversity, whether negative or positive. In this sense, the research seeks to evaluate the inventory of greenhouse gas emissions from a photovoltaic solar plant in operation in Rio Grande do Norte, Brazil, over the last three years, identifying the activities that generate the highest emissions and proposing the adoption of strategies to reduce them.

Keywords: Renewable energy, climate change, inventory of greenhouse gas emissions, photovoltaic solar plant.

INTRODUCTION

Over the years, the world has seen a gradual increase in the planet's average temperature. According to the WMO Global Annual to Decadal Climate Updatena, a report prepared by the United Nations (UN), there is a 66% probability that the average annual warming will exceed 1.5°C between 2023 and 2027. According to the Instituto Nacional de Pesquisas Espaciais (INPE), since the end of the 18th century, during the Industrial Revolution, there has been an expansion in industrial production, which has led to a large increase in greenhouse gas emissions into the atmosphere.

Among the human activities that generate the most greenhouse gas (GHG) emissions, the burning of fossil fuels is the main one, because during combustion, carbon dioxide (CO_2) is released, which retains heat in the atmosphere, making it the main pollutant responsible for global warming and climate change.

The Amazon Environmental Research Institute (IPAM) shows that the second most important contributor is deforestation, since it emits the carbon contained in forest biomass into the environment in the form of CO_2. The rest of the pollutants that have already had a large contribution, called fluorinated gases, such as hydrofluorocarbons, perfluorocarbons and sulphur hexafluoride, have been under control due to international pressure to reduce them in the atmosphere, as established in the Montreal Protocol.

In this context, the Sustainable Development Goals (SDGs) have emerged, established by the UN General Assembly (UNGA) as part of the 2030 Agenda for Sustainable Development, which include key targets and indicators for combating climate change as they provide a global, integrated and long-term framework for climate action.

Of the 17 Sustainable Development Goals (SDGs) formulated, SDG 13 is specifically focused on climate action, as it sets targets and guidelines for combating climate change, including reducing greenhouse gas emissions and promoting education initiative on climate change. In addition, it is of the utmost importance to consider SDG 7 (Affordable and Clean Energy) as an essential part of the global strategy to reduce GHG emissions, since renewable energies reduce dependence on fossil fuels for energy generation.

However, it is known that, to date, there is no renewable energy that is 100% clean and does not generate any environmental impact throughout its production and consumption. In the case of photovoltaic solar energy, GHG emissions can occur at certain stages of its life cycle, such as the production of materials, transportation and the energy needed to manufacture the components, build the plant, operate it and dispose of it at the end of its useful life as Schreiber (2019) and Schultz (2022) note. Given this scenario, it is possible to carry out a Greenhouse Gas Emissions Inventory, an instrument that makes it possible to identify and quantify the profile of GHG emissions resulting from certain activities in different sectors, which can be

drawn up on an institutional and/or community scale (IPCC, 2006).

Drawing up inventories is the fundamental starting point for an institution or company to contribute to tackling climate change, because by understanding the emissions profile through the diagnosis provided by the inventory, it is possible to establish strategies, plans and targets to reduce and manage greenhouse gas emissions, thus committing to solving the great challenge of global sustainability.

Through the Brazilian GHG Protocol Program (Programa Brasileiro GHG Protocol), adapted from the GHG Protocol, several organizations in Brazil are already able to draw up and account for their greenhouse gas emissions inventories in order to manage their emissions more accurately.

The purpose of this paper is therefore to analyze the GHG emissions inventory of a solar photovoltaic complex over the last three years, identifying opportunities to reduce harmful impacts resulting from activities carried out in the operation phase, including electricity consumption for monitoring, control and maintenance of the systems, as well as the use of equipment and vehicles among other examples.

METHODS

The research has an analytical approach, using a literature review and an inventory analysis of greenhouse gas emissions from a solar photovoltaic plant as the main tools for collecting and processing data.

Based on the GHG inventories provided by the renewable energy company responsible for operating the plant under study, it was possible to obtain the information needed to analyze GEES emissions, based on the specifications of the Programa Brasileiro GHG Protocol.

The company identifies and classifies the emissions associated with its operations, which can be direct (Scope 1) or indirect (Scopes 2 and 3) for accounting and drawing up the emissions inventory. Direct GHG emissions result from sources that belong to the organization, such as equipment, vehicles and refrigeration systems, while indirect emissions result from sources that belong to or are controlled by another organization. In scope 2, emissions come from the generation of energy purchased from third parties and consumed by the organization and in scope 3 they come from sources outside the organization, such as transport and distribution, employee commuting, waste management, effluents, among other activities (Programa Brasileiro GHG Protocol, 2008).

After evaluating the emissions inventory for the last three years, proposals for preventing and reducing the impacts identified were studied, given that it is now of the utmost importance to understand the effects of renewable energies on climate change.

The project is located in the municipality of Assú (RN) and has 30 MW of installed capacity, divided into three circuits, the first two of 9 MW and the third of 12 MW.



Figure 1. Plant Location *(Google Maps, May-2024)*

FINDINGS AND ARGUMENT

The study analyzed three inventories of the plant under study, with the reference period being 2021 to 2023, during the project's operating phase, which began in 2018. The Table 1 below shows the total emissions by scope over the last 3 years.

A critical analysis of the results shows a drastic increase (23,528.9%) in the plant's emissions compared to 2021 (base year). This factor can be explained by the inclusion of new emission sources that were not previously included in the calculation, such as purchased goods and services, capital goods, transportation and distribution, fuel and energy-related activities not included in Scopes 1 and 2 and finally, indirect waste.

Table 1. Evolution of Emissions (tCO_2eq)

Emissions Inventory			
Emission Source	Total emissions		
	2021	2022	2023
	tCO_2eq	tCO_2eq	tCO_2eq
Scope 1	**35,57**	**7,23**	**10,5**
stationary combustion	-	0,23	-
mobile combustion	7,28	6,2	10,4
effluents	0,2	0,75	0,09
fugitive emissions	28,1	0,05	0,01
Scope 2	**84,22**	**28,54**	**-**
purchasing electricity	84,22	28,54	-
Scope 3	**0,28**	**211,48**	**28.355,34**
purchased goods and services	-	151,69	19.847,63
capital goods	-	44,23	8.455,37
energy-related activities not included in Scopes 1 and 2	-	13,78	29,1
business travel	0,28	1,78	12,5
transportation and distribution (upstream)	-	-	10,67
indirect waste	-	-	0,08
Total	**120,07**	**247,25**	**28.365,84**

(Casanova, 2024.05.04)

On the other hand, in 2022, Scope 2 emissions were reduced by 66.1% compared to 2021, the explanation for which is related to the purchase of energy from the Sistema Interligado Nacional (SIN), a positive change that is essential for reducing

emissions. The Scope 1 emissions were reduced, with particular attention to fugitive emissions, which contributed significantly to this reduction.

It is also worth mentioning that due to the purchase of I-RECs (International Renewable Energy Certificates) for the plant, guaranteeing that the electricity consumed comes from a renewable energy source, 100% of scope 2 emissions were offset in 2023, resulting in the neutralization of these emissions.

The plant's biogenic emissions were also recorded for the three reference years and can be seen in the table below.

Table 2. Evolution of Biogenic Emissions (tCO_2e)

Emissions Inventory			
Emission Source	Total emissions		
	2021	2022	2023
	tCO_2eq	tCO_2eq	tCO_2eq
Scope 1	**1,73**	**3,83**	**11,77**
stationary combustion	-	0,02	-
mobile combustion	1,73	3,81	11,77
Scope 3	**0,07**	**0,05**	**5,48**
business travel	0,07	0,05	2,86
transportation and distribution (upstream)	-	-	2,62
Total	**1,8**	**3,88**	**17,25**

(Casanova, 2024.05.04)

Based on the results presented, we can see a progressive increase in biogenic emissions, with a 116% increase in 2022 compared to 2021 and a 344.7% increase in 2023 compared to 2022. This is mainly related to the increase in fuel consumption by vehicles controlled by the company and employee travel.

Below is a graph showing total emissions in tCO_2eq over the three year period.

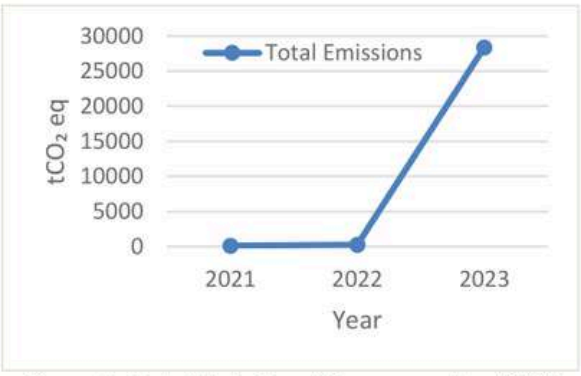


Figure 2. Total Emissions *(Casanova, May-2024)*

CONCLUSIONS

Based on the results examined, it can be concluded that a large part of the company's emissions are concentrated in Scope 3, which can be explained by the significant number of activities belonging to this scope, especially in relation to purchased goods and services and capital.

It is therefore important to think of ways to avoid and reduce these emissions, such as changing the fuels used in transportation to those from renewable sources, consuming renewable energy in your establishments and, above all, demanding that your suppliers and service providers also commit to reducing GHG emissions through sustainable practices.

Through this study, it was possible to prove that solar photovoltaic plants cannot be considered 100% clean, as they emit greenhouse gases at various stages of their life cycle, with the case study being the operation and maintenance stage, thus proving a certain degree of emission.

It is also necessary to consider the prospect of growth of photovoltaic solar energy in the Brazilian electricity matrix, making it essential to consider the cumulative and synergistic impacts of such plants.

REFERENCES

Schreiber, Andrea, and Josefine Marx. "Comparative life cycle assessment of electricity generation by different wind turbine types". *Journal of Cleaner Production* 233 (2019): 561-572. doi: https://doi.org/10.1016/j.jclepro.2019.06.058

Schultz, Herwin, and Monica Carvalho. "Design, Greenhouse Emissions, and Environmental Payback of a Photovoltaic Solar Energy System". *MDPI* (2022), 15(16), 6098. doi: https://doi.org/10.3390/en15166098

Intergovernmental Panel on Climate Change (IPCC). "Guidelines for National Greenhouse Gas Inventories, Intergovernmental Panel on Climate Change." *IPCC website*, 2006. doi: https://www.ipcc-nggip.iges.or.jp/public/2006gl/

Monzoni, Mario. "Contabilização, quantificação e publicação de inventários corporativos de emissões de gases de efeito estufa." *Sistema de Bibliotecas FGV*, 2008. doi: https://hdl.handle.net/10438/15413.

ENGIE Brasil Energia. "Inventário de Emissões de Gases de Efeito Estufa 2021 ENGIE Brasil Energia." ENGIE Brasil website, 2022. doi: https://www.engie.com.br/uploads/2022/04/Inventario-de-GEE-ENGIE-2021.pdf

ENGIE Brasil Energia. "Inventário de Emissões de Gases de Efeito Estufa 2022 ENGIE Brasil Energia." ENGIE Brasil website, 2023. doi: https://www.engie.com.br/uploads/2023/04/Relatorio_Engie_21.03.2023_v03.pdf

ENGIE Brasil Energia. "Inventário de Emissões de Gases de Efeito Estufa 2022 ENGIE Brasil Energia." ENGIE Brasil website, 2024. Doi: https://www.engie.com.br/uploads/2024/04/Inventario-de-emissoes-ENGIE-2023_10.04.2024.pdf

AIR POLLUTION CONFERENCE BRAZIL
CMAS SOUTH AMERICA
COMMUNITY MODELING AND ANALYSIS SYSTEM

OZONE AND PM2.5 MODELİNG İN QUİTO, ECUADOR

Gabriela Mancheno[1], Héctor Jorquera[2]
[1]Pontificia Universidad Católica de Chile
gamancheno@uc.cl
[2]Pontificia Universidad Católica de Chile
jorquera@ing.puc.cl

Abstract:

The goal of this work was to model ozone and aerosol chemistry in Quito, Ecuador and estimate improved emission inventories for this city; as far as we know of, this is the first time that this advanced air quality modeling is applied in Quito. For achieving this goal, the WRF-Chem (Version 4.4) model was setup for Quito, using three nested spatial domains at 32, 8 and 2 km of horizontal resolution. The emission inventories were taken from EDGAR and processed using HERMES-v3 software. The inventory for the innermost domain was spatially distributed according to: a) for industrial point sources (including energy sector), their geographical locations, b) for residential sources, population density data from the Global Human Settlement Layer, c) for traffic sources, vehicle counts at 110 measuring points throghout the city (these were also used for temporal distribution of traffic sources). Total emission inventories in the innermost domain were varied between EDGAR estimates and local estimates for Quito. In addition, biogenic emissions were estimated online by WRF-Chem (using MEGAN model). The chemical mechanism chosen was CBMZ with MADE/SORGAM aerosols (mechanism 30 in WRF-Chem).

We found that SO_2 was the most challenging gas species to model, because there was a lack of detailed information on stack source parameters, and we did not have information on industrial sources located south of Quito, which were also relevant. For CO and NOX species, reasonable results were achieved (r: 0.6-0.8 and r: 0.4-0.7, respectively). Ozone was the gas species with better modeled performance (r: 0.7-0.8). For total PM2.5, performance was lower (r: 0.4-0.5). In order to improve model performance, the local emission inventories for CO, NOx, and PM2.5 were modified by factors of 1.5, 0.75 and 3.0 approximately. On the other hand, the lack of ambient VOC and NH3 measurements prevented to further improve these emission estimates. The impact of biomass emissions on ozone and PM2.5 was positive but small, and the inclusion of aerosol radiative feedback was minor, becasue of the relatively small ambient PM2.5 concentrations in Quito.

Keywords: Quito; WRF-Chem; ozone, PM2.5; emission inventories.

INTRODUCTION

Urban air quality management is an imperative facet of contemporary environmental stewardship, particularly in rapidly growing cities where the confluence of industrial activities, vehicular emissions, and natural geographical features can significantly impact atmospheric dynamics and public health (Franco et al., 2019). Within this context, our study focuses on the burgeoning metropolis of Quito, Ecuador, located within the Andean landscape. Quito remains relatively underexplored in the domain of air quality research, prompting the need for localized modelling efforts tailored to its specific context.

The primary objective of our study is twofold: first, to model the gas and aerosol chemistry within Quito's atmospheric domain and, second, to refine emission inventories for the city through advanced air quality modeling techniques.

METHODS

2.1 Study Area and Monitoring Stations.

Quito (0°13'23"S and 78°30'45"W), situated on the eastern slopes of the Pichincha volcano within the Andes Mountain range, served as the study area. Ambient air quality data were gathered from five automatic monitoring stations managed by the Environmental Secretariat of the Metropolitan District of Quito (Table 1).

Table 1. Monitoring Stations for Quito.

Code	Station	Longitude	Latitude	Altitude (m asl)
BEL	Belisario	-78.495677	-0.1851697	2 835
CAR	Carapungo	-78.449413	-0.09548	2 660
COT	Cotocollao	-78.49954	-0.11051	2 795
CAM	El Camal	-78.517214	-0.2518482	2 840
GUA	Guamaní	-78.553478	-0.3342668	3 066

Source: https://ambiente.quito.gob.ec/.

2.2 The Weather Research and Forecasting Model (WRF).

The WRF-Chem (Version 4.4) (Skamarock et al., 2021) model was employed with three nested spatial domains at 32, 8, and 2 km horizontal resolutions (Figure 1). Emission inventories from EDGAR were processed using HERMES-v3 software (Guevara et al., 2019). The innermost domain's inventory was spatially distributed based on industrial point sources locations, residential sources using population density data, and traffic sources utilizing vehicle counts at 110 measuring points across the city. Biogenic emissions were

estimated online by WRF-Chem using the MEGAN model, while the chosen chemical mechanism was CBMZ with MADE/SORGAM aerosols (mechanism 30 in WRF-Chem) (Grell, 2005).

Simulations were conducted for the base year 2018, testing emission inventories in April and December. Various planetary boundary layer (PBL) schemes were tested, including YSU, MYJ, MYNN, and urban canopy parameterization through the BEP module, combined with YSU, MYJ, and Bougault-LaCarrere PBL options. Cumulus and aerosol radiative feedbacks were included in the model configuration. Simulations included 2 days of spin off and a full week of model evaluation each month.

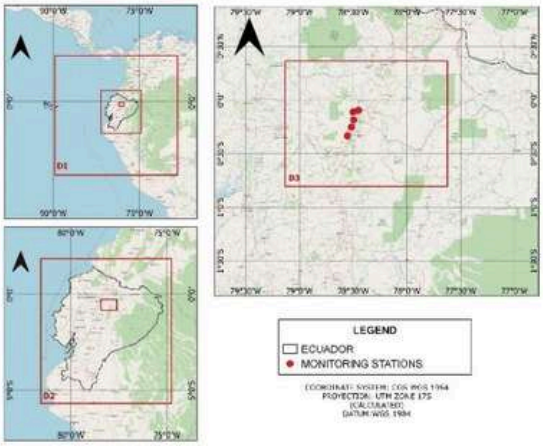


Figure 1. Nested domains employed in WRF simulations, with exclusive utilization of the innermost domain for retrospective simulations.

2.3 Evaluation of Air Quality Model Performance.

To evaluate the model's performance, the simulated concentrations of various pollutants were compared with observational data from the air quality stations shown on Table 1. The pollutants considered included sulfur dioxide (SO2), carbon monoxide (CO), nitrogen oxides (NOx), ozone (O3), and particulate matter with a diameter of 2.5 micrometers or less (PM2.5).

FINDINGS AND ARGUMENT

Prior to the analysis, it's important to note that the results presented here are for December, reflecting the best-modeled scenario, using the Bou-Lac PBL option.

3.1 CO

Figure 2 and Table 2 show that the average performance of the model was acceptable (R>0.65, NMB $\in$ [-0.2 0.2]) and there was good aggreement between observed and modeled hourly concentrations, except at Guamani station located on the southern side of Quito (Fig. 1).

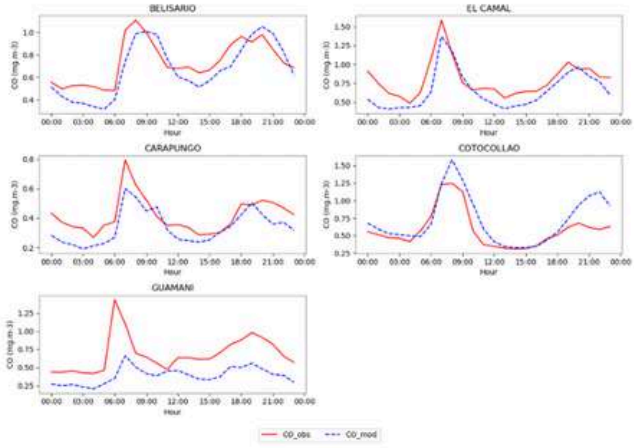


Figure 2. Comparison of observed (red) and modeled (blue) hourly CO concentrations.

3.2 NO_2

For NO2, the model had better performance in station Cotocollao. Nonetheless, the model underestimated observations (NMB $\in$ [-0.44, -0.07]) except for Cotocollao (NMB=0.28). Thus, model performance is lower in R metrics, as compared with CO modeling results.

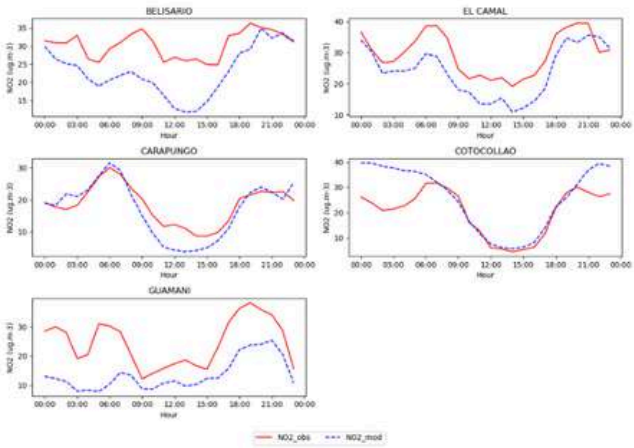


Figure 3. Comparison of observed (red) and modeled (blue) NO_2 concentrations.

3.3 SO_2 Analysis

Fos this pollutant, the model underestimates observed concentrations at most stations. The model performance is acceptable for the purpose of the diurnal variability (R >0.6, except for Guamaní station), considering the lack of detailed information about industrial SO2 emissions (stack size, gas exit velocity, etc.) for Quito.

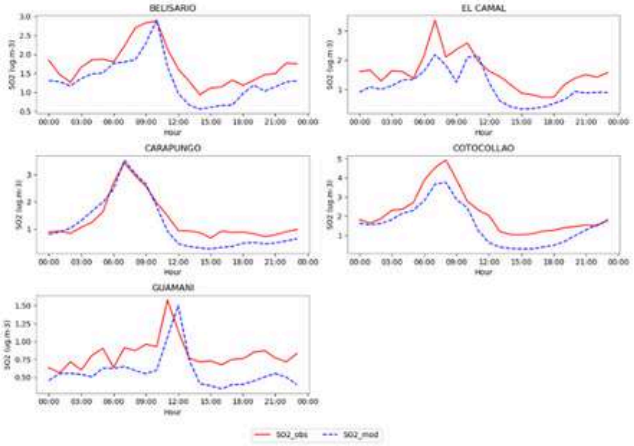


Figure 4. Comparison of observed (red) and modeled (blue) SO_2 concentrations.

3.4 O_3 Analysis

For this pollutant, the model performance was good, with R values between 0.67 and 0.84, and NMB between -0.06 and 0.15.

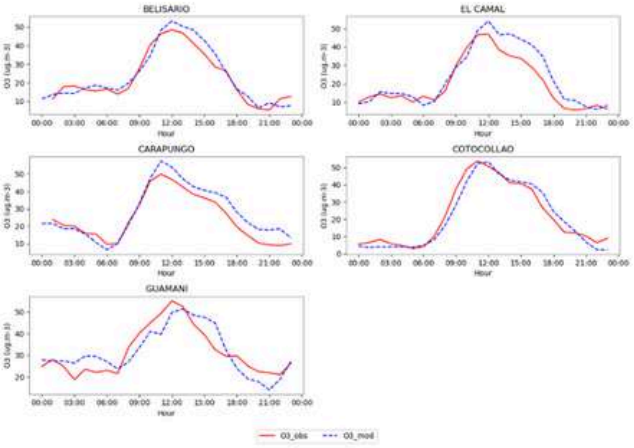


Figure 5. Comparison of observed (red) and modeled (blue) O_3 concentrations.

3.5 $PM_{2.5}$ Analysis

For this pollutant, model performance was weak, specially in capturing the rise of ambient concentrations in the afternoon, likely due to underestimation of secondary $PM_{2.5}$ generation (R values between 0.3 and 0.4).

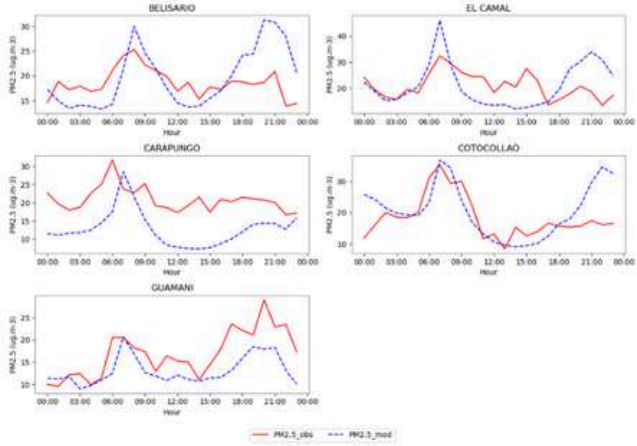


Figure 6. Comparison of observed (red) and modeled (blue) $PM_{2.5}$ concentrations.

CONCLUSIONS

This study shows the challenges of employing advanced air quality modeling techniques in a complex urban environment like Quito, Ecuador. While the WRF-Chem model demonstrates effectiveness in simulating certain pollutants, notably ozone and CO, limitations arise in accurately modeling PM2.5 and NO2 concentrations due to gaps in emission data and monitoring information. The improved estimates of annual emissions were 300, 27 and 6.8 kton for CO, NOx and PM2.5, respectively.

REFERENCES

Franco, J., Gidhagen, L., Morales, R. & Behrentz, E. (2019). Towards a better understanding of urban air quality management capabilities in Latin America. Environmental Science & Policy. 102, 43-53, ISSN 1462-9011, https://doi.org/10.1016/j.envsci.2019.09.011.

Grell, G.A., Peckham, S., Schmitz, R., McKeen, S., Frost, G., Skamarock, W., & Eder, B. (2005). Fully coupled "online" chemistry within the WRF model. Atmospheric Environment, 39 (37), 6957-6975. https://doi.org/10.1016/j.atmosenv.2005.04.027.

Guevara, M., Tena, C., Porquet, M., Jorba, O., & Pérez, C. (2019). HERMESv3, a stand-alone multi-scale atmospheric emission modelling framework - Part 1: global and regional module. Geosci. Model Dev., 12, 1885–1907. https://doi.org/10.5194/gmd-12-1885-2019

Skamarock, W. C., Klemp, J. B., Dudhia, J., Gill, D. O., Liu, Z., Berner, J., Wang, W., Powers, J. G., Duda, M. G., Barker, D., & Huang, X.-y. (2021). A Description of the Advanced Research WRF Model Version 4.3 [Technical report]. Retrieved from http://dx.doi.org/10.5065/1dfh-6p97

AIR POLLUTION CONFERENCE BRAZIL
CMAS SOUTH AMERICA
COMMUNITY MODELING AND ANALYSIS SYSTEM

IDENTİFİCATİON AND QUANTİFİCATİON OF FİNE PARTİCLES İN THE TULA-TEPEJİ İNDUSTRİAL CORRİDOR İN TULA, USİNG PMF RECEPTOR MODEL

Rubio Gomez Yrany[1], Vega Rangel Elizabeth[2]
[1]*Programa de Maestría y Doctorado en Ingeniería, Universidad Nacional Autonoma de México*
maye_rg@comunidad.unam.mx
[2]*Instituto de Ciencias de la Atmósfera y Cambio Climático, Universidad Nacional Autonoma de México*
evega@atmosfera.unam.mx

Abstract: A Receptor models are widely used to identify and quantify major emissions sources of fine particulate matter ($PM_{2.5}$), the chemical composition and specifically the so-called tracers allow the identification of specific processes that emit this pollutant. In this work, the Positive Matrix Factorization (PMF) model was used as a tool to identify and quantify the contribution of potential $PM_{2.5}$ emission sources in the industrial corridor Tula-Vito Apaxco de Tula, Hidalgo, Mexico.Environmental data from three sampling campaigns with 24-hour average measurement were used in 8 sites with different land use, such as urban, industrial and rural areas as well as in two seasons of the year, dry-warm and dry-cold. The methodological process included: 1) collection and analysis of $PM_{2.5}$ concentrations and chemical composition; 2) validation and processing of data for input to the model; and 3) identification and quantification of possible sources.The results revealed that during the highest PM2.5 concentrations, there was a higher contribution of organic carbon (28 %) and secondary inorganic aerosols (NH_4^+, NO_3^- y SO_4^{2-}) (51 %). The chemical composition of the particles collected during the three sampling campaigns was 51 % secondary inorganic aerosols, 28 % organic carbon, 9 % elements of geological material, 8 % elemental carbon, 3 % trace elements and 1 % salts. The PMF model indicated that fossil fuel burning is the main contributor of $PM_{2.5}$ at approximately 30 % during the two study periods. This finding is consistent with the industrial activities present in the area, such as refineries, thermoelectric plants, cement and metallurgical plants. Other notable sources included vehicular emissions, secondary inorganic aerosols and industrial dusts. These results are valuable for policy makers as they provide essential information to address emission reduction in the industrial area and mitigate health risks.

Keywords: Receptor model, Positive Matrix Factorization, fine particulate matter, emission sources, industrial zone.

INTRODUCTION

The United States Environmental Protection Agency (USEPA) established six criteria pollutants to assess air quality, including fine ($PM_{2.5}$) and coarse (PM_{10}) particulate matter fractions. This particulate matter, emitted by both anthropogenic and natural sources, constitute a complex pollutant with diverse physical, chemical, and biological compositions. Exposure to this particulate matter has been linked to various health problems, including respiratory and cardiovascular diseases, as evidenced by epidemiological studies showing significant correlations between particle concentrations and hospital admissions, as well as mortality (Ferreira et al., 2019).

Particularly, $PM_{2.5}$, due to their tiny size, have a significant impact on health by penetrating deeply into the respiratory system. They have been associated with various diseases such as lung cancer, nervous system damage, and cardiorespiratory diseases (Ali et al., 2019; Ferreira et al., 2019; Groma et al., 2022).

Industrial areas are hubs of intense human activity that generate a wide variety of atmospheric. In Mexico, Tula is one of the country's largest industrial areas (Vega et al., 2021), deemed critical since 1989 due to multiple sources emitting high concentrations of pollutants into the atmosphere, especially SO_2 and $PM_{2.5}$ (Sosa et al., 2020). Additionally, its demographic condition exposes approximately 476,000 inhabitants to industrial pollution (Toledo et al., 2020). The area hosts industries such as refineries, cement plants, and a thermal power plant, along with others including chemical, pharmaceutical, metallurgical, and steel industries. Therefore, quantifying emissions from these sources is crucial for managing air quality in the region.

The receptor models are based on the premise that pollution sources release a mixture of particles with specific chemical characteristics. These particles can be collected at a sampling site (receptor) and then related to potential sources using mathematical methods that consider their chemical properties (Hopke, 2015).

Among these receptor models, the Positive Matrix Factorization (PMF) developed by the USEPA stands out as the most widely used by researchers for particulate matter analysis, in addition to being open access. The latest version, PMF 5.0, requires a robust database and enables simultaneous analysis

of data from multiple sites. This receptor modelling approach facilitates the identification of potential pollution sources and the estimation of their contribution to the observed concentrations at the sampling site (Hopke, 2015). In this regard, the present study utilized the PMF model as a tool to identify and quantify the contribution of potential $PM_{2.5}$ emission sources in the Tula-Vito Apaxco industrial corridor in Tula, Hidalgo, Mexico.

METHODS

Study Area: The industrial zone is in the Hidalgo state of Mexico, within the influence area of the Atitalaquia-Tula-Apaxco region, where the Tula-Tepeji and Tula-Vito-Apaxco industrial corridors are located. In Figure 1, the study area is shown.

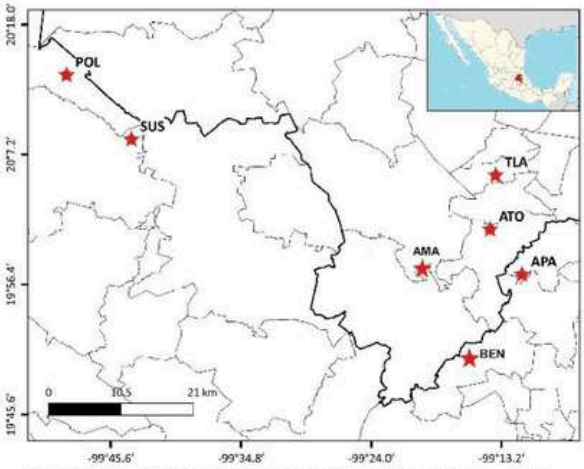


Figure 1. Study area and sampling sites: AMA, APA, ATO, BEN, POL, SUS, TLA.

The collection of $PM_{2.5}$: Environmental data from three sampling campaigns with 24-hour average measurement were used in 8 sites (Figure 1) with different land use, such as urban, industrial, and rural areas as well as in two seasons of the year, dry-warm and dry-cold. The sampling was conducted using portable low-volume equipment (MiniVol) at a flow rate of 5 L/min.

Analysis of $PM_{2.5}$ concentrations and chemical composition: Gravimetry was used to determination $PM_{2.5}$ concentrations (USEPA, 1997). Three groups of chemical species were analyzed: the Inductively coupled plasma mass spectrometry method (ICP-MS) was used for trace elements; the High-performance liquid chromatography (HPLC) method (HPLC) for soluble ions, and Thermal/Optical Reflectance method (TOR) served for the determination of organic carbon (OC) and elemental carbon (EC).

Validation and processing of data for input to the model: The concentration values and chemical composition of the particles analyzed were validated to ensure the quality of the data used as input for the receptor model application. The validation was carried out as described in (Chow et al., 2022).

Identification and quantification of possible sources

PMF version 5.0 software was applied to identify $PM_{2.5}$ emission sources. The basic equation is:

$$X_{ij} = \sum_{k=1}^{p} g_{ik} f_{kj} + e_{ij} \quad (1)$$

where X_{ij} is the concentration of species j measured on sample i; p is the number of factors contributing to the samples; f_{kj} is the concentration of species j in factor profile k; g_{ik} is the relative contribution of profile k to sample i; and e_{ij} is error of the PMF model for the j species measured on sample i. To obtain the best solution that met the goodness-of-fit parameters, the procedure explained by Vega et al., (2022) was followed.

FINDINGS AND ARGUMENT

Average $PM_{2.5}$ concentrations are shown in Figure 2. The concentrations of the dry-warm season were higher than those of the dry-cold season. This is possibly due to the rains that occurred on some sampled days of the dry-cold season.

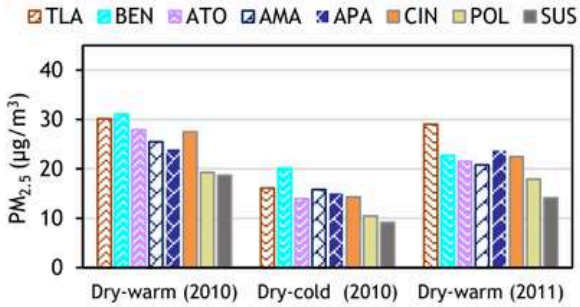


Figure 2. Average concentrations of $PM_{2.5}$.

The results revealed that during the highest $PM_{2.5}$ concentrations, there was a higher contribution of secondary inorganic aerosols (NH_4^+, NO_3^- y SO_4^{2-}) (32%) and OC (28%). The chemical composition of the particles collected during the three sampling campaigns are shown in Figure 3.

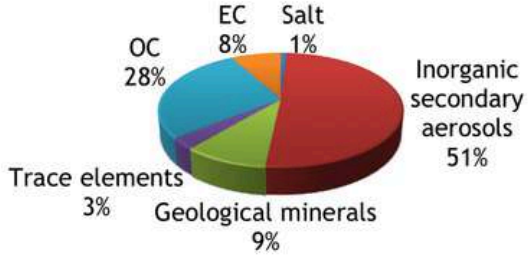


Figure 2. Percentages of the 24-hour average chemical composition of PM2.5.

The identification of $PM_{2.5}$ emission sources through the PMF model revealed differences among land use types. Urban sites (APA, ATO, and TLA) exhibited the highest contributions from sources such as fossil fuel burning, industrial emissions, and industrial dust. Meanwhile, rural sites (SUS and POL) were characterized by the highest contributions from secondary aerosols, biomass burning, and soil dust. Table 1 presents the contributions of $PM_{2.5}$ sources at each site.

Table 1. Contributions (%) of potential $PM_{2.5}$ emission sources

Source	Urban			Rural	
	APA	ATO	TLA	SUS	POL
Fossil fuel burning	30%	19%	21%	7%	6%
Vehicles	24%	7%	12%	12%	21%
Road dust	13%	-	-	4%	10%
Cement industry	-	13%	-	-	-
Soil dust	-		10%	9%	19%
Industrial	-	13%	-	-	-
Industrial dust	9%	14%	14%	-	-
Waste burning	4%	13%	16%	-	-
Biomass burning	20%	21%	12%	33%	17%
Secondary aerosols			15%	35%	27%

CONCLUSIONS

The PMF model revealed that fossil fuel combustion constitutes the primary source of $PM_{2.5}$, accounting for roughly 30% during both study periods. This result aligns with the prevalent industrial activities in the region. Additionally, significant contributors to $PM_{2.5}$ were vehicular emissions, secondary inorganic aerosols, and industrial dust. These results are valuable for policy makers as they provide essential information to address emission reduction in the industrial area and mitigate health risks.

REFERENCES

Ali, Liu, Yousaf, Ullah, Abbas, & Munir. "A systematic review on global pollution status of particulate matter-associated potential toxic elements and health perspectives in urban environment." *Environmental Geochemistry and Health* 41 (2019): 1131-1162S. https://doi.org/10.1007/s10653-018-0203-z

Chow, Liao, Huang, Leung, Lau, & Yu. "Measurement report: The 10-year trend of PM2.5 major components and source tracers from 2008 to 2017 in an urban site of Hong Kong, China." *Atmospheric Chemistry and Physics* 22 (2022): 11557-11577. https://doi.org/10.5194/acp-22-11557-2022

Ferreira, Paixão, Figueiredo, Moreira, & Caldeira. "Environment air quality and health." *Annals of Medicine* 51 (2019): 70-70. https://doi.org/10.1080/07853890.2018.1561625

Groma, Alföldy, Börcsök, Czömpöly, Füri, Horváthné Kéri, Kovács, Török, & Osán. "Sources and health effects of fine and ultrafine aerosol particles in an urban environment." *Atmospheric Pollution Research* 13 (2022). https://doi.org/10.1016/j.apr.2021.101302

Hopke. "Applying multivariate curve resolution to source apportionment of the atmospheric aerosol." In *40 Years of Chemometrics - From Bruce Kowalski to the Future, American Chemical Society* (2015): 129-157. https://doi.org/10.1021/bk-2015-1199.ch006

Sosa, Vega, Wellens, Jaimes, Fuentes, Granados, Alarcón, Torres, Sánchez, Rosas, & Mateos. "Reduction of atmospheric emissions due to switching from fuel oil to natural gas at a power plant in a critical area in Central Mexico." *Journal of the Air and Waste Management Association*, 70 (2020): 1043-1059. https://doi.org/10.1080/10962247.2020.1808113

Toledo, Trujillo, Martínez, Ruiz, Ortinez, Iniestra, Rico, Ramírez, Pérez, Páramo, Barrios, & Calva. *Calidad del Aire en la Cuenca Atmosférica de Tula* (2020). https://www.gob.mx/cms/uploads/attachment/file/571616/Calidad_del_Aire_Cuenca_Atm_de_Tula-FINAL.pdf

USEPA. "40 CFR Part 50 National Primary and Secondary Ambient Air Quality Standards." (1997): 244. https://www.ecfr.gov/current/title-40/chapter-I/subchapter-C/part-50

Vega, López, Ramírez, Chow, & Watson. "Particle-bound pahs and chemical composition, sources, and health risk of PM2.5 in a highly industrialized area." *Aerosol and Air Quality Research*, 21 (2021). https://doi.org/10.4209/AAQR.210047

Vega, Ramírez, Sánchez, Chow, Watson, López, & Jaimes-Palomera. "Volatile Organic Compounds and Carbonyls Pollution in Mexico City and an Urban Industrialized Area of Central Mexico." *Aerosol and Air Quality Research*, 22 (2022). https://doi.org/10.4209/aaqr.210386

AIR POLLUTION CONFERENCE BRAZIL
CMAS SOUTH AMERICA
COMMUNITY MODELING AND ANALYSIS SYSTEM

Impact of COVID-19 on methane emissions over the US

Sergio Ibarra-Espinosa[1,2*], Lei Hu[2*], Colin Harkins[1,3], Brian McDonald[3], Scot Miller[4], Youmi Oh[1,2], Lori Bruhwiler[1,2], Kathryn McKain[2], Colm Sweeney[2], Arlyn Andrews[2]

1 Cooperative Institute for Research in Environmental Sciences, University of Colorado-Boulder, Boulder, CO, United States.
2 Global Monitoring Laboratory, National Oceanic and Atmospheric Administration (NOAA), Boulder, CO, United States.
3 Chemical Science Laboratory, National Oceanic and Atmospheric Administration (NOAA), Boulder, CO, United States.
4 Johns Hopkins University
sergio.ibarra-espinosa@noaa.gov

Abstract: Methane, a potent greenhouse gas, has a short lifetime of approximately 9 years, a global warming potential of 30 over 100 years, and has contributed to a radiative forcing of 0.650 Wm^{-2} since 1750. Recently, the US pledged in the COP26 to reduce methane emissions by 30% by 2030 compared to 2020 levels, emphasizing the urgency of monitoring and quantifying these emissions for effective greenhouse gas mitigation. The COVID-19 pandemic led to reduced human activity globally, resulting in lower air pollutant concentrations. However, the pandemic's direct and indirect effects on greenhouse gas emissions require further investigation. In this study, we present a detailed analysis of methane emissions across the contiguous US. Using NOAA CH_4 ObsPack GLOBALVIEWplus data from December 2017 to January 2022, and employing the Hybrid Single-Particle Lagrangian Integrated Trajectory (HYSPLIT) model with meteorological data from the NAM and Global Forecast System, we conducted inverse modeling analyses. Our results indicate a reduction of -6.1% in 2020 and -4.6% in 2021 compared to 2019, particularly in regions dominated by oil and gas activities, consistent with external data.

Keywords: COVID-19, methane, emissions, oil and gas, in-situ, inversion, modeling, lockdown

INTRODUCTION

The COVID-19 pandemic swiftly disrupted global socioeconomic activities, prompting governments worldwide to implement lockdowns and quarantines to contain the spread of the virus. This led to a notable reduction in human mobility, reflected in improved air quality in many cities (Alessandretti, 2022; Ibarra-Espinosa et al., 2022). Despite these measures, greenhouse gas emissions, particularly methane, continued to rise (Foster et al., 2020, NOAA, 2023). Methane, a potent greenhouse gas with a short lifespan and significant radiative forcing since 1750, has become a focal point for emission reduction efforts, exemplified by the US signing the Global Methane Pledge at COP26. In the US, anthropogenic methane emissions, primarily from energy and agricultural sectors, are a major concern, with conflicting estimates necessitating robust quantification methods. Amidst the pandemic, studies reported varied impacts on methane emissions globally, highlighting the need for further investigation (U.S. White House, 2021).

In this context, our study focuses on quantifying methane emissions over the US from 2018 to 2021. Leveraging comprehensive observational data and employing a Lagrangian inverse modeling framework (Hu et al., 2023), we aim to provide accurate assessments of methane emissions, considering both natural and anthropogenic sources. By integrating various emission estimates and investigating the influence of COVID-19 on methane emissions, we contribute to a deeper understanding of emission dynamics and aid in devising effective mitigation strategies.

METHODS

We used the Hybrid Single-Particle Lagrangian Integrated Trajectory (HYSPLIT) (Stein et al., 2015) to calculate the atmosphere's sensitivity to the surface fluxes. We used meteorology from NAMS(12km) with GFS0.25. Then, we used NOAA CH4 ObsPack GLOBALVIEW+ v5 to determine the sensitivity for each 2:00pm for surface, and eerie 20 seconds for aircraft, shown on figure 1. Usually, aircraft and surface flasks observation are assimilated, but in this case we added surface continuous, doubling the amount of observations assimilated (Ibarra-Espinosa and Hu, 2024). Then we applied a Lagrangian Inverse modeling (Hu et al., 2023) approach to produce an ensemble of 6 posterior estimates. We additionally compiled natural estimates for North America with values from literature (L. Liu et al., 2020; Sanderson, 1996; Houweling et al., 1999; Etiope et al., 2019; Bloom et al., 2017; Miller et al., 2014, 2016; Pickett-Heaps et al., 2011; Zhang et al., 2023).

.

AIR POLLUTION CONFERENCE BRAZIL

CMAS SOUTH AMERICA

COMMUNITY MODELING AND ANALYSIS SYSTEM

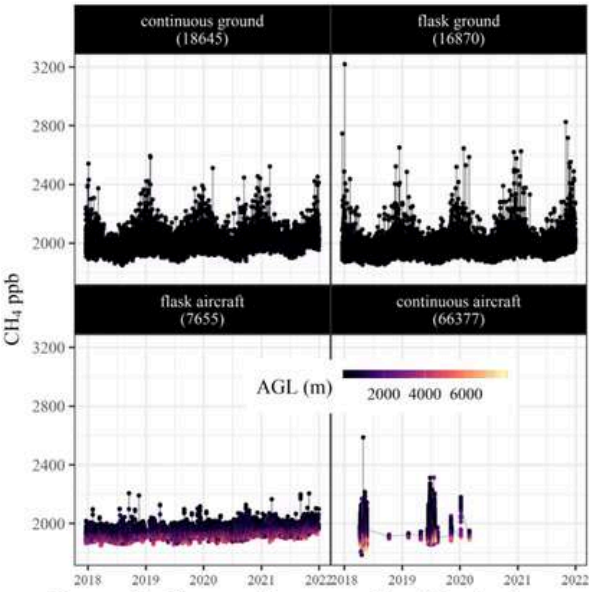


Figure 1. Observations used in this study. continuous observations were reserved for evaluation. The color shows altitude above ground level (AGL)

FINDINGS

The average methane emissions in the US during 2018-2021 were 53.6 (±3.3), 55.2 (±2.9), 51.8 (±3.6), and 52.6 (±3.3) Tgy^{-1}, respectively. Comparing these to the pre-pandemic levels of 2019, there was a decrease of 3.4 Tgy^{-1} in 2020 and 2.6 Tgy^{-1} in 2021. Despite these reductions being smaller than the uncertainty range, they are statistically significant across all ensemble members. The average percentage change from 2019 to 2020 and 2021 was -5.3%.

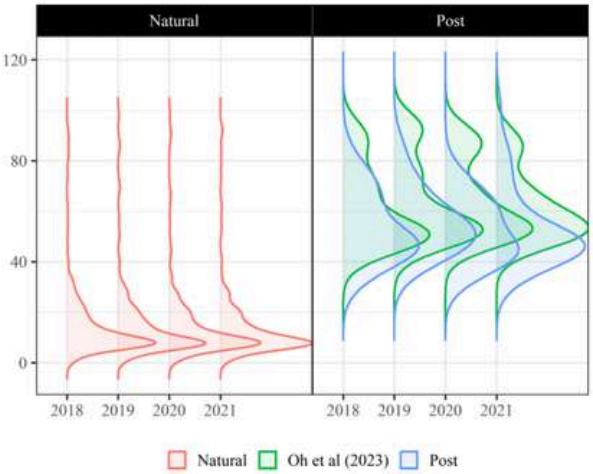


Figure 2. Natural and posterior density of estimates between 2018 to 2021 (Tgy^{-1}) including values from Oh et al (2023).

Figure 2 shows the density of monthly observations in Tgy^{-1} for our ensemble estimations, named Post, values from Carbon Tracker (Oh et al., 2023), and natural estimates. First, we see that the mean of natural values is lower than the total posterior, but with high dispersion and low interannual variability. We see a general agreement between our estimates and values from Oh et al. (2023) in the case of posterior estimates.

The spatial analyses, consisting of the average of the differences 2020/2021 with 2019, revealed clear patterns, as shown in Figure 3. Reductions in emissions are found in the South and Northeast US, in the Oil and Gas region, specifically the Permian, Eagle Ford, Niobara, and Appalachia regions[1]. The official US/EPA (2023) emissions inventory data shows a similar magnitude reduction focused over the South and North East US due to changes in the Energy sector, coincidentally the same locations. Finally, we compared our results with the Fuel Oil and Gas NOAA/CSL emissions inventory (Francoeur et al., 2021). The FOG inventory separates methane emissions by drilling and production activities, finding reduction for the period 2020-2021, in comparison to 2019, in the same order of magnitude, specifically due to drilling in South and North East US.

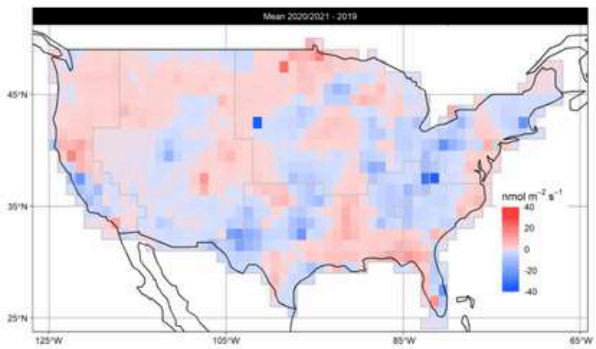


Figure 3. The average of the differences in the posterior emissions

CONCLUSIONS

Our study analyzes COVID-19's impact on US methane emissions, revealing trends: -5% in 2020/2021 compared to 2019. Despite consistent yearly changes, varied datasets reflect complex methane sources across the US. The study emphasizes the energy sector's role, especially drilling, in influencing emissions and suggests targeted mitigation can aid environmental goals amidst pandemic challenges.

[1] https://www.eia.gov/petroleum/drilling/

REFERENCES

1. Alessandretti, L. (2022). What human mobility data tell us about COVID-19 spread. Nature Reviews Physics, 4(1), 12-13. https://doi.org/10.1038/s42254-021-00407-1
2. Ibarra-Espinosa, S., Dias de Freitas, E., Ropkins, K., Dominici, F., & Rehbein, A. (2022). Negative-Binomial and quasi-poisson regressions between COVID-19, mobility and environment in São Paulo, Brazil. Environmental Research, 112369. https://doi.org/10.1016/j.envres.2021.112369
3. NOAA. (2023, August 1). Trends in Atmospheric Methane. https://gml.noaa.gov/ccgg/trends_ch4/
4. Forster, P. M., Forster, H. I., Evans, M. J., Gidden, M. J., Jones, C. D., Keller, C. A., ... & Turnock, S. T. (2020). Current and future global climate impacts resulting from COVID-19. Nature Climate Change, 10(10), 913-919.
5. U.S. White House. (2021, September). Joint US-EU press release on the Global Methane Pledge. The White House. The United States Government. Retrieved from https://www.whitehouse.gov/briefing-room/statements-releases/2021/09/18/joint-us-eu-press-release-on-the-global-methane-pledge/
6. Hu, Ottinger, D., Bogle, S., Montzka, S. A., DeCola, P. L., Dlugokencky, E., et al. (2023). Declining, seasonal-varying emissions of sulfur hexafluoride from the United States. Atmos. Chem. Phys., 23(2), 1437-1448. https://doi.org/10.5194/acp-23-1437-2023
7. Stein, A. F., Draxler, R. R., Rolph, G. D., Stunder, B. J. B., Cohen, M. D., & Ngan, F. (2015). NOAA's HYSPLIT atmospheric transport and dispersion modeling system. Bulletin of the American Meteorological Society, 96(12), 2059-2077.
8. Ibarra-Espinosa, S., Hu ,L. (2024). _rtorf: 'rtorf' ObspackGLOBALView+_. https://noaa-gml.github.io/rtorf/
9. Oh, Y., Bruhwiler, L., Lan, X., Basu, S., Schuldt, K., Thoning, K., et al. (2023). CarbonTracker CH4 2023. NOAA Global Monitoring Laboratory. https://doi.org/10.25925/40JT-QD67
10. Bloom, A. A., Bowman, K. W., Lee, M., Turner, A. J., Schroeder, R., Worden, J. R., et al. (2017). A global wetland methane emissions and uncertainty dataset for atmospheric chemical transport models (WetCHARTs version 1.0). Geoscientific Model Development, 10(6), 2141-2156. https://doi.org/10.5194/gmd-10-2141-2017
11. Etiope, G., Ciotoli, G., Schwietzke, S., & Schoell, M. (2019). Gridded maps of geological methane emissions and their isotopic signature. Earth System Science Data, 11(1), 1-22. https://doi.org/10.5194/essd-11-1-2019
12. Houweling, S., Kaminski, T., Dentener, F., Lelieveld, J., & Heimann, M. (1999). Inverse modeling of methane sources and sinks using the adjoint of a global transport model. Journal of Geophysical Research: Atmospheres, 104(D21), 26137-26160. https://doi.org/https://doi.org/10.1029/1999JD900428
13. Liu, L., Zhuang, Q., Oh, Y., Shurpali, N. J., Kim, S., & Poulter, B. (2020). Uncertainty Quantification of Global Net Methane Emissions From Terrestrial Ecosystems Using a Mechanistically Based Biogeochemistry Model. Journal of Geophysical Research: Biogeosciences, 125(6), e2019JG005428. https://doi.org/https://doi.org/10.1029/2019JG005428
14. Pickett-Heaps, C. A., Jacob, D. J., Wecht, K. J., Kort, E. A., Wofsy, S. C., Diskin, G. S., et al. (2011). Magnitude and seasonality of wetland methane emissions from the Hudson Bay Lowlands (Canada). Atmospheric Chemistry and Physics, 11(8), 3773-3779. https://doi.org/10.5194/acp-11-3773-2011
15. Sanderson, M. G. (1996). Biomass of termites and their emissions of methane and carbon dioxide: A global database. Global Biogeochemical Cycles, 10(4), 543-557. https://doi.org/https://doi.org/10.1029/96GB01893
16. U.S. EPA. (2023, August). Greenhouse Gas Inventory Data Explorer. US. EPA. Retrieved from https://cfpub.epa.gov/ghgdata/inventoryexplorer/
17. Francoeur, C. B., et al. (2021). Quantifying Methane and Ozone Precursor Emissions from Oil and Gas Production Regions across the Contiguous US. Environmental Science & Technology, 55(13), 9129-9139. https://doi.org/10.1021/acs.est.0c07352

AIR POLLUTION CONFERENCE BRAZIL
CMAS SOUTH AMERICA
COMMUNITY MODELING AND ANALYSIS SYSTEM

CFD MODELING OF A PARTICULATE EMISSIONS MONITOR DEVICE IN QUENCH TOWERS EXHAUST

Willian Lemker Andreão[1], Maria Eduarda Oliveira, Rafael Sartim
ArcelorMittal Tubarão, Serra, Espírito Santo, Brazil
[1]*willian.andreao@arcelormittal.com.br*

Abstract: Wet quenching is the most common method of coke cooling, for economic and technological reasons, although the quench tower becomes a source of several gases and particulate emissions. Measuring the amount of dust generated during coke quenching is extremely difficult because the quench vapor velocity and dust concentration change greatly during the quench process, which lasts only a few minutes, and are different at certain points in the tower cross section. When coke is quenched, most of the dust is usually generated during the first 20 sec. A passive sampling method, using Mohrhauer probes based on German former standard VDI 2303, has been recommended by the Best Available Techniques (BAT) reference document for iron and steel production to measure this emission. However, few results using this method are reported in scientific literature. The well know major deficiency of Mohrhauer method is the capture of fine dust, PM_{10} and $PM_{2.5}$, which can represent up to 30% of total PM mass. In this context, this work aims to investigate, thought a computational fluid dynamic analysis, the flow distribution inside of the current shape of Mohrhauer probe, verifying if the flow conditions allow small particles deposition, and how the device can be improved to increase this efficiency, ensuring the passive flow.

Keywords: coke, wet quenching, atmospheric pollution, pollutant emissions, computational fluid dynamics.

INTRODUCTION

Most coke plants are located within or nearby iron and steel production facilities, and the demand for coke relates with iron and steel production. After carbonization in furnace batteries, the coke is taken out of the oven and must be cooled. Wet quenching is the most common method of coke cooling, for economic and technological reasons, although the quench tower is a source of several gases and particulate emissions [1-3].

When coke is quenched, dust is not evenly generated throughout the quench process. Usually, the highest amount of dust is generated during the first 20 sec. The total amount of dust generated differs from system to system. Measuring the amount of dust generated during coke quenching is extremely difficult because the quench vapor velocity and dust concentration change during the quench process, which lasts only a few minutes, and are different at certain points in the tower cross section.

A passive sampling was developed using Mohrhauer probes (Mohrhauer's non-isokinetic method, Figure 1), based on German former standard VDI 2303 Limiting of dust emissions in the extinguishing of coke; coking plants and gas works [4], in accordance with the Best Available Techniques (BAT) reference document for iron and steel production [5].

However, the Mohrhauer method is recognized for its inability to capture fine dust. It is still not clear the efficiency of measure PM_{10} and $PM_{2.5}$ with such method, for example, which can represent up to 30% of total PM mass [6]. In this context, this work aims to investigate, thought a computational fluid dynamic analysis, the flow distribution inside of the current shape of Mohrhauer probe, verifying if the flow conditions allow small particles deposition, and how the device can be improved to increase this efficiency, ensuring the passive flow.

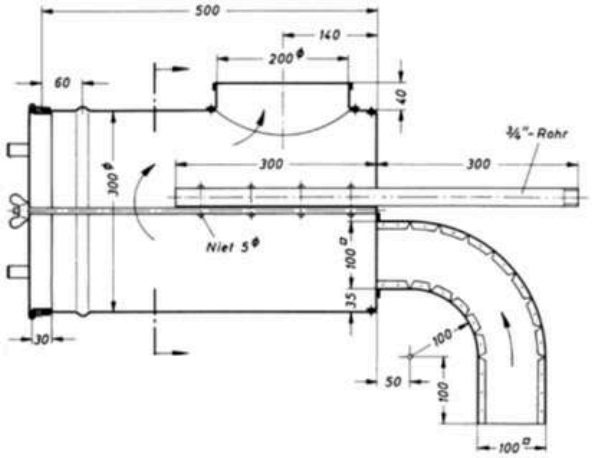


Figure 1 - Mohrhauer sampling probe.

METHODS

ANSYS Fluent 2020R1 was used to solve the governing equations. Equations were solved for isothermal (80 °C) and incompressible flow. The thermodynamic properties used for the fluid are those of steam, as shown in Table 1. The flow was assumed turbulent, and the SST k-ω turbulence model was used. Mass, momentum, and turbulence model equations were solved considering steady state conditions.

Table 1 - Gas and particle properties.

Property	Steam	Coke particle
Density [kg/m³]	0.2935	650
Viscosity [Pa·s]	1.16E-05	-

To model the sampling device, the outlet was extended by two diameters to prevent recirculation at the exit. The internal walls were treated with a no-slip condition, while zero shear stress was applied to the external wall. A ΔP = 0 Pa was set at the outlet. At the inlet, two velocities profiles obtained by simulating an outer domain were used.

Three modifications in Mohrhauer sampling probe were also evaluated, according to Figure 2: (ID #1) an extension of the probe and plate lengths in 30%; (ID #2) a second stage plate, moving the exit close to the back side; and (ID #3) a perforated plate closing the middle of the device.

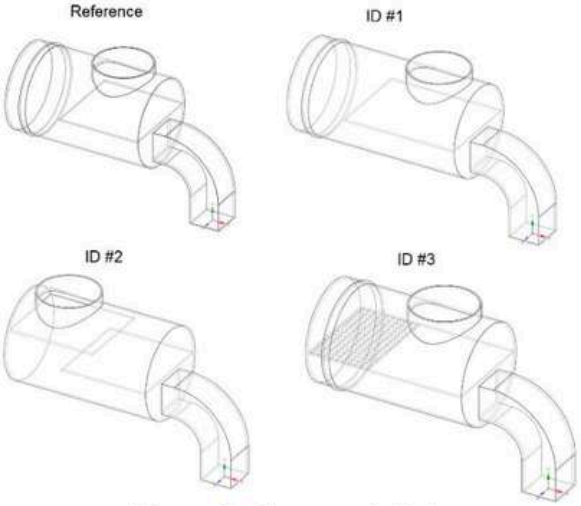


Figure 2 - Cases modelled.

To simulate particles dispersed in the fluid, the discrete phase model (DPM) was adopted, with particle diameters varying between 2.5 µm and 100 µm. Wet coke density was considered (650 kg/m³). For the coefficient of restitution on the walls, the value of 0.7 was adopted.

One relevant aspect to evaluate the efficiency of Mohrhauer sampling probe is evaluate the complete and incomplete particles, which determines the percentage of particles captured. A maximum residence time was stablished to simulate the DPM, based on each geometry and mean inlet velocity, according to Table 2.

After grid sensitivity tests, a mesh with 3.6 million nodes was selected for the reference geometry.

Table 2 - Particle residence time for each inlet mean velocity.

Geometry	1.0 m/s	4.2 m/s
Reference	5.3 s	1.3 s
ID #1	5.3 s	1.3 s
ID #2	6 s	1.4 s
ID #3	5.3 s	1.3 s

FINDINGS AND ARGUMENT

The particle capture efficiency for each mean inlet velocity modelled is presented in Figures 3 and 4. As expected, higher the particle diameter, higher the capture efficiency. For the smaller diameters (2.5 to 10 µm), efficiency was around 40%, except for ID #1, which presented the worst particle capture capacity. For smaller inlet velocity, modifications 2 and 3 presented comparable results as the reference geometry, while for higher inlet velocities, the reference geometry still presented better particle capture efficiencies.

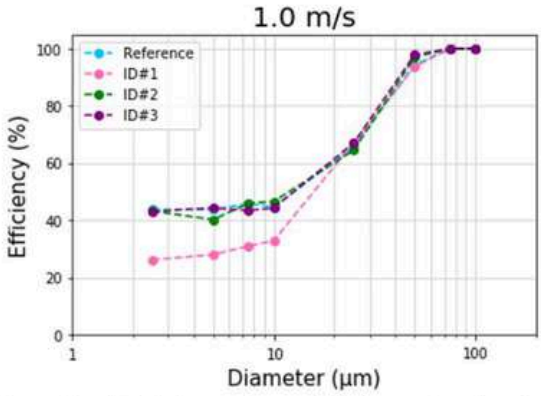


Figure 3 - Particle capture efficiency for 1 m/s of inlet mean velocity.

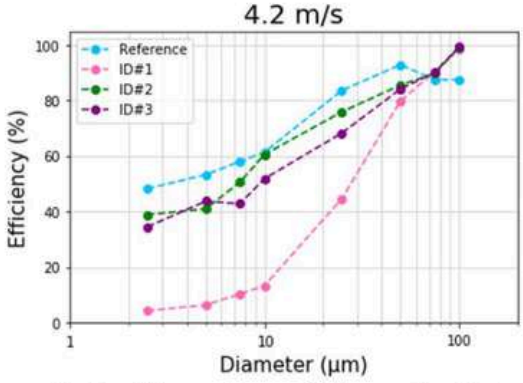


Figure 4 - Particle capture efficiency for 4.2 m/s of inlet mean velocity.

Figure 5 and 6 present the flow distribution for inlet velocity of 1.0 m/s and 4.2 m/s, respectively. For the mean inlet velocity of 1.0 m/s, a larger recirculated zone at the back of the sampling device

has been observed for ID #1 compared to the reference geometry, with smaller velocities. However, the flow still preserved the preferential path, accelerating close to the plate and leaving the exit. An analogous situation was observed with the two stage plates (ID #2). With the perforated plate, the velocity is reduced, but quickly leaves the device, not been enough to reflect in the smaller particle capture efficiency.

Considering the mean inlet velocity of 4.2 m/s, for the reference geometry, after the inlet curve, the flow hits the back of the sampling device and splits into two directions. A small part recirculates to down, but most part accelerate and goes to the exit above the plate. Extending the domain (ID #1), this acceleration decreased, but also the recirculation bellow, which favorited the flow direction to the exit. The presence of a second stage (ID #2) created other recirculation zones, but the flow did not loose velocity. The perforate plate (ID #3) reduced the velocity after the flow passed thought it, but it was not enough to impact the capture efficiency estimated.

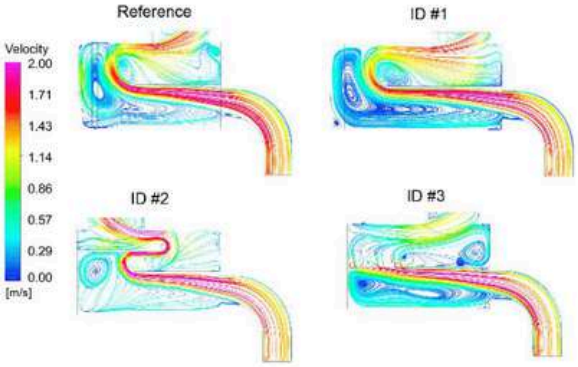


Figure 5 - Fluid flow distribution for mean inlet velocity of 1.0 m/s.

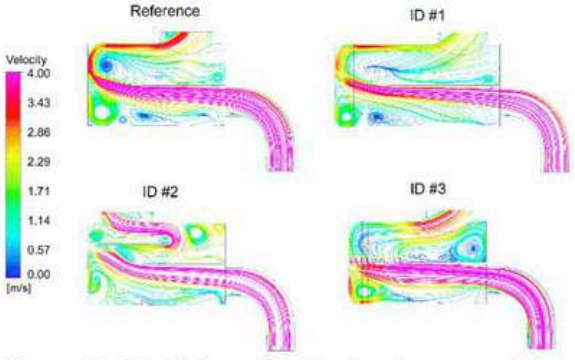


Figure 6 - Fluid flow distribution for mean inlet velocity of 4.2 m/s.

Figure 7 presents the particle tracking for the reference case and for mean inlet velocity of 4.2 m/s. Larger particles remained in the bottom of the sampling device, while most part of the finer particles is still transported with the fluid and leave the sampling device. Comparable results were obtained with the modifications evaluated.

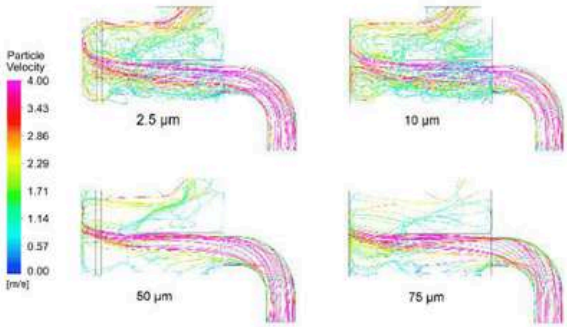


Figure 7 - Particle tracking for the reference geometry and mean inlet velocity of 4.2 m/s.

CONCLUSIONS

For the first time, an efficiency of the Mohrhauer sampling probe used in wet quenching towers has been estimated using CFD. Overall, efficiencies over 50% were obtained with particle diameters higher than 50 µm. However, for finer particles, increase the capture efficiency is still challenging, with most part of the particles leaving the sampling device.

The tested modifications did not improve the efficiencies, and other solutions is still necessary to increase the sampling performance. A field test can be performed to validate the simulation and assess the appropriate modification when found.

REFERENCES

[1] Kwiecinska A. et al. (2014). The Impact of Cooling Water Parameters on the Wet-Quenched Coke Quality. Coke and Chemistry, 57 (11), 425–428.
[2] Kishore K., Mukhopadhyay G. (2019). Failure Analysis of Liner Plates of Wet Coke Quenching Car. J Fail. Anal. and Preven., 19, 771–776.
[3] Miroshnichenko I.V. et al. (2020). Calorific Value of Coke 5. Quenching Method. Coke and Chemistry, 63 (4), 177–182.
[4] Verein Deutscher Ingenieure (VDI). VDI 2303 Limiting of dust emissions in the extinguishing of coke; coking plants and gas works. 1966.
[5] Remus R. et al. Best Available Techniques (BAT) Reference Document for Iron and Steel Production: Industrial Emissions Directive 2010/75/EU: (Integrated Pollution Prevention and Control). 2013.
[6] U.S. Environmental Protection Agency (2008). Background Report AP-42 Section 12.2 Coke Production. US EPA: Research Triangle Park, NC, 2008.

AIR POLLUTION CONFERENCE BRAZIL
CMAS SOUTH AMERICA
COMMUNITY MODELING AND ANALYSIS SYSTEM

Road transportation emissions in Brazil between 1960 and 2100 and impacts on air quality

Sergio Ibarra-Espinosa[1,2], Edmilson Dias de Freitas[3], Benjamin Gaubert[4], Pablo Lichtig[5,6], Louisa Emmons[4], Guy Brasseur[6,7]

1. Cooperative Institute for Research in Environmental Sciences, University of Colorado-Boulder, Boulder, CO, United States sergio.ibarra-espinosa@noaa.gov
2. Global Monitoring Laboratory, National Oceanic and Atmospheric Administration (NOAA), Boulder, CO, United States
3. Departamento de Ciências Atmosféricas, Universidade de São Paulo. São Paulo, Brazil.
4. National Center for Atmospheric Research (NCAR/ACOM), Boulder, CO, United States
5. Consejo Nacional de Ciencia y Tecnología, Buenos Aires, Argentina
6. Comisión Nacional de Energía Atómica, Buenos Aires, Argentina
7. Max Plank Institute for Meteorology, Hamburg, Germany

Abstract: Road transportation is the main source of air pollution in urban centers. However, air pollutant concentration relies on the transport of pollutants across scales. Brazil, the biggest country in Latin America, presents high levels of PM2.5 and ozone. Global anthropogenic emission inventories can present shortcomings due to the limited availability of local activity data and vehicle fleet-specific emission factors. In this study, we estimated road transportation emissions in Brazil between 1960 and 2100 considering different Shared Socioeconomic Pathways (SSP). We used the VEIN model with emission factors adjusted with observed local measurements made in tunnels in São Paulo. The air quality modeling was done using the Multi-Scale Infrastructure for Chemistry and Aerosols (MUSICA). This model is a configuration of the Community Atmosphere Model with chemistry (CAM-chem), a global model with a nominal resolution of 1 degree with a mesh refinement down to around 0.25 degree for the whole of South America with emissions from VEIN over Brazil and global emissions inventories elsewhere. Our results indicate the peak of CO, NMHC and $PM_{2.5}$ transportation emissions occurred during the 90's.

Keywords: Brazil, vehicular, emissions, inventory, vein, musica, ncar, air pollution

INTRODUCTION

Road transportation has a huge impact on air quality and greenhouse gasses. This was demonstrated with the lockdowns during the COVID-19 pandemic, where there was a reduction of air pollutants globally (Foster et al., 2020). However, long term studies about emissions trends are scarce, and their impact on air quality even more, specially in Latin America.

Brazil, one of the biggest countries in world, has a population of over 200 million and a huge fleet. Despite that there are studies focusing on vehicular emissions and air quality at city level (Gavidia-Calderon et al, 2023;, Ibarra-Espinosa etc al., 2022, Lichtig et al., 2024), information covering the county is limited or restricted for specific years (Hoinaski et al., 2022, 2023). Therefore, in this study we provide a long-term vehicular emissions inventory, between 1960 to 2080, and evaluate the air quality.

METHODS

To estimate the vehicular emissions in Brazil we used the Vehicular Emissions INVentories model (VEIN) (Ibarra-Espinosa et al., 2018). In Brazil, gasoline contains 27% of ethanol then we need local emissions factors. The emission factors comes from official dynamometer measurements corrected with real-world measurements (Nogueira et al., 2021). We used fleet information at state level from the department of transportation (DENATRAN) at state and annual level between 1980 and 2020. Then we applied survival functions to account for the scrapped fleet and generate data by age of use. We used monthly road transportation fuel consumption for ethanol, gasoline and diesel by state between 2000 and 2020. We projected the fuel consumption, fitting a logistic equation to the data. Emissions were allocated to streets from Open Streets Maps. Air quality was simulated for the year 20199 using the MUSICA model (Pfister et al., 2020), which refinement with spectral element dynamical core. The emissions from VEIN were gridded with 0.1 degree of spatial resolution too match the CAMS inventory, and then merge without road transportation from CAMS.

FINDINGS AND ARGUMENT

The projection of fuel consumption is shown on Figure 1, where it is assumed a stable consumption after the year 2020, which can be considered an optimistic scenario. Diesel is the fuel most consumed, followed by gasoline and then ethanol.

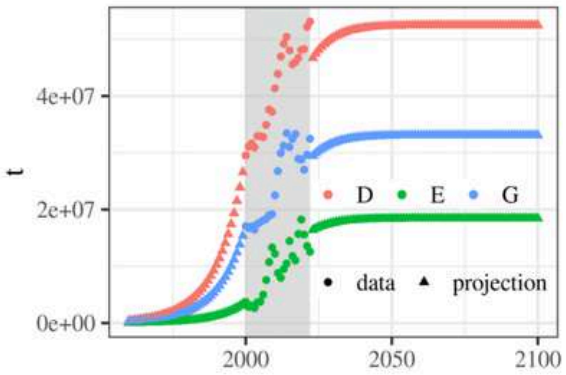


Figure 1. Fuel consumption in Brazil from 1960 to 2100 (t/year)

The emissions for the year 2018 are shown in for $PM_{2.5}$, where exhaust is the most important source for diesel vehicles, however wear from tires, brakes and road plays an important role for non-diesel fleet. Hence, the most important category is trucks semi heavy diesel (TRUCKS_SH_D), followed by heavy trucks (TRUCKS_H_D).

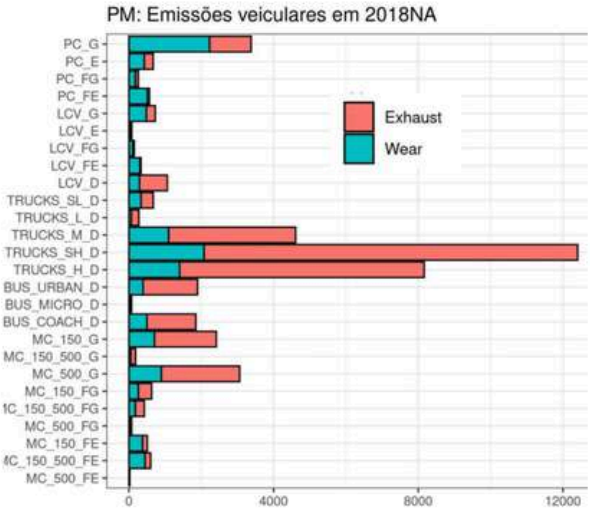


Figure 2. Emissions of $PM_{2.5}$ in Brazil in 2018 category and process (t/year), denoted as PM.

The emissions were estimated between 1960 and 2080, because there was a problem in the code in the last year. We are currently investigating the problem. The time series of total emissions in Brazil between 1960 and 2080 can be seen in Figure 3 for the pollutants CO, NMHC and $PM_{2.5}$ by type of of fuel in kt/year. Then we see that CO peaked during the 90's with 2.5 Mt/year with the gasoline as the biggest contributor. Then NMHC peaked at the beginning of the 90's with biggest contribution from gasoline and ethanol. Lastly, $PM_{2.5}$ reached its peak at the beginnings of the 2000 with a huge contribution from diesel, however, towards the year 2030, the contribution from diesel, mostly exhaust, and gasoline, mostly wear will be similar due to the effectiveness of environmental policies in the technologies associated with the emissions standards and the fleet turnover.

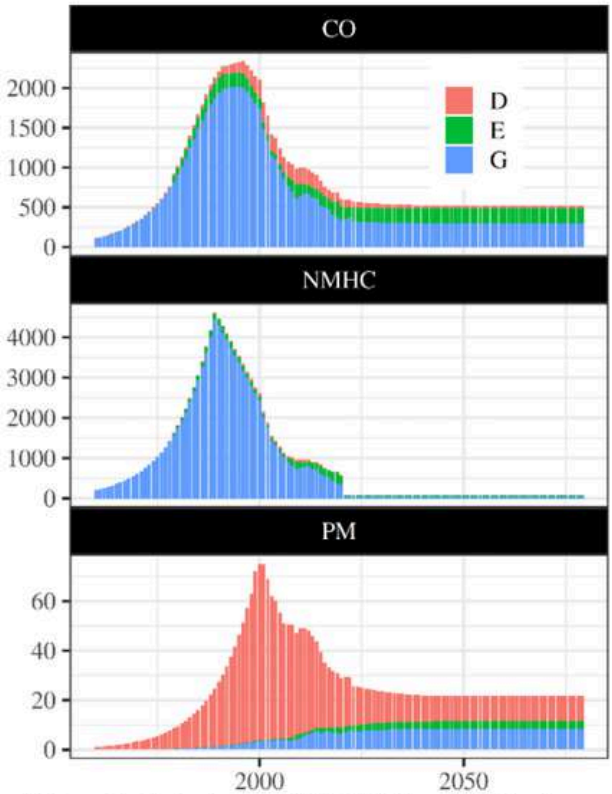


Figure 3. Emissions of CO, NMHC and $PM_{2.5}$ in Brazil between 1960 and 2080 by type of fuel (kt/year).

We compared road transportation emissions from VEIN and CAMS emissions in Brazil as shown in Figure 4. We see that CAMS emissions are highly concentrated in the biggest cities, as shown by the darker blue colors, specially in Sao Paulo. On the other side, red colors are found in the northeast region. This may indicate that the use of fuel consumption and fleet by region, in conjunction with emissions factors based on real-world measurements made in Brazil, may be more representative.

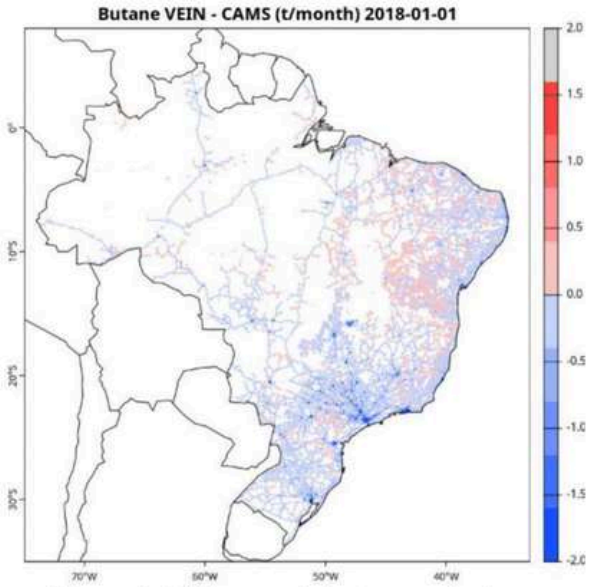


Figure 4. Difference in butane emissions between VEIN and CAMS (t/month), January of 2018.

Figure 5 shows the monthly mean surface concentrations of $PM_{2.5}$ over south america using the model MUSICA and road transportations emissions from VEIN over Brazil. The most important source sare the wildfire in central south america as show by the high concentrations of this pollutant, with values above 1000 μg/m3.

CONCLUSIONS

The use of local fuel consumption data, fleet and local emissions factors based on real-world measurements produce estimates reliable and representative. CO, NMHC and $PM_{2.5}$ transportation emissions peaked during the 90's. Towards 2030 the exhaust and wear emissions will be equally important for $PM_{2.5}$.

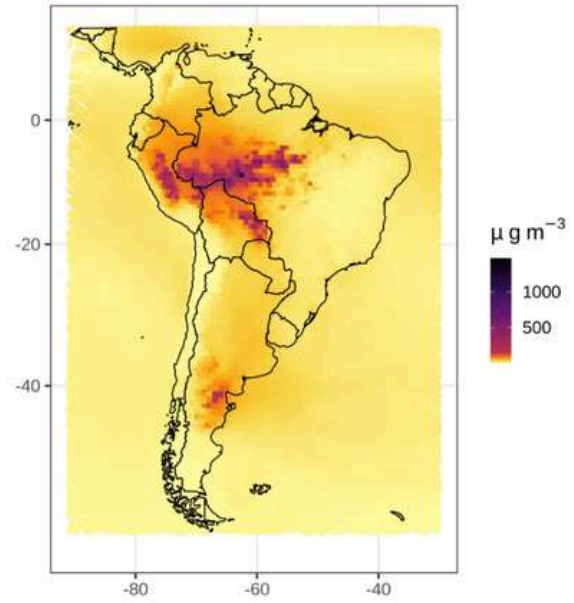


Figure 5. Monthly mean of $PM_{2.5}$ for 2020-08 over south america using MUSICA $\mu g/m^3$.

REFERENCES

Forster, P. M., Forster, H. I., Evans, M. J., Gidden, M. J., Jones, C. D., Keller, C. A., ... & Turnock, S. T. (2020). Current and future global climate impacts resulting from COVID-19. Nature Climate Change, 10(10), 913-919.

Gavidia-Calderón, Mario, et al. "Air quality modeling in the metropolitan area of São Paulo, Brazil: A review." Atmospheric Environment (2023): 120301.

Ibarra-Espinosa, Sergio, et al. "Atmospheric effects of air pollution during dry and wet periods in são paulo." Environmental Science: Atmospheres 2.2 (2022): 215-229.

Lichtig, Pablo, et al. "Multiscale CO budget estimates across South America: quantifying local sources and long range transport." Journal of Geophysical Research: Atmospheres 129.8 (2024): e2023JD040434.

Hoinaski, Leonardo, et al. "Multispecies and high spatiotemporal resolution database of vehicular emissions in Brazil." Earth System Science Data Discussions 2022 (2022): 1-29.

Hoinaski, Leonardo, Robson Will, and Camilo Bastos Ribeiro. "Brazilian Atmospheric Inventories-BRAIN: A comprehensive database of air quality in Brazil." Earth System Science Data Discussions 2023 (2023): 1-22.

Ibarra-Espinosa, Sergio, et al. "VEIN v0. 2.2: an R package for bottom-up vehicular emissions inventories." Geoscientific Model Development 11.6 (2018): 2209-2229.

Pfister, Gabriele G., et al. "The multi-scale infrastructure for chemistry and aerosols (MUSICA)." *Bulletin of the American Meteorological Society* 101.10 (2020): E1743-E1760.

Nogueira, Thiago, et al. "Evolution of vehicle emission factors in a megacity affected by extensive biofuel use: results of tunnel measurements in São Paulo, Brazil." Environmental Science & Technology 55.10 (2021): 6677-6687.

AIR POLLUTION CONFERENCE BRAZIL
CMAS SOUTH AMERICA
COMMUNITY MODELING AND ANALYSIS SYSTEM

SÃO PAULO URBAN GREENHOUSE GAS NETWORK – METROCLIMA PRELIMINARY RESULTS AND PROCESSES

Lucas Gatti Domingues[1], Maria de Fátima Andrade[1], Eduardo Landulfo[2], Noele Leonardo[1], Carlos Oliveira [3].
lgtdomingues@gmail.com
[1]*Instituto de Astronomia, Geofísica e Ciências Atmosféricas (IAG) - Universidade de São Paulo*
[2]*Instituto de Pesquisas Energéticas e Nucleares (IPEN);*
[3]*SCINK – Carbon Management through Science*

Keywords: Urban Network; Greenhouse gas; METROCLIMA; São Paulo emission

INTRODUCTION

Cities cover only ~3% of the world's surface yet originate 70% to 80% of global CO2 emissions[1,2] and are expected to continue growing as urban migration continues and intensifies. Cities are projected to shelter ~70% of world's population by 2050[3]. Managing urban emissions is vital to address the climate crisis and meet the objectives established by the United Nations Framework Convention on Climate Change and the Paris Agreement. To achieve this, we need to not only quantify and monitor emissions[4], but most importantly, attribute them to specific sources[5-10].

The current state-of-art-method uses "inverse modelling"[11] to infer emissions through a combination of bottom-up emission inventories[12-14] and a small number of strategically placed high-precision direct atmospheric measurements[15-17].

There are several different approaches for top-down methods. Some of these methods include aircraft mass balance, in situ tower networks, and remote sensing. Each method presents its own strengths, weaknesses, and level of repeatability to other urban areas. The main strength that top-down methods have is measuring the concentrations directly, so it is getting an accurate level of concentrations. However, depending on the method, it can be hard to assign which sources are contributing to the overall emissions and by what magnitude.

The cavity ring-down spectroscopy (CRDS) appeared in the late 1890's and is a well stablished technique used for the high precision trace gas measurements. It consists in a laser-based technique which is used to excite a ring-down cavity, in which the infrared absorption loss caused by a gas in the sample cell is measured to quantify the gas mole fraction[18,19]. It generates a quasi-real-time data set, performing measurements from different species every approximately 2 seconds. This generates large data sets and to extract the best information from it, scripts from programs as R a Python must be used. In the program development, it also must be taken in account the packages and tools to applied due to the computing time.

In terms of comparability, The World Meteorological Organization (WMO) has stablished a high accuracy and compatibility goals for atmospheric CO_2 and CH4 measurements to ±0.1 ppm for CO_2 (±0.05 ppm in the southern hemisphere) and ±2 ppb for CH_4[20]. Achieving WMO goals is not a trivial task. Atmospheric water vapor must be taking in account due to its large variability, which can cover any signal in the trace gases. There are several methods to reach the desired dryness as cooling or streaming the sampling air but the limitations and specifications of the sites conditions must be considered and meticulously evaluated.

Different urban networks have developed their own method to continuously measure greenhouse gas mole fractions across the city, including the background mole fraction measurements from all wind directions and resolving spatial patterns[21]. The same logic follows the calibration method to be applied relying on optimizing the measurement equipment to its best response.

A recent study comparing the combination of measurements and modelling with inventories result, showed that cities using only bottom-up emission inventories are under-reporting emissions on an average of 18,3% ranging from -145,5% to +63,5%[22]. São Paulo city is among the biggest cities in the world and it can not rely only on bottom-up estimations to report and understand its emissions.

Here we present the network structure, the implemented modifications along with the calibration plan and primary results from the first urban greenhouse gas in Latin America.

METHODS

The METROCLIMA-GHG Network commenced its operations in early January 2020, initially setting up stations at UNICID (UND) and Pico do Jaraguá (PDJ). Subsequently, in April 2020, instruments for measuring CO_2 and CH_4 concentrations, along with carbon isotopes in both gases, were added at IAG. It's worth noting that prior measurements of CO_2 and CH_4 (2019) existed at PDJ and IAG stations; however, these lacked calibration gas checks. In August 2020, the ICESP station (ICP) was successfully installed (Figure 1).

Since November 2022, modifications have been carried out in the greenhouse gas monitoring systems aimed at increasing the reliability of measurements. These monitors are sensitive to the material applied to the system during sample injection and also to the amount of water contained in the samples.

To enhance measurement reliability, physical modifications are being made to the measurement systems, primarily concerning the previously installed tubes and connections. Additionally, a drying system is being added to reduce water content in the samples. Given that these are continuous monitoring stations, methodologies are being developed for automatic

calibration and continuous verification of data quality. Figure 2 presents the scheme applied for the stations application.

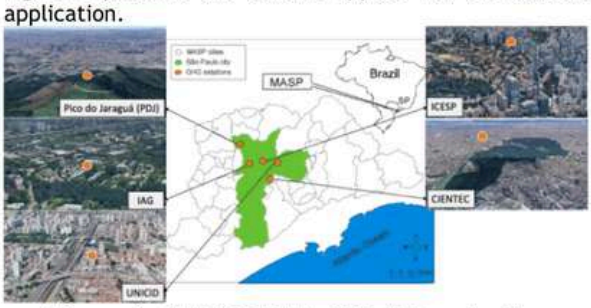


Figure 1. METROCLIMA-GHG Network sites overview. 4 greenhouse gas monitoring stations distributed throughout the city of São Paulo.



Figure 2. General scheme for the new configuration of the sampling sites.

FINDINGS AND ARGUMENT

The diurnal cycle of CO_2 is a widely utilized method for studying the variability of gas concentrations throughout the day. It helps to understand the main factors affecting these concentrations, such as sources, sinks, and atmospheric dynamics like the planetary boundary layer [19]. Consequently, the diurnal CO_2 cycle is influenced by local, regional, and seasonal characteristics, making it a crucial record of gas dynamics in a specific area.

Figure 3 presents the annual diurnal cycles of the PDJ, IAG, and UND stations. These cycles showed characteristic and distinct distributions for each station, mainly related to amplitudes (peak-trough), periods of maximum concentrations, and variations in the annual mean cycles. The maximum hourly concentrations were observed during the night and early morning hours at all stations. However, at UND, a characteristic peak (Fig. 3C) was observed during the morning rush hour (7-9 AM), associated with the source of heavy vehicular traffic on avenues near the station, characteristic of this station (Fig. 1). At the PDJ station, the smallest amplitude and the lowest values of maximum concentrations were observed compared to the others (Fig. 3A, D).

At the IAG station, the highest amplitude and maximum values were observed during the night. This station is located in a suburban area within the University of São Paulo (USP), which includes a semi-vegetated area with heavy vehicular traffic approximately 2 km away, exhibiting characteristics intermediate to the other two stations. Therefore, the peak concentrations at night may indicate the combined contributions of vegetation and vehicles. Meanwhile, the minimum concentrations, with values similar to those at the PDJ station, observed in the early afternoon (1-3 PM), are possibly due to more intense photosynthetic activity compared to the UND station (Fig. 3D).

The differences in average hourly values for each station between 2020 and 2021 were considerable at PDJ, with a slight increase from 2020 to 2021, possibly indicating a greater influence of global fluxes at this station. For the IAG and UND stations, there was no significant difference over the last two years (Fig. 3D). This may indicate that vehicular sources are the main contributors to CO2 at these stations.

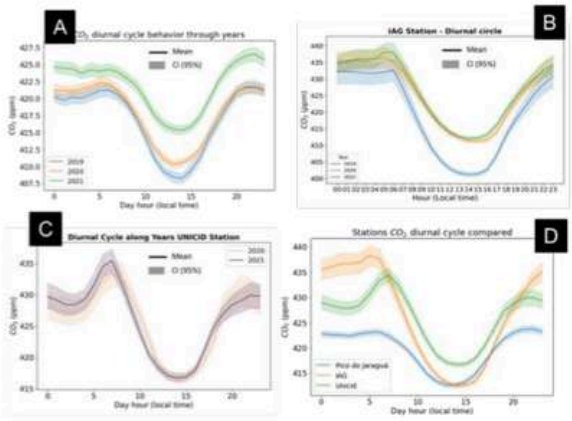


Figure 3. Annual diurnal cycle of CO_2 for the PDJ (A), IAG (B), and UND (C) stations. Comparison of the three stations for the period.

CONCLUSIONS

Significant adjustments have been made to the stations to enhance their accuracy. However, further critical adjustments are necessary. Implementing a calibration method and routine is crucial to achieve a more precise representation of the city's emissions. Clearly, important challenges still need to be pursued for the improvement of the network and understanding of the results. This includes evaluating other potential sites that may represent the CO2 background for the RMSP, assessing the dynamics of CH4, and identifying the main sources of the gas for the RMSP, among other important aspects. Additionally, publishing in indexed international journals and disseminating the results to the scientific community are continuous goals of the project.

REFERENCES

[11] Cassol, H. L. G., Domingues, L. G., Sanchez, A. H., Basso, L. S., Marani, L., Tejada, G. P., Arai, E., Correia, C., Alden, C. B., Miller, J. B., Gloor, M., Anderson, L. O., Aragão, L. E. O. C., & Gatti, L. V. Determination of region of influence obtained by aircraft vertical profiles using the density of trajectories from the hysplit model. Atmosphere, 11(10). https://doi.org/10.3390/atmos11101073, 2020.

[12] Gately, C. K., & Hutyra, L. R. Large Uncertainties in Urban-Scale Carbon Emissions. Journal of Geophysical Research: Atmospheres,2017
[13] Gurney, K. R., Razlivanov, I., Song, Y., Zhou, Y., Benes, B., & Abdul-Massih, M. Quantification of fossil fuel CO2 emissions on the building/street scale for a large U.S. City. Environmental Science and Technology, 46(21), 12194–12202. https://doi.org/10.1021/es3011282, 2012.
[10] Pacala SW, Breidenich C, Brewer PG, Fung IY, Gunson MR, Heddle G, Law BE, Marland G, Paustian K, Prather M. Verifying greenhouse gas emissions: Methods to support international climate agreements; committee on methods for estimating greenhouse gas emissions; national research council. Washington, DC: National Academies Press, 2010.
[14] Pugliese, S. C., Murphy, J. G., Vogel, F. R., Moran, M. D., Zhang, J., Zheng, Q., Stroud, C. A., Ren, S., Worthy, D., & Broquet, G. High-resolution quantification of atmospheric CO2 mixing ratios in the Greater Toronto Area, Canada. Atmospheric Chemistry and Physics, 18(5), 3387–3401. https://doi.org/10.5194/acp-18-3387-2018, 2018.
[15] McKain, K., Wofsy, S. C., Nehrkorn, T., Eluszkiewicz, J., Ehleringer, J. R., & Stephens, B. B. Assessment of ground-based atmospheric observations for verification of greenhouse gas emissions from an urban region. Proceedings of the National Academy of Sciences of the United States of America, 109(22), 8423–8428. https://doi.org/10.1073/pnas.1116645109, 2012.
[16] Lauvaux, T., Miles, N. L., Deng, A., Richardson, S. J., Cambaliza, M. O., Davis, K. J., Gaudet, B., Gurney, K. R., Huang, J., O'Keefe, D., Song, Y., Karion, A., Oda, T., Patarasuk, R., Razlivanov, I., Sarmiento, D., Shepson, P., Sweeney, C., Turnbull, J., & Wu, K. High-resolution atmospheric inversion of urban CO2 emissions during the dormant season of the Indianapolis flux experiment (INFLUX). Journal of Geophysical Research, 121(10), 2016.
[17] Sargent, M., Barrera, Y., Nehrkorn, T., Hutyra, L. R., Gately, C. K., Jones, T., Mckain, K., Sweeney, C., Hegarty, J., Hardiman, B., Wang, J. A., & Wofsy, S. C. Anthropogenic and biogenic CO2 fluxes in the Boston urban region. Proceedings of the National Academy of Sciences of the United States of America, 115(40), E9507. https://doi.org/10.1073/pnas.1815348115, 2018.
[18] Wastine, Benoit & Kaiser, Claire & Vuillemin, C. & Lavrič, Jošt & Schmidt, Martina & Ramonet, Michel. Evaluation of the Picarro EnviroSense 3000i analysers (now called G1301) for continuous CO2/CH4 measurements, (2009).
[19] Miles, N. L., Martins, D. K., Richardson, S. J., Rella, C. W., Arata, C., Lauvaux, T., Davis, K. J., Barkley, Z. R., McKain, K., and Sweeney, C.: Calibration and field testing of cavity ring-down laser spectrometers measuring CH4, CO2, and δ13CH4 deployed on towers in the Marcellus Shale region, Atmos. Meas. Tech., 11, 1273–1295, https://doi.org/10.5194/amt-11-1273-2018, 2018.
[1] United Nations, UN-Habitat: The Strategic Plan 2020 – 2023, 2019.
[2] United Nations, Department of Economic and Social Affairs, Population Division. World Population Prospects 2019: Highlights, 2019.
[20] Turnbull, J. C., et al., Toward quantification and source sector identification of fossil fuel CO2 emissions from an urban area: Results from the INFLUX experiment, J. Geophys. Res. Atmos., 120, 292– 312, doi:10.1002/2014JD022555, 2015.
[21] Reum, F., Gerbig, C., Lavric, J. V., Rella, C. W., and Göckede, M.: An improved water correction function for Picarro greenhouse gas analyzers, Atmos. Meas. Tech. Discuss. https://doi.org/10.5194/amt-2017-174, 2017.
[22] Gurney, K.R., Liang, J., Roest, G. et al. Under-reporting of greenhouse gas emissions in U.S. cities. Nat Commun 12, 553.. https://doi.org/10.1038/s41467-020-20871-0.
[3] United Nations, Human Settlement Programme: Hot Cities: Battle- Ground for Climate Change, 2011.
[4] Hutyra, L. R., Duren, R., Gurney, K. R., Grimm, N., Kort, E. A., Larson, E., & Shrestha, G. Urbanization and the carbon cycle: Current capabilities and research outlook from the natural sciences perspective. Earth's Future, 2(10), 473-495. https://doi.org/10.1002/2014ef000255, 2014.
[5] Turner, A. J., Shusterman, A. A., McDonald, B. C., Teige, V., Harley, R. A., & Cohen, R. C. Network design for quantifying urban CO2 emissions: Assessing trade-offs between precision and network density. Atmospheric Chemistry and Physics, 16(21), 2016.
[6] Nathan, B., Lauvaux, T., Turnbull, J., & Gurney, K. Investigations into the use of multi-species measurements for source apportionment of the Indianapolis fossil fuel CO2 signal. Elementa. https://doi.org/10.1525/elementa.131, 2018.
[7] Ciais, P., Dolman, A. J., Bombelli, A., Duren, R., Peregon, A., Rayner, P. J., Miller, C., Gobron, N., Kinderman, G., Marland, G., Gruber, N., Chevallier, F., Andres, R. J., Balsamo, G., Bopp, L., Bréon, F. M., Broquet, G., Dargaville, R., Battin, T. J., … Zehner, C. Current systematic carbon-cycle observations and the need for implementing a policy-relevant carbon observing system. Biogeosciences, 11(13), 3547–3602. https://doi.org/10.5194/bg-11-3547-2014, 2014.
[8] Bai, X., Dawson, R. J., Ürge-Vorsatz, D., Delgado, G. C., Barau, A. S., Dhakal, S., Dodman, D., Leonardsen, L., Masson-Delmotte, V., Roberts, D., & Schultz, S. Six research priorities for cities. Nature, 555, 23–25, 2018.
[9] Hoornweg, D., Sugar, L., & Gómez, C. L. T.. Cities and greenhouse gas emissions: moving forward. Environment and Urbanization, 23(1), 2011

PROCEEDINGS OF THE

2024 AIR POLLUTION CONFERENCE

And 5th CMAS South America

SESSION 05
Environmental Odours

Most of the research on atmospheric dispersion is concerned with the examination of mean concentrations over a given time, typically minutes or hours in length. However, many studies have shown that the mean concentration field alone is not sufficient for estimating the potential hazards from pollutant releases in the atmosphere, for example in the case of flammability, malodour nuisance and, often, toxicity. Odour is an increasingly sensitive issue and complaints of odour nuisance emitted by domestic and industrial wastewater treatment plants. The problems associated with malodour nuisance occur with sufficient frequency and severity to warrant regulatory intervention. It is therefore important to develop, validate and use appropriate dispersion modelling approaches in order to investigate odour dispersion and provide regulatory authorities with relevant information.

- Odour perception and odour impact
- Odour regulation and policy
- Odour formation and emission
- Odour dispersion modelling

SESSION 05

K-9 UNIT: DOGS TRAINING IN STEEL PLANT ODOUR DETECTION 158

AIR POLLUTION CONFERENCE BRAZIL
CMAS SOUTH AMERICA
COMMUNITY MODELING AND ANALYSIS SYSTEM

K-9 UNIT: DOGS TRAINING IN STEEL PLANT ODOUR DETECTION

Willian Lemker Andreão[1*], Erick Lopes[1], Antônio José de Miranda Magalhães[2], Gustavo Machado Jantorno[3], Rafael Sartim[1]

[1]*ArcelorMittal Tubarão, Serra, Espírito Santo, Brazil*

[2]*HPDogs-Solutions, Brasília, Distrito Federal, Brazil*

[3]*Base K9 Working Dogs, Serra, Espírito Santo, Brazil*

**willian.andreao@arcelormittal.com.br*

Abstract: Odorous compounds, such as hydrogen sulfide, ammonia, benzene, toluene, naphthalene, indene, acetylene, and others, can be emitted during certain processes in the steel industry, such as the coke manufacturing process. To investigate the potential nuisance impact of these emissions, the ability of K-9s to recognize and alert has been assessed. Several studies have demontrated canine sensitivity is within the same order of magnitude of analytical instrumentation, showing the advantage of using detection canines in field-based examinations. The K-9s can learn to respond to odours similar to those used in training, based on recognizing common odour components of the particular target. Getxent tubes were used to impregnate the odour compounds present in the air, exposing the tubes in the areas of interest for 24 hours. A gas chromatography coupled to mass spectroscopy of the odours absorbed in the tubes showed a variety of volatile organic compounds, in accordance with literature. All impregnated Getxent tubes showed a strong and complex signal, which demonstrates the applicability of the impregnation methodology. A VOC meter will be used to assess whether odour was still present in the tube, in order to evaluate the time that each tube can be used for training. If a positive response from the K-9s' identification of industrial site odours signal is achieved, the perspective of a new environmental impact assessment method will be possible.

Keywords: odour, steel plant, VOC, canine.

INTRODUCTION

Iron, steel, and coke industry activities can lead to olfactory pollution in the atmosphere due to emissions of several odorous compounds, such as hydrogen sulfide, ammonia, benzene, toluene, naphthalene, indene, and acetylene, for example [1-3].

Humans and animals recognize the presence of chemical contaminants through stimulation of their smell organs. There are several advantages of using detection canines in field-based examinations due to canine sensitivity. They can learn up to at least ten odour discriminations without difficulty and maintain high levels of olfactory memory even after months without refresher training, although they do not distinguish between low and high concentrations of odorants (detection threshold). The detection canine (the most well-known and widely used biological sensor) is successfully employed for rapidly searching large scenes for the presence of target volatile compounds [4,5]. Canines are trained and utilized for detection purposes in a wide variety of fields including explosives, narcotics, contraband, living and deceased humans, agriculture, currency, pests, and more recently medical diagnostic fields [6].

To investigate the potential nuisance impact of a steel plant odour emissions, the ability of canines to recognize and alert has been investigated for detection. In this sense, this study focuses, through analytical chemistry and odour capture and release materials, on understanding the unique odour profile of a steel plant and, from there, developing a safe and effective training aid for canine detection teams (K-9 Units), in a project for a new environmental assessment method.

METHODS

The research is being developed based on five pillars: (1) Selection of a non-contaminating, odour-capturing, and releasing material for use in K-9 training as VOC samples; (2) Protocol for target material collection, handling, and storage; (3) Target odor identification - reference VOCs; (4) Sample Validation Protocol for use in K-9 training; (5) K-9 Training Protocol detailing the phases, learning goals and method validation procedures defined.

For canine trainers, it is essential to select the most appropriate materials for odour capture and release. Getxent tubes (Figure 1) are an absorption-based polymer that are blank when purchased and require imprinting. The patented technology (WO2018206808) is based on a polymer able to capture all the molecules constituting an odour. Once captured, the Getxent tube releases them continuously up to several weeks. For passive imprinting, the Getxent tube should be exposed to the target odour for 24-48 h [7].



Figure 1 - Getxent tubes (8×35 mm; 0.93 g each).

Getxent tubes were used to impregnate the odour compounds present in the ambient air in five different points, exposing the tubes in the areas of interest for 24 hours, as shown in Figures 2 and 3.



Figure 2. Getxent tube exposed at a quenching tower exit.



Figure 3. Getxent tubes exposed in a coke plant area.

To identify the main possible odour compounds imprinted, a gas chromatography coupled to mass spectroscopy of the odours absorbed in the tubes were performed with Biodesiv Laboratory, using an Agilent GC-MS, model 6890, single quadrupole, injector split/splitless. Triplicate samples for each of the five points were performed.

Empty glass vials (machine blanks) were placed at the beginning of each batch of three replicates. All samples were analyzed by SPME GC-MS with method "Tube40RDV1Splitless". Only peaks integrated by the software were considered. Molecules were identified using NIST 2023 database.

To assist the training and avoid false negative response (when a K-9 fails to respond in the presence of a target odour), TIGER XT 10.6eV Handheld VOC Detector will be used to detect the odour in all Getxent tubes imprinted before making them valid and available for training. False responses are undesirable as they decrease the reliability of detector dogs [5]. TIGER XT can respond to over 750 VOCs and toxic compounds, from 1 ppb to 20.000 ppm.

The training initially consists of conditioning the K-9 to a specific behavior when it identifies the presence of a target odor in a box with a reward-based method. After that, the K-9 is leading along a trail of different odours (Figure 4). If the target odour is recognized and pointed out by the K-9 (with a sitting action), it will be rewarded. The training is performed for several weeks, in different conditions. Two German Shepherd were selected and are being trained in a specialized K-9 training center.

With the K-9s trained, Getxent tubes can be placed in potential areas of nuisance to imprint and then the same tubes can be taken for K-9 evaluation. If the target odour is presented in the imprinted tubes, even mixed with other odours compounds, a positive response by the canine can indicate a potential influence of the target odour in that area.



Figure 4. Training trials.

FINDINGS AND ARGUMENT

For each sample, the chromatograms of the replicates were superimposed, meaning that the impregnation was reproducible. All impregnated Getxent tubes showed a strong and complex signal, which demonstrates the applicability of the impregnation methodology. More than 180 potential chemical species were identified. Figure 5 shows the overlay chromatograms.

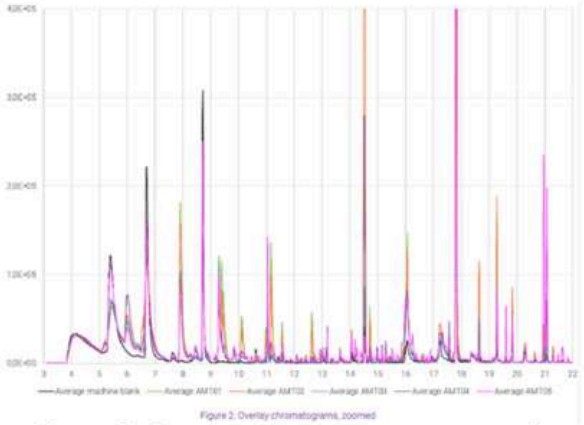


Figure 5. Overlay chromatograms, zoomed.

The highlighted chemical species with the highest potential of occurrence were: cyclotrisiloxane, propane, toluene, hexanal, cyclopentasiloxane, ethylbenzene, p-xylene, benzene, acetic acid, pyridine, styrene, indene, benzonitrile, benzaldehyde, naphthalene, 2,4-di-tert-butylphenol, isoquinoline, and phenol. Results is in accordance with those reported in the literature for the main compounds [1-3].

For the K-9s to be able to distinguish the imprinting target odour from others, like a wastewater treatment inlet system odour, it is essential the differentiation of sources by the use of a training aid with the presence of a well-known specific markers compounds, as an odour signature, even that in several different sources it can found some of the same compounds, as sulfide hydrogen, for example.

CONCLUSIONS

Getxent tubes has been demonstrated as a good odour capture and release material. They were able to capture the steel plant odour mixed characteristics, which is important to distinguish from other odour sources, as wastewater treatment plants, for example. However, due to odour low concentrations in the air, the impregnated odour ends in a few training sessions with the dogs, requiring more frequently impregnation with new tubes.

If a positive response from the K-9s' identification of industrial site odours signal is achieved, the perspective of a new environmental impact assessment method will be possible.

REFERENCES

[1] Lin, C. et al. (2007). Fugitive coke oven gas emission profile by continuous line averaged open-path Fourier Transform infrared monitoring. Journal of the Air & Waste Management Association, 57:4, 472-479.
[2] Jiun-Horng T. L. et al. (2008). Volatile organic compound constituents from an integrated iron and steel facility. Journal of Hazardous Materials 157, 569-578.
[3] Hermia J. et al. (1992). Odour Characterization and control of volatile odoriferous compounds in coke and steel industries. Studies in Environmental Science 51, 225-230.
[4] Leitch O. et al. (2013). Biological organisms as volatile compound detectors: A review. Forensic Science International 232, 92-103.
[5] Leung D. et al. (2019). Volatile organic compound analysis of accelerant detection canine distractor odours. Forensic Science International 303, 109953.
[6] Gallegos, S.F. (2022). Odor signature evaluation: Perspectives encompassing explosives and pathogen detection. Texas Tech University: Dissertation in Environmental Toxicology.
[7] Simon A.G. (2022). Analysis of non-hazardous canine training aids for triacetone triperoxide (TATP). Forensic Chemistry 30, 100440.

PROCEEDINGS OF THE

2024 AIR POLLUTION CONFERENCE

And 5th CMAS South America

SESSION 06
Indoor air quality and its implications

Indoor air pollution poses a threat to human health, causing millions of deaths every year. The COVID-19 pandemic underscored the critical role of ventilation in mitigating the transmission of respiratory disease and highlighted the importance of improving indoor air quality. Worldwide, around 2.4 billion people still cook using polluted fuels such as solid fuels and kerosene. Each year, 3.2 million people die prematurely from illnesses attributable to household air pollution caused by the incomplete combustion of solid fuels and kerosene used for cooking. Session topics include:

- Monitoring of indoor air quality
- Air cleaning, ventilation and filtration
- COVID-19 and Viral Transmission
- Health Outcomes and Exposure Assessment
- Indoor microbiological exposure
- Thermal Comfort
- Indoor air Policy, Regulation and Standards

SESSION 06

STUDYING INDOOR AIR QUALITY IN A HOME IMPROVEMENT AND GARDENING STORE 163

FUTURE URBAN VENTILATION NETWORK: OPEN REPOSITORY 166

ANALYSİS OF İNDOOR AND OUTDOOR PM2.5 CONCENTRATİON İN SOME SCHOOLS İN SÃO PAULO, BRAZİL 170

AIR QUALITY ASSESSMENT IN INDOOR ENVIRONMENTS: STUDY IN A HIGHER EDUCATION INSTITUTION 173

MICROORGANISMS PRESENT IN THE AIR IN INTENSIVE CARE UNITS, SURVEILLANCE OR MONITORING? 176

AIR POLLUTION CONFERENCE BRAZIL
CMAS SOUTH AMERICA
COMMUNITY MODELING AND ANALYSIS SYSTEM

STUDYING INDOOR AIR QUALITY IN A HOME IMPROVEMENT AND GARDENING STORE

Leonardo Furst [1], Yago Cipoli [1], Eduardo Yubero [2], Nuria Galindo [2], Teresa Nunes [1], Getúlio Igrejas [3 5], Manuel Feliciano [4 5], Célia Alves [1]

[1]Centre for Environmental and Marine Studies (CESAM), Department of Environment, University of Aveiro, 3810-193 Aveiro, Portugal

[2]Atmospheric Pollution Laboratory (LCA), Department of Applied Physics, Miguel Hernández University, 03202 Elche, Spain

[3]Centro de Investigação em Digitalização e Robótica Inteligente (CeDRI), Instituto Politécnico de Bragança, Campus de Santa Apolónia, 5300-253 Bragança, Portugal

[4]Centro de Investigação de Montanha (CIMO), Instituto Politécnico de Bragança, Campus de Santa Apolónia, 5300-253 Bragança, Portugal

[5]Laboratório Associado para a Sustentabilidade e Tecnologia em Regiões de Montanha (SusTEC), Instituto Politécnico de Bragança, Campus de Santa Apolónia, 5300-253 Bragança, Portugal

Abstract: In urban areas, stores/shops play an important role in people's daily routines, whether it is for work, leisure, or shopping. As urban dwellers tend to spend most of their time indoors, it becomes crucial to ensure good indoor air quality (IAQ) for a comfortable and healthy environment for both employees and customers. Proper air quality is an essential part of human health protection, and the first step in achieving this is through monitoring. Understanding the composition of the air one breathes is critical to establish effective measures to maintain good air quality. The most commonly studied IAQ pollutants are carbon dioxide (CO_2), carbon monoxide (CO), particulate matter smaller than 10 and 2.5 µm (PM_{10} and $PM_{2.5}$), volatile organic compounds (VOCs), polycyclic aromatic hydrocarbons (PAHs), nitrogen dioxide (NO_2), radon, microorganisms and pollen. Many studies have investigated the sources of air pollution in stores, particularly those caused by smoking and cooking. However, the IAQ of several other frequently visited stores and shops remains largely unexplored. This study focuses on the IAQ of a type of commercial establishment that is becoming increasingly popular: home improvement and gardening stores. The aim of this research was to characterise the indoor and outdoor air quality of such stores using two monitoring systems, one indoors and one outdoors. The indoor system consisted of a low-volume sampler (FAI Instruments, SILENT Sequential Air Sampler) for collection of PM_{10} on 47 mm quartz fibre filters, and an air quality probe (GrayWolf, WolfSense IQ-610) for CO_2, temperature and relative humidity. The outdoor system included a low-volume sampler (Tecora, Echo PM) for PM_{10} sampling and an optical particulate matter monitor (TSI, DustTrak DRX 8533). Data acquisition was performed every minute. A total of 17 filter pairs were sampled, 14 filter pairs during opening hours (daytime) and 3 filter pairs during closing hours (nighttime), collected simultaneously indoors and outdoors. The indoor system was positioned in three locations to give a better representation of the home improvement store, while the outdoor system remained fixed throughout the entire sampling campaign. In addition, diffusion tubes (Radiello) for passive sampling of volatile organic compounds (VOCs) and carbonyls were installed at three indoor and one outdoor site. Indoors, the diffusion tubes were installed in the paint and adhesives, wood, and bathroom furniture sections. PM_{10} concentrations were higher than the WHO guideline and the protection threshold stipulated by the national legislation (45 and 50 µg/m^3, respectively), reaching 92.4 ± 22 µg/m^3 indoors and 46.8 ± 19.1 µg/m^3 outdoors during labour hours. Outdoor contributions to PM_{10} were mainly related to resuspension, non-exhaust emissions from traffic and biomass burning, while the indoor composition was linked to resuspension and the type of product sold in each section. Indoors, the dominant VOCs were α-pinene, limonene, and hexanal, especially in the wood section, with indoor-to-outdoor (I/O) ratios of 612, 634 and 72, respectively. The most abundant elements in PM_{10} inside the store were Ca, Fe and Zn, with values of 637 ± 307, 260 ± 148, 176 ± 69.5 ng/m^3 and I/O ratios of 1.95, 0.78 and, 3.81, respectively. The average temperature and relative humidity were 18.3 °C and 41.7%, respectively, values in accordance with the standard EN 16798-1. The average CO_2 concentration during labour hours was less than 850 ppm, well below the protection limit of 1250 ppm set by the Portuguese Ordinance No. 138-G/2021 on IAQ. This study showed that the type of product sold in the premises has a strong influence on the concentration of VOCs, while particulate matter is associated with the number of customers and the type of activity carried out indoors.

Keywords: Retail store, monitoring, gravimetric sampling, VOCs, PM_{10}

Acknowledgements: The authors are grateful to the Foundation for Science and Technology (FCT, Portugal) for financial support by national funds FCT/MCTES to CESAM (UIDP/50017/2020, UIDB/50017/2020 and LAP/0094/2020), SusTEC (LA/P/0007/2020), CIMO (UIDB/00690/2020), CeDRI (UIDB/05757/2020 and UIDP/05757/2020) and to PhD fellow students Leonardo Furst (SRFH/BD/08461/2020) and Yago Cipoli (SFRH/BD/04992/2021).

INTRODUCTION

Indoor air quality (IAQ) is crucial for human health and well-being, with pollutants like particulate matter (PM) posing significant risks. Urban populations spend a large portion of their time indoors, making indoor environments, including retail stores, vital for ensuring a healthy and attractive environment. While studies often focus on smoke-filled establishments like bars, other highly frequented stores remain understudied. IAQ

in retail stores can be compromised by various pollutants, including, PM, volatile organic compounds (VOCs) and microorganisms. The objective of this study was to characterise the indoor and outdoor air quality of a home improvement and gardening store, a type of establishment that has not yet been studied extensively. The monitoring campaign included the analysis of volatile organic compounds, particulate matter, and its bond elements.

METHODOLOGY

This study was conducted in December 2021 and January 2022 within a home improvement store located in the northern region of Portugal. Home improvement stores are specialised in selling products for repair, maintenance, construction, and gardening. The store operated from Monday to Saturday, from 09:00 to 20:00, and on Sundays from 09:00 to 17:00.

Indoor sampling involved the use of a low-volume sampler (FAI Instruments, SILENT Sequential Air Sampler) to collect PM_{10} on 47 mm quartz fibre filters, together with an air quality probe (GrayWolf, WolfSense IQ-610) for monitoring CO_2 levels, temperature, and relative humidity. Outdoor sampling utilized a low-volume sampler (Tecora, Echo PM) for PM_{10} collection and an optical particulate matter monitor (TSI, DustTrak DRX 8533). A total of 17 filter pairs were sampled, with 14 pairs collected during store operating hours (daytime) and 3 pairs during closing hours (nighttime). The indoor monitoring system was positioned in three locations to provide a better coverage of the store, while the outdoor system remained stationary. Additionally, diffusion tubes (Radiello) were deployed for passive sampling of VOCs. They were installed at three indoor locations and one outdoor site. Indoor diffusion tubes were placed in the paint and adhesives, wood, and bathroom furniture sections.

Quartz fibre filters used for PM_{10} sampling underwent weighing using a microbalance (RADWAG, MYA 5/2Y/F) with a precision of 1 µg. The mass of the filters was determined based on the average of six weightings conducted after a stabilisation period of two days at 20 °C and 50% relative humidity. Additionally, X-ray fluorescence (XRF) analysis of the quartz fibre filters was performed to assess the concentration of various elements. The analyses of diffusive samplers were carried out at Fondazione Salvatore Maugeri in Padova, Italy. Carbonyls were quantified through desorption with acetonitrile followed by high-performance liquid chromatography (HPLC), while VOCs were measured via thermal desorption followed by gas chromatography–mass spectrometry (GC/MS).

RESULTS AND DISCUSSION

The indoor PM_{10} concentrations were much higher than those measured outdoors, averaging 92.4 ± 22 µg/m^3 during the opening hours (diurnal period) and 46.8 ± 19.1 µg/m^3 (outdoors). When the store was closed (night period), the indoor and outdoor averages were 81.7 ± 21.52 and 34 ± 7.9 µg/m^3, respectively. These indoor concentrations were well above those recommended by the World Health Organisation (WHO, 2021), which specifies a 24-h average of 45 µg/m^3. Due to the central heating system, temperature and relative humidity indoors presented a smaller amplitude than outdoors, with mean values of 18.3 °C and 41.7%, respectively.

CO_2 concentrations followed the occupancy patterns, increasing with the opening of the shop (09:00), slightly decreasing during lunchtime (12:00 - 14:00), rising again at 14h00 and declining after 18h00. The Portuguese Decree Law No. 101-D/2020, 2020), aiming to improve energy performance of buildings, applies a lower limit, stipulating a protection threshold of 1250 ppm. The highest CO_2 values were close to 850 ppm, and the maximum 8-h average was 680 ppm, well below the national threshold.

In general, indoor elemental concentrations were higher than the outdoor levels, even for elements commonly related to vehicular emissions and mineral dust. The most predominant elements were Ca, Fe, Zn, K, Cl, S and Ti with average indoor concentrations during opening hours of 637 ± 307, 260 ±.148, 176 ± 69.5, 117 ± 78.4, 123 ± 175, 66.4 ± 32.8, and 74.4 ±2 2.1 ng/m^3, respectively.

Both the indoor and outdoor Ti were associated with crustal origin, linked with resuspension. Studies have also shown that pellets and wood from the genus *Pinus* have high concentrations of Ca and K, but lower levels of Ti (Chandrasekaran et al., 2012; Saarela et al., 2005). Zn showed the highest indoor/outdoor (I/O) ratio, pointing to anthropogenic sources. Infiltration of vehicular emissions and the contribution of a diverse range of galvanized steel products that use Zn as a protective coat are likely the main sources of Zn (John et al., 2007).

The most prevalent VOCs in the indoor air were α-pinene, ethylbenzene, formaldehyde, hexanal, limonene, m,p-xylene, o-xylene, and toluene. All VOCs presented I/O ratios higher than 1, indicating the contribution of indoor sources to their concentrations. α-Pinene and limonene are mainly released by plants. Their presence in indoor environments is generally related to wooden emissions and the use of air fresheners (Król et al., 2014). The higher concentrations of hexanal and formaldehyde in the wood section, may also be associated with wood particleboard emissions (Jiang et al., 2017). Limonene and α-pinene showed indoor concentrations 415 and 365 times higher than those recorded outdoors, respectively. If only the wood section is considered, the I/O ratios reached values

634 and 612 times higher, pointing the wood materials as the sources of emissions.

CONCLUSIONS

This analysis sheds light on the diverse sources contributing to PM_{10} levels both indoors and outdoors in a home improvement and gardening store. The results showed a high concentration of particulate matter, exceeding the PM_{10} threshold of the World Health Organisation (45 $\mu g/m^3$), while CO_2 levels remained below the protective threshold of 1250 ppm by Portuguese regulations.

Outdoor sources predominantly included emissions from both exhaust and non-exhaust traffic, along with biomass burning. Indoor PM_{10} originated from dust resuspension and various products stocked in the store. PM_{10}-bound elements derived from crustal material and emissions from metal alloys, while VOCs were primarily associated with paints and wood materials.

This work also showed that various stores may have high concentrations of particulate matter and demonstrates the need to study environments that are part of the daily life of the urban population.

REFERENCES

Chandrasekaran, S. R., Hopke, P. K., Rector, L., Allen, G., & Lin, L. (2012). Chemical composition of wood chips and wood pellets. *Energy & Fuels*, *26*(8), 4932–4937. https://doi.org/10.1021/ef300884k

Decree Law No. 101-D/2020, 7(21) (2020).

Jiang, C., Li, D., Zhang, P., Li, J., Wang, J., & Yu, J. (2017). Formaldehyde and volatile organic compound (VOC) emissions from particleboard: Identification of odorous compounds and effects of heat treatment. *Building and Environment*, *117*, 118–126. https://doi.org/10.1016/J.BUILDENV.2017.03.004

John, S. G., Genevieve Park, J., Zhang, Z., & Boyle, E. A. (2007). The isotopic composition of some common forms of anthropogenic zinc. *Chemical Geology*, *245*(1–2), 61–69. https://doi.org/10.1016/j.chemgeo.2007.07.024

Król, S., Namieśnik, J., & Zabiegała, B. (2014). α-Pinene, 3-carene and d-limonene in indoor air of Polish apartments: The impact on air quality and human exposure. *Science of The Total Environment*, *468–469*, 985–995. https://doi.org/10.1016/J.SCITOTENV.2013.08.099

Saarela, K.-E., Harju, L., Rajander, J., Lill, J.-O., Heselius, S.-J., Lindroos, A., & Mattsson, K. (2005). Elemental analyses of pine bark and wood in an environmental study. *Science of The Total Environment*, *343*(1–3), 231–241. https://doi.org/10.1016/j.scitotenv.2004.09.043

WHO. (2021). *WHO global air quality guidelines: particulate matter (PM2. 5 and PM10), ozone, nitrogen dioxide, sulfur dioxide and carbon monoxide*. https://www.google.com/books?hl=pt-PT&lr=&id=s5pREAAAQBAJ&oi=fnd&pg=PR5&dq=World+Health+Organization+2021+Guidelines+pm10&ots=qzVC9AIivn&sig=0RN5P-TcdTNJMqvDg3LG-qZ9UMc

AIR POLLUTION CONFERENCE BRAZIL
CMAS SOUTH AMERICA
COMMUNITY MODELING AND ANALYSIS SYSTEM

FUTURE URBAN VENTILATION NETWORK: OPEN REPOSITORY

Vitor Lavor[1,3], Saad Inam[2], Janet Barlow[3], Zheng-Tong Xie[2]
[1]School of the Built Environment, University of Reading, Reading, UK
v.f.lavor@pgr.reading.ac.uk
[2]Aerodynamics and Flight Mechanics, University of Southampton, Southampton, UK
[3]Department of Meteorology, University of Reading, Reading, UK

Abstract: The Future Urban Ventilation Network (FUVN) is a collaborative research initiative in the UK dedicated to addressing the critical issue of managing exposure to air quality by considering the airflow between indoor and outdoor environments. To facilitate well-informed decision-making in the pursuit of clean air, FUVN has established an Open Repository, currently in its beta version, accessible through the web-based portal at breathingcity.org (google.com). The repository currently has over 40 datasets and their associated journal papers, serving as a valuable resource for researchers and stakeholders. The Open Repository contains high-quality datasets from field experiments, laboratory & physical modelling, and computational fluid dynamics (CFD) studies. Notably, it provides access to direct numerical simulation (DNS) data, which is often not readily available elsewhere and we are committed to advancing this resource and plan to double the number of datasets in the coming year. Moreover, the network intends to publish a concise review paper summarizing the key findings and contributions of these datasets.

Keywords: Urban Ventilation, Indoor, Outdoor, Air Quality, Open Repository

INTRODUCTION

The Future Urban Ventilation Network (FUVN) operates across three interconnected themes: 1) Coupled indoor-outdoor environments, 2) Health-centred ventilation design and 3) Breathing City into practice. Its goal is to define the scientific, technological and practice innovations for Breathing City approach – an integrated health evidence approach to urban and building ventilation designs for vulnerable communities.

FUVN has established an Open Repository, currently in its beta version, to support well-informed decision-making in the pursuit of clean air. The Open Repository contains key papers and datasets from field experiments, laboratory & physical modelling, and computational fluid dynamics (CFD) studies and it is accessible through the web-based portal at breathingcity.org (google.com). Users of the repository have multiple ways to search and access the datasets: they can filter them based on various criteria, explore a geographical map to visualize the data's spatial distribution and access scientific articles related to the datasets in chronological order. The Open Repository currently has over 40 entries and associated journal papers, serving as a valuable resource for researchers and stakeholders.

This work summarizes the content of the Open Repository into three main sections: studies focused on indoor environments, outdoor environments and investigations exploring the coupling between indoor and outdoor ventilation and pollutant exchange dynamics.

INDOOR ENVIRONMENT STUDIES

Indoor environment studies covered in the Open Repository encompass many influencing factors indoor dynamics such as the effect of building design on internal airflow, dispersion modelling and internal buoyancy-driven airflows.

Examples are the evaluation of indoor airborne material dispersion using an eddy diffusion method in mechanically ventilated rooms (Foat et al., 2020), the influence of induced hinged door motion on the airflow between two rooms (Papakonstantis et al.,2018) and internal buoyancy-driven flow in unconfined and unventilated confined spaces (Parker et al., 2021a; Parker et al., 2021b). Also, on-site tracer gas measurements and cross-infection risk assessment between horizontal inter-household transmission (Wu et al., 2016).

Other factors can influence the indoor dynamics and a more comprehensive focus on additional papers addressing building designs, occupant activities, HVAC systems, airflow pathways, sources of heating and pollution would enhance the repository's coverage and utility.

OUTDOOR ENVIRONMENT STUDIES

The Open Repository covers key factors affecting the microscale airflow and pollutant dynamics within urban areas. These include building characteristics, urban heterogeneity, which accounts for diverse urban compositions and land use types, effects of meteorological conditions and anthropogenic heat effects (Table 1).

Building characteristics (BC), such as building size (Hertwig et al., 2019; Lim et al., 2022), aspect ratio (Lavor et al., 2023), and spacing between building (Mishra, Placidi, Carpentieri, & Robins, 2023) plays an important role in shaping the outdoor flow pattern. Urban heterogeneity (UH), such as varied building arrangements introduces further

complexity (Goular et al., 2016; Sütz et al, 2021) Also the effect of street trees on pollutant concentration and street canyon ventilation (Fellini et al., 2022). Urban elements, such as street trees (Fellini et al., 2022), add a natural element affecting the pollutant levels. Also, readily available DSN data by (Coceal, et al., 2006; Goulart et al., 2016) provides important insights into airflow and pollutant dispersion over arrays of building.

Meteorological conditions (MC), such as variations of wind speed and direction (Drew et al., 2013; Gough et al., 2017), and atmospheric stability (Ding et al., 2023; Marucci & Carpentieri, 2019, 2020b) contribute significantly to the dispersion of pollutants outdoors. Wind tunnel datasets further explore the development of stable and convective boundary layers for urban arrays (Marucci & Carpentieri, 2020b) and their effect on the airflow and pollutant dispersion in street canyons (Marucci & Carpentieri, 2019) and urban building arrays (Marucci & Carpentieri, 2020a).

Table 1. Studies on outdoor airflow and pollutant dispersion by influential group and method.

Study	Method	Group
Lavor et al. (2023)	CFD: RANS	BC
Lappa & Inam (2020)	CFD: RANS	MC
Sütz et al. (2021)	CFD: LES	UH
Grylls et al. (2019)	CFD: LES	UH
Coceal et al. (2006)	CFD: DNS	UH
Lim et al. (2022)	CFD: LES Wind tunnel	BC
Goulart et al. (2016)	CFD: DNS	UH
Drew et al. (2013)	Field campaign	MC
Ding et al. (2023)	Wind tunnel	MC
Fellini et al. (2022)	Wind tunnel	UH
Mishra et al. (2023)	Wind tunnel	UH, BC
Hertwig et al. (2019)	Wind tunnel	BC
Gough et al. (2018)	Field	MC
Marucci & Carpentieri (2020b)	Wind tunnel	MC
Marucci & Carpentieri (2020a)	Wind tunnel	MC
Marucci & Carpentieri (2019)	Wind tunnel	MC
Gronemeier et al. (2021)	Wind tunnel	UH

COUPLING INDOOR AND OUTDOOR

The Open Repository also have studies that integrate the indoor and outdoor dynamics ventilation (Table 2).

Architectural design elements, such as the positioning of windows (W), deployment of louvres (L), and the configuration of roofs (R), have an important impact on ventilation rates and airflow pathways (Kosutova et al., 2019; Murakami, et al., 2018; Peren et al, 2015; Zaki et al, 2018; Zhang et al., 2022). The strategic placement of these features influences the effectiveness of natural ventilation and determines the extent of indoor-outdoor air exchange.

Beyond architectural considerations, studies also highlight the role of internal and external thermal forces (F) in shaping the dynamics of pollutant exchange and indoor ventilation performance (Durrani et al., 2015; Higton et al., 2021; Mu et al., 2018).

Table 2. Studies on coupled indoor-outdoor airflow and pollutant dispersion by influential group and method.

Study	Method	Group
Murakami et al. (2018)	CFD: RANS	W
Hang et al. (2023)	CFD: RANS	F
Kosutova et al. (2019)	CFD: RANS Water flume	L, W
Zhang et al. (2022)	CFD: RANS	W
Wang et al. (2017)	CFD: RANS	W
Perén et al. (2015a)	CFD: RANS	R, W
Peren et al. (2015b)	CFD: RANS	R
Ai & Mak (2014)	CFD: RANS	I
Song et al. (2018)	CFD: LES Wind tunnel	F
Durrani et al. (2015)	CFD: RANS LES	F
Mu et al. (2018)	CFD: RANS	F
Zaki et al. (2018)	CFD: RANS	W
Chu & Chiang (2014)	CFD: LES	F
Cui et al. (2021)	Wind Tunnel	F
Shirzadi et al. (2019)	Wind tunnel	F
Shirzadi et al. (2020)	Wind tunnel	F
Manolesos et al. (2018)	Wind tunnel	W
Tominaga & Blocken (2015)	Wind tunnel	F
Albuquerque et al. (2021)	Wind tunnel	W
Chan (2002)	Field	F
Fan et al. (2021)	Field/ Wind tunnel	CV
Higton et al. (2021)	Water flume	F
Cui et al. (2016)	Wind tunnel	F
O'Sullivan & Kolokotroni (2017)	Field	L, W

CONCLUSIONS

The Open Repository is in its Beta version and fosters more than 40 studies concerning indoor and outdoor ventilation dynamics. These studies offer a valuable resource for researchers and stakeholders. Furthermore, we are committed to advancing this resource.

ACKNOWLEDGEMENTS

The authors are grateful for the support (NE/V002082/1) on setting up the repository.

REFERENCES

Ai, Z. T., & Mak, C. M. (2014). A study of interunit dispersion around multistory buildings with single-sided ventilation under different wind directions. *Atmospheric Environment*, *88*, 1–13.

Albuquerque, D. P., O'Sullivan, P. D., & da Graça, G. C. (2021). Effect of window geometry on wind driven single sided ventilation through one opening. *Energy and Buildings*, *245*, 111060.

Chan, A. T. (2002). Indoor-outdoor relationships of particulate matter and nitrogen oxides under different outdoor meteorological conditions. *Atmospheric Environment*, *36*, 1543–1551.

Chu, C.-R., & Chiang, B.-F. (2014). Wind-driven cross ventilation in long buildings. *Building and Environment*, *80*, 150–158.

Coceal, O., Thomas, T. G., Castro, I. P., & Belcher, S. E. (2006). Mean Flow and Turbulence Statistics Over Groups of Urban-like Cubical Obstacles. *Boundary-Layer Meteorology*, *121*, 491–519.

Cui, P.-Y., Li, Z., & Tao, W.-Q. (2016). Wind-tunnel measurements for thermal effects on the air flow and pollutant dispersion through different scale urban areas. *Building and Environment*, *97*, 137–151.

Cui, P.-Y., Zhang, Y., Chen, W.-Q., Zhang, J.-H., Luo, Y., & Huang, Y.-D. (2021). Wind-tunnel studies on the characteristics of indoor/outdoor airflow and pollutant exchange in a building cluster. *Journal of Wind Engineering and Industrial Aerodynamics*, *214*, 104645.

Ding, S.-S., Placidi, M., Carpentieri, M., & Robins, A. (2023). Neutrally- and stably-stratified boundary layers adjustments to a step change in surface roughness. *Experiments in Fluids*, *64*, 86.

Drew, D. R., Barlow, J. F., & Lane, S. E. (2013). Observations of wind speed profiles over Greater London, UK, using a Doppler lidar. *Journal of Wind Engineering and Industrial Aerodynamics*, *121*, 98–105.

Durrani, F., Cook, M. J., & McGuirk, J. J. (2015). Evaluation of LES and RANS CFD modelling of multiple steady states in natural ventilation. *Building and Environment*, *92*, 167–181.

Fan, S., Davies Wykes, M. S., Lin, W. E., Jones, R. L., Robins, A. G., & Linden, P. F. (2021). A full-scale field study for evaluation of simple analytical models of cross ventilation and single-sided ventilation. *Building and Environment*, *187*, 107386.

Fellini, S., Marro, M., Del Ponte, A. V., Barulli, M., Soulhac, L., Ridolfi, L., & Salizzoni, P. (2022). High resolution wind-tunnel investigation about the effect of street trees on pollutant concentration and street canyon ventilation. *Building and Environment*, *226*, 109763.

Foat, T., Drodge, J., Nally, J., & Parker, S. (2020). A relationship for the diffusion coefficient in eddy diffusion based indoor dispersion modelling. *Building and Environment*, *169*, 106591.

Gough, H., Sato, T., Halios, C., Grimmond, C. S. B., Luo, Z., Barlow, J. F., … Quinn, A. (2018). Effects of variability of local winds on cross ventilation for a simplified building within a full-scale asymmetric array: Overview of the Silsoe field campaign. *Journal of Wind Engineering and Industrial Aerodynamics*, *175*, 408–418.

Gough, Hannah. (2017). *Effects of meteorological conditions on building natural ventilation in idealised urban settings* (Phd, University of Reading). University of Reading.

Goulart, E. V., Coceal, O., Branford, S., Thomas, T. G., & Belcher, S. E. (2016). Spatial and Temporal Variability of the Concentration Field from Localized Releases in a Regular Building Array. *Boundary-Layer Meteorology*, *159*, 241–257.

Gronemeier, T., Surm, K., Harms, F., Leitl, B., Maronga, B., & Raasch, S. (2021). Evaluation of the dynamic core of the PALM model system 6.0 in a neutrally stratified urban environment: Comparison between LES and wind-tunnel experiments. *Geoscientific Model Development*, *14*, 3317–3333.

Grylls, T., Le Cornec, C. M. A., Salizzoni, P., Soulhac, L., Stettler, M. E. J., & van Reeuwijk, M. (2019). Evaluation of an operational air quality model using large-eddy simulation. *Atmospheric Environment: X*, *3*, 100041.

Hang, J., Yang, X., Ou, C.-Y., Luo, Z.-W., Fan, X.-D., Zhang, X.-L., … Li, X.-X. (2023). Assessment of exhaled pathogenic droplet dispersion and indoor-outdoor exposure risk in urban street with naturally-ventilated buildings. *Building and Environment*, *234*, 110122.

Hertwig, D., Gough, H. L., Grimmond, S., Barlow, J. F., Kent, C. W., Lin, W. E., … Hayden, P. (2019). Wake Characteristics of Tall Buildings in a Realistic Urban Canopy. *Boundary-Layer Meteorology*, *172*, 239–270.

Higton, T. D., Burridge, H. C., & Hughes, G. O. (2021). Natural ventilation flows established by a localised heat source in a room with a doorway and a high-level vent. *Building and Environment*, *203*, 108093.

Kosutova, K., van Hooff, T., Vanderwel, C., Blocken, B., & Hensen, J. (2019). Cross-ventilation in a generic isolated building equipped with louvers: Wind-tunnel experiments and CFD simulations. *Building and Environment*, *154*, 263–280.

Lappa, M., & Inam, S. (2020). Thermogravitational and hybrid convection in an obstructed compact cavity. *International Journal of Thermal Sciences*, *156*, 106478.

Lavor, V., Coceal, O., Grimmond, S., Hang, J., & Luo, Z. (2023). Possible high COVID-19 airborne infection risk in deep and poorly ventilated 2D street canyons. *Building Simulation*, *16*, 1617–1628.

Lim, H. D., Hertwig, D., Grylls, T., Gough, H., Reeuwijk, M. van, Grimmond, S., & Vanderwel, C. (2022). Pollutant dispersion by tall buildings: Laboratory experiments and Large-Eddy Simulation. *Experiments in Fluids*, *63*, 92.

Manolesos, M., Gao, Z., & Bouris, D. (2018). Experimental investigation of the atmospheric boundary layer flow past a building model with openings. *Building and Environment*, *141*, 166–181.

Marucci, D., & Carpentieri, M. (2019). Effect of local and upwind stratification on flow and dispersion inside and above a bi-dimensional street canyon. *Building and Environment*, *156*, 74–88.

Marucci, D., & Carpentieri, M. (2020a). Dispersion in an array of buildings in stable and convective atmospheric conditions. *Atmospheric Environment*, *222*, 117100.

Marucci, D., & Carpentieri, M. (2020b). Stable and convective boundary-layer flows in an urban array. *Journal of Wind Engineering and Industrial Aerodynamics*, *200*, 104140.

Mishra, A., Placidi, M., Carpentieri, M., & Robins, A. (2023). Wake Characterization of Building Clusters Immersed in Deep Boundary Layers. *Boundary-Layer Meteorology*. https://doi.org/10.1007/s10546-023-00830-0

Mu, D., Gao, N., & Zhu, T. (2018). CFD investigation on the effects of wind and thermal wall-flow on pollutant transmission in a high-rise building. *Building and Environment*, *137*, 185–197.

Murakami, Y., Ikegaya, N., Hagishima, A., & Tanimoto, J. (2018). Coupled Simulations of Indoor-Outdoor Flow Fields for Cross-Ventilation of a Building in a Simplified Urban Array. *Atmosphere*, *9*, 217.

O'Sullivan, P. D., & Kolokotroni, M. (2017). A field study of wind dominant single sided ventilation through a narrow slotted architectural louvre system. *Energy and Buildings*, *138*, 733-747.

Papakonstantis, I. G., Hathway, E. A., & Brevis, W. (2018). An experimental study of the flow induced by the motion of a hinged door separating two rooms. *Building and Environment*, *131*, 220-230.

Parker, D. A., Burridge, H. C., Partridge, J. L., Hacker, J. N., & Linden, P. F. (2021). Vertically distributed wall sources of buoyancy. Part 2. Unventilated and ventilated confined spaces. *Journal of Fluid Mechanics*, *907*, A16.

Parker, D. A., Burridge, H. C., Partridge, J. L., & Linden, P. F. (2021). Vertically distributed wall sources of buoyancy. Part 1. Unconfined. *Journal of Fluid Mechanics*, *907*, A15.

Perén, J. I., van Hooff, T., Leite, B. C. C., & Blocken, B. (2015). CFD analysis of cross-ventilation of a generic isolated building with asymmetric opening positions: Impact of roof angle and opening location. *Building and Environment*, *85*, 263-276.

Peren, J. I., van Hooff, T., Ramponi, R., Blocken, B., & Leite, B. C. C. (2015). Impact of roof geometry of an isolated leeward sawtooth roof building on cross-ventilation: Straight, concave, hybrid or convex? *Journal of Wind Engineering and Industrial Aerodynamics*, *145*, 102-114.

Shirzadi, M., Tominaga, Y., & Mirzaei, P. A. (2019). Wind tunnel experiments on cross-ventilation flow of a generic sheltered building in urban areas. *Building and Environment*, *158*, 60-72.

Shirzadi, M., Tominaga, Y., & Mirzaei, P. A. (2020). Experimental study on cross-ventilation of a generic building in highly-dense urban areas: Impact of planar area density and wind direction. *Journal of Wind Engineering and Industrial Aerodynamics*, *196*, 104030.

Song, J., Fan, S., Lin, W., Mottet, L., Woodward, H., Davies Wykes, M., ... Linden, P. F. (2018). Natural ventilation in cities: The implications of fluid mechanics. *Building Research & Information*, *46*, 809-828.

Sützl, B. S., Rooney, G. G., & van Reeuwijk, M. (2021). Drag Distribution in Idealized Heterogeneous Urban Environments. *Boundary-Layer Meteorology*, *178*, 225-248.

Tominaga, Y., & Blocken, B. (2015). Wind tunnel experiments on cross-ventilation flow of a generic building with contaminant dispersion in unsheltered and sheltered conditions. *Building and Environment*, *92*, 452-461.

Wang, J., Zhang, T., Wang, S., & Battaglia, F. (2017). Gaseous pollutant transmission through windows between vertical floors in a multistory building with natural ventilation. *Energy and Buildings*, *153*, 325-340.

Wu, Y., Tung, T. C. W., & Niu, J. (2016). On-site measurement of tracer gas transmission between horizontal adjacent flats in residential building and cross-infection risk assessment. *Building and Environment*, *99*, 13-21.

Zaki, S. A., Kasim, N. F. M., Ikegaya, N., Hagishima, A., & Ali, M. S. M. (2018). Numerical Simulation on Wind-Driven Cross Ventilation in Square Arrays of Urban Buildings with Different Opening Positions. *Journal of Advanced Research in Fluid Mechanics and Thermal Sciences*, *49*, 101-114.

Zhang, X., Weerasuriya, A. U., Wang, J., Li, C. Y., Chen, Z., Tse, K. T., & Hang, J. (2022). Cross-ventilation of a generic building with various configurations of external and internal openings. *Building and Environment*, *207*, 108447.

AIR POLLUTION CONFERENCE BRAZIL
CMAS SOUTH AMERICA
COMMUNITY MODELING AND ANALYSIS SYSTEM

ANALYSİS OF İNDOOR AND OUTDOOR $PM_{2.5}$ CONCENTRATİON İN SOME SCHOOLS İN SÃO PAULO, BRAZİL

Luana Ferreira Vasconcelos[1], , Maria de Fátima Andrade[2], Rubens Fabio Pereira[2], Regina Maura de Miranda[1]

[1]*School of Arts, Sciences and Humanities, University of São Paulo*
E-mail: luana.vasc88@usp.br; remaura@usp.br

[2]*Instituto de Astronomia, Geofísica e Ciências Atmosférias da Universidade de São Paulo (IAG-USP)*
E-mail: maria.andrade@iag.usp.br; rubens.pereira@usp.br

Abstract: Vehicles and industries are the main sources of pollutants in large cities, but the burning of garbage and biomass is also a problem in some regions, such as São Paulo, Brazil. In the analysis of health effects, fine particulate matter ($PM_{2.5}$) must be considered, since studies show that this pollutant has a significant effect on morbidity and mortality of populations, especially for children under six years old, including impaired learning. In addition, this pollutant can also influence the earth's climate. This study monitored $PM_{2.5}$ concentrations, using a low-cost sensor (Airbeam), in five schools in the Metropolitan Area of São Paulo, in order to know the concentration of the pollutant inside and outside the classrooms. In addition, $PM_{2.5}$ was sampled with a specific equipment to know the chemical composition and identify the main sources, in order to subsidize the public authorities for future actions to reduce vulnerability in early childhood. The results showed that concentrations of the pollutant can be higher indoors, especially if the school is located near roads with heavy vehicle traffic. Meteorological conditions also have a strong influence on the concentration of particulate matter. Regarding the sources of $PM_{2.5}$ in the outdoor environments near the schools, the analysis using Positive Matrix Factorization (PMF) showed that 19.5% is due to local sources, 45.1% soil resuspension, 9.3% light vehicles, and 26.1% heavy vehicles

Keywords: low-cost sensors, air pollution, early childhood, São Paulo.

INTRODUCTION

The Metropolitan Area of São Paulo (MASP) has several environmental problems, including air pollution, due to high urbanization and population density, generating large vehicular and industrial emissions that increases the concentration of gases and particles in the atmosphere, affecting health and the environment on a regional and global scale (CETESB, 2023; BARROS e LOMBARDO, 2016; SEINFELD e PANDIS, 2006).

Air pollution has a damaging effect on the health of children, especially those under the age of three, including impaired learning. Children in this age group do not yet have a well-formed immune system and have a higher breathing rate, which leads to greater inhalation of air pollutants. Another important factor is that they are at a height close to vehicle exhaust and sidewalk resuspension. As such, children, especially under six years old, are considered part of the population most vulnerable to the effects of air pollution (SHARMA and KUMAR, 2018).

Monitoring air quality in environments where children spend most of their time, such as schools, and subsequently including measures that can minimize the effects of high concentrations of pollutants in school environments is extremely necessary to maintain children's quality of life.

Low-cost sensors used in this research, are alternative tools for monitoring atmospheric environmental quality in real time, especially in those regions where the environmental agency does not have equipment. However, they may have limitations in terms of data accuracy and precision, and there should be some kind of calibration and validation of the data to ensure that they are providing reliable data (LI, J. et al, 2020).

The monitoring data provides input for subsides the development of new policies and practical actions that make it possible to minimize exposure to pollutants by the most vulnerable population, mainly children and elderly, to maintain the population's quality of life. This research was carried out in partnership with WRI-Brazil.

METHODS

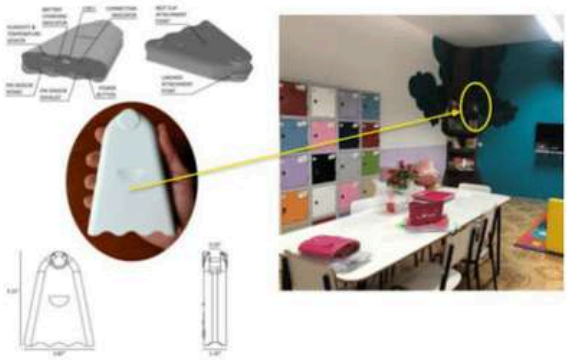
This research consisted of monitoring $PM_{2.5}$ concentrations with low-cost sensors, Airbeam from AirCasting (Figure 1), indoors and outdoors, in five schools around MASP, in the period between June and November 2021 (Figure 2). The sensors are connected to a cell phone via Bluetooth and the cell phone is connected to a local Wi-Fi network. Data is generated every 3 minutes.

The $PM_{2.5}$ outdoor samples were collected over a 24-h period (24:00 to 24:00) onto 47-mm Teflon membrane filters with a specific equipment (Tupiniquim), in four schools, to study the chemical composition to determine the main elements and their sources.

The "Tupiniquim" sampler was developed at the Laboratory for the Analysis of Atmospheric

Processes (LAPAt) at IAG-USP (http://www.lapat.iag.usp.br/), where also, the chemical analysis of the particulate matter samples was performed.

Figure 1 - Sensor Airbeam and an indoor sampling site School 4.



Source: Airbeam - User's Guide (habitatmap.org)

Figure 2 - Location of the five schools where the monitoring was carried out



The Positive Matrix Factor (PMF), version 5.0 was used to determine the main sources of pollutants in the areas.

FINDINGS AND ARGUMENT

$PM_{2.5}$ monitoring with the Airbeans sensors was placed between June and November 2021.

Table 1 shows the average concentrations of $PM_{2.5}$ in the schools, indoors and outdoors, the number of measurements days and the standard deviation.

There were some technical failures and data loss, mainly at School 2 and the measurements were compromised in this site.

With the exception of Schools 4 and 5, concentrations were higher outdoors.

At School 5, the indoor concentration was higher, as the sensor was located in the school's covered patio, an open area with a lot of movement of people and air exchange with the surrounding area, where the teachers' parking lot is located.

At School 4 the internal sensor was located in a room, with some windows facing directly onto the street, with a lot of movement of children, adults and vehicles, including shcool transportation.

This fact shows that the indoor air circulation is not appropriate.

Table 2 shows the meteorological parameters during the sampling period: temperature (T), relative humidity (RH), wind speed (W) and accumulated rainfall (P). Meteorological conditions during the monitoring period showed low rainfall, few cold fronts and atmospheric stability, which favors the concentration of pollutants. Until the end of August, temperatures were lower, less wind and little precipitation. The month with the most rain was October. The predominant direction was SE.

Table 1 - Local, sampling period, average $PM_{2.5}$ concentration, number of measurement days (N) and standard deviation (SD) for the entire monitoring period, outdoor and indoor, at the school sites

Local/ School	*Date 2021*	*Area*	*N*	*$PM_{2.5}$ ($\mu g/m^3$)*	*SD*
1	16jun-19nov	Outdoor	144	15.3	7.87
	16jun-30nov	Indoor	132	10.78	6.68
2	26aug-28oct	Outdoor	25	8.41	5.13
	26aug-15oct	Indoor	14	4.85	2.15
3		Outdoor	111	9.08	4.69
	19aug-30nov	Indoor	111	7.23	4.42
4		Outdoor	111	9.02	4.84
	06jul-30nov	**Indoor**	149	**10.25**	3.61
5		Outdoor	50	11.2	4.8
	16jul-11aug	**Indoor**	27	**16.09**	7.2

Table 2 - Average meteorological parameters and standard deviation (SD) for the entire period.

	T (°C)	*RH (%)*	*W (m/s)*	*Prec (mm)*
Avarege	18.58	67.14	1,32	0.08
SD	4.74	19.10	1.22	0.59

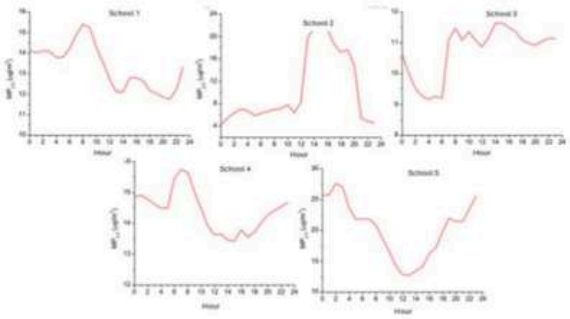
Source of data: INMET (2021) (https://portal.inmet.gov.br/)

The current São Paulo State air quality standard for 24 hours (50 $\mu g/m^3$) was not exceeded at any time during monitoring, however, the air quality standard suggested by the World Health

Organization (WHO) (15 $\mu g/m^3$) was exceeded several times in all schools, internally and externally (WHO, 2018).

The analysis of the time profiles of the indoor environment (Figure 3), shows that in School 5 there were high concentrations of pollutants during the early hours of the morning, probably related to the parking lot and local sources in the surrounding area, which contributes to the worsening of air quality in the environment where children and teachers must be expend most of their time in week. In Schools 4 and 1, concentrations were highest in the early morning, when there is a high flow of vehicles, typical of the region. In Schools 2 and 3, the time profile is related to the period when the schools are open and people are circulating.

Figure 3 - Time profile of $PM_{2.5}$ concentration indoor in schools.



The elemental concentration revealed the presence of soil elements as well as others related to local sources and vehicles for all sites. The application of a statistical model (PMF) applied to data from all sites identified that 19.5% of $PM_{2.5}$ is due to local sources, 45.1% soil resuspension, 9.3% light vehicles and 26.1% heavy vehicles (PAATERO;TAPPER, 1994; REFF et al, 2007; BROWN et al, 2015).

CONCLUSIONS

We can conclude the results of the monitoring and sampling showed that the WHO air quality standard was exceeded in all sites, including indoors, even though the sensors were installed in relatively open places, showing the air circulation was not appropriate in these environments. The elemental concentration revealed the presence of soil elements as well as others related heavy vehicles and local sources for all sites, respectively.

In the area surrounding of the sampling sites there are industries and other activities that can contribute to worsening air quality, but a much longer sampling period would be necessary to identify possible chemical species to identify possible chemical species related to these activities.

REFERENCES

BARROS, H. R., LOMBARDO, M. A. "*A ilha de calor urbana e o uso e cobertura do solo em São Paulo*". 2016. Rev. Geo USP espaço e tempo. V. 20, nº1, p.160-177. São Paulo

BROWN, S.G.; EBERLY, S.; PAATERO, P.; NORRIS, G. A. Methods for estimating uncertainty in PMF solutions: Examples with ambient air and water quality data and guidance on reporting PMF results. Science of The Total Environment. v. 518-519, p. 626-635, 2015. DOI: https://doi.org/10.1016/j.scitotenv.2015.01.022.

CETESB. "*Relatório de Qualidade do ar, 2022*". São Paulo, 2023. Available in: http://cetesb.sp.gov.br/ar/publicacoes-relatorios/

LI, J.; MATTEWAL, S. K.; PATEL, S.; BISWAS, P. "*Evaluation of nine low-cost-sensor-based particulate matter monitors*". Aerosol and Air Quality Research. v. 20. p. 254-270. 2020. doi: 10.4209/aaqr.2018.12.048

PAATERO, P., TAPPER, U. 1994. "*Positive matrix factorization: A non-negative factor model with optimal utilization of error estimates of data values*". Environmetrics, 5: 111-126.

REFF, A., EBERLY, S., BHAVE, P. "*Receptor modeling of ambient particulate matter data using Positive Matrix Factorization: review of existing mehods*". J. Air Waste Manage. Assoc. 57: 146-154. 2007.

SHARMA, A., KUMAR, P. "*A review of factors surrounding the air pollution exposure to in-pram babies and mitigation strategies*". Environment International. v. 120. p. 262-278. 2018. DOI: 10.1016/J.ENVINT.2018.07.038

SEINFELD, J. H., PANDIS, S. N. "Atmospheric chemistry and physics: from air pollution to climate change". 2006. Ed. 2°. Wiley, New Jersey.

WORLD HEALTH ORGANIZATION. "*Clean air for health: Geneva Action Agenda*". 2018. Available in: https://www.who.int/phe/news/clean-air-for-health/en/

AIR POLLUTION CONFERENCE BRAZIL
CMAS SOUTH AMERICA
COMMUNITY MODELING AND ANALYSIS SYSTEM

AIR QUALITY ASSESSMENT IN INDOOR ENVIRONMENTS: STUDY IN A HIGHER EDUCATION INSTITUTION

Franciele Ribeiro Cavalcante[1], Geisiely do Espírito Santo[1], Marilia Gueler da Penha[1], Thayná Prata Oliveira[1], Brenda Santos Tonon[1], Andressa Curto Marques Dessaune[1], Bruno Furieri[1]

[1]Federal University of Espírito Santo, Vitória, ES, Brazil.

E-mails: franciele97rc@gmail.com, geisielyes@gmail.com, mariigueler@gmail.com, prata.thayna11@gmail.com, bstonon@gmail.com, andressacm@gmail.com, furieribruno@gmail.com

Abstract: It is evident that individuals spend a large part of their time indoors, especially in work and study environments. In artificially air-conditioned places, the concentration of atmospheric pollutants is influenced by internal and external emissions. Therefore, it is crucial not to underestimate the importance of understanding indoor air quality and its associated parameters, as neglecting this issue can present risks to health and efficiency in the workplace. From this perspective, the main objective of this study is to investigate Indoor Air Quality (IAQ) by monitoring PM (PTS, 2.5 and 10), CO_2, bioaerosols and thermal comfort parameters (temperature and humidity air) in two offices of a Higher Education Institution (HEI) that use mechanical ventilation. To monitor bioaerosols, an Andersen CF-6 impactor and petri dishes prepared with Potato Dextrose Agar (PDA) and Chloramphenicol (antibiotic) were used. The petri dishes were subjected to growth in an oven. Particulates and CO_2 were monitored using continuous monitors, Ecopm and Aeroqual, respectively. Air speed and temperature were measured using an anemometer at different points in the environments of interest. The results revealed that air quality and thermal comfort parameters showed variations in the two environments analyzed. When comparing the data obtained with current IAQ standards, particulate matter concentrations remained stable within acceptable limits. CO_2 levels varied between offices, potentially indicating IAQ concerns in Office 1. Bioaerosol analysis highlighted the impact of occupancy and influences of outdoor concentrations. And, finally, comfort parameters were often outside recommended ranges, emphasizing the need for well-maintained ventilation systems. This study contributes valuable information that enables the implementation of practices aimed at improving air quality in indoor environments.

Keywords: Indoor air quality, thermal comfort, environmental monitoring.

INTRODUCTION

Indoor air quality (IAQ) is a critical concern for building occupants' health and comfort, with potential health effects, including, for example eyes irritation, fatigue and respiratory diseases (US EPA, 2024). In university settings, the dynamic nature of office spaces accommodating students and professors can lead to ventilation issues, exacerbating IAQ concerns. These spaces pose multiple sources of indoor air pollutants, including CO_2 from human breathing, Particulate Matter (PM) infiltration from outdoor air, and the proliferation of biological particulate matter due to humidity or mold presence (Sung et al., 2022).

From this perspective, this study aims to investigate IAQ by monitoring PM (PTS, 2.5 and 10), CO_2, bioaerosols and thermal comfort parameters (temperature and humidity air) in two offices of a Higher Education Institution (HEI) that use mechanical ventilation.

METHODS

Study Area Description: The study area, located in Vitória, Espírito Santo State, Brazil, is characterized by a tropical climate. Two workspaces, Office 1 (18 m^2) and Office 2 (20.6 m^2), situated in separate buildings on the university campus, were chosen for analysis. These spaces, utilized by professors and students for research activities, are equipped with essential amenities and air conditioning units, typically operated between 8 AM and 6 PM with an average occupancy of around 4 individuals, with Office 1 showing greater variability in occupancy compared to Office 2.

Sampling: Sampling focused on sections of the offices with consistent occupancy. Continuous monitoring of PM and CO_2 levels was conducted using a laser particle counter (ECOPM) and a Portable Air Quality Monitor (Aeroqual S500) respectively, alongside integrated temperature and humidity sensors. For these parameters, sampling occurred during the following periods: Office 1 was sampled from February 19th, 2024, to February 23th, 2024, and Office 2 from February 26th, 2024 to March 1st, 2024. Results are presented as hourly averages for particulate matter, and 5-minute averages for CO_2 and thermal comfort parameters. Bioaerosols were monitored using an Andersen CF-6 impactor, with sampling taking place on November 17th, 2023, at two points within each office and one outdoors to assess the Indoor/Outdoor (I/O) ratio.

Analyses: Collected data were compared with IAQ and comfort regulations to evaluate compliance with established limits ensuring the health and well-being of office occupants. Recommendations for enhancing IAQ were derived from the analysis to address any identified concerns.

RESULTS

Particulate Matter: Table 1 presents the results of monitoring particulate matter. The results reveal relatively stable concentrations across both offices, with occasional peaks for large particles correlating with increased human activity, particularly during entry, exit, and lunchtime. Office 1 exhibits higher peaks and standard deviations, particularly evident during the short-duration weekly cleaning (PTS=87.1 µg/m³ and PM_{10}=36.0 µg/m³), aligning with Velasco's (2020) findings suggesting a correlation between human movement and particulate concentration variations. Despite these fluctuations, all average concentrations remain below the reference values established by both Brazilian regulation (Anvisa=80 µg/m³ for Total Airborne Particulate Matter) and WHO Air Quality Guidelines (50 µg/m³ for PM_{10} and 25 µg/m³ for $PM_{2.5}$ to 24-hour averages), suggesting IAQ overall.

Table 1. Descriptive statistics related to particulate matter concentrations

Descriptive statistics	PM_1 (µg/m³)	$PM_{2.5}$ (µg/m³)	PM_{10} (µg/m³)	PTS (µg/m³)
Office 1				
Minimum	0.2	0.5	1.0	1.0
Maximum	1.2	5.0	36.0	87.1
Mean	0.6	1.3	2.7	5.2
St. Deviation	0.3	0.6	3.6	9.6
Office 2				
Minimum	0.3	0.4	0.5	0.5
Maximum	2.0	3.4	5.1	15.8
Mean	0.8	1.4	2.2	3.3
St. Deviation	0.4	0.6	1.1	3.0

Carbon dioxide CO_2: Figure 1 shows the variability in carbon dioxide (CO_2) concentration within the monitored environments. Despite both offices maintaining average concentrations below the Brazilian regulation limit of 1000 ppm (Brasil, 2003), office 1 demonstrates higher variability, with a standard deviation of 218.6 compared to 81.7 for office 2.

Examining global legislation, Dimitroulopoulou et al. (2023) highlighted thresholds for CO_2 levels, with concentrations below 1000 ppm considered indicative of good indoor air quality (IAQ). In this study, office 2 consistently maintained CO_2 levels below this threshold, with a maximum concentration of 800 ppm, reflecting good IAQ throughout the monitoring period. However, office 1 experienced peaks reaching 1659.0 ppm, indicating poor IAQ during these instances, with a duration of 2 continuous hours. This prolonged exposure to elevated CO_2 concentrations in office 1 poses concerns, as discussed by Sahu and Gujar (2020), who noted adverse effects such as drowsiness, lethargy, and potential impacts on cognitive performance and productivity in similar settings.

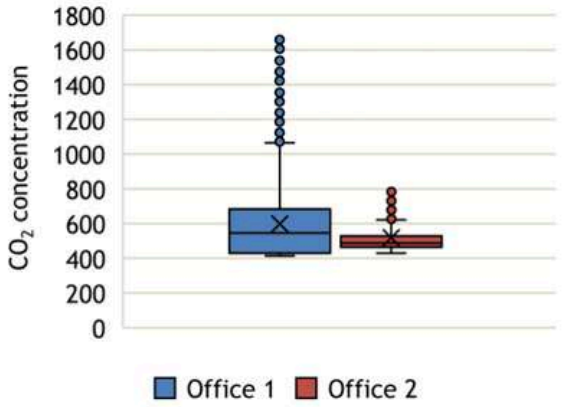


Figure 1. Concentration of carbon dioxide (CO_2)

Bioaerosols: Table 2 presents the outcomes of bioaerosol monitoring in the two office environments. Higher concentrations were observed in areas with increased occupant density, reaching 735 CFU/m³ in Office 1 and 643.11 CFU/m³ in Office 2. Variances between the spaces were influenced by outdoor conditions and office occupancy density, with Office 1 exhibiting higher levels, potentially due to its ground-floor location and higher occupancy. These results support Velasco's (2020) research, emphasizing the impact of building characteristics and ventilation on indoor fungal concentrations.

Comparison with regulatory standards (Brasil, 2003), which specify a limit of 750 CFU/m³ or an I/O ratio of 1.5, indicates compliance and satisfactory air quality regarding fungal concentration in both offices.

Table 2: Bioaerosol monitoring results

Description	Number of colonies	CFU/m³	I/O
Office 1			
Samp. point 1 - Indoor	104	734,98	0,59
Samp. point 2 - Indoor	76	537,10	0,43
Outdoor	176	1243,82	
Office 2			
Samp. point 1 - Indoor	91	643,11	0,64
Samp. point 2 - Indoor	77	544,17	0,54
Outdoor	143	1010,60	

Comfort parameters: The monitoring of comfort parameters revealed temperature ranges of 22.6°C to 27.0°C for Office 1 and 20.2°C to 25.9°C for Office 2, along with relative humidity varying from 46.2% to 82.6% for Office 1 and 54.0% to 84.7% for

Office 2. Despite established standards by Brazilian Regulatory Standards NBR 6401, specifying temperature ranges of 22.5°C to 25.5°C and 65% RH in summer conditions (ABNT, 1980), our observations indicate deviations from these standards in both offices during the analyzed period.

Wolkoff et al. (2021) emphasize the impact of indoor temperature and humidity on health and work performance, highlighting increased risks of respiratory and cardiovascular diseases associated with deviations from optimal conditions. Office 1 consistently maintained higher temperatures during occupancy, while Office 2 experienced prolonged periods of lower temperatures. It was found that Office 1 exhibited elevated temperature and humidity levels for over 2 hours, whereas Office 2 recorded temperatures below 21.0°C persisting for more than 6 hours.

Strategies to promote better IAQ: In the analyzed workspaces, IAQ parameters meet current regulations, particularly in Brazil. However, at least two points should be considered for improving IAQ:

Firstly, addressing occupant density is essential, especially in small offices. WHO (1990) highlights the risk of airborne disease transmission in densely populated spaces. It was found that the current air conditioning system in these offices merely insufflates air to enhance thermal comfort. In Office 1, prolonged CO_2 concentrations above 1000 ppm indicate the need for enhanced ventilation systems or occasional natural ventilation. Additionally, higher temperatures during peak occupancy suggest potential ventilation system limitations in maintaining thermal comfort.

Secondly, ensuring cleanliness of air conditioning systems is vital. Sung et al. (2022) emphasize the risk of pollution from neglected filters, hindering airflow and PM10 removal. WHO (1990) warns of unchanged filters becoming breeding grounds for microbes.

CONCLUSIONS

This study underscores the importance of IAQ monitoring and management in office environments. While particulate matter and bioaerosol concentrations generally remained within acceptable limits, peaks in carbon dioxide levels and comfort parameters outside the recommended range, especially in densely occupied areas, raise concerns about IAQ adequacy. The findings highlight the need for improved ventilation strategies and regular maintenance of air conditioning systems to mitigate potential health risks associated with poor IAQ. By addressing these issues, workplaces can create healthier and more comfortable indoor environments, promoting occupant well-being and productivity.

REFERENCES

Associação Brasileira de Normas Técnicas (ABNT). *NBR 6401 - Instalações centrais de ar-condicionado para conforto: parâmetros básicos de projeto*. Rio de Janeiro: ABNT, 1980.

Brasil. *Resolução nº 09, de 16 de janeiro de 2003*. Agência Nacional de Vigilância Sanitária. Orientação Técnica sobre Padrões Referenciais de Qualidade do Ar Interior, em ambientes climatizados artificialmente de uso público e coletivo. Diário Oficial da República Federativa do Brasil, Section 1, n. 14, p. 35, 2003.

Dimitroulopoulou, S. et al. Indoor air quality guidelines from across the world: An appraisal considering energy saving, health, productivity, and comfort. *Environment International*, 108127, 2023.

Sahu, V., and Gurjar, B. R. Spatial and seasonal variation of air quality in different microenvironments of a technical university in India. *Building and Environment*, *185*, 107310, 2020.

Sung, W. P., Chen, T. Y., & Liu, C. H. Strategy for improving the indoor environment of office spaces in subtropical cities. *Buildings*, 12(4), 412, 2022.

United States Environmental Protection Agency (US-EPA). *Indoor Air Quality (IAQ)*. Available in: <https://www.epa.gov/indoor-air-quality-iaq/introduction-indoor-air-quality#:~:text=Indoor%20Air%20Quality%20(IAQ)%20refers,risk%20of%20indoor%20health%20concerns>. Accessed in april 23, 2024.

VELASCO, M. L. Z. *Estudo exploratório da qualidade do ar interior em escolas públicas de Ensino Fundamental*. Dissertação de Metrado em Engenharia Ambiental, Universidade Federal do Espírito Santo, Vitória, ES, 2020.

Wolkoff, P., Azuma, K., and Carrer, P. Health, work performance, and risk of infection in office-like environments: The role of indoor temperature, air humidity, and ventilation. *International Journal of Hygiene and Environmental Health*, *233*, 113709, 2021.

World Health Organization. *Indoor air quality: biological contaminants*: report on a WHO meeting, Rautavaara, 29 August-2 September 1988 (No. ICP/CEH 073). World Health Organization. Regional Office for Europe, 1990.

AIR POLLUTION CONFERENCE BRAZIL
CMAS SOUTH AMERICA
COMMUNITY MODELING AND ANALYSIS SYSTEM

"Microorganisms present in the air in intensive care units, surveillance or monitoring?"

Valter Batista Duo Filho[1], Ana Carolina Souza Ramos de Carvalho[1], Ellen Dreger Cardoso[2], Diego Oliveira Pessoa[2], Dulcilena de Matos Castro e Silva[1]

[1]Mycology Department, Adolfo Lutz Institute; São Paulo, Brazil- dulcilena.silva@ial.sp.gov.br
[2]Emílio Ribas Institute for Infectious Diseases; São Paulo, Brazil- diego.pessoa@emilioribas.sp.gov.br

Abstract: *Microbiological monitoring of hospital environments, particularly intensive care units (ICUs), is essential for understanding microbial behavior and controlling cross-infections. This study conducted a six-month analysis of air quality in ten rooms within an infectious disease institute's ICU. Samples were collected before and after cleaning, as well as 36 hours post-cleaning, using culture media for bacterial and fungal analysis. A total of xxx samples were isolated and identified using mass spectrometry. Findings revealed differing microbial concentrations between rooms with and without patients, with cleaning reducing microbial load, albeit to varying extents. Pathogenic microorganisms were identified both before and after cleaning, emphasizing the importance of continuous monitoring. The study underscores the necessity of tailored cleaning protocols based on microbiological monitoring to mitigate cross-infection risks in hospital environments.*

Keywords: Microbiology, hospital air hygiene, environmental contamination, Fungi and bacteria.

INTRODUCTION

Intensive Care Units (ICUs) have always struggled to keep patients out of the risk of cross infections, especially those involving microorganisms dispersed in the hospital environment. (ROSTAMI et al., 2017; VANETTI et al., 2008) Microbiological monitoring of various hospital areas usually occur as a complement, and its records are considered additional documents in the certification folder. However, when they occur, they are randomly scaled, not recording the true circulation of microorganisms. (RUSSELL; AYLIFFE´S, 2004) Epidemiological surveillance always suggests that in order to prevent unbalanced dispersion of microorganisms, biosafety tools should be adequately utilized. However, what has been observed is that professionals in the sector often fail to perceive the microbial discharge they themselves make in their workplace. (CUMHUR et al., 2019; ROSTAMI et al., 2017) The professionals who circulate in the ICUs are mostly those who provide assistance to patients. The percentage distribution of professionals and the professional/patient ratio are established by legislation, as should be the case with the hospital hygiene maintenance team, since this team varies according to the institution. ("RESOLUÇÃO COFEN N 0543/2017", 2017) Regarding surveillance and control of microorganism dispersion, hospital air can be one of the most neglected items in the hospital area. Controlling the air in the environment involves not only monitoring its circulation or cleaning the air conditioning system but also collecting samples and identifying viable microorganisms present at the time of monitoring. (ADAMS et al., 2013; CUMHUR et al., 2019; MAREKOVIĆ, 2023; TAOUFIQ, 2021) Since these analyses are not frequently performed, it is necessary to monitor the microbiological behaviour of the air in a specific ICU at different times.

METHODS

During six months of monitoring, 10 rooms in the ICU of an Infectious Disease Institute, a reference for infectious diseases, currently with 70 beds, were analyzed. The ICU of this hospital consists of 12 beds, with a unidirectional air circulation system from the corridor to the internal environments of the beds, with individual isolation of each room. The study sampled five empty rooms and five beds with admitted patients.

In each room, three air samples were taken: before and after cleaning, and the third air sample was collected 36 hours after delivery for use. All collections were performed using specific culture media, Modified Dichloran Rose Bengal Agar (DRBCm) for fungal impact and Tryptic Soy Broth (TSB) for bacteria. (Castro e Silva DM et al., 2015).

To collect the air sample, the agar plate was placed inside the impactor, MAS 100 Merck®. The final volume of air collected was 250L ($0.25m^3$), allowing for the analysis of CFU/m3 and the isolation of colony-forming units. Plates with air samples were sent to the Mycology Laboratory of the Adolfo Lutz Institute (IAL) and incubated in a bacteriological incubator set at 30° ± 2°C for up to 7 days for isolation and identification of genus and species. Following the principle that each viable

organism present in the air has the ability to form a colony, the concentration was expressed in CFU/m^3.
During the study, a total of xxx samples of fungi and bacteria were isolated, characterized by polyblastic taxonomy and mass spectrometry by the MALDI-TOF System for species identification. MALDI-TOF MS is a rapid, simple, inexpensive, and high-throughput proteomic technique for identification of both bacteria and fungi, but it is important to highlight that its application is dependent on the reference strains included in the database. (ASHFAQ; DA'NA; AL-GHOUTI, 2022; DE ALMEIDA JÚNIOR et al., 2014; NORMAND et al., 2020)

FINDINGS AND ARGUMENT

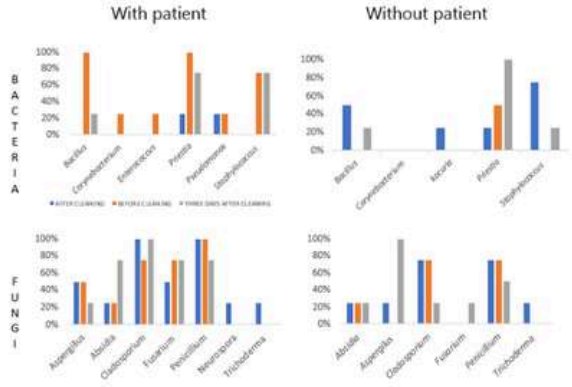
In the results obtained during this study, rooms without patients showed a lower concentration of CFU/m^3 of bacteria compared to rooms with patients before cleaning, whereas the opposite was observed for fungal concentrations. After cleaning, there was a reduction in microbial load in both groups, but in different proportions: 94% (N=3/54) of bacteria in rooms without patients and 41,42% (N= 87/210) in rooms with patients. Regarding fungi, there was a reduction of 91% (N=31/358) in rooms without patients and 78% (N=) in rooms with patients. The quantity of CFU/m^3 of bacteria in the air after three days of cleaning showed an increase of 84% (N=186/221), while fungal concentrations decreased by 17% (N=296/358) compared to the initial analysis before cleaning. The analyses showed that the presence of patients is a factor that modifies the concentration of microorganisms present in the air of the rooms, increasing the diversity of isolated genera (Table 1).

Table1: Concentration of UFC/m^3 of fungi and bacteria before, after, and three days after standard cleaning in a hospital room at Hospital São Paulo, Brazil

Period	Average UFC/BAC	Average UFC/FU
Before Cleaning		
Without patient	54	358
With patient	210	82
After cleaning		
Without patient	3	31
With patient	87	18
Three days after cleaning		
Without patient	186	296
With patient	221	63

Non-cleaned rooms exhibited pathogenic microorganisms of the genera *Pseudomonas*, *Staphylococcus*, *Fusarium*, and *Aspergillus*; however, after cleaning, other pathogenic microorganisms were identified, such as *Enterococcus* and *Corynebacterium* in rooms with newly admitted patients, indicating this as the source of these findings. Three days after cleaning, the entire microbial load was renewed in all rooms, regardless of the presence of patients, revealing that cleaning requires monitoring. The identification and monitoring of the microbiota present in hospital environments are essential for understanding and tracing the cleanliness conditions, as well as for controlling cross-infections (Figure 1).

Figure 1: Distribution of genera of fungi and bacteria in rooms with and without patients during the cleaning protocols



CONCLUSIONS

Numerous cleaning processes can be employed for the decontamination and sanitation of hospital ICUs to achieve success. However, this study revealed that microbiological monitoring can signal which environments should be controlled and/or cleaned with differentiated frequency. It also showed that microbial proliferation is more intense in rooms with patients than in rooms without patients.

REFERENCES

ADAMS, R. I. et al. Dispersal in microbes: Fungi in indoor air are dominated by outdoor air and show dispersal limitation at short distances. **ISME Journal**, v. 7, n. 7, p. 1262–1273, 2013.

ASHFAQ, M. Y.; DA'NA, D. A.; AL-GHOUTI, M. A. Application of MALDI-TOF MS for identification of environmental bacteria: A review. **Journal of Environmental Management**, v. 305, n. December 2021, p. 114359, 2022.

CUMHUR, Y. E. et al. Epidemiology of bacterial contamination of inert hospital surfaces and equipment in critical and non-critical care units: a Brazilian multicenter study. **Journal of Wind Engineering and Industrial Aerodynamics**, v. 26, n. 1, p. 1–4, 2019.

DE ALMEIDA JÚNIOR, J. N. et al. Usefulness of matrix-assisted laser desorption ionisation-time-of-flight mass spectrometry for identifying clinical Trichosporon isolates. **Clinical Microbiology and Infection**, v. 20, n. 8, p. 784–790, 2014.

MAREKOVIĆ, I. What's New in Prevention of Invasive Fungal Diseases during Hospital Construction and Renovation Work: An Overview. **Journal of Fungi**, v. 9, n. 2, 2023.

MATOS, D. DE et al. A new culture medium for recovering the agents of Cryptococcosis from environmental sources. v. 358, p. 355–358, 2015.

NORMAND, A. C. et al. Optimization of MALDI-ToF mass spectrometry for yeast identification: a multicenter study. **Medical mycology**, v. 58, n. 5, p. 639–649, 1 jul. 2020.

RESOLUÇÃO COFEN N 0543/2017. , 2017. Disponível em: <https://ci.nii.ac.jp/naid/120006927694/>

ROSTAMI, N. et al. Assessment of indoor and outdoor airborne fungi in an Educational, Research and Treatment Center. **Italian Journal of Medicine**, 2017.

RUSSELL, H.; AYLIFFE´S. Principles and Practice of Disinfection, Preservation & Sterilization. p. 689, 2004.

TAOUFIQ, A. H. T. **AVALIAÇÃO DA EFICÁCIA DE UM DESCONTAMINANTE DE PARTÍCULAS OXIDANTES APLICADO POR AEROSSOL GASOSO EM ESPOROS DE Bacillus cereus**. [s.l.] UNIVERSIDADE DE LISBOA FACULDADE DE MEDICINA VETERINÁRIA, 2021.

VANETTI, M. D. et al. Bioaerossóis em ambientes hospitalares. **Journal of Hospital Infection**, v. 63, n. 1, p. 24–30, 2008.

PROCEEDINGS OF THE

2024 AIR POLLUTION CONFERENCE

And 5th CMAS South America

SESSION 07
Machine Learning and Reduced Form Models Developments and Applications

Typically, a limited number of specific simulations using chemical transport models (CTMs) or Gaussian plume models are used to derive relationships between emissions from particular sources and a response variable (pollutant concentration, health impact, etc.) for specific locations. We want to discuss here the potential usages/applications of Machine Learning (ML) and Reduced form models (RFM) that are computationally efficient and allow users to rapidly assess air quality impacts for a large number of emission scenarios, making them especially useful as screening tools for evaluating policy scenarios.

There have been many ML and RFM implementations on air quality forecasting in recent years and this session focuses on the development, evaluation, and application of ML and RFMs. Topics include, but are not limited to, the following:

- Developing and evaluating ML and RFMs
- Inter-comparison of ML and RFMs
- Global or regional application of ML and RFMs on air quality, human health, ecosystem or other impacts

SESSION 07

ENHANCING PM2.5 CONCENTRATION ACCURACY IN LIMA CITY, PERU THROUGH MACHINE LEARNING CALIBRATION OF DATASETS FROM LOW-COST SENSORS 181

AN AI SYSTEM TO PREDICT STREET-LEVEL AIR QUALITY: INTRODUCTION TO THE QUALARIA PROJECT 184

THE CO-IMPACTS OF DROUGHT AND HEAT WAVES ON WILDFIRES IN THE BRAZILIAN CERRADO BIOME 187

AIR POLLUTION CONFERENCE BRAZIL
CMAS SOUTH AMERICA
COMMUNITY MODELING AND ANALYSIS SYSTEM

ENHANCING $PM_{2.5}$ CONCENTRATION ACCURACY IN LIMA CITY, PERU THROUGH MACHINE LEARNING CALIBRATION OF DATASETS FROM LOW-COST SENSORS

Odon R. Sanchez-Ccoyllo[1], Heydy J. Espinoza Huamani[1], Winnie R. Islachin Aquise[1], Rosa L. Chaparro Huilca[1], Ever E. Castillo Osorio[2]

[1]*Atmospheric Pollution Research Group, Universidad Nacional Tecnologica de Lima Sur, Lima, Peru*
osanchez@untels.edu.pe

[2]*School of Civil and Environmmental Engineering, Yonsei University. Seoul, South Korea*
ecastillo@yonsei.ac.kr

Abstract: The Metropolitan Area of Lima-Callao (MALC) stands out as one of the most environmentally challenged regions in Latin America and the Caribbean (LAC), characterized by elevated concentrations of the $PM_{2.5}$ pollutant. This study aims to refine the accuracy of $PM_{2.5}$ measurements obtained through a low-cost sensor (LCS), employing machine learning (ML) technique with reference data provided by the Meteorology and Hydrology National Service of Peru (SENAMHI) in the MALC.

To train and evaluate the ML model, we utilized hourly $PM_{2.5}$ concentrations from SENAMHI's reference measurements and those from the LCS operated by the Urban Transportation Authority for Lima-Callao (ATU) during the period from July 16th, 2023, to August 26th, 2023. The dataset was split into training (80%) and testing (20%) sets to construct a linear regression model using the scikit-learn package in Python.

In the experimental results, our ML model has revealed a robust correlation between the LCS $PM_{2.5}$ concentrations and the reference $PM_{2.5}$ concentrations, implying its efficacy in predicting and calibrating $PM_{2.5}$ measurements. Despite the intercept and the Root Mean Squared Error (RMSE) values falling short of the Environmental Protection Agency (EPA) guidelines, the slope and Coefficient of Determination (R^2) values adhere to them, underscoring the resilience of our model. These findings highlight the potential of ML technique in refining air quality measurements and addressing pollution concerns in the MALC region.

Keywords: $PM_{2.5}$ concentrations, Low-cost Sensor, Machine Learning, Lima-Callao Metropolitan Area

INTRODUCTION

Low-Cost sensors (LCS) for air quality are small portable instrumental in enhancing the spatial-temporal distribution of air quality monitoring efforts (Lee et al., 2024). LCS are popular for their affordability and low maintenance, less than $ 350 per unit (Aix et al., 2023). However, their widespread use raises concerns about data reliability due to potential undetected malfunctions more than one year (Liang, 2021). LCS cannot achieve the same accuracy as reference instruments, so the LCS data should be calibrated before it uses. Once calibrated the LCS data must compare with reference instrument (Aix et al., 2023). Several methods are used to calibrate the LCS data that are linear regression, multiple linear regression, and Machine learning (ML) (Aix et al., 2023). A Random Forest ML used to correct of $PM_{2.5}$ and PM_{10} data measured with LCS in Oxford, UK (Bush et al., 2023). Particles measured from TEOM instrument are used as dependent variables and measurements from LCS as predictor variables in New York, US in order to use ML method by (Johnson et al., 2018).

METHODOLOGY

The CERES air quality station (AQS) is situated to the east of the Metropolitan Area of Lima, as depicted in Figure 1. The CERES AQS is located near heavy traffic. Reference measurements of hourly data on $PM_{2.5}$ concentration was retrieved from the website of the Meteorology and Hydrology National Service of Peru (SENAMHI), accessible at https://www.senamhi.gob.pe/?p=calidad-del-aire. The $PM_{2.5}$ is measured using beta attenuation Monitor 5014i. On the other hand, the hourly data on $PM_{2.5}$ mass concentrations measured with the LCS is obtained from the Urban Transportation Authority for Lima and Callao (ATU).

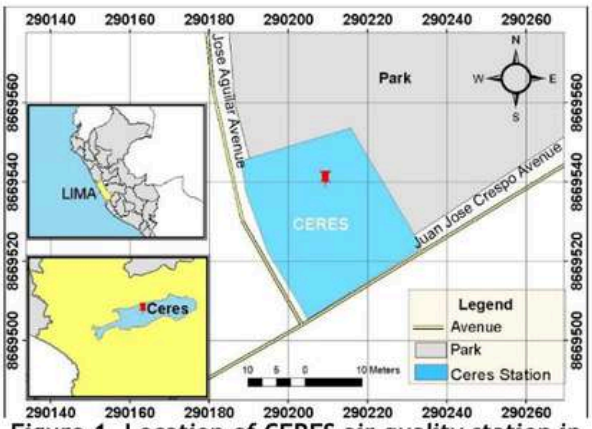


Figure 1. Location of CERES air quality station in Lima

The methodology for data processing, particularly the partitioning of data in ML, holds a pivotal role

in influencing the accuracy of the model (Panneerselvam et al., 2023). To address this critical aspect, 80% of the available data were allocated for training the ML model, while the remaining 20% were designated for evaluating the model's performance. This partitioning strategy aims to mitigate the risk of overfitting in the ML model, as emphasized by (Panneerselvam et al., 2023). The ML technique is employed for calibrating particulate LCS datasets (Liang, 2021). Limited data fails to accurately estimate parameters, while increased data enhances accuracy. Notably, accuracy improves from one to two months of data. However, accuracy declines with durations exceeding half a year, possibly due to degraded LCS performance and heightened seasonal variation (Liang, 2021).

The ML model employed in this study discerns the influence of input variables, specifically $PM_{2.5}$ concentration data measured from reference air quality stations, on the predictive outcomes derived from the $PM_{2.5}$ concentrations recorded by the LCS instrument. Linear Simple Regression (LSR) is a statistical technique used to uncover and quantify the linear relationship between two variables: the response variable, also known as the dependent variable, and the predictor variable, or the independent variable. This method assumes that changes in the response variable are directly proportional to changes in the predictor variable, following a straight-line pattern. The particles measured with the reference instrument is chosen as dependent variable, while the aerosol measured with LCS datasets as predictor variable for calibrating studies (Aix et al., 2023), expressed as:

$$PM2.5Reference = \theta 0 + \theta 1(PM2.5LCS)$$

Where: *PM2.5Reference* represents the response variable; *PM2.5LCS* represents the predictor variable; $\theta 0$ is the intercept, indicating the value of *PM2.5Reference* when *PM2.5LCS* equals zero; $\theta 1$ is the slope, representing the rate of change in *PM2.5Reference* for each unit change in *PM2.5LCS*. The objective of LSR is to estimate the parameters $\theta 0$ and $\theta 1$ that minimize the sum of squared errors between the observed and predicted values of the response variable. This is typically achieved using the method of least squares. By fitting a linear model to the data, LSR allows us to make predictions about the response variable based on the values of the predictor variable. The coefficient of determination (R^2) and root mean squared error (RMSE) were used to evaluate the accuracy of the relationship between particles of the reference and particles of the LCS (Johnson et al., 2018).

FINDINGS AND ARGUMENT

Figure 2 displays the outcome of the ML model, illustrating the scatter plot of the LCS $PM_{2.5}$ concentrations against the reference $PM_{2.5}$ concentrations. A clear and favorable correlation is observed, indicating that LCS $PM_{2.5}$ concentrations serve as a reliable predictor. In this analysis, the reference $PM_{2.5}$ concentrations are employed as the dependent variable.

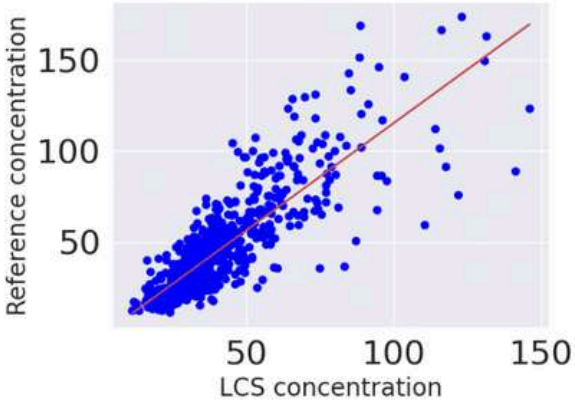


Figure 2. Hourly values of reference and LCS $PM_{2.5}$ concentrations ($\mu g/m^3$). The red line is the best linear fit

Although the statistical values of intercept and RMSE fall short of the accuracy criteria outlined by the Environmental Protection Agency (EPA) guidelines, the slope and R^2 values effectively meet these criteria (table 1).

Table 1. Accuracy metrics for $PM_{2.5}$ concentrations ($\mu g/m^3$)

Statistical metrics		EPA guidelines
R^2	0.7	≥ 0.7
RMSE	10.03	≤ 7.0
Slope	0.61	1.0 ± 0.35
Intercept	13.6	$-5 \leq B \leq 5$

CONCLUSION

In conclusion, our ML model demonstrates a strong correlation between LCS $PM_{2.5}$ concentrations and reference $PM_{2.5}$ concentrations, suggesting their effectiveness in predicting and calibrating $PM_{2.5}$ measurements. Although intercept and RMSE values do not fully meet EPA guidelines, the slope and R^2 values comply, indicating the robustness of our model. This highlights the potential utility of LCS $PM_{2.5}$ concentrations as a reliable proxy for calibration, despite the need for further refinement to meet regulatory standards.

REFERENCES

Aix, M. L., Schmitz, S., & Bicout, D. J. (2023). Calibration methodology of low-cost sensors for high-quality monitoring of fine particulate matter. *Science of the Total Environment*, *889*. https://doi.org/10.1016/j.scitotenv.2023.164063

Bush, T., Bartington, S., Pope, F. D., Singh, A., Thomas, G. N., Stacey, B., Economides, G., Anderson, R., Cole, S., Abreu, P., & Leach, F. C. P. (2023). The impact of COVID-19 public health restrictions on particulate matter pollution measured by a validated low-cost sensor network in Oxford, UK. *Building and Environment*, *237*. https://doi.org/10.1016/j.buildenv.2023.110330

Johnson, N. E., Bonczak, B., & Kontokosta, C. E. (2018). Using a gradient boosting model to improve the performance of low-cost aerosol monitors in a dense, heterogeneous urban environment. *Atmospheric Environment*, *184*, 9–16. https://doi.org/10.1016/j.atmosenv.2018.04.019

Lee, Y. M., Lin, G. Y., Le, T. C., Hong, G. H., Aggarwal, S. G., Yu, J. Y., & Tsai, C. J. (2024). Characterization of spatial-temporal distribution and microenvironment source contribution of PM2.5 concentrations using a low-cost sensor network with artificial neural network/kriging techniques. *Environmental Research*, *244*. https://doi.org/10.1016/j.envres.2023.117906

Liang, L. (2021). Calibrating low-cost sensors for ambient air monitoring: Techniques, trends, and challenges. In *Environmental Research* (Vol. 197). Academic Press Inc. https://doi.org/10.1016/j.envres.2021.111163

Panneerselvam, B., Ravichandran, N., Dumka, U. C., Thomas, M., Charoenlerkthawin, W., & Bidorn, B. (2023). A novel approach for the prediction and analysis of daily concentrations of particulate matter using machine learning. *Science of the Total Environment*, *897*. https://doi.org/10.1016/j.scitotenv.2023.166178

AIR POLLUTION CONFERENCE BRAZIL
CMAS SOUTH AMERICA
COMMUNITY MODELING AND ANALYSIS SYSTEM

AN AI SYSTEM TO PREDICT STREET-LEVEL AIR QUALITY: INTRODUCTION TO THE QUALARIA PROJECT

Cathy W. Y. Li[1], Gabriel M. P. Perez[2], Thomas C. M. Martin[3], Victória M. L. Peli[4], Amanda V. de Lucena[5], Edson L. S. Y. Barbosa[6], Mario Gavidia-Calderón[7], Edmilson Dias de Freitas[8], Maria de Fatima Andrade[9], Matthias Schindler[10], Felix Laimer[11], Karim Tarraf[12], Guy Brasseur[13]

[1]*Max Planck Institute for Meteorology, Hamburg, Germany*
cathy.li@mpimet.mpg.de
[2]*MeteoIA Data Science, São Paulo, Brazil*
gabriel@meteoia.com
[3]*MeteoIA Data Science, São Paulo, Brazil*
thomas@meteoia.com
[4]*MeteoIA Data Science, São Paulo, Brazil*
victoria@meteoia.com
[5]*MeteoIA Data Science, São Paulo, Brazil*
amanda@meteoia.com
[6]*MeteoIA Data Science, São Paulo, Brazil*
edson@meteoia.com
[7]*Instituto de Astronomia, Geofísica e Ciências Atmosféricas, Universidade de São Paulo, Brazil*
mario.calderon@iag.usp.br
[8]*Instituto de Astronomia, Geofísica e Ciências Atmosféricas, Universidade de São Paulo, Brazil*
edmilson.freitas@iag.usp.br
[9]*Instituto de Astronomia, Geofísica e Ciências Atmosféricas, Universidade de São Paulo, Brazil*
maria.andrade@iag.usp.br
[10]*Bernard Technologies GmbH, Munich, Germany*
matthias.schindler@bernard-gruppe.com
[11]*Bernard Technologies GmbH, Munich, Germany*
felix.laimer@bernard-gruppe.com
[12]*Bernard Technologies GmbH, Munich, Germany*
karim.tarraf@bernard-gruppe.com
[13]*Max Planck Institute for Meteorology, Hamburg, Germany*
National Center for Atmospheric Research, Boulder, USA
guy.brasseur@mpimet.mpg.de

Abstract:

Here we present the joint German-Brazilian project QUALARIA (Sistema baseado em Inteligência Artificial para a previsão de qualidade do ar em escala sub-urbana/Artificial Intelligence based system for sub-urban scale air quality prediction).
With joint effort between research and business partners in Brazil and Germany, QUALARIA proposes to develop an operational artificial intelligence-based system for monitoring, simulation and prediction of air quality in urban environments with unprecedented spatial resolution and temporal availability. The system will be first testbedded in São Paulo/ SP. Brazil and made it applicable for other cities in the world. Its features will be designed in consultation with national and international stakeholders in the public and private sectors, mainly aiming at policy-makers, city planners and citizens. The system will combine a low-cost sensor network, existing observational networks, regional atmospheric models and state-of-the-art artificial intelligence (AI) to transform coarse resolution air quality maps (10 km) to street-level (100 m) maps. Advanced global and regional chemical-transport models will be applied to derive the climatological state of air composition, specifically the average level of air pollutant levels based on existing emission inventories. An artificial intelligence pipeline will be designed to downscale air quality information in space and time, simulating sub-grid atmospheric processes. The system will account for fast-changing local forcing factors and provide predictive estimates of hourly air pollution variability relative to the climatology. Observational data from in-situ monitoring networks and remote sensing data will be used to train the QUALARIA system. Low-cost sensors will be deployed to increase the spatial coverage of the observational network. From its simulated and predicted pollutant concentration fields, QUALARIA will provide its users with relevant air quality indicators through an online interactive dashboard, informing about the impacts of air pollution in human health and activities.

AIR POLLUTION CONFERENCE BRAZIL
CMAS SOUTH AMERICA
COMMUNITY MODELING AND ANALYSIS SYSTEM

Keywords: artificial intelligence, air quality monitoring and prediction, street-level scale

INTRODUCTION

According to the World Health Organization (WHO), 91% of the world population lives in areas where air pollution exceeds international guideline limits, and every year approximately 4.2 million people die prematurely from outdoor air pollution. Based on 2016 pollution patterns from six Brazilian metropolitan regions, which constitute 23% of the country's population, the Brazilian Instituto Saúde e Sustentabilidade estimated the number of premature deaths due to air pollution to reach 128,000 between 2018 and 2025, costing R$51.5 billion ($9.8 billion) in productivity loss. In terms of mortality, air pollution has become one of the most acute environmental problems facing humanity today. Citizens in big cities are more vulnerable to the mortality and health risks caused by air pollution, due to the intense pollutant emissions by human activities and dense populations. São Paulo, being the most populous city in Brazil, is not only challenged by the local traffic emissions, but also under the threat from regional sources from the biomass burning from the states west of São Paul, e.g., Mato Grosso, Mato Grosso do Sul and Goiás. Air quality mitigation becomes one of the key concerns for city planning and public health in the metropolitan area.

In the past two decades, substantial efforts have been conducted to develop predictive models to provide forecasts of air quality, which allows regional and local decision-makers to take actions to adopt the necessary measures to decrease air pollution. Regional chemical transport models provide predicted fields at spatial resolutions typically between 5 and 50 km, and providing information for a large metropolitan area and its surrounding region (Gavidia-Calderón et al., 2024). The performance of these predictive models is considerably improved by assimilating observations and other locally refined input data (such as local emission inventories). Models can provide reliable short-term predictions for air quality and longer-term projections for the development of mitigation policies. However, citizens and stakeholders in public and private sectors often prefer to receive information for the relatively small area in which they live and/or work. Therefore, there are now significant attempts to further downscale the data provided by regional models into data that are valid at the city block and even the street scale. One downscaling attempt is to use data-driven approaches based on artificial intelligence (AI) and machine learning (ML) models. With the aid of high-resolution geospatial datasets, the distributions of air pollutants will be correlated to certain local spatial and temporal features. This ML approach also requires a dense coverage of available observations, of which local monitoring stations may not provide sufficient data for model training. The deployment of low-cost sensors provides a cost-effective solution to expand the observation capacities in diverse regions in the city. With the cost-effectiveness of data-driven models and low-cost sensors, the system can be easily adapted to any cities or regions in the world.

METHODS

The QUALARIA system, which is an AI-based air quality monitoring and forecasting system, will first be driven by climatological outputs of a regional chemical transport model (CTM) at spatial resolution of 10 km. An up-to-date refined emission inventory will be employed for the climatological simulations. A machine learning-based workflow using linear and non-linear feature extraction techniques (e.g., Principal Component Analysis (PCA) and Uniform Manifold Approximation and Projection (UMAP) (Martin et al., 2020) will be applied on different data sources, including high-resolution satellite images, network observations, CTM output data and local based emission data in artificial neural network models to simulate sub-grid scale atmospheric and chemical processes. The downscaling methodology will provide a high-resolution air quality monitoring and forecasts at street-level in the future 10 days. Low-cost sensors will be deployed throughout the city of São Paulo to expand the observational coverage and to increase the data volume available for the training of the AI-based air quality model. The forecast system will also provide air quality indicators in relation to city planning and public health, and long-term projection of air quality scenarios for mitigation purposes. Stakeholder engagement will be ensured in different production development phases, so that the online interactive dashboard can optimally fulfil the needs and requirements of the end-users in public and private sectors.

FINDINGS AND ARGUMENT

Currently, QUALARIA is deploying the BERNARD Air Analyser low-cost sensors in data-deficient areas that are not covered by the Air Quality Automatic Stations of the Environmental Company of São Paulo State (CETESB). Together with the CETESB stations, the high-resolution network of observational data of PM_{10}, $PM_{2.5}$, NO_2 and O_3 concentrations will be analysed to disentangle the spatio-temporal variability of air quality conditions over the city of São Paulo. On the other hand, QUALARIA will implement regional chemical-transport models initialised with reanalyses data and refined local emissions to capture the climatological variabilities

and long-range influence of relevant air quality parameters in the São Paulo Metropolitan Area and its surrounding area. Artificial Intelligence will then provide downscaling from the model-driven coarse-resolution air quality maps at a horizontal resolution of 10 km to street-level maps with an increased resolution to 100 m by generalising small-scale variabilities in time and space from high-resolution observational and auxiliary data. The QUALARIA system will account for fast-changing local forcing factors and provide predictive estimates of hourly air pollution variability relative to the climatology.

With the QUALARIA street-level air quality predictions, an interactive online dashboard will then be developed to disseminate relevant information of air quality monitoring and prediction in the Metropolitan Area of São Paulo, mainly targeting decision makers, legislators, and population as potential users. To achieve the optimal dashboard design, QUALARIA will invite public and private sector stakeholders to identify and co-develop dashboard features and to test different versions of the dashboard. The dashboard will provide relevant air quality indicators to its users and inform about atmospheric pollution impacts on human health and daily activities. With the Metropolitan Area of São Paulo as its first testbed, the QUALARIA system will be made applicable for other cities in the world.

CONCLUSIONS

QUALARIA will develop an efficient and accurate AI-based air quality monitoring and forecasting system that includes local and regional influences and generate hourly neighbourhood and street-level operational air quality monitoring and forecasting over the Metropolitan Area of São Paulo. By combining the benefits of regional chemical transport models and high-resolution network of observational data complementing in-situ monitoring network with low-cost sensors, the QUALARIA AI model will downscale coarse-resolution regional air quality maps to street level air quality monitoring and predictions at horizontal resolution of 100 m. The high-resolution monitoring and forecasting will then be displayed and disseminated through an interactive online dashboard with features and design co-developed by public and private stakeholders. The QUALARIA system will provide important air quality indicators to its users about air pollution impacts on their health and daily activities. The developed prototype system can also be applied to other regions of the world to provide a quick and efficient solution to monitor, predict and understand air pollution scenarios around the world.

REFERENCES

Gavidia-Calderón, Mario, Daniel Schuch, Angel Vara-Vela, Rita Inoue, Edmilson D. Freitas, Taciana Toledo de A. Albuquerque, Yang Zhang, Maria de Fatima Andrade, and Michelle L. Bell. "Air quality modeling in the metropolitan area of São Paulo, Brazil: A review." *Atmospheric Environment* 319 (2024): 120301.

Martin, Thomas C. M., Humberto R. Rocha, and Gabriel M. P. Perez. "Fine scale surface climate in complex terrain using machine learning." *Int J Climatol*. 41 (2021): 233–250.

AIR POLLUTION CONFERENCE BRAZIL
CMAS SOUTH AMERICA
COMMUNITY MODELING AND ANALYSIS SYSTEM

THE CO-IMPACTS OF DROUGHT AND HEAT WAVES ON WILDFIRES IN THE BRAZILIAN CERRADO BIOME

Katyelle F. S. Bezerra[1], Helber B. Gomes[1], Janaína M. P. Nascimento[2], Alessandro Banducci[3], Lucas H. S. Rocha[1], Hakki Baltaci[4], Maria Cristina L. Silva[1]

[1]*Institute of Atmospheric Sciences, Federal University of Alagoas, Maceió, Brazil*
Katyelle.silva@icat.ufal.br; helber.gomes@icat.ufal.br; lucas.santos@icat.ufal.br; cristina.lemos@icat.ufal.br

[2]*National Oceanic and Atmospheric Administration, Boulder, USA*
Janaina.nascimento@noaa.gov

[3]*Physics Department, Colorado State University, Boulder, USA*
alessandro.lindahl@gmail.com

[4]*Institute of Earth and Marine Sciences, Gebze Technical University, Kocaeli, Turkey*
baltacihakki@gmail.com

Abstract: The Cerrado biome is the second largest biome in South America and most of its territory represents the largest savannah in the world. It plays a vital role in the Brazilian ecosystem, harbouring a rich biodiversity and contributing significantly to stabilising the climate and water availability. The Cerrado biome has faced challenges as a result of climate change in the last decade, evidenced by extreme events such as prolonged heatwaves, periods of drought and an increased risk of fires. Given this context, this study aims to analyse the impact of compound drought and heatwave events on fires in the Brazilian Cerrado biome from 2012 to 2022. Monthly and annual analyses of heat waves (HW), Fire Radiative Power (FRP) and drought were carried out for 164 stations located in the Brazilian Cerrado biome. Maximum and minimum temperature and rainfall were observed data collected from the National Meteorological Institute (INMET), and the FRP variable was obtained from the Visible Infrared Imaging Radiometer Suite VIIRS satellite on board the NOAA-20 and the sunsynchronous Suomi NPP satellites. This study adopted the CTX90pct and CTN90pct calculations, which define a heatwave as a period of at least three consecutive days with maximum and minimum temperatures above the 90th percentile. To characterise drought events, we used the Standardised Precipitation Index (SPI) over periods of 6 and 12 months. In general, the results of the SPI-6 and SPI-12 analyses showed values throughout the series that varied from moderately humid to extremely humid, with the most intense values from January to March. Negative values indicate the presence of mild drought, with the most intense values from July to September. These periods coincided with more intense periods of heatwaves, resulting in a greater frequency of these events, especially in August, September and October. These periods of drought and heatwave events had a direct impact on the FRP variables. The month of July had the highest Fire Radiative Energy (FRE), which is considered a critical period of drought, which anticipates the months with the highest average FRP. Above all, the results highlight the urgent importance of understanding the joint dynamics of drought and heatwaves in order to better assess and prevent fires in this region.

Keywords: Compound events, fires, heatwaves, droughts, Cerrado bioma.

INTRODUCTION

The Cerrado biome, the second largest in South America and home to the largest savannah in the world, plays a fundamental role in the Brazilian ecosystem by contributing significantly to climate stability, water availability and biodiversity (DeBano et al., 1998). Although fires are a natural part of this biome, human intervention has drastically altered their patterns, impacting not only ecosystem structure, but also energy balance, biogeochemical cycles and human and economic health (Hantson et al., 2015). Studies have shown a clear relationship between fire activity and climate, with extreme events, such as the 2020 fires in the Pantanal, being the result of the interaction between extreme climatic conditions, such as heat and drought, and the inappropriate use of fire (Libonati et al., 2022). Given this scenario, this research aims to analyse the impact of compound drought and heatwave events on fires in the Brazilian Cerrado from 2012 to 2022, highlighting the importance of understanding this interaction for fire prevention and mitigation in the region.

METHODS

Monthly and annual analyses of heat waves (HW), Fire Radiative Power (FRP) and drought were carried out for 164 stations located in the Brazilian Cerrado biome (Fig. 1) during the period 2012-2022. Maximum and minimum temperature and rainfall were observed data collected from the National Meteorological Institute (INMET), and the 375m Fire Radiative Power (FRP) product from the Visible

Infrared Imaging Radiometer Suite VIIRS on board the NOAA-20 and Suomi NPP satellites, synchronous to the sun.

In this study, the CTX90 pct and CTN90 pct calculations were used to define a heatwave as a period of at least three consecutive days with maximum and minimum temperatures above the 90th percentile. To characterise drought events, the Standardised Precipitation Index (SPI) was used for periods of 6 and 12 months.

Fire patterns in the Cerrado were analysed based on FRP data greater than zero, excluding fires lasting less than 24 hours. A Machine Learning (ML) approach was used for clustering, as developed by Nascimento et al. (in prep), using the DBSCAN algorithm (Density-Based Spatial Clustering of Applications with Noise, ESTER et al., 1996).

In order to cluster fires using the DBSCAN algorithm, the latitude, longitude and time variables were transformed into the same Cartesian space. To do this, time was converted by multiplying it by an empirical constant with units of degrees per hour. This procedure resulted in the assignment of unique group identifiers (fire_id) to each fire detection point, allowing the identification and grouping of the FRP data points into different fires.

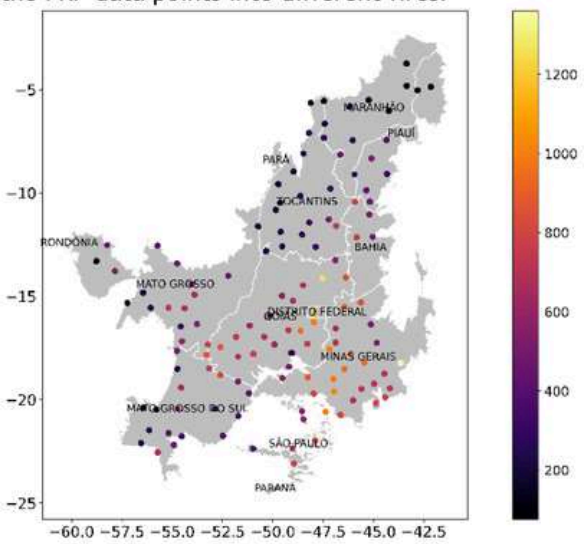


Figure 1. Study area: Brazilian Cerrado

FINDINGS AND ARGUMENT

Figure 2 shows the frequency and duration of heatwaves over the period studied. In Figure 2 (a), 2015 stands out as the year with the highest frequency (CTX90pct), attributed in part to the strong El Niño that occurred at the time. The years 2016, 2017, 2019 and 2020 also showed high frequencies. It is notable that, in most years, the duration of the heatwaves was greater than the frequency, with 2019 standing out in particular as having the longest duration during the period studied for CTX90pct.

Figure 2 (b) shows the frequencies and durations for CTN90pct. The year 2016 was marked by the highest frequency, although high frequencies were also observed in the years 2015, 2017, 2018, 2019 and 2020, with frequencies exceeding 200 heatwaves throughout 2012-2022. The analyses show long heatwave durations from 2015 onwards, with a decrease in 2022, returning to values close to those of 2012. This trend may be associated with inappropriate land use and deforestation (Geirinhas et al., 2017). According to Libonati (2022), heatwaves are increasingly related to droughts in the Northeast, Southeast, Amazon and the Brazilian Pantanal (Libonati et al., 2022).

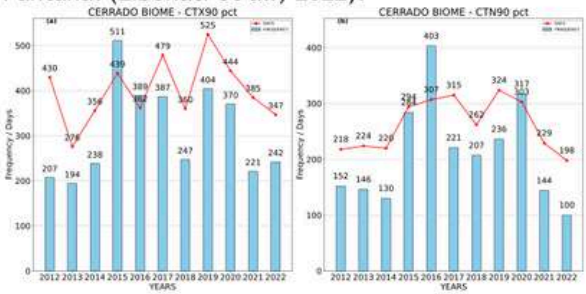


Figure 2. Annual heat wave frequency and duration in the Cerrado Biome: (a) CTX90pct and (b) CTN90pct

Figure 3 shows the seasonality of the frequency and duration of heat waves in the Cerrado, Fig. 3(a) refers to CTX90pct and Fig. 3(b) to CTN90pct. According to Fig. 3 (a), the highest frequencies occurred from August to December, with a peak in September, followed by October, where it can be seen that the duration of the OCs for September and October were similar. In Fig. 3 (b) the highest peak was in October, but the months of November and December also stand out. The months of January, February and March also showed high frequencies. As for the duration (in days) of the CTN90 pct, it was most intense in January and December, but showed high durations in the months of January to March and September to December. Some studies in Brazil agree and are in line with the higher occurrence and duration of OC in spring and summer in recent decades (Bitencourt et al., 2020; Oliveira et al., 2021).

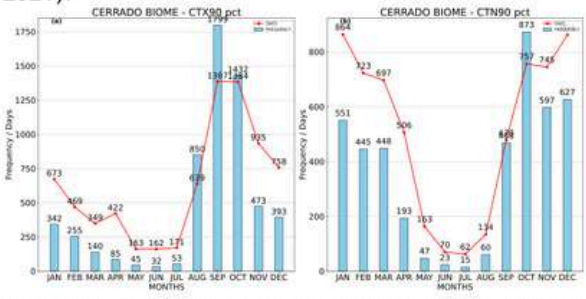


Figure 3. Frequency and monthly duration of heat waves in the Cerrado: (a) CTX90pct and (b)CTX90pct

To characterise drought events, the Standardised Precipitation Index (SPI) was used for 6 and 12 month periods. Analyses of the SPI-6 and SPI-12 revealed a variation in values throughout the series, ranging from moderately humid to extremely humid, with the most intense values recorded from January to March. The negative values indicate the presence of a mild drought, which in some years began in May and in others in June, persisting in most years until October and November.

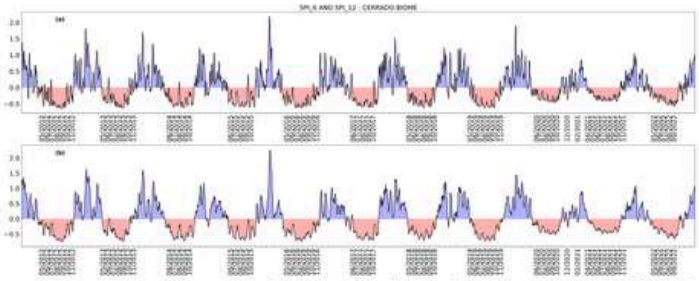


Figure 4. Standardised precipitation index (SPI): (a) SPI-6 and (b) SPI-12

Fig. 5 shows the climatology of the FRP. Regions with wider violins indicate a higher concentration of data, while narrow violins indicate a low concentration. The lower and upper ends of each violin represent the lower and upper limits of the data, respectively. It is noteworthy that the months of August, September and October recorded the highest average FRP, and the distribution over the months varies significantly. The Cerrado has a well-defined dry season which directly influences the fire regime.

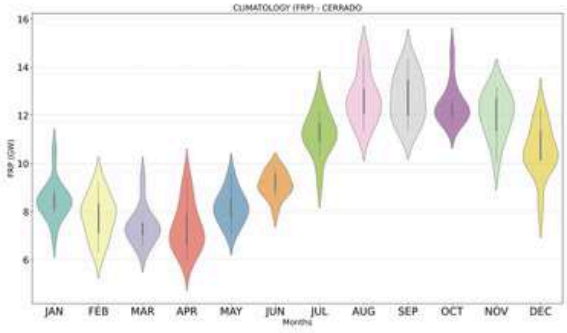


Figure 5. FRP climatology in the Cerrado during the period 2012-2022

Figure 6 shows the average fire radiative energy (FRE) over the months. The highest average is seen in July, which can be explained by the dry season in the Cerrado. This month sees a decrease in rainfall and an increase in temperatures, creating favourable conditions for the occurrence and spread of fires.
In addition, the months of August and September also show significant concentrations of FRE. This suggests that, even after the start of the drought in July, climatic conditions remain favourable for the spread of fires.

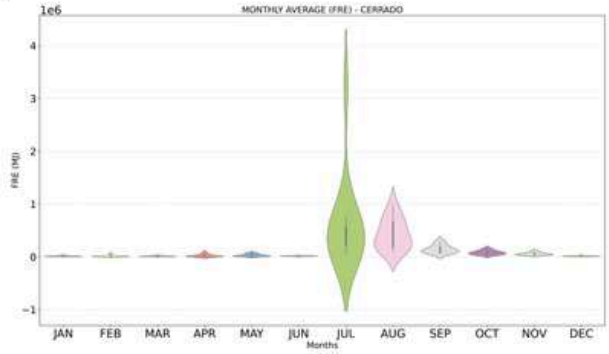


Fig 6. Average monthly Fire Radiative Energy (FRE) over the period 2012-2022

CONCLUSIONS

The results show that heatwave and drought events coincide with the fire season in the Cerrado, especially in August, September and October, increasingly impacting this region. Land use practices and deforestation are likely factors contributing to these trends. The dry season in the Cerrado, which influences the fire regime, further exacerbates the impact of these events.

REFERENCES

BITENCOURT, et al. The climatology of cold and heat waves in Brazil from 1961 to 2016. International Journal of Climatology, v. 40, n. 4, p. 2464-2478, 2020.
DeBano et al. (1998). The ERA-Interim reanalysis: configuration and performance of the data assimilation system. Q. J. R. Meteorol. Soc. 137, 553-597. https://doi.org/10.1002/qj.828
ESTER, M., KRIEGEL, H. P., SANDER, J., & XU, X. (1996, August). A density-based algorithm for discovering clusters in large spatial databases with noise. In kdd (Vol. 96, No. 34, pp. 226-231)
GEIRINHAS, J.L.; TRIGO, R.M.; LIBONATI, R.; COELHO, C.A.S.; PALMEIRA, A.C. Climatic and synoptic characterization of heat waves in Brazil. International Journal of Climatology, v. 38, n. 4, p. 1760-1776, 2017
Hantson, S., et al. (2015). Global fire size distribution is driven by human impact and climate. Glob. Ecol. Biogeogr. 24, 77-86. https://doi.org/10.1111/geb. 12246
Libonati, et al. (2020). Natureza 588, 217-219. http://dx.doi.org/ 10.1038/d41586-020-03464-1.
Libonati, R., et al. (2022). Assessing the role of compound drought and heatwave events on unprecedented 2020 wildfires in the pantanal. Environ. Res. Lett. 17, 015005. http://dx.doi.org/10.1088/1748-9326/ac462e.
NASCIMENTO J P., et al (in prep). Machine Learning Model for Forecasting Hourly Fire Radiative Power and Improving Biomass Burning Emissions in Air Quality Forecast Models.
OLIVEIRA, et al. (2021). Ondas de calor mais quentes, duradouras e frequentes: Um estudo observacional para a cidade brasileira de Campinas, São Paulo. Revista Brasileira de Meteorologia, v. 36, n. 2, p. 305-316, 2021.

PROCEEDINGS OF THE

2024 AIR POLLUTION CONFERENCE

And 5th CMAS South America

SESSION 09
Modeling to Support Exposure and Health Studies and Community-scale Applications

The purpose of this session is to present modeling approaches for various applications ranging from exposure assessments in support of health studies to near-source assessments such as near-roadway studies or community-scale applications. A variety of models can provide these detailed, spatially-, and temporally-resolved concentrations in support of environmental health studies. Models also provide an opportunity to examine how changes in emissions affect near-road air quality or other near-to-source impacts. Local governments and community groups may be interested in what if scenarios such as how to optimize traffic patterns around heavily polluted areas. For example, when schools are located near roadways, models can help to examine potential impacts on children's health or the relative contribution of school-related exposure compared to, or combined with, home-related exposure. The topics for this session will involve development, evaluation and application of models with the following focal areas:

- Air quality modeling for exposure assessments in support of environmental health studies
- Dispersion model development for applications with near-source complexities
- Evaluation and inter-comparison of models for near roadway applications
- Decision support tools to quantify risk of human exposure
- Air quality applications focused on inequitable pollution exposures in different communities

SESSION 09

RISK IDENTIFICATION FROM AIR TOXIC EMISSIONS IN THE TULA REGION, HIDALGO, MEXICO 192

AIREXPOSURE: AN R PACKAGE FOR AIR POLLUTION EXPOSURE ASSESSMENT CONSIDERING DYNAMIC VARIABLES 195

ANALYZİNG PM2.5 SOURCE AREAS THROUGH THE CONCENTRATİON WEİGHTED TRAJECTORY (CWT) MODEL DURİNG THE COVID-19 OUTBREAK İN SÃO PAULO 198

RISKS IDENTIFICATION FROM AIR TOXIC EMISSIONS IN THE TULA REGION, HIDALGO, MEXICO 201

AIR POLLUTION CONFERENCE BRAZIL
CMAS SOUTH AMERICA
COMMUNITY MODELING AND ANALYSIS SYSTEM

RISKS IDENTIFICATION FROM AIR TOXIC EMISSIONS IN THE TULA REGION, HIDALGO, MEXICO

Faviola Altúzar-Villatoro[1], José Agustín García-Reynoso[1]
[1]*Institute of Atmospheric Sciences and Climate Change, National Autonomous University of Mexico*
faviola.altuzar@atmosfera.unam.mx, agustin@atmosfera.unam.mx

Abstract: Industrial activity in the Tula de Allende region, Mexico, has resulted in high levels of air pollution, which could pose significant risks to human health and the environment. This study focuses on assessing the impact of air toxics emissions on public health, using data from industrial emissions and atmospheric dispersion models such as CALPUFF. Eight industries with significant emissions were identified, and it was found that the highest concentrations of heavy metals and organic compounds were located near the refinery and the power plant. Furthermore, the inhalation cancer risk was found to be at unacceptable levels at various sites, especially for nickel, chromium, and benzene. These findings highlight the need to take measures to control industrial emissions and protect the health of the population in this region.

Keywords: Risk assessment, air toxics, Tula.

INTRODUCTION

In Mexico, the Tula de Allende region in Hidalgo has been characterized by high industrial activity, which has resulted in it being considered one of the most polluted areas in the country (Vega et al., 2021). However, in terms of health risk assessment from air toxics (pollutants that even in small concentrations, are known or suspected to cause cancer or other serious health damage (US EPA, 2018)), limited information is available.

On the other hand, in a summary of studies on the relationship between cancer mortality and industrial emissions in Spain reported in the European Pollutant Release and Transfer Register, it was suggested that there is an excess of cancer mortality of approximately 17% in regions exposed to industrial emissions compared to those that are not. However, it's important to note the limitations of these findings, particularly the omission of meteorological and topographical variables (Fernández-Navarro et al., 2017). One way to take them into account, is the use of pollutant dispersion modeling, and one of these models is CALPUFF, which is of puff, Lagrangian, Gaussian, non-stationary type, which has been employed in different applications (Arregoces et al., 2018).

The objective of this study was to estimate the risk of cancer and non-cancer health effects due to exposure to air toxics. The aim was to determine whether populations residing near industrial sources are at risk of developing cancer and/or experiencing chronic non-cancer effects.

METHODS

2.1 Identifying Establishments Reporting Air Toxics in the PRTR.

The PRTR 2019 database was reviewed, where the industrial facilities present in the study area that emitted air toxics were identified, as well as the quantities reported.

2.2 Identification of establishments requiring risk assessment.

Scores for carcinogenic effects (S_{cancer}) and chronic non-cancer effects ($S_{noncancer}$) were calculated to identify companies requiring detailed risk assessments. The following equations were utilized for this purpose (Gratt, 1996):

$$S_{cancer} = \sum_c (Q_c)(URF_C)(RP)(1.7x10^3) \quad \text{Eq. 1}$$

$$S_{noncancer} = \sum_c (\frac{Q_c}{RELc})(RP)(150) \quad \text{Eq. 2}$$

Where:
Q_c = emission rate of chemical c (lb/year);
URF_C = Unit Risk Factor of chemical c $(\mu g/m^3)^{-1}$;
REL_C = Reference exposure level of chemical c with chronic toxicity ($\mu g/m^3$);
RP = receptor proximity adjustment factor (dimensionless).

Qc emissions were obtained from the PRTR; URFc and chronic RELc values were obtained from the Consolidated Table of California Office of Environmental Health Hazard Assessment/ California Air Resources Board Approved Risk Assessment Health Values (CARB, 2022). The proximity factor (RP), which refers to the distance from the source to the nearest receptor, was assumed to be approximately 100 to 250 m, corresponding to an RP of 0.25 (Gratt, 1996). Finally, the industries were classified according to the criteria listed in Table 1.

Table 1. Classification criteria according to the obtained score.

S_{cancer}	$S_{noncancer}$	Classification
> 100	> 10	Required assessment
≥10 to ≤ 100	≥ 1 to ≤ 10	Potential candidates for assessment
< 10	< 1	Probably no need for assessment

Reference: Gratt, 1996.

2.3 Annual average concentrations of air toxics.
To derive concentrations in the area, we employed Version 6 of the CALPUFF model. Prior to this, meteorological data was processed using the WRF (Weather Research and Forecasting) model, utilizing data from the North American Mesoscale Forecast System (NAM) at a 12 km resolution. The CALMET module was then executed using the WRF results to generate meteorological data for the study area utilized by CALPUFF. Emissions data were sourced from the PRTR 2019. This process involved defining a domain covering 26 x 26 km with a resolution of 1 km was defined, covering both industrial plants and the surrounding towns.

In the CALPUFF module, sources were entered as area sources. And the localities of Apaxco, Atitalaquia, Atotonilco, Bomintzha, Jasso, La Joya, Tlaxcoapan, and Tula de Allende were designated as discrete receptors.

2.4 Risk characterization
Cancer Risk
Cancer Risk (R_{cancer}) was estimated through the application of the following equation (EPA, 2018):

$$R_{cancer} = Exposure\ concentration * URF \quad \text{Eq. 3}$$

Where Rcancer is the probability of an individual developing cancer due to exposure to an atmospheric toxicant, in addition to the overall risk of suffering cancer. Likewise, assuming that the population surrounding the identified industries is simultaneously exposed to all the substances reported in the PRTR, the total cancer risk was estimated as follows (EPA, 2018):

$$R_{total-cancer} = \sum_{c=1}^{n} Conc._c * URF_c \quad \text{Eq. 4}$$

In this work, R_{cancer} or $R_{total\text{-}cancer}$ is considered acceptable when it is less than $1x10^{-6}$. Furthermore, in order to have a better understanding of R_{cancer}, different metrics were used, such as Cancer Population Risk (CPR), which is the increase in the number of cancer cases; or the loss of life expectancy (LLE), which indicates the number of days subtracted from life expectancy. The CPR was obtained by multiplying Rtotal-cancer by $1x10^6$ (assuming an exposed population of 1 million), while the LLE was estimated with the equation (Gratt, 1996):

$$LLE = 1.1x10^6 * R_{total-cancer} \quad \text{Eq. 5}$$

Non cancer Risk
The hazard quotient (HQ) was used to characterize the non-carcinogenic chronic effects risk, with the equation (EPA, 2018):

$$HQ_c = \frac{Exposure\ concentration}{REL_c} \quad \text{Eq. 6}$$

HQ is applicable for an individual pollutant, whereas, for exposure to multiple substances, the hazard index (HI) was used which is equal to the sum of all HQs:

$$HI = \sum HQ_c \quad \text{Eq. 7}$$

When HQ or HI is less than 1, it indicates that the risk is acceptable, while a value greater than 1 indicates the extent to which the reference level is exceeded, so there is a possibility of adverse health effects. (EPA, 2018).

Spatial distribution of cancer risk
Finally, with the distribution of concentrations obtained through CALPUFF in the study region, the areas cancer risk levels were identified.

FINDINGS AND ARGUMENT

3.1 Industries in RETC that reported air toxics
Eight industries emitting air toxics were identified in the region: an oil refinery, a thermal power plant, three cement factories (Cemex, Cruz Azul, and Holcim), a rubber articles factory, a lime factory, and a hazardous waste collection company called Actium. Together, they reported the emission of 11 air toxics: arsenic, cadmium, chromium, mercury, nickel, furans, benzene, dioxins, formaldehyde, acetaldehyde and lead. The refinery and the power plant reported the highest emissions, corresponding to nickel, formaldehyde, and acetaldehyde, while Cemex and Holcim reported the highest values of benzene.

3.2 Industries requiring a risk assessment
Based on the scores for carcinogenic effects and chronic non-carcinogenic effects shown in Table 2, the lime factory and the rubber industry were discarded in order to continue the risk assessment of the rest of the establishments.

Table 2. Scores of carcinogenic and chronic non-carcinogenic effects.

Nombre	S_{cancer}	$S_{noncancer}$
Oil refinery	46,808	166,636,880
Thermal power plant	25,381	83,388,510
Cemex	8,356	261,742
Actium	237	699
Cruz Azul	48.0	113,811
Holcim	42.9	75,406
Lime factory	0.0314	1.823
Rubber industry	0.0007	0.0422

3.3 Annual average concentrations of air toxics
The results of the CALPUFF modeling show that the highest concentrations correspond to Ni, which is emitted by the refinery and the thermoelectric plant. Figure 1 shows the annual average concentration isolines for this metal, where it can be seen that the emissions from the aforementioned sources are distributed towards the south-

southwest, reaching the town of Bomintzha, where the highest average concentrations of most pollutants were recorded, with the exception of benzene, dioxins and furans. On the other hand, the lowest concentrations were recorded in Tula.

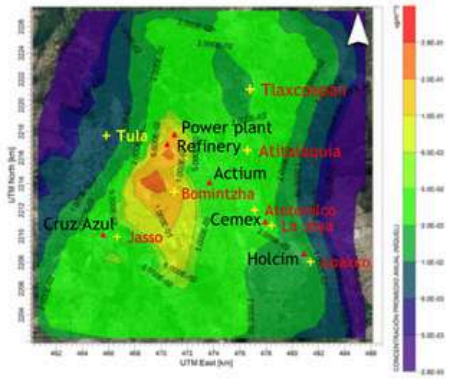


Figure 1. Nickel annual average concentration isolines during 2019

3.4 Risk characterization

In all populations, the R_{cancer} due to Cr and Ni, exceeded acceptable level, although in La Joya and Apaxco, there was also an unacceptable R_{cancer} due to benzene. The highest $R_{total\text{-}cancer}$ was found in Bomintzha, corresponding to a CPR of approximately 275 new cancer cases in the population as a result of inhaling the reported air toxics. Figure 2a shows the increase in the number of cancer cases per million inhabitants in each population, it can be observed that Tula has the lowest number of cases. Additionally, it was found that the range of days subtracted from life expectancy was from 15 to 302 (Fig. 2b).

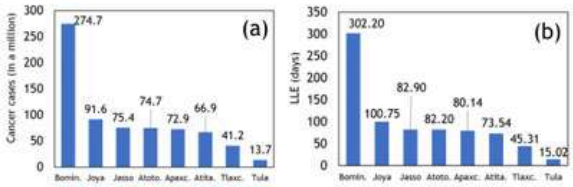


Figure 2. (a) Cancer cases (in a million) and (b) LLE (days) per locality

Regarding the non-cancer risk, Ni was the only pollutant with a HQ greater than 1 in almost all sites (except for Apaxco and Tula). The difference between HI and HQ ranged from 1.5 to 0.2%, which could indicate a low contribution to Rnon-cancer from the other substances. These results indicate the possibility of adverse health effects. Once again, Bomintzha recorded the highest HQ.

With respect to the spatial distribution of unacceptable R_{cancer}, it was found that, for Ni and Cr, this area covers almost the entire study domain, while for benzene, it only extends in the vicinity of the emission sources (Cemex and Holcim). Figure 3 shows the ranges of chromium inhalation cancer cases that could occur in the area. These results suggest that besides the sites considered as receptors, other communities could also be at risk of developing cancer.

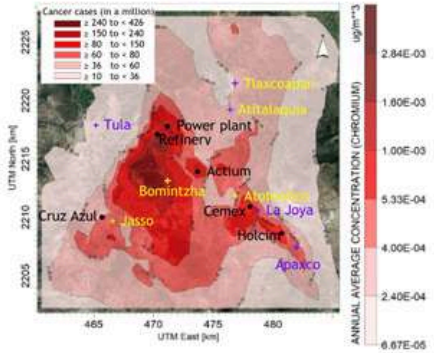


Figure 3. R_{cancer} spatial distribution due to chromium inhalation.

CONCLUSIONS

The results suggest that emissions of some air toxics reported in the RETC may affect the health of the population located around industrial establishments, with Cr, Ni, and benzene being the pollutants representing the highest cancer risk, in addition to the chronic effects produced by Ni. Therefore, it is important to pay greater attention to controlling the emissions of these pollutants in order to protect the people health. Finally, it is necessary to mention that one of the limitations of this work is the lack of evaluation of the model's performance since there are no measurements of the substances evaluated during the study period.

REFERENCES

Arregoces, Heli A., Mendoza, Yoma I. and Rojano, Roberto E. *"Evaluación del CALPUFF para Estimar Concentraciones Ambientales de PM10 de una Cantera en Terrenos Complejos."* Información Tecnológica 29(5) (2018): 131-142.

California Air Resources Board. *Consolidated table of OEHHA/CARB approved risk assessment health values.* (2022).

Environmental Protection Agency. *Technical Support Document EPA's Air Toxics Screening Assessment 2018 AirToxScreen TSD.* (2018).

Fernández-Navarro, P., García-Pérez, J., Ramis, R., Boldo, E., and López-Abente, G. *"Industrial pollution and cancer in Spain: An important public health issue".* Environmental Research 15 (2017): 555-563. https://doi.org/10.1016/j.envres.2017.08.049

Gratt, Lawrence B. *Air. Toxic risk Assessment and Management: public health risks from normal operations.* Estados Unidos: Wiley, 1996.

Vega, E., López-Veneroni, D., Ramírez, O., Chow, J. C., and Watson, J. G. *"Particle-bound PAHs and chemical composition, sources and health risk of $PM_{2.5}$ in a highly industrialized area".* Aerosol and Air Quality Research, 21(10), (2021): 1-24. https://doi.org/10.4209/AAQR.210047

AIR POLLUTION CONFERENCE BRAZIL
CMAS SOUTH AMERICA
COMMUNITY MODELING AND ANALYSIS SYSTEM

AirExposure: AN R PACKAGE FOR AIR POLLUTION EXPOSURE ASSESSMENT CONSIDERING DYNAMIC VARIABLES

Josefina Urquiza[1,2], María Florencia Tames[1], Enrique Puliafito[1,2], Sebastian Diez[3], Maela Lupo[2,4], Alfredo Rigalli[2,4]

[1] *Grupo de Estudios de la Atmósfera y el Ambiente (GEAA), Universidad Tecnológica Nacional, Facultad Regional Mendoza (UTN-FRM)*

jurquiza@conicet.gov.ar

mtames@mendoza-conicet.gob.ar

epuliafito@frm.utn.edu.ar

[2] *Consejo Nacional de Investigaciones Científicas y Técnicas (CONICET)*

[3] *Universidad del Desarrollo, Chile*

sebastian.diez@udd.cl

[4] *Centro Universitario de Estudios Medioambientales (CUEM)*

maela.lupo@gmail.com

arigalli@unr.edu.ar

Abstract: Atmospheric pollution faces significant spatial and temporal variability, especially concerning vehicular pollutants. This complexity limits the accuracy of the assessment due to the lack of reliable data and challenges associated with collecting high-resolution information. Taking this issue into account, we've created AirExposure, an open-source model based on the .R language. The aim of this model is to estimate exposure to atmospheric pollutants using dynamic variables.

The approach of AirExposure focuses on integrating people's daily activities, urban mobility, and hourly concentrations of specific pollutants in urban areas. The model requires users to input information about their daily activities and the modes of transportation used, including details about origins and destinations as well as activity schedules. One of the most important settings employed by AirExposure is the TomTom API. TomTom API is a free Application Programming Interface (API) provided by TomTom which facilitates the creation of urban mobility patterns, providing a more comprehensive and detailed view of movements within urban environments based on user-entered data. It provides, through the programming language (in our case .R), real-time traffic data and allows for the calculation of optimal routes between two or more locations, considering real-time traffic, type of transportation, and other user-input preferences.

As input data, users must provide their own hourly concentration maps to enhance the accuracy of exposure estimation at specific sites of interest. These maps should be grids stored in shapefile format for each hour of the day. The atmospheric pollutants considered thus far are the criteria pollutants: carbon monoxide (CO), nitrogen dioxide (NO_2), particulate matter ($PM_{2.5}$ and PM_{10}), ozone (O_3), sulfur dioxide (SO_2) due to their potential health effects on the population.

The model results highlights that excluding information about human mobility and the spatiotemporal variability of air pollution, could lead to inaccurate estimations of total exposure, biasing health risk assessments. In contrast, AirExposure's innovative approach represents a more realistic assessment of personal exposure levels and potential health effects.

The results obtained through AirExposure hold significant potential for diverse applications such as socio-environmental vulnerability analysis, health studies, and decision-making processes. This tool not only provides a more precise and detailed view of air pollution exposure but also offers a better approximation of the real geographic and temporal context in which individuals are exposed to these pollutants, thereby enhancing comprehension and decision-making in this critical field.

Keywords: Urban mobility, Human exposure, Atmospheric pollutants, Daily activities.

INTRODUCTION

In urban areas, air pollution is a growing problem, and public concern has significantly increased in recent years. Atmospheric pollution has become one of the leading causes of serious health issues, including cardiovascular diseases and respiratory problems (Manisalidis et al., 2020). For air pollution, exposure occurs whenever a person breathes air containing traces of one or more contaminants (Bigazzi & Figliozzi, 2014). Traditionally, studies evaluating exposure to air pollutants have relied on pollutant measurements from specific locations, focusing on residential sites (Gorai et al., 2014; Pinichka et al., 2017). These studies provide valuable information about the potential health effects of pollutants. However, this approach has some limitations because it uses static variables that do not consider the spatio-temporal variation of pollutants and the interactions between pollutants and people (Lu, 2021; Nyhan et al., 2019). In particular, this approach assumes that people do not move, so the estimation is limited to measurements of concentrations at home, excluding areas beyond the neighborhood. In recent years, the importance of using dynamic variables to estimate exposure has been emphasized, taking into account activity patterns and the variability of pollutants(Park & Kwan, 2017).

Therefore, we present *AirExposure* package, a tool developed in .R language incorporating an innovative model for estimating exposure to atmospheric pollutants with dynamic variables. Its aim is to integrate daily activities, urban mobility, hourly pollutant concentrations, and other conventional parameters. Additionally, the model includes an approach enabling exposure assessment through static variables while considering residential location. Thus, this work aims to: 1) introduce AirExposure to .R users; 2) provide details on the model and its implementation; 3) demonstrate AirExposure's usage through sample data analysis.

METHODS

In the package, two methodologies are presented: i) static variables; ii) dynamic variables.

Static exposure assessment

Where the average concentrations over 24 hours are used, assigning them to people's residences.

$$E_i = \sum_{j=1}^{m} T_{ij}\, C_{ij} \qquad \text{(Eq. 1)}$$

Where T_{ij} is the time that an individual i spends in each environment j (24 h), C_{ij} is the concentration experienced by individual i in the environment j, E_i represents the time-integrated exposure of a person i, and m is the number of environments considered (i.e. the address location).

Dynamic exposure assessment

Exposure with dynamic variables takes into account three moments: i) origin; ii) commuting; and iii) destination(s). During these moments, varying concentrations in time and space are expected.

$$E'_i = E_{ori} + E_{com} + E_{dest} \qquad \text{(Eq. 2)}$$

Where exposure at origin point is calculated as:

$$E_{ori} = \sum_{t_{i=0}}^{t_i = T_0} C_i\,(s_o, t_i) x\, \Delta t\,(s_o, t_i) \qquad \text{(Eq. 3)}$$

Where E_{ori} is the hourly mean concentration at the individual's residence (C_{ori}), multiplied by the mean time that the person spends at home (T_{ori}). The commuting exposure is the sum of the concentration $C_i(s_i,t_i)$ multiplied by the exposure time (Δt) for each path segment(s) between origin and destination:

$$E_{com} = \sum_{i=1}^{i=n} C_i\,(s_i, t_i) x\, \Delta t\,(s_i, t_i) \qquad \text{(Eq. 4)}$$

where $C(s,t)$ is the concentration for segment s_i at time t_i; $s_i = (x_i,y_i)$ is the position of each segment coordinates; and $\Delta t(s_i,t_i)$ is the time spent in each segment; n is the number of possible segments in each path. After concluding all activities at each destination, the return home is calculated, taking into account the point of origin. This parameter is configured through the free TomTom API, allowing users to select the mode of transportation (e.g., car, walking) and route preference (e.g., fastest). The destination exposure represents the sum of the hourly concentrations of the pollutant at each destination point (C_{dest}), multiplied by the duration of each activity considered (T_{dest}).

$$E_{dest} = \sum_{j=1}^{m} T_{dest}\; C_{dest} \qquad \text{(Eq. 5)}$$

Figure 1 shows the space-time representation of the models in the *AirExposure* package.

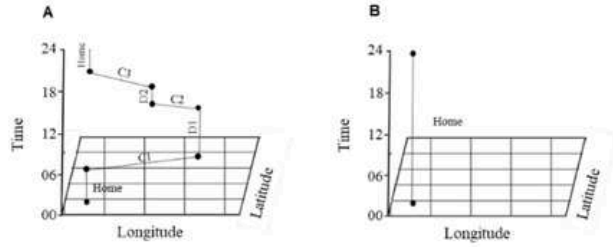


Figure 1. Representation. A: dynamic variables model. B: Static exposure assessment.

FINDINGS AND ARGUMENT

Below, practical examples will be presented on how to use some functions of the *AirExposure* package.

Request about commuting alternatives

The commuting information is retrieved using the *trajectories_tomtom* functions through the Tom-Tom API. Subsequently, the *alternative_trajectories* function present it in a more user-friendly visualization. Figure 2 shows an interactive grid map featuring different routes classified for August 1, 2018, at 3:00 PM, presented in HTML format. The map on the left displays travel alternatives by car, while walking routes are on the right. In the upper right corner, there is a checkbox that allows users to show or hide the different travel alternatives. It can be observed that there are more routes on the left than on the right, for the same input data. This is because in some cases, the options may overlap. For example, the fastest route might coincide with the most polluted. Also, there are distinctions between the travel options, as walking considers sidewalks, parks, and pedestrian areas, which avoid streets with vehicles. Regarding the grid color, it represents a color palette indicating pollutant concentration levels, as determined by the EPA's AQI. In these maps, $PM_{2.5}$ concentrations are visualized.



Figure 2. Output of *alternative_trajectories* function.

In Table 1, a selection of the model output detailing the exposure in each available route is presented. It is observed that in *alternative_1*, both the concentration and exposure are significantly lower (0.11 $\mu g/m^3$, 0.07 $\mu g/m^3$ h) compared to *alternative_3* (8.83 $\mu g/m^3$, 6.58 $\mu g/m^3$ h), where

the values are over 100% higher. However, one point to consider is that this will also depend on the hourly maps and the pixel size to be considered by the user.

Table 1. Output of *alternative_trajectories*.

Alternative	Concentration	Exposure
alternative_1	0.11	0.07
alternative_3	8.83	6.58

Dynamic exposure assessment

The estimation of exposure to air pollutants from dynamic variables is carried out by the *total_exposure()* function. This function estimating exposure at three moments mentioned through an iterative process. Although the input parameters are very similar to those presented above, in this case, the information for the entire 24-hour period is detailed. Figure 3 illustrates the output of the function in an interactive map format. The map on the right represents travel by car, while the one on the left shows results for bicycle travel. At the top edge, a box summarizes the daily exposure according to the entered pollutant, as well as the total time at each moment of interest. Although the results reflect minimal differences in exposure, it is crucial to note that most points along the route show low concentration levels in this sector. On the other hand, the background pollutant map is based on a daily average obtained from the 24 hourly grids.



Figure 3. Output of the total_exposure function

Traditional exposure assessment

The *traditional_model* function allows us to calculate the total daily exposure using a traditional methodology, where it is assumed that a person remains at home or nearby throughout the day. Using the same input data as in the calculation of total exposure with dynamic variables, we obtained a daily concentration of 41.36 µg/m³ over 24 hours. Comparing these results with those obtained previously, we see that exposure considering mobility by car is 29.35% higher, while by foot it is 26.82% higher than exposure calculated with the traditional methodology. This suggests that our approach provides more realistic results as it takes into account mobility and travel in daily exposure.

CONCLUSIONS

AirExposure package presents an alternative tool for studying exposure to atmospheric pollutants based on dynamic variables. The set of functions in the package facilitates the estimation process, taking into account mobility and spatiotemporal variability of pollutants. The traditional method of exposure estimation based on residence is a preliminary approach for individuals with low mobility. However, we believe that ignoring human mobility, variations in air pollution, or both may introduce biases in exposure estimation.

REFERENCES

Bigazzi, A. Y., & Figliozzi, M. A. (2014). Review of Urban Bicyclists' Intake and Uptake of Traffic-Related Air Pollution. *Transport Reviews*, *34*(2), 221–245. https://doi.org/10.1080/01441647.2014.897772

Gorai, A. K., Tuluri, F., & Tchounwou, P. B. (2014). A GIS based approach for assessing the association between air pollution and asthma in New York State, USA. *International Journal of Environmental Research and Public Health*, *11*(5), 4845–4869. https://doi.org/10.3390/ijerph110504845

Lu, Y. (2021). Beyond air pollution at home: Assessment of personal exposure to PM2.5 using activity-based travel demand model and low-cost air sensor network data. *Environmental Research*, *201*(May), 111549. https://doi.org/10.1016/j.envres.2021.111549

Manisalidis, I., Stavropoulou, E., Stavropoulos, A., & Bezirtzoglou, E. (2020). Environmental and Health Impacts of Air Pollution: A Review. *Frontiers in Public Health*, *8*(February), 1–13. https://doi.org/10.3389/fpubh.2020.00014

Nyhan, M. M., Kloog, I., Britter, R., Ratti, C., & Koutrakis, P. (2019). Quantifying population exposure to air pollution using individual mobility patterns inferred from mobile phone data. *Journal of Exposure Science and Environmental Epidemiology*, *29*(2), 238–247. https://doi.org/10.1038/s41370-018-0038-9

Park, Y. M., & Kwan, M. P. (2017). Individual exposure estimates may be erroneous when spatiotemporal variability of air pollution and human mobility are ignored. *Health and Place*, *43*(September 2016), 85–94. https://doi.org/10.1016/j.healthplace.2016.10.002

Pinichka, C., Makka, N., Sukkumnoed, D., Chariyalertsak, S., Inchai, P., & Bundhamcharoen, K. (2017). Burden of disease attributed to ambient air pollution in Thailand: A GIS-based approach. *PLoS ONE*, *12*(12), 1–18. https://doi.org/10.1371/journal.pone.0189909

AIR POLLUTION CONFERENCE BRAZIL
CMAS SOUTH AMERICA
COMMUNITY MODELING AND ANALYSIS SYSTEM

ANALYZİNG $PM_{2.5}$ SOURCE AREAS THROUGH THE CONCENTRATİON WEİGHTED TRAJECTORY (CWT) MODEL DURİNG THE COVID-19 OUTBREAK İN SÃO PAULO

Anderson P. Rudke[1], Ronaldo A. Alves[2], Leila D. Martins[3], Jorge A. Martins[3], Taciana T. De Almeida Albuquerque[1]
[1]*Federal University of Minas Gerais*
rudke@ufmg.br, taciana@desa.ufmg.br
[2]*State University of Londrina*
ronaldo.adriano@uel.br
[3]*Federal University of Thechnology - Paraná*
leilamartins@utfpr.edu.br, jmartinseae@gmail.com

Abstract: Due to the high transmission rate of the virus causing COVID-19 (SARS-CoV-2), several measures were adopted to reduce its spread, among which mobility restrictions were highlighted. These measures, besides proving effective in reducing viral transmission, had a significant impact on decreasing pollutant levels in major urban centers, owing to the substantial reduction in vehicular traffic. In São Paulo, one of the world's largest urban centers, significant reductions in primary pollutants such as carbon monoxide (CO) and nitrogen oxides (NO_X) were observed during the restriction period. However, surprisingly, some areas experienced increases in fine particulate matter ($PM_{2.5}$) concentrations, indicating a complex dynamic of atmospheric pollution sources. Given this scenario and considering the relevance of $PM_{2.5}$ to human health, particularly amidst the mobility restrictions imposed by the pandemic, this study proposed a detailed assessment of $PM_{2.5}$ sources using the Concentration Weighted Trajectory (CWT) model. The analysis period covered the phase of the strictest mobility restrictions, spanning from March 16 to June 30. Trajectories of air masses at 100 m and 1000 m above ground level (AGL) reaching São Paulo were meticulously considered. The HYSPLIT dispersion model, coupled with the CWT model, was utilized to gain a deeper understanding of the origins and transport patterns of pollutants. Air quality monitoring stations (20) distributed across the State of São Paulo served as the locations of arrival of the air masses. Analyses included not only air mass trajectories but also the Weighted Average Concentration (WAC) of particles, providing a comprehensive view of sources and impacts on air quality. CWT results indicated that regions with significant emissions from biomass burning had a notable impact on pollutant concentrations in São Paulo. These elevated concentrations were attributed primarily to airflows from the northwest and west directions, traversing biomes such as the Pantanal, as well as territories in Bolivia and Paraguay. While the impact of biomass burning is evident, the analysis of primary pollutant sources (WAC) revealed that local sources, including nearby biomass burning, played a more prominent role in concentrations than fires in remote areas. WAC analysis also highlighted that the influx of air masses from regions like Minas Gerais, Rio de Janeiro, and São Paulo is crucial for pollutant transport to the receptor site, adding to local emissions. Therefore, although the impact of wildfires on particle concentrations in São Paulo is notable during specific times of the year, it seems that they did not have a significant impact during the strictest mobility restrictions imposed by the COVID-19 pandemic. Consequently, $PM_{2.5}$ concentrations during that time appear to be more influenced by local sources, particularly industrial and biomass burning, as well as regional sources, especially from Rio de Janeiro and Minas Gerais. These results underscore the complexity of the interaction between atmospheric emissions, meteorological patterns, and local responses to human interventions, providing valuable insights into understanding atmospheric pollutant behavior in urban contexts and during significant global events such as the COVID-19 pandemic.

Keywords: Weighted Average Concentration, Concentration Weighted Trajectory, Mobility Restrictions, Biomass Burning.

INTRODUCTION

The emergence of the COVID-19 pandemic in late 2019 brought about unprecedented changes in human behavior and societal operations worldwide (Pak et al., 2020; The Lancet, 2020). As governments implemented strict lockdown measures to curb the spread of the virus, significant alterations in daily activities, transportation patterns, and industrial operations ensued (Blumenthal et al., 2020; de Oliveira Andrade, 2020). One notable consequence of these measures was the substantial impact on air quality across various regions globally (Collivignarelli et al., 2020; Gkatzelis et al., 2021).

In the context of São Paulo state, home to one of the world's largest urban hubs, São Paulo city, studies unveil a persistent reality, albeit with varying intensity across different timeframes (Rudke et al., 2021, 2022, 2023). While there's been a decline in primary pollutants like CO and NO_x, there's been a notable surge in $PM_{2.5}$ and O_3 ozone concentrations (Rudke et al., 2021, 2022). This uptick in O_3 has been noted not only in São Paulo but also in numerous other regions, particularly in major urban centers, and is linked to alterations in ozone formation regimes (VOC-limited and NO_x-limited regimes) (Rudke et al., 2021, 2022). Conversely, evidence is lacking regarding the factors driving $PM_{2.5}$ concentration increases, even during mobility restrictions.

Amidst the significance of $PM_{2.5}$ concerning human health, especially in light of pandemic-induced

mobility restrictions, this study embarks on a comprehensive examination of $PM_{2.5}$ sources. Employing the Concentration Weighted Trajectory (CWT) model, we aim to provide detailed insights. The analysis encompasses the period of the strictest mobility constraints, spanning from March 16 to June 30. Consequently, our research seeks to elucidate the intricate dynamics of $PM_{2.5}$ pollution during this critical timeframe, shedding light on its sources and contributing factors.

METHODS

The HYSPLIT model (Stein et al., 2015) of the National Oceanic and Atmospheric Administration (NOAA) was used to assess the backward atmospheric trajectories, thereby enabling the inference of pollutant origins and their long-range transport. In this sense, 3-day backward atmospheric trajectories were used to verify wildfire smoke originating in South America's northern and central regions. Seeking to evaluate the impacts on the surface observed by the air quality stations, trajectories of air masses reaching São Paulo at 100 m Above Ground Level (AGL) were considered. The trajectories obtained through HYSPLIT were used together with the Concentration Weighted Trajectory (CWT) algorithm (Brereton & Johnson, 2012; Hsu et al., 2003) to locate significant sources of pollutants degrading air quality in São Paulo. The Weighted Average Concentration (WAC) (Brereton & Johnson, 2012) was also used to locate the sources of pollutants that had the most impact for the period. In these stages, the locations of the air quality monitoring stations capable of monitoring PM2.5 (20) were considered the places of arrival of the air masses. The equations and more information about CWT and WAC can be obtained from (Brereton & Johnson, 2012).

The fire outbreaks provided by the National Institute for Space Research (INPE, accessible at: https://terrabrasilis.dpi.inpe.br/queimadas/) were evaluated to assess the impact of the wildfires that occurred during the period. The wildfire data, the assessment of $PM_{2.5}$ concentrations, and the application of CWT and WAC techniques considered the period with the strictest mobility restrictions (from March 16 to June 30, 2020).

FINDINGS AND ARGUMENT

The CWT algorithm was used to evaluate the primary sources of $PM_{2.5}$ and the effect of biomass burning on their concentrations. The results of the model that uses air mass trajectories at 100 m height from HYSPLIT are shown in **Error! Reference source not found.**. It is observed that regions with high biomass burning emissions (**Error! Reference source not found.**) impacted the concentrations of $PM_{2.5}$ analyzed for São Paulo. High air pollutant concentrations related to biomass burning are mainly attributed to northwest and west airflows through the Pantanal biome, besides Bolivia and Paraguay. The high number of fire outbreaks in the Pantanal was reported worldwide due to the unprecedented devastation of the Biome (da Silva Junior et al., 2020; Ferreira Barbosa et al., 2022; Marques et al., 2021). In addition, fires in this region were associated with deteriorating air quality in several Brazilian states, such as São Paulo, Rio de Janeiro, and Paraná (Beringui et al., 2022; Rudke et al., 2021). These findings corroborate previous studies that demonstrate the impacts of long-range transport of pollutants emitted from burning biomass areas over South America, especially those originating in the Amazon and central-west region of Brazil, and their effects on southern and southeastern regional air quality (Martins et al., 2018; Vara-Vela et al., 2018). Some of these studies show that fires significantly impact São Paulo, doubling the $PM_{2.5}$ concentrations compared to the period without fire episodes.

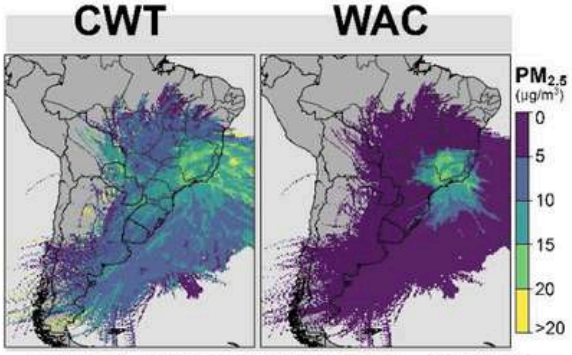


Figure 1. CWT and WAC for $PM_{2.5}$ at 100 m.

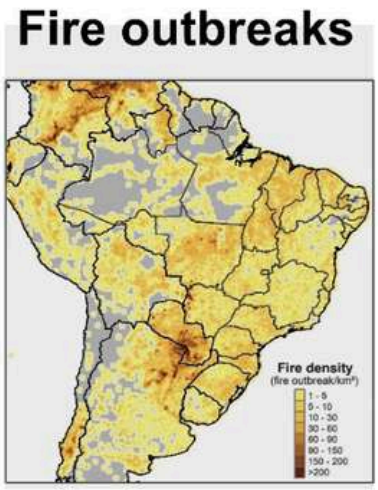


Figure 2. Spatial distribution of the fire outbreaks density.

Although the impact of the fires is evident, when evaluating the primary sources of pollutants for the period, WAC (CWT weighted by the number of trajectories in each cell of the grid), it is noticed that local sources have more impact on the

concentration (including biomass burning in proximate areas) than fire outbreaks in remote areas. Analyzing WAC (Figure 1), it is observed that the inflow of air masses traveling over Minas Gerais, Rio de Janeiro, and São Paulo is primarily responsible for the transport of pollutants to the receiver site, which is added on top of those locally emitted (Pedruzzi, 2020).

Additionally, both CWT and WAC demonstrate a significant impact of trajectories over the ocean, suggesting a possible influence of sea salt on PM2.5 concentrations. The effect of sea salt on PM2.5 concentrations has been previously demonstrated by studies conducted primarily in the city of São Paulo (e.g., Souza et al., 2014).

CONCLUSIONS

This study aimed to comprehensively examine the sources of $PM_{2.5}$ pollution during the period of pandemic-induced mobility restrictions in São Paulo. Utilizing the CWT model, we analyzed the impact of biomass burning emissions on $PM_{2.5}$ concentrations. Our findings revealed that regions with high biomass burning emissions, including the Pantanal biome, Bolivia, and Paraguay, significantly contributed to elevated $PM_{2.5}$ levels in São Paulo. Despite the observed impact of remote sources, our analysis also highlighted the substantial influence of local emissions, particularly from proximate areas such as Minas Gerais, Rio de Janeiro, and São Paulo itself. These results underscore the complex interplay between local and remote sources of air pollutants in urban areas, emphasizing the need for comprehensive air quality management strategies.

Additionally, our study identified a potential influence of sea salt on $PM_{2.5}$ concentrations, as indicated by significant trajectories over the ocean. This observation suggests a multifaceted nature of $PM_{2.5}$ pollution, involving both terrestrial and maritime sources. Overall, our findings contribute to a deeper understanding of $PM_{2.5}$ dynamics during pandemic-induced mobility restrictions, highlighting the importance of addressing both local and remote sources of air pollutants for effective air quality management. Further research is needed to explore the underlying mechanisms driving $PM_{2.5}$ pollution and its implications for human health and environmental sustainability in urban environments like São Paulo.

REFERENCES

Blumenthal, D., Fowler, E. J., Abrams, M., & Collins, S. R. (2020). Covid-19 — Implications for the Health Care System. *New England Journal of Medicine*, *383*(15), 1483–1488. https://doi.org/10.1056/NEJMsb2021088

Brereton, C. A., & Johnson, M. R. (2012). Identifying sources of fugitive emissions in industrial facilities using trajectory statistical methods. *Atmospheric Environment*, *51*, 46–55. https://doi.org/10.1016/j.atmosenv.2012.01.057

Collivignarelli, M. C., Abbà, A., Bertanza, G., Pedrazzani, R., Ricciardi, P., & Carnevale Miino, M. (2020). Lockdown for CoViD-2019 in Milan: What are the effects on air quality? *Science of The Total Environment*, *732*, 139280. https://doi.org/10.1016/j.scitotenv.2020.139280

Gkatzelis, G. I., Gilman, J. B., Brown, S. S., Eskes, H., Gomes, A. R., Lange, A. C., McDonald, B. C., Peischl, J., Petzold, A., Thompson, C. R., & Kiendler-Scharr, A. (2021). The global impacts of COVID-19 lockdowns on urban air pollution: A critical review and recommendations. *Elementa: Science of the Anthropocene*, *9*(1). https://doi.org/10.1525/elementa.2021.00176

Hsu, Y.-K., Holsen, T. M., & Hopke, P. K. (2003). Comparison of hybrid receptor models to locate PCB sources in Chicago. *Atmospheric Environment*, *37*(4), 545–562. https://doi.org/10.1016/S1352-2310(02)00886-5

Marques, J. F., Alves, M. B., Silveira, C. F., Amaral e Silva, A., Silva, T. A., dos Santos, V. J., & Calijuri, M. L. (2021). Fires dynamics in the Pantanal: Impacts of anthropogenic activities and climate change. *Journal of Environmental Management*, *299*(August), 113586. https://doi.org/10.1016/j.jenvman.2021.113586

Martins, L. D., Hallak, R., Alves, R. C., de Almeida, D. S., Squizzato, R., Moreira, C. A. B., Beal, A., da Silva, I., Rudke, A., & Martins, J. A. (2018). Long-range Transport of Aerosols from Biomass Burning over Southeastern South America and their Implications on Air Quality. *Aerosol and Air Quality Research*, *18*(7), 1734–1745. https://doi.org/10.4209/aaqr.2017.11.0545

Pak, A., Adegboye, O. A., Adekunle, A. I., Rahman, K. M., McBryde, E. S., & Eisen, D. P. (2020). Economic Consequences of the COVID-19 Outbreak: the Need for Epidemic Preparedness. *Frontiers in Public Health*, *8*(May), 1–4. https://doi.org/10.3389/fpubh.2020.00241

Pedruzzi, R. (2020). Atmospheric transport of air pollutants over southeastern Brazil: the impact of metropolitan areas emissions on air quality. In *SMARH*. UFMG.

Rudke, A. P., de Almeida, D. S., Alves, R. A., Beal, A., Martins, L. D., Martins, J. A., Hallak, R., & de Almeida Albuquerque, T. T. (2022). Impacts of Strategic Mobility Restrictions Policies during 2020 COVID-19 Outbreak on Brazil's Regional Air Quality. *Aerosol and Air Quality Research*, *22*(4), 210351. https://doi.org/10.4209/aaqr.210351

Rudke, A. P., Martins, J. A., Hallak, R., Martins, L. D., de Almeida, D. S., Beal, A., Freitas, E. D., Andrade, M. F., Koutrakis, P., & Albuquerque, T. T. A. (2023). Evaluating TROPOMI and MODIS performance to capture the dynamic of air pollution in São Paulo state: A case study during the COVID-19 outbreak. *Remote Sensing of Environment*, *289*(October 2022), 113514. https://doi.org/10.1016/j.rse.2023.113514

Souza, D. Z., Vasconcellos, P. C., Lee, H., Aurela, M., Saarnio, K., Teinilä, K., & Hillamo, R. (2014). Composition of PM2.5 and PM10 Collected at Urban Sites in Brazil. *Aerosol and Air Quality Research*, *14*(1), 168–176. https://doi.org/10.4209/aaqr.2013.03.0071

Stein, A. F., Draxler, R. R., Rolph, G. D., Stunder, B. J. B., Cohen, M. D., & Ngan, F. (2015). NOAA's HYSPLIT Atmospheric Transport and Dispersion Modeling System. *Bulletin of the American Meteorological Society*, *96*(12), 2059–2077. https://doi.org/10.1175/BAMS-D-14-00110.1

The Lancet. (2020). COVID-19 in Latin America: a humanitarian crisis. *The Lancet*, *396*(10261), 1463. https://doi.org/10.1016/S0140-6736(20)32328-X

AIR POLLUTION CONFERENCE BRAZIL
CMAS SOUTH AMERICA
COMMUNITY MODELING AND ANALYSIS SYSTEM

RISKS IDENTIFICATION FROM AIR TOXIC EMISSIONS IN THE TULA REGION, HIDALGO, MEXICO

Faviola Altúzar-Villatoro[1], José Agustín García-Reynoso[1]
[1]*Institute of Atmospheric Sciences and Climate Change, National Autonomous University of Mexico*
faviola.altuzar@atmosfera.unam.mx, agustin@atmosfera.unam.mx

Abstract: Industrial activity in the Tula de Allende region, Mexico, has resulted in high levels of air pollution, which could pose significant risks to human health and the environment. This study focuses on assessing the impact of air toxics emissions on public health, using data from industrial emissions and atmospheric dispersion models such as CALPUFF. Eight industries with significant emissions were identified, and it was found that the highest concentrations of heavy metals and organic compounds were located near the refinery and the power plant. Furthermore, the inhalation cancer risk was found to be at unacceptable levels at various sites, especially for nickel, chromium, and benzene. These findings highlight the need to take measures to control industrial emissions and protect the health of the population in this region.

Keywords: Risk assessment, air toxics, Tula.

INTRODUCTION

In Mexico, the Tula de Allende region in Hidalgo has been characterized by high industrial activity, which has resulted in it being considered one of the most polluted areas in the country (Vega et al., 2021). However, in terms of health risk assessment from air toxics (pollutants that even in small concentrations, are known or suspected to cause cancer or other serious health damage (US EPA, 2018)), limited information is available.

On the other hand, in a summary of studies on the relationship between cancer mortality and industrial emissions in Spain reported in the European Pollutant Release and Transfer Register, it was suggested that there is an excess of cancer mortality of approximately 17% in regions exposed to industrial emissions compared to those that are not. However, it's important to note the limitations of these findings, particularly the omission of meteorological and topographical variables (Fernández-Navarro et al., 2017). One way to take them into account, is the use of pollutant dispersion modeling, and one of these models is CALPUFF, which is of puff, Lagrangian, Gaussian, non-stationary type, which has been employed in different applications (Arregoces et al., 2018).

The objective of this study was to estimate the risk of cancer and non-cancer health effects due to exposure to air toxics. The aim was to determine whether populations residing near industrial sources are at risk of developing cancer and/or experiencing chronic non-cancer effects.

METHODS

2.1 Identifying Establishments Reporting Air Toxics in the PRTR.

The PRTR 2019 database was reviewed, where the industrial facilities present in the study area that emitted air toxics were identified, as well as the quantities reported.

2.2 Identification of establishments requiring risk assessment.

Scores for carcinogenic effects (S_{cancer}) and chronic non-cancer effects ($S_{noncancer}$) were calculated to identify companies requiring detailed risk assessments. The following equations were utilized for this purpose (Gratt, 1996):

$$S_{cancer} = \sum_c (Q_c)(URF_C)(RP)(1.7x10^3) \quad \text{Eq. 1}$$

$$S_{noncancer} = \sum_c (\frac{Q_c}{RELc})(RP)(150) \quad \text{Eq. 2}$$

Where:
Q_c = emission rate of chemical c (lb/year);
URF_C = Unit Risk Factor of chemical c $(\mu g/m^3)^{-1}$;
REL_C = Reference exposure level of chemical c with chronic toxicity ($\mu g/m^3$);
RP = receptor proximity adjustment factor (dimensionless).

Qc emissions were obtained from the PRTR; URFc and chronic RELc values were obtained from the Consolidated Table of California Office of Environmental Health Hazard Assessment/ California Air Resources Board Approved Risk Assessment Health Values (CARB, 2022). The proximity factor (RP), which refers to the distance from the source to the nearest receptor, was assumed to be approximately 100 to 250 m, corresponding to an RP of 0.25 (Gratt, 1996). Finally, the industries were classified according to the criteria listed in Table 1.

Table 1. Classification criteria according to the obtained score.

S_{cancer}	$S_{noncancer}$	Classification
> 100	> 10	Required assessment
≥10 to ≤ 100	≥ 1 to ≤ 10	Potential candidates for assessment
< 10	< 1	Probably no need for assessment

Reference: Gratt, 1996.

2.3 Annual average concentrations of air toxics.
To derive concentrations in the area, we employed Version 6 of the CALPUFF model. Prior to this, meteorological data was processed using the WRF (Weather Research and Forecasting) model, utilizing data from the North American Mesoscale Forecast System (NAM) at a 12 km resolution. The CALMET module was then executed using the WRF results to generate meteorological data for the study area utilized by CALPUFF. Emissions data were sourced from the PRTR 2019. This process involved defining a domain covering 26 x 26 km with a resolution of 1 km was defined, covering both industrial plants and the surrounding towns.

In the CALPUFF module, sources were entered as area sources. And the localities of Apaxco, Atitalaquia, Atotonilco, Bomintzha, Jasso, La Joya, Tlaxcoapan, and Tula de Allende were designated as discrete receptors.

2.4 Risk characterization
Cancer Risk
Cancer Risk (R_{cancer}) was estimated through the application of the following equation (EPA, 2018):

$$R_{cancer} = Exposure\ concentration * URF \quad \text{Eq. 3}$$

Where Rcancer is the probability of an individual developing cancer due to exposure to an atmospheric toxicant, in addition to the overall risk of suffering cancer. Likewise, assuming that the population surrounding the identified industries is simultaneously exposed to all the substances reported in the PRTR, the total cancer risk was estimated as follows (EPA, 2018):

$$R_{total-cancer} = \sum_{c=1}^{n} Conc._c * URF_c \quad \text{Eq. 4}$$

In this work, R_{cancer} or $R_{total\text{-}cancer}$ is considered acceptable when it is less than $1x10^{-6}$. Furthermore, in order to have a better understanding of R_{cancer}, different metrics were used, such as Cancer Population Risk (CPR), which is the increase in the number of cancer cases; or the loss of life expectancy (LLE), which indicates the number of days subtracted from life expectancy. The CPR was obtained by multiplying Rtotal-cancer by $1x10^6$ (assuming an exposed population of 1 million), while the LLE was estimated with the equation (Gratt, 1996):

$$LLE = 1.1x10^6 * R_{total-cancer} \quad \text{Eq. 5}$$

Non cancer Risk
The hazard quotient (HQ) was used to characterize the non-carcinogenic chronic effects risk, with the equation (EPA, 2018):

$$HQ_c = \frac{Exposure\ concentration}{REL_c} \quad \text{Eq. 6}$$

HQ is applicable for an individual pollutant, whereas, for exposure to multiple substances, the hazard index (HI) was used which is equal to the sum of all HQs:

$$HI = \sum HQ_c \quad \text{Eq. 7}$$

When HQ or HI is less than 1, it indicates that the risk is acceptable, while a value greater than 1 indicates the extent to which the reference level is exceeded, so there is a possibility of adverse health effects. (EPA, 2018).

Spatial distribution of cancer risk
Finally, with the distribution of concentrations obtained through CALPUFF in the study region, the areas cancer risk levels were identified.

FINDINGS AND ARGUMENT

3.1 Industries in RETC that reported air toxics
Eight industries emitting air toxics were identified in the region: an oil refinery, a thermal power plant, three cement factories (Cemex, Cruz Azul, and Holcim), a rubber articles factory, a lime factory, and a hazardous waste collection company called Actium. Together, they reported the emission of 11 air toxics: arsenic, cadmium, chromium, mercury, nickel, furans, benzene, dioxins, formaldehyde, acetaldehyde and lead. The refinery and the power plant reported the highest emissions, corresponding to nickel, formaldehyde, and acetaldehyde, while Cemex and Holcim reported the highest values of benzene.

3.2 Industries requiring a risk assessment
Based on the scores for carcinogenic effects and chronic non-carcinogenic effects shown in Table 2, the lime factory and the rubber industry were discarded in order to continue the risk assessment of the rest of the establishments.

Table 2. Scores of carcinogenic and chronic non-carcinogenic effects.

Nombre	S_{cancer}	$S_{noncancer}$
Oil refinery	46,808	166,636,880
Thermal power plant	25,381	83,388,510
Cemex	8,356	261,742
Actium	237	699
Cruz Azul	48.0	113,811
Holcim	42.9	75,406
Lime factory	0.0314	1.823
Rubber industry	0.0007	0.0422

3.3 Annual average concentrations of air toxics
The results of the CALPUFF modeling show that the highest concentrations correspond to Ni, which is emitted by the refinery and the thermoelectric plant. Figure 1 shows the annual average concentration isolines for this metal, where it can be seen that the emissions from the aforementioned sources are distributed towards the south-

southwest, reaching the town of Bomintzha, where the highest average concentrations of most pollutants were recorded, with the exception of benzene, dioxins and furans. On the other hand, the lowest concentrations were recorded in Tula.

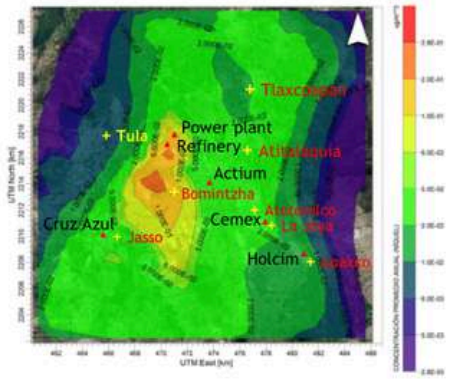


Figure 1. Nickel annual average concentration isolines during 2019

3.4 Risk characterization

In all populations, the R_{cancer} due to Cr and Ni, exceeded acceptable level, although in La Joya and Apaxco, there was also an unacceptable R_{cancer} due to benzene. The highest $R_{total\text{-}cancer}$ was found in Bomintzha, corresponding to a CPR of approximately 275 new cancer cases in the population as a result of inhaling the reported air toxics. Figure 2a shows the increase in the number of cancer cases per million inhabitants in each population, it can be observed that Tula has the lowest number of cases. Additionally, it was found that the range of days subtracted from life expectancy was from 15 to 302 (Fig. 2b).

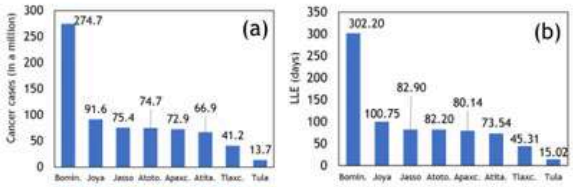


Figure 2. (a) Cancer cases (in a million) and (b) LLE (days) per locality

Regarding the non-cancer risk, Ni was the only pollutant with a HQ greater than 1 in almost all sites (except for Apaxco and Tula). The difference between HI and HQ ranged from 1.5 to 0.2%, which could indicate a low contribution to Rnon-cancer from the other substances. These results indicate the possibility of adverse health effects. Once again, Bomintzha recorded the highest HQ.

With respect to the spatial distribution of unacceptable R_{cancer}, it was found that, for Ni and Cr, this area covers almost the entire study domain, while for benzene, it only extends in the vicinity of the emission sources (Cemex and Holcim). Figure 3 shows the ranges of chromium inhalation cancer cases that could occur in the area. These results suggest that besides the sites considered as receptors, other communities could also be at risk of developing cancer.

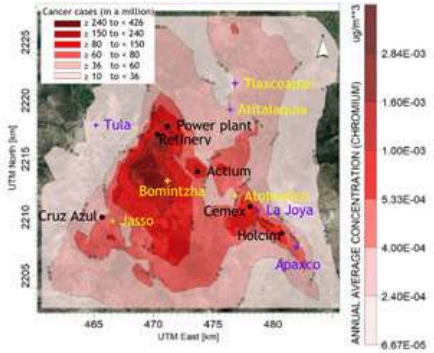


Figure 3. R_{cancer} spatial distribution due to chromium inhalation.

CONCLUSIONS

The results suggest that emissions of some air toxics reported in the RETC may affect the health of the population located around industrial establishments, with Cr, Ni, and benzene being the pollutants representing the highest cancer risk, in addition to the chronic effects produced by Ni. Therefore, it is important to pay greater attention to controlling the emissions of these pollutants in order to protect the people health. Finally, it is necessary to mention that one of the limitations of this work is the lack of evaluation of the model's performance since there are no measurements of the substances evaluated during the study period.

REFERENCES

Arregoces, Heli A., Mendoza, Yoma I. and Rojano, Roberto E. *"Evaluación del CALPUFF para Estimar Concentraciones Ambientales de PM10 de una Cantera en Terrenos Complejos."* Información Tecnológica 29(5) (2018): 131-142.

California Air Resources Board. *Consolidated table of OEHHA/CARB approved risk assessment health values.* (2022).

Environmental Protection Agency. *Technical Support Document EPA's Air Toxics Screening Assessment 2018 AirToxScreen TSD.* (2018).

Fernández-Navarro, P., García-Pérez, J., Ramis, R., Boldo, E., and López-Abente, G. *"Industrial pollution and cancer in Spain: An important public health issue".* Environmental Research 15 (2017): 555-563. https://doi.org/10.1016/j.envres.2017.08.049

Gratt, Lawrence B. *Air. Toxic risk Assessment and Management: public health risks from normal operations.* Estados Unidos: Wiley, 1996.

Vega, E., López-Veneroni, D., Ramírez, O., Chow, J. C., and Watson, J. G. *"Particle-bound PAHs and chemical composition, sources and health risk of $PM_{2.5}$ in a highly industrialized area".* Aerosol and Air Quality Research, 21(10), (2021): 1-24. https://doi.org/10.4209/AAQR.210047

SESSION 10
Multiscale Model Applications and Evaluations

Both observations and modeling studies have demonstrated the long-range inter-continental transport of pollutants. Changes in emission patterns over different regions of the world are likely to exacerbate the impacts of long-range pollutant transport on background pollutant levels in another region, which may then impact the attainment of local air quality standards. Additionally, increased concerns of climate impacts on regional and local ecosystem disciplines have driven the need to utilize outputs from global models into regional modeling systems with different temporal and spatial scales. In such applications, downscaling approaches have been used to link the two modeling systems, with different physical and dynamical characteristics, to bridge the gap between global and local effects. This session seeks papers that discuss key issues related to the consistent coupling of atmospheric physical and chemical processes on local-to-global scales and related modeling applications. Topics of interest in this session include:

- Hemispheric chemistry transport models
- Multi-scale climate and air quality modeling applications
- Earth System Modeling and Feedbacks
- Dynamical and statistical downscaling
- Model evaluation and inter-comparison

Also, evaluation of air quality modeling systems (including meteorological and emissions models) is a key to verify the integrity of such modeling systems for various applications at various spatial and temporal resolutions. Abstracts are invited that present results of model evaluation studies, with emphasis on new techniques for model evaluation. Session topics include:

- Diagnostic tools
- Analyses and comparisons with data from measurement networks
- Process evaluation, including dynamic evaluation
- Sensitivity of air quality models to meteorological inputs

SESSION 10

THE DYNAMICS AND PHOTOCHEMISTRY OZONE PRODUCTION IN THE AMAZON REGION: A MODELING STUDY WITH WRF-CHEM MODEL 206

VALIDATION OF THE RIO DE JANEIRO METROPOLITAN REGION METEOROLOGICAL DATA USING THE WEATHER RESEARCH AND FORECASTING MODEL 209

ANALYSIS OF THE TRANSPORT OF PRIMARY POLLUTANTS AMONG THE METROPOLITAN REGIONS OF SÃO PAULO, CAMPINAS, AND BAIXADA SANTISTA 209

INFLUENCE OF ATMOSPHERIC WINDS DYNAMIC OVER THE CONCENTRATIONS OF PM10 AND PM2.5 IN A OPENCAST COAL MINING AREA OF COLOMBIA FOR A NEUTRAL ENSO PERIOD 215

MULTİSCALE MODEL EVALUATİON İN SUPPORT OF AN ANALYSİS AND FORECAST SYSTEM FOR LATİN AMERİCA 218

IMPACT OF WRF MODELED PBLH ERRORS ON CMAQ AIR QUALITY SIMULATIONS 221

QUANTIFYING THE IMPACT OF AEROSOLS ON THE PREDICTIVE SKILL OF SUBSEASONAL GLOBAL ATMOSPHERIC AND AIR QUALITY SIMULATIONS 224

AIR POLLUTION CONFERENCE BRAZIL
CMAS SOUTH AMERICA
COMMUNITY MODELING AND ANALYSIS SYSTEM

THE DYNAMICS AND PHOTOCHEMISTRY OZONE PRODUCTION IN THE AMAZON REGION: A MODELING STUDY WITH WRF-CHEM MODEL

Lucas H. S. Rocha[1], Helber B. Gomes[1], Janaína M. P. Nascimento[2], Alessandro Banducci[3], Katyelle F. S. Bezerra[1], Maria Cristina L. Silva[1]

[1]*Institute of Atmospheric Sciences, Federal University of Alagoas, Maceió, Brazil*
lucas.santos@icat.ufal.br; helber.gomes@icat.ufal.br; katyelle.silva@icat.ufal.br; cristina.lemos@icat.ufal.br.

[2]*National Oceanic and Atmospheric Administration, Boulder, USA*
janaina.nascimento@noaa.gov.

[3]*Physics Department, Colorado State University, Boulder, USA*
alessandro.lindahl@gmail.com

Abstract: The Manaus region is surrounded by a vast expanse of tropical forest, exhibiting a complex interplay of geographical, climatic, and ecosystem factors that render it unique. The forest naturally emits a substantial amount of biogenic volatile organic compounds (BVOCs), frequently interacting with anthropogenic air pollution originating from the city of Manaus, significantly favoring the production of O3 in downwind regions of the city. According to Nascimento et al. (2022), the peak O3 concentration is observed southwest of Manaus, reaching approximately 47 ppbv at 2:00 PM (local time - UTC-4), with approximately 150-200 km from the city and in the direction of the prevailing wind. Conversely, in the center of Manaus during the same timeframe, O3 concentrations were observed to be close to 10 ppbv. For the calibration and validation of simulations using WRF-Chem, data from stations in the Green Ocean Amazon experiment (GoAmazon 2014-2015) were employed, including a total of 4 stations in addition to the Amazon Tall Tower Observatory (ATTO-T0a). In this context, tracking and analyzing the plume produced in the urban center of Manaus and its dispersion into pasture and forest regions at different times reveal variations in O3 concentrations. Air masses leaving Manaus at 7:00 AM (local time) reach their maximum development (~55 ppbv) at 3:00 PM (local time) due to a significant amount of available solar radiation during their transit. Conversely, air masses leaving later exhibit lower development in O3 production. To better understand the dynamics and photochemistry of O3 production in the Amazon region, experiments utilizing the WRF-Chem model are being developed and investigated. To assess how radiation interacts in the O3 formation process, maintaining a fixed radiation value, numerical experiments with the WRF-Chem model have been chosen.

Keywords: Ozone, Photochemistry, WRF-CHEM, Amazon region.

INTRODUCTION

Interaction between solar radiation and chemical agents in the Amazon Rainforest and various other places around the world plays an important role in maintaining ecological balance. One of the essential processes is the formation and decomposition of ozone in the stratosphere and troposphere. In the troposphere, nitrogen dioxide (NO2) is a fairly common precursor that can interact with atmospheric gases and, through chemical reactions, generate tropospheric ozone. Through the burning of fossil fuels, NO2 is released, which preferably reacts with oxygen (O2) to generate NO + O3. At this reaction stage, consumption of O3 can occur, so that it donates an oxygen atom (O) to NO. This oxygen atom can 'recover', through photochemical reaction, to atmospheric O2, generating O3 again (Rodrigues and Martins, 2001). This work focuses on tropospheric ozone and aims, through the use of a numerical model, to model the interaction of O3 present in the Manaus region and the surrounding forest with solar radiation, with solar radiation having a fixed value throughout the day in time and space.

METHODS

The main modeling tool used was the Weather Research and Forecasting model with coupled chemistry (WRF-Chem). The simulation was conducted starting on March 8th and ending on March 15th, 2014, with an hourly time step; however, the first day was discarded from all analyses, serving only as spin-up. For calibration and validation of the simulations using WRF-Chem, data from stations of the Green Ocean Amazon experiment (GoAmazon 2014-2015) were employed, including a total of 4 stations in addition to the Amazon Tall Tower Observatory (ATTO-T0a). This simulation was the same as that used by Nascimento et al. (2021 and 2022). Based on the control simulation by Nascimento et al. (2021 and 2022), normal radiation patterns were calculated for some areas of the study region described later.

FINDINGS AND ARGUMENT

When analyzing and tracking at different times the plume emanating from the urban center of Manaus towards the forest, it is discovered that ozone (O3)

concentrations behave differently, as shown in Figure 1. The air parcel leaving Manaus at 7 a.m. (local time) experiences greater development in O3 concentration, reaching around 55 ppbv with peak maximum at 3 p.m. (local time), as there is a significant amount of solar radiation available during the morning and afternoon while the parcel travels, favoring O3 production along the path through photochemical interactions. On the other hand, parcels leaving later experience lesser development in O3 production because they are exposed to solar radiation for less time, resulting in lower O3 production.

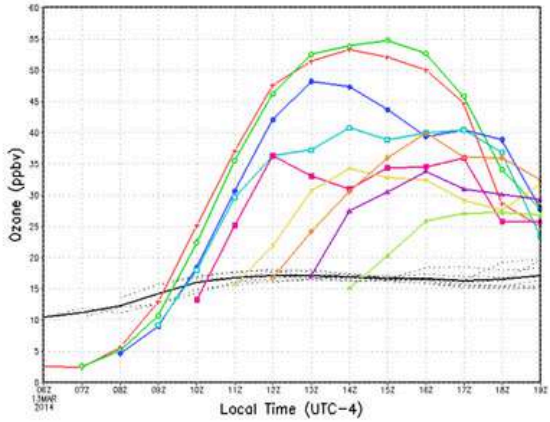


Figure 1. Tracking O3 concentration in air parcels leaving Manaus at different times of the day.

The analyses of solar radiation near the surface for the entire study region, i.e., the Manaus region and surrounding forest, show a peak radiation value just slightly above 1000 W/m² occurring at 12-13 hours local time, as depicted in Figure 2. Interestingly, in the best-case scenario where parcel development occurs (green line in Figure 1), the peak O3 concentration occurs 2 to 3 hours after the peak radiation (14-15 hours local time), with a value of 55 ppbv.

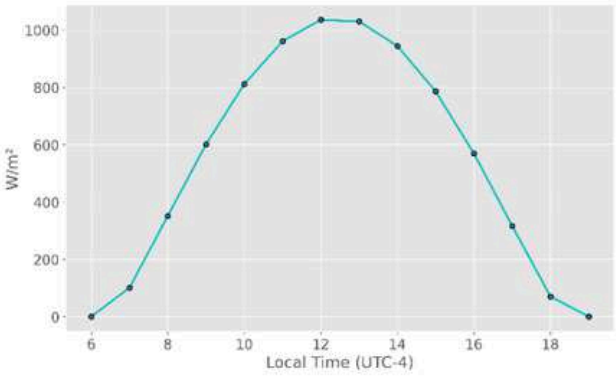


Figure 2. Hourly variation (local time) of surface radiation throughout the study area.

Spatially, it's possible to notice radiation values with a subtle attenuation towards the southwest of Manaus (Figure 3), at approximately 150-200 km from the city, which corresponds to the region where the O3 concentration is higher, reaching average values of about 47 ppbv.

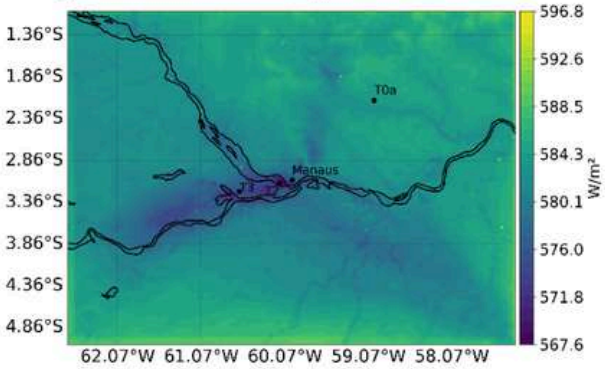


Figure 3. Spatial visualization of surface radiation across the entire study domain. T3 and T2: surface stations; Manaus: station within the city; T0a: Amazon Tall Tower Observatory.

CONCLUSIONS

Based on what has been done so far, it's possible to observe the interaction of O3 and the behavior of solar radiation at the surface in the region of interest. Radiation decreases towards the dense forest region southwest of Manaus, the same direction in which the city's pollution plume, driven by local dynamics, travels during the night and begins to develop in the early morning hours. Due to the significant amount of available radiation throughout the region's domain, O3 production is favored in this downstream area of Manaus. Subsequently, a simulation will be conducted with fixed solar radiation in time and space to further observe and explore the dynamics and production of O3 for the region.

REFERENCES

Nascimento, J. P., Bela, M. M., Meller, B. B., Banducci, A. L., Rizzo, L. V., Vara-Vela, A. L., Barbosa, H. M. J., Gomes, H., Rafee, S. A. A., Franco, M. A., Carbone, S., Cirino, G. G., Souza, R. A. F., McKeen, S. A., Artaxo, P. "Aerosols from anthropogenic and biogenic sources and their interactions - modeling aerosol formation, optical properties, and impacts over the central Amazon basin", Atmos. Chem. Phys., 2021, 6755-6779, https://doi.org/10.5194/acp-21-6755-2021.

Nascimento, J. P., Barbosa, H. M., Banducci, A. L., Rizzo, L. V., Vara-Vela, A. L., Meller, B. B., Gomes, H., Cezar, A., Franco, M. A., Ponczek, M., Wolff, S., Bela M. M., Artaxo, P. "Major regional-scale production of O3 and secondary organic aerosol in remote Amazon regions from the dynamics and photochemistry of urban and forest emissions". Environmental Science & Technology, 2022, 56(14), 9924-9935.

AIR POLLUTION
CONFERENCE BRAZIL
CMAS SOUTH AMERICA
COMMUNITY MODELING AND ANALYSIS SYSTEM

Rodrigues, G. S., Martins, R. A. "Efeitos potenciais do ozônio troposférico sobre as plantas cultivadas e o biomonitoramento ambiental". 2001.

AIR POLLUTION CONFERENCE BRAZIL
CMAS SOUTH AMERICA
COMMUNITY MODELING AND ANALYSIS SYSTEM

Validation of the Rio de Janeiro Metropolitan Region meteorological data using the Weather Research and Forecasting model

Thiago Fonseca da Costa [1*], Rizzieri Pedruzzi[1], Taciana Toledo de Almeida Albuquerque[2,3], Eduardo Martins[1]

[1] Department of Sanitary and Environmental Engineering, State University of Rio de Janeiro, 20950-000, Brasil Rio de Janeiro, Brazil.

[2] Department of Sanitary and Environmental Engineering, Federal University of Minas Gerais, 31270-901, Belo Horizonte, Brazil

[3] Postgraduate Program in Environmental Engineering, Federal University of Espírito Santo, 29075-710, Vitória, Brazil.

tfc0sta20@gmail.com; rizzieri.pedruzzi@gmail.com; edmmartins@gmail.com

Abstract: The Metropolitan Region of Rio de Janeiro is a densely urbanized area, characterized by a high concentration of mobile and fixed sources of pollution, as well as vast expanses impermeabilized by concrete and asphalt, contributing to local air quality issues. In this context, validating a meteorological model becomes crucial, as the data obtained can feed into chemical transport models, relating meteorological variables to emissions and atmospheric chemistry. This allows for predicting and creating scenarios for controlling air pollution through legislation and public policies. Based on this premise, the present study aims to validate the meteorological data generated by the Weather Research and Forecasting (WRF) model to understand local meteorology. For this purpose, two nested domains were developed, one with a horizontal resolution of 9km and another more refined one with a resolution of 3km, both containing 40 vertical layers. The simulation was conducted from August 28th to September 3rd, 2018, characterized by low precipitation and fewer extreme weather events. The validation of the results was performed using indices of agreement, mean absolute error, square root of the mean squared error, and mean bias for variables such as temperature, specific humidity, wind speed, and direction. For this, simulated values were compared with observed data from 36 stations distributed across the study domain. The results obtained showed good agreement between simulated and observed data for temperature and specific humidity, but less agreement for wind speed and direction. This discrepancy may be related to the location of meteorological stations. However, the model still yielded satisfactory results in representing local meteorology.

*Keywords:*WRF, Weather Research and Forecasting, Meteorological Validation, Metropolitan Region of Rio de Janeiro, Air Quality.

INTRODUCTION

The WRF, a mesoscale model developed by a consortium of scientific and governmental entities, has been widely used to predict meteorological scenarios, simulate meteorological variables for energy utilization studies, and provide data for air quality models, among other applications(SKAMAROCK et al., 2017).

In the context of energy utilization, the model has been prominently applied in Brazil. Duarte Jacondino et al. (2021) employed the WRF to evaluate wind patterns in the Northeast for use in wind energy generation. Through analysis of wind farms, the researchers identified optimized model configurations for wind patterns in the region. Tuchtenhagen et al. (2020) conducted a similar study in the southern region, focusing on the coastal area, where they compared WRF data with direct measurements of wind speed over the oceans. While the model showed satisfactory results near the coast, with an average difference in wind speed between -10% and 10%, greater distances showed significant errors, reaching 80% due to currents near the region of the Malvinas. This result highlights the need to incorporate an oceanic wind model coupled with the WRF in such situations.

Regarding the generation of data for air quality models, the WRF is widely used, especially in the meteorological fields of the CMAQ. Loriato et al. (2018) used SMOKE to feed the CMAQ model in a study on ozone formation precursors in the metropolitan region of Vitória, Espírito Santo. De Toledo et al. (2018) employed the CMAQ-WRF to model various pollutants in the city of São Paulo and assess atmospheric conditions in this megacity. Pedruzzi et al. (2019) used the CMAQ-WRF to create different prediction scenarios, varying the model conditions regarding ozone and particulate matter concentrations.

The WRF model has been applied in the Rio de Janeiro metropolitan area and in other areas of the Brazilian territory ((PEDRUZZI et al., 2019; TACIANA et al., 2019; MAIA; BAPTISTA; MARTINS, 2020). However, it is necessary to simulate for different times of the year and different periods of the historical series in order to generate comparisons with the data already generated by other

simulations, monitored data, and data from other regions.

METHODS

The methodology consisted of the following steps: construction of the modeling domain and simulation period, establishment of the physical parameters applied to the simulation, and validation of the data with observed data from 36 stations within the domain.

The horizontal domain used is nested with a coarse resolution of 9 x 9 km to smooth boundary conditions from neighboring states of Minas Gerais, São Paulo, and Espirito Santo, and a more detailed resolution in the interior of 3 x 3 km to encompass the Rio de Janeiro Metropolitan Region (RMRJ) along with some neighboring cities from different states that influence the tropospheric chemistry of Rio. Figure 1 presents the domain configurations for the study.



Figure 1. WRF's domains. Domain 1(blue line) 9 km resolution. Domain 2 (red line) 3 km resolution.

The temporal resolution will be the month of September 2018 as this month represents spring in the southern hemisphere, a season which, due to its lower rainfall compared to summer, is the time of year with the highest ozone peaks.

Meteorological data validation will be based on the studies of Tai; Yarwood (2001); Mcnally (2009). The parameters was: Mean bias (MB), Index of Agreement (IOA), Root Mean Square Error (RMSE), Bias, Mean Absolute Gross Error (MAGE).

FINDINGS AND ARGUMENT

The validation assays were conducted according to the parameters outlined in the methodology. Values within the benchmarks were found for all evaluated meteorological parameters. Table 2 shows the percentage of stations with data within the values. The boxplot of the evaluated data for each parameter is presented in Figure 13: temperature in Kelvin, specific humidity in grams per kilogram, wind direction in degrees, and wind speed in meters per second.

Regarding temperature and specific humidity, these showed good benchmarks for over 90% of their stations, indicating good representations of the observed data.

Regarding wind speed and direction, these are the meteorological variables with the greatest validation difficulty. For this study, wind direction showed few stations within the benchmark, namely: Campos dos Goytacazes, São Tomé, and Arraial do Cabo. All stations with benchmarks are located in suitable places according to the parameters specified by the World Meteorological Organization, showing the absence of nearby buildings, open fields, and little influence of terrain. Due to the locality providing an appropriate configuration, it is believed that for these reasons, these stations may present values following the simulations.

Regarding areas that obtained benchmarks outside the advisable range, several factors may have occurred. Pedruzzı et al. (2019) as well as Pıno-cortés et al. (2022) believe that large relief masses or obstacles, both natural and anthropogenic, influence the parameter and cause differences in vector orientation. Tuchtenhagen et al. (2020) also believe that high-intensity low-troposphere jets from the Andes influence the wind regime of the southeastern region, potentially causing changes in wind direction, which are poorly simulated by the WRF. Another factor that may influence wind direction simulation is wind speed. Chen et al. (2020) present that wind speeds lower than 5 m/s result in values with lower accuracy. As observed in the daily profile, the WRF overestimated wind speed, but still with values below those mentioned by the author. This overestimation of wind speed can also be linked to the location of stations with low-speed winds incident on them and complex terrain as mentioned earlier (PEDRUZZI et al., 2019; JIMÉNEZ; DUDHIA, 2013). Figure 2 shows the boxplot of the benchmarks from each parameter.

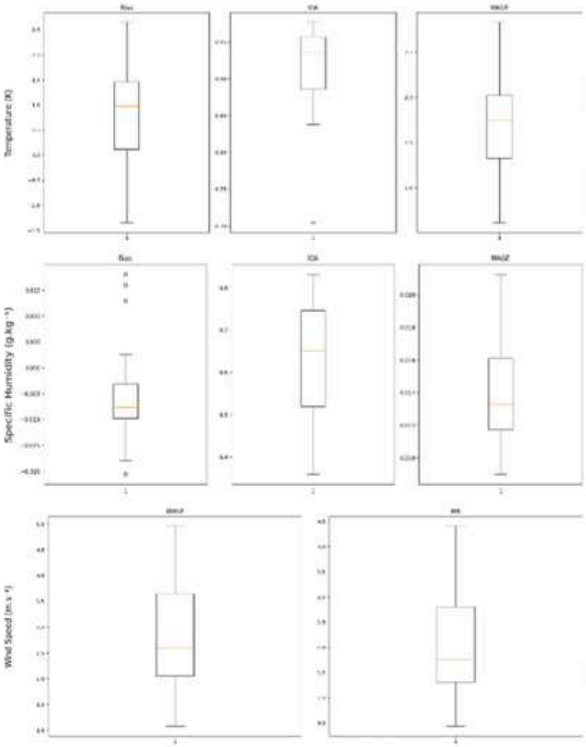


Figure 2. Boxplots for temperature, wind speed, and specific humidity with the data of all stations within the domain.

Variable	Benchmarks	Total stations	Percentage of stations within the benchmarks
Wind Direction [°]	MB <± 10.0	35	74.29%
	MAGE < 55,.		8.57%
Temperature (K)	Bias ≤± 2.0	36	91.67%
	MAGE ≤ 3.5		100.00%
	IOA ≥ 0.8		97.22%
Specific Humidity [g.k^{-1}]	Bias ≤± 1.0	34	100.00%
	MAGE ≤ 2.0		100.00%
	IOA ≥ 0.6		67.64%
Wind speed [m.s^{-1}]	MB ± 1.5	35	68.57%
	RMSE < 2.5		45.71%

Table 1. Percentage of stations within the benchmarks for the main parameters stipulated by Tai; Yarwood, (2001); Mcnally, (2009)

CONCLUSIONS

Regarding the validation of the WRF meteorological model, the results show good reproduction of temperature and specific humidity at over 95% of the stations. However, the similarity with observed data concerning wind direction and speed is lower, something already reported in the literature. This disparity may be attributed to model errors, difficulties in simulating rugged terrain, and even inaccuracies in observed data due to station locations in areas with many obstacles.

REFERENCES

CHEN, C. et al. Comparative study on WRF model simulations from the viewpoint of optimum ship routing. *Ocean Engineering*, v. 207, 2020.

DUARTE JACONDINO, W. et al. Hourly day-ahead wind power forecasting at two wind farms in northeast Brazil using WRF model. *Energy*, v. 230, 1 set. 2021.

JIMÉNEZ, P. A.; DUDHIA, J. On the ability of the WRF model to reproduce the surface wind direction over complex terrain. *Journal of Applied Meteorology and Climatology*, v. 52, n. 7, p. 1610–1617, jul. 2013.

LORIATO, A. G. et al. Inventário de Emissões com Alta Resolução para a Região da Grande Vitória Utilizando o Sistema de Modelagem Integrada WRF-SMOKE-CMAQ. *Revista Brasileira de Meteorologia*, v. 33, n. 3, p. 521–536, 2018.

MAIA, R.; BAPTISTA, L.; MARTINS, E. PREPARAÇÃO E VALIDAÇÃO DE ARQUIVOS DE ENTRADA PARA USO NO SIMULADOR DE QUALIDADE DO AR (CMAQ). *Química Nova*, v. 43, n. 10, p. 1375–1384, 2020. Disponível em: <http://quimicanova.sbq.org.br/audiencia_pdf.asp?aid2=9191&nomeArquivo=AR2020-0050.pdf>.

MCNALLY, D. *Meteorological modeling performance guidelines to replace old standards*. [s.l: s.n.]. Disponível em: <https://www3.epa.gov/scram001/adhoc/mcnally2009.pdf>.

PEDRUZZI, R. et al. Performance evaluation of a photochemical model using different boundary conditions over the urban and industrialized metropolitan area of Vitória, Brazil. *Environmental Science and Pollution Research*, v. 26, n. 16, p. 16125–16144, 2019.

PINO-CORTÉS, E. et al. An evaluation of the photochemical air quality modeling using CMAQ in the industrial area of Quintero-Puchuncavi-Concon, Chile. *Atmospheric Pollution Research*, v. 13, n. 3, 1 mar. 2022.

SKAMAROCK, W. C. et al. *A Description of the Advanced Research WRF Version 2NCAR TECHNICAL NOTE*. [s.l: s.n.].

TACIANA, T. T. et al. Analysis of PM2.5 concentrations under pollutant emission control strategies in the metropolitan area of São Paulo, Brazil. *Environmental Science and Pollution Research*, v. 26, n. 32, p. 33216–33227, 2019.

TAI, C. E. E.; YARWOOD, G. *Air Sciences Final Report ENHANCED METEOROLOGICAL MODELING AND PERFORMANCE EVALUATION FOR TWO TEXAS OZONE EPISODES*. [s.l: s.n.].

TOLEDO, T. et al. WRF-SMOKE-CMAQ modeling system for air quality evaluation in São Paulo megacity with a 2008 experimental campaign data. *Environmental Science and Pollution Research*, v. 25, p. 36555–36569, 2018.

TUCHTENHAGEN, P. et al. WRF model assessment for wind intensity and power density simulation in the southern coast of Brazil. *Energy*, v. 190, 2020.

AIR POLLUTION CONFERENCE BRAZIL
CMAS SOUTH AMERICA
COMMUNITY MODELING AND ANALYSIS SYSTEM

ANALYSIS OF THE TRANSPORT OF PRIMARY POLLUTANTS AMONG THE METROPOLITAN REGIONS OF SÃO PAULO, CAMPINAS, AND BAIXADA SANTISTA

Natasha Murgu Valdambrini[1], Flávia Noronha Dutra Ribeiro[2]
[1]*School of Arts, Sciences and Humanities University of São Paulo*
natasha.valdambrini@usp.br
[2]*School of Arts, Sciences and Humanities University of São Paulo*
flaviaribeiro@usp.br

Abstract: Air pollution is a global concern and is not limited to the geographical boundaries of a region: the pollutants in the atmosphere are subject to transport processes and chemical transformations that affect their composition and the level of contamination in a specific area. Pollutants transported from distant regions can affect local atmospheric concentrations. High concentrations of ozone (O_3) are challenging to control, because, as a secondary pollutant, produced through photochemical reactions between its precursors, nitrogen oxides (NO_x) and Volatile Organic Compounds (VOCs), O_3 concentrations depend on the emission of its precursors, favorable weather conditions for its formation and the geographical location that influences its dispersion. Therefore, there is no long-term spatial distribution trend. This study aims to investigate the transportation of primary pollutants among the metropolitan regions of São Paulo, Campinas, and Baixada Santista to understand the implications of precursor transportation for O_3 formation. The spring and summer seasons show higher concentrations of O_3 from September to March, due to conditions that favor its formation: high solar incidence, due to low cloudiness; temperatures above 20° C; and low humidity. Frequent episodes of O3 levels being exceeded throughout the state are measured and reported daily through CETESB's Air Quality Information System (QUALAR). A preliminary analysis of the total days of exceedances of state air quality standards for O3 throughout the state of São Paulo showed a significant decrease from 2014 to 2016; in 2017, there was a slight increase, decreasing again in 2018. However, in 2019, there was a sudden increase in these exceedances, making it clear that O3 is a difficult pollutant to control, which generated interest in this study period. To analyze the interaction of air pollution by O3 among more than one region, the three main metropolitan regions of the state of São Paulo were chosen, which are not only close to each other but also have great political and economic importance: Metropolitan Region of São Paulo (MRSP), Metropolitan Region of Campinas (MRC) and the Metropolitan Region of Baixada Santista (MRBS). To perform the simulations, we chose a week with high daily O_3 concentrations episodes during spring, from 1 to 8/Oct/2019, a favorable season for the formation of O_3. Meteorological simulations were carried out with the WRF (Weather Research Forecasting Model) using two domains: one of 271 × 271 km and a smaller one of 150 × 150 km, covering the entire State of São Paulo, centered at coordinates -23.21° S, -46.44° W. The transport of primary precursors was represented by three tracers with continuous and constant emission, one in each region. The meteorological simulations during the study period showed good agreement with observations, representing the temperature profiles adequately, especially the high temperatures in the first five days, which favors the formation of O_3. Considering the geographical location, the sea breeze, and the wind predominant direction of the studied regions, it can be seen that during the day, part of the pollution plume from the MRSP will be transported to the MRC; the plume from the MRC will be transported to the northwest; and the plume from the MRBS, will climb the Serra do Mar escarpment arriving at the MRSP. At night, the wind direction changes to northwest, reversing the dispersion direction. The results indicate an interaction between the primary pollutants in these regions, which has implications for the concentrations of secondary pollutants such as O_3.

Keywords: Metropolitan regions, pollutant transport, air pollutant dispersion modeling, interregional pollutants transport.

INTRODUCTION

An atmospheric pollution is a global concern and is not restricted to the geographical boundaries of a region, the pollutants present in the atmosphere, whether primary or secondary, are subject to transport processes and chemical transformations that affect their composition and the level of contamination of a given region.

Unfavorable meteorological conditions combined with high pollutant emissions can be responsible for the dispersion of these pollutants, affecting local air quality in other regions, leading to low air quality. Therefore, it is essential to consider the topographical characteristics of each region (JACOB; WINNER, 2009; SANTOLAYA et al., 2019). In urban areas, wind patterns are influenced by changes in ground roughness, wind channelization between buildings, building barrier effects, and urban heat island (UHI) circulations. The sea breeze plays an important role in this process, increasing turbulence and the transport of pollutants to areas far from the emission sources. However, in some cases, it can hinder dispersion, creating a circulation that does not dissipate completely, leading to the stagnation of high concentrations of pollutants near cities. (CHIQUETTO et al., 2018; FREITAS et al., 2007; NAIR et al., 2004; OLIVEIRA et al., 2003).

The ozone (O_3) is a secondary pollutant, formed by photochemical reactions between its precursors, nitrogen oxides (NO_x) and Volatile Organic Compounds (VOCs), which are emitted directly into

the lower troposphere by both anthropogenic and biogenic sources (CHIQUETTO et al., 2019; SCHUCH et al., 2019). The O_3 formation process is complex and nonlinear, depending on the concentrations of its precursors, favorable meteorological conditions, and geographic location that favor pollutant dispersion. Once in the atmosphere, it can remain for up to two hours after the emission of its precursors, which continue to be transported by the wind, leading to high concentrations of O_3 in regions distant from its emission or its precursors (SEINFELD; PANDIS, 2006; SIMON et al., 2015).

There are locations with an abundance of Volatile Organic Compounds (VOCs) emissions compared to NO_x, known as NO_x-limited areas, where a decrease in NO_x results in a decrease in O_3 production. In regions called VOCs-limited areas, where there are high concentrations of NO_x compared to VOCs, a decrease in VOCs can lead to a decrease in O_3 concentrations (ALVIM et al., 2017; 2018; MARTINS; ANDRADE, 2008; MASSAGUÉ et al., 2021; 2024; ORLANDO et al., 2010).

Therefore, this study aims to analyze the dispersion behavior of primary pollutants through tracers with continuous and constant emission between the main metropolitan regions of the State of São Paulo. These regions have a history of exceeding air quality standards in 2019, based on air quality monitoring data available in the State of São Paulo. This analysis aims to understand the implications of precursor transport for O_3 formation.

METHODS

A preliminary analysis of the total number of days exceeding the state air quality standards for O_3 throughout the State of São Paulo from 2014 to 2019 showed a significant decrease in O_3 exceedances from 2014 to 2016 across the state. In 2017, there was a slight increase, followed by another decrease in 2018. However, in 2019, there was a sudden increase in these exceedances, indicating that O_3 is a pollutant that is difficult to control. This increase sparked interest in this study period.

To analyze the interaction of atmospheric pollution by O_3 across multiple regions, the three main metropolitan regions of the State of São Paulo were selected. These regions, in addition to being close to each other, are of great political and economic importance: Metropolitan Region of São Paulo (MRSP), Metropolitan Region of Campinas (MRC), and Metropolitan Region of Baixada Santista (MRBS). In order to conduct the simulations in a representative manner, we decided to choose a week that showed episodes of high daily O_3 concentrations during spring, a favorable season for O_3 formation. Therefore, the period from October 1st to October 8th, 2019, was chosen. Meteorological simulations were performed using the WRF (Weather Research Forecasting Model) with two nested domains: a larger domain of 271 × 271 km, with a horizontal grid spacing of 5 km, and a smaller domain of 150 × 150 km, with a grid spacing of 1 km by 1 km, covering the entire State of São Paulo, centered at coordinates -23.21° S, -46.44° W. The transport of primary precursors was represented using three tracers with continuous and constant emissions in the study regions.

FINDINGS AND ARGUMENT

Analyzing the images generated by the WRF output, as shown in Figure 1, during the morning, it is possible to verify that the predominant wind direction is from the northwest, indicating that the tracer plume located in the RMSP (tracer 1) is transported to the RMC. In the RMC (tracer 2), it is possible to observe that the plume was transported to the northwest, passing through the RMSP, and reaching the RMBS. The tracer 3, located in the RMBS, ascends the escarpment of the Serra do Mar, reaching the RMSP. During the night, there is a change in wind direction, resulting in the inversion of the plumes, but they are still being transported between the regions.

The results demonstrate that there is interaction of primary pollutants between the study regions; thus, this interaction will also affect O3 concentrations.

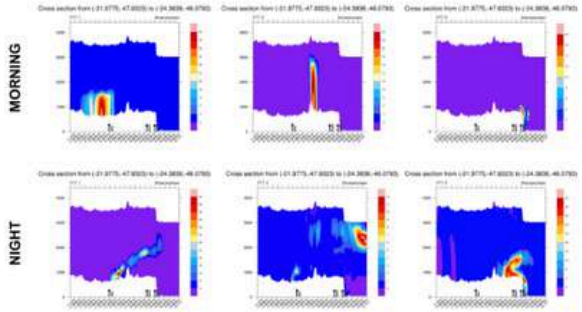


Figure 1. WRF model simulations for the regions: tr17_1 - São Paulo Metropolitan Region; tr17_2 - Campinas Metropolitan Region; and tr17_3 - Baixada Santista Metropolitan Region during morning and night periods.

CONCLUSIONS

Although there are significant sources of pollutants in other regions within the analyzed grid domain, the tracers were placed only in the areas corresponding to the study regions, MRSP, MRC, and MRBS. It is important to emphasize that pollutants emitted in other areas can be transported to the study regions. However, the main objective of this analysis is to investigate the interaction of the pollution plume between the study regions in order to understand the implications of precursor transport on O_3

formation. In future work, we intend to use a more realistic emission inventory and include photochemical modeling of pollutants to better understand O_3 formation.

Finally, this study highlights the need for public policies to jointly address air pollution, considering not only existing economic relations but also the interaction between regions.

REFERENCES

Alvim, Débora Souza; Gatti, Luciana Vanni; Corrêa, Sérgio Machado et al. "Main ozone-forming VOCs in the city of Sao Paulo: observations, modelling and impacts." Air Quality, Atmosphere and Health, 10 (2017): 421–435. Accessed June 13, 2022. doi: 10.1007/s11869-016-0429-9.

Alvim, Débora Souza; Gatti, Luciana Vanni; Corrêa, Sérgio Machado et al. "Determining VOCs reactivity for ozone forming potential in the megacity of São Paulo." *Aerosol and Air Quality Research*, 18 (2018) 2460–2474. Accessed October 28, 2022. doi: 10.4209/aaqr.2017.10.0361.

Chiquetto, Júlio Barboza; Ribeiro, Flávia Noronha Dutra; Alvim, Débora Souza, et al. "Transport of Pollutants by the Sea Breeze in São Paulo under the South Atlantic High." *Revista do Departamento de Geografia*, Volume Especial (2018): 148-161. Accessed February 22, 2024. doi: 10.11606/rdg.v0ispe.143050.

Chiquetto, Júlio Barboza; Silva, Maria Elisa Siqueira; Cabral-Miranda, William et al. "Air Quality Standards and Extreme Ozone Events in the São Paulo Megacity". *Sustainability*, 11 (2019): 3725. Accessed September 04, 2021. doi: 10.3390/su11133725.

Freitas, Edmilson, Dias; Rozoff, Christopher M.; Cotton, William R. et al. "Interactions of an urban heat island and sea-breeze circulations during winter over the metropolitan area of São Paulo, Brazil." *Boundary-Layer Meteorology*, 122 (2007):43–65. Accessed March 01, 2024. doi: 10.1007/s10546-006-9091-3.

Jacob, Daniel J. and Winner, Darrel A. "Effect of climate change on air quality." *Atmospheric Environment*, 43 (2009): 51-63. Accessed July 23, 2022. doi: 10.1016/j.atmosenv.2008.09.051.

Martins, Leila Droprinchinski; Andrade, Maria de Fátima. "Ozone formation potentials of volatile organic compounds and ozone sensitivity to their emission in the megacity of São Paulo, Brazil." Water, Air, and Soil Pollution, 195 (2008): 201213. Accessed July 02, 2022. doi: 10.1007/s11270-008-9740-x.

Massagué, Jordi; Contreras, Juan; Campos, Alberto et al. "2005–2018 trends in ozone peak concentrations and spatial contributions in the Guadalquivir Valley, southern Spain." Atmospheric Environment, 254 (2021): 118385. Accessed January 12, 2024. doi: 10.1016/j.atmosenv.2021.118385.

Massagué, Jordi; Escudero, Miguel; Alastuey, Andrés et al. "Drivers of divergent trends in tropospheric ozone hotspots in Spain, 2008–2019". Air Quality, Atmosphere & Health, 17 (2024): 621–639. Accessed April 22, 2024. doi: 10.1007/s11869-023-01468-0.

Nair, K. N.; Freitas, Edmilson, Dias; Sánchez-Ccoyllo, Odon et al. Dynamics of urban boundary layer over São Paulo associated with mesoscale processes. Meteorology and Atmospheric Physics, 86 (2004): 87–98 Accessed April 03, 2024. doi: 10.1007/s00703-003-0617-7.

Oliveira, Amauri, P.; Bornstein, Robert, D.; Soares, Jacyra. "ANNUAL AND DIURNAL WIND PATTERNS IN THE CITY OF SÃO PAULO." Water, Air, and Soil Pollution: Focus, 3 (2003): 3-15. Accessed April 03, 2024. doi: 10.1023/A:1026090103764.

Orlando, João Paulo; Alvim, Débora Souza; Yamazaki, Amélia et al. "Ozone precursors for the São Paulo Metropolitan Area." *Science of the Total Environment*, 408 (2010): 1612–1620. Accessed February 18, 2023. doi: 10.1016/j.scitotenv.2009.11.060.

Santolaya, Caroline; Oliveira, Maria Carla Queiroz Diniz; Rizzo, Luciana Varanda; Miraglia, Simone Georgers El Khouri. "CONTRIBUTION OF CHEMICAL AND METEOROLOGICAL FACTORS TO TROPOSPHERIC OZONE FORMATION IN SÃO PAULO". *Brazilian Journal of Environmental Sciences*, 54 (2019): 90–104. Accessed August 01, 2022. doi: 10.5327/Z2176-947820190577.

Schuch, Daniel; Freitas, Edmilson Dias; Ibarra-Espinosa, Sérgio et al. "A two decades study on ozone variability and trend over the main urban areas of the São Paulo state, Brazil." *Environmental Science and Pollution Research*, 26 (2019): 31699–31716. Accessed August 11, 2023. doi: 10.1007/s11356-019-06200-z.

Seinfeld, John H. and Pandis, Spyros, N. *Atmospheric chemistry and physics: from air pollution to climate change*. New York: J. Wiley, 2006.

Simon, Heather; Reff, Adam; Wells, Benjamin et al. Ozone trends across the United States over a period of decreasing NOx and VOC emissions. *Environmental Science and Technology*, 49 (2015): 186–195. Accessed January 27, 2022. doi: 10.1021/es504514z.

AIR POLLUTION CONFERENCE BRAZIL
CMAS SOUTH AMERICA
COMMUNITY MODELING AND ANALYSIS SYSTEM

INFLUENCE OF ATMOSPHERIC WINDS DYNAMIC OVER THE CONCENTRATIONS OF PM10 AND PM2.5 IN A OPENCAST COAL MINING AREA OF COLOMBIA FOR A NEUTRAL ENSO PERIOD

José Luis Rodríguez Castilla[1], José Franklin Ruiz Murcia[2], Alex Andres Murillo Villamizar[3], Luis Carlos Angulo Argote[4]

[1]Universidad Nacional de Colombia
Universidad Popular del Cesar
[2]Universidad Nacional de Colombia
jfruizm@unal.edu.co
[3]Universidad Popular del Cesar
aamurillo@unicesar.edu.co
[4]Universidad Popular del Cesar
lcangulo@unicesar.edu.co

Abstract: In a open-pit coal mining area of Colombia country, there is a significant impact on the air quality of its population centers due to PM10 and PM2.5 particulate matter emitted by open-pit coal mines; In the present work, the YSU and MYNN2 planetary boundary layer schemes of the WRF model were validated and it was determined how wind dynamics influence the concentration of particulate material that is monitored in the area. Transport routes for particulate matter PM10 and PM2.5 were found in a period of neutral ENSO and the influence of regional and local winds on these routes was estimated. In addition, the behavior of winds at different height levels was analyzed, taking as reference the planetary boundary layer; Finally, during the study period, local-scale wind dynamics patterns were identified that could be implemented to forecast episodes of high concentration of particulate matter in the area. The results showed that on the days of peak concentration of particulate matter PM10 and PM2.5 occurred under conditions of atmospheric stability and slow movement of local air masses, which caused the particulate matter to remain suspended in the atmosphere for a considerable time.

Keywords: Wind simulation, WRF, Hysplit,PM10, PM2.5.

INTRODUCTION

In Colombia there is great interest in studying the dimension of the environmental impact generated by open pit coal mining companies on the air resource, but in most cases the lack of primary information does not make this work possible. It is for this reason that the implementation of technological tools and the use of mathematical models of air quality must be taken into account as an alternative to help solve problems that affect communities established near mining projects.

Although, in one of the open-pit coal mining areas of Colombia, located in the department of Cesar, there are a series of surface weather stations that can give us an idea of what the behavior of the meteorology is like in the area, these do not have radiosonde campaigns to measure meteorological variables in the vertical. It is for this reason that it is necessary to develop and apply mathematical modeling tools that adequately represent the meteorology of the study area and that make it possible to reveal the behavior of the dispersion of the pollutants present in it. In this work, the WRF meteorological model (Skamarock, Klemp, & Dudhia, 2001) was implemented, which adapts to the needs of the study area. The WRF is a dynamic model with the capacity to simulate the behavior of the different variables of the atmosphere in a non-hydrostatic manner and that also allows monitoring the behavior of winds and non-reactive atmospheric pollutants such as particulate matter PM10 and PM2.5.

METHODS

A downscaling was carried out by applying the WRF model to determine the behavior of the surface wind, taking the planetary boundary layer as a reference and evaluating two of its parameterizations in the study area; the planetary boundary layer parameterizations to be evaluated were YSU and MYNN2 (Hong, S. Y., 2010); (Hong, Noh, Dudhia, 2006); (Nakanishi, M., and H. Niino., 2006).For the simulations, the CFSR (Climate Forecast System Reanalysis) reanalysis data from the NCEP (National Centers for Environmental Prediction) were used as initial and boundary conditions at a horizontal spatial resolution of 0.25°, 37 levels of vertical resolution and a departure frequency of 6 hours (Saha, 2010; Saha et. al., 2010). A set of three nested domains was centered on the coal zone of the Cesar

department. A mother domain that covers a large part of the north of Colombian territory with 9 km of spatial resolution, a second smaller domain of 3 km resolution and a third domain of 1 km resolution that covers the Cesar opencast coal mining area.



Figure 1. Domains in the coal mining area of the department of Cesar, Colombia (Autor).

The period of 2019-2020 was chosen to carry out the modeling taking into account different vertical levels depending on the planetary boundary layer; this period was characterized by having a neutral ENSO phase (NOAA). The results returned by the WRF served as input to run the Hysplit trajectory model Draxler, R. R., Hess, G. D. (1998).

Statistical analyzes like the mean square error and the mean absolute error were used to evaluate the results of the WRF model; the data provided by the WRF were compared with the existing surface meteorological information in the study area for the study months of the 2019-2020 period. The validation was carried out with hourly average values of the variables: temperature, relative humidity, wind speed and wind direction. In addition, a wind analysis was carried out for each meteorological station applying trend diagrams; this was compared with the wind data produced by the WRF model. To analyze the behavior of the planetary boundary layer in the study area, the mixed layer height variable "PBLH" produced by the WRF model was plotted at different times (6:00 AM, 1:00 PM, 9:00 PM) on the simulated days. The vertical profiles of the virtual potential temperature, wind speed and direction were graphed, taking the town of La Jagua de Ibirico as a study point for the creation of these profiles. Through the graphed profiles it was possible to identify the evolution of the boundary layer vertically and its relationship with the speed and direction of the wind.

FINDINGS AND ARGUMENT

The dry, wet and transition seasons of the region were taken into account to evaluate the parameterizations of the YSU and MYNN2 planetary boundary layer in different meteorological situations.

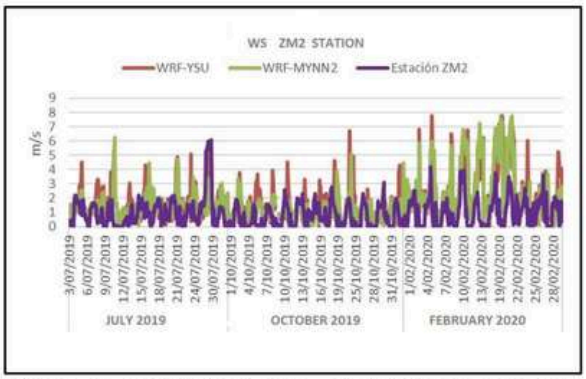


Figure 2. trend diagrams of wind speed in the validation of WRF model for the weather superficial station ZM2 (Autor).

Table 1. Statistical analysis of the MYNN2 parameterization for the meteorological study variables at the ZM2 station.

Weather station ZM2	PBL-MYNN2			
	Temp.	RH	WS	WD
MB, Bias	1,1590	0,0118	-0,7465	-0,0366
NMB	0,0401	0,0002	-0,7969	-0,0002
RMSE	1,9533	8,7948	1,7713	117,4358
NMSE	0,0047	0,0137	1,7982	0,3953

Reference: Autor.

The WRF model in its YSU and MYNN2 planetary boundary layer schemes represented adequately the meteorology of the open pit coal mining area of the Cesar department in the study period. The data of the studied variables produced by the two CLP schemes showed correspondence with the data of the five surface stations with which the model was compared, however, the surface wind direction variable presented a high bias.

The transport routes of the PM10 and PM2.5 particulate matter that entered the mining area of department of Cesar for the study period were identified, implementing a retro-trajectory analysis with the Hysplit model. The stations ZM3 (Loma Caribe), ZM2 (La Jagua center) and ZM15 (Chiriguaná) at 00:00 hours (UTC) or 19:00 hours (UTC-5) were taken as the final point of the particles in the retrotrajectories. at a height of 50 meters. It was found that one of the main transport routes comes from the east-west direction, which means that an important part of the particulate matter that entered the area in the

months of study crossed the Perijá mountain range in this direction.

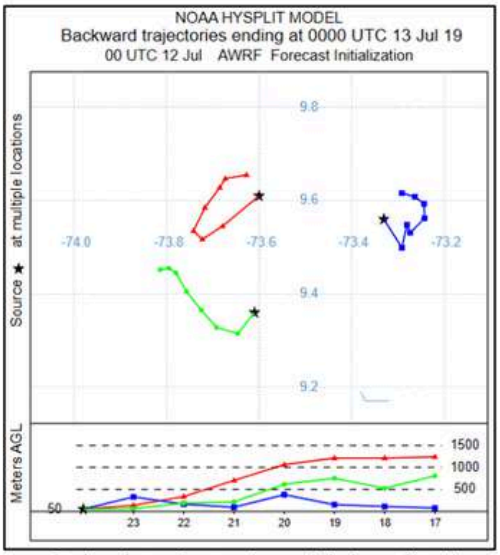


Figure 3. back trajectories with hysplit (Autor).

CONCLUSIONS

The atmospheric dynamics in the area is influenced by the intensity in which the north-east trade winds can occur; When its influence is greater, there is a displacement of humidity in the atmosphere of the area and conditions of atmospheric stability occur (at night and early morning) which, together with a low height of the boundary layer, can lead to an increase in PM10 concentrations. and PM2.5. When the trade winds are less intense, convective processes occur in the area that cause precipitation to fall, which helps to attenuate the concentrations of particulate matter. Another process that influences the dynamics of the atmosphere in the area is the valley-mountain interaction. In the area of the foothills closest to the Perijá mountain range, a notable influence of the katabatic winds coming from this mountain formation was observed during the night and early morning hours. In addition, the influence of the winds coming from the south-east stands out in the area, which predominate in rainy seasons and that even in dry seasons manage to influence the area at night and early morning.

The results of the retro-trajectory modeling with the Hysplit showed a predominance of transport of air masses from the east-west direction, where it was observed how the air masses cross the Perijá mountain range to arrive at the study area. However, it was not found that the pollution peaks presented in the study period were due to particulate matter transported from long distances. This study made it possible to verify that the dynamics of the local atmosphere was the cause of these pollution peaks due to PM10 and PM2.5 particulate matter.

REFERENCES

Draxler, R. R., Hess, G. D. (1998). An overview of the HYSPLIT_4 modeling system for trajectories, dispersion, and deposition. Australian Meteorological Magazine, 47, 295-308.

Hong, S. Y. (2010). A new stable boundary layer mixing scheme and itsimpact on the simulated East Asian summer monsoon. Quart. J. Roy.Meteor. Soc.,136(651), 1481–1496.

Hong, S. Y., Noh, Y., & Dudhia, J. (2006). A new vertical diffusion package with an explicit treatment of entrainment processes. Monthly Weather Review, 134,, 2318-2341.

Nakanishi, M., and H. Niino. (2006). An improved Mellor-Yamada level 3 model: its numericalstability and application to a regional prediction of advecting fog. Bound. Layer Meteor. 119,397–407.

NOAA.https://origin.cpc.ncep.noaa.gov/products/analysis_monitoring/ensostuff/ONI_v5.php

Saha, S. (2010). Climate Forecast System Reanalysis. . Bulletin of the American Meteorological Society, 91(8), , 1015–1057.

Skamarock, W. C., Klemp, J. B., Dudhia, J. (2001). Prototypes for the WRF (Weather Research and Forecasting) model. Ninth Conference on Mesoscale Processes, Amer. Met. Soc., Ft. Lauderdale, (págs. 11-15).

AIR POLLUTION CONFERENCE BRAZIL
CMAS SOUTH AMERICA
COMMUNITY MODELING AND ANALYSIS SYSTEM

MULTİSCALE MODEL EVALUATİON İN SUPPORT OF AN ANALYSİS AND FORECAST SYSTEM FOR LATİN AMERİCA

Jorge E. Pachon[1], Mariel A. Opazo[2], Pablo Lichtig[3], Nicolas Huneeus[4], Idir Bouarar[5], Guy Brasseur[6]

[1] Universidad de La Salle, Bogota, Colombia
E-mail: jpachon@unisalle.edu.co
[2] Universidad de Chile, Santiago, Chile
E-mail: mariel.opazo@uchile.cl
[3] Consejo Nacional de Energía Atómica - CNEA, Buenos Aires, Argentina
E-mail: pablo.lichtig@gmail.com
[4] Universidad de Chile, Santiago, Chile
E-mail: nhuneeus@uchile.cl
[5] Max Planck Institute for Meteorology, Hamburg, Germany
E-mail: idir.bouarar@mpimet.mpg.de
[6] Max Planck Institute for Meteorology, Hamburg, Germany
E-mail: guy.brasseur@mpimet.mpg.de

Abstract:
A multi-scale model evaluation has been conducted in Latin America in 2015 (January and July) with the purpose to assess the performance of global and regional air quality models and set a pathway for an analysis and forecasting system in the region. Two global and three regional models were implemented and compared over a shared domain (120W-28W, 60S-30N) by different research groups in Latin America and Europe as part of the PAPILA (Prediction of Air Pollutants in Latin America) project (https://papila-h2020.eu/papila). Observations from local air quality monitoring networks in Mexico, Colombia, Ecuador, Perú, Chile, Brazil, and Uruguay were used for model evaluation. An ensemble, created from the median value of the individual models, was assessed on its performance.

Most models were able to adequately reproduce air quality observations even with the adopted coarse resolution (0.2 x 0.2°) used in this work. However, no single model or ensemble had the best performance among pollutants and sites available. In general, ozone achieved high scores across sites while SO_2 had the lowest performance. The median ensemble showed superior results for NO_2 than individual models. Large urban areas (> 3500 km^2) outperformed smaller urban zones (area between 500 and 1000 km^2), suggesting an accurate portrayal of the temporal and spatial variability in large cities and the need for a finer resolution in smaller cities.

This study identified certain limitations in global emissions inventories that should be addressed with the involvement and experience of local researchers. For example, NO_2 and CO were substantially underestimated by all models in Bogota due to the lack of local emission sources in global inventories, especially from on-road sources. Similarly, $PM_{2.5}$ levels were overestimated in Sao Paulo due to overestimation of biomass burning activity.

This work will present the results of the first multiscale model intercomparison in Latin America, highlighting the main outcomes and challenges for the setting of an analysis and forecasting system for the region.

Keywords: model intercomparison, ensemble, Latin America, evaluation scores, air quality forecasting

INTRODUCTION

This report presents the results of the different modeling test cases in Latin America and their validation. Two global and three regional models were selected to simulate ambient air concentrations of CO, NO_2, SO_2, O_3, and $PM_{2.5}$ in Latin America and the Caribbean in 2015 at 0.2 degrees spatial resolution. The model set up and executions were conducted by different groups from Europe and Latin America with complement expertise. A protocol was prepared to guide the activities and facilitate postprocessing analysis. Simulated concentrations were compared with observations from different air quality monitoring networks in the region.

In general, there is a good agreement between models and observations in terms of order of magnitude, but correlation coefficients are relatively low ($0.2 < R < 0.6$). The pollutants best and worst simulated by the models are ozone and SO_2 (lowest and highest mean bias and error). Latin America and the Caribbean represent a challenge for air quality modeling, due to a complex topography and diverse meteorological conditions.

METHODS

The model inter-comparison task for Latin America included the execution of two global and three regional air quality models in a domain that covered

Latin America and the Caribbean (120W-28W, 60S-30N, spatial resolution 0.2°). The modeling period was January and July of 2015. Pollutant concentrations were available from several air quality monitoring networks in the region, but major cities were more robust in terms of number of monitoring sites and data quantity and quality. The tests cases for this study are describe in Table 1. All modeling fields are available in an open repository (Pachon et al., 2024).

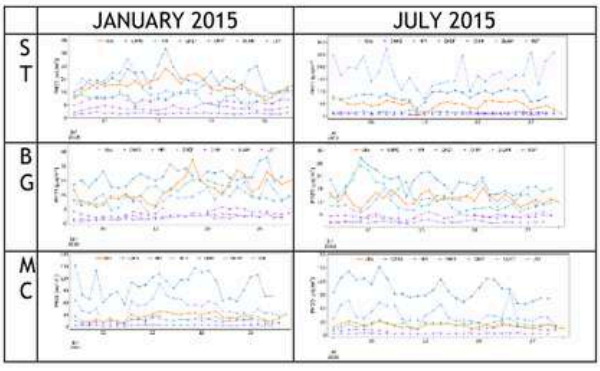
Table 1. Header

Modeling periods	Cities	Pollutants	Metrics
January	Bogota	PM2.5	BIAS
July	Mexico	NO2	NMBIAS
	Santiago	O3	RMSE
	Sao Paulo	CO	FGE

FINDINGS AND ARGUMENT

With the purpose to evaluate similarities and differences in the simulation of pollutants among cities in LAC, time series between models and observations were constructed and analyzed. The inter-model variability (IMV) was estimated as the range between predicted values (maximum - minimum) and normalized by the observations. This extended abstract only shows results for $PM_{2.5}$.

The largest $PM_{2.5}$ predicted values and IMV are found in Mexico City (MC) and Sao Paulo (SP), as well as Santiago (ST) during winter time. However, the IMV for $PM_{2.5}$ is approximately four times the average of observations. In Santiago in July the large IMV value (213 ug/m^3) is caused by one model, if that prediction is removed the IMV descends to 95.2 ug/m^3, which corresponds to 1.6 the average of observations. In the summer in Santiago (January) and in Bogota, the IMV is the lowest and corresponds to approximately 1.3 times the observations. The predicted $PM_{2.5}$ concentrations are also lower. Most models in Santiago, Bogota and Mexico City simulate $PM_{2.5}$ above and below the observations, but in Sao Paulo overprediction is more commonv (Figure 1).



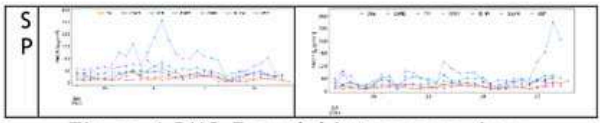


Figure 1 PM2.5 model intercomparison

CONCLUSIONS

A model inter-comparison exercise was conducted for Latin America during January and July of 2015 with the purpose to evaluate global and regional models and set a path for an air quality analysis and forecast system in the region. Two global and three regional models were executed with a spatial resolution of 0.2 x 0.2° (~20 km in the equator) and predict concentrations of $PM_{2.5}$, NO_2, O_3, CO and SO_2. The models were able to reproduce pollutants at the same order of magnitude than observations especially in the largest urban areas (Sao Paulo and Mexico City). Santiago and Bogota showed larger differences with the observations, probably due to the complex topography and meteorological conditions, requiring a finer, but more computationally expensive resolution. Nevertheless, problems with global emission inventories were observed, such as the severe overestimation of SO_2 by all models in all cities (except Bogota), the underprediction of NO_2 in Bogota and Santiago and the underprediction of CO in Bogota. Local expertise can be useful to understand and solve gaps in global emissions (Álamos et al., 2022; Castesana et al., 2022; Puliafito et al., 2015, 2017; Rojas et al., 2023).

REFERENCES

Álamos, N., Huneeus, N., Opazo, M., Osses, M., Puja, S., Pantoja, N., Denier van der Gon, H., Schueftan, A., Reyes, R., & Calvo, R. (2022). High-resolution inventory of atmospheric emissions from transport, industrial, energy, mining and residential activities in Chile. *Earth Syst. Sci. Data*, *14*(1), 361–379. https://doi.org/10.5194/essd-14-361-2022

Castesana, P., Diaz Resquin, M., Huneeus, N., Puliafito, E., Darras, S., Gómez, D., Granier, C., Osses Alvarado, M., Rojas, N., & Dawidowski, L. (2022). PAPILA dataset: a regional emission inventory of reactive gases for South America based on the combination of local and global information. *Earth System Science Data*, *14*(1), 271–293. https://doi.org/10.5194/essd-14-271-2022

Pachon, J. E., Opazo, M. A., Lichtig, P., Huneeus, N., Boaurar, I., Li, C. W. Y., Brasseur, G., Flemming, J., Menut, L., menares menares, camilo, Gallardo, L., Gauss, M., Sofiev, M., Kouznetsov, R., Palamarchuk, J., Dawidowski, L., Rojas, N. Y., Andrade, M. de F., Gavidia-Calderón, M. E., … Schuch, D. (2024). *Supplementary Dataset: Air quality*

modeling intercomparison and multi-scale ensemble chain for Latin America. Zenodo. https://doi.org/10.5281/zenodo.10934490

Puliafito, S. E., Allende, D. G., Castesana, P. S., & Ruggeri, M. F. (2017). High-resolution atmospheric emission inventory of the argentine energy sector. Comparison with edgar global emission database. *Heliyon*, *3*(12), e00489. https://doi.org/https://doi.org/10.1016/j.heliyon.2017.e00489

Puliafito, S. E., Allende, D., Pinto, S., & Castesana, P. (2015). High resolution inventory of GHG emissions of the road transport sector in Argentina. *Atmospheric Environment*, *101*, 303–311. https://doi.org/https://doi.org/10.1016/j.atmosenv.2014.11.040

Rojas, N. Y., Mangones, S. C., Osses, M., Granier, C., Laengle, I., Alfonso A., J. V, & Mendez, J. A. (2023). Road transport exhaust emissions in Colombia. 1990–2020 trends and spatial disaggregation. *Transportation Research Part D: Transport and Environment*, *121*, 103780. https://doi.org/https://doi.org/10.1016/j.trd.2023.103780

AIR POLLUTION CONFERENCE BRAZIL
CMAS SOUTH AMERICA
COMMUNITY MODELING AND ANALYSIS SYSTEM

Impact of WRF Modeled PBLH Errors on CMAQ Air Quality Simulations

Robson Will[1], Leonardo Hoinaski[2]
[1]UFSC
Robson.will@posgrad.ufsc.br
[2]UFSC
Leonardo.hoinaski@ufsc.br

In the realm of air quality modeling, accurately representing the planetary boundary layer height (PBLH) is pivotal for assessing pollutant levels with precision. Given the limited availability of PBLH data, meteorological modeling emerges as a viable alternative. However, this approach introduces errors and modeling bias, and the extent of their influence on CMAQ (Community Multiscale Air Quality) results remains to be determined. Our study quantifies the impact of propagated errors from WRF (Weather Research and Forecasting) PBLH simulations on CMAQ air quality modeling. We calculated biases between WRF PBLH outputs and meteorological balloon data, as well as biases between CMAQ ozone (O3) concentration simulations and ground measurements in the São Paulo metropolitan region, Brazil. Employing the Spearman correlation index, we examined the relationship between these biases to unravel the intricate interplay between the two models. Our results reveal a significant relationship, shedding light on the substantial influence of modeling errors in WRF on CMAQ concentration outcomes. These results underscore the critical role of the planetary boundary layer's height in shaping the dispersion of pollutants. These findings not only contribute to advancing our understanding of air quality modeling intricacies but also hold implications for refining future modeling approaches in pollution assessment.

Keywords: CMAQ, WRF, PBLH, error

INTRODUCTION

The study of emissions, dispersion, and reception of atmospheric pollutants in developing countries faces technical barriers, mainly due to the need for more data at appropriate temporal and spatial scales (Long et al., 2022).

In Brazil, available air quality data is limited to atmospheric pollutant control stations restricted to a few urban centers with limited or unknown spatial representativeness (Andreao and Toledo de Almeida Albuquerque, 2020). The advent of models, inventories, and diagnoses on air quality in the country makes it possible to develop studies on the relationship between air quality and the health risks posed by pollutants (Will et al., 2022).

The lack of data is not limited to pollutant measurement; PBLH measurements are also scarce, making it necessary to couple models like WRF with CMAQ. As a consequence, errors propagate between the two models, potentially deteriorating the quality of the results.

Measuring the possible errors propagated between the two models becomes necessary to ensure that the findings have well-defined applications. Under the hypothesis that different PBLH configuration options can reduce propagated errors, our objective is to measure these errors using two distinct WRF configurations and calculate the difference between CMAQ simulations and data measured at reference stations in the state of São Paulo.

METHODOLOGY

We conducted meteorological simulations using the Weather Research and Forecasting (WRF) model. This model utilizes files from the Global Forecast System (GFS) of the National Center for Atmospheric Research (NCAR), providing inputs with a spatial resolution of 0.25° x 0.25° and a temporal resolution of six hours for WRF simulations (Skamarock et al., 2019). Land use data and classification parameters from the Moderate Resolution Imaging Spectroradiometer (MODIS) of the United States Geological Survey (USGS) were also employed. We used bl_pbl_physics settings of 1 for the first model (model A) and 11 for the second model (model B). Thirty-three vertical levels were employed, spaced at 50 hPa intervals. The remaining vertical levels followed a hybrid modeling scheme, accounting for terrain in the lower layers and gradually minimizing its influence in the upper levels. Similar to CMAQ, the spatial resolution used was 20x20 km. The simulation domain is the same one used for CMAQ, shown in Figure 1.

The remaining inputs for CMAQ are the emissions inventories, which include vehicular (BRAVES), industrial, biogenic (MEGAM), and biomass-burning emissions (FINN). In this work, we utilized CMAQ results for ozone (O3). All files are available on the Brazilian Atmospheric INventories (BRAIN) platform (Hoinaski et al., 2024).

We collected sounding data from https://ruc.noaa.gov/raobs/ for station SBMT (MARTE) 83779 23.52S 46.63W 722. METAR data was collected from https://hoinaski.prof.ufsc.br/BRAIN/getMETAR.

We processed this data using AERMET to obtain the boundary layer height; we used the platform

https://hoinaski.prof.ufsc.br/AERMOD_online/AERMET_web to run AERMET and intermediate processes.
Ozone concentration data was obtained from the platform https://energiaeambiente.org.br/qualidadedoar/.
The analysis period was from July 1st, 2020, to July 31st, 2020. We collected data from all air pollution measurement stations in the state of São Paulo.
Data analysis was performed using Python with the Scipy library. Figures were created using the MATPLOTLIB library.



Figure 1 - WRF/CMAQ modeling domain.

FINDINGS AND ARGUMENT

Our initial results pertain to PBLH. We used the Spearman correlation index between the meteorological monitoring station at SBMT airport and the WRF simulations. Our results show a difference of 0.007 between the Spearman correlation indexes found for the two WRF configurations: model A—0.5798 and model B—0.5724, a percentage difference of 1.27% between the indexes. This difference, although small, propagated to the results of the CMAQ simulations.
The correlation values between the CMAQ simulations using models A and B as input and the reference stations can be found in Table 1. These results show an average difference of 1.07% between the Spearman indexes, with the most significant difference occurring at the Sorocaba reference station (2.88%) and the smallest at the Presidente Prudente station (0.08%). Due to the lack of upper air and METAR data for these locations, it was not possible to measure the difference between simulated and measured PBLH at the ground level. Thus, we assume that the difference in PBLH within the state of São Paulo is similar across all air quality measurement stations.

Table 1. spearman correlation and difference between model A and B for CMAQ.

Air quality station	MODEL A	MODEL B	difference %
Bauru	0.4225	0.4129	2.26%
Campinas - Taquaral	0.5367	0.5288	1.46%
Carapicuíba	0.6351	0.6325	0.41%
Catanduva	0.4806	0.4798	0.17%
Grajaú - Parelheiros	0.6337	0.6162	2.77%
Guaratinguetá	0.5474	0.5322	2.79%
Guarulhos - Paço Municipal	0.5595	0.5563	0.58%
Ibirapuera	0.6662	0.6648	0.22%
Interlagos	0.6644	0.6627	0.25%
Itaim Paulista	0.5684	0.5639	0.79%
Itaquera	0.6127	0.6084	0.69%
Jundiaí	0.6803	0.6739	0.95%
Limeira	0.6648	0.6569	1.19%
Mauá	0.4893	0.4768	2.56%
Mooca	0.5300	0.5285	0.28%
Nossa Senhora do Ó	0.6455	0.6344	1.72%
Paulínia	0.6162	0.6092	1.12%
Pinheiros	0.5628	0.5586	0.75%
Piracicaba	0.7754	0.7735	0.25%
Presidente Prudente	0.2889	0.2887	0.08%
Rio Claro - Jardim Guanabara	0.7107	0.7082	0.35%
Santana	0.5826	0.5712	1.95%
Santo Amaro	0.6196	0.6105	1.48%
Santos - Ponta da Praia	0.4645	0.4599	1.00%
Santos	0.4510	0.4474	0.79%
Sorocaba	0.5514	0.5355	2.88%
São Bernardo do Campo - Centro	0.5701	0.5687	0.25%
São Caetano do Sul	0.5557	0.5510	0.84%
São José dos Campos - J.S.	0.3950	0.3902	1.19%
São José dos Campos	0.4827	0.4817	0.21%

Figure 2 illustrates the spatial distribution of the analyzed stations and their respective percentage differences in correlation index results. We observe that most points are concentrated in the capital, where the role of boundary layer height seems more relevant. At the same time, more minor differences appear in locations farther from the capital in less urbanized areas.

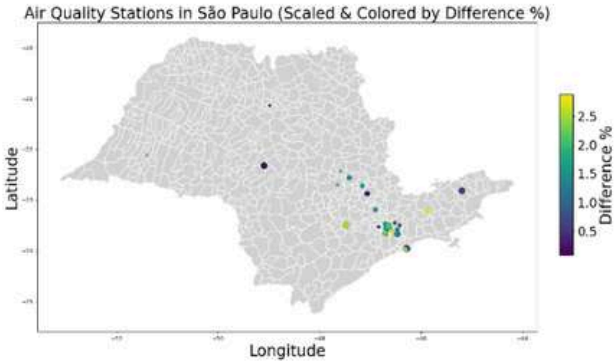


Figure 2 – Air quality stations in São Paulo.

We considered only one variable change between the two simulations; therefore, the difference in CMAQ modeling results should be explained solely by the PBLH calculation configuration in WRF. This preliminary indication suggests that errors in PBLH modeling are a significant factor in atmospheric pollutant modeling errors. Further, more precise, and in-depth tests should be conducted.

CONCLUSIONS

This study demonstrated that errors in WRF-modeled PBLH can propagate to CMAQ air quality simulations, affecting the accuracy of ozone predictions. The choice of PBLH parameterization in WRF can influence CMAQ results, and this sensitivity can vary spatially and temporally. Further studies should be conducted to measure this error propagation.

REFERENCES

Andreão, Willian Lemker, and Taciana Toledo de Almeida Albuquerque. "Avoidable mortality by implementing more restrictive fine particles standards in Brazil: An estimation using satellite surface data." Environmental Research 192 (2021): 110288.

Hoinaski, Leonardo, Robson Will, and Camilo Bastos Ribeiro. "Brazilian Atmospheric Inventories–BRAIN: a comprehensive database of air quality in Brazil." Earth System Science Data 16.5 (2024): 2385-2405.

Long, Haichuan et al. Evaluation of the Planetary Boundary Layer Height in China Predicted by the CMA-GFS Global Model. Atmosphere, v. 13, n. 5, p. 845, 2022.

Skamarock, William C., et al. "A description of the advanced research WRF version 4." NCAR tech. note ncar/tn-556+ str 145 (2019).

Will, Robson, et al. "Socioeconomic development role in hospitalization related to air pollution and meteorology: A study case in southern Brazil." Science of The Total Environment 826 (2022): 154063.

AIR POLLUTION CONFERENCE BRAZIL
CMAS SOUTH AMERICA
COMMUNITY MODELING AND ANALYSIS SYSTEM

QUANTIFYING THE IMPACT OF AEROSOLS ON THE PREDICTIVE SKILL OF SUBSEASONAL GLOBAL ATMOSPHERIC AND AIR QUALITY SIMULATIONS

Ariane Frassoni[1] and Frederic Vitart[2]
1-Brazilian National Institute for Space Research
2-European Centre for Medium-Range Weather Forecasts
ariane.frassoni@inpe.br

Abstract: Subseasonal forecasts have been fundamental in bridging the gap between numerical weather predictions and seasonal forecasts, offering a wide range of products and services, particularly within the intraseasonal timescale. Recognizing the significance of atmospheric composition in enhancing weather and climate prediction capabilities for the global climate system, the World Climate Research Programme Core Project Earth System Modeling and Observations-Working Group on Numerical Experimentation (WGNE), the WCRP-World Weather Research Programme (WWRP) S2S Steering Group (S2S-SG) and the Global Atmosphere Watch Programme Scientific Advisory Group on Applications (SAG APPs) have collaboratively led the WGNE Aerosol Project. This initiative aims to gain a deeper understanding of the role of aerosols in the predictive skill of models within the S2S timescale. The WGNE Aerosol Project involves operational meteorological centers worldwide, contributing their state-of-the-art climate-chemistry-aerosol-cloud-radiation coupled modeling systems. Modeling groups participants contributed with an ensemble of retrospective predictions (hindcasts) considering distinct model configurations, taking into account the feedback between radiation/microphysics parametrization and aerosols. No-feedback between radiation/microphysics and aerosols experiments were considered as reference experiments. These reference experiments serve as a baseline to evaluate and understand the impact of incorporating feedback mechanisms in the modeling systems. We propose to assess the performance of the WGNE Aerosol project modeling contributions, specifically focusing on the global domain within the S2S timescale. This work will present preliminart results of the assessment, focusing on the main atmospheric variables near the surface, and aerosol properties. The WGNE Aerosol Project offers an opportunity to comprehend the feedback represented in current climate-chemistry-aerosol-cloud-radiation coupled systems and their impact on predicting climate variability, air quality, and extreme meteorological events within the S2S timescale. Moreover, it aims to identify the uncertainties associated with model predictions of feedback, providing insights for future developments and addressing the complexities of coupled modeling systems that impact predictive skill within the S2S timescale.

***Keywords*:** *Subseazonal prediction, climate prediction, aerosols, aerosol-climate feedbacks*

INTRODUCTION

Atmospheric aerosols are one of the main uncertainties on Earth's energy budget and radiative forcing for climate change estimation. Increased confidence in the quantification of changes in the Effective Radiation Forcing (that indicated the strength of a climate driver) due to aerosols based in new observations and model-based studies, however, have been indicating the decrease of uncertainty due to a better understanding of the aerosol radiative feedbacks.

The role of aerosols as a climate driver is associated with their direct interaction with radiation (direct effect) (Zuidema et al., 2016) and changes in cloud lifecycle and precipitation (indirect effect).

However, despite the importance of aerosols on the climate variability, their impact on Numerical Weather (NWP) and Climate Prediction (CP) have been addressed in the last two decades. The incorporation of climatologies of aerosols to improve the skill of global models were the first approximation to take into account the effects of aerosols. Later, the development of real-time treatment (or interactive aerosols with respect of dynamics, radiation and microphysics) in operational forecasting systems in regional and global models was carried out. There is still uncertainty regarding the magnitude of the impact as well as the degree of model sophistication that is needed to fully capture the effects of aerosols.

Understanding these complex interactions is crucial for improving numerical models' ability to simulate and predict weather and climate patterns accurately. The numerical representation of atmospheric composition is also fundamental to the performance of air quality forecast models. Chemical reactions involving atmospheric constituents have implications for air quality, weather and climate. For instance, the oxidation of pollutants can lead to the formation of secondary pollutants such as O_3 and aerosols, which impact both air quality and atmospheric patterns. Accurately representing these chemical processes in

numerical models is essential for simulating and predicting air pollution levels and their environmental impacts.

Despite the unprecedented opportunities to provide relevant information on key climate characteristics within the Subseasonal to Seasonal (S2S) timescale, there remains room for improvement in the predictive skill of S2S forecasts. One potential avenue for enhancement is the numerical representation of two-way aerosol-climate interactions. Atmospheric aerosols play a crucial role as climate forcing due to their interactions with radiation (direct effect) and influences on cloud life cycle and precipitation (indirect effect). Acknowledging the role of atmospheric composition in enhancing forecast capabilities in meteorological centres, a collaborative effort was initiated in 2019 by WGNE jointly with the WWRP Subseasonal to Seasonal (S2S) Steering Group and the GAW Scientific Advisory Group (SAG) on Modelling Applications (SAG-APP). The research goals encompass a comprehensive investigation of the potential benefits of applying atmospheric composition forecasts within the subseasonal timescale. Therefore, the WGNE- Aerosol Project fosters collaboration among operational meteorological centres and research institutions worldwide. It brings together experts who contribute their cutting-edge integrated chemistry-meteorology numerical models.

Subseasonal experiments in the global-scale were performed by several meteorological centres, using the re-forecast ensemble approach. These experiments aim to simulate the direct and (optionally) indirect effects of aerosols, allowing for comparisons between simulations with climatological aerosols and those incorporating the effect of aerosol interactively.

METHODS

A systematic study has been conducted considering the diversity and complexity of participating modelling groups based on the fixed model version, computational and human resources available in each participating institution. The present study considered those experiments focused on biomass burning smoke over South America and the Africa continents. To this end, the analysed period encompasses the month of September, the peak of the dry season in both continents.

The S2S experiments considered as forecast length about 32-days from 00:00 UTC, with time resolution of 6 hours. Different start dates and number of ensemble members were considered, depending on the capability of the modeling groups. In this study, the European Centre for Medium-Range Weather Forecasts (ECMWF) Integrated Forecast System (IFS), the National Aeronautics and Space Administration (NASA) and the National Oceanic and Atmospheric Administration (NOAA) of the United States of America (USA) global models were analysed. The number of ensemble members considered was 15, 5 and 4 for IFS, NOAA and NASA, respectively.

Daily data from the ERA5 reanalysis were used to assess 2-meter temperature hindcasts quality (Hersbach et al., 2019). The spatial resolution of ERA5 is 25km of lat/lon. To assess the skill of Aerosol Optical Depth (AOD), daily data from the Copernicus Atmosphere Monitoring Service (CAMS) (Flemming et al., 2015) and Modern-Era Retrospective analysis for Research and Applications, Version 2 (MERRA2, GMAO, 2005) from NASA were used.

A case study was analysed in order to identify the ability of the models in predict the anomalies of AOD in the S2S timescale. September 2019 was chosen as the case study due to the intense biomass burning smoke released to the atmosphere. The forecasted anomalies were compared with CAMS and MERRA2 reanalysis.

2-meter temperature and AOD hindcasts of the three models were evaluated using a determinist metric. It was calculated for four weekly average lead times counting from the hindcast start dates of each model as follows: days 1–7 (week-1), days 8–14 (week-2), days 15–21 (week-3) and days 22–28 (week-4). Lead time dependent hindcast weekly averages for these days (and for the corresponding matching reference data) were computed considering the start dates of each model. The correlation between predicted and observed 2-meter temperature and AOD anomalies at each grid point were selected to measure the linear association between the models and reference datasets.

FINDINGS AND ARGUMENT

The spatial distribution of correlation values between the predicted and observed AOD (CAMS) anomalies for NOAA model produced for the first (left upper panel) to the fourth weeks (right bottom panel) is shown in Figure 1. Predicted anomalies used for producing the correlation maps of Fig. 1 are based on the ensemble mean of 5 hindcast members for NOAA model. It is observed high correlation values during the first week in most regions, and these values decrease as the lead time increases. This behavior is well-documented

in other weekly variable predictions like precipitation at the sub-seasonal time scale, as the initial conditions used to run the models during the first two weeks have a major impact on prediction performance than those used during the last two weeks (Andrade et al. 2019).

In addition to NOAA, NASA and ECMWF correlation maps (not shown) also indicate similar behavior, with higher values of correlation for the first lead time and lower correlation values for the 4th lead time. Biomass burning emissions contributing to black carbon and organic matter loads came from global biomass burning emissions provided by satellite datasets for NOAA and NASA and are prescribed from the Global Fire Assimilation System for IFS.

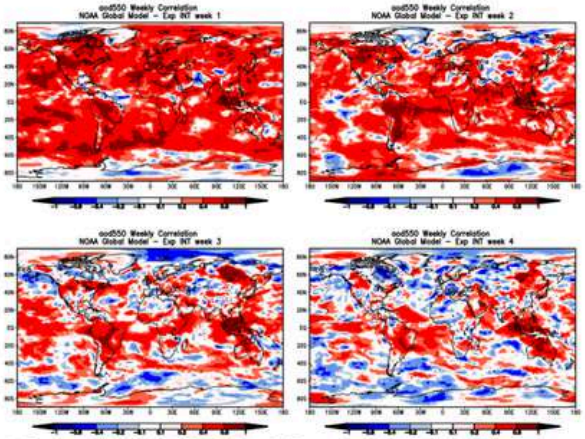


Figure 1. AOD weekly correlation maps – NOAA model x CAMS

As both modeling groups provided an interactive prognostic aerosol run with prognostic aerosols and a second run in which aerosols come from a fixed climatology, it is possible to identify the impact of prognostic and climatological aerosols on the 2-meter temperature anomalies prediction. The difference between the spatial distribution of correlation values between the predicted and observed (ERA5) 2-meter temperature anomalies for ECMWF model produced for the first (left upper panel) to the fourth weeks (right bottom panel) is shown in Figure 2. Red colors indicate degradation while blue colors indicate improvement when using interactive aerosols. Different from NOAA model (not shown), ECMWF correlation map differences indicate degradation over the areas mostly influenced by biomass burning smoke in September, e.g., over South America and South Africa. These results might be related with the implementation of aerosol properties in the IFS radiative scheme and should be better investigated.

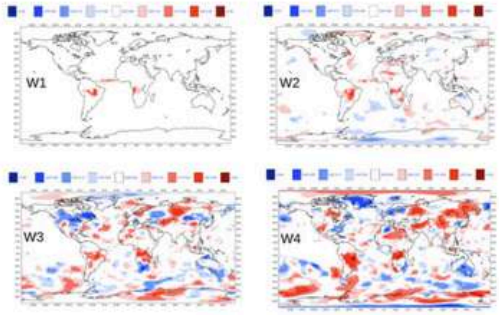


Figure 2. 2-meter temperature weekly correlation map differences (Control – Interactive aerosols)– ECMWF model x ERA5

The case study of September 2019 indicated negative anomalies of AOD are better forecasted by the models, however, positive AOD anomalies in central South America and South Africa are not represented. There is also differences among the anomalies observed in CAMS and MERRA2, indicating that scores like correlation and other deterministic scores can be sensitive to the reference used.

CONCLUSIONS

Differences in reanalysis might impact bias results. Models show a mix of improvements and degradations globally; however, significant improvements were observed in key regions such as the USA, Canada, and South America (NASA model, not shown). There is a need for better adjustments in models to account for the impact of aerosols. The next steps of our work include extending the assessment to the KMA model and evaluating the skill of atmospheric dynamics, atmospheric composition, and other aerosol optical properties.

REFERENCES

Andrade F.M., Coelho C.A.S., Cavalcanti I.F. Global precipitation hindcast quality assessment of the Subseasonal to Seasonal (S2S) prediction project models. Clim Dyn 52:5451–5475, 2019

Flemming, J. et al., Tropospheric chemistry in the integrated forecasting system of ECMWF. Geoscientific model development, Copernicus GmbH, v. 8, n. 4, p., 975–1003, 2015.

GMAO (Global Modeling and Assimilation Office), *inst3_3d_asm_Cp: MERRA-2 3D IAU State, Meteorology Instantaneous 3-hourly (p-coord, 0.625x0.5L42), version 5.12.4*, Greenbelt, MD, USA: Goddard Space Flight Center Distributed Active Archive Center (GSFC DAAC), 2015.

Hersbach, H. et al., Global reanalysis: goodbye ERA-Interim, hello ERA5. ECMWF Newsletter, n. 159, p. 17–24, 2019. 34, 44

Zuidema P. et al., Smoke and clouds above the southeast atlantic: Upcoming field campaigns probe absorbing aerosol's impact on climate. Bul. Amer. Met. Soc., v. 97, n. 7, p. 1131–1135, 2016

SESSION 11
Particulate matter and its effects on human health and the environment

Particulate matter (PM) plays an important role in the chemistry and physics of the atmosphere, as well as climate and public health. Atmospheric particulate matter affects the biogeochemistry of ecosystems, the hydrological cycle, atmospheric circulation, rainfall acidification, and also cloud formation.
In addition, exposure to aerosols can lead to both respiratory and cardiovascular diseases, furthermore, it also presents genotoxic effects. These effects depend on factors such as the size, concentration, structure, and chemical composition of the particles.
Session topics include:

- Effects of PM on radiative forcing
- Monitoring and modeling of Black Carbon
- Air quality and respiratory health
- Measuring PM-bound potentially toxic species
- Oxidative potential of PM
- Cytotoxicity of PM
- Bioassays

SESSION 11

CARCİNOGENİCİTY OF PESTİCİDES AND PM2.5 COLLECTED İN BRAZİLİAN CİTİES. EVALUATİON USİNG CELLS BEAS-2B AND SOFT AGAR COLONY FORMATİON ASSAY 231

REDUCTION OF HEALTH IMPACT OF AMBIENT PM10 AND PM2.5- CONCENTRATIONS IN SANTOS-SP, BRAZIL 234

PARTICULATE MATTER-BOUND PAHS AND MUTAGENCITY IN THE LARGEST BRAZILIAN METROPOLITAN AREA 237

ASSESSMENT OF AİRBONE MERCURY LEVELS İN PRESERVED AND ANTHROPOGENİCALLY İMPACTED AREAS (RİO DE JANEİRO STATE, BRAZIL) 240

USE OF PLANTS AS BIOMONITORS OF PARTICULATE MATTER TOXICITY IN URBAN REGIONS INFLUENCED BY MINNING 243

SOCIOENVIRONMENTAL VULNERABILITIES AND AIR POLLUTION IN THE CITY OF SÃO PAULO FROM 2019 TO 2023 246

ASSESSMENT OF AİRBONE MERCURY LEVELS İN PRESERVED AND ANTHROPOGENİCALLY İMPACTED AREAS (RİO DE JANEİRO STATE, BRAZIL) 249

COMPREHENSIVE EVALUATION OF MAIAC 1KM AOD PRODUCT FOR PM2.5 ESTIMATION IN LATIN AMERICAN URBAN AREAS 252

AİR POLLUTİON ANALYSİS İN LATİN AMERİCA: IMPLİCATİONS FOR HEALTH AND SOCİO-ENVİRONMENTAL INEQUALİTİES 256

ASSESSMENT OF PM2.5 OXIDATIVE POTENTIAL, COMPOSITION, AND EMISSION SOURCES IN THE URBAN AIR OF SÃO PAULO, BRAZIL 259

EVALUATING THE OXIDATIVE POTENTIAL OF PM2.5 IN SÃO PAULO, BRAZIL: A COMPARATIVE ANALYSIS BETWEEN DIFFERENT ASSAYS 262

ANALYSIS OF FINE PARTICULATE MATTER (PM2.5) IN SAO PAULO CITY 265

ASSESSMENT OF MERCURY CONTENT IN ATMOSPHERIC PARTICULATE MATTER NEAR A COAL-FIRED POWER PLANT IN FIGUEIRA, SOUTHERN BRAZIL 268

CARCİNOGENİCİTY OF PESTİCİDES AND PM2.5 COLLECTED İN BRAZİLİAN CİTİES. EVALUATİON USİNG CELLS BEAS-2B AND SOFT AGAR COLONY FORMATİON ASSAY 271

SESSION 11

REDUCTION OF HEALTH IMPACT OF AMBIENT PM10 AND PM2.5- CONCENTRATIONS IN SANTOS-SP, BRAZIL 274

PARTICULATE MATTER-BOUND PAHS AND MUTAGENCITY IN THE LARGEST BRAZILIAN METROPOLITAN AREA 277

ASSESSMENT OF AİRBONE MERCURY LEVELS İN PRESERVED AND ANTHROPOGENİCALLY İMPACTED AREAS (RİO DE JANEİRO STATE, BRAZIL) 280

USE OF PLANTS AS BIOMONITORS OF PARTICULATE MATTER TOXICITY IN URBAN REGIONS INFLUENCED BY MINNING 283

SOCIOENVIRONMENTAL VULNERABILITIES AND AIR POLLUTION IN THE CITY OF SÃO PAULO FROM 2019 TO 2023 286

ASSESSMENT OF AİRBONE MERCURY LEVELS İN PRESERVED AND ANTHROPOGENİCALLY İMPACTED AREAS (RİO DE JANEİRO STATE, BRAZIL) 289

COMPREHENSIVE EVALUATION OF MAIAC 1KM AOD PRODUCT FOR PM2.5 ESTIMATION IN LATIN AMERICAN URBAN AREAS 292

AİR POLLUTİON ANALYSİS İN LATİN AMERİCA: IMPLİCATİONS FOR HEALTH AND SOCİO-ENVİRONMENTAL INEQUALİTİES 296

ASSESSMENT OF PM2.5 OXIDATIVE POTENTIAL, COMPOSITION, AND EMISSION SOURCES IN THE URBAN AIR OF SÃO PAULO, BRAZIL 299

EVALUATING THE OXIDATIVE POTENTIAL OF PM2.5 IN SÃO PAULO, BRAZIL: A COMPARATIVE ANALYSIS BETWEEN DIFFERENT ASSAYS 302

ANALYSIS OF FINE PARTICULATE MATTER (PM2.5) IN SAO PAULO CITY 305

POST-LOCKDOWN PARTICULATE MATTER COMPOSITION AND SOURCE APPORTIONMENT IN THE METROPOLITAN AREA OF SÃO PAULO 308

EFFECTS OF AİR QUALİTY ON HUMAN HEALTH AND AVOİDABLE DEATHS IN THE METROPOLİTAN REGİON OF RİO DE JANEİRO: 2015 2019 311

PHYSICAL-CHEMICAL CHARACTERIZATION OF FINE PARTICULATE MATTER(2,5 IN AMAZONIA: A STUDY IN FOUR MUNICIPALITIES IN NORTHEASTERN PARÁ DURING THE TRANSITION BETWEEN THE SUMMER AND WINTER PERIOD AMAZONIAN 314

SESSION 11

ANNOYANCE DUE TO SEDIMENTED PARTICULATE MATTER AND ITS INFLUENCING FACTORS EXPERIENCED BY COMMUNITIES IN AN INDUSTRIALIZED AREA 317

INFLUENCE OF WIND DIRECTION, RECEPTOR POINT HEIGHT AND TIME INTERVAL ON PREDICTING THE MAXIMUM SHORT-TERM AVERAGE CONCENTRATION AND ON THE INTEGRAL TIME SCALE OF CONCENTRATION 320

ASSESSMENT OF AIR POLLUTION RISKS AND ITS SPATIAL CORRELATION WITH SOCIOECONOMIC CONDITIONS, GREEN AREAS AND ATMOSPHERIC EMISSIONS IN BRAZIL 323

IMPACT OF LIGHTNING-NOX ON AEROSOL PRODUCTION IN THE AMAZON 326

BEHAVIOR OF METEOROLOGICAL VARIABLES IN CRITICAL AIR POLLUTION EVENTS IN A MINING CITY 329

CORRELATİON BETWEEN EXPOSURE TO PARTİCULATE MATTER AND HOSPİTALİZATİONS FOR CİRCULATORY DİSEASES İN THE ELDERLY İN THE STATE OF SÃO PAULO, FROM 2016 TO 2020. 332

ANALYSIS OF PM2.5 AND PM10 ATMOSPHERIC CONCENTRATIONS RATIOS IN THE METROPOLITAN AREA OF BELO HORIZONTE 335

ASSESSMENT OF PM2.5 COMPOSITION AND PAH SOURCES IN THREE CONTINENTS: IMPLICATIONS FOR AIR QUALITY AND HUMAN HEALTH 338

USE OF PLANTS AS BIOMONITORS OF PARTICULATE MATTER TOXICITY IN URBAN REGIONS INFLUENCED BY MINING 341

UNRAVELING AEROSOLS: EXPLORING SIZE, NUMBER, AND PARTICLE FORMATION EVENTS IN SÃO PAULO 344

USE OF PLANTS AS BIOMONITORS OF PARTICULATE MATTER TOXICITY IN URBAN REGIONS INFLUENCED BY MINING 347

COMPARISON OF THE EFFECTS OF URBAN AFFORESTATION ON AIR QUALITY IN TWO REGIONS OF A BRAZILIAN CITY 350

AIR POLLUTION CONFERENCE BRAZIL
CMAS SOUTH AMERICA
COMMUNITY MODELING AND ANALYSIS SYSTEM

CARCİNOGENİCİTY OF PESTİCİDES AND $PM_{2.5}$ COLLECTED İN BRAZİLİAN CİTİES. EVALUATİON USİNG CELLS BEAS-2B AND SOFT AGAR COLONY FORMATİON ASSAY

Aleinnys Marys Barredo Yera[1], Pérola de Castro Vasconcellos[1] and Ana Paula de Melo Loureiro[2]

[1]*Institute of Chemistry, University of São Paulo, Brazil*
[2] *School of Pharmaceutical Sciences, University of São Paulo, Brazil*
aleinnysb@usp.br

Abstract: Since 2008, Brazil has become one of the largest consumers of pesticides in the world. Many of these compounds have already been banned in several countries due to the negative effects they have on human health. Studies show that pesticides have a broad relationship with the increase in cases of diseases that mostly involve the nervous system and cancer. Soft Agar Colony Formation Assay is a test used to determine the carcinogenicity of a compound. It is based on the hypothesis that healthy cells cannot grow off a solid surface, but modified cells (malignant transformations) will have this ability and form colonies. To study the cytotoxicity and carcinogenicity of $PM_{2.5}$ collected in cities in the state of São Paulo (São Paulo, Piracicaba, and Capuava), human lung cells (BEAS-2B) were separately exposed for 7 days to both $PM_{2.5}$ collected at these sites, and different pesticide patterns that were found in representative concentrations in the samples. For this, the violet crystal assay and Solft Agar were used. The $PM_{2.5}$ samples collected at all sampling sites with concentrations (C_1 = 5 µg/m^3, C_2 = 25 µg/m^3, and C_3 = 50 µg/m^3) showed cytotoxicity from 72h of exposure. Piracicaba was the site with the highest cytotoxicity, followed by Capuava and São Paulo. In the case of pesticides (C_1=300 pg/m^3 and C_2=3000 pg/m^3), during the first 4 days of exposure no significant differences were found between pesticides and control. From the 5th day on, different behaviors were observed, but further studies are needed to understand the cytotoxicity of these compounds. Based on the hypothesis that more carcinogenic compounds can form more colonies in the soft agar, the results show the tumorigenic effect of $PM_{2.5}$ (C=5 µg/m^3), with Piracicaba again being the site with the greatest effects. In the case of pesticides, only Atrazine (ATRA) and the substance containing a mixture of 25 pesticides (MIXG) showed tumorigenic effects for both concentrations, this effect was smaller than that found for $PM_{2.5}$. Statistically, there are no significant differences between the results for exposure to ATRA and MIXG. This indicates that the tumorigenic effect found in MIXG may be influenced by the presence of ATRA. To date, no references have been found to similar studies carried out on samples of particulate matter collected at sites in the state of São Paulo, nor on the pesticides of interest, thus having great relevance to the results found in this research.

Keywords: **Particulate matter, Pesticide inhalation, Cytotoxicity, Carcinogenicity, Soft agar**

INTRODUCTION

Since 2008, Brazil has become the largest consumer of pesticides in the world (Bombardi, Larissa, 2017). However, of the 50 most consumed active ingredients in the country, 22 have been banned in Europe and North America (Carneiro & Lia Giraldo da Silva Augusto, Raquel Maria Rigotto, 2018). The state of São Paulo is the second largest consumer of pesticides in Brazil, using approximately 110,000 tons in 2016 (Bombardi, Larissa, 2017).

Many of these compounds have already been banned in several countries due to their negative impact on human health. Studies have shown that pesticides are closely related to the increase in cases of diseases that mostly involve the nervous system, with Hodgkin's Disease, Parkinson's Disease, and Alzheimer's being the most related (Mostafalou & Abdollahi, 2013). Other studies also include these pesticides in the list of endocrine-disrupting chemical compounds (EDCs)(Patisaul et al., 2018).

Soft Agar test is used to determine the carcinogenicity of a compound. It is based on the hypothesis that healthy cells cannot grow outside of a solid surface, but modified cells (malignant transformations) will have this ability (Borowicz et al., 2014). This test is done on a viscous cellular medium. After a certain time of exposure, the growth of cells is observed, which indicates that the compound has modified them, and this mutation is the beginning of the development of cancer.

To assess the cytotoxicity and carcinogenicity of $PM_{2.5}$ collected at sites in cities in the state of São Paulo (São Paulo, Piracicaba, and Capuava), human lung cells (BEAS-2B) were exposed to $PM_{2.5}$ collected at these sites, and to different pesticide patterns found in representative concentrations in the samples. For this, the violet crystal test and the Soft Agar test were used.

METHODS

Site characterization and sampling

Piracicaba (PRB) is an urban-agricultural city located 300 km from São Paulo, with over 150,000 ha of sugarcane and orange crops (IBGE, 2018). During the dry season in July 2018, $PM_{2.5}$ (particles with a diameter equal or smaller than 2.5 micrometers) were collected, and the total number of samples was 16.

The second location chosen was São Paulo (SPA), the capital of the state of São Paulo, and the largest city in Brazil. $PM_{2.5}$ samples (n = 15) were collected in July 2018, simultaneously with the PRB samples.

The third location was Capuava (CAP), a large urban area with an industrial complex of high economic importance, with nearly 80,000 people living in around 14 chemical industries (Zaccarelli-Marino et al., 2016). $PM_{2.5}$ samples (n = 17) were collected between July and August 2018.

Culture of BEAS-2B cells
The BEAS-2B strain was provided by Prof. Fekadu Kassie (Masonic Cancer Center, University of Minnesota, Minneapolis, United States). Cultures are maintained in BEGM (Bronchial Epithelial Growth Medium®) medium, supplemented with the kit's set of cofactors (bovine pituitary extract, insulin, hydrocortisone, hEGF, epinephrine, transferrin, retinoic acid, triiodothyronine, gentamicin, and amphotericin). The cells are kept in bottles and incubated at 37°C in an atmosphere containing 5% CO_2.

Exposure of cells to pesticides and $PM_{2.5}$
The cells were plated at a density of 2 x 10^4/well in 96-well plates. After the cell adhesion period (1 day), pesticide exposures (1.5 x 10^{-4} pg/µL and 1.5 x 10^{-3} pg/µL) were performed. For the case of exposure to $PM_{2.5}$ the concentrations were 2.5 pg/µL, 12.5 pg/µL, and 25 pg/µL. Control incubations (culture medium and DMSO) were also performed. The cells were exposed for 1 - 7 days, with renewal of the culture medium containing pesticides and $PM_{2.5}$ every 24 h.

Cytotoxicity, Crystal Violet Dye (CVD) Assay
After different exposure periods, the culture medium is removed and the cell layer is carefully washed twice with PBS. Then, the PBS solution was removed from the wells, and methanol (100 µL) was added as a fixative, which was aspirated after 40 seconds of contact. Cells were stained with 50 µL/well of CVD solution (1 % CVD in 20 % methanol) for 10 min at room temperature. After incubation, the dye is carefully removed, and each well is washed 4 times with 200 µL of a PBS solution. The dye adhered to the cells is dissolved by adding 200 µL of a 30 % (v/v) acetic acid solution.

To construct the standard curve, 1 x 10^4 to 19 x 10^4 cells/well were plated, and quantification was performed in a spectrophotometer with a microplate reader (SpectraMAX). The microplates were read at wavelengths 570 nm and 690 nm, the latter corresponding to the signal from the plates.

Carcinogenicity study
Commercial BEAS-2B lung cell lines were exposed for 7 days of growth to the pesticides atrazine (ATRA), permethrin (PER), malathion (MAL), a mixture of organochlorine pesticides (20 compounds, MIXO), and a mixture with all of the above compounds (MIXG). The pesticide concentrations were 300 pg/m^3 = 1.5 x 10^{-4} pg/µL and 3000 pg/m^3 = 1.5 x 10^{-3} pg/µL). In the other part of the assay, other BEAS-2B cells were exposed for 7 days to the $PM_{2.5}$ collected at the 3 sampling sites. For exposure to $PM_{2.5}$, the concentration of 5 µg/m^3 = 2.5 pg/µL was used, the lowest concentration of PM2.5 found at the sampling sites and which presented relevant results in the CV test performed previously.

Colony formation in Soft-agar
The assay was performed as described in (Borowicz et al., 2014). After 7 days of exposure to PM2.5 and pesticides, in addition to the controls for each exposure, BEAS-2B cells were trypsinized and plated at densities of 15000 cells per well in a culture medium containing 0.35% low-melting agarose in 6-well plates with a base layer of 0.5% high-melting agarose. The plates were incubated for 20 days at 37°C in an atmosphere containing 5% CO_2. Culture medium was added every 3 days. After the growth period in a semisolid medium, the colonies were fixed in 200 µL of paraformaldehyde (4% v/v) for 45 minutes. Subsequently, colonies with a diameter greater than or equal to 100 µm were counted under an inverted microscope, using a 100-fold magnification.

RESULTS

Cytotoxicity
It was observed that $PM_{2.5}$ can prevent cell growth after 72 h of exposure in all sampling sites and concentrations. The $PM_{2.5}$ collected in PRB had the most significant effect and caused the highest number of cells to die. Samples from CAP and SPA followed in that order. The latter remained stable in the last two days of exposure, but further studies are needed to understand this behavior.

For pesticides, there were no significant differences between exposure and controls for the first 4 days. However, different behaviors were observed from the 5th day of exposure. The lowest concentration of all formulations showed significant differences, and on the 6th day of exposure, the Mix containing all pesticides caused the highest cell death. This result may be due to the synergistic effect between the pesticides, which makes them more toxic when reacting together.

Carcinogenicity
The number of colonies in the soft agar increased significantly after exposure to $PM_{2.5}$ compared to the control group ($p<0.0001$). The $PM_{2.5}$ collected in PRB showed the most significant tumorigenic effect followed by CAP and SPA (Figure 1). It is worth

noting that the $PM_{2.5}$ concentration used was the lowest, so, the tumorigenic effects would increase on days with higher concentrations.

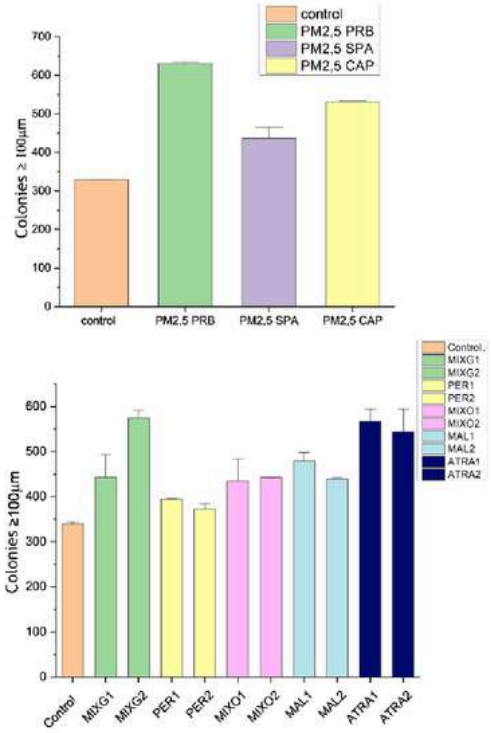


Figure 1. Analysis of colony formation in Soft Agar semisolid medium after 7 days of exposure of BEAS-2B cells to $PM_{2.5}$ and pesticide standards.

The second test showed that colony formation was higher in pesticide exposure than in the control, but statistically significant differences were found only for the mixture containing all pesticides (MIXG) and atrazine (ATRA). The presence of atrazine in particulate matter caused tumorigenic effects and the tumorigenic effect found in MIXG may be exclusive to the presence of atrazine. Further studies should be done to corroborate this result. Comparing these results with those obtained for $PM_{2.5}$, we can see how the effect of $PM_{2.5}$ is even greater than that caused by individual or mixed pesticides.

An important result is that the pesticide with the greatest tumorigenic effect, ATRAZ, was the compound that had one of the highest concentrations (163 pg/m^3) and detection frequency (100%) in PRB samples. For SPA samples (93 pg/m^3) and CAP (not detected), the concentration of ATRAZ was much lower (Yera & de Castro Vasconcellos, 2021). This result may be relevant to explain the differences found between $PM_{2.5}$ in PRB, CAP, and SPA.

Further tests would be needed to determine whether the tumorigenic effect of $PM_{2.5}$ is influenced more by the particle itself or its chemical composition.

CONCLUSIONS

The study found that after 3 days of exposure, the tested concentrations of $PM_{2.5}$ induced growth arrest of BEAS-2B cells, indicating the presence of cytotoxicity in the particulate matter. In comparison, while pesticides also showed significant cytotoxicity, it was much lower than that caused by $PM_{2.5}$. However, when pesticides were mixed together, a synergistic effect was observed, leading to greater cytotoxicity, which better simulates what happens in ambient air.

The greater cytotoxicity of $PM_{2.5}$ for pesticides may be due to its complex composition, which includes ions, metals, bacteria, and a hundred organic compounds. The study also revealed that $PM_{2.5}$ had tumorigenic effects for concentrations 5 $\mu g/m^3$, with PRB having the greatest effects followed by CAP and SPA. Among the pesticides studied, only atrazine exhibited tumorigenic effects, which may be responsible for the difference in the tumorigenic effect found at each site since it is one of the main pesticides detected in PRB.

This research is of great relevance as no similar studies have been conducted on samples of particulate matter collected at sites in the state of São Paulo or on the pesticides of interest.

REFERENCES

Bombardi, Larissa, M. (2017). *Geografia de uso de agrotoxicos no brasil e conexoes com a uniao europeia*.

Borowicz, S., Van Scoyk, M., Avasarala, S., Karuppusamy Rathinam, M. K., Tauler, J., Bikkavilli, R. K., & Winn, R. A. (2014). The soft agar colony formation assay. *Journal of Visualized Experiments*, *92*, 1–6.

IBGE, I. B. de G. e E. (2018). *Panorama e Pesquisa de Piracicaba*.

Mostafalou, S., & Abdollahi, M. (2013). Pesticides and human chronic diseases: Evidences, mechanisms, and perspectives. *Toxicology and Applied Pharmacology*, *268*(2), 157–177.

Patisaul, H. B., Fenton, S. E., & Aylor, D. (2018). Animal models of endocrine disruption. *Best Practice & Research Clinical Endocrinology & Metabolism*, *32*(3), 283–297.

Yera, A. M. B., & de Castro Vasconcellos, P. (2021). Pesticides in the atmosphere of urban sites with different characteristics. *Process Safety and Environmental Protection*, *156*, 559–567.

Zaccarelli-Marino, M. A., André, C. D. S., & Singer, J. M. (2016). Overt primary hypothyroidism in an industrial area in São Paulo, Brazil: The impact of public disclosure. *International Journal of Environmental Research and Public Health*, *13*(11).

AIR POLLUTION CONFERENCE BRAZIL
CMAS SOUTH AMERICA
COMMUNITY MODELING AND ANALYSIS SYSTEM

REDUCTION OF HEALTH IMPACT OF AMBIENT PM_{10} AND $PM_{2.5}$-CONCENTRATIONS IN SANTOS-SP, BRAZIL

Andreas F. Grauer[1], Débora L. Perazzoli[1], Marcos V. O. de Figueiredo[1], Jacqueline A. Schraier[1], André Luciano Malheiros[1], Helder Rafael Nocko[1]

[1]*Envex Engenharia e Consultoria*

andreas.grauer@envexengenharia.com.br

debora.perazzoli@envexengenharia.com.br

Abstract:

The city of Santos/SP is a densely populated area with the largest port in Latin America. This port is characterized by a high volume of vegetable dry bulk exports, and the handling of these products is known as a source of particulate matter emissions (PM_{10} and $PM_{2.5}$). The air quality in Santos (with regard to PM_{10} and $PM_{2.5}$) is influenced by the contribution of a natural portion, related to the sea mist, and an anthropogenic portion, including mainly vehicular traffic and commercial and industrial activities. Due to the availability of fuels and raw material, there are large industrial activities with the potential to influence air quality in the metropolitan region around Santos, which is called Baixada Santista. The emission of atmospheric pollutants in the Baixada Santista is especially critical due to the topographical conditions, notably the Serra do Mar mountain range, which forms an obstacle to the pollutants's dispersion. In recent years there have been a number of improvements in industrial processes and in the facilities at the Port of Santos, which caused a reduction in the concentrations of PM_{10} and $PM_{2.5}$, and consequently in the impact on the population's health. The aim of this study is to quantify the benefits of these improvements in terms of reducing the impact on health. In order to do this, the deaths attributable to the pollutants PM_{10} and $PM_{2.5}$ were calculated for the period from 2013 to 2019. The years 2020 to 2022 were not included due to the effect of COVID-19 on health data, which caused a significant increase in cases of illnesses and deaths. The tool used for this analysis was the World Health Organization's (WHO) AirQ+ software.The input data included average annual concentrations measured at two automatic air quality stations operated by CETESB, São Paulo's state environmental agency: Estação Santos and Estação Santos - Ponta da Praia. Death data was obtained from DataSUS, a system linked to the Brazilian Ministry of Health. The effects studied were: total deaths >30 years; deaths from diseases of the circulatory system >30 years; deaths from diseases of the respiratory system >30 years; and deaths from lung cancer >20 years. The results showed that the average annual concentrations of PM_{10} ranged from 48 $\mu g/m^3$ in 2013 to 22 $\mu g/m^3$ in 2019 in the Ponta da Praia Estuary, while the average concentrations of $PM_{2.5}$ ranged from 19 $\mu g/m^3$ to 14 $\mu g/m^3$ in the same period. The concentrations considered as cut-off (No observed effect level) for each pollutant were: 10 $\mu g/m^3$ for $PM_{2.5}$ and 21.7 $\mu g/m^3$ for PM_{10}. In relation to health impact, the highest resulting attributable fraction was 17.80% for respiratory system diseases in 2014. In general, the attributable fractions decreased during the study period. In 2019, the impact with the highest calculated attributable fraction was lung cancer for the population >20 years, with 4.43%. In the reference period, there was a reduction in total deaths attributed to the effects of pollution, from 266 cases in 2013 to 124 in 2019 (a reduction of 53.4%). When comparing PM_{10} and $PM_{2.5}$, the pollutant $PM_{2.5}$ proved to have a greater impact on health. Deaths from circulatory problems were reduced from 123 in 2013 to 49 in 2019 (60.2% reduction). Deaths from respiratory problems were reduced from 92 in 2013 to 17 in 2019 (81.5% reduction). It is interesting to note that the pollutant PM_{10} was the main cause of deaths in this category until 2015, however, from 2016 onwards the impact calculated for the pollutant $PM_{2.5}$ exceeded the impact calculated for PM_{10}. Deaths from lung cancer were reduced from 17 in 2013 to 5 in 2019 (a 70.6% reduction). Excluding the specific deaths studied from the total number attributed to particulate air pollution, between 32 and 53 cases attributed to PM_{10} or $PM_{2.5}$ remained, without appearing in the categories studied. Despite the significant improvements observed in the period 2013-2019, still 124 cases attributable to $PM_{2.5}$ were calculated for 2019, which reinforces the importance of continuing improvements in reducing emissions of this pollutant.

Keywords: Epidemiological study, Fine particles, AirQ+ model, air quality health impact.

INTRODUCTION

Accounting for the effects of air pollution has been made possible today by the availability of air quality data and dose-response curves that link the impact studied on the affected population with the concentrations they are exposed to. Analysis of the effects of air pollution on the morbidity and mortality of the population is not typically addressed in environmental reports from the public agencies responsible for monitoring air quality. They usually simply compare measured concentrations with air quality standards. However, compliance with the standards does not mean the absence of an impact, which can be accounted for using dose-response relationship curves drawn up in epidemiological studies. This study provides results on the impact of PM_{10} and $PM_{2.5}$ on the mortality of the population of Santos, Brazil from 2013 to 2019.

METHODS

Air quality data was obtained from São Paulo's state environmental agency's reports (CETESB, 2023). CETESB operates two air quality stations in Santos: Santos Station, which measures PM_{10}; and Santos - Ponta da Praia Station, which measures PM_{10} and $PM_{2.5}$. The arithmetic mean of the annual averages of both stations was calculated for the pollutant PM_{10}; and in the case of $PM_{2.5}$ the annual average of

Ponta da Praia Station was used for the period 2013 to 2019.The evolution of measured concentrations over the period are shown in Figure 1, as well as the cut-off (No observed effect level) for both pollutants. The cut-off was 10 µg/m³ for $PM_{2.5}$ (default AirQ+) and 21.7 µg/m³ for PM_{10}. This second value was based on the ratio $PM_{2.5}/PM_{10}$=0.46 (WHO, 2016), valid for Brazil.

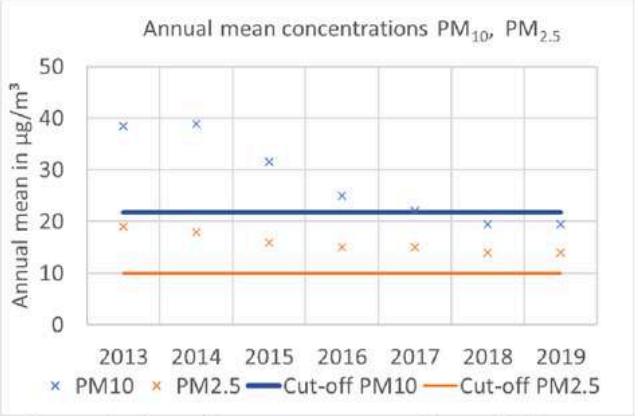


Figure 1. Annual mean concentrations of PM_{10} and $PM_{2.5}$ in Santos, Brazil.
Reference: Adapted from CETESB (2023)

Using these averages and the AirQ+ software (WHO, 2022), five impacts were calculated:

1. total deaths >30 years;
2. deaths from diseases of the circulatory system >30 years;
3. deaths from diseases of the respiratory system >30 years;
4. deaths from lung cancer >20 years and
5. deaths from unknown causes by the difference between the total value and the numbers in categories 2 to 4.

This age group was chosen because there is in the AirQ+-software a dose-response relationship curve for this part of the population.
The impacts calculated by AirQ+, expressed as attributable fractions, were multiplied by the number of cases reported by the Ministry of Health through the DataSUS system for the municipality of Santos (BRASIL, 2023). For example, in 2013, 3971 deaths were recorded in Santos, of which, according to the AirQ+ log-linear relationship, 6.38% were caused by the pollutant PM_{10} and 6.69% by the pollutant $PM_{2.5}$,. The higher of the two results (266 cases) was considered to be deaths attributable to particles in the atmosphere.

FINDINGS AND ARGUMENT

According to the reduction in ambient particle concentrations shown in Figure 1, there was also a reduction in calculated attributable deaths, as shown in Figure 2. Since 2018, PM_{10} concentrations have been below the cut-off, so there have been no more attributable deaths for this pollutant since that year. In absolute numbers, total attributable deaths decreased from 266 in 2013 to 124 in 2019. This corresponded to a reduction in the percentage of attributable cases calculated in Santos from 6.69% to 3.03%.

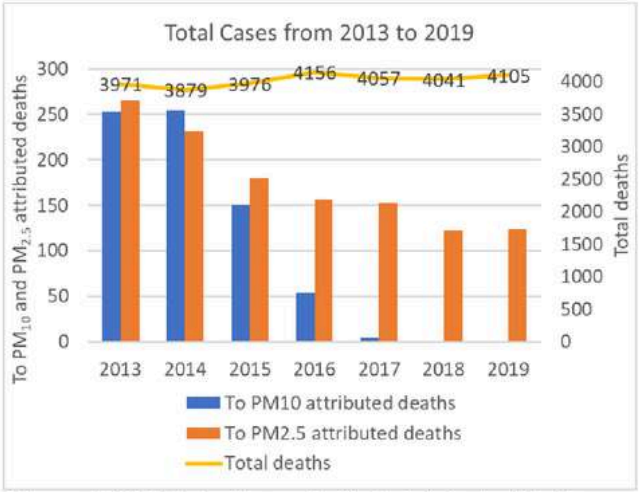


Figure 2. Total deaths and attributable deaths to PM_{10} and $PM_{2.5}$ in Santos, Brazil.
Reference: The authors (2024)

For the specific effects, lung cancer showed the greatest impact reduction expressed as attributable fractions, from 9.70% in 2013 to 4.43% in 2019, as shown in Figure 3. However, in all the studied years it represented the highest percentage of impact among the specific effects studied, which highlights the existence of a strong link between $PM_{2.5}$ and lung cancer.

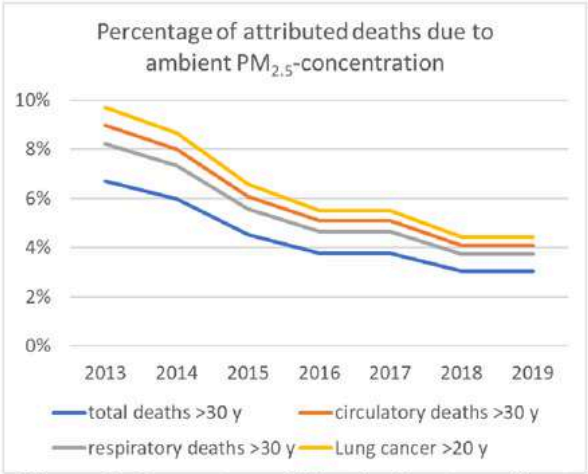


Figure 3. Percentage of deaths due to ambient $PM_{2.5}$-concentration in Santos, Brazil.
Reference: EnvEx (2024)

Looking at the attributable deaths between 2013 and 2019 in Figure 4, we see a reduction in the categories: total deaths (>30 years), deaths due to circulatory system problems (>30 years), deaths due to respiratory system problems (>30 years) and deaths due to lung cancer (>20 years). The

difference between the sum of the specific causes and the total attributable deaths is shown by the green column, which represents the cases of other deaths potentially caused by atmospheric particles, but not included in the above categories, i.e. deaths attributable to unknown causes. These unknown causes increased from 34 in 2013 to 54 in 2019.

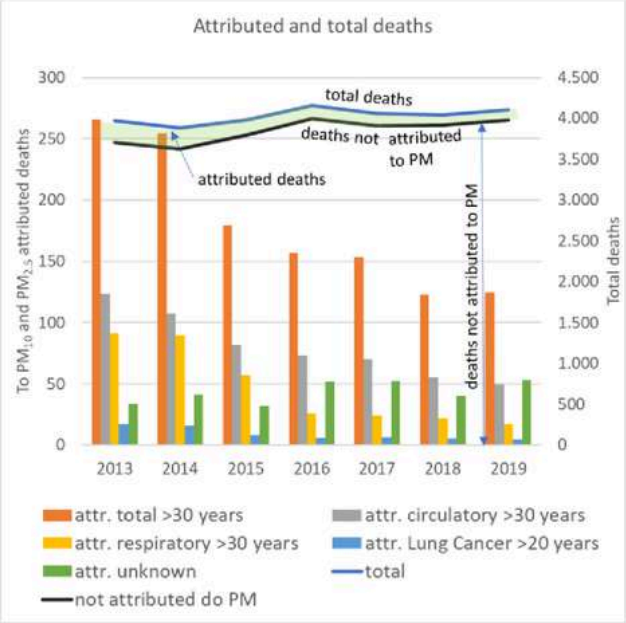


Figure 4. Attributed and total deaths.
Reference: The authors (2024)

Figure 5 compares the percentages of deaths from the causes studied in 2013 and 2019. There was a significant drop in causes attributed to the respiratory system from 35% in 2013 to 14% in 2019. At the same time, there was an increase in unknown causes from 13% to 43% in the period. In 2013, of the 124 cases of deaths attributable from particles in the atmosphere, 49 were from circulatory problems, 17 from respiratory problems and 5 from lung cancer. The remaining 53 cases, or 43%, had other causes.

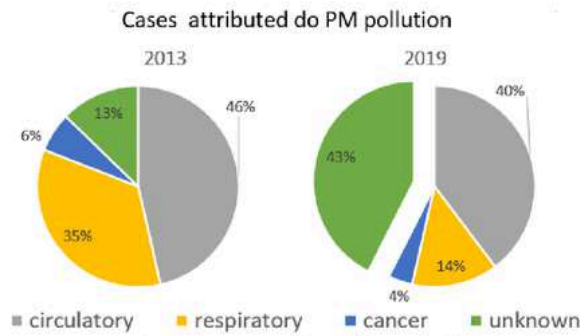


Figure 5. Percentage of attributed deaths for each category studied in 2013 and 2019.
Reference: The authors (2024)

CONCLUSIONS

Between 2013 and 2019 there was a substantial reduction in PM_{10} and $PM_{2.5}$ concentrations in Santos. The reduction in environmental concentrations was fed into the AirQ+ software and the share of deaths attributable to these pollutants for the population over 30 was computed.

The calculations showed that there was a reduction in deaths attributable to particles in the atmosphere from 266 cases in 2013, or 6.69%, to 3.03% in 2019 (124 cases). Among the specific effects, the greatest benefit was seen in reduction of deaths from respiratory system problems, which accounted for 35% of attributable deaths in 2013, a figure that fell to 14% in 2019. At the same time, deaths from unknown causes increased from 13 to 43%, which reinforces the need for further studies into the dose-response relationships for low concentrations of particles in the atmosphere.

It was not possible, in this study, to identify possible effects of atmospheric particles other than circulatory problems, respiratory problems and lung cancer on mortality. One hypothesis is that these additional effects exist, but there is still a lack of data to quantify them. Another possible explanation for the increase in unknown cases is the limitation of dose-effect curves when they are used near their lower limit. Any tool used at the lower limit of its applicability has high uncertainty.

REFERENCES

BRASIL. Ministério da Saúde. DATASUS. Tabnet. Brasília, DF: Ministério da Saúde, 2023. (Sistema de Informações sobre Mortalidade - SIM). http://tabnet.datasus.gov.br/cgi/deftohtm.exe?sim/cnv/obt10uf.def. Accessed November 2023.

CETESB. Relatórios de Qualidade do ar no Estado de São Paulo. São Paulo, 2023. (Série Relatórios). https://cetesb.sp.gov.br/ar/publicacoes-relatorios/. Accessed November 2023.

WHO Regional Office for Europe, European Centre for Environment and Health (2022). AirQ+: software tool for health risk assessment of air pollution. Bonn (Germany): WHO Regional Office for Europe. https://www.who.int/europe/tools-and-toolkits/airq---software-tool-for-health-risk-assessment-of-air-pollution
Accessed November 2023

WHO - World Health Organization. Ambient air quality database 2016. https://www.who.int/data/gho/data/themes/air-pollution/who-air-quality-database/2016. Accessed August 2023.

AIR POLLUTION CONFERENCE BRAZIL
CMAS SOUTH AMERICA
COMMUNITY MODELING AND ANALYSIS SYSTEM

PARTICULATE MATTER-BOUND PAHS AND MUTAGENICITY IN THE LARGEST BRAZILIAN METROPOLITAN AREA

Guilherme Martins Pereira[1,2], Gabriely F. Groto Militão[3], Jessica Cardoso[3], Thayná da Silva Santos[1], Daniel A. Morales[3], Gisela de A. Umbuzeiro[3], Edmilson Dias de Freitas[2], Maria de F. Andrade[2], Pérola de C. Vasconcellos[1]

[1]*Institute of Chemistry - University of São Paulo*
[2]*Institute of Astronomy, Geophysics and Atmospheric Sciences - University of São Paulo*
guilherme.martins.pereira@usp.br
perola@iq.usp.br
[3]*Laboratory of Ecotoxicology and Genotoxicity - State University of Campinas*
grotogabi@gmail.com
giselau@unicamp.br

Abstract: The Metropolitan Area of São Paulo is often affected by high particulate matter levels due to the influence of its large vehicular fleet and pollution events are more common during drier periods of the year due to the influence of the increase of biomass burning events and less favorable meteorological conditions for pollutant dispersion. Polycyclic aromatic hydrocarbons (PAHs) in particulate matter have been associated with mutagenic properties. In 2019, an intensive campaign was performed in the drier months of the year (June to September) with a high-volume sampler (Hi-Vol), collecting fine particulate matter ($PM_{2.5}$). Organic extracts were obtained after solvent extraction and polycyclic aromatic hydrocarbons (PAHs) were determined with a Gas Chromatograph coupled to a Mass Spectrometer (GC/MS). In order to study which particulate matter sources are more associated with mutagenic effects, some samples were selected as representative of specific particulate matter sources (secondary formation, vehicular exhaust and non-exhaust, industrial and biomass burning) and tested for mutagenicity through Salmonella/microsome assay in the miniaturized version, microplate agar (MPA), without and with metabolic activation (rat liver S9 5%, Phenobarbital/5,6-Benzoflavone induced). The SPA13 sample presented the lowest mutagenic potency and was associated with secondary formation by the receptor model. The SPA29 sample presented the highest mutagenic potency and was characterized by the influence of biomass burning. Despite the different mutagenic potencies, these samples present similar concentrations of $PM_{2.5}$, benzo(a)pyrene (BaP), and theoretically calculated equivalent mutagenicity (BaP-MEQ) and carcinogenicity (BaP-TEQ). Furthermore, correlations were not found between mutagenicity results and PAHs or BaP-MEQ, and the increase in the observed concentrations of PAHs was not related to higher mutagenicity of the samples, suggesting the effect of other not determined species in the study or a complex interaction of different chemical species in the extract. When the experiment is performed with metabolic activation (+S9), the SPA15 sample presents a decrease in mutagenicity, while SPA33 increases, which may be related to the effects of nitro-PAHs in the experiment without activation (Figure 1A). For the assays with S9, the samples with lower mutagenicity potencies (SPA13, SPA15, and SPA64) were often related to higher $PM_{2.5}$ concentrations (above 25 μg m^{-3}), suggesting that high $PM_{2.5}$ concentrations not always are associated with higher mutagenicity.

Keywords: Polycyclic aromatic hydrocarbons, pollution, sources, Salmonella/microsome assay, microplate agar, YG1041, Benzo(a)pyrene

INTRODUCTION

Urban particulate matter often contains high levels of polycyclic aromatic hydrocarbons (PAHs) and other toxic species, which are mainly associated with vehicular exhaust in the Metropolitan Area of São Paulo (MASP) (Pereira et al., 2017, 2023). PAHs and their nitrated and oxygenated derivatives are associated with mutagenic and carcinogenic effects (Ravindra et al., 2008). Mutagenicity assays can be performed to detect reverse-type mutations. Different strains of *Salmonella enterica* serovar Typhimurium bacteria (Ames, 1971). These tests can be applied to environmental samples, including particulate matter (Alves et al., 2016).

Different strains can be used to detect different types of mutations, the most common are TA100 and TA98, which are useful for the detection of the majority of mutagens (William et al., 2019). The strain YG1041, derived from the TA98 strain, overproduces nitroreductase and O-acetyltransferase enzymes and is very sensitive to certain compounds, including nitroarenes and aromatic amines, and is the most sensitive strain to the detect aerosol-related mutagenicity (Maselli et al., 2019, Hagiwara et al., 1993).

The objective of this study was the application of Microplate Agar (MAP), a miniaturized technique, with the YG1041 strain to evaluate the mutagenicity of organic extracts of fine particulate matter ($PM_{2.5}$) collected in the MASP.

METHODS

Particulate matter was sampled and analyzed by researchers at the University of São Paulo

(*Laboratório do Grupo de Estudos em Química Atmosférica* - GEQAt/USP).

A sampling campaign was performed in a dry period in 2019 (June to September), inside the university campus, near a busy expressway and a green area. The passing fleet included light- and heavy-duty vehicles running on gasoline, diesel, biodiesel, and ethanol. $PM_{2.5}$ was collected in quartz fiber filters, with a high-volume sampler (Hi-Vol, 1.13 m^3 min^{-1} flow). Sampling started at 9 AM, followed by a 24-hour collection.

After the sampling, PAHs were extracted from the filters under sonication with dichloromethane, followed by a clean-up process with silica gel column chromatography. A Gas Chromatograph coupled to a Mass Spectrometer (GC-MS) was employed to quantify these species. More details are found in Pereira et al. (2017) and Vasconcellos et al. (2010).

The Positive Matrix Factorization (PMF) receptor model was applied to apportion the sources affecting $PM_{2.5}$ in this site and some samples were selected as representative of specific particulate matter sources (secondary formation, local vehicular, vehicular + road dust, industrial and biomass burning).

After the chemical analysis, the organic extracts were analyzed for mutagenicity by researchers at the State University of Campinas (*Laboratório de Ecotoxicologia e Genotoxicidade - LAEG/UNICAMP)*.

The assay was conducted according to Zwarg et al. (2018), using concentration-response experiments for each sample, with and without metabolic activation (5% of S9, a rat liver mix, induced by Phenobarbital/5,6-Benzoflavone, Moltox®). The selected strain was the YG1041. Complementally, tests with TA98 were conducted for comparison.

Overnight bacterial cultures were five times concentrated (10000g, 4°C, and 10 min) and resuspended in 0.015M sodium phosphate buffer. 50µL of cell suspension (0.5 to $2x10^{10}$ cells per mL) was added to a tube containing 2 µL of the organic extract. Half of this was transferred to a new tube. In the first tube, 25 µL of 0.015M sodium phosphate was added, and in the second tube, 25 µL of S9 mix. All tubes were incubated with shaking (180 rpm, 37°C, and 90 min). Afterward, 1mL of molten agar was added to each tube and 250 µL of the mixture was distributed in 4 wells in microplates, each containing 2.8 mL of minimal agar. Revertants colonies were manually counted after incubation (66 h, 37°C). Dimethyl sulfoxide was used as negative control and positive controls were 4-nitro-o-diamino-phenylinphenylenediamine, without S9, and 2-aminoanthracene (2AA), with S9. The data was analyzed using ANOVA/Tukey, followed by a linear regression. Samples were considered as positive if the responses were statistically significant ($p < 0.05$). The results were expressed as the minimum effective concentration (MEC2), capable of doubling the revertant number in ng of $PM_{2.5}$ per µL. For better understanding, the mutagenic potencies were presented as 1/MEC2.

FINDINGS AND ARGUMENT

Benzo(a)pyrene equivalent mutagenicity (BaP-MEQ) and toxicity (BaP-TEQ), benzo(a)pyrene (BaP) concentrations and mutagenic potencies (1/MEC2 in ng of PM) with S9 and without S9 are presented in Figure 1. Overall, BaP-MEQ, BaP-TEQ, and BaP ranges were 0.02-0.08 ng μg^{-1}, 0.01-0.09 ng μg^{-1}, and 0.000-0.026 ng μg^{-1}, respectively.

Regarding the mutagenic potencies, with and without metabolic activation (+S9) (Figure 1A and 1B), the sample SPA13, associated with secondary formation by the PMF receptor model, presented the lowest 1/MEC2. On the other hand, sample SPA29, associated with the influence of biomass burning, presented the highest value. Despite the different mutagenic potencies, these samples presented similar concentrations of $PM_{2.5}$ (35 and 31 µg m^{-3}), BaP (0.026 and 0.023 ng μg^{-1}), BaP-MEQ (0.08 and 0.08 ng μg^{-1}) and BaP-TEQ (0.09 and 0.06 ng μg^{-1}).

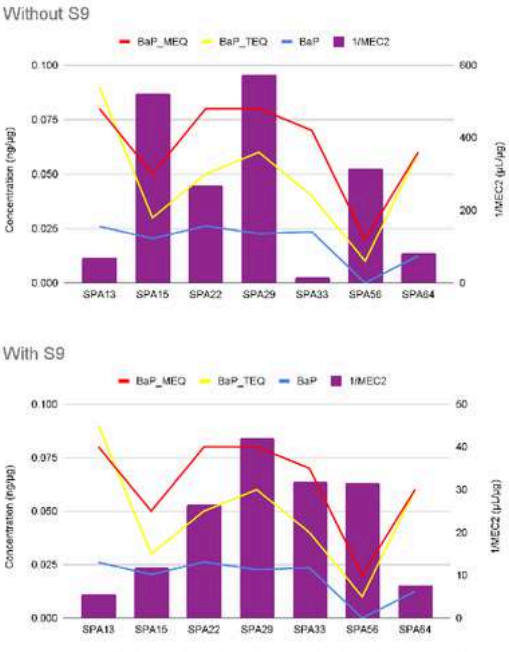


Figure 1. BaP-MEQ, BaP–TEQ, BaP (ng μg^{-1}) concentrations (left Y axis) and mutagenic potencies (1/MEC2 in ng of PM) with S9 (A) and without S9 (B) (right Y axis).

Furthermore, no correlations were found between mutagenicity results and PAHs or BaP-MEQ, and the increase in the observed concentrations of PAHs was not related to higher mutagenicity of the samples, suggesting the effect of other species, not determined in the study or a complex

interaction of different chemical species in the extract, that may have synergistic interactions (de Oliveira Alves et al., 2020).
When the experiment is performed with metabolic activation (+S9), the SPA15 sample presents a decrease in mutagenicity, while SPA33 presents the opposite effect, which may be related to the effects of the presence of nitrated PAHs in the experiment performed without activation. For the assays with S9, the samples with lower mutagenicity potencies (SPA13, SPA15, and SPA64) were often related to higher $PM_{2.5}$ concentrations (above 25 μg m^{-3}), suggesting that high $PM_{2.5}$ concentrations not always are associated with higher mutagenicity.

CONCLUSIONS

A miniaturized technique, with the YG1041 strain, was applied to evaluate the mutagenicity of organic extracts of $PM_{2.5}$ collected inside the University of São Paulo campus. It was possible to observe that relatively higher $PM_{2.5}$, BaP concentrations, and equivalent toxicities were not always associated with higher mutagenic potencies. The lack of correlations between mutagenicity results and the measured species suggests the effect of other species, not determined in this study, and a complex interaction of the different species present in this type of sample.

REFERENCES

Alves, Debora Kristina et al. Mutagenicity profile of atmospheric particulate matter in a small urban center subjected to airborne emission from vehicle traffic and sugar cane burning. *Environmental and Molecular Mutagenesis* 57 (2016): 41-50.

Ames, Bruce. *The Detection of Chemical Mutagens with Enteric Bacteria. Chemical Mutagens.* Boston: Springer, 1971.

Hagiwara, Yuji et al. Specificity and sensitivity of *Salmonella typhimurium* YG1041 and YG1042 strains possessing elevated levels of both nitroreductase and acetyltransferase activity. *Mutation Research/Environmental Mutagenesis and Related Subjects* 291 (1993): 171-180.

Maselli, Bianca et al. Comparative mutagenic activity of atmospheric particulate matter from Limeira, Stockholm and Kyoto. *Environmental and Molecular Mutagenesis* 60 (2019): 607-616.

de Oliveira Alves, Nilmara et al. Inflammation response, oxidative stress and DNA damage caused by urban air pollution exposure increase in the lack of DNA repair XPC protein. *Environment International* 145 (2020): 106150.

Pereira, Guilherme Martins et al. Particulate pollutants in the Brazilian city of São Paulo: 1-year investigation for the chemical composition and source apportionment. *Atmospheric Chemistry and Physics* 17 (2017): 11943–11969.

Pereira, Guilherme Martins et al. Emission factors for a biofuel impacted fleet in South America's largest metropolitan area. *Environmental Pollution* 331 (2023): 121826.

Ravindra, Khaiwal et al. Atmospheric polycyclic aromatic hydrocarbons: Source attribution, emission factors and regulation. *Atmospheric Environment* 42 (2008): 2895–2921.

Vasconcellos, Pérola et al. Determination of anthropogenic and biogenic compounds on atmospheric aerosol collected in urban, biomass burning and forest areas in São Paulo, Brazil. *Science of the Total Environment* 408 (2010): 5836–5844.

Williams, Richard et al. Are all bacterial strains required by OECD mutagenicity test guideline TG471 needed? *Mutation Research/Genetic Toxicology and Environmental Mutagenesis* 848 (2019): 503081.

Zwarg, José Ricardo et al. Miniaturization of the microsuspension *Salmonella*/microsome assay in agar microplates. *Environmental and Molecular Mutagenesis* 59 (2018): 488-501.

AIR POLLUTION CONFERENCE BRAZIL
CMAS SOUTH AMERICA
COMMUNITY MODELING AND ANALYSIS SYSTEM

ASSESSMENT OF AİRBONE MERCURY LEVELS İN PRESERVED AND ANTHROPOGENİCALLY İMPACTED AREAS (RİO DE JANEİRO STATE, BRAZIL)

Luis Fhernando Mendonça da Silva[1], Caio da Silva Assis Felix[4,6], Rodrigo Stellet Ferreira[2], Hellen Gonçalves da Silva[2], Maria Cristina Canela[2], Cibele Maria Stivanin de Almeida[2], Luiz Francisco Pires Guimarães Maia[3], Gisele Olímpio da Rocha[4,5,6,7], Jailson Bittencourt de Andrade[4,5,6,7], Renato da Silva Carreira[1], Adriana Gioda[1].

[1] Pontifical Catholic University of Rio de Janeiro (PUC-Rio), Departamento de Química. 22451-900 Rio de Janeiro-RJ, Brazil
agioda@puc-rio.br

[2] Universidade Estadual do Norte Fluminense Darcy Ribeiro (UENF), Centro de Ciência e Tecnologia, Laboratório de Ciências Químicas. Campos dos Goytacazes-RJ-Brazil

[3] Universidade Federal do Rio de Janeiro (UFRJ), Departamento de Meteorologia, Instituto de Geociências, Rio de Janeiro, Brasil

[4] Centro Interdisciplinar de Energia e Ambiente-CIEnAm, Universidade Federal da Bahia, 40170-115, Salvador, BA, Brazil

[5] Universidade Federal da Bahia, Instituto de Química, Programa de Pós-Graduação em Química, 40170-115, Salvador, BA, Brazil

[6] Instituto Nacional de Ciência e Tecnologia em Energia e Ambiente-INCT E&A, Universidade Federal da Bahia, 40170-115, Salvador, BA, Brazil

[7] Centro Universitário SENAI-CIMATEC, Av. Orlando Gomes, 1845 Piatã, 41650-010, Salvador, BA, Brazil

Abstract: Although present in low concentrations in the atmosphere, mercury in particulate matter (PM) plays an important role in the biogeochemical process of mercury. With this in mind, this study aims to investigate mercury concentrations in particulate matter ($PM_{2.5}$) samples from the regions of Campos dos Goycatazes (CG), Gávea (GA) and Serra dos Órgãos National Park (PARNASO). All samples were collected according to Brazilian standards (ABNT-NBR 9547/86) and the methods of the United States Environmental Protection Agency (US EPA) (Method IO - 2.1). PM concentrations were determined by gravimetric technique. The Direct Mercury Analyzer (DMA-80, Milestone Helpind Chemists) was used for total Hg analysis. Daily $PM_{2.5}$ concentrations ranged from 13 to 36 μg m^{-3}, with a mean of 24 ± 12 μg m^{-3} for the GA region, and from 24 to 46 μg m^{-3}, with a mean of 33 ± 12 μg m^{-3} for the PARNASO region, and from 14 to 19 μg m^{-3}, with a mean of 17 ± 11 μg m^{-3} for the CG for the days sampled from July to October 2022. High levels of PM concentrations at PARNASO indicate a contribution from anthropogenic sources. Considering these values, no day sampled exceeded the value suggested by Brazilian legislation (60 μg m^{-3}), but 65 % of the samples showed higher daily concentrations than suggested by World Health Organization (WHO, 15 μg m^{-3}). Hg concentrations ranged from 223 to 366 pg m^{-3}, with a mean of 274 ± 65 pg m^{-3} for the GA region, and from 119 to 190 pg m^{-3}, with a mean of 155 ± 29 pg m^{-3} for the PARNASO region, and from 164 to 315 pg m^{-3}, with a mean of 258 ± 67 pg m^{-3} for the CG for the days sampled. Hg concentrations in the atmosphere showed significant spatial variation, with much higher values in urban areas than in the natural zone. The results showed that Hg concentrations in particulate matter are at the same level as those found in urban and industrial areas in US and northern Europe. At Parnaso, the presence of Hg may be due to anthropogenic sources, which may be local sources and/or long-range transport contributions. There exists an intriguing meteorological facet warranting consideration, pertaining to the atmospheric transport facilitated by mountain-valley interactions and sea-land breezes within the southern region of the Serra dos Órgãos. This phenomenon merits further in-depth exploration. In addition, the high concentrations of Hg found in Campos dos Goytacazes may be associated with the burning of biomass, since sugar cane is burned throughout the year in the region and also due to the application of pesticides in the most diverse crops in the municipality, many times without due control.

Keywords: Mercury, particulate matter, $PM_{2.5}$, Rio de Janeiro.

INTRODUCTION

Mercury (Hg) is a pervasive environmental contaminant with significant repercussions for both human health and ecosystems globally. Its persistence, ability to accumulate in organisms, and capability for long-distance atmospheric movement make it a particularly concerning pollutant. Mercury exists in various forms, such as elemental mercury (Hg^0), reactive gaseous mercury (RGM), and particle-bound mercury (PHg). Of these, PHg is of particular concern because it can settle into ecosystems and water bodies. Once there, it undergoes transformations, ultimately converting into methylmercury—a potent neurotoxin easily absorbed by aquatic organisms and subsequently magnified through the food chain (Galappaththi and Suraweera 2020; Henriques et al. 2019).

A comprehensive comprehension of particle-bound mercury dynamics, encompassing its sources, transport mechanisms, and deposition patterns, is

essential for crafting effective mitigation strategies to alleviate its harmful effects (Brocza et al. 2024). This study seeks to enhance our understanding of these dynamics by specifically focusing on quantifying concentrations, delineating seasonal variations, and discerning potential emission sources on both a global scale and within the context of Brazil. By delving into these aspects, we aim to provide insights crucial for developing targeted interventions to address the adverse impacts of particulate mercury on ecosystems and human health.

METHODS

$PM_{2.5}$ samples were collected from three monitoring sites situated at Gávea (GÁVEA, 22°58'50" S and 43°13'58" W), Campos dos Goytacazes (CAMPOS, 21°45'39.1''S 41°17'31.1'' W), and the Serra dos Órgãos National Park (PARNASO, 22°29'47.5'' S and 43°00'05.2'' W) (Fig. 1) from July to October 2022. $PM_{2.5}$ samples were gathered employing quartz microfiber filters with a pore size of 1.6 µm (Whatman, Fisher Scientific, Maidstone, United Kingdom) over 24 hours, monthly, utilizing monitoring equipment following Brazilian standards (ABNT-NBR 129 9547/86) and methods outlined by the United States Environmental Protection Agency (US EPA) under method 130 (Method IO – 2.1). This process utilized a High-Volume air sampler (Hi-Vol 3000, Energética, Sao Paulo, Brazil) with an average air flow rate of 1.07 m^3 per minute. The filters underwent a conditioning process in a desiccator for 24 hours and they were subjected to gravimetric analysis before and after the sampling sessions using an analytical balance (Gehaka AG200 ± 0.0001, Marte Científica, Brazil) to ensure accurate measurement of particulate mass. The relative humidity levels were maintained between 20 % and 30 %, and temperatures ranged from 20 °C to 25 °C during the filter weighing procedures. This study examined all available $PM_{2.5}$ samples to assess their particulate mass content.

Total Hg concentrations in $PM_{2.5}$ were determined using a Direct Mercury Analyzer - DMA-80 (Milestone, Sorisole (BG), Italy).

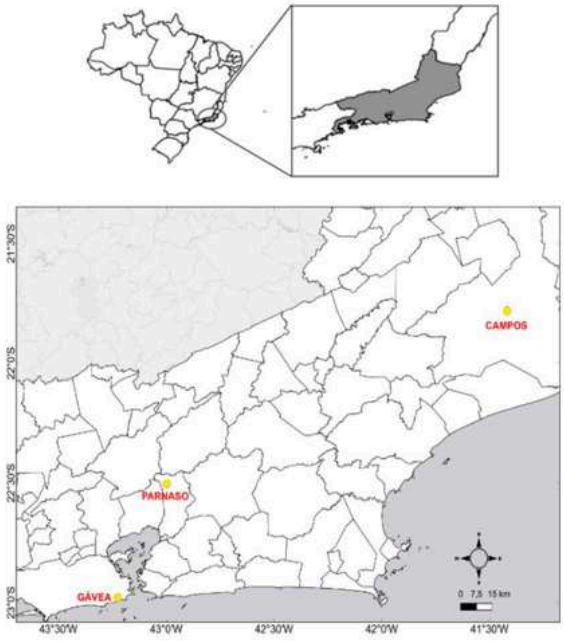


Figure 1. $PM_{2.5}$ monitoring stations: GAVEA: Gávea, PARNASO: Serra dos Órgãos National Park, and CAMPOS: Campos dos Goytacazes.

FINDINGS AND ARGUMENT

The average concentration of $PM_{2.5}$ in Gávea was 24±12 µg m^{-3} (with values ranging from 133 to 26 µg m-3, in PARNASO, it was 33±12 µg m^{-3} (with values ranging from 24 to 46 µg m^{-3}), and in Campos, it was 17±11 µg m^{-3} (with values ranging from 14 to 19 µg m^{-3}). Given these values, none of the days sampled exceeded the threshold recommended by Brazilian regulations (60 µg m^{-3}). However, 65 % of the samples exhibited daily concentrations surpassing the guidelines set by the WHO (15 µg m^{-3}).

$PM_{2.5}$ concentrations were observed to be relatively elevated during the dry season (July - August) in contrast to the wet season (September-October). This pattern has been documented in numerous prior studies (Beringui et al. 2021; De La Cruz et al. 2024; Mateus et al. 2013). Many researchers attribute this phenomenon to the cleansing impact of rainfall, which captures and deposits suspended particles in the atmosphere.

The average PHg concentrations (range) were 274±65 (223–366) pg m^{-3}, 155±29 (119–190) pg m^{-3} and 258±67 (164–315) pg m^{-3} at the urban region of the capital, interior with sugarcane burning and forest sites during the sampling period, respectively. The average concentration of PHg in the urban with sugarcane burning (CAMPOS) and

forest (PARNASO) sites was approximately two times higher than in the urban site (GAVEA).

The results showed that PHg concentrations at urban sites in coastal cities are considerably lower than those in other cities, such as Gávea. The surface winds in coastal areas influence the concentrations of PM in these regions (Wang et al. 2023). PHg concentrations in urban areas were 5.9-11.3 times higher than the nearby values found in Asian countries (Xu et al. 2019), and North America (Detroit, USA) (Liu et al. 2007), indicating that a large amount of anthropogenic mercury has been released into the atmosphere in Brazil.

The highest levels of PHg were found in Campos and PARNASO, while the lowest concentrations of PHg were present in Gavea. The high concentration of PHg at the sites may be associated with anthropogenic emissions. In Campos, the most significant contributions may come from vehicular traffic, the port area and, above all, the burning of sugar cane. PARNASO, despite being an environmental conservation area, usually receives many visitors to the park, with vehicles being the primary commuter. In addition, it is less than 200 m away from BR-116, one of the main avenues linking the metropolitan region of Rio de Janeiro to the Serra and other states in the country, with heavy vehicle traffic.

CONCLUSIONS

During the sampling period, it was observed that $PM_{2.5}$ concentrations varied among the locations under study. In Gávea, PARNASO, and Campos, the average concentrations remained within acceptable limits as per Brazilian regulations, with none exceeding the specified threshold. However, a significant proportion of samples from all locations exceeded the daily concentration standards recommended by the World Health Organization, raising potential health concerns.

Mercury concentrations also exhibited variations across different environments, with higher levels detected in areas associated with sugarcane burning compared to urban and preserved sites. Urban fire sites recorded the highest mercury levels, surpassing those in both urban and preserved areas.

REFERENCES

Beringui, Karmel et al. 2021. "Assessment of the Concentration and Inorganic Composition of Particulate Matter Collected in the State of Rio De Janeiro." *Quimica Nova* 44(6): 737–54.

Brocza, Flora Maria et al. 2024. "Global Scenarios of Anthropogenic Mercury Emissions." *EGUsphere [preprint]* (41). https://doi.org/10.5194/egusphere-2024-4 (February 21, 2024).

Galappaththi, Himan K.A., and Inoka Suraweera. 2020. "Risk of Mercury Exposure during Childhood: A Review of Sri Lankan Situation." *Reviews on Environmental Health* 35(3): 229–32. https://www.degruyter.com/document/doi/10.1515/reveh-2020-0024/html (January 31, 2024).

Henriques, Magda Carvalho, Susana Loureiro, Margarida Fardilha, and Maria Teresa Herdeiro. 2019. "Exposure to Mercury and Human Reproductive Health: A Systematic Review." *Reproductive Toxicology* 85: 93–103.

De La Cruz, Alex H. et al. 2024. "Black Carbon and Particulate Matter Concentrations: Air Pollution Levels in Rio de Janeiro, Brazil." *Article J. Braz. Chem. Soc.* 35: 1–12. https://dx.doi.org/10.21577/0103-5053.20240029 (March 31, 2024).

Liu, Bian et al. 2007. "Temporal Variability of Mercury Speciation in Urban Air." *Atmospheric Environment* 41: 1911–23. www.elsevier.com/locate/atmosenv (February 1, 2024).

Mateus, Vinícius Lionel et al. 2013. "Study of the Chemical Composition of Particulate Matter from the Rio de Janeiro Metropolitan Region, Brazil, by Inductively Coupled Plasma-Mass Spectrometry and Optical Emission Spectrometry." *Spectrochimica Acta Part B: Atomic Spectroscopy* 86: 131–36.

Wang, Ju et al. 2023. "Impact Analysis of Meteorological Variables on PM2.5 Pollution in the Most Polluted Cities in China." *Heliyon* 9(7): e17609.

Xu, H. M. et al. 2019. "Mercury Stable Isotope Compositions of Chinese Urban Fine Particulates in Winter Haze Days: Implications for Hg Sources and Transformations." *Chemical Geology* 504: 267–75.

AIR POLLUTION CONFERENCE BRAZIL
CMAS SOUTH AMERICA
COMMUNITY MODELING AND ANALYSIS SYSTEM

USE OF PLANTS AS BIOMONITORS OF PARTICULATE MATTER TOXICITY IN URBAN REGIONS INFLUENCED BY MINNING

Santos, Emannuelly Ap. Amaral[1]; Neves, Thiago de Alencar[2]; Oliveira, Dângelle Makelle[3]; Passos, Ricardo Gomes[4]; Albuquerque, Taciana Toledo de Almeida[5]; Starling, Maria Clara Vieira Martins[6]
[1]*Department of Sanitary and Environmental Engineering, Federal University of Minas Gerais.* *emannuellyufmg@gmail.com*
[2]*Department of Sanitary and Environmental Engineering, Federal University of Minas Gerais.* *thiago@desa.ufmg.br*
[3]*Department of Sanitary and Environmental Engineering, Federal University of Minas Gerais.* *dangelleem@yahoo.com.br*
[4]*Nuclear Technology Development Center, Federal University of Minas Gerais* *ricardo.passos@cdtn.br*
[5]*Department of Sanitary and Environmental Engineering, Federal University of Minas Gerais.* *tacianatoledo26@gmail.com*
[6]*Department of Sanitary and Environmental Engineering, Federal University of Minas Gerais.* *mariaclara@desa.ufmg.br*

Abstract: Regarding air quality, biomonitoring applies plant species for which standard assays enable tracking direct and immediate effect of pollutants, as well as the release of toxic compounds, such as metals found in particulate matter (PM), into the ecosystem. This is extremely relevant considering that ecosystem health is linked to human health as according to the One Health Approach. Given the above, this research aims to conduct biomonitoring of air quality by using the standard grass species *Lolium multiflorum* as a tool for air quality monitoring in the city of Brumadinho (Minas Gerais, Brazil). The region is impacted by mining activities that release high loads of particulate matter into the atmosphere. The plants were cultivated and exposed according to the VDI 3957 - part 2 standard, with adaptations. Three sampling points were selected: S1 - City center; S2 - Tejuco neighborhood, surrounded by mining sites; S3 - an Indigenous community area, along with a reference point - S4 (a natural reserve). Additionally, $PM_{2.5}$ were sampled throughout the exposure period using a medium-volume sampler (ARA Instrument). S3 showed the highest concentrations of $PM_{2.5}$ (median of 40.15 $\mu g/m^3$), while S4 had the lowest concentrations (median of 31.40 $\mu g/m^3$). However, the medians did not differ significantly between the monitoring points. Visual analyses of the plants after exposure demonstrate a possible correlation between the presence of metals in atmospheric particles and their growth, indicating the accumulation of trace elements.

Keywords: Biomonitoring, One Health, Mining, Particulate Matter, *Lolium multiflorum*.

INTRODUCTION

Air pollution is a current challenge, representing one of the greatest risks to human health and environmental integrity (WHO, 2023). In mining regions, the impacts and emission of atmospheric pollutants, especially particulate matter (PM), from anthropogenic activities are intensified. In Brazil, mining plays a pivotal role in the country's economy, especially in the state of Minas Gerais. However, indiscriminate activities and lack of control and monitoring lead to the exacerbated release of atmospheric pollutants, highly detrimental to health.

The bottleneck in conventional air quality monitoring techniques, which rely on physicochemical analyses, does not allow for direct conclusions about the potential effects of pollutants to the environment (Klumpp *et al.*, 2003). Thus, alternatives supported by Nature-Based Solutions (NbS) can contribute to the diagnosis and reduction of air pollution (Theophilo *et al.*, 2021).

Biomonitoring is an efficient technique for assessing environmental contamination by using living organisms. Considering the concept of One Health (Multisanti *et al.*, 2022), environmental health threats detected by biomonitoring can serve as an early warning for human health threats, contributing to preventive measures. PM containing potentially toxic trace elements such as cadmium (Cd), copper (Cu), lead (Pb), and zinc (Zn) (Theophilo *et al.*, 2021), are easily inhaled by humans and animals, as well as deposited in plants, resulting in direct and indirect problems for the environment and public health.

Regarding air quality (bio)monitoring, plants are cost-effective indicators that allow for the assessment of the risk of complex mixtures of pollutants and analyses of those with very low environmental concentrations, which are difficult to measure by traditional methods (De Temmerman *et al.*, 2004). In addition, biomonitoring can be implemented in locations which lack access to high-tech equipment which require frequent maintenance. Besides, they promote environmental education and raise community awareness related to air pollution.

AIR POLLUTION CONFERENCE BRAZIL
CMAS SOUTH AMERICA
COMMUNITY MODELING AND ANALYSIS SYSTEM

The forage grass *Lolium multiflorum* Lam. (ryegrass) is used for animal consumption and due to its resistance to atmospheric pollutants, it has a high rate of bioaccumulation of toxic substances, such as sulfur, trace metals, polycyclic aromatic hydrocarbons (PAHs), gases, and PM (Bulbovas; Camargo; Domingos, 2015; Nakazato et al., 2018). Thus, it is ideal for monitoring and risk assessment in industrial and urban areas.

Considering the foregoing, this research aims to conduct air quality biomonitoring using the standard grass species *Lolium multiflorum* in a mining region located in the city of Brumadinho, metropolitan region of Belo Horizonte, in the state of Minas Gerais, Brazil.

METHODS

Biomonitoring was actively conducted in March and April of 2024, with grass cultivation and exposure following the VDI 3957 - part 2 standard (2003) (adapted). The plants were cultivated for 3 weeks before exposure in a natural reserve selected as a reference site (S4) and exposed for 28 days at 3 sampling points in Brumadinho: S1 - City center, S2 - Tejuco neighborhood, surrounded by mining sites, S3 – an Indigenous community area near a ferry line used for mining ore transportation.

Plant growth was observed during the exposure period. Subsequently, they were manually cut and subjected to laboratory analyses to evaluate the presence of metals, following EPA 3050B (1996) (adapted). The plant material was submitted to wet-opened digestion with a HNO_3 and H_2O_2 solution (1:1), and the extracts will be analyzed by ICP-OES.

In addition to plant exposure, fine particulate matter (<2.5 micrometers in diameter; $PM_{2.5}$) were sampled using a medium-volume sampler (ARA Instrument) equipped with quartz filters. $PM_{2.5}$ sampling was carried out for 24 hours in the same locations of plant exposure, throughout the exposure period. Subsequently, the $PM_{2.5}$ concentration was determined by gravimetric method (INPE, 2012), and the concentration of metals using the aforementioned methodology. Results were submitted to statistical analysis by Kruskal-Wallis analysis of variance followed by Dunn's mean test.

FINDINGS AND ARGUMENT

The concentration of particulate matter $PM_{2.5}$ varied among the sampling sites, with a maximum of 43.77 µg/m³ in the Indigenous community area (S3) and a minimum of 16.23 µg/m³ in the reference area (S4). Figure 1 illustrates the variation found among the monitoring points in the city of Brumadinho and the comparison with air quality reference value of WHO (2021).

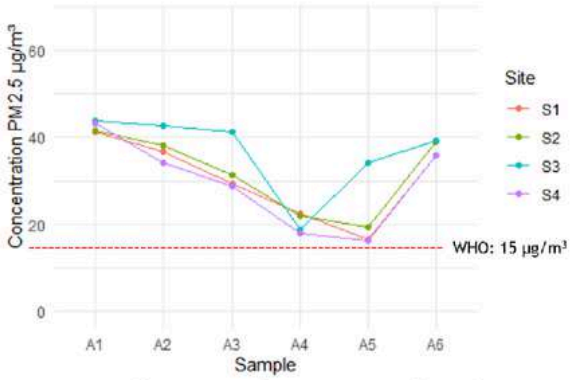


Figure 1. Illustrates the variation found among the monitoring points in the city of Brumadinho compared with WHO air quality reference value (2021) (15 µg/m³ in 24 hours).

All samples exceeded the WHO reference value for $PM_{2.5}$. This suggests poor air quality in the region, requiring more attention to monitoring and source control. Furthermore, it is important to highlight that PM concentrations are also associated with other factors, such as climatic conditions, and correlation studies with such factors should be performed.

S3 showed the highest median of 40.15 µg/m³ among the sampling points (Figure 2). The lowest median was at the reference point (S4) of 31.40 µg/m³. However, there was no significant differences according to the Kruskal-Wallis test ($p<0.05$).

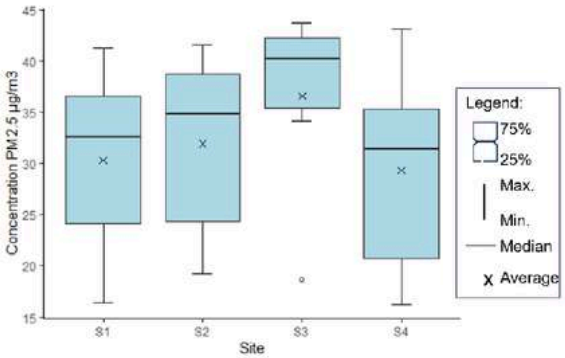


Figure 2. Boxplot of $PM_{2.5}$ concentration in each monitoring point.

Site 3 represents an Indigenous community area located near the ore loading and transportation area. Additionally, the region was affected by the tailings dam collapse on January 26th, 2019. So, it still suffers the consequences of tailings deposit in the region. Such factors may be associated with the resuspension of contaminated particulate matter. However, further studies should be conducted to test this hypothesis, such as studies involving soil sampling.

The preliminary qualitative analysis of plants (visual analysis) contributed to an initial understanding of the impacts of air pollution to bioindicators, as toxic components can cause biomass reduction, growth inhibition, and organism death (Ghosh; Dutta; Mukhopadhyay, 2023). Figure 3 demonstrates the state of plants exposed in each of the sampling sites after 28 days.



Figure 3. Visual plants after exposure in each of the sampling sites after 28 days.

It can be observed that plants exposed in Points 2 and 3 exhibited more leaf injuries and are smaller than the other points. Borowiak *et al.* (2020) noted that the accumulation of trace elements presents in the atmosphere in ryegrass reduced the net photosynthesis rate and stomatal conductance of the plants.

Although S3 presented the highest PM concentrations, it is worth noting that the plants were exposed in a wooded area and toxic elements may have encountered barriers in taller plants compared to the sampler. Thus, the analysis of metals in ryegrass leaves will provide more elaborate data for understanding metal contamination at this and the other sampling sites.

CONCLUSIONS

Preliminary analyses demonstrate that particulate matter concentration may influence plant development, taking into consideration other processes such as land use in the surroundings. The high concentrations of particulate matter in the city of Brumadinho reflect air pollution in urban areas influenced by mining.

Analyses of metals in plants leaves and quartz filters will be used to better discuss the relationships between atmospheric pollutant concentration and ecosystem health. Biomonitoring data along with chemical characterization will be of great significance in devising strategies for controlling and mitigating pollution.

REFERENCES

Arsenic, Aluminum Magnesium, et al. "Method 3050B acid digestion of sediments, sludges, and soils 1.0 scope and application." *Washington, DC, USA* (1996).

Borowiak, Klaudia, et al. "Accumulation of airborne toxic elements and photosynthetic performance of Lolium multiflorum L. leaves." *Processes* 8.9 (2020): 1013.

Bulbovas, Patricia, Carla ZS Camargo, and Marisa Domingos. "Ryegrass cv. Lema and guava cv. Paluma biomonitoring suitability for estimating nutritional contamination risks under seasonal climate in Southeastern Brazil." *Ecotoxicology and Environmental Safety* 118 (2015): 149-157.

Nakazato, Ricardo Keiichi, et al. "Efficiency of biomonitoring methods applying tropical bioindicator plants for assessing the phytoxicity of the air pollutants in SE, Brazil." *Environmental Science and Pollution Research* 25 (2018): 19323-19337.

De Temmerman, Ludwig, and Michel Hoenig. "Vegetable crops for biomonitoring lead and cadmium deposition." Journal of Atmospheric Chemistry 49 (2004): 121-135.

Ferreira, Tatiane Morais, Maria Cristina Forti, and Plinio Carlos Alvala. "Protocolo para coleta de material particulado atmosférico." *INPE, São José dos Campos* (2012).

Ghosh, Sayantan, Ratna Dutta, and Shritama Mukhopadhyay. "A Review on Seasonal Changes in Particulate Matter Accumulation by Plant Bioindicators: Effects on Leaf Traits." *Water, Air, & Soil Pollution* 234.8 (2023): 529.

Klumpp, Andreas. "European network for the assessment of air quality by the use of bioindicator plants. LIFE99 ENV/D/000453". University of Hohenheim. 2003.

Multisanti, Cristiana Roberta, et al. "Sentinel species selection for monitoring microplastic pollution: A review on one health approach." Ecological Indicators 145 (2022): 109587.

Theophilo, Carolina Yume Sawamura, et al. "Biomonitoring as a Nature-Based Solution to Assess Atmospheric Pollution and Impacts on Public Health." Bulletin of Environmental Contamination and Toxicology 107 (2021): 29-36.

VDI - Verein Deutscher Ingenieure. "Biological Measuring Techniques for the Determination and Evaluation of Effects of Air Pollutants on Plant (Bioindication). Method of Standardized Grass Exposure. VDI-Guideline 3957 Part 2. *Beuth Verlag, Berlin*, 2003.

WHO. "Air quality and health. Type of pollutants." *Available at: Air quality and health (who.int)*. Accessed on March 8, 2024.

WHO. "WHO global air quality guidelines." *Particulate Matter (PM2.5 and PM10), Ozone, Nitrogen Dioxide, Sulfur Dioxide and Carbon Monoxide* (2021).

AIR POLLUTION CONFERENCE BRAZIL
CMAS SOUTH AMERICA
COMMUNITY MODELING AND ANALYSIS SYSTEM

SOCIOENVIRONMENTAL VULNERABILITIES AND AIR POLLUTION IN THE CITY OF SÃO PAULO FROM 2019 TO 2023

Vinícius de Souza Oliveira[1], Paulo Eduardo Alves Camargo-Cruz[2], Regina Maura de Miranda[3]
[1]*Escola de Artes, Ciências e Humanidades, Universidade de São Paulo*
vinicius_so@usp.br
[2]*Escola de Artes, Ciências e Humanidades, Universidade de São Paulo*
negresse@usp.br
[3]*Escola de Artes, Ciências e Humanidades, Universidade de São Paulo*
remaura@usp.br

Abstract: It's inherent that air quality has been a highly discussed and researched topic over time, becoming a determining environmental indicator. Thus, this study aimed to analyze the possible relationship between air quality in the city of São Paulo and the socioeconomic and environmental conditions of its inhabitants from 2019 to 2023. The indicators of socioenvironmental vulnerability from the map of inequality and the annual average concentrations of PM_{10} (inhalable particles), $PM_{2.5}$ (fine inhalable particles), NO_2 (nitrogen dioxide), and O_3 (ozone) were correlated using the Spearman method in the Statistica software. Few events with high correlation between pollution parameters and vulnerability indicators were observed, which may indicate a low correlation between the sample data. Despite low values, the correlations provide an indication that socio-environmental vulnerabilities may be influenced by poor air quality, as 36% of the results obtained correspond to strong or moderate correlations, with higher values for the correlation of NO_2 with the proportion of black people (-0.708) and formal employment opportunities (0.737), indicating these as factors that intensify the correspondence to possible disturbances in areas where NO_2 concentrations are higher and with low formal employment opportunities for black people. Thus, the relevance of the topic must be emphasized in scientific production, political discussions, and public awareness, especially among the most vulnerable populations.

Keywords: Socioenvironmental vulnerabilities, São Paulo, atmospheric pollution, Spearman correlation.

INTRODUCTION

Exposure to atmospheric pollutants produced in cities is one of the factors contributing to poor quality of life in urban centers. It is inherent that air quality has been a much discussed and researched topic over time, becoming a determining environmental indicator (Russo, 2010). Thus, this study aimed to analyze the possible relationship between air quality in the city of São Paulo and the socioeconomic and environmental conditions of its inhabitants from 2019 to 2023.

Air pollution is linked to respiratory diseases, cardiovascular diseases, central nervous system diseases, premature births, among other aggravating factors. Environmental impact should also be considered, such as climate changes, leading to ecological imbalances (Abe and Miraglia, 2016).

In addition to industrial activities, urban "immobility" should be highlighted as a triggering factor for high concentrations of pollutants, responsible for about 60% of the pollutants people breathe in cities (Andrade *et al.*, 2012; Saldiva, 2018).

There is a gap in understanding how air pollution can affect people according to their position in society, considering aspects that characterize their level of socioenvironmental vulnerability (Castelhano, 2021). Some case studies have delved into this line of research, such as studies conducted in Uganda, Africa (Clark *et al.*, 2022), and in New Jersey, United States (Sabrin *et al.*, 2020). In Brazil, a notable study related economic inequalities to exposure to pollutants generated by vehicular traffic in São Paulo (Habermann *et al.*, 2014).

In this study, it was possible to identify correlations at different levels for the concentrations of PM_{10}, $PM_{2.5}$, NO_2, and O_3 and the variables selected through Spearman's correlation. Despite the presence of low values, the correlations provide an indication that socioenvironmental vulnerabilities may be influenced by poor air quality, where 36% of the results obtained correspond to strong or moderate correlations.

With higher values for the correlation of NO_2 with the proportion of black people (-0.708) and formal employment opportunities (0.737), this finding may indicate that these factors intensify the correspondence to possible disturbances in areas where NO_2 concentrations are higher and with low formal employment opportunities for black people. Thus, the relevance of the topic must be emphasized in scientific production, political discussions, and public awareness, especially among the most vulnerable populations.

METHODS

The exploratory research was limited to the Web of Science database, without data systematization. The selection of socioeconomic indicators (Table 1)

was made based on the understanding of risk, susceptibility, and exposure to atmospheric pollutants (Ge *et al.*, 2017).

Table 1. Socioeconomic indicators

Variable	
1	Female population
2	Black population
3	Average time for consultations in Primary Care (SUS)
4	Mortality from respiratory system diseases
5	Formal employment opportunities
6	Average monthly income from formal employment
7	Shantytowns

Reference: RNSP, 2019, 2020, 2021, 2022, 2023.

The data for the indicators were obtained through the annual publications of the Map of Inequality campaign by the Rede Nossa São Paulo (RNSP). The average concentrations of the analyzed parameters - PM_{10}, $PM_{2.5}$, NO_2, and O_3 - were obtained from the QUALAR system and the air quality reports by the Environmental Company of the State of São Paulo (CETESB) published from 2019 to 2022. For the year 2023, the monthly average concentrations published in CETESB's monthly bulletins were used.

To analyze the possible relationship between the parameters and indicators, Spearman correlation was conducted using the Statistica software, which statistically compares the selected independent variables by revealing the degree of association between them (Bermúdez Pastor, 2023; Xiao *et al.*, 2015).

FINDINGS AND ARGUMENT

Few events with high correlation between pollution parameters and vulnerability indicators were observed, which may indicate a low correlation between the sample data. However, there is a possible indication that NO_2 is the pollutant with the highest correlation with the indicators (Table 2).

Within a 95% confidence interval and a significance level of 5%, the average concentration of NO_2 in the study period indicates a high negative correlation with the black and brown population (-0.708), suggesting a possible vulnerability of the black and brown population to NO_2 exposure. Using the same criteria, the correlation with the indicator of formal employment opportunities showed a high positive correlation (0.737), indicating a relationship with NO_2 concentration.

In this regard, it is inferred that the black population residing in districts of São Paulo where there are higher concentrations of NO_2, such as Campo Belo and Vila Leopoldina districts, with average concentrations of 62 and 54 µg/m³, and approximately 12.21% and 14.41% of black residents, respectively, over a five-year period.

Furthermore, for these districts, the employment opportunities were at median and high rates compared to other districts, with 8.75 and 14.86, respectively, per ten participants in the labor force aged fifteen years or older, indicating that it may not negatively influence the vulnerability of its inhabitants.

The correlation between $PM_{2.5}$ and the average monthly income from formal employment also showed a high negative correlation coefficient (-0.506), indicating a relationship between the average $PM_{2.5}$ concentration monitored by CETESB and the indicator of average monthly income from formal employment.

It is observed that the highest concentration of $PM_{2.5}$ during the analyzed period was found in the Vila Leopoldina district, with an average of 18 µg/m³, while the lowest occurred in Santo Amaro, with an average value of 12 µg/m³. The average monthly salary for formal employment was R$ 3,890.00 for Vila Leopoldina and R$ 4,854.27 for Santo Amaro, which does not capture a clear relationship between pollutant concentration and the indicator.

Table 2. Correlation coefficients

Variable	NO_2	O_3	$MP_{2,5}$	MP_{10}
1	0.301	-0.093	-0.425	-0.403
2	-0.708	-0.090	0.266	0.274
3	0.192	0.233	0.063	-0.240
4	-0.177	-0.159	0.250	0.374
5	0.737	0.031	-0.037	-0.039
6	0.396	0.108	-0.506	-0.319
7	-0.529	0.163	0.192	0.055

**The marked values are the correlation coefficients found within a 95% confidence interval and 5% significance level.*

The data collection process was challenging due to the limited census data collected by institutions such as the Instituto Brasileiro de Geografia e Estatística (IBGE). Therefore, the data analysis may have resulted in few correlation coefficients with a 95% confidence interval due to data scarcity, which was one of the main barriers to conducting this research. Due to the limited number of studies conducted in Brazil on this topic, access to research that could contribute to the interpretation of these results is also limited, highlighting the need for more studies as this one.

CONCLUSIONS

The relationship between atmospheric pollution and socioenvironmental vulnerabilities indicates that few of the sampled data are well correlated. It is inferred that further statistical analyses may be necessary for a better visualization of the possible relationship between the parameters and selected indicators.

The reliance on the publication of open data regarding the characteristics of the population and city infrastructure posed challenges in conducting the study. On the other hand, campaigns monitoring the spatial characterization of cities and their inhabitants, such as the Map of Inequality, are essential for understanding reality.

Finally, these preliminary results could already suggest the creation of an index of socioenvironmental vulnerability to atmospheric pollution. This tool could aid in understanding the relationship between socioenvironmental vulnerabilities and atmospheric pollution in cities, contributing to public agendas and measures for managing issues related to poor air quality.

REFERENCES

Abe, Carina C., and Simone G. El K. Miraglia. "Health Impact Assessment of Air Pollution in São Paulo, Brazil." *Int. J. Environmental Research and Public Health* 694 (2016): 1-10. Acessed May 03, 2024. doi: 10.3390/ijerph13070694.

Andrade, Maria de F., Regina M. de Miranda, Adalgiza Fornaro, Americo Kerr, Beatriz Oyama, Paulo A. de Andre and Paulo Saldiva. "Vehicle emissions and PM2.5 mass concentrations in six Brazilian cities." *Air Qual Atmos Health* 5 (2012): 79-88. Acessed May 03, 2024. doi: 10.1007/s11869-010-0104-5.

Bermúdez Pastor, Pablo. "Contaminación atmosférica y vulnerabilidad social en la ciudad de Madrid." *Revista Internacional de Ciencia y Tecnología de la Información Geográfica* 31 (2023): 115-145. Acessed May 03, 2024. doi: 10.21138/GF.797.

Castelhano, Francisco J. "Riscos e vulnerabilidades sob a perspectiva da qualidade do ar." *Finisterra* 56 (2021): 253-269. Acessed May 03, 2024. doi: 10.18055/Finis20231.

CETESB. "Qualidade do ar no estado de São Paulo 2019-23" *CETESB* (2020-3). Acessed May 03, 2024.

Clarke, Kayan, Kevin Ash, Eric S. Coker, Tara Sabo-Attwood and Engineer Bainomugisha. "A Social Vulnerability Index for Air Pollution and Its Spatially Varying Relationship to PM2.5 in Uganda." *Atmosphere* 13 (2022): 1-16. Acessed May 03, 2024. doi: 10.3390/atmos13081169.

Ge, Yi, Haibo Zhang, Wen Dou, Wenfang Chen, Ning Liu, Yuan Wang, Yulin Shi and Wenxin Rao. "Mapping Social Vulnerability to Air Pollution: A Case Study of the Yangtze River Delta Region, China." *Sustainability* 109 (2017): 1-15. Acessed May 03, 2024. doi: 10.3390/su9010109.

Habermann, Mateus, Míriam Souza, Rogério Prado and Nelson Gouveia. "Socioeconomic inequalities and exposure to traffic-related air pollution in the city of São Paulo, Brazil." *Cad. Saúde Pública* 30 (2014): 119-125. Acessed May 03, 2024. doi: 10.1590/0102-311X00168412.

RNSP, Rede Nossa São Paulo. "Mapa da desigualdade 2019-23". *Rede Nossa São Paulo* (2020-24). Acessed May 03, 2024.

Russo, Paulo R. "A qualidade do ar no município do Rio de Janeiro: análise espaço-temporal de partículas em suspensão na atmosfera." *Revista de Ciências Humanas* 1 (2010): 78-93.

Sabrin, Samin, Maryam Karimi e Rouzbeth Nazari. "Developing Vulnerability Index to Quantify Urban Heat Islands Effects Coupled with Air Pollution: A Case Study of Camden, NJ." *International Journal of Geo-Information* 9 (2020): 1-14. Acessed May 03, 2024. doi:10.3390/ijgi9060349.

Xiao, Chengwei, Jiaqi Ye, Rui M. Esteves and Chunming Rong. "Using Spearman's correlation coefficients for exploratory data analysis on big dataset" *Concurrency Computat.: Pract. Exper.* 28 (2015): 3866-3878. Acessed May 03, 2024. doi: 10.1002/cpe.3745.

AIR POLLUTION CONFERENCE BRAZIL
CMAS SOUTH AMERICA
COMMUNITY MODELING AND ANALYSIS SYSTEM

ASSESSMENT OF AİRBONE MERCURY LEVELS İN PRESERVED AND ANTHROPOGENİCALLY İMPACTED AREAS (RİO DE JANEİRO STATE, BRAZIL)

Luis Fhernando Mendonça da Silva[1], Caio da Silva Assis Felix[4,6], Rodrigo Stellet Ferreira[2], Hellen Gonçalves da Silva[2], Maria Cristina Canela[2], Cibele Maria Stivanin de Almeida[2], Luiz Francisco Pires Guimarães Maia[3], Gisele Olímpio da Rocha[4,5,6,7], Jailson Bittencourt de Andrade[4,5,6,7], Renato da Silva Carreira[1], Adriana Gioda[1].

[1] Pontifical Catholic University of Rio de Janeiro (PUC-Rio), Departamento de Química. 22451-900 Rio de Janeiro-RJ, Brazil
agioda@puc-rio.br

[2] Universidade Estadual do Norte Fluminense Darcy Ribeiro (UENF), Centro de Ciência e Tecnologia, Laboratório de Ciências Químicas. Campos dos Goytacazes-RJ-Brazil

[3] Universidade Federal do Rio de Janeiro (UFRJ), Departamento de Meteorologia, Instituto de Geociências, Rio de Janeiro, Brasil

[4] Centro Interdisciplinar de Energia e Ambiente-CIEnAm, Universidade Federal da Bahia, 40170-115, Salvador, BA, Brazil

[5] Universidade Federal da Bahia, Instituto de Química, Programa de Pós-Graduação em Química, 40170-115, Salvador, BA, Brazil

[6] Instituto Nacional de Ciência e Tecnologia em Energia e Ambiente-INCT E&A, Universidade Federal da Bahia, 40170-115, Salvador, BA, Brazil

[7] Centro Universitário SENAI-CIMATEC, Av. Orlando Gomes, 1845 Piatã, 41650-010, Salvador, BA, Brazil

Abstract: Although present in low concentrations in the atmosphere, mercury in particulate matter (PM) plays an important role in the biogeochemical process of mercury. With this in mind, this study aims to investigate mercury concentrations in particulate matter ($PM_{2.5}$) samples from the regions of Campos dos Goycatazes (CG), Gávea (GA) and Serra dos Órgãos National Park (PARNASO). All samples were collected according to Brazilian standards (ABNT-NBR 9547/86) and the methods of the United States Environmental Protection Agency (US EPA) (Method IO - 2.1). PM concentrations were determined by gravimetric technique. The Direct Mercury Analyzer (DMA-80, Milestone Helpind Chemists) was used for total Hg analysis. Daily $PM_{2.5}$ concentrations ranged from 13 to 36 μg m^{-3}, with a mean of 24 ± 12 μg m^{-3} for the GA region, and from 24 to 46 μg m^{-3}, with a mean of 33 ± 12 μg m^{-3} for the PARNASO region, and from 14 to 19 μg m^{-3}, with a mean of 17 ± 11 μg m^{-3} for the CG for the days sampled from July to October 2022. High levels of PM concentrations at PARNASO indicate a contribution from anthropogenic sources. Considering these values, no day sampled exceeded the value suggested by Brazilian legislation (60 μg m^{-3}), but 65 % of the samples showed higher daily concentrations than suggested by World Health Organization (WHO, 15 μg m^{-3}). Hg concentrations ranged from 223 to 366 pg m^{-3}, with a mean of 274 ± 65 pg m^{-3} for the GA region, and from 119 to 190 pg m^{-3}, with a mean of 155 ± 29 pg m^{-3} for the PARNASO region, and from 164 to 315 pg m^{-3}, with a mean of 258 ± 67 pg m^{-3} for the CG for the days sampled. Hg concentrations in the atmosphere showed significant spatial variation, with much higher values in urban areas than in the natural zone. The results showed that Hg concentrations in particulate matter are at the same level as those found in urban and industrial areas in US and northern Europe. At Parnaso, the presence of Hg may be due to anthropogenic sources, which may be local sources and/or long-range transport contributions. There exists an intriguing meteorological facet warranting consideration, pertaining to the atmospheric transport facilitated by mountain-valley interactions and sea-land breezes within the southern region of the Serra dos Órgãos. This phenomenon merits further in-depth exploration. In addition, the high concentrations of Hg found in Campos dos Goytacazes may be associated with the burning of biomass, since sugar cane is burned throughout the year in the region and also due to the application of pesticides in the most diverse crops in the municipality, many times without due control.

Keywords: Mercury, particulate matter, $PM_{2.5}$, Rio de Janeiro.

INTRODUCTION

Mercury (Hg) is a pervasive environmental contaminant with significant repercussions for both human health and ecosystems globally. Its persistence, ability to accumulate in organisms, and capability for long-distance atmospheric movement make it a particularly concerning pollutant. Mercury exists in various forms, such as elemental mercury (Hg^0), reactive gaseous mercury (RGM), and particle-bound mercury (PHg). Of these, PHg is of particular concern because it can settle into ecosystems and water bodies. Once there, it undergoes transformations, ultimately converting into methylmercury—a potent neurotoxin easily absorbed by aquatic organisms and subsequently magnified through the food chain (Galappaththi and Suraweera 2020; Henriques et al. 2019).

A comprehensive comprehension of particle-bound mercury dynamics, encompassing its sources, transport mechanisms, and deposition patterns, is

essential for crafting effective mitigation strategies to alleviate its harmful effects (Brocza et al. 2024). This study seeks to enhance our understanding of these dynamics by specifically focusing on quantifying concentrations, delineating seasonal variations, and discerning potential emission sources on both a global scale and within the context of Brazil. By delving into these aspects, we aim to provide insights crucial for developing targeted interventions to address the adverse impacts of particulate mercury on ecosystems and human health.

METHODS

$PM_{2.5}$ samples were collected from three monitoring sites situated at Gávea (GÁVEA, 22°58'50" S and 43°13'58" W), Campos dos Goytacazes (CAMPOS, 21°45'39.1''S 41°17'31.1'' W), and the Serra dos Órgãos National Park (PARNASO, 22°29'47.5'' S and 43°00'05.2'' W) (Fig. 1) from July to October 2022. $PM_{2.5}$ samples were gathered employing quartz microfiber filters with a pore size of 1.6 µm (Whatman, Fisher Scientific, Maidstone, United Kingdom) over 24 hours, monthly, utilizing monitoring equipment following Brazilian standards (ABNT-NBR 129 9547/86) and methods outlined by the United States Environmental Protection Agency (US EPA) under method 130 (Method IO – 2.1). This process utilized a High-Volume air sampler (Hi-Vol 3000, Energética, Sao Paulo, Brazil) with an average air flow rate of 1.07 m^3 per minute. The filters underwent a conditioning process in a desiccator for 24 hours and they were subjected to gravimetric analysis before and after the sampling sessions using an analytical balance (Gehaka AG200 ± 0.0001, Marte Científica, Brazil) to ensure accurate measurement of particulate mass. The relative humidity levels were maintained between 20 % and 30 %, and temperatures ranged from 20 °C to 25 °C during the filter weighing procedures. This study examined all available $PM_{2.5}$ samples to assess their particulate mass content.

Total Hg concentrations in $PM_{2.5}$ were determined using a Direct Mercury Analyzer - DMA-80 (Milestone, Sorisole (BG), Italy).

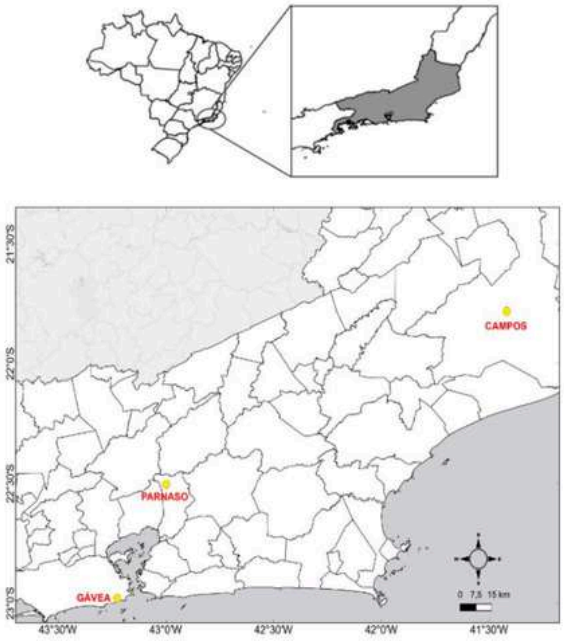


Figure 1. $PM_{2.5}$ monitoring stations: GAVEA: Gávea, PARNASO: Serra dos Órgãos National Park, and CAMPOS: Campos dos Goytacazes.

FINDINGS AND ARGUMENT

The average concentration of $PM_{2.5}$ in Gávea was 24±12 µg m^{-3} (with values ranging from 13 to 36 µg m^{-3}, in PARNASO, it was 33±12 µg m^{-3} (with values ranging from 24 to 46 µg m^{-3}), and in Campos, it was 17±11 µg m^{-3} (with values ranging from 14 to 19 µg m^{-3}). Given these values, none of the days sampled exceeded the threshold recommended by Brazilian regulations (60 µg m^{-3}). However, 65 % of the samples exhibited daily concentrations surpassing the guidelines set by the WHO (15 µg m^{-3}).

$PM_{2.5}$ concentrations were observed to be relatively elevated during the dry season (July - August) in contrast to the wet season (September-October). This pattern has been documented in numerous prior studies (Beringui et al. 2021; De La Cruz et al. 2024; Mateus et al. 2013). Many researchers attribute this phenomenon to the cleansing impact of rainfall, which captures and deposits suspended particles in the atmosphere.

The average PHg concentrations (range) were 274±65 (223–366) pg m^{-3}, 155±29 (119–190) pg m^{-3} and 258±67 (164–315) pg m^{-3} at the urban region of the capital, interior with sugarcane burning and forest sites during the sampling period, respectively. The average concentration of PHg in the urban with sugarcane burning (CAMPOS) and

forest (PARNASO) sites was approximately two times higher than in the urban site (GAVEA).

The results showed that PHg concentrations at urban sites in coastal cities are considerably lower than those in other cities, such as Gávea. The surface winds in coastal areas influence the concentrations of PM in these regions (Wang et al. 2023). PHg concentrations in urban areas were 5.9-11.3 times higher than the nearby values found in Asian countries (Xu et al. 2019), and North America (Detroit, USA) (Liu et al. 2007), indicating that a large amount of anthropogenic mercury has been released into the atmosphere in Brazil.

The highest levels of PHg were found in Campos and PARNASO, while the lowest concentrations of PHg were present in Gavea. The high concentration of PHg at the sites may be associated with anthropogenic emissions. In Campos, the most significant contributions may come from vehicular traffic, the port area and, above all, the burning of sugar cane. PARNASO, despite being an environmental conservation area, usually receives many visitors to the park, with vehicles being the primary commuter. In addition, it is less than 200 m away from BR-116, one of the main avenues linking the metropolitan region of Rio de Janeiro to the Serra and other states in the country, with heavy vehicle traffic.

CONCLUSIONS

During the sampling period, it was observed that $PM_{2.5}$ concentrations varied among the locations under study. In Gávea, PARNASO, and Campos, the average concentrations remained within acceptable limits as per Brazilian regulations, with none exceeding the specified threshold. However, a significant proportion of samples from all locations exceeded the daily concentration standards recommended by the World Health Organization, raising potential health concerns.

Mercury concentrations also exhibited variations across different environments, with higher levels detected in areas associated with sugarcane burning compared to urban and preserved sites. Urban fire sites recorded the highest mercury levels, surpassing those in both urban and preserved areas.

REFERENCES

Beringui, Karmel et al. 2021. "Assessment of the Concentration and Inorganic Composition of Particulate Matter Collected in the State of Rio De Janeiro." *Quimica Nova* 44(6): 737–54.

Brocza, Flora Maria et al. 2024. "Global Scenarios of Anthropogenic Mercury Emissions." *EGUsphere [preprint]* (41). https://doi.org/10.5194/egusphere-2024-4 (February 21, 2024).

Galappaththi, Himan K.A., and Inoka Suraweera. 2020. "Risk of Mercury Exposure during Childhood: A Review of Sri Lankan Situation." *Reviews on Environmental Health* 35(3): 229–32. https://www.degruyter.com/document/doi/10.1515/reveh-2020-0024/html (January 31, 2024).

Henriques, Magda Carvalho, Susana Loureiro, Margarida Fardilha, and Maria Teresa Herdeiro. 2019. "Exposure to Mercury and Human Reproductive Health: A Systematic Review." *Reproductive Toxicology* 85: 93–103.

De La Cruz, Alex H. et al. 2024. "Black Carbon and Particulate Matter Concentrations: Air Pollution Levels in Rio de Janeiro, Brazil." *Article J. Braz. Chem. Soc.* 35: 1–12. https://dx.doi.org/10.21577/0103-5053.20240029 (March 31, 2024).

Liu, Bian et al. 2007. "Temporal Variability of Mercury Speciation in Urban Air." *Atmospheric Environment* 41: 1911–23. www.elsevier.com/locate/atmosenv (February 1, 2024).

Mateus, Vinícius Lionel et al. 2013. "Study of the Chemical Composition of Particulate Matter from the Rio de Janeiro Metropolitan Region, Brazil, by Inductively Coupled Plasma-Mass Spectrometry and Optical Emission Spectrometry." *Spectrochimica Acta Part B: Atomic Spectroscopy* 86: 131–36.

Wang, Ju et al. 2023. "Impact Analysis of Meteorological Variables on PM2.5 Pollution in the Most Polluted Cities in China." *Heliyon* 9(7): e17609.

Xu, H. M. et al. 2019. "Mercury Stable Isotope Compositions of Chinese Urban Fine Particulates in Winter Haze Days: Implications for Hg Sources and Transformations." *Chemical Geology* 504: 267–75.

AIR POLLUTION CONFERENCE BRAZIL
CMAS SOUTH AMERICA
COMMUNITY MODELING AND ANALYSIS SYSTEM

Comprehensive Evaluation of MAIAC 1km AOD Product for $PM_{2.5}$ Estimation in Latin American Urban Areas

Sebastian Diez[1] Josefina Urquiza[2,3],
[1]*Universidad del Desarrollo, Chile*
sebastian.diez@udd.cl
[2]*Grupo de Estudios de la Atmósfera y el Ambiente (GEAA), Universidad Tecnológica Nacional, Facultad Regional Mendoza (UTN-FRM)*
jurquiza@conicet.gov.ar
[3]*Consejo Nacional de Investigaciones Científicas y Técnicas (CONICET)*

Abstract: In Latin America, limited PM2.5 monitoring stations hinder air quality assessment and understanding health impacts. This study utilizes the Aerosol Optical Depth (AOD) measured by satellite platforms, particularly focusing on the MAIAC product with its high spatial resolution (1 km), often used as a PM proxy. Our aim is to evaluate the uncertainty of the MAIAC 1km product in six densely populated cities: Sao Paulo, Santiago, Buenos Aires, Medellín, La Paz, and México, over 2015-2022. We employed typical global metrics (R2, RMSE, bias) and the detailed Relative Expanded Uncertainty (REU) for a comprehensive assessment. Unlike common metrics, REU provides insights into the error structure across the AOD's dynamic range. Our findings indicate relatively low AOD values (< 0.2) with moderate correlation (R < 0.6) with AERONET sun photometers. In the AOD range of 0.05 to 0.15, the relative uncertainty exceeded 50% for all locations. Additionally, we compared MAIAC with the MODIS DT 3km product, finding consistently lower uncertainties (REU~20-30%) for MODIS in the same dynamic range. Despite MAIAC showing slightly better RMSE and R2 (~0.08 and ~0.55) than MODIS (~0.1 and ~0.49), regression analysis revealed a greater bias in MAIAC. We conclude that at lower aerosol loads, the MAIAC algorithm exhibits higher uncertainty and bias compared to MODIS DT, highlighting the importance of considering uncertainties when using AOD products for PM estimation and spatial PM2.5 distribution characterization.

Keywords: MAIAC 1km, AOD, Uncertainty, Latin American cities.

INTRODUCTION

Aerosols are solid and liquid particles suspended in the atmosphere originating from both natural and anthropogenic sources (Liu & Yi, 2022). These particles play a significant role in climate change, air quality and human health. Therefore, understanding the distribution and variation of aerosols in different regions is essential for improving human quality of life. Aerosol Optical Depth (AOD) is an indicator used in the study of particles, as it provides a quantitative measure of the amount of direct sunlight that is blocked on its way to the Earth's surface due to the scattering and/or absorption of atmospheric aerosols. The global network of solar photometers, AERONET, offers measurements at the surface with a sampling frequency of 15 minutes. However, the limited number of stations restricts its application to regional and local studies. In contrast, satellite product typically provides information with global coverage but with a more limited temporal resolution due to the satellite's pass frequency. This is the case with the Multi-Angle Implementation of Atmospheric Correction (MAIAC) product, which retrieves AOD with a spatial resolution of 1 km and daily temporal resolution for studying urban air quality (Lyapustin et al., 2018).

In recent years, MAIAC has been widely used globally due to improvements in the spatial resolution of aerosol products, primarily serving as a proxy for particulate matter (PM) (Damascena et al., 2021). Comprehensive evaluations of MAIAC have been conducted on both global (Qin et al., 2021) and regional scales (Martins et al., 2017). Results have shown good agreement with surface measurements, with some differences depending on land use and aerosol levels. In Latin America, several countries are in a position of increased vulnerability due to scarce or none existent air quality measurements (Carmona et al., 2021; Pinder et al., 2019), making it difficult to determine aerosol behaviour and distribution at local and regional scales. In countries lacking extensive monitoring networks, MAIAC could be useful for deriving indirect estimates of $PM_{2.5}$ in the air from aerosol optical properties, overcoming spatial limitations of traditional measurements. Such estimates can be seen as a complementary and cost-effective method for $PM_{2.5}$ monitoring (Carmona et al., 2021). Several studies have evaluated MAIAC's performance in different Latin American locations. However, in situations using proxies to estimate PM2.5, there's a lack of comprehensive quantitative analysis on uncertainty. This absence could lead to potentially inappropriate use of satellite products and improper conclusions (Sayer et al., 2020). Given that surface characteristics and aerosol properties are unknown and must be evaluated as part of the retrieval process, inherent uncertainty arises, making it difficult to distinguish true spatiotemporal aerosol variability. Therefore, the aim is to evaluate the uncertainty of the MAIAC 1km product in six densely populated cities: São Paulo, Santiago, Buenos Aires, Medellín, La Paz, and Mexico, over the period 2015-2022.

AIR POLLUTION CONFERENCE BRAZIL
CMAS SOUTH AMERICA
COMMUNITY MODELING AND ANALYSIS SYSTEM

METHODS

The AOD data were acquired from the surface network of the AERONET, using L2.0 level records available for the period 2015-2022 for: São Paulo (SP), Santiago (ST), Buenos Aires (BA), Medellín (MD), La Paz (LP), and Mexico (MX). These sites were selected considering their location in major Latin American cities and the availability of measurements. Since the data bands provided by AERONET do not match those of the satellite product, interpolation was performed to obtain AOD_{550} using the Ångström exponent at wavelengths close to 500 and 675 nm. Regarding the satellite product, MCD19A2 was used, which provides AOD at 550 nm. Multiple tiles were downloaded from the Terra and Aqua missions in Hierarchical Data Format (HDF) and the images were filtered by selecting those of better quality (QA = 0000). Subsequently, a performance evaluation was carried out by comparing the space-time (1 km² - 60 min) of both satellite datasets C6.0 and C6.1 using the AERONET network as a reference to analyze the associated uncertainty and the modifications made in the algorithm. To evaluate performance, typical global metrics (R^2, RMSE, bias) were used, and a more detailed metric called Relative Expanded Uncertainty (REU) was used for a more comprehensive assessment of performance.

FINDINGS AND ARGUMENT

The Figure 1 shows the temporal evolution of AERONET AOD_{550} between 2015 and 2022, obtained from daily averages. A significant lack of data is observed, especially in MD (48.5%) and MX (15.3%), while in other locations, this deficiency is less than 13%. AOD levels for the region are generally low (<0.2), with higher values in MX and MD. Although most AOD levels are close to the average, there is greater dispersion in MX and possibly less in BA and LP. No clear cycle is evident in the temporal patterns, with variable peaks at each location. Peaks with maximum aerosol load levels greatly exceed the period's averages, especially in ST, LP, MX, MD, and SP, where increases of up to six times higher than the mean levels are observed. Similar trends to previous research are observed, such as seasonal increases during the summer attributed to factors like biomass burning and regional transport of combustion products. In SP and BA, these increases could be due to long-distance transport of biomass burning smoke in the Amazon, which typically occurs from August to November(Mendez-Espinosa et al., 2019). In ST, peaks could also be attributable to wildfires in surrounding areas (Lapere et al., 2021). Meanwhile, LP and MX did not show significant increases above the mean.

The Figure 2 depicts a scatter plot comparing the performance of the C6.0 and C6.1 collections to determine if the new MAIAC product offers improvements for the analyzed Latin American cities. Analyzing R^2, both versions exhibit moderate performance, with values ranging from 0.3 to 0.8. An enhancement is detected in the values for the cities of ST and MX, which are the sites with the highest AOD levels, with increases of 6.6% and 15% respectively.

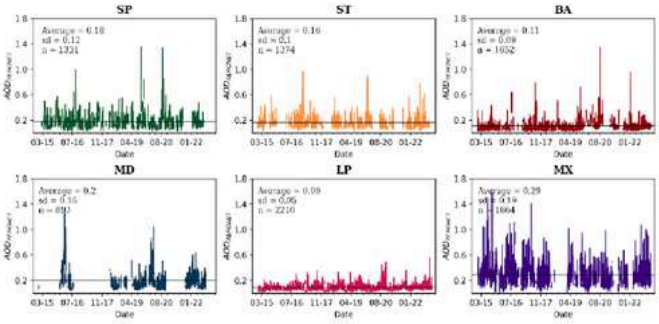


Figure 1. Daily averages of AERONET AOD_{550}.

However, for the rest of the sites (except MD), the R^2 values remain uniform. In MD, it is the only site experiencing a performance decrease, with a reduction of 34.62%, possibly due to data gaps. Regarding RMSE and the dispersion, no significant differences are observed between both collections. However, a moderate dispersion persists, mainly below the 1:1 reference line, indicating a tendency to underestimate values in all cases. Additionally, it is noted that the points tend to concentrate at lower AOD levels (<0.2), except in MX, where the variability range is higher. As for bias, a slight reduction is observed, implying an improvement compared to version C6.1. Although values remain underestimated and below the 1:1 reference line, this underestimation has decreased in magnitude. This difference is more evident in some cities, particularly notable in LP, followed by MX and BA. Furthermore, the regression line shows that C6.0 values are more biased than those of C6.1 in all cases. In summary, in Latin American cities, MAIAC C6.1 exhibits slightly better RMSE, R^2, and bias values (~0.06, ~0.54, ~-0.008) than C6.0 (~0.07, ~0.5, and ~-0.027).

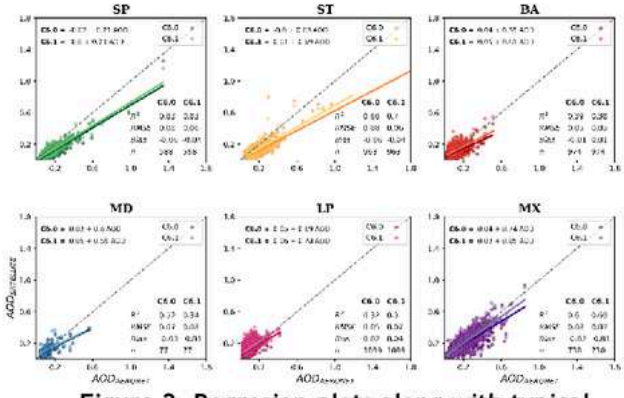


Figure 2. Regresion plots along with typical single valued metrics for the 6 LatAm cities.

Figure 3 presents the relative uncertainty (REU), with the x-axis representing AODAERONET reference levels. Both versions of MAIAC consistently show relative uncertainty exceeding 25%, while in the range of 0.05 to 0.15, it exceeds

50% for all cities. As AOD levels increase and reach approximately 0.1, the uncertainty stabilizes. This is crucial, given that the regional average of $AOD_{AERONET}$ is 0.17, and cities like BA and LP have averages below AOD = 0.1, suggesting that the uncertainty at these levels could be very high and could lead to erroneous results and conclusions. Specifically, it is observed that in ST, SP, and BA, the highest minimum values are recorded for version C6.1 (62.18%, 54.19%, and 53.35% respectively), and even higher in version C6.0 (75%, 60.38%, and 68.28% respectively). In contrast, the lowest results were obtained for LP and MX. This finding differs from what is shown by single-value metrics, where, generally, sites with higher AOD levels (SP, MX, and ST) show better performance. A trend of decreasing uncertainty is observed in all cases, improving performance in C6.1. The sites where uncertainty decreased significantly are SP with 10.3%, ST with 17.1%, BA with 21.9%, LP with 30.7%, and MX with 40.2%. In the case of MD, similar to traditional metrics, a similar pattern is maintained between both versions.

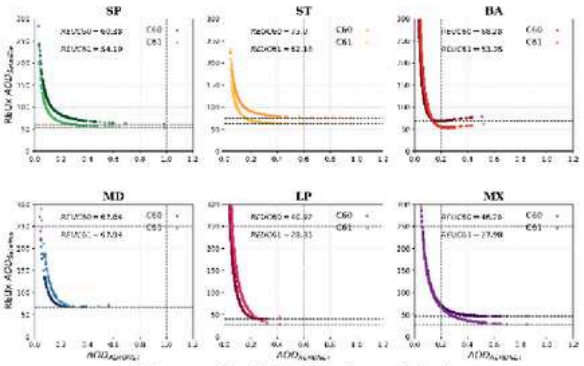


Figure 3. REU C6.0 vs C6.1

CONCLUSIONS

These findings reveal a significant data gap in the region. The AOD levels were relatively low, with an average of 0.2. Regarding performance according to traditional metrics, a generally moderate to low performance is observed, although an improvement is noted in sites with higher AOD levels. REU always exceeds 25%, and in the range of 0.05 to 0.15, it exceeds 50%. When comparing product versions, subtle improvements are observed in certain metrics for C6.1, but improvements in bias and REU are mainly highlighted. However, the magnitude of these improvements may vary depending on the city and AOD levels. Reductions between 10% (SP) and 40% (MX) were recorded in REU between both versions. It is observed that as AOD levels increase and reach approximately 0.1, uncertainty stabilizes. This is crucial since the regional average of $AOD_{AERONET}$ is 0.17, suggesting high uncertainty at these levels. Therefore, these results highlight the importance of considering uncertainties when using satellite-derived AOD products to estimate PM and characterize the spatial distribution of PM, as it could lead to erroneous conclusions.

REFERENCES

Carmona, J. M., Gupta, P., Lozano-García, D. F., Vanoye, A. Y., Hernández-Paniagua, I. Y., & Mendoza, A. (2021). Evaluation of modis aerosol optical depth and surface data using an ensemble modeling approach to assess pm2.5 temporal and spatial distributions. *Remote Sensing*, *13*(16). https://doi.org/10.3390/rs13163102

Damascena, A. S., Yamasoe, M. A., Martins, V. S., Rosas, J., Benavente, N. R., Sánchez, M. P., Tanaka, N. I., & Saldiva, P. H. N. (2021). Exploring the relationship between high-resolution aerosol optical depth values and ground-level particulate matter concentrations in the Metropolitan Area of São Paulo. *Atmospheric Environment*, *244*(September 2020). https://doi.org/10.1016/j.atmosenv.2020.117949

Lapere, R., Mailler, S., & Menut, L. (2021). The 2017 mega-fires in central chile: Impacts on regional atmospheric composition and meteorology assessed from satellite data and chemistry-transport modeling. *Atmosphere*, *12*(3). https://doi.org/10.3390/atmos12030344

Liu, Y., & Yi, B. (2022). Aerosols over East and South Asia: Type Identification, Optical Properties, and Implications for Radiative Forcing. *Remote Sensing*, *14*(9). https://doi.org/10.3390/rs14092058

Lyapustin, A., Wang, Y., Korkin, S., & Huang, D. (2018). MODIS Collection 6 MAIAC algorithm. *Atmospheric Measurement Techniques*, *11*(10), 5741–5765. https://doi.org/10.5194/amt-11-5741-2018

Martins, V. S., Lyapustin, A., De Carvalho, L. A. S., Barbosa, C. C. F., & Novo, E. M. L. M. (2017). Validation of high-resolution MAIAC aerosol product over South America. *Journal of Geophysical Research*, *122*(14), 7537–7559. https://doi.org/10.1002/2016JD026301

Mendez-Espinosa, J. F., Belalcazar, L. C., & Morales Betancourt, R. (2019). Regional air quality impact of northern South America biomass burning emissions. *Atmospheric Environment*, *203*(February), 131–140. https://doi.org/10.1016/j.atmosenv.2019.01.042

Pinder, R. W., Klopp, J. M., Kleiman, G., Hagler, G. S. W., Awe, Y., & Terry, S. (2019). Opportunities and challenges for filling the air quality data gap in low- and middle-income countries. *Atmospheric Environment*, *215*(February), 116794. https://doi.org/10.1016/j.atmosenv.2019.06.032

Qin, W., Fang, H., Wang, L., Wei, J., Zhang, M., Su, X., Bilal, M., & Liang, X. (2021). MODIS high-resolution MAIAC aerosol product: Global validation and analysis. *Atmospheric Environment*, *264*. https://doi.org/10.1016/j.atmosenv.2021.118684

Sayer, A. M., Govaerts, Y., Kolmonen, P., Lipponen, A., Luffarelli, M., Mielonen, T., Patadia, F., Popp, T., Povey, A. C., Stebel, K., & Witek, M. L. (2020). A review and framework for the evaluation of pixel-level uncertainty estimates in satellite aerosol remote sensing. *Atmospheric Measurement*

Techniques, *13*(2), 373–404.
https://doi.org/10.5194/amt-13-373-2020

AIR POLLUTION CONFERENCE BRAZIL
CMAS SOUTH AMERICA
COMMUNITY MODELING AND ANALYSIS SYSTEM

AİR POLLUTİON ANALYSİS İN LATİN AMERİCA: IMPLİCATİONS FOR HEALTH AND SOCİO-ENVİRONMENTAL INEQUALİTİES

Josefina Urquiza[1,2], Tailine Corrêa dos Santos[3], Sebastian Diez[4]
[1]*Grupo de Estudios de la Atmósfera y el Ambiente (GEAA), Universidad Tecnológica Nacional, Facultad Regional Mendoza (UTN-FRM)*
jurquiza@conicet.gov.ar
[2]*Consejo Nacional de Investigaciones Científicas y Técnicas (CONICET)*
[3]*Universidade de São Paulo - USP*
tailine.santos@usp.br
[4]*Universidad del Desarrollo, Chile*
sebastian.diez@udd.cl

Abstract: Air pollution has a wide range of adverse impacts on public health, covering issues from respiratory and cardiovascular problems to metabolic and neurological disorders, where it is estimated to be associated with 4 million annual deaths in urban areas. However, the distribution of pollution impacts differently in those vulnerable communities, due to socio-economic inequalities and the limited availability of essential health services. Understanding the effects of pollution and the current information scenario is crucial to designing effective policies that address both environmental and social issues. This paper aims to investigate the monitoring scenario of available $PM_{2.5}$ air quality data and associated disease records in the context of social inequality, discussing possible relationships due to lack of information and/or access to health services. This study focuses on Latin America, where the region's vulnerability is exacerbated by limited access to health care and lack of information on air quality and medical records. To conduct this analysis, information on pollutants was collected, using data from reference monitors from the OpenAQ database, as well as information from national registries in order to examine the evolution of the number of sensors in the region. In addition, these data were combined with measures from the Global Burden of Disease study (i.e. years of life lost due to premature mortality (YLLs); and disability-adjusted life years (DALYs), to perform a comprehensive analysis of correlations and trends. Our initial analysis indicates that in the 41% of the region where there are no air quality monitoring systems, the mortality rate is about 20% higher than in those places with monitoring, and about 35% higher than in countries where data is fully accessible. However, in those countries that do have measurement systems, sensors are limited, averaging only 0.2 sensors per 100,000 inhabitants. This situation highlights the differences in the availability and density of air quality sensors in the region. The absence of reference station monitoring is not only related to data availability, but also reflects deeper socio-economic challenges. Specifically, we observe that the burden of disease is significantly higher in less developed nations, highlighting the importance of the socio-economic dimension in understanding and addressing the health effects of air pollution. Countries with a low Social Development Index (SDI) have DALYs rates for ischaemic heart disease and stroke more than five times higher than high SDI countries. Likewise, nations in the lowest economic bracket have almost seven times higher DALY rates for stroke compared to those with very high incomes. These results highlight the relationship between a country's socio-economic status and health risks linked to air pollution. However, it is essential to stress that these findings do not indicate causality, but rather provide a snapshot of the current situation. Moreover, to fully understand these differences, factors such as public health policies, economic development and socio-environmental conditions must be taken into account. In order to develop strategies to improve the overall health of the region, it is vital to consider other relevant factors. This study could serve as a starting point for further research and the formulation of more informed and effective policies in the region.

Keywords: Public health, Air Quality Data, Health risks, Monitoring Systems.

INTRODUCTION

Currently, approximately 57% of the global population resides in urban areas, with Latin America having around 81% of its population living in cities, ranking as the second most urbanized region (UN-DESA-PD, 2022). In urban areas, air pollution has become one of the leading causes of serious health issues, such as cardiovascular diseases, respiratory problems, diabetes, and even premature death (Juginović et al., 2021; Sang et al., 2022). Despite efforts to reduce pollution levels globally, it remains one of the most significant factors affecting both health and the economy. However, over 90% of the world's population was exposed to air quality levels exceeding the World Health Organization (WHO) Air Quality Guidelines in 2016 (WHO, 2022).

Disparities in air quality have been observed based on a country's income level. While air pollution in developed countries poses a significant public health problem, it is even more pronounced in developing countries where rapid population expansion alongside widespread industrialization has led to areas with poor air quality, posing a serious health threat (Mannucci & Franchini, 2017). In Latin America, this issue is exacerbated as many countries face a range of additional challenges. Data availability on air quality is scarce, with limited measurements primarily concentrated in major cities of the countries (Gómez Peláez et al., 2020; Pinder et al., 2019). Moreover, access to healthcare is limited, and information regarding the

relationship between air quality and its health effects is insufficient to address this issue. Therefore, this work aims to investigate the state of available information on air quality in Latin America and examine its relationship with the effects of exposure to these pollutants. We will focus on monitoring available air quality data and records of associated diseases, especially considering the context of social inequality. Possible relationships due to lack of information and/or access to healthcare services will be discussed to identify areas for improvement and address existing challenges in the region.

METHODS

Information on pollutants was collected using data from reference air quality monitors from the OpenAQ database, an organization dedicated to providing universal access to air quality data. These data were combined with measures from the Global Burden of Disease study obtained from the Institute for Health Metrics and Evaluation (IHME) and the Health Effects Institute (HEI). Specifically, data were collected for 35 Latin American countries on general mortality, years of life lost (YLLs), and disability-adjusted life years (DALYs) attributable to air pollution by age, year, and sex between 1990 and 2019. Additionally, estimates of ambient $PM_{2.5}$ ($aPM_{2.5}$) exposure levels were obtained. To analyze disparities in terms of air pollution and disease burden, countries were divided based on their Social Development Index (SDI)

FINDINGS AND ARGUMENT

In Latin America, the availability of reference sensor measurements is limited. In Figure 1, the proportions of the countries performing air quality monitoring are presented. Approximately 44% of countries are regularly generating and sharing air quality data, while 41% of countries do not conduct direct measurements. The remaining countries (15%) carry out measurements but do not make this information public.This lack of transparency may lead to the population being unaware of the risks associated with air quality in their environment. However, in countries with measurement systems, sensors are limited, with an average of only 0.2 sensors per 100,000 inhabitants. Belize and Puerto Rico stand out with 1.2 and 0.76 sensors per 100,000 people, respectively. Countries like El Salvador, Paraguay, Uruguay, and Venezuela have a lower number of sensors per 100,000 inhabitants (<0.03). Looking at the geographical distribution of sensors, there is a predominance in South America, with countries like Peru, Brazil, Colombia, and Chile, except for Mexico, which has more than 70 sensors in each country. However, these numbers are small compared to each country's population (Chile and Peru~0.3, Colombia ~0.2, Mexico and Brazil <0.07 sensors per 100,000 inhabitants). This situation highlights differences in the availability and density of air quality sensors in the region.

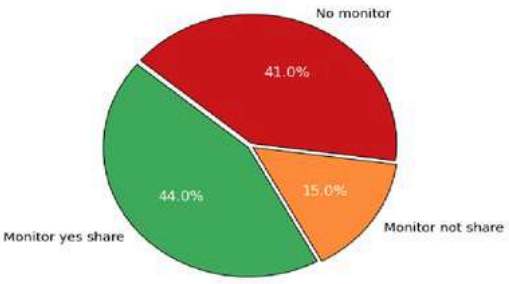


Figure 1. Air Quality monitoring OpenAQ

Figure 2 presents the average annual population-weighted $aPM_{2.5}$ for year 2019, according to the availability of information on air quality. Despite the existence of many countries without measurements, the concentrations are quite uniform compared to those that do monitor. Countries that monitor and have full access to information present an average of 19.55 ug/m^3, while those that monitor but do not share data record 16.94 ug/m^3. Those that do not conduct direct monitoring have average concentrations of 18.08 ug/m^3. This raises questions about whether countries without monitoring actually have better air quality conditions or if estimates and projections are also skewed due to lack of data for proper model validation. However, this is not the focus of this work and does not have an easy answer. In all cases, the concentrations considerably exceed the WHO limits of 5 ug/m^3. In fact, in all three cases, they exceed the limits by more than 250%. Only Puerto Rico (6.85ug/m^3) y Bemuda(7.07 ug/m^3) are close to the WHO guidelines limit.

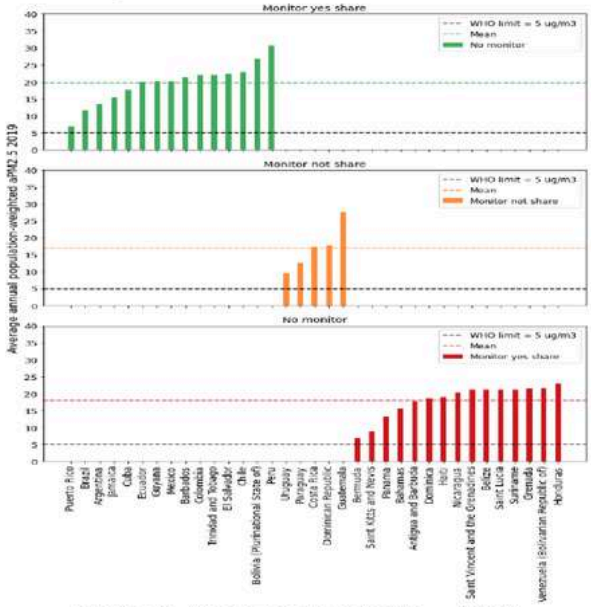


Figure 2. Average annual $aPM_{2.5}$ 2019

Figure 3 presents the mortality rate attributable to air pollution. Countries that monitor and share their data have an average mortality rate of 38.79 per 100,000 inhabitants. In contrast, countries that monitor but do not share their data have a slightly higher mortality rate, reaching 43.19 per 100,000

inhabitants. However, the most notable disparity is evident in countries that do not monitor air quality directly, recording a higher mortality rate of 54.77. Analyzing these figures reveals that in 41% of the countries in the region where there is no monitoring, the mortality rate is 26.86% higher than in those places that do conduct monitoring. Additionally, this rate is approximately 41.18% higher than in countries where data is fully accessible.

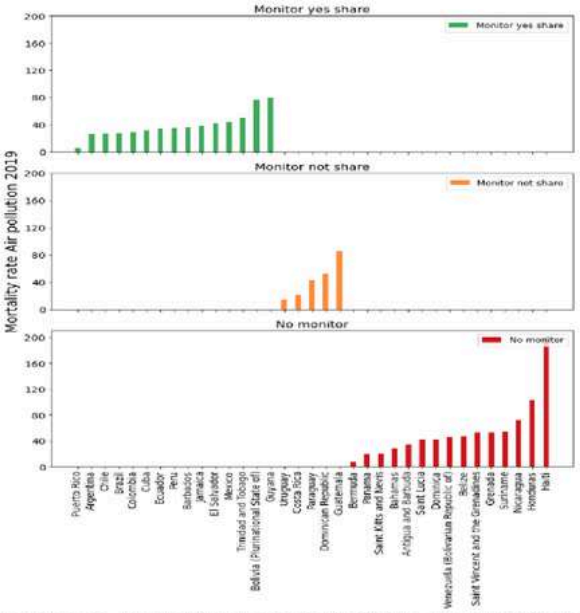


Figure 3. Mortality rate atributable Air Pollution

The absence of monitoring is not only limited to data availability but also reveals profound socioeconomic challenges. Specifically, the disease burden is significantly higher in less developed nations, highlighting the importance of addressing the socioeconomic dimension when tackling the effects of air pollution on health. In the left-hand of the Figure 3, the DALYs rate attributed to air pollution for the year 2019 is presented by country. In the right-hand en the Figure 3, the Social Development Index (SDI) by country is shown. An inverse relationship between DALYs rates and SDI is observed.

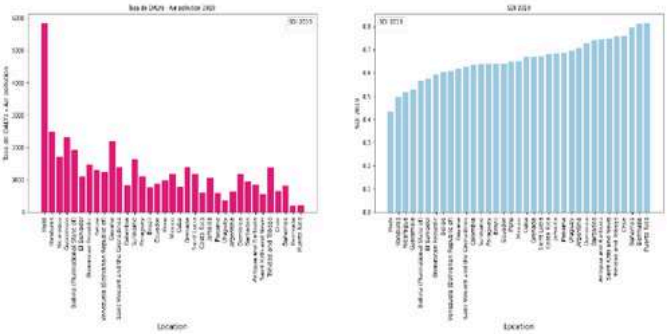


Figure 4. DALYs rate and SDI per country

As DALYs attributed to air pollution decrease, SDI increases. Countries with a low SDI (0.4-0.5) have a DALY of 4157.18, while those with a high SDI (>0.8) have a DALY of 193.63. This difference highlights that countries with a low SDI have a DALY 21.47 times higher than countries with a high SDI, emphasizing the urgency of addressing socioeconomic disparities to improve environmental and human health.

CONCLUSIONS

These findings underscore the relationship between a country's socioeconomic status and the health risks associated with air pollution. However, it's crucial to emphasize that these findings do not imply causation but rather provide a snapshot of the current scenario. Furthermore, to fully understand these differences, factors such as public health policies, economic development, and socio-environmental conditions must be taken into account. This study could serve as a stepping stone for further research and the crafting of more informed and efficacious policies in the region.

REFERENCES

Gómez Peláez, L. M., Santos, J. M., de Almeida Albuquerque, T. T., Reis, N. C., Andreão, W. L., & de Fátima Andrade, M. (2020). Air quality status and trends over large cities in South America. *Environmental Science and Policy*, *114*(September), 422–435. https://doi.org/10.1016/j.envsci.2020.09.009

Juginović, Alen; Vuković, Miro; Aranza, Ivan; Biloš, V. (2021). *Health impacts of air pollution exposure from 1990 to 2019 in 43 European countries*. https://doi.org/https://doi.org/10.1038/s41598-021-01802-5

Mannucci, P. M., & Franchini, M. (2017). Health effects of ambient air pollution in developing countries. *International Journal of Environmental Research and Public Health*, *14*(9), 1-8. https://doi.org/10.3390/ijerph14091048

Pinder, R. W., Klopp, J. M., Kleiman, G., Hagler, G. S. W., Awe, Y., & Terry, S. (2019). Opportunities and challenges for filling the air quality data gap in low- and middle-income countries. *Atmospheric Environment*, *215*(February), 116794. https://doi.org/10.1016/j.atmosenv.2019.06.032

Sang, S., Chu, C., Zhang, T., Chen, H., & Yang, X. (2022). The global burden of disease attributable to ambient fine particulate matter in 204 countries and territories, 1990–2019: A systematic analysis of the Global Burden of Disease Study 2019. *Ecotoxicology and Environmental Safety*, *238*(April). https://doi.org/10.1016/j.ecoenv.2022.113588

UN-DESA-PD. (2022). World Population Prospects 2022. In *United Nation* (Issue 9). www.un.org/development/ desa/pd/.

WHO. (2022). *Ambient (outdoor) air pollution*. https://www.who.int/news-room/fact-sheets/detail/ambient-(outdoor)-air-quality-and-health

AIR POLLUTION CONFERENCE BRAZIL
CMAS SOUTH AMERICA
COMMUNITY MODELING AND ANALYSIS SYSTEM

ASSESSMENT OF PM2.5 OXIDATIVE POTENTIAL, COMPOSITION, AND EMISSION SOURCES IN THE URBAN AIR OF SÃO PAULO, BRAZIL

Caroline F.H. Wikuats[1], Rafaela Squizzato[1], Iara da Silva[1], Thiago Nogueira[2], Daan L.A.C. Leseman[3], A. John F. Boere[3], Lucia da Conceição Andrade[4], Edmilson Dias de Freitas[1], Alessandra Tammaro[5], Flemming R. Cassee[3,6], Maria de Fatima Andrade[1]

[1]*Institute of Astronomy, Geophysics, and Atmospheric Sciences, University of São Paulo, São Paulo, Brazil*

caroline.wikuats@usp.br

[2]*School of Public Health, University of São Paulo, São Paulo, Brazil*

[3]*National Institute for Public Health and the Environment, Bilthoven, The Netherlands*

[4]*Faculty of Medicine, University of São Paulo, São Paulo, Brazil*

[5]*Amsterdam University Medical Centers, University of Amsterdam, Amsterdam, The Netherlands*

[6]*Institute for Risk Assessment Sciences, Utrecht University, Utrecht, The Netherlands*

Abstract: Particulate matter (PM) presents numerous chemical and physical properties, such as composition, size, and surface area, that may induce several adverse effects on human health. Fine particles (PM2.5) can oxidize target molecules and result in oxidative stress and (systemic) inflammation. The oxidative potential (OP) quantifies particle reactivity that is expected to correlate with biological responses and related adverse health effects induced by exposure to PM. The Metropolitan Area of São Paulo (MASP), Southeastern Brazil, is the fourth largest urban area in the world in terms of population. Little is known about the toxicological properties of PM2.5 from MASP, but it is expected to depend on the chemical composition. Therefore, we evaluated the OP, composition, and emission sources of PM2.5 collected during an extensive sampling campaign (from May 2021 to August 2022) at the Faculty of Medicine of the University of São Paulo (FMUSP), located in an area highly impacted by vehicular emissions. We sampled PM2.5 with a Partisol 2025i Sequential Air Sampler. We analyzed the OP using electron spin resonance (OP-ESR) and dithiothreitol (OP-DTT) assays, while the composition was measured via energy-dispersive X-ray fluorescence (EDXRF). PM2.5 at FMUSP is mainly composed of OC > EC > S > Na > K > Fe > Si > Al > Zn. The primary sources identified with Principal Component Analysis (PCA) were vehicular emissions, resuspension, and biomass burning (factor 1), engine oil burning (factor 2), sea salt (factor 3), vehicle exhaust and non-exhaust (brake and tire wear) emissions (factor 4). These factors explained 46, 16, 11, and 27% of the PCA variance. Our results show that PM collected in April and May of 2022 exhibited the highest monthly mean OP values for ESR (OP-ESRv: 3.6_x10^4 and 3.9_x10^4 a.u. m^{-3}, respectively) and DTT (OP-DTTv: 3.0 and 3.8 nmol min^{-1} m^{-3}), whereas the highest PM2.5 concentrations were recorded in July and August of 2021 (18.4 and 21.1 µg m^{-3}, respectively). Furthermore, there is no characteristic seasonal profile for OP-ESR and OP-DTT, as observed for PM2.5. Regarding the days of the week, Sundays presented lower values for PM2.5 (13.3 µg m^{-3}), OP-ESRv (1.4_x10^4 a.u. m^{-3}), and OP-DTTv (1.6 nmol min^{-1} m^{-3}) compared to Monday through Saturday, attributed to a 70% reduction in vehicle traffic in the region. Applying a Generalized Linear Model (GLM) with gamma distribution showed that different PM2.5 species are significantly correlated (p-value ≤ 0.05) with OP-ESR and OP-DTT, such as OC, EC, Na, Mg, Cl, K, Fe, Cu, Br, Sr, Cd, and Sb. In conclusion, OP is mainly influenced by PM2.5 composition and its emission sources. Moreover, the weak correlation between OP-ESR, OP-DTT, and PM2.5 mass indicates that the oxidative potential assays could be used as alternative metrics in observational studies.

Keywords: Oxidative potential, particulate matter pollution, health effects, chemical characterization, emission sources.

INTRODUCTION

Particulate matter (PM) presents numerous chemical and physical properties, such as composition, size, and surface area, that may induce several adverse effects on human health. Fine particles (PM2.5) can oxidize target molecules and result in oxidative stress and (systemic) inflammation (Borlaza et al., 2018; Gao et al., 2020). The oxidative potential (OP) quantifies particle reactivity that is expected to correlate with biological responses and related adverse health effects induced by exposure to PM (Calas et al., 2018).

The Metropolitan Area of São Paulo (MASP), located in Southeastern Brazil, is the fourth largest urban area in the world in terms of population (United Nations, 2019). While studies in the MASP have focused on the distribution and composition of PM, air quality modeling, associations with meteorological variables, and health effects (Andrade et al., 2012; Nogueira et al., 2020; Vara-Vela et al., 2016), there is limited knowledge about the toxicological properties of PM2.5 from MASP.

To address this gap, we evaluated the OP, chemical composition, and emission sources of PM2.5 collected during an extensive sampling campaign

(from May 2021 to August 2022) at the Faculty of Medicine of the University of São Paulo (FMUSP).

METHODS

We collected daily PM2.5 samples on Teflon filters at FMUSP using a Partisol 2025i Sequential Air Sampler (Figure 1a). OP analysis was performed using electron spin resonance (OP-ESR) and dithiothreitol (OP-DTT) assays with spectrophotometers (Figure 1b, 1c). The composition was determined via energy-dispersive X-ray fluorescence (EDXRF) (Figure 1d). Furthermore, Principal Component Analysis (PCA) was employed to identify the main emission sources.



Figure 1. Partisol 2025i Sequential Air Sampler (a), MiniScope MS400 (b), SpectraMax 190 Microplate Reader (c), and Epsilon 5 Energy-Dispersive X-Ray Fluorescence Analyzer (d).

FINDINGS AND ARGUMENT

PCA results showed four primary emission sources based on the predominance of specific PM2.5 components (Figure 2). Factor 1 indicated influences from vehicular emissions, resuspension, and biomass burning, characterized by BC, Mg, Al, Si, K, Ca, Cr, Mn, Fe, Se, Br, and Rb. Factor 2 is associated with engine oil burning due to the presence of P, S, V, and Ni.

In contrast, Factor 3 is possibly linked to sea salt emissions indicated by Na, Mg, and Cl. Factor 4 is related to vehicle exhaust and non-exhaust (brake and tire wear) emissions, with significant amounts of BC, Cr, Mn, Ni, Cu, Zn, As, and Sb. These factors explained 46, 16, 11, and 27% of the PCA variance, respectively. Therefore, PCA analysis confirms that while other sources may contribute, vehicular traffic is the primary emission source of particles at FMUSP.

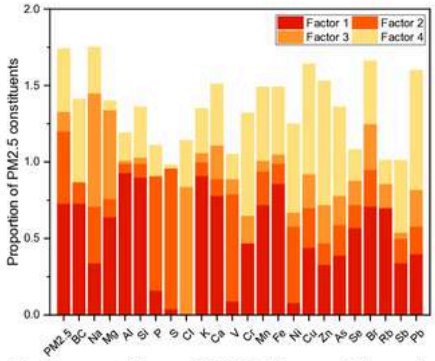


Figure 2. Proportion of PM2.5 constituents to the emission sources (factors) at FMUSP.

PM collected in April and May of 2022 exhibited the highest monthly mean volume-based OP values for ESR (OP-ESRv: $3.6x10^4$ and $3.9x10^4$ a.u. m^{-3}, respectively) (Figure 3a) and DTT (OP-DTTv: 3.0 and 3.8 nmol min^{-1} m^{-3}) (Figure 3c), whereas the highest PM2.5 concentrations were recorded in July and August of 2021 (18.4 and 21.1 µg m^{-3}, respectively) (Figure 3e).

Furthermore, OP-ESR and OP-DTT did not exhibit a characteristic seasonal profile, as was observed for PM2.5, which presented higher values in winter due to reduced precipitation rates and stable atmospheric conditions. Thus, the composition and emission sources of PM2.5, rather than its concentration, significantly influence OP reactions.

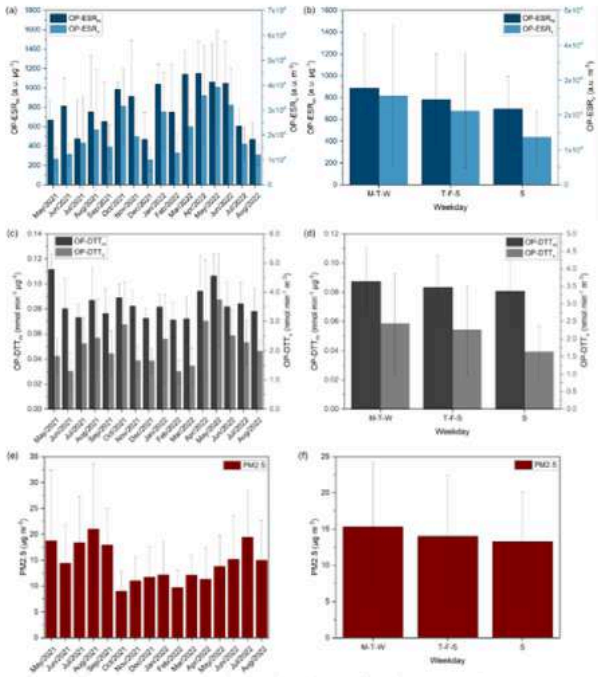


Figure 3. Monthly and day-of-the-week mean values for OP-ESR (a, b), OP-DTT (c, d), and PM2.5 (e, f) at FMUSP. In the OP representation, darker shades indicate results based on mass, while lighter shades represent results based on volume.

Analysis of the days of the week revealed that Sundays had lower values for OP-ESRv ($1.4x10^4$ a.u. m^{-3}) (Figure 3b), OP-DTTv (1.6 nmol min^{-1} m^{-3}) (Figure 3d), and PM2.5 (13.3 µg m^{-3}) (Figure 3f), compared to Monday through Saturday. This reduction is attributed to a 70% decrease in vehicle traffic in the region on Sundays (Wikuats et al., 2023). The reduced emission levels observed on Sundays possibly influence both PM2.5 atmospheric reactions and OP responses. Notably, OP results based on volume exhibited statistically significant differences across the days of the week (p-value ≤ 0.05) according to the Kruskal-Wallis test.

Chemical analysis using EDXRF on Teflon filters indicated that PM2.5 at the sampling site is primarily composed of OC > EC > S > Na > K > Fe > Si > Al > Zn, with daily concentrations ranging from $1.5x10^{-3}$ to 21.2 µg m^{-3}. A Generalized Linear Model (GLM) with gamma distribution showed that different PM2.5 species are significantly correlated (p-value ≤ 0.05) with OP-ESR and OP-DTT, such as OC, EC, Na, Mg, Cl, K, Fe, Cu, Br, Sr, Cd, and Sb (Table 1). This preliminary analysis confirms that PM composition has a greater influence on OP reactions than its mass concentration.

Table 1. Preliminary results from the GLM regression analysis for PM2.5 species and OP results at FMUSP.

PM2.5	OP-ESRm	OP-ESRv	OP-DTTm	OP-DTTv
	p-value			
OC	**$5.00x10^{-7}$**	**$6.10x10^{-6}$**	**0.02**	**0.02**
EC	**$7.00x10^{-4}$**	**0.05**	0.16	0.92
Na	**0.04**	0.40	0.34	0.67
Mg	0.30	0.71	0.24	**0.04**
Cl	0.24	0.07	**$3.40x10^{-3}$**	**$3.6x10^{-3}$**
K	**0.03**	0.09	0.81	0.99
Fe	0.85	0.46	**0.02**	0.71
Cu	**$1.00x10^{-4}$**	**$4.90x10^{-3}$**	0.49	0.84
Br	**0.03**	**0.03**	0.08	0.75
Sr	0.48	0.27	0.59	**0.02**
Cd	**0.05**	0.53	**0.03**	0.94
Sb	**$2.35x10^{-5}$**	**$1.77x10^{-5}$**	**$1.80x10^{-3}$**	**$8.00x10^{-4}$**

Values with statistical significance (p-value ≤ 0.05) are highlighted in blue and bold.

CONCLUSIONS

OP is mainly influenced by PM2.5 chemical composition, which in turn is affected by the contribution of emission sources. PM2.5 mass concentration alone does not fully reflect the variation in PM's intrinsic oxidative potential. Additionally, the weak correlation between OP and PM2.5 mass suggests that oxidative potential assays, specifically OP-ESR and OP-DTT, could serve as alternative metrics in observational studies, as they better reflect chemical composition. This may provide valuable insights into the variation in health impacts due to exposure to PM2.5.

REFERENCES

Andrade, Maria de Fatima, Regina Maura de Miranda, Adalgiza Fornaro, Americo Kerr, Beatriz Oyama, Paulo Afonso de Andre, and Paulo Saldiva. "Vehicle emissions and PM 2.5 mass concentrations in six Brazilian cities." *Air Quality, Atmosphere & Health* 5 (2012): 79-88.

Borlaza, Lucille Joanna S., Enrique Mikhael R. Cosep, Seojong Kim, Kwangyul Lee, Hungsoo Joo, Minhan Park, Daphne Bate, Mylene G. Cayetano, and Kihong Park. "Oxidative potential of fine ambient particles in various environments." *Environmental Pollution* 243 (2018): 1679-1688.

Calas, Aude, Gaëlle Uzu, Frank J. Kelly, Stephan Houdier, Jean MF Martins, Fabrice Thomas, Florian Molton et al. "Comparison between five acellular oxidative potential measurement assays performed with detailed chemistry on PM 10 samples from the city of Chamonix (France)." *Atmospheric Chemistry and Physics* 18, no. 11 (2018): 7863-7875.

Gao, Dong, Krystal J. Godri Pollitt, James A. Mulholland, Armistead G. Russell, and Rodney J. Weber. "Characterization and comparison of PM 2.5 oxidative potential assessed by two acellular assays." *Atmospheric Chemistry and Physics* 20, no. 9 (2020): 5197-5210.

Nations, United. "World urbanization prospects: The 2018 revision. " Department of Economic and Social Affairs, Population Division, United Nations (2019).

Nogueira, Thiago, Prashant Kumar, Adelaide Nardocci, and Maria de Fatima Andrade. "Public health implications of particulate matter inside bus terminals in Sao Paulo, Brazil." *Science of the total environment* 711 (2020): 135064.

Vara-Vela, Angel, Maria F. Andrade, Prashant Kumar, Rita Y. Ynoue, and Angel G. Munoz. "Impact of vehicular emissions on the formation of fine particles in the Sao Paulo Metropolitan Area: a numerical study with the WRF-Chem model." *Atmospheric Chemistry and Physics* 16, no. 2 (2016): 777-797.

Wikuats, Caroline Fernanda Hei, Thiago Nogueira, Rafaela Squizzato, Edmilson Dias de Freitas, and Maria de Fatima Andrade. "Health Risk Assessment of Exposure to Air Pollutants Exceeding the New WHO Air Quality Guidelines (AQGs) in São Paulo, Brazil." *International Journal of Environmental Research and Public Health* 20, no. 9 (2023): 5707.

AIR POLLUTION CONFERENCE BRAZIL
CMAS SOUTH AMERICA
COMMUNITY MODELING AND ANALYSIS SYSTEM

EVALUATING THE OXIDATIVE POTENTIAL OF PM2.5 IN SÃO PAULO, BRAZIL: A COMPARATIVE ANALYSIS BETWEEN DIFFERENT ASSAYS

Caroline F.H. Wikuats[1], Sumit K. Dey[2], Daan L.A.C. Leseman[2], A. John F. Boere[2], Thiago Nogueira[3], Lucia da Conceição Andrade[4], Edmilson Dias de Freitas[1], Alessandra Tammaro[5], Flemming R. Cassee[2,6], Maria de Fatima Andrade[1]

[1]*Institute of Astronomy, Geophysics, and Atmospheric Sciences, University of São Paulo, São Paulo, Brazil*

caroline.wikuats@usp.br

[2]*National Institute for Public Health and the Environment, Bilthoven, The Netherlands*

[3]*School of Public Health, University of São Paulo, São Paulo, Brazil*

[4]*Faculty of Medicine, University of São Paulo, São Paulo, Brazil*

[5]*Amsterdam University Medical Centers, University of Amsterdam, Amsterdam, The Netherlands*

[6]*Institute for Risk Assessment Sciences, Utrecht University, Utrecht, The Netherlands*

Abstract: Characterizing particulate matter (PM) based on its chemical composition, especially the fine PM (PM2.5) that penetrates deeper into the respiratory system, can be an effective procedure to evaluate its impacts on human health and elucidate efficient mitigation and control procedures. While PM2.5 mass concentration has been a conventional metric for correlating exposure levels with health outcomes, it fails to capture the variation in the intrinsic toxic potential of PM, emphasizing the need for alternative assessment methods. The oxidative potential (OP) has gained attention for its ability to evaluate the redox-active organic and metal content and toxic responses of PM2.5, which may vary based on composition, emission sources, and multi-component interactions. In the traditional acellular OP assays, the estimation of OP derives from the consumption of cellular reductant proxies (dithiothreitol – DTT) and the generation and detection of hydroxyl radicals (electron spin resonance – ESR). These assays provide good correlations between the composition of organic and metal species and emission sources of PM2.5. As both tests require a considerable amount of mass, an alternative and robust bioassay developed by Dey et al. (2021) not only consumes less PM but also is close to a biological response, i.e., it simulates other oxidative damage as it is based on lipid peroxidation (LPO). The current study focused on the Metropolitan Area of São Paulo (MASP), South America's most industrialized and developed urban area, where knowledge of the toxicological properties of PM2.5 is still limited. We aimed to assess and compare the results obtained from conventional OP methods (OP^{DTT} and OP^{ESR}) with those from a newly developed, pathologically relevant bioassay designed to quantify the LPO index (OP^{LPO}). We analyzed PM2.5 samples collected at the Faculty of Medicine of the University of São Paulo (FMUSP) from May 2021 to August 2022. Various sources influenced the sampling site, including vehicular emissions, biomass and engine oil burning, soil and road resuspension, and sea salt. Our results indicated that the OP^{LPO} assay is more sensitive in identifying the toxicity of PM2.5 in a dose-dependent manner (100 to 3 μg mL^{-1}), particularly at lower concentrations where the traditional OP methods showed no significant responses. Further analyses will help to elucidate the mechanisms of action of PM2.5 in São Paulo, providing insights for future epidemiological studies and air quality management strategies.

Keywords: Oxidative potential, health outcomes, bioassays, particle toxicity, lipid peroxidation.

INTRODUCTION

Characterizing particulate matter (PM), particularly fine (≤ 2.5 μm) and ultrafine particles (< 100 nm), based on their chemical and toxicological properties, provides valuable insights into their impact on human health. These smaller particles penetrate deeper into the respiratory system, making it crucial to understand their effects for effective mitigation and control procedures (Borlaza et al., 2018). However, the mechanisms of action and toxicity of health effects related to PM2.5 are still poorly understood (Bates et al., 2019; Simonetti et al., 2018).

While PM2.5 mass concentration has been a conventional metric for correlating exposure levels with health outcomes, it fails to capture the variation in the intrinsic toxic potential of PM, emphasizing the need for alternative assessment methods (Dey et al., 2021; Janssen et al., 2014). Oxidative potential (OP) has gained attention for its ability to evaluate the redox-active organic and metal content and toxic responses of PM2.5, which may vary based on composition, emission sources, and multi-component interactions (Bates et al., 2019; Borlaza et al., 2018).

Traditional acellular OP assays estimate OP by measuring the consumption of cellular reductant proxies (dithiothreitol – DTT) and the generation and detection of hydroxyl radicals (electron spin resonance – ESR) (Figure 1a) (Borlaza et al., 2018; Gao et al., 2020a, 2020b). These assays provide good correlations between the composition of organic and metal species and emission sources of PM2.5 (Bates et al., 2019; Borlaza et al., 2018; Janssen et al., 2014).

Given that both tests require a considerable amount of mass, Dey et al. (2021) developed an alternative, robust bioassay that consumes less PM and closely simulates biological responses, particularly oxidative damage, as it is based on lipid peroxidation (LPO) (Figure 1b).

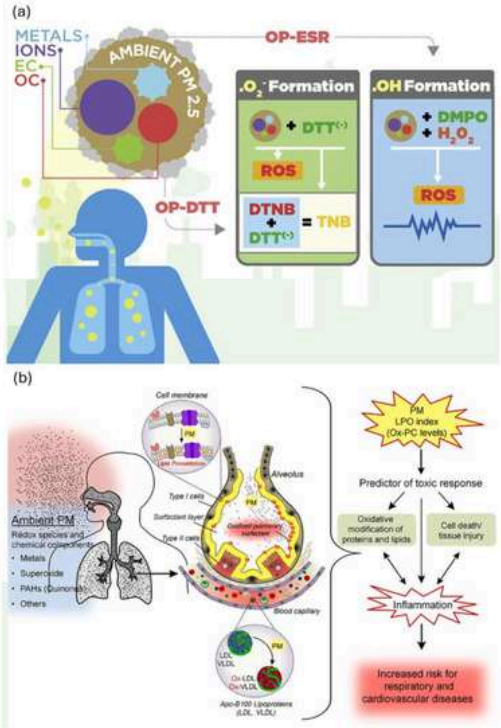


Figure 1. Schematic of the different mechanisms of action for traditional (a) and alternative (b) OP assays. Reference: Modified from Borlaza et al. (2018) and Dey et al. (2021).

The current study focused on the Metropolitan Area of São Paulo (MASP), South America's most industrialized and developed urban area, where knowledge of the toxicological properties of PM2.5 remains limited. Our objective was to assess and compare the results of conventional OP methods with those of a newly developed, pathologically relevant bioassay designed to quantify the LPO index.

METHODS

We analyzed selected PM2.5 samples collected on Teflon filters using a Partisol 2025i Sequential Air Sampler at the Faculty of Medicine of the University of São Paulo (FMUSP) from May 2021 to August 2022. Traditional assays, including dithiothreitol (OP^{DTT}) and electron spin resonance (OP^{ESR}), were used alongside the alternative LPO method (OP^{LPO}) for OP assessment.

DTT reacts with PM2.5 and 5,5'-dithiobis-(2-nitrobenzoic) acid (DTNB), forming 2-nitro-5-thiobenzoic acid (TNB) that is quantified at 412 nm. OP^{DTT} is evaluated as the DTT consumption rate, which is proportional to the concentration of redox-active species. In contrast, OP^{ESR} is quantified based on the first derivative of the ESR signal of the 5,5-dimethyl-1-pyrroline N-oxide and hydroxyl radical (DMPO-OH) quartet as the sum of the total amplitudes (Gao et al., 2020a, 2020b).

For the OP^{LPO} assay, we followed the method by Dey et al. (2021), subjecting captured serum apoB-100 lipoprotein particles to 3-100 μg mL^{-1} of PM solution from the summer and winter seasons. DOFA and Fenton reagent ($FeCl_2$:H_2O_2) were incubated as the positive controls. The data were represented as oxidized phospholipids (Ox-PCs) normalized to the vehicle (serum without PM).

In our analyses, a domestic oil-burning furnace (DOFA) solution was the positive control, while ultrapure water was the negative control.

FINDINGS AND ARGUMENT

Various sources influenced the sampling site, including vehicular emissions, biomass and engine oil burning, soil and road resuspension, and sea salt. However, vehicles were the predominant emission source of PM2.5 at FMUSP, located near roads with heavy traffic and no industrial sources.

Our results indicated that the OP^{LPO} assay is more sensitive in identifying the toxicity of PM2.5 in a dose-dependent manner (100 to 3 μg mL^{-1}) (Figure 2), particularly at lower concentrations where the traditional OP methods showed no significant responses. Winter samples exhibited up to 35 times higher responses than the serum vehicle (Figure 2c, 2d). Winter values differed significantly from summer values for all concentrations tested based on the Mann-Whitney U test (p-value ≤ 0.05).

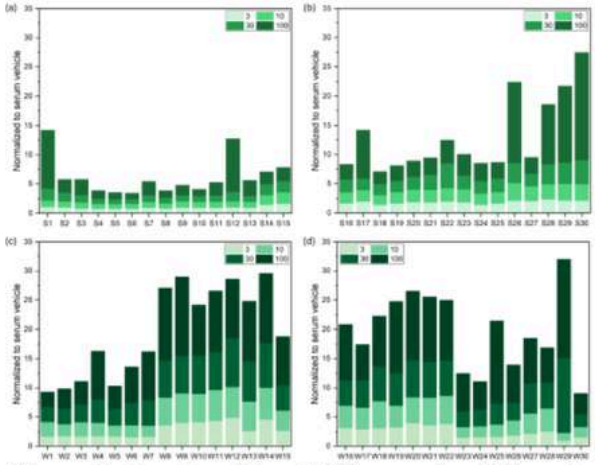


Figure 2. Results of the OP^{LPO} assay for different concentrations (3, 10, 30, and 100 μg mL^{-1}) for summer (a, b) and winter (c, d) samples at FMUSP.

Despite using different PM2.5 concentrations in each method (100 μg mL^{-1} for OP^{LPO}, 500 μg mL^{-1} for OP^{DTT}, and 1000 μg mL^{-1} for OP^{ESR}), the OP^{LPO} assay showed significantly higher values for winter samples (p-value ≤ 0.05), particularly those associated with biomass burning (Figure 3). This finding suggests a response possibly driven more by organic compounds than metals. There was no statistical difference between summer and winter results for OP^{DTT} and OP^{ESR}.

The biomass-burning samples were collected at FMUSP during a massive wildfire at Juquery State Park in the MASP in August 2021. OP^{DTT} results were also elevated during this period, while OP^{ESR} values decreased (samples W8 to W16 in Figure 3b). Our ongoing investigation aims to explore further the relationship between specific OP responses and PM2.5 composition and sources through regression analysis.

While the traditional OP^{DTT} and OP^{ESR} methods focus on ROS generation and radical species, OP^{LPO} provides complementary information by assessing oxidative damage to lipids. This evaluation is directly linked to cellular membrane integrity, making it a technique of high physiological relevance. However, it remains to be established if this novel metric indeed predicts toxicity and health effects.

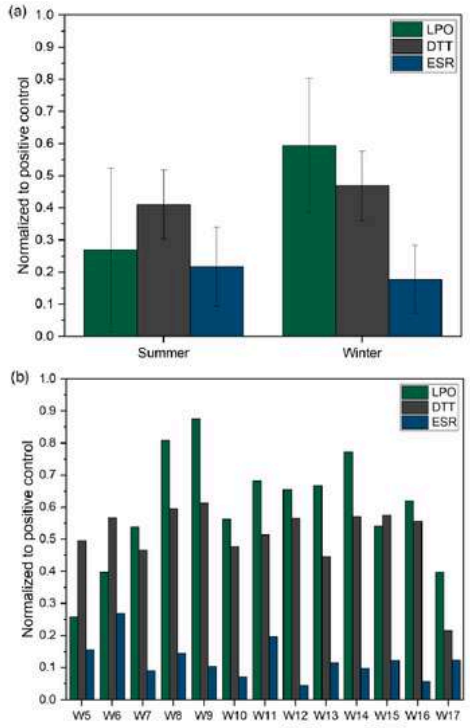


Figure 3. Mean values for OP^{LPO}, OP^{DTT}, and OP^{ESR} assays normalized to the positive control for summer and winter (a) and a biomass burning period (b) at FMUSP.

CONCLUSIONS

The sensitivity of the OP^{LPO} assay highlights its potential as an effective tool for assessing PM2.5 toxicity and guiding public health interventions in urban areas. Integrating results from OP^{LPO} and traditional methods (OP^{DTT} and OP^{ESR}) can offer a more comprehensive understanding of PM's oxidative potential and associated health risks. These findings contribute to elucidating the mechanisms of action of PM2.5 in São Paulo, providing insights for future epidemiological studies and air quality management strategies.

REFERENCES

Bates, Josephine T., Ting Fang, Vishal Verma, Linghan Zeng, Rodney J. Weber, Paige E. Tolbert, Joseph Y. Abrams et al. "Review of acellular assays of ambient particulate matter oxidative potential: methods and relationships with composition, sources, and health effects." *Environmental Science & Technology* 53, no. 8 (2019): 4003-4019.

Borlaza, Lucille Joanna S., Enrique Mikhael R. Cosep, Seojong Kim, Kwangyul Lee, Hungsoo Joo, Minhan Park, Daphne Bate, Mylene G. Cayetano, and Kihong Park. "Oxidative potential of fine ambient particles in various environments." *Environmental Pollution* 243 (2018): 1679-1688.

Dey, Sumit K., et al. "Lipid peroxidation index of particulate matter: Novel metric for quantifying intrinsic oxidative potential and predicting toxic responses." *Redox Biology* 48 (2021): 102189.

Gao, Dong, Krystal J. Godri Pollitt, James A. Mulholland, Armistead G. Russell, and Rodney J. Weber. "Characterization and comparison of PM 2.5 oxidative potential assessed by two acellular assays." *Atmospheric Chemistry and Physics* 20, no. 9 (2020a): 5197-5210.

Gao, Dong, Susannah Ripley, Scott Weichenthal, and Krystal J. Godri Pollitt. "Ambient particulate matter oxidative potential: Chemical determinants, associated health effects, and strategies for risk management." *Free Radical Biology and Medicine* 151 (2020b): 7-25.

Janssen, Nicole AH, Aileen Yang, Maciej Strak, Maaike Steenhof, Bryan Hellack, Miriam E. Gerlofs-Nijland, Thomas Kuhlbusch et al. "Oxidative potential of particulate matter collected at sites with different source characteristics." *Science of the Total Environment* 472 (2014): 572-581.

Simonetti, Giulia, Elena Conte, Cinzia Perrino, and Silvia Canepari. "Oxidative potential of size-segregated PM in an urban and an industrial area of Italy." *Atmospheric Environment* 187 (2018): 292-300.

AIR POLLUTION CONFERENCE BRAZIL
CMAS SOUTH AMERICA
COMMUNITY MODELING AND ANALYSIS SYSTEM

ANALYSIS OF FINE PARTICULATE MATTER ($PM_{2.5}$) IN SAO PAULO CITY

Vitoria Rodilha Leão[1], Maria de Fatima Andrade[1], Dayane da Fonseca[2], José Vinicius Martins[3], Thiago Nogueira[2],

[1]*Instituto de Astronomia, Geofísica e Ciências Atmosféricas*

[2]*Faculdade de Saúde Pública*

[3]*Instituto de Geociências*

Universidade de Sao Paulo, Sao Paulo, Brazil

E-mail: vitorialeao.iag@usp.br

Abstract: This work aims to characterize the chemical composition of $PM_{2.5}$, using Inductively Coupled Plasma Mass Spectrometry (ICP-MS), apportioning its sources and relation with the atmospheric conditions in the Metropolitan Area of Sao Paulo. $PM_{2.5}$ samples were collected in the *Faculdade de Saúde Pública* (FSP; School of Public Health) from the University of Sao Paulo, a region next to avenues and natural parks, with a large fleet of light and heavy-duty vehicles, from 2022 to 2023. After sampling, element concentrations were determined with ICP-MS, and source apportionment was performed using Principal Component Analysis (PCA) and Positive Matrix Factorization (PMF) model. There were higher $PM_{2.5}$ concentrations during winter when temperature and total rainfall were lower; the concentrations decreased in summer, along with an increase in temperatures and total rainfall. The mean concentration of $PM_{2.5}$ surpassed the annual air quality standard and the WMO guidelines. Strong correlations between resuspension-related compounds and vehicular-emitted compounds were found. The PCA as well as PMF results, suggested the following sources: heavy-duty and light-duty vehicles explaining most of PM2.5 mass;, road dust resuspension and civil construction. Meteorological seasonal conditions explain the variations of $PM_{2.5}$ coordinate with the expected function of meteorological conditions. The main sources of $PM_{2.5}$ in the region of FSP are heavy-duty and light-duty vehicles, and road dust resuspension and civil construction. These new sources evaluated through receptor models for recent years made available the evolution of the vehicular sources in Sao Paulo.

Keywords: $PM_{2.5}$, ICP-MS, PCA, PMF, Sao Paulo.

INTRODUCTION

Particulate matter (PM) pollution is the most pressing issue in air quality regulation worldwide (Fuzzi et al., 2015). Atmospheric aerosols have local and global effects, affecting the life cycle and albedo of clouds, precipitation, and lightning, degrading air quality, and impacting Earth energy budget. Aerosols have optical effects as well, impacting visibility (Zhang et al., 2015).

Fine particulate matter ($PM_{2.5}$) is the fraction of aerosols that have aerodynamic diameters below 2.5 μm (Colbeck & Lazaridis, 2014). In the Metropolitan Area of Sao Paulo (MASP), vehicle exhaust heavily contributes to $PM_{2.5}$, emitting Cu, Pb, Zn, and oxygenated polycyclic aromatic hydrocarbons (Oxi-PAHs). Other sources of $PM_{2.5}$ in MASP are resuspension of road dust, with high levels of Al, and brake wear, related to Sb, Zn, and Ba (Pereira, Kamigauti et al., 2023; Pereira, Nogueira et al., 2023). $PM_{2.5}$ is also heavily impacted by remote sources, such as biomass combustion from the Amazon Forest and Pantanal or within the state of Sao Paulo, and wood burning in restaurants, bakeries, and residences (Kumar et al., 2016; Martins Pereira et al., 2017; Souto-Oliveira et al., 2023).

Considering that PM concentrations change according to human behavior and atmospheric conditions, this work aims to create an updated study of the sources of $PM_{2.5}$, characterizing its composition using Inductively Coupled Plasma Mass Spectrometry (ICP-MS), and apportioning its sources and relation with the atmospheric conditions in the Metropolitan Area of Sao Paulo.

METHODS

Samples were collected in the *Faculdade de Saúde Pública* (FSP; School of Public Health; 23°33'S, 46°40'W) from the University of Sao Paulo from 2022 to 2023. Samples were digested in a microwave oven and element concentrations were obtained with Inductively Coupled Plasma Mass Spectrometry (ICP-MS). The procedure is described in Pereira, Nogueira et al. (2023).

The source apportionment was performed through Enrichment Factor (EF; Nishida, 2017) and Principal Component Analysis (PCA; Hetem, 2014) calculations, and application of the Positive Matrix Factorization (PMF; de Miranda et al., 2018) model.

RESULTS

Time series of $PM_{2.5}$ concentration is presented in Figure 1 with the total precipitation and temperature. There were higher concentrations during the winter of the Southern Hemisphere when the temperatures and total precipitation were lower. For the summer, concentrations were pointedly lower, along with an increase in temperatures and total precipitation. The mean was approximately 19.09 μg/m³, overtaking the

annual air quality standard and the annual guideline WMO value.

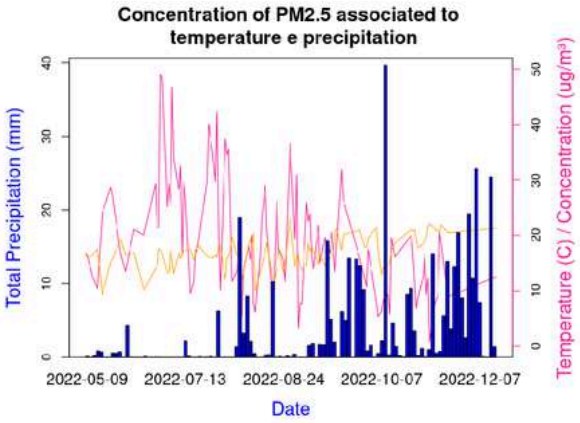


Figure 1. Time series of $PM_{2.5}$ concentrations (pink line) measured in FSP from 05/09/2022 to 01/11/2023 with temperature (orange line) and total precipitation (blue line) time series from ERA5 model from ECMWF.

The EF results are shown in Table 1. Only Cr, Cu, Pb, Zn, and Na were associated with anthropogenic sources, related to vehicular emissions such as fuel and lubricant oil combustion, and brake wear (Pereira, Kamigauti, et al., 2023).

The PCA was run for 5 components. The first showed a mixed source of road dust resuspension, diesel, and biomass combustion (Artaxo et al., 1994; de Miranda et al., 2018; Pereira, Kamigauti, et al., 2023). The second factor showed also road dust resuspension and civil construction (Wang et al., 2006). The third concerned a vehicular source, in special brake wear, exhaustion, and lubricant oil from heavy-duty vehicles (Pereira, Kamigauti, et al., 2023). The fourth factor was possibly an oil combustion source from generators in the region (Nishida, 2017). The last indicated a vehicle-emitted source, from light-duty vehicles (Pereira, Nogueira, et al., 2023). The highest fractions of $PM_{2.5}$ were in the factors associated with resuspension, biomass combustion, and vehicle sources.

The PMF was also run for 5 factors. The first was characteristic of vehicular sources, such as gasohol exhaust, brake wear, and lubricant oil (Pereira, Kamigauti, et al., 2023). The second component was a light-duty vehicle source, from gasoline and diesel exhaust, and brakes and tire wear (Pereira, Kamigauti, et al., 2023). The third factor indicated a road dust resuspension and civil construction source. The fourth was also a road dust resuspension source, in addition to a diesel-powered vehicle source (de Miranda et al., 2018; Pereira, Kamigauti, et al., 2023). The last presented a heavy-duty vehicle source. The contribution of the $PM_{2.5}$ sources is shown in Figure 2. The main source was vehicular, with major contributions of factors 2 (32.4%), light-duty vehicles, and 4 (31.6%), heavy-duty vehicles.

Table 1. Emission Factor (EF) results for median concentrations of elements in $PM_{2.5}$.

Element	EF	Classification
Al	1.00	Natural
Fe	0.95	Natural
Mn	1.29	Natural
Cr	16.97	Anthropogenic
Cu	95.82	Anthropogenic
Ni	6.52	Natural
Zn	209.19	Anthropogenic
Pb	120.08	Anthropogenic
Na	26.22	Anthropogenic
Ca	0.69	Natural
K	2.39	Natural
Mg	4.44	Natural
Ti	0.38	Natural

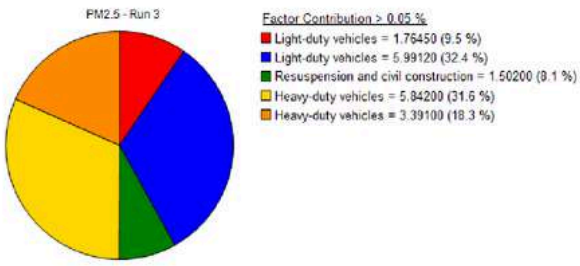


Figure 2. Contributions of sources to $PM_{2.5}$ from the PMF model.

CONCLUSIONS

There were higher concentrations of $PM_{2.5}$ during the winter months in the southern hemisphere, while temperatures and total precipitation were lower; on the other hand, the concentrations decreased in summer while temperatures and total precipitation increased. PCA results indicated the main sources of $PM_{2.5}$ to be light and heavy-duty vehicles, local, and road dust resuspension and civil construction, in this order. The PMF denoted light and heavy-duty vehicle sources, and a road dust resuspension and civil construction source. That way, seasonal changes in $PM_{2.5}$ concentrations occurred according to the expected function of meteorological conditions. The main source of $PM_{2.5}$ in FSP is vehicular, followed by a smaller contribution of road dust resuspension and civil construction.

REFERENCES

Artaxo, P. et al. "Fine mode aerosol composition at three long-term atmospheric monitoring sites in the Amazon Basin." *Journal of Geophysical Research*, 99(D11) (1994).

Colbeck, I., & Lazaridis, M. *Aerosol Science: Technology and Applications*. New Jersey: Wiley, 2014.

de Miranda, R. M. et al. "Source apportionment of fine particulate matter by positive matrix factorization in the metropolitan area of São Paulo, Brazil". *Journal of Cleaner Production*, 202 (2018): 253–263.

Fuzzi, S. et al. "Particulate matter, air quality and climate: Lessons learned and future needs." *Atmospheric Chemistry and Physics*, 15(14) (2015): 8217–8299.

Hetem, I. "Quantificação da contribuição veicular para as concentrações atmosféricas de material particulado fino e black carbon em São Paulo." (2014).

Kumar, P. et al. "New directions: From biofuels to wood stoves: The modern and ancient air quality challenges in the megacity of São Paulo." *Atmospheric Environment*, 140 (2016): 364–369.

Martins Pereira, G. et al. "Particulate pollutants in the Brazilian city of São Paulo: 1-year investigation for the chemical composition and source apportionment." *Atmospheric Chemistry and Physics* (2017): 11943–11969.

Nishida, R. B. "Análise Do Material Particulado Emitido Na Cidade De Ponta Grossa." *Atmospheric Environment*, 53(1) (2017): 1–5.

Pereira, G. M. et al. "Emission factors for a biofuel impacted fleet in South America's largest metropolitan area." *Environmental Pollution*, 331 (2023).

Pereira, G. M. et al. "Particulate matter fingerprints in biofuel impacted tunnels in South America's largest metropolitan area." *Science of the Total Environment*, 856 (2023).

Souto-Oliveira, et al. "Impact of extreme wildfires from the Brazilian Forests and sugarcane burning on the air quality of the biggest megacity on South America." *Science of the Total Environment*, 888 (2023).

Zhang, R. et al. "Formation of Urban Fine Particulate Matter." *Chemical Reviews*, 115(10) (2015): 3803–3855.

AIR POLLUTION CONFERENCE BRAZIL
CMAS SOUTH AMERICA
COMMUNITY MODELING AND ANALYSIS SYSTEM

ASSESSMENT OF MERCURY CONTENT IN ATMOSPHERIC PARTICULATE MATTER NEAR A COAL-FIRED POWER PLANT IN FIGUEIRA, SOUTHERN BRAZIL

Bianca Dutra de Lima[1], Rita de Cássia Marques Alves[2], Fernanda Pereira Machado[3], Leandro Kolling[4], Morgana Bazzan Dessuy[5], Bruna Lüdtke Paim[6]

[1]*Centro de Pesquisas em Sensoriamento Remoto e Meteorologia,Universidade Federal do Rio Grande do Sul*
bianca_duli@hotmail.com
[2]*Instituto de Geociências, Universidade Federal do Rio Grande do Sul*
rita.cma@terra.com.br
[3]*Instituto de Química,Universidade Federal do Rio Grande do Sul*
fernandamachado2701@gmail.com
[4]*Instituto de Química,Universidade Federal do Rio Grande do Sul*
mrleandrors@gmail.com
[5]*Instituto de Química,Universidade Federal do Rio Grande do Sul*
mbdessuy@ufrgs.br
[6]*Centro de Pesquisas em Sensoriamento Remoto e Meteorologia,Universidade Federal do Rio Grande do Sul*
bruhpaim20@gmail.com

Abstract: Particulate matter (PM) stands out as a pollutant capable of affecting various physical-chemical cycles in the atmosphere and posing significant risks to human health. It is known that the production of energy through the burning of fossil fuels, such as coal and diesel oil, is responsible for producing increased emissions of PM over short periods of time. This burning process can contribute to the increase of heavy metals, such as mercury (Hg), in the atmosphere. The south of Brazil is the region with the largest stockpiles of mineral coal, consequently, the number of thermal power plants is higher than in the rest of the country. The aim of this study was to determine the mercury content in atmospheric PM ($PM_{2.5}$ and PM_{10}) collected near a coal-fired power station in Figueira, located in the south of Brazil. The sampling sites were determined based on wind direction, population density and mine location (site 01: at a hotel next to the thermal power plant; site 02: near the center of the municipality; and site 03: inside the coal mine). The sampling campaigns were carried out in summer (February/2023) and winter (September/2023). Low-volume dichotomous stacked filter unit (SFU) samplers were used. Collections were performed for 24-hour periods using PTFE membrane filters with pore sizes of 1 µm and 10 µm for $PM_{2.5}$ and PM_{10}, respectively. Particulate matter concentrations were measured by gravimetric analysis. For total mercury determination, 2/4 of each filter was analyzed directly by atomic absorption spectrometry using a Direct Mercury Analyzer (model DMA-80, Milestone, Italy). The results showed that particulate matter concentrations were higher in the winter period ($PM_{2.5max}$ = 13.77 µg/m³; PM_{10max} = 110.38 µg/m³) compared to the summer ($PM_{2.5max}$ = 4.35 µg/m³; PM_{10max} = 97.21 µg/m³), with peaks occurring mainly in downtown and at the mine. The presence of mercury was detected in $PM_{2.5}$ samples at the three studied sites, in both periods (<39.33 pg/m³ Hg), and in PM_{10} samples from the mine (collected during the summer) and at the hotel, downtown and mine collected in the winter (<108.63 pg/m³ Hg).

Keywords: Air pollution, coal, mercury, PM.

INTRODUCTION

Air pollution is one of the most challenging environmental and public health issues of our time. With the growth of industrialization, along with population density in urban areas, there has been a significant increase in demand for energy and transport and, consequently, higher levels of gas and particle emissions generated by these processes. Mercury (Hg) is a metal with a residence time of 0.5 to 2 years that is toxic to human health and the environment. It exists in the air predominantly in the gaseous elemental phase (GEM, around 95% of its concentration) but is also present in the gaseous oxidized phase (RGM, called the reactive phase) and in the particulate phase (PHg). PHg and RGM together make up 5% of total atmospheric Hg (Siudek et al., 2016). Both RGM and PHg are more water-soluble and less volatile, which means that their vertical distributions in the lower atmosphere are limited to emission areas due to rapid removal through dry and wet deposition. Thus, considering the system formed by atmospheric emission, transformation, transportation and deposition, RGM and PHg end up contributing more directly to the pollution process even though they are less abundant than GEM (Schroeder and Munthe, 1998).

AIR POLLUTION CONFERENCE BRAZIL
CMAS SOUTH AMERICA
COMMUNITY MODELING AND ANALYSIS SYSTEM

The increase in atmospheric Hg emissions caused by anthropogenic activities compared to natural levels is estimated at 450% (Yang et al., 2020), with coal combustion being one of the main sources, accounting for around 22% of emissions, according to the latest Global Mercury Assessment carried out by the United Nations Environment Programme (UNEP). In Brazil, in 2018 approximately 1.97 tons of mercury were emitted by thermal power plants. In view of this, and considering that the southern region has the largest coal stocks in the country, the aim of this study was to determine the Hg content in particulate matter (PM_{10} and $PM_{2.5}$) collected near a coal-fired thermal power station in Figueira, Paraná.

METHODS

Sampling

The three sampling sites were determined based on wind direction, population density and mine location: Site 01- at a hotel next to the thermal power plant, Site 02- near the center of the municipality, and Site 03- inside the coal mine. PM samples were collected in summer (February 2023) and winter (September 2023), in campaigns lasting one week each with low-volume dichotomous stacked filter unit (SFU) samplers, that consist of sets of two sequential filters connected to vacuum pumps with a flow rate of 18 L min^{-1}. Collections were carried out over 24-hour periods, using 47 mm diameter PTFE membrane filters with pore sizes of 1 µm and 10 µm for $PM_{2.5}$ and PM_{10}, respectively. Before campaigns, PTFE filters were heated at 110 °C for 3 h, in an oven, to remove any deposited compounds. Before and after the samplings, the filters were conditioned in a desiccator for at least 24 hours in order to obtain a constant weight for gravimetric analysis.

Analysis

Particulate matter concentrations were determined by gravimetric analysis. The volume values were corrected for the standard conditions of air temperature and atmospheric pressure in accordance with Method IO-2.4 - EPA/625/R-96/010a. For total mercury determination, 2/4 of each filter were analyzed directly by atomic absorption spectrometry using a Direct Mercury Analyzer (DMA-80 model, Milestone, Italy), without any prior preparation. The certified reference material (CRM) BCR 176R was used for the calibration curve and to check the accuracy of the DMA method, and the NIST 695 was used for its validation. Limits of detection (LOD) and quantification (LOQ) were calculated using the sample standard deviation of 10 blank measurements and the angular coefficient of the calibration curve (sensitivity).

FINDINGS AND ARGUMENT

Table 1 shows the concentrations of particulate matter collected in Figueira in the summer and winter of 2023.

Table1. Summary of PM concentrations (µg/m³)

Seasons		$PM_{2.5}$	PM_{10}
Summer	Mean ±	**1,19**	**27,70**
	Min	0,37	2,08
	Max	4,35	97,21
Winter	Mean ±	**3,47**	**37,28**
	Min	0,24	5,11
	Max	13,77	110,38

As expected, higher concentrations of particulate matter were recorded in the colder period, probably favored by the low temperatures that enhance atmospheric stability (Young et al., 2012). During the summer, $PM_{2.5}$ concentrations showed great variation between sites, while PM_{10} concentrations followed a pattern, being significantly higher in the coal mine and lower in the hotel. On the other hand, for samples from winter, two patterns were observed: $PM_{2.5}$ concentrations were ordered as: downtown > mine > hotel, indicating a notable increase in finer particles in the central area of the city, and PM_{10} concentrations repeated the same behavior as previously seen: mine > downtown > hotel. The results of the analysis of mercury in the summer samples are displayed in figures 1 and 2.

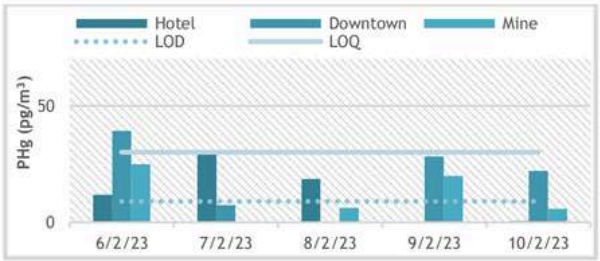


Figure 1. PHg in $PM_{2.5}$ - Summer



Figure 2. PHg in PM_{10} - Summer

The mercury averaged concentration in samples from summer was 10.01 pg/m³ for $PM_{2.5}$ and 19.37 pg/m³ for PM_{10}, both above the detection limits ($LOD_{PM2.5}$ = 9.03 pg/m³; LOD_{PM10} = 19.32 pg/m³) but below the quantification limits ($LOQ_{PM2.5}$ = 30.11

pg/m³; LOQ_{PM10} = 64.38 pg/m³). Within this period, Hg was detected at least once in $PM_{2.5}$ at all the sites monitored and in PM_{10} only at the coal mine. The maximum concentration quantified in summer was 39.33 pg/m³ in $PM_{2.5}$ in downtown. This value is comparable to that reported by studies on $PM_{2.5}$ in urban areas, such as those by Liu et al. (2007) in the United States (20.80 pg/m³), but around 10 times lower than that recorded by Gao et al. (2016) in $PM_{2.5}$ near a thermal power plant in China (309.50 pg/m³). The results for the winter samples are presented below, in figures 3 and 4.



Figure 3. PHg in $PM_{2.5}$ - Winter

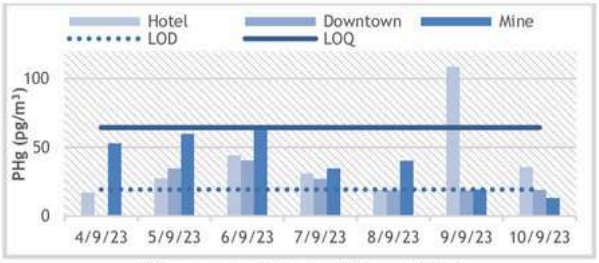


Figure 4. PHg in PM_{10} - Winter

During the winter, the average concentration of mercury identified in $PM_{2.5}$ was 10.42 pg/m³, very similar to the summer, but its presence was less frequent, rising above the LOD on only four of the seven days. The maximum concentration of Hg recorded in $PM_{2.5}$ was 29.29 pg/m³ in downtown. The average amount of mercury found in PM_{10} samples during the winter (31.61 pg/m³) followed the increase in particulate matter concentrations and was considerably higher than in the summer.The highest concentration of mercury quantified in PM_{10} was 108.63 pg/m³ at the hotel, which was also the highest in the entire study. This value is very similar to that identified by Pyta et al. (2009) in $PM_{2.5}$ samples from an urban area in Poland (100.40 pg/m³) but still much lower than the 387.50 pg/m³ of mercury found by Gao et al. (2016) in PM_{10} near a Chinese thermal power plant. The mean recovery from the DMA-80 analysis was of 109%.

CONCLUSIONS

The mercury content in particulate matter (PM) shows that there is Hg associated with PM, even though in lower concentrations than those reported by other authors in similar areas. Both the concentration of particulate matter and the mercury content are quite variable and possibly influenced by factors that need to be examined in more detail, such as meteorological and environmental conditions and the presence of external sources other than those of interest. In addition, in order to provide a more comprehensive understanding of the presence of mercury in the region's thermoelectric process, the Hg content in the coal mined in the region, in the ash produced and in the wet deposition (precipitation) should also be analyzed.

REFERENCES

Gao, J., Wang, H., Caı, W., Wu, J.; He, Y. "Pollution characteristics of atmospheric particulate mercury near a coal-fired power plant on the southeast coast of China". Atmospheric Pollution Research 7 (2016):1119-1127. Accessed March 29, 2024. 10.1016/j.apr.2016.07.003

Lıu, Bian, Keeler, Gerald J., Dvonch, J.T., Barres, James A., Lynam, Mary M., Marsık, Frank J., Morgan, Joy T. ''Temporal variability of mercury speciation in urban air''. Atmospheric Environment 41 (2007): 1911-1923. Accessed March 28, 2024. 10.1016/j.atmosenv.2006.10.063

Pyta, H., Rosık-Dulewska, C., Czaplicka, M. ''Speciation of ambient mercury in the upper silesia region, Poland''. Water Air Soil & Pollution 197 (2009): 233-240. Accessed March 27, 2024. 10.1007/s11270-008-9806-9 & M.

Schroeder, William H., Munthe, John. ''Atmospheric mercury—An overview.'' Atmospheric Environment 32 (1998): 809-22. Accessed March 30, 2024. doi: 10.1016/S1352-2310(97)00293-8.

Siudek, Patrycja.,Kurzyca, Iwona.,Sıepak, Jerzy. ''Atmospheric deposition of mercury in central Poland: Sources and seasonal trends.'' Atmospheric Research 170 (2016): 14-22. Accessed March 27, 2024. doi:10.1016/j.atmosres.2015.11.004.

United Nations Environment Programme(UNEP). ''Global Mercury Assessment 2018''. UNEP Chemical Branch, Geneva, Switzerland. 2019. Accessed March 27, 2024.

Yang, Yingju., Liu,Jing., Wang, Zhen. ''Reaction mechanisms and chemical kinetics of mercury transformation during coal combustion''. Progress in Energy and Combustion Science 79 (2020): 100844. Accessed March 30, 2024. doi:10.1016/j.pecs.2020.100844

Young, Li-Hao., Wang, Yi-Ting., Hsu, Hung-Chieh., Lin, Ching-Hui., Liou, Yi-Jyun., Lai, Ying-Chung., Lin, Yun-Hua., Chang, Wei-Lun., Chiang, Hung-Lung., Cheng, Man-Ting. ''Spatiotemporal variability of submicrometer particle number size distributions in an air quality management district''. Science of The Total Environment 425 (2012): 135-145. Accessed March 30, 2024. doi:10.1016/j.scitotenv.2012.02.063

AIR POLLUTION CONFERENCE BRAZIL
CMAS SOUTH AMERICA
COMMUNITY MODELING AND ANALYSIS SYSTEM

CARCİNOGENİCİTY OF PESTİCİDES AND $PM_{2.5}$ COLLECTED İN BRAZİLİAN CİTİES. EVALUATİON USİNG CELLS BEAS-2B AND SOFT AGAR COLONY FORMATİON ASSAY

Aleinnys Marys Barredo Yera[1], Pérola de Castro Vasconcellos[1] and Ana Paula de Melo Loureiro[2]

[1]Institute of Chemistry, University of São Paulo, Brazil
[2] School of Pharmaceutical Sciences, University of São Paulo, Brazil
aleinnysb@usp.br

Abstract: Since 2008, Brazil has become one of the largest consumers of pesticides in the world. Many of these compounds have already been banned in several countries due to the negative effects they have on human health. Studies show that pesticides have a broad relationship with the increase in cases of diseases that mostly involve the nervous system and cancer. Soft Agar Colony Formation Assay is a test used to determine the carcinogenicity of a compound. It is based on the hypothesis that healthy cells cannot grow off a solid surface, but modified cells (malignant transformations) will have this ability and form colonies. To study the cytotoxicity and carcinogenicity of $PM_{2.5}$ collected in cities in the state of São Paulo (São Paulo, Piracicaba, and Capuava), human lung cells (BEAS-2B) were separately exposed for 7 days to both $PM_{2.5}$ collected at these sites, and different pesticide patterns that were found in representative concentrations in the samples. For this, the violet crystal assay and Solft Agar were used. The $PM_{2.5}$ samples collected at all sampling sites with concentrations (C_1 = 5 µg/m^3, C_2 = 25 µg/m^3, and C_3 = 50 µg/m^3) showed cytotoxicity from 72h of exposure. Piracicaba was the site with the highest cytotoxicity, followed by Capuava and São Paulo. In the case of pesticides (C_1=300 pg/m^3 and C_2=3000 pg/m^3), during the first 4 days of exposure no significant differences were found between pesticides and control. From the 5th day on, different behaviors were observed, but further studies are needed to understand the cytotoxicity of these compounds. Based on the hypothesis that more carcinogenic compounds can form more colonies in the soft agar, the results show the tumorigenic effect of $PM_{2.5}$ (C=5 µg/m^3), with Piracicaba again being the site with the greatest effects. In the case of pesticides, only Atrazine (ATRA) and the substance containing a mixture of 25 pesticides (MIXG) showed tumorigenic effects for both concentrations, this effect was smaller than that found for $PM_{2.5}$. Statistically, there are no significant differences between the results for exposure to ATRA and MIXG. This indicates that the tumorigenic effect found in MIXG may be influenced by the presence of ATRA. To date, no references have been found to similar studies carried out on samples of particulate matter collected at sites in the state of São Paulo, nor on the pesticides of interest, thus having great relevance to the results found in this research.

Keywords: **Particulate matter, Pesticide inhalation, Cytotoxicity, Carcinogenicity, Soft agar**

INTRODUCTION

Since 2008, Brazil has become the largest consumer of pesticides in the world (Bombardi, Larissa, 2017). However, of the 50 most consumed active ingredients in the country, 22 have been banned in Europe and North America (Carneiro & Lia Giraldo da Silva Augusto, Raquel Maria Rigotto, 2018). The state of São Paulo is the second largest consumer of pesticides in Brazil, using approximately 110,000 tons in 2016 (Bombardi, Larissa, 2017).

Many of these compounds have already been banned in several countries due to their negative impact on human health. Studies have shown that pesticides are closely related to the increase in cases of diseases that mostly involve the nervous system, with Hodgkin's Disease, Parkinson's Disease, and Alzheimer's being the most related (Mostafalou & Abdollahi, 2013). Other studies also include these pesticides in the list of endocrine-disrupting chemical compounds (EDCs)(Patisaul et al., 2018).

Soft Agar test is used to determine the carcinogenicity of a compound. It is based on the hypothesis that healthy cells cannot grow outside of a solid surface, but modified cells (malignant transformations) will have this ability (Borowicz et al., 2014). This test is done on a viscous cellular medium. After a certain time of exposure, the growth of cells is observed, which indicates that the compound has modified them, and this mutation is the beginning of the development of cancer.

To assess the cytotoxicity and carcinogenicity of $PM_{2.5}$ collected at sites in cities in the state of São Paulo (São Paulo, Piracicaba, and Capuava), human lung cells (BEAS-2B) were exposed to $PM_{2.5}$ collected at these sites, and to different pesticide patterns found in representative concentrations in the samples. For this, the violet crystal test and the Soft Agar test were used.

METHODS

Site characterization and sampling

Piracicaba (PRB) is an urban-agricultural city located 300 km from São Paulo, with over 150,000 ha of sugarcane and orange crops (IBGE, 2018). During the dry season in July 2018, $PM_{2.5}$ (particles with a diameter equal or smaller than 2.5 micrometers) were collected, and the total number of samples was 16.

The second location chosen was São Paulo (SPA), the capital of the state of São Paulo, and the largest city in Brazil. $PM_{2.5}$ samples (n = 15) were collected in July 2018, simultaneously with the PRB samples.

The third location was Capuava (CAP), a large urban area with an industrial complex of high economic importance, with nearly 80,000 people living in around 14 chemical industries (Zaccarelli-Marino et al., 2016). $PM_{2.5}$ samples (n = 17) were collected between July and August 2018.

Culture of BEAS-2B cells
The BEAS-2B strain was provided by Prof. Fekadu Kassie (Masonic Cancer Center, University of Minnesota, Minneapolis, United States). Cultures are maintained in BEGM (Bronchial Epithelial Growth Medium®) medium, supplemented with the kit's set of cofactors (bovine pituitary extract, insulin, hydrocortisone, hEGF, epinephrine, transferrin, retinoic acid, triiodothyronine, gentamicin, and amphotericin). The cells are kept in bottles and incubated at 37°C in an atmosphere containing 5% CO_2.

Exposure of cells to pesticides and $PM_{2.5}$
The cells were plated at a density of 2 x 10^4/well in 96-well plates. After the cell adhesion period (1 day), pesticide exposures (1.5 x 10^{-4} pg/µL and 1.5 x 10^{-3} pg/µL) were performed. For the case of exposure to $PM_{2.5}$ the concentrations were 2.5 pg/µL, 12.5 pg/µL, and 25 pg/µL. Control incubations (culture medium and DMSO) were also performed. The cells were exposed for 1 - 7 days, with renewal of the culture medium containing pesticides and $PM_{2.5}$ every 24 h.

Cytotoxicity, Crystal Violet Dye (CVD) Assay
After different exposure periods, the culture medium is removed and the cell layer is carefully washed twice with PBS. Then, the PBS solution was removed from the wells, and methanol (100 µL) was added as a fixative, which was aspirated after 40 seconds of contact. Cells were stained with 50 µL/well of CVD solution (1 % CVD in 20 % methanol) for 10 min at room temperature. After incubation, the dye is carefully removed, and each well is washed 4 times with 200 µL of a PBS solution. The dye adhered to the cells is dissolved by adding 200 µL of a 30 % (v/v) acetic acid solution.

To construct the standard curve, 1 x 10^4 to 19 x 10^4 cells/well were plated, and quantification was performed in a spectrophotometer with a microplate reader (SpectraMAX). The microplates were read at wavelengths 570 nm and 690 nm, the latter corresponding to the signal from the plates.

Carcinogenicity study
Commercial BEAS-2B lung cell lines were exposed for 7 days of growth to the pesticides atrazine (ATRA), permethrin (PER), malathion (MAL), a mixture of organochlorine pesticides (20 compounds, MIXO), and a mixture with all of the above compounds (MIXG). The pesticide concentrations were 300 pg/m^3 = 1.5 x 10^{-4} pg/µL and 3000 pg/m^3 = 1.5 x 10^{-3} pg/µL). In the other part of the assay, other BEAS-2B cells were exposed for 7 days to the $PM_{2.5}$ collected at the 3 sampling sites. For exposure to $PM_{2.5}$, the concentration of 5 µg/m^3 = 2.5 pg/µL was used, the lowest concentration of PM2.5 found at the sampling sites and which presented relevant results in the CV test performed previously.

Colony formation in Soft-agar
The assay was performed as described in (Borowicz et al., 2014). After 7 days of exposure to PM2.5 and pesticides, in addition to the controls for each exposure, BEAS-2B cells were trypsinized and plated at densities of 15000 cells per well in a culture medium containing 0.35% low-melting agarose in 6-well plates with a base layer of 0.5% high-melting agarose. The plates were incubated for 20 days at 37°C in an atmosphere containing 5% CO_2. Culture medium was added every 3 days. After the growth period in a semisolid medium, the colonies were fixed in 200 µL of paraformaldehyde (4% v/v) for 45 minutes. Subsequently, colonies with a diameter greater than or equal to 100 µm were counted under an inverted microscope, using a 100-fold magnification.

RESULTS

Cytotoxicity
It was observed that $PM_{2.5}$ can prevent cell growth after 72 h of exposure in all sampling sites and concentrations. The $PM_{2.5}$ collected in PRB had the most significant effect and caused the highest number of cells to die. Samples from CAP and SPA followed in that order. The latter remained stable in the last two days of exposure, but further studies are needed to understand this behavior.

For pesticides, there were no significant differences between exposure and controls for the first 4 days. However, different behaviors were observed from the 5th day of exposure. The lowest concentration of all formulations showed significant differences, and on the 6th day of exposure, the Mix containing all pesticides caused the highest cell death. This result may be due to the synergistic effect between the pesticides, which makes them more toxic when reacting together.

Carcinogenicity
The number of colonies in the soft agar increased significantly after exposure to $PM_{2.5}$ compared to the control group ($p<0.0001$). The $PM_{2.5}$ collected in PRB showed the most significant tumorigenic effect followed by CAP and SPA (Figure 1). It is worth

noting that the $PM_{2.5}$ concentration used was the lowest, so, the tumorigenic effects would increase on days with higher concentrations.

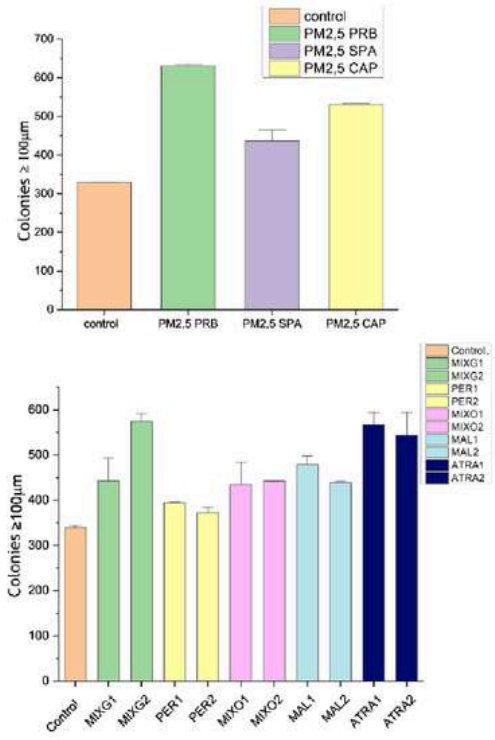


Figure 1. Analysis of colony formation in Soft Agar semisolid medium after 7 days of exposure of BEAS-2B cells to $PM_{2.5}$ and pesticide standards.

The second test showed that colony formation was higher in pesticide exposure than in the control, but statistically significant differences were found only for the mixture containing all pesticides (MIXG) and atrazine (ATRA). The presence of atrazine in particulate matter caused tumorigenic effects and the tumorigenic effect found in MIXG may be exclusive to the presence of atrazine. Further studies should be done to corroborate this result. Comparing these results with those obtained for $PM_{2.5}$, we can see how the effect of $PM_{2.5}$ is even greater than that caused by individual or mixed pesticides.

An important result is that the pesticide with the greatest tumorigenic effect, ATRAZ, was the compound that had one of the highest concentrations (163 pg/m^3) and detection frequency (100%) in PRB samples. For SPA samples (93 pg/m^3) and CAP (not detected), the concentration of ATRAZ was much lower (Yera & de Castro Vasconcellos, 2021). This result may be relevant to explain the differences found between $PM_{2.5}$ in PRB, CAP, and SPA.

Further tests would be needed to determine whether the tumorigenic effect of $PM_{2.5}$ is influenced more by the particle itself or its chemical composition.

CONCLUSIONS

The study found that after 3 days of exposure, the tested concentrations of $PM_{2.5}$ induced growth arrest of BEAS-2B cells, indicating the presence of cytotoxicity in the particulate matter. In comparison, while pesticides also showed significant cytotoxicity, it was much lower than that caused by $PM_{2.5}$. However, when pesticides were mixed together, a synergistic effect was observed, leading to greater cytotoxicity, which better simulates what happens in ambient air.

The greater cytotoxicity of $PM_{2.5}$ for pesticides may be due to its complex composition, which includes ions, metals, bacteria, and a hundred organic compounds. The study also revealed that $PM_{2.5}$ had tumorigenic effects for concentrations 5 $\mu g/m^3$, with PRB having the greatest effects followed by CAP and SPA. Among the pesticides studied, only atrazine exhibited tumorigenic effects, which may be responsible for the difference in the tumorigenic effect found at each site since it is one of the main pesticides detected in PRB.

This research is of great relevance as no similar studies have been conducted on samples of particulate matter collected at sites in the state of São Paulo or on the pesticides of interest.

REFERENCES

Bombardi, Larissa, M. (2017). *Geografia de uso de agrotoxicos no brasil e conexoes com a uniao europeia*.

Borowicz, S., Van Scoyk, M., Avasarala, S., Karuppusamy Rathinam, M. K., Tauler, J., Bikkavilli, R. K., & Winn, R. A. (2014). The soft agar colony formation assay. *Journal of Visualized Experiments*, *92*, 1–6.

IBGE, I. B. de G. e E. (2018). *Panorama e Pesquisa de Piracicaba*.

Mostafalou, S., & Abdollahi, M. (2013). Pesticides and human chronic diseases: Evidences, mechanisms, and perspectives. *Toxicology and Applied Pharmacology*, *268*(2), 157–177.

Patisaul, H. B., Fenton, S. E., & Aylor, D. (2018). Animal models of endocrine disruption. *Best Practice & Research Clinical Endocrinology & Metabolism*, *32*(3), 283–297.

Yera, A. M. B., & de Castro Vasconcellos, P. (2021). Pesticides in the atmosphere of urban sites with different characteristics. *Process Safety and Environmental Protection*, *156*, 559–567.

Zaccarelli-Marino, M. A., André, C. D. S., & Singer, J. M. (2016). Overt primary hypothyroidism in an industrial area in São Paulo, Brazil: The impact of public disclosure. *International Journal of Environmental Research and Public Health*, *13*(11).

AIR POLLUTION CONFERENCE BRAZIL
CMAS SOUTH AMERICA
COMMUNITY MODELING AND ANALYSIS SYSTEM

REDUCTION OF HEALTH IMPACT OF AMBIENT PM_{10} AND $PM_{2.5}$- CONCENTRATIONS IN SANTOS-SP, BRAZIL

Andreas F. Grauer[1], Débora L. Perazzoli[1], Marcos V. O. de Figueiredo[1], Jacqueline A. Schraier[1], André Luciano Malheiros[1], Helder Rafael Nocko[1]

[1]*Envex Engenharia e Consultoria*

andreas.grauer@envexengenharia.com.br

debora.perazzoli@envexengenharia.com.br

Abstract:

The city of Santos/SP is a densely populated area with the largest port in Latin America. This port is characterized by a high volume of vegetable dry bulk exports, and the handling of these products is known as a source of particulate matter emissions (PM_{10} and $PM_{2.5}$). The air quality in Santos (with regard to PM_{10} and $PM_{2.5}$) is influenced by the contribution of a natural portion, related to the sea mist, and an anthropogenic portion, including mainly vehicular traffic and commercial and industrial activities. Due to the availability of fuels and raw material, there are large industrial activities with the potential to influence air quality in the metropolitan region around Santos, which is called Baixada Santista. The emission of atmospheric pollutants in the Baixada Santista is especially critical due to the topographical conditions, notably the Serra do Mar mountain range, which forms an obstacle to the pollutants's dispersion. In recent years there have been a number of improvements in industrial processes and in the facilities at the Port of Santos, which caused a reduction in the concentrations of PM_{10} and $PM_{2.5}$, and consequently in the impact on the population's health. The aim of this study is to quantify the benefits of these improvements in terms of reducing the impact on health. In order to do this, the deaths attributable to the pollutants PM_{10} and $PM_{2.5}$ were calculated for the period from 2013 to 2019. The years 2020 to 2022 were not included due to the effect of COVID-19 on health data, which caused a significant increase in cases of illnesses and deaths. The tool used for this analysis was the World Health Organization's (WHO) AirQ+ software.The input data included average annual concentrations measured at two automatic air quality stations operated by CETESB, São Paulo's state environmental agency: Estação Santos and Estação Santos - Ponta da Praia. Death data was obtained from DataSUS, a system linked to the Brazilian Ministry of Health. The effects studied were: total deaths >30 years; deaths from diseases of the circulatory system >30 years; deaths from diseases of the respiratory system >30 years; and deaths from lung cancer >20 years. The results showed that the average annual concentrations of PM_{10} ranged from 48 $\mu g/m^3$ in 2013 to 22 $\mu g/m^3$ in 2019 in the Ponta da Praia Estuary, while the average concentrations of $PM_{2.5}$ ranged from 19 $\mu g/m^3$ to 14 $\mu g/m^3$ in the same period. The concentrations considered as cut-off (No observed effect level) for each pollutant were: 10 $\mu g/m^3$ for $PM_{2.5}$ and 21.7 $\mu g/m^3$ for PM_{10}. In relation to health impact, the highest resulting attributable fraction was 17.80% for respiratory system diseases in 2014. In general, the attributable fractions decreased during the study period. In 2019, the impact with the highest calculated attributable fraction was lung cancer for the population >20 years, with 4.43%. In the reference period, there was a reduction in total deaths attributed to the effects of pollution, from 266 cases in 2013 to 124 in 2019 (a reduction of 53.4%). When comparing PM_{10} and $PM_{2.5}$, the pollutant $PM_{2.5}$ proved to have a greater impact on health. Deaths from circulatory problems were reduced from 123 in 2013 to 49 in 2019 (60.2% reduction). Deaths from respiratory problems were reduced from 92 in 2013 to 17 in 2019 (81.5% reduction). It is interesting to note that the pollutant PM_{10} was the main cause of deaths in this category until 2015, however, from 2016 onwards the impact calculated for the pollutant $PM_{2.5}$ exceeded the impact calculated for PM_{10}. Deaths from lung cancer were reduced from 17 in 2013 to 5 in 2019 (a 70.6% reduction). Excluding the specific deaths studied from the total number attributed to particulate air pollution, between 32 and 53 cases attributed to PM_{10} or $PM_{2.5}$ remained, without appearing in the categories studied. Despite the significant improvements observed in the period 2013-2019, still 124 cases attributable to $PM_{2.5}$ were calculated for 2019, which reinforces the importance of continuing improvements in reducing emissions of this pollutant.

Keywords: Epidemiological study, Fine particles, AirQ+ model, air quality health impact.

INTRODUCTION

Accounting for the effects of air pollution has been made possible today by the availability of air quality data and dose-response curves that link the impact studied on the affected population with the concentrations they are exposed to. Analysis of the effects of air pollution on the morbidity and mortality of the population is not typically addressed in environmental reports from the public agencies responsible for monitoring air quality. They usually simply compare measured concentrations with air quality standards. However, compliance with the standards does not mean the absence of an impact, which can be accounted for using dose-response relationship curves drawn up in epidemiological studies. This study provides results on the impact of PM_{10} and $PM_{2.5}$ on the mortality of the population of Santos, Brazil from 2013 to 2019.

METHODS

Air quality data was obtained from São Paulo's state environmental agency's reports (CETESB, 2023). CETESB operates two air quality stations in Santos: Santos Station, which measures PM_{10}; and Santos - Ponta da Praia Station, which measures PM_{10} and $PM_{2.5}$. The arithmetic mean of the annual averages of both stations was calculated for the pollutant PM_{10}; and in the case of $PM_{2.5}$ the annual average of

Ponta da Praia Station was used for the period 2013 to 2019.The evolution of measured concentrations over the period are shown in Figure 1, as well as the cut-off (No observed effect level) for both pollutants. The cut-off was 10 µg/m³ for $PM_{2.5}$ (default AirQ+) and 21.7 µg/m³ for PM_{10}. This second value was based on the ratio $PM_{2.5}/PM_{10}$=0.46 (WHO, 2016), valid for Brazil.

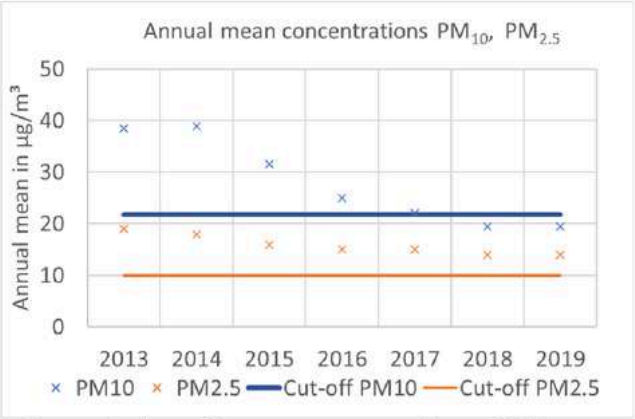


Figure 1. Annual mean concentrations of PM_{10} and $PM_{2.5}$ in Santos, Brazil.
Reference: Adapted from CETESB (2023)

Using these averages and the AirQ+ software (WHO, 2022), five impacts were calculated:

1. total deaths >30 years;
2. deaths from diseases of the circulatory system >30 years;
3. deaths from diseases of the respiratory system >30 years;
4. deaths from lung cancer >20 years and
5. deaths from unknown causes by the difference between the total value and the numbers in categories 2 to 4.

This age group was chosen because there is in the AirQ+-software a dose-response relationship curve for this part of the population.
The impacts calculated by AirQ+, expressed as attributable fractions, were multiplied by the number of cases reported by the Ministry of Health through the DataSUS system for the municipality of Santos (BRASIL, 2023). For example, in 2013, 3971 deaths were recorded in Santos, of which, according to the AirQ+ log-linear relationship, 6.38% were caused by the pollutant PM_{10} and 6.69% by the pollutant $PM_{2.5}$,. The higher of the two results (266 cases) was considered to be deaths attributable to particles in the atmosphere.

FINDINGS AND ARGUMENT

According to the reduction in ambient particle concentrations shown in Figure 1, there was also a reduction in calculated attributable deaths, as shown in Figure 2. Since 2018, PM_{10} concentrations have been below the cut-off, so there have been no more attributable deaths for this pollutant since that year. In absolute numbers, total attributable deaths decreased from 266 in 2013 to 124 in 2019. This corresponded to a reduction in the percentage of attributable cases calculated in Santos from 6.69% to 3.03%.

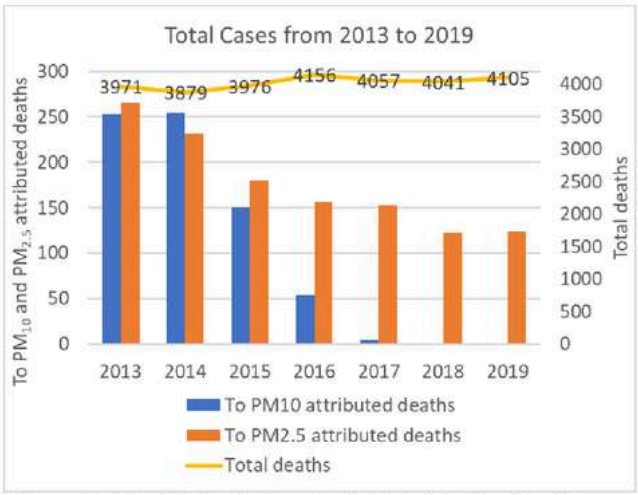


Figure 2. Total deaths and attributable deaths to PM_{10} and $PM_{2.5}$ in Santos, Brazil.
Reference: The authors (2024)

For the specific effects, lung cancer showed the greatest impact reduction expressed as attributable fractions, from 9.70% in 2013 to 4.43% in 2019, as shown in Figure 3. However, in all the studied years it represented the highest percentage of impact among the specific effects studied, which highlights the existence of a strong link between $PM_{2.5}$ and lung cancer.

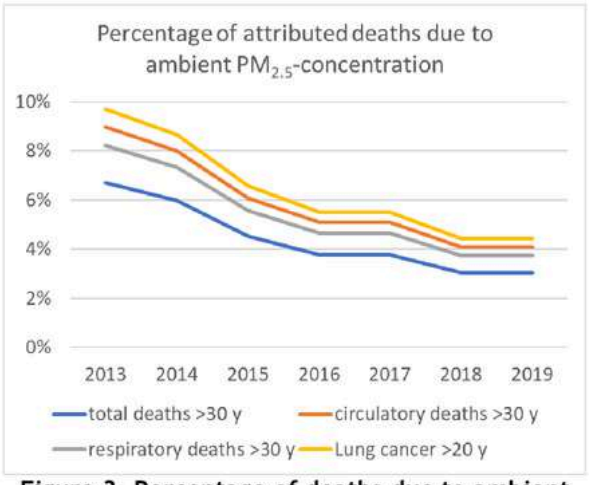


Figure 3. Percentage of deaths due to ambient $PM_{2.5}$-concentration in Santos, Brazil.
Reference: EnvEx (2024)

Looking at the attributable deaths between 2013 and 2019 in Figure 4, we see a reduction in the categories: total deaths (>30 years), deaths due to circulatory system problems (>30 years), deaths due to respiratory system problems (>30 years) and deaths due to lung cancer (>20 years). The

difference between the sum of the specific causes and the total attributable deaths is shown by the green column, which represents the cases of other deaths potentially caused by atmospheric particles, but not included in the above categories, i.e. deaths attributable to unknown causes. These unknown causes increased from 34 in 2013 to 54 in 2019.

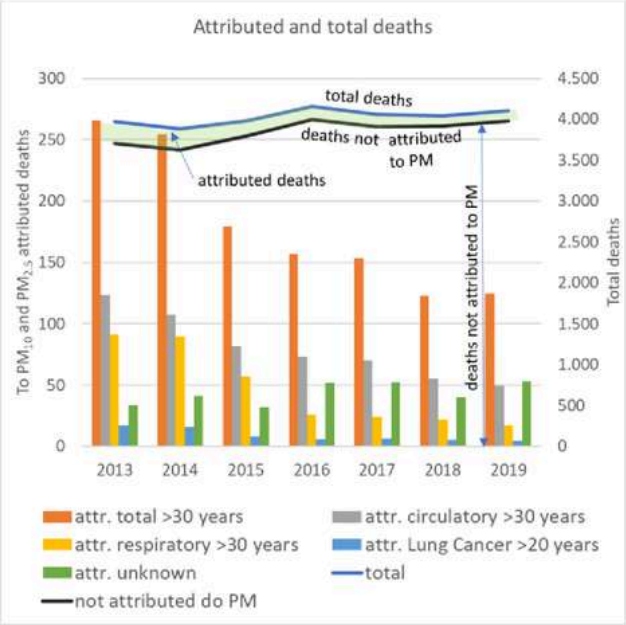


Figure 4. Attributed and total deaths.
Reference: The authors (2024)

Figure 5 compares the percentages of deaths from the causes studied in 2013 and 2019. There was a significant drop in causes attributed to the respiratory system from 35% in 2013 to 14% in 2019. At the same time, there was an increase in unknown causes from 13% to 43% in the period. In 2013, of the 124 cases of deaths attributable from particles in the atmosphere, 49 were from circulatory problems, 17 from respiratory problems and 5 from lung cancer. The remaining 53 cases, or 43%, had other causes.

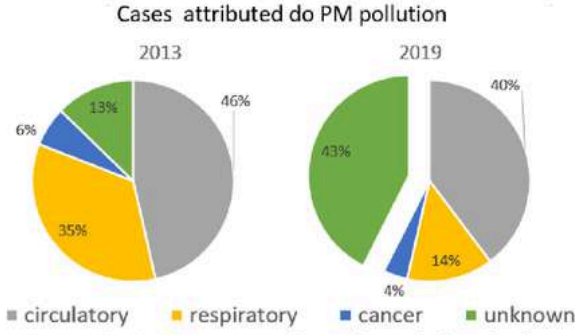


Figure 5. Percentage of attributed deaths for each category studied in 2013 and 2019.
Reference: The authors (2024)

CONCLUSIONS

Between 2013 and 2019 there was a substantial reduction in PM_{10} and $PM_{2.5}$ concentrations in Santos. The reduction in environmental concentrations was fed into the AirQ+ software and the share of deaths attributable to these pollutants for the population over 30 was computed.

The calculations showed that there was a reduction in deaths attributable to particles in the atmosphere from 266 cases in 2013, or 6.69%, to 3.03% in 2019 (124 cases). Among the specific effects, the greatest benefit was seen in reduction of deaths from respiratory system problems, which accounted for 35% of attributable deaths in 2013, a figure that fell to 14% in 2019. At the same time, deaths from unknown causes increased from 13 to 43%, which reinforces the need for further studies into the dose-response relationships for low concentrations of particles in the atmosphere.

It was not possible, in this study, to identify possible effects of atmospheric particles other than circulatory problems, respiratory problems and lung cancer on mortality. One hypothesis is that these additional effects exist, but there is still a lack of data to quantify them. Another possible explanation for the increase in unknown cases is the limitation of dose-effect curves when they are used near their lower limit. Any tool used at the lower limit of its applicability has high uncertainty.

REFERENCES

BRASIL. Ministério da Saúde. DATASUS. Tabnet. Brasília, DF: Ministério da Saúde, 2023. (Sistema de Informações sobre Mortalidade - SIM). http://tabnet.datasus.gov.br/cgi/deftohtm.exe?sim/cnv/obt10uf.def. Accessed November 2023.

CETESB. Relatórios de Qualidade do ar no Estado de São Paulo. São Paulo, 2023. (Série Relatórios). https://cetesb.sp.gov.br/ar/publicacoes-relatorios/. Accessed November 2023.

WHO Regional Office for Europe, European Centre for Environment and Health (2022). AirQ+: software tool for health risk assessment of air pollution. Bonn (Germany): WHO Regional Office for Europe. https://www.who.int/europe/tools-and-toolkits/airq---software-tool-for-health-risk-assessment-of-air-pollution
Accessed November 2023

WHO - World Health Organization. Ambient air quality database 2016. https://www.who.int/data/gho/data/themes/air-pollution/who-air-quality-database/2016. Accessed August 2023.

AIR POLLUTION CONFERENCE BRAZIL
CMAS SOUTH AMERICA
COMMUNITY MODELING AND ANALYSIS SYSTEM

PARTICULATE MATTER-BOUND PAHS AND MUTAGENICITY IN THE LARGEST BRAZILIAN METROPOLITAN AREA

Guilherme Martins Pereira[1,2], Gabriely F. Groto Militão[3], Jessica Cardoso[3], Thayná da Silva Santos[1], Daniel A. Morales[3], Gisela de A. Umbuzeiro[3], Edmilson Dias de Freitas[2], Maria de F. Andrade[2], Pérola de C. Vasconcellos[1]

[1]*Institute of Chemistry - University of São Paulo*
[2]*Institute of Astronomy, Geophysics and Atmospheric Sciences - University of São Paulo*
guilherme.martins.pereira@usp.br
perola@iq.usp.br
[3]*Laboratory of Ecotoxicology and Genotoxicity - State University of Campinas*
grotogabi@gmail.com
giselau@unicamp.br

Abstract: The Metropolitan Area of São Paulo is often affected by high particulate matter levels due to the influence of its large vehicular fleet and pollution events are more common during drier periods of the year due to the influence of the increase of biomass burning events and less favorable meteorological conditions for pollutant dispersion. Polycyclic aromatic hydrocarbons (PAHs) in particulate matter have been associated with mutagenic properties. In 2019, an intensive campaign was performed in the drier months of the year (June to September) with a high-volume sampler (Hi-Vol), collecting fine particulate matter ($PM_{2.5}$). Organic extracts were obtained after solvent extraction and polycyclic aromatic hydrocarbons (PAHs) were determined with a Gas Chromatograph coupled to a Mass Spectrometer (GC/MS). In order to study which particulate matter sources are more associated with mutagenic effects, some samples were selected as representative of specific particulate matter sources (secondary formation, vehicular exhaust and non-exhaust, industrial and biomass burning) and tested for mutagenicity through Salmonella/microsome assay in the miniaturized version, microplate agar (MPA), without and with metabolic activation (rat liver S9 5%, Phenobarbital/5,6-Benzoflavone induced). The SPA13 sample presented the lowest mutagenic potency and was associated with secondary formation by the receptor model. The SPA29 sample presented the highest mutagenic potency and was characterized by the influence of biomass burning. Despite the different mutagenic potencies, these samples present similar concentrations of $PM_{2.5}$, benzo(a)pyrene (BaP), and theoretically calculated equivalent mutagenicity (BaP-MEQ) and carcinogenicity (BaP-TEQ). Furthermore, correlations were not found between mutagenicity results and PAHs or BaP-MEQ, and the increase in the observed concentrations of PAHs was not related to higher mutagenicity of the samples, suggesting the effect of other not determined species in the study or a complex interaction of different chemical species in the extract. When the experiment is performed with metabolic activation (+S9), the SPA15 sample presents a decrease in mutagenicity, while SPA33 increases, which may be related to the effects of nitro-PAHs in the experiment without activation (Figure 1A). For the assays with S9, the samples with lower mutagenicity potencies (SPA13, SPA15, and SPA64) were often related to higher $PM_{2.5}$ concentrations (above 25 μg m^{-3}), suggesting that high $PM_{2.5}$ concentrations not always are associated with higher mutagenicity.

Keywords: Polycyclic aromatic hydrocarbons, pollution, sources, Salmonella/microsome assay, microplate agar, YG1041, Benzo(a)pyrene

INTRODUCTION

Urban particulate matter often contains high levels of polycyclic aromatic hydrocarbons (PAHs) and other toxic species, which are mainly associated with vehicular exhaust in the Metropolitan Area of São Paulo (MASP) (Pereira et al., 2017, 2023). PAHs and their nitrated and oxygenated derivatives are associated with mutagenic and carcinogenic effects (Ravindra et al., 2008). Mutagenicity assays can be performed to detect reverse-type mutations. Different strains of *Salmonella enterica* serovar Typhimurium bacteria (Ames, 1971). These tests can be applied to environmental samples, including particulate matter (Alves et al., 2016).
Different strains can be used to detect different types of mutations, the most common are TA100 and TA98, which are useful for the detection of the majority of mutagens (William et al., 2019). The strain YG1041, derived from the TA98 strain, overproduces nitroreductase and O-acetyltransferase enzymes and is very sensitive to certain compounds, including nitroarenes and aromatic amines, and is the most sensitive strain to the detect aerosol-related mutagenicity (Maselli et al., 2019, Hagiwara et al., 1993).
The objective of this study was the application of Microplate Agar (MAP), a miniaturized technique, with the YG1041 strain to evaluate the mutagenicity of organic extracts of fine particulate matter ($PM_{2.5}$) collected in the MASP.

METHODS

Particulate matter was sampled and analyzed by researchers at the University of São Paulo

(*Laboratório do Grupo de Estudos em Química Atmosférica* - GEQAt/USP).

A sampling campaign was performed in a dry period in 2019 (June to September), inside the university campus, near a busy expressway and a green area. The passing fleet included light- and heavy-duty vehicles running on gasoline, diesel, biodiesel, and ethanol. $PM_{2.5}$ was collected in quartz fiber filters, with a high-volume sampler (Hi-Vol, 1.13 m^3 min^{-1} flow). Sampling started at 9 AM, followed by a 24-hour collection.

After the sampling, PAHs were extracted from the filters under sonication with dichloromethane, followed by a clean-up process with silica gel column chromatography. A Gas Chromatograph coupled to a Mass Spectrometer (GC-MS) was employed to quantify these species. More details are found in Pereira et al. (2017) and Vasconcellos et al. (2010).

The Positive Matrix Factorization (PMF) receptor model was applied to apportion the sources affecting $PM_{2.5}$ in this site and some samples were selected as representative of specific particulate matter sources (secondary formation, local vehicular, vehicular + road dust, industrial and biomass burning).

After the chemical analysis, the organic extracts were analyzed for mutagenicity by researchers at the State University of Campinas (*Laboratório de Ecotoxicologia e Genotoxicidade - LAEG/UNICAMP)*.

The assay was conducted according to Zwarg et al. (2018), using concentration-response experiments for each sample, with and without metabolic activation (5% of S9, a rat liver mix, induced by Phenobarbital/5,6-Benzoflavone, Moltox®). The selected strain was the YG1041. Complementally, tests with TA98 were conducted for comparison.

Overnight bacterial cultures were five times concentrated (10000g, 4°C, and 10 min) and resuspended in 0.015M sodium phosphate buffer. 50µL of cell suspension (0.5 to $2x10^{10}$ cells per mL) was added to a tube containing 2 µL of the organic extract. Half of this was transferred to a new tube. In the first tube, 25 µL of 0.015M sodium phosphate was added, and in the second tube, 25 µL of S9 mix. All tubes were incubated with shaking (180 rpm, 37°C, and 90 min). Afterward, 1mL of molten agar was added to each tube and 250 µL of the mixture was distributed in 4 wells in microplates, each containing 2.8 mL of minimal agar. Revertants colonies were manually counted after incubation (66 h, 37°C). Dimethyl sulfoxide was used as negative control and positive controls were 4-nitro-o-diamino-phenylinphenylenediamine, without S9, and 2-aminoanthracene (2AA), with S9.

The data was analyzed using ANOVA/Tukey, followed by a linear regression. Samples were considered as positive if the responses were statistically significant ($p < 0.05$). The results were expressed as the minimum effective concentration (MEC2), capable of doubling the revertant number in ng of $PM_{.5}$ per µL. For better understanding, the mutagenic potencies were presented as 1/MEC2.

FINDINGS AND ARGUMENT

Benzo(a)pyrene equivalent mutagenicity (BaP-MEQ) and toxicity (BaP-TEQ), benzo(a)pyrene (BaP) concentrations and mutagenic potencies (1/MEC2 in ng of PM) with S9 and without S9 are presented in Figure 1. Overall, BaP-MEQ, BaP-TEQ, and BaP ranges were 0.02-0.08 ng μg^{-1}, 0.01-0.09 ng μg^{-1}, and 0.000-0.026 ng μg^{-1}, respectively.

Regarding the mutagenic potencies, with and without metabolic activation (+S9) (Figure 1A and 1B), the sample SPA13, associated with secondary formation by the PMF receptor model, presented the lowest 1/MEC2. On the other hand, sample SPA29, associated with the influence of biomass burning, presented the highest value. Despite the different mutagenic potencies, these samples presented similar concentrations of $PM_{2.5}$ (35 and 31 µg m^{-3}), BaP (0.026 and 0.023 ng μg^{-1}), BaP-MEQ (0.08 and 0.08 ng μg^{-1}) and BaP-TEQ (0.09 and 0.06 ng μg^{-1}).

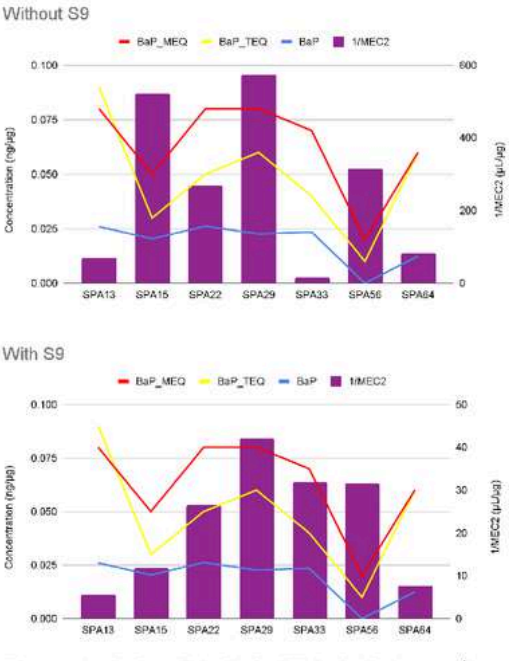


Figure 1. BaP-MEQ, BaP–TEQ, BaP (ng μg^{-1}) concentrations (left Y axis) and mutagenic potencies (1/MEC2 in ng of PM) with S9 (A) and without S9 (B) (right Y axis).

Furthermore, no correlations were found between mutagenicity results and PAHs or BaP-MEQ, and the increase in the observed concentrations of PAHs was not related to higher mutagenicity of the samples, suggesting the effect of other species, not determined in the study or a complex

interaction of different chemical species in the extract, that may have synergistic interactions (de Oliveira Alves et al., 2020).
When the experiment is performed with metabolic activation (+S9), the SPA15 sample presents a decrease in mutagenicity, while SPA33 presents the opposite effect, which may be related to the effects of the presence of nitrated PAHs in the experiment performed without activation. For the assays with S9, the samples with lower mutagenicity potencies (SPA13, SPA15, and SPA64) were often related to higher $PM_{2.5}$ concentrations (above 25 µg m^{-3}), suggesting that high $PM_{2.5}$ concentrations not always are associated with higher mutagenicity.

CONCLUSIONS

A miniaturized technique, with the YG1041 strain, was applied to evaluate the mutagenicity of organic extracts of $PM_{2.5}$ collected inside the University of São Paulo campus. It was possible to observe that relatively higher $PM_{2.5}$, BaP concentrations, and equivalent toxicities were not always associated with higher mutagenic potencies. The lack of correlations between mutagenicity results and the measured species suggests the effect of other species, not determined in this study, and a complex interaction of the different species present in this type of sample.

REFERENCES

Alves, Debora Kristina et al. Mutagenicity profile of atmospheric particulate matter in a small urban center subjected to airborne emission from vehicle traffic and sugar cane burning. *Environmental and Molecular Mutagenesis* 57 (2016): 41-50.

Ames, Bruce. *The Detection of Chemical Mutagens with Enteric Bacteria. Chemical Mutagens.* Boston: Springer, 1971.

Hagiwara, Yuji et al. Specificity and sensitivity of *Salmonella typhimurium* YG1041 and YG1042 strains possessing elevated levels of both nitroreductase and acetyltransferase activity. *Mutation Research/Environmental Mutagenesis and Related Subjects* 291 (1993): 171-180.

Maselli, Bianca et al. Comparative mutagenic activity of atmospheric particulate matter from Limeira, Stockholm and Kyoto. *Environmental and Molecular Mutagenesis* 60 (2019): 607-616.

de Oliveira Alves, Nilmara et al. Inflammation response, oxidative stress and DNA damage caused by urban air pollution exposure increase in the lack of DNA repair XPC protein. *Environment International* 145 (2020): 106150.

Pereira, Guilherme Martins et al. Particulate pollutants in the Brazilian city of São Paulo: 1-year investigation for the chemical composition and source apportionment. *Atmospheric Chemistry and Physics* 17 (2017): 11943–11969.

Pereira, Guilherme Martins et al. Emission factors for a biofuel impacted fleet in South America's largest metropolitan area. *Environmental Pollution* 331 (2023): 121826.

Ravindra, Khaiwal et al. Atmospheric polycyclic aromatic hydrocarbons: Source attribution, emission factors and regulation. *Atmospheric Environment* 42 (2008): 2895–2921.

Vasconcellos, Pérola et al. Determination of anthropogenic and biogenic compounds on atmospheric aerosol collected in urban, biomass burning and forest areas in São Paulo, Brazil. *Science of the Total Environment* 408 (2010): 5836–5844.

Williams, Richard et al. Are all bacterial strains required by OECD mutagenicity test guideline TG471 needed? *Mutation Research/Genetic Toxicology and Environmental Mutagenesis* 848 (2019): 503081.

Zwarg, José Ricardo et al. Miniaturization of the microsuspension *Salmonella*/microsome assay in agar microplates. *Environmental and Molecular Mutagenesis* 59 (2018): 488-501.

AIR POLLUTION CONFERENCE BRAZIL
CMAS SOUTH AMERICA
COMMUNITY MODELING AND ANALYSIS SYSTEM

ASSESSMENT OF AİRBONE MERCURY LEVELS İN PRESERVED AND ANTHROPOGENİCALLY İMPACTED AREAS (RİO DE JANEİRO STATE, BRAZIL)

Luis Fhernando Mendonça da Silva[1], Caio da Silva Assis Felix[4,6], Rodrigo Stellet Ferreira[2], Hellen Gonçalves da Silva[2], Maria Cristina Canela[2], Cibele Maria Stivanin de Almeida[2], Luiz Francisco Pires Guimarães Maia[3], Gisele Olímpio da Rocha[4,5,6,7], Jailson Bittencourt de Andrade[4,5,6,7], Renato da Silva Carreira[1], Adriana Gioda[1].

[1] Pontifical Catholic University of Rio de Janeiro (PUC-Rio), Departamento de Química. 22451-900 Rio de Janeiro-RJ, Brazil
agioda@puc-rio.br

[2] Universidade Estadual do Norte Fluminense Darcy Ribeiro (UENF), Centro de Ciência e Tecnologia, Laboratório de Ciências Químicas. Campos dos Goytacazes-RJ-Brazil

[3] Universidade Federal do Rio de Janeiro (UFRJ), Departamento de Meteorologia, Instituto de Geociências, Rio de Janeiro, Brasil

[4] Centro Interdisciplinar de Energia e Ambiente-CIEnAm, Universidade Federal da Bahia, 40170-115, Salvador, BA, Brazil

[5] Universidade Federal da Bahia, Instituto de Química, Programa de Pós-Graduação em Química, 40170-115, Salvador, BA, Brazil

[6] Instituto Nacional de Ciência e Tecnologia em Energia e Ambiente-INCT E&A, Universidade Federal da Bahia, 40170-115, Salvador, BA, Brazil

[7] Centro Universitário SENAI-CIMATEC, Av. Orlando Gomes, 1845 Piatã, 41650-010, Salvador, BA, Brazil

Abstract: Although present in low concentrations in the atmosphere, mercury in particulate matter (PM) plays an important role in the biogeochemical process of mercury. With this in mind, this study aims to investigate mercury concentrations in particulate matter ($PM_{2.5}$) samples from the regions of Campos dos Goycatazes (CG), Gávea (GA) and Serra dos Órgãos National Park (PARNASO). All samples were collected according to Brazilian standards (ABNT-NBR 9547/86) and the methods of the United States Environmental Protection Agency (US EPA) (Method IO - 2.1). PM concentrations were determined by gravimetric technique. The Direct Mercury Analyzer (DMA-80, Milestone Helpind Chemists) was used for total Hg analysis. Daily $PM_{2.5}$ concentrations ranged from 13 to 36 μg m^{-3}, with a mean of 24 ± 12 μg m^{-3} for the GA region, and from 24 to 46 μg m^{-3}, with a mean of 33 ± 12 μg m^{-3} for the PARNASO region, and from 14 to 19 μg m^{-3}, with a mean of 17 ± 11 μg m^{-3} for the CG for the days sampled from July to October 2022. High levels of PM concentrations at PARNASO indicate a contribution from anthropogenic sources. Considering these values, no day sampled exceeded the value suggested by Brazilian legislation (60 μg m^{-3}), but 65 % of the samples showed higher daily concentrations than suggested by World Health Organization (WHO, 15 μg m^{-3}). Hg concentrations ranged from 223 to 366 pg m^{-3}, with a mean of 274 ± 65 pg m^{-3} for the GA region, and from 119 to 190 pg m^{-3}, with a mean of 155 ± 29 pg m^{-3} for the PARNASO region, and from 164 to 315 pg m^{-3}, with a mean of 258 ± 67 pg m^{-3} for the CG for the days sampled. Hg concentrations in the atmosphere showed significant spatial variation, with much higher values in urban areas than in the natural zone. The results showed that Hg concentrations in particulate matter are at the same level as those found in urban and industrial areas in US and northern Europe. At Parnaso, the presence of Hg may be due to anthropogenic sources, which may be local sources and/or long-range transport contributions. There exists an intriguing meteorological facet warranting consideration, pertaining to the atmospheric transport facilitated by mountain-valley interactions and sea-land breezes within the southern region of the Serra dos Órgãos. This phenomenon merits further in-depth exploration. In addition, the high concentrations of Hg found in Campos dos Goytacazes may be associated with the burning of biomass, since sugar cane is burned throughout the year in the region and also due to the application of pesticides in the most diverse crops in the municipality, many times without due control.

Keywords: Mercury, particulate matter, $PM_{2.5}$, Rio de Janeiro.

INTRODUCTION

Mercury (Hg) is a pervasive environmental contaminant with significant repercussions for both human health and ecosystems globally. Its persistence, ability to accumulate in organisms, and capability for long-distance atmospheric movement make it a particularly concerning pollutant. Mercury exists in various forms, such as elemental mercury (Hg^0), reactive gaseous mercury (RGM), and particle-bound mercury (PHg). Of these, PHg is of particular concern because it can settle into ecosystems and water bodies. Once there, it undergoes transformations, ultimately converting into methylmercury—a potent neurotoxin easily absorbed by aquatic organisms and subsequently magnified through the food chain (Galappaththi and Suraweera 2020; Henriques et al. 2019).

A comprehensive comprehension of particle-bound mercury dynamics, encompassing its sources, transport mechanisms, and deposition patterns, is

essential for crafting effective mitigation strategies to alleviate its harmful effects (Brocza et al. 2024). This study seeks to enhance our understanding of these dynamics by specifically focusing on quantifying concentrations, delineating seasonal variations, and discerning potential emission sources on both a global scale and within the context of Brazil. By delving into these aspects, we aim to provide insights crucial for developing targeted interventions to address the adverse impacts of particulate mercury on ecosystems and human health.

METHODS

$PM_{2.5}$ samples were collected from three monitoring sites situated at Gávea (GÁVEA, 22°58'50" S and 43°13'58" W), Campos dos Goytacazes (CAMPOS, 21°45'39.1''S 41°17'31.1'' W), and the Serra dos Órgãos National Park (PARNASO, 22°29'47.5'' S and 43°00'05.2'' W) (Fig. 1) from July to October 2022. $PM_{2.5}$ samples were gathered employing quartz microfiber filters with a pore size of 1.6 µm (Whatman, Fisher Scientific, Maidstone, United Kingdom) over 24 hours, monthly, utilizing monitoring equipment following Brazilian standards (ABNT-NBR 129 9547/86) and methods outlined by the United States Environmental Protection Agency (US EPA) under method 130 (Method IO – 2.1). This process utilized a High-Volume air sampler (Hi-Vol 3000, Energética, Sao Paulo, Brazil) with an average air flow rate of 1.07 m^3 per minute. The filters underwent a conditioning process in a desiccator for 24 hours and they were subjected to gravimetric analysis before and after the sampling sessions using an analytical balance (Gehaka AG200 ± 0.0001, Marte Científica, Brazil) to ensure accurate measurement of particulate mass. The relative humidity levels were maintained between 20 % and 30 %, and temperatures ranged from 20 °C to 25 °C during the filter weighing procedures. This study examined all available $PM_{2.5}$ samples to assess their particulate mass content.

Total Hg concentrations in $PM_{2.5}$ were determined using a Direct Mercury Analyzer - DMA-80 (Milestone, Sorisole (BG), Italy).

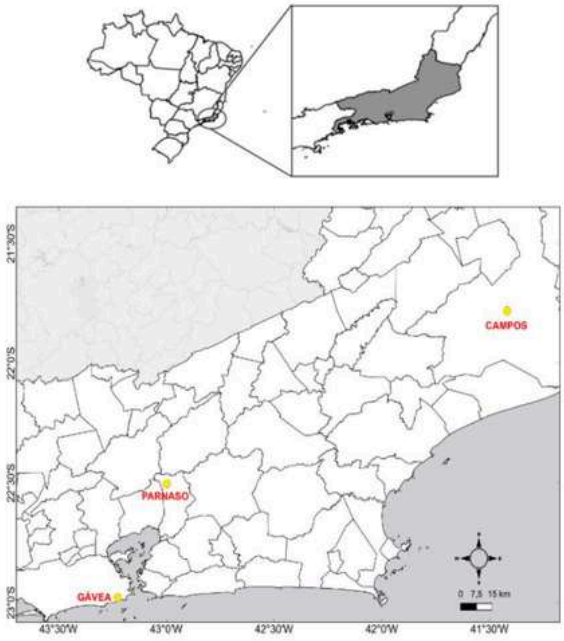


Figure 1. $PM_{2.5}$ monitoring stations: GAVEA: Gávea, PARNASO: Serra dos Órgãos National Park, and CAMPOS: Campos dos Goytacazes.

FINDINGS AND ARGUMENT

The average concentration of $PM_{2.5}$ in Gávea was 24±12 µg m^{-3} (with values ranging from 133 to 26 µg m-3, in PARNASO, it was 33±12 µg m^{-3} (with values ranging from 24 to 46 µg m^{-3}), and in Campos, it was 17±11 µg m^{-3} (with values ranging from 14 to 19 µg m^{-3}). Given these values, none of the days sampled exceeded the threshold recommended by Brazilian regulations (60 µg m^{-3}). However, 65 % of the samples exhibited daily concentrations surpassing the guidelines set by the WHO (15 µg m^{-3}).

$PM_{2.5}$ concentrations were observed to be relatively elevated during the dry season (July - August) in contrast to the wet season (September-October). This pattern has been documented in numerous prior studies (Beringui et al. 2021; De La Cruz et al. 2024; Mateus et al. 2013). Many researchers attribute this phenomenon to the cleansing impact of rainfall, which captures and deposits suspended particles in the atmosphere.

The average PHg concentrations (range) were 274±65 (223–366) pg m^{-3}, 155±29 (119–190) pg m^{-3} and 258±67 (164–315) pg m^{-3} at the urban region of the capital, interior with sugarcane burning and forest sites during the sampling period, respectively. The average concentration of PHg in the urban with sugarcane burning (CAMPOS) and

forest (PARNASO) sites was approximately two times higher than in the urban site (GAVEA).

The results showed that PHg concentrations at urban sites in coastal cities are considerably lower than those in other cities, such as Gávea. The surface winds in coastal areas influence the concentrations of PM in these regions (Wang et al. 2023). PHg concentrations in urban areas were 5.9-11.3 times higher than the nearby values found in Asian countries (Xu et al. 2019), and North America (Detroit, USA) (Liu et al. 2007), indicating that a large amount of anthropogenic mercury has been released into the atmosphere in Brazil.

The highest levels of PHg were found in Campos and PARNASO, while the lowest concentrations of PHg were present in Gavea. The high concentration of PHg at the sites may be associated with anthropogenic emissions. In Campos, the most significant contributions may come from vehicular traffic, the port area and, above all, the burning of sugar cane. PARNASO, despite being an environmental conservation area, usually receives many visitors to the park, with vehicles being the primary commuter. In addition, it is less than 200 m away from BR-116, one of the main avenues linking the metropolitan region of Rio de Janeiro to the Serra and other states in the country, with heavy vehicle traffic.

CONCLUSIONS

During the sampling period, it was observed that $PM_{2.5}$ concentrations varied among the locations under study. In Gávea, PARNASO, and Campos, the average concentrations remained within acceptable limits as per Brazilian regulations, with none exceeding the specified threshold. However, a significant proportion of samples from all locations exceeded the daily concentration standards recommended by the World Health Organization, raising potential health concerns.

Mercury concentrations also exhibited variations across different environments, with higher levels detected in areas associated with sugarcane burning compared to urban and preserved sites. Urban fire sites recorded the highest mercury levels, surpassing those in both urban and preserved areas.

REFERENCES

Beringui, Karmel et al. 2021. "Assessment of the Concentration and Inorganic Composition of Particulate Matter Collected in the State of Rio De Janeiro." *Quimica Nova* 44(6): 737–54.

Brocza, Flora Maria et al. 2024. "Global Scenarios of Anthropogenic Mercury Emissions." *EGUsphere [preprint]* (41). https://doi.org/10.5194/egusphere-2024-4 (February 21, 2024).

Galappaththi, Himan K.A., and Inoka Suraweera. 2020. "Risk of Mercury Exposure during Childhood: A Review of Sri Lankan Situation." *Reviews on Environmental Health* 35(3): 229–32. https://www.degruyter.com/document/doi/10.1515/reveh-2020-0024/html (January 31, 2024).

Henriques, Magda Carvalho, Susana Loureiro, Margarida Fardilha, and Maria Teresa Herdeiro. 2019. "Exposure to Mercury and Human Reproductive Health: A Systematic Review." *Reproductive Toxicology* 85: 93-103.

De La Cruz, Alex H. et al. 2024. "Black Carbon and Particulate Matter Concentrations: Air Pollution Levels in Rio de Janeiro, Brazil." *Article J. Braz. Chem. Soc.* 35: 1–12. https://dx.doi.org/10.21577/0103-5053.20240029 (March 31, 2024).

Liu, Bian et al. 2007. "Temporal Variability of Mercury Speciation in Urban Air." *Atmospheric Environment* 41: 1911–23. www.elsevier.com/locate/atmosenv (February 1, 2024).

Mateus, Vinícius Lionel et al. 2013. "Study of the Chemical Composition of Particulate Matter from the Rio de Janeiro Metropolitan Region, Brazil, by Inductively Coupled Plasma-Mass Spectrometry and Optical Emission Spectrometry." *Spectrochimica Acta Part B: Atomic Spectroscopy* 86: 131–36.

Wang, Ju et al. 2023. "Impact Analysis of Meteorological Variables on PM2.5 Pollution in the Most Polluted Cities in China." *Heliyon* 9(7): e17609.

Xu, H. M. et al. 2019. "Mercury Stable Isotope Compositions of Chinese Urban Fine Particulates in Winter Haze Days: Implications for Hg Sources and Transformations." *Chemical Geology* 504: 267–75.

AIR POLLUTION CONFERENCE BRAZIL
CMAS SOUTH AMERICA
COMMUNITY MODELING AND ANALYSIS SYSTEM

USE OF PLANTS AS BIOMONITORS OF PARTICULATE MATTER TOXICITY IN URBAN REGIONS INFLUENCED BY MINNING

Santos, Emannuelly Ap. Amaral[1]; Neves, Thiago de Alencar[2]; Oliveira, Dângelle Makelle[3]; Passos, Ricardo Gomes[4]; Albuquerque, Taciana Toledo de Almeida[5]; Starling, Maria Clara Vieira Martins[6]
[1]*Department of Sanitary and Environmental Engineering, Federal University of Minas Gerais.* *emannuellyufmg@gmail.com*
[2]*Department of Sanitary and Environmental Engineering, Federal University of Minas Gerais.* *thiago@desa.ufmg.br*
[3]*Department of Sanitary and Environmental Engineering, Federal University of Minas Gerais.* *dangelleem@yahoo.com.br*
[4]*Nuclear Technology Development Center, Federal University of Minas Gerais* *ricardo.passos@cdtn.br*
[5]*Department of Sanitary and Environmental Engineering, Federal University of Minas Gerais.* *tacianatoledo26@gmail.com*
[6]*Department of Sanitary and Environmental Engineering, Federal University of Minas Gerais.* *mariaclara@desa.ufmg.br*

Abstract: Regarding air quality, biomonitoring applies plant species for which standard assays enable tracking direct and immediate effect of pollutants, as well as the release of toxic compounds, such as metals found in particulate matter (PM), into the ecosystem. This is extremely relevant considering that ecosystem health is linked to human health as according to the One Health Approach. Given the above, this research aims to conduct biomonitoring of air quality by using the standard grass species *Lolium multiflorum* as a tool for air quality monitoring in the city of Brumadinho (Minas Gerais, Brazil). The region is impacted by mining activities that release high loads of particulate matter into the atmosphere. The plants were cultivated and exposed according to the VDI 3957 - part 2 standard, with adaptations. Three sampling points were selected: S1 - City center; S2 - Tejuco neighborhood, surrounded by mining sites; S3 - an Indigenous community area, along with a reference point - S4 (a natural reserve). Additionally, $PM_{2.5}$ were sampled throughout the exposure period using a medium-volume sampler (ARA Instrument). S3 showed the highest concentrations of $PM_{2.5}$ (median of 40.15 $\mu g/m^3$), while S4 had the lowest concentrations (median of 31.40 $\mu g/m^3$). However, the medians did not differ significantly between the monitoring points. Visual analyses of the plants after exposure demonstrate a possible correlation between the presence of metals in atmospheric particles and their growth, indicating the accumulation of trace elements.

Keywords: Biomonitoring, One Health, Mining, Particulate Matter, *Lolium multiflorum*.

INTRODUCTION

Air pollution is a current challenge, representing one of the greatest risks to human health and environmental integrity (WHO, 2023). In mining regions, the impacts and emission of atmospheric pollutants, especially particulate matter (PM), from anthropogenic activities are intensified. In Brazil, mining plays a pivotal role in the country's economy, especially in the state of Minas Gerais. However, indiscriminate activities and lack of control and monitoring lead to the exacerbated release of atmospheric pollutants, highly detrimental to health.

The bottleneck in conventional air quality monitoring techniques, which rely on physicochemical analyses, does not allow for direct conclusions about the potential effects of pollutants to the environment (Klumpp *et al.*, 2003). Thus, alternatives supported by Nature-Based Solutions (NbS) can contribute to the diagnosis and reduction of air pollution (Theophilo *et al.*, 2021).

Biomonitoring is an efficient technique for assessing environmental contamination by using living organisms. Considering the concept of One Health (Multisanti *et al.*, 2022), environmental health threats detected by biomonitoring can serve as an early warning for human health threats, contributing to preventive measures. PM containing potentially toxic trace elements such as cadmium (Cd), copper (Cu), lead (Pb), and zinc (Zn) (Theophilo *et al.*, 2021), are easily inhaled by humans and animals, as well as deposited in plants, resulting in direct and indirect problems for the environment and public health.

Regarding air quality (bio)monitoring, plants are cost-effective indicators that allow for the assessment of the risk of complex mixtures of pollutants and analyses of those with very low environmental concentrations, which are difficult to measure by traditional methods (De Temmerman *et al.*, 2004). In addition, biomonitoring can be implemented in locations which lack access to high-tech equipment which require frequent maintenance. Besides, they promote environmental education and raise community awareness related to air pollution.

AIR POLLUTION CONFERENCE BRAZIL
CMAS SOUTH AMERICA
COMMUNITY MODELING AND ANALYSIS SYSTEM

The forage grass *Lolium multiflorum* Lam. (ryegrass) is used for animal consumption and due to its resistance to atmospheric pollutants, it has a high rate of bioaccumulation of toxic substances, such as sulfur, trace metals, polycyclic aromatic hydrocarbons (PAHs), gases, and PM (Bulbovas; Camargo; Domingos, 2015; Nakazato et al., 2018). Thus, it is ideal for monitoring and risk assessment in industrial and urban areas.

Considering the foregoing, this research aims to conduct air quality biomonitoring using the standard grass species *Lolium multiflorum* in a mining region located in the city of Brumadinho, metropolitan region of Belo Horizonte, in the state of Minas Gerais, Brazil.

METHODS

Biomonitoring was actively conducted in March and April of 2024, with grass cultivation and exposure following the VDI 3957 - part 2 standard (2003) (adapted). The plants were cultivated for 3 weeks before exposure in a natural reserve selected as a reference site (S4) and exposed for 28 days at 3 sampling points in Brumadinho: S1 - City center, S2 - Tejuco neighborhood, surrounded by mining sites, S3 - an Indigenous community area near a ferry line used for mining ore transportation.

Plant growth was observed during the exposure period. Subsequently, they were manually cut and subjected to laboratory analyses to evaluate the presence of metals, following EPA 3050B (1996) (adapted). The plant material was submitted to wet-opened digestion with a HNO_3 and H_2O_2 solution (1:1), and the extracts will be analyzed by ICP-OES.

In addition to plant exposure, fine particulate matter (<2.5 micrometers in diameter; $PM_{2.5}$) were sampled using a medium-volume sampler (ARA Instrument) equipped with quartz filters. $PM_{2.5}$ sampling was carried out for 24 hours in the same locations of plant exposure, throughout the exposure period. Subsequently, the $PM_{2.5}$ concentration was determined by gravimetric method (INPE, 2012), and the concentration of metals using the aforementioned methodology. Results were submitted to statistical analysis by Kruskal-Wallis analysis of variance followed by Dunn's mean test.

FINDINGS AND ARGUMENT

The concentration of particulate matter $PM_{2.5}$ varied among the sampling sites, with a maximum of 43.77 µg/m³ in the Indigenous community area (S3) and a minimum of 16.23 µg/m³ in the reference area (S4). Figure 1 illustrates the variation found among the monitoring points in the city of Brumadinho and the comparison with air quality reference value of WHO (2021).

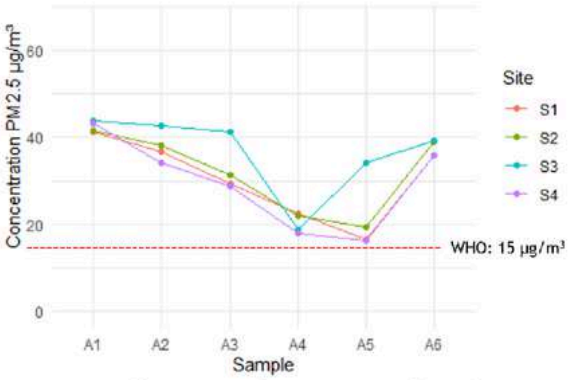


Figure 1. Illustrates the variation found among the monitoring points in the city of Brumadinho compared with WHO air quality reference value (2021) (15 µg/m³ in 24 hours).

All samples exceeded the WHO reference value for $PM_{2.5}$. This suggests poor air quality in the region, requiring more attention to monitoring and source control. Furthermore, it is important to highlight that PM concentrations are also associated with other factors, such as climatic conditions, and correlation studies with such factors should be performed.

S3 showed the highest median of 40.15 µg/m³ among the sampling points (Figure 2). The lowest median was at the reference point (S4) of 31.40 µg/m³. However, there was no significant differences according to the Kruskal-Wallis test ($p<0.05$).

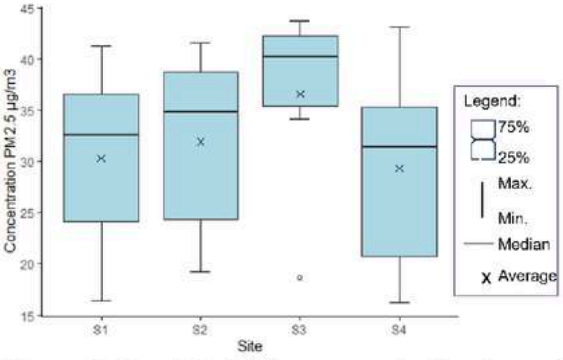


Figure 2. Boxplot of $PM_{2.5}$ concentration in each monitoring point.

Site 3 represents an Indigenous community area located near the ore loading and transportation area. Additionally, the region was affected by the tailings dam collapse on January 26th, 2019. So, it still suffers the consequences of tailings deposit in the region. Such factors may be associated with the resuspension of contaminated particulate matter. However, further studies should be conducted to test this hypothesis, such as studies involving soil sampling.

The preliminary qualitative analysis of plants (visual analysis) contributed to an initial understanding of the impacts of air pollution to bioindicators, as toxic components can cause biomass reduction, growth inhibition, and organism death (Ghosh; Dutta; Mukhopadhyay, 2023). Figure 3 demonstrates the state of plants exposed in each of the sampling sites after 28 days.



Figure 3. Visual plants after exposure in each of the sampling sites after 28 days.

It can be observed that plants exposed in Points 2 and 3 exhibited more leaf injuries and are smaller than the other points. Borowiak *et al.* (2020) noted that the accumulation of trace elements presents in the atmosphere in ryegrass reduced the net photosynthesis rate and stomatal conductance of the plants.

Although S3 presented the highest PM concentrations, it is worth noting that the plants were exposed in a wooded area and toxic elements may have encountered barriers in taller plants compared to the sampler. Thus, the analysis of metals in ryegrass leaves will provide more elaborate data for understanding metal contamination at this and the other sampling sites.

CONCLUSIONS

Preliminary analyses demonstrate that particulate matter concentration may influence plant development, taking into consideration other processes such as land use in the surroundings. The high concentrations of particulate matter in the city of Brumadinho reflect air pollution in urban areas influenced by mining.

Analyses of metals in plants leaves and quartz filters will be used to better discuss the relationships between atmospheric pollutant concentration and ecosystem health. Biomonitoring data along with chemical characterization will be of great significance in devising strategies for controlling and mitigating pollution.

REFERENCES

Arsenic, Aluminum Magnesium, et al. "Method 3050B acid digestion of sediments, sludges, and soils 1.0 scope and application." *Washington, DC, USA* (1996).

Borowiak, Klaudia, et al. "Accumulation of airborne toxic elements and photosynthetic performance of Lolium multiflorum L. leaves." *Processes* 8.9 (2020): 1013.

Bulbovas, Patricia, Carla ZS Camargo, and Marisa Domingos. "Ryegrass cv. Lema and guava cv. Paluma biomonitoring suitability for estimating nutritional contamination risks under seasonal climate in Southeastern Brazil." *Ecotoxicology and Environmental Safety* 118 (2015): 149-157.

Nakazato, Ricardo Keiichi, et al. "Efficiency of biomonitoring methods applying tropical bioindicator plants for assessing the phytoxicity of the air pollutants in SE, Brazil." *Environmental Science and Pollution Research* 25 (2018): 19323-19337.

De Temmerman, Ludwig, and Michel Hoenig. "Vegetable crops for biomonitoring lead and cadmium deposition." Journal of Atmospheric Chemistry 49 (2004): 121-135.

Ferreira, Tatiane Morais, Maria Cristina Forti, and Plinio Carlos Alvala. "Protocolo para coleta de material particulado atmosférico." *INPE, São José dos Campos* (2012).

Ghosh, Sayantan, Ratna Dutta, and Shritama Mukhopadhyay. "A Review on Seasonal Changes in Particulate Matter Accumulation by Plant Bioindicators: Effects on Leaf Traits." *Water, Air, & Soil Pollution* 234.8 (2023): 529.

Klumpp, Andreas. "European network for the assessment of air quality by the use of bioindicator plants. LIFE99 ENV/D/000453". University of Hohenheim. 2003.

Multisanti, Cristiana Roberta, et al. "Sentinel species selection for monitoring microplastic pollution: A review on one health approach." Ecological Indicators 145 (2022): 109587.

Theophilo, Carolina Yume Sawamura, et al. "Biomonitoring as a Nature-Based Solution to Assess Atmospheric Pollution and Impacts on Public Health." Bulletin of Environmental Contamination and Toxicology 107 (2021): 29-36.

VDI - Verein Deutscher Ingenieure. "Biological Measuring Techniques for the Determination and Evaluation of Effects of Air Pollutants on Plant (Bioindication). Method of Standardized Grass Exposure. VDI-Guideline 3957 Part 2. *Beuth Verlag, Berlin*, 2003.

WHO. "Air quality and health. Type of pollutants." *Available at: Air quality and health (who.int)*. Accessed on March 8, 2024.

WHO. "WHO global air quality guidelines." *Particulate Matter (PM2.5 and PM10), Ozone, Nitrogen Dioxide, Sulfur Dioxide and Carbon Monoxide* (2021).

AIR POLLUTION CONFERENCE BRAZIL
CMAS SOUTH AMERICA
COMMUNITY MODELING AND ANALYSIS SYSTEM

SOCIOENVIRONMENTAL VULNERABILITIES AND AIR POLLUTION IN THE CITY OF SÃO PAULO FROM 2019 TO 2023

Vinícius de Souza Oliveira[1], Paulo Eduardo Alves Camargo-Cruz[2], Regina Maura de Miranda[3]
[1]*Escola de Artes, Ciências e Humanidades, Universidade de São Paulo*
vinicius_so@usp.br
[2]*Escola de Artes, Ciências e Humanidades, Universidade de São Paulo*
negresse@usp.br
[3]*Escola de Artes, Ciências e Humanidades, Universidade de São Paulo*
remaura@usp.br

Abstract: It's inherent that air quality has been a highly discussed and researched topic over time, becoming a determining environmental indicator. Thus, this study aimed to analyze the possible relationship between air quality in the city of São Paulo and the socioeconomic and environmental conditions of its inhabitants from 2019 to 2023. The indicators of socioenvironmental vulnerability from the map of inequality and the annual average concentrations of PM_{10} (inhalable particles), $PM_{2.5}$ (fine inhalable particles), NO_2 (nitrogen dioxide), and O_3 (ozone) were correlated using the Spearman method in the Statistica software. Few events with high correlation between pollution parameters and vulnerability indicators were observed, which may indicate a low correlation between the sample data. Despite low values, the correlations provide an indication that socio-environmental vulnerabilities may be influenced by poor air quality, as 36% of the results obtained correspond to strong or moderate correlations, with higher values for the correlation of NO_2 with the proportion of black people (-0.708) and formal employment opportunities (0.737), indicating these as factors that intensify the correspondence to possible disturbances in areas where NO_2 concentrations are higher and with low formal employment opportunities for black people. Thus, the relevance of the topic must be emphasized in scientific production, political discussions, and public awareness, especially among the most vulnerable populations.

Keywords: Socioenvironmental vulnerabilities, São Paulo, atmospheric pollution, Spearman correlation.

INTRODUCTION

Exposure to atmospheric pollutants produced in cities is one of the factors contributing to poor quality of life in urban centers. It is inherent that air quality has been a much discussed and researched topic over time, becoming a determining environmental indicator (Russo, 2010). Thus, this study aimed to analyze the possible relationship between air quality in the city of São Paulo and the socioeconomic and environmental conditions of its inhabitants from 2019 to 2023.

Air pollution is linked to respiratory diseases, cardiovascular diseases, central nervous system diseases, premature births, among other aggravating factors. Environmental impact should also be considered, such as climate changes, leading to ecological imbalances (Abe and Miraglia, 2016).

In addition to industrial activities, urban "immobility" should be highlighted as a triggering factor for high concentrations of pollutants, responsible for about 60% of the pollutants people breathe in cities (Andrade *et al.*, 2012; Saldiva, 2018).

There is a gap in understanding how air pollution can affect people according to their position in society, considering aspects that characterize their level of socioenvironmental vulnerability (Castelhano, 2021). Some case studies have delved into this line of research, such as studies conducted in Uganda, Africa (Clark *et al.*, 2022), and in New Jersey, United States (Sabrin *et al.*, 2020). In Brazil, a notable study related economic inequalities to exposure to pollutants generated by vehicular traffic in São Paulo (Habermann *et al.*, 2014).

In this study, it was possible to identify correlations at different levels for the concentrations of PM_{10}, $PM_{2.5}$, NO_2, and O_3 and the variables selected through Spearman's correlation. Despite the presence of low values, the correlations provide an indication that socioenvironmental vulnerabilities may be influenced by poor air quality, where 36% of the results obtained correspond to strong or moderate correlations.

With higher values for the correlation of NO_2 with the proportion of black people (-0.708) and formal employment opportunities (0.737), this finding may indicate that these factors intensify the correspondence to possible disturbances in areas where NO_2 concentrations are higher and with low formal employment opportunities for black people. Thus, the relevance of the topic must be emphasized in scientific production, political discussions, and public awareness, especially among the most vulnerable populations.

METHODS

The exploratory research was limited to the Web of Science database, without data systematization. The selection of socioeconomic indicators (Table 1)

was made based on the understanding of risk, susceptibility, and exposure to atmospheric pollutants (Ge *et al.*, 2017).

Table 1. Socioeconomic indicators

Variable	
1	Female population
2	Black population
3	Average time for consultations in Primary Care (SUS)
4	Mortality from respiratory system diseases
5	Formal employment opportunities
6	Average monthly income from formal employment
7	Shantytowns

Reference: RNSP, 2019, 2020, 2021, 2022, 2023.

The data for the indicators were obtained through the annual publications of the Map of Inequality campaign by the Rede Nossa São Paulo (RNSP). The average concentrations of the analyzed parameters - PM_{10}, $PM_{2.5}$, NO_2, and O_3 - were obtained from the QUALAR system and the air quality reports by the Environmental Company of the State of São Paulo (CETESB) published from 2019 to 2022. For the year 2023, the monthly average concentrations published in CETESB's monthly bulletins were used.
To analyze the possible relationship between the parameters and indicators, Spearman correlation was conducted using the Statistica software, which statistically compares the selected independent variables by revealing the degree of association between them (Bermúdez Pastor, 2023; Xiao *et al.*, 2015).

FINDINGS AND ARGUMENT

Few events with high correlation between pollution parameters and vulnerability indicators were observed, which may indicate a low correlation between the sample data. However, there is a possible indication that NO_2 is the pollutant with the highest correlation with the indicators (Table 2).
Within a 95% confidence interval and a significance level of 5%, the average concentration of NO_2 in the study period indicates a high negative correlation with the black and brown population (-0.708), suggesting a possible vulnerability of the black and brown population to NO_2 exposure. Using the same criteria, the correlation with the indicator of formal employment opportunities showed a high positive correlation (0.737), indicating a relationship with NO_2 concentration.
In this regard, it is inferred that the black population residing in districts of São Paulo where there are higher concentrations of NO_2, such as Campo Belo and Vila Leopoldina districts, with average concentrations of 62 and 54 µg/m³, and approximately 12.21% and 14.41% of black residents, respectively, over a five-year period.
Furthermore, for these districts, the employment opportunities were at median and high rates compared to other districts, with 8.75 and 14.86, respectively, per ten participants in the labor force aged fifteen years or older, indicating that it may not negatively influence the vulnerability of its inhabitants.
The correlation between $PM_{2.5}$ and the average monthly income from formal employment also showed a high negative correlation coefficient (-0.506), indicating a relationship between the average $PM_{2.5}$ concentration monitored by CETESB and the indicator of average monthly income from formal employment.
It is observed that the highest concentration of $PM_{2.5}$ during the analyzed period was found in the Vila Leopoldina district, with an average of 18 µg/m³, while the lowest occurred in Santo Amaro, with an average value of 12 µg/m³. The average monthly salary for formal employment was R$ 3,890.00 for Vila Leopoldina and R$ 4,854.27 for Santo Amaro, which does not capture a clear relationship between pollutant concentration and the indicator.

Table 2. Correlation coefficients

Variable	NO_2	O_3	$MP_{2,5}$	MP_{10}
1	0.301	-0.093	-0.425	-0.403
2	-0.708	-0.090	0.266	0.274
3	0.192	0.233	0.063	-0.240
4	-0.177	-0.159	0.250	0.374
5	0.737	0.031	-0.037	-0.039
6	0.396	0.108	-0.506	-0.319
7	-0.529	0.163	0.192	0.055

**The marked values are the correlation coefficients found within a 95% confidence interval and 5% significance level.*

The data collection process was challenging due to the limited census data collected by institutions such as the Instituto Brasileiro de Geografia e Estatística (IBGE). Therefore, the data analysis may have resulted in few correlation coefficients with a 95% confidence interval due to data scarcity, which was one of the main barriers to conducting this research. Due to the limited number of studies conducted in Brazil on this topic, access to research that could contribute to the interpretation of these results is also limited, highlighting the need for more studies as this one.

CONCLUSIONS

The relationship between atmospheric pollution and socioenvironmental vulnerabilities indicates that few of the sampled data are well correlated. It is inferred that further statistical analyses may be necessary for a better visualization of the possible relationship between the parameters and selected indicators.

The reliance on the publication of open data regarding the characteristics of the population and city infrastructure posed challenges in conducting the study. On the other hand, campaigns monitoring the spatial characterization of cities and their inhabitants, such as the Map of Inequality, are essential for understanding reality.

Finally, these preliminary results could already suggest the creation of an index of socioenvironmental vulnerability to atmospheric pollution. This tool could aid in understanding the relationship between socioenvironmental vulnerabilities and atmospheric pollution in cities, contributing to public agendas and measures for managing issues related to poor air quality.

REFERENCES

Abe, Carina C., and Simone G. El K. Miraglia. "Health Impact Assessment of Air Pollution in São Paulo, Brazil." *Int. J. Environmental Research and Public Health* 694 (2016): 1-10. Acessed May 03, 2024. doi: 10.3390/ijerph13070694.

Andrade, Maria de F., Regina M. de Miranda, Adalgiza Fornaro, Americo Kerr, Beatriz Oyama, Paulo A. de Andre and Paulo Saldiva. "Vehicle emissions and PM2.5 mass concentrations in six Brazilian cities." *Air Qual Atmos Health* 5 (2012): 79-88. Acessed May 03, 2024. doi: 10.1007/s11869-010-0104-5.

Bermúdez Pastor, Pablo. "Contaminación atmosférica y vulnerabilidad social en la ciudad de Madrid." *Revista Internacional de Ciencia y Tecnología de la Información Geográfica* 31 (2023): 115-145. Acessed May 03, 2024. doi: 10.21138/GF.797.

Castelhano, Francisco J. "Riscos e vulnerabilidades sob a perspectiva da qualidade do ar." *Finisterra* 56 (2021): 253-269. Acessed May 03, 2024. doi: 10.18055/Finis20231.

CETESB. "Qualidade do ar no estado de São Paulo 2019-23" *CETESB* (2020-3). Acessed May 03, 2024.

Clarke, Kayan, Kevin Ash, Eric S. Coker, Tara Sabo-Attwood and Engineer Bainomugisha. "A Social Vulnerability Index for Air Pollution and Its Spatially Varying Relationship to PM2.5 in Uganda." *Atmosphere* 13 (2022): 1-16. Acessed May 03, 2024. doi: 10.3390/atmos13081169.

Ge, Yi, Haibo Zhang, Wen Dou, Wenfang Chen, Ning Liu, Yuan Wang, Yulin Shi and Wenxin Rao. "Mapping Social Vulnerability to Air Pollution: A Case Study of the Yangtze River Delta Region, China." *Sustainability* 109 (2017): 1-15. Acessed May 03, 2024. doi: 10.3390/su9010109.

Habermann, Mateus, Míriam Souza, Rogério Prado and Nelson Gouveia. "Socioeconomic inequalities and exposure to traffic-related air pollution in the city of São Paulo, Brazil." *Cad. Saúde Pública* 30 (2014): 119-125. Acessed May 03, 2024. doi: 10.1590/0102-311X00168412.

RNSP, Rede Nossa São Paulo. "Mapa da desigualdade 2019-23". *Rede Nossa São Paulo* (2020-24). Acessed May 03, 2024.

Russo, Paulo R. "A qualidade do ar no município do Rio de Janeiro: análise espaço-temporal de partículas em suspensão na atmosfera." *Revista de Ciências Humanas* 1 (2010): 78-93.

Sabrin, Samin, Maryam Karimi e Rouzbeth Nazari. "Developing Vulnerability Index to Quantify Urban Heat Islands Effects Coupled with Air Pollution: A Case Study of Camden, NJ." *International Journal of Geo-Information* 9 (2020): 1-14. Acessed May 03, 2024. doi:10.3390/ijgi9060349.

Xiao, Chengwei, Jiaqi Ye, Rui M. Esteves and Chunming Rong. "Using Spearman's correlation coefficients for exploratory data analysis on big dataset" *Concurrency Computat.: Pract. Exper.* 28 (2015): 3866-3878. Acessed May 03, 2024. doi: 10.1002/cpe.3745.

AIR POLLUTION CONFERENCE BRAZIL
CMAS SOUTH AMERICA
COMMUNITY MODELING AND ANALYSIS SYSTEM

ASSESSMENT OF AİRBONE MERCURY LEVELS İN PRESERVED AND ANTHROPOGENİCALLY İMPACTED AREAS (RİO DE JANEİRO STATE, BRAZIL)

Luis Fhernando Mendonça da Silva[1], Caio da Silva Assis Felix[4,6], Rodrigo Stellet Ferreira[2], Hellen Gonçalves da Silva[2], Maria Cristina Canela[2], Cibele Maria Stivanin de Almeida[2], Luiz Francisco Pires Guimarães Maia[3], Gisele Olímpio da Rocha[4,5,6,7], Jailson Bittencourt de Andrade[4,5,6,7], Renato da Silva Carreira[1], Adriana Gioda[1].

[1] Pontifical Catholic University of Rio de Janeiro (PUC-Rio), Departamento de Química. 22451-900 Rio de Janeiro-RJ, Brazil
agioda@puc-rio.br

[2] Universidade Estadual do Norte Fluminense Darcy Ribeiro (UENF), Centro de Ciência e Tecnologia, Laboratório de Ciências Químicas. Campos dos Goytacazes-RJ-Brazil

[3] Universidade Federal do Rio de Janeiro (UFRJ), Departamento de Meteorologia, Instituto de Geociências, Rio de Janeiro, Brasil

[4] Centro Interdisciplinar de Energia e Ambiente-CIEnAm, Universidade Federal da Bahia, 40170-115, Salvador, BA, Brazil

[5] Universidade Federal da Bahia, Instituto de Química, Programa de Pós-Graduação em Química, 40170-115, Salvador, BA, Brazil

[6] Instituto Nacional de Ciência e Tecnologia em Energia e Ambiente-INCT E&A, Universidade Federal da Bahia, 40170-115, Salvador, BA, Brazil

[7] Centro Universitário SENAI-CIMATEC, Av. Orlando Gomes, 1845 Piatã, 41650-010, Salvador, BA, Brazil

Abstract: Although present in low concentrations in the atmosphere, mercury in particulate matter (PM) plays an important role in the biogeochemical process of mercury. With this in mind, this study aims to investigate mercury concentrations in particulate matter ($PM_{2.5}$) samples from the regions of Campos dos Goycatazes (CG), Gávea (GA) and Serra dos Órgãos National Park (PARNASO). All samples were collected according to Brazilian standards (ABNT-NBR 9547/86) and the methods of the United States Environmental Protection Agency (US EPA) (Method IO - 2.1). PM concentrations were determined by gravimetric technique. The Direct Mercury Analyzer (DMA-80, Milestone Helpind Chemists) was used for total Hg analysis. Daily $PM_{2.5}$ concentrations ranged from 13 to 36 μg m^{-3}, with a mean of 24 ± 12 μg m^{-3} for the GA region, and from 24 to 46 μg m^{-3}, with a mean of 33 ± 12 μg m^{-3} for the PARNASO region, and from 14 to 19 μg m^{-3}, with a mean of 17 ± 11 μg m^{-3} for the CG for the days sampled from July to October 2022. High levels of PM concentrations at PARNASO indicate a contribution from anthropogenic sources. Considering these values, no day sampled exceeded the value suggested by Brazilian legislation (60 μg m^{-3}), but 65 % of the samples showed higher daily concentrations than suggested by World Health Organization (WHO, 15 μg m^{-3}). Hg concentrations ranged from 223 to 366 pg m^{-3}, with a mean of 274 ± 65 pg m^{-3} for the GA region, and from 119 to 190 pg m^{-3}, with a mean of 155 ± 29 pg m^{-3} for the PARNASO region, and from 164 to 315 pg m^{-3}, with a mean of 258 ± 67 pg m^{-3} for the CG for the days sampled. Hg concentrations in the atmosphere showed significant spatial variation, with much higher values in urban areas than in the natural zone. The results showed that Hg concentrations in particulate matter are at the same level as those found in urban and industrial areas in US and northern Europe. At Parnaso, the presence of Hg may be due to anthropogenic sources, which may be local sources and/or long-range transport contributions. There exists an intriguing meteorological facet warranting consideration, pertaining to the atmospheric transport facilitated by mountain-valley interactions and sea-land breezes within the southern region of the Serra dos Órgãos. This phenomenon merits further in-depth exploration. In addition, the high concentrations of Hg found in Campos dos Goytacazes may be associated with the burning of biomass, since sugar cane is burned throughout the year in the region and also due to the application of pesticides in the most diverse crops in the municipality, many times without due control.

Keywords: Mercury, particulate matter, $PM_{2.5}$, Rio de Janeiro.

INTRODUCTION

Mercury (Hg) is a pervasive environmental contaminant with significant repercussions for both human health and ecosystems globally. Its persistence, ability to accumulate in organisms, and capability for long-distance atmospheric movement make it a particularly concerning pollutant. Mercury exists in various forms, such as elemental mercury (Hg^0), reactive gaseous mercury (RGM), and particle-bound mercury (PHg). Of these, PHg is of particular concern because it can settle into ecosystems and water bodies. Once there, it undergoes transformations, ultimately converting into methylmercury—a potent neurotoxin easily absorbed by aquatic organisms and subsequently magnified through the food chain (Galappaththi and Suraweera 2020; Henriques et al. 2019).

A comprehensive comprehension of particle-bound mercury dynamics, encompassing its sources, transport mechanisms, and deposition patterns, is

essential for crafting effective mitigation strategies to alleviate its harmful effects (Brocza et al. 2024). This study seeks to enhance our understanding of these dynamics by specifically focusing on quantifying concentrations, delineating seasonal variations, and discerning potential emission sources on both a global scale and within the context of Brazil. By delving into these aspects, we aim to provide insights crucial for developing targeted interventions to address the adverse impacts of particulate mercury on ecosystems and human health.

METHODS

$PM_{2.5}$ samples were collected from three monitoring sites situated at Gávea (GÁVEA, 22°58'50" S and 43°13'58" W), Campos dos Goytacazes (CAMPOS, 21°45'39.1''S 41°17'31.1'' W), and the Serra dos Órgãos National Park (PARNASO, 22°29'47.5'' S and 43°00'05.2'' W) (Fig. 1) from July to October 2022. $PM_{2.5}$ samples were gathered employing quartz microfiber filters with a pore size of 1.6 µm (Whatman, Fisher Scientific, Maidstone, United Kingdom) over 24 hours, monthly, utilizing monitoring equipment following Brazilian standards (ABNT-NBR 129 9547/86) and methods outlined by the United States Environmental Protection Agency (US EPA) under method 130 (Method IO – 2.1). This process utilized a High-Volume air sampler (Hi-Vol 3000, Energética, Sao Paulo, Brazil) with an average air flow rate of 1.07 m^3 per minute. The filters underwent a conditioning process in a desiccator for 24 hours and they were subjected to gravimetric analysis before and after the sampling sessions using an analytical balance (Gehaka AG200 ± 0.0001, Marte Científica, Brazil) to ensure accurate measurement of particulate mass. The relative humidity levels were maintained between 20 % and 30 %, and temperatures ranged from 20 °C to 25 °C during the filter weighing procedures. This study examined all available $PM_{2.5}$ samples to assess their particulate mass content.

Total Hg concentrations in $PM_{2.5}$ were determined using a Direct Mercury Analyzer - DMA-80 (Milestone, Sorisole (BG), Italy).

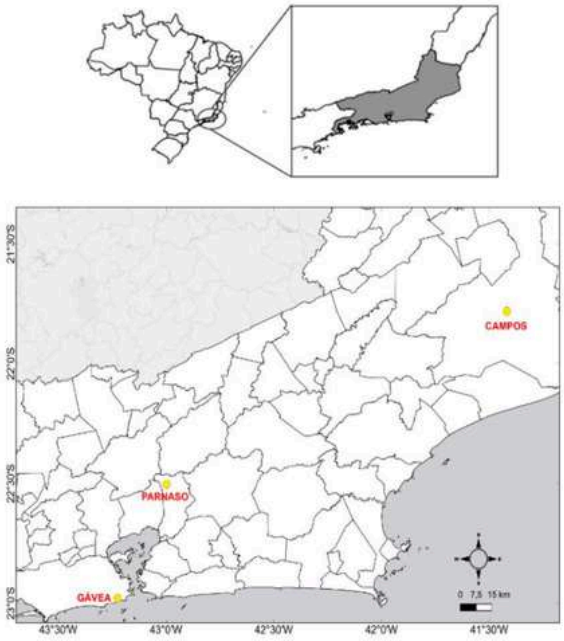


Figure 1. $PM_{2.5}$ monitoring stations: GAVEA: Gávea, PARNASO: Serra dos Órgãos National Park, and CAMPOS: Campos dos Goytacazes.

FINDINGS AND ARGUMENT

The average concentration of $PM_{2.5}$ in Gávea was 24±12 µg m^{-3} (with values ranging from 13 to 36 µg m^{-3}, in PARNASO, it was 33±12 µg m^{-3} (with values ranging from 24 to 46 µg m^{-3}), and in Campos, it was 17±11 µg m^{-3} (with values ranging from 14 to 19 µg m^{-3}). Given these values, none of the days sampled exceeded the threshold recommended by Brazilian regulations (60 µg m^{-3}). However, 65 % of the samples exhibited daily concentrations surpassing the guidelines set by the WHO (15 µg m^{-3}).

$PM_{2.5}$ concentrations were observed to be relatively elevated during the dry season (July - August) in contrast to the wet season (September-October). This pattern has been documented in numerous prior studies (Beringui et al. 2021; De La Cruz et al. 2024; Mateus et al. 2013). Many researchers attribute this phenomenon to the cleansing impact of rainfall, which captures and deposits suspended particles in the atmosphere.

The average PHg concentrations (range) were 274±65 (223–366) pg m^{-3}, 155±29 (119–190) pg m^{-3} and 258±67 (164–315) pg m^{-3} at the urban region of the capital, interior with sugarcane burning and forest sites during the sampling period, respectively. The average concentration of PHg in the urban with sugarcane burning (CAMPOS) and

forest (PARNASO) sites was approximately two times higher than in the urban site (GAVEA).

The results showed that PHg concentrations at urban sites in coastal cities are considerably lower than those in other cities, such as Gávea. The surface winds in coastal areas influence the concentrations of PM in these regions (Wang et al. 2023). PHg concentrations in urban areas were 5.9-11.3 times higher than the nearby values found in Asian countries (Xu et al. 2019), and North America (Detroit, USA) (Liu et al. 2007), indicating that a large amount of anthropogenic mercury has been released into the atmosphere in Brazil.

The highest levels of PHg were found in Campos and PARNASO, while the lowest concentrations of PHg were present in Gavea. The high concentration of PHg at the sites may be associated with anthropogenic emissions. In Campos, the most significant contributions may come from vehicular traffic, the port area and, above all, the burning of sugar cane. PARNASO, despite being an environmental conservation area, usually receives many visitors to the park, with vehicles being the primary commuter. In addition, it is less than 200 m away from BR-116, one of the main avenues linking the metropolitan region of Rio de Janeiro to the Serra and other states in the country, with heavy vehicle traffic.

CONCLUSIONS

During the sampling period, it was observed that $PM_{2.5}$ concentrations varied among the locations under study. In Gávea, PARNASO, and Campos, the average concentrations remained within acceptable limits as per Brazilian regulations, with none exceeding the specified threshold. However, a significant proportion of samples from all locations exceeded the daily concentration standards recommended by the World Health Organization, raising potential health concerns.

Mercury concentrations also exhibited variations across different environments, with higher levels detected in areas associated with sugarcane burning compared to urban and preserved sites. Urban fire sites recorded the highest mercury levels, surpassing those in both urban and preserved areas.

REFERENCES

Beringui, Karmel et al. 2021. "Assessment of the Concentration and Inorganic Composition of Particulate Matter Collected in the State of Rio De Janeiro." *Quimica Nova* 44(6): 737–54.

Brocza, Flora Maria et al. 2024. "Global Scenarios of Anthropogenic Mercury Emissions." *EGUsphere [preprint]* (41). https://doi.org/10.5194/egusphere-2024-4 (February 21, 2024).

Galappaththi, Himan K.A., and Inoka Suraweera. 2020. "Risk of Mercury Exposure during Childhood: A Review of Sri Lankan Situation." *Reviews on Environmental Health* 35(3): 229–32. https://www.degruyter.com/document/doi/10.1515/reveh-2020-0024/html (January 31, 2024).

Henriques, Magda Carvalho, Susana Loureiro, Margarida Fardilha, and Maria Teresa Herdeiro. 2019. "Exposure to Mercury and Human Reproductive Health: A Systematic Review." *Reproductive Toxicology* 85: 93–103.

De La Cruz, Alex H. et al. 2024. "Black Carbon and Particulate Matter Concentrations: Air Pollution Levels in Rio de Janeiro, Brazil." *Article J. Braz. Chem. Soc.* 35: 1–12. https://dx.doi.org/10.21577/0103-5053.20240029 (March 31, 2024).

Liu, Bian et al. 2007. "Temporal Variability of Mercury Speciation in Urban Air." *Atmospheric Environment* 41: 1911–23. www.elsevier.com/locate/atmosenv (February 1, 2024).

Mateus, Vinícius Lionel et al. 2013. "Study of the Chemical Composition of Particulate Matter from the Rio de Janeiro Metropolitan Region, Brazil, by Inductively Coupled Plasma-Mass Spectrometry and Optical Emission Spectrometry." *Spectrochimica Acta Part B: Atomic Spectroscopy* 86: 131–36.

Wang, Ju et al. 2023. "Impact Analysis of Meteorological Variables on PM2.5 Pollution in the Most Polluted Cities in China." *Heliyon* 9(7): e17609.

Xu, H. M. et al. 2019. "Mercury Stable Isotope Compositions of Chinese Urban Fine Particulates in Winter Haze Days: Implications for Hg Sources and Transformations." *Chemical Geology* 504: 267–75.

AIR POLLUTION CONFERENCE BRAZIL
CMAS SOUTH AMERICA
COMMUNITY MODELING AND ANALYSIS SYSTEM

Comprehensive Evaluation of MAIAC 1km AOD Product for $PM_{2.5}$ Estimation in Latin American Urban Areas

Sebastian Diez[1] Josefina Urquiza[2,3],
[1]*Universidad del Desarrollo, Chile*
sebastian.diez@udd.cl
[2]*Grupo de Estudios de la Atmósfera y el Ambiente (GEAA), Universidad Tecnológica Nacional, Facultad Regional Mendoza (UTN-FRM)*
jurquiza@conicet.gov.ar
[3]*Consejo Nacional de Investigaciones Científicas y Técnicas (CONICET)*

Abstract: In Latin America, limited PM2.5 monitoring stations hinder air quality assessment and understanding health impacts. This study utilizes the Aerosol Optical Depth (AOD) measured by satellite platforms, particularly focusing on the MAIAC product with its high spatial resolution (1 km), often used as a PM proxy. Our aim is to evaluate the uncertainty of the MAIAC 1km product in six densely populated cities: Sao Paulo, Santiago, Buenos Aires, Medellín, La Paz, and México, over 2015-2022. We employed typical global metrics (R2, RMSE, bias) and the detailed Relative Expanded Uncertainty (REU) for a comprehensive assessment. Unlike common metrics, REU provides insights into the error structure across the AOD's dynamic range. Our findings indicate relatively low AOD values (< 0.2) with moderate correlation (R < 0.6) with AERONET sun photometers. In the AOD range of 0.05 to 0.15, the relative uncertainty exceeded 50% for all locations. Additionally, we compared MAIAC with the MODIS DT 3km product, finding consistently lower uncertainties (REU~20-30%) for MODIS in the same dynamic range. Despite MAIAC showing slightly better RMSE and R2 (~0.08 and ~0.55) than MODIS (~0.1 and ~0.49), regression analysis revealed a greater bias in MAIAC. We conclude that at lower aerosol loads, the MAIAC algorithm exhibits higher uncertainty and bias compared to MODIS DT, highlighting the importance of considering uncertainties when using AOD products for PM estimation and spatial PM2.5 distribution characterization.

Keywords: MAIAC 1km, AOD, Uncertainty, Latin American cities.

INTRODUCTION

Aerosols are solid and liquid particles suspended in the atmosphere originating from both natural and anthropogenic sources (Liu & Yi, 2022). These particles play a significant role in climate change, air quality and human health. Therefore, understanding the distribution and variation of aerosols in different regions is essential for improving human quality of life. Aerosol Optical Depth (AOD) is an indicator used in the study of particles, as it provides a quantitative measure of the amount of direct sunlight that is blocked on its way to the Earth's surface due to the scattering and/or absorption of atmospheric aerosols. The global network of solar photometers, AERONET, offers measurements at the surface with a sampling frequency of 15 minutes. However, the limited number of stations restricts its application to regional and local studies. In contrast, satellite product typically provides information with global coverage but with a more limited temporal resolution due to the satellite's pass frequency. This is the case with the Multi-Angle Implementation of Atmospheric Correction (MAIAC) product, which retrieves AOD with a spatial resolution of 1 km and daily temporal resolution for studying urban air quality (Lyapustin et al., 2018).

In recent years, MAIAC has been widely used globally due to improvements in the spatial resolution of aerosol products, primarily serving as a proxy for particulate matter (PM) (Damascena et al., 2021). Comprehensive evaluations of MAIAC have been conducted on both global (Qin et al., 2021) and regional scales (Martins et al., 2017). Results have shown good agreement with surface measurements, with some differences depending on land use and aerosol levels. In Latin America, several countries are in a position of increased vulnerability due to scarce or none existent air quality measurements (Carmona et al., 2021; Pinder et al., 2019), making it difficult to determine aerosol behaviour and distribution at local and regional scales. In countries lacking extensive monitoring networks, MAIAC could be useful for deriving indirect estimates of $PM_{2.5}$ in the air from aerosol optical properties, overcoming spatial limitations of traditional measurements. Such estimates can be seen as a complementary and cost-effective method for $PM_{2.5}$ monitoring (Carmona et al., 2021). Several studies have evaluated MAIAC's performance in different Latin American locations. However, in situations using proxies to estimate PM2.5, there's a lack of comprehensive quantitative analysis on uncertainty. This absence could lead to potentially inappropriate use of satellite products and improper conclusions (Sayer et al., 2020). Given that surface characteristics and aerosol properties are unknown and must be evaluated as part of the retrieval process, inherent uncertainty arises, making it difficult to distinguish true spatiotemporal aerosol variability. Therefore, the aim is to evaluate the uncertainty of the MAIAC 1km product in six densely populated cities: São Paulo, Santiago, Buenos Aires, Medellín, La Paz, and Mexico, over the period 2015-2022.

AIR POLLUTION CONFERENCE BRAZIL

CMAS SOUTH AMERICA

COMMUNITY MODELING AND ANALYSIS SYSTEM

METHODS

The AOD data were acquired from the surface network of the AERONET, using L2.0 level records available for the period 2015-2022 for: São Paulo (SP), Santiago (ST), Buenos Aires (BA), Medellín (MD), La Paz (LP), and Mexico (MX). These sites were selected considering their location in major Latin American cities and the availability of measurements. Since the data bands provided by AERONET do not match those of the satellite product, interpolation was performed to obtain AOD_{550} using the Ångström exponent at wavelengths close to 500 and 675 nm. Regarding the satellite product, MCD19A2 was used, which provides AOD at 550 nm. Multiple tiles were downloaded from the Terra and Aqua missions in Hierarchical Data Format (HDF) and the images were filtered by selecting those of better quality (QA = 0000). Subsequently, a performance evaluation was carried out by comparing the space-time (1 km² - 60 min) of both satellite datasets C6.0 and C6.1 using the AERONET network as a reference to analyze the associated uncertainty and the modifications made in the algorithm. To evaluate performance, typical global metrics (R^2, RMSE, bias) were used, and a more detailed metric called Relative Expanded Uncertainty (REU) was used for a more comprehensive assessment of performance.

FINDINGS AND ARGUMENT

The Figure 1 shows the temporal evolution of AERONET AOD_{550} between 2015 and 2022, obtained from daily averages. A significant lack of data is observed, especially in MD (48.5%) and MX (15.3%), while in other locations, this deficiency is less than 13%. AOD levels for the region are generally low (<0.2), with higher values in MX and MD. Although most AOD levels are close to the average, there is greater dispersion in MX and possibly less in BA and LP. No clear cycle is evident in the temporal patterns, with variable peaks at each location. Peaks with maximum aerosol load levels greatly exceed the period's averages, especially in ST, LP, MX, MD, and SP, where increases of up to six times higher than the mean levels are observed. Similar trends to previous research are observed, such as seasonal increases during the summer attributed to factors like biomass burning and regional transport of combustion products. In SP and BA, these increases could be due to long-distance transport of biomass burning smoke in the Amazon, which typically occurs from August to November(Mendez-Espinosa et al., 2019). In ST, peaks could also be attributable to wildfires in surrounding areas (Lapere et al., 2021). Meanwhile, LP and MX did not show significant increases above the mean.

The Figure 2 depicts a scatter plot comparing the performance of the C6.0 and C6.1 collections to determine if the new MAIAC product offers improvements for the analyzed Latin American cities. Analyzing R^2, both versions exhibit moderate performance, with values ranging from 0.3 to 0.8. An enhancement is detected in the values for the cities of ST and MX, which are the sites with the highest AOD levels, with increases of 6.6% and 15% respectively.

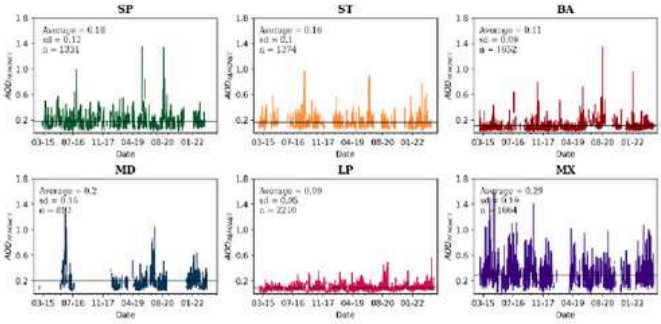


Figure 1. Daily averages of AERONET AOD_{550}.

However, for the rest of the sites (except MD), the R^2 values remain uniform. In MD, it is the only site experiencing a performance decrease, with a reduction of 34.62%, possibly due to data gaps. Regarding RMSE and the dispersion, no significant differences are observed between both collections. However, a moderate dispersion persists, mainly below the 1:1 reference line, indicating a tendency to underestimate values in all cases. Additionally, it is noted that the points tend to concentrate at lower AOD levels (<0.2), except in MX, where the variability range is higher. As for bias, a slight reduction is observed, implying an improvement compared to version C6.1. Although values remain underestimated and below the 1:1 reference line, this underestimation has decreased in magnitude. This difference is more evident in some cities, particularly notable in LP, followed by MX and BA. Furthermore, the regression line shows that C6.0 values are more biased than those of C6.1 in all cases. In summary, in Latin American cities, MAIAC C6.1 exhibits slightly better RMSE, R^2, and bias values (~0.06, ~0.54, ~-0.008) than C6.0 (~0.07, ~0.5, and ~-0.027).

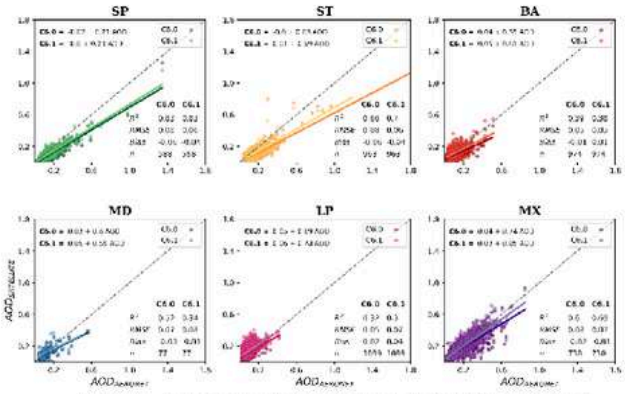


Figure 2. Regresion plots along with typical single valued metrics for the 6 LatAm cities.

Figure 3 presents the relative uncertainty (REU), with the x-axis representing AODAERONET reference levels. Both versions of MAIAC consistently show relative uncertainty exceeding 25%, while in the range of 0.05 to 0.15, it exceeds

50% for all cities. As AOD levels increase and reach approximately 0.1, the uncertainty stabilizes. This is crucial, given that the regional average of $AOD_{AERONET}$ is 0.17, and cities like BA and LP have averages below AOD = 0.1, suggesting that the uncertainty at these levels could be very high and could lead to erroneous results and conclusions. Specifically, it is observed that in ST, SP, and BA, the highest minimum values are recorded for version C6.1 (62.18%, 54.19%, and 53.35% respectively), and even higher in version C6.0 (75%, 60.38%, and 68.28% respectively). In contrast, the lowest results were obtained for LP and MX. This finding differs from what is shown by single-value metrics, where, generally, sites with higher AOD levels (SP, MX, and ST) show better performance. A trend of decreasing uncertainty is observed in all cases, improving performance in C6.1. The sites where uncertainty decreased significantly are SP with 10.3%, ST with 17.1%, BA with 21.9%, LP with 30.7%, and MX with 40.2%. In the case of MD, similar to traditional metrics, a similar pattern is maintained between both versions.

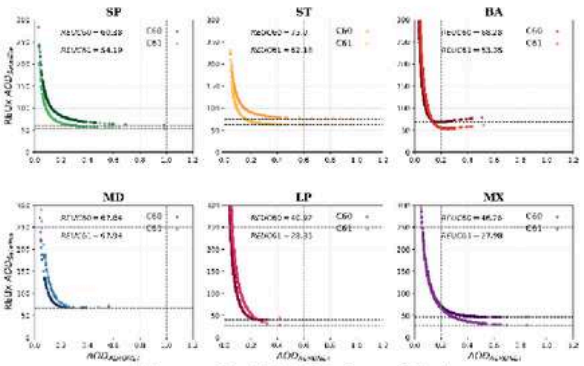


Figure 3. REU C6.0 vs C6.1

CONCLUSIONS

These findings reveal a significant data gap in the region. The AOD levels were relatively low, with an average of 0.2. Regarding performance according to traditional metrics, a generally moderate to low performance is observed, although an improvement is noted in sites with higher AOD levels. REU always exceeds 25%, and in the range of 0.05 to 0.15, it exceeds 50%. When comparing product versions, subtle improvements are observed in certain metrics for C6.1, but improvements in bias and REU are mainly highlighted. However, the magnitude of these improvements may vary depending on the city and AOD levels. Reductions between 10% (SP) and 40% (MX) were recorded in REU between both versions. It is observed that as AOD levels increase and reach approximately 0.1, uncertainty stabilizes. This is crucial since the regional average of $AOD_{AERONET}$ is 0.17, suggesting high uncertainty at these levels. Therefore, these results highlight the importance of considering uncertainties when using satellite-derived AOD products to estimate PM and characterize the spatial distribution of PM, as it could lead to erroneous conclusions.

REFERENCES

Carmona, J. M., Gupta, P., Lozano-García, D. F., Vanoye, A. Y., Hernández-Paniagua, I. Y., & Mendoza, A. (2021). Evaluation of modis aerosol optical depth and surface data using an ensemble modeling approach to assess pm2.5 temporal and spatial distributions. *Remote Sensing*, *13*(16). https://doi.org/10.3390/rs13163102

Damascena, A. S., Yamasoe, M. A., Martins, V. S., Rosas, J., Benavente, N. R., Sánchez, M. P., Tanaka, N. I., & Saldiva, P. H. N. (2021). Exploring the relationship between high-resolution aerosol optical depth values and ground-level particulate matter concentrations in the Metropolitan Area of São Paulo. *Atmospheric Environment*, *244*(September 2020). https://doi.org/10.1016/j.atmosenv.2020.117949

Lapere, R., Mailler, S., & Menut, L. (2021). The 2017 mega-fires in central chile: Impacts on regional atmospheric composition and meteorology assessed from satellite data and chemistry-transport modeling. *Atmosphere*, *12*(3). https://doi.org/10.3390/atmos12030344

Liu, Y., & Yi, B. (2022). Aerosols over East and South Asia: Type Identification, Optical Properties, and Implications for Radiative Forcing. *Remote Sensing*, *14*(9). https://doi.org/10.3390/rs14092058

Lyapustin, A., Wang, Y., Korkin, S., & Huang, D. (2018). MODIS Collection 6 MAIAC algorithm. *Atmospheric Measurement Techniques*, *11*(10), 5741–5765. https://doi.org/10.5194/amt-11-5741-2018

Martins, V. S., Lyapustin, A., De Carvalho, L. A. S., Barbosa, C. C. F., & Novo, E. M. L. M. (2017). Validation of high-resolution MAIAC aerosol product over South America. *Journal of Geophysical Research*, *122*(14), 7537–7559. https://doi.org/10.1002/2016JD026301

Mendez-Espinosa, J. F., Belalcazar, L. C., & Morales Betancourt, R. (2019). Regional air quality impact of northern South America biomass burning emissions. *Atmospheric Environment*, *203*(February), 131–140. https://doi.org/10.1016/j.atmosenv.2019.01.042

Pinder, R. W., Klopp, J. M., Kleiman, G., Hagler, G. S. W., Awe, Y., & Terry, S. (2019). Opportunities and challenges for filling the air quality data gap in low- and middle-income countries. *Atmospheric Environment*, *215*(February), 116794. https://doi.org/10.1016/j.atmosenv.2019.06.032

Qin, W., Fang, H., Wang, L., Wei, J., Zhang, M., Su, X., Bilal, M., & Liang, X. (2021). MODIS high-resolution MAIAC aerosol product: Global validation and analysis. *Atmospheric Environment*, *264*. https://doi.org/10.1016/j.atmosenv.2021.118684

Sayer, A. M., Govaerts, Y., Kolmonen, P., Lipponen, A., Luffarelli, M., Mielonen, T., Patadia, F., Popp, T., Povey, A. C., Stebel, K., & Witek, M. L. (2020). A review and framework for the evaluation of pixel-level uncertainty estimates in satellite aerosol remote sensing. *Atmospheric Measurement*

Techniques, *13*(2), 373–404.
https://doi.org/10.5194/amt-13-373-2020

AIR POLLUTION CONFERENCE BRAZIL
CMAS SOUTH AMERICA
COMMUNITY MODELING AND ANALYSIS SYSTEM

AİR POLLUTİON ANALYSİS İN LATİN AMERİCA: IMPLİCATİONS FOR HEALTH AND SOCİO-ENVİRONMENTAL INEQUALİTİES

Josefina Urquiza[1,2], Tailine Corrêa dos Santos[3], Sebastian Diez[4]
[1]*Grupo de Estudios de la Atmósfera y el Ambiente (GEAA), Universidad Tecnológica Nacional, Facultad Regional Mendoza (UTN-FRM)*
jurquiza@conicet.gov.ar
[2]*Consejo Nacional de Investigaciones Científicas y Técnicas (CONICET)*
[3]*Universidade de São Paulo - USP*
tailine.santos@usp.br
[4]*Universidad del Desarrollo, Chile*
sebastian.diez@udd.cl

Abstract: Air pollution has a wide range of adverse impacts on public health, covering issues from respiratory and cardiovascular problems to metabolic and neurological disorders, where it is estimated to be associated with 4 million annual deaths in urban areas. However, the distribution of pollution impacts differently in those vulnerable communities, due to socio-economic inequalities and the limited availability of essential health services. Understanding the effects of pollution and the current information scenario is crucial to designing effective policies that address both environmental and social issues. This paper aims to investigate the monitoring scenario of available $PM_{2.5}$ air quality data and associated disease records in the context of social inequality, discussing possible relationships due to lack of information and/or access to health services. This study focuses on Latin America, where the region's vulnerability is exacerbated by limited access to health care and lack of information on air quality and medical records. To conduct this analysis, information on pollutants was collected, using data from reference monitors from the OpenAQ database, as well as information from national registries in order to examine the evolution of the number of sensors in the region. In addition, these data were combined with measures from the Global Burden of Disease study (i.e. years of life lost due to premature mortality (YLLs); and disability-adjusted life years (DALYs), to perform a comprehensive analysis of correlations and trends. Our initial analysis indicates that in the 41% of the region where there are no air quality monitoring systems, the mortality rate is about 20% higher than in those places with monitoring, and about 35% higher than in countries where data is fully accessible. However, in those countries that do have measurement systems, sensors are limited, averaging only 0.2 sensors per 100,000 inhabitants. This situation highlights the differences in the availability and density of air quality sensors in the region. The absence of reference station monitoring is not only related to data availability, but also reflects deeper socio-economic challenges. Specifically, we observe that the burden of disease is significantly higher in less developed nations, highlighting the importance of the socio-economic dimension in understanding and addressing the health effects of air pollution. Countries with a low Social Development Index (SDI) have DALYs rates for ischaemic heart disease and stroke more than five times higher than high SDI countries. Likewise, nations in the lowest economic bracket have almost seven times higher DALY rates for stroke compared to those with very high incomes. These results highlight the relationship between a country's socio-economic status and health risks linked to air pollution. However, it is essential to stress that these findings do not indicate causality, but rather provide a snapshot of the current situation. Moreover, to fully understand these differences, factors such as public health policies, economic development and socio-environmental conditions must be taken into account. In order to develop strategies to improve the overall health of the region, it is vital to consider other relevant factors. This study could serve as a starting point for further research and the formulation of more informed and effective policies in the region.

Keywords: Public health, Air Quality Data, Health risks, Monitoring Systems.

INTRODUCTION

Currently, approximately 57% of the global population resides in urban areas, with Latin America having around 81% of its population living in cities, ranking as the second most urbanized region (UN-DESA-PD, 2022). In urban areas, air pollution has become one of the leading causes of serious health issues, such as cardiovascular diseases, respiratory problems, diabetes, and even premature death (Juginović et al., 2021; Sang et al., 2022). Despite efforts to reduce pollution levels globally, it remains one of the most significant factors affecting both health and the economy. However, over 90% of the world's population was exposed to air quality levels exceeding the World Health Organization (WHO) Air Quality Guidelines in 2016 (WHO, 2022).

Disparities in air quality have been observed based on a country's income level. While air pollution in developed countries poses a significant public health problem, it is even more pronounced in developing countries where rapid population expansion alongside widespread industrialization has led to areas with poor air quality, posing a serious health threat (Mannucci & Franchini, 2017). In Latin America, this issue is exacerbated as many countries face a range of additional challenges. Data availability on air quality is scarce, with limited measurements primarily concentrated in major cities of the countries (Gómez Peláez et al., 2020; Pinder et al., 2019). Moreover, access to healthcare is limited, and information regarding the

relationship between air quality and its health effects is insufficient to address this issue. Therefore, this work aims to investigate the state of available information on air quality in Latin America and examine its relationship with the effects of exposure to these pollutants. We will focus on monitoring available air quality data and records of associated diseases, especially considering the context of social inequality. Possible relationships due to lack of information and/or access to healthcare services will be discussed to identify areas for improvement and address existing challenges in the region.

METHODS

Information on pollutants was collected using data from reference air quality monitors from the OpenAQ database, an organization dedicated to providing universal access to air quality data. These data were combined with measures from the Global Burden of Disease study obtained from the Institute for Health Metrics and Evaluation (IHME) and the Health Effects Institute (HEI). Specifically, data were collected for 35 Latin American countries on general mortality, years of life lost (YLLs), and disability-adjusted life years (DALYs) attributable to air pollution by age, year, and sex between 1990 and 2019. Additionally, estimates of ambient $PM_{2.5}$ ($aPM_{2.5}$) exposure levels were obtained. To analyze disparities in terms of air pollution and disease burden, countries were divided based on their Social Development Index (SDI)

FINDINGS AND ARGUMENT

In Latin America, the availability of reference sensor measurements is limited. In Figure 1, the proportions of the countries performing air quality monitoring are presented. Approximately 44% of countries are regularly generating and sharing air quality data, while 41% of countries do not conduct direct measurements. The remaining countries (15%) carry out measurements but do not make this information public.This lack of transparency may lead to the population being unaware of the risks associated with air quality in their environment. However, in countries with measurement systems, sensors are limited, with an average of only 0.2 sensors per 100,000 inhabitants. Belize and Puerto Rico stand out with 1.2 and 0.76 sensors per 100,000 people, respectively. Countries like El Salvador, Paraguay, Uruguay, and Venezuela have a lower number of sensors per 100,000 inhabitants (<0.03). Looking at the geographical distribution of sensors, there is a predominance in South America, with countries like Peru, Brazil, Colombia, and Chile, except for Mexico, which has more than 70 sensors in each country. However, these numbers are small compared to each country's population (Chile and Peru~0.3, Colombia ~0.2, Mexico and Brazil <0.07 sensors per 100,000 inhabitants). This situation highlights differences in the availability and density of air quality sensors in the region.

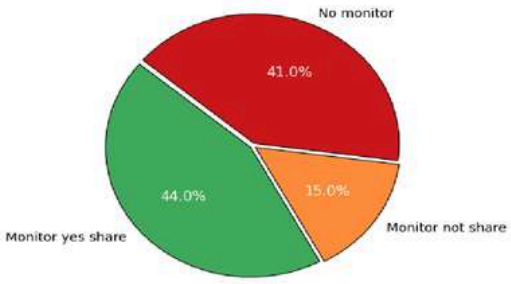


Figure 1. Air Quality monitoring OpenAQ

Figure 2 presents the average annual population-weighted $aPM_{2.5}$ for year 2019, according to the availability of information on air quality. Despite the existence of many countries without measurements, the concentrations are quite uniform compared to those that do monitor. Countries that monitor and have full access to information present an average of 19.55 ug/m^3, while those that monitor but do not share data record 16.94 ug/m^3. Those that do not conduct direct monitoring have average concentrations of 18.08 ug/m^3. This raises questions about whether countries without monitoring actually have better air quality conditions or if estimates and projections are also skewed due to lack of data for proper model validation. However, this is not the focus of this work and does not have an easy answer. In all cases, the concentrations considerably exceed the WHO limits of 5 ug/m^3. In fact, in all three cases, they exceed the limits by more than 250%. Only Puerto Rico (6.85ug/m^3) y Bemuda(7.07 ug/m^3) are close to the WHO guidelines limit.

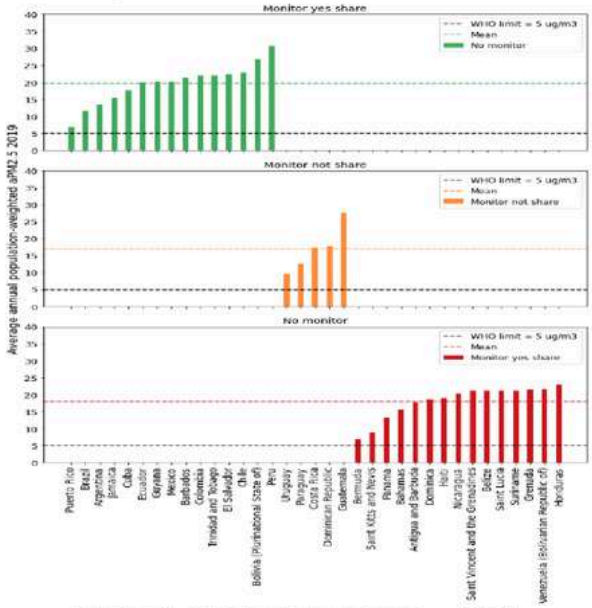


Figure 2. Average annual $aPM_{2.5}$ 2019

Figure 3 presents the mortality rate attributable to air pollution. Countries that monitor and share their data have an average mortality rate of 38.79 per 100,000 inhabitants. In contrast, countries that monitor but do not share their data have a slightly higher mortality rate, reaching 43.19 per 100,000

inhabitants. However, the most notable disparity is evident in countries that do not monitor air quality directly, recording a higher mortality rate of 54.77. Analyzing these figures reveals that in 41% of the countries in the region where there is no monitoring, the mortality rate is 26.86% higher than in those places that do conduct monitoring. Additionally, this rate is approximately 41.18% higher than in countries where data is fully accessible.

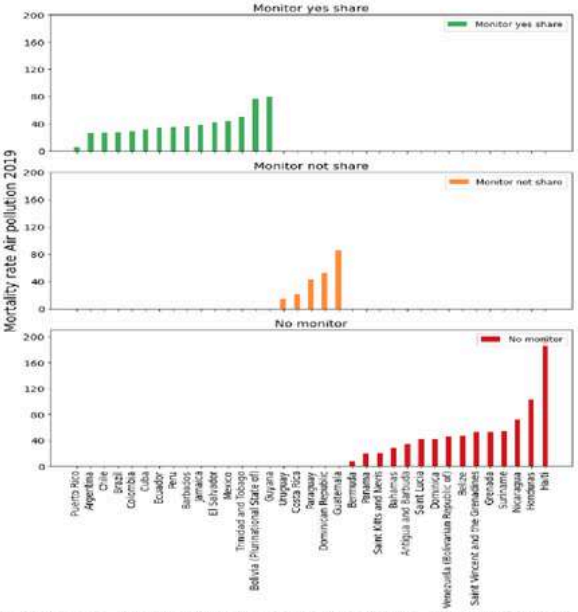


Figure 3. Mortality rate atributable Air Pollution

The absence of monitoring is not only limited to data availability but also reveals profound socioeconomic challenges. Specifically, the disease burden is significantly higher in less developed nations, highlighting the importance of addressing the socioeconomic dimension when tackling the effects of air pollution on health. In the left-hand of the Figure 3, the DALYs rate attributed to air pollution for the year 2019 is presented by country. In the right-hand en the Figure 3, the Social Development Index (SDI) by country is shown. An inverse relationship between DALYs rates and SDI is observed.

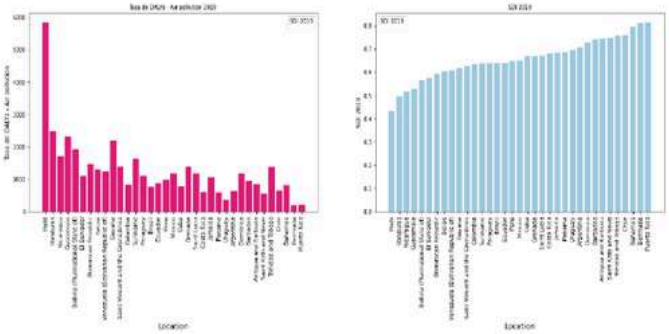


Figure 4. DALYs rate and SDI per country

As DALYs attributed to air pollution decrease, SDI increases. Countries with a low SDI (0.4-0.5) have a DALY of 4157.18, while those with a high SDI (>0.8) have a DALY of 193.63. This difference highlights that countries with a low SDI have a DALY 21.47 times higher than countries with a high SDI, emphasizing the urgency of addressing socioeconomic disparities to improve environmental and human health.

CONCLUSIONS

These findings underscore the relationship between a country's socioeconomic status and the health risks associated with air pollution. However, it's crucial to emphasize that these findings do not imply causation but rather provide a snapshot of the current scenario. Furthermore, to fully understand these differences, factors such as public health policies, economic development, and socio-environmental conditions must be taken into account. This study could serve as a stepping stone for further research and the crafting of more informed and efficacious policies in the region.

REFERENCES

Gómez Peláez, L. M., Santos, J. M., de Almeida Albuquerque, T. T., Reis, N. C., Andreão, W. L., & de Fátima Andrade, M. (2020). Air quality status and trends over large cities in South America. *Environmental Science and Policy*, *114*(September), 422–435. https://doi.org/10.1016/j.envsci.2020.09.009

Juginović, Alen; Vuković, Miro; Aranza, Ivan; Biloš, V. (2021). *Health impacts of air pollution exposure from 1990 to 2019 in 43 European countries.* https://doi.org/https://doi.org/10.1038/s41598-021-01802-5

Mannucci, P. M., & Franchini, M. (2017). Health effects of ambient air pollution in developing countries. *International Journal of Environmental Research and Public Health*, *14*(9), 1–8. https://doi.org/10.3390/ijerph14091048

Pinder, R. W., Klopp, J. M., Kleiman, G., Hagler, G. S. W., Awe, Y., & Terry, S. (2019). Opportunities and challenges for filling the air quality data gap in low- and middle-income countries. *Atmospheric Environment*, *215*(February), 116794. https://doi.org/10.1016/j.atmosenv.2019.06.032

Sang, S., Chu, C., Zhang, T., Chen, H., & Yang, X. (2022). The global burden of disease attributable to ambient fine particulate matter in 204 countries and territories, 1990–2019: A systematic analysis of the Global Burden of Disease Study 2019. *Ecotoxicology and Environmental Safety*, *238*(April). https://doi.org/10.1016/j.ecoenv.2022.113588

UN-DESA-PD. (2022). World Population Prospects 2022. In *United Nation* (Issue 9). www.un.org/development/ desa/pd/.

WHO. (2022). *Ambient (outdoor) air pollution.* https://www.who.int/news-room/fact-sheets/detail/ambient-(outdoor)-air-quality-and-health

AIR POLLUTION CONFERENCE BRAZIL
CMAS SOUTH AMERICA
COMMUNITY MODELING AND ANALYSIS SYSTEM

ASSESSMENT OF PM2.5 OXIDATIVE POTENTIAL, COMPOSITION, AND EMISSION SOURCES IN THE URBAN AIR OF SÃO PAULO, BRAZIL

Caroline F.H. Wikuats[1], Rafaela Squizzato[1], Iara da Silva[1], Thiago Nogueira[2], Daan L.A.C. Leseman[3], A. John F. Boere[3], Lucia da Conceição Andrade[4], Edmilson Dias de Freitas[1], Alessandra Tammaro[5], Flemming R. Cassee[3,6], Maria de Fatima Andrade[1]

[1]*Institute of Astronomy, Geophysics, and Atmospheric Sciences, University of São Paulo, São Paulo, Brazil*

caroline.wikuats@usp.br

[2]*School of Public Health, University of São Paulo, São Paulo, Brazil*

[3]*National Institute for Public Health and the Environment, Bilthoven, The Netherlands*

[4]*Faculty of Medicine, University of São Paulo, São Paulo, Brazil*

[5]*Amsterdam University Medical Centers, University of Amsterdam, Amsterdam, The Netherlands*

[6]*Institute for Risk Assessment Sciences, Utrecht University, Utrecht, The Netherlands*

Abstract: Particulate matter (PM) presents numerous chemical and physical properties, such as composition, size, and surface area, that may induce several adverse effects on human health. Fine particles (PM2.5) can oxidize target molecules and result in oxidative stress and (systemic) inflammation. The oxidative potential (OP) quantifies particle reactivity that is expected to correlate with biological responses and related adverse health effects induced by exposure to PM. The Metropolitan Area of São Paulo (MASP), Southeastern Brazil, is the fourth largest urban area in the world in terms of population. Little is known about the toxicological properties of PM2.5 from MASP, but it is expected to depend on the chemical composition. Therefore, we evaluated the OP, composition, and emission sources of PM2.5 collected during an extensive sampling campaign (from May 2021 to August 2022) at the Faculty of Medicine of the University of São Paulo (FMUSP), located in an area highly impacted by vehicular emissions. We sampled PM2.5 with a Partisol 2025i Sequential Air Sampler. We analyzed the OP using electron spin resonance (OP-ESR) and dithiothreitol (OP-DTT) assays, while the composition was measured via energy-dispersive X-ray fluorescence (EDXRF). PM2.5 at FMUSP is mainly composed of OC > EC > S > Na > K > Fe > Si > Al > Zn. The primary sources identified with Principal Component Analysis (PCA) were vehicular emissions, resuspension, and biomass burning (factor 1), engine oil burning (factor 2), sea salt (factor 3), vehicle exhaust and non-exhaust (brake and tire wear) emissions (factor 4). These factors explained 46, 16, 11, and 27% of the PCA variance. Our results show that PM collected in April and May of 2022 exhibited the highest monthly mean OP values for ESR (OP-ESRv: $3.6_{x}10^{4}$ and $3.9_{x}10^{4}$ a.u. m^{-3}, respectively) and DTT (OP-DTTv: 3.0 and 3.8 nmol min^{-1} m^{-3}), whereas the highest PM2.5 concentrations were recorded in July and August of 2021 (18.4 and 21.1 µg m^{-3}, respectively). Furthermore, there is no characteristic seasonal profile for OP-ESR and OP-DTT, as observed for PM2.5. Regarding the days of the week, Sundays presented lower values for PM2.5 (13.3 µg m^{-3}), OP-ESRv ($1.4_{x}10^{4}$ a.u. m^{-3}), and OP-DTTv (1.6 nmol min^{-1} m^{-3}) compared to Monday through Saturday, attributed to a 70% reduction in vehicle traffic in the region. Applying a Generalized Linear Model (GLM) with gamma distribution showed that different PM2.5 species are significantly correlated (p-value ≤ 0.05) with OP-ESR and OP-DTT, such as OC, EC, Na, Mg, Cl, K, Fe, Cu, Br, Sr, Cd, and Sb. In conclusion, OP is mainly influenced by PM2.5 composition and its emission sources. Moreover, the weak correlation between OP-ESR, OP-DTT, and PM2.5 mass indicates that the oxidative potential assays could be used as alternative metrics in observational studies.

Keywords: Oxidative potential, particulate matter pollution, health effects, chemical characterization, emission sources.

INTRODUCTION

Particulate matter (PM) presents numerous chemical and physical properties, such as composition, size, and surface area, that may induce several adverse effects on human health. Fine particles (PM2.5) can oxidize target molecules and result in oxidative stress and (systemic) inflammation (Borlaza et al., 2018; Gao et al., 2020). The oxidative potential (OP) quantifies particle reactivity that is expected to correlate with biological responses and related adverse health effects induced by exposure to PM (Calas et al., 2018).

The Metropolitan Area of São Paulo (MASP), located in Southeastern Brazil, is the fourth largest urban area in the world in terms of population (United Nations, 2019). While studies in the MASP have focused on the distribution and composition of PM, air quality modeling, associations with meteorological variables, and health effects (Andrade et al., 2012; Nogueira et al., 2020; Vara-Vela et al., 2016), there is limited knowledge about the toxicological properties of PM2.5 from MASP.

To address this gap, we evaluated the OP, chemical composition, and emission sources of PM2.5 collected during an extensive sampling campaign

(from May 2021 to August 2022) at the Faculty of Medicine of the University of São Paulo (FMUSP).

METHODS

We collected daily PM2.5 samples on Teflon filters at FMUSP using a Partisol 2025i Sequential Air Sampler (Figure 1a). OP analysis was performed using electron spin resonance (OP-ESR) and dithiothreitol (OP-DTT) assays with spectrophotometers (Figure 1b, 1c). The composition was determined via energy-dispersive X-ray fluorescence (EDXRF) (Figure 1d). Furthermore, Principal Component Analysis (PCA) was employed to identify the main emission sources.



Figure 1. Partisol 2025i Sequential Air Sampler (a), MiniScope MS400 (b), SpectraMax 190 Microplate Reader (c), and Epsilon 5 Energy-Dispersive X-Ray Fluorescence Analyzer (d).

FINDINGS AND ARGUMENT

PCA results showed four primary emission sources based on the predominance of specific PM2.5 components (Figure 2). Factor 1 indicated influences from vehicular emissions, resuspension, and biomass burning, characterized by BC, Mg, Al, Si, K, Ca, Cr, Mn, Fe, Se, Br, and Rb. Factor 2 is associated with engine oil burning due to the presence of P, S, V, and Ni.

In contrast, Factor 3 is possibly linked to sea salt emissions indicated by Na, Mg, and Cl. Factor 4 is related to vehicle exhaust and non-exhaust (brake and tire wear) emissions, with significant amounts of BC, Cr, Mn, Ni, Cu, Zn, As, and Sb. These factors explained 46, 16, 11, and 27% of the PCA variance, respectively. Therefore, PCA analysis confirms that while other sources may contribute, vehicular traffic is the primary emission source of particles at FMUSP.

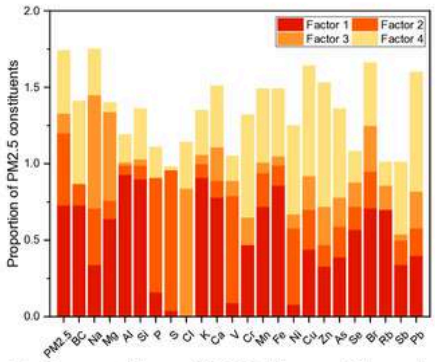


Figure 2. Proportion of PM2.5 constituents to the emission sources (factors) at FMUSP.

PM collected in April and May of 2022 exhibited the highest monthly mean volume-based OP values for ESR (OP-ESRv: 3.6×10^4 and 3.9×10^4 a.u. m^{-3}, respectively) (Figure 3a) and DTT (OP-DTTv: 3.0 and 3.8 nmol min^{-1} m^{-3}) (Figure 3c), whereas the highest PM2.5 concentrations were recorded in July and August of 2021 (18.4 and 21.1 µg m^{-3}, respectively) (Figure 3e).

Furthermore, OP-ESR and OP-DTT did not exhibit a characteristic seasonal profile, as was observed for PM2.5, which presented higher values in winter due to reduced precipitation rates and stable atmospheric conditions. Thus, the composition and emission sources of PM2.5, rather than its concentration, significantly influence OP reactions.

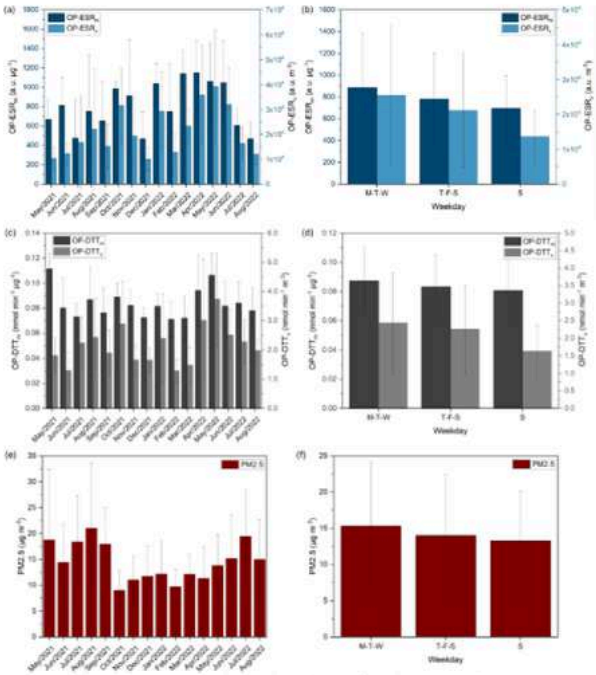


Figure 3. Monthly and day-of-the-week mean values for OP-ESR (a, b), OP-DTT (c, d), and PM2.5 (e, f) at FMUSP. In the OP representation, darker shades indicate results based on mass, while lighter shades represent results based on volume.

Analysis of the days of the week revealed that Sundays had lower values for OP-ESRv ($1.4x10^4$ a.u. m^{-3}) (Figure 3b), OP-DTTv (1.6 nmol min^{-1} m^{-3}) (Figure 3d), and PM2.5 (13.3 µg m^{-3}) (Figure 3f), compared to Monday through Saturday. This reduction is attributed to a 70% decrease in vehicle traffic in the region on Sundays (Wikuats et al., 2023). The reduced emission levels observed on Sundays possibly influence both PM2.5 atmospheric reactions and OP responses. Notably, OP results based on volume exhibited statistically significant differences across the days of the week (p-value ≤ 0.05) according to the Kruskal-Wallis test.

Chemical analysis using EDXRF on Teflon filters indicated that PM2.5 at the sampling site is primarily composed of OC > EC > S > Na > K > Fe > Si > Al > Zn, with daily concentrations ranging from $1.5x10^{-3}$ to 21.2 µg m^{-3}. A Generalized Linear Model (GLM) with gamma distribution showed that different PM2.5 species are significantly correlated (p-value ≤ 0.05) with OP-ESR and OP-DTT, such as OC, EC, Na, Mg, Cl, K, Fe, Cu, Br, Sr, Cd, and Sb (Table 1). This preliminary analysis confirms that PM composition has a greater influence on OP reactions than its mass concentration.

Table 1. Preliminary results from the GLM regression analysis for PM2.5 species and OP results at FMUSP.

PM2.5	OP-ESRm	OP-ESRv	OP-DTTm	OP-DTTv
	p-value			
OC	**$5.00x10^{-7}$**	**$6.10x10^{-6}$**	**0.02**	**0.02**
EC	**$7.00x10^{-4}$**	**0.05**	0.16	0.92
Na	**0.04**	0.40	0.34	0.67
Mg	0.30	0.71	0.24	**0.04**
Cl	0.24	0.07	**$3.40x10^{-3}$**	**$3.6x10^{-3}$**
K	**0.03**	0.09	0.81	0.99
Fe	0.85	0.46	**0.02**	0.71
Cu	**$1.00x10^{-4}$**	**$4.90x10^{-3}$**	0.49	0.84
Br	**0.03**	**0.03**	0.08	0.75
Sr	0.48	0.27	0.59	**0.02**
Cd	**0.05**	0.53	**0.03**	0.94
Sb	**$2.35x10^{-5}$**	**$1.77x10^{-5}$**	**$1.80x10^{-3}$**	**$8.00x10^{-4}$**

Values with statistical significance (p-value ≤ 0.05) are highlighted in blue and bold.

CONCLUSIONS

OP is mainly influenced by PM2.5 chemical composition, which in turn is affected by the contribution of emission sources. PM2.5 mass concentration alone does not fully reflect the variation in PM's intrinsic oxidative potential. Additionally, the weak correlation between OP and PM2.5 mass suggests that oxidative potential assays, specifically OP-ESR and OP-DTT, could serve as alternative metrics in observational studies, as they better reflect chemical composition. This may provide valuable insights into the variation in health impacts due to exposure to PM2.5.

REFERENCES

Andrade, Maria de Fatima, Regina Maura de Miranda, Adalgiza Fornaro, Americo Kerr, Beatriz Oyama, Paulo Afonso de Andre, and Paulo Saldiva. "Vehicle emissions and PM 2.5 mass concentrations in six Brazilian cities." *Air Quality, Atmosphere & Health* 5 (2012): 79-88.

Borlaza, Lucille Joanna S., Enrique Mikhael R. Cosep, Seojong Kim, Kwangyul Lee, Hungsoo Joo, Minhan Park, Daphne Bate, Mylene G. Cayetano, and Kihong Park. "Oxidative potential of fine ambient particles in various environments." *Environmental Pollution* 243 (2018): 1679-1688.

Calas, Aude, Gaëlle Uzu, Frank J. Kelly, Stephan Houdier, Jean MF Martins, Fabrice Thomas, Florian Molton et al. "Comparison between five acellular oxidative potential measurement assays performed with detailed chemistry on PM 10 samples from the city of Chamonix (France)." *Atmospheric Chemistry and Physics* 18, no. 11 (2018): 7863-7875.

Gao, Dong, Krystal J. Godri Pollitt, James A. Mulholland, Armistead G. Russell, and Rodney J. Weber. "Characterization and comparison of PM 2.5 oxidative potential assessed by two acellular assays." *Atmospheric Chemistry and Physics* 20, no. 9 (2020): 5197-5210.

Nations, United. "World urbanization prospects: The 2018 revision. " Department of Economic and Social Affairs, Population Division, United Nations (2019).

Nogueira, Thiago, Prashant Kumar, Adelaide Nardocci, and Maria de Fatima Andrade. "Public health implications of particulate matter inside bus terminals in Sao Paulo, Brazil." *Science of the total environment* 711 (2020): 135064.

Vara-Vela, Angel, Maria F. Andrade, Prashant Kumar, Rita Y. Ynoue, and Angel G. Munoz. "Impact of vehicular emissions on the formation of fine particles in the Sao Paulo Metropolitan Area: a numerical study with the WRF-Chem model." *Atmospheric Chemistry and Physics* 16, no. 2 (2016): 777-797.

Wikuats, Caroline Fernanda Hei, Thiago Nogueira, Rafaela Squizzato, Edmilson Dias de Freitas, and Maria de Fatima Andrade. "Health Risk Assessment of Exposure to Air Pollutants Exceeding the New WHO Air Quality Guidelines (AQGs) in São Paulo, Brazil." *International Journal of Environmental Research and Public Health* 20, no. 9 (2023): 5707.

AIR POLLUTION CONFERENCE BRAZIL
CMAS SOUTH AMERICA
COMMUNITY MODELING AND ANALYSIS SYSTEM

EVALUATING THE OXIDATIVE POTENTIAL OF PM2.5 IN SÃO PAULO, BRAZIL: A COMPARATIVE ANALYSIS BETWEEN DIFFERENT ASSAYS

Caroline F.H. Wikuats[1], Sumit K. Dey[2], Daan L.A.C. Leseman[2], A. John F. Boere[2], Thiago Nogueira[3], Lucia da Conceição Andrade[4], Edmilson Dias de Freitas[1], Alessandra Tammaro[5], Flemming R. Cassee[2,6], Maria de Fatima Andrade[1]

[1]*Institute of Astronomy, Geophysics, and Atmospheric Sciences, University of São Paulo, São Paulo, Brazil*

caroline.wikuats@usp.br

[2]*National Institute for Public Health and the Environment, Bilthoven, The Netherlands*

[3]*School of Public Health, University of São Paulo, São Paulo, Brazil*

[4]*Faculty of Medicine, University of São Paulo, São Paulo, Brazil*

[5]*Amsterdam University Medical Centers, University of Amsterdam, Amsterdam, The Netherlands*

[6]*Institute for Risk Assessment Sciences, Utrecht University, Utrecht, The Netherlands*

Abstract: Characterizing particulate matter (PM) based on its chemical composition, especially the fine PM (PM2.5) that penetrates deeper into the respiratory system, can be an effective procedure to evaluate its impacts on human health and elucidate efficient mitigation and control procedures. While PM2.5 mass concentration has been a conventional metric for correlating exposure levels with health outcomes, it fails to capture the variation in the intrinsic toxic potential of PM, emphasizing the need for alternative assessment methods. The oxidative potential (OP) has gained attention for its ability to evaluate the redox-active organic and metal content and toxic responses of PM2.5, which may vary based on composition, emission sources, and multi-component interactions. In the traditional acellular OP assays, the estimation of OP derives from the consumption of cellular reductant proxies (dithiothreitol – DTT) and the generation and detection of hydroxyl radicals (electron spin resonance – ESR). These assays provide good correlations between the composition of organic and metal species and emission sources of PM2.5. As both tests require a considerable amount of mass, an alternative and robust bioassay developed by Dey et al. (2021) not only consumes less PM but also is close to a biological response, i.e., it simulates other oxidative damage as it is based on lipid peroxidation (LPO). The current study focused on the Metropolitan Area of São Paulo (MASP), South America's most industrialized and developed urban area, where knowledge of the toxicological properties of PM2.5 is still limited. We aimed to assess and compare the results obtained from conventional OP methods (OP^{DTT} and OP^{ESR}) with those from a newly developed, pathologically relevant bioassay designed to quantify the LPO index (OP^{LPO}). We analyzed PM2.5 samples collected at the Faculty of Medicine of the University of São Paulo (FMUSP) from May 2021 to August 2022. Various sources influenced the sampling site, including vehicular emissions, biomass and engine oil burning, soil and road resuspension, and sea salt. Our results indicated that the OP^{LPO} assay is more sensitive in identifying the toxicity of PM2.5 in a dose-dependent manner (100 to 3 μg mL^{-1}), particularly at lower concentrations where the traditional OP methods showed no significant responses. Further analyses will help to elucidate the mechanisms of action of PM2.5 in São Paulo, providing insights for future epidemiological studies and air quality management strategies.

Keywords: Oxidative potential, health outcomes, bioassays, particle toxicity, lipid peroxidation.

INTRODUCTION

Characterizing particulate matter (PM), particularly fine (≤ 2.5 μm) and ultrafine particles (< 100 nm), based on their chemical and toxicological properties, provides valuable insights into their impact on human health. These smaller particles penetrate deeper into the respiratory system, making it crucial to understand their effects for effective mitigation and control procedures (Borlaza et al., 2018). However, the mechanisms of action and toxicity of health effects related to PM2.5 are still poorly understood (Bates et al., 2019; Simonetti et al., 2018).

While PM2.5 mass concentration has been a conventional metric for correlating exposure levels with health outcomes, it fails to capture the variation in the intrinsic toxic potential of PM, emphasizing the need for alternative assessment methods (Dey et al., 2021; Janssen et al., 2014). Oxidative potential (OP) has gained attention for its ability to evaluate the redox-active organic and metal content and toxic responses of PM2.5, which may vary based on composition, emission sources, and multi-component interactions (Bates et al., 2019; Borlaza et al., 2018).

Traditional acellular OP assays estimate OP by measuring the consumption of cellular reductant proxies (dithiothreitol – DTT) and the generation and detection of hydroxyl radicals (electron spin resonance – ESR) (Figure 1a) (Borlaza et al., 2018; Gao et al., 2020a, 2020b). These assays provide good correlations between the composition of organic and metal species and emission sources of PM2.5 (Bates et al., 2019; Borlaza et al., 2018; Janssen et al., 2014).

Given that both tests require a considerable amount of mass, Dey et al. (2021) developed an alternative, robust bioassay that consumes less PM and closely simulates biological responses, particularly oxidative damage, as it is based on lipid peroxidation (LPO) (Figure 1b).

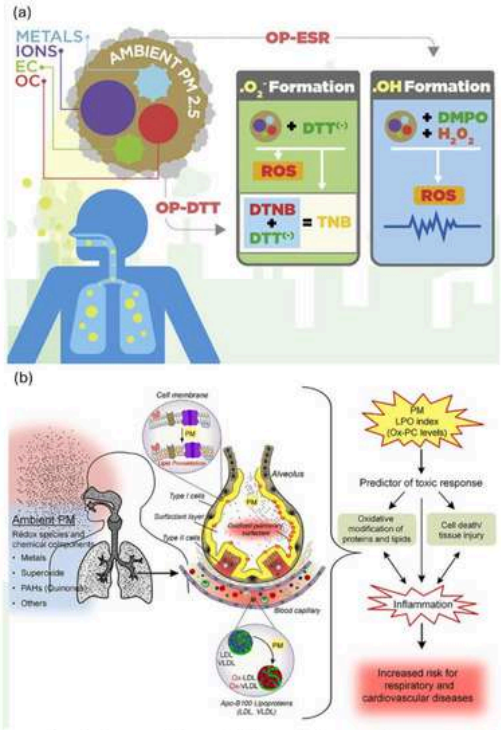


Figure 1. Schematic of the different mechanisms of action for traditional (a) and alternative (b) OP assays. Reference: Modified from Borlaza et al. (2018) and Dey et al. (2021).

The current study focused on the Metropolitan Area of São Paulo (MASP), South America's most industrialized and developed urban area, where knowledge of the toxicological properties of PM2.5 remains limited. Our objective was to assess and compare the results of conventional OP methods with those of a newly developed, pathologically relevant bioassay designed to quantify the LPO index.

METHODS

We analyzed selected PM2.5 samples collected on Teflon filters using a Partisol 2025i Sequential Air Sampler at the Faculty of Medicine of the University of São Paulo (FMUSP) from May 2021 to August 2022. Traditional assays, including dithiothreitol (OP^{DTT}) and electron spin resonance (OP^{ESR}), were used alongside the alternative LPO method (OP^{LPO}) for OP assessment.

DTT reacts with PM2.5 and 5,5'-dithiobis-(2-nitrobenzoic) acid (DTNB), forming 2-nitro-5-thiobenzoic acid (TNB) that is quantified at 412 nm. OP^{DTT} is evaluated as the DTT consumption rate, which is proportional to the concentration of redox-active species. In contrast, OP^{ESR} is quantified based on the first derivative of the ESR signal of the 5,5-dimethyl-1-pyrroline N-oxide and hydroxyl radical (DMPO-OH) quartet as the sum of the total amplitudes (Gao et al., 2020a, 2020b).

For the OP^{LPO} assay, we followed the method by Dey et al. (2021), subjecting captured serum apoB-100 lipoprotein particles to 3-100 μg mL^{-1} of PM solution from the summer and winter seasons. DOFA and Fenton reagent ($FeCl_2$:H_2O_2) were incubated as the positive controls. The data were represented as oxidized phospholipids (Ox-PCs) normalized to the vehicle (serum without PM).

In our analyses, a domestic oil-burning furnace (DOFA) solution was the positive control, while ultrapure water was the negative control.

FINDINGS AND ARGUMENT

Various sources influenced the sampling site, including vehicular emissions, biomass and engine oil burning, soil and road resuspension, and sea salt. However, vehicles were the predominant emission source of PM2.5 at FMUSP, located near roads with heavy traffic and no industrial sources.

Our results indicated that the OP^{LPO} assay is more sensitive in identifying the toxicity of PM2.5 in a dose-dependent manner (100 to 3 μg mL^{-1}) (Figure 2), particularly at lower concentrations where the traditional OP methods showed no significant responses. Winter samples exhibited up to 35 times higher responses than the serum vehicle (Figure 2c, 2d). Winter values differed significantly from summer values for all concentrations tested based on the Mann-Whitney U test (p-value ≤ 0.05).

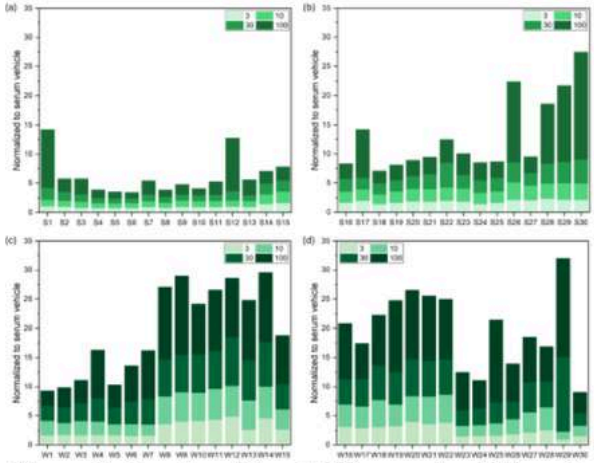


Figure 2. Results of the OP^{LPO} assay for different concentrations (3, 10, 30, and 100 μg mL^{-1}) for summer (a, b) and winter (c, d) samples at FMUSP.

Despite using different PM2.5 concentrations in each method (100 μg mL^{-1} for OP^{LPO}, 500 μg mL^{-1} for OP^{DTT}, and 1000 μg mL^{-1} for OP^{ESR}), the OP^{LPO} assay showed significantly higher values for winter samples (p-value ≤ 0.05), particularly those associated with biomass burning (Figure 3). This finding suggests a response possibly driven more by organic compounds than metals. There was no statistical difference between summer and winter results for OP^{DTT} and OP^{ESR}.

The biomass-burning samples were collected at FMUSP during a massive wildfire at Juquery State Park in the MASP in August 2021. OP^{DTT} results were also elevated during this period, while OP^{ESR} values decreased (samples W8 to W16 in Figure 3b). Our ongoing investigation aims to explore further the relationship between specific OP responses and PM2.5 composition and sources through regression analysis.

While the traditional OP^{DTT} and OP^{ESR} methods focus on ROS generation and radical species, OP^{LPO} provides complementary information by assessing oxidative damage to lipids. This evaluation is directly linked to cellular membrane integrity, making it a technique of high physiological relevance. However, it remains to be established if this novel metric indeed predicts toxicity and health effects.

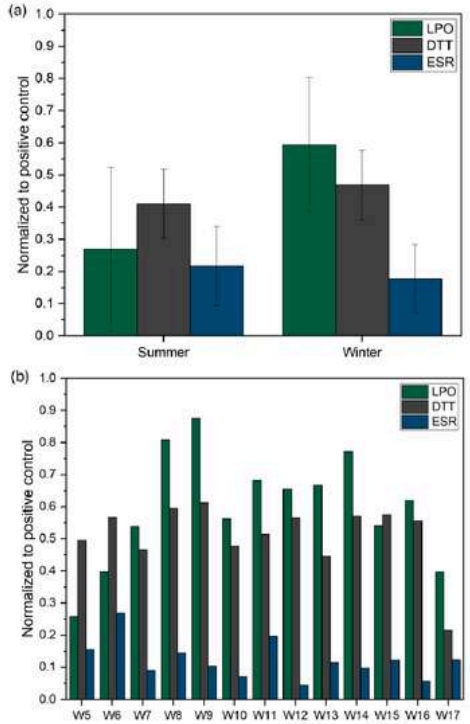


Figure 3. Mean values for OP^{LPO}, OP^{DTT}, and OP^{ESR} assays normalized to the positive control for summer and winter (a) and a biomass burning period (b) at FMUSP.

CONCLUSIONS

The sensitivity of the OP^{LPO} assay highlights its potential as an effective tool for assessing PM2.5 toxicity and guiding public health interventions in urban areas. Integrating results from OP^{LPO} and traditional methods (OP^{DTT} and OP^{ESR}) can offer a more comprehensive understanding of PM's oxidative potential and associated health risks. These findings contribute to elucidating the mechanisms of action of PM2.5 in São Paulo, providing insights for future epidemiological studies and air quality management strategies.

REFERENCES

Bates, Josephine T., Ting Fang, Vishal Verma, Linghan Zeng, Rodney J. Weber, Paige E. Tolbert, Joseph Y. Abrams et al. "Review of acellular assays of ambient particulate matter oxidative potential: methods and relationships with composition, sources, and health effects." *Environmental Science & Technology* 53, no. 8 (2019): 4003-4019.

Borlaza, Lucille Joanna S., Enrique Mikhael R. Cosep, Seojong Kim, Kwangyul Lee, Hungsoo Joo, Minhan Park, Daphne Bate, Mylene G. Cayetano, and Kihong Park. "Oxidative potential of fine ambient particles in various environments." *Environmental Pollution* 243 (2018): 1679-1688.

Dey, Sumit K., et al. "Lipid peroxidation index of particulate matter: Novel metric for quantifying intrinsic oxidative potential and predicting toxic responses." *Redox Biology* 48 (2021): 102189.

Gao, Dong, Krystal J. Godri Pollitt, James A. Mulholland, Armistead G. Russell, and Rodney J. Weber. "Characterization and comparison of PM 2.5 oxidative potential assessed by two acellular assays." *Atmospheric Chemistry and Physics* 20, no. 9 (2020a): 5197-5210.

Gao, Dong, Susannah Ripley, Scott Weichenthal, and Krystal J. Godri Pollitt. "Ambient particulate matter oxidative potential: Chemical determinants, associated health effects, and strategies for risk management." *Free Radical Biology and Medicine* 151 (2020b): 7-25.

Janssen, Nicole AH, Aileen Yang, Maciej Strak, Maaike Steenhof, Bryan Hellack, Miriam E. Gerlofs-Nijland, Thomas Kuhlbusch et al. "Oxidative potential of particulate matter collected at sites with different source characteristics." *Science of the Total Environment* 472 (2014): 572-581.

Simonetti, Giulia, Elena Conte, Cinzia Perrino, and Silvia Canepari. "Oxidative potential of size-segregated PM in an urban and an industrial area of Italy." *Atmospheric Environment* 187 (2018): 292-300.

AIR POLLUTION CONFERENCE BRAZIL
CMAS SOUTH AMERICA
COMMUNITY MODELING AND ANALYSIS SYSTEM

ANALYSIS OF FINE PARTICULATE MATTER ($PM_{2.5}$) IN SAO PAULO CITY

Vitoria Rodilha Leão[1], Maria de Fatima Andrade[1], Dayane da Fonseca[2], José Vinicius Martins[3], Thiago Nogueira[2],

[1]*Instituto de Astronomia, Geofísica e Ciências Atmosféricas*

[2]*Faculdade de Saúde Pública*

[3]*Instituto de Geociências*

Universidade de Sao Paulo, Sao Paulo, Brazil

E-mail: vitorialeao.iag@usp.br

Abstract: This work aims to characterize the chemical composition of $PM_{2.5}$, using Inductively Coupled Plasma Mass Spectrometry (ICP-MS), apportioning its sources and relation with the atmospheric conditions in the Metropolitan Area of Sao Paulo. $PM_{2.5}$ samples were collected in the *Faculdade de Saúde Pública* (FSP; School of Public Health) from the University of Sao Paulo, a region next to avenues and natural parks, with a large fleet of light and heavy-duty vehicles, from 2022 to 2023. After sampling, element concentrations were determined with ICP-MS, and source apportionment was performed using Principal Component Analysis (PCA) and Positive Matrix Factorization (PMF) model. There were higher $PM_{2.5}$ concentrations during winter when temperature and total rainfall were lower; the concentrations decreased in summer, along with an increase in temperatures and total rainfall. The mean concentration of $PM_{2.5}$ surpassed the annual air quality standard and the WMO guidelines. Strong correlations between resuspension-related compounds and vehicular-emitted compounds were found. The PCA as well as PMF results, suggested the following sources: heavy-duty and light-duty vehicles explaining most of PM2.5 mass;, road dust resuspension and civil construction. Meteorological seasonal conditions explain the variations of $PM_{2.5}$ coordinate with the expected function of meteorological conditions. The main sources of $PM_{2.5}$ in the region of FSP are heavy-duty and light-duty vehicles, and road dust resuspension and civil construction. These new sources evaluated through receptor models for recent years made available the evolution of the vehicular sources in Sao Paulo.

Keywords: $PM_{2.5}$, ICP-MS, PCA, PMF, Sao Paulo.

INTRODUCTION

Particulate matter (PM) pollution is the most pressing issue in air quality regulation worldwide (Fuzzi et al., 2015). Atmospheric aerosols have local and global effects, affecting the life cycle and albedo of clouds, precipitation, and lightning, degrading air quality, and impacting Earth energy budget. Aerosols have optical effects as well, impacting visibility (Zhang et al., 2015).

Fine particulate matter ($PM_{2.5}$) is the fraction of aerosols that have aerodynamic diameters below 2.5 μm (Colbeck & Lazaridis, 2014). In the Metropolitan Area of Sao Paulo (MASP), vehicle exhaust heavily contributes to $PM_{2.5}$, emitting Cu, Pb, Zn, and oxygenated polycyclic aromatic hydrocarbons (Oxi-PAHs). Other sources of $PM_{2.5}$ in MASP are resuspension of road dust, with high levels of Al, and brake wear, related to Sb, Zn, and Ba (Pereira, Kamigauti et al., 2023; Pereira, Nogueira et al., 2023). $PM_{2.5}$ is also heavily impacted by remote sources, such as biomass combustion from the Amazon Forest and Pantanal or within the state of Sao Paulo, and wood burning in restaurants, bakeries, and residences (Kumar et al., 2016; Martins Pereira et al., 2017; Souto-Oliveira et al., 2023).

Considering that PM concentrations change according to human behavior and atmospheric conditions, this work aims to create an updated study of the sources of $PM_{2.5}$, characterizing its composition using Inductively Coupled Plasma Mass Spectrometry (ICP-MS), and apportioning its sources and relation with the atmospheric conditions in the Metropolitan Area of Sao Paulo.

METHODS

Samples were collected in the *Faculdade de Saúde Pública* (FSP; School of Public Health; 23°33'S, 46°40'W) from the University of Sao Paulo from 2022 to 2023. Samples were digested in a microwave oven and element concentrations were obtained with Inductively Coupled Plasma Mass Spectrometry (ICP-MS). The procedure is described in Pereira, Nogueira et al. (2023).

The source apportionment was performed through Enrichment Factor (EF; Nishida, 2017) and Principal Component Analysis (PCA; Hetem, 2014) calculations, and application of the Positive Matrix Factorization (PMF; de Miranda et al., 2018) model.

RESULTS

Time series of $PM_{2.5}$ concentration is presented in Figure 1 with the total precipitation and temperature. There were higher concentrations during the winter of the Southern Hemisphere when the temperatures and total precipitation were lower. For the summer, concentrations were pointedly lower, along with an increase in temperatures and total precipitation. The mean was approximately 19.09 μg/m³, overtaking the

annual air quality standard and the annual guideline WMO value.

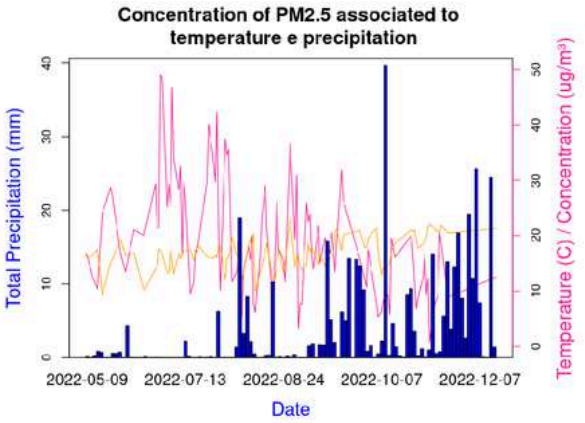


Figure 1. Time series of $PM_{2.5}$ concentrations (pink line) measured in FSP from 05/09/2022 to 01/11/2023 with temperature (orange line) and total precipitation (blue line) time series from ERA5 model from ECMWF.

The EF results are shown in Table 1. Only Cr, Cu, Pb, Zn, and Na were associated with anthropogenic sources, related to vehicular emissions such as fuel and lubricant oil combustion, and brake wear (Pereira, Kamigauti, et al., 2023).

The PCA was run for 5 components. The first showed a mixed source of road dust resuspension, diesel, and biomass combustion (Artaxo et al., 1994; de Miranda et al., 2018; Pereira, Kamigauti, et al., 2023). The second factor showed also road dust resuspension and civil construction (Wang et al., 2006). The third concerned a vehicular source, in special brake wear, exhaustion, and lubricant oil from heavy-duty vehicles (Pereira, Kamigauti, et al., 2023). The fourth factor was possibly an oil combustion source from generators in the region (Nishida, 2017). The last indicated a vehicle-emitted source, from light-duty vehicles (Pereira, Nogueira, et al., 2023). The highest fractions of $PM_{2.5}$ were in the factors associated with resuspension, biomass combustion, and vehicle sources.

The PMF was also run for 5 factors. The first was characteristic of vehicular sources, such as gasohol exhaust, brake wear, and lubricant oil (Pereira, Kamigauti, et al., 2023). The second component was a light-duty vehicle source, from gasoline and diesel exhaust, and brakes and tire wear (Pereira, Kamigauti, et al., 2023). The third factor indicated a road dust resuspension and civil construction source. The fourth was also a road dust resuspension source, in addition to a diesel-powered vehicle source (de Miranda et al., 2018; Pereira, Kamigauti, et al., 2023). The last presented a heavy-duty vehicle source. The contribution of the $PM_{2.5}$ sources is shown in Figure 2. The main source was vehicular, with major contributions of factors 2 (32.4%), light-duty vehicles, and 4 (31.6%), heavy-duty vehicles.

Table 1. Emission Factor (EF) results for median concentrations of elements in $PM_{2.5}$.

Element	EF	Classification
Al	1.00	Natural
Fe	0.95	Natural
Mn	1.29	Natural
Cr	16.97	Anthropogenic
Cu	95.82	Anthropogenic
Ni	6.52	Natural
Zn	209.19	Anthropogenic
Pb	120.08	Anthropogenic
Na	26.22	Anthropogenic
Ca	0.69	Natural
K	2.39	Natural
Mg	4.44	Natural
Ti	0.38	Natural

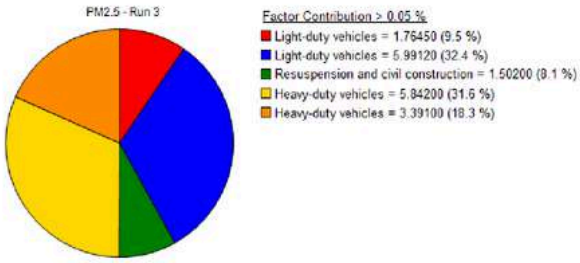


Figure 2. Contributions of sources to $PM_{2.5}$ from the PMF model.

CONCLUSIONS

There were higher concentrations of $PM_{2.5}$ during the winter months in the southern hemisphere, while temperatures and total precipitation were lower; on the other hand, the concentrations decreased in summer while temperatures and total precipitation increased. PCA results indicated the main sources of $PM_{2.5}$ to be light and heavy-duty vehicles, local, and road dust resuspension and civil construction, in this order. The PMF denoted light and heavy-duty vehicle sources, and a road dust resuspension and civil construction source. That way, seasonal changes in $PM_{2.5}$ concentrations occurred according to the expected function of meteorological conditions. The main source of $PM_{2.5}$ in FSP is vehicular, followed by a smaller contribution of road dust resuspension and civil construction.

REFERENCES

Artaxo, P. et al. "Fine mode aerosol composition at three long-term atmospheric monitoring sites in the Amazon Basin." *Journal of Geophysical Research*, 99(D11) (1994).

Colbeck, I., & Lazaridis, M. *Aerosol Science: Technology and Applications*. New Jersey: Wiley, 2014.

de Miranda, R. M. et al. "Source apportionment of fine particulate matter by positive matrix factorization in the metropolitan area of São Paulo, Brazil". *Journal of Cleaner Production*, 202 (2018): 253–263.

Fuzzi, S. et al. "Particulate matter, air quality and climate: Lessons learned and future needs." *Atmospheric Chemistry and Physics*, 15(14) (2015): 8217–8299.

Hetem, I. "Quantificação da contribuição veicular para as concentrações atmosféricas de material particulado fino e black carbon em São Paulo." (2014).

Kumar, P. et al. "New directions: From biofuels to wood stoves: The modern and ancient air quality challenges in the megacity of São Paulo." *Atmospheric Environment*, 140 (2016): 364–369.

Martins Pereira, G. et al. "Particulate pollutants in the Brazilian city of São Paulo: 1-year investigation for the chemical composition and source apportionment." *Atmospheric Chemistry and Physics* (2017): 11943–11969.

Nishida, R. B. "Análise Do Material Particulado Emitido Na Cidade De Ponta Grossa." *Atmospheric Environment*, 53(1) (2017): 1–5.

Pereira, G. M. et al. "Emission factors for a biofuel impacted fleet in South America's largest metropolitan area." *Environmental Pollution*, 331 (2023).

Pereira, G. M. et al. "Particulate matter fingerprints in biofuel impacted tunnels in South America's largest metropolitan area." *Science of the Total Environment*, 856 (2023).

Souto-Oliveira, et al. "Impact of extreme wildfires from the Brazilian Forests and sugarcane burning on the air quality of the biggest megacity on South America." *Science of the Total Environment*, 888 (2023).

Zhang, R. et al. "Formation of Urban Fine Particulate Matter." *Chemical Reviews*, 115(10) (2015): 3803–3855.

AIR POLLUTION CONFERENCE BRAZIL
CMAS SOUTH AMERICA
COMMUNITY MODELING AND ANALYSIS SYSTEM

POST-LOCKDOWN PARTICULATE MATTER COMPOSITION AND SOURCE APPORTIONMENT IN THE METROPOLITAN AREA OF SÃO PAULO

Guilherme Martins Pereira[1], Rafaela Squizzato[1], Caroline Fernanda Hei Wikuats[1], Vitoria Rodilha Leão[1], Jayne Sousa Silva[1], Mario Gavidia-Calderon[1], Adriana Grandis[2], Marcos S. Buckeridge[2], Thiago Nogueira[3], Paulo Artaxo[4], Marco Aurelio de Menezes Franco[1], Maria de Fátima Andrade[1] and Edmilson Dias de Freitas[1]

[1]*Institute of Astronomy, Geophysics and Atmospheric Sciences, University of São Paulo, São Paulo, Brazil*
guilherme.martins.pereira@usp.br; maria.andrade@iag.usp.br; edmilson.freitas@iag.usp.br
[2]*Institute of Biosciences, University of São Paulo, São Paulo, Brazil*
[3]*School of Public Health, University of São Paulo, São Paulo, Brazil*
[4]*Institute of Physics, University of São Paulo, São Paulo, Brazil*

Abstract: In most Latin American metropolises, the largest source of pollutant emissions is the vehicle fleet. In Brazil, atmospheric concentrations of primary pollutants emitted by vehicular exhaust have been reduced after enforcing emission control laws. However, some pollutant levels are still above the values the World Health Organization (WHO) recommended. Extensive monitoring has been performed with the measurement of particulate matter in the Faculty of Medicine of the University of São Paulo, located in the central area of São Paulo (Brazil), since 2021, allowing us to observe the effects of the changes in the fleet circulating in the city. Fine particulate matter ($PM_{2.5}$) was collected with low-volume samplers (Partisol 2025i Sequential Air Sampler) and then subjected to analysis with an XRF (X-ray fluorescence) spectrometer to determine element concentrations. Black carbon (BC) was monitored with an aethalometer, and biomass burning-related BC was estimated. Carbohydrates are quantified after aqueous extraction and analysis with high-performance anion-exchange chromatography with pulsed amperometric detection (HPAEC). $PM_{2.5}$ concentrations increased with northeast winds, where the central area of São Paulo is located, with intense vehicle traffic. The most abundant elements in $PM_{2.5}$ between 2021 and 2022 were S, Na, K, Fe, Si, Zn, and Al. The profile is similar to a previous study performed in the same sampling site when an abundance of Al, K, Fe, and Ca was observed in $PM_{2.5}$. The high abundance of sulfur is associated with the presence of secondarily formed sulfate in the aerosol, and elements such as Si, Al, and K may have crustal origin. In addition to marine aerosol, sodium has already been linked to resuspension associated with paving, vehicular emissions, and, specifically, the combustion of ethanol and gasohol. Potassium may also be associated with biomass burning and marine aerosol. The element Fe has already been associated with emissions from vehicles powered by ethanol and gasohol, which are widely used in Brazil and are also related to crustal sources. Receptor model Positive Matrix Factorization (PMF) was applied, and five factors were obtained. Adding the source's contribution related to vehicle emissions, such as two vehicular-associated factors, secondary formation, and lubricating oil, it is possible to observe that it represents the majority of the contribution for fine particulate matter in the city (above 60%), while the other sources were biomass burning + soil resuspension, marine aerosol, and industrial source. Vehicular-related sources remain dominant after the pandemic lockdown period and are associated with the high particulate matter levels measured at the site.

Keywords: Particulate matter, source apportionment, receptor model, positive matrix factorization, black carbon.

INTRODUCTION

Atmospheric particulate matter (PM) influences the chemistry and physics of the atmosphere, as well as public health and climate (Andreae and Crutzen, 1997). This type of pollutant also has an impact on the atmospheric circulation, hydrological cycle, cloud formation, and the study of the biogeochemistry of ecosystems (Pöschl, 2005). In large Brazilian cities, the largest source of emissions is the vehicle fleet. Despite the reduction in atmospheric concentrations of primary substances emitted by exhaust after the implementation of emission control laws, these are above the values recommended by the World Health Organization. Secondarily formed compounds have an important role in impacting health and the climate (Andrade et al., 2017).

The objective of the study is to obtain the chemical composition of fine particulate matter in the Metropolitan Area of São Paulo (MASP) to determine the emission sources. Receptor models were applied to differentiate primary from secondary sources, and long-range transport.

METHODS

A sampling campaign was performed at the Faculty of Medicine of the University of São Paulo (USP), located in the central area of São Paulo, between 2021 and 2023 with the collection of fine particulate matter ($PM_{2.5}$) with a low-volume sampler (Partisol 2025i Sequential Air Sampler). The collection of particulate matter was performed in 24-hour periods. Teflon filters collected with Partisol were analyzed by energy-dispersive X-ray fluorescence (ED-XRF) to determine the elemental composition, and black carbon (BC) was monitored with an aethalometer

(Magee AE33). The contributions of fossil fuel and biomass burning were apportioned for BC.
The Positive Matrix Factorization (PMF) receptor model was applied for source apportionment and six emission sources were identified.
Carbohydrate compounds are quantified after aqueous extraction under sonication and analysis with high-performance anion-exchange chromatography with pulsed amperometric detection (HPAEC/PAD).

FINDINGS AND ARGUMENT

The most abundant elements in $PM_{2.5}$ in the 2021-2022 period were S, Na, K, Fe, Si, Al and Zn. The profile is similar to a previous study performed in the same sampling site when an abundance of Al, K, Fe, and Ca was observed in fine particulate matter (de Oliveira Alves et al., 2020). The high abundance of sulfur is associated with the presence of secondarily formed sulfate in the aerosol, and elements such as Si, Al, and K may have crustal origin (Miranda et al, 2012). In addition to marine aerosol, sodium has already been linked to resuspension associated with paving, vehicular emissions, and, specifically, the combustion of ethanol and gasohol (Vieira-Filho et al., 2016; Pereira et al., 2023a). Potassium may also be associated with biomass burning and marine aerosol. The element Fe has already been associated with emissions from vehicles powered by ethanol and gasohol, which are widely used in Brazil and are also related to crustal sources (Pereira et al., 2017. Brito et al., 2013).
BC represented 2% to 64% of $PM_{2.5}$ (averaging 14%). The diagnostic ratio BC/Cu averaged 106, approaching the observed EC/Cu ratio obtained in 2018 for a rather diesel-impacted heavy-duty fleet tunnel (149, ranging from 80 to 189) (Pereira et al., 2023b), indicating an impact of heavy diesel vehicles in the studied region. The minimum BC/Cu value (20) was closer to that observed for light-duty vehicles in 2018 (7). In 2018, the EC/Cu diagnostic ratio showed a significant correlation with the fraction of heavy diesel vehicles in the tunnel, suggesting that it could be used to mark the predominance of light or heavy vehicles. EC is associated with emissions from heavy-duty diesel-powered vehicles, while copper is related to light-duty vehicles powered by ethanol and gasohol (Brito et al., 2013).
A six-factor solution was obtained with the PMF receptor model and polar plots (concentrations in function of wind speed and direction) were obtained for each factor (Figure 1). Factor 1 attributed to vehicle exhaust emissions, with the presence of elements such as Cr, Ni, As, Br, Sr, Cd, Sb, and the fossil-fuel-related BC (BC_{ff}), this factor did not present a seasonality trend and the polar plot suggests an association with a local contribution. Factor 2 was attributed to marine aerosol due to the presence of Cl, Na, and Mg increasing with strong winds from the southeast, suggesting the entry of sea breezes. Factor 3 was characterized by chemical species associated with Vehicle sources, including BC_{ff}, Pb, and Zn, which have increased their contribution with northwest winds, where the city's central area is located. Factor 4 may be associated with secondary formation due to the presence of S, and the burning of lubricating oil, due to the presence of P, this factor increased with winds coming from the east and southeast, but in conditions of lower wind speed, suggesting a secondary formation from precursor pollutants. Factor 5 presented a profile marked by a mixture of species associated with soil dust (Fe, Mg, Al, and Si) and biomass burning (Pereira et al., 2017), and was the most associated with biomass-burning-related BC (BC_{bb}). The contribution increases with higher wind speeds from the north, northeast, and northwest, more associated with low humidity conditions, in addition, there are regions with frequent forest fires and burning in the northwest of the state. Factor 6 presented the loading of vanadium and can be attributed to the burning of lubricating oil or industrial sources, the contributions of this factor increased with easterly winds, in a similar way to the V/Ni ratio.

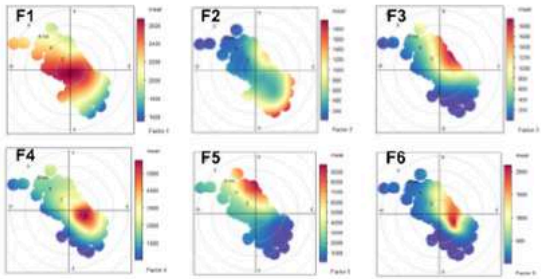


Figure 1. Polar plots for PMF contributions.

Figure 2 presents the contributions of each type of source to $PM_{2.5}$ and their variation between sampling days. Adding the sources related to vehicle emissions such as vehicle exhaust 1 (7%), vehicle 2 (23%), secondary formation and lubricating oil (30%), there is the majority of the contribution for fine particulate matter in the city (n60%). The remaining sources were biomass burning + soil resuspension (24%), industrial (10%), and marine aerosol (5%).

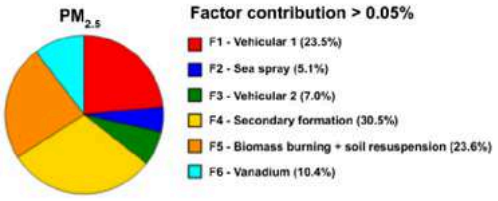


Figure 2.PMF factor contributions for $PM_{2.5}$.

CONCLUSIONS

An extensive $PM_{2.5}$ sampling campaign was performed in the central area of São Paulo. The receptor model (PMF) was updated with these recent results, providing a comprehensive analysis of sources for the period between 2021 and 2022. It was possible to identify six distinct factors, two related to vehicles, one associated with marine aerosol, the other to secondary formation, one to biomass burning + soil resuspension, and the last one related to industries. The inclusion of the recalculated estimate of black carbon from biomass burning allowed the identification of a specific factor for this source. Vehicular-related sources remain dominant after the pandemic lockdown period and are associated with the high particulate matter levels measured at the site.

REFERENCES

Andrade, Maria de Fatima et al. Air quality in the megacity of São Paulo: Evolution over the last 30 years and future perspectives. *Atmospheric Environment* 159 (2017): 66-82.

Andreae, Meinrat, and Crutzen, Paul. Atmospheric Aerosols: Biogeochemical Sources and Role in Atmospheric Chemistry. *Science* (1997): 276.

Brito, Joel et al. Physical-chemical characterization of the particulate matter inside two road tunnels in the São Paulo Metropolitan Area. *Atmospheric Chemistry and Physics* 13 (2013): 12199-12213.

de Miranda, Regina Maura et al. Urban air pollution: a representative survey of $PM_{2.5}$ mass concentrations in six Brazilian cities. *Air Quality, Atmosphere and Health* 5 (2012): 63-77.

de Oliveira Alves, Nilmara, et al. Inflammation response, oxidative stress and DNA damage caused by urban air pollution exposure increase in the lack of DNA repair XPC protein. *Environment International* 145 (2020): 106150.

Pereira, Guilherme Martins et al. Emission factors for a biofuel impacted fleet in South America's largest metropolitan area. *Environmental Pollution* 331 (2023a): 121826.

Pereira, Guilherme Martins et al. Particulate matter fingerprints in biofuel impacted tunnels in South America's largest metropolitan area. *Science of The Total Environment* 856 (2023b): 159006.

Pereira, Guilherme Martins et al. Particulate pollutants in the Brazilian city of São Paulo: 1-year investigation for the chemical composition and source apportionment. *Atmospheric Chemistry and Physics* 17 (2017): 11943-11969.

Pöschl, Ulrich. Atmospheric aerosols: Composition, transformation, climate and health effects. *Angewandte Chemie* 44 (2005): 7520-7540.

Vieira-Filho, Marcelo et al. Water-soluble ions species of size-resolved aerosols: Implications for the atmospheric acidity in São Paulo megacity, Brazil. *Atmospheric Research* 181 (2016): 281-287.

AIR POLLUTION CONFERENCE BRAZIL
CMAS SOUTH AMERICA
COMMUNITY MODELING AND ANALYSIS SYSTEM

EFFECTS OF AİR QUALİTY ON HUMAN HEALTH AND AVOİDABLE DEATHS IN THE METROPOLİTAN REGİON OF RİO DE JANEİRO: 2015-2019.

Ana Drummond1, Brenda Novaes1, Rebekah Bon Oliveira1, Taciana Toledo de Almeida Albuquerque2, Leonardo Hoinaski3, Rizzieri Pedruzzi1
1Department of Sanitary and Environmental Engineering - UERJ
2Department of Sanitary and Environmental Engineering - UFMG
3Department of Sanitary and Environmental Engineering - UFSC
Corresponding author: anasofiaengambiental@gmail.com, rizzieri.pedruzzi@gmail.com

Abstract: Air quality has been strongly influenced by anthropogenic activities since the Industrial Revolution. Air quality management remains without efficient control strategies by public authorities to reduce the concentration of environmental pollutants, which can cause serious health problems and lead to fatalities. Rio de Janeiro also suffers from air pollution, especially the metropolitan area, which contributes 65% of the GDP of Rio de Janeiro and comprises 21 municipalities, with an estimated population in 2019 of 12,899,152 inhabitants. According to the Portal da Indústria, in 2021, around 38,2% of industrial companies in the state were extracting oil and natural gas, and 14.9% were oil derivatives and biofuels. To assess the air pollutant concentration, the Rio de Janeiro state has 125 air quality monitoring stations, which have consistently violated Brazilian air quality standards and the WHO guidelines, which are more restricted than Brazilian standards. According to the WHO, the recommended concentrations for $PM_{2.5}$ are 15 and 5 µg/m³ for 24h and annual average, respectively, to ensure fewer adverse health effects. Among the health effects that $PM_{2.5}$ can cause are cardiovascular, cerebrovascular, and respiratory problems, according to the WHO. This work aims to estimate avoidable deaths in the RMRJ from 2015 to 2019 if the actual concentrations of $PM_{2.5}$ were brought to the WHO limits. To achieve this objective, the relative risk equation will be applied as a function of the concentration of the pollutants PM2.5 related to the ICD of the diseases. The diseases that will be analyzed are all causes (ICD-10, A00-Y98), non-accidental (ICD-10: A00-R99), lung cancer (ICD-10, C33-C34), diseases of the circulatory system (ICD-10, I20-I79) and ischemic heart diseases (ICD-10, C33-C34). The analysis will be based on relative risks already concluded from other studies involving the same diseases and the same group of human beings used as base and exposure. The data on Mortality was taken from DATASUS, and the air quality data came from the INEA database. The results met the expectations of the literature, since the results of avoidable deaths were compared with those of a study that used the same relative risk but with a higher average annual concentration, so the results of this study were slightly lower than those compared. Rio de Janeiro, Duque de Caxias, Niterói, São João de Meriti and Itaboraí were the cities that had valid annual average concentrations of $PM_{2.5}$ and for lung cancer, Rio de Janeiro had the highest value of 59.68(22.3) in 2017, although the highest concentration was 15.86 $\mu g/m^3$in São João de Meriti in 2016, but the result is due to the highest number of deaths in all years for this disease being in Rio de Janeiro, the largest population in the metropolitan region of Rio. For all causes it was 1500 in Rio and for cardiovascular diseases for Rio, it ranged from 288.9 to 726.4 in 2017 depending on the relative risk used, making it important to emphasize that epidemiological studies should be carried out for Brazilian metropolises in order to have a more accurate relative risk for deaths.

Keywords: Air pollution, Air quality standards, Mortality, Rio de Janeiro.

INTRODUCTION

Brazil was considered one of the developing countries in the latest Human Development Report 2021/2022 of the United Nations Development Programme. Countries that are still developing have not seen considerable improvements in air quality, thus demonstrating the urgency of debating the issue (VALLERO, 2014). In addition, the WHO announced in April 2022 that 99% of the population is exposed to air quality that is not in line with the parameters suggested by the WHO itself, so air pollution is a problem of global relevance (PAHO, 2022).

Among the pollutants that the WHO states are high enough to harm the population's health and quality of life are nitrogen dioxide and fine particulate matter. The health effects of exposure to fine particulate matter, considering $MP_{2,5}$, include cardiovascular, cerebrovascular, and respiratory problems and nitrogen dioxide associated with respiratory tract problems that can lead to asthma and coughing (PAHO, 2022).

Air pollution across the country can vary based on the region. Some areas are influenced by industry emissions and cases where vehicular emissions play a crucial role in air pollution.

According to the 1st National Inventory of Atmospheric Emissions by Road Motor Vehicles, Brazil's main source of particulate matter emissions is heavy-duty diesel vehicles, accounting for 45% of emissions in 2009 and 53% in 2020 (ANTT, 2011).

Andreão et al. (2020) found higher PM2.5 concentrations in cities from São Paulo and Rio de Janeiro in 2015 than comparing to the metropolitan regions of São Paulo (MASP), Rio de Janeiro (MARJ),

Belo Horizonte (MABH), and Great Vitória (MAGV), this study concluded 10,300(1,700) to all causes avoidable deaths and 360(100) avoidable deaths of lung cancer, therefore, it is clear the necessity of keep the monitoring and better analyze this scenario.

In this context, this study aims to analyze the air quality of the Metropolitan Region of Rio de Janeiro between 2015 and 2019, focusing on the pollutant $PM_{2.5}$, correlating through relative risks from the literature the deaths related to codes for all causes (ICD10, A00-Y98), cardiovascular (ICD-10, I20-I79), lung cancer (ICD-10: C33-C34), ischaemic heart disease (ICD-10, I20-I25) and nonaccidental deaths (ICD-10: A00-R99) to conclude the quantities of avoidable deaths from the same period.

METHODS

The calculations of avoidable deaths are based on annual deaths based on the specific ICD, air quality data, and the relative risk of the specific ICD related to the pollutant.

The Mortality data was collected from the DATASUS database, filtered by municipalities in the MARJ, and each of the five ICD-10 disease groups from 2015 to 2019. The $PM_{2,5}$ concentrations were taken from the Rio de Janeiro State Environmental Protection Agency (INEA) database, free and available at: (http://200.20.53.25/qualiar/home/index). Therefore, only INEA monitoring stations were considered.

The relative risks were adopted from the study of Andreão et al. (2018) (Table 1). Since there have been no cohort studies in Brazil relating to air pollution and health, these relative risks were considered, all from the long term $PM_{2.5}$:

Table 1 - Relative Risks

Health outcome	ICD-10	Relative Risk	Age Range	From
All Causes	(ICD-10:A00-Y98)	1.08 (1.06-1.11)	>=30	Pope et al. (2019b)
Non-Accidental	(ICD-10: A00-R99)	1.04 (1.03-1.05)	>=30	Cesaroni et al. (2013)
Nonaccidental	(ICD-10: A00-R99)	1.15 (1.13-1.16)	>=25	Crouse et al. (2012)
Cardiovascular	(ICD-10: I20-I79)	1.06 (1.04-1.08)	>=30	Cesaroni et al. (2013)
Cardiovascular	(ICD-10: I20-I79)	1.16 (1.13-1.18)	>=25	Crouse et al. (2012)
Ischemic Heart Disease	(ICD-10: I20-I25)	1.18 (1.14-1.23)	30-99	Pope et al. (2004)
Lung Cancer	(ICD-10: C33-C34)	1.13 (1.07-1.20)	>=30	Pope et al. (2019)

Reference: Drummond, 2024.

Equation (1) was used to find the avoidable deaths in this study since this is the expected health impact function to estimate the health effects in long-term (annual) (Sacks et al., 2018):

$$\Delta y = Y_0 * Pop * (1 - e^{-\beta * \Delta PM}) \quad (1)$$

Where Y_0 is the incidence rate of deaths in the year, (amount of deaths)/(population in that year which is represented as Pop in Equation 1), then the population can be considered, then ΔY is the number of cases avoided (deaths). ΔPM is the air quality final standard of CONAMA 491/2018 for $PM_{2.5}$ which has been considered 10 $\mu g/m^3$, subtracting the average concentration of that year. The value of β can be found by the equation 2:

$$\beta = \frac{\ln(RR)}{\Delta Q} \quad (2)$$

The validation of the annual concentrations of $PM_{2.5}$ were based on the Environment Ministry guide. However, the stations collected data only per six days a year. Therefore, it was considered 50% of valid concentrations per 365/(24) by each four-month period.

FINDINGS AND ARGUMENT

These are the annual concentrations of $PM_{2.5}$ for the cities of the metropolitan region of Rio de Janeiro (Table2):

Table 2 - $PM_{2.5}$ Annual concentrations

City	2015	2016	2017	2018	2019
Rio de Janeiro	11,24	11,83	13,84	10,19	12,37
São Gonçalo	No data	No data	No data	No data	No data
Duque de Caxias	15,67	12,80	9,63	10,30	No data
Nova Iguaçu	No data	No data	No data	No data	No data
Niterói	9,34	11,26	Invalid	Invalid	Invalid
Belford Roxo	No data	No data	No data	No data	No data
São João de Meriti	11,51	15,86	11,39	11,88	13,37
Itaboraí	7,50	14,99	10,02	10,69	No data
Nilópolis	No data	No data	No data	No data	No data
Maricá	No data	No data	No data	No data	No data
Itaguaí	No data	No data	No data	No data	No data
Japeri	No data	No data	No data	No data	No data
Seropédica	No data	No data	No data	No data	No data
Angra dos reis	Invalid	No data	No data	Invalid	Invalid
Barra Mansa	No data	No data	No data	No data	No data

Reference: Drummond, 2024.

And the avoidable deaths considering only the valid data can be checked by figure 1.

	Município	2015	2016	2017	2018	2019
Lung Cancer Pope et al. (2019)	Rio de Janeiro	19,36 (7,35)	29,33 (11,1)	59,68 (22,3)	2,907 (1,11)	36,08 (13,8)
	Duque de Caxias	6,359 (2,34)	3,566 (1,34)	Up to standard	0,413 (0,15)	No data
	Niterói	Up to standard	1,966 (0,74)	Invalid	Invalid	Invalid
	São João de Meriti	1,189 (0,45)	4,006 (1,47)	0,977 (0,37)	1,427 (0,54)	2,582 (0,96)
	Itaboraí	Up to standard	1,655 (0,61)	0,004 (0,00)	0,267 (0,10)	No data
Non-accidental Crouse et al. (2012)	Rio de Janeiro	832,5 (64,415)	1293, (99,663)	2536, (192,96)	129,5 (10,093)	1713, (131,61)
	Duque de Caxias	407,9 (30,660)	218,8 (16,762)	Up to standard	23,85 (1,8566)	No data
	Niterói	Up to standard	71,72 (5,5481)	Invalid	Invalid	Invalid
	São João de Meriti	66,70 (5,1517)	270,5 (20,308)	59,92 (4,6318)	84,37 (6,50)	157,64 (12,02)
	Itaboraí	Up to standard	95,58 (7,21)	0,319 (0,02)	15,61 (1,21)	No data
Non-accidental Cesaroni et al. (2013)	Rio de Janeiro	233,1 (45,559)	363,1 (72,428)	720,2 (143,09)	36,11 (7,2260)	482,6 (96,170)
	Duque de Caxias	116,7 (23,108)	61,75 (12,284)	Up to standard	6,624 (1,3252)	No data
	Niterói	Up to standard	20,15 (4,0248)	Invalid	Invalid	Invalid
	São João de Meriti	18,69 (3,7304)	77,23 (15,285)	16,70 (3,3352)	23,61 (4,70)	44,558 (8,861)
	Itaboraí	Up to standard	27,32 (5,41)	0,088 (0,01)	4,360 (0,87)	No data
All causes Pope et al. (2019)	Rio de Janeiro	486,6 (119,04)	756,6 (268,77)	1500, (362,85)	75,59 (18,577)	1002, (244,02)
	Duque de Caxias	243,2 (58,3)	129,4 (31,4)	Up to standard	14,04 (3,45)	No data
	Niterói	Up to standard	41,98 (10,2)	Invalid	Invalid	Invalid
	São João de Meriti	38,89 (9,50)	159,8 (38,3)	35,04 (8,56)	48,81 (11,9)	91,90 (22,2)
	Itaboraí	Up to standard	58,31 (14,0)	0,188 (0,04)	9,252 (2,26)	No data
Cardiovascular Cesaroni et al. (2013)	Rio de Janeiro	96,75 (25,4)	152,7 (40,1)	288,9 (75,5)	14,34 (3,78)	190,2 (49,9)
	Duque de Caxias	52,35 (13,6)	29,47 (7,73)	Up to standard	2,203 (0,58)	No data
	Niterói	Up to standard	7,334 (1,93)	Invalid	Invalid	Invalid
	São João de Meriti	8,010 (2,10)	32,47 (8,44)	6,443 (1,69)	7,921 (2,08)	13,51 (3,53)
	Itaboraí	Up to standard	11,62 (3,03)	0,034 (0,00)	1,655 (0,43)	No data
Cardiovascular Crouse et al. (2012)	Rio de Janeiro	245,8 (29,2)	387,1 (45,8)	726,4 (84,86)	36,61 (4,387)	481,2 (56,79)
	Duque de Caxias	130,8 (15,0)	74,26 (8,73)	Up to standard	5,654 (0,676)	No data
	Niterói	Up to standard	18,65 (2,21)	Invalid	Invalid	Invalid
	São João de Meriti	20,36 (2,41)	81,09 (9,34)	16,37 (1,945)	20,11 (2,382)	34,04 (3,990)
	Itaboraí	Up to standard	29,10 (3,37)	0,087 (0,010)	4,213 (0,503)	No data
Ischemic Heart Disease Pope et al. (2004)	Município	2015	2016	2017	2018	2019
	Rio de Janeiro	101,2 (18,8)	163,7 (30,2)	319,1 (57,9)	17,39 (3,26)	235,3 (43,2)
	Duque de Caxias	50,15 (8,95)	26,27 (4,81)	Up to standard	1,926 (0,36)	No data
	Niterói	Up to standard	9,740 (1,80)	Invalid	Invalid	Invalid
	São João de Meriti	8,222 (1,52)	34,00 (6,06)	6,715 (1,24)	8,311 (1,53)	15,13 (2,75)
	Itaboraí	Up to standard	11,64 (2,09)	0,035 (0,00)	1,810 (0,33)	No data

Figure1-Avoidable deaths and standard deviation

There is a difference between the relative risks even when comparing the same disease, for example, in the case of cardiovascular diseases, the highest relative risk (Crouse et al. 2012) results in a greater number of avoidable deaths, considering the same year, as well as for nonaccidental deaths, which in the case of Crouse et. al 2012, it is possible to see a more significant number of avoidable deaths than the all-causes cases itself, since the relative risk of Crouse is greater than that of Pope et. al (2019).

Furthermore, when comparing with the results of Andreão, et al. 2020, the deaths of cardiovascular diseases, RR of Crouse et al., 2012 and Cesaroni et al. (2013) were lower in this study in 2015, and the concentration of $PM_{2.5}$ in this study was lower, 11,24 μ/m^3, compared to 12 μ/m^3 in Andreão study, so it was already expected that all the results would be lower, considering the same cities, RR, and year.

CONCLUSIONS

Therefore, air quality deserves more effort and attention in Rio de Janeiro, mainly in metropolitan regions as the cities belong to the state of Rio de Janeiro, as it was possible to find significant avoidable death results if $PM_{2.5}$ concentration was up to the standard 10 μ/m^3. Therefore, it is urgent that there are cohort studies in Brazil for Mortality and thus, to have a more faithful result of avoidable deaths since there is a significant difference between avoidable deaths from different RR even for the same disease.

REFERENCES

Andreão et al. Excess deaths associated with fine particulate matter in Brazilian cities Atmos, 71-81. Environ., 194 (2018), doi:10.1016/j.atmosenv.2018.09.034.

Andreão *et al.* Quantifying the impact of particle matter on Mortality and hospitalizations in four Brazilian metropolitan areas, Journal of Environmental Management, Volume 270, 2020, 110840, doi: https://doi.org/10.1016/j.jenvman.2020.110840.

ANTT. 1st National Inventory of atmospheric emissions by road motor vehicles, 2011. Available at:http://anuario.antt.gov.br/index.php/content/view/5632/1__Inventario_Nacional_de_Emissoes_Atmosfericas_por_Veiculos_Automotores_Rodoviarios.html.

Brazil. Ministry of the Environment. Environmental Quality Secretariat. Technical guide for monitoring and evaluating air quality / Ministry of the Environment. Department of Environmental Quality. Department of Environmental Quality and Waste Management. - Brasília, DF: MMA, 2020. 136 p. : ill. colour.

Cesaroni et al. Long-term exposure to urban air pollution and Mortality in a cohort of more than a million adults in Rome. Environ. Health Perspect., 121 (2013), pp. 324-331, doi:10.1289/ehp.1205862.

Crouse et al. Risk of nonaccidental and cardiovascular Mortality in relation to long-term exposure to low concentrations of fine particulate matter: a Canadian national-level cohort study Environ. Health Perspect., 120 (2012), pp. 708-714, 10.1289/ehp.1104049.

PAHO. Billions of people still breathe unhealthy air: new WHO data. Available in: <https://www.paho.org/pt/noticias/4-4-2022-novos-dados-da-oms-revelam-que-bilhoes-pessoas-ainda-respiram-ar-insalubre>.

Pope et al. Cardiovascular Mortality and long-term exposure to particulate air pollution: epidemiological evidence of general pathophysiological pathways of disease Circulation, 109 (2004), pp. 71-77, doi: 10.1161/01.CIR.0000108927.80044.7F.

Pope et al. Fine particulate air pollution and human mortality: 25+ years of cohort studies. Environmental Research (2019), doi:10.1016/j.envres.2019.108924.

Sacks *et al.* The Environmental Benefits Mapping and Analysis Program e Community Edition (BenMAPeCE): a tool to estimate the health and economic benefits of reducing air pollution Environ. Model. Software, 104 (2018), pp. 118-129, doi: 10.1016/j.envsoft.2018.02.009.

VALLERO, D. Fundamentals of Air Pollution. 5. ed. EUA, 2014.

AIR POLLUTION CONFERENCE BRAZIL
CMAS SOUTH AMERICA
COMMUNITY MODELING AND ANALYSIS SYSTEM

PHYSICAL-CHEMICAL CHARACTERIZATION OF FINE PARTICULATE MATTER($_{2,5}$ IN AMAZONIA: A STUDY IN FOUR MUNICIPALITIES IN NORTHEASTERN PARÁ DURING THE TRANSITION BETWEEN THE SUMMER AND WINTER PERIOD AMAZONIAN

Francisco Daniel Mota Lima [1] , Glauber Guimarães Cirino [2] , Julia Clarinda Paiva Cohen [3] , David Kenton Adams [4]

[1] *Federal University of Pará*
francisco.lima@ifpa.edu.br
[2] *Federal University of Pará*
glaubercirino@ufpa.edu.br
[3] *Federal University of Pará*
jcpcohen@ufpa.edu.br
[4]*University of Arizona*
dave.k.adams@gmail.com

Abstract: Atmospheric aerosols, also called Particulate Matter (PM), attract great interest in studies on climate and air quality, being important indicators of environmental pollution. The objective of this study is to characterize PM $_{(2.5)}$ in terms of concentration, chemical composition, black carbon content and morphology of particulate matter during the transition between summer and winter in the Amazon of Pará (months of November and December 2022).In the Amazon, this type of study is scarce, especially during the transition period between seasons. The Minivol, manufactured by Airmetrics, was used to collect particulate matter, and polycarbonate filters with a diameter of 47mm and pores of 0.4µm with filter changes every 24h. 22 measurements were carried out in locations with different land uses: an urbanized area in Belém-Pa; a coastal mangrove area located in Bragança-Pa, an area close to the sea located in Salinópolis-Pa and a pasture area, affected by mineral exploration, in Barcarena-Pa. These sampling locations are strategic for evaluating the influence of local and regional PM-emitting sources, as well as long-distance aerosol transport. Concentration was determined by the gravimetric method. Scanning electron microscopy (MeV) was used to determine the morphology of the PM. The chemical composition of the PM and the black carbon (BC) content will be determined using X-ray fluorescence (XRF) and reflectance, respectively. The analyzes were carried out in collaboration with several partner laboratories, such as the Mineral Characterization Laboratory at the UFPA Institute of Geosciences (LCM), Atmospheric Processes Analysis Laboratory, at the Institute of Astronomy, Geophysics and Atmospheric Sciences at USP (LAPAt). The average concentrations of PM $_{2.5}$ and BC were: Belém (10.71µg/m ^{3} ; 1.04 µg/m ^{3})- urban area; Barcarena (2.13 µg/m ^{3} ; 1.13 µg/m ^{3})-industrial area; Bragança (10.93 µg/m ^{3} ; 0.26 µg/m ^{3})-coastal mangrove area and Salinópolis (2.13 µg/m ^{3} ; 0.028 µg/m ^{3})- area close to the sea. The (MeV) result revealed spherical particles, small clusters, pointed particles, ovals, rods, particles overlapping layers and biogenic particles. The chemical composition of MP revealed the predominance of macroelements such as Na, K, Cl, Si, Ca and S revealed some of the properties of PM in the Amazon of Pará in the transition period between winter and Amazon summer.

Keywords : Particulate matter, atmospheric chemistry, physical-chemical characterization, land use, Pará Amazon.

INTRODUCTION

In the Amazon Pollution in Pará atmospheric constitutes one of the most serious and complex problems current environmental issues, although yet little searched . Pollutants as you Aerossóis Athmospheric(AA) or Particulate Matter (PM) is responsible per many different effects on climate , environment environment and in health human . The (AA) constitute mixtures particle complexes solid It is liquid in sus p e n is œat atmosphere coming in varied types in sources (SEINFELD, 2016). In the climate, MP can act as an aerosol scatterer or absorber of solar radiation. O operation of the ecosystems am azônics, reducing the amount in r a d i a ç ã o solar required to the process in photosynthesis (CIRINO et al. , 2014 ; EZHOVA et al. , 2018 ; RAP MUSIC et al. , 2018 ; ARTAXO et al. , 2021) It is properties microphysics of clouds impacting , indirectly , the cycle h i d r o l g i c .There is also evident impacts about health human . Brazil recorded around 52 thousand deaths in 2019 alone (WHO, 2021). The chemical composition of PM presents a wide variety of substances, mainly due to the fine particles that associate with secondary gaseous pollutants through nucleation and condensation processes, forming larger particles (JACOBSON, 2002; GODISH 2003; BAIRD, 2006, SEINFELD, 2016).The fine particles have predominant concentrations of nitrate and sulfate ions, condensed organic compounds, elemental carbon and a variety of metals. Depending on the chemical composition of the particulate material, the morphology and shape of the particles vary. On the other hand, in Brazil, a bottleneck important limits very much ours capacity predictive current: the lack of an investment of emissions in MP in lots of regions from the the Amazon Brazilian. Missing information basics about the main sources,

concentrations and composition MP chemistry (ANNA et al. , 2021). Therefore, this research aims to characterize fine particulate matter in 4 municipalities in the northeast of the Amazon Pará during the transition period between the Amazon winter and summer, which corresponds to the months of November and December.

METHODS

Location and description of the study area

Figure 01 illustrates the four municipalities that are the subject of this study.

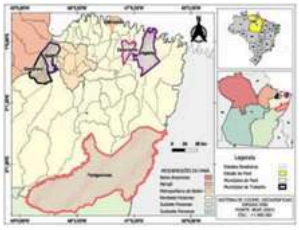


Figure 01. Location of the 4 municipalities covered by this study.

The 04 municipalities have different land uses and occupation. Bragança (close to the mangroves and the sea; and firewood burning in various production processes), Capanema (presence of a large cement factory), Salinópolis (coastal region) and the state capital, Belém (the city is undergoing an intense process of metropolization, and numerous works due to COP 30), that is, there is a notable diversity of land uses, with urban areas, agricultural areas amidst fragments of native forest, combined mainly with the increase in the number of vehicles and the increase of around 85% in the motorcycle fleet, places Belém as the fourth city in the country in terms of vehicle fleet growth, currently with 511 thousand vehicles and approximately 150 thousand motorcycles (IBGE, 2022).

Instrumentation and techniques analytics at characterization of $_{PM\ 2.5}$

The Minivol manufactured for the *Airmetrics* it was the equipment used at carrying out the research with filter changes every 24 hours, operates with a flow rate of 5 L/min. They were used polycarbonate filters with a diameter of 47mm and pores of 0.4µm. The determination of the mass concentration of particulate matter was carried out using the gravimetric method . After being sampled, the filter with the collected particulate matter was weighed again and the result of the difference in weight between the dirty filter and the clean filter (in µg) divided by the volume of total air sampled (in m^3), thus estimating the average concentration of particulate matter dispersed in the air during the period, expressed in $\mu g/m^3$. For weighing, a Mettler Toledo model MX5 precision scale with 6 decimal places was used. In reflectance analysis a Smoke reflectometer was used Stain Reflectometer, Diffusion System, model M43D. The analysis was used to estimate the concentration of BC present in the sampled filters. Epsilon 5, PANalytical BV, was used in chemical characterization using X-ray Fluorescence (XRF), an instrumental analytical technique used in the qualitative and quantitative assessment of chemical composition in various types of studies (ARANA et al., 2016; LIMA et al., 2020). The morphological characterization of the samples was obtained using the Scanning Electron Microscopy (MeV), providing high-resolution information on morphology, such as particle texture, size and shape.

FINDINGS AND ARGUMENTS

Figure 02 reveals the concentrations of PM and BC in the 4 municipalities for the campaign period, the months of November and December, the transition between summer and winter in the Amazon. The highest average concentrations of PM and BC were quantified in Belém (10.71 $\mu g/m^3$;1.04 $\mu g/m^3$) ,Bragança (10.73 $\mu g/m^3$; 0.27 $\mu g/m^3$),Barcarena (10.01 $\mu g/m^3$; 1.13 $\mu g/m^3$) and Salinópolis (2.13 $\mu g/m^3$;0.028 $\mu g/m^3$), respectively.

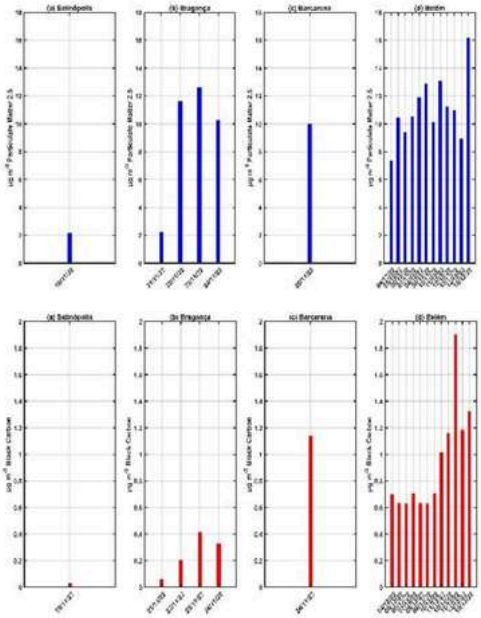
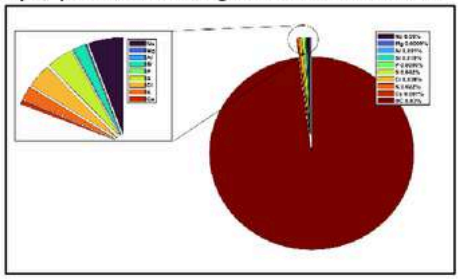


Figure 02. Concentration of MP and BC in the municipalities of Salinópils, Bragança, Barcarena and Belém, campaign period between November and December 2022.

Regarding the composition of Particulate Material, figure 03 illustrates the percentage of the elemental composition of the PM of Belém and Bragança, places with higher concentrations.



AIR POLLUTION CONFERENCE BRAZIL
CMAS SOUTH AMERICA
COMMUNITY MODELING AND ANALYSIS SYSTEM

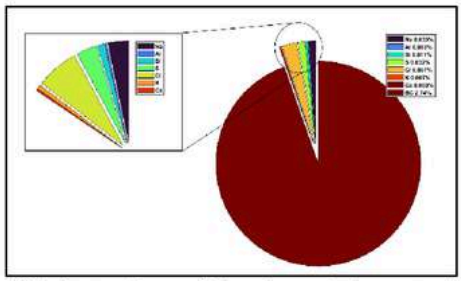
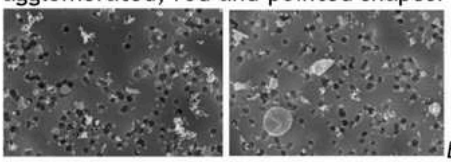
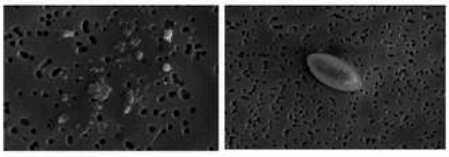


Figure 03. Percentage of the elemental composition of the MP of Belém and Bragança, places with higher concentrations.

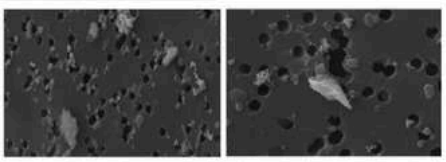
Belém presents more intense land use and occupation, with a greater variety and number of pollution sources, population size beyond the current verticalization process, growth of the city and metropolitan region, especially on the way to the COP 30. Barcarena, an industrial and mining region, uses different types of fossil fuels, such as natural gas and oil, in addition to the presence of the largest port in the State of Pará, justifying the concentrations of PM and BC. In Bragança there are brickworks and flour mills, with firewood burning in the production processes, in addition to the intense burning of oil in small and medium-sized boats to meet the largest fish production in the State. Added to this is the proximity to the sea and mangrove vegetation as a potential emission of biogenic particles. Salinópolis is one of the main tourist routes in the State, its main sources of emissions are the sea. The city has no potential anthropogenic sources of air pollution, although civil construction activities are growing in the city. The chemical composition revealed the predominance of macro elements such as K, S, Al, Ca, Cl, Si and Na, elements associated with anthropogenic and biogenic emissions. Figure 04 shows the micrographs of the particles and revealed oval, spherical, agglomerated, rod and pointed shapes.



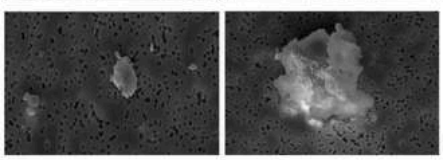
Belém



Bragança



Barcarena



Salinópolis

CONCLUSIONS

Air pollution is a topic that is still little researched in the northeast of the Pará Amazon, and this study is a pioneer in the physical-chemical characterization in 04 municipalities with different land uses and occupation, from coastal areas and mangrove regions (Salinópolies and Bragança), through through a large urban center (Belém) to an industrial and mining area (Barcarena). The results revealed concentrations of PM and BC in the order of: Belém (10.71µg/m^3; 1.04µg/m^3), Bragança (10.73µg/m^3 ; 0.27µg/m^3), Barcarena (10.01µg/m^3; 1.13 µg/m^3) Salinópolis (2.13µg/m^3 ; 0.028µg/m^3). The elemental composition revealed the predominance of macroelements such as Na, K, Cl, Si, Ca and S and micrographs of spherical particles, small clusters, pointed particles, ovals, rods, particles overlapping layers and biogenic particles. And it reinforces the need to monitor the region in view of the need for measures and campaigns throughout the year.

REFERENCES

Arana, A. Atmospheric Aerosols in the Amazon: Composition. PhD, p. 153, 2014.

Baird, Colin. Environmental Chemistry, 2006 2

Cırıno, Guimarãe.G., SOUZA, RAF, ADAMS, DK, Artaxo, P., 2014. The effect of atmospheric aerosol particles and clouds on net ecosystem exchange in the Amazon. Atmos. Chem. Phys. 14, 6523-6543. https://doi.org/10.5194/acp-14-6523-2014.

Godısh, T. Air quality. Boca Raton: CRC Press, LLC, 3 ed, 2003.

IBGE: Brazilian Institute of Geography and Statistics, 2022.

Jacobson, MZ Atmospheric Pollution - History, Science and Regulation, Cambridge University Press, 2002.

Lıma, Francısco Danıel Mota Lıma., Pedro José Perez-Martınez., Marıa De Fátıma Andrade., Prashant Kumar., Regına Maura DE Mıranda. Characterization of particles emitted by pizzerias burning wood and briquettes: a case study at São Paulo, Brazil. Environmental Science and Pollution Research. 2020. https://doi.org/10.1007/s11356-019-07508-6.

Rap, A.; Scott, CE; Reddington, C.L.; Mercado, L.; Ellıs, RJ; Garraway, S.; Evans, M.J.; Beerling, DJ; Mackenzıe, AR; HewıtT, CN;

Spracklen, DV Enhanced global primary production by biogenic aerosol via diffuse radiation fertilization. Nature Geoscience, Springer US, v. 11, no. 9, p. 640-644, 2018. ISSN 17520908

Spracklen, DV Enhanced global primary production by biogenic aerosol via diffuse radiation fertilization. Nature Geoscience, Springer US, v. 11, no. 9, p. 640-644, 2018. ISSN 17520908

Seınfeld, JH Atmospheric chemistry and physics: from air pollution to climate change. Third. Hoboken, New Jersey: John-Wiley & Sons, Inc., 2016. 1963 p. ISBN 9781626239777.

AIR POLLUTION CONFERENCE BRAZIL
CMAS SOUTH AMERICA
COMMUNITY MODELING AND ANALYSIS SYSTEM

Annoyance due to sedimented particulate matter and its influencing factors experienced by communities in an industrialized area

Milena Machado[1], Franciele Ribeiro Cavalcante[2], Valderio Anselmo Reisen[3, 5], Paulo Roberto Prezotti Filho[1], Jane Meri Santos[2], Márton Ispány[4] and Pascal Bondon[3]

[1]Federal Institute of Science and technology of Espírito Santo, Brazil.
E-mail:milenamm@ifes.edu.br
[2]Department of Environmental Engineering, Federal University of Espírito Santo, Brazil.
[3]Université Paris-Saclay, CNRS, CentraleSupélec, Laboratoire des signaux et systèmes, 91190, Gif-sur-Yvette, France.
E-mail:
[4]Faculty of Informatics, University of Debrecen, Debrecen, Hungary.
E-mail:
[5]Institute of Mathematics and Statistics, Federal University of Bahia, Salvador, Brazil
E-mail:

Abstract: This study investigates annoyance caused by air pollution according to the perception of the exposed community and also investigates variables that determine the perceived nuisance caused by sedimented dust. Face-to-face surveys obtained the data set before and after the pelletizing plant interruption. The Pearson chi-square test and the logistic regression model were applied. Comparing the surveys, the population perceived air quality improvement after the industry interruption and also noticed that the main source of settled dust had changed. The logistic regression model identifies air quality assessment, frequency of perceived air pollution caused by dust, seeing the doctor with problems caused by dust, and the quantity of dust inside the house, as the variables determining the annoyance caused by dust. The results prove that the interruption at the pelletizing plant reduced the complaints about nuisance due to dust. However, the communities complain about the loss of work and income. This study presents results that reconcile the various approaches to quantify annoyance caused by air pollution and provide information to improve future community involvement policies.

Keywords: annoyance, dust, community perception, quality of life.

INTRODUCTION

The proximity of industries to communities in developing regions often triggers complaints about air pollution, particularly regarding particulate matter (PM)(Seinfeld and Pandis, 2016). Numerous studies have shown that PM concentration exposure causes adverse health and quality of life effects, for example, respiratory and cardiovascular diseases, as well as annoyance and impacts on daily activities. According to the World Health Organization (WHO, 2006), health is a "state of complete physical, mental, and social well-being, and not simply the absence of disease or illness." Thus, air pollution-related annoyance has an impact on quality of life and is a public health issue.

Despite the documented relationship between annoyance and PM concentration levels (Blanes-Vidal et al., 2012; Machado et al., 2018), there are few studies exploring details about many variables that can influence people's opinions. Inspired by Stenlund et al.'s (2009) research, this study investigates the perceived air pollution impact of an unplanned intervention halting operations at a pelletizing plant in southern Espírito Santo, Brazil. This event offers a unique opportunity to assess community perception changes regarding air pollution reduction, risk perception, and economic consequences. The objective of this study is to explore community annoyance due to air pollution and investigate factors associated with perceived nuisance from sedimented dust.

METHODS

The study was conducted in the southern region of Espírito Santo, Brazil, specifically in the municipalities of Anchieta and Guarapari. Surveys were conducted in 2014 and 2017, before and after the interruption of activities at a pelletizing plant caused by a mining industry accident in Mariana, MG (the city where the mining process begins). The research radius was defined as 1.5 km around six air quality monitoring stations. These areas are identified as sub-regions Anchieta-sede (E-1), Belo Horizonte (E-2), Guanabara (E-3), Maembá (E-4), Meaípe (E-5), and Ubu (E-6). A simple stratified random sampling method with proportional allocation was employed, resulting in representative sample sizes of n = 258 in 2014 and n = 553 in 2017.

The questionnaire comprised closed-ended questions covering air pollution perception, dust annoyance, dust impact, health problems, and respondent profiles (Machado et. al 2014).

Statistical analyses, including the chi-square test of homogeneity and independence, were applied to compare the two surveys and identify associations between annoyance caused by air pollution and questionnaire variables.

RESULTS

Figure 1 compares the annoyance due to air pollution and the assessment of air quality before and after the interruption of pelletizing plant activities. The findings indicate that air pollution annoyance was higher in the 2014 survey, and in the 2017 survey, an improvement in the assessment of air quality. These findings are consistent with those of Stenlund et al. (2009), who showed that a higher proportion of respondents were not annoyed with air pollution and perceived better air quality after the interruption of a sinter plant.

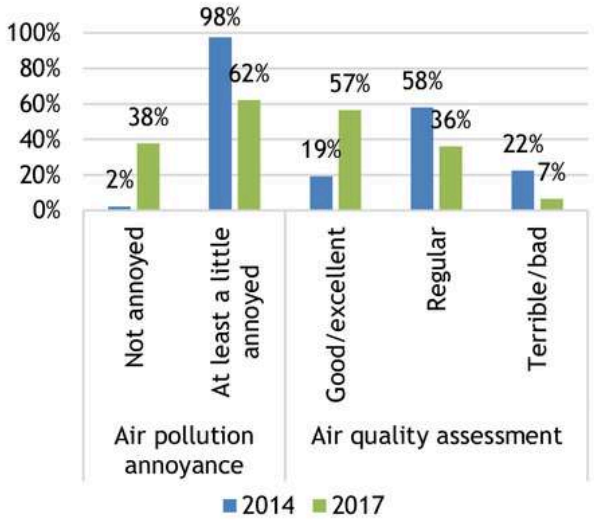


Figure 1. Annoyance and air quality perception

Statistical comparisons between the two surveys were conducted using a chi-square homogeneity test. The tested hypothesis (H_1) was that perceptions of air pollution and its impacts had changed following the intervention. A summary of the homogeneity test results is presented in Table 1. As expected, changes in the frequency of perceptions of dust, annoyance due to dust, and air pollution were statistically significant. Reductions in the impact on daily activities were also observed, such as a decreased frequency of house cleaning to remove dust, less frequent closing of windows to prevent dust from outside. While visits to the doctor appeared to be less frequent, less severe symptoms related to dust, such as allergies, rhinitis, sinusitis, coughs, throat irritations, and shortness of breath, remained a problem even before dust reduction.

Regarding the source of dust, in 2014, 79.5% of respondents identified the industry as the main source in the region. In 2017, this scenario changed, and a higher proportion of respondents identified vehicles, unpaved roads, and construction work as the main source of air pollution. Research in various contexts has also found that people in metropolitan areas have identified vehicular traffic and industry as sources of dust (Orru et al., 2016; Vlasov et al., 2022).

Table 1. Homogeneity test results

Hypotheses	Variables
H_1 (Statistically significant (>0.05)	Perception of dust, annoyance, sources or air pollution, impact in daily activities (cleaning, closing windows), visiting doctor
H_0(Not significant (<0.05)	Health symptoms related to dust and perception of air pollution through odor

Table 2 presents the results of independence tests, revealing associations between various factors and the degree of annoyance with air pollution. Before and after the closure of the pelletizing plant, variables related to air quality perception, risk exposure, perception of other forms of air pollution (opacity and odor), and dust impacts on daily activities showed significant associations ($p < 0.05$). Moreover, gender was also significant, aligning with previous studies like those by Machado et al. (2021, 2022), which linked higher levels of annoyance with dust pollution to the female gender, likely due to women's roles in cleaning and dust removal.

In 2017, the importance of air quality was found to be associated with annoyance, suggesting that social and financial issues were more dominant in this context. Despite the improvement in air quality following the closure of the pelletizing plant, the loss of jobs and economic impact in the region were noteworthy, and more than 90% of respondents expressed a desire for the industry to resume operations.

Table 2. Independence test results

Variables	2014 P-value	2017 P-value
Air Quality Importance	0.00	0.49
Air Quality Assessment	0.00	0.00
Industrial Risk Exposure	0.00	0.00
Dust Deposition Perception	0.00	0.00
Odor Perception	0.02	0.00
Opacity Perception	0.00	0.00
Indoor Dust Annoyance	0.00	0.00
Dust Source	0.00	0.26
House Cleaning Frequency	0.00	0.00
Closing Windows	0.00	0.07
Doctor Visits Frequency	0.00	0.00
Health Problems Frequency	0.00	0.00
Air Pollution Source	0.00	0.18
Dust Reduction Perception	-	0.00
Occupation	0.17	0.05
Smoking	0.21	0.95
Gender	0.05	0.02
Age Group	0.44	0.02
Education	0.20	0.78

Also, a significant result of air pollution perception and dust sources was only observed in the 2014 survey, coinciding with the period when industrial activities contributed to MP concentration in the region.

CONCLUSIONS

The study investigated community annoyance due to air pollution and the factors associated with perceived nuisance from air pollution before and after the unplanned closure of a pelletizing plant in southern Espírito Santo, Brazil.

The study highlighted the changes in air pollution sources perception, from industrial to vehicles and construction activities comparing both scenarios. Statistical analyses identified factors associated with the degree of annoyance with air pollution, including air quality assessment, industrial risk, perceptions of dust and other forms of air pollution, impacts on quality of life (health, cleaning the house, opening windows) and gender.

These findings underscore the complex nature of air pollution due to air pollution and emphasize the importance of comprehensive strategies addressing both environmental and socioeconomic dimensions to foster healthier and more sustainable communities.

REFERENCES

Blanes-Vidal, V., Suh, H., Nadimi, E. S., Løfstrøm, P., Ellermann, T., Andersen, H. V., & Schwartz, J. (2012). Residential exposure to outdoor air pollution from livestock operations and perceived annoyance among citizens. *Environment international*, *40*, 44-50.

Machado, M., Santos, J. M., Frere, S., Chagnon, P., Reisen, V. A., Bondon, P., ... & Reis Jr, N. C. (2021). Deconstruction of annoyance due to air pollution by multiple correspondence analyses. *Environmental Science and Pollution Research*, *28*(35), 47904-47920.

Machado, M., Santos, J. M., Reisen, V. A., e Silva, A. F. P., Junior, N. C. R., Bondon, P., ... & Lima, A. T. (2022). Parameters influencing population annoyance pertaining to air pollution. *Journal of Environmental Management*, *323*, 115955.

Machado, M., Santos, J. M., Reisen, V. A., Reis Jr, N. C., Mavroidis, I., & Lima, A. T. (2018). A new methodology to derive settleable particulate matter guidelines to assist policy-makers on reducing public nuisance. *Atmospheric environment*, *182*, 242-251.

Orru, K., Orru, H., Maasikmets, M., Hendrikson, R., and Ainsaar, M. (2016). Well-being and environmental quality: Does pollution affect life satisfaction? *Quality of Life Research*, 25(3):699–705.

Seinfeld, J. H., & Pandis, S. N. (2016). *Atmospheric chemistry and physics: from air pollution to climate change*. John Wiley & Sons.

Stenlund, T., Lidén, E., Andersson, K., Garvill, J., & Nordin, S. (2009). Annoyance and health symptoms and their influencing factors: A population-based air pollution intervention study. *Public Health*, *123*(4), 339-345.

Vlasov, D., Ramírez, O., & Luhar, A. (2022). Road dust in urban and industrial environments: Sources, pollutants, impacts, and management. *Atmosphere*, *13*(4), 607.

World Health Organization. (2006). *Air quality guidelines: global update 2005: particulate matter, ozone, nitrogen dioxide, and sulfur dioxide*. World Health Organization.

AIR POLLUTION CONFERENCE BRAZIL
CMAS SOUTH AMERICA
COMMUNITY MODELING AND ANALYSIS SYSTEM

Influence of wind direction, receptor point height and time interval on predicting the maximum short-term average concentration and on the integral time scale of concentration

Renata Pilon Cevolani[1], Elisa Valentim Goulart [2]
[1]*Affiliation: Federal University of Espirito Santo*
E-mail: renatapc.09@gmail.com
[2]*Affiliation: Federal University of Espirito Santo*
E-mail: elisa.goulart@ufes.br

Abstract: Atmospheric turbulence on a micrometeorological scale can lead to concentration peaks in very short time intervals, on the order of seconds or minutes. Exposure to these peaks can cause discomfort and immediate serious impacts, depending on the emitted pollutant, when the peak exceeds sanitary limits. Short-term individual exposure is especially crucial in cases of release of toxic, flammable, and odorous gases into the air, as they can be dangerous and harmful to health at relatively low concentrations and short exposure times. Additionally, it is even more concerning in urban areas, where the presence of buildings significantly alters the structure of atmospheric turbulent flow. To analyze the impacts of atmospheric emission of toxic substances, flammables, or odor fluctuations on health, it is necessary to calculate the average concentration over a short time interval, on the order of seconds or minutes. As legislation and dispersion models typically use at least hourly average concentration, alternative techniques have been developed to estimate short-term individual exposure. Among them is the Power Law function (peak-to-mean ratio), which relates the average concentration over a longer time interval to the maximum average concentration over a shorter time interval. Another model, developed by Bartzis et al. (2008), derived from the Power Law function, relates the maximum average concentration to parameters such as turbulence intensity and integral time scale of concentration. The objective of this article is to analyze the influence of wind direction, receptor point height, and time interval on predicting the maximum short-term average concentration, using these two models, and on the integral time scale of concentration. For this purpose, wind tunnel data from the works of Castro et al. (2017) and Fuka et al. (2018) were utilized, where the authors conducted flow and dispersion experiments in an idealized urban model, composed of 14x21=294 rectangular blocks with a width of 2H, length of H, and height of H, where H=70mm. When comparing the performance of the two models for two exposure time intervals, 0.01 and 0.1, considering the wind direction 15° and height of the receiving point equal to H/2, the Bartzis's model obtained a performance (FAC2) much higher than Power Law Function.

Keywords: *Air pollution, Exposures, Modeling, Short-term exposure*

INTRODUCTION

Knowing how to predict the maximum short-term average concentration is especially important in cases of release of toxic, flammable and odorous gases into the air, as such substances can be dangerous at relatively low concentrations and over short periods of exposure. This parameter is essential for analyzing the consequences of these cases, which are even more worrying in urban areas, and planning countermeasures. In fact, to analyze such impacts, it is necessary to calculate the average concentration over a short period of time, on the order of seconds or minutes. However, the exposure periods used by legislation, Gaussian models and the World Health Organization (WHO) Global Air Quality Guidelines are generally at least 1 hour. Therefore, alternative techniques have been developed to estimate the maximum short-term average concentration. Among them, the Power Law function (peak-mean ratio), originally presented by Singer (1961), which relates the average concentration in a longer time interval to the maximum average concentration in a shorter time interval, and the model developed by Bartzis et al. (2008), resulting from the Power Law function and which relates the maximum average concentration to parameters such as turbulence intensity and concentration integral time scale.

After being originally presented by Singer (1961), the Power Law function was applied in the works of Santos et al. (2009a), Santos et al. (2019), Mello et al. (2023), Bartzis et al. (2008), among others. In Bartzis et al. (2008), the author seeks to estimate, in cases of emissions of toxic substances, the maximum expected dosage in a short period of exposure, a problem that is converted to the calculation of the maximum average concentration. Using the concept of concentration integral time scale and making some substitutions in the Power Law function, the author developed a new deterministic model, applying it to field experimental data covering neutral stability conditions. However, the values and variability of its parameters had an indicative referential character and, according to the author, need to be refined with additional data. In Bartzis et al. (2010), Efthimiou et al. (2015a), Efthimiou et al. (2015b) and Bartzis et al. (2015), the authors applied the model by Bartzis et al. (2008) using different experimental data sets, but also cite the need for more validation studies.

The main objective of this work was to analyze the influence of wind direction, receptor point height, and time interval on predicting the maximum short-term average concentration, using these two models, and on the integral time scale of concentration. Using wind tunnel data, the performance of the two models in predicting the maximum short-term average concentration was compared for exposure time interval equal to 0.01s and 0.1s, considering the scenario of a regular network of streets, wind direction equal to $15°$ and height of the receiving point equal to H/2. Furthermore, concentration integral time scale values were compared for the H/2 and H heights.

METHODS

In the present work, wind tunnel data from the work of Castro et al. (2017) and Fuka et al. (2018), where the authors carried out flow and dispersion experiments in the EnFlo wind tunnel, at the University of Surrey, England, were used. For these experiments, an idealized urban model was organized, consisting of 14x21=294 rectangular blocks (buildings) with width 2H, length H and height H, where H=70mm. Figure 1 shows the representation of part of these blocks, equipped with a coordinate system, and the entire scenario based on the present work. The emission source, represented by the black star, is located at $(-70, -105, 0)$, the wind direction is equal to $15°$ and each point in green is a sensor (343 in total), located at height H/2=35mm. For each sensor, the authors estimated concentration and velocity sequentially over time, resulting in concentration and velocity time series. The measurements were made at high frequency, with collection times of 150 seconds, in general, and the data available has a temporal resolution of 0.01 seconds.

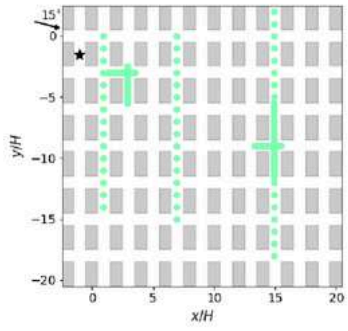


Figure 1. analyzed scenario

To calculate $C_{max}(\Delta\tau)$, the Power Law function and the Bartzis'smodel (2008) were used, considering $\Delta\tau = 0.01s$ and $\Delta\tau = 0.1s$ e the total measurement time interval of, generally, $\Delta T = 150s$. The Power Law function relates the value of $C_{max}(\Delta\tau)$ in a shorter averaging time $\Delta\tau$ with the average concentration $\overline{C}(\Delta T)$ for the entire sampling period or for a longer period of time ΔT through of the equation

$$\frac{C_{max}(\Delta\tau)}{\overline{C}(\Delta T)} = \left(\frac{\Delta\tau}{\Delta T}\right)^{-\nu} \qquad (1)$$

where ν is given experimentally. The model developed by Bartzis et al. (2008), derived from this equation, is given by

$$\frac{C_{max}(\Delta\tau)}{\overline{C}} = 1 + bI\left(\frac{\Delta\tau}{T_C}\right)^{-\nu} \qquad (2)$$

where $\overline{C}$ is the average concentration, b and ν are experimental parameters, I is the turbulence intensity, given by $I = \frac{\sigma_C^2}{\overline{C}^2}$, $\sigma_C^2 = \overline{C'}^2$, whith σ_C^2 concentration variance and C' concentration fluctuations, and T_C is the concentration integral time scale, originating from the concentration autocorrelation function $R_C(\tau)$

$$T_C = \int_0^\infty R_C(\tau)d\tau \qquad (3)$$

To compare the performance of the models, the maximum average concentration $C_{max}(0.01)$ and $C_{max}(0.1)$, the average concentration $\overline{C}$ considering the entire sampling time, the turbulence intensity I and the concentration integral time scale T_C (Equation 3) was calculated directly from each concentration time series. The ν parameter of the Bartzis et al. (2008) model was set at $\nu = 0.3$ by experimental evidence of its relatively slight variability and the fact that it is absorbed in the additional variability of the parameter b (Bartzis et al., 2008, Bartzis et al., 2010, Bartzis et al., 2015, Efthimiou et al., 2015a, Efthimiou et al., 2015b). As a result, the ν exponent of the Power Law function and the parameter b of the Bartzis et al. (2008) model varied freely, making it possible to identify a value for each of these parameters that minimizes the NMSE (Normalized Mean Square Error) metric when comparing the respective modeled data with the measured data. Thus, it was verified which of the two models presented a better performance in predicting $C_{max}(0.01)$ and $C_{max}(0.1)$.

FINDINGS AND ARGUMENT

For $\Delta\tau = 0.01$, when comparing the measured data with the data modeled by the Power law function, the value $\nu = 0.27$ was the one that generated the lowest NMSE. On the other hand, comparing the measured data with those modeled by Bartzis et al. (2008), the value $b = 1.28$ was the one that generated the lowest value of this metric. The graph in figure 2 shows the performance of the two models. For $\Delta\tau = 0.1$, the parameters found were the same ($\nu = 0.27$ and $b = 1.28$). The graph in figure 3 shows the performance of the two models.

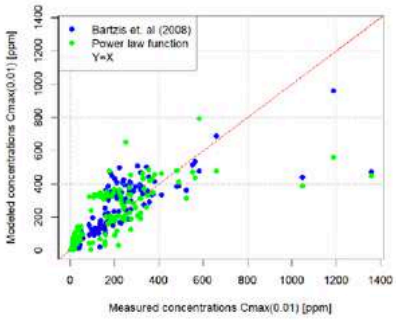


Figure 2. $C_{max}(0.01)$ measured versus modeled.

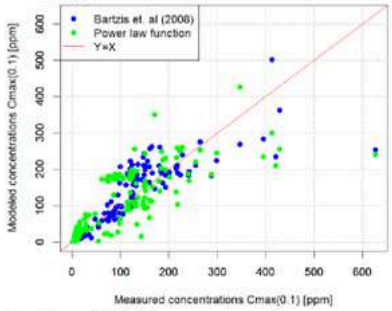


Figure 3. $C_{max}(0.1)$ measured versus modeled.

Table 3 also shows the performance of the two models in the two time intervals analyzed. It is possible to see that, in both cases, the Bartzis's model (B) presented a much higher FAC2 compared to the Power Law function (PLF). Regarding NMSE, both models presented satisfactory results, with all values below 1. Finally, all FB values were slightly negative, which may indicate a tendency for both models to underestimate the observed data values.

Table 1. Bartzis's model (B) and Power Law Function (PLF)

Model/time	FAC2	NMSE	FB
B (0.01)	0.902	0.545	-0.095
B(0.1)	0.985	0.295	-0.029
PLF (0.01)	0.364	0.736	-0.219
PLF (0.1)	0.430	0.481	-0.142

Finally, the maximum, minimum and average values of the concentration integral time scale obtained for the analyzed scenario were, respectively, 131.98, 0.92 and 44.4. Changing the height for H and maintaining the same scenario, these values were 69.19, 0.67 and 20.65, showing a decrease.

CONCLUSIONS

The studies carried out indicated the much higher performance (FAC2) of the model developed by Bartzis et al. (2008), compared to the role of the power law in predicting the maximum short-term average concentration. This can be explained by the fact that Bartzis's model have more parameters that represent the effects of atmospheric turbulence on concentration fluctuations. Both models presented good results when analyzing the NMSE metric (all values were less than 1) and, in both cases analyzed, they presented slightly negative FB values. This may indicate a tendency for models to underestimate observed data values. The values of the parameter v and b (Bartzis et al., 2008) that best adjusted the respective modeled data to the measured data were, respectively, 0.27 and 1.28 for the two time intervals analyzed. Finally, when changing the height to H, the average value of the concentration integral time scale decreased.It is worth mentioning that in this work, to analyze the performance of the models, only the scenario with wind direction equal to 15°, reception point height equal to H/2, exposure time intervals equal to 0.01s and 0.1s and a single source position was analyzed. Other cases need to be analyzed to prove the results obtained.

REFERENCES

Bartzis, J.G.; Sfetsos, A.; Andronopoulos, S. *On the individual exposure from airborne hazardous releases: The effect of atmospheric turbulence*. Journal of Hazardous Materials, 150, 76–82, 2008.

Bartzis, J.G.; Efthimiou, G.C. *Maximum individual exposure estimation using CFD RANS modelling*. 2010.

Bartzis, J.G.; Efthimiou, G.C.; Andronopoulos, S. *Modelling short term individual exposure from airborne hazardousreleases in urban environments*. Journal of Hazardous Materials, 300, 182–188, 2015.

Castro, I. P.,Xie, Z. T., Fuka, V.,Robins, A. R., Carpentieri, M.,Hayden, P., Hertwig, D.,Coceal, *O. Measurements and computations of flow in an urban street system.* Boundary Layer Meteorology,162,207-230, 2017.

Efthimiou, G.C.; Bartzis, J.G.; Palaiokostas, M. *Modeling Short-Term Maximum Individual Exposure from Airborne Hazardous Releases in Urban Environments. Part I: Validation of a Deterministic Model with Field Experimental Data*. Toxics, 3, 249-258, 2015a.

Efthimiou, G. C.; Bartzis, J.G.; Berbekar, E.; Hertwig, D.; Harms, F.; Leitl, B. *Modelling Short-Term Maximum Individual Exposure from Airborne Hazardous Releases in Urban Environments. Part II: Validation of a Deterministic Model with Wind Tunnel Experimental Data*. Toxics, 3, 259-267, 2015b.

Fuka, V.; Xie, Z. T.; Castro, I. P.; Hayden, P.; Carpentieri, M.; Robins, A. G. *Scalar Fluxes Near a Tall Building in an Aligned Array of Rectangular Buildings*. Boundary Layer Meteorology, v. 167, p.53-76, 2018.

Mello, A.L.V.; Santos, J.M.; Reis, N.C.JR.; Castro, I.P., Goulart, E.V.; Xie, Z.T. *Influence of wind direction and source location on peak-to-mean concentration ratios in urban environments*. Journal of wind Engineering and Industrial Aerodynamics, 232, 2023.

Santos, J. M.; Griffiths, R.F.; Robert, I.D.; Reis, N. C. JR. *A field experiment on turbulent concentration fluctuations of an atmospheric tracer gas in the vicinity of a complex-shaped building*. Atmospheric Environment v.39, p. 4999-5012, 2005.

Santos, J. M.; Griffiths, R.F.; Reis, N. C. JR.; Mavroidis, I. *Experimental investigation of averaging time effects on building influenced atmospheric dispersion under different meteorological stability conditions*. Building and Environment, v.44, p. 1295–1305, 2009a.

Santos, J.M.; Reis, N.C.Jr.; Castro, I.P.; Goulart, E.V.; Xie, Z.T. *Using Large-Eddy Simulation and Wind-Tunnel Data to Investigate Peak-to-Mean Concentration Ratios in an Urban Environment*. Boundary-Layer Meteorology, 172, 333–350, 2019.

AIR POLLUTION CONFERENCE BRAZIL
CMAS SOUTH AMERICA
COMMUNITY MODELING AND ANALYSIS SYSTEM

Assessment of air pollution risks and its spatial correlation with socioeconomic conditions, green areas and atmospheric emissions in Brazil

Julia Placido Moore[1], Leonardo Hoinaski[2], Robson Will[2], Camilo Bastos Ribeiro[2], Rizzieri Pedruzzi[3], Taciana Toledo de Almeida Albuquerque[4]
1Center for Environmental and Public Health Studies (CEMASP)
(moorepjuliaa@gmail.com)
2Federal University of Santa Catarina - Brazil
(leonardo.hoinaski@ufsc.br)
3Rio de Janeiro State Univeristy - Brazil
4Federal University of Minas Gerais- Brazil

Abstract: Air pollution is an environmental worldwide threat that has deleterious effects on human health. The risks of poor air quality harm populations distinctively; they can vary by different levels of air pollution exposure but also change according to how they can adapt to the events. Socioeconomic conditions reflect how populations are more susceptible to these events, whether in terms of access to health care or education to protect themselves from environmental hazards. Brazil has an extensive territory characterized by large socioeconomic, biomes, air quality, and emission disparities. We aimed to identify hotspots where social disadvantage, air pollution emissions, and lower levels of green areas correlate with the risks of being hospitalized due to air pollution in Brazilian municipalities. Using a spatial method, we employed bivariate analysis of Moran's I. We associate the risks of being hospitalized with PM2.5 emissions, the Human Development Index of Municipality, and green areas in Brazil. The hospitalizations relative risks of each Brazilian city were obtained from a combination a Principal Component Analysis (PCA), Generalized Linear Model and Autoregressive Integrated Moving Average (ARIMA). Moreover, we utilized EDGAR's inventory of air pollution emissions and the land use cover from MAPBIOMAS to obtain the variable data of the analysis. We found that higher risks of hospitalization were spatially correlated with lower socioeconomic conditions in North and Northeast, higher air pollution emissions and lower green areas in South and Southeast. This work identifies possible drivers of the cardiorespiratory health risks of air pollution and elucidate the hotspots of harm that require attention to prioritize health public policies areas.

Keywords: Air pollution, Respiratory hospitalizations, industrial and vehicular emissions, green areas, M-HDI

INTRODUCTION

Researchers widely document the association between air pollution and human health. Poor air quality is considered the most significant environmental threat to health (WHO, 2021). Other factors are decisive in this relationship, such as the ability to respond to environmental threats and exposure to atmospheric pollutants (Makri & Stilianakis, 2008).

Among the social determinants of health, socioeconomic factors play a fundamental role in building the vulnerability of communities (Boing et al., 2022). Thus, access to health and education are essential resources to mitigate the impacts of poor air quality (EEA, 2018).

Place of residence, work, and study determine exposure factors (Fecht et al., 2015; Ma et al., 2020). Since the temporal variation in atmospheric pollutant emissions and factors that control these concentrations, such as the presence of green areas (Barbosa et al., 2024), proximity to highways (Requia et al., 2016), or other sources of pollutant emissions (Reis et al., 2017; Ye et al., 2021).

Brazil is a country characterized by vast social, human, economic, and environmental disparities, and different levels of atmospheric pollutant emissions, given its continental dimensions (IBGE, 2023). Therefore, understanding the intersection of these factors is extremely important to seek solutions to challenges related to air quality.

This study seeks to identify spatial patterns in Brazil where social inequalities, atmospheric emissions sources, the absence of green areas converge with the risks of hospitalization due to respiratory diseases related to air pollution. Using spatial analysis techniques, we employed Moran's bivariate analysis to explore the spatial relationships between morbidity risks, vegetation cover, specific sources of PM2.5 emissions, and the human development index in Brazil.

METHODS

Data

We analyzed the air pollution exposure using the $PM_{2.5}$ database by the MERRA-2 project from 2008 to 2019 (Randles et al., 2017). The air pollution data has a spatial resolution of 0.500°x0.625° and the analysis were conducted using this resolution. We calculated the average daily concentration of $PM_{2.5}$.

The Department of Informatics of the Brazilian National Health System (DATASUS) shares data on respiratory (ICD-10) hospital admissions. We collected these data using the microdatasus library in R software (Rocha et al., 2018; Saldanha et al., 2019), which facilitates the downloading and data preprocessing. Our analysis used daily hospitalizations of all municipalities from 2008 and 2019. Using the worldpop database (https://hub.worldpop.org/geodata/listing?id=75), we calculated the hospitalization rate per 10000 inhabitants. Both health and population data were reggrided to $PM_{2.5}$ grid. To conduct the spatial analysis, we also utilized the Municipal Human Development Index (M-HDI), which is estimated according to 2010 Nacional Census (PNUD, IPEA, FJP, 2013). Also, we extract the forest cover, by the MapBiomas land use and cover database from the 2019

year (Souza at. al.,2020). Finally, we used the industrial and transport emission of $PM_{2.5}$ emissions by the Emissions Database for Global Atmospheric Research (EDGAR) (Crippa et al., 2019)

Statistical Analysis

To estimate the relative risks of being hospitalized by $PM_{2.5}$, we developed a multilinear model to find the associations between $PM_{2.5}$ (independent variable) and hospitalization rate (dependent variable). To remove the collinearity effects, we applied the *Principal Component Analysis* (PCA), which transform a set of variables in fewer groups not correlated (Bro & Smilde, 2014). After that, we employed a generalized linear model (GLM) with a Poisson distribution to analyze the relationship between the PCs and the hospital admissions data. Also, to remove the serial correlations in the residual GLM model, we applied an Autoregressive Integrated Moving Average (ARIMA) model. We developed a model for each pixel in the selected grid.

Spatial Analysis

To identify spatial patterns of relative risks of being hospitalized between socioeconomic conditions, green areas coverage and, PM2.5 by transport and industrial emissions, we conducted a spatial analysis. we conducted a spatial autocorrelation analysis. The Moran's Index (Moran, 1950) was employed to develop a bivariate analysis. We adopted the PySAL python package (Rey and Anselin, 2010) to create spatial clusters visualizations.

FINDINGS AND ARGUMENT

We estimated the spatial correlation between the M-HDI, green areas, two sources of PM2.5 emission, and the relative risk of being hospitalized by respiratory disease due to PM2.5. Our research could identify hotspots in the Brazilian territory, where those variables may play a role in the risk of respiratory morbidity by $PM_{2.5}$. Figure 1 shows the Relative Risks (RR) of being hospitalized by respiratory diseases due to PM2.5 The highest RR are in the South and Southeast region.

Figure 2 displays the results of the Moran spatial correlation, which the darkest yellow balls represent pixels with the highest RR and values of the analyzed variable (HH symbol). The lighter yellow balls indicate pixels with the lowest RR but highest values of the indicated variable (LH symbol). Light purple balls denote pixels with the lowest RR and values of the specified variable (LL symbol). Finally, the darkest purple balls signify the highest RR and the lowest values of the mentioned variable.

When analyzing the Moran's - I between $PM_{2.5}$ transportation emissions and the RR, the highest values of this variable are mainly in the southeast region. For years, the southeast region faces the challenges related to vehicular emission, especially in the Metropolitan Area of Sao Paulo (MASP) (Gavidia-Calderón et al., 2024). Several studies have found association between these types of emissions and the health outcomes (Leirião et al., 2020; Leirião & Miraglia, 2019). Additionally, we highlight that the places with highest risks and the highest transport emissions are also in the South region, the northeast coastline, and the metropolitan region of the Federal District. Ribeiro and Hoinaski (2024) reported high vehicular density in large urban spots located in the South, Northeast, and Midwest regions, which seems related to the HH values in these regions (Figure 2a).

Regarding the industrial $PM_{2.5}$ emissions, the highest risks and the highest emissions are in the southeast and the south. Those are regions with the most industrialized states in the country (Freitas et al., 2024) and these types of emissions may be contributing to enhance the respiratory hospitalizations on these places (Fernandes et al., 2020). The clusters of the highest RR and the lowest emissions, as in North and the South Region may suggest that the emission sources of $PM_{2.5}$ are others, which can be wildfires in North or vehicles in South (Hoinaski et al., 2022; Silva et al., 2021).

The pixels with the highest coverage of forests and the lowest RR are placed in the North (Amazon Rainforest), which is consistent with findings of (Barbosa et al., 2024), and mainly in the northeast. Hotspots of highest risks and lowest forest coverage are especially in the south and southeast region, regions in a context of severe air pollution emissions and elevated number of respiratory hospital admissions. Green areas are an important barrier to air pollution, since tree leaves may absorb PM2.5 particles or intercept them on their surfaces (Kumar et al., 2019; Nowak et al., 2006). These ecosystem services avoid and help to mitigate the impacts on air quality, thus in the health of the population (Requia et al., 2023). For example, Carvalho & Szlafsztein (2019) identified that the decrease in dense and moderate vegetation coverage in Brazil was concurrent with the increase of air pollution.

Finally, regarding the M-HDI, the regions with the lowest index and highest RR are in the north and northeast region. Given that these regions have lower M-HDI, they may face greater challenges in adapting to air pollution events (Will et al., 2022). Few spots in the South and Southeast region had lower RR and higher M-HDI values, which are not in the most air polluted areas. The areas with the highest M-HDI and RR values, although they present higher index, do not demonstrate adequate adaptation to the effects of atmospheric pollution.

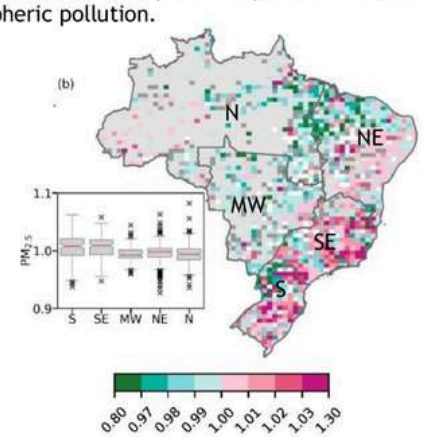


Figure 1: Respiratory hospitalization Relative Risk (RR) associated with PM2.5. South (S), Southeast (SE), Midwest (MW), Northeast (NE), and North (N) Region.

CONCLUSIONS

Our research that the Southern and Southeastern regions exhibited the highest RR and atmospheric emissions from vehicles and industries, as well as the lowest vegetation coverage. When evaluating the M-HDI, the greatest risks were identified in the North and Northeast regions, which

have the lowest M-HDI and thus are more susceptible to atmospheric pollution. This work contributes to accumulating evidence of the challenges posed by atmospheric pollution on human health. It is important that further studies be developed to assess vulnerable populations in terms of age, race, and gender.

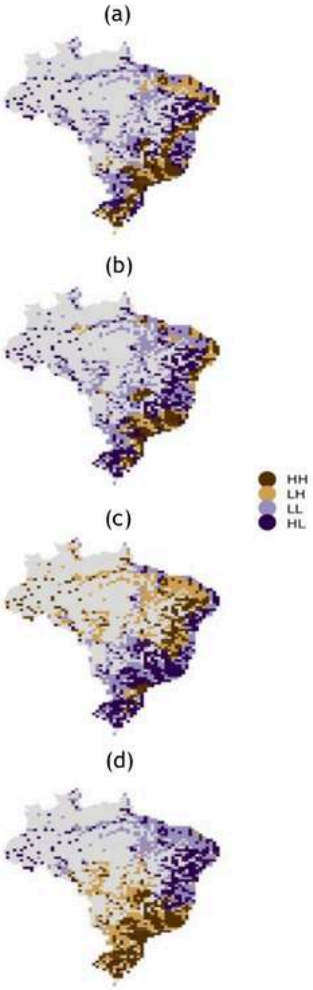


Figure 1: Relative risk of being hospitalized by PM2.5 and the spatial correlation of with (a) PM2.5 by transport emission, (b) PM2.5 by industrial emission, (c) forests, and (d) M-HDI.

REFERENCES

Barbosa, V. R. F., Damasceno, R. M., Dias, M. A., Castelhano, F. J., Roig, H. L., & Requia, W. J. (2024). Ecosystem services provided by green areas and their implications for human health in Brazil. *Ecological Indicators*, *161*. https://doi.org/10.1016/j.ecolind.2024.111975

Carvalho, R. M. de, & Szlafsztein, C. F. (2019). Urban vegetation loss and ecosystem services: The influence on climate regulation and noise and air pollution. *Environmental Pollution*, *245*, 844–852. https://doi.org/10.1016/j.envpol.2018.10.114

Fernandes, M. A. de O., Andreão, W. L., Maciel, F. M., & Albuquerque, T. T. de A. (2020). Avoiding hospital admissions for respiratory system diseases by complying to the final Brazilian air quality standard: an estimate for Brazilian southeast capitals. *Environmental Science and Pollution Research*, *27*(29), 35889–35907. https://doi.org/10.1007/s11356-020-07772-x

Freitas, E., Britto, G., & Amaral, P. (2024). Related industries, economic complexity, and regional diversification: An application for Brazilian microregions. *Papers in Regional Science*, *103*(1). https://doi.org/10.1016/j.pirs.2024.100011

Gavidia-Calderón, M., Schuch, D., Vara-Vela, A., Inoue, R., Freitas, E. D., Albuquerque, T. T. de A., Zhang, Y., Andrade, M. de F., & Bell, M. L. (2024). Air quality modeling in the metropolitan area of São Paulo, Brazil: A review. In *Atmospheric Environment* (Vol. 319). Elsevier Ltd. https://doi.org/10.1016/j.atmosenv.2023.120301

RIBEIRO, C.B.; HOINASKI, L. PM2.5 decadal changes in Brazil: influence of vehicular fleet growth and policy to control vehicular emissions. **Clean Technologies and Environmental Policy**, 2024. https://doi.org/10.1007/s10098-024-02805-2

Kumar, P., Druckman, A., Gallagher, J., Gatersleben, B., Allison, S., Eisenman, T. S., Hoang, U., Hama, S., Tiwari, A., Sharma, A., Abhijith, K. V., Adlakha, D., McNabola, A., Astell-Burt, T., Feng, X., Skeldon, A. C., de Lusignan, S., & Morawska, L. (2019). The nexus between air pollution, green infrastructure and human health. In *Environment International* (Vol. 133). Elsevier Ltd. https://doi.org/10.1016/j.envint.2019.105181

Leirião, L. F. L., Debone, D., Pauliquevis, T., Rosário, N. M. É. do, & Miraglia, S. G. E. K. (2020). Environmental and public health effects of vehicle emissions in a large metropolis: Case study of a truck driver strike in Sao Paulo, Brazil. *Atmospheric Pollution Research*, *11*(6), 24–31. https://doi.org/10.1016/j.apr.2020.02.020

Leirião, L. F. L., & Miraglia, S. G. E. K. (2019). Environmental and health impacts due to the violation of Brazilian emissions control program standards in Sao Paulo Metropolitan Area. *Transportation Research Part D: Transport and Environment*, *70*, 70–76. https://doi.org/10.1016/j.trd.2019.03.006

Nowak, D. J., Crane, D. E., & Stevens, J. C. (2006). Air pollution removal by urban trees and shrubs in the United States. *Urban Forestry and Urban Greening*, *4*(3–4), 115–123. https://doi.org/10.1016/j.ufug.2006.01.007

Requia, W. J., Vicedo-Cabrera, A. M., Amini, H., da Silva, G. L., Schwartz, J. D., & Koutrakis, P. (2023). Short-term air pollution exposure and hospital admissions for cardiorespiratory diseases in Brazil: A nationwide time-series study between 2008 and 2018. *Environmental Research*, *217*. https://doi.org/10.1016/j.envres.2022.114794

Silva, C. A., Santilli, G., Sano, E. E., & Laneve, G. (2021). Fire occurrences and greenhouse gas emissions from deforestation in the Brazilian Amazon. *Remote Sensing*, *13*(3), 1–18. https://doi.org/10.3390/rs13030376

Will, R., Hirota, M., Chaffe, P. L. B., dos Santos, O. N., & Hoinaski, L. (2022). Socioeconomic development role in hospitalization related to air pollution and meteorology: A study case in southern Brazil. *Science of The Total Environment*, *826*, 154063. https://doi.org/10.1016/j.scitotenv.2022.154063

AIR POLLUTION CONFERENCE BRAZIL
CMAS SOUTH AMERICA
COMMUNITY MODELING AND ANALYSIS SYSTEM

IMPACT OF LIGHTNING-NOX ON AEROSOL PRODUCTION IN THE AMAZON

(TREBUCHET MS, 14 FONT SIZE, BOLD, ALL CAPS, CENTERED)

Wanda I.D.Valenti[1], Rachel Albrecht[1] , Lucas Camargo[1], Thibaut Dauhut[2] Luiz A.T. Machado[3,4], Micael Cecchini[1] , Marco A.M. Franco[1], Caroline Monteiro[1,4], Hartwig Harder[4], Raquel C. Bueno[1]

[1]*Department of Atmospheric Sciences, Astronomy Institute, Atmospheric and Geophysical Sciences, University of São Paulo (USP), São Paulo, São Paulo, Brazil*

[2]*Aérology laboratory, Midi -Pyrénées Observatory -Toulouse France*

[3]*Institute of Physics, University of São Paulo (USP), São Paulo, São Paulo, Brazil*

[4]*Atmospheric Chemistry Department, Max Planck Institute for Chemistry, Mainz, Germany*

isabella.dvalenti@usp.br
rachel.albrecht@iag.usp.br

Abstract: This study investigates the impact of lightning-generated nitrogen oxides (LNOx) on aerosol formation in the Amazon region during dry and rainy seasons. Utilizing data from ACRIDICON-CHUVA and CAFE-Brazil experiments, alongside lightning frequency data from GLD360 and GLM, the study analyzes correlations between lightning characteristics and NOx concentrations. Aerosol measurements from ATTO tower and aircraft instruments, including data on NOx, provide insights into aerosol concentration. The study focuses on deep convection events, aiming to understand the role of LNOx in ultrafine particle production. Preliminary results show October as the month with highest NOx presence, with morning peaks. This research contributes to understanding the Amazon's role in the global climate system.

Keywords: Lightning-NOx, Amazon, aerosol

INTRODUCTION

The study of the relationship between the aerosol and clouds in the Amazon has been growing in the atmosphere scientific community in the last years, mainly after the ACRIDICON-CHUVA (Aerosol, Cloud, Precipitation, and Radiation Interactions and Dynamics of Convective Cloud Systems - Cloud processes of tHe main precipitation systems in Brazil: A contribUtion to cloud resolVing modeling and to the GPM - GlobAl Precipitation Measurement) (Wendisch et al. 2016) and GoAmazon2014/5 (Green Ocean Amazon 2014/5) (Martin et al. 2016) field campaigns. As a result of this campaign, a significant amount of aerosols was observed (about 20,000 particles per cm^3) at high altitudes (12-14 km), in the Amazonian Upper Troposphere (UT), raising the scientific question: *how is it possible to observe such high aerosol concentrations at these altitudes, when the expectation was much less (around 100 #/cm^2)?* (Andreae et al., 2018). Observations made in other regions (Clarke and Kapustin, 2010; Yin et al., 2005 etc) associated the boundary layer (BL) upward transport as a source of the UT aerosols (Yin et al., 2005). On the other hand, over Amazon, Andreae et al (2018) showed that the aerosols seen in the UT were not coming from the Low Troposphere (LT), that are fundamentally different from the aerosols in the UT, indicating that upward transport of BL aerosols, including combustion aerosols from biomass burning, is not an important source of aerosols to the Amazonian UT. The number of concentrations of particles in the UT also was very different, being orders of magnitude higher than in the LT, and their size distribution was in the ultrafine (UFP) size range (<90 nm), far exceeding typical concentrations in the BL and are generally too short-lived to survive deep convection and long-range transport (Andreae et al., 2018). The particles observed in UT, compared to LT, were predominantly volatile at 250°C and had much more organics and nitrate contents, and were very effective CCN (Andreae et al., 2018). Recently, several studies, using observations and simulations, focused in understanding the complex interactions between aerosol-cloud-precipitation and the main pathways of transport between the boundary layer and the upper troposphere in Amazon of the conceptual model (Kumar et al., 2015; Wang et al., 2016; Andreae et al., 2018; Bardakov et al 2022; Liu et al., 2023 and others). Considering that Lightning as a source of Nitrogen Oxides (LNOx) and LNOx by interactions with Volatile Organic Compounds (VOCs) emitted by the Amazon forest can interact with them and produce ultrafine particles (UFP) both in Upper troposphere (UT) and in the Boundary Layer (BL). The hypothesis that concern this work is first, that various electrification processes, dictated by a

combination of large-scale and local thermodynamics occurring during dry and wet seasons, will modulate the concentration of LNOx throughout the troposphere and second, in the absence of anthropogenic sources, such as during low aerosol concentration periods and/or remote regions with high lightning activity, lightning will be the major source of NOx in the BL for the new UFP chain of production. And in the UT, LNOx is the only source. IN this way, the objective of this work is to investigate the impact of the LNOx on aerosol life cycle during the dry and rainy season in the Amazon region on upper and in the boundary layer troposphere.

METHODS

Observational data collected during the ACRIDICON-CHUVA (dry period) and CAFE-Brazil (rainy period) experiments will be used for NOx in the upper troposphere and NOx samples will be collected along the ATTO tower, for the analysis of the contribution of LNOx in the PBL.The study involves evaluating time series data, spanning 10 years of lightning frequency from GLD360 and 6 years (2018-2023) of GLM, using various synchrony metrics and techniques. These include Pearson correlation, time-lagged cross-correlation (TLCC), windowed TLCC, dynamic time warping, and instantaneous phase synchrony. The analysis explores potential correlations between lightning characteristics and NOx concentrations, considering factors like flash rate, peak current, flash area, and flash energy. An equation is proposed for estimating Lightning-NOx production (LNOxPE) in the Amazon. Additionally, the study analyzes NOx measurements from ACRIDICON-CHUVA and CAFE-Brazil for the upper troposphere, evaluating HALO flight track NOx for synchrony with lightning features. A sensitivity analysis is conducted to determine the flight track footprint for retrieving spatially and temporally collocated lightning data. Aerosols measurements also collected at ATTO tower, by the instruments SMPS and MAAP will provide the aerosol concentration in BL, and for UT we will use collected data from the instruments NOAH (Nitrogen Oxides Analyzer on Halo), ATTILA (Airborne Tropospheric Tracer In-situ Laser Absorption) and AENEAS, all aboard at the aircraft used in the both campaigns (ACRIDCON and CAFE-BRAZIL). We will select events with high lightning activity and statistically correlate them with UFP concentrations observed in the UT and BL.The analysis focuses on deep convection events exhibiting abrupt changes in surface UFP concentration and/or NOx levels.

FINDINGS AND ARGUMENT

The goal is to assess the potential impact of deep convection as a generator of Lightning-NOx (LNOx) on UFP production. The study will examine the temporal evolution of physical characteristics, electrical activity, and environmental variables (e.g., NOx, aerosols) during deep convection events, emphasizing temporal windows before, during, and after these sudden changes. The results obtained with the observational data will provide more detailed information on how the LNOx cycle is in storms in different seasons. In events of high electrical activity, LNOx is expected to be the leader in concentration compared to NOx coming from the surface, and we will investigate how the NOx flow behaves in these events within the canopy. This type of evaluation will contribute to the understanding, from the point of view of the role of LNOX, of a larger scientific question about how UFP are produced in the UT of the Amazon and whether these particles are part of a feedback loop of convection itself in this region. This question is of paramount importance to understand the role of the Amazon region in the global climate scenario.

At this moment, we are analyzing the series data of NOx and UFP to understand the type of the data and its characteristics for this region. As a result, we have the seasonal (Figure 1) and diurnal cycle of NOx for 2018 to 2020 (Figure 2 and 3) and the UFP concentration at 60 m of height also for 2018 to 2021 (Figure 4).

Figure 1 presents the monthly average concentration of NO, NO2, and NOx for the years 2018 through 2020 solely for the first level, i.e., at the surface of the 80-meter tower. What could be observed is that for NOx, especially NO, there is a characteristic seasonal cycle with peaks found in October, another in August, and smaller peaks in March and May. The peaks found in August and October may be related to the fact that during this time of the year in the Amazon, there is a significant presence of pollutants due to wildfires, which can increase the concentration of NOx in the region. Another factor occurring during this period is that it is also the month with the widest radius in the region and the presence of deeper clouds, which could also, to some extent, increase the observed NOx concentration. However, as this is only the first level, and likely more affected by interactions with the surface than the atmosphere, it is intended to analyze the other levels to observe the behavior of this pattern.

Figure 2 presents the diurnal average concentration of NO, NO2, and NOx for the first measurement level of the tower (surface). It can be observed that there are two moments during the day where an increase in concentration is observed, around 11 and 20 UTC, which would be approximately 7 and 16 local time.

AIR POLLUTION CONFERENCE BRAZIL

CMAS SOUTH AMERICA

COMMUNITY MODELING AND ANALYSIS SYSTEM

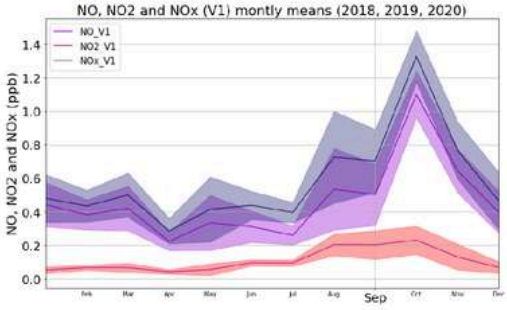


Figure 1. No, NO2 and NOx Seasonal cycle

This result needs further analysis and comparison with other levels to better understand this behavior, and to determine if there is any relationship with NOx production from the ground or if there is any connection with deep clouds and their lightning, as these times are known to have a greater presence of rain clouds in this region.

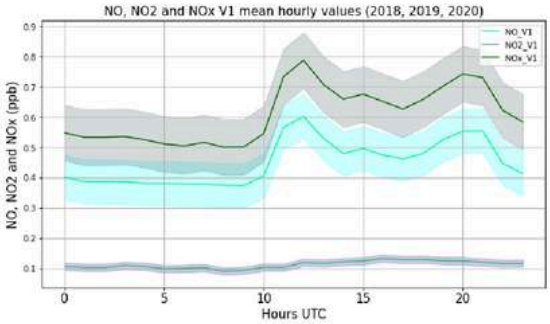


Figure 2. Diurnal cycle of NO, NO2 and Nox concentration between 2018 to 2020.

To observe this diurnal behavior and its differences throughout the months, the diurnal cycle was examined for the rainy season (Figure 3 b)) and the dry season (Figure 3 a)). It can be observed that the dry period exhibits a behavior similar to the overall average, perhaps indicating a standard pattern of NOx concentration near the surface. In contrast, during the rainy season, a third peak around 15 UTC (11 local time) is observed, prompting us to question whether this peak could be related to some meteorological factor. For all these results presented so far, analyses will be conducted for the other levels throughout the boundary layer, up to 80 meters, to obtain more information about the behavior of NOx concentration.

a) b)

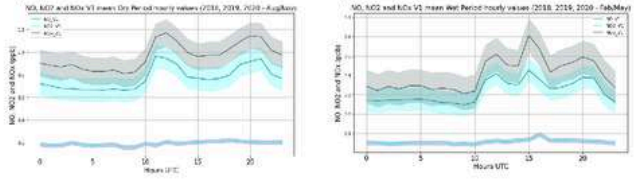
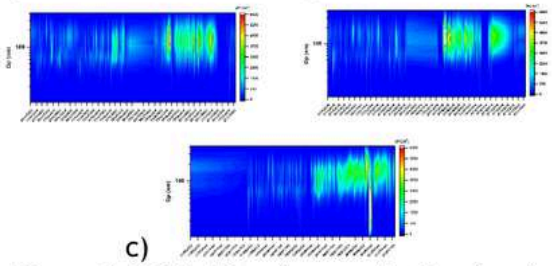


Figure 3. Diurnal cycle of NO, NO2 and Nox concentration between 2018 to 2020 to a) dry and b) wet season.

We obtained UFP data from 2018 to 2020 (we will receive the remaining data in the next few days). So far, we have only evaluated the concentration of these particulates over the years, and for the three years analyzed, they followed somewhat distinct patterns from each other. Notably, in 2020, there was a significant peak in September. Selecting specific days, especially those with high electrical activity and NOx, will contribute to a more robust analysis of UFP.

a) b)



c)

Figure 4. UFP (<50 nm) concentration for a) 2018, b) 2019 and c) 2020 Seasonal cycle.

CONCLUSIONS

Considering it a work that is in progress, we don't have final conclusions at this moment. But it is possible to see that NOx has a characteristic behavior over the Amazon troposphere and it can be related with lightning. For the next steps of this research we will Verify other levels for NOx concentration, as well as analyze lightning data. Through them, we also intend to analyze vertical wind flow and UFP concentrations

REFERENCES

Andreae, M. O., et al. Aerosol characteristics and particle production in the upper troposphere over the Amazon Basin. Atmos. Chem. Phys., 18,2018.

Bardakov, R., et al. The role of convective up- and downdrafts in the transport of trace gases in the Amazon. Journal of Geophysical Research: Atmospheres 2022 127, e2022JD037265. https://doi.org/10.1029/2022JD037265.

Clarke, A., & Kapustin, V. (2010). Hemispheric aerosol vertical profiles: Anthropogenic impacts on optical depth and cloud nuclei. Science, 329, 1488-1492. DOI: 10.1126/science.1188838.

Kumar, V. V., Jakob, C., Protat, A., Williams, C. R., & May, P. T. (2015). Mass-Flux Characteristics of Tropical Cumulus Clouds from Wind Profiler Observations at Darwin, Australia. J. Atmos. Sci., 72, 1837-1855. https://doi.org/10.1175/JAS-D-14-0259.1.

Martin, S. T., et al. (2016). Introduction: Observations and Modeling of the Green Ocean Amazon (GoAmazon2014/5). Atmos. Chem. Phys., 16, 4785-4797. https://doi.org/10.5194/acp-16-4785-2016.

Wendisch, M., et al. (2016). ACRIDICON-CHUVA Campaign: Studying Tropical Deep Convective Clouds and Precipitation over Amazonia Using the New German Research Aircraft HALO. Bull. Am. Meteorol. Soc., 97,

AIR POLLUTION CONFERENCE BRAZIL
CMAS SOUTH AMERICA
COMMUNITY MODELING AND ANALYSIS SYSTEM

Behavior of meteorological variables in critical air pollution events in a mining city.

Angie Natali Zambrano Ovalle[1], Erick Giovani Sperandio Nascimento[2], Boris René Galvis Remolina[3], Taciana Toledo de Almeida Albuquerque[4]

[1] *Graduate program in Sanitation, Environment and Water Resources, Av. Presidente Antônio Carlos, 6627, Belo Horizonte, 31270-901, MG, Brazil*

natalizambrano512@gmail.com

[2] *Clean Air Systems at the Surrey Institute for People-Centred AI, University of Surrey, United Kingdom*

es0047@surrey.ac.uk

[3] *Escuela de Ingenieria de Recursos Naturales y del Ambiente - Universidad del Valle in Cali, Colombia*

bgalvis@gmail.com

[4] *Graduate program in Sanitation, Environment and Water Resources, Av. Presidente Antônio Carlos, 6627, Belo Horizonte, 31270-901, MG, Brazil*

tacianatoledo26@gmail.com

Abstract: There are various sources of air pollution, including mining. This activity is responsible for emitting concentrations of atmospheric pollutants that commonly exceed the standards established by current legislation, causing critical pollution events. Thus, characterization, monitoring, modeling and prediction of pollutant concentrations together with the study of meteorological variables are aspects of interest for decision-making aimed at predicting effects on people's health. In this sense, this research seeks to analyze the behavior of meteorological variables in critical pollution events and their correlation with atmospheric pollutants in Congonhas, a city with activity of the two largest iron mining producers in the country. The study will be carried out in three stages. The first stage is data collection, organization and preliminary analysis from four air quality stations in the city between 2017 and 2022. The second stage is analysis of the current air quality situation in the city, considering the temporal and spatial variation of air pollutant concentrations. The last stage is identification of critical pollution events and their relationship with atmospheric variables, considering the concentrations for these events covered by legislation. In this stage Spearman's correlations are calculated to find correlation between the environmental variables and the concentrations of the contaminants under these events. Python programming language and GoogleColab tool are used to develop the study. The expected results of this work are: (i) Data follow a non-parametric distribution; ii) Concentrations have decreased over the years but are still above the reference values; iii) Concentrations are higher at the stations nearest to the mining. (iv) The correlation with variables such as wind speed and humidity are greater in events of critical concentrations of atmospheric pollutants. In the future, we intend to use the meteorological variables with the best correlation and the concentrations of atmospheric pollutants as input variables for the development of machine learning models for the prediction of concentrations of atmospheric pollutants in the region.

Keywords: Minning, air pollution, meteorological variables, critical pollution events.

INTRODUCTION

Mining activities provide funding for other industrial sectors that are essential to sustaining both the general well-being of the populace and the smooth operation of the world economies (MANCINI; SALA, 2018). The open-pit mining in the state of Minas Gerais is an integral element of the history and development of the region, as well as a significant contributor to the economic development of Brazil. (CUNHA; CORREA; MARTINS VIEIRA, 2021).

Particularly, the two largest producers of iron mining in the country, Vale and CSN, are operating in Congonhas municipality, transforming the city into one that has been reliant on the mining industry for than a century (ANGOTTI et al., 2022).

Due to the production of significant amounts of dust, both surface and underground mining operations are among the major sources of atmospheric contamination. (LUO et al., 2021).The amount of pollution that has accumulated in various areas inside and beyond the mining zone has led to a significant decline in the variety of plants and animals that inhabit the area. Additionally, to lowering crop production, it may also contaminate the water underneath the affected area (ABDOLLAHISHARIF; BAKHTAVAR; NOURIZADEH, 2016).

In this context, the objective of this study is to examine the dynamics of meteorological variables during critical pollution events and explore their relationship with atmospheric pollutants in Congonhas.

AIR POLLUTION CONFERENCE BRAZIL
CMAS SOUTH AMERICA
COMMUNITY MODELING AND ANALYSIS SYSTEM

METHODS

Data collection, organization, and preliminary analysis for the study utilized meteorological and air quality data obtained from stations operated by the State Foundation for the Environment - Minas Gerais (FEAM). The municipality's air quality network comprised six stations monitoring atmospheric pollutants and meteorological variables. Data from station located in the municipality of Ouro Preto were also used. The study used data between 2017 and 2022, as most stations began operating in 2017. Python programming language and GoogleColab tool were used in this stage.

The hourly data available on the FEAM website were organized in tables by station for use in subsequent stages. Preliminary analysis of these data included three substages. The first involved the calculation of descriptive statistics. The second stage verified statistical representativeness based on the recommendation of the Technical Guide for Monitoring and Evaluation of air quality (MMA, 2019). After this verification, daily, monthly, and annual averages were calculated. The final substage included the Shapiro-Wilk Test with a significance level of 5% to evaluate whether a distribution was similar to a normal distribution.

Spatial and temporal analysis was divided into two sub-stages. The first sub stage involved comparing stations with hourly data to validate the variance of PM_{10} concentrations at each station. The second stage aimed to compare the behavior of PM_{10} concentrations per day and per year. Comparisons were performed using the Kruskal-Wallis and Dunn's test.

The critical pollution events were identified based on reports made by the city's municipality regarding the occurrences of each event. Hourly data were utilized to achieve this objective. Finally, the correlation between the environmental variables and the concentrations of the contaminants under the described conditions was investigated. The Spearman correlation was calculated to find relationships.

FINDINGS AND ARGUMENT

The results from the Shapiro-Wilk test indicate that the data distribution is non-parametric. This observation is further supported by the histograms generated for each station (see Figure 1), revealing a notable occurrence of low-frequency data points, thus indicating a departure from normal distribution.

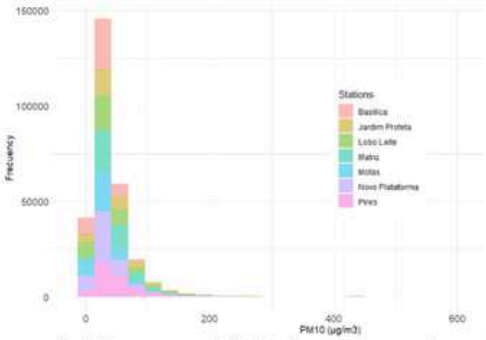


Figure 1. Histogram PM10 data for each station

The comparison of PM10 concentrations across the air quality stations revealed significant variations among them, as indicated by the results of Dunn's test. Figure 2 illustrates that stations such as Pires, Lobo Leite, Jardim Profeta, and Matriz exhibit notably higher concentrations. Notably, these stations are situated closer to the mining activities conducted within the city.

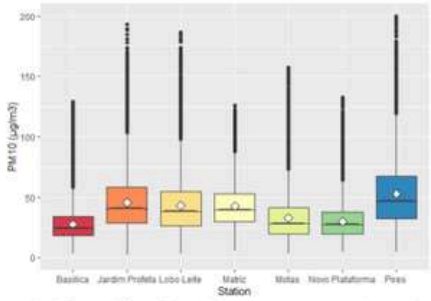


Figure 2. Box Plot PM10 concentrations in each station

The Pires station stands out not only for recording the highest concentrations but also for having a greater number of outliers, as depicted in Figure 2. Situated within an urban neighborhood, this station serves a significant portion of the Congonhas population and lies in close proximity to two major mining companies operating in the region.

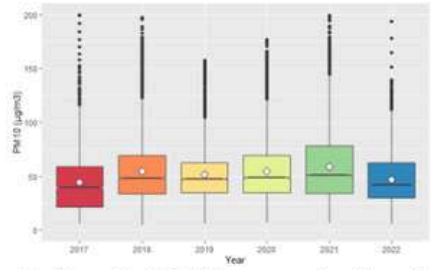


Figure 3. Box Plot PM10 concentrations in each year in Pires Station

The concentrations were compared across years for this season, as illustrated in Figure 3. The analysis revealed that the year 2022 exhibited the highest concentration levels, whereas 2017 recorded the

lowest. This trend indicates a gradual increase in concentrations over time.

Based on the findings from Figure 4, critical contamination events were identified, revealing that a majority of these occurrences transpire during the dry season, spanning from April to September. Notably, the peak concentrations are observed between 10 am and 7 pm. This aligns with reports from the mayor's office, which indicate that these events typically manifest between 11 am and 6 pm. Thus, it becomes apparent that concentrations at the Pires station are significantly influenced by these events.

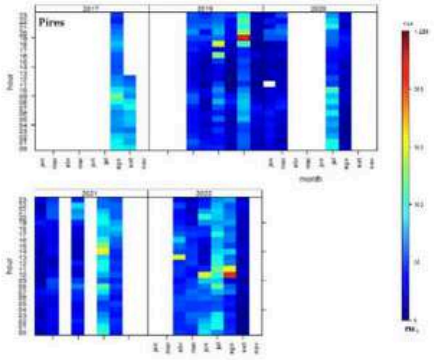


Figure 4. Trend plot of PM10 maximum concentrations hours vs months in pollution critical events in Pires Station

Figure 5 reveals that varying PM10 concentrations do not alter the prevailing wind direction on critical event days. However, it is evident that wind speeds are notably higher within concentration ranges of 56 to 87 and 87 to 331 ug/m3.

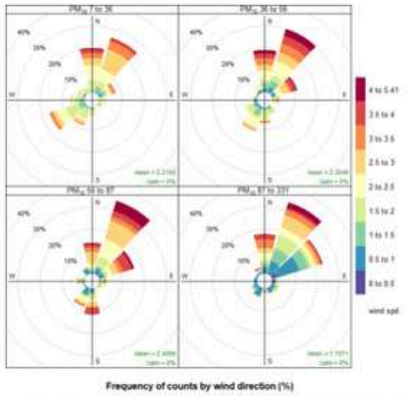


Figure 5. Wind roses in specific PM10 concentrations in pollution critical events in Pires Station

Finally, no significant correlations were discerned between pollutant concentrations and meteorological variables during critical pollution events (Figure 6). However, it is imperative to note that the presence of missing data may have influenced these findings. Thus, further investigation utilizing additional data sources is warranted to ascertain the existence of such correlations. This underscores the importance of comprehensive data collection and analysis in understanding the complex dynamics of air pollution.

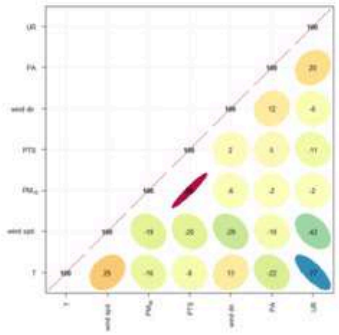


Figure 6. Meteorological variables and pollutants correlation in pollution critical events in Pires Station

CONCLUSIONS

The findings unveil a correlation between critical pollution events and PM10 concentrations at the Pires station. A consistent trend of heightened concentrations is evident during the dry season, notably between 10 am and 7 pm. Nonetheless, there are exceptions and potential issues, including anomalies during this season and disparities in pollution event reporting. Moreover, no significant correlations emerged between pollutant concentrations and meteorological variables during critical pollution events. However, it's crucial to acknowledge the potential influence of missing data on these findings. Thus, further investigation utilizing additional data sources is essential to validate these correlations. These discoveries underscore the significance of comprehending temporal and spatial fluctuations in air quality, advocating for enhanced data collection and proactive measures to safeguard public health and the environment.

REFERENCES

ABDOLLAHISHARIF, J.; BAKHTAVAR, E.; NOURIZADEH, H. *Green biocompatible approach to reduce the toxic gases and dust caused by the blasting in surface mining.*Environmental Earth Sciences, v. 75, n. 3, p. 1–12, 1 feb. 2016.

ANGOTTI, M. et al. *A narrative approach for reporting social and environmental accounting impacts in the mining sector - giving marginalized communities a voice*. Meditari Accountancy Research, 2022.

CUNHA, B.; CORREA, F.; MARTINS VIEIRA, N. *A mineração em Congonhas-MG: análise da influência da mineração no desenvolvimento da cidade e as perspectivas do setor na região Mining activity in Congonhas-MG*. O eco da graduação, v. 6, n. 1, 11 oct. 2021.

CORRELATİON BETWEEN EXPOSURE TO PARTİCULATE MATTER AND HOSPİTALİZATİONS FOR CİRCULATORY DİSEASES İN THE ELDERLY İN THE STATE OF SÃO PAULO, FROM 2016 TO 2020.

Paulo Eduardo Alves Camargo-Cruz[1], Regina Maura de Miranda[2]
[1] *School of Arts, Sciences and Humanities, University of São Paulo*
negresse@usp.br
[2]*School of Arts, Sciences and Humanities, University of São Paulo*
remaura@usp.br

Abstract: The association between exposure to particulate matter and hospitalizations for diseases caused or aggravated by this effect is a topic in which several studies that address this correlation have focused on searching for evidence that proves this direct relationship. Under the general name of particulate matter (PM) is a group of pollutants made up of dust, smoke and all types of solid and liquid material that remain suspended in the atmosphere because of their small size. For this study, fine particulate matter (PM2.5) was analyzed. Several studies have analyzed the correlation between inhaling this pollutant and its implications for human health. Piracicaba is a city located in the Northwest Region of the State of São Paulo, an important industrial, agro-industrial and sugar-alcohol hub, with a large vehicle fleet, as well as industries with high pollutant emissions. Due to these characteristics, the city (and the territory in which it is located, the Piracicaba Mesoregion) has an ideal profile for studying these correlations between health problems and atmospheric pollution. This study evaluates hospitalizations for circulatory diseases (Chapter IX of ICD-10, codes I00-I99) in the Piracicaba Mesoregion and their correlation with emissions of fine particulate matter (PM2.5) between the years 2016 and 2020, in the period called "expanded winter", where the characteristics of the winter season (low air humidity, light winds and low-altitude thermal inversions) are already and/or still present. All hospitalizations that occurred in the 26 constituent municipalities of the Piracicaba mesoregion were selected, by those over 60 years of age, without distinction of gender or race, residing in the constituent municipalities. These hospitalizations occurred from June 1st to September 30th, for each year. These hospitalization data were obtained from the Ministry of Health and hospitalization rates were calculated with the populations for the respective years, per ten thousand inhabitants. PM2.5 concentrations (monthly averages) were obtained at the air quality station in the municipality of Piracicaba, for the same period. Maps were produced with the incidence of hospitalizations and for the analysis of spatial statistics, which made it possible to find spatial clusters with lower or higher incidence of hospitalizations. The monthly averages of PM2.5 do not coincide with the longest periods of hospitalization for diseases of the circulatory system. Average gross hospitalizations are also much higher during the extended winter period than in others. The distribution of hospitalizations was high throughout the mesoregion, with greater prominence in the central, western and southern portions of the territory. In 2016 and 2018, a cluster of hospitalizations was found in the southern part of the mesoregion. In 2020, this cluster formed in the eastern portion of the mesoregion. The diseases studied here are diseases of the circulatory system, although studies and research in this area indicate diseases of the respiratory system as those that present the greatest variations, depending on air quality. The findings of this study provide a vision of the importance that limiting the emission of atmospheric pollutants can bring, through public policies, effectively impacting the health of elderly people in the interior of the State of São Paulo. Likewise, there is the observation that the correlation between the increase in hospitalizations due to diseases of the circulatory system and the emission of PM2.5, when studied in smaller territories, may be of greater proportion than that estimated in other studies, carried out on national bases or state, reinforcing the use of more adequate and appropriate analyzes for the study in these dimensions.
Keywords: *p*articulate matter, circulatory diseases, elderly, hospitalizations, correlation.

INTRODUCTİON

The association between exposure to particulate matter and hospitalizations for diseases caused or aggravated by this effect is a topic in which several studies that address this correlation have focused on searching for evidence that proves this direct relationship. Under the general name of particulate matter (PM) is a group of pollutants made up of dust, smoke and all types of solid and liquid material that remain suspended in the atmosphere because of their small size. The main sources of particulate matter emissions into the atmosphere are: motor vehicles, industrial processes, biomass burning, among others. Regions with high concentrations of this pollutant have been the focus of studies and works that correlate them - in particular - with diseases of the respiratory and circulatory systems and cardiovascular diseases[1,2,3,4]. This association produces deleterious effects on the health of communities that are close to sources of this type of air pollution, mainly affecting elderly populations and children. Exposure to particulate matter can lead to an increase in the risk of hypertension, one of the main causes of circulatory diseases, and indicates that this pollutant is one of those that most contribute to the worsening of the conditions of patients sensitive to cardiovascular diseases[5,6].
Piracicaba is a city located in the Northwest Region of the State of São Paulo, an important industrial, agro-industrial and sugar-alcohol hub, with a large vehicle fleet, as well as industries with high pollutant emissions. Due to these characteristics, the city (and the territory in which it is located, the Piracicaba Mesoregion) has an ideal profile for studying these correlations between health problems and atmospheric pollution.

METHODS

This study evaluates hospitalizations for circulatory diseases (Chapter IX of ICD-10, codes I00-I99) in the Piracicaba Mesoregion and their correlation with emissions of fine particulate matter (PM2.5) between the years

2016 and 2020, in the period called “expanded winter”, where the characteristics of the winter season (low air humidity, light winds and low-altitude thermal inversions) are already and/or still present. All hospitalizations that occurred in the 26 constituent municipalities of the Piracicaba mesoregion were selected, by those over 60 years of age, without distinction of gender or race, residing in the constituent municipalities. These hospitalizations occurred from June 1st to September 30th, for each year. These hospitalization data were obtained from the Ministry of Health and hospitalization rates were calculated with the populations for the respective years, per ten thousand inhabitants. PM2.5 concentrations (monthly averages) were obtained at the air quality station in the municipality of Piracicaba, for the same period. Maps were produced with the incidence of hospitalizations and for the analysis of spatial statistics, which made it possible to find spatial clusters with lower or higher incidence of hospitalizations.

FINDINGS AND ARGUMENT

The diseases studied here are diseases of the circulatory system, although studies and research in this area indicate diseases of the respiratory system as those that present the greatest variations, depending on air quality. The monthly averages of PM2.5 did not coincide with the longest periods of hospitalizations for diseases of the circulatory system, however the average gross hospitalizations found were much higher during the extended winter period than in others. The distribution of hospitalizations was high throughout the mesoregion, with greater prominence in the central, western and southern portions of the territory, as we can see in image 1, which represents the incidences in 2016 and 2020. With the spatial analysis tool, we can see that, in 2016 (and also in 2018), a cluster of hospitalizations (hotspot) was found in the southern part of the mesoregion. In the last year of the analyzed series (2020) this cluster was formed in the eastern portion of the mesoregion, as image 2 demonstrates.

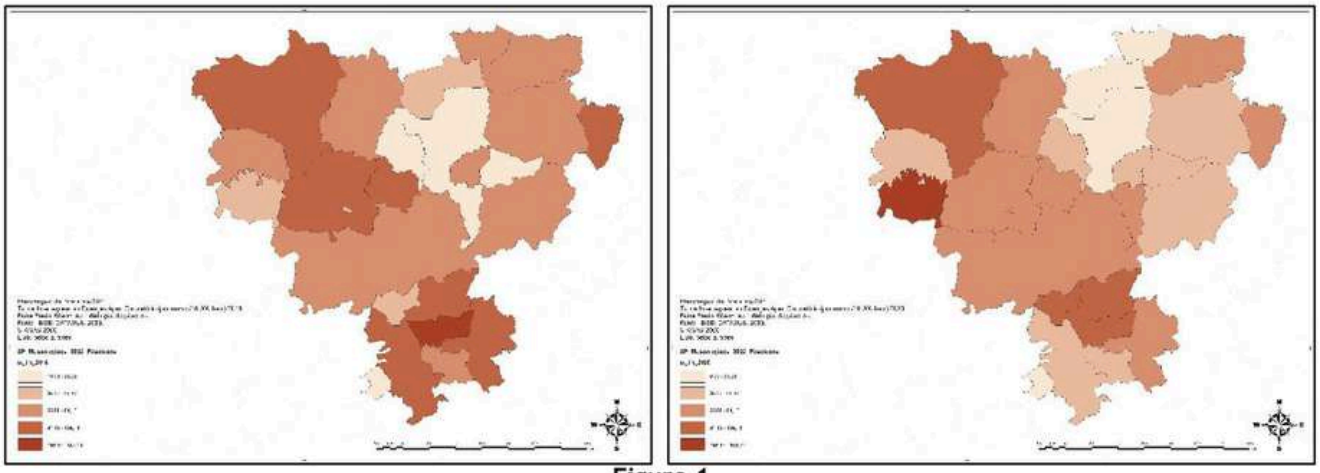


Figure 1

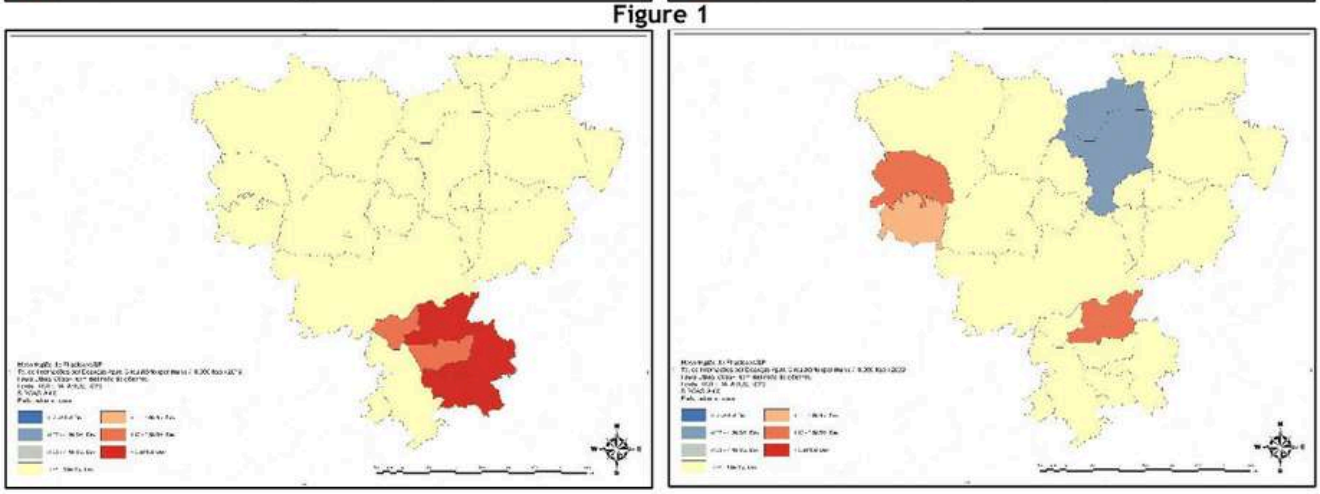
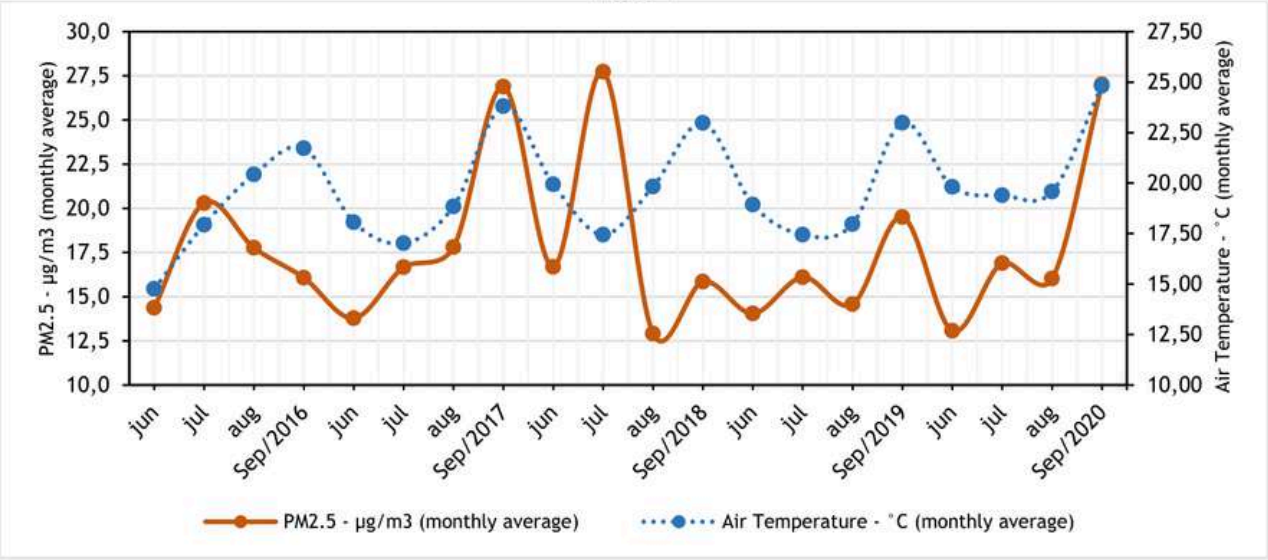


Figure 2

The variations in temperature and PM2.5 were coincident, except between July 2018 and July 2019, where there was an increase in average temperatures and a decrease in the concentration of PM2.5, as we can see in table 1. The rates of hospitalizations varied much closer to the air temperature averages (higher temperature, higher hospitalization rate) than to the average concentrations of particulate matter, due to less ease in the dispersion

of pollutants. We found periods of coincidence between the average pollutant concentrations and hospitalization rates, as listed in the literature[7,8,9] and reinforced by the data found here.

Table 1



CONCLUSIONS

The findings of this study provide a vision of the importance that limiting the emission of atmospheric pollutants can bring, through public policies, effectively impacting the health of elderly people in the interior of the State of São Paulo. Likewise, there is the observation that the correlation between the increase in hospitalizations due to diseases of the circulatory system and the emission of PM2.5, when studied in smaller territories, may be of greater proportion than that estimated in other studies, carried out on national bases or state, reinforcing the use of more adequate and appropriate analyzes for the study in these dimensions.

REFERENCES

1. Cançado J.E.D., Saldiva P.H.N., Braga A.L.F. et al. The impact of sugar cane-burning emissions on the respiratory system of children and the elderly. (2006) Environmental Health Perspectives, 114(5), p.725-729, DOI: 10.1289/ehp.8485.
2. Cesar A.C.G., Nascimento L.F.C., Carvalho Jr J.A. Association between exposure to particulate matter and hospital admissions for respiratory disease in children. (2013) Revista de Saúde Pública, 47(6):1-4, DOI:10.1590/S0034-8910.2013047004713.
3. Mantovani K.C., Nascimento L.F.C., Moreira D.S. et al. Poluentes do ar e internações devido a doenças cardiovasculares em São José do Rio Preto, Brasil. (2016) Ciência & Saúde Coletiva, 21(2):509-515, DOI: 10.1590/1413-81232015212.16102014.
4. Cesar A.C.G., Nascimento L.F.C. Coarse particles and hospital admissions due to respiratory diseases in children. An ecological time series study. (2018) São Paulo Medical Journal, 36(3):245-50, DOI: 10.1590/1516-3180.2017.0362080218.
5. Abdul-Rahman T., Roy P., Bliss Z.S.B. et al. The impact of air quality on cardiovascular health: A state of the art review. Current Problems in Cardiology. (2023), 49(2):102174. DOI: 10.1016/j.cpcardiol.2023.102174.
6. Krittanawong C., Qadeer Y.K., Hayes R.B. et al. PM2.5 and cardiovascular diseases: State-of-the-Art review. International Journal of Cardiology: Cardiovascular Risk and Prevention. (2023), 19:200217. DOI: 10.1016/j.ijcrp.2023.200217.
7. Lara L.L., Artaxo P., Martinelli L.A. et al. Properties of aerosols from sugar-cane burning emissions in Southeastern Brazil. (2005) Atmospheric Environment, 39(26), p.4627-4637, DOI: 10.1016/j.atmosenv.2005.04.026.
8. Andreão W.L., Albuquerque T.T.A. Fine particles as a public health indicator in Brazil: from monitoring to modeling. (2020) Air Quality, Atmosphere & Health, 13:1453–1463, DOI: 10.1007/s11869-020-00899-3.
9. Barbosa Neto A., Ferraro A.A., Vieira S.E. Acute and subchronic exposure to urban atmospheric pollutants aggravate acute respiratory failure in infants. (2023) Scientific Reports, 13:16888, DOI: 10.1038/s41598-023-43670-1.

AIR POLLUTION CONFERENCE BRAZIL
CMAS SOUTH AMERICA
COMMUNITY MODELING AND ANALYSIS SYSTEM

Analysis of $PM_{2.5}$ and PM_{10} atmospheric concentrations ratios in the Metropolitan Area of Belo Horizonte

Otavio Medeiros Sobrinho[1], Angie Natali Zambrano Ovalle[1], William Vizuete[2], Rizzieri Pedruzzi[3], Leila Droprinchinski Martins[4], Taciana Toledo de Almeida Albuquerque[1,5]

[1] *Graduate program in Sanitation, Environment and Water Resources, Av. Presidente Antônio Carlos, 6627, Belo Horizonte, 31270-901, MG, Brazil*
sobrinhotavio@gmail.com; anatalizo@ufmg.br
[2] *Department of Environmental Science and Engineering, University of North Carolina at Chapel Hill, 135 Dauer Dr, Chapel Hill, 27599, NC, United States*
vizuete@unc.edu
[3] *Department of Sanitary and Environmental Engineering, Faculty of Engineering, Rio de Janeiro State University, PJLF - 5° andar - Sala 5029 Bloco F*
rizzieri.pedruzzi@gmail.com
[4] *Graduate Program in Environmental Engineering, Campus Londrina, Federal University of Technology, Paraná, Av. dos Pioneiros, 3131, Londrina, 86036-370, Brazil*
leiladromartins@gmail.com
[5] *Graduate program in Sanitation, Environment and Water Resources, Av. Presidente Antônio Carlos, 6627, Belo Horizonte, 31270-901, MG, Brazil*
tacianatoledo26@gmail.com

Abstract:
In the Metropolitan Area of Belo Horizonte (MABH), various activities including wind-blown dust resuspension, mining, industrial operations, and vehicular emissions significantly contribute to air pollution deterioration, particularly in mining regions where particulate matter (PM) is the main pollutant. Studies have revealed significant proportions of crustal elements, indicating a mixture of natural iron enrichment and urban-industrial pollution in air particulate matter. The primary objective of the study was to analyze spatiotemporal variations in the $PM_{2.5}/PM_{10}$ ratio in the MABH. Daily average ratios were computed from hourly data obtained between 2016 and 2021 from seventeen air quality stations. Analysis identified higher $PM_{2.5}/PM_{10}$ ratios near human activity-related pollutant sources and lower ratios near mining activities, attributed to wind-blown emissions. On the industrial air quality station an increment on ratios year by year was identified. A dust storm event on September 26th, 2021, showed varying ratios across different air quality station classes, indicating the usefulness of the ratio as an indicator of PM emission sources.

Keywords: Dust storm, air quality data, mining activities.

INTRODUCTION

Each year, more than nine million fatalities are associated with air quality issues, with almost half attributed to the chronic or acute effects of exposure to particulate matter with aerodynamic diameter of 2.5 microns or less ($PM_{2.5}$) (Lelieveld et al., 2019). The origin and composition of particulate matter are complex, as it can be directly emitted by emissions sources (mainly the particulate matter with aerodynamic diameter of 10 microns or less, PM_{10}) or formed secondarily on the atmosphere (mainly $PM_{2.5}$) (Tan et al., 2019).

Within the Metropolitan Area of Belo Horizonte (MABH), primary sources of $PM_{2.5}$ include vehicles (26,941 tons.year^{-1}), industries (293 tons.year^{-1}), households (226 tons.year^{-1}), and biomass burning (116 tons.year^{-1}) (FEAM, 2018). In the MABH, contributions to air pollution from wind-blown dust resuspension, dust emissions from mining activities, industrial operations, and vehicular emissions are substantial, particularly in mining regions where particulate matter is the primary air pollutant emitted in open pit mining areas. Experimental studies have revealed significant proportions of crustal elements, indicating a strong presence of natural iron enrichment alongside contamination from local urban-industrial pollution in $PM_{2.5}$ range (Andrade et al., 2012; and Miranda et al., 2012).

Being part of the Brazilian iron quadrangle, MABH is a key player in iron ore production (Morozesk et al., 2021). The iron quadrangle is a critical area for iron deposit that annually extracts 228 million tons of iron through open pit mining, representing over 70% of Brazilian iron production, with more than 50% exported to Asia (Alkmim, 2018; Minas Gerais, 2020). Consequently, the MABH is heavily impacted by human activities, characterized by the proximity of active mining operations, industries, and urban areas. This proximity creates a unique synergy of various air pollutant emissions, resulting in continuous spatial-temporal variations in air pollutant emissions and compositions (Tang and Werner, 2023).

Therefore, the primary aim of the study was to identify spatiotemporal variations in the $PM_{2.5}/PM_{10}$ ratio in the MABH across three different air quality stations.

METHODS

The MABH comprises 34 cities in 15,000 km^2 and approximately 6 million people in the Minas Gerais state, being reference in iron ore mining and processing (IBGE, 2019). Along this area, there are seventeen air quality stations supported by the *Fundação Estadual do Meio Ambiente do Estado de Minas Gerais* (FEAM), which obtain hourly data (Figure 1).

In this context, daily averages were computed based on hourly data spanning from 2016 to 2021, being calculated when more than ¾ of the daily hourly data were available. Then, the daily average of $PM_{2.5}/PM_{10}$ ratio was calculated. Following, in the computer software "R" by using the package "openair", which is an open-source tool for analyzing air pollution data, polar plots were elaborated to identify the relationship between wind direction and $PM_{2.5}/PM_{10}$ ratios and to analyze the ratios behaviors in the data series.

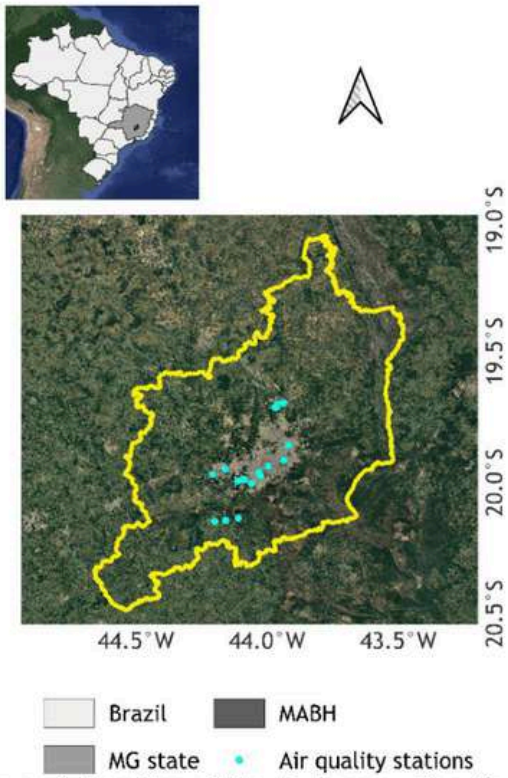


Figure 1. Location of the study area. The site of air quality stations from *Fundação Estadual do Meio Ambiente - Minas Gerais* (FEAM) is in the blue points. The yellow outline corresponds to the Metropolitan Area of Belo Horizonte (MABH). Note: MG state: Minas Gerais state; MABH: Metropolitan Area of Belo Horizonte.

Fallowing the same approach of Sobrinho et al., (2024), the main focus of our work will be on the fallow air quality stations:

- Petrovale (industrial): in a radius smaller than one kilometer is observed high industrialized area with petroleum refinery, gas filing, vehicle manufacturer, power plant, mining, and industries;
- Av. Contorno (vehicular): has a trick urban road network;
- Célvia (mining), is highly influenced by mining activities, once in addition to industries, there are a lot of mining operations near to this station.

FINDINGS AND ARGUMENT

The analysis of the $PM_{2.5}/PM_{10}$ ratio indicates high values in air quality stations near human activity-related pollutant sources (industrial station), conversely, when moving away from the air pollutants sources air quality stations near mining activities exhibited low ratios (mining station), attributed to wind-blown emissions dominated by particle sizes in the PM_{10} range, and the dust storms, corroborating with Zhao et al. (2018). Monthly and weekly time variation data showed high ratios in the industrial air quality station, and low in the mining station as presented on Figure 2. The lower ratios on industrial and vehicular stations were in the wintertime (from June to September), and the higher ratios on these stations were in the summertime. Conversely, mining air quality station registered the opposite behavior, as observed on China by Fun et al. (2021). Annual average showed an increase in $PM_{2.5}/PM_{10}$ ratios, since 2016 for the industrial air quality station, and for the others, a stability was observed.

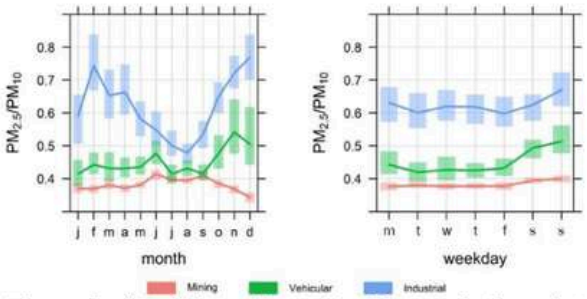


Figure 2. Monthly and weekly time variation plot of $PM_{2.5}/PM_{10}$ ratio for mining, vehicular and industrial stations.

On the Figure 3, bivariate polar plots show the $PM_{2.5}/PM_{10}$ ratios for the three air quality stations. In the vehicular station, the higher contribution of ratios' increase was when wind blowing from southwest, probably due to the direct emissions of $PM_{2.5}$ from the vehicles. Li and Managi (2021) highlighted that $PM_{2.5}$ direct emissions originates mainly from combustion emissions, being on-road

transportation one of the primary sources of $PM_{2.5}$ emissions.

In the industrial station, higher ratios were identified by winds blowing from east to south, due to emissions from industries operating in the region, as previously observed in a Chinese study (Xu, et al. 2017).

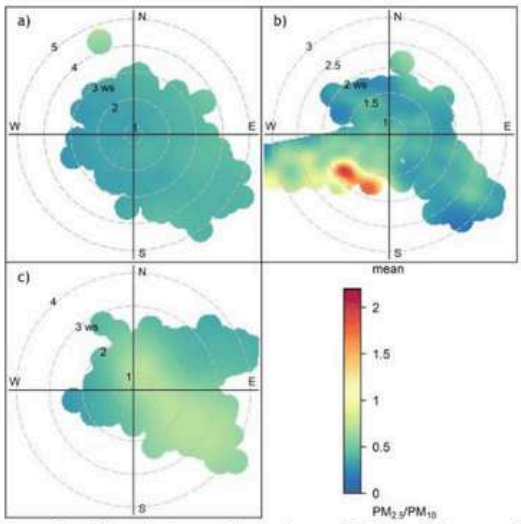


Figure 3. Bivariate polar plot of $PM_{2.5}/PM_{10}$ ratios for a) mining; b) vehicular; and c) industrial stations.

On 2021 September 26th, a dust storm in the MABH was identified, and the average $PM_{2.5}/PM_{10}$ ratio for each air quality station class was 0.36 < 0.60 < 0.70 for mining, vehicular, and industrial staions. In this regard, the $PM_{2.5}/PM_{10}$ ratio serves as a valuable indicator of the sources of PM emissions, whether they are caused by human activity (greater ratio) or by natural processes (lower ratio).

CONCLUSIONS

Utilizing PM_{10} and $PM_{2.5}$ concentration data gathered from three air quality stations in the MABH, we conducted an analysis of the spatiotemporal patterns of $PM_{2.5}/PM_{10}$ ratios. Our findings reveal that $PM_{2.5}/PM_{10}$ ratios peak during summer and reach their lowest levels in spring. Additionally, these ratios exhibit distinct spatial distribution trends, with mining sites displaying the lowest ratios, followed by vehicular sources, and then industrial areas throughout the period of our study. This pattern remained consistent even during a dust storm recorded on September 26th, 2021. Our research outcomes contribute to a deeper understanding of the mechanisms underlying air pollution formation and aid in the assessment of its impacts on human health, as well as on weather and climate conditions.

REFERENCES

Alkmim, F. F. História Geológica de Minas Gerais. 2018.

Andrade, M. F. de A., et al. "Vehicle emissions and $PM_{2.5}$ mass concentrations in six Brazilian cities." *Air Quality, Atmosphere & Health* 5 (2012): 79-88. doi:10.1007/s11869-010-0104-5.

Fan, H., et al. "Spatio-Temporal Variations of the $PM_{2.5}/PM_{10}$ Ratios and Its Application to Air Pollution Type Classification in China." *Frontiers in Environmental Science* 9 (2021). doi:10.3389/fenvs.2021.692440.

FEAM - Fundação Estadual do Meio Ambiente. Relatório Técnico Atualização do Inventário das Fontes de Emissão de Poluentes Atmosféricos da Região de Belo Horizonte, Contagem e Betim. Belo Horizonte, MG, 2008.

IBGE - Instituto Brasileiro de Geografia e Estatística, 2019. Censo Demográfico: Características da população – amostra.

Li, C. and Managi, S. "Contribution of on-road transportation to $PM_{2.5}$." *Scientific Reports* 11 (2021). doi: 10.1038/s41598-021-00862-x.

Lelieveld, J., et al. "Effects of fossil fuel and total anthropogenic emission removal on public health and climate." *Earth, Atmospheric, and Planetary Sciences* 116 (2019): 7192-7197.

Minas Gerais, 2020. DIAGNÓSTICO DO SETOR MINERAL DE MINAS GERAIS: Documento-base para Formulação do Plano Estadual da Mineração. Belo Horizonte.

Miranda, R. M. de, et al. "Urban air pollution: a representative survey of $PM_{2.5}$ mass concentrations in six Brazilian cities." *Air Quality, Atmosphere & Health* 5 (2012): 63-77. doi: 10.1073/pnas.181998911.

Morozesk, M., et al. "Airborne particulate matter in an iron mining city: Characterization, cell uptake and cytotoxicity effects of nanoparticles from $PM_{2.5}$, PM_{10} and PM_{20} on human lung cells." *Environmental Advances* 6 (2021): 100125. doi: 10.1016/j.envadv.2021.100125.

Sobrinho, O. M., et al. "From mining to fire outbreaks: The relative impact of pollutants sources on air quality in the metropolitan area of Belo Horizonte." *Atmospheric Pollution Research* 15 (2024): 102118-. doi: 10.1016/j.apr.2024.102118.

Tan, W., et al. "Potential of Polarization Lidar to Profile the Urban Aerosol Phase State during Haze Episodes." *Environmental Science & Technology Letters* 7 (2020): 54-59. doi: 10.1021/acs.estlett.9b00695.

Tang, L., and Werner, T. T. "Global mining footprint mapped from high-resolution satellite imagery." *Communications Earth & Environment* 134 (2023). doi:10.1038/s43247-023-00805-6

Xu, G., et al. "Spatial and Temporal Variability of the $PM_{2.5}/PM_{10}$ Ratio in Wuhan, Central China". *Aerosol and Air Quality Research* 17 (2017): 741-751. doi:10.4209/aaqr.2016.09.0406.

Zhao, D., et al. "$PM_{2.5}/PM_{10}$ Ratios in Eight Economic Regions and Their Relationship with Meteorology in China." *Advances in Meteorology* 2019 (2019). doi: 10.1155/2019/5295726.

AIR POLLUTION CONFERENCE BRAZIL
CMAS SOUTH AMERICA
COMMUNITY MODELING AND ANALYSIS SYSTEM

ASSESSMENT OF $PM_{2.5}$ COMPOSITION AND PAH SOURCES IN THREE CONTINENTS: IMPLICATIONS FOR AIR QUALITY AND HUMAN HEALTH

Caroline Scaramboni[1,2*], Camila N. Farias[3], Pérola C. Vasconcellos[3], Ioannis Sadiktsis[4], Simone A. Pozza[5], Gisela A. Umbuzeiro[5], Tetsushi Watanabe[6], Poliany C. O. Rodrigues[7], M. Lucia A. M. Campos[2], Kristian Dreij[1], M. Felipe de Oliveira Galvão[1].
*e-mail: carolinesc@alumni.usp.br
[1]*Institute of Environmental Medicine, Karolinska Institutet, Stockholm, Sweden.*
[2]*Departamento de Química - FFCLRP, Universidade de São Paulo, Ribeirão Preto, Brasil*
[3]*Instituto de Química, Universidade de São Paulo, São Paulo, Brasil*
[4]*Department of Materials and Environmental Chemistry, Stockholm University, Stockholm, Sweden*
[5]*Faculdade de Tecnologia, Universidade Estadual de Campinas, Limeira, Brasil*
[6]*Department of Public Health, Kyoto Pharmaceutical University, Kyoto, Japan*
[7]*Faculdade de Ciências da Saúde, Universidade do Estado de Mato Grosso, Cáceres, Brasil*

Abstract: Atmospheric ($PM_{2.5}$) is a critical indicator of air quality, with substantial implications for human health. Polycyclic aromatic hydrocarbons (PAH) and their oxygenated (OPAH) derivatives represent one of the largest contributors to the harmful effects attributed to PM. The objective of this study was to assess the concentrations of PAHs and OPAHs in $PM_{2.5}$ collected at five cities on three continents: Stockholm (Sweden), Kyoto (Japan), Limeira, Ribeirão Preto, and Cáceres (Brazil), in order to identify the main sources of particulate air pollution at these cities during the winter/dry seasons. $PM_{2.5}$ sampling campaigns were carried out in 2020, 2021, and 2022, using high-volume air samplers. PAHs and OPAHs were extracted and determined by gas chromatography coupled to mass spectrometry (GC/MS) following the methodology described by Santos et al. (2016). The highest mass concentrations of $PM_{2.5}$ were found in Ribeirão Preto (49.5 ± 18.4 μg m^{-3}; n = 6) and Limeira (33.7 ± 17.9 μg m^{-3}; n = 9), followed by Stockholm (19.7 ± 6.3 μg m^{-3}; n = 5), and the lowest in Kyoto (9.9 ± 4.9 μg m^{-3}; n = 9). Cáceres exhibited the highest variability in $PM_{2.5}$ levels, ranging from 2.2 to 122.3 μg m^{-3} (n = 6) showing occasional high inputs. Comparisons with WHO short-term air quality guideline (AQG 24 h: 15 μg m^{-3}) revealed several exceedances of the threshold, particularly in the Brazilian cities. Winter/dry season sampling indicated higher $PM_{2.5}$ levels compared to annual means reported by local agencies, with all cities surpassing the WHO annual AQG. This underscores the need for continuous monitoring, especially in regions lacking a comprehensive air quality network. Limeira had the highest median of total PAHs (Σ_{16}PAH) (11.8 ng m^{-3}), followed by Ribeirão Preto (5.50 ng m^{-3}), Stockholm (2.07 ng m^{-3}), Kyoto (1.68 ng m^{-3}), and Cáceres (1.29 ng m^{-3}). Cáceres exhibited the lowest Σ_{16}PAH median but displayed high variability, correlating with the observed variability in $PM_{2.5}$ levels. Since the site in Cáceres is located at a remote area, the main drivers of the elevated concentrations detected in certain samples were occasional $PM_{2.5}$ inputs by biomass burning, as evidenced by the high concentrations of retene, associated with biomass burning. Among the individual PAHs, human exposure to high-molecular-weight PAHs (HMW-PAHs) are of special health concern due to their higher mutagenic and carcinogenic activity compared to smaller PAHs. A prevalence of HMW-PAHs was observed in Ribeirão Preto, Limeira, and Kyoto samples, with benzo[*b*]fluoranthene (BbF) and benzo[*ghi*]perylene (BPer) being the most abundant. The carcinogenic activity of PAHs mixtures, measured in terms of benzo[*a*]pyrene equivalent (BaP_{eq}) concentrations, was notably elevated in Brazilian cities. In Ribeirão Preto, the BaP_{eq} concentrations reached up to 13.5 ng m^{-3}, highlighting the city's susceptibility to heightened risk due to biomass burning, as previously demonstrated (Scaramboni et al., 2024). In contrast to Σ_{16}PAH, total oxygenated PAHs (Σ_4OPAH) showed different patterns, with Cáceres having nearly twice the concentrations of Σ_4OPAH compared to Kyoto and Stockholm. In Cáceres, 2-methylanthraquinone was the predominant OPAH, exhibiting a median concentration 2-8 times greater than that observed in other cities. The primary source of this compound is attributed to the teak tree, widely cultivated in the city. However, the specific emission processes, whether through burning or biogenic emissions, remain to be investigated. In all five cities studied, diagnostic ratios (DRs) consistently indicated a dominance of pyrogenic sources over petrogenic sources in the measured PAHs, aligning with expectations given the prevalence of pyrogenic sources in air samples compared to petrogenic sources associated with sediment deposition from petroleum activities. DRs also suggested that the pyrogenic sources were a combination of vehicle emissions and biomass combustion. The BaP/BPer ratio, associated with traffic-related emissions, was highest in Stockholm, in line with its proximity to a highway. The BaP/(BaP + BeP) ratio indicated fresh PM emissions in Cáceres > Ribeirão Preto > Limeira > Stockholm and more aged particles in Kyoto, aligning with fire spots in Cáceres and long-range air mass trajectories from China and South Korea to Kyoto. Brazilian cities showed a notable influence of biomass burning, likely attributable to widespread Amazon and Cerrado wildfires added to local fires. Our results support the importance of improving the air quality especially during the emission-intense winter/dry season to reach air quality standards and limit human health effects from air pollution.

Keywords: Particulate Matter, Biomass Burning, Monitoring.

INTRODUCTION

Atmospheric fine particulate matter ($PM_{2.5}$) is a critical indicator of air quality, with substantial implications for human health. Polycyclic aromatic hydrocarbons (PAHs) and their oxygenated (OPAHs) derivatives represent one of the largest contributors to the harmful effects attributed to PM (WHO et al., 2021). The objective of this study was to assess the

concentrations of PAHs and OPAHs in $PM_{2.5}$ collected at five cities on three continents: Stockholm (Sweden), Kyoto (Japan), Limeira, Ribeirão Preto, and Cáceres (Brazil), in order to identify the main sources of particulate air pollution and infer about health impacts. We have previously shown markedly different PAC concentrations in total suspended particles (TSP) collected at Stockholm, Kyoto, and Limeira, implying that the residents of these urban environments are exposed to different levels of genotoxic pollutants (Maselli et al., 2020). Our present study extended this research by conducting new $PM_{2.5}$ samplings in these three cities and in two additional Brazilian cities: Ribeirão Preto, a midsized agro-industrial city, and Cáceres, a town surrounded by state parks and an ecological reserve.

METHODS

The $PM_{2.5}$ sampling campaigns were carried out in 2020, 2021, and 2022, using high-volume air samplers. An area of 3.5 cm^2 of the samples and blank filters were extracted using micro-extraction devices with 500 µL of acetonitrile:dichloromethane mixture (18:82%) for 23 minutes in an ultrasonic bath. Sixteen PAHs and 4 OPAHs were determined by gas chromatography coupled to mass spectrometry (GC/MS) following the methodology described by Santos et al. (2016). The carcinogenic activity was expressed in terms of the benzo[*a*]pyrene equivalent concentration ($B[a]P_{eq}$), calculated according to Equation 1 (USEPA, 2010).

$$B[a]P_{eq} = \sum_{i}^{n=i} (C_i \times RPF_i) \qquad \text{Equation 1}$$

where, C_i is the concentration and RPF_i is the relative potency factor of the individual 'i' PAHs classified as carcinogenic by IARC.

FINDINGS AND ARGUMENT

The highest mass concentrations of $PM_{2.5}$ were found in Ribeirão Preto and Limeira, followed by Stockholm, and the lowest in Kyoto (Figure 1). Cáceres exhibited the highest variability in $PM_{2.5}$ levels due to occasional high inputs.

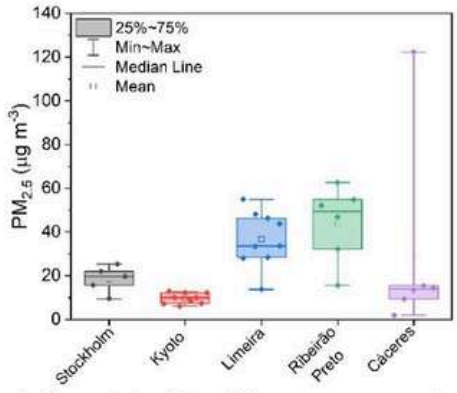


Figure 1. Box plots of the $PM_{2.5}$ mass concentrations determined in the five studied cities.

Comparisons with WHO short-term air quality guideline (AQG 24 h: 15 µg m^{-3}) revealed several exceedances of the threshold, particularly in the Brazilian cities. Winter/dry season sampling indicated higher $PM_{2.5}$ levels compared to annual means reported by local agencies, with all cities surpassing the WHO annual AQG. Cáceres had no available annual data from local monitoring, but it showed elevated $PM_{2.5}$ levels during the study. This underscores the need for continuous monitoring, especially in regions lacking a comprehensive air quality network.

Limeira had the highest median of total PAHs (Σ_{16}PAH), followed by Ribeirão Preto, Stockholm, Kyoto, and Cáceres (Table 1). Σ_{16}PAH median in Limeira was ~6 times higher than Stockholm and Kyoto, consistent with previous findings (Maselli et al., 2020). Cáceres exhibited the lowest Σ_{16}PAH median but displayed high variability, correlating with the observed variability in $PM_{2.5}$ levels. Although low concentrations were expected at the rural Cáceres site due to its remote location, it is likely that the main drivers of the elevated concentrations detected in certain samples were occasional $PM_{2.5}$ inputs by biomass burning, as evidenced by the high concentrations of retene (Ret), associated with biomass burning.

Table 1 - Ranges and medians of the total concentrations of PAHs and OPAHs determined in the five studied cities

	Σ_{16}PAH (ng m^{-3})		Σ_4OPAH (ng m^{-3})	
	min-max	**med**	**min-max**	**med**
Stockholm (*n* = 5)	0.56 - 2.7	2.1	0.06 - 0.25	0.13
Kyoto (*n* = 9)	0.42 - 3.2	1.7	0.02 - 0.25	0.14
Limeira (*n* = 9)	1.9 - 22.4	11.8	0.07 - 2.1	0.64
Ribeirão Preto (*n* = 6)	3.6 - 24.5	5.5	0.08 - 6.5	0.32
Cáceres (*n* = 6)	0.23 - 22.1	1.3	0.05 - 5.2	0.23

Scaramboni et al. (2024a)

Among the individual PAHs, human exposure to high-molecular-weight PAHs (HMW-PAHs) are of special health concern due to their higher mutagenic and carcinogenic activity compared to smaller PAHs. A prevalence of HMW-PAHs was observed in Limeira (77%), Ribeirão Preto (76%), and Kyoto samples (58%), with benzo[b]fluoranthene (BbF) and benzo[ghi]perylene (BPer) being the most abundant. In contrast to Σ_{16}PAH, total oxygenated PAHs (Σ_4OPAH) showed different patterns, with Cáceres having nearly twice the concentrations of Σ_4OPAH compared to Kyoto and Stockholm. In Cáceres, 2-methylanthraquinone was the predominant OPAH, exhibiting a median concentration 2-8 times greater than that observed in other cities. The primary source of this compound

is attributed to the teak tree, widely cultivated in the city. However, the specific emission processes, whether through burning or biogenic emissions, remain to be investigated.

The carcinogenic activity of the PAHs mixtures, measured in terms of BaP_{eq} concentrations, was notably elevated in Brazilian cities (Figure 2). In Ribeirão Preto, the BaP_{eq} concentrations reached up to 13.5 ng m^{-3}, highlighting the city's susceptibility to heightened risk due to biomass burning, as previously demonstrated (Scaramboni et al., 2024b).

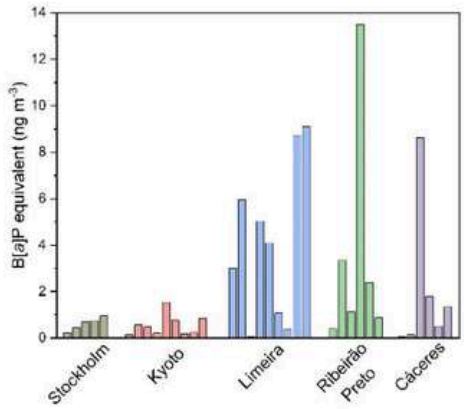


Figure 2. B[*a*]P_{eq} concentrations found for individual $PM_{2.5}$ samples from the studied cities.

In all five cities studied, diagnostic ratios (DRs) consistently indicated a dominance of pyrogenic sources over petrogenic sources in the measured PAHs, aligning with expectations given the prevalence of pyrogenic sources in air samples compared to petrogenic sources associated with sediment deposition from petroleum activities (Table 2).

Table 2. Diagnostic ratios (DRs) calculated for PAHs determined in the $PM_{2.5}$ samples from the studied cities.

DR	Stockholm ($n = 5$)	Kyoto ($n = 9$)	Limeira ($n = 9$)	Ribeirão Preto ($n = 6$)	Cáceres ($n = 6$)
Flt / (Flt + Pyr)[a]	0.52–0.62 (0.59)	0.53–0.66 (0.60)	0.43–0.61 (0.54)	0.43–0.56 (0.54)	0.50–0.70 (0.60)
BaA / (BaA + Chr)[b]	0.43–0.58 (0.47)	0.09–0.47 (0.37)	0.21–0.49 (0.35)	0.34–0.50 (0.44)	0.59–0.76 (0.64)
InP / (InP + BPer)[c]	0.24–0.41 (0.34)	0.08–0.44 (0.36)	0.08–0.41 (0.30)	0.04–0.42 (0.28)	0.30–0.42 (0.37)
BaP / BPer[d]	0.25–0.71 (0.60)	0.08–0.56 (0.44)	0.19–0.68 (0.35)	0.13–0.58 (0.47)	0.16–0.67 (0.45)
BaP / (BaP + BeP)[e]	0.31–0.49 (0.45)	0.23–0.41 (0.35)	0.34–0.54 (0.45)	0.38–0.51 (0.47)	0.39–0.68 (0.52)
Ret / (Ret + Chr)[f]	0.25–0.47 (0.32)	0.09–0.71 (0.17)	0.05–0.61 (0.19)	0.07–0.58 (0.29)	0.46–0.84 (0.68)

[a] < 0.4: petrogenic; 0.4–0.5: fossil fuel combustion; > 0.5: grass, wood, and coal combustion.
[b] < 0.2: petrogenic;> 0.35: pyrogenic.
[c] < 0.2: petrogenic; 0.2–0.5: petroleum combustion; > 0.5: grass, wood, and coal combustion.
[d] < 0.6: non-traffic emissions; > 0.6: traffic emissions.
[e] < 0.5: aged particles; > 0.5: fresh particles.
[f] 0.15–0.50: petroleum combustion; 0.30–0.45 coal combustion; ~1: wood burning.

Scaramboni et al. (2024a)

DRs also suggested that the pyrogenic sources were a combination of vehicle emissions and biomass combustion. The BaP/BPer ratio, associated with traffic-related emissions, was highest in Stockholm, in line with its proximity to a highway. The BaP/(BaP + BeP) ratio indicated fresh PM emissions in Cáceres > Ribeirão Preto > Limeira > Stockholm and more aged particles in Kyoto, aligning with fire spots in Cáceres and long-range air mass trajectories from China and South Korea to Kyoto. Brazilian cities showed a notable influence of biomass burning, likely attributable to widespread Amazon and Cerrado wildfires added to local fires.

CONCLUSIONS

Despite regional disparities, Stockholm and the three Brazilian cities exhibited $PM_{2.5}$ levels above WHO short-term guidelines, with the Brazilian cities experiencing the highest air pollution. Brazilian cities also exhibited the highest levels of total PAHs and OPAHs, and consequently, the highest carcinogenic activity based on B[*a*]P equivalent concentrations. Our results support the importance of improving the air quality especially during the emission-intense winter/dry season to reach air quality standards and limit human health effects from air pollution.

REFERENCES

Maselli, B.S. et al. “Similar polycyclic aromatic hydrocarbon and genotoxicity profiles of atmospheric particulate matter from cities on three different continents”. Environmental and Molecular Mutagenesis 61 (2020): 560-573.

Santos, A.G. et al. “A simple, comprehensive, and miniaturized solvent extraction method for determination of particulate-phase polycyclic aromatic compounds in air”. Journal of Chromatography A 1435 (2016): 6-17.

Scaramboni, C. et al. “Characterization of cross-continental $PM_{2.5}$: Insights into emissions and chemical composition”. Atmospheric Research 305 (2024a): 107423.

Scaramboni et al. "Particulate matter from a tropical city in southeast Brazil: Impact of biomass burning on polycyclic aromatic compounds levels, health risks, and in vitro toxicity". Chemosphere 350 (2024b): 141072.

USEPA - United States Environmental Protection Agency, 2010. Development of a Relative Potency Factor (RPF) Approach for Polycyclic Aromatic Hydrocarbon (PAH) Mixtures (External Review Draft). Washington, DC.

WHO - World Health Organization. “Human health effects of polycyclic aromatic hydrocarbons as ambient air pollutants: report of the Working Group on Polycyclic Aromatic Hydrocarbons of the Joint Task Force on the Health Aspects of Air Pollution”. Copenhagen: WHO Regional Office for Europe, 2021.

AIR POLLUTION CONFERENCE BRAZIL
CMAS SOUTH AMERICA
COMMUNITY MODELING AND ANALYSIS SYSTEM

USE OF PLANTS AS BIOMONITORS OF PARTICULATE MATTER TOXICITY IN URBAN REGIONS INFLUENCED BY MINING

Santos, Emannuelly Ap. Amaral[1]; Neves, Thiago de Alencar[2]; Oliveira, Dângelle Makelle[3]; Passos, Ricardo Gomes[4]; Albuquerque, Taciana Toledo de Almeida[5]; Starling, Maria Clara Vieira Martins[6]
[1]*Department of Sanitary and Environmental Engineering, Federal University of Minas Gerais.*
emannuellyufmg@gmail.com
[2]*Department of Sanitary and Environmental Engineering, Federal University of Minas Gerais.*
thiago@desa.ufmg.br
[3]*Department of Sanitary and Environmental Engineering, Federal University of Minas Gerais.*
dangelleem@yahoo.com.br
[4]*Nuclear Technology Development Center, Federal University of Minas Gerais*
ricardo.passos@cdtn.br
[5]*Department of Sanitary and Environmental Engineering, Federal University of Minas Gerais.*
tacianatoledo26@gmail.com
[6]*Department of Sanitary and Environmental Engineering, Federal University of Minas Gerais.*
mariaclara@desa.ufmg.br

Abstract: Regarding air quality, biomonitoring applies plant species for which standard assays enable tracking direct and immediate effect of pollutants, as well as the release of toxic compounds, such as metals found in particulate matter (PM), into the ecosystem. This is extremely relevant considering that ecosystem health is linked to human health as according to the One Health Approach. Given the above, this research aims to conduct biomonitoring of air quality by using the standard grass species *Lolium multiflorum* as a tool for air quality monitoring in the city of Brumadinho (Minas Gerais, Brazil). The region is impacted by mining activities that release high loads of particulate matter into the atmosphere. The plants were cultivated and exposed according to the VDI 3957 - part 2 standard, with adaptations. Three sampling points were selected: S1 - City center; S2 - Tejuco neighborhood, surrounded by mining sites; S3 - an Indigenous community area, along with a reference point - S4 (a natural reserve). Additionally, $PM_{2.5}$ were sampled throughout the exposure period using a medium-volume sampler (ARA Instrument). S3 showed the highest concentrations of $PM_{2.5}$ (median of 40.15 $\mu g/m^3$), while S4 had the lowest concentrations (median of 31.40 $\mu g/m^3$). However, the medians did not differ significantly between the monitoring points. Visual analyses of the plants after exposure demonstrate a possible correlation between the presence of metals in atmospheric particles and their growth, indicating the accumulation of trace elements.

Keywords: Biomonitoring, One Health, Mining, Particulate Matter, *Lolium multiflorum*.

INTRODUCTION

Air pollution is a current challenge, representing one of the greatest risks to human health and environmental integrity (WHO, 2024). In mining regions, the impacts and emission of atmospheric pollutants, especially particulate matter (PM), from anthropogenic activities are intensified. In Brazil, mining plays a pivotal role in the country's economy, especially in the state of Minas Gerais. However, indiscriminate activities and lack of control and monitoring lead to the exacerbated release of atmospheric pollutants, highly detrimental to health.

The bottleneck in conventional air quality monitoring techniques, which rely on physicochemical analyses, does not allow for direct conclusions about the potential effects of pollutants to the environment (Klumpp *et al.*, 2003). Thus, alternatives supported by Nature-Based Solutions (NbS) can contribute to the diagnosis and reduction of air pollution (Theophilo *et al.*, 2021).

Biomonitoring is an efficient technique for assessing environmental contamination by using living organisms. Considering the concept of One Health (Multisanti *et al.*, 2022), environmental health threats detected by biomonitoring can serve as an early warning for human health threats, contributing to preventive measures. PM containing potentially toxic trace elements such as cadmium (Cd), copper (Cu), lead (Pb), and zinc (Zn) (Theophilo *et al.*, 2021), are easily inhaled by humans and animals, as well as deposited in plants, resulting in direct and indirect problems for the environment and public health.

Regarding air quality (bio)monitoring, plants are cost-effective indicators that allow for the assessment of the risk of complex mixtures of pollutants and analyses of those with very low environmental concentrations, which are difficult to measure by traditional methods (De Temmerman *et al.*, 2004). In addition, biomonitoring can be implemented in locations which lack access to high-tech equipment which require frequent maintenance. Besides, they promote environmental education and raise community awareness related to air pollution.

AIR POLLUTION CONFERENCE BRAZIL
CMAS SOUTH AMERICA
COMMUNITY MODELING AND ANALYSIS SYSTEM

The forage grass *Lolium multiflorum* Lam. (ryegrass) is used for animal consumption and due to its resistance to atmospheric pollutants, it has a high rate of bioaccumulation of toxic substances, such as sulfur, trace metals, polycyclic aromatic hydrocarbons (PAHs), gases, and PM (Nakazato *et al.*, 2018). Thus, it is ideal for monitoring and risk assessment in industrial and urban areas.

Considering the foregoing, this research aims to conduct air quality biomonitoring using the standard grass species *Lolium multiflorum* in a mining region located in the city of Brumadinho, metropolitan region of Belo Horizonte, in the state of Minas Gerais, Brazil.

METHODS

Biomonitoring was actively conducted in March and April of 2024, with grass cultivation and exposure following the VDI 3957 - part 2 standard (2003) (adapted). The plants were cultivated for 3 weeks before exposure in a natural reserve selected as a reference site (S4) and exposed for 28 days at 3 sampling points in Brumadinho: S1 - City center, S2 - Tejuco neighborhood, surrounded by mining sites, S3 - an Indigenous community area near a ferry line used for mining ore transportation.

Plant growth was observed during the exposure period. Subsequently, they were manually cut and subjected to laboratory analyses to evaluate the presence of metals, following EPA 3050B (1996) (adapted). The plant material was submitted to wet-opened digestion with a HNO_3 and H_2O_2 solution (1:1), and the extracts will be analyzed by ICP-OES.

In addition to plant exposure, fine particulate matter (<2.5 micrometers in diameter; $PM_{2.5}$) were sampled using a medium-volume sampler (ARA Instrument) equipped with quartz filters. $PM_{2.5}$ sampling was carried out for 24 hours in the same locations of plant exposure, throughout the exposure period. Subsequently, the $PM_{2.5}$ concentration was determined by gravimetric method (INPE, 2012), and the concentration of metals using the aforementioned methodology. Results were submitted to statistical analysis by Kruskal-Wallis analysis of variance followed by Dunn's mean test.

FINDINGS AND ARGUMENT

The concentration of particulate matter $PM_{2.5}$ varied among the sampling sites, with a maximum of 43.77 µg/m³ in the Indigenous community area (S3) and a minimum of 16.23 µg/m³ in the reference area (S4). Figure 1 illustrates the variation found among the monitoring points in the city of Brumadinho and the comparison with air quality reference value of WHO (2021).

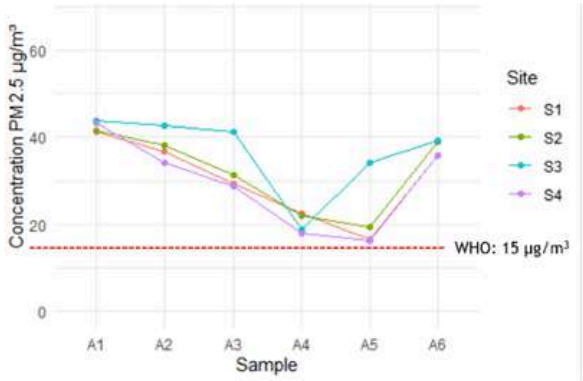


Figure 1. $PM_{2.5}$ concentrations detected in each of the monitoring points (S1- S4) in the city of Brumadinho compared with WHO air quality guidelines (2021) (15 µg/m³ in 24 hours).

All samples exceeded the WHO reference value for $PM_{2.5}$. This suggests poor air quality in the region, requiring more attention to monitoring and source control. Furthermore, it is important to highlight that PM concentrations are also associated with other factors, such as climatic conditions, and correlation studies with such factors should be performed.

S3 showed the highest median of 40.15 µg/m³ among the sampling points (Figure 2). The lowest median was at the reference point (S4) of 31.40 µg/m³. However, there was no significant differences according to the Kruskal-Wallis test ($p<0.05$).

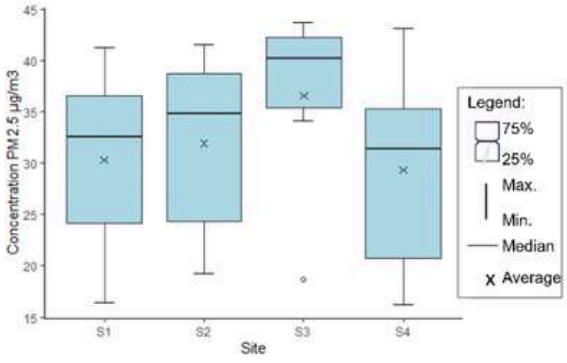


Figure 2. Boxplot of $PM_{2.5}$ concentration in each monitoring point.

Site 3 represents an Indigenous community area located near the ore loading and transportation area. Additionally, the region was affected by the tailings dam collapse on January 26th, 2019. So, it still suffers the consequences of tailings deposit in the region. Such factors may be associated with the resuspension of contaminated particulate matter. However, further studies should be conducted to test this hypothesis, such as studies involving soil sampling.

The preliminary qualitative analysis of plants (visual analysis) contributed to an initial understanding of the impacts of air pollution to bioindicators, as toxic components can cause biomass reduction, growth inhibition, and organism death (Ghosh; Dutta; Mukhopadhyay, 2023). Figure 3 demonstrates the state of plants exposed in each of the sampling sites after 28 days.



Figure 3. Plants after exposure in each of the sampling sites after 28 days, some are visually affected (injuries).

It can be observed that plants exposed in Points 2 and 3 exhibited more leaf injuries and are smaller than the other points. Borowiak *et al.* (2020) noted that the accumulation of trace elements presents in the atmosphere in ryegrass reduced the net photosynthesis rate and stomatal conductance of the plants.

Although S3 presented the highest PM concentrations, it is worth noting that the plants were exposed in a wooded area and toxic elements may have encountered barriers in taller plants compared to the sampler. Thus, the analysis of metals in ryegrass leaves will provide more elaborate data for understanding metal contamination at this and the other sampling sites.

CONCLUSIONS

Preliminary analyses demonstrate that particulate matter concentration may influence plant development, taking into consideration other processes such as land use in the surroundings. The high concentrations of particulate matter in the city of Brumadinho reflect air pollution in urban areas influenced by mining. Analyses of metals in plants leaves and quartz filters will be used to better discuss the relationships between atmospheric pollutant concentration and ecosystem health. Biomonitoring data along with chemical characterization will be of great significance in devising strategies for controlling and mitigating pollution.

ACKNOWLEDGMENTS

The authors would like to thank the FAPEMIG (Minas Gerais Research Funding Foundation) and CAPES program for funding the project.

REFERENCES

Arsenic, Aluminum Magnesium, et al. "Method 3050B acid digestion of sediments, sludges, and soils 1.0 scope and application." *Washington, DC, USA* (1996).

Borowiak, Klaudia, et al. "Accumulation of airborne toxic elements and photosynthetic performance of Lolium multiflorum L. leaves." *Processes* 8.9 (2020): 1013.

Nakazato, Ricardo Keiichi, et al. "Efficiency of biomonitoring methods applying tropical bioindicator plants for assessing the phytotoxicity of the air pollutants in SE, Brazil." *Environmental Science and Pollution Research* 25 (2018): 19323-19337.

De Temmerman, Ludwig, and Michel Hoenig. "Vegetable crops for biomonitoring lead and cadmium deposition." Journal of Atmospheric Chemistry 49 (2004): 121-135.

Ferreira, Tatiane Morais, Maria Cristina Forti, and Plinio Carlos Alvala. "Protocolo para coleta de material particulado atmosférico." *INPE, São José dos Campos* (2012).

Ghosh, Sayantan, Ratna Dutta, and Shritama Mukhopadhyay. "A Review on Seasonal Changes in Particulate Matter Accumulation by Plant Bioindicators: Effects on Leaf Traits." *Water, Air, & Soil Pollution* 234.8 (2023): 529.

Klumpp, Andreas. "European network for the assessment of air quality by the use of bioindicator plants. LIFE99 ENV/D/000453". University of Hohenheim. 2003.

Multisanti, Cristiana Roberta, et al. "Sentinel species selection for monitoring microplastic pollution: A review on one health approach." Ecological Indicators 145 (2022): 109587.

Theophilo, Carolina Yume Sawamura, et al. "Biomonitoring as a Nature-Based Solution to Assess Atmospheric Pollution and Impacts on Public Health." Bulletin of Environmental Contamination and Toxicology 107 (2021): 29-36.

VDI - Verein Deutscher Ingenieure. "Biological Measuring Techniques for the Determination and Evaluation of Effects of Air Pollutants on Plant (Bioindication). Method of Standardized Grass Exposure. VDI-Guideline 3957 Part 2. *Beuth Verlag, Berlin*, 2003.

WHO. "Air quality and health. Type of pollutants." *Available at: Air quality and health (who.int).* Accessed on March 8, 2024.

WHO. "WHO global air quality guidelines." *Particulate Matter (PM2.5 and PM10), Ozone, Nitrogen Dioxide, Sulfur Dioxide and Carbon Monoxide* (2021).

AIR POLLUTION CONFERENCE BRAZIL
CMAS SOUTH AMERICA
COMMUNITY MODELING AND ANALYSIS SYSTEM

Unraveling Aerosols: Exploring Size, Number, and Particle Formation Events in São Paulo

Rubens Fabio Pereira[1,1], Maria de Fatima Andrade [1,2], Luciana Varanda Rizzo[2,3]
[1]*Institute of Astronomy, Geophysics and Atmospheric Sciences, University of Sao Paulo*
[2]*Institute of Physics, University of Sao Paulo*
E-mail: [1]rubens.pereira@usp.br , [2]maria.andrade@iag.usp.br, [3]lrizzo@usp.br

Abstract: The city of São Paulo, located in the southeast of Brazil, covers an area of 1,521.11 km², with an estimated population of 11.4 million inhabitants and a fleet of approximately 8 million vehicles. This fleet is the main contributor to atmospheric pollutant emissions in the city, followed by sources such as biomass burning and the transport of pollutants from nearby industrial centers. In the context of emission control programs for conventional atmospheric pollutants implemented in São Paulo, satisfactory progress has been observed over the years. However, certain pollutant classes, such as ultrafine particles, still lack similar policies. Characterizing the size and number distributions of atmospheric particles (PNSD), combined with the analysis of chemical composition and trajectories, is crucial for understanding the diverse influences of aerosols on the climate and human health. This ongoing master's project aims to characterize the size distributions of submicrometer aerosols in the Metropolitan Region of São Paulo. For this purpose, PNSD data were obtained using a Scanning Mobility Particle Sizer (SMPS) in the size range of 10.6 to 429.6 nanometers from June 2019 to January 2020 at the University of São Paulo. Meteorological variables and the concentrations of other atmospheric constituents, such as black carbon, ozone, and nitrogen oxides, were also monitored. Data analysis methods included algorithms for identifying modes and clustering PNSDs into five different clusters. From a total of 72,330 PNSDs, log-normal curves were successfully fitted to nucleation, Aitken, and accumulation modes in 96.97 %, 97.57%, and 99.44% of cases, with mean particle number concentrations (PNC) observed as (4.7 ± 3.8) x 10^3 (#/cm³), (5.2 ± 3.5) x 10^3 (#/cm³), and (3.0 ± 3.2) x 10^3 (#/cm³) for each mode, respectively. The average size and number distributions of particles (PNSD) for weekdays (WD) and weekends (WE) revealed a slightly smaller geometric mean diameter in WD, with an average of 49±2 nm, compared to the average of 51±2 nm in WE. The difference in mean particle concentrations between the two periods was not significant, only 800 (#/cm³) (WD: 1.09 ± 0.4, WE: 1.01 ± 0.4) x 10^3 #/cm³ Log-normal curve fitting to these mean distributions showed particle number concentrations for nucleation, Aitken, and accumulation modes of (5.0 ± 3.9, 5.2 ± 3.5, 3.1 ± 3.4) x 10^3 #/cm³ in WD and (4.0 ± 3.5, 4.6 ± 3.4, 2.8 ± 2.7) x 10^3 #/cm³ in WE. Regarding the geometric mean diameter (Dpg), values were (18.2 ± 5.0 nm, 52.5 ± 14.5 nm, and 168.5 ± 54.2 nm) in WD and (18.1 ± 5.3 nm, 52.1 ± 14.5 nm, and 168.4 ± 58.7 nm) in WE for the three modes. A possible explanation for this is the reduction in the number of vehicles in circulation during weekends, which is a source of precursor gases for particle formation and growth. The application of the K-means clustering algorithm to PNSDs revealed the presence of five distinct clusters, each characterized by variations in predominant modes and their frequencies throughout the diurnal cycle. These results suggest potential influences from various sources, as well as dynamic and physicochemical processes. In a subsequent stage, we plan to refine and expand our analysis, conducting a more detailed investigation of each of these clusters and establishing connections with the meteorological variables and aforementioned atmospheric constituents. Mask R-CNN model identified 16 of 32 visually identified NPF events. However, it also falsely identified NPF events 33 times.

Keywords: Air Pollution, Ultrafine Aerosols, Cluster Analysis, Particle Number and Size Distribution

INTRODUCTION

Aerosols are critical in atmospheric composition, impacting climate, air quality, and human health. These suspended particles vary in size, composition, and origin, affecting radiative balance, cloud formation, and visibility. Depending on the portions of the body they access, they can have deleterious effects. Understanding their properties is essential for developing effective strategies to mitigate the impacts of anthropogenic emissions on the environment (ZHENG et al., 2015; THORNHILL et al., 2021).

The city of São Paulo (23.5S; 46.6W) is the largest population center in the São Paulo Metropolitan Region (RMSP), located in the southeast region of Brazil. The region is influenced by mesoscale phenomena (urban heat island and sea breeze circulations) and synoptic scale phenomena (South Atlantic convergence zone (ZCAS) and frontal systems) (SANCHEZ-CCOYLLO; ANDRADE, 2002).

Regarding aerosol sources, the largest contributions come from the vehicle fleet, with approximately 8 million vehicles, emitting both particles directly and precursor gases that will give rise to particles in new particle formation events (NPF). Other relevant sources include biomass burning (agricultural residues and wood burning in restaurants) and the transport of pollutants from industrial centers near the capital (EMYGDIO et al., 2018; MIRANDA et al., 2018).

Despite the progress made by some megacities like São Paulo in controlling conventional atmospheric pollutant emissions, the emergence of new pollutants such as ultrafine (UF) particles has introduced a new challenge in this context (KUMAR et al., 2014). Identifying NPF events visually is labor-intensive, time-consuming, and subject to human bias, which necessitates the use of automatic methods to optimize this process.

This work has two main objectives. The first is to characterize the particle number and size distributions (PNSD) obtained at the Institute of Astronomy, Geophysics, and Atmospheric Sciences of the University of São Paulo in 2019, analyzing possible sources and the meteorological and environmental variables that influence the formation of these distributions. Subsequently, with the PNSD data in hand, we will employ an image segmentation model to automatically detect new particle formation (NPF) events and evaluate its applicability for this purpose.

METHODS

The data were collected by the Laboratory of Atmospheric Processes Analysis (LAPAt) of the Department of Atmospheric Sciences at IAG-USP, on the terrace of its main building (23.55S; 46.73W). The campaign took place from June 26, 2019, to January 7, 2020, intermittently, totaling 152 days of collection. Aerosol size and number distributions were obtained using an SMPS, in the range of 10.6 to 429.6 nanometers, and Black Carbon (BC) concentration was measured with an Aethalometer model AE33. Meteorological data (temperature, relative humidity, wind speed and direction, and solar radiation) were provided by the Micrometeorology Laboratory of IAG-USP and recorded at the automatic station installed on the institute's terrace. Additionally, ozone concentration and fine particulate matter data were collected at the automatic monitoring station of CETESB, located at the Institute of Energy and Nuclear Research of University City USP (23.56S; 46.72W).

To quantify the representativeness of each mode individually in each PNSD, an algorithm that fits multi-modal log-normal functions was applied ***(RIZZO et al., 2018)****. The original distribution was extrapolated up to 600 nm based on these fits. The K-means clustering method was applied and according to clustering quality indices, the optimal number of clusters for the dataset was five.*

As a first attempt to automatically detect NPF events, we utilized the Mask R-CNN model originally trained by (SU et al., 2022), who used an extensive dataset obtained from stations in Finland and Italy between 1997 and 2021. In later stages, we will apply the same approach with data collected in São Paulo. The training method involves manually segmenting the characteristic shapes of NPF events (such as the banana-shaped patterns), feeding the model with training and validation datasets, and checking its accuracy in identifying these events, as shown in Figure 1.

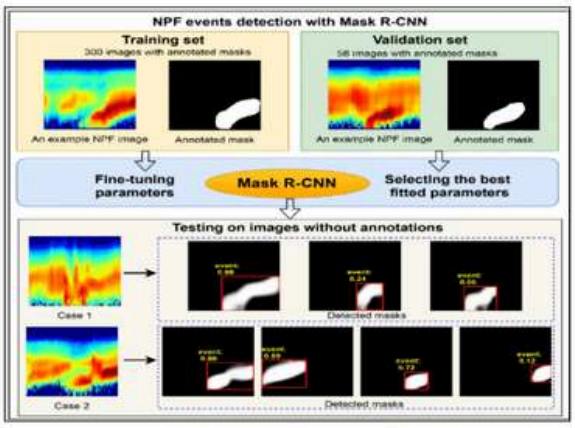


Figure 1. Flowchart of new particle formation event detection via Mask R-CNN. All rights to the author *(SU et al., 2022).*

FINDINGS AND ARGUMENT

Table 1 presents the average characteristic indices of the PNSD and their respective modes. The average particle number concentration (PNC) observed was (1.15 ± 0.54) × 10^4 particles per cubic centimeter, with a geometric mean diameter of (49 ± 1.2) nanometers. Regarding the modes, the Aitken mode shows the highest number concentration of particles, with (5.2 ± 3.5) × 10^3 particles, while the Accumulation mode was the most frequently observed, appearing in 99.44% of the distributions.

Table 1. Statistical data of the PNSD. We have the total number of samples obtained and the number of times it was possible to fit that mode to the distribution, the frequency with which that mode was present concerning all samples, concentration (N), geometric mean diameter (D_{pg}), and geometric standard deviation (σ_g).

Distribution	Samples	Occurrence (%)	Parameters	Mean ± Std
PNSD	72330	*	N	$(1.15 \pm 0.54)10^4$
			D_{pg}	$(4.9 \pm 1.2)10^1$
Nucleation mode	70138	96.97	N	$(4.7 \pm 3.8)10^3$
			D_{pg}	$(1.8 \pm 0.5)10^1$
			σ_g	(1.6 ± 0.1)
Aitken mode	70572	97.57	N	$(5.2 \pm 3.5)10^3$
			D_{pg}	$(5.25 \pm 1.45)10^1$
			σ_g	(1.6 ± 0.1)
Accumulation mode	71924	99.44	N	$(3.0 \pm 3.2)10^3$
			D_{pg}	$(1.68 \pm 0.54)10^2$
			σ_g	(1.6 ± 0.07)

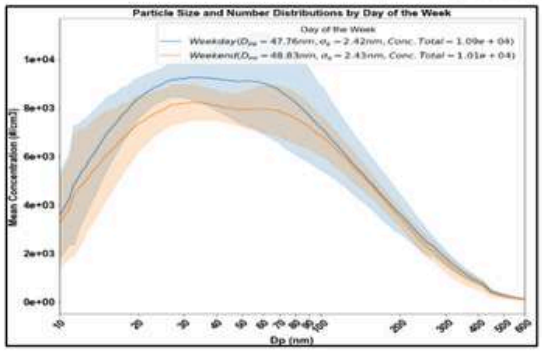


Figure 2. Particle size and number distributions by Day of the Week. Along with the legend, we have the values of the geometric mean diameter (D_{pg}), the geometric standard deviation (σ_g), and the total concentration of the PNSD.

The curves in Figure 2 show the PNSD for weekdays (WD) and weekends (WE), with 82 WD and 30 WE. The geometric mean diameter of the particles is slightly smaller on WD, averaging 47.76 nm, compared to 48.8 nm on WE. The difference in average particle concentrations between WD and WE is not significant, being only 800 particles per cubic centimeter

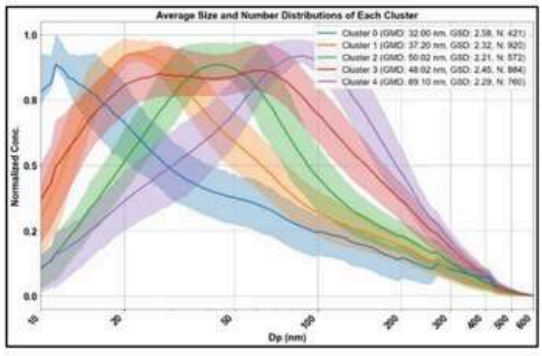
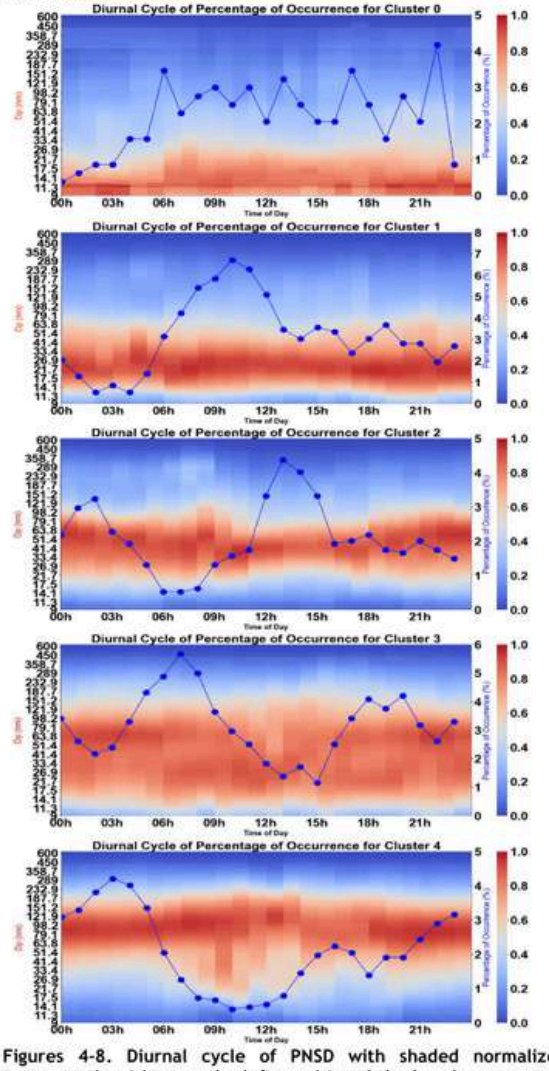


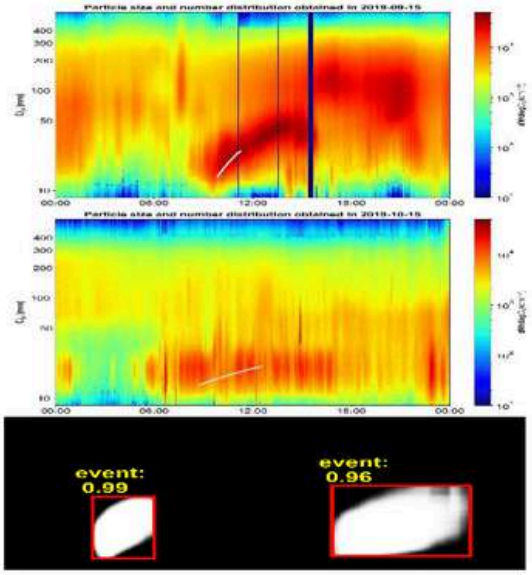
Figure 3. Average PNSD for each of the five clusters obtained with the k-means classification. The shaded areas on each graph represent the 25th and 75th percentiles. Along with the legend, we have the values of (D_{pg}), (σ_g), and the total PNSD per cluster.

In Figure 3, we have five PNSDs representing the mean value and 25th and 75th percentiles of each cluster obtained by the K-means method. The (Dpg) varies between 32 and 69 nm, indicating that they may have different sources and degrees of aerosol processing. Out of a total of 3557 grouped samples, the most frequently observed ones are in clusters 1 and 3, with 920 and 884 samples, respectively.



Figures 4-8. Diurnal cycle of PNSD with shaded normalized concentration (sizes on the left y-axis) and the hourly percentage frequency of this PNSD on the blue line (scale on the right y-axis).

Cluster number 0 presents a size range consistent with the nucleation mode (10.9 nm to 27 nm), indicating newly formed or lightly processed particles. They are predominant between 6:00 AM and 9:00 PM local time. Clusters 1 and 3 exhibit peaks in the early morning hours, with a new peak recorded late in the afternoon in the case of cluster 3, moments that coincide with rush hour. Cluster number 2 records a more pronounced peak around noon, with a secondary peak in the early hours of the day. This pattern may be related to the growth process of particles originating from nucleation during the day and the increase in humidity during the night. Finally, Cluster 4 harbors aerosols with diameters of both the Aitken mode and accumulation mode (41.4 nm to 151.2 nm). This cluster is more observed in the nighttime period, from 11:00 PM to 5:00 AM, but already shows an increase in its frequency from 7:00 PM. These characteristics can be attributed to the mixture of already aged particles brought by the sea breeze with aerosols from the Aitken mode, and its higher nocturnal frequency explained by the stabilization of the Planetary Boundary Layer



Figures 9-11. PNSD for September 15 and October 15, 2019. The white line indicates the region where the NPF event was identified. The lower panel shows the masks that the model associated with the respective days

Figures 9 and 10 show two examples of PNSD where the Mask R-CNN model identified NPF events. The first identification was correct, while the second was not. Figure 11 shows the two masks the model associated with the NPF events. Out of 32 visually identified NPF events, the model correctly detected 16. However, it also falsely identified NPF events 33 times.

CONCLUSIONS

The PNSD analysis revealed that the geometric mean diameter of the particles is slightly smaller on WD, with no significant differences observed between the average particle concentrations during WD and WE. The log-normal curve fitting showed that the highest concentrations are seen in the Aitken mode, indicating that the region receives particles at various aging stages.

Applying the K-means clustering algorithm to the PNSD resulted in the identification of five distinct clusters with variations in frequency throughout the diurnal cycle. This suggests the influence of different sources, as well as dynamic and physicochemical processes involved in their formation.

Although the model successfully identified 50% of the NPF events, it showed a high rate of false positives due to being trained with PNSD data from regions with different characteristics than RMSP. Future work will involve training the model with PNSD data from RMSP to see if performance improves.

REFERENCES

EMYGDIO, A. P. M. et al. Biomarkers as indicators of fungal biomass in the atmosphere of sao paulo, brazil. The Science of the total environment, Elsevier B.V, Netherlands, v. 612,p. 809-821, 2018

MIRANDA, R. M. de et al. Source apportionment of fine particulate matter by positive matrix factorization in the metropolitan area of sao paulo, brazil. Journal of cleaner production, Elsevier Ltd, v. 202, p. 253-263, 2018.

KUMAR, P. et al. Ultrafine particles in cities. Environment International, v. 66,

P. Su et al. "New particle formation event detection with Mask R-CNN". Em: Atmospheric Chemistry and Physics 22.2 (2022), pp. 1293-1309. DOI: 10.5194/acp- 22- 1293- 2022.

RIZZO, L. et al. Multi-year statistical and modeling analysis of submicrometer aerosol number size distributions at a rain forest site in amazonia. Atmospheric Chemistry and Physics, v. 18, 07 2018.

SANCHEZ-CCOYLLO, O.; ANDRADE, M. The influence of meteorological conditions on the behavior of pollutants concentrations in sao paulo, brazil. Environmental Pollution, v. 116, 01 2002

THORNHILL, G. D. et al. Effective radiative forcing from emissions of reactive gases and aerosols - a multi-model comparison. Atmospheric Chemistry and Physics, v. 21, n. 2, p.853-874, 2021

ZHENG, S. et al. Long-term (2001-2012) concentrations of fine particulate matter (pm2.5) and the impact on human health in beijing, china. Atmospheric chemistry and physics, Copernicus Gesellschaft Mbh,

AIR POLLUTION CONFERENCE BRAZIL
CMAS SOUTH AMERICA
COMMUNITY MODELING AND ANALYSIS SYSTEM

USE OF PLANTS AS BIOMONITORS OF PARTICULATE MATTER TOXICITY IN URBAN REGIONS INFLUENCED BY MINING

Santos, Emannuelly Ap. Amaral[1]; Neves, Thiago de Alencar[2]; Oliveira, Dângelle Makelle[3]; Passos, Ricardo Gomes[4]; Albuquerque, Taciana Toledo de Almeida[5]; Starling, Maria Clara Vieira Martins[6]
[1]*Department of Sanitary and Environmental Engineering, Federal University of Minas Gerais.* *emannuellyufmg@gmail.com*
[2]*Department of Sanitary and Environmental Engineering, Federal University of Minas Gerais.* *thiago@desa.ufmg.br*
[3]*Department of Sanitary and Environmental Engineering, Federal University of Minas Gerais.* *dangelleem@yahoo.com.br*
[4]*Nuclear Technology Development Center, Federal University of Minas Gerais* *ricardo.passos@cdtn.br*
[5]*Department of Sanitary and Environmental Engineering, Federal University of Minas Gerais.* *tacianatoledo26@gmail.com*
[6]*Department of Sanitary and Environmental Engineering, Federal University of Minas Gerais.* *mariaclara@desa.ufmg.br*

Abstract: Regarding air quality, biomonitoring applies plant species for which standard assays enable tracking direct and immediate effect of pollutants, as well as the release of toxic compounds, such as metals found in particulate matter (PM), into the ecosystem. This is extremely relevant considering that ecosystem health is linked to human health as according to the One Health Approach. Given the above, this research aims to conduct biomonitoring of air quality by using the standard grass species *Lolium multiflorum* as a tool for air quality monitoring in the city of Brumadinho (Minas Gerais, Brazil). The region is impacted by mining activities that release high loads of particulate matter into the atmosphere. The plants were cultivated and exposed according to the VDI 3957 - part 2 standard, with adaptations. Three sampling points were selected: S1 - City center; S2 - Tejuco neighborhood, surrounded by mining sites; S3 – an Indigenous community area, along with a reference point - S4 (a natural reserve). Additionally, $PM_{2.5}$ were sampled throughout the exposure period using a medium-volume sampler (ARA Instrument). S3 showed the highest concentrations of $PM_{2.5}$ (median of 40.15 $\mu g/m^3$), while S4 had the lowest concentrations (median of 31.40 $\mu g/m^3$). However, the medians did not differ significantly between the monitoring points. Visual analyses of the plants after exposure demonstrate a possible correlation between the presence of metals in atmospheric particles and their growth, indicating the accumulation of trace elements.

Keywords: Biomonitoring, One Health, Mining, Particulate Matter, *Lolium multiflorum*.

INTRODUCTION

Air pollution is a current challenge, representing one of the greatest risks to human health and environmental integrity (WHO, 2024). In mining regions, the impacts and emission of atmospheric pollutants, especially particulate matter (PM), from anthropogenic activities are intensified. In Brazil, mining plays a pivotal role in the country's economy, especially in the state of Minas Gerais. However, indiscriminate activities and lack of control and monitoring lead to the exacerbated release of atmospheric pollutants, highly detrimental to health.

The bottleneck in conventional air quality monitoring techniques, which rely on physicochemical analyses, does not allow for direct conclusions about the potential effects of pollutants to the environment (Klumpp *et al.*, 2003). Thus, alternatives supported by Nature-Based Solutions (NbS) can contribute to the diagnosis and reduction of air pollution (Theophilo *et al.*, 2021).

Biomonitoring is an efficient technique for assessing environmental contamination by using living organisms. Considering the concept of One Health (Multisanti *et al.*, 2022), environmental health threats detected by biomonitoring can serve as an early warning for human health threats, contributing to preventive measures. PM containing potentially toxic trace elements such as cadmium (Cd), copper (Cu), lead (Pb), and zinc (Zn) (Theophilo *et al.*, 2021), are easily inhaled by humans and animals, as well as deposited in plants, resulting in direct and indirect problems for the environment and public health.

Regarding air quality (bio)monitoring, plants are cost-effective indicators that allow for the assessment of the risk of complex mixtures of pollutants and analyses of those with very low environmental concentrations, which are difficult to measure by traditional methods (De Temmerman *et al.*, 2004). In addition, biomonitoring can be implemented in locations which lack access to high-tech equipment which require frequent maintenance. Besides, they promote environmental education and raise community awareness related to air pollution.

The forage grass *Lolium multiflorum* Lam. (ryegrass) is used for animal consumption and due to its resistance to atmospheric pollutants, it has a high rate of bioaccumulation of toxic substances, such as sulfur, trace metals, polycyclic aromatic hydrocarbons (PAHs), gases, and PM (Nakazato *et al.*, 2018). Thus, it is ideal for monitoring and risk assessment in industrial and urban areas.

Considering the foregoing, this research aims to conduct air quality biomonitoring using the standard grass species *Lolium multiflorum* in a mining region located in the city of Brumadinho, metropolitan region of Belo Horizonte, in the state of Minas Gerais, Brazil.

METHODS

Biomonitoring was actively conducted in March and April of 2024, with grass cultivation and exposure following the VDI 3957 - part 2 standard (2003) (adapted). The plants were cultivated for 3 weeks before exposure in a natural reserve selected as a reference site (S4) and exposed for 28 days at 3 sampling points in Brumadinho: S1 - City center, S2 - Tejuco neighborhood, surrounded by mining sites, S3 - an Indigenous community area near a ferry line used for mining ore transportation.

Plant growth was observed during the exposure period. Subsequently, they were manually cut and subjected to laboratory analyses to evaluate the presence of metals, following EPA 3050B (1996) (adapted). The plant material was submitted to wet-opened digestion with a HNO_3 and H_2O_2 solution (1:1), and the extracts will be analyzed by ICP-OES.

In addition to plant exposure, fine particulate matter (<2.5 micrometers in diameter; $PM_{2.5}$) were sampled using a medium-volume sampler (ARA Instrument) equipped with quartz filters. $PM_{2.5}$ sampling was carried out for 24 hours in the same locations of plant exposure, throughout the exposure period. Subsequently, the $PM_{2.5}$ concentration was determined by gravimetric method (INPE, 2012), and the concentration of metals using the aforementioned methodology. Results were submitted to statistical analysis by Kruskal-Wallis analysis of variance followed by Dunn's mean test.

FINDINGS AND ARGUMENT

The concentration of particulate matter $PM_{2.5}$ varied among the sampling sites, with a maximum of 43.77 µg/m³ in the Indigenous community area (S3) and a minimum of 16.23 µg/m³ in the reference area (S4). Figure 1 illustrates the variation found among the monitoring points in the city of Brumadinho and the comparison with air quality reference value of WHO (2021).

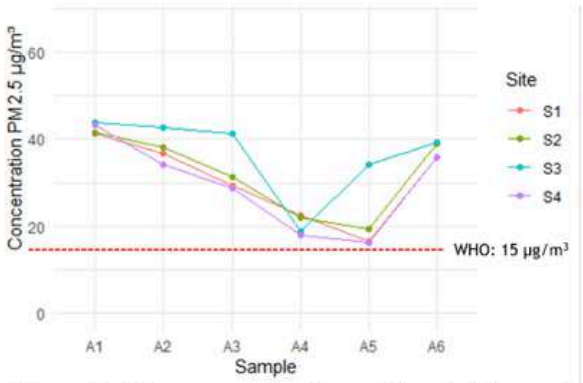


Figure 1. $PM_{2.5}$ concentrations detected in each of the monitoring points (S1- S4) in the city of Brumadinho compared with WHO air quality guidelines (2021) (15 µg/m³ in 24 hours).

All samples exceeded the WHO reference value for $PM_{2.5}$. This suggests poor air quality in the region, requiring more attention to monitoring and source control. Furthermore, it is important to highlight that PM concentrations are also associated with other factors, such as climatic conditions, and correlation studies with such factors should be performed.

S3 showed the highest median of 40.15 µg/m³ among the sampling points (Figure 2). The lowest median was at the reference point (S4) of 31.40 µg/m³. However, there was no significant differences according to the Kruskal-Wallis test ($p<0.05$).

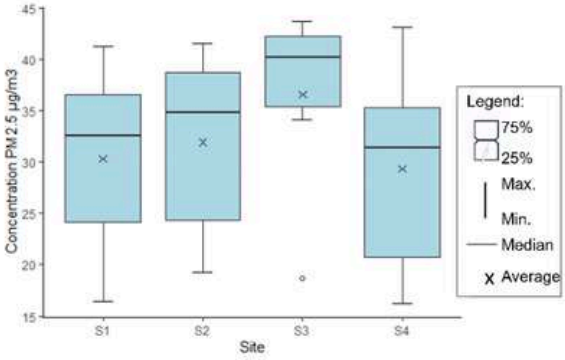


Figure 2. Boxplot of $PM_{2.5}$ concentration in each monitoring point.

Site 3 represents an Indigenous community area located near the ore loading and transportation area. Additionally, the region was affected by the tailings dam collapse on January 26th, 2019. So, it still suffers the consequences of tailings deposit in the region. Such factors may be associated with the resuspension of contaminated particulate matter. However, further studies should be conducted to test this hypothesis, such as studies involving soil sampling.

The preliminary qualitative analysis of plants (visual analysis) contributed to an initial understanding of the impacts of air pollution to bioindicators, as toxic components can cause biomass reduction, growth inhibition, and organism death (Ghosh; Dutta; Mukhopadhyay, 2023). Figure 3 demonstrates the state of plants exposed in each of the sampling sites after 28 days.



Figure 3. Plants after exposure in each of the sampling sites after 28 days, some are visually affected (injuries).

It can be observed that plants exposed in Points 1 and 2 exhibited more leaf injuries and are smaller than the other points. Borowiak *et al.* (2020) noted that the accumulation of trace elements presents in the atmosphere in ryegrass reduced the net photosynthesis rate and stomatal conductance of the plants.

Although S3 presented the highest PM concentrations, it is worth noting that the plants were exposed in a wooded area and toxic elements may have encountered barriers in taller plants compared to the sampler. Thus, the analysis of metals in ryegrass leaves will provide more elaborate data for understanding metal contamination at this and the other sampling sites.

CONCLUSIONS

Preliminary analyses demonstrate that particulate matter concentration may influence plant development, taking into consideration other processes such as land use in the surroundings. The high concentrations of particulate matter in the city of Brumadinho reflect air pollution in urban areas influenced by mining. Analyses of metals in plants leaves and quartz filters will be used to better discuss the relationships between atmospheric pollutant concentration and ecosystem health. Biomonitoring data along with chemical characterization will be of great significance in devising strategies for controlling and mitigating pollution.

ACKNOWLEDGMENTS

The authors would like to thank the FAPEMIG (Minas Gerais Research Funding Foundation) and CAPES program for funding the project.

REFERENCES

Arsenic, Aluminum Magnesium, et al. "Method 3050B acid digestion of sediments, sludges, and soils 1.0 scope and application." *Washington, DC, USA* (1996).

Borowiak, Klaudia, et al. "Accumulation of airborne toxic elements and photosynthetic performance of Lolium multiflorum L. leaves." *Processes* 8.9 (2020): 1013.

Nakazato, Ricardo Keiichi, et al. "Efficiency of biomonitoring methods applying tropical bioindicator plants for assessing the phytotoxicity of the air pollutants in SE, Brazil." *Environmental Science and Pollution Research* 25 (2018): 19323-19337.

De Temmerman, Ludwig, and Michel Hoenig. "Vegetable crops for biomonitoring lead and cadmium deposition." Journal of Atmospheric Chemistry 49 (2004): 121-135.

Ferreira, Tatiane Morais, Maria Cristina Forti, and Plinio Carlos Alvala. "Protocolo para coleta de material particulado atmosférico." *INPE, São José dos Campos* (2012).

Ghosh, Sayantan, Ratna Dutta, and Shritama Mukhopadhyay. "A Review on Seasonal Changes in Particulate Matter Accumulation by Plant Bioindicators: Effects on Leaf Traits." *Water, Air, & Soil Pollution* 234.8 (2023): 529.

Klumpp, Andreas. "European network for the assessment of air quality by the use of bioindicator plants. LIFE99 ENV/D/000453". University of Hohenheim. 2003.

Multisanti, Cristiana Roberta, et al. "Sentinel species selection for monitoring microplastic pollution: A review on one health approach." Ecological Indicators 145 (2022): 109587.

Theophilo, Carolina Yume Sawamura, et al. "Biomonitoring as a Nature-Based Solution to Assess Atmospheric Pollution and Impacts on Public Health." Bulletin of Environmental Contamination and Toxicology 107 (2021): 29-36.

VDI - Verein Deutscher Ingenieure. "Biological Measuring Techniques for the Determination and Evaluation of Effects of Air Pollutants on Plant (Bioindication). Method of Standardized Grass Exposure. VDI-Guideline 3957 Part 2. *Beuth Verlag, Berlin*, 2003.

WHO. "Air quality and health. Type of pollutants." *Available at: Air quality and health (who.int)*. Accessed on March 8, 2024.

WHO. "WHO global air quality guidelines." *Particulate Matter (PM2.5 and PM10), Ozone, Nitrogen Dioxide, Sulfur Dioxide and Carbon Monoxide* (2021).

AIR POLLUTION CONFERENCE BRAZIL
CMAS SOUTH AMERICA
COMMUNITY MODELING AND ANALYSIS SYSTEM

COMPARİSON OF THE EFFECTS OF URBAN AFFORESTATİON ON AİR QUALİTY İN TWO REGİONS OF A BRAZİLİAN CİTY

Priscila Boleta Gonçalves[1], Danilo Covaes Nogarotto[2], Vitor Eduardo Molina Junior[3], Felippe Benavente Canteras[4], Simone Andrea Pozza[5]
Universidade Estadual de Campinas
[1]*p148922@dac.unicamp.br*
[2]*danilocn@unicamp.br*
[3]*vemolina@unicamp.br*
[4]*canteras@unicamp.br*
[5]*spozza@unicamp.br*

Abstract: The urbanization process has caused a major change in land use and occupation, increasing impervious areas, and decreasing the afforestation of urban centers. This phenomenon has caused several environmental consequences, one of which is the negative impact related to air pollution. One of the computational tools that uses remote sensing to relate air quality to the quantity of local tree individuals is the i-Tree Canopy. This tool allows one to identify features in satellite imagery that define the land cover in each region. The objective of this research was to use this software to compare two urban regions (Taquaral and Downtown) within the same city, but with different forest cover characteristics, to verify the differences in environmental and economic benefits between them. Under this scenario, it was calculated with i-Tree Canopy that the Taquaral region removes 48% more Carbon, CO, NO_2, O_3, SO_2 and $PM_{2.5}$ and 55% more PM_{10} from the atmosphere annually than the Downtown region.The difference in the average pollutant concentrations obtained from the monitoring stations reinforces the importance of the afforestation, since the average PM_{10} last year (data from 10/01/2022 to 09/30/2023) in Downtown was 24.1 μm/m³ and in Taquaral in 19.0 μm/m³ (significant t-test, p-value < 0.0001). In view of the above, the environmental and socio-economic importance of urban reforestation and maintenance of parks and gardens in cities is clear. It is also concluded that the i-Tree Canopy, despite some limitations, is a good tool for the valuation of ecosystem services.

Keywords: Environmental monitoring, Atmospheric pollution, i-Tree Canopy, Campinas.

INTRODUCTION

Urbanization has led to a significant change in the pattern of land use and occupation, resulting in an increase in impervious surfaces and a decrease in urban wooded areas. This has led to several environmental impacts, including the negative effects associated with air pollution and, consequent damage to human health (Martelli and Delbim, 2022).

The i-Tree Canopy is a tool to classify land cover that uses remote sensing techniques to establish a relationship between the number of trees present in a given area and air quality (i-Tree, 2023). This tool is freely distributed and developed by the United States Department of Agriculture Forest Service (USDA). It uses the random sampling method and allows the identification of features in satellite images that define land cover in each region. Due to its ease of use and simple data collection, it is a tool widely used tool worldwide (Costemalle, Candido and Carvalho, 2023; Crosby, McConnell and Holderieath, 2020; Ghorbankhani, Zarrabi and Ghorbankhani,2023).

Therefore, the objective of this research was to use the i-Tree Canopy to compare two regions of Campinas in order to verify the differences in environmental and economic benefits between them.

METHODS

The study site is the city of Campinas (Figure 1), located in the state of São Paulo, with an area of 794,571 km² and current population of 1,139,047 inhabitants (2022 data) (IBGE, 2024). The city presents distinct characteristics of tree cover in its different regions, standing out among them Downtown, with densely urbanization, and Taquaral, notable for the presence of an extensive urban park, highlighting contrasts in terms of vegetation and urban environment. Urbanization has led to a significant change in the pattern of land use and occupation, resulting in an increase in impervious surfaces and a decrease in urban wooded areas and overall tree cover.



Figure 1. Campinas location map

The i-Tree website recommends that between 500 and 1000 points be marked in each area, in order to increase the reliability of the data generated (i-Tree, 2023). Therefore, to estimate land cover with i-Tree Canopy, 750 points were marked in each of the sites, within a 1 km radius of the monitoring stations. The points were classified into the following categories: Grass/Herbaceous (H), Impervious Buildings (IB), Impervious Other (IO), Impervious Road (IR), Soil/Bare Ground (S), Tree/Shrub (T), and Water (W). The proportions test was used to compare the two sites (Downtown and Taquaral) in each category.

Taquaral and Downtown have automatic monitoring stations of the São Paulo Environmental Company (CETESB). The data from these stations are made available through QUALAR System, which has the history and also real-time data on various parameters (QUALAR, 2024). In this way, it is possible to make comparisons between i-Tree results and station data. The t-test was used to compare the mean concentrations of the two sites with each other.

FINDINGS AND ARGUMENT

Figure 2 shows the geographical distribution of the points classified in the i-Tree Canopy within the area delimited for Taquaral and the Downtown. The figure shows that Taquaral has a larger area covered by green points that are Trees/Shrubs, when compared to the Downtown.

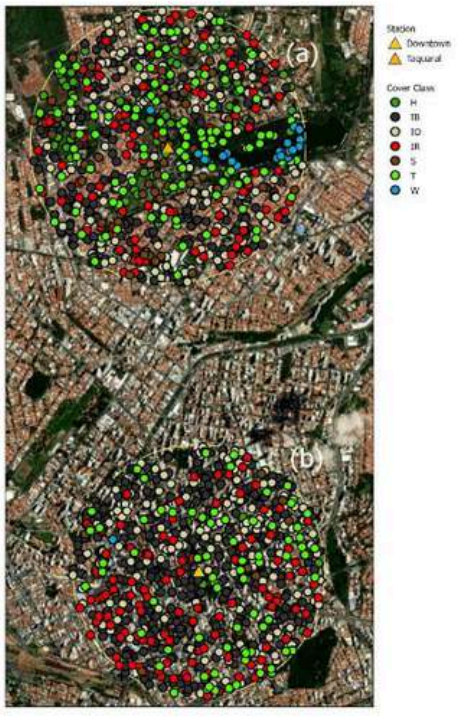


Figure 2. Distribution of points according to land cover in Taquaral (a) and Downtown (b) stations.

Figure 3 show the percentage of land cover for each of the classifications in each of the locations. It can be seen that for the Downtown most of the area is covered by Impervious Buildings (48.4%), followed by Impervious Other (22%) and Impervious Road (15.5%). Most of the Taquaral region is also covered by Impervious Buildings, but with a much smaller percentage (29.7%), followed by Impervious Other (20.3%) and Tree/Shrub (16.9%). The p-value of the proportion test is shown in Table 1. The proportion of category IB was significantly higher in Downtown than in Taquaral, while categories H, S, T and W were significantly higher in Taquaral (Table 1).

Table 1. p-value for each land cover category

Land Cover Categories	p-value
H	<0.0001
IB	<0.0001
IO	0.2861
IR	0.2098
S	<0.0001
T	0.0002
W	<0.0001

In the other words, it should be noted that the impervious area of the Downtown is much larger and that Taquaral has a larger cover tree area. Under this scenario, it was calculated with i-Tree Canopy that the Taquaral region removes 48% more Carbon, CO, NO_2, O_3, SO_2 and $PM_{2.5}$ and 55% more PM_{10} from the atmosphere annually than the Downtown region.

In monetary terms, Taquaral Station has 48% lower costs for carbon emissions, 40% lower for CO, 56% lower for NO_2, 48% llower for O_3, 50% lower for SO_2 and, 48% lower for $PM_{2.5}$ and PM_{10} than the Downtown Station.

The difference in the average pollutant concentrations obtained from the monitoring stations reinforce the importance of preservation, planning, and expansion of urban tree cover (afforestarion and wooded areas). Table 2 shows the monthly and annual averages of PM_{10} in the period between 10/01/2022 and 09/30/2023. It can be seen that the average for all months is higher in the center region (Downtown) than in park region (Taquaral), with the exception of April 2023. This phenomenon can be explained by the large amount of missing hourly data for that month in the Downtown station. The annual average in the Downtown was 23 $\mu m/m^3$ and in Taquaral it was 19 $\mu m/m^3$ (significant t-test, p-value < 0.0001).

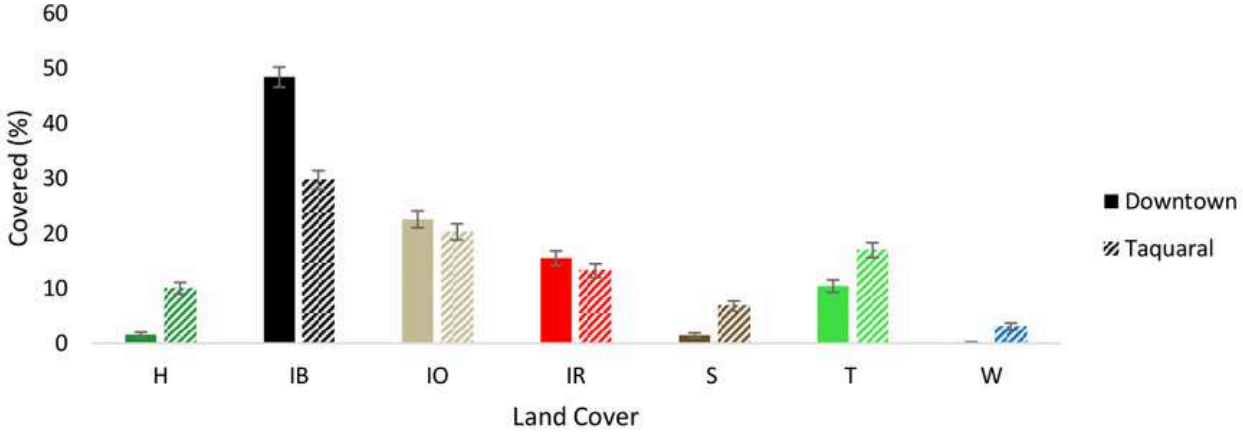


Figure 3. Land Cover Classification using i-Tree Canopy

Table 2. Monthly and annual averages of PM_{10} ($\mu m/m^3$) in Taquaral and Downtown

Year	Month	PM_{10} ($\mu m/m^3$)	
		Taquaral	Downtown
2022	October	19	23
	November	15	19
	December	-	18
2023	January	12	18
	February	11	18
	March	16	17
	April	15	14
	May	21	25
	June	22	26
	July	-	29
	August	31	35
	September	26	29
Mean		**19**	**23**

- Missing data

CONCLUSIONS

It is also concluded that the i-Tree Canopy, despite some limitations, is a good tool for the valuation of ecosystem services. Considering its free access and ease of use, it can be used by public authorities as a tool for initial analysis in urban areas, supporting decision making and the development of more detailed specific studies that can guide urban planning, mainly related to the maintenance and expansion of green spaces. It also highlights the importance of increasing the number of air quality monitoring stations is pointed out, since if they are located in different areas of the same city, they can reveal different realities depending on their surroundings.

ACKNOWLEDGMENTS

This study was financed in part by the Coordenação de Aperfeiçoamento de Pessoal de Nível Superior – Brasil (CAPES) – Finance Code 001. The authors thank the CETESB for providing access to the QUALAR database.

REFERENCES

Costemalle, Valéria B.; Candido, Helder M. N.; Carvalho, Fabrício A. "An estimation of ecosystem services provided by urban and peri-urban forests: a case study in Juiz de Fora, Brazil". Ciência Rural 53:4 (2023). Accessed February 10, 2024. https://doi.org/10.1590/0103-8478cr20210208.

Crosby, M. K.; McConnell, T. E.; Holderieath, J. J. "Forest canopy benefits in small urban areas of Louisiana." Mathematical and Computational Forestry & Natural-Resource Sciences 12:2 (2020): 79-91. ISSN 1946-7664.

Ghorbankhani, Zahra; Zarrabi, Mohamad M.; Ghorbankhani, Melika. "The significance and benefits of green infrastructures using I-Tree canopy software with a sustainable approach". Environment, Development and Sustainability. (2023) https://doi.org/10.1007/s10668-023-03226-9

IBGE. "Cidades e Estados". https://www.ibge.gov.br/cidades-e-estados/sp/campinas.html. Acessed February 14, 2024.

i-Tree. A tree canopy assessment tool. https://canopy.itreetools.org/. Acessed November 16, 2023.

Martelli, Anderson; Delbim, Lucas. "Arborização favorece redução de doenças cardiovasculares em moradores dos centros urbanos." PhD Scientific Review 2:9 (2022): 22-35.

QUALAR. Qualidade do ar. https://cetesb.sp.gov.br/ar/qualar/. Acessed 16 February, 2024.

SESSION 12
Policy and regulatory frameworks for air pollution control

Air pollution poses significant challenges to public health, the environment, and overall quality of life. To address these concerns, governments around the world have developed policy and regulatory frameworks aimed at controlling and reducing air pollution. These frameworks are essential in guiding actions to mitigate the adverse effects of air pollution and ensure cleaner, healthier air for present and future generations. Some components are key to control air pollution: emissions standards, monitoring and data collection, air quality standards, technology and innovation, public awareness and finally Equity and Environmental Justice.

In recent years, there has been a growing recognition of the urgent need to combat air pollution and its associated health and environmental consequences. Consequently, many countries are strengthening their policy and regulatory frameworks to achieve cleaner and healthier air for their citizens.

The effectiveness of these frameworks ultimately depends on their enforcement, public support, and the commitment of governments and industries to prioritize air quality. By implementing comprehensive and forward-thinking policies, societies can reduce the impact of air pollution and create a more sustainable and healthy future.

SESSÃO 12

SPATIAL AND TEMPORAL MAPPING OF TRANSPORT EMISSIONS AND APPLICATION OF AIR QUALITY MODELS USING LOW-COST SENSORS DATA 355

STRATEGIC PLANNING IN DATA MANAGEMENT FOR INVENTORYING STATIONARY SOURCES IN THE STATE OF SÃO PAULO 358

TECHNİCAL CHALLENGES OF NEW REGULATORY SCHEMES TO İMPROVE AİR QUALİTY - A CASE STUDY OF LOW EMİSSİON ZONES İN BOGOTA COLOMBİA 362

REAL WORLD LABORATORİES AND THE SOCİAL CONTROL OF AİR POLLUTİON 365

TRENDS AND CHALLENGES FOR AIR QUALITY RESEARCH IN LATIN AMERICA 368

AIR POLLUTION CONFERENCE BRAZIL
CMAS SOUTH AMERICA
COMMUNITY MODELING AND ANALYSIS SYSTEM

SPATIAL AND TEMPORAL MAPPING OF TRANSPORT EMISSIONS AND APPLICATION OF AIR QUALITY MODELS USING LOW-COST SENSORS DATA

Janini Oliveira Dias da Silva[1], Pedro José Perez Martinez[2], Regina Maura de Miranda[3]
[1]PhD Student, FECFAU UNICAMP
E-mail j263548@dac.unicamp.br
[2]Professor, FECFAU UNICAMP
E-mail pjperez@unicamp.br
[3]Professor EACH USP
E-mail remaura@usp.br

Abstract: The transport sector is known for being one of the biggest contributors to greenhouse gas (GHG) emissions and other atmospheric pollutants. In this sense, research and mitigation policies have been developed to minimize the effects of climate change and to meet the sector's decarbonization targets. However, Brazil still doesn't have a well-developed air quality monitoring system with a wide territorial reach. In São Paulo State, most of the stations in the air quality network of the Environmental Company of the State of São Paulo are concentrated in the São Paulo Metropolitan Region. Therefore, to fill this gap, this research proposes a mapping of transportation flows and emissions on the main highways of the Campinas Metropolitan Region of Campinas (São Paulo State, Brazil) using low-cost sensors. The sensors map atmospheric emissions of greenhouse gases (GHGs) and toxic air pollutants (APs) related mainly to traffic emissions. This data collection method will be associated with socioeconomic data and aligned with the main policies of the Integrated Urban Development Plan of the region. In this way, it will be possible to present a temporal and spatial analysis aimed at contributing to sustainable urban mobility planning and the development of mitigation policies related to the transportation sector.

Keywords: transport emissions, low-cost sensors, spatial and temporal mapping.

INTRODUCTION

The air quality in Brazilian metropolises has become one of the main concerns in discussions about climate change. Controlling atmospheric pollution is one of the greatest urban environmental challenges, directly impacting the health and quality of life of the population (OMS, 2022).

The transportation sector is the largest contributor to greenhouse gas emissions (GHG) and other atmospheric pollutants (AP)(BEN, 2023). Particulate Matter (PM) is one of the main pollutants emitted by vehicles and is capable of causing cardiovascular, cerebrovascular, and respiratory diseases (OMS, 2022).

With Brazil's economic growth over the past decades, the vehicle fleet and, parallel to it, the consumption of fossil fuels have significantly increased, directly affecting air pollution levels and urban quality of life (CETESB, 2023; SIMS et al., 2014).

In addition to the degradation of air quality, the expansion of motorized vehicle fleets has introduced further adverse effects on urban living standards, including traffic accidents, congestion, longer commuting times, urban sprawl, and social inequality concerns (CARVALHO, 2016; KAHN RIBEIRO, S., 2007).

In the State of São Paulo, the Environmental Company of the State of São Paulo (CETESB) operates air quality monitoring networks that assess atmospheric pollution levels across various scales since 1970. However, due to the high cost of equipment, most of this network is located only in the São Paulo Metropolitan Region (Figure 1).



Figure 1. Location of air quality stations from CETESB in the State of São Paulo. Source: CETESB, 2024.

The Metropolitan Region of Campinas (MRC) is the second largest in the State of São Paulo, covering 20 municipalities and with an estimated population of 3.2 million inhabitants (IBGE, 2022). It accounts for approximately 9% of the state GDP and 3% of the Brazilian GDP and is one of the most important hubs for research and technological development in the country (SÃO PAULO, 2018).

The total vehicle fleet in the MRC is approximately 2.3 million vehicles, with 79% comprised of cars and motorcycles. When compared to the estimated population, the region has a rate of 1.3 persons per vehicle (DENATRAN, 2020).

The MRC is one of the most urbanized regions in the country and has high rates of daily commuting trips. According to the Origin-Destination Survey, approximately 4.7 million trips occur in the MRC daily, with 60.2% (2.07 million) of these trips by individual modes, 39.8% (1.3 million) by collective modes, and 27.6% (1.2 million) by non-motorized modes (SÃO PAULO, 2012).
Currently, there are only six air quality monitoring stations operated by CETESB in the MRC, three in Campinas, two in Paulínia, and one in Americana (Figure 2).

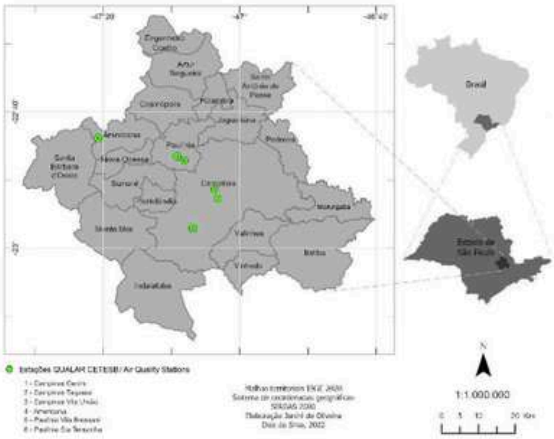


Figure 2. Location of air quality stations from CETESB in MRC. Source: CETESB, 2024.

In this context, policies aimed at controlling vehicle emissions, combined with urban planning and mobility policies, tend to be an excellent alternative for mitigating pollutant emissions, as well as improving safety, health, and the well-being of the population.
However, for the design of appropriate public policies, it is necessary for the databases to be reliable, standardized, and up-to-date, as they are essential for the development of appropriate analyses. This has been the main barrier that authors have encountered in developing methodologies using urban mobility and air quality data (OMS, 2022; PACHECO et al., 2017).
Thus, to address this gap, this research proposes mapping the flows and emissions of transportation on the main highways of the MRC, using low-cost sensors (NOTS) (Figure 3), it will be possible to present an analysis of sustainability indicators aimed at contributing to regional urban mobility planning and the development of transport-related public policies.
In this context, a temporal and spatial mapping of transportation flows and pollutant emissions on the main road axes of the MRC will be achieved, with the aim of developing an air quality model associated with land use, socioeconomic variables, and urban mobility dynamics in the MRC.

METHODS

The NOTS sensors, developed in partnership with UNICAMP, USP, and the University of Surrey (UK) (Fapesp grants 2018/10714-4 and 2022/04619-4), allow atmospheric monitoring of CO2, CO, NO2, NO, and O3 concentrations, particulate matter (PM) in the PM1, PM2.5, and PM10 fractions, temperature, and relative humidity.
To achieve the goals outlined in this project, georeferenced socioeconomic data from the OD Survey, IBGE Senso, and the Center for Metropolitan Studies (CEM) will be utilized. For vehicle volume data will be gathered from road concessionaires, radar systems and São Paulo State Highway Department (DER). CETESB's monitoring networks and NOTS sensors and will be employed for traffic emissions data along the MRC's seven main roads (Figure 3).

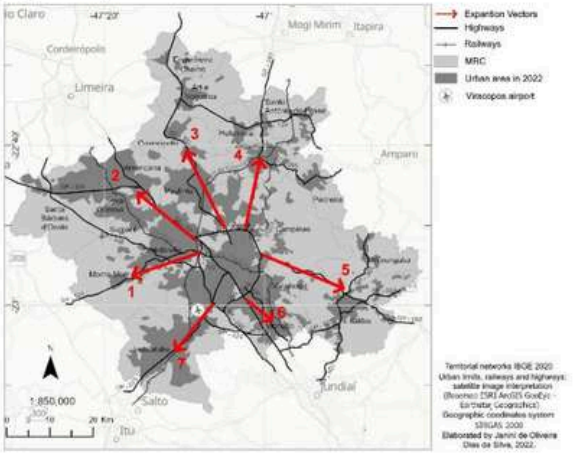


Figure 3. Main expantion axes in MRC.

These datasets will be incorporated into a regional land use model alongside land use and land cover data, enabling a temporal and spatial analysis to identify critical areas for air quality. This analysis aims to inform regional urban mobility planning and the formulation of mitigation policies pertaining to transportation and the environment.
The emissions model will undergo validation through the utilization of low-cost sensors, collecting data along routes on the primary highways connecting the municipalities of the MRC over a two-year period.
This methodology will integrate with socioeconomic data and aligned with the main policies of the Integrated Urban Development Plan (PDUI) of the region.

EXPECTED RESULTS

The project is currently in the phase of structuring the methodologies that will be employed. The first data collection phase is scheduled for July 2024. It is expected that the analyses conducted in this research will identify critical areas of pollutant

emissions along the main road axes of the MRC, enabling the development of policies for urban mobility planning, regional integration, and reduction of emissions from the transportation sector.

From the data collection and calculation of descriptive measures of the selected variables, it will be possible to visualize spatial distributions in tables and maps. These initial results will be useful for obtaining an overview of the variables, allowing the visualization of the most critical areas in the MRC. These maps will indicate the different relationships and behaviours of the variables in the region.

Based on this analysis, a mathematical model capable of indicating the main variables that influence the region's mobility will be adjusted. This model will estimate and quantify the influence of these variables in the region, as well as determine trends. Thus, it is possible to analyse the main indicators determining the situation of sustainable urban mobility and the air quality in the MRC.

Based on these results, it is expected that this research will contribute to identifying the current situation, forecasting scenarios, and producing inputs capable of assisting in the development of public policies aimed at improving sustainable urban mobility on a regional scale and mitigating pollutants.

REFERENCES

Balanço Energético Nacional 2023. Disponível em: <https://www.epe.gov.br/pt/publicacoes-dados-abertos/publicacoes/balanco-energetico-nacional-2023>. Acesso em: 6 abr. 2024.

CARVALHO, C. H. R. DE. Desafios da mobilidade urbana no Brasil. **IPEA**, 2016.

CETESB. **Emissões veiculares no estado de São Paulo 2022**. São Paulo, SP: Cetesb, 2023.

DENATRAN. **Frota de Veículos - 2020**. Disponível em: <https://www.gov.br/transportes/pt-br/assuntos/transito/conteudo-Senatran/frota-de-veiculos-2020>. Acesso em: 2 maio. 2024.

IBGE. **Panorama do Censo 2022**. Disponível em: <https://censo2022.ibge.gov.br/panorama/>. Acesso em: 2 maio. 2024.

KAHN RIBEIRO, S. **Transport and its infrastructure. In Climate Change 2007: Mitigation.** Disponível em: <https://www.researchgate.net/publication/235360467_Transport_and_its_infrastructure>. Acesso em: 1 maio. 2024.

OMS. **Novos dados da OMS revelam que bilhões de pessoas ainda respiram ar insalubre - OPAS/OMS | Organização Pan-Americana da Saúde**. Disponível em: <https://www.paho.org/pt/noticias/4-4-2022-novos-dados-da-oms-revelam-que-bilhoes-pessoas-ainda-respiram-ar-insalubre>. Acesso em: 1 maio. 2024.

PACHECO, M. T. et al. A review of emissions and concentrations of particulate matter in the three major metropolitan areas of Brazil. **Journal of Transport & Health**, v. 4, p. 53–72, 1 mar. 2017.

SÃO PAULO. **Pesquisa de Origem e Destino da Região Metropolitana de Campinas**. , 2012. Disponível em: <https://www.mobilize.org.br/midias/pesquisas/pesquisa-origem-e-destino-2011---regiao-metropolit.pdf>

SÃO PAULO. **PDUI-RMC (Região Metropolitana de Campinas) - Plano de Desenvolvimento Urbano Integrado**. Disponível em: <https://rmc.pdui.sp.gov.br/wp-content/uploads/RELATORIO-3-%E2%80%93-Diagnostico-Final-dos-Problemas-Metropolitanos.pdf>. Acesso em: 20 set. 2023.

SIMS, R. et al. Transport. In: Climate Change 2014: Mitigation of Climate Change. Contribution of Working Group III to the Fifth Assessment Report of the Intergovernmental Panel on Climate Change.

AIR POLLUTION CONFERENCE BRAZIL
CMAS SOUTH AMERICA
COMMUNITY MODELING AND ANALYSIS SYSTEM

Strategic planning in data management for inventorying stationary sources in the state of São Paulo

Tailine Corrêa dos Santos[1,2], Iara da Silva[1], Leila Droprinchinski Martins[3], Edmilson Dias de Freitas[1]
[1]*Institute of Astronomy, Geophysics and Atmospheric Sciences/University of São Paulo - IAG/USP, São Paulo - SP, Brazil*
iaradasilva@usp.br; edmilson.freitas@iag.usp.br
[2]*Superintendency of Environmental Management/University of São Paulo - SGA/USP, São Paulo - SP, Brazil*
tailine.santos@usp.br
[3]*Federal University of Technology - Paraná/UTFRP, Londrina - PR, Brazil*
leilamartins@utfpr.edu.br

Abstract: **Introduction:** The first challenge of diagnosing and managing air quality is to understand, quantify and identify the contribution of sources, as well as the main pollutants associated with them. This survey becomes even more complex in regions with a wide diversity of sources, such as large urban and industrial centers. This identification is extremely important for formulating data-based actions to control and reduce the impact on human health, natural ecosystems, and climate change. In 2013, the state of São Paulo changed its regulations, which implemented intermediate targets to achieve the final target recommended by the World Health Organization (2005), such as a threshold. In 2021, the air quality standard in the state became the second, more restrictive, intermediate target. To achieve these goals, it is important to plan and develop control strategies, mainly associated with reducing the sources of pollutant emissions and precursors. To promote discussions and solutions related to air quality in the state of São Paulo, this project focused on the challenges of surveying pollutant emission factors and inventories. Inventories are important environmental management tools that allow us to identify significant sources of atmospheric pollutants, provide a basis for decision-making, formulate control strategies, and are essential for projections of climate and air quality scenarios.
Objective: In this context, the objective of this project was to create a strategic plan for managing data, provided by the industries listed in the Stationary Source Emissions Reduction Plan (PREFE), to organize and automate the construction of a state inventory, to prepare a diagnosis of the sources pollutant emissions in the state of São Paulo.
Method: This work has been carried out in partnership with state environmental agencies, CETESB (Environmental Company of the State of São Paulo). Important parts of this project have been developed by this collaboration, where we are working, mainly, in the monitoring and analysis of CETESB Board Decisions (no. 118/2021/I/C and 119/2021/ I/C) associated with PREFE. Therefore, we point out here discussions and solutions related to air quality in the control regions listed in PREFE, as well as the main challenges encountered for planning in this context. To manage the information received by industries, the fundamental stages of compilation, analysis, validation and visualization of emission data from fixed sources were outlined, aiming to formulate strategic planning that can be applied in other locations in Brazil to build an inventory. The construction of definitions and description of procedures associated with fundamental steps begins from planning data capture to their visualization. This process was listed in cyclical schemes, as this data is reviewed and, in many cases, requires updates and corrections by industries.
Findings: Within the air quality theme regarding emission inventories, the scope and strategies have directed towards the generation of applicable products, such as interactive analysis dashboards and methodological strategies for the emission inventories of industries listed in PREFE. These products have worked to improve the analysis and inspection of emission inventories delivered by industries, being tools for agility and reliability in complying with Board Decisions for the effectiveness of PREFE. The compilation of this data has generated effective actions in the reduction plan. Furthermore, these compiled, checked data, sectorized by category of industrial activity and type of sources, are strategies that have allowed, in addition to reduction actions, the development of local scientific studies with real data. Of these, the identification of the main sources by type of pollutants emitted stands out, such as large tanks emitting hydrocarbons, as well as the main activities, where emphasis was placed on the refinery. Data management and inventory has impacted several aspects and generated effectiveness in the administrative, political and scientific process. Planning has allowed the inclusion of different actors, managers and skills in the applicability and effectiveness of the control policy. And from this new inventory generated with industrial data, it is expected to have a better basis for environmental research, formulation of mitigation and emission reduction strategies, as well as subsidies for decision-making and regulatory guidance.

Keywords: Emissions Inventory, São Paulo State, Pollution Control Plan, Information management

INTRODUCTION

To promote discussions and solutions related to air quality in the state of São Paulo-SP, Brazil, this project focused on the challenges of surveying pollutant emission factors and inventories. Inventories are important environmental management tools that allow us to identify significant sources of atmospheric pollutants, provide a basis for decision-making, formulate control strategies and are essential for projections of climate and air quality scenarios (EPA, 2022). Air quality is directly related to quality of life, with air pollution being the greatest environmental risk to health (COHEN et al., 2017; LELIEVELD et al., 2020). In 2013, the state of SP changed its regulations to include PM2.5 in its air quality standards and also changed the reference values for other pollutants. Intermediate goals were implemented to reach the final goal recommended by WHO (2005), as the threshold of no or minor health effects (SÃO PAULO, 2013). In 2021, the air quality standard in the state becomed the second intermediate target, more restrictive (CETESB, 2021). And to achieve these targets, planning and developing control strategies are important, mainly associated with the reduction of air pollutants emission and its precursors in sources. In this context, the objective of this project was to create a strategic plan for managing data to organize and automate the construction of a state inventory, and prepare a diagnosis of the pollutant emissions sources in the state of São Paulo. We point out in this discussion ,solutions related to the inventory of industrial sources in the state of São Paulo, as well as the main challenges encountered in planning.

METHODS

The project is being developed in partnership with CETESB by agreement signed for 2 years to work on inventory analyses, information validation and on the effectiveness of improvements in public policies. The work has been done by acting on the Stationary Source Emissions Reduction Plan (PREFE 2021) fixed source (industrial) inventories, with the monitoring of associated board decisions (DD).

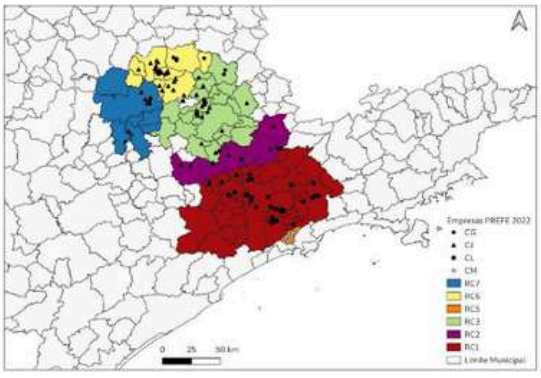


Figure 1. Control Regions and Industries PREFE 2021

The DD 118 (BOARD DECISION No. 118/2021/I/C) (CETESB, 2021b), referring to companies listed in the control regions that are in the condition of not meeting intermediate target 2 (MI2) (Figure 1). This decision already had its first phase in 2014, in PREFE 2014. Incorporated in this second phase of 2021 is DD 119 (BOARD DECISION No. 119/2021/I/C - CETESB, 2021c), referring to the "Plan Sector for Controlling Emissions of Volatile and Semi-Volatile Organic Compounds from Fuel Storage, Distribution and Wholesale Trade Units".

FINDINGS AND ARGUMENT

Due to the constant and cyclical nature of PREFE inventories, the information formulation and construction process was developed based on cyclical planning with 4 main stages, as shown in the diagram in figure 2:



Figure 2. Strategic diagram of the steps involved in the inventory - PREFE 2021

Inventory consists of collecting and receiving data. This begins as soon as the industries called in each of the six control regions send their emissions inventories to CETESB. After receiving these forms with information relating to each company provided to CETESB, the forms are compiled and tabulated in a spreadsheet format for data analysis.

Verification, which involves manipulating spreadsheets and data analysis. At this stage, interactive dashboards were built with pivot tables, figures and filters in excel and power BI, to facilitate data visualization. Visual automation tools were used to speed up and support the monitoring of initial and updated information received throughout the process. These interactive areas made it possible to visualize a scale from macro to micro, that is, from the general scenario of the data received grouped by centers of control regions or agencies, to a detailed individual condition of each industry.

Validation, considered as a third step, uses these visualization tools to make detailed summaries and analyzes of the data, mainly associated with data that presented discrepancies. To this end, internal documents were also collected for verification and comparison with information already provided to CETESB in other processes related to the industry, such as licensing, environmental impact studies,

dispersion studies, etc. Another check was carried out with calculation spreadsheets for methodological conferences.

At this stage, divergences were raised in the information provided by the companies that were nominated for corrections. It is worth noting that the CETESB/USP team did not change any data presented, and in the case of corrections being necessary, they were opened communicate, an administrative instrument for the request of information within CETESB's administrative folder, so that the respective department could make corrections within a given period and forward it back to CETESB.

Audit, phase in which meetings were held with the entire CETESB team involved, including representatives of environmental agencies and respective departments, as well as assistants from the Environmental Control and Licensing Directorate to check the information collected. Environmental agencies received information to monitor and verify companies related to their area of coverage. In case of non-fulfillment of requirements or inconsistencies in the information provided, companies were notified. This process is associated with the communications sent to companies for corrections, and in some specific cases the on-site inspection.

Although the steps followed a sequence, the methodology used to process the data consisted of a circular and constant updating process. Thus, all the steps used were monitored throughout the period from the beginning of the data transmission to the present day, and many of the activities described were repeated with each update.

Here we present two products produced within these steps:

Automated Form for completing DD 119 inventories: The automated form for industries to complete DD 119 inventories related to the fuel base was designed (Figure 3). In this process, the selection of essential information and the best efficiency in collecting information were worked on in order to minimize errors at this stage. The user's guide was provided along with the form.



Figure 3. Electronic form created to collect the information provided for in DD 119, delivered to CETESB. Available online on the PREFE page: <https://cetesb.sp.gov.br/ar/plano-de-reducao-de-emissao-de-fontes-estacionarias-prefe/> (CETESB, 2024)

Dashboards of DD 118 inventories: Dashboards of DD 118 inventories: Developed interactive analyses ("dashboard") of the general and detailed PREFE 2021 inventories for each control region. This also includes a comparison with PREFE 2014 of the companies listed in DD 118. These analyses were presented at board meetings and made available to decision makers to accelerate the review and intervention of environmental control policies in the inventoried industries. Figure 1 illustrates the product created.

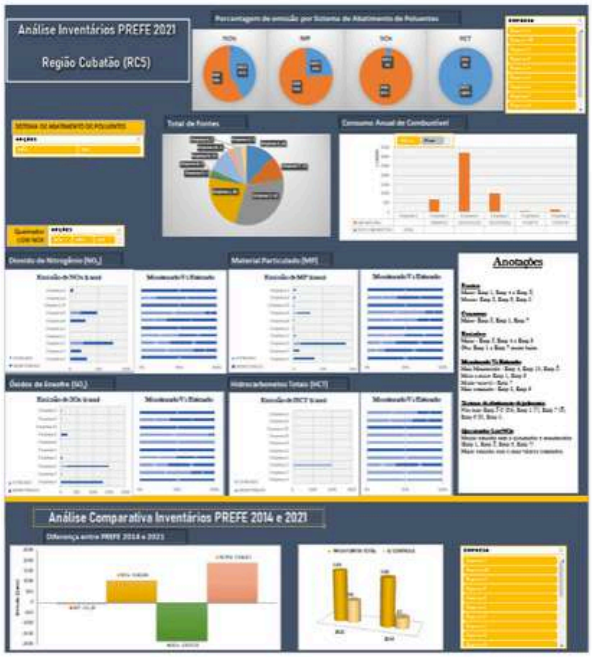


Figure 4. Interactive Dashboard for decision-making within the PREFE 2021 for the Cubatão region (RC5).

CONCLUSIONS

The strategies and products developed in the field of air quality in relation to emission inventories have allowed a direction towards the generation of applicable and modifiable products. The survey of inventories, whether at PREFE or as part of another public policy, is a cyclical and constant process, which requires automation tools that speed up and reduce errors. Thus, as strategic planning that involves everything from data selection to methodology during the process of structuring this information. These products have worked to improve the analysis and inspection of emission inventories, being tools for agility and reliability that allow greater effectiveness in complying with Board Decisions. This allows for agile and effective data-based decision making.

Acknowledgment

We would like to thank Companhia Ambiental do Estado de São Paulo - CETESB, for the work in partnership, for the experience and technical support regarding the content present in this chapter. To the USP Sustainability Program of the

Environmental Management Superintendency (SGA) for financial support. To the Institute of Astronomy, Geophysics and Atmospheric Sciences for academic support.

REFERENCES

CETESB - Environmental Company of the State of São Paulo. BOARD DECISION No. 289/2014/p, October 8, 2014. Provides for the approval of the "Stationary Source Emission Reduction Plan - PREFE 2014", prepared in compliance with State Decree No. 59,113, of April 23, 2013 . São Paulo, Brazil, 2014. Available at: <https://cetesb.sp.gov.br/decisoes-de-direitoia/>

CETESB - Environmental Company of the State of São Paulo. Technical study to evaluate and propose a deadline for the entry into force of the Intermediate Target stage 2 (MI2) in accordance with Article 8 of State Decree no. 59,113/2013. Updated in May 2021. São Paulo, 2021b. Available at: <https://cetesb.sp.gov.br/ar/wp-content/uploads/sites/28/2021/12/Estudo-Tecnico-para-viabilizar-a-Etapa-MI2-.pdf>.

CETESB - Environmental Company of the State of São Paulo. BOARD DECISION No. 118/2021/I/C, of November 26, 2021. Provides for the approval of the "Stationary Source Emission Reduction Plan - PREFE 2021". São Paulo, 2021b. Available at: <https://cetesb.sp.gov.br/decisoes-de-directia/>

CETESB - Environmental Company of the State of São Paulo. BOARD DECISION No. 119/2021/I/C, of November 26, 2021. Provides for the Sectoral Plan for Emission Control of Volatile and Semi-Volatile Organic Compounds from Fuel Storage, Distribution and Wholesale Trade Units. São Paulo, 2021c. Available at: <https://cetesb.sp.gov.br/decisoes-de-directia/>

CETESB - Environmental Company of the State of São Paulo. BOARD DECISION No. 120/2021/I/C, of November 26, 2021. Provides for the expansion of the coverage area of the Stationary Source Emission Reduction Plan - Ceramic Flooring and Clay Mining Industries Sector. São Paulo, 2021d. Available at: <https://cetesb.sp.gov.br/decisoes-de-directia/>

CETESB - Environmental Company of the State of São Paulo. Air Quality. Emission Reduction Plan from Stationary Sources - PREFE 2024. Available at: <https://cetesb.sp.gov.br/ar/plano-de-reducao-de-emissao-de-fontes-estacionarias- prefer/>. Accessed on: May 1st. 2024.

COHEN, A. J. et al. Estimates and 25-year trends of the global burden of disease attributable to ambient air pollution: an analysis of data from the Global Burden of Diseases Study 2015. The Lancet, v. 389, n. 10082, p. 1907–1918, 2017. DOI: /10.1016/S0140-6736(17)30505-6

LELIEVELD, J. et al. Loss of life expectancy from air pollution compared to other risk factors: A worldwide perspective. Cardiovascular Research, v. 116, n. 11, p. 1910–1917, 2020. DOI: /10.1093/cvr/cvaa025

SÃO PAULO, E. DECRETO Nº 59.113, DE 23 DE ABRIL DE 2013. Estabelece novos padrões de qualidade do ar e dá providências correlatas. Assembleia Legislativa de São Paulo (ALESP). PODER Executivo. Diário Oficial. São Paulo, Brasil, 2013. Disponível em: <https://www.al.sp.gov.br/repositorio/legislacao/decreto/2013/decreto-59113-23.04.2013.html>

WHO - World Health Organization. Air quality guidelines: global update 2005 - Particulate matter, ozone, nitrogen dioxide, and sulfur dioxide. ISBN 92 890 2192 6. 496 p. Europe, 2005. Disponível em: <https://www.who.int/publications/i/item/WHO-SDE-PHE-OEH-06.02>

EPA- U.S. Environmental Protection Agency. Managing Air Quality - Emissions Inventories. Last updated on december 21, 2022. Disponível em: <https://www.epa.gov/air-quality-management-process/managing-air-quality-emissions-inventories>. Acesso em: 20 jun. 2023.

AIR POLLUTION CONFERENCE BRAZIL
CMAS SOUTH AMERICA
COMMUNITY MODELING AND ANALYSIS SYSTEM

TECHNİCAL CHALLENGES OF NEW REGULATORY SCHEMES TO İMPROVE AİR QUALİTY - A CASE STUDY OF LOW EMİSSİON ZONES İN BOGOTA COLOMBİA

Mónica Espinosa[1], Juliana Hernández[2], Luis Morales[3], Juan Felipe Franco[4]

[1]*Hill Consulting*
mespinosa@hill.com.co
[2]*Scientific Level Consultant Association*
juliana.hernandez@slcaconsultores.com
[4]*Scientific Level Consultant Association*
luamoralesri@gmail.com
[4]*Hill Consulting*
jfranco@hill.com.co

Abstract: In 2023, Bogotá created a new regulatory scheme for air quality management called Urban Zones for Better Air Quality (ZUMA).This program aims to manage air quality in small urban areas, striving to meet air quality standards while achieving other sustainability goals for the community. These goals, among others, include reducing exposure to air pollution, lowering greenhouse gas emissions and promoting a more inclusive and equal community.

This research paper explores the primary challenges faced by technical evaluation processes when conducting multi-criteria analysis and cost-benefit analysis for air pollution control strategies for small urban areas. The definition of a new regulatory scheme has resulted in various technical barriers including: 1. Technical features of the existing data to monitor and evaluate the impacts of specific interventions in small regulatory areas. 2. The selection of air quality models that can represent the effects at a small scale while dealing with new data requirements. 3.The methodology to monitor air quality. 4. Evaluating and interpreting health impacts assessment at such a small scale and estimating their economic benefits. 5. Incorporating equity and inclusion criteria in the technical assessment of the ex-ante evaluation of the actions to be implemented; among others. The research paper discusses the technical features of the programs that must align with the new regulatory framework to enhance air quality at the community level. The analysis is based on what was conducted during the definition of the First ZUMA in Bogotá.

The assessment of the first ZUMA in Bogotá revealed that traditional methods of data collection and analysis at the city level are inadequate for exploring small urban areas. New options for data collection and cost-benefit analyses were suggested. It is essential to balance the cost of collecting data and running air quality models with the actual use of the data for air quality management. This case study highlights the need for modified methodologies to assess projects and meet the requirements of the impact pathway methodology. As cities adopt new approaches to air quality management, there is an opportunity to develop standardized and practical methods for evaluating the ex-ante impact of the programs and monitoring their technical, health, and economic performance, particularly in the context of developing countries.

Keywords: Regulatory Schemes, Developing countries, Air quality managment, Cost-benefit methodologies.

INTRODUCTION

Low Emission Zones (LEZs) have emerged as a complementary approach to air pollution management, being implemented across various cities worldwide. Unlike conventional approaches, LEZs involve specific strategies according to each area type, needs and opportunities. A common characteristic is the delineation of urban areas afflicted with high air pollution levels, which significantly impact sizeable populations or groups susceptible to air pollution. Within designated LEZs, tailored emission reduction schemes target the primary pollution sources. Notably, most LEZ initiatives concentrate on city center areas heavily impacted by vehicular emissions (Steimer & Kothari, 2022; Xue, 2021). Consequently, most LEZ focus on limiting the circulation of the most polluting vehicles through diverse regulatory mechanisms.

Bogotá, Colombia's capital, recently undertook a similar air quality management strategy. The objective is to mitigate pollution in areas historically exhibiting the city's highest pollution levels, concentrating emission´s mitigation efforts in relatively small urban areas. The local government established the Urban Zones for Better Air Strategy (ZUMA), targeting areas with high pollution and socioeconomic vulnerability. The actions of the ZUMA Strategy cover multiple dimensions, including territorial planning, climate action, mobile sources, fixed sources, resuspended particulate matter, air governance and social management, and non-conventional technologies

for air cleaning. Local Decree 492 of 2023 serves as the regulatory foundation, declaring the ZUMA Bosa-Apogeo as Bogotá's first ZUMA, with additional areas projected for implementation in the coming years.

This new air quality management scheme comes with technical challenges in the approaches employed throughout the policy lifecycle. The analysis presented herein centers on identifying the primary technical barriers, data collection challenges, and proposals to overcome key obstacles related to the ZUMA definition, implementation, and monitoring. This paper is based on a technical assistance process, conducted with C40 support, for the District Secretariat of Environment and District Secretariat of Mobility in developing the technical analysis to define the ZUMA Bosa-Apogeo. The insights will prove valuable for other cities in the developing world pursuing the implementation of approaches such as LEZs or ZUMA. The analyses point out that substantial technical challenges remain to be addressed from a technical standpoint.

METHOLOGY

A central part of the first ZUMA technical assessment was to prioritize and define the mitigation actions that will be taken in the micro-zone in the short and medium term. The proposed measures for the project are divided into four portfolios, which are: i) reducing children's exposure to $PM_{2.5}$, ii) sustainable logistics, iii) providing clean and high-quality transportation for all, and iv) nature-based solutions and surface/road improvements. To assess the technical feasibility of these strategies for reducing local pollution and population exposure, a cost-benefit analysis and a multi-criteria analysis were conducted. Table 1 provides an overview of the criteria used in the assessment for the ZUMA Bosa-Apogeo.

Table 1. Multicriteria assessmente to prioritize the mitigation actions for the ZUMA.

Criteria	Analysis	
	Quantitative	Qualitative
Reduction of $PM_{2.5}$ emissions	✓	
Reduction of ambient $PM_{2.5}$ concentration	✓	
Reduction of $PM_{2.5}$ levels to which the population is exposed in microenvironments within the ZUMA		✓
Health benefits from improved air quality	✓	
Co-benefits in GHG emissions mitigation	✓	
Environmental co-benefits	✓	✓
Considerations in equity and inclusion		✓
Cost analysis	✓	
Actors		✓

Main challenges and alternatives proposed to conduct the analyses

While the general methodology to develop cost-benefit analysis and a multi-criteria analysis remains consistent for varying geographic scales, it's important to note that a ZUMA covers an area of approximately 1 km^2, and therefore it requires different approaches for data acquisition and evaluation of each criterion.

Below are examples of the main challenges in conducting multicriteria analyses, along with proposed alternatives.

- **Determination of the baseline $PM_{2.5}$ concentration at the ZUMA.** Data derived from the citywide air quality monitoring network does not necessarily provide an accurate approximation for analyzing a micro-zone. Consequently, a monitoring campaign was undertaken, utilizing a network of microsensors to estimate the baseline $PM_{2.5}$ levels. Furthermore, this analysis is pertinent as it enables estimating the potential for reducing $PM_{2.5}$ concentrations by mitigating emission sources within the ZUMA, while accounting for $PM_{2.5}$ contributions from sources external to the designated zone. The network of microsensors is the tool proposed to monitor the effectiveness of mitigation actions during the ZUMA implementation phase.

- **Mobile emissions inventory within the ZUMA.** Simulations of air quality within the ZUMA necessitate data representative of emission dynamics at a localized scale, which is not always feasible with the information available from the city-scale emissions inventory. Moreover, the design of traffic source management strategies at a micro-scale requires comprehensive knowledge of traffic flows as well as the characteristics of the vehicle fleet circulating within the specific zone. The data collection methodology employed for the city's emissions inventory does not provide the requisite spatial resolution for a ZUMA. Through computerized video-based counting techniques implemented within the ZUMA, vehicular activity was determined for four distinct road types. This alternative approach proves more cost-effective than the conventional manual counting methods currently utilized by the city.

- **Estimation of changes in air quality in the ZUMA with the mitigation actions.** To quantify the anticipated impact on air quality resulting from mitigation actions, changes in $PM_{2.5}$ concentration were estimated across various scenarios. The AERMOD dispersion model was selected for this purpose, as it can accurately represent the concentration gradients that manifest in the vicinity of emission sources over short temporal

scales immediately after an emission event. Based on the CMAQ Model, the current modeling system employed by the environmental authority is not appropriate for representing the processes that affect the concentration levels of pollutants at a micro-scale (Silveira et al., 2019).

- **Impacts on public health expected with the interventions within the ZUMA**. Health analyses were conducted using the AIRQ+ Program developed by the World Health Organization. The long-term effects were evaluated based on the expected improvements in air quality in the Bosa-Apogeo ZUMA. The health analysis relied on exposure-response functions to estimate the disease burden caused by long-term exposure to $PM_{2.5}$ under different ambient air scenarios. The focus of the analyses was on the impacts of mortality. However, data from larger areas in the city were used, and thus, they may not be the best representation of the ZUMA population. Due to limitations in the health data available for the ZUMA, the effects on morbidity were not included in the analysis. Another challenge was interpreting and communicating the results in terms of the number of potential deaths avoided with the actions taken in the ZUMA. The monitoring phase will also be limited by the lack of sources to obtain data at the ZUMA resolution. Alternatives, such as perception surveys, were proposed for the monitoring scheme.

- **Equity and inclusion**. This analysis identified whether the measures contribute to improving the quality of life of the population in Zuma. Possible risks of excluding vulnerable populations from the benefits or generating negative impacts on certain community groups were identified. This analysis helped to avoid creating additional conditions that increase inequity and guided the design of mechanisms that allow individuals from vulnerable groups to access the benefits of Zuma. Although there is currently no information system at the Zuma level that can answer all the guiding questions designed, the best possible approximation to each question was used to improve the ZUMA design interventions.

The application of conventional project evaluation methodologies to the context of the ZUMA Bosa-Apogeo highlighted the necessity to adapt these methodologies to ensure their applicability at the micro-scale level. Similarly, the need for novel information management mechanisms that facilitate the acquisition of representative data for the study area became evident. Data-intensive exercises typically entail higher costs for data procurement, which poses a relevant limitation for environmental authorities in developing countries.

CONCLUSIONS AND RECOMENDATIONS

Throughout the ZUMA definition process, several methodologies and technical tools were proposed to help make decisions about the design and prioritization of measures to be implemented. However, due to the Strategy's focus on relatively small geographic areas, conventional evaluation methodologies for the ex-ante assessment and the information sources used at the city level fail to adequately represent the various processes that generate emissions or the expected impacts. Similar barriers in terms of data acquisition were identified and anticipated for the monitoring phase.

There is an opportunity to develop standardized, practical, and cost-efficient methods for evaluating the impact of this type of strategies to serve similar air quality management strategies across cities in the developing world. Under a novel policy framework, it is crucial to ensure that the preeminent objective remains achieving substantive improvements in air quality, while the methodological limitations of ex-ante analyses can be gradually resolved. The ZUMA Strategy is a unique initiative that requires some flexibility in its initial stages to ensure it can be adjusted and monitored effectively.

The experienced in Bogota also shows that it is imperative to look for a balance between the technical effort devoted to build data supporting the policies and the tangible utilization of the technical analysis results to achieve the desired air quality objectives.

REFERENCES

District Decree 492 of 2023 “By means of which Article 120 of District Decree 555 of 2021 is regulated in relation to the Urban Zones for Better Air (ZUMA) in Bogotá D.C., the ZUMA Bosa-Apogeo is declared, and other regulations are issued”.

Sarmiento, L., Wägner, N., & Zaklan, A. (2023). The air quality and well-being effects of low emission zones. Journal of Public Economics, 227, 105014.

Silveira, C. , Ferreira, J. , & Miranda, A. I. (2019). The challenges of air quality modelling when crossing multiple spatial scales. Air Quality, Atmosphere & Health, 12, 1003-1017.

Steimer, H., & Kothari, V. (2022). Zero-Emission Delivery Zones: A New Way to Cut Traffic, Air Pollution and Greenhouse Gases.

Xue, L. (2021). Lessons from Shenzhen's Green Logistic Zones: Fast-Tracking Zero-Emissions Freight.

AIR POLLUTION CONFERENCE BRAZIL
CMAS SOUTH AMERICA
COMMUNITY MODELING AND ANALYSIS SYSTEM

REAL WORLD LABORATORİES AND THE SOCİAL CONTROL OF AİR POLLUTİON

Ana Paula Koury[1], Renato Luis Sobral Anelli[2], Fabio Carlos Martins[3]
[1]*São Judas University/ Mackenzie Presbyterian University*
apkoury@gmail.com
[2] *Mackenzie Presbyterian University*
renato.anelli@mackenzie.br
[3] *São Judas University*
fabio.martins@saojudas.br

Abstract: This proposal discusses the social control of air pollution through real-world laboratory experience. The issue of air pollution occupies the center of the debate on climate change. The main challenges for controlling pollution are 1) the capillarity of economic processes based on the burning of fossil fuels. 2) the intangibility of air pollution compared to other forms of environmental pollution. This poster aims to discuss the issue of social control of air pollution based on real-world laboratory experiences. The Real World Laboratories is considered an essential device for city change and can contribute to air pollution regulation. The Real World Laboratories differs from other forms of civil society engagement popularized in Latin America, such as the Participatory Process and Social Urbanism. It belongs to a field of Labs developed to support societal change through disciplinary approaches and connection with science and urban Labs. It usually connects civil society, academics, and local authorities to co-design and co-produce solutions for the cities. The themes of mobility (micro and macro mobility) and the challenges of air pollution in informal settlements will be discussed in the Well Being Wuppertal experiment and Itaim Paulista Lab. These are themes present in the real-world experiments to be analyzed. Both cases highlight important stakeholders in regulating climate change, organized and unorganized civil society sectors, and large transport companies.

Keywords: : Air Pollution Control, Real World Laboratory, Climate Change, Societal Control

INTRODUCTION

As per the Elsevier Analytical Report "Pathways to Net Zero: The Impact of Clean Energy Research on NØEnergy research" (Elsevier, 2021, p. 2), achieving net zero emissions globally requires two key actions: reducing greenhouse gas (GHG) emissions from human activities and extracting carbon from the atmosphere. While the solution to the climate crisis seems straightforward in theory, reports such as the Hamburg Climate Futures Outlook suggest it is challenging to meet the decarbonization targets set by the Paris agreement to limit the global temperature rise to 1.5°C (Engels et al., 2023, p. 5).

Greenhouse gases contribute significantly to air pollution, a major public health issue associated with ailments like heart attacks and respiratory diseases, which are among the leading causes of mortality worldwide. Addressing air pollution is critical not only for reducing health risks but also for combating climate change and ensuring a sustainable future for upcoming generations (Afifa et al., 2024; El Morabet, 2019).

According to data from Climate Watch, the primary sectors influencing GHG emissions are energy production (61%) and transportation (13%), which have extensive interconnectedness with other economic activities. This complexity underscores the challenges in reducing emissions due to their significant economic impacts. Moreover, social control poses another hurdle as awareness of air pollution among the general population is not always high (Noël, Vanroelen, Gadeyne, 2021).The main challenges for controlling the GEE emissions are 1) the capillarity of economic processes based on the burning of fossil fuels. 2) the intangibility of air pollution compared to other forms of environmental pollution.

Addressing this substantial global challenge requires placing it within the urban context, considering that the majority of the world's population resides in cities currently, with projections indicating that by 2050, 68% of the global population will be urban dwellers (Nations, 2018).

To contribute to social transformation and implement measures that directly impact greenhouse gas (GHG) emissions, particularly in urban settings, we will delve into two Real World Laboratory (RWL) experiences. One RWL initiative is situated in Wuppertal, Germany, while the other is located in Itaim Paulista, an area facing significant vulnerabilities in the eastern region of São Paulo. Both experiments focus on mobility as a central theme, offering a valuable opportunity to address the urgent need for effective control measures in vital economic sectors to meet the pressing challenges of urban decarbonization.

AIR POLLUTION
CONFERENCE BRAZIL
CMAS SOUTH AMERICA
COMMUNITY MODELING AND ANALYSIS SYSTEM

METHODS

RWLs often integrate diverse forms of knowledge, encompassing both scientific and non-scientific insights. Their primary objective is to contribute to sustainable urban development at the local level while empowering local change agents to spearhead transformations within their communities. The knowledge generated through RWL experiments enables the evaluation of existing theories and the development of new theoretical frameworks and intervention strategies in the realms of urban and social realities. Each RWL experiment is unique and non-repeatable due to the distinctive cultural, social, and political characteristics of each setting. As noted by Wanner et al. (2018), the effectiveness of action and problem-solving within RWLs is closely linked to the narrative logic and spirit of the specific place.

The evolution of this research approach has led to the proliferation of diverse types of laboratories, each with distinct characteristics and objectives aimed at catalyzing urban transformation towards a more sustainable society. Schäpke et al. (2018) conducted a study on 14 laboratories in the state of Baden-Württemberg, Germany, comparing them based on type and key characteristics to refine the methodological approaches employed by these labs. According to the authors, laboratories like RWLs play a crucial role in bridging varying methods of transformative research, designing and implementing experiments, evaluating outcomes, ensuring reproducibility, and facilitating social learning. The authors delineate four main types of experimental laboratories: Real World Laboratory (RWL), Urban Transition Lab (UTL), Sustainable Living Lab (SLL), and Transformation Lab (T-LAB).

The characterization conducted by the authors offers insights into distinguishing between various types of urban laboratories and how each type can be effectively applied to address the challenges related to air pollution. The appended table is an interpretative adaptation of the original authors' work, categorizing laboratories based on their emphasis on social or technological transformations. All these laboratory types prioritize interactive and participatory methodologies.

In tackling the identified "problem situations," which include the abstract nature of pollution and the intricate linkages of economic processes reliant on carbon emissions, these laboratories aim to delineate local impacts that foster iterative learning cycles to shape a fresh blueprint for social organization. Hence, the Real World Laboratory (RWL) emerges as a fitting choice in this scenario to realize the intended objectives effectively.

Table 1. Comparative table of the types of Labs

	social centered	
	Real World Laboratory (RWL)	**Urban Transition Lab (UTL)**
focus	**Governance for sustainability**	**Social change theory**
method	Participatory (Multiperspectivism)	Participatory
actors	Civil society, academia and public authorities	Pioneers of change and public authorities
duration and reproduc.	Long term. It must be transferred to society. Generalization of results via strategic partnerships, local empowerment and social learning.	Long term. It must be transferred to society. Generalization of results via strategic partnerships, local empowerment and social learning.
learning	Experimental learning cycles. Protected spaces for negotiations. Construction of common meanings and reciprocal trust between those involved.	Knowledge of strategies oriented to problem situations. Transdisciplinary learning environment based on interaction between society and academia.
	techincal centered	
	Sustainable Living Lab (SLL)	**Transformation Lab (T-LAB)**
focus	**socio-technical innovations**	**prototyping socio-ecological solutions**
method	Field tests	Prototypes
actors	Residents and companies	Facilitators and key actors
duration and reproduc.	Long term through permanent infrastructures. Generalization via market	Temporaries. Change perceptions
learning	Tacit knowledge about sustainable practices in system users through their integration in experiments	It depends on the design of the Design Thinking Lab. Innovations in processes and systems.

Source: Author. Adapted from SCHÄPKE, 2018.

These laboratory models, predominantly established in Germany to catalyze urban transformations through social processes, markedly differ from the modes of social engagement prevalent in Latin American nations.

Moving forward, two exemplary experiments will be presented: the Well Being Wuppertal initiative in Germany and the Itaim Paulista Lab in São Paulo, Brazil. Both endeavors were implemented in vulnerable communities and revolve around the central theme of transforming mobility systems. They feature locally institutionalized hubs dedicated to effecting transformative change, alongside engaging a diverse array of local stakeholders.

THE REAL WOLD EXPERIMENTS.

The "Well-being Transformation Wuppertal" (WTW) project is situated at the Center for Transformation Research and Sustainability, a collaborative initiative between the University of Wuppertal and the Wuppertal Institute. The project's objective is to establish a set of Urban Well-Being indicators in partnership with the local community. Key participants include organized civil society groups, municipal authorities, and visionary advocates for change. The project comprises three Real World Laboratories (RWLs). In the Mark district with 8,100 residents, pervasive

social issues like poverty and unemployment are prominent. Here, socio-cultural institutions play a central role in community development. Notably, the creative collective Utopiastadt, known as "Utopia City," stands out as a key contributor. Utopiastadt, a WTW partner, organizes inclusive cultural events that inspire local progress, encompassing initiatives such as culinary endeavors, urban gardening, open data projects, active mobility solutions, and shared co-working spaces. Utopiastadt is housed within a disused railway station dating back to 1882, where the former tracks now double as a cross-city bike path, symbolizing both active mobility and enhanced connectivity between the district and the urban core (Haake, 2018).

Itaim Paulista, comprising approximately 400,000 residents, is an administrative region delineated by two districts in the far-eastern sector of São Paulo. The area is marked by community vulnerability, particularly among residents living in high-risk zones alongside the streams that traverse the region from north to south. Estrada Dom João Nery, a principal thoroughfare oriented in the same direction, runs along the boundary of the two districts parallel to the Ribeirão do Lageado creek. Since 2013, concerted efforts and investments have been directed towards road infrastructure enhancements along this route. The Itaim Paulista laboratory was established with the objective of conducting research aimed at aligning planned transformations with the core tenets of co-design, co-production, and sustainable real-world experiments. The proposed strategy incorporates green and blue infrastructure elements to shape an urban environmental corridor capable of addressing decarbonization objectives alongside the infrastructure needs outlined by municipal and state entities. Additionally, the initiative includes a pilot community study in response to local opposition to government proposals. Recognizing the significance of further exploration into an integrated model of green and blue infrastructure and local governance, key stakeholders such as organized civil society groups, local governance bodies, municipal urban development departments, and academic institutions are actively engaged through the Klimapolis project.

The proposal did not yield the intended outcomes, despite active engagement from various social sectors involved in the experiment, the community encountered palpable challenges that resonated on a local scale. Issues such as enhancing the transportation system, fortifying local community cohesion, and addressing drainage concerns were concrete and easily comprehensible to community members without the need for complex abstractions.

CONCLUSIONS

We believe that these instances, demonstrating the collaboration between societal stakeholders and urban revitalization initiatives concerning mobility, governance, and community cohesion, hold significant potential to enhance social influence and reshape local social, cultural, and political frameworks. By fostering connections and tangible improvements, these endeavors can pave the way for transformative changes, fostering community engagement needed to address urban policy obstacles that impede effective decarbonization efforts.

REFERENCES

Afifa et al. Air pollution and climate change as grand challenges to sustainability. Science of The Total Environment, v. 928, p. 172370, 10 jun. 2024.

El Morabet, R. Effects of Outdoor Air Pollution on Human Health. Em: NRIAGU, J. (Ed.). Encyclopedia of Environmental Health (Second Edition). Oxford: Elsevier, 2019. p. 278–286.

Elsevier. Pathways to Net Zero: The Impact of Clean Energy Research. Amsterda: Elsevier, 2021. . Acesso em: 4 maio. 2024.

Engels, A. et al. Hamburg Climate Futures Outlook: The plausibility of a 1.5°C limit to global warming - social drivers and physical processes. [s.l.] [object Object], 1 fev. 2023.

Haake, H. WTW_Broschüre_Einzelseiten_2018.pdf. Zentrum für Transformationsforschung und Nachhaltigkeit (TransZent), , 2018.

Nations, U. 68% of the world population projected to live in urban areas by 2050, says UN.

Noël, C.; Vanroelen, C.; Gadeyne, S. Qualitative research about public health risk perceptions on ambient air pollution. A review study. SSM - Population Health, v. 15, p. 100879, 1 set. 2021.

Schäpke, N. et al. Jointly Experimenting for Transformation? Shaping Real-World Laboratories by Comparing Them. GAIA - Ecological Perspectives for Science and Society, v. 27, n. 1, p. 85–96, 1 jan. 2018.

Wanner, M. et al. Towards a Cyclical Concept of Real-World Laboratories: A Transdisciplinary Research Practice for Sustainability Transitions. disP - The Planning Review, v. 54, n. 2, p. 94–114, 3 abr. 2018.

This work is funded by Fapesp (22/00580-6) is a direct contribution to the research themes of the **CIAM Clima** and the National Institute for Science and Technology - INCT **Klimapolis** funded by the Brazilian Ministry of Science, Technology, and Innovation (MCTI), National Council for Scientific and Technological Development (CNPq) (406728/2022-4), as well as the initial German Brazilian Klimapolis Laboratory (klimapolis.net), funded by the German Federal Ministry of Education and Research (BMBF).

AIR POLLUTION CONFERENCE BRAZIL
CMAS SOUTH AMERICA
COMMUNITY MODELING AND ANALYSIS SYSTEM

TRENDS AND CHALLENGES FOR AIR QUALITY RESEARCH IN LATIN AMERICA

Thalia Alejandra Montejo[1], Juan Felipe Franco[1]
[1]*Hill Consulting, Colombia*
Corresponding author: *jfranco@hill.com.co*

Keywords: Air pollution, Research trends, Bibliometric analysis, VOSviewer, CiteSpace.

INTRODUCTION

The present study is a bibliometric analysis of distribution and the state of research on air pollution in Latin America. It focuses on a comprehensive literature review of key air-quality terms during the last decade, emphasizing current aspects to drive future research. The main objective is to delve into the most relevant issues and trends identified from the key topics found in air-quality-related publications in the region and highlight those that need further attention. The bibliometric analysis of such publications provides a direction for hot topics and future research trends. The results of this exercise will serve to understand the dynamics of air pollution studies in Latin American countries and as a starting point for proposing future approaches and topics on which to focus. Findings will help guide researchers and other stakeholders towards a more comprehensive vision to manage air quality problems in the region.

METHODS

We conducted a literature review covering 6260 articles that includes the terms air quality, air pollution, air pollutants, indoor air quality, particulate matter and all countries names of Latin America in their title, keywords and abstract, and published between 2013 and 2023 in Scopus and Web of Science databases. Initially, a bibliometric analysis was conducted to delineate prevailing research trends. Subsequently, content analysis was undertaken to elucidate relationships among key terms extracted from the reviewed literature, thereby exposing recent air quality research trends in Latin America. This assessment incorporated Time Trend Analysis, Word Frequency Analysis, and statistical linguistic identification and clustering techniques.

Three bibliometric analysis tools were used: VOSviewer (version 1.6.20), CiteSpace (5.5.R2) and Python text data analysis. VOSviewer is widely recognized for its ability to perform keyword co-occurrence analysis (Escorcia Hernández et al., 2023; Zhang et al., 2019). The "minimum of occurrences of a term" refers to the threshold set for the number of times a term must appear in the dataset to be considered in the analysis. In this study, a minimum of 80 occurrences of a term was chosen. Additionally, the "number of terms to be selected" indicates the number of terms chosen for inclusion in the analysis. Here, 100 terms were selected, focusing the analysis on a manageable and relevant set of terms. CiteSpace V5.5 is noted for its robust document co-citation analysis (Chen, 2006; Pierpaoli & Ruello, 2018). We used both tools to map thematic trends in literature and highlight key areas of knowledge (clusters) related to air quality conditions and impacts.

FINDINGS AND ARGUMENT

The findings reveal a significant upward trend in air quality publications, giving signals of a growing interest in research on air pollution characterization and effects. On average, about 496 papers were published per year during this period. An increasing trend in the number of publications is observed over the years, with a steady increase from 2013 to 2023. Peak productivity was recorded in 2021, with 722 publications, representing approximately 13% of the cumulative total.

Brazil emerges as the country with the highest frequency, mentioned 1796 times, followed by Mexico with 1295 mentions, and Chile with 565. Colombia and Peru follow with 456 and 262 mentions, respectively, while Argentina is mentioned 259 times (see Figure 1).

We identified 100 key terms with the highest co-occurrence and relevance using VOSviewer software. As depicted in Figure 2, this visual representation illustrates the structure and relationships among terms within extensive datasets. The size of each circle (or node) indicates the significance or frequency of the corresponding term in the dataset, with larger circles representing more frequent terms. The distance between terms signifies the similarity or proximity between them, with closer terms indicating stronger relationships. Color-coded groups denote sets of terms sharing cluster connections, often indicating thematic areas or specific categories. These visualizations greatly aid in interpreting complex datasets.

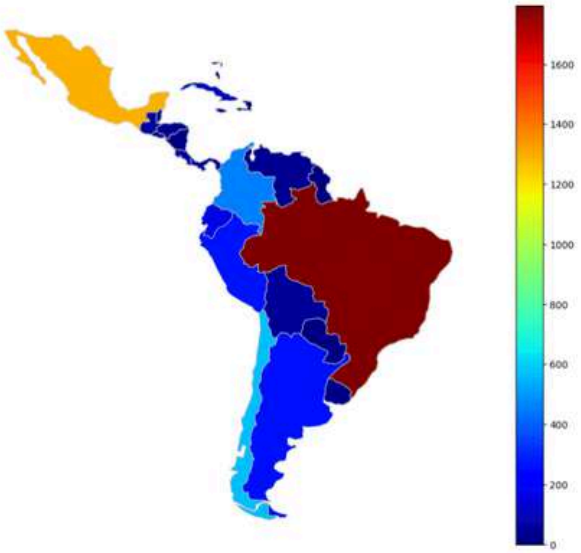


Figure 1. Geographical distribution of country frequencies in abstracts on air pollution publications in Latin America.

This analysis provides valuable insights into the interconnectedness of various themes within the research landscape of air pollution. Notably, the analysis revealed the presence of five distinct clusters, each characterized by a unique concentration of interrelated themes. Clusters represent groups of closely interconnected nodes within a network.

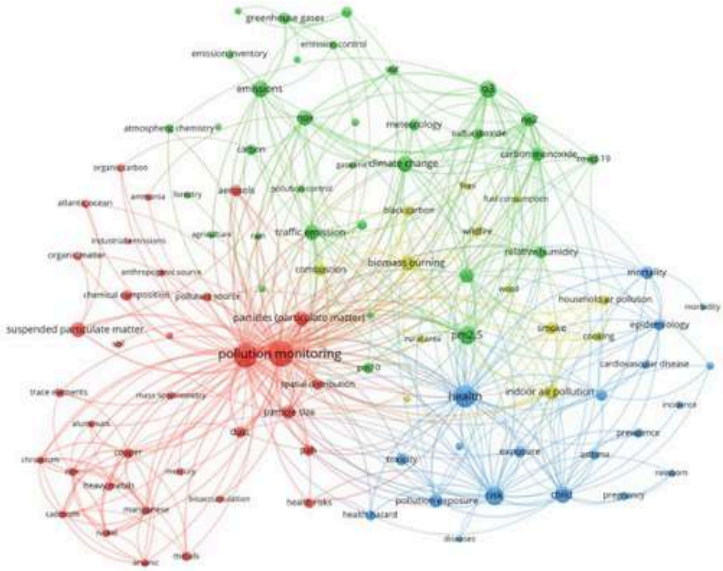


Figure 2. Term co-occurrence map of key terms.

These clusters are visually depicted through color-coded sets of nodes with stronger connections, typically indicating thematic or closely associated elements. Upon examination, it is evident that the research theme of air pollution has formed four distinct clusters: Cluster 1 (Red, contaminant characterization), Cluster 2 (Green, contaminant sources), Cluster 3 (Blue, environmental health and epidemiology), Cluster 4 (Yellow, biomass burning and household pollution). Table 1 summarizes the analysis of keywords with the highest total link strength, revealing also significant trends in the field of air quality in the region.

Systematic analysis of keywords in specific research fields offers a clear understanding of the developmental trends and research distinctions within the domain. By scrutinizing the prevalence and interrelationships of keywords across clusters, researchers can discern emerging patterns, thematic focuses, and evolving areas of interest. This approach enables the identification of key themes, research gaps, and priorities within the field, facilitating informed decision-making, strategic planning, and targeted interventions to address pressing issues and advance knowledge in the respective domain.

Table 1. Keywords with the highest total link strength.

Words	Cluster	Total Link strength
Pollution monitoring	Red	6664
Concentration (comp.)	Red	5891
Health	Blue	3991
Risk	Blue	3423
PM2.5	Green	2641
Traffic Emission	Green	2583
Child	Blue	2363
O3	Green	2287
NO2	Green	2211
Biomass Burning	Yellow	2141

Research in the region is responding to these trends. Various strategies and measures have been scientifically proposed to address air pollution challenges, including regulation of industrial emissions (Mardones & Cabello, 2019) control of vehicular emissions (Davis, 2008; Morales Betancourt et al., 2022), and promotion of clean and renewable energies (Koengkan et al., 2021). In addition, the implementation of air quality monitoring systems has become increasingly important in the region, allowing the collection of accurate and real-time data on the concentration of air pollutants in urban and rural areas (Yarce Botero et al., 2023). Finally, atmospheric modelling studies have played a crucial role in understanding pollutant dispersion patterns and predicting air quality in different scenarios (Ballesteros-González et al., 2020). All these tools provide valuable information for decision making in environmental management and public health by identifying high-

risk areas and assessing the impact of policies and mitigation measures, as well as understanding the dynamics of the problem.

CONCLUSIONS

The comprehensive analysis conducted on air quality in Latin America has yielded significant insights into various aspects of the topic. Key findings include the notable prevalence of countries such as Brazil, Mexico, and Chile in air quality literature, indicating their substantial contributions to research in this field. The exploration of bigrams and trigrams has revealed important associations, such as those between biomass concentration and indoor air pollution, shedding light on critical themes within the region. Moreover, the identification of citation bursts underscores periods of intense research focus on topics like urban air pollution and its long-term health impacts, highlighting areas of particular concern and interest. These findings collectively provide a comprehensive and contemporary overview of air quality research in Latin America, offering valuable insights for policymakers and stakeholders seeking to address environmental and public health challenges effectively.

REFERENCES

Ballesteros-González, K., Sullivan, A. P., & Morales-Betancourt, R. (2020). Estimating the air quality and health impacts of biomass burning in northern South America using a chemical transport model. Science of The Total Environment, 739, 139755. https://doi.org/10.1016/j.scitotenv.2020.139755

Chen, C. (2006). CiteSpace II: Detecting and visualizing emerging trends and transient patterns in scientific literature. Journal of the American Society for Information Science and Technology, 57(3), 359–377. https://doi.org/10.1002/asi.20317

Davis, L. W. (2008). The Effect of Driving Restrictions on Air Quality in Mexico City. Journal of Political Economy, 116(1), 38–81. https://doi.org/10.1086/529398

Escorcia Hernández, J. R., Torabi Moghadam, S., Sharifi, A., & Lombardi, P. (2023). Cities in the times of COVID-19: Trends, impacts, and challenges for urban sustainability and resilience. Journal of Cleaner Production, 432, 139735. https://doi.org/10.1016/j.jclepro.2023.139735

Koengkan, M., Fuinhas, J. A., & Silva, N. (2021). Exploring the capacity of renewable energy consumption to reduce outdoor air pollution death rate in Latin America and the Caribbean region. Environmental Science and Pollution Research, 28(2), 1656–1674. https://doi.org/10.1007/s11356-020-10503-x

Mardones, C., & Cabello, M. (2019). Effectiveness of local air pollution and GHG taxes: The case of Chilean industrial sources. Energy Economics, 83, 491–500. https://doi.org/10.1016/j.eneco.2019.08.007

Morales Betancourt, R., Galvis, B., Mendez-Molano, D., Rincón-Riveros, J. M., Contreras, Y., Montejo, T. A., Rojas-Neisa, D. R., & Casas, O. (2022). Toward Cleaner Transport Alternatives: Reduction in Exposure to Air Pollutants in a Mass Public Transport. Environmental Science & Technology, 56(11), 7096–7106. https://doi.org/10.1021/acs.est.1c07004

Pierpaoli, M., & Ruello, M. (2018). Indoor Air Quality: A Bibliometric Study. Sustainability, 10(11), 3830. https://doi.org/10.3390/su10113830

Yarce Botero, A., Lopez Restrepo, S., Sebastian Rodriguez, J., Valle, D., Galvez-Serna, J., Montilla, E., Botero, F., Henzing, B., Segers, A., Heemink, A., Quintero, O. L., & Pinel, N. (2023). Design and Implementation of a Low-Cost Air Quality Network for the Aburra Valley Surrounding Mountains. Pollutants, 3(1), 150–165. https://doi.org/10.3390/pollutants3010012

Zhang, X., Estoque, R. C., Xie, H., Murayama, Y., & Ranagalage, M. (2019). Bibliometric analysis of highly cited articles on ecosystem services. PLOS ONE, 14(2), e0210707. https://doi.org/10.1371/journal.pone.0210707

SESSION 13
Remote Sensing/Sensor Technology and Measurements Studies

Papers in this session are devoted to analyzing data from both conventional and remote-sensing observational platforms. In particular, presentations are invited on the integration of data collected from different platforms, and on the use of new satellite data products in air quality modeling. Session topics include:

- Satellite processing products and its use
- Monitoring air pollution and meteorology
- Field measurement studies
- Laboratory smog chamber experiments
- Aerosol detection and sampling

In addition, new sensor technologies, due to their characteristics (e.g., low cost, small size, high portability), are becoming increasingly important for individual exposure assessment, especially since this kind of instrument can provide measurements at high spatial and temporal resolution, which is a notable advantage when approaching assessment of exposure to environmental contaminants.

This session will provide information about advancements on the developments and use of sensor technology for air quality and health studies.
Topics include, but are not limited to, the following:

- Novel air sensor technologies for monitoring air quality and health conditions
- Evaluation and validation of sensor performance
- Application of sensor network on air quality, exposure and health studies

SESSÃO 13

VALIDATION OF ATMOSPHERIC POLLUTANT CONCENTRATION REANALYSIS DATA IN THE METROPOLITAN AREA OF SÃO PAULO 373

DEVELOPMENT OF ENVIRONMENTAL QUALITY MONITORING SYSTEMS FOR SMART CITIES 376

MEASURING INDOOR AIR QUALITY IN RETAIL STORES: MEASUREMENTS RECOMMENDATIONS BASED ON FIELD EXPERIENCE 379

MODELING AND SCENARIO ANALYSIS APPLIED TO THE DYNAMICS OF LAND USE AND TRANSPORT USING CELLULAR AUTOMATA AND LANDSAT DATA 382

ESTIMATIVE OF URBAN PLUME DISPERSION PARAMETERS FOR THE CITY OF MANAUS BASED ON AIRPLANE OBSERVATIONS 385

PERFORMANCE ASSESSMENT OF A LOW-COST AIR QUALITY SENSOR IN A SEMI-URBAN AREA OF SÃO PAULO 388

CARBON DIOXIDE AND METHANE LEVELS IN SURFACE WATERS ALONG THE SÃO VICENTE ISLAND IN COASTAL REGION OF SÃO PAULO STATE 391

ASSEMBLY RESULTS ON GHG AND PARTICULATED MATTER MONITORING USING LOW-COST SENSORS 394

LONG-TERM ISOPRENE (BVOC) FLUXES IN THE AMAZON RAINFOREST BY RELAXED EDDY ACCUMULATION COUPLED TO GC/PID (REAPER) 397

CARBON DIOXIDE AND METHANE LEVELS IN SURFACE WATERS ALONG THE SÃO VICENTE ISLAND IN COASTAL REGION OF SÃO PAULO STATE 399

AIR POLLUTION CONFERENCE BRAZIL
CMAS SOUTH AMERICA
COMMUNITY MODELING AND ANALYSIS SYSTEM

VALIDATION OF ATMOSPHERIC POLLUTANT CONCENTRATION REANALYSIS DATA IN THE METROPOLITAN AREA OF SÃO PAULO

Marina Spina Paiva[1], Luciana Varanda Rizzo[2]
[1]*Institute of Physics/Universidade de São Paulo*
marinaspinapaiva@usp.br
[2]*Institute of Physics/Universidade de São Paulo*
lrizzo@usp.br

Abstract: The objective of this project is to validade CAMS and MERRA-2 reanalysis products againt in situ air quality data in the Metropolitan Area of São Paulo between 2015 and 2019, for the pollutants O_3, NO_2, $PM_{2.5}$ and PM_{10}. For each reanaysis product, the most representative grid point was selected according to multiple metrics such as Pearson Correlation coefficients, slopes and offsets, relative mean bias and standard deviations. CAMS data overestimated concentrations of O_3, $PM_{2.5}$, and PM_{10} and underestimated NO_2. MERRA-2 overestimated O_3 but underestimated $PM_{2.5}$ and PM_{10}. CAMS data reproduced the seasonal variation observed in situ for all pollutant concentrations, showing squared correlation coefficents above 0.70 for PM. MERRA-2 had a worse performance, failing to reproduce the PM seasonal variability and showed lower correlation coefficients all pollutants against in situ observations.

Keywords: Air quality, tropospheric ozone, particulate matter, CAMS, MERRA-2

INTRODUCTION

Reanalysis products can be an alternative to characterize air quality in regions where in situ monitoring is insufficient. Through advanced data assimilation methods, reanalysis combines data from atmospheric transport models with observations from around the world, both remote sensed or in situ. Before reanalysis data can be used to assess air quality at local and regional scales, its accuracy must be evaluated by comparing it with temporally and spatially co-located in situ data to assess correlations and biases. The objective of this project is to validate Copernicus Atmosphere Monitoring Service (CAMS) and Modern-Era Retrospective Analysis for Research and Applications (MERRA-2) reanalysis data near surface against in situ data collected in the Metropolitan Area of São Paulo (MASP) by Companhia Ambiental no Estado de São Paulo (CETESB) between 2015 and 2019, focusing on the pollutants ozone (O_3), nitrogen dioxide (NO_2) and particulate matter ($PM_{2.5}$ and PM_{10}). It should be noted that MERRA-2 does not provide NO_2 data, so comparisons with in situ data were made using only CAMS. This analysis is unprecedented in MASP.

METHODS

Eight air quality monitoring stations operated by CETESB were selected to represent MASP in terms of air pollutant concentrations. Daily and monthly averages of air pollutant concentrations were calculated from the hourly in-situ and MERRA-2 data and from the 3-hourly CAMS data. For MERRA-2, $PM_{2.5}$ *and* PM_{10} concentrations were calculated following the recommendations of the data provider, which include organics and inorganics components of aerosol.

Six grid points from CAMS and other six from MERRA-2 intersecting the metropolitan were selected, with spatial resolutions of 0.75°x 0.75° and 0.5°x 0.625°, respectively. In order to select the most representative CAMS and MERRA-2 grid points, it was performed a correlation analysis between the MASP in situ data and the concentrations in each grid point for the four air pollutants under analysis. Metrics to evaluate the performance of reanalysis data in representing in situ observations included: Pearson correlation coefficients, slopes and offsets, relative mean bias ($RMB = \frac{\overline{\text{REANALYSIS}-\text{CETESB}}}{\overline{\text{CETESB}}}$) and standard deviations. Taylor diagrams were used to support the choice of the best CAMS and MERRA-2 grid points to represent air quality conditions in the MASP, allowing for simultaneous comparison of different metrics.

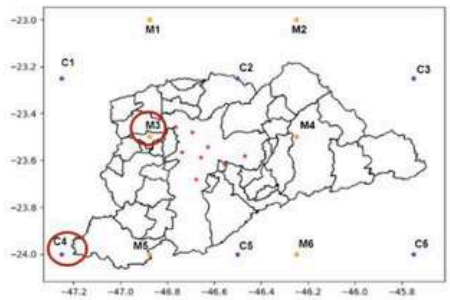


Figure 1. Map of MASP showing municipal divisions. Selected stations in MASP are marked in red, CAMS grid centroids in purple, and MERRA-2 grid centroids in yellow. All CAMS grid points are over land areas, except for point C6, which is over the Atlantic Ocean. Point C5 is in the Baixada Santista area. The chosen points were C4 from CAMS and M3 from MERRA-2.

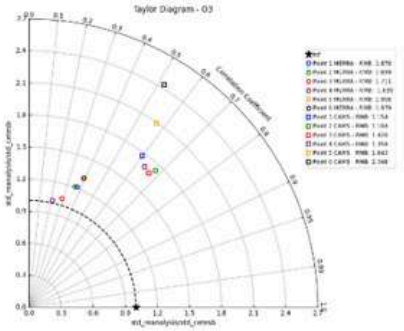


Figure 2. Taylor diagram for O_3, comparing CAMS and MERRA-2 data with CETESB, as an example of the diagrams created for the four pollutants.

Additionally, the seasonal variability of reanalysis products were compared against in situ observations.

RESULTS AND DISCUSSION

Grid points C4 and M3, according to Figure 1, were most suitable for representing the CETESB data. Table 1 shows the RMB for the comparison between reanalysis and in situ data, as well as the squared correlation coefficients R^2. CAMS overestimates the concentrations of O_3, $PM_{2.5}$, and PM_{10} and underestimated NO_2. MERRA-2 overestimated O_3 and underestimated $PM_{2.5}$ and PM_{10}. Each pollutant will be discussed in the following.

Table 1: Relative mean bias (RMB) and squared correlation coefficient (R^2) for the comparison between reanalysis and in situ monthly data.

		O_3	NO_2	$PM_{2.5}$	PM_{10}
CAMS	RMB	136%	-45%	50%	16%
	R^2	0.58	0.55	0.73	0.80
MERRA-2	RMB	171%	---	-20%	-11%
	R^2	0.19	---	0.04	0.08

1. O_3

Spring and summer are the seasons with the highest ozone formation (Schuch et al., 2019). It is observed that the CAMS and MERRA-2 data reproduced the expected seasonality in comparison with CETESB data (Fig 3).



Figure 3. Monthly averages from 2015-2019 of O3 data from MERRA-2, CAMS, and CETESB.

However, the reanalysis products generally overestimate the in situ concentrations throughout all months. As a comparison, Wagner et al.(2021) reported RMB values between -40% and 20% for CAMS O_3 concentrations in mid-latitude regions of the Northern Hemisphere. Wang et al. (2020) found overestimations of up to 30% in the lower troposphere in tropical regions. Given a 136% overestimation for CAMS in MASP, O_3 concentrations over this region are significantly more overestimated than in other parts of the world.

The coefficients of determination were R^2 = 0.40 for CAMS and R^2 = 0.08 for MERRA-2, according to the daily analysis. For the monthly averages, these values improved to R^2 = 0.58 and R^2 = 0.19, respectively. It is concluded that these two reanalysis models better represent concentration variations on a monthly scale. However, these values still indicate a limited ability of MERRA-2 to represent the variability in ozone concentrations as recorded in the CETESB data.

2. NO_2

Like other primary pollutants, NO_2 shows higher concentrations during the winter (Carvalho et al., 2015).

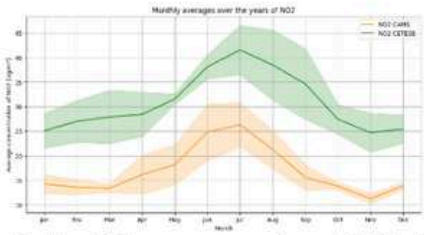


Figure 4. Monthly averages from 2015-2019 of NO_2 data from CAMS and CETESB.

CAMS reanalysis followed the same seasonal pattern as CETESB but consistently underestimates NO_2 concentrations throughout the study months (Fig 4). According to the product's documentation, the estimated NO_2 concentrations rely mostly on the quality of the global emission inventories considered in the model, whereas in situ concentrations are heavily influenced by local emissions, since NO_2 has a relatively short lifespan in the atmosphere. Local emissions may not be well represented in global emission inventories. Another point to discuss is that O_3 is produced in the atmosphere from NO_2 and hydrocarbons (HC). In São Paulo, O_3 production is limited by hydrocarbons, so the amount of O_3 produced depends on the HC/NO_X ratio (Alvim, D.S et al., 2017). Therefore, since CAMS underestimates NO_2, it consequently overestimates O_3, which aligns with the analysis in the previous subsection.

The CAMS x CETESB coefficients of determination for this pollutant improved from 0.43 to 0.55 from daily to monthly data.

3. $PM_{2.5}$ and PM_{10}

As winter is a colder and drier period, the dispersion of pollutants is hindered, favoring the accumulation of predominantly primary pollutants such as NO_2 and PM (Oliveira, M.C.Q.D. *et al.*, 2022). CAMS superestimates concentrations of $PM_{2.5}$ and PM_{10}, but it reproduces the seasonal variability of CETESB data with higher concentrations in winter, showing July as the peak month for these pollutants in the atmosphere. MERRA-2 data often subestimates PM concentrations and exhibit a seasonal pattern opposite to the expected for PM_{10}, with lower concentrations in July (Fig 5).

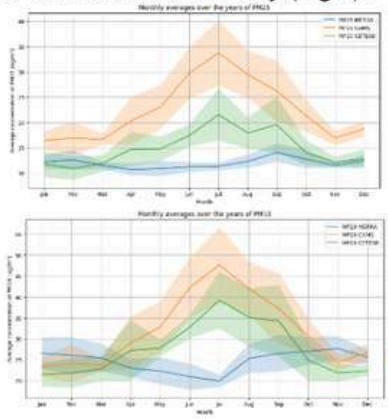


Figure 5. Monthly averages from 2015-2019 of $PM_{2.5}$ and PM_{10} data from MERRA-2, CAMS and CETESB.

Concerning R^2 (Tab 1), CAMS's correlation were above 0.73 for $PM_{2.5}$ and PM_{10}, considering monthly data. In contrast, the R^2 value was below 0.08 for MERRA-2. To investigate possible reasons behind the poor performance of MERRA-2 for PM, the seasonal pattern for each component that constitutes the pollutants $PM_{2.5}$ and PM_{10} was conducted to more deeply examine the sources of these discrepancies.

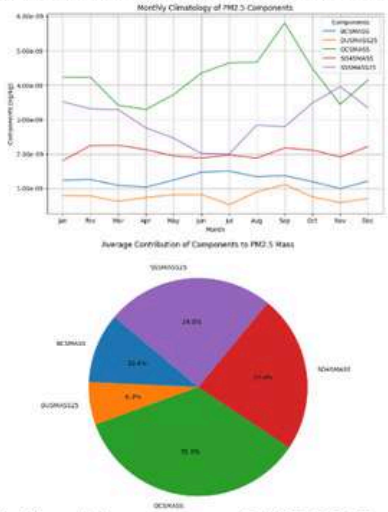


Figure 6. Monthly averages 2015-2019 of $PM_{2.5}$ components and average contribution to the total mass according to MERRA-2.

The MERRA-2 data shows an inverted seasonal pattern for sea salt mass concentration compared to in situ observations, with only black carbon reflecting the correct seasonality (Fig 6). Organics are the dominant component of $PM_{2.5}$ in MERRA-2. Previous observational studies in the MASP showed that organics represent 55% of the mass, followed by sulfate (15%) and equivalent black carbon (14%) (D. Monteiro dos Santos *et al.*,2021). This analysis suggests an overestimation of sea salt by MERRA-2 and a distortion in $PM_{2.5}$ seasonality, needing further research to address these discrepancies. In the conducted analysis of PM_{10} components, it was concluded once again that MERRA-2 overestimates sea salt in the MASP.

CONCLUSIONS

CAMS successfully replicates the seasonality observed in situ for the pollutants concentrations, with Point C4 being the most accurate to represent surface concentrations. Regarding MERRA-2, this product performed poorly in representing O_3 data (R^2 = 0.08) and didn't reproduce the seasonal variability of PM concentrations. Therefore, CAMS reanalysis data is recommended for representing air quality data in São Paulo, in the montly time scale. Expanding the research to other regions in Brazil is also crucial for a better understanding of the results obtained.

REFERENCES

[1] Alvim, D.S *et al.* Main ozone-forming VOCs in the city of Sao Paulo: observations, modelling and impacts. Air Qual Atmos Health 10, 421–435 (2017).
[2] Carvalho, V.S.B. *et al.* Air quality status and trends over the metropolitan area of São Paulo, Brazil as a result of emission control policies. Environ. Sci. Policy, 47:68–79, 2015.
[3] Monteiro dos Santos, D. *et al.* Physical and chemical properties of urban aerosols in São Paulo, Brazil: links between composition and size distribution of submicron particles. Atmospheric Chemistry and Physics, 21(11):8761–8773, 2021.
[4] Oliveira, M.C.Q.D. *et al.* Air pollution persistent exceedance events in the Brazilian metropolis of Sao Paulo and associated surface weather patterns. Int. J. Environ. Sci. Technol. 19, 9495–9506 (2022).
[5] Schuch, D. *et al.* A two decades study on ozone variability and trend over the main urban areas of the São Paulo state, Brazil. Environ Sci Pollut Res 26, 31699–31716 (2019).
[6] Wagner, Annette *et al.* Comprehensive evaluation of the Copernicus atmosphere monitoring service (CAMS) reanalysis against independent observations: Reactive gases. Elem Sci Anth, 9(1):00171, 2021.
[7] Wang, Y. *et al.* Evaluation of the cams global atmospheric trace gas reanalysis 2003–2016 using aircraft campaign observations. Atmos. Chem. Phys., 20:4493–4521, 2020.

We thank FAPESP for their support (process number 2022/16238-5).

AIR POLLUTION CONFERENCE BRAZIL
CMAS SOUTH AMERICA
COMMUNITY MODELING AND ANALYSIS SYSTEM

DEVELOPMENT OF ENVIRONMENTAL QUALITY MONITORING SYSTEMS FOR SMART CITIES

Leila D. Martins[1], André F. Pastório[2], Mateus M. Roncaglio[2], Marcos V.R. da Silva[3], João C.M de Sá[3], Camili R.B.de Sá[3], Giuseppe D.P de Souza[3], Fábio A. Spanhol[3], Marcio S. Oyamada[2], Cleber A. Lindino[4], Alessandro B. Bovo[1], Paulo C. Gonçalves[5], Maria de Fátima Andrade[6], Edson Tavares de Camargo[3]

[1]*Federal University of Technology - Paraná (UTFPR) – Londrina, Brazil*
leilamartins@utfpr.edu.br, alessandrobovo@utfpr.edu.br
[2]*State University of Western Parana (UNIOESTE) – Cascavel, Brazil*
a.f.past@hotmail.com, engenheiromateusmaruzka@gmail.com, marcio.oyamada@unioeste.br
[3]*Federal University of Technology - Paraná (UTFPR) – Toledo, Brazil*
marcosviniciusrochadasilva@gmail.com, joaosa@alunos.utfpr.edu.br, camilirita1@gmail.com, giuseppediniz@alunos.utfpr.edu.br, faspanhol@utfpr.edu.br, edson@utfpr.edu.br
[4]*State University of Western Parana (UNIOESTE) – Toledo, Brazil*
lindino99@gmail.com
[5]*Federal University of Technology - Paraná (UTFPR) – Campo Mourão, Brazil,*
paulogoncalves@utfpr.edu.br
[6]*Institute of Astronomy, Geophysics and Atmospheric Sciences/University of São Paulo - IAG/USP, São Paulo - SP, Brazil*
mftandra@model.iag.usp.br

Abstract: **Introduction**: Environmental pollution is the leading cause of death worldwide. This problem is exacerbated by the pollution to which many people in urban areas are exposed. Another aspect is the high cost of purchasing and maintaining conventional monitoring stations, which makes networks with adequate spatial distribution economically impractical. To address this problem, low-cost sensors (LCS) have been proposed as an alternative. They have gained popularity and have been used worldwide for several purposes.
Objective: In this direction, the main objective of the EnvCity project (FAPESP, process 2020/05135-5) is to investigate LCS, their performance, and machine learning methods for data correction to support the development of a low-cost environmental quality monitoring system that provides real-time data and information.
Methods: The literature on LCS was reviewed using the main scientific databases and several intercomparison tests were conducted between LCS and reference stations or devices. Machine learning methods were evaluated as a tool to correct the dataset and were used to investigate and improve the performance of the measurements performed by the developed devices. The architecture of the system, firmware, circuit board and housing of the devices were also developed.
Findings: i) the LCS for air quality sensors are sensitive to measurements and suffer from the influence of temperature and relative humidity. To minimize these effects, they need to be housed in a box with sufficient size and air circulation in addition to the necessary corrections; ii) although some LCS are calibrated at the factory, the measurements should be corrected in the local; iii) the performance of LCS for particulate matter (PM) shows consistency between them; iv) machine learning methods for data processing are the most viable alternatives identified to correct the measurements; v) the cost of the DustAI developed for PM is about USD 320, while the station (CO, NOx, O3, SO2, PM) costs about USD 850; vi) the devices developed are plug-and-play devices, making sensor replacement more accessible and less expensive; vii) the use of low-cost air quality and particulate matter stations can be useful in locations with few or no reference stations, which, along with other ways of obtaining environmental data, contribute to the study of air pollution and health. We have also found interesting results for water quality. It can be emphasized that few studies have evaluated the sensors against reference devices in the applications and efforts should be made to conduct long-term studies for multiple comparisons in the laboratory and in the field. Also, studies need to be conducted to support the development of calibration and correction protocols for low-cost water quality devices. In addition, the network architecture has been developed with various dashboards to visualize the dataset, including the *EnvCity app* for mobile, with various features and tools from real-time data visualization to interactive map features and detailed reports. Finally, securing further financial support is crucial to improve the developed systems and facilitate their implementation in cooperation with public environmental agencies.

Keywords: low-cost sensors, water and air quality, internet of things, machine learning, particulate matter.

INTRODUCTION

Currently air pollution, both indoor and outdoor, is the greatest health risk. According to the World Health Organization (WHO) almost all the world's population has been living and breathing air above the security guidelines levels. However, around 40% of countries don't have systematic air quality monitoring. The high cost of acquiring and maintaining conventional monitoring stations makes networks with adequate spatial distribution economically unviable, especially in low-middle-income countries. To implement and mainly

evaluate the efficiency of public policies for mitigating air quality problems, the first step is to know the scope of the problem (in the spatial, time, and pollutants); therefore, air quality monitoring systems are imperative.

To deal with this issue low-cost sensors (LCS) have been pointed out as an alternative, have gained notoriety, and have been used worldwide for several purposes. In this direction, the main objective of the EnvCity project (FAPESP, process 2020/05135-5) is to investigate LCS, its performance, and machine learning methods for data correction to support the development of low-cost monitoring systems for environmental quality, including air and water quality, that provide real-time data and information in real-time (see Fig. 1). The objective overtakes the aid of the EnvCity project and consists of a study topic.

METHODS

The literature on LCS was revised using the main scientific databases and several intercomparison tests between LCS and reference (equipment) stations were performed. As a tool to correct the dataset, machine learning methods were evaluated and used to study and improve the performance of the measurements done by the devices developed. The system's architecture, the firmware, the printed circuit board, and the case of devices were also developed.

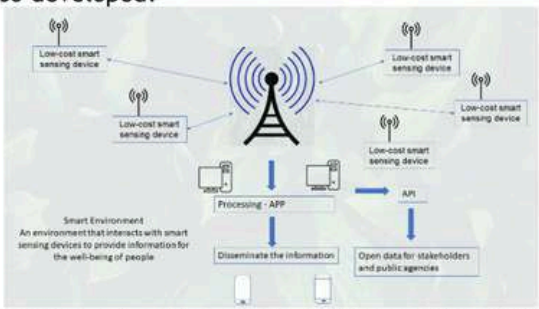


Figure 1. The concept of environmental quality monitoring for a smart Environment.

For air quality were evaluated five LCS of particulate matter (PM): SDS011, SDS018, HPMA115S0, PMS7003, and MIX6070, which cost around $20 and use the light scattering principle (Pastório, et al., 2022). For other classical pollutants, we use Alphasense B family sensors (CO-B4, NO2-B43F, OX-B431, SO2-B4) and its ISB (Individual Sensor Board). The prototypes, one for PM and another for air quality target pollutants (a low-cost air quality station) were developed. The description of DustAI (Monitor de Material Particulado de Baixo Custo com Calibração via Aprendizado de Máquina) prototype development can be found in Pastório (2023), while the development of the low-cost air quality station in Roncaglio et al., (2023). The prototypes were evaluated with a colocation procedure and using machine learning methods to correct the measurements. The DustAI measurements were compared with Beta Attenuation Monitor (BAM 1020 Met One Instruments) from Aires Serviços Ambientais in Vitória, ES; while the air quality station gas measurements (March to June, 2023) were compared with Thermo-Fisher Model 42i NOx Analyzer, Model 48i CO Analyzer, Model 49i Ozone Analyzer and Model 43i SO2 Analyzer that is part of a reference station (LuMIAR, mobile laboratory for air quality monitoring and research), located at the University of São Paulo School of Medicine.

For water quality, it was developed a first prototype (Xavier et al., 2022) that has been supporting other developments. The device consists of a floating buoy with electronic components, sensors, and a transmission system. The parameters selected for measurement were temperature, dissolved oxygen, pH, and turbidity, with SEN0189 water turbidity sensor (US$9.90), ENV-50-DO dissolved oxygen sensor (US$234.99), SEN0237 dissolved oxygen sensor (US$169.00) and SEN0161-V2 pH sensor (US$39.50).

FINDINGS AND ARGUMENT

The results for low-cost air quality station indicate that the random forest (RF) machine learning method is able to correct the measurements done by station (see Figure 2a). As an example, Figure 2b shows the Ozone (O_3) concentration of reference and those corrected with the trained RF model through the last 15 days of June.

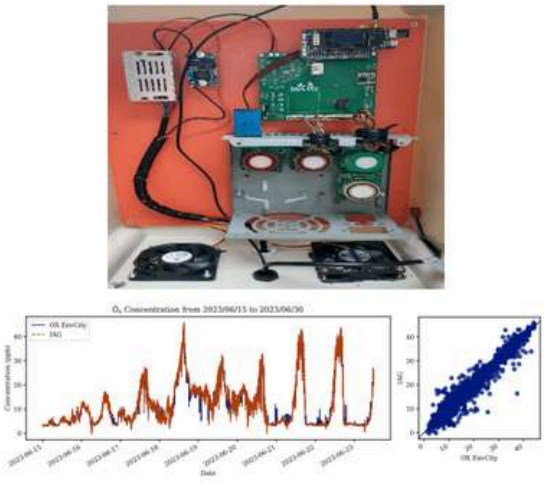


Figure 2. EnvCity low-cost air quality station. A) Photography of prototype. B) O_3 concentrations predicted by RF (blue line) in comparison with reference (red line). Adapted from Roncaglio et al., (2023).

The cost estimated for the DustAI prototype is around 320 US$ (see Figure 3). The machine learning methods applied indicated a great improvement in the performance, with RF resulting in the highest correlation.



Figure 3. DustAI monitor. Adapted from Pastório (2023).

Figure 4 presents an example of PM_{10} concentrations measured by LCS without any correction (Fig. 4A) and those corrected (or calibrated) by RF model (Fig. 4B).

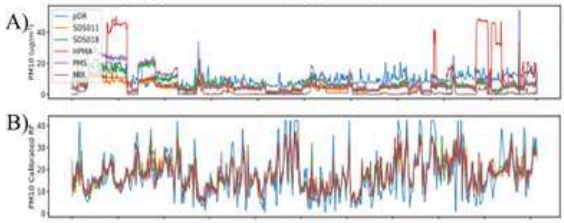


Figure 4. PM_{10} concentrations. A) measured by the LCS (raw data) and B) After corrected by RF method (reference values in blue). Adapted from Pastório et al., (2022).

For water quality, we also found interesting results, among them is those presented in the systematic review of low-cost water quality sensors for IoT (De Camargo et al., 2023). The results indicated that most of the work uses commercial sensors such as those from Atlas Scientific, Vernier, and DfRobot, and only some works have made comparisons with reference devices. However, the applications are growing fast (19 works in 2019 against 64 in 2022) for measurements (56) on natural water bodies, with a specific emphasis on rivers (23), lakes, and ponds (18). In another study, which is currently under review, comparisons were made between LCS and reference values, the results of which demonstrate the accuracy of LCS. The error found was generally ≤ 5% for most LCS.



Figure 5. Example of visualization provided by *EnvCity app*.

Finally, as a result, the network architecture with several dashboards to visualize the dataset was developed, including the *EnvCity app* (see Fig. 5) for mobile, with various features and tools from real-time data visualization (air and water variables) to interactive mapping capabilities and detailed reporting.

CONCLUSIONS

In conclusion, low-cost air quality and particulate matter stations can be useful in low-density locations or without reference stations. Together with other ways of obtaining environmental data, they help to improve monitoring and are recommended for the study of air pollution and health. Combining several low-cost stations with some reference stations and machine learning methods is our recommendation to improve air quality monitoring. For water quality, we believe that LCS sensors presented accuracy enough to be used as a complementary alternative to measuring water quality parameters. Finally, it is essential to obtain additional support for the optimization of the developed systems (e.g., to perform tests with other sensors, to create technical guides, measurement and maintenance procedures, and calibration protocols) and to enable the solution to be implemented and evaluated in collaboration with public environmental authorities.

REFERENCES

De Camargo, E.T., Spanhol, F.A, Slongo J.S., et al. (2023). Low-cost water quality sensors for iot: A systematic review. Sensors 23(9).

Pastório, A.F., Spanhol, F.A., Martins, L.D. De Camargo, E.T. "A machine learning-based approach to calibrate low-cost particulate matter sensors." Paper presented at XII Brazilian Symposium on Computing Systems Engineering (SBESC), Fortaleza, Ceará, Brazil, November, 21-24, 2022.

Pastório, A.F. "DustAI: Monitor de Material Particulado de Baixo Custo com Calibração via Aprendizado de Máquina" MSc. diss., Unioeste, Cascavel, 2023.

Roncaglio, M.M., De Camargo, E.T., Martins, L.D. Oyamada, M. S. "Development of an air quality station using low-cost sensors." Paper presented at XIII Brazilian Symposium on Computing Systems Engineering (SBESC), Porto Alegre, RS, Brazil, November, 21-24, 2023.

Xavier F., Martins L.D., Oyamada M.S., et al. "Evaluation of low-cost sensors for real-time water quality monitoring." Paper presented at XII Brazilian Symposium on Computing Systems Engineering (SBESC), Fortaleza, Ceará, Brazil, November, 21-24, 2022.

AIR POLLUTION CONFERENCE BRAZIL
CMAS SOUTH AMERICA
COMMUNITY MODELING AND ANALYSIS SYSTEM

MEASURING INDOOR AIR QUALITY IN RETAIL STORES: RECOMMENDATIONS BASED ON FIELD EXPERIENCE

Leonardo Furst [1], Yago Cipoli [1], Getúlio Igrejas [3 4], Manuel Feliciano[2 4], Célia Alves [1]
[1]Centre for Environmental and Marine Studies (CESAM), Department of Environment, University of Aveiro, 3810-193 Aveiro, Portugal
[2]Centro de Investigação de Montanha (CIMO), Instituto Politécnico de Bragança, Campus de Santa Apolónia, 5300-253 Bragança, Portugal
[3]Centro de Investigação em Digitalização e Robótica Inteligente (CeDRI), Instituto Politécnico de Bragança, Campus de Santa Apolónia, 5300-253 Bragança, Portugal
[4]Laboratório Associado para a Sustentabilidade e Tecnologia em Regiões de Montanha (SusTEC), Instituto Politécnico de Bragança, Campus de Santa Apolónia, 5300-253 Bragança, Portugal

Abstract: In recent years, there has been a growing awareness of the effects of indoor air quality (IAQ) on human health, driven by the various pollutants that can accumulate in enclosed spaces, including particulate matter (PM), volatile organic compounds (VOCs), carbon dioxide (CO_2), carbon monoxide (CO), and microorganisms. IAQ in retail shops has been a topic of interest for researchers, with most studies centring on establishments that are prone to high indoor pollutant levels, such as restaurants and waterpipes cafes. Monitoring IAQ in a retail store is essential for ensuring a comfortable and healthy environment for both customers and employees. Retail stores are physical establishments that directly sell a wide range of products to consumers, including department stores, supermarkets, boutiques, convenience stores, and many more. In this regard, this work discusses the challenges of monitoring air quality in retail shops, based on measurements obtained from different establishments, such as a gardening and home improvement store, a clothing store, and a supermarket. Also, ways to improve air quality monitoring procedures are highlighted. When it comes to installing an IAQ monitoring system, there are several key factors to consider. One of the most important is the physical space where the equipment will be located. It is crucial to ensure that the monitoring system does not interfere with the normal functioning of the shop or business. This will largely depend on the size of the equipment being used. For instance, compact IAQ stations can be easily installed on walls, columns or above shelves, while larger equipment like gravimetric samplers and gas analysers may require their own structures. It is also desirable that the system is not installed too close to the walls. In the case of small stores, the system may be positioned in the centre of the store for greater representativeness, while in larger stores, such as supermarkets, the system should be installed in different sections for wider sampling. It is important to also consider the power source needed for the equipment. For optimal performance, it is advisable to install IAQ monitoring systems near a power source to ensure uninterrupted operation. However, power outages can occur, which can disrupt data collection. Therefore, it is recommended to use an uninterruptible power supply (UPS) to prevent any disturbances when the region does not have a stable power grid. In a silent retail store, such as a pharmacy or clothing store, any noise generated can be quite disruptive. So, it is important to ensure that equipment is insulated to reduce noise, especially those with electric motors or vacuum pumps. The use of an acoustically insulated cabinet can be a useful solution in such cases. Additionally, appearance and safety are two other factors to consider. A visually interesting equipment can attract unwanted attention and tampering, especially in crowded areas with children. Also, in places where safety is a concern, it is necessary to install a cabinet with a locking mechanism to ensure the safety of the equipment. Still considering equipment safety and maintenance, if the location is prone to insects, installing a PTFE net at the air inlet is highly recommended to prevent them from entering the equipment and damaging it. Additionally, with the advancement of compact air monitoring stations, having Wi-Fi connectivity on site can be extremely beneficial, allowing for real-time data visualisation and reducing the need for frequent operator visits to the site.

Keywords: IAQ, air pollutants, instrumentation, sampling, recommendations

Acknowledgements: The authors are grateful to the Foundation for Science and Technology (FCT, Portugal) for financial support by national funds FCT/MCTES to CESAM (UIDP/50017/2020, UIDB/50017/2020 and LAP/0094/2020), SusTEC (LA/P/0007/2020), CIMO (UIDB/00690/2020), CeDRI (UIDB/05757/2020 and UIDP/05757/2020) and to PhD fellow students Leonardo Furst (SRFH/BD/08461/2020) and Yago Cipoli (SFRH/BD/04992/2021).

INTRODUCTION

Indoor air quality has substantial implications for human health and wellbeing (Tham, 2016). To ensure data quality and support meaningful interpretations, it is essential to plan thoroughly the indoor air study. This involves careful consideration of factors such as target pollutants, instrument selection, temporal and spatial sampling strategies, calibration procedures, and data analysis. While established guidelines exist, identifying best practices and developing measurement protocols remain an essential part of the scientific progress. This study examined the challenges associated with the practical implementation of IAQ monitoring, based on field experience, and seeks to provide recommendations to facilitate IAQ measurement in retail stores.

INDOOR AIR POLLUTANTS

Indoor air quality can be impacted by several pollutants such as CO_2, VOCs, particulate matter, NO_X, CO, and microorganisms. Some of these are easier to measure due to the availability of equipment for the usual concentration ranges. CO_2 is one of the most studied pollutants since it can be used to check air ventilation and indoor air quality overall. The accumulation of CO_2 implies a low air change rate, and probably the concomitant increase in concentration of other air pollutants. VOCs can be measured for their total concentration (TVOCs) or can be speciated. Speciation provides information on individual concentrations, which can help identifying sources of potentially harmful compounds. However, this last option has a high associated cost. Particulate matter is usually measured using gravimetric sampling, which requires one filter to be weighted before and after collection. It is more precise, but do not provide short time resolution. For this, particulate matter monitors based on optical principles can be used to measure both PM mass and number concentrations.
Before selecting which pollutants to measure, it is necessary to carry out a prior inspection of the store's specific environment. For instance, waterpipe cafes are known to have high levels of particulate matter and VOCs. In bakeries, workers are exposed to high concentrations of particulate matter, which can lead to respiratory diseases with chronic exposure.

SYSTEM INSTALATION

To set up an indoor air quality system, two important factors are the instruments required (or available) for the study and the conditions of the store. The first requirement for instrumentation is energy. Depending on the type of instrument, there may be a high energy consumption, such as in the case of high-volume particulate matter samplers that operate with a strong pump. This makes it very unlikely to rely on batteries. However, this requirement is usually not a problem as retail stores have access to power. In areas where power outages are frequent, it is recommended to use an uninterruptible power supply (UPS). The capacity of the UPS should match the power needs of the equipment, or at least for those that are desired to remain on.
Another important factor to consider is the noise level of the equipment. The ISO 16000-1 (ISO, 2004) states that low noise levels are an important factor for indoor environments. Gas analysers and particulate matter samplers tend to generate high levels of noise, which can be disruptive and unpleasant for both clients and employees. In some cases, the noise level may be lower than the ambient noise of the building, but in other instances, it is necessary to isolate the instruments to reduce the sound. This can be achieved using materials such as wooden boxes or polystyrene foam. However, it is important to monitor the equipment operation as this may cause overheat during long-term operation.
Attention must be paid to the height at which air quality measurements are taken, particularly measurements of the breathing zone. Several guidelines provide recommendations for the ideal height. According to ASHRAE 62.1 (ASHRAE, 2022), the breathing zone height indoors should be between 7,5 and 180 cm, and no closer than 60 cm from walls. The Directive 2008/50/EC (European Union, 2008) suggests placing the air inlets for microscale measurements between 1.5 to 4 m, and taking breathing zone measurements between 1.5 to 2 m. Similarly, the ISO 16000-1 (ISO, 2004) recommends a height between 1.0 and 1.5 m, and no closer than 1 m from walls. For larger rooms, multiple location measurements are recommended.
A review of CO_2 measurement procedures conducted by Mahyuddin & Awbi (2012) found that the most common height of measurement in articles was from 1.0 to 1.2 m, with the second most common height being between 1.3 and 1.8 m.
Also, it is important to consider the security of the monitoring system, especially if it is installed in a location that is easily accessible by clients and employees. People may be curious and try to explore or press buttons. To avoid this, it is recommended to add a plate explaining the purpose of the system and a sign not to touch it or even warning of danger. Also, the employees should be informed about the system to avoid any interference without prior communication.
Another point, often overlooked, is the presence of insects. In certain cases, insects can enter the equipment, usually in those that require an air intake. This problem is normally more serious in optical particle monitors, which have no filter before the optical cell. This can result in interference on the detection system or even cause an obstruction, requiring the equipment to be repaired. In particulate samplers, insects that enter the air inlet will be stopped by the sampling filter, which will lead to contamination and loss of the sample. In those cases, it is necessary to install a mesh at the air inlet, ideally from PTFE. Figure 1 show a summary of the important factor when monitoring indoor air quality.

CONCLUSIONS

The retail industry is a diverse sector that encompasses various types of businesses. Some of these, such as restaurants, cafes, shopping malls, and laundries, have more sources of emissions, and therefore, have been studied in greater depth. However, there are several types of stores that have been less studied, or do not have indoor air quality detailed studies. Additionally, there are numerous franchises around the world, and studying the air quality in these stores would not only provide a local

perspective but also give an idea of the air quality in these buildings globally.
And to reach that goal is essential to know how to install a monitoring system and the main challenges faced during the research.

REFERENCES

ASHRAE. (2022). ANSI/ASHRAE 62.1-2022, Ventilation and acceptable indoor air quality.

European Union. (2008). Directive 2008/50/EC of the European Parliament and of the Council of 21 May 2008 on ambient air quality and cleaner air for Europe.

ISO. (2004). ISO 16000-1:2004 Indoor air Part 1: General aspects of sampling strategy.

Mahyuddin, N., & Awbi, H. (2012). A Review of CO 2 Measurement Procedures in Ventilation Research. International Journal of Ventilation, 10(4), 353-370. https://doi.org/10.1080/14733315.2012.11683961

Tham, K. W. (2016). Indoor air quality and its effects on humans—A review of challenges and developments in the last 30 years. Energy and Buildings, 130, 637-650. https://doi.org/10.1016/j.enbuild.2016.08.071

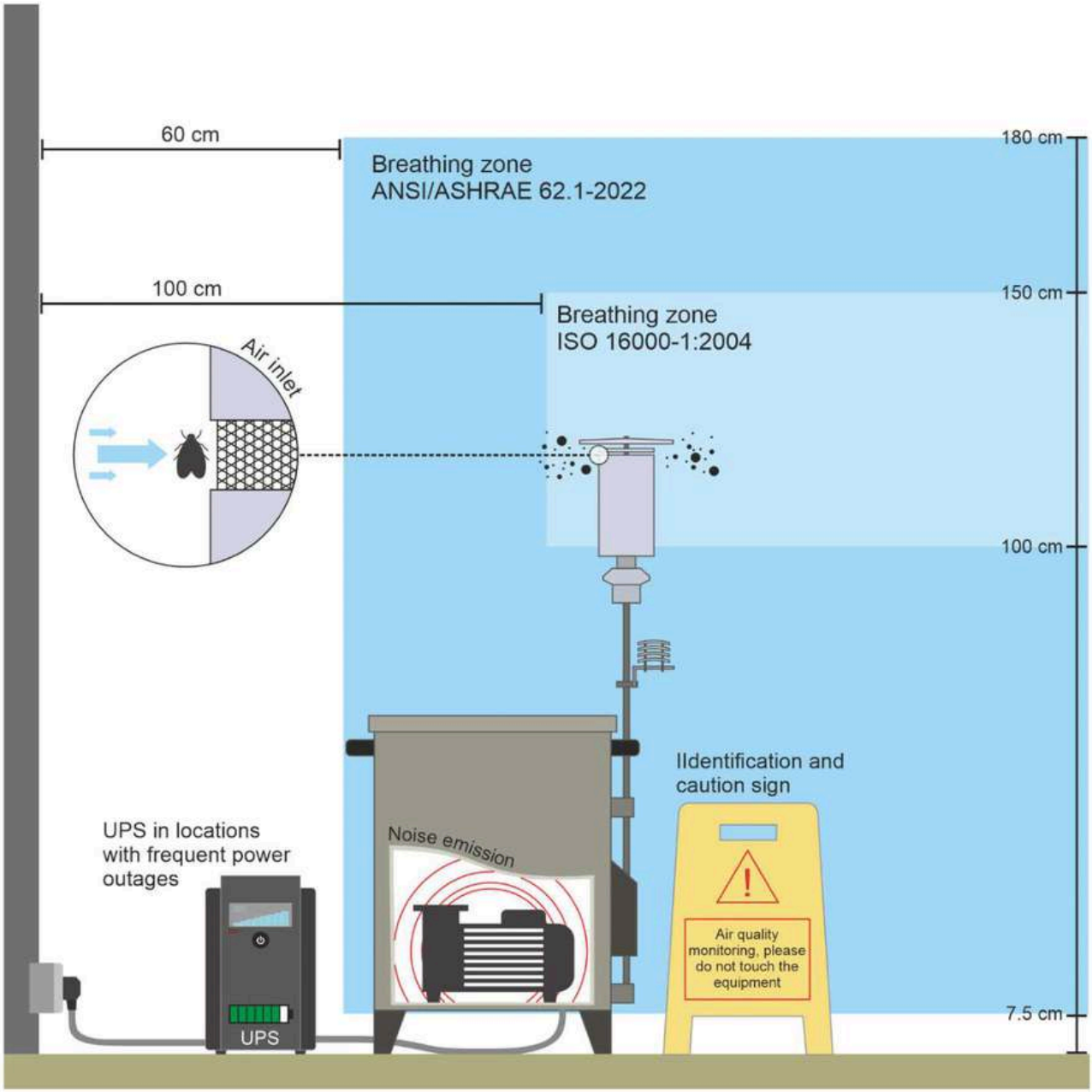


Figure 1. Important factors for air quality sampling in retail stores

AIR POLLUTION CONFERENCE BRAZIL
CMAS SOUTH AMERICA
COMMUNITY MODELING AND ANALYSIS SYSTEM

MODELING AND SCENARIO ANALYSIS APPLIED TO THE DYNAMICS OF LAND USE AND TRANSPORT USING CELLULAR AUTOMATA AND LANDSAT DATA

F. R. Teixeira[1], P. J. Pérez Martínez[1], R. M. Miranda[2] (10 font size)
[1]*Faculty of Civil Engineering, University of Campinas, Rua Saturnino de Brito, 224, Cidade Universitária Zeferino Vaz, CEP 13083-889, Campinas, Brazil.*
E-mail f150041@dac.unicamp.br ; pjperez@unicamp.br
[2]*Department of Astronomy, Geophysics and Atmospheric Sciences, University of São Paulo, Rua do Matão, 1226. CEP 05508-090, São Paulo, Brazil.*
E-mail remaura@usp.br

Abstract: Interactions involving land use and transport have been increasingly studied by researchers who deal with dynamic phenomena, in favor of global sustainability. One method that represents this phenomenon consists of the Land Use Transport Interaction - LUTI model, which provides predictions of these interactions and identifies causal relationships for policy formulation. LUTI models identify the patterns that best relate land use to transport, projecting the evolution of the urban area. The goal of this research is to obtain a calibrated dynamic model capable of simulating scenarios, based on the interaction of land use and transport, in the Metropolitan Region of São Paulo. The application of the NDBI index demonstrated a high capacity to discretize natural and artificial materials, resulting in excellent separability, generating negative values on surfaces formed by vegetation and positive values for built-up areas. This result indicated that the NDBI index is the most appropriate choice for use in the band difference method, when used in the change detection algorithm, highlighting the type, extent and location of the change for each pixel in this time series. The generated product consists of a change detection output raster file, which represents the difference in pixels between scenes, the type or intensity of the change. The samples of changes that represent expansion and densification showed high separability with the application of the M statistical test, regarding the separability capacity of the NDBI index in discretizing the classes of changes. The scars of the changes was be used as references for collecting and training pixels, in Landsat reflectance scenes, for use in the Deep Learning supervised classification method (Figure 3a), consisting of three phases: 1st) Sample training, 2nd) Deep Learning model training and 3rd) Performance. As a result, a specific land use classification model will be obtained for the RMSP, .dlpk file (Depp Learning Package). The raster classified by the ".dlpk" model and other transport parameters (accessibility, distance traveled, gradient between roads and transport zones) will be used as input parameters for the AC - TRAZ model, for calibration, optimizing the characteristics of the RMSP. As a future perspective, transition maps between the real and the simulated will be generated to support the formulation of policy and urban planning.

Keywords: Change detection, Deep learning, Dynamic systems, Accessibility, Public policy.

INTRODUCTION

The dynamics of urban sprawl have been increasingly affected by the economy, promoted through changes in land use, which require new technologies to improve the efficiency of transport systems, for a more compact environment, constituting one of the greatest challenges for global sustainability (Yan et al., 2020).

Cities that show intense growth in the road vehicle fleet are impacted by atmospheric pollution, making air quality more degraded in peripheral regions, with the export of sources of Greenhouse Gas (GHG) emissions and pollutants from the urban core to these regions of the surroundings (Pérez-Martínez et al., 2022).

One of the points explored in urban mobility studies is how the transport system is affected by changes in the territory and estimating how new developments in transport and land regulation can interfere by modifying human activities and land uses (Guzman et al., 2020).

The method used to deal with this problem consists of the interaction model of land use, transport and environment, called LUTI - Land Use Transport Interaction, which was developed with the purpose of providing predictability of interactions based on development and accessibility. of the transport system, (Cordera et al., 2018). LUTI models, in addition to providing a predictive approach to planning, are appropriate for identifying causal relationships at all levels and domains for decision-making in policy formulation for the benefit of society (Kii et al., 2019).

The development of models that simulate reliable scenarios for large metropolises is necessary to analyse the impacts of changes at various levels, caused by economic transformations and changes in land use (Li et al., 2017).

Based on this approach, this research aims to obtain a calibrated dynamic model, based on cellular automaton (CA), which relates the interactions of land use and transport, simulating scenarios of the evolution of the urban area, in the Metropolitan Region of São Paulo (RMSP). To achieve this objective, this research presents the following specific objectives: 1) Increase performance in change detection, with the algorithm optimized for

urban surfaces, in relation to the separability of classes of changes and land uses; 2) Obtain optimal calibration parameters for the TRAZ (Transport Zones) dynamic model, which relates land use and transport, when applied to RMSP; 3) Obtain maps with the transition potential, based on trends and model performance, representative of the RMSP, relating the level of transition potential and future transformation, with the transport and building infrastructure projects foreseen in the master plan and the development plan urban Development.

METHODS

This research is organized into four sessions: 1st) Systematic literature review and definition of the data set; 2) Treatment of spectral data; 3rd) Model calibration and simulations; 4th) Scenario analysis.
To assist in the spectral characterization of targets on the surface, data relating to the spectral properties of natural and artificial materials were obtained according to the following classification from the ECOSTRESS library (Figure 1 e 2).

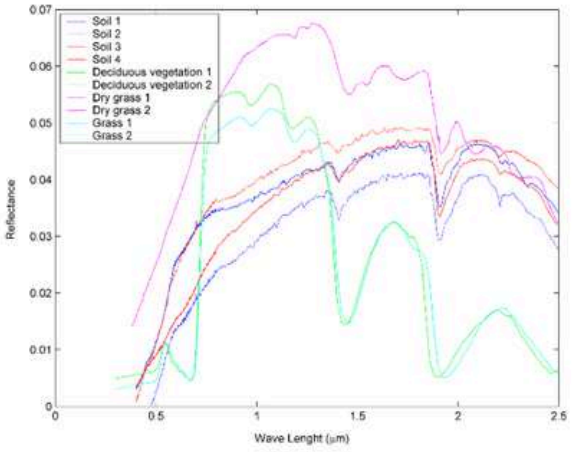


Figure 1: Reflectance curve of ECOSTRESS natural materials. Elaboration in Octave.

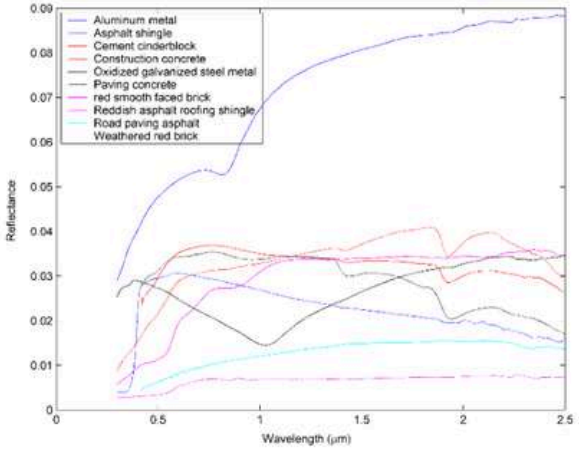


Figure 2. : Reflectance curve of ECOSTRESS artificial materials. Elaboration in Octave.

The purpose of using the ECOSTRESS spectral library is to form a reference of the spectral behavior, with specific patterns, of materials of known constitution. In Figure 1, the spectral curve of natural materials in SWIR-2 (2.1μm) showed a drop in the brightness response. For this reason, the reflectance in the SWIR-1 band in the short-wave infrared was better evaluated for characterizing the materials of the analyzed surfaces, together with the NIR band in the near-infrared for natural surfaces.
The NIR and SWIR-1 bands, present in the TM/Landsat and OLI/Landsat sensors, have a sensitive response function for spectral characterization of changes in land use, with most artificial materials in built areas being detected with greater band response in SWIR-1(1.6μm) due to increased spectral information.
The sensor response function provides quantitative information corresponding to the spectral bands that each sensor is most sensitive to the phenomenon of interest, that is, how the satellite sensor detects a surface feature in each spectral band (Figure 3). Furthermore, SWIR-1 is considered one of the parameters of Equation 1 used in calculating the NDBI index (Normalized Difference Built-Up Index) to discretize built-up areas.

$$\mathrm{NDBI} = \frac{(\mathrm{SWIR1}-\mathrm{NIR})}{(\mathrm{SWIR1}+\mathrm{NIR})} \quad (\mathrm{Eq.}\,1)$$

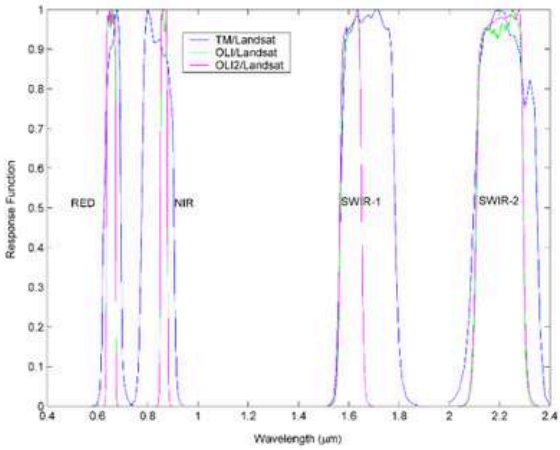


Figure 3. Graph with the response function of the Landsat series sensors. Elaboration in Octave.

FINDINGS AND ARGUMENT

The NDBI values are the result of a ratio operation between bands, based on surface reflectance values, which aims to minimize the variation of these reflectances throughout the time series, for lower ratio index values, achieving greater consistency of the values in each pixel, with the smallest variation between dates.
The result of the change detection process in Figure 4 (a) e (b) is expressed in NDBI values from the method of difference between bands of TM/Landsat and OLI/Landsat sensor images obtained in the years 1985-2010 and 2013-2023, highlighting the

type, extent and location of the change. change for each pixel in this time series.

NDBI values are represented on a scale from -1 to 1, with positive values represented by built areas and negative values by vegetation. A Figure 4 (a) e (b) shows the areas with positive NDBI values, resulting from a filtering of negative values during the application of the change detection algorithm using the frequency histogram. The areas represented in red with NDBI values indicate that expansion of the urban area is occurring in regions where changes are detected from some non-urbanized class to low or medium density built areas.

These changes occur as a result of the degree of anthropization, originating from transformations of surfaces covered by vegetation or exposed soil, to a built surface, as can be seen in Figure 4 (a), with the inauguration of Guarulhos airport in 1985 and the transformations until 2010. These NDBI values may also indicate densification, starting from a transition from a low-density built area to a medium or high-density built area.

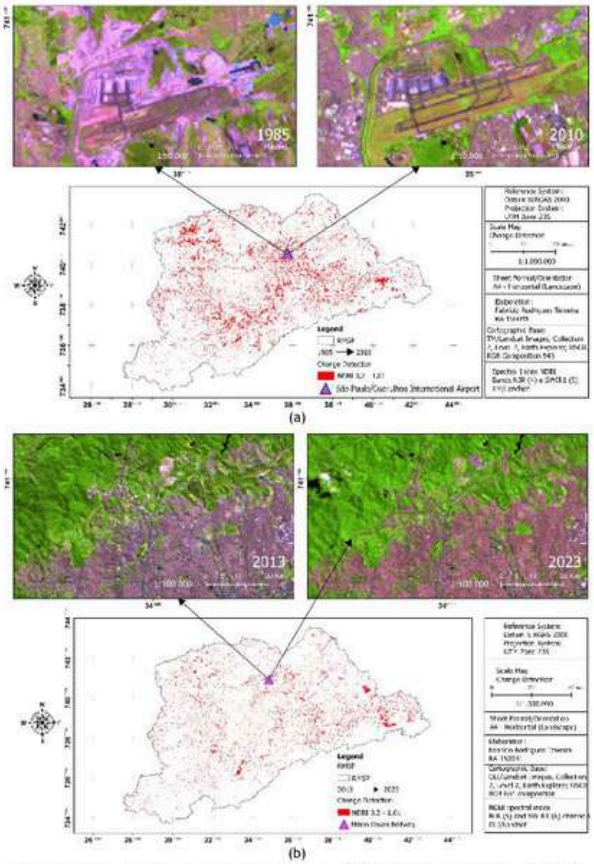


Figure 4. Change detection (a) TM/Landsat 1985-2010 (b) OLI/Landsat 2013-2023.

CONCLUSIONS

The generated product consists of a change detection output raster file, which represents the difference in pixels between scenes, the type or intensity of the change. As a future perspective, changes that represent expansion and densification will be subjected to statistical testing using the M index to test the separability capacity of the NDBI index in the discretization of classes of changes. The scars of the changes will be used as references for collecting and training pixels, in Landsat reflectance scenes, for use in the Deep Learning supervised classification method, consisting of three phases: 1st) Sample training, 2nd) Deep Learning model training and 3rd) Performance. The product of this classification and other transport parameters (accessibility, distance travelled, gradient between roads and transport zones) will be used as input parameters for the AC - TRAZ model (Figure 5), for calibration, optimizing the characteristics of the RMSP.

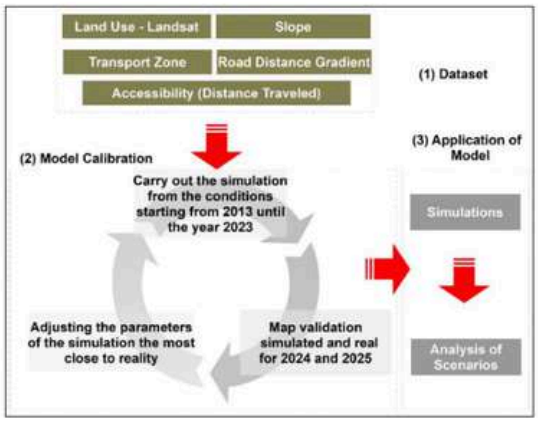


Figure 5. Steps for applying the RMSP cellular automata model. Prepared by the author.

REFERENCES

Cordera, R., Ibeas, Á., dell'Olio, L., & Alonso, B. (2017) Land Use-Transport Interaction Models (1st ed.). CRC Press.

Guzman, L. A.; Escobar, F.; Peña, J.; Cardona, R. (2020) Cellular automata-based land-use model as an integrated spatial decision support system for urban planning in developing cities: The case of the Bogotá region. Elsevier, *Land Use Policy*, 92, 104445.

Kii, M., Moeckel, R., & Thill, J.-C. (2019) Land use, transport, and environment interactions: WCTR 2016 contributions and future research directions. *Computers, Environment and Urban Systems*, *77*, 101335.

Li, X., Yu, L., Sohl, T., Clinton, N., Li, W., Zhu, Z., Liu, X., & Gong, P. (2016) A Cellular Automata downscaling based 1 km global land use datasets (2010-2100). *Science Bulletin*, *61*(21), 1651-1661.

Pérez-Martínez, P. J., Dunck, J. A., de Assunção, J. V., Connerton, P., Slovic, A. D., Ribeiro, H., & Miranda, R. M. (2022). Long-term commuting times and air quality relationship to COVID-19 in São Paulo. *Journal of transport geography*, *101*, 103349.

Yang, J.; Gong, J.; Tang, W.; Liu, C. (2020). Patch-based cellular automata model of urban growth simulation: Integrating feedback between quantitative composition and spatial configuration. *Computers, Environment and Urban Systems*, n. 79.

AIR POLLUTION CONFERENCE BRAZIL
CMAS SOUTH AMERICA
COMMUNITY MODELING AND ANALYSIS SYSTEM

ESTIMATIVE OF URBAN PLUME DISPERSION PARAMETERS FOR THE CITY OF MANAUS BASED ON AIRPLANE OBSERVATIONS

Artur Libanio de Araujo Yordaky[1], Luciana Varanda Rizzo[2]
[1]*University of São Paulo*
arturyordaky@usp.br
[2]*University of São Paulo*
lrizzo@usp.br

Abstract: The pollutants emitted from the city of Manaus, an industrialized city in the central region of the Amazon, form an urban plume that can be tens of kilometers long. This Scientific Initiation project uses airplane data from the GoAmazon2014/5 experiment in order to estimate dispersion parameters of pollutants for the wet season, focusing on NOx, CO and particle number concentration. With the implementation of a Gaussian plume model, dispersion along both longitudinal and transversal directions is analyzed. Results show that NOx disperses more rapidly than the other pollutants studied. Finally, NOx emission rate was estimated through the cross-sectional flux method and the value obtained was 1.4 kg/s.

Keywords: Amazon, urban emissions, air pollutants, urban plume.

INTRODUCTION

In the central region of the Amazon, Manaus is a highly industrialized city that daily emits tons of pollutants that disperses through its surroundings, which are mostly rainforest, and form an urban plume which can be tens of kilometers long. This interaction between anthropic and natural pollutants has been a subject of scientific research for the last decades. Based on this, this Scientific Initiation project aims to estimate the dispersion parameters of the urban plume of the city of Manaus using airplane data obtained in situ by the GoAmazon2014/5 experiment [1]. Obtaining these parameters is a necessary step towards a better understanding of the impacts of the urban plume on the forest and on the regional climate.

METHODS

Average horizontal distributions of the concentration of the pollutants NOx (nitrogen oxides), CO (carbon monoxide) and N (particle number concentration) were evaluated over an area of about 1x1° in the downwind region of Manaus, during the wet season in 2014, when the aircraft measurements of the GoAmazon2014/5 experiment [1] were carried out (Fig. 1). Spatially interpolated aircraft data was used from 16 flights carried out during the wet season [2] (Fig. 2). In the interpolation, only observations made below 1500m altitude were considered in order to incorporate only data within the Planetary Boundary Layer (PBL), in which it is assumed that there is a vertical homogeneity of concentration. Thus, the data can be analyzed considering only latitude and longitude, in a plane.

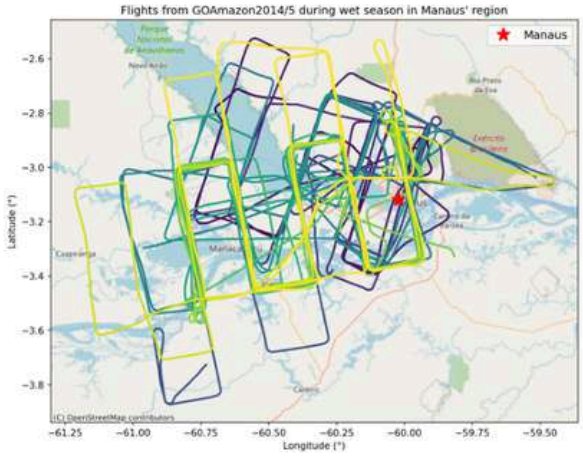


Figure 1. GoAmazon 2014/5 flights trajectories around Manaus for the wet season. For this plot, it was only considered data with altitude below 1500m.

Using an article [3] as a basis, a plume mask model was used to establish which data belong to the plume and which do not. From this, the centerline of the plume (which is aligned with the average wind direction) was determined by the weighted average of the concentration along the plume. A linear regression was used to obtain the plume center line. The next step was to apply the gaussian plume model. Concentration data was retrieved from this line and an exponential function (Eq. 1) was fitted, representing the attenuation of air pollutant concentration as a function of the distance from the emission source. In addition, the dispersion of concentration along transversal lines was analyzed by fitting a gaussian function to the data (Eq. 2). In the equations below, z represents the concentration, x and y represent distances along the plume central and

transversal lines, and a, b, c, d, σ are coefficients to be fitted.

$$z(x) = ae^{bx} + c \quad (1)$$

$$z(y) = ae^{-\frac{1}{2}\left(\frac{y-c}{\sigma}\right)^2} + d \quad (2)$$

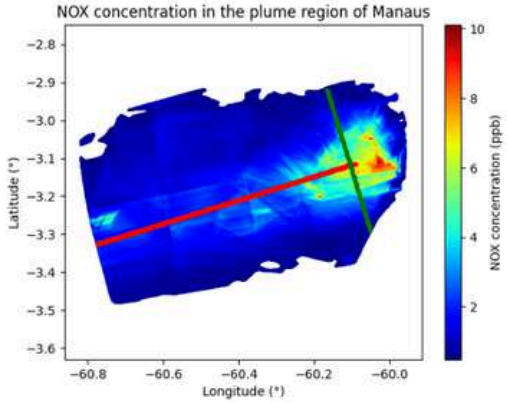


Figure 2. Average distribution of NO_X concentrations downwind the Manaus city in the wet season of 2014. The red line represents the plume center line.

The cross-sectional flux method [3] was used to estimate the emission rate of NOx based on the average spatial distribution of the urban plume. The emission rate (Q) was calculated by the integration of the concentration (z) minus the background (z_b) observed along a transverse line within the plume, multiplied by the average wind speed (U) and PBL height (h), estimated as 1000 m (Eq. 3).

$$Q = Uh\sum_j (z_j - z_b)\Delta y_j \quad (3)$$

This equation is valid under the assumptions that wind is constant along the transverse line and that the concentration is constant vertically inside the PBL. Aircraft measurements of wind speed and direction were linearly interpolated to retrieve the necessary information. The data was processed and analyzed using Python codes.

RESULTS AND DISCUSSION

The method for obtaining the dispersion parameters was applied for NOx, CO and N. The dispersion parameters in the plume center line (x) and transversal line (y) are represented by b and σ , respectively. The transversal line analyzed in this work is centered in the point (-60.74°, -3.32°). As shown in Tab. 1, the parameter b indicates that the attenuation of NOx along the plume centerline occurs faster than the other pollutants. This is expected, as NOx is highly reactive, suffering chemical loss in addition to turbulent dispersion as the plume moves downwind Manaus. In the transverse direction, the dispersion coefficients (σ) were similar for the three air pollutants.

Table 1. Dispersion parameters of pollutant concentration along the directions longitudinal (b) and transversal (σ) to the plume, and R^2.

Pollutant	b (Km^{-1})	R^2	σ (Km)	R^2
NOx	-0.127	0.91	8.14	0.96
CO	-0.0754	0.96	7.64	0.96
N	-0.0552	0.95	6.65	0.97

Analyzing the exponential fits, represented by Figure 3, R^2 varied between 0,91 and 0,96, while for the gaussian fits, shown in Figure 4, it ranged from 0,96 to 0,97. This shows that the gaussian plume model was adequate to the dataset.

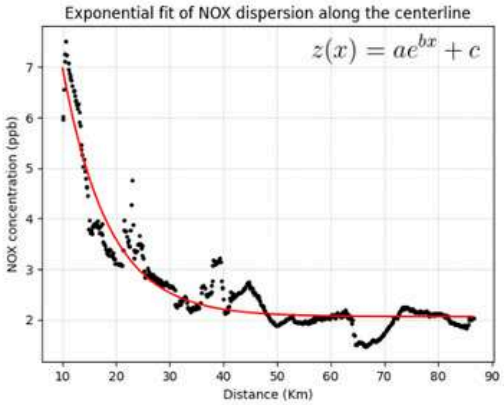


Figure 3. Exponential fit of NOX dispersion along the centerline shown in Fig. 2.

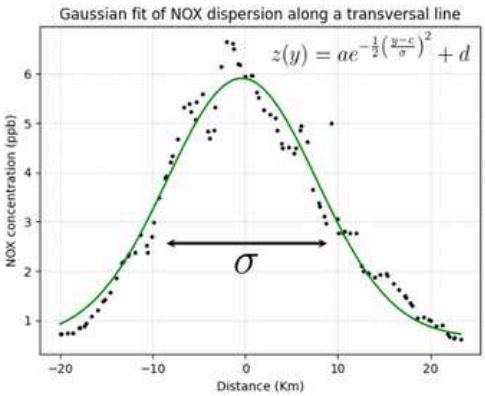


Figure 4. Gaussian fit of NOX dispersion along the transverse line shown in Fig. 2.

Fig. 5 shows the linear interpolation for the wind. The wind direction was homogeneous, consistent with the plume central line and with the expected circulation during the wet season [1]. The wind magnitude was 6(1) m/s. Based on the

cross-sectional flux method, the NOx emission rate was estimated in 1.4 kg/s. In comparison, previous research by Medeiros et al. (2017) estimated the NOx emission rate as 0.60 kg/s [4]. This is a preliminary result that could be improved by refining the representation of the vertical distribution of NOx in the PBL.

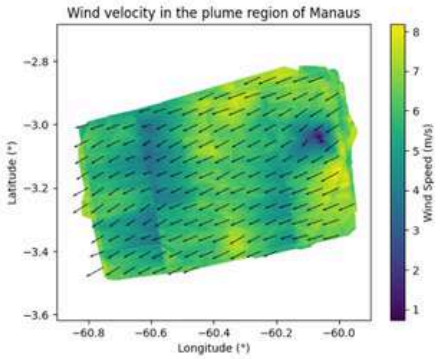


Figure 5. Interpolated data of wind velocity in the plume region of Manaus for the wet season

CONCLUSIONS

The method implemented for obtaining the dispersion parameters was able to adequately determine the central line of the plume and the transverse lines. The pollutant dispersion model proved to be compatible with the data, both along the central line of the plume and in relation to a transverse line. Overall, aircraft data fitted well to the exponential and the gaussian functions, and it was possible to conclude that NOx disperses more rapidly than CO and number of particles. Finally, it was possible to estimate the average NOx emission rate for Manaus.

REFERENCES

[1] Martin et al., Bulletin of the American Meteorological Society, 98(5), pp.981-997, 2017

[2] Okabayashi Miyaji, R. et al. Spatial Interpolation of Air Pollutant and Meteorological Variables in Central Amazonia. Data, v. 6, n. 12, p. 126, 30 nov. 2021.

[3] Varon, Daniel J. et al. Quantifying methane point sources from fine-scale satellite observations of atmospheric methane plumes. Atmospheric Measurement Techniques, v. 11, n. 10, p. 5673-5686, 2018.

[4] Medeiros, A. S. S. et al. Power plant fuel switching and air quality in a tropical, forested environment. Atmospheric Chemistry and Physics, v. 17, n. 14, p. 8987–8998, 26 jul. 2017.

ACKNOWLEDGEMENTS

Many thanks to the support of FAPESP (process 2023/06157-0).

AIR POLLUTION CONFERENCE BRAZIL
CMAS SOUTH AMERICA
COMMUNITY MODELING AND ANALYSIS SYSTEM

PERFORMANCE ASSESSMENT OF A LOW-COST AIR QUALITY SENSOR IN A SEMI-URBAN AREA OF SÃO PAULO

Márcio Farias[1], Adalgiza Fornaro[2]
[1]*University of São Paulo*
marciomatheus23@usp.br
[2]*University of São Paulo*
adalgiza.fornaro@iag.usp.br

Abstract: This study aimed to evaluate the performance of the low-cost sensor Vaisala AQT530, which measures trace gases and aerosols, along with meteorological variables, by comparing them to reference instruments. The assessment was made from 1st March to 15th April 2024 in São Paulo, with the standard instruments located at IAG, and IPEN and Pinheiros stations. O_3 values agreed unexpectedly well with the reference (R^2 = 0.94) in contrast to the obtained by Petäjä et al. (2021) in Helsinki (R^2 = 0.42), indicating that the accuracy of this pollutant increase in a warmer climate. On the other hand, poor performances of NO_2 (y = 0.8x + 2.5, R^2 = 0.53) and PM_{10} (y = 0.5x + 2.5, R^2 = 0.59) were also observed. A rigorous co-location study is needed, however, to assess the performance of the sensor more adequately.

Keywords: Air quality, low-cost sensor, particulate matter, trace gases

INTRODUCTION

Air pollution is the main environmental risk of early death globally, with stronger impact on low and middle-income countries (Health Effects Institute, 2020). Air quality monitoring plays an important role in identifying and reducing these health risks, thereby improving the general quality of life. High acquisitional and operational costs of conventional instruments, however, hinders their deployment in monitoring networks by those governments (Ionascu et al., 2021).

In comparison to standard instruments, low-cost sensors (LCS) are cheaper, smaller, less power-demanding, measure in high frequency, and often comprise multiple detectors. These characteristics enable them to achieve a greater and denser spatial coverage in less favorable regions (Carotenuto, 2023). However, they need to be calibrated, since the measures are affected by temperature, relative humidity and some pollutants. The calibration is typically made through a co-location study, in which the low-cost sensor is collocated at the same site with the reference for a certain period. The data obtained is then adjusted using linear, non-linear, or machine learning regression methods (Ionascu et al., 2021, DeSouza et al., 2022).

In this study, our goal was to assess the performance of the Vaisala AQT530 low-cost sensor of trace gases and aerosols in a semi-urban area of São Paulo. The only peer-reviewed assessment of the sensor was conducted by Petäjä et al. (2021) in Helsinki. They performed a long-term study with 5 sensors against a downtown air quality station, and most pollutants correlated well with R^2 values above 0.8. Still, artifact peaks of PM_{10} due to fog events and long-term drifting of CO were also observed.

METHODS

The assessment was made from 1st March to 15th April 2024 in São Paulo. The Vaisala AQT530 sensor was installed at the Institute of Astronomy, Geophysics and Atmospheric Sciences at the University of São Paulo (IAG/USP). Its measurements of temperature (T), relative humidity (RH), ozone (O_3), nitrogen dioxide (NO_2) and inhalable particulate matter (PM_{10}) were compared against reference instruments located in three sites (Table 1). Data of the sensor were hourly averaged, and then the time series and linear regression were made using the programming language R (version 4.3.3). Despite that only the meteorological variables could be evaluated in a rigorous co-location study, the pollutants were evaluated against two nearby air monitoring stations of São Paulo, one at the same campus (IPEN) and the other just across the Pinheiros river that separates the campus from the rest of the city (Pinheiros).

Table 1. List of reference instruments and their locations.

Local	Instrument	Variable
IAG, USP	Humidity and temperature probe HUMICP 155 (Vaisala)	T [°C], RH [%]
Station IPEN, USP	UV Photometric ozone analyser 49C (Thermo E. I. I.)	O_3 [ppb]

Station Pinheiros	NO-NO2-NOx analyser 42C (Thermo E. I. I.)	NO_2 [ppb]
Station Pinheiros	PM10 Beta attenuation monitor FH621-N (Andersen Inst.)	PM_{10} [µg/m^3]

Reference: Laboratory of Micrometeorology - IAG, Xavier (2011)

FINDINGS AND ARGUMENT

There was an excellent agreement between meteorological variables measured by the Vaisala AQT530 and those measured by the HUMICP 155 (temperature: y = 0.99x + 0.22 and R2 = 0.99, relative humidity: y = 0.99x - 1.76 and R^2 = 0.99). Temperature and relative humidity influence the accuracy of the pollutant measurements, therefore it's important that this variable has a good performance (Petäjä et al., 2021).

The NO_2 values measured by the low-cost sensor do not follow the diurnal evolution observed by the reference (Figure 1). Although both slope and intercept had low values, the residuals were intense (y = 0.8x + 2.5, R2 = 0.53). Since NO_2 is a primary pollutant emitted mainly by vehicles in the city, and station Pinheiros is impacted by heavy traffic, unlike IAG site, it becomes difficult to assess the sensor's performance regarding this pollutant (Carvalho et al., 2015). The hourly averaged AQT530 concentration was 18.1 ± 11.0 ppb, ranging between 0.7 and 65.8 ppb. The corresponding reference value was 20 ± 11 ppb, with range between 4 and 62 ppb.

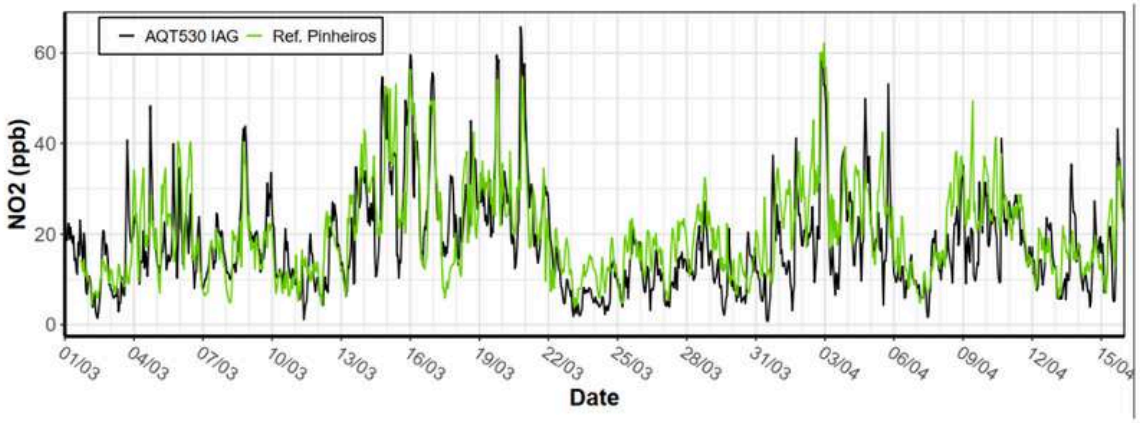


Figure 1. Time series of NO_2 from AQT530 (in black) and Pinheiros station (in green).

The O_3 showed the best performance of all pollutants, agreeing clearly well with the reference station (Figure 2), with regression equation y = 0.73x + 0.66, and R^2 = 0.94. O_3 is not derived directly from vehicular emissions, but rather by photochemical oxidation of them, and then it has a wider spatial distribution in the city, enabling its evaluation (Andrade et al., 2017). The good correlation contrasts with the poor one from Petäjä (2021), who obtained a mean R^2 of 0.42, suggesting that O_3 measurements are more accurate at a warmer climate. The hourly averaged AQT530 concentration was 18.1 ± 15.2 ppb, ranging between 0.0 and 77.0 ppb. The corresponding IPEN value was 25 ± 20 ppb, with range between 0 and 128 ppb.

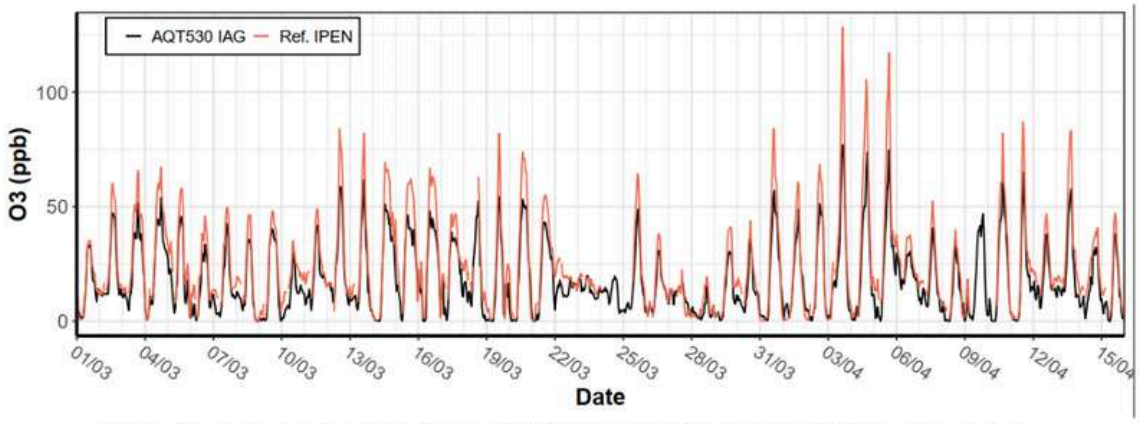


Figure 2. Time series of O_3 from AQT530 (in black) and IPEN station (in orange).

The PM_{10} measured by the low-cost sensor does not match very well with the reference (Figure 3). Despite the diurnal mismatch, in some periods of 4-6 days the AQT530 signal increased along with the reference, probably due to meteorological factors that affected both locations. The intercept and the coefficient of determination were relatively low ($y = 0.5x + 2.5$, $R^2 = 0.59$), but they cannot be properly assessed given that PM_{10} is a primary pollutant derived mainly from local traffic emissions and dust resuspension (Carvalho et al., 2015). The hourly averaged AQT530 concentration was 12.2 ± 7.8 µg/m³, ranging between 1.0 and 55.9 µg/m³. The corresponding reference value was 24 ± 13 µg/m³, with a range between 1 and 74 µg/m³.

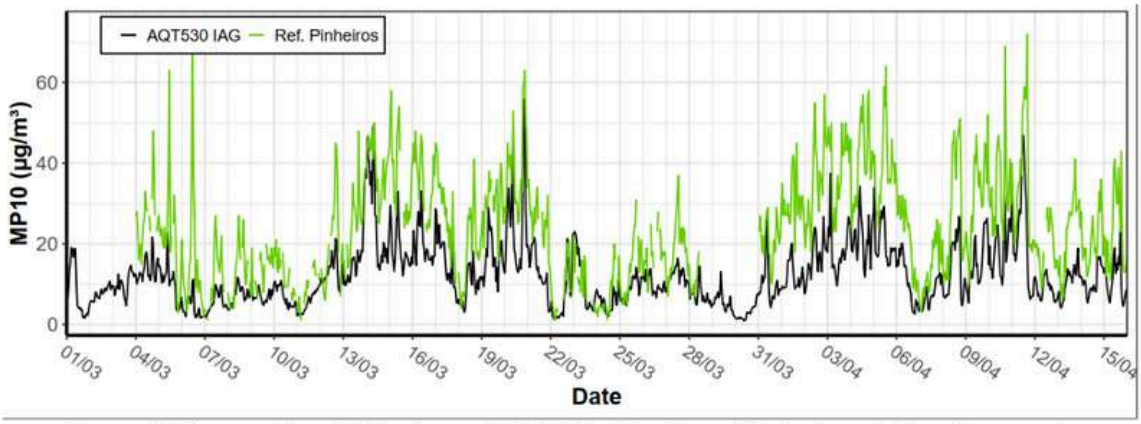


Figure 3. Time series of PM_{10} from AQT530 (in black) and Pinheiros station (in green).

CONCLUSIONS

Assessment of the low-cost sensor Vaisala AQT530 was made in the city of São Paulo. The meteorological variables showed excellent agreement with the reference instruments, with slope and coefficient of determination almost equal to unity and quite low intercept. The measurements of pollutants varied in performance, with O3 showing a good one as shown by time series and linear regression, and with NO2 and PM10 showing a bad one. However, the results are not definitively true, due to the fact that these both constituents are associated with local emissions and the sensor and their reference instruments were in sites with emission profiles likely different from each other. A proper assessment and calibration of the sensor's measurements should therefore be made through a co-location study, with standard instruments at the same site. A longer period of comparison is also recommended to evaluate the stability of the sensor in other ranges of temperature and relative humidity and to see if there is a long-term drift. Once calibrated and having enough stability, the sensor units can maybe be deployed in standard air quality networks in other cities and regions of Brazil or for research purposes.

REFERENCES

Andrade, Maria F. and Kumar, Prashant, and Freitas, Edmilson D. and Ynoue, Rita Y. and Martins, Jorge, and Martins, Leila D. and Nogueira, Thiago, and Perez-Martinez, Pedro, and Miranda, Regina M. and Albuquerque, Taciana, and Gonçalves, Fabio L. T. and Oyama, Beatriz, and Zhang, Yang. "Air quality in the megacity of São Paulo: Evolution over the last 30 years and future perspectives." *Atmospheric Environment* 159 (2017): 66-82.

Carotenuto, F. and Bisignano, A. and Brilli, L. and Gualtieri, G. and Giovannini, L. "Low-cost air quality monitoring networks for long-term field campaigns: A review." *Meteorological Applications* 30 (2023): e2161.

DeSouza, Priyanka, and Kahn, Ralph and Stockman, Tehya, and Obermann, William, and Crawford, Ben, and Wang, An, and Crooks, James, and Li, Jing, and Kinney, Patrick. "Calibrating networks of low-cost air quality sensors." *Atmospheric Measurement Techniques* 15 (2022): 6309-6328.

Carvalho, Vanessa S. B. and Freitas, Edmilson D. and Martins, Leila D. and Martins, Jorge A. and Mazzoli, Caroline R. and Andrade, Maria F. "Air quality status and trends over the Metropolitan Area of São Paulo, Brazil as a result of emission control policies." *Environmental Science & Policy* 47 (2015): 68-79

Ionascu, Marian-Emanuel, and Castell, Nuria, and Boncalo, Oana, and Schneider, Philipp, and Darie, Marius, and Marcu, Marius. "Calibration of CO, NO_2, and O_3 Using Airify: A Low-Cost Sensor Cluster for Air Quality Monitoring." *Sensors* 21 (2021): 7977.

Health Effects Institute. State of Global Air 2020: Special Report. Boston: Health Effects Institute, 2020.

Petäjä, Tuukka, and Ovaska, Aino, and Fung, Pak L. and Poutanen, Pyry, and Yli-Ojanperä, Jaakko, and Suikkola, Jari, and Laakso, Mikko, and Mäkelä, Taneli, and Niemi, Jarkko V. and Keskinen, Jorma, and Järvinen, Anssi, and Kuula, Joel, and Kurppa, Mona, and Hussein, Tareq, and Tarkoma, Sasu, and Kulmala, Markku, and Karppinen, Ari, and Manninen, Hanna E. and Timonen, Hilkka. "Added Value of Vaisala AQT530 Sensors as a Part of a Sensor Network for Comprehensive Air Quality Monitoring." *Frontiers in Environmental Science* 9 (2021): 719657.

Xavier, José. "Análise da disponibilidade da rede automática de monitoramento da qualidade do ar e seus reflexos no licenciamento ambiental realizado em São Paulo." MSc diss., Aeronautics Institute of Technology, 2011.

AIR POLLUTION CONFERENCE BRAZIL
CMAS SOUTH AMERICA
COMMUNITY MODELING AND ANALYSIS SYSTEM

CARBON DIOXIDE AND METHANE LEVELS IN SURFACE WATERS ALONG THE SÃO VICENTE ISLAND IN COASTAL REGION OF SÃO PAULO STATE

Elaine Cristina Araujo[1], Izabel da Silva Andrade[1] Fernanda de M. Macedo[4], Thaís Corrêa[1], Thais Andrade[1], Elisabete S. Braga[3], Maria de F. Andrade[2], Eduardo Landulfo[1]

[1]*Nuclear and Energy Research Institute*
elaine.c.araujo@usp.br
izabel.andrade@usp.br
correa-thais@usp.br
thais.andradedasilva@usp.br
elandulf@ipen.br
[2]*Institute of Astronomy, Geophysics and Atmospheric Sciences*
maria.andrade@iag.usp.br
[3]*University of Sao Paulo, Institute Oceanography, Brazil*
edsbraga@usp.br
[4]*FATEC - Faculty of Technology of the State of São Paulo*
fernanda.m.macedo@alumni.usp.br

Abstract: Various studies explore the relationship between the rising levels of CO_2 and CH_4 (greenhouse gasses) in the atmosphere and climate changes, and how these increases are connected to human activities. The escalation of these gas species may have implications for the environment. Concerning coastal systems, the rise in greenhouse gas emissions could impact the environment through multiple pathways because the atmosphere and superficial ocean waters also have significant exchanges. The main purpose of this work is to study Greenhouse gasses (GHG), such as CO_2 and CH_4, on the superficial waters of the coastal region of São Paulo coast. The data were collected in situ on a vessel provided by the Institute of Oceanography of São Paulo University (IOUSP). The campaign was conducted in spring 2022 (10 -11 October) in the south of the coast of São Paulo state, traveling through cities with anthropogenic impacts in principal Santos city, which is located the main port of Sul America. For these in situ measurements a portable gas analyzer Microportable Greenhouse Gas Analyzers (LGR-ICOS ™ GLA Series) - was used to detect the CO_2 and CH_4 spectra through the Off-Axis Integrated Cavity Output Spectroscopy (OA-ICOS) technique.

***Keywords*:** Methane, Carbon Dioxide, Estuary, GHG, Microportable Gas Analyzers.

INTRODUCTION

According to the IPCC 2013, carbon dioxide concentration increased from 278 ppm in 1750 to 390.5 ppm in 2011, making it one of the largest contributors to the anthropogenic greenhouse effect. Another important gas in the process of greenhouse effect is methane (CH_4), which had an increase since the pre-industrial era (1750), from 722 ppb to 1803 ppb in 2011 [1]. This escalating concentration of greenhouse gasses (GHGs) and their significant impact on radiative forcing has spurred extensive research into GHG dynamics, particularly in coastal areas and estuaries. Coastal regions, comprising only 7% of the total ocean surface, play a crucial role in biogeochemical cycles linking continents, the atmosphere, and oceans [2]. The main purpose of this work is to study Greenhouse gasses (GHG), such as CO_2 and CH_4, on the waters of the coastal region of São Paulo. The data were collected in situ on a vessel provided by the Institute of Oceanography of São Paulo University (IOUSP). The campaign was carried out in October 2022 on São Vicente island, where the cities of Santos and São Vicente are inside, two cities with greater anthropic impact in the Metropolitan Region of Baixada Santista. For these in situ measurements a portable gas analyzer - Microportable Greenhouse Gas Analyzers (LGR-ICOS ™ GLA Series) - was installed in the vessel Alpha Delphini for to detect the CO_2 and CH_4 concentrations through the Off-Axis Integrated Cavity Output Spectroscopy (OA-ICOS) technique.

AIR POLLUTION CONFERENCE BRAZIL

CMAS SOUTH AMERICA

COMMUNITY MODELING AND ANALYSIS SYSTEM

METHODS

The Delphini I Campaign, which took place in an approximately 28-hour Journey along the cities São Vicente and Santos in the Coast of São Paulo state, Brazil. The route crossed the coast of cities with greater anthropic impact in the Metropolitan Region of Baixada Santista. (Figure 1).

For data gathering, a portable gas analyzer - Microportable Greenhouse Gas Analyzer LGR-ICOS™ GLA Series - was used. This instrument has a high sensibility, resulting in a very fast gas flow response time (1 second) [3], it's based on the Off-Axis, Integrated Cavity Output Spectroscopy (OA-ICOS), where the light beam is placed at an angle off the axis of the cavity and its output signal is a sinusoidal modulation in light intensity, it's a technique that is widely utilized for gas detection due to its rapid response, high sensitivity, and stability [4], achieve obtain a precision of <0.9 ppb (1 second) for CO_2 and <350 ppb for CH_4 (1 second).

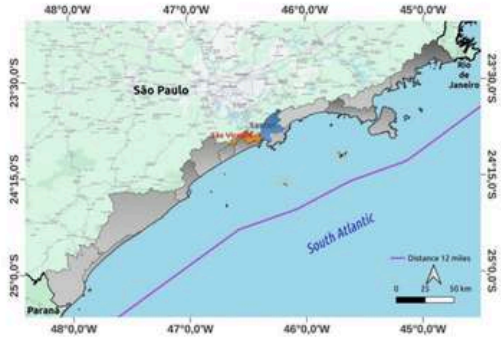


Figure 1. Map coast of São Paulo. In highlight the cities São Vicente and Santos



Figure 2. Vessel Alpha Delphini IOUSP, in destak the position inlet of portable gas analyzer

A Teflon tube of ¼ was coupled to the INLET, which extended up to about ~8 meters above sea level and was positioned above the cabin of the captain of the vessel at half ship. At the end of this tube a PFA 47-mm Savillex filter holder was attached, and inside this support a Zefluor membrane of 2.0 µm was used (Figure 2).

FINDINGS AND ARGUMENT

Data was continuously obtained during the campaign, which was divided into two days. The initial day (10th, october) of the project was spent around the Port of Santos, and the measurements began at 3 pm. The vessel returned to the pier about 8 pm. The GHG analyzer maintained continuous measures until the second day around 7 am and the journey was around Santos submarine emissary and São Vicente city. The campaign finished on October 11th at approximately 6 pm. The analysis inserted a minimum and maximum limit by calculating the Interquartile Range (IQR), which is the difference between the Third Quartile (Q3) and the First Quartile (Q1) - representing the amplitude of the interval in which the central half of the data is concentrated, ignoring the extremes (Figure 3 and 4).

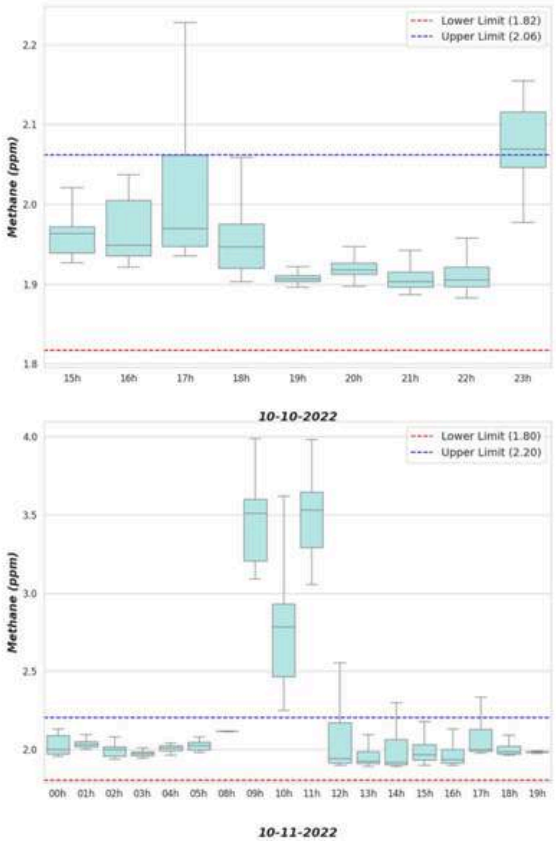


Figure 3. Boxplot for daily data of CH4 concentrations per hour for the two days of campaign.

After excluding highly descriptive data, methane values on the first day of the campaign mostly remained within the lower and upper limits calculated by the interquartile range (1.82 ppm and 2.06 ppm,

respectively), deviating from this range only after 10 pm. Regarding CH_4, in the second day of analysis, most data points still fell within the range established by the interquartiles. However, between 9 am and 12 pm, it was evident that values significantly exceeded the maximum limit, reaching up to 4 ppm (Figure 3).

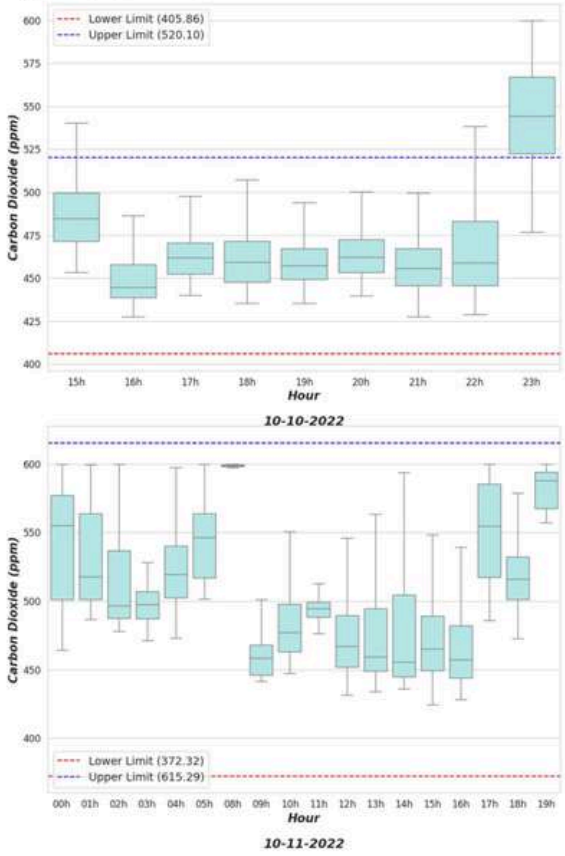


Figure 4. Boxplot for daily data of CO2 concentrations per hour for the two days of campaign.

Carbon dioxide data exhibited results that surpassed the upper limits of the interquartile range, which was approximately 520 ppm, peaking close to 600 ppm by 11 pm on the first day of measurement (October 10th). On the final day of the campaign, concentrations did not surpass the maximum interquartile value of around 615 ppm. However, there were very few data points within this range between 6 and 9 am, suggesting that most of the data during this time exceeded 600 ppm (Figure 4).

The highs methane data, were recorded when the vessel was positioned between the cities of Santos and São Vicente. It is noteworthy that these two cities are the most populous in the region, and between them lies the submarine outfall of Santos, where residential sewage is discharged. As for CO_2, concentrations exceeding 500 ppm occurred when the vessel navigated through the channel of the Port of Santos, near the ferry crossing, and in close proximity to bulk carriers.

CONCLUSIONS

The data presented here are from the first campaign that utilized a portable GHG analyzer to assess CO_2 and CH_4 concentrations in the Santos and São Vicente cities. The campaign aimed to explore a coastal region heavily influenced by anthropogenic factors, such as a high population density and proximity to the Port of Santos. Despite being the initial use of this equipment in the region, the results were promising, as they revealed high concentrations of both gasses that align with potential sources near the vessel. However, it is crucial to consider certain factors in future research. Parameters like wind direction should be accounted for to pinpoint the origins of the highest concentration peaks in each region. Additionally, conducting more extensive sampling over multiple days in the same areas would facilitate a more thorough analysis of the results.

REFERENCES

[1] IPCC, 2021: *Climate Change 2021: The Physical Science Basis. Contribution of Working Group I to the Sixth Assessment Report of the Intergovernmental Panel on Climate Change* [Masson-Delmotte, V., P. Zhai, A. Pirani, S.L. Connors, C. Péan, S. Berger, N. Caud, Y. Chen, L. Goldfarb, M.I. Gomis, M. Huang, K. Leitzell, E. Lonnoy, J.B.R. Matthews, T.K. Maycock, T. Waterfield, O. Yelekçi, R. Yu, and B. Zhou (eds.)]. Cambridge University Press, Cambridge, United Kingdom and New York, NY, USA, In press, doi.org/10.1017/9781009157896.

[2] Burgos, M., Ortega, T., & Forja, J. (2018). *Carbon dioxide and methane dynamics in three coastal systems of Cadiz Bay (SW Spain). Estuaries and Coasts,* 41(4), 1069-1088. doi.org/10.1007/s12237-017-0330-2.

[3] ABB Inc. Measurement & Analytics.GLA131 Series *Microportable Analyzers User Manual. ABB Inc. Measurement & Analytics*, 2020.

[4] Krishnan R. P., David I. R., Mark G. A.,1 Alan M. G. & Terence H. R. (2009). *Off-axis integrated cavity output spectroscopy with a mid-infrared interband cascade laser for real-time breath ethane measurements.* Applied optics - Vol. 48, No. 4.-549, 2007.

AIR POLLUTION CONFERENCE BRAZIL
CMAS SOUTH AMERICA
COMMUNITY MODELING AND ANALYSIS SYSTEM

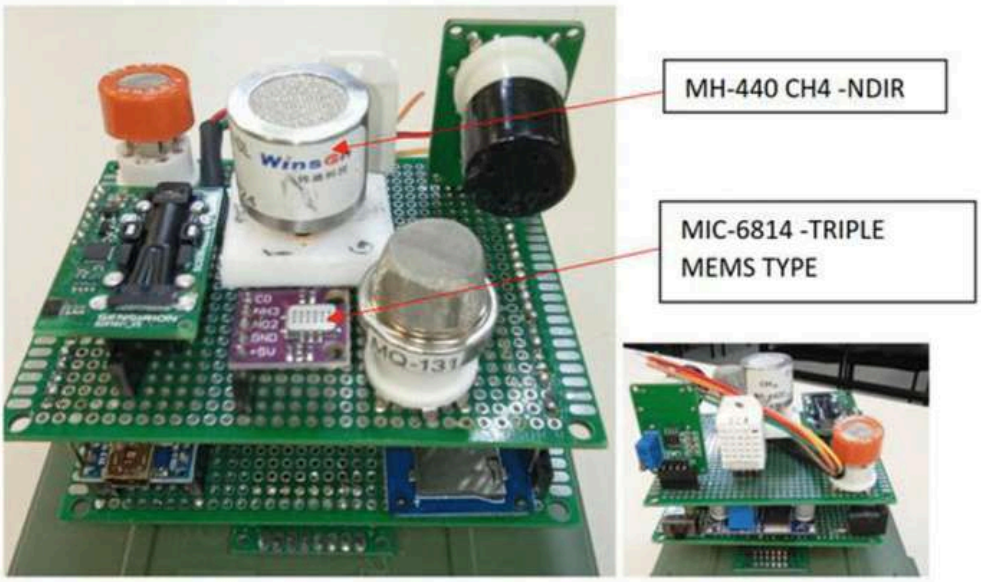
ASSEMBLY RESULTS ON GHG AND PARTICULATED MATTER MONITORING USING LOW-COST SENSORS

Jose C. Santos[1], Jose A.S. da Matta[2], Eduardo Landulfo[2]
[1]*Polytechnic School - University of São Paulo - USP*
eng.josesantos@usp.br
[2]*Nuclear and Energy Research Institute - IPEN*
elandulfo@ipen.gov.br; jasmatta@ipen.gov.br

Abstract: Abstract should be written with 8 font size, Trebuchet MS, justified, single line spacing. **Objective, method** and **findings** are summarized in this section.

Objective: This project aims to develop a tropospheric gas monitoring system with a focus on greenhouse gas emissions (GHG), through remote sensing with drones. Measurements will be will be taken to assess the concentration of these gases in areas such as landfills, sewers, areas with industrial facilities, roads, rivers and gas pipelines. The system in question will operate using electrochemical, electronic and optical sensor methods[1]. This survey will be used to map critical emission points and then monitored using the same sensors used in drones, but stationary for a long period of time. This sensing methodology, known as "STAND-ALONE", should be applied to the study of daily thermal inversions by identifying the moments of maximum concentrations (present in the decrease in night-time temperature) and subsequent dilution during warming throughout the day. Thus we will utilise the complementarity between the first prospecting done by the drone and the monitoring of continuous emissions recorded in sensor modules placed on poles. The fact is that the technologies available today offer rapid processing and diagnostics so that we can to build a scenario in which we can systematically monitor the emissions and can mitigate the effects they generate[2,3], such an application becomes a significant device for promoting attitudes on the part of the various organisations interested in improving natural and social ecosystems.

Method: Initially, as a test, a conditioning study was carried out on some of the main sensors. Summarised here the main procedures carried out during assembly of the three main protoboards: sensor board (surface), power supply \& acquisition (middle) and real time clock, RTC (bottom board). This assembly tested the electrical connection between the various components, the collection of individual data with alternating sensores and operating autonomy using all of them connected to a single power supplied by four Li-ion batteries. All measurements will be taken inside a protective module carried by the drone or positioned on poles, with no additional instruments required. This initial test proved the viabilityfeasibility of implementing this project, defining the main sensors to be used for monitoring sensors to be used for monitoring, as well as establishing a payload of 430 g for the drone used. The main parameters measured are: pressure, temperature, humidity, soot (PM2.5 and PM10), CH_4, CO and CO_2 emissions. The set of sensors includes carbon monoxide sensor, WinSen-SENSORS ZE07-CO, Particulate PM2.5 Plantower PMS5003, ZH06-IV also from WinSen-SENSORS (Laser Dust Sensor), GPS Neo-6m/antenna board with a dedicated Arduino Nano microcontroller, one Sensirion CO_2 sensor and the BOSH BME-680 for monitoring pressure, temperature and humidity. Since the set will be taking measurements at fixed points using poles, its power supply relies on six 7.3 V Li-18650 Li-ion batteries, so longer autonomy is expected, which is being worked on at the moment, as well as the construction of the code ("scripts") for acquiring and logging data extracted from the sensors.



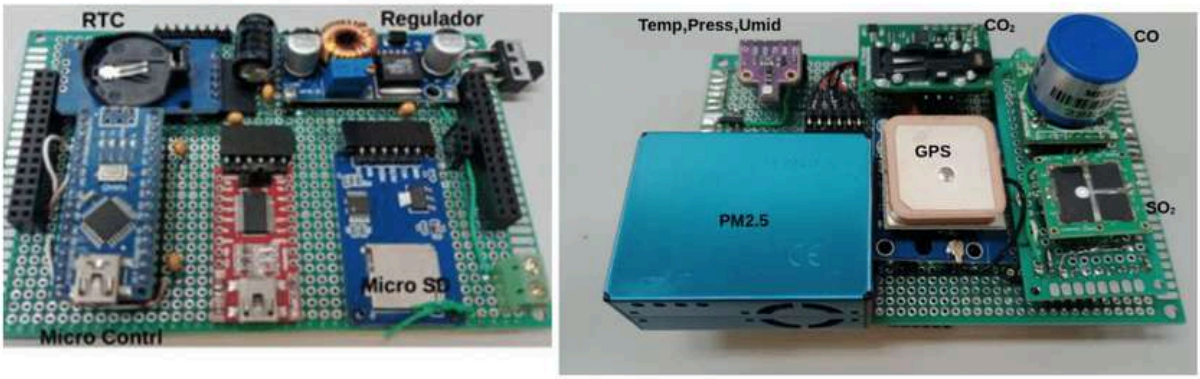
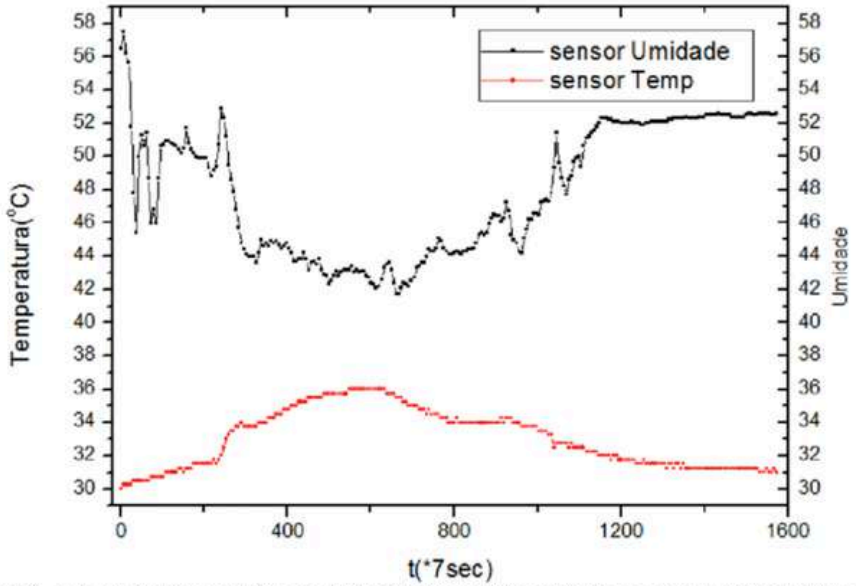
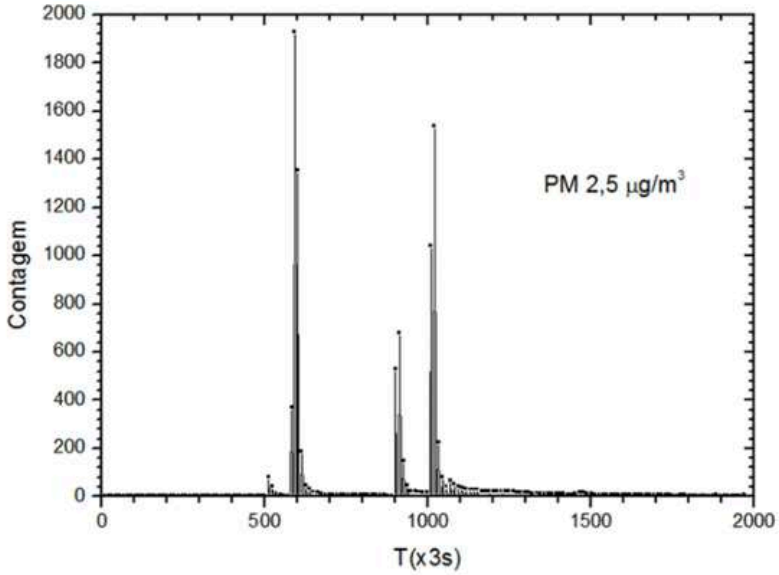


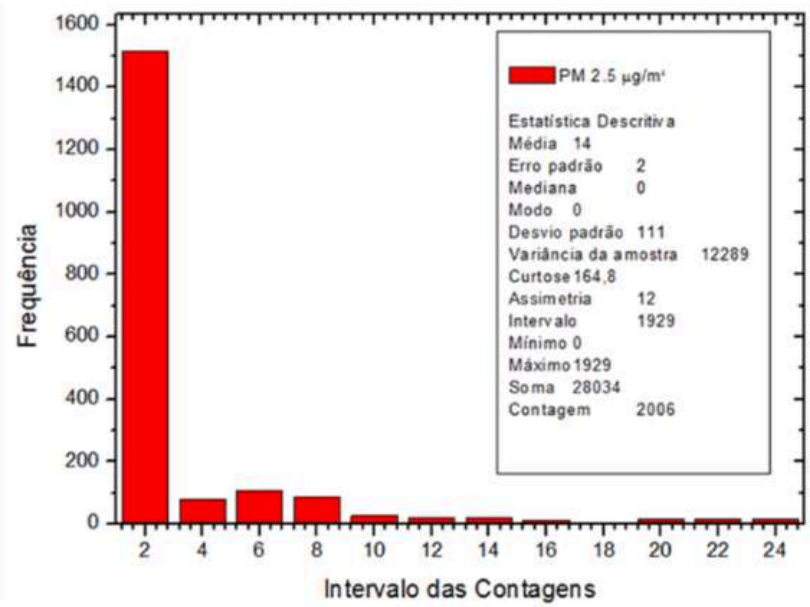
Figure 1: Three main Protoboards.

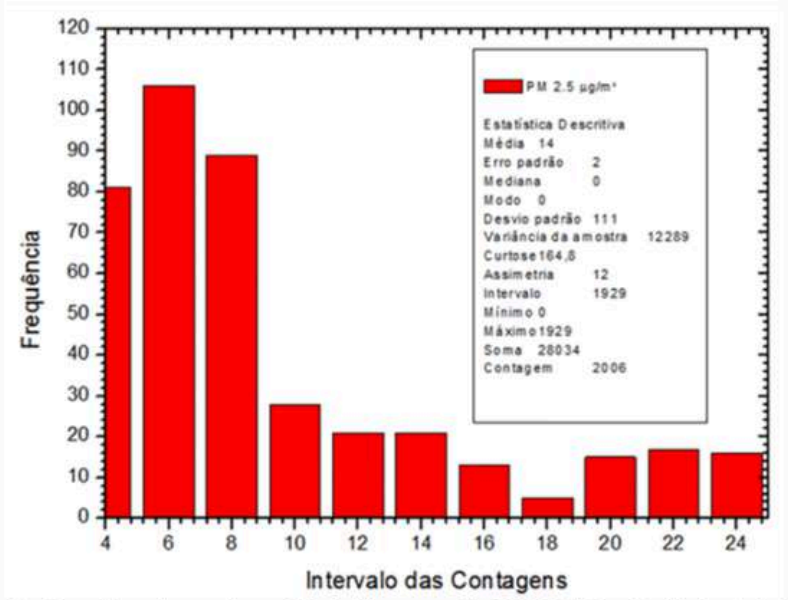


Graph of the BOSH BME-680 sensor, for temperature and humidity measurements in operation on board the Phanton 3 drone over the IPEN area (11/03/2024). The two profiles show complementarity as we change the drone's height between 0 and 50 meters.



In the bench test, two ways of stimulating the sensors were tried (i) the burning of wood incense (first peaks in the figure) and then (ii) and then tin solder vapour (peaks around 3000s).





As result for example in the above figure it was observed in the histograms for PM2.5 (right detail) that both the concentrations of 12 and 14 µg/m^3 and those of 20, 22 and 24 µg/m^3 show presence frequencies between 15 and 20 and the intermediate concentration of 18 µg/m^3 represents a gap (frequency of presence around 5) in the continuity decay to higher concentrations.

References

[1] Burgués, J.; Marco, S.; Environmental chemical sensing using small drones: A review. Sci. Total Environ. 2020, 748, No. 141172.

[2] Kunz, M.; Larvic, J. V.; Gerbig, C.; et al.; COCAP: a carbon dioxide analyser for small unmanned aircraft systems. Atmos. Meas. Tech. 2018, 11, 1833-1849.

[3] Ali, N. B. H.; Abichou, T.; Green, R.; Comparing estimates of fugitive landfill methane emissions using inverse plume modeling obtained with Surface Emission Monitoring (SEM), Drone Emission Monitoring (DEM), and Downwind Plume Emission Monitoring (DWPEM). J. Air Waste Manage. Assoc. 2020, 70, 410-424.

Keywords: *GHG emissions, Low-Cost Sensor, Arduino Platform, Particulate* Matter.

AIR POLLUTION CONFERENCE BRAZIL
CMAS SOUTH AMERICA
COMMUNITY MODELING AND ANALYSIS SYSTEM

LONG-TERM ISOPRENE (BVOC) FLUXES IN THE AMAZON RAINFOREST BY RELAXED EDDY ACCUMULATION COUPLED TO GC/PID (REAPER)

Caroline Ostermann[1], Alex Guenther[2], Scot Martin [3], Jonathan William[4], Valerio Ferracci[2], Sanjeevi Nagalingam[2], Hui Wang[2], Pitchayawee Kittitananuvong[2], Alvin Laa[2], Nora Zanoni[5], Sergio Duvoisin[6],Silvana Nascimento[6], Francisco Alcinei[6], Rodrigo Souza[6] and Oscar Vega Bustillos[1]

[1]*Instituto de Pesquisas Energéticas e Nucleares*
ovega@ipen.br
[2]*University of California, Irvine*
alex.guenther@uci.edu
[3]*Harvard University*
scot_martin@harvard.edu,
[4]*Max Planck Institute*
jonathan.william@mpic.de
[5]*Universita de Bologna*
n.zanonni@isac.cnr.it
[6]*Universidade Estadual do Amazonas*
rafsouza@uea.edu.br

Abstract: Understanding the role of Biogenic Volatile Organic Compounds (BVOCs) in atmospheric chemistry and their impact on oxidants and aerosol formation is essential for global environmental research. BVOC emissions, primarily sourced from biogenic processes, pose a challenge due to the vast diversity of vegetation and ecosystems, as well as temporal changes in land use. While prevalent BVOC emission models categorize vegetation into functional types, the variability in environmental parameters and temporal fluctuations within natural canopies remains inadequately represented. This study introduces an innovative device system designed to address these challenges by integrating the Relaxed Eddy Accumulator and Gas Chromatograph Photoionization Detector (REAPER) in real-time measurement of isoprene fluxes. The system is portable, cost-effective and lightweight, easily to deploy in remote environments. By enabling high temporal resolution measurements, this device overcomes limitations associated with traditional techniques and offers accurate chromatograms. The novel instrument also facilitates real-time data transmission through a cloud-based platform, allowing access to meteorological data, calculated parameters, chromatograms and flux results. This feature supports the deployment of these systems across a wide range of sites and integrates them into existing flux tower networks. In conclusion, this research contributes to the advancement of isoprene fluxes measurement techniques and validation of satellite-based retrievals of isoprene abundances providing a valuable tool for scientists studying atmospheric chemistry and its impacts on the environment in diverse ecosystems, ultimately aiding in our understanding of the complex interplay between biogenic processes and atmospheric chemistry. The REAPER is installed in the ATTO tower in the Amazon rainforest and continuously measures Isoprene every hour within parts per billion (ppb) content. All the meteorology and chemistry data are sent through the Internet anywhere in the world to measure the BVOCs fluxes.

Keywords: BVOC, Amazon, REA, Isoprene, GC/PID.

INTRODUCTION

Global reactive carbon emissions are estimated at 2.4 Pg annually, with significant contributions from carbon monoxide (0.6 Pg), methane (0.5 Pg), isoprene (0.5 Pg), and other volatile organic compounds (0.8 Pg). About half of these emissions are from terrestrial vegetation, with the rest from technological sources, biomass burning, and microbes. Isoprene, primarily emitted by tropical vegetation, plays a crucial role in plant physiology and atmospheric chemistry due to its high reactivity, leading to various oxidation products and secondary organic aerosols that impact climate. The Amazon rainforest is a significant source of isoprene but estimating its emissions is challenging due to biodiversity and limited observational data. Accurate isoprene modeling is hindered by uncertainties in emission factors and the effects of extreme weather conditions, which are expected to increase with climate change. Current measurement techniques using gas chromatographs and mass spectrometers, though precise, are not well-suited for long-term field use in remote areas like the Amazon, necessitating the development of new, robust instruments for better spatial and temporal coverage.

AIR POLLUTION CONFERENCE BRAZIL
CMAS SOUTH AMERICA
COMMUNITY MODELING AND ANALYSIS SYSTEM

METHODS

This research aims to develop and evaluate an instrument based on the REA methodology to measure BVOC fluxes globally in real-time, addressing the lack of empirical data in current climate models. The REAPER device segregates atmospheric air based on vertical wind velocity, collecting samples into reservoirs for upward and downward air currents. Designed to be cost-effective, energy-efficient, and robust, the REAPER channels air samples to an online GC-PID, focusing on isoprene and other VOCs. It generates real-time data on meteorological parameters, stores the information on Google Drive, and interfaces with the GC-PID via a Raspberry Pi or Ethernet connection. The REAPER, deployed in the Amazon rainforest in May 2023 at the ATTO site, includes three main components: a control unit, a segregator enclosure, and a GC unit with a PID. This innovative system provides crucial data for improving climate models by capturing detailed BVOC flux measurements in remote locations.

FINDINGS AND ARGUMENT

During the initial testing phase of the REAPER instrument in Dr. Alex Gunther's laboratory at the University of California Irvine, comprehensive evaluations ensured that the system met anticipated parameters, generating new β values. Verification involved introducing the heat flux equation to rigorously assess the β coefficient's accuracy. Data was collected every two seconds and synchronized through Google Drive, with new β coefficients calculated every 30 minutes. Chromatograms generated every 50 minutes allowed real-time monitoring of flux results. Data was organized into two sheets on Google Drive: "Segregation Data," containing meteorological observations, and "REA Data," storing critical study parameters, including β coefficients and heat flux. Custom-coded analysis in RStudio revealed a notable correlation between heat flux, diurnal and nocturnal cycles, and temperature variations, with β coefficients ranging from 0.30 to 0.45, indicating proper system functioning. These insights are crucial for accurately determining the flux of compounds like isoprene, with consistent patterns observed during the Amazon rainforest campaign from September 12, 2023, to the present, across different seasons.

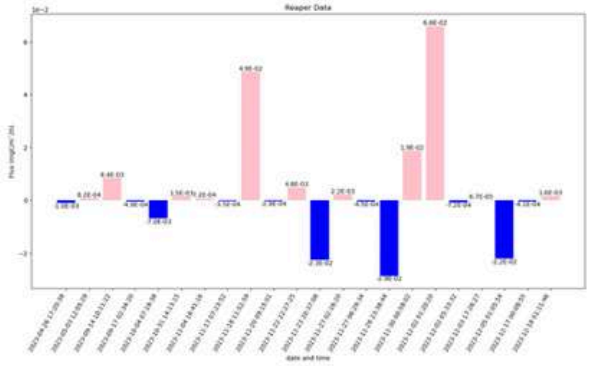


Figure 1 shows the magnitude of the fluxes captured by the REAPER over the period of deployment in the Amazon.

CONCLUSIONS

The study highlights the successful validation of the REAPER instrument, demonstrating its capability to accurately measure and segregate BVOC fluxes based on vertical wind velocity (Figure 1). The system's performance, as indicated by consistent β coefficient values and reliable correlations with heat flux and temperature variations, confirms its potential for real-time, high-resolution monitoring. The instrument's robustness and effectiveness were proven during the Amazon rainforest campaign, showing consistent results across different seasonal transitions. This suggests that the REAPER can significantly enhance empirical data collection for climate models, particularly in remote and diverse environments.

REFERENCES

CARLTON, A. G.; WIEDINMYER, C.; KROLL, J. H. A review of Secondary Organic Aerosol (SOA) formation from isoprene. Atmospheric Chemistry and Physics, v. 9, n. 14, p. 4987-5005, 2009.

FERRACCI, V. et al. Continuous isoprene measurements in a UK temperate forest for a whole growing season: Effects of drought stress during the 2018 heatwave. Geophysical Research Letters, v. 47, n. 15, p. e2020GL088885, 2020.

GREENBERG, J. P. et al. Eddy flux and leaf-level measurements of biogenic VOC emissions from mopane woodland of Botswana. Journal of Geophysical Research: Atmospheres, v. 108, n. D13, 2003.

SARKAR, C. ; TURNIPSEED, A. ; SHERTZ, S. ; KARL, T. ; POTOSNAK, M. ; BAI, J. ; SERÇA, D. ; BONAL, D. ; BURBAN, B. ; LOPES, P.R.C. ; VEGA, O. ; GUENTHER, A.B. . A portable, low-cost relaxed eddy accumulation (REA) system for quantifying ecosystem-level fluxes of volatile organics. ATMOSPHERIC ENVIRONMENT, v. 240, p. 117764, 2020.

AIR POLLUTION CONFERENCE BRAZIL
CMAS SOUTH AMERICA
COMMUNITY MODELING AND ANALYSIS SYSTEM

CARBON DIOXIDE AND METHANE LEVELS IN SURFACE WATERS ALONG THE SÃO VICENTE ISLAND IN COASTAL REGION OF SÃO PAULO STATE

Elaine Cristina Araujo[1], Izabel da Silva Andrade[1] Fernanda de M. Macedo[4], Thaís Corrêa[1], Thais Andrade[1], Elisabete S. Braga[3], Maria de F. Andrade[2], Eduardo Landulfo[1]

[1]*Nuclear and Energy Research Institute*
elaine.c.araujo@usp.br
izabel.andrade@usp.br
correa-thais@usp.br
thais.andradedasilva@usp.br
elandulf@ipen.br
[2]*Institute of Astronomy, Geophysics and Atmospheric Sciences*
maria.andrade@iag.usp.br
[3]*University of Sao Paulo, Institute Oceanography, Brazil*
edsbraga@usp.br
[4]*FATEC - Faculty of Technology of the State of São Paulo*
fernanda.m.macedo@alumni.usp.br

Abstract: Various studies explore the relationship between the rising levels of CO_2 and CH_4 (greenhouse gasses) in the atmosphere and climate changes, and how these increases are connected to human activities. The escalation of these gas species may have implications for the environment. Concerning coastal systems, the rise in greenhouse gas emissions could impact the environment through multiple pathways because the atmosphere and superficial ocean waters also have significant exchanges. The main purpose of this work is to study Greenhouse gasses (GHG), such as CO_2 and CH_4, on the superficial waters of the coastal region of São Paulo coast. The data were collected in situ on a vessel provided by the Institute of Oceanography of São Paulo University (IOUSP). The campaign was conducted in spring 2022 (10 -11 October) in the south of the coast of São Paulo state, traveling through cities with anthropogenic impacts in principal Santos city, which is located the main port of Sul America. For these in situ measurements a portable gas analyzer Microportable Greenhouse Gas Analyzers (LGR-ICOS ™ GLA Series) - was used to detect the CO_2 and CH_4 spectra through the Off-Axis Integrated Cavity Output Spectroscopy (OA-ICOS) technique.

***Keywords*:** Methane, Carbon Dioxide, Estuary, GHG, Microportable Gas Analyzers.

INTRODUCTION

According to the IPCC 2013, carbon dioxide concentration increased from 278 ppm in 1750 to 390.5 ppm in 2011, making it one of the largest contributors to the anthropogenic greenhouse effect. Another important gas in the process of greenhouse effect is methane (CH_4), which had an increase since the pre-industrial era (1750), from 722 ppb to 1803 ppb in 2011 [1]. This escalating concentration of greenhouse gasses (GHGs) and their significant impact on radiative forcing has spurred extensive research into GHG dynamics, particularly in coastal areas and estuaries. Coastal regions, comprising only 7% of the total ocean surface, play a crucial role in biogeochemical cycles linking continents, the atmosphere, and oceans [2]. The main purpose of this work is to study Greenhouse gasses (GHG), such as CO_2 and CH_4, on the waters of the coastal region of São Paulo. The data were collected in situ on a vessel provided by the Institute of Oceanography of São Paulo University (IOUSP). The campaign was carried out in October 2022 on São Vicente island, where the cities of Santos and São Vicente are inside, two cities with greater anthropic impact in the Metropolitan Region of Baixada Santista. For these in situ measurements a portable gas analyzer - Microportable Greenhouse Gas Analyzers (LGR-ICOS ™ GLA Series) - was installed in the vessel Alpha Delphini for to detect the CO_2 and CH_4 concentrations through the Off-Axis Integrated Cavity Output Spectroscopy (OA-ICOS) technique.

AIR POLLUTION CONFERENCE BRAZIL
CMAS SOUTH AMERICA
COMMUNITY MODELING AND ANALYSIS SYSTEM

METHODS

The Delphini I Campaign, which took place in an approximately 28-hour Journey along the cities São Vicente and Santos in the Coast of São Paulo state, Brazil. The route crossed the coast of cities with greater anthropic impact in the Metropolitan Region of Baixada Santista. (Figure 1).

For data gathering, a portable gas analyzer - Microportable Greenhouse Gas Analyzer LGR-ICOS™ GLA Series - was used. This instrument has a high sensibility, resulting in a very fast gas flow response time (1 second) [3], it's based on the Off-Axis, Integrated Cavity Output Spectroscopy (OA-ICOS), where the light beam is placed at an angle off the axis of the cavity and its output signal is a sinusoidal modulation in light intensity, it's a technique that is widely utilized for gas detection due to its rapid response, high sensitivity, and stability [4], achieve obtain a precision of <0.9 ppb (1 second) for CH_4 and <350 ppb for CO_2 (1 second).



Figure 1. Map coast of São Paulo. In highlight the cities São Vicente and Santos



Figure 2. Vessel Alpha Delphini IOUSP, in destak the position inlet of portable gas analyzer

A Teflon tube of ¼ was coupled to the INLET, which extended up to about ~8 meters above sea level and was positioned above the cabin of the captain of the vessel at half ship. At the end of this tube a PFA 47-mm Savillex filter holder was attached, and inside this support a Zefluor membrane of 2.0 µm was used (Figure 2).

FINDINGS AND ARGUMENT

Data was continuously obtained during the campaign, which was divided into two days. The initial day (10th, october) of the project was spent around the Port of Santos, and the measurements began at 3 pm. The vessel returned to the pier about 8 pm. The GHG analyzer maintained continuous measures until the second day around 7 am and the journey was around Santos submarine emissary and São Vicente city. The campaign finished on October 11th at approximately 6 pm. The analysis inserted a minimum and maximum limit by calculating the Interquartile Range (IQR), which is the difference between the Third Quartile (Q3) and the First Quartile (Q1) - representing the amplitude of the interval in which the central half of the data is concentrated, ignoring the extremes (Figure 3 and 4).

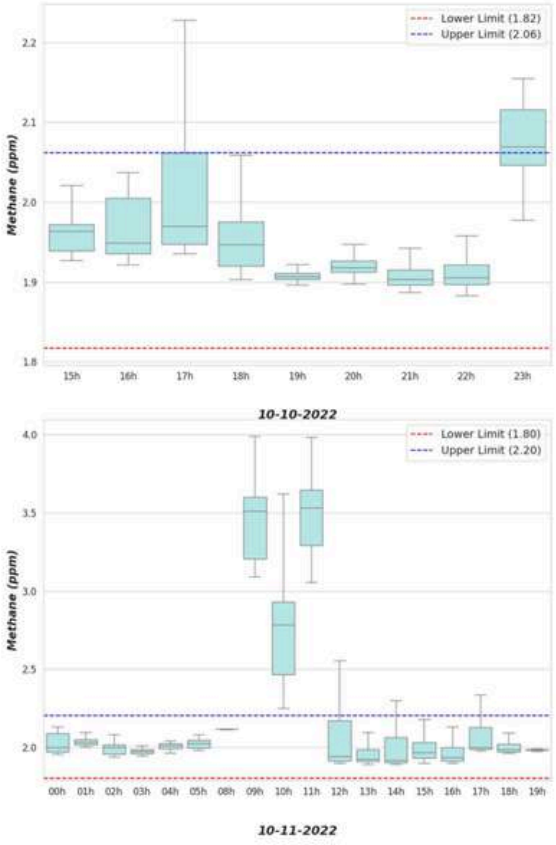


Figure 3. Boxplot for daily data of CH4 concentrations per hour for the two days of campaign.

After excluding highly descriptive data, methane values on the first day of the campaign mostly remained within the lower and upper limits calculated by the interquartile range (1.82 ppm and 2.06 ppm,

respectively), deviating from this range only after 10 pm. Regarding CH_4, in the second day of analysis, most data points still fell within the range established by the interquartiles. However, between 9 am and 12 pm, it was evident that values significantly exceeded the maximum limit, reaching up to 4 ppm (Figure 3).

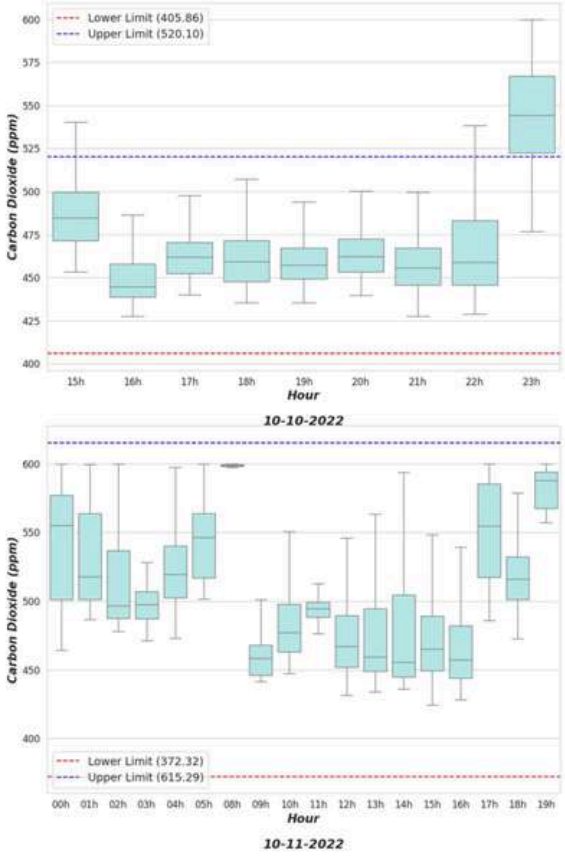


Figure 4. Boxplot for daily data of CO2 concentrations per hour for the two days of campaign.

Carbon dioxide data exhibited results that surpassed the upper limits of the interquartile range, which was approximately 520 ppm, peaking close to 600 ppm by 11 pm on the first day of measurement (October 10th). On the final day of the campaign, concentrations did not surpass the maximum interquartile value of around 615 ppm. However, there were very few data points within this range between 6 and 9 am, suggesting that most of the data during this time exceeded 600 ppm (Figure 4).

The highs methane data, were recorded when the vessel was positioned between the cities of Santos and São Vicente. It is noteworthy that these two cities are the most populous in the region, and between them lies the submarine outfall of Santos, where residential sewage is discharged. As for CO_2, concentrations exceeding 500 ppm occurred when the vessel navigated through the channel of the Port of Santos, near the ferry crossing, and in close proximity to bulk carriers.

CONCLUSIONS

The data presented here are from the first campaign that utilized a portable GHG analyzer to assess CO_2 and CH_4 concentrations in the Santos and São Vicente cities. The campaign aimed to explore a coastal region heavily influenced by anthropogenic factors, such as a high population density and proximity to the Port of Santos. Despite being the initial use of this equipment in the region, the results were promising, as they revealed high concentrations of both gasses that align with potential sources near the vessel. However, it is crucial to consider certain factors in future research. Parameters like wind direction should be accounted for to pinpoint the origins of the highest concentration peaks in each region. Additionally, conducting more extensive sampling over multiple days in the same areas would facilitate a more thorough analysis of the results.

REFERENCES

[1] IPCC, 2021: *Climate Change 2021: The Physical Science Basis. Contribution of Working Group I to the Sixth Assessment Report of the Intergovernmental Panel on Climate Change* [Masson-Delmotte, V., P. Zhai, A. Pirani, S.L. Connors, C. Péan, S. Berger, N. Caud, Y. Chen, L. Goldfarb, M.I. Gomis, M. Huang, K. Leitzell, E. Lonnoy, J.B.R. Matthews, T.K. Maycock, T. Waterfield, O. Yelekçi, R. Yu, and B. Zhou (eds.)]. Cambridge University Press, Cambridge, United Kingdom and New York, NY, USA, In press, doi.org/10.1017/9781009157896.

[2] Burgos, M., Ortega, T., & Forja, J. (2018). *Carbon dioxide and methane dynamics in three coastal systems of Cadiz Bay (SW Spain). Estuaries and Coasts,* 41(4), 1069-1088. doi.org/10.1007/s12237-017-0330-2.

[3] ABB Inc. Measurement & Analytics.GLA131 Series *Microportable Analyzers User Manual. ABB Inc. Measurement & Analytics*, 2020.

[4] Krishnan R. P., David I. R., Mark G. A.,1 Alan M. G. & Terence H. R. (2009). *Off-axis integrated cavity output spectroscopy with a mid-infrared interband cascade laser for real-time breath ethane measurements.* Applied optics - Vol. 48, No. 4.-549, 2007.

SESSION 14
Urban climate processes and Methods

- Boundary layer and urban canopy layer processes
  - Surface and subsurface urban processes
  - Boundary-layer effects
- Urban air quality
  - Pollutant dispersion in the urban canopy layer
  - Urban greenhouse gas emissions and uptakes in cities
- Extreme weather and disasters in the urban environment
  - Forecasting and impact assessment of extreme weather events in cities
  - Influence of cities on precipitations and thunderstorms
- Modelling
  - Multi-scale numerical studies of urban environments
  - Cities in global- and regional-scale climate models
  - Urban canopy parameterizations and models
  - Local Climate Zones Applications
- Observations
  - New observational techniques to study urban climate
  - Field campaigns, sensor and network development
  - Urban remote sensing
  - Wind tunnel and scale model outdoor experiments

SESSÃO 14

IMPROVİNG URBAN METEOROLOGY SİMULATİON BY UPDATİNG URBAN GEOMORPHOLOGİCAL AND RADİATİVE PROPERTİES İN WRF-CHEM: A STUDY CASE İN SÃO PAULO 404

ASSESSMENT OF METEOROLOGICAL EFFECTS ON FINE PARTİCLE POLLUTİON İN A BRAZİLİAN URBAN CENTER 407

POLLUTANTS MASS TRANSFER AT THE TOP OF URBAN CANOPY 410

DISPERSION ANALYSIS OF PARTICLE EMISSION FROM A SINTERING MAIN STACK: IMPACT OF A BAGHOUSE INSTALLATION 413

APPLICATION OF THE UWRF MODEL FOR THE EVALUATION OF THE MITIGATION OF THE URBAN HEAT ISLAND OF CDMX THROUGH A SYSTEM OF LAKES IN THE AREA OF THE EX-LAKE OF TEXCOCO 416

STOCHASTIC FLOW IN AN IDEALIZED STREET NETWORK 419

REGIONAL CLIMATE SIMULATIONS FOR SOUTH AMERICA IN THE CONTEXT OF THE FOCI PROJECT 422

AIR POLLUTION CONFERENCE BRAZIL
CMAS SOUTH AMERICA
COMMUNITY MODELING AND ANALYSIS SYSTEM

IMPROVING URBAN METEOROLOGY SIMULATIONS BY UPDATING URBAN GEOMORPHOLOGICAL AND RADIATIVE PROPERTIES IN WRF-CHEM: A STUDY CASE IN SÃO PAULO

Mario E. Gavidia-Calderón[1], Prashant Kumar[2], Maria de Fatima Andrade[1], and Edmilson Dias de Freitas[1]

[1] *Instituto de Astronomia, Geofísica e Ciências Atmosféricas, Universidade de São Paulo, São Paulo, Brazil*

mario.calderon@iag.usp.br; maria.andrade@iag.usp.br; edmilson.freitas@iag.usp.br

[2]*Global Centre for Clean Air Research (GCARE), School of Sustainability, Civil and Environmental Engineering, Faculty of Engineering and Physical Sciences, University of Surrey, Guildford GU2 7XH, United Kingdom*

p.kumar@surrey.ac.uk

Abstract: Simulation of air pollutants concentration depends on the correct representation of both atmospheric emissions and the urban weather. To represent the urban atmosphere in WRF-Chem, the urban physics option needs to be activated. Nevertheless, the correct configuration required updating the default values of the geomorphological and radiative properties of the urban classes inside the simulated domain. In this work, we gather global and local databases to create the domain urban classification and to estimate the building height, the anthropogenic heat, the urban fraction, the albedo, and the road-width parameters for this new urban classification. We performed simulations with WRF-Chem for a week in July 2021. The simulation domain is centered in the Metropolitan Area of São Paulo and has a spatial resolution of 1 km. Three simulations are carried out, a scenario without urban physics, and two scenarios using the Urban Canopy Model (UCM) and the Building Environment Parameterization (BEP) with updated urban parameters values. Meteorological parameters are compared against observations from CETESB air quality network. Preliminary results showed an improvement in the spatial variation of meteorological parameters. In the case of air temperature, the updated scenario of UCM and BEP presents a better representation of nocturnal temperature. The BEP scenario produces a better representation of the magnitude of the planetary boundary layer height and improves the representation of the wind speed. The database is useful for urban studies and the methodology is suitable to estimate different properties for other urban classification like Local Climate Zones (LCZ) or other urban physics models such as or Building Energy Model (BEM), not only in São Paulo but in other cities of the region.

Keywords: WRF-Chem, BEP, UCM, Urban Climate, São Paulo.

INTRODUCTION

In air quality modeling, the simulation of pollutant concentrations in urban areas depends on the correct representation of urban emissions and the urban weather. Many efforts have been done to improve the representation of anthropogenic emissions, especially vehicular emissions, in the Metropolitan Area of São Paulo (MASP) but the remaining question of improving the urban weather has not been addressed (Gavidia-Calderón et al., 2024). As a matter of fact, Pellegati-Franco et al. (2019) is the only work that deals with improving urban representation to improve air quality modeling in the MASP.

To represent the urban weather, WRF-Chem counts with three urban physics parameterizations schemes. But to correctly configure these schemes, it is required to classify the urban area in at least three classes and to estimate and provide the geomorphological and radiative properties of those urban subclasses. Therefore, with the aim of improving the air quality simulations in the MASP, this work improves the urban meteorological representation inside WRF-Chem by testing and configuring two urban models.

METHODS

We carried out three simulation scenarios: without activating the urban physics (No urban), activating the Urban Canopy Model urban model (UCM), and activating the Building Environment Parameterization (BEP) urban model. The simulation domain is centered in the MASP with a spatial resolution of 1 km. The simulation period is a week from July 8th to 16th, 2021. In this period, planetary boundary height (PBLH) measures are available.

By default, in the WRF-Chem model, the MASP area is classified by a single urban area (Urban and built-up). We subclassify this urban area in high-density residential (HD Res.), low-density residential (LD Res.), and industrial/commercial (CI). These three classes are based on the percentage of constructed materials area (Tewari et al., 2007). We used the impervious surface area for MASP from Kawakubo et

al. (2019) as a proxy to perform the urban classification.

Based on Masson et al. (2020), we updated the geomorphological and radiative properties of these three urban subclasses using the following databases: Global Human Settlement Layer (European Commission, 2023), global anthropogenic database (Varquez et al., 2021), and urban fraction (Kawakubo et al., 2019). These values are added to the URBPARAM.TBL file.

Simulation results are compared against the measurement of São Paulo State Environmental Agency (CETESB) air quality network. We focused on temperature (T2), relative humidity (RH), wind speed (WS) and direction (WD). PBLH is also analyzed. We used the mean bias (MB), root square error (RMSE), and Pearson correlation (R) to analyze model performance.

FINDINGS AND ARGUMENT

Figure 1 shows the difference between the default urban classification and the updated urban classification. Table 1 also shows an example of differences between the default values and updated in the URBPARM.TBL file for anthropogenic heat and building height.

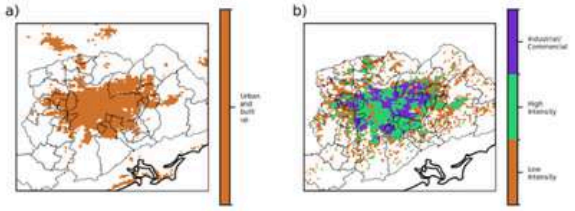


Figure 1. Urban classification in a) WRF default and b) Updated in this work.

Table 1. Example of updated values in URBAMPARM.TBL

Parameter	Case	Urban classes		
		BD Res.	HD Res.	IC
Anthropogenic heat (W/m^2)	Default	20	50	90
	Updated	50	55	60
Buildings height (m)	Default	5	7.5	10
	Updated	4	12	13

Figure 2 shows the results in representing the PBLH. UCM results are close to the No-Urban scenario, and both scenarios underpredict PBLH. However, using BEP results in a better representation of diurnal PBLH magnitude. All simulations underpredict nocturnal PBLH and in the three scenarios peak PBLH happens around two hours earlier than the observations.

Figure 3 shows simulation results for temperature, relative humidity, and wind speed for Parque D. Pedro II station. In the case of temperature, daily maximum temperature is underpredicted in all cases, but BEP results in a better representation of nocturnal temperature (daily minimum). BEP scenario produces a lower overestimation of wind speed.

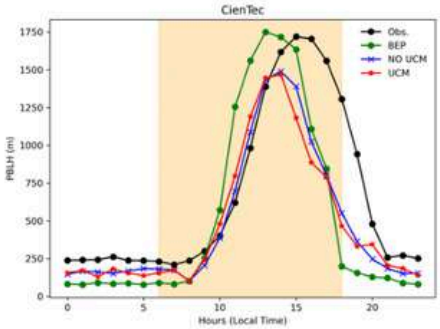


Figure 2. Simulation of planetary boundary layer height for the three scenarios.

Table 2 shows the performance statistics for three evaluated air quality stations. Using UCM or BEP improve in most of the cases the representation of T2, RH, and WS. UCM and BEP get similar performance statistics values, being UCM slightly better for T2 and RH. Nevertheless, when using BEP, there is an improvement in the representatiton of wind speed in almost all the stations by reducing the error and increasing the linear correlation coefficient.

Table 2: Performance statistics

		T2 (K)			RH (%)			WS (m/s)		
		No-Urb	UCM	BEP	No-Urb	UCM	BEP	No-Urb	UCM	BEP
Capão Redondo	MB	1.2	**-0.4**	0.5	**-13.3**	-9.0	**-8.7**	0.9	1.3	**0.7**
	RMSE	2.3	**1.6**	2.0	22.6	**19.3**	20.4	1.3	1.7	**1.2**
	R	0.9	**0.9**	0.9	0.7	**0.8**	0.8	**0.7**	0.7	0.6
Marg.Tietê Pte Remédios	MB	0.8	**-0.5**	-0.6	-5.8	**-0.3**	3.2	0.7	0.9	**0.2**
	RMSE	**1.6**	1.8	2.0	**14.0**	14.1	16.3	1.3	1.5	**0.9**
	R	**1.0**	0.9	0.9	**0.8**	0.8	**0.8**	0.5	0.5	**0.7**
Parque D.Pedro II	MB	0.7	-0.4	**-0.3**	-6.4	-2.3	**-0.2**	1.3	1.6	**0.7**
	RMSE	1.7	1.7	**1.4**	14.0	**13.6**	13.8	1.6	1.9	**1.1**
	R	**1.0**	0.9	**1.0**	**0.8**	0.8	**0.9**	0.5	0.5	**0.7**

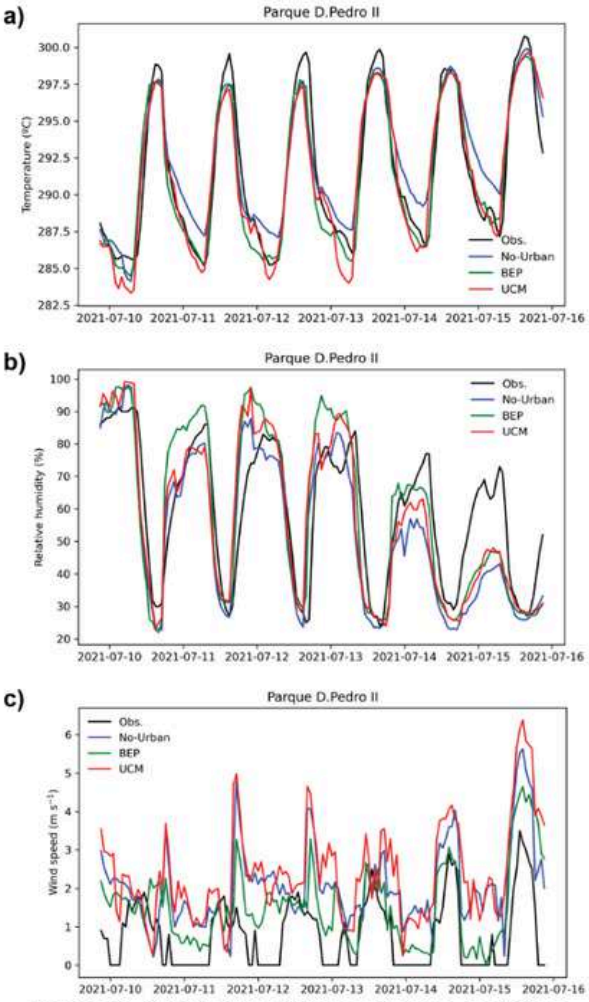


Figure 3. Simulation of temperature, relative humidity, and wind speed in Parque D. Pedro II station for the three scenarios.

CONCLUSIONS

Preliminary results show that even improving the urban classification can improve meteorological simulation inside the city. The biggest improvement is in the spatial variation of meteorological parameters. The UCM and BEP scenarios improve the simulation of T2 and RH. BEP scenario results in better representation of wind speed and planetary boundary layer. Given that these parameters are important variables that affect pollutant concentration, we recommend using the BEP urban model with updated URBPARAM.TBL when performing air quality simulations. Next steps involve increasing the number of evaluated stations and test BEP in simulating air quality in the MASP.

REFERENCES

European Commission. Joint Research Centre. (2023). GHSL data package 2023. https://doi.org/doi:10.2760/098587

Gavidia-Calderón, M., Schuch, D., Vara-Vela, A., Inoue, R., Freitas, E. D., Albuquerque, T. T. de A., Zhang, Y., Andrade, M. de F., & Bell, M. L. (2024). Air quality modeling in the metropolitan area of São Paulo, Brazil: A review. Atmospheric Environment, 319, 120301. https://doi.org/10.1016/j.atmosenv.2023.120301

Kawakubo, F., Morato, R., Martins, M., Mataveli, G., Nepomuceno, P., & Martines, M. (2019). Quantification and Analysis of Impervious Surface Area in the Metropolitan Region of São Paulo, Brazil. Remote Sensing, 11(8), 944. https://doi.org/10.3390/rs11080944

Masson, V., Heldens, W., Bocher, E., Bonhomme, M., Bucher, B., Burmeister, C., de Munck, C., Esch, T., Hidalgo, J., Kanani-Sühring, F., Kwok, Y. T., Lemonsu, A., Lévy, J. P., Maronga, B., Pavlik, D., Petit, G., See, L., Schoetter, R., Tornay, N., … Zeidler, J. (2020). City-descriptive input data for urban climate models: Model requirements, data sources and challenges. In Urban Climate (Vol. 31). Elsevier B.V. https://doi.org/10.1016/j.uclim.2019.100536

Pellegatti Franco, D. M., Andrade, M. de F., Ynoue, R. Y., & Ching, J. (2019). Effect of Local Climate Zone (LCZ) classification on ozone chemical transport model simulations in Sao Paulo, Brazil. Urban Climate, 27(December 2018), 293–313. https://doi.org/10.1016/j.uclim.2018.12.007

Tewari, M., Chen, F., Kusaka, H., & Miao, S. (2007). Coupled WRF/Unified Noah/Urban-Canopy Modeling System.

Varquez, A. C. G., Kiyomoto, S., Khanh, D. N., & Kanda, M. (2021). Global 1-km present and future hourly anthropogenic heat flux. Scientific Data, 8(1). https://doi.org/10.1038/s41597-021-00850-w

AIR POLLUTION CONFERENCE BRAZIL
CMAS SOUTH AMERICA
COMMUNITY MODELING AND ANALYSIS SYSTEM

ASSESSMENT OF METEOROLOGICAL EFFECTS ON FINE PARTİCLE POLLUTİON İN A BRAZİLİAN URBAN CENTER

Amanda Ribeiro[1], Taciana Albuquerque[2]
[1] *Post Graduate Program in Sanitation, Environment and Water Resources, Federal University of Minas Gerais, Belo Horizonte, Brazil*
amandakcr@ufmg.br
[2] *Department of Sanitary and Environmental Engineering, Federal University of Minas Gerais*
Av. Pres. Antônio Carlos, 6627, 31270-901, Belo Horizonte, Brazil
taciana@desa.ufmg.br

Abstract: : A large body of evidence has pointed to the effects of particle pollution on human health, particularly in urban centers. Fine particles are responsible for approximately 6.4 million deaths each year, and of the total number of deaths, approximately 95% occur in countries in the Global South. The concentration of pollutants in the troposphere is influenced by dynamic atmospheric processes, with precipitation and relative humidity being the main mechanisms for removing particles from the air. Therefore, the present work aims to map atmospheric dynamics in the city of Belo Horizonte, with a simultaneous focus on climate processes and air pollution, to contribute to debates on air quality control in the city. Hourly particle concentration data from the Minas Gerais automatic air quality monitoring network were used, for the central station located in the Belo Horizonte, capital of the state. The analysis of the annual intensity classification based on the Standard Year classification and annual anomaly verification was based on daily meteorological data from the local station of the National Institute of Meteorology and the groupings were carried out using the Standard Deviation. Regarding mapping, this step was carried out using spatial interpolation methods, the Voronoi Diagram, when data from automatic stations across the entire Metropolitan Area of Belo Horizonte (MABH) were included in the analysis, to minimize problems of edge effects in the Belo Horizonte. Statistical techniques were used, such as the Mann-Kendall trend test ($\alpha = 0.05$) to investigate climate and pollution trends. A bottleneck analysis technique was carried out to evaluate the influence of influential factors on pollution, starting with an annual analysis and moving on to monthly and daily analyses, filtering the worst situations. Despite the lower concentrations of $PM_{2.5}$ in Belo Horizonte, compared to other municipalities in the MABH, the $PM_{2.5}$ concentrations were above those recommended by the World Health Organization's Global Air Quality Guidelines (WHO-AQG), with no prospects for improvement. The results explained the possibility of the occurrence of fire outbreaks as a predominant factor for the relevant increases in PM2.5 pollution in September, combined with meteorological conditions of low precipitation and air humidity. It is also important to assess the seasonal variability of atmospheric emissions from all relevant sources and analyze the influences throughout the other months of the dry period, due to the recurrence of concentrations above the WHO-DQA, not ensuring health protection. Expanding the analysis to the remaining months and understanding the spatial variability of all relevant atmospheric sources is important to complete the understanding of the factors that influence the dynamics of particle pollution to thereby step toward establishing strategies to control and improve the local air quality.

Keywords: Fine particle pollution, Meteorological influence, Air pollution in a Brazilian urban center, Geostatistical analysis of air quality.

INTRODUCTION

Particle air pollution has become an important risk factor for human health, with a large body of evidence of a causal association between short-term (hours/days) and long-term (months/years) exposure to pollutants and hospitalizations, reduced life expectancy, and mortality (RODRIGUES et al., 2015; POPE et al., 2020; FERNANDES et al., 2020). The concentration of pollutants in the troposphere is influenced by dynamic atmospheric processes, and meteorological and climatic conditions can influence both the pollutant dispersion process and the dilution and removal process. Therefore, to study atmospheric pollution, it is necessary to understand climate dynamics and clarify their influence on pollutant concentration. Ribeiro et al. (2021), with a statistical analysis evaluating the meteorological influence on particle concentrations in the Metropolitan Area of Belo Horizonte (MABH), demonstrated that their concentrations tend to be lower in rainy months and the concentrations tend to reduce with intensification of precipitation and relative humidity, which are associated with wet deposition processes of particulate matter. Thus, statistics and geostatistics methods allow, in a temporal and regionalized way, to carry out mapping, quantification, and modeling of the climatic and pollution aspects, which if applied simultaneously to sampled points of atmospheric pollution, allow to contribute to discussions on understanding the dynamics pollution to identify its possible causes, influences and consequences.

Therefore, this study sought to understand the relationship between atmospheric dynamics and PM2.5 pollution in Belo Horizonte, the capital of the

state of Minas Gerais, using statistical and geostatistical methods.

METHODS

Pollutants concentration data was obtained from the automatic air quality monitoring network of Minas Gerais (FEAM, 2023). The station considered was Avenida do Contorno station, and for the meteorological analysis, data from the station of the National Institute of Meteorology, code 83587, was used, both located in Belo Horizonte. The analysis of the annual evolution was carried out considering the concentrations of $PM_{2.5}$, accumulated precipitation, and average relative humidity. The methods consisted of spatio-temporal evaluation using geostatistical techniques of spatial interpolation and classification statistics of standard years and annual anomalies. The verification of anomalies was carried out through the application of the Standard Deviation technique concerning the average, using five classes for precipitation (Too Dry, Dry, Usual, Rainy, and Too Rainy) and three classes for the other parameters (Low, Usual, and High). Regarding mapping, due to the small number of points available concerning the pollution network, the method applied was Voronoi Diagrams. At this stage, data from automatic stations across the entire MRBH were also included in the analysis, to minimize problems with edge effects in the municipality that is the focus of this study, Belo Horizonte. Statistical methods were applied to confirm the evaluations of evolution and correlation, the Mann-Kendall trend test and Spearman correlation test, both with a confidence level of 95% (α=0.05). The analysis was carried out following a temporal funneling methodology, starting with the annual analysis and continuing to monthly and daily, based on the temporal decomposition of the worst situations for $PM_{2.5}$ air concentrations.

FINDINGS AND ARGUMENT

The spatial interpolation of the Voronoi Polygon technique showed that the Belo Horizonte is located in the polygons with the lowest concentrations of MABH area (**Figure *1***).

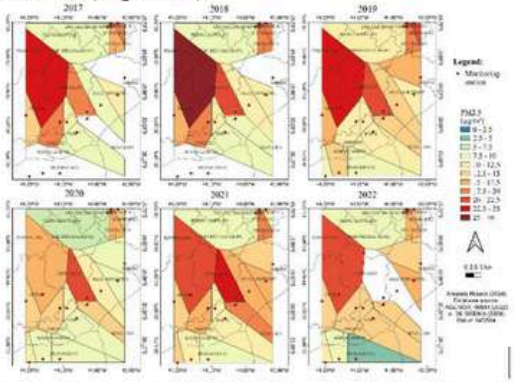


Figure 1 - Voronoi diagrams for $PM_{2.5}$ concentrations from 2017 to 2022.

However, in all the MABH and all years, the concentrations were above the World Health Organization's Global Air Quality Guidelines (WHO-AQG), which is 5 µg/m³ for annual $PM_{2.5}$ averages. With the Mann-Kendall statistical test results, it was verified that there is no prospect of improvement or worsening in concentrations of $PM_{2.5}$ in the municipality of Belo Horizonte, considering the period from 2015 to 2022. There was no direct relationship between $PM_{2.5}$ concentration and accumulated precipitation over the years and between the diagrams (***Figure 2***).

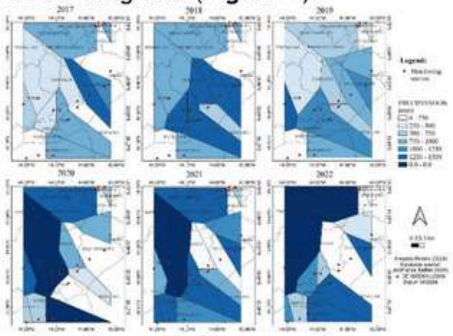
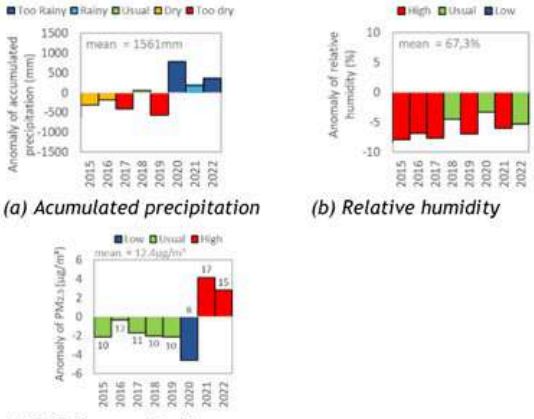


Figure 2 - Voronoi diagrams for accumulated precipitation from 2017 to 2022.

To Belo Horizonte, the annual anomaly profiles demonstrated the year 2021 as the worst year for $PM_{2.5}$ pollution, which was a rainy year, but with low average annual relative humidity (***Figure 3***). The year 2020 was the year with the best air quality situation, which may be associated both with the fact that it was a rainy year and with higher average relative humidity, as well as with the reduction in emissions from urban traffic due to air restriction measures tackling COVID-19.



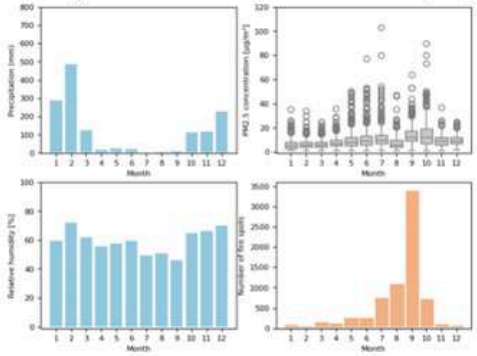
(a) Acumulated precipitation *(b) Relative humidity*

(c) PM2.5 concentration

Figure 3 - Anomaly and Standard Years by the Standard Deviation Method.

Due to the worst situation observed for the year 2021, the temporal bottleneck analysis will be carried out for the ST01 station, central to the municipality, and for the year 2021 (***Figure 4***). The highest concentrations of $PM_{2.5}$ were observed mainly in September and October 2021, but a frequency of higher concentrations was also

observed in June and July. The month of September, with the highest average monthly concentrations, also had the lowest average monthly relative humidity and low precipitation, at the same time as the highest occurrence of fire outbreaks was observed, with 51% of the percentage of outbreaks recorded in 2021, with a 220% increase in fire outbreaks compared to the second month with the highest number of fire outbreaks, August.



Note: Precipitation and Relative humidity by INMET, $PM_{2.5}$ concentration by ST01, and Number of fire spots by Terra Brasilis.

Figure 4 - Mensal temporal series to 2021.

It is worth noting that October, which also represented the month with the highest recorded concentrations, was the month with the fourth highest record of fire outbreaks, although it recorded greater precipitation and greater relative humidity.



Figure 5 - Time series of daily maximums of 24h moving average of $PM_{2.5}$ concentrations in ST01 for 2021.

The months of July and August were also two months with low precipitation and relative humidity. Furthermore, August had a higher number of fire outbreaks (second highest monthly record in 2021) than July (third highest monthly record), and despite that, $PM_{2.5}$ concentrations in August were lower than in July. However, in ***Figure 5*** it is possible to verify the frequency of concentrations above WHO-AQG from May to October, but with more intense increases during September. However, during almost the entire month of September, concentrations were above the WHO-AQG. During this period there was no rainfall, and it was a period of lower relative humidity than usual. When observing the synoptic charts between the 18th and 19th, it is not possible to verify the presence of a cold wave arrival or a high-pressure zone.

Thus, this work explains the possibility of the occurrence of fire outbreaks as a predominant factor for the relevant increases in $PM_{2.5}$ pollution in September, combined with meteorological conditions of low precipitation and air humidity. However, it is also important to assess the seasonal variability of atmospheric emissions from all relevant source sectors in the region and analyze the influences throughout the other months of the dry period, due to the recurrence of concentrations above the WHO-DQA, not ensuring health protection for the local population.

CONCLUSIONS

The annual geostatistical analysis did not indicate a direct relationship between pollution and accumulated precipitation, while the analysis of standard years and annual anomalies demonstrated the year 2021 as the year with the highest pollution between 2015 and 2022, with meteorological conditions of lower rainfall and relative humidity. The month with the highest $PM_{2.5}$ pollution in 2021 was September, which may be associated with low precipitation, low relative air humidity, and a significant increase in the number of fire outbreaks. It is also important to assess the seasonal variability of atmospheric emissions from all relevant sources and analyze the influences throughout the other months of the dry period, due to the recurrence of concentrations above the WHO-DQA, not ensuring health protection.

REFERENCES

FEAM. (2023, Sep 5). Dados de monitoramento da qualidade do ar.

FERNANDES, Matheus Augusto de Oliveira et al. Avoiding hospital admissions for respiratory system diseases by complying to the final Brazilian air quality standard: an estimate for Brazilian southeast capitals. http://dx.doi.org/10.1007/s11356-020-07772-x.

INMET. (2023, Sep 5). Banco de dados meteorológicos do INMET.

Ribeiro, A. K. C. et al. (2021). Influence of Meteorology on Fine Particles Concentration in an Urban Center in Southeast of Brazil (pp. 199-204). https://doi.org/10.1007/978-3-031-12786-1_28.

POPE, C. Arden et al. Fine particulate air pollution and human mortality: 25+ years of cohort studies. Elsevier BV. http://dx.doi.org/10.1016/j.envres.2019.108924.

RODRIGUES, C.G. et al. Projeção da mortalidade e internações hospitalares na rede pública de saúde atribuíveis à poluição atmosférica no Estado de São Paulo entre 2012 e 2030. http://dx.doi.org/10.1590/s0102-3098201500000029.

WHO. 2021. WHO global air quality guidelines: particulate matter (MP2,5 e MP10), ozone, nitrogen dioxide, sulfur dioxide and carbon monoxide.

AIR POLLUTION CONFERENCE BRAZIL
CMAS SOUTH AMERICA
COMMUNITY MODELING AND ANALYSIS SYSTEM

POLLUTANTS MASS TRANSFER AT THE TOP OF URBAN CANOPY

Fernanda Cezana Capucho[1], Neyval Costa Reis Júnior[2], Jane Meri Santos[3], Elson Silva Galvão[4] , Elisa Valentim Goulart[5]

[1]*Instituto Federal do Espírito Santo - Coordenadoria de Formação Geral - São Mateus/ES - Brazil*
fecezana@edu.ifes.br[1]

[2, 3, 4, 5]*Universidade Federal do Espírito Santo - Centro Tecnológico - Programa de Pós-Graduação em Engenharia Ambiental - Vitória/ES - Brazil*
neyval.reis@ufes.br[2]
jane.m.santos@ufes.br[3]
elsongalvao@gmail.com[4]
elisa.goulart@edu.ufes.br[5]

Abstract: Air quality in urban areas is strongly influenced by the cities architectural planning or by the lack of a planning. It is important to involve researchers with the aim of better understanding the mechanisms that are present in the dispersion of pollutants in urban areas so that decisions can be made to improve air quality in these regions. The aim of this work is to investigate the scalar transfer velocity parametrizations at the top of urban canopies with aligned buildings and uniforme heigths, for using numerical simulation results obtained from Direct Numerical Simulation (DNS) and two different empirical algebraic formulations presented in existing literature. The domain is composed of 64 buildings with the following dimensions: 16 H (length, L), 16 H (width, W) and 8 H (height, H) where $H = 10\ mm$ is the building height. The distance between buildings is $10\ mm$. Source is located at the canyon region at ground level and the external wind direction is aligned to the buildings (0°) and oblique (45°). The findings reveal that, for the scenario of aligned buildings and wind direction equal to 45°, there was good agreement for both models (using σ_w and U_c calculated through DNS) in the region of streets. However, there was a poor agreement in the region of intersections. For the scenario of aligned buildings and wind direction equal to 0°, the same pattern was observed.

Keywords: Transfer velocity, DNS, street newtork model.

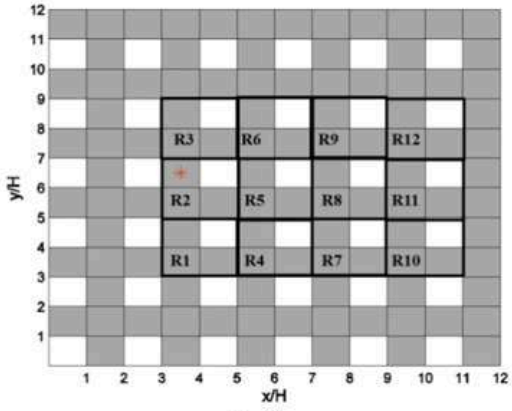
INTRODUCTION

Various studies have been concerned with the mass transfer processes within the canopies. This is due to the need to understand how the pollutant disperses in an urban area. Concerning the mass transfer process across the canopy, the transfer velocity U_T has been used as a parameter to represent the mass transfer to outside the canopy (Soulhac et al., 2011).

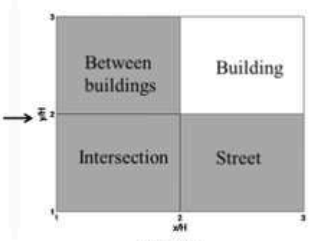
The aim of this work is to investigate the scalar transfer velocity parametrizations at the top of urban canopies with aligned buildings and uniforme heigths, for using numerical simulation results obtained from Direct Numerical Simulation (DNS) and two different empirical algebraic formulations presented in existing literature.

METHODS

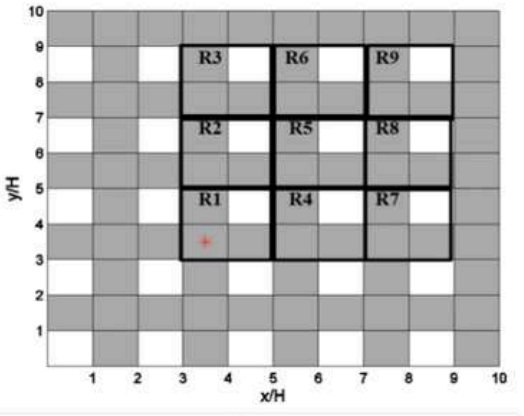
A data set from Direct Numerical Simulations (DNS) performed by Branford *et al.* (2011), Coceal *et al.* (2006) and Yao *et al.* (2001) was used in the analyses. This data set involves an array of uniform building heights, aligned configurations and wind directions of 0° and 45° relative to the building's orientation. Figure 1 shows the schematic configurations of the scenarios analyzed. The source locations for each flow direction are indicated by asterisks (*) in Figure 1. The domain is composed of 64 buildings with the following dimensions: 16 H (length, L), 16 H (width, W) and 8 H (height, H) where $H = 10\ mm$ is the building height. The distance between buildings is $10\ mm$. For analyses repeating unities closest to the source of pollutants were used.



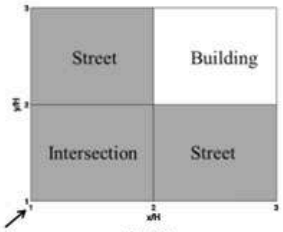
(a.1)



(a.2)



(b.1)



(b.2)

Figure 1. Schematic representation of the computational domain and repeating units in which the scalar transfer velocity was calculated for the aligned buildings configuration, (a) 0° and (b) 45° wind directions. * indicates the source locations.

FINDINGS AND ARGUMENT

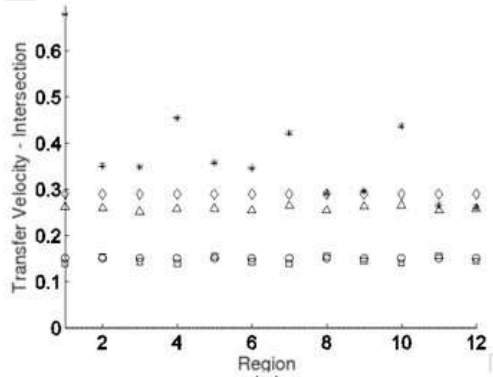
The transfer velocity, U_T, was calculated for the repeating units according to the building array configuration and it is called mean scalar transfer. The repeating units were composed by four blocks each and chosen based on the source location as shown in Figure 1.

The DNS results were compared with the models proposed by Soulhac *et al.* (2011) and Bentham and Britter (2003), as shown in Table 1.

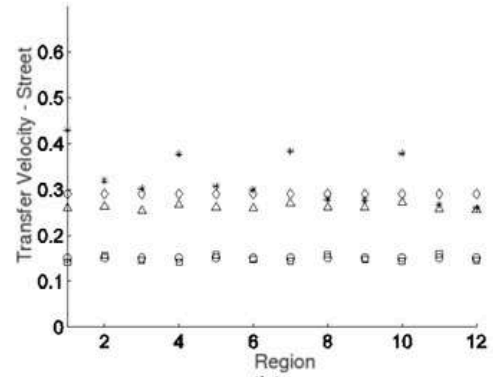
Figure 2(a), (b) and (c) show U_T at the top of the urban canopy at the intersections, streets and between buildings, respectively, considering aligned buildings and wind direction of 0°. The best agreement with DNS data is given by SOULHAC02 for calculating U_T in the streets, whilst the worst agreement was found for U_T between buildings. The best agreement with DNS data occurs with the parametrization proposed by Soulhac *et al.* (2011). The mean transfer velocity calculated by DNS is 0.35, while by SOULHAC01 is 0.25 and by SOULHAC02 is 0.29. The result obtained using B&B01 or B&B02 is 0.15. Therefore, among the parametrizations investigated in this work, SOULHAC02 gives the best results.

Table 1. Different formulae for the scalar transfer velocity.

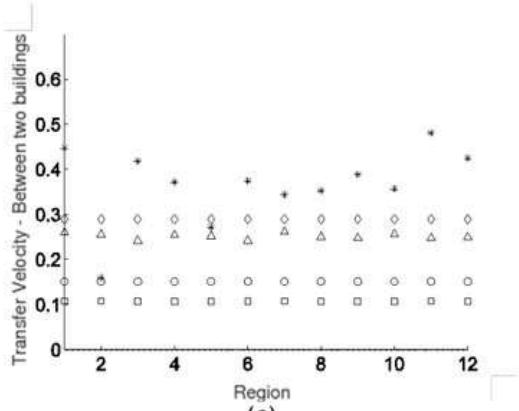
Parametrization identification	U_T *formulae*
SOULHAC01 (SOULHAC *et al.*, 2011)	$U_T = \frac{\sigma_w}{\sqrt{2\pi}}$, σ_w is the standard deviation of w at the top of the canopy and is calculated based on the numerical simulations results.
SOULHAC02 (SOULHAC *et al.*, 2011)	$U_T = \frac{\sigma_w}{\sqrt{2\pi}}$, where $\sigma_w = 1.3u_*$ and u_* is the friction velocity.
B&B01 (BENTHAM; BRITTER, 2003)	$\frac{U_T}{u^*} = \left(\frac{U_{ref} - U_c}{u^*}\right)^{-1}$, U_{ref} e U_c are calculated based on the numerical simulation results. U_{ref} is the reference velocity at $z_{ref} = 2{,}5H$ and U_c is the characteristic velocity for the mean flow within the array.
B&B02 (BENTHAM; BRITTER, 2003)	$\frac{U_T}{u^*} = \left(\frac{U_{ref} - U_c}{u^*}\right)^{-1}$, U_{ref} is calculated based on the numerical simulation results and U_c is calculated based on $\frac{U_c}{u_*} = \left(\frac{\lambda_f}{2}\right)^{-1/2}$.



(a)



(b)



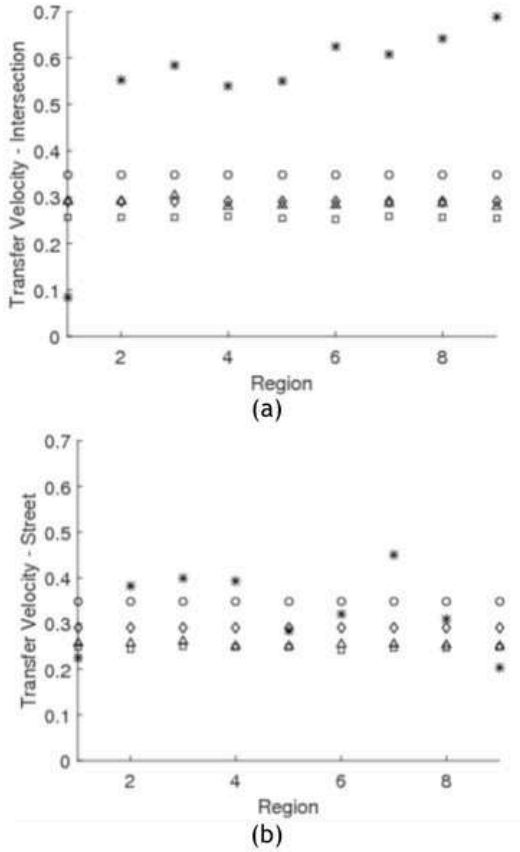
(c)

Figure 2. Scalar transfer velocity at the top of the urban canopy at (a) the intersections, (b) streets and (c) between buildings, considering aligned buildings and wind direction of 0°. The symbols represent the data obtained from (*) DNS; (Δ) SOULHAC01; (◇) SOULHAC02; (□) B&B01 and (○) B&B02.

Figure 3(a) and Figure 3(b) present U_T at the top of the urban canopy at intersections and streets, respectively, considering aligned buildings and wind direction of 45°. The DNS data indicates a global mean U_T equal to 0.5 whilst the other parameterizations indicate values between 0.25 and 0.34. However, the mean U_T at the streets calculated by DNS is 0.3, showing a better agreement with the other parametrizations. This can be explained by the fact that Soulhac *et al.* (2011) considered the vertical transfer only in the streets. The intersections were treated as two-dimensional and therefore not included in the calculation. U_T in the streets calculated using the parametrization proposed by Bentham and Britter (2003) based on U_c as a function of λ_f shows better agreement with the DNS than the other parametrizations.

CONCLUSIONS

Two distinct empirical algebraic models were assessed for estimating the scalar transfer velocity at the top of an urban canopy. It was observed that, for the configuration of aligned buildings and wind direction of 45°, there was good agreement for both models (using σ_w and U_c calculated by DNS data) in the region of streets. However, poor agreement was observed in the region of intersections. This was expected as the models were developed for an urban canyon, which is a different configuration from an urban area comprising buildings, streets, and intersections. A similar pattern was found for the configuration of aligned buildings and wind direction equal to 0°.



(a)

(b)

Figure 3. Scalar transfer velocity at the top of the urban canopy at (a) the intersections and (b) streets, considering aligned buildings and wind direction of 45°. The symbols represent the data obtained from (*) DNS; (Δ) SOULHAC01; (◇) SOULHAC02; (□) B&B01 and (○) B&B02.

REFERENCES

Branford, S. *et al.* Dispersion of a Point-Source Release of a Passive Scalar Through an Urban-Like Array for Different Wind Directions. *Boundary-Layer Meteorology*, Lido, v. 139, n. 3, p. 367-394, 2011.

Bentham, T.; Britter, R. Spatially averaged flow within obstacle arrays. Atmospheric Environment, v. 37, n. 15, p. 2037-2043, 2003.

Coceal, O. *et al.* Mean flow and turbulence statistics over groups of urban-like cubical obstacles. *Boundary-Layer Meteorology*, v. 121, n. 3, p. 491-519, 2006.

Soulhac, L. *et al.* The model SIRANE for atmospheric urban pollutant dispersion; part I, presentation of the model. *Atmospheric Environment*, v. 45, n. 39, p. 7379-7395, 2011.

Yao, Y. F.; Thomas, T. G.; Sandham, N. D. Direct numerical simulation of turbulent flow over a rectangular trailing edge. *Theoretical and Computational Fluid Dynamics*, v. 14, p. 337-358, 2001.

AIR POLLUTION CONFERENCE BRAZIL
CMAS SOUTH AMERICA
COMMUNITY MODELING AND ANALYSIS SYSTEM

DISPERSION ANALYSIS OF PARTICLE EMISSION FROM A SINTERING MAIN STACK: IMPACT OF A BAGHOUSE INSTALLATION

Willian Lemker Andreão[1], Erick Lopes, José Gustavo da Costa, Rafael Sartim
ArcelorMittal Tubarão, Serra, Espírito Santo, Brazil
[1]willian.andreao@arcelormittal.com.br

Abstract: Atmospheric pollutants are subject to transport processes that are dependent on meteorological conditions, which determine how quickly the pollutants emitted by a given source will mix and how far they will reach. Thus, atmospheric dispersion studies are of fundamental importance for air quality management, being widely used by private, governmental and research institutions to monitor air quality trends. This study investigated the dispersion impact of particle emissions from a sintering main stack with AERMOD View® mathematical model. Two different scenarios represented the particulate emissions emissions, one prior the installation of a baghouse (2015: average emission of 35.6 mg/Nm^3) and another after five years of the baghouse operation (2022: average emission of 3.7 mg/Nm^3). In all scenarios, short- and long-term national and state-level standards were not exceeded. With the scenario considering the PM emission rate for 2015, the highest PM daily average was 3.24 µg/m^3 and the highest annual average was 0.46 µg/m^3, while for the scenario considering the PM emission rate for 2022, the highest PM daily average was 0.37 µg/m^3 and the highest annual average was 0.05 µg/m^3. Compared to the first scenario, there was a reduction of 2.87 µg/m^3 in the maximum daily average, which is equivalent to a reduction of 88.6%. Accross the entire modeling domain, the average PM reduction was 87.7% (range from 87.4% to 90.9%). At the discrete receptors, located at the coordinates of the automatic air quality monitoring stations, it was found that for the 2015 emissions scenario, the average representation was 0.71% of the average daily concentrations observed at the stations, while for the scenario of 2022, the average representation was 0.09%. In conclusion, the results demonstrated that emissions from the sintering main stack have a small influence on local air quality, compared to air quality standards and compared to the maximum observed in automatic stations. Furthermore, it was possible to demonstrate that the implementation of the baghouse achieved its objective of reducing emissions and consequently eliminating the visibility of the stack plume and improving air quality in the region.

Keywords: dispersion, modeling, Aermod, sintering, emission.

INTRODUCTION

The sintering process essentially consists of mixing and homogenizing a set of raw materials with adequate humidity and a certain fuel content, submitting this homogenized mixture to an oxidizing reductive semi-fusion in a grill car oven. As consequence, particulate matter emission is generated.

In turn, the AERMOD model is a computational tool that simulates the dispersion of pollutants in the atmosphere, representing physical processes through equations. This study aimed to evaluate the impact of particulate matter on air quality, originating exclusively from emissions from the main sintering stack, over three years (2020 - 2022), considering scenarios before and after the implementation of a bag filter.

METHODS

The computational domain, with dimensions of 20 km × 20 km, was centered on the sintering stack. The surface characteristics, land use and occupation and its physical parameters were defined, as well as topography data.

To classify land use and occupation, the modeling domain was divided into two sectors to group similar characteristics. Considering the sintering stack in the center, the northeast to southwest portions were considered water. The southwest to northeast portions were considered predominantly urban. Each sector was characterized according to aerodynamic roughness, albedo, and Bowen ratio.

The study period covered the period from January 1st, 2020, to December 31st, 2022. The meteorological data were from the Vitória surface meteorological station (A612) of the National Institute of Meteorology (INMET), located at -20.27° and -40.31°. This station is located approximately 8 km away from the center of the domain. The missing data were complemented with meteorological data from the RAMQAr 02 station, from the Espírito Santo State Institute of Environment and Water Resources (IEMA), aiming to obtain a consistent and complete database. After processing by the AERMET meteorological module, a percentage of 5.75% of missing data was verified, which meets the US EPA criteria, which requires less than 10% of missing meteorological data. Regarding altitude meteorological data, processing with radiosonde data from Vitória Eurico de Aguiar Salles Airport generated a final percentage of missing data outside the US EPA criteria. For this reason, it was decided to enable the reconstitution of vertical variables using the AERMET model itself.

Figure 1 shows the wind rose with all meteorological data monitored during the three years of study (2020 - 2022). Low winds predominated, with the average vector at 353 degrees (north). The highest intensities were mainly observed in the north and

northeast quadrants. In January, February and December, the predominant wind was north, with greater intensities coming from the northeast. Between March and November, there was a greater presence of northwest and south winds. Calms (winds less than 0.5 m/s) were more frequent during drier periods.

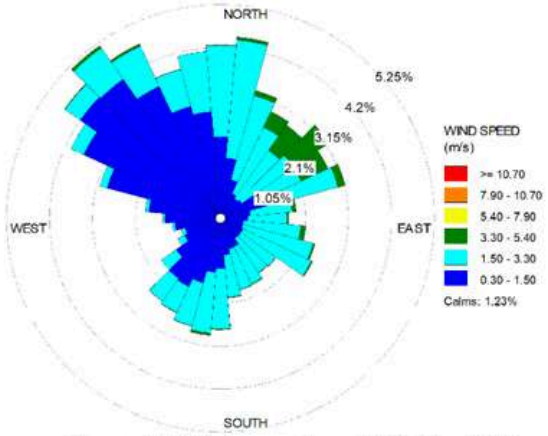


Figure 1. Wind rose from 2018 to 2020.

The modelling scenarios considered were: (1) Scenario 01, average emission rate for the year 2015, equivalent to 35.6 mg/Nm^3; (2) Scenario 02, average emission rate for the year 2022, equivalent to 3.7 mg/Nm^3. Table 1 presents the geometric characteristics of the stack and the physical characteristics of the gaseous effluent, as well as the emission rate for each modeled scenario.

Table 1. PM emission rates and information needed for dispersion modeling for each scenario

Scenario	01	02
E [mg/Nm^3]	35.6	3.7
T [°C]	160	
H [m]	80	
D [m]	7.32	
Q [m^3/h]	2,076,514.5	2,499,594.2
v [m/s]	13.7	16.5
FE	1.00	0.93
E [g/s]	12.95	1.62

The effect of building downwash close to the sintering main stack was considered. The calculation of PM concentrations was restricted to a grid of receptors spaced every 250 m throughout the modeling domain, thus forming a grid with 25921 receptor points. Discreet receptors were established at the coordinates of the automatic air quality monitoring stations (RAMQAr) that presented results for monitoring PM_{10}.
The AERMOD View software, a dispersion modeling package developed by Lakes Environmental, which incorporates the US EPA model, was used (AERMOD version 22112, AERMAP version 18081 and AERMET version 22112).

FINDINGS AND ARGUMENT

Figure 2 shows the maximum daily average concentrations of PM for Scenario 01 (emission rate for the year 2015 of 35.6 mg/Nm^3, 12.95 g/s). The highest average daily concentration modeled was 3.24 µg/m^3, approximately 2 km west of the emitting source, but being within the standards of CONAMA Resolution 491/2018 (final standard (FS): 240 µg/m^3) and State Decree 3463/R/2013 MI1 (180 µg/m^3) and FS (150 µg/m^3). This concentration represents only 2.16% of the state FS. Two others, but smaller, concentration peaks of 2.5 µg/m^3 were observed 2.5 km north away of the emitting source.

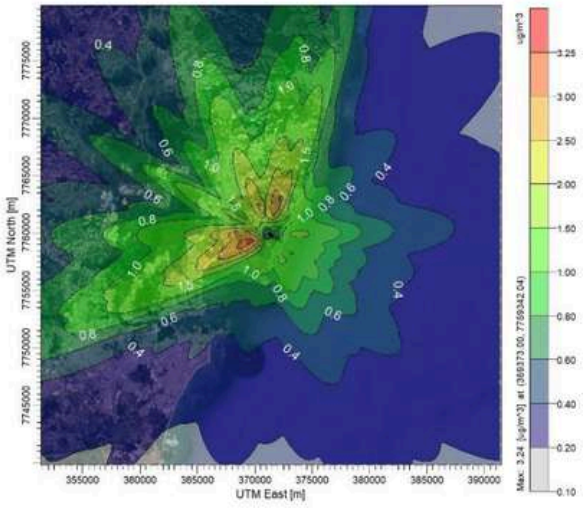


Figure 2. Maximum daily average for Scenario 01: emission rate equivalent to 35.6 mg/Nm^3.

Figure 3 shows the maximum daily average concentrations of PM for Scenario 02 (emission rate for the year 2022 of 3.7 mg/Nm^3, 1.62 g/s). The highest average daily concentration modeled was only 0.37 µg/m^3, therefore, within the standards of CONAMA Resolution 491/2018 (FS: 240 µg/m^3) and State Decree 3463/R/2013 MI1 (180 µg/m^3) and FS (150 µg/m^3). This concentration represents only 0.25% of the state FS. Compared to Scenario 01, there was a reduction of 2.87 µg/m^3 in the maximum daily average, which is equivalent to a reduction of 88.6%. Considering all receivers in the grid, the average reduction was 87.7% (range from 87.4% to 90.9%).

Figure 4 shows the evolution of daily averages of PM_{10} in one of the automatic air quality monitoring stations and the respective daily averages modeled in each scenario for the same coordinates. For the 2015 emissions scenario, the average representation was 0.71% of the observed concentrations, while for the 2022 scenario, the average representation was 0.09%.

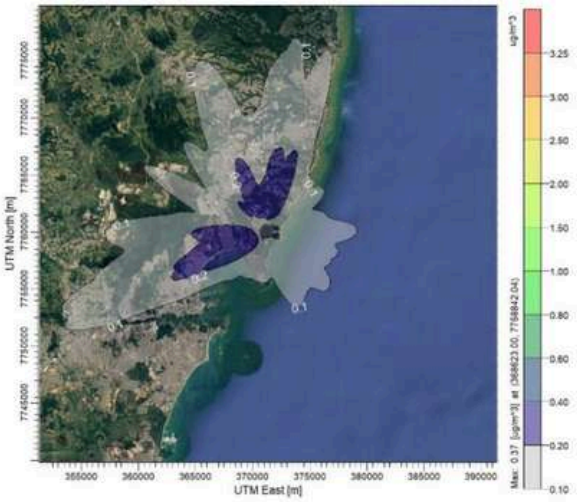


Figure 3. Maximum daily average for Scenario 02: emission rate equivalent to 3.7 mg/Nm³.

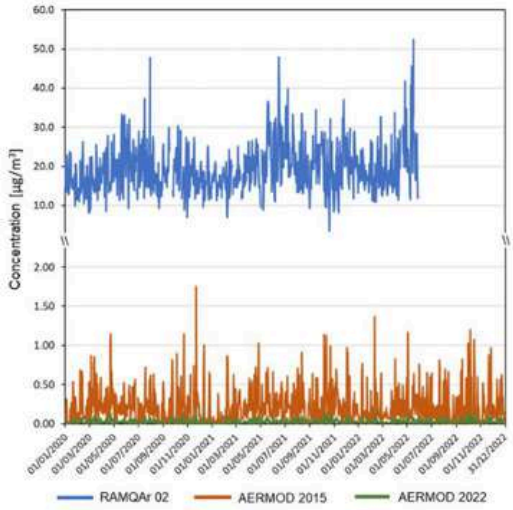


Figure 4. Average daily concentration of PM in RAMQAr 02.

The dispersion maps for the maximum annual average PM are presented in Figures 5 and 6 for the scenarios referring to average emissions in 2015 and 2022, respectively. The highest modeled concentration had a maximum annual average of 0.46 µg/m³ (Scenario 01), a value already below that recommended by CONAMA Resolution 491/2018 (80 µg/m³) and State Decree 3463/R/2013 MI1 (65 µg/m³) and FS (60 µg/m³). This value represents 0.8% of the state FS. Furthermore, this value occurs approximately 1.5 km from the emission source in the east direction, just after the coal yard towards the sea. Scenario 02 obtained a maximum annual average of 0.05 µg/m³ (0.08% of the state FS), which represents a reduction of 89% compared to Scenario 01.

The average representativeness of the maximum modeled annual concentration compared to the annual maximums observed in the automatic stations (2020 and 2021) would be 0.8% and 0.1% for the 2015 and 2022 emissions scenarios, respectively.

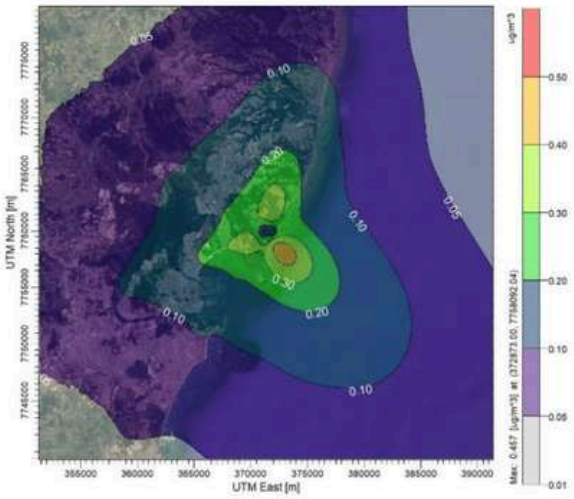


Figure 5. Maximum annual average for Scenario 01: emission rate equivalent to 35.6 mg/Nm³.

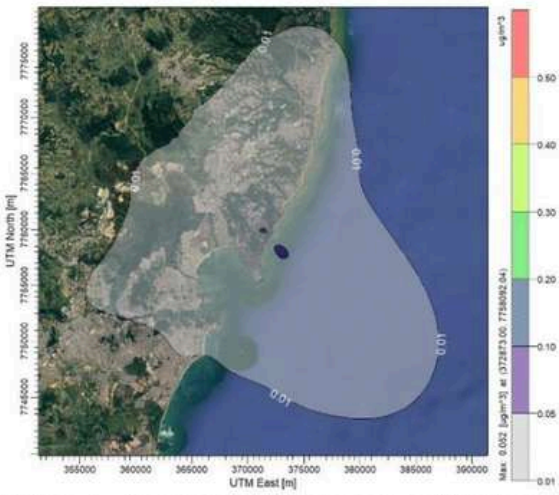


Figure 6. Maximum annual average for Scenario 02: emission rate equivalent to 3.7 mg/Nm³.

CONCLUSIONS

The continental portion of the modelling domain presented the highest concentrations for daily averages, but all within national and state air quality limits. Throughout the modelling domain, the average reduction in maximum concentrations in receptors was 87.7% (range from 87.4% to 90.9%), which demonstrates that the implementation of the bag filter achieved its objective of reducing emissions and consequently eliminating the visibility of the stack plume and improving air quality in the region. Emissions are on a local scale, which would hardly result in a significant worsening of air quality, which was demonstrated when data measured at automatic monitoring stations were compared with averages modeled for the same coordinates.

AIR POLLUTION CONFERENCE BRAZIL
CMAS SOUTH AMERICA
COMMUNITY MODELING AND ANALYSIS SYSTEM

Application of the UWRF model for the evaluation of the mitigation of the Urban Heat Island of CDMX through a system of lakes in the area of the ex-lake of Texcoco

Mariana Zavaleta Palacios[1], Arón Jazcilevich Diamant[2], Víctor Almanza Veloz[3] y José Agustín García Reynoso[4]

[1] *Instituto de Ciencias de la Atmósfera y Cambio Climático, Universidad Nacional Autónoma de México, Ciudad de México*
mariana.zavaleta@comunidad.unam.mx

[2] *Instituto de Ciencias de la Atmósfera y Cambio Climático, Universidad Nacional Autónoma de México, Ciudad de México*
jazcilev@unam.mx

[3] *Instituto de Ciencias de la Atmósfera y Cambio Climático, Universidad Nacional Autónoma de México, Ciudad de México*
victor.almanza@atmosfera.unam.mx

[4] *Instituto de Ciencias de la Atmósfera y Cambio Climático, Universidad Nacional Autónoma de México, Ciudad de México*
agustin@atmosfera.unam.mx

Abstract: In CDMX, the Urban Heat Island (UHI) reaches intensities up to 10°C, which influences the local meteorology and aggravates health problems. Through numerical modeling, it has been concluded that one of the main factors of the increase in local temperature in the city was the extinction of Texcoco's Lake. However, there are still no studies where a high resolution model (500 m) is used to analyze this phenomenon. Likewise, there is a proposal for partial lake regeneration through a system of lakes in the Zona Federal del ex-Lago de Texcoco (ZFLT) that indicates this system could modulate the local temperature in some areas of the city. Based on the above, the WRF-urban model was used at 500 m resolution with the Local Climatic Zones (LCZ) scheme and the Building Environment Parameterization (BEP) scheme in order to evaluate more accurately the mitigation of the CDMX's UHI through water bodies. A scenario was generated during the dry season of the current meteorological and urban conditions, and another was made based on the land use change of the aforementioned lake regeneration proposal. Preliminary results show that the presence of the proposed lake system results in a temperature decrease in the surrounding areas of between 0.5°C and 1.5°C.

Keywords: UHI, LCZ, WRF, urban, climate.

INTRODUCTION

In Mexico City (CDMX), the current Urban Heat Island (UHI) can reach intensities up to 10°C (Ballinas), which can trigger a series of environmental and health problems (Oke et al.). Until today, there are few researches that study the reduction of CDMX UHI through urban vegetation (Ballinas and Barradas; Vázquez Morales et al.) and even fewer those that consider water bodies, which, according to Sun and Chen, are more effective for UHI mitigation than vegetation.

In addition, Jazcilevich Diamant et al. mention that a lakes system in the Federal Zone of the former Lake of Texcoco (ZFLT by its acronym in Spanish) could increase wind speed and modulate local temperature. This statement is based on the thermal properties of the water and on the simulation results of the lakes that made up the Metropolitan Area of Mexico City lake system 500 years ago (Ruiz-Angulo and López-Espinoza).

Based on the above, the objective of this work is to evaluate, through numerical modeling and during the warm dry season, the behavior of the CDMX ICU due to the local thermal response of the lake system in the ZFLT proposed by Jazcilevich Diamant et al.

METHODS

Model configuration

For the present study, the Weather Research and Forecasting (WRF) model version 4.5.1 with the Advanced Research WRF (ARW) core was used. A mother domain and two one-way nested domains were generated. The horizontal resolution of the domains was increased from 7.5 km for Domain 1 (D01) to 1.5 km for Domain 2 (D02) and finally to 0.5 km for Domain 3 (D03). Domain D03 has a dimension of 76x76 cells, which cover the area of interest, that is, the Federal Zone of the former Lake of Texcoco and its surroundings. Also, from the surface to 50hPa, each domain presents a total of 62 atmospheric levels of Eta (dzbot=10 m, dzstrech_s = 1.2, dzstrech_u = 1.02).

For the initial and boundary conditions, the final forecast data and global operational analysis, NCEP Final Analysis (GFS-FNL), were used, with a spatial resolution of 0.25°x0.25° and a temporal resolution of six hours. In addition, the Lambert Conformal

projection and a time step of 30s were used. For land use and vegetation cover data, CGLC-MODIS-LCZ data were used.

Scenarios

Taking as criteria days with zero precipitation and clear skies, the period of March 22 - 25, 2023 was selected for the simulations.

A total of three scenarios were carried out. The first was called "Base_WRF-urban Scenario" ($E_{Base\text{-}urban}$) and considers both the use of land and vegetation presents currently at the ZMCDMX and the BEP scheme for the urban surface. The second scenario, named "Base_WRF Scenario" ($E_{Base\text{-}wrf}$), presents the same configuration as the EBase-urban except that the BEP urban scheme was not activated. The third scenario, "Lagos System Scenario" (E_{Lagos}), contemplates the proposal for partial recovery of Texcoco's Lake in the ZFLT. For this, a total of 4,600 hectares of land classified as "open shrublands" or "sterile or sparsely vegetated" were replaced by the "water" category.

Model validation

The evaluation of the model performance was done through a qualitative and quantitative comparison of the simulated results against observed data. The parameters evaluated were surface temperature and wind speed. For this, information from 14 stations of the Meteorology and Solar Radiation Network (REDMET by its acronym in Spanish) was used.

For the qualitative evaluation, daily profile graphs and wind rose graphs were used. The quantitative evaluation consisted of a statistical analysis through the calculation of metrics such as the root mean square error (RMSE), the mean bias (MBE), the Pearson correlation coefficient (R), and the improved concordance index. (dr) from Willmott et al.

FINDINGS AND ARGUMENT

Model validation

Regarding temperature, the time series show that both the EBase-urban and EBase-wrf scenarios manage to represent the daily cycle in a similar way to the observed data. However, both scenarios tend to overestimate minimum temperatures and underestimate maximum temperatures. Despite this, $E_{Base\text{-}urban}$ shows better approximations, which is reaffirmed with the statistical analysis, since $E_{Base\text{-}urban}$ presents lower values of the RMSE, higher values of R and higher values of dr.

In the case of wind speed, although there are notable differences with the observed data, again the $E_{Base\text{-}urban}$ shows better approximations than the $E_{Base\text{-}wrf}$.

Comparison between the $E_{Base\text{-}urban}$ and the E_{Lagos}

The temperature difference between E_{Lagos} and $E_{Base\text{-}urban}$ (E_{Lagos} minus $E_{Base\text{-}urban}$) shows that the proposed lake system in the ZFLT induces a temperature decrease of up to 1.0 °C, which is especially noticeable in the northwest of the body of water and during the afternoon and evening, around 17:00 h - 23:00 h. (Figure 1). This cooling, although has a greater impact in the vicinity of the proposed lake, also has a radius of influence close to 10 km.

Likewise, the difference in wind speed and wind direction between E_{Lagos} and $E_{Base\text{-}urban}$ shows that, throughout the day, air currents are generated from the surface of the proposed lake. These currents can reach speeds close to 1.8 m/s, with maximum intensities occurring during the afternoon and night. In general, these winds have a predominant southeast direction, which coincides with and explains the temperature decreases in these areas due to the proposed lake (Figure 2). However, it is also observed that the direction of these winds can become radial between 08:00 h and 10:00 h (Figure 3).

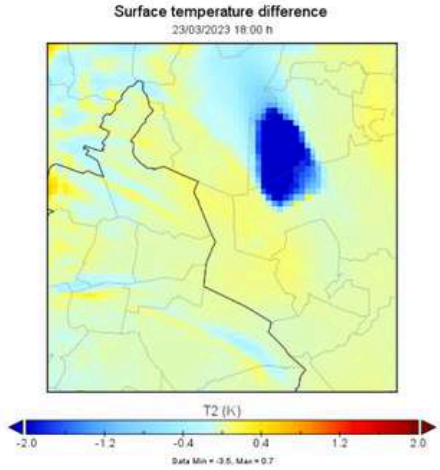


Figure 1. Surface temperature difference between E_{Lagos} and E_{Base} at 18:00 h.

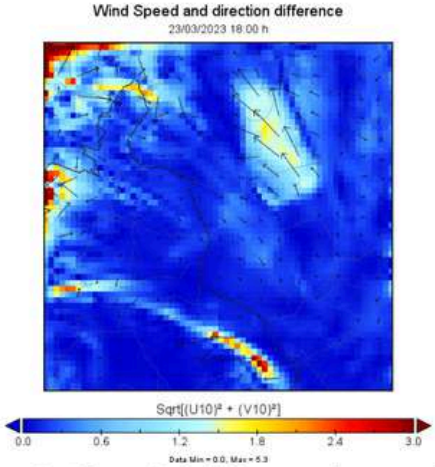


Figure 2. 10 m wind difference between E_{Lagos} and E_{Base} at 18:00 h.

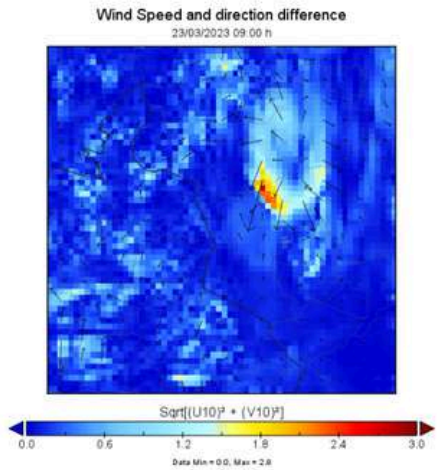


Figure 3. 10 m wind difference between E_{Lagos} and E_{Base} at 09:00 h.

CONCLUSIONS

According to the results, using the urban parameterization of the WRF allows the simulated data to present greater agreement with the observed data. Likewise, a recovery of 4,600 hectares of water in the ZFLT could cause a decrease in local temperature by up to 1°C. This cooling will be greater in the vicinity of the proposed lake, however, due to the action of the wind, its influence could reach a radius of up to 10 km. In this sense, the proposal for the partial recovery of the former Lake of Texcoco will help regulate the temperature not only of the State of Mexico but also of CDMX and therefore, it will contribute to reduce the intensities of their respective UHI.

Also, 4,600 hectares of water in the ZFLT will generate local air currents, with a predominantly southeast direction, although also radially at some hours of the day. These air currents, in addition to transporting cold air masses to nearby areas, will also transport surrounding particulate matter. Therefore, the proposed lake in the ZFLT will also help reduce local air pollution.

Finally, although the results obtained in the simulations are acceptable, they have some biases. The reason for the overestimation of minimum temperatures and the underestimation of maximum temperatures could be multifactorial, such as the use of a land cover different from the observed, use of a slightly erroneous urban scheme, or discordance in the surface temperature of simulated water bodies. Therefore, it is recommended to improve these aspects for future works.

REFERENCES

Ballinas, Mónica. *Mitigación de La Isla de Calor Urbana: Estudio de Caso de La Zona Metropolitana de La Ciudad de México*. Universidad Nacional Autónoma de México, 2011.

Ballinas, Mónica, and Víctor L. Barradas. "The Urban Tree as a Tool to Mitigate the Urban Heat Island in Mexico City: A Simple Phenomenological Model." *Journal of Environmental Quality*, vol. 45, no. 1, 2016, pp. 157–66, https://doi.org/https://doi.org/10.2134/jeq2015.01.0056.

Córdova Sáez, Karenia. "Impactos de Las Islas Térmicas o Islas de Calor Urbano, En El Ambiente y La Salud Humana. Análisis Estacional Comparativo: Caracas, Octubre - 2009, Marzo - 2010." *Terra. Nueva Etapa*, vol. XXVII, 2011, pp. 95–122, https://www.redalyc.org/articulo.oa?id=72121706005.

Jazcilevich Diamant, Aaron, et al. "Retos y Oportunidades Para El Aprovechamiento y Manejo Ambiental Del Ex Lago de Texcoco." *Boletín de La Sociedad Geológica Mexicana*, vol. 67 (2), no. ISSN-e 1405-3322, 2015, pp. 145–66, https://dialnet.unirioja.es/servlet/articulo?codigo=5295954.

Oke, T. R., et al. *Urban Climates*. Cambridge University Press, 2017, https://doi.org/10.1017/9781139016476.

Ruiz-Angulo, Angel, and Erika Danaé López-Espinoza. "Estimación de La Respuesta Térmica de La Cuenca Lacustre Del Valle de México En El Siglo XVI: Un Experimento Numérico." *Boletín de La Sociedad Geológica Mexicana*, vol. 67, 2015, pp. 215–25, https://www.redalyc.org/articulo.oa?id=94340680006.

Sun, Ranhao, and Liding Chen. "How Can Urban Water Bodies Be Designed for Climate Adaptation?" *Landscape and Urban Planning*, vol. 105, no. 1, 2012, pp. 27–33, https://doi.org/https://doi.org/10.1016/j.landurbplan.2011.11.018.

Vázquez Morales, Williams, et al. "Influence of Green Roofs on Early Morning Mixing Layer Depths in Mexico City." *Journal of Solar Energy Engineering*, vol. 138, no. 6, 2016, https://doi.org/10.1115/1.4034807.

Willmott, Cort J., et al. "A Refined Index of Model Performance." *International Journal of Climatology*, vol. 32, no. 13, 2012, pp. 2088–94, https://doi.org/https://doi.org/10.1002/joc.2419.

AIR POLLUTION CONFERENCE BRAZIL
CMAS SOUTH AMERICA
COMMUNITY MODELING AND ANALYSIS SYSTEM

STOCHASTIC FLOW İN AN IDEALIZED STREET NETWORK

Karine Klippel[1], Elisa Valentim Goulart[1], Torsten Auerswald[2], Elson Silva Galvão[1], Neyval Costa Reis Jr.[1], Omduth Coceal[2]

[1]*Federal University of Espirito Santo, BR*
karine.klippel@edu.ufes.br
elisa.goulart@ufes.br
elsongalvao@gmail.com
neyval.reis@ufes.br
[2]*University of Reading, UK*
t.auerswald@reading.ac.uk
o.coceal@reading.ac.uk

Abstract: Turbulent fluctuations dominate the flow within urban canopies and impact the dispersion of passive scalars. This study aims to better understand the stochastic nature of the turbulent flow in idealized street networks using direct numerical simulations. Turbulent flow for a fixed wind direction of 45 degrees over a regular array of cuboidal buildings was simulated. The probability density functions (PDFs) characterizing the 3D velocity components were analyzed at different horizontal locations and heights. The differences in the shape of the PDFs for the wind velocity components reflect the three-dimensionality of the stochastic flow. The distributions generally depart from Gaussian, especially within the canopy. However, the shape of the distribution also depends on the location within the street network. Beyond a transition zone above the canopy approximately Gaussian behavior is observed. Switching flow patterns were identified at the intersections near the ground, with two bistable states in wind direction. Preliminary analyses showed a switching time scale of approximately 12 eddy turnover times.

Keywords: Urban areas, DNS, stochastic flow, Gaussian distribution.

INTRODUCTION

Atmospheric flow is turbulent, with turbulence being characterised by its stochastic, three-dimensional and anisotropic nature (Wyngaard, 2010). Small particles in the atmosphere follow the flow direction and also diffuse randomly through the surrounding fluid due to turbulence. In consequence, pollutant concentration is a highly variable quantity. In urban areas the pollutant transport is more complex due to the presence of obstacles that produce more irregularity in the flow. Coceal et al. (2006) and Coceal et al. (2014) showed the complexity of the turbulent motions and, consequently, of the scalar transport around cubic building-like obstacles by visualisations of the velocity field from Direct Numerical Simulation (DNS). Auerswald et al. (2024) identified variability of the instantaneous flow structures between streets of the same type within a simplified street network, and also systematic larger-scale variations oriented along the forcing direction. Hng et al. (2022) and Hirose et al. (2022) reported that the Gaussian distribution can characterise the urban velocity fluctuations in some cases; however, the distribution more usually tends to be skewed at negative values. Building on these previous studies, this work aims to characterize flow fluctuations in an urban area by analyzing the moments and probability density functions of wind velocity and direction within an urban street network, using data from Direct Numerical Simulations (DNS). We specifically investigate the impact of location in particular streets and at different heights on the results.

METHODS

Direct numerical simulations (DNS) were performed within the DIPLOS (Dispersion of Localized Releases in a Street Network) project (Auerswald et al., 2024). The domain, shown in Figure 1, consists of a regular array of rectangular buildings elongated in y-direction and with an aspect ratio of $h/L = 0.5$ and $h/w = 1$, where h is the building height, $L = 2h$ is the length and $W = 1h$ is the width. The horizontal extent of the domain is $24h \times 24h$ and the domain height is $8h$. The simulation was run in parallel using computational block units of size $1h \times 1h \times 1h$ each resolved by $32 \times 32 \times 32$ grid points, with periodic horizontal boundaries. The simulations were run with a time step of $\Delta t = 0.00025\,T$ and data were collected every 20 time steps $(0.005\,T)$, with $T = \frac{h}{u_\tau} = 1.23$ the non-dimensional time scale, where u_τ is the wall friction velocity. The wind direction was 45 degrees to the street directions.

The stochastic characteristics of the turbulent flow field were studied here using the time series of velocity for each street typology and height. We calculated the theoretical probability density function (PDF) that characterizes the velocity components u, v and w, and compared it with the Gaussian PDF:

$$f(x) = \frac{1}{\sigma\sqrt{2\pi}} \exp -\frac{1}{2}\left(\frac{x-\mu}{\sigma}\right)^2$$

where μ is the mean velocity and σ is the standard deviation for each time series.

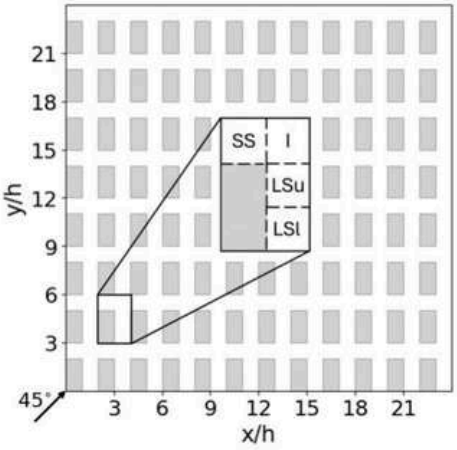


Figure 1 - Schematic of the computational domain. SS, I, LSu and LSl indicate the location of the short streets, intersections, long streets upper and long streets lower, respectively.

Additionally, the PDF and the power spectrum of the horizontal wind direction at the intersections was analysed, as we could identify switching patterns that can help in understanding the street scale fluctuations.

FINDINGS AND ARGUMENT

Probability density functions (PDFs) characterizing the 3D velocity components were analyzed at different horizontal locations. Figure 2 shows the PDFs of velocity u, v and w for each type of street at z = 0.5h. Within the canopy, for all cases, the velocity components deviate from the Gaussian distribution at both tails. The w velocity component especially has more pronounced fat tails near the ground (z = 0.125h, not shown here). In general, the upper long street has the larger asymmetry for u, v and w; for v, the distribution has a more elongated right tail (positive skewness). The opposite occurs for u and w, where the left tail is more elongated (negative skewness). For u and v, the short street and the upper long street have higher kurtosis (> 3), indicating again a greater concentration of data in the tails of the distribution, which means there is higher probability of observing extreme values compared to the Gaussian theoretical PDF. For w, the upper long street exhibits the highest kurtosis (4.7 at z = 0.5h and 6.7 at z = 0.125h), while the other streets have large, but similar kurtosis (> 3.7 in all cases). Only in two locations (intersections at z = 0.125h and z = 0.25h) and for v velocity the kurtosis is less then 3 (2.9 and 2.7), showing reduced fluctuations in the instantaneous flow and more Gaussian behaviour.

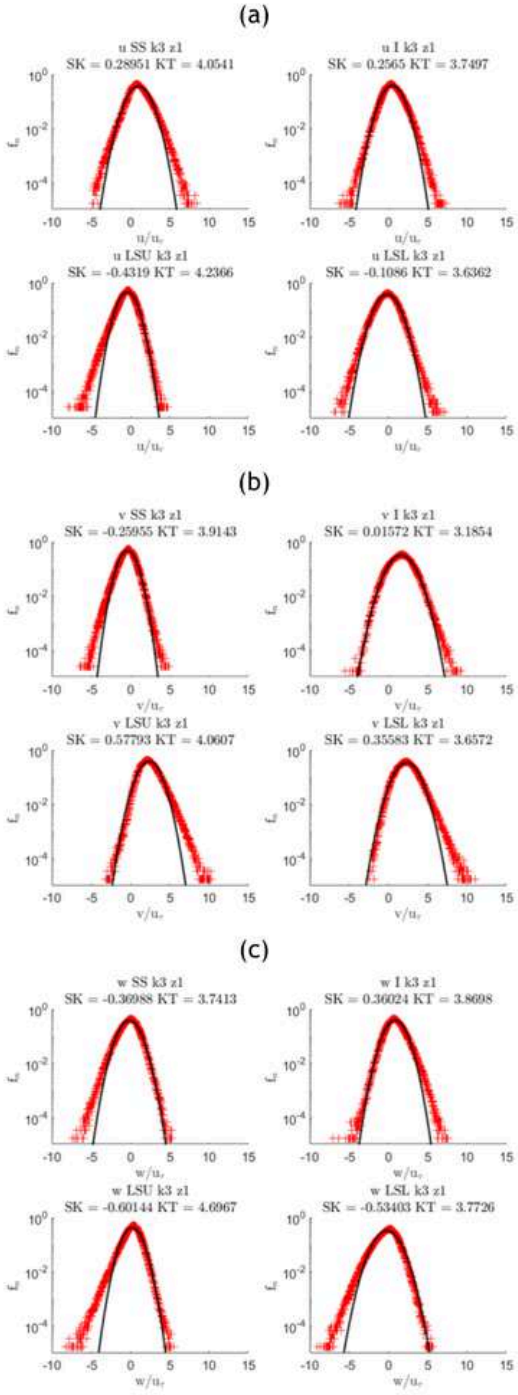


Figure 2 - Probability density functions (PDFs) of wind velocity components a) u, b) v, and c) w, at z = 0.5h and for each street type: short street (SS), intersection (I), upper long street (LSU) and lower long street (LSL).

In all cases, the variation in the wind direction in each street within the canopy exhibits characteristics distinct from a Gaussian distribution.

Wind tunnel experiments and CFD simulations have shown that fluctuations in wind direction significantly influence air flow across an intersection (Soulhac et al., 2009). Focusing on the specific case of an intersection, especially closer to the ground at z = 0.125h (Figure 3), we find evidence of the prevalence of two favorable states, with peaks in positive and negative wind directions. This is more evident when we apply a moving average (with a window of one eddy turnover time used here) to remove the noise of the time series. The bimodal histogram of wind direction (Figure 4) at this height shows that the peaks are at approximately -16° and 117°. At z = 0.25h (not shown here), the peaks are approximately at -5° and 95°, indicating that the flow is switching between the adjacent short and long streets, with a higher probability along the latter. Preliminary analyses of the power spectrum of wind direction (Figure 5) indicated a peak at a frequency of 0.083 Hz, corresponding to a switching time scale of approximately 12T.

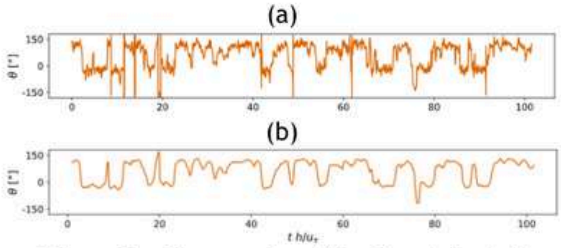


Figure 3 - Time series of horizontal wind direction at (x, y, z) = (2h, 3h, 0.125h): a) original, b) smoothed using a moving average with a window equal to an eddy turnover time.

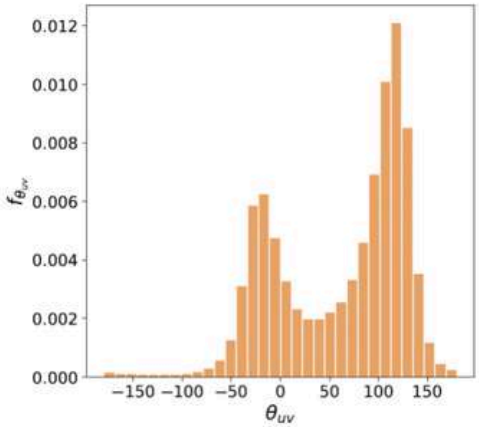


Figure 4 - Histogram of horizontal wind direction at the intersections at z = 0.125h.

CONCLUSIONS

The differences in the shapes of the PDFs for the wind velocity components reflect the three-dimensionality of the stochastic flow. The shape of the distribution also depends on location within the street network. The distributions generally depart from Gaussian within the canopy, exhibiting fat tails, especially for the upper long streets and velocity w. Above the canopy (above z = 1.25h), approximately Gaussian behavior is observed. Since the flow is approaching 45°, the u and v PDFs are very similar. At the intersections, we observed a bimodal distribution of instantaneous wind direction, with two bistable states, and preliminary analyses show a switching time scale of approximately 12T.

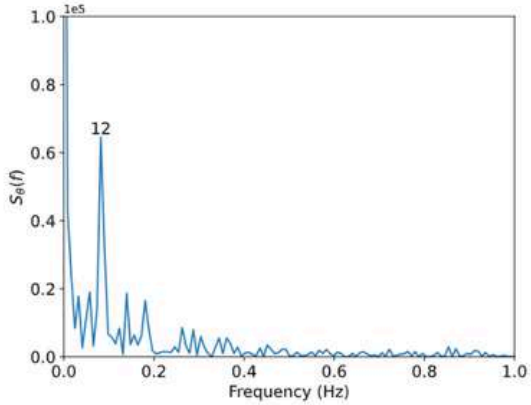


Figure 5 - Power spectrum of wind direction.

REFERENCES

Auerswald, T., Klippel, K., Thomas, T. G., Goulart, E. V., Carpentieri, M., Hayden, P. and Coceal, O. Effect of Flow Variability on Dispersion of Continuous and Puff Releases in a Regular Street Network. Boundary-Layer Meteorology, 190(4), 20. 2024.

Coceal, O., Goulart, E. V., Branford, S., Thomas, T. G. and Belcher, S. E. Flow structure and near-field dispersion in arrays of building-like obstacles. Journal of Wind Engineering and Industrial Aerodynamics, Elsevier, v. 125, p. 52-68, 2014.

Coceal, O., Thomas, T., Castro, I. and Belcher, S. Mean flow and turbulence statistics over groups of urban-like cubical obstacles. Boundary-Layer Meteorology, Springer, v. 121, n. 3, p. 491-519, 2006.

Hirose, C., Nomichi, T. and Ikegaya, N. Distributions of gust and peak factors at a pedestrian level in a simplified urban canopy obtained by particle image velocimetry. Building and Environment, Elsevier, p. 109350, 2022.

H'ng, Y. M., Ikegaya, N., Zaki, S. A., Hagishima, A. and Mohammad, A. F. Wind-tunnel estimation of mean and turbulent wind speeds within canopy layer for urban campus. Urban Climate, Elsevier, v. 41, p. 101064, 2022.

Soulhac, L.; Garbero, V.; Salizzoni, P.; Mejean, P.; Perkins, R. Flow and dispersion in street intersections. Atmospheric Environment, Elsevier, v. 43, n. 18, p. 2981-2996, 2009.

AIR POLLUTION CONFERENCE BRAZIL
CMAS SOUTH AMERICA
COMMUNITY MODELING AND ANALYSIS SYSTEM

REGIONAL CLIMATE SIMULATIONS FOR SOUTH AMERICA IN THE CONTEXT OF THE FOCI PROJECT

Natália Machado Crespo[1], Rosmeri Porfírio da Rocha[2], Peter Huszár[1], Michal Belda[1], Tomáš Halenka[1]

[1] *Department of Atmospheric Physics, Faculty of Mathematics and Physics, Charles University, V Holešovičkách 747/2, 180 00, Prague, Czech Republic*
natalia.machado-crespo@matfyz.cuni.cz; peter.huszar@matfyz.cuni.cz; michal.belda@matfyz.cuni.cz; tomas.halenka@matfyz.cuni.cz
[2] *Departamento de Ciências Atmosféricas, Instituto de Astronomia, Geofísica e Ciências Atmosféricas, Universidade de São Paulo, Rua do Matão 1226, Cidade Universitária, São Paulo, Brazil*
rosmerir.rocha@iag.usp.br

Abstract: The FOCI project (https://www.project-foci.eu/wp/) aims to better understand the impacts of key non-CO2 radiative forcers, to assess where and how they arise, and their impact on the climate system. The project will find and test an effective implementation of them into global Earth System Models (ESMs) and into Regional Climate Models (RCMs) and hopes to subsequently use these tools to investigate mitigation and adaptation policies incorporated in selected scenarios of future development, targeted at Europe and other regions of the world. In this context, one contemplated region of FOCI interests is Central/South America. In this study, we will focus on South America, specifically in southeastern Brazil, where one of the most populated cities in the world is located: the Metropolitan Area of São Paulo. The new version of RegCM5 will be used for both climate and climate-chemistry mode simulations in high resolution, with nested domain around São Paulo city for a convection-permitting simulation. The aim is to explore results of one year simulation driven by "perfect" boundary conditions of ERA5 and from assimilated chemistry by Copernicus Atmosphere Monitoring Service (CAMS) in terms of selected climate characteristics and chemical species concentrations, that is, to assess the impact of chemistry on atmospheric variables, such as temperature and precipitation. RegCM5 is one of the assigned RCMs involved in FOCI and performs remarkably well in the South America domain; moreover, is being actively used under the CORDEX initiative.

Keywords: South America, FOCI project, RegCM5, convection-permitting, CAMS

INTRODUCTION

The FOCI project ("Non-CO_2 Forcers and their Climate, Weather, Air Quality and Health Impacts", https://www.project-foci.eu/) aims to better understand the impacts of key non-CO_2 radiative forcings, to assess where and how they arise, and their impact on the climate system. The final goal is to provide tools to investigate mitigation and adaptation policies incorporated in selected scenarios of future development. In this study, the focus is the South America domain (Figure 1), one of the contemplated regions of FOCI interests. The goal of this preliminary analysis is to assess the impact of chemistry and high model resolution on local climate representation.

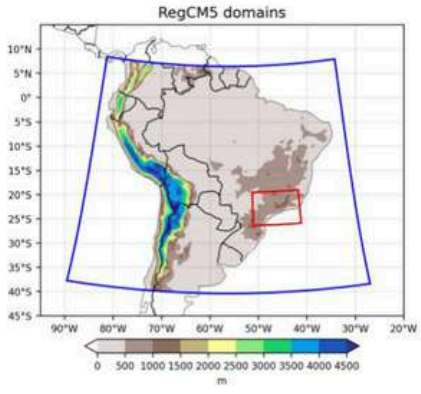


Figure 1. South America simulation domains in 0.2° (blue line) and 0.03° of horizontal resolutions (red line). The shaded colors represent the orography (m) of RegCM.

AIR POLLUTION CONFERENCE BRAZIL

CMAS SOUTH AMERICA

COMMUNITY MODELING AND ANALYSIS SYSTEM

METHODS

The fifth generation of the Regional Climate Model System (RegCM5; Giorgi et al., 2023) is used for climate, climate-chemistry and convection-permitting (CP) mode simulations. The common configurations among the experiments are the dynamical core, microphysics, radiation and surface scheme set as MOLOCH, NoTo, CCM3 and CLM4.5, respectively.

For the three 0.2° horizontal resolution experiments the convection scheme (Tiedke) and number of grid points (261 x 235 x 31) are the same. For the two 0.03° horizontal resolution experiments the convection is turned off and the moist convection is solved explicitly by NoTo scheme (CP simulation) in a grid with 300 x 230 x 41 points. Table 1 presents further differences between the experiments. Both CP simulations are nested by their respective coarser simulation with the same PBL scheme.

The period of simulation covers the whole **year of 2010, starting in December 2009**. The driving boundary conditions are given by ERA5 (Hersbach et al., 2020) and the Copernicus Atmosphere Monitoring Service (CAMS; Inness et al., 2019). The reference dataset for the evaluation is the Multi-Source Weighted-Ensemble Precipitation (MSWEP; Beck et al., 2019), Multi-Source Weather (MSWX) (Beck et al., 2022).

Table 1. Experiment names and their further configurations.

Experiment	PBL	Chemistry
Chem	Holtslag	Activate gas phase and sulfate, 4 dust bins scheme, 4 species black/anthropic carbon simulation
Holt		-
CPHolt		
UW	UW	
CPUW		

The analysis is conducted over the smaller domain (Figure 1), since a broader overview from the bigger domain was presented by Crespo et al. (2024).

FINDINGS AND ARGUMENT

Chem shows the strongest (positive) bias for precipitation (Figure 2). Except for *Chem*, the other two coarser experiments show relatively small biases compared with the CP ones, that are wetter than observations. The overestimation of precipitation by the CP simulations might be related to the enhancement of the spatial resolution especially in regions of complex orography (such as regions closer to the coast of São Paulo state).

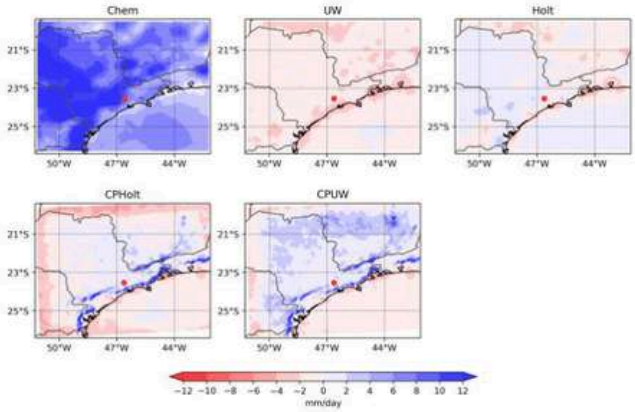


Figure 2. Annual bias of precipitation (mm/day) for each simulation with MSWEP as reference. The red dot indicates the city of São Paulo.

Most simulations present positive bias in temperature, i.e. warmer than observed (Figure 3). *UW* has the smallest bias over great part of São Paulo state when compared with the other simulations. In this case, CP experiments decrease the bias near the coast.

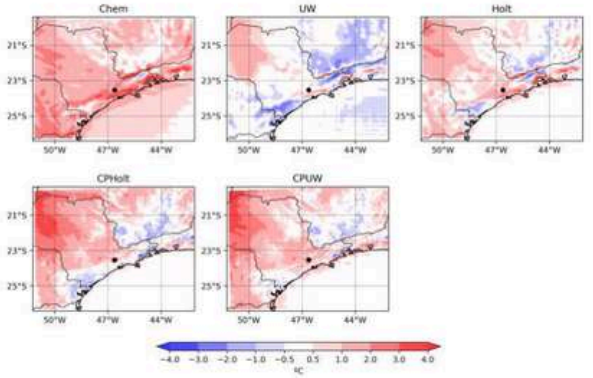


Figure 3. Annual bias of temperature at 2-m height (°C) for each simulation with MSWX as reference. The black dot indicates the city of São Paulo.

All simulations have a good representation of the annual cycle of temperature averaged over the CP domain (Figure 4). Nevertheless, *Chem* overestimates the temperature by 2°C for almost the whole year. For the precipitation, all simulations capture the phase and amplitude of observed annual cycle, except for *Chem* (Figure 4).

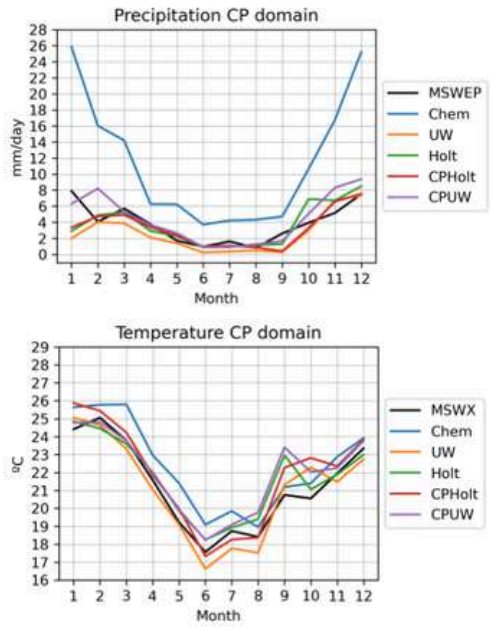


Figure 4. Annual cycle of precipitation (mm/day) and temperature at 2-m height (°C) averaged over the CP domain.

CONCLUSIONS

All the experiments were able to reproduce the annual cycle of precipitation (except for *Chem*) and temperature over the domain centered in the state of São Paulo. The *UW* simulation (coarser resolution) was the ones less biased in terms of annual mean temperature, whereas in terms of annual precipitation both *UW* and *Holt* performed similarly. The CP simulations presented a wet bias basically over the whole domain.

A possible reason for the strong bias in the *Chem* experiment might be related to the fact that RegCM is well tuned for running without chemistry whereas with the addition of aerosols pushes the model off balance, especially when activating the feedback from aerosols on radiative, thermodynamic and dynamic fields. Moreover, further sensitivity tests in the chemistry mode (as well as in CP) shall be performed by changing the microphysics scheme, for instance.

ACKNOWLEDGEMENT

This study has been co-funded by the European Union with funding from the European Union's Horizon Europe research and innovation Programme under grant agreement No. 101056783.

REFERENCES

Beck, Hylke E., Wood, Eric F., Pan, Ming et al. (2019) "MSWEP V2 Global 3-Hourly 0.1° Precipitation: Methodology and Quantitative Assessment". *Bulletin of the American Meteorological Society* 100(3), 473-500. https://doi.org/10.1175/BAMS-D-17-0138.1

Beck, Hylke E., van Dijk, Albert I. J. M., Larraondo, Pablo R. et al. (2022) "MSWX: Global 3-Hourly 0.1° Bias-Corrected Meteorological Data Including Near-Real-Time Updates and Forecast Ensembles". *Bulletin of the American Meteorological Society* 103(3), E710-E732. https://doi.org/10.1175/BAMS-D-21-0145.1

Crespo, Natália M., da Rocha, Rosmeri P., Huszár, Peter et al. (2024) "Regional climate simulations for South America in the FOCI Project". Poster presented in *the 14th International Conference on Air Quality, May 13-17, 2024, Helsinki, Finland.* DOI: 10.13140/RG.2.2.16111.65447

Giorgi, Filippo, Coppola, Erika, Giuliani, Graziano, et al. (2023) "The fifth generation regional climate modeling system, RegCM5: Description and illustrative examples at parameterized convection and convection-permitting resolutions". *Journal of Geophysical Research: Atmospheres*, 128, e2022JD038199. https://doi.org/10.1029/2022JD038199

Hersbach, Hans, Bell, Bill, Berrisford, Paul, et al. (2020) "The ERA5 global reanalysis". *Quarterly Journal of the Royal Meteorological Society*, 146(730), 1999-2049. https://doi.org/10.1002/qj.3803

Inness, Antje, Ades, Melanie, Agustí-Panareda, Anna, et al. (2019) "The CAMS reanalysis of atmospheric composition". *Atmospheric Chemistry and Physics*, 19, 3515-3556, https://doi.org/10.5194/acp-19-3515-2019.

SESSION 15
Street Scale Air Quality Modeling

- Regional air quality models can not calculate pollutant concentration at street scale. Street air quality modeling requires simulating pollutant concentrations inside the urban canyons. Urban canyons are compartments formed by the street and its flanked buildings. They are expected to have high pollutant concentrations for their closeness to vehicular emissions and for being a space with reduced dispersion. Currently, there are many street-scale air quality models, with different assumptions and formulations, that describe the dynamics and chemistry inside urban canyons. These models usually require street-level emission and urban morphology information. The representation of pollutant concentration at street scale is essential for estimating pollutant exposure to pedestrians, developing urban planning policies, and studying different vehicular fuel-emission scenarios.
- This session's topics include:
- The Model of Urban Network of Intersecting Canyons and Highways (MUNICH)
- The Street-in-Grid model (SinG)

SESSÃO 15

INFLUENCE OF TRAFFIC EMISSIONS OVER AIR QUALITY INSIDE STREET CANYONS: A MUNICH APPLICATION IN A NEIGHBORHOOD IN BRAZIL 427

AIR POLLUTION CONFERENCE BRAZIL
CMAS SOUTH AMERICA
COMMUNITY MODELING AND ANALYSIS SYSTEM

INFLUENCE OF TRAFFIC EMISSIONS OVER AIR QUALITY INSIDE STREET CANYONS: A MUNICH APPLICATION IN A NEIGHBORHOOD IN BRAZIL

Karina Tonoli Cevolani[1], Elisa Valentim Goulart[2], Lya Lugon Cornejo Von Marttens[3] and Jane Meri Santos[4]

[1]*Federal University of Espírito Santo*
karinatonolic@gmail.com

[2]*Federal University of Espírito Santo*
elisavalentim@gmail.com

[3]*CEREA, École des Ponts ParisTech, EDF R&D, 77455 Marne la Vallée, France*
lya.lugon@enpc.fr

[4]*Federal University of Espírito Santo*
jmerisantos@yahoo.com.br

Abstract: Air pollution is a concern worldwide especially in urban areas, in which dispersion is limited and outdoor activities take place essentially at the street-level and close to traffic emissions. In order to analyze the impact of traffic emissions on the $PM_{2.5}$, PM_{10} e NO_2 concentrations inside street canyons, MUNICH model was executed for an urban neighborhood in the Southeast of Brazil. In addition, MUNICH was used to investigate the sensibility of street concentrations by (i) changing meteorology, urban geometry, background concentrations, and emissions, and (ii) to verify the impact of distinct mobility urban scenarios. In order to perform these analyses, meteorology and background concentrations were obtained from WRF-Urban model v.4.1.5 and CMAQ v. 5.3.2, respectively. Emissions data were determined based on the latest local inventory released by the State Institute of Environment and Water Resources. Particularly, volatile organic emissions were chemically speciated following factors associated with combustion of Brazilian fuels available in the literature. Street network and buildings were defined considering the data from the local city hall database. MUNICH simulations indicated peaks of concentrations associated with low values of planetary boundary layer and/or friction velocity. A decrease by roughly 30% on the aspect ratio in street close to the air quality station used in validation caused a reduction in about 13% and 9% on average particles and NO_2 concentration, respectively. Street concentrations proved to be sensible to input data mostly on low traffic roads. Regarding PM_{10} and $PM_{2.5}$, MUNICH simulations suggested a potential overestimation of resuspension emission determined by the local agency inventory. Finally, scenarios changing the urban mobility could reduce up to 93%, 80% and 66%, respectively, of NO_2, $PM_{2.5}$ and PM_{10} concentrations at the street-level. However, these scenarios were not strong enough to respect the international recommendations on air quality, and more ambitious restrictions are needed.

Keywords: MUNICH model, particulate matter, nitrogen dioxide, urban area, traffic emission scenarios.

INTRODUCTION

Particulate Matter (PM) is associated with respiratory and cardiovascular diseases (US EPA, 2023b). Nitrogen dioxide (NO_2) can irritate airways in the human respiratory, contributing to development of respiratory diseases (including asthma) and increasing of hospital admissions (Holgate et al., 1999; US EPA, 2023a). In urban areas, deterioration of air quality together with the expectation to increase the urban population may potentially increase the number of vulnerable people who breathe unhealthy air. In order to determine the level of air pollution, air quality models were created. Model of Urban Network of intersecting Canyons and Highways (MUNICH) was developed (Kim et al., 2018) and improved (Lugon et al., 2020; Lugon et al., 2021b; Kim et al., 2022) to overcome the limitations present in other models by integrating a non-stationary approach (Lugon et al., 2020) and allowing air dispersion modeling over a whole city (Lugon et al., 2021a; Wang, T. et al., 2022; Liang, J. et al., 2023) with a relatively low computational cost. In face of the new air quality guidelines recommended by WHO (WHO, 2021), understanding the actual level of deterioration of air quality and establishing distinct emissions scenarios may support public strategies for pollution control. In this context, this study employs MUNICH over a Brazilian neighborhood (Vitoria, ES) to (i) evaluate the influence of traffic emissions on the $PM_{2.5}$, PM_{10} and NO_2 concentrations in streets (ii) investigate the sensibility of street-level concentrations by changing meteorology, urban geometry, background concentrations and emissions and (iii) verify the impact of different mobility urban scenarios on the air quality inside street canyon. It is the second application of MUNICH in South America.

SİMULATİONS SET UP

MUNICH was applied to simulate NO_2, PM_{10} and $PM_{2.5}$ concentrations during November and December, 2019. The choice for these months was based on the data availability. For all simulations, gas-phase chemistry is considered using the MUNICH photochemistry module.

Site description

Study was performed at Enseada do Suá (illustrated at **Fig. 1**), a neighborhood in the Great Vitória Region, an urban area located in the southeast coast

of Brazil. Air quality in this region is influenced by traffic and industrial emissions (IEMA, 2022). Enseada Suá's station was used to validate MUNICH simulations.



Figure 1. Study area (Blue lines). Brown polygons indicate the urban area. Dots show the location of two air quality stations and one meteorological station (Cevolani et al., 2024).

Input data

Fig. 2 shows all the input data needed to run MUNICH. The street network and their characteristics were determined from Vitória city's hall website (see in: https://geoweb.vitoria.es.gov.br/, composed by 193 streets segments. Last access in: November, 16th, 2021). Length and width for each street were defined by utilizing QGis software v.3.10.10 (https://qgis.org/pt_BR/site/). Emissions for each street segment were quantified based on the emission inventory released by the State Institute of Environment and Water Resources for the base year 2015 (IEMA, 2019). Emissions were quantified for primary, streets with high road traffic, and secondary streets, low traffic roads. Volatile organic compounds were speciated based on Martins (2006). Background concentrations were obtained from simulation performed and validated by Kitagawa et al. (2021,2022), using the Community Multiscale Air Quality (CMAQ) model version 5.3.2 (US EPA, 2022a) together with the Integrated Source Apportionment Method (ISAM) tool (US EPA, 2022b). Meteorological data was obtained from WRF-Urban model version 4.1.5 (Skamarock et al., 2008; Skamarock et al., 2019), which was performed and validated by Kitagawa et al. (2021,2022).

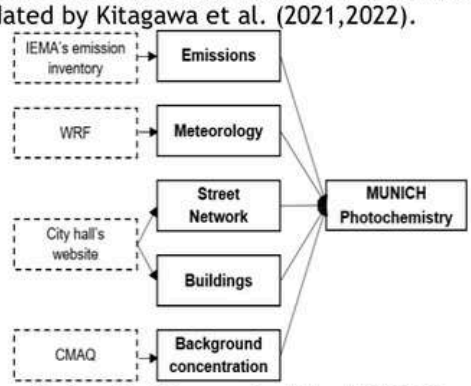


Figure 2. Input data required for MUNICH model.

Simulations performed

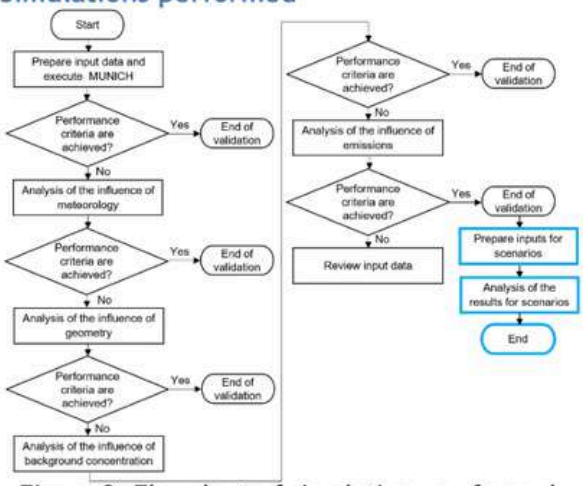


Figure 3. Flowchart of simulations performed.

FINDINGS AND ARGUMENT

Influence of meteorological variables

Peaks of simulated concentrations were associated with low values of Planetary Boundary Layer height (PBL height) and friction velocity (u*). Minimum values (0.03m/s for u* and 61m for PBL height) were defined. However, all validation criteria proposed by Hanna and Chang (2012) and Herring and Huq (2018) have not met.

Influence of geometry

Sensibility tests changing the geometry of two primary street segments close to Enseada Suá's station were performed. Increase of street width by 40% caused reduction by roughly 9% and 13% of average NO_2 and PM concentrations over the two street segments.

Influence of background concentrations

As mentioned in Kitagawa et al. (2021,2022), the resulting CMAQ concentrations for NO_2 are overestimated compared to observations in Vitória. After a correction of background concentrations, all acceptance criteria were reached. Largest reduction of average NO_2 concentrations were simulated for secondary streets, with low traffic emissions.

Influence of resuspension emissions

Particle resuspension was estimated based on the local agency emission inventory, and totalized more than 80% of total particle emissions in streets. Good model performance overall was achieved with null resuspension emission, which indicates an overestimation of resuspension emission and it emphasizes the need for better estimation for this source type.

Mobility scenarios

Three mobility scenarios were simulated: (i) no vehicular traffic in the main roads, (ii) no vehicular traffic in the secondary roads and (iii) no vehicular traffic in important roads on the weekends during a specific period. Changes in urban mobility could reduce up to 93%, 80% and 66%, respectively, of NO_2, $PM_{2.5}$ and PM_{10} concentrations at the street-

level. However, even with the most ambitious scenario, violations to national standards and to new air quality guidelines recommended by WHO (WHO, 2021) were noted.

CONCLUSIONS

MUNICH proved to be an important tool to evaluate air quality in streets and evaluate the impact of different mobility scenarios in South America. The model is sensitive to input data, such as meteorological (u*, PBLH), background concentrations and emissions, which highlights the importance of an accurate input dataset and the uncertainties that street-level simulations are submitted to. This study suggested a potential overestimation of resuspension emission. Finally, different emission scenarios performed indicated an improvement on the air quality levels but it was not enough to meet air quality standards.

REFERENCES

Cevolani, K. T. et al. "Influence of distinct mobility scenarios on NO_2, $PM_{2.5}$ and PM_{10} street-level concentrations—A case study in a Brazilian urban neighborhood". *Atmospheric Pollution Research*, v. 15, 2024.

Hanna, S.; Chang, J. Acceptance criteria for urban dispersion model evaluation.Meteorology and *Atmospheric Physics*, Springer, v. 116, n. 3, p. 133-146, 2012.

Herring, S.; Huq, P. A review of methodology for evaluating the performance of atmospheric transport and dispersion models and suggested protocol for providing more informative results. *Fluids*, MDPI, v. 3, n. 1, p. 1-21, 2018.

Holgate, S. T. et al. *Air pollution and health*: Academic Press, 1999.

IEMA. Air quality: "Emission inventory 2015". 2019. Available in: <https://iema.es.gov.br/qualidadedoar/inventariodefontes/2015>. Accessed in: May 24th, 2022.

IEMA. "Air quality report in Great Vitoria: 2021". 2022. Available in: <https://https://iema.es.gov.br/qualidadedoar/relatorios>. Accessed in: May 29th, 2023.

Kim, Y. et al. "MUNICH v2.0: A street-network model coupled with SSH-aerosol (v1.2) for multi-pollutant modelling". *Geoscientific model development discussions*, Copernicus GmbH, p. 1-33, 2022.

Kim, Y. et al. "Multi-scale modeling of urban air pollution: Development and application of a Street-in-Grid model (v1.0) by coupling MUNICH (v1.0) and Polair3D (v1.8.1)". *Geoscientific model development*, Copernicus GmbH, v. 11, n. 2, p. 611-629, 2018.

Kitagawa, Y. K. L. et al. "Exposure and dose assessment of school children to air pollutantsin a tropical coastal-urban area". *Science of The Total Environment*, Elsevier, v. 803, p.1-12, 2022.

Kitagawa, Y. K. L. et al. "Source apportionment modelling of $PM_{2.5}$ using CMAQ-ISAM over a tropical coastal-urban area". *Atmospheric Pollution Research*, Elsevier, v. 12, n. 12, p. 1-12, 2021.

Liang, J. et al. "Combined effects of photochemical processes, pollutant sources and urban configuration on photochemical pollutant concentrations". *Sustainability*, MDPI, v. 15, n. 4, p. 3281, 2023.

Lugon, L. et al. "Nonstationary modeling of NO_2, NO and NO_X in Paris using the Street-in-Grid model: coupling local and regional scales with a two-way dynamic approach". *Atmospheric chemistry and physics*, Copernicus GmbH, v. 20, n. 13, p. 7717-7740, 2020.

Lugon, L. et al. "Simulation of primary and secondary particles in the streets of Paris using MUNICH". *Faraday discussions*, Royal Society of Chemistry, v. 226, p. 432-456, 2021.

Lugon, L. et al. "Black carbon modeling in urban areas: investigating the influence of resuspension and non-exhaust emissions in streets using the Street-in-Grid model for inert particles (SinG-inert)". *Geoscientific Model Development*, Copernicus GmbH, v. 14, n. 11, p. 7001-7019, 2021.

Martins, L. D. "Sensibility of tropospheric ozone formation to traffic emissions in the metropolitan region of São Paulo". *PHD thesis* – University of São Paulo, São Paulo, 2006.

Skamarock, W. C. et al. "A description of the Advanced Research WRF version 3". *NCARTechnical note-475+* STR. Citeseer, 2008.

Skamarock, W. C. et al. "A description of the advanced research WRF model version 4". *National Center for Atmospheric Research:* Boulder, CO, USA, 2019.

US EPA. "Basic Information about NO_2". 2023. Available in: <https://www.epa.gov/no2-pollution/basic-information-about-no2#Effects>. Accessed in: August 8th, 2023.

US EPA. "CMAQ models". 2022. Available in: <https://www.epa.gov/cmaq/ cmaq-models-0>. Accessed in: July 31th, 2022.

US EPA. "Particulate Matter (PM) Basics". 2023. Available in: <https://www.epa.gov/pm-pollution/particulate-matter-pm-basics#effects>. Accessed in: August 8th, 2023.

US EPA. "The Integrated Source Apportionment Method (CMAQ-ISAM)". 2022. Available in:<$https://www.epa.gov/cmaq/integrated-source-apportionment-method-cmaq-isam$>. Accessed in: July 31th, 2022.

Wang, T. et al. "An integrated air quality modeling system coupling regional-urban and street models in Beijing". *Urban climate*, Elsevier, v. 43, p. 101-143, 2022.

WHO. "WHO global air quality guidelines: particulate matter ($PM_{2.5}$ and PM_{10}), ozone, nitrogen dioxide, sulfur dioxide and carbon monoxide: executive summary". 2021. Available in: <https://apps.who.int/iris/handle/10665/345334> Accessed in: June 20th, 2023.

AIR POLLUTION CONFERENCE
5th CMAS SOUTH AMERICA
COMMUNITY MODELING ANALYSIS SYSTEM

PROCEEDINGS OF THE

AIR POLLUTION CONFERENCE 2024

And 5th CMAS South America









Maria de Fátima Andrade
Taciana Toledo de A. Albuquerque
Jane Meri Santos

ISBN: 978-65-985800-0-1